# *Studies on the Molecular Structures of Some Cyanuric Compounds by Electron Diffraction*

By Yûmi AKIMOTO*)

(Received April 13, 1954)

Recently, heterocyclic compounds have been studied theoretically from various points of view. We cannot admit, however, that we have so many experimental data available for this theory as for other spheres of study. In order to obtain such data, it may be necessary that more electron diffraction investigations be made on such heterocyclic compounds.

In this paper two kinds of cyanuric compounds, that is, cyanuric chloride and melamine are taken up. These compounds have a good symmetry, which makes it possible to measure the whole scheme of the molecules by comparatively few parameters. Therefore these compounds may be considered to be quite suitable for electron diffraction investigations.

Several crystalline cyanuric compounds have been investigated by the X-ray diffraction method[1-5]. We will mention here only the value given in Hughes' report of 1941 on melamine as it is directly related to this paper, which suggests that[1], C-$N_{ring}$=1.33–1.35 Å, C-$N_{outer}$=1.35–1.36 Å and $\angle N_r$-C-$N_r$=123–125° within the error limit of about 0.02 Å. Reports concerning other cyanuric compounds will be quoted hereafter, when necessary.

## Experimental

Each sample, cyanuric chloride (bp. 190°C) and melamine (sublimed over 300°C), was recrystallized before use. The electron diffraction photographs were made with these crystalline samples, which were vaporized into the apparatus previously described, with the help of a high temperature nozzle, newly designed for this purpose[7,8]. Gold foils were used for calibration of the electron wave length which was approximately 0.05–0.06 Å. The positions of halos were measured visually, and listed in Table I. The characteristic features of the photographs were represented by the visual curves $I_{vis}(q)$ and shown at the top of Fig. 3 and Fig. 5. From these curves, radial distribution curves were obtained by punched card summation of the formula

$$rD(r)=\sum_q I_{vis}(q)\exp(-aq^2)\sin(\pi qr/10)$$

with $a$ chosen to give $\exp(-aq^2)=0.20$ at $q=80$.

The theoretical intensity curves

$$I(q)=\sum_{i\neq j}\sum(Z_iZ_j/r_{ij})\exp(-b_{ij}q^2)\sin(\pi qr_{ij}/10)$$

were calculated also for various models and compared with the visual curves.

TABLE I

THE OBSERVED $q$-VALUES FOR CYANURIC CHLORIDE AND MELAMINE

| Max. | Min. | Cyanuric chloride | Melamine |
|---|---|---|---|
| 1 | | 17.2 | 18.6 |
| 2 | | (20.1) | (20.4) |
| | 2 | 22.2 | 23.8 |
| 3 | | 24.0 | 26.2 |
| | 3 | 26.1 | 28.1 |
| 4 | | 28.0 | 31.1 |
| | 4 | 30.2 | 33.1 |
| 5 | | 32.6 | 35.9 |
| | 5 | 36.0 | |
| 6 | | 38.9 | (39.2) |
| | 6 | | 41.9 |
| 7 | | (43.0) | 45.6 |
| | 7 | 45.2 | 49.8 |
| 8 | | 47.8 | 53.2 |
| | 8 | 52.9 | 57.4 |
| 9 | | 55.3 | 62.0 |
| 10 | | (59.7) | |
| 11 | | 64.0 | |
| 12 | | 70.2 | |
| 13 | | 74.9 | |
| 14 | | 78.9 | |

The values in the branckets were not used for quantitative comparisons.

## Interpretation

In 1935, Knaggs[5] suggested that cyanuric triazide requires two unequal C-$N_r$ distances of 1.31 and 1.38 Å, corresponding essentially

* Present address: Hosokura Smelter, Mitsubishi Metal Mining Co. Ltd., Miyagi-ken, Japan.

1) E.W. Hughes, *J. Am. Chem. Soc.*, **63**, 1737 (1941).
2) J.L. Hoard, ibid., **60**, 1194 (1938).
3) E.H. Wiebenga and N.F. Moremann, *Z. Krist.*, **99**, 217 (1938).
4) E.W. Hughes. *J. Chem. Phys.*, **3**, 1 (1935).
5) J.E. Knaggs, *Proc. Roy. Soc.* (London), **A150**, 576 (1935).
6) T. Yuzawa and M. Yamaha, This Bulletin, **26**, 414 (1953).
7) H. Oosaka and Y. Akimoto, ibid., **26**, 433(1953).
8) L. Pauling and Sturdivant, *Proc. Nat. Acad. Sci.*, **23**, 615 (1937).

to alternating double and single bonds. However, throughout all the X-ray diffraction investigation on various cyanuric compounds, this is the only work that suggested the inequality of cyanuric bonds. As the theoretical treatment of Pauling and Sturdivant[8] showed, such inequality seems very unusual, especially in the gaseous state. Moreover our result on the radial distribution curves does not support such a conclusion anyway. Therefore, in this work, we assumed the $D_{3h}$ symmetry of the cyanuric ring: namely the equality of all cyanuric bonds. The same symmetry and co-planality were assumed throughout the whole molecular shapes[9]. Therefore, for cyanuric chloride only 3 parameters: C-$N_r$, C-Cl, and $N_r$-C-$N_r$, and for melamine 5 parameters: C-$N_r$, C-$N_o$, $N_o$-H, $\angle N_r$-C-$N_r$, and $\angle$H-$N_o$-H, are sufficient to determine the complete shapes of these molecules.

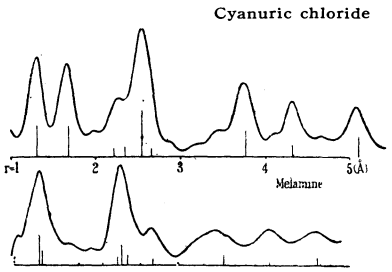



Fig. 1. Radial distribution curves for cyanuric chloride and melamine.

TABLE II
ASSUMED $<l^2_{ij}>^{1/2}_{AV}$ VALUES
($b_{ij}=(\pi^2/200)<l^2_{ij}>_{AV}$)

| Cyanuric chloride | | Melamine | |
|---|---|---|---|
| C-$N_r$ | 0.044 | All C-N, N-N, and C-C distances | 0 |
| C-C′ | 0.053 | | |
| $N_r$-$N_r$′ | 0.056 | $N_o$-H | 0.060 |
| C-$N_r$″ | 0.061 | All the other H-containing distances | 0.083 |
| C-Cl | 0.045 | | |
| $N_r$-Cl′ | 0.057 | | |
| C-Cl″ | 0.072 | | |
| $N_r$-Cl‴ | 0.084 | | |
| Cl-Cl‴ | 0.095 | | |

**Cyanuric Chloride.**—The radial distribution curve is shown at the upper part of Fig. 1. The following parameter set was the best obtained: C-$N_r$=1.33 Å, C-Cl=1.68 Å, and $\angle N_r$-C-$N_r$=125°.

The theoretical intensity curves were calculated for 32 models over the following parameter ranges: C-$N_r$=1.30–1.37 Å, C-Cl=1.60–1.70 Å, $\angle N_r$-C-$N_r$=115–130°, with $b_{ij}$ values shown in Table II[10]. The $q_{calc}/q_{obs}$ values and mean deviations of maxima and minima were calculated over all theoretical curves respectively. The relations of these values are picturized in Fig. 2 as a parameter chart which is essential for all models in the following parameter ranges: C-Cl=1.70–1.64 Å and $\angle N_r$-C-$N_r$=120–130°. C-$N_r$=1.33 Å, and $N_r$′-Cl=2.59 Å are the best values established from this chart. Several theoretical curves are shown in Fig. 3, and their parameters in Table III. Curve R has the best parameter set obtained from the radial distribution computation. Curves A–C were chosen to explain the differences of particular features from the visual curves. For such differences of features, a parameter chart was

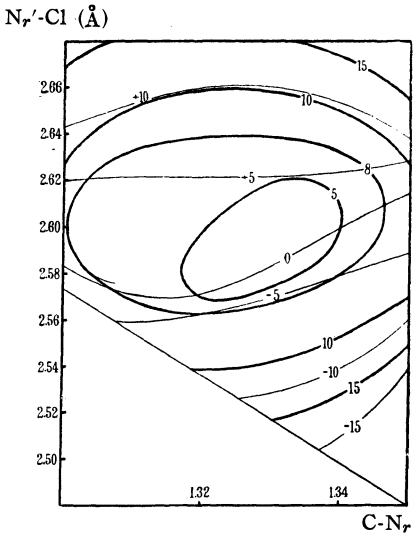



Fig. 2. Parameter chart of $q_{calc.}/q_{obs.}$ and mean deviations for cyanuric chloride.* *Heavy lines are for $q_{calc.}/q_{obs.}$; and light curves for mean deviations. Numerical values must be multiplied by $10^{-3}$.

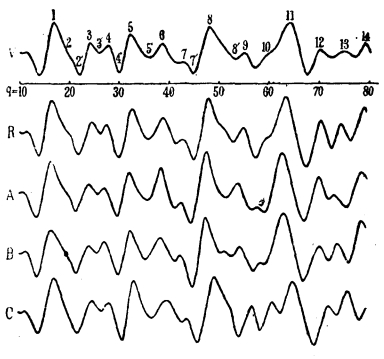



Fig. 3. Intensity curves for cyanuric chloride.

9) For melamine, several models, in which the planes through the $N_o$ atom and the two H atoms are perpendicular with the ring plane, were also tested but with no sufficient changes of the curves.

10) In both cases, the curves are almost insensitive to slight changes of $b_{ij}$ values.

TABLE III
MODELS FOR CYANURIC CHLORIDE

| Model | C-$N_r$ (Å) | C-Cl (Å) | $\angle N_r$-C-$N_r$ |
|---|---|---|---|
| R | 1.33 | 1.68 | 125° |
| A | 1.32 | 1.70 | 120° |
| B | 1.34 | 1.68 | 122.5° |
| C | 1.34 | 1.66 | 130° |

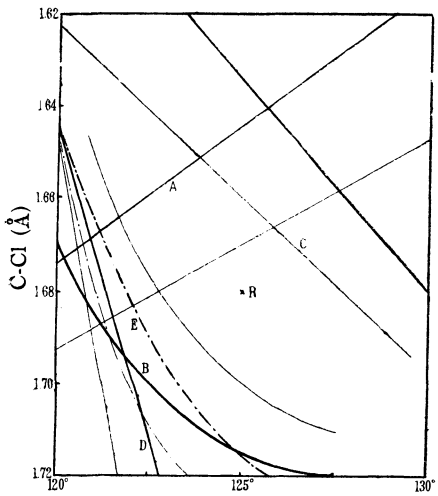



Fig. 4. Parameter chart of particular features for cyanuric chloride. Heavy lines indicate the border lines of models which have 1.34Å for C-$N_r$, and light lines 1.32Å for C-$N_r$.
Relative intensities of max. 3 and max. 4 (A), max. 5 and max.6 (B), and min. 8′ and 9′ (C), positions and shapes of max. 10 (D) and max. 13 (E) were quoted for the comparisons.

also made and shown in Fig. 4. Each line indicates where a particular feature of the intensity curves is sufficiently different from the visual curves to make them unacceptable.

Comparison of the two parameter charts leads us to the final set, C-$N_r$=1.33±0.02 Å, C-Cl=1.68±0.03 Å, and $\angle N_r$-C-$N_r$=125±3°. which is in complete agreement with the conclusion of the radial distribution argument.

**Melamine.**—The radial distribution curve is shown at the bottom of Fig. 1. The increase of the number of atoms makes the interpretation more difficult than that of the former. Overmore, the existence of hydrogen atoms makes almost all peaks considerably ambiguous. Therefore the direct determination of the 5 parameters is next to impossible. Assuming 120° for H-$N_o$-H and 1.04 Å for $N_o$-H, we can barely get to the following most possible parameter set: C-$N_r$= 1.34 Å, C-$N_o$=1.36–1.37 Å, and $\angle N_r$-C-$N_r$= 120–125°.

Twelve theoretical curves were calculated over the following ranges: C-$N_r$=1.32–1.38 Å, C-$N_o$=1.34–1.40 Å and $\angle N_r$-C-$N_r$=115–130°. $N_o$-H=1.04 Å and $\angle$H-$N_o$-H=120° were kept over all models. The $b_{ij}$ values were taken as shown in Table II [10]. An effective value $Z$=1.25 was used for hydrogen atoms. Representative theoretical curves are shown in Fig. 5. The positions of several peaks are only sensitive for the change of the C-$N_r$ distances. As these peaks are hardly affected by the change of the other parameters (for example, 0.02 Å changes of C-$N_r$ distance is enough to shift Max. 5 by 1$q$, while 0.5 $q$ shifts of the same peak requires the change

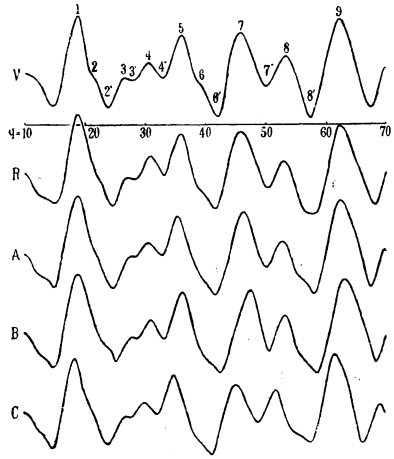



Fig. 5. Intensity curves for melamine.

TABLE IV
MODELS FOR MELAMINE

| Model | C-N (Å) | C-$N_o$ (Å) | $\angle N_r$-C-$N_r$ |
|---|---|---|---|
| R | 1.34 | 1.37 | 123° |
| A | 1.34 | 1.36 | 120° |
| B | 1.32 | 1.34 | 120° |
| C | 1.36 | 1.36 | 120° |

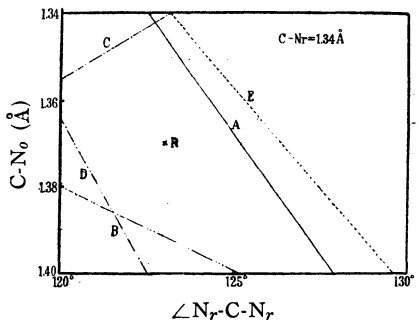



Fig. 6. Parameter chart of particular features for melamine.
Positions of max. 3 (A), max. 4 (B), max. 7 (C) and max. 8 (D), and existence of shelf between 8′ and 9 (E) were quoted for the comparisons.

of about 0.05 Å of C-$N_o$ distance or 5° of $\angle N_r$-C-$N_r$), we can conclude safely that the C-$N_r$ distance is 1.34±0.01 Å. To decide the other two parameters, the particular features are compared in Fig. 6 as a parameter chart.

Final conclusions are C-$N_r$=1.34±0.01 Å, C-$N_o$=1.37±0.03 Å and $\angle N_r$-C-$N_r$=123±3°.

## Molecular Orbital Calculation

In order to discuss our results theoretically, simple MO calculations were applied to these compounds as well as to *sym*-trichlorobenzene and *sym*-triaminobenzene. The energy and wave function of each molecular orbital were obtained by the usual LCAO method. In the actual calculation, the exchange integral between non-adjacent atoms was neglected. Furthermore, for the Coulomb integral ($\alpha_r$) and the exchange integral ($\beta_{rs}$) between two adjacent atoms, Sandorfy's values were employed, as shown in Table V[11]. Induction effect was assumed for $\alpha_r$ of the atoms which are next to hetero atoms to be 1/10.

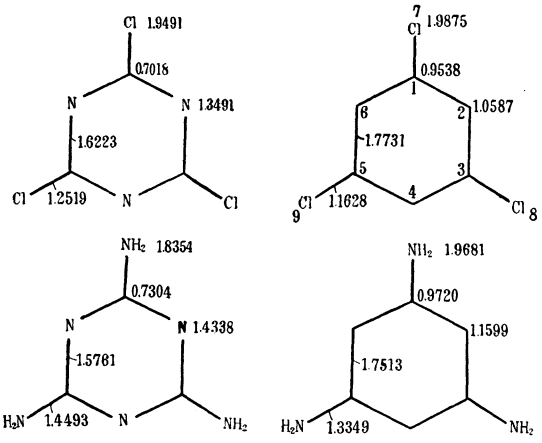



Fig. 7. Molecular diagrams by MO calculations.

By use of the molecular orbital wave function thus obtained, the electron density ($q_r$) and bond order ($p_{rs}$) were evaluated by the following equations:

$$q_r = 2\sum_n c^2_{rn}, \quad p_{rs} = 2\sum_n c_{rn}c_{sn}.$$

where $C_{rn}$ is the coefficient of the $r$-th atomic wave function in the molecular orbital and the summation extends over the filled orbitals in the ground state. The results are shown in Fig 7.

TABLE V
SANDORFY'S INTEGRAL VALUES IN UNIT OF $\beta$[11]

| Atom or bond | Integral value |
|---|---|
| C | 4.10 |
| $N_r$,$N_o$ | 5.17 |
| Cl | 5.08 |
| C-C | 1.00 |
| C-$N_r$ | 1.22 |
| C-$N_o$ | 0.80 |
| C-Cl | 0.39 |

## Discussion

In Table VI, the results of the present investigations are compared with those of earlier works on the related compounds. About cyanuric chloride, the C-Cl distance (1.68 Å) is somewhat shorter than that of *sym*-trichlorobenzene (1.69 Å). On the C-N distance (1.33 Å), the same tendency is observed as compared with that of melamine (1.34 Å). We have not any accurate data to compare with the C-$N_o$ distance (1.37 Å), but the inaccurate value (1.4 Å) for *p*-iodoaniline will serve to let us observe the similar tendency as the C-Cl distance of cyanuric chloride. Comparison of the bond order obtained above endorses these aspects.

11) M.C. Sandorfy., *Bull. chim. phys.*, **16**, 615 (1949).
12) L. O. Brockway and K. J. Palmer., *J. Am. Chem. Soc.*, **59**, 2181 (1937).
13) H. M. Powell, G. Huse and P. W. Cooke., *J. Chem. Soc.*, **1943**. 153

TABLE VI
COMPARISON OF PARAMETER VALUES ON THE RELATED COMPOUNDS (Å)

| Molecule | | | | method | reference |
|---|---|---|---|---|---|
| Cyanuric chloride | C-N=1.33±0.02, | C-Cl=1.68±0.03, | ∠N-C-N=125±3°,. | E | |
| Melamine | C-$N_r$=1.34±0.01, | C-$N_o$=1.37±0.03, | $\angle N_r$-C-$N_r$=123±3°,. | E | |
| | C-$N_r$=1.33~1.35, | C-$N_o$=1.35~1.36, | $\angle N_r$-C-$N_r$=123~125°,. | X | 1 |
| Cyanuric acid | C-$N_r$=1.36, | | | X | 3 |
| Cyanuric triazide | C-$N_r$=1.33, | C-$N_o$=1.50, | $\angle N_r$-C-$N_r$=137°,. | X | 4 |
| | C-$N_r$=1.31,1.38, | C-$N_o$=1.38. | | X | 5 |
| Trisodium tricyan melamine trihydrate | C-$N_r$=1.34,1,35, | C-$N_o$=1.40,. | | X | 2 |
| *sym*-Trichlorobenzene | C-C=1.41(assum.), | C-Cl=1,69±0.03,. | | E | 11 |
| *m*,*p*-Dichlorobenzene | C-C=1.40(assum.), | C-Cl=1.69±0.03,. | | E | 11 |
| Chlorobenzene | C-C=1.39±0.02, | C-Cl=1.69±0.03,. | | E | 11 |
| *p*-Iodoaniline | C-C=1.4, | C-N=1.4$_3$,. | | X | 12 |

E indicates the electron diffraction method and X the X-ray diffraction method.

In the case of benzene derivatives, C-C distance of the ring is almost independent of the number or the species of the substituent. On the other hand, the cyanuric ring seemingly cannot stand invariably against the change of circumstances. The certificate of this phenomenon can be obtained also from the MO treatment. The bond order of cyanuric C-$N_r$ distance is more easily affected by the introduction of new $\pi$-electron systems than that of benzene C-C distance as shown in Fig. 7. The distortion of the cyanuric ring from the regular hexagon, may be understood as the effect of a lone pair which is located on each $N_r$ atom.

## Summary

1. The molecular structure of cyanuric chloride and melamine were investigated by the electron diffraction. The following values were obtained by the analysis based on $D_{3h}$ symmetry of the molecules: C-$N_r$=1.33±0.02 Å, C-Cl=1.68±0.03 Å, and $\angle N_r$-C-$N_r$=125±3° for cyanuric chloride: C-$N_r$=1.34±0.01 Å, C-$N_0$=1.37±0.03 Å, and $\angle N_r$-C-$N_r$=123±3° for melamine assuming $N_o$-H=1.04 Å, $\angle$C-$N_o$-H=$\angle$H-$N_0$-H=120°, and the coplanarity of all atoms.

2. Simple MO calculations were applied for both molecules as well as for *sym*-trichlorobenzene and *sym*-triaminobenzene. The resulted molecular diagrams were discussed together with the data obtained in the present experiment.

We are deeply indepted to Prof. A. Kotera and Assist. Prof. K. Suzuki for their continued encouragement and valuable advice for this study. The kindness of Dr. M. Uenaka who gave us the samples is gratefully acknowledged. Thanks are also due to Mr. M. Yamaha and Mr. M. Igarashi for their helpful discussion.

*Chemical Laboratory, Tokyo Bunrika University, Tokyo*

# *The Effect of Layered Water on the Color Reaction of Benzidine or Other Similar Compounds with Montmorillonite*

By Hiroshi TAKAHASHI

(Received May 10, 1954)

## Introduction

It is well known that certain clay minerals form stable complexes with some organic compounds. Complexes between montmorillonite and aromatic amines are particularly well known, because of their deep colors.[1,2] Investigations on the structure of the complexes as well as their color reactions have been reported by several authors. It has been clarified[3,4,5] through the X-ray diffraction method, that in these complexes organic molecules lie along can be held between two adjacent sheets of successive silicate layers, generally as a single layer or double layers just similar to the behavior of water molecules in natural montmorillonite. A schematic illustration of a montmorillonite complex after Hendricks and Jefferson[4,6] is shown in Fig. 1.

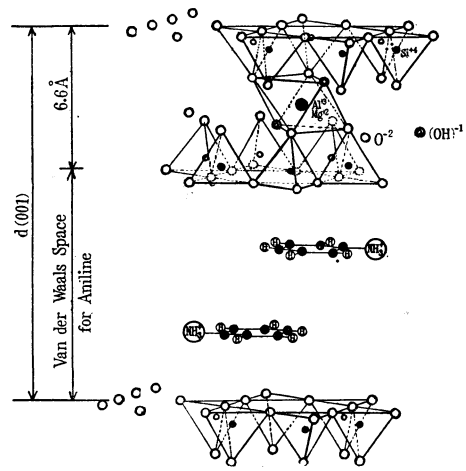



Fig. 1. Schematic drawing showing organic molecules between silicate layers of montmorillonite after Hendricks and Jefferson.

1) K. Kobayashi and K. Yamamoto, *J. Soc. Chem. Ind. Japan*, **26**, 289 (1921).
2) E. A. Hauser and M. B. Leggett, *J. Am. Chem. Soc.*, **62**, 1811 (1940).
3) J. B. Gieseking, *Soil Sci.*, **47**, 1 (1941).
4) S. B. Hendricks, *J. Phys. Chem.*, **45**, 65 (1941).
5) D. M. C. MacEwan, *Trans. Farad. Soc.*, **44**, 349 (1948).
6) S. B. Hendricks and M. E. Jefferson, *Am. Mineral.*, **23**, 863 (1938).

In regard to the mechanism of the coloration displayed in the complex between montmorillonite and benzidine, Kameyama and Oka[7] have assumed that the benzidine molecule is colored in the semiquinone form due to the oxidation by the manganese ion which is present in clay as impurity, while, Weil-Malherbe and Weiss[8] ascribed it to the oxidation by the ferric ion present in the octahedral layer of the clay mineral. The present author, however, has found that the coloration is influenced remarkably by the amount of the absorbed water, i.e., interlayer water which is present between the adjacent silicate layers.[9,10] From this point of view, the present article will report on the mechanism of the formation of complexes as well as the color reactions between some montmorillonite and benzidine or some related compounds, discussing them in comparison with each other.

**Clay Samples.**—The clays used in this experiment are Wyoming bentonite, Bodai acid clay and Numata clay, from Osage, Wyoming, U.S.A., Bodai, Naya-mura, Ishikawa Prefecture and Shimokawada, Kawada-mura, Gunma Prefecture, respectively. The refined samples have been obtained from these clays after having thoroughly elutriated them in the usual way. The X-ray powder patterns of these samples have shown that they have montmorillonite for the main ingredient.[11] Bodai acid clay alone, however, contains $\alpha$-cristobalite and quartz as impurities. (Cf. Table I)

Their differential thermal analysis curves (Fig. 2) reveal that they are montmorillonite type, and the rate of heating is 12°C per minute.[12] In this figure, however, Numata clay alone has an endothermic peak at 560°C, which may be due to the possible presence of illite or kaolin minerals as an impurity in Numata clay,[13] though its presence has not yet been found in the X-ray powder pattern.

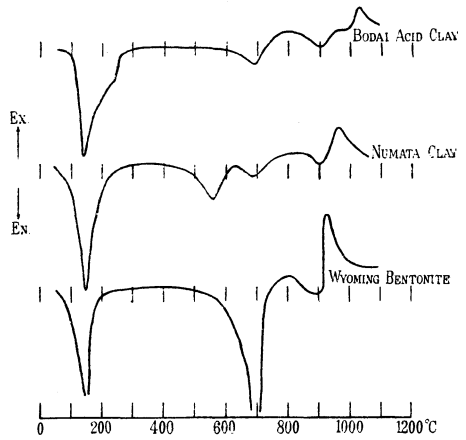



Fig. 2. Differential thermal analysis curves of clay samples.

The chemical formulas[14,15] obtained from the chemical analysis of these clay samples, all of which are assumed as montmorillonite, are given below:

Wyoming bentonite:

$(Al_{1.50}Fe_{.18}Mg_{.32})\ (Al_{.01}Si_{3.99})O_{10}(OH)_2X^{I}_{.33}$

Bodai acid clay:

TABLE I

THE X-RAY POWDER PATTERNS OF CLAY SAMPLES

| Indices | Bodai acid clay | | Numata clay | | Wyoming bentonite | |
|---|---|---|---|---|---|---|
| | *d* | *I* | *d* | *I* | *d* | *I* |
| 001 | 15.4 | 10 | 15.4 | 10 | 15.4 | 10 |
| 003 | 5.14 | 2 | 5.15 | 1 | 5.16 | 1 |
| 02,11 | 4.46 | 6 | 4.50 | 5 | 4.51 | 5 |
| | 4.21 (Q) | | | | | |
| | 4.04 ($\alpha$-C) | | | | | |
| | 3.35 (Q) | | | | | |
| 005 | 3.09 | 2 | 3.05 | 1 | 3.07 | 2 |
| 13,20 | 2.56 | 3 | 2.57 | 2 | 2.58 | 2 |
| 31,15,24 | 1.72 | 0.5 | 1.69 | 0.5 | 1.70 | 0.5 |
| 33,06 | 1.498 | 3 | 1.496 | 2 | 1.500 | 3 |

Key to abbreviations: *d*=spacing in kx, *I*=intensity, Q=quartz pattern, $\alpha$−C=$\alpha$−cristobalite pattern

7) N. Kameyama and S. Oka, *J. Soc. Chem. Ind. Japan*, **32**, 294 (1929).
8) H. Weil-Malherbe and J. Weiss, *J. Chem. Soc.*, **1948**, 2164.
9) S.B. Hendricks, R.A. Nelson and L.T. Alexander, *J. Am. Chem. Soc.*, **62**, 1457 (1940).
10) J. Mering, *Trans. Farad. Soc.*, **42-B**, 205 (1946).
11) D.M.C. MacEwan, "X-ray Identification and Crystal Structures of Clay Minerals", edited by G.W. Brindley, The Mineralogical Society (Clay Mineral Group). London, (1951) p. 124.
12) R.E. Grim, "Clay Mineralogy", McGraw-Hill Book Co., Inc., New York, N.Y., (1953), p. 197.
13) T. Sudo et al., *J. Geol. Soc. Japan*, **58**, 115 (1952).
14) C.S. Ross and S.B. Hendricks, *U.S. Geol. Surv. Bull.*, Prof. Paper, **205-B**, 23 (1945).
15) Y. Otsubo, "Chemical Researches, No. 8", Asakura Book Co., Tokyo, (1950), p. 85.

$(Al_{1.64}Fe._{15}Mg._{32})$ $(Al._{13}Si_{3.87})O_{10}(OH)_2X^{I}._{34}$

Numata clay:

$(Al_{1.55}Fe._{16}Mg._{33})$ $(Al._{08}Si_{3.92})O_{10}(OH)_2X^{I}._{29}$

Exchangeable cation is sodium in Wyoming bentonite and Numata clay, while it may be both sodium and calcium in Bodai acid clay. However, as it may be considered to have the least effect on the color reaction of complexes, further discussion on cation exchange seems to be unnecessary for the present purpose.

Of the plate type and fluffy type which usually characterize the shape of montmorillonite, these clays are considered to belong to the latter type, from the electron micrographs of them.[16,17,18]

As a result of all the experiments above, it seems to be certain that these clay samples are montmorillonite.

**Preparation of Specimens.**—Complexes between montmorillonite and every one of the following organic substances such as benzidine, *r*-diphenol, aniline, phenol, *p*-phenylenediamine and monomethyl-*p*-aminophenol were prepared for the present investigation. To prepare a complex, the water-alcohol solution of a given organic compound is poured into an aqueous suspension of clay. The amount of the organic compound which is added is as much as several times the base exchange capacity of the clay (5–10 milliequivalent per one gram of clay). The suspension of the complex thus prepared was centrifuged after left over twenty four hours. The precipitates obtained were washed with alcohol and water repeatedly until free compounds were no longer present, and dried in air. From every kind of these air dried complexes, four kinds of specimens were made by the following processes:

(1) Absorption of water by standing in the saturated water vapor at 20°C for about a week,

(2) complete absorption of water by direct wetting,

(3) dehydration by standing over phosphorus pentoxide,

(4) absorption of water by wetting again after (3) procedure was applied.

The specimens prepared by these processes will hereinafter be abbreviated as S-1, S-2, S-3 and S-4 for every complex.

## Experimental and Discussion

It was found that the color of the complex is varied remarkably, in some cases, accordingly to the way of preparation of the specimen, and in other cases, it is not. The colors of specimens of each complex are shown in Table II, along with the values of their (001) spacings obtained by a Philips X-ray Geiger counter spectrometer. Filtered copper radiation, 35 Kv. 15 Ma, scan speeds 2° and 1/2° per minute, angular aperture 1°, receiving slit 0.006 inch, time constant 4 second.

TABLE II

THE (001) SPACINGS AND THE COLORS OF THE SPECIMENS FOR EACH COMPLEX

| | | Bodai acid clay | Numata clay | Wyoming bentonite | color |
|---|---|---|---|---|---|
| benzidine | S-1 | 15.4 kx | 15.4 | 15.3 | blue |
| | S-2 | 19 | 19 | 19 | blue |
| | S-3 | 13.8 | 13.9 | 13.2 | yellow~colorless |
| | S-4 | 19 | 19 | 19 | blue |
| *r*-diphenol | S-1 | 16.1 | | | green |
| | S-2 | 19.5 | | | green |
| | S-3 | 14.7 | | | colorless |
| | S-4 | 19.5 | | | green |
| aniline | S-1 | 15.3 | 15.2 | 15.2 | very light violet |
| | S-2 | 18 | 18 | 19 | very light violet |
| | S-3 | 13.5 | 13.5 | 12·4 | very light violet~colorless |
| | S-4 | 18 | 18 | 19 | very light violet |
| phenol | S-1 | 15.2 | 15.2 | 15.2 | colorless |
| | S-2 | 18 | 19 | 18.5 | colorless |
| | S-3 | 14.5 | 14.5 | 13.4 | colorless |
| | S-4 | 19 | 18 | 18.5 | colorless |
| *p*-phenylene diamine | S-1 | 15.4 | 15.4 | 15.4 | violet (blue) |
| | S-2 | 15.4 | 15.4 | 15.4 | violet |
| | S-3 | 15.2 | 14.5 | 14.7 | violet |
| | S-4 | 15.4 | 15.4 | 15.4 | violet |
| mono-methyl -*p*-amino phenol | S-1 | 15.4 | 15.3 | 15.3 | violet (light green) |
| | S-2 | 15.4 | 15.3 | 15.4 | violet |
| | S-3 | 15.1 | 13.3 | 14.0 | violet |
| | S-4 | 15.4 | 15.2 | 15.4 | violet |

With respect to the benzidine complex, Table II reveals that the color reaction is caused by the presence of water and when dehydrated as S-3 the color can not be developed. The color of the air dried complex when it is further dried over calcium chloride becomes yellowish green and the (001) spacing is 14.5–15.0 kx. The yellowish green color gradually turns to blue when the complex is in equilibrium with water vapor, and

16) R.P. Humbert and B.T. Shaw, *Soil Sci.*, 52, 481 (1941).

17) B.T. Shaw, *J. Phys. Chem.*, 46, 1032 (1942).

18) P.F. Kerr et al., "API Report Project 49", No. 6 (1950).

TABLE III
THE VARIATION OF (001) SPACINGS OF CLAYS AND THEIR BENZIDINE COMPLEXES WITH THE ABSORPTION OF WATER

| | Bodai acid clay | | Numata clay | | Wyoming bentonite | |
|---|---|---|---|---|---|---|
| | natural clay | complex | natural clay | complex | natural clay | complex |
| absorbed water vapor | 15.4 kx | 15.4 | 15.4 | 15.4 | 15.4 | 15.3 |
| saturated with water | 19 | 19 | 19 | 19 | | 19 |
| dried over $CaCl_2$ | 13.6 | 14.8 | 13.7 | 14.9 | 13.3 | 14.5 |
| dried over $P_2O_5$ | 12.4 | 13.8 | 12.4 | 13.9 | 12.0 | 13.2 |

the (001) spacing becomes equal to the value of S-1. It is inferred from this fact that, in the case of the benzidine complex, the color varies, depending on the amount of water held between two neighbouring sheets of successive silicate layers.

Table III shows the variation of the (001) spacings of the clay samples with the absorption of water, in comparison with their benzidine complexes. The (001) spacing of natural clays are 15.4 kx when they are in equilibrium with water vapor. This implies that they have two water layers between two adjacent silicate layers. When the clays are saturated with water, they swell and in the case of Bodai acid clay and Numata clay, the (001) spacing increases to 19 kx, which corresponds to the increment of one or two water layers, whereas, in Wyoming bentonite, the (001) spacing becomes too large to estimate its value. When benzidine complex is saturated with water, the increment in the number of water layers is one or two, just as in the case of natural Bodai and Numata clay. As well as in the case of Wyoming bentonite; it is of interest to note that it can not swell so much as in the natural state when it forms a complex.

Table III shows also that even in the dehydrated state there still remain the benzidine molecules themselves between the silicate layers. Therefore, decoloration is caused, not by the absence of benzidine molecules themselves, but by the absence of water.

The presence of the layered water is necessary for the color reaction; moreover, it was found that some liquids other than water also show the same effect. For the purpose of estimating the absorbed water thoroughly, the clay was heated to 300–400°C. That the layered water is no longer present in it, is demonstrated by its X-ray diffraction diagram, by which, its (001) spacing was found to be 9.5 kx. When a water solution, an alcohol solution and an acetone solution of benzidine were added to the dehydrated clay respectively, it was found that the color of the complex became blue, greenish blue and yellow according to the solvent. This fact means that the color reaction of this complex changes according to the kind of liquid which is present between layers.

The same effect is also demonstrated in the following way. When water, alcohol and acetone are added respectively to a benzidine complex which has been dehydrated thoroughly to a colorless state, it becomes blue, greenish blue and yellow respectively as above. In this case, however, if benzene is added to the complex, the appearence of color can not be observed.

*r*-diphenol whose construction approximates to benzidine, shows similar behavior in the formation of complex with these clays. However, amino-radical has a greater effect of deepening the color of the complex than in the case of hydroxyl-radical as revealed from Table II.

*p*-Phenylenediamine(paramine)-montmorillonite and monomethyl-*p*-aminophenol(methol)-montmorillonite complexes have deep colors, which do not change even when they are dried, in contrast with the case of benzidine or *r*-diphenol complex. It is worthy to note that there is no difference in the value of (001) spacing between S-2 and S-3 (the dried state and the water saturated state). It is presumably because of the fact that these complexes in themselves have little layered water, and even when they are dried or saturated with water, it dose not affect the quantity of the layered water in them. What deserves particular attention here is the fact that, in the paramine and methol complexes, their colors are blue and green respectively when they are made freshly in the clay suspension, and then these colors change to violet as time passes or if they are dehydrated. This fact may lead to an assumption that in the first stage of the formation, these complexes temporarily make benzidine-like coloration, but in the next stage their colors change as the molecules of paramine or methol fix on both sides of the silicate layers, no longer permitting the water molecules to get into them. It is, however, ascertained through X-rays that in the case where the quantity of paramine and of methol is not saturated, the shrinkage or swelling occurs to some extent of movement of the water getting into or out of them.

In contrast with paramine and methol, the coloration of the aniline complex is not so remarkable. In the case of phenol, which is believed to be able to form a complex with montmorillonite,[2,5] the coloration can not be recognized by the naked eye. This unremarkable coloration is due to the fact that aniline and phenol are monofunctional compounds, and the amino- or hydroxyl-radical

fixes on one side of the silicate layer. When these complexes are saturated with water, the increment in the number of water layers is one or two just as in the case of benzidine complex.

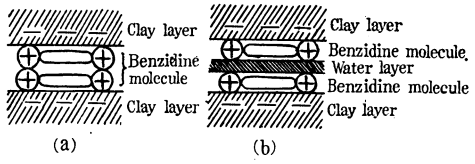



Fig 3. The process of benzidine complex formation with montmorillonite.
(a) Complex is formed.
(b) Saturated with water.

The benzidine and paramine complexes show a remarkable coloration, as they are bifunctional compounds. In the case of the benzidine complex, a benzidine molecule fixes on one side of the silicate layer, and then when it is saturated with water, the water molecules get into the silicate layer. From this fact, a schematic drawing of the process of benzidine complex formation with montmorillonite is shown in Fig. 3.

## Summary

The relationship between layered water and coloration of some complexes between montmorillonite and benzidine or other similar compounds has been discussed, and it is shown that they may be divided into types according to the structures of organic compounds. The shrinkage and swelling of the layer distance of the complex caused by its dehydration and hydration are observed.

The coloration of the monofunctional-complex is not so remarkable and that of the bifunctional-complex is remarkable. In the case of monofunctional-complex or the bifunctional-complex with benzidine, the amino- or hydroxyl-radical fixes on one side of the silicate layer, and then, when it is saturated with water, the water molecules get into the silicate layer. On the other hand, in the bifunctional-complex with paramine, as the amino- or hydroxyl-radical fixes on both sides of the silicate layers, the water molecules no longer get into it.

The author wishes to express his hearty thanks to Prof. H. Akamatu for his kind guidance and encouragement.

*Department of Chemistry, Faculty of Science, the University of Tokyo, Tokyo*

# *Surface Chemistry of Synthetic Protein Analogues. V. On the Effect of Salt on the Monolayers of the Copolypeptide of L-Lysine, L-Phenylalanine and L-Glutamic Acid*

By Kozo HAMAGUCHI and Toshizo ISEMURA

(Received May 22, 1954)

## Introduction

In the previous paper,[1] we have reported on the behaviour of the monolayers of the electrolytic polypeptides, poly-L-glutamic acid and a copolypeptide of L-lysine, L-leucine and L-glutamic acid, in relation to the pH's of substrates. In the present paper, we shall report on the effect of salts on the monolayers of the copolypeptide of L-lysine, L-phenylalanine and L-glutamic acid. The interaction between natural proteins and salts is important in biological systems. The numerous investigations on these interactions have been carried out in bulk solution,[2] but few in interfaces.[3,4] In the recent investigations of protein by spreading monolayer, concentrated solutions of salts such as ammonium sulphate, are generally used as substrates in order to prevent the proteins from passing into substrate water.[5] Since there exist also some interactions between protein and salts at interface, a detailed knowledge of the interaction between protein molecules and salts in the substrate is indispensable for a thorough understanding of the behaviour of protein monolayers on salt solution.

For these reasons we have examined the effect of salt, i.e., potassium chloride, on the

1) T. Isemura and K. Hamaguchi, This Bulletin, **27**, 339 (1954).

2) F. Haurowitz, "Chemistry and Biology of Proteins," pp. 66 (1950).

3) A. Lajtha and E. K. Rideal, *Arch. Biochem. Biophys.*, **33**, 252 (1951).

4) E. Fredericq, *Biochim. et Biophys. Acta*, **9**, 601 (1952).

5) H. B. Bull, *J. Am. Chem. Soc.*, **67**, 4, 8, (1945).

monolayers of the amphoteric polypeptide which appears very promising as a protein model.

## Experimental

**Material and Methods.**—The copolypeptide of L-lysine, L-phenylalnine and L-glutamic acid was prepared by Dr. H. Tani and Mr. H. Yuki[6] and was used without any further purification. This copolypeptide was spread from a solution in N/100 hydrochloric acid to which 10 per cent of isopropyl alcohol was added. Surface pressure and surface viscosity measurements were carried out by the method of hanging plate and of damped oscillatory motion of disc, as reported in the previous papers.[7,8] Potassium chloride was recrystallized three times from water. The pH's of the substrates were adjusted by hydrochloric acid for lower pH values and by potassium bicarbonate or potassium carbonate for higher pH's, which were used by Langmuir and Shaefer for the studies of the effect of salts on the fatty acid monolayers.[9] The areas per amino-acid residue of the copolypeptide were calculated by assuming that the same ratio of L-lysine, L-phenylalanine and L-glutamic acid as the initial monomer concentration, 1:3:1, was maintained in the copolymer. This assumption turned out to be probably true throughout the analysis of the results.

**Results.**—The copolypeptide of L-lysine, L-phenylalanine and L-glutamic acid was soluble in the substrates which did not contain any salts. The stable monolayers were obtained when aqueous solutions of potassium chloride were used as substrates. To find out the concentration of potassium chloride, in the substrate solution necessary for giving a stable monolayer, the areas at constant surface pressure (1 dyne/cm.) against the concentration of potassium chloride are plotted as in Fig. 1. From this figure, one per cent of potassium chloride in the substrate was found to be sufficient to obtain a stable monolayer.

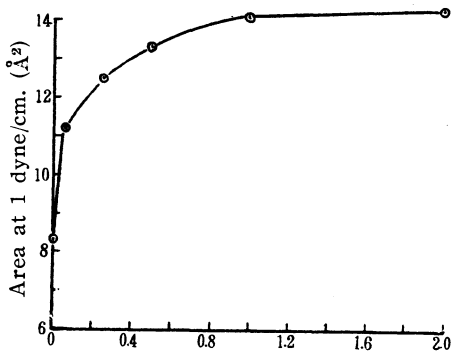



Fig. 1. Effect of the concentration of potassium chloride on the area per residue at 1 dyne/cm (pH 5.6).

6) H. Tani, H. Yuki, K. Okawa, S. Sakakibara and C. Oizumi, *Sen-i Kagaku Kenkyusho Nempo* (*Mem. Inst. Fiber Research*), 7, 98 (1953).

7) T. Isemura and K. Hamaguchi, This Bulletin, 25, 40 (1952).

8) T. Isemura and K. Hamaguchi, ibid., 27, 125 (1954).

9) I. Langmuir and V. J. Shaefer, *J. Am. Chem. Soc.*, 59, 2400 (1937).

The variations of the surface pressure-area (F-A) curves with the pH's of the substrates of constant KCl concentration (0.07 mole/litre), are shown in Fig. 2.

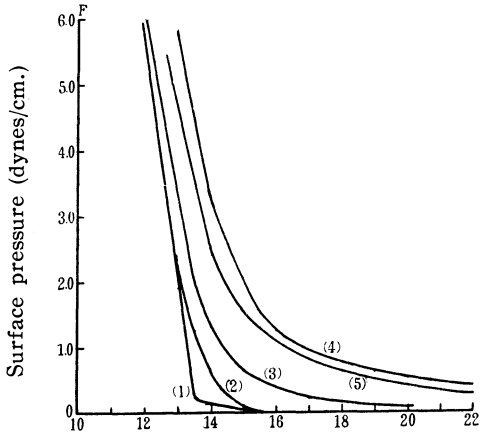



Fig. 2. Variations of F-A curves with the pH's of substrates; (1) pH 5.6—8.0, (2) pH 5.0, (3) pH 3.8, (4) pH 2.2, (5) pH 10.3 (0.07 mol. of KCl/litre).

A single F-A curve of condensed type was obtained in the pH range between 5.6 and 8.0. Changing the pH values of the substrate out of this pH range, F-A curves expanded gradually. The areas per residue at 1 dyne/cm. against pH's of the substrates are plotted in Fig. 3.

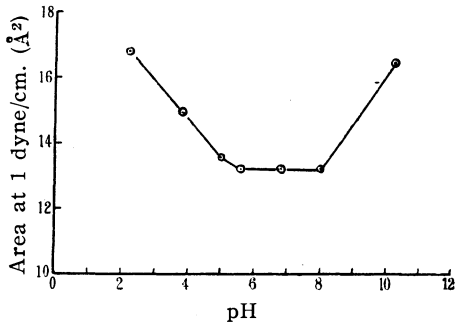



Fig. 3. Effect of pH of the substrate on the area per residue at 1 dyne/cm. (0.07 M KCl).

In this figure the minimum area region which is parallel to the pH axis, appears between pH 5.6 and 8.0.

The variations of F-A curves as the function of the concentration of potassium chloride in the substrate at constant pH (pH 2.2) are shown in Fig. 4.

It would be clear from this figure that the film expands with the decrease in the concentration of potassium chloride.

The surface viscosity-area ($\eta$-A) curves of the copolypeptide on the substrates of different concentrations of potassium chloride (at pH 5.6) are shown in Fig. 5. Fig. 6 shows the curve of $\eta$ at constant area (at 17 Å²/residue) plotted against the concentration of potassium chloride.

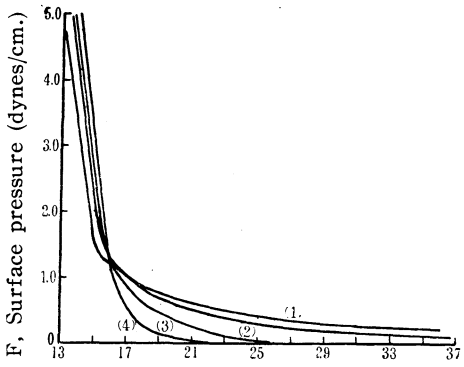



Fig. 4. Variations of F-A curves with concentration of KCl. (1) 0.035 M, (2) 0.07 M, (3) 0.13 M, (4) 0.40 M KCl. (pH 2.2)

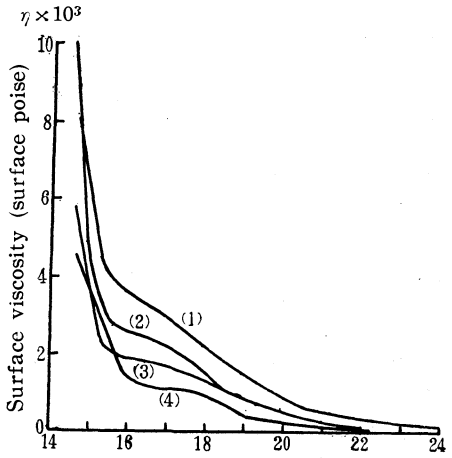



Fig. 5. Effect of KCl on the $\eta$-A curves of the copolypeptide. (1) 0.07 M, (2) 0.14 M, (3) 0.28 M, (4) 0.56 M KCl. (pH 5.6)

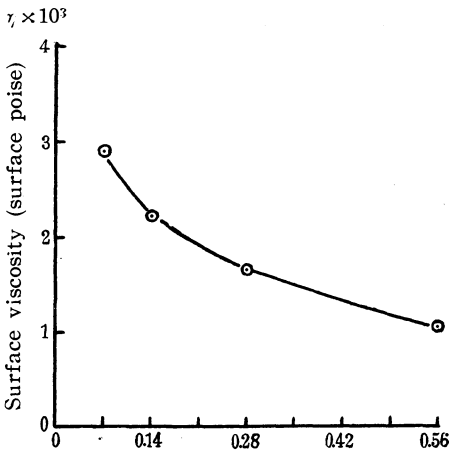



Fig. 6. Effect of the concentration of KCl on the surface viscosity (at 17Å²/residue). (pH 5.6)

The greater the concentration of potassium chloride becomes, the lower is the surface viscosity at constant area. Thus, the effect of potassium chloride on the $\eta$-A curves could be detected markedly while no effect on the F-A curves was observed when more than 1% potassium chloride was present in the substrates (Fig. 1). The fact recognized in common with all these $\eta$-A curves was that the surface viscosity begins to increase steeply at the area of 15.9 Å²/residue, irrespective of the concentration of potassium chloride.

The $\eta$-A curves of the copolypeptide on the substrates of different pH values, maintaining the concentration of KCl to be constant (0.28 M/litre), are shown in Fig. 7. Fig. 8 shows the surface viscosities at constant area (17 Å²/residue) against pH curve.

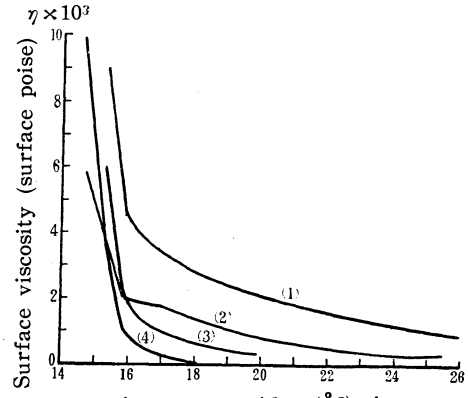



Fig. 7. Effect of pH on $\eta$-A curves of the copolypeptide (1) pH 6.8, (2) pH 5.6, (3) pH 8.0, (4) pH 2.2 (0.28 M KCl).

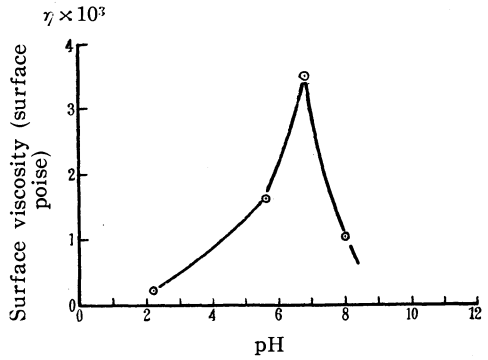



Fig. 8. Effect of pH of the substrate on surface viscosity (at 17Å²/residue). (0.28 M KCl)

It has been found from these figures that the surface viscosity becomes maximum at pH 6.8. On a more acidic substrate, the value of surface viscosity rather fluctuated and reproducible $\eta$-A curves could not be obtained in the pH range between 5.0 and 3.8.

## Discussion

### The Relationships between F-A Curves and pH's of Substrates (at Constant Con-

**centration of KCl**).—As shown in Fig. 2, the monolayers of the copolypeptide at pH between 5.6 and 8.0 of the substrates gave the same F-A curve of condensed type and in both the outsides of this pH range the F-A curves were of expanded type. The minimum area region appearing in the area (at constant pressure) against pH's of substrates curve (Fig. 3), corresponds to the region in which F-A curves have condensed type. This region between pH 5.6 and 8.0 corresponds to the isoelectric region and would be designated as the "isoelectric band" of the copolypeptide at this salt concentration (0.07 M/litre). When salts are contained in the substrate the isoelectric "band" appears rather than a "point" and the width of this band is the function of the salt concentration; an increase in the concentration of salt in the substrate widened the band. Even at pH 2.2, therefore, the F-A curves were of condensed type and it was expected that the F-A curves would represent the isoelectric property throughout all the pH's of the substrates, if potassium chloride was present in the concentration of more than 0.42 M/litre. This is due to the effect that an increase in ionic strength would reduce the coulombic force between the ionized groups of the copolypeptide. The fact that the film expands at each side outer than the isoelectric region is due to the electrostatic repulsion of $-COO^-$ or $-NH_3^+$ ions themselves when the one group exceeds the other.

In the previous paper,[1] it was pointed out that in the case of the copolypeptide of L-lysine, L-leucine and L-glutamic acid, the area at constant pressure against pH curve is of W-shape in the absence of salts in the substrate and that this fact can be interpreted in terms of free charge ($\Delta\alpha=|\alpha_L-\alpha_G|$) and of salt linkage ($\alpha_L\cdot\alpha_G$), if $\alpha_L$ and $\alpha_G$ represent the ionization degree of amino and carboxyl groups. Referring to the present results, salts would have the effect of depressing the maximum point appearing in the $(A)_F$-pH curve. Detailed considerations about this effect will be present in the later part of this paper.

**The Relationships between F-A Curves and Ionic Strength of Substrates (at Constant pH)**.—The effect of potassium chloride on the F-A curves of this copolypeptide is shown in Fig. 4. It may be found from this figure that the films are more expanded at low ionic strength in the substrates. This fact can be interpreted by the increment of the surface pressure due to the free energy of the electrical double layer which is formed between the ionized groups of the monolayer (in this case, $-NH_3^+$ ions of lysine residues) and the counter ions ($Cl^-$).

We can calculate the electrical potential difference of the double layer underneath the film from the F–A curves by the procedure adopted by J. T. Davies.[10,11]

According to Verwey and Overbeek,[12] the free energy of the double layer is represented by

$$G_s=-\frac{8nkT}{\kappa}\left(\cosh\frac{ze\psi_0}{2kT}-1\right), \qquad (1)$$

where $k$ is the Boltzmann constant, $T$ the absolute temperature, $n$ the number of ions in 1 cc. of bulk solution, i.e., $n=NC/1000$ ($C$: mol./litre, $N$: Avogadro number), $z$ the valency of salt, $e$ the electronic charge, $\psi_0$ the surface potential and $\kappa=\sqrt{\frac{8\pi nz^2e^2}{\varepsilon kT}}$ ($\varepsilon$: dielectric constant).

The surface tension is equivalent to the surface free energy per unit area. When the electrical double layer is formed, the surface tension is decreased by $G_s$ (because of the negative sign of equation (1)) and correspondingly the surface pressure is increased by $\Delta F$, namely

$$\Delta F=-G_s=\frac{8nkT}{\kappa}\left(\cosh\frac{ze\psi_0}{2kT}-1\right). \qquad (2)$$

After numerical substitution with $k=1.38\times10^{-16}$ erg/°K, $T=293$°K, $\varepsilon=80$, $e=4.8\times10^{-10}$ e.s.u., $z=1$, the following relation is obtained:

$$\Delta F=6.1\sqrt{c}\left(\cosh\frac{ze\psi_0}{2kT}-1\right). \qquad (3)$$

From Eq. (3)

$$\psi_0=51.2\ \cosh^{-1}\left(1+\frac{\Delta F}{6.1\sqrt{c}}\right) \qquad (4)$$

is obtained, where $\psi_0$ is expressed in millivolt units.

The surface pressure increment ($\Delta F$) due to the presence of the electrical double layer is written

$$\Delta F=F^+-F^\circ, \qquad (5)$$

where $F^+$ is the observed pressure and $F^\circ$ the pressure if the film had no charged groups. $F^\circ$ is a negative quantity, as shown in the later part, so it might be recognized as the cohesional force between film molecules.

On the other hand, the Gouy potential $\psi_G$, which is at a uniformly charged surface when uni-univalent salts are present, is expressed as

10) J. T. Davies, *Proc. Roy. Soc.*, **A208**, 224 (1951).
11) K. Hamaguchi, *Mem. Inst. Sci. Ind. Res., Osaka University*, **11**, 175 (1954).
12) H. R. Kruyt, "Colloid Science," Elsevier, Vol. I, pp. 140 (1952).

$$\psi_G = 2.303\frac{kT}{e}\log\left(\frac{134^2\times 4}{A^2C}\right), \quad (6)$$

where $A$ is the area per ion of film-forming substance in Å$^2$ unit.

If we assume that $\psi_G$ is the same as $\psi_0$, we can calculate $\psi_0$ by Eq. (6). However, the following two assumptions are necessary: (a) At pH 2.2 all the -$NH_2$ groups of lysine residues are ionized to -$NH_3^+$ ions. (b) It is difficult to find out the area per ion in the case of polyampholytes. In the present case, we assume in regard to the first approximation as described above, that the initial monomer concentration ratio of lysine, phenylalanine and glutamic acid residues, i.e., 1 : 3 : 1, is maintained in the copolymer produced, so that the area per -$NH_3^+$ ion may be five times the area per residue. By these assumptions $\psi_0$ can be calculated by Eq. (6) for the case of 20 Å$^2$/residue, namely 100 Å$^2$/-$NH_3^+$ ion. $\psi_0$ becomes 115 mv. when $c=0.075$ mol./litre. Substituting this figure in Eq. (4) and then in Eq. (5) we obtain $F^\circ=-5.8$ dynes/cm. Using this $F^\circ$ value $\psi_0$ can be calculated by Eq. (4) at different salt concentrations. The results are summarized in Table I.

TABLE I

| $c$ (mol./litre) | $F$ (dynes/cm.) at 20 Å$^2$/residue | $\psi_0$ (mv.) calculated from eq. (4) | $\psi_0$ (mv.) calculated from eq. (6) |
|---|---|---|---|
| 0.04 | 0.65 | 130 | 131 |
| 0.075 | 0.55 | 115 | 115 |
| 0.135 | 0.30 | 102 | 100 |
| 0.405 | 0.05 | 80.4 | 72.8 |

The values of $\psi_0$ calculated from Eq. (4) are in close agreement with those of $\psi_G$ from (6). Therefore, the following equation, which is readily derived from Eq. (6), is also applied for $\psi_0$ values calculated from the F–A curves.

$$\left(\frac{\partial\psi_0}{\partial\log c}\right)_A = -59\ mv. \quad (7)$$

This relation was found for the monolayers of $\alpha$-brompalmitic acid[13] and of octadecyltrimethylammonium chloride[10] on the substrates containing sodium chloride.

**The Relationships between $\eta$-A Curves and Ionic Strength or pH's of Substrates.**— As shown in Figs. 5 and 6 an increase of the ionic strength in the substrate accompanied the decrease of the surface viscosity and the surface viscosity began to increase steeply at the area of about 15.9 Å$^2$/residue. This area corresponds to the area per residue calculated with the X-ray data for close packed arrangement of peptide of $\beta$-configuration.[7]

Cumper and Alexander[14,15] showed that although the effect of the ionic strength of salts could not be detected for the spreading monolayers of proteins, in the case of adsorbed protein films an increase in ionic strength decreased the surface viscosities. We could find out the same effect for the spreading monolayers of the copolypeptide as for the adsorbed films found by them.

There are two possibilities to explain why the surface viscosity decreased by an increase in ionic strength of salts in the substrate.

(a) In the case of polyelectrolyte solutions, the viscosity is generally decreased by an increase in salt concentration, and this might attributed to the coiling of polyelectrolyte molecules, for salt reduces the electrostatic repulsion between the intramolecular charged groups.[16] The relation between the surface viscosities and the salt concentration which was found in the present experiments (Fig. 6), is analogous to the bulk viscometric behaviour of polyelectrolytes just mentioned. The surface viscometric behaviour would be, therefore, explained by the same reason as for bulk viscosities.

(b) There exist many salt-linkages between -$NH_3^+$ and -$COO^-$ ions at pH 5.6, for this pH value lies in the isoelectric band as described previously. The high surface viscosities would be the result of the great resistance due to these inter- or intramolecular salt-linkages. By the presence of salts, however, the coulombic force between -$NH_3^+$ and -$COO^-$ ions is minimized. Therefore, the effect of salt on the surface viscosities would be interpreted in terms of this reducing effect of electrostatic interaction.

The former possibility (a) cannot be admitted for the following reasons. The areas where the effect of salts appears, are smaller than 21 Å$^2$/residue and this smaller area region corresponds to the state in which polymer molecules are very close to each other. In such a state it could not be considered that the surface viscosity depends on the shape of each polymer molecule. Furthermore, if the increase in surface viscosity by the decrease in the concentration of salt would be due to the elongation of a polymer molecule, the reason why a maximum point appears in the $(\eta)_{\frac{}{A}}$ pH curve (Fig. 8), cannot be ex-

13) D. J. Crisp, Surface Chemistry (*Research Supplement*), Butterworth, (1949) p. 65.

14) C. W. N. Cumper and A. E. Alexander, *Trans. Faraday Soc.*, **46**, 235 (1950).

15) C. W. N. Cumper and A. E. Alexander, *Revs. Pure and Applied Chem.* (Australia), **1**, 121 (1951).

16) A. Katchalsky, *J. Polymer Sci.*, **7**, 393 (1951.).

plained. These facts support the possibility (b). Davies,[17] in his paper on the shape of protein molecules at interfaces, considered that the surface viscosity of protein at oil-water interface is very much higher than at air-water interface, is one of the evidences that the protein molecules are to a greater extent unfolded into long chains of considerable flexibility at the former than at the latter. He compared, however, the surface viscosity at oil-water interface with that at air-water interface in a region of very small area. Furthermore, he referred to Joly's data[18] of surface viscosities at air-water interface in which the substrate was acidified by N/100 HCl and also to the data of Cumper and Alexander[14] at oil-water interface in which the pH's of the aqueous phase were not described explicitly. However, in view of our results mentioned above, we cannot agree with his opinion. Inokuchi[19] pointed out that the area at which the instantaneous elasticity of egg albumin films appears on 5% ammonium sulphate solution at pH 5.5, was three times the area as on 0.1 N HCl. This would also be interpreted in terms of salt-linkages when we take into account that the isoelectric point of the protein lies at pH 4.8.

The decrease in surface viscosities at constant area is approximately proportional to the square root of the ionic strength in the substrate. This fact corresponds to the bulk viscosity or rigidity of very concentrated gelatin solutions.

**The Relationships between $(A)_F$-pH, $(\eta)_A$-pH, $\Delta\alpha$-pH and $\alpha_L \cdot \alpha_G$-pH Curves.**—In the previous paper,[1] it was pointed out that the $(A)_{F or \eta}$ (at constant $F$ or at constant $\eta$)-pH curve which was obtained with the films of the copolypeptide of L-lysine, L-leucine and L-glutamic acid on the substrate which did not contain any salts, was of W-shape and the maximum point in this curve corresponded to its isoelectric point. We calculated the ionization degrees of $-NH_2$ groups of lysine residue ($\alpha_L$) and of -COOH groups of glutamic acid residue ($\alpha_G$) at each pH by the following simple approximate equation

$$pH - pK_0 = \log\frac{\alpha}{1-\alpha}, \qquad (8)$$

where $K_0$ is the intrinsic dissociation constant which is assumed to be 10.5 and 4.3 for $-NH_2$ and -COOH groups, respectively. $\Delta\alpha = |\alpha_L - \alpha_G|$ might be assumed to give a measure of effective free charges and $\alpha_L \cdot \alpha_G$ the probability of salt-linkages. This assumption might be justified if the polymerization ratio of lysine and glutamic acid is 1 : 1. The W-shaped $(A)_{F or \eta}$-pH curve could be interpreted as follows in terms of the $\Delta\alpha$-pH and $\alpha_L \cdot \alpha_G$-pH curves. $\alpha_L \cdot \alpha_G$-pH curve showed a maximum at pH 7.0 and the $(A)_{F or \eta}$-pH curve also showed a maximum at this pH. When the substrate becomes more acidic or alkaline from this isoelectric point, the area becomes smaller and this region corresponds to the droop $\alpha_L \cdot \alpha_G$-pH curve. In this region the effect of $\alpha_L \cdot \alpha_G$ is more predominant than that of $\Delta\alpha$, i.e., the effect of salt-linkages is more pronounced than that of electrical repulsion by free charges. When the substrate becomes still more acidic or alkaline, the area becomes larger again and these regions correspond to the rise of the $\Delta\alpha$-pH curve, i.e., the effect of electrical repulsion is more predominant than that of salt-linkages.

When salt is present in the substrate, however, the maximum in the W-shaped $(A)_F$-pH curve disappeared and the curve had a minimum $(A)_F$ region between pH 5.6 and 8.0 which is parallel to the pH axis (Fig. 3). As described above, salt ions have the effect of reducing the electrostatic interaction between $-NH_3^+$ and $-COO^-$ ions. Therefore, it is very probable that a maximum point which should appear in the $(A)_F$-pH curve, is depressed by salt ions and so the portion corresponding to the $\alpha_L \cdot \alpha_G$-pH curve which

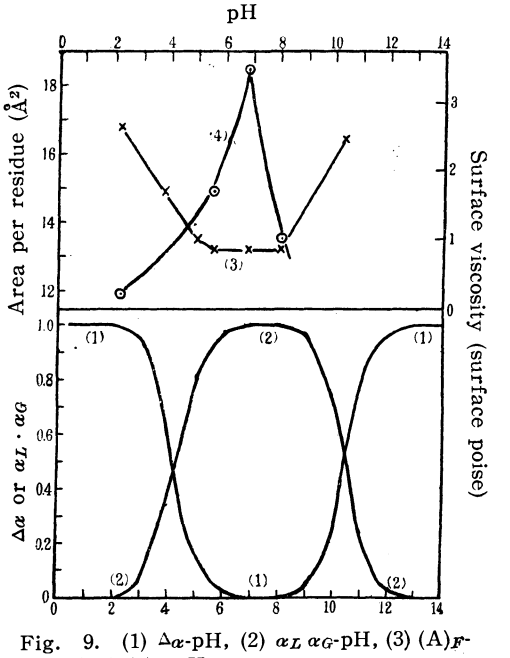



Fig. 9. (1) $\Delta\alpha$-pH, (2) $\alpha_L \alpha_G$-pH, (3) $(A)_F$-pH, (4) $(\eta)_A$-pH curves.

17) J. T. Davies, *Biochim. et Biophys. Acta*, **11**, 165 (1953).
18) M. Joly, "Surface Chemistry" (*Research Supplement*), Butterworth, (1949) p. 157.
19) K. Inokuchi, This Bulletin, **26**, 500 (1953).

represents the term of salt-linkages, disappears. Then as shown in Fig. 3 the $(A)_F$-pH curve has only the portion corresponding to the $\Delta\alpha$-pH curve. Ellis and Pankhurst[20] showed that the $(F)_A$-pH curve obtained with collagen films, showed a maximum at pH 2.2 and sodium chloride in the substrate caused the maximum to be depressed and finally to disappear. The $(\eta)_A$-pH curve has a maximum point at pH 6.8 and corresponds to the $\alpha_L \cdot \alpha_G$-pH curve. This fact also supports the consideration that the surface viscosities depend markedly on the number of inter- or intra- molecular salt likages. The $(A)_F$-pH, $(\eta)_A$-pH, $\Delta\alpha$-pH and $\alpha_L \cdot \alpha_G$-pH curves are shown together in Fig. 9.
These relationships show that the isoelectric point of the copolypeptide lies near pH 6.8.

## Summary

By studying the surface pressure-area and surface viscosity-area curves of the copolypeptide of L-lysine, L-phenylalanine and L-glutamic acid over a range of pH values and salt contents in the substrate, the following four distinct results were obtained:

(1) When the concentration of potassium chloride in the substrate was kept constant (0.07 M/litre), the $(A)_F$-pH curve has a minimum area region between pH 5.6 and 8.0 which is parallel to the pH axis and this region corresponds to the isoelectric band of this copolypeptide at this salt concentration. The width of this band was the function of the salt concentration; when the salt content was increased this band became wider.

(2) When the pH's of the substrates was kept constant (pH 2.2), the F-A curves were more expanded at low salt concentrations. This fact could be interpreted by the increment of surface pressure due to the free energy of the electrical double layer which is formed between the ionized groups of the monolayer ($NH_3^+$ ions) and the counter ions ($Cl^-$ ions). The values of surface potentials calculated from the F-A curves and from Gouy's equation agreed with each other.

(3) The surface viscosities became higher when the salt concentrations in the substrate at constant pH's were decreased and became maximum at its isoelectric point. The surface viscosity depends markedly on the number of inter- or intra-salt-linkages between $-NH_3^+$ and $COO^-$ ions and not on the shape of each polymer molecule.

(4) The $(A)_F$-pH and $(\eta)_A$-pH curves could be interpreted in terms of effective free charges and the number of salt-linkages.

The authors wish to express their sincere thanks to Dr. H. Tani and Mr. H. Yuki, of the Faculty of Science at Osaka University, who gave them the valuable sample of synthetic polypeptide. A part of the expense for the experiment has been defrayed from grants given by the Ministry of Education, and the Asahi Press to which the authors' thanks are also due.

*The Institute of Scientific and Industrial Research, Osaka, University, Sakai, Osaka*

20) S. C. Ellis and K. G. A. Pankhurst, *Nature*, **163**, 600 (1949); *Trans. Faraday Soc.*, **50**, 82 (1954).

# *Heats of Combustion and Formation of Some Organosilicon Compounds*

By Toshio TANAKA, Ukiko TAKAHASHI, Rokuro ŌKAWARA

and Takeo WATASE

(Received June 4, 1954)

Recently the heats of combustion of organosilicon compounds have been reported by a few investigators[1,2,3,4] using the bomb calorimeter. We measured the heats of combustion of organosilicon compounds in order to derive the bond energies between silicon and other elements. In this paper we shall summerize the conditions of complete burning of organosilicon compounds and the data obtained in our measurements for the heats of combustion of the five following substances; i.e. dimethyl diethoxysilane $(CH_3)_2Si(OC_2H_5)_2$, di-*n*-propyl diethoxysilane $(n\text{-}C_3H_7)_2Si(OC_2H_5)_2$, diethyl silanediol $(C_2H_5)_2Si(OH)_2$, hexamethyl cyclotrisiloxane $[(CH_3)_2SiO]_3$ and hexaphenyl cyclotrisiloxane $[(C_6H_5)_2SiO]_3$.

1) H. Reuther, *Chem. Tech. (Berlin)*, **2**, 331 (1950).

2) S. Tannenbaum, S. Kaye and G. F. Lewenz, *J. Am. Chem. Soc.*, **75**, 3753 (1953).

3) R. Thompson, *J. Chem. Soc.*, 1953 1908.

4) T. Tanaka, U. Takahashi, R. Ōkawara and T. Watase, *J. Chem. Phys.*, **19**, 1330 (1951); **22**, 957 (1954).

### Method and Apparatus

The apparatus was the commercial Berthelot Mahler-type bomb calorimeter, incorporating a 300-ml. stainless-steel-made bomb and a Beckmann thermometer. The calorimeter was set in the thermostat (20±0.2°C), and it was held for an hour in the thermostat before measurement. The temperature rise in the calorimeter was measured through the magnifying-glass attached in front of the thermometer, using a telescope. In order to prevent "sticking" of the mercury of the thermometer, the capillary was continuously kept in a slight vibratory motion[5], that is, the thermometer was ticked by an electromagnetic instrument, placed over the top of it, 150 times per minute, and read with an accuracy of 0.001°C.

Iron wire was employed as the ignition medium, and the value 1490 cal./g. was adopted for the heat of its combustion[6]. For the complete burning of solid organosilicon compounds it was not a desirable method to burn the tablet. The silica produced during the early stage of combustion floated over the surface of the tablet so that there was no access of oxygen beneath it and incompletely burnt residues were left on the base of the crucible. Each solid sample was stuffed into a bag of Ganpi-paper, which was burned with it. The heat of combustion of Ganpi-paper was found to be 3971 cal./g.

After some preliminary work on the method of burning under various pressures, it was successfully found to burn completely under 30 atm. pressure. Before each combustion 1 ml. of water was in the bomb, which was then filled with pure oxygen up to the pressure of 30 atm. at 20°C. In our experiments the air initially present in the bomb was not driven out by filling the bomb with oxygen, bacause of the considerable volatility used for measurements. Accordingly there was always present a small amount of nitrogen within the bomb and the nitric acid produced in the combustion process was titrated with N/14.55-sodium carbonate solution. The magnitude of the thermal correction for this nitric acid, calculated on the basis of an evolution of 14.55 kcal./mole of aqueous nitric acid formed[6], was about 10 calories. The corrected temperature rise was calculated by the method described by Dickinson[7].

To determine the water equivalent of the calorimeter at 20°C, we used the value 6319.0 cal./g.[8] for the heat of combustion of standard benzoic acid (Kahlbaum, *zur Analyse*). Eight calibration experiments of calorimeter were performed with these materials, and its water equivalent value was determined to be 2348 cal./degree (the relative mean deviation ±1.0 cal./degree).

**Complete Burning of Liquid Compounds.**—Reuther[1] measured the heats of combustion of six organosilicon compounds. However, it is difficult to understand why he did not refer to the technique for the combustion of liquid. For the purpose of complete combustion of polydimethyl siloxane, which could be itself employed as the promoter, Thompson[3] divided the sample into two glass ampoules of nearly the same volume, the more breakable one of which was collapsed at an oxygen pressure of several atm. to produce a pool of liquid in the crucible, and the other stronger ampoule was burnt after firing, owing to the heat produced by the combustion of the liquid pool. But in our experimemt, when the weaker ampoule collapsed, a portion of liquid was scattered, and the liquid attached to the inside surface of the bomb ended in incomplete combustion.

In our experiments the liquid samples were sealed into a thin walled glass ampoule of soft glass. We filled up the ampoule with the liquid so that there might be no air left within it and so that the ampoule might remain filled up at the temperature in the calorimeter. We performed its preliminary ignition by using a cotton string tied to an iron wire, the string being soaked with promoter which was kept in touch with the ampoule. In the combustion measurements of volatile carbon compounds Moore and his coworkers[9] employed specially formed glass capsules, 0.5 to 0.8 ml. in volume and 0.065 to 0.085 g., in empty weight while in our experiments the ampoules were of a single spherical form and the relation of weight to volume was similar to Moore's. The ampoules must be made so as to withstand the oxygen pressure (30 atm.) within the bomb, and also when one weighed more than 0.100 g. it tended to explode on ignition, and then the liquid therein was splashed out of the crucible resulting in incomplete burning. In our combustion measurements about 0.02 g. of liquid paraffin was used as a promoter, and its heat of combustion was found to be 10,868 cal./g. as the average of six measurements. Even under these conditions about half the experiments ended in incomplete combustion, so it was found to be necessary to carry out 10 or more experiments before several consistent values were obtained.

**Materials.**—Dimethyl diethoxysilane was prepared as follows; the Grignard solution was added drop by drop to diethoxy dichlorosilane diluted with ether for three hours[10,11]. For the preparation of di-*n*-propyl diethoxysilane, the procedure of addition was reversed, that is, diethoxy dichlorosilane dissolved in dry ether was dropped into the Grignard solution for an hour while keeping the reacting mixture below 10°C under cooling and vigorous stirring[10]. Hexamethyl cyclotrisiloxane[12] and hexaphenyl cyclotrisiloxane[13] were prepared by the hydrolysis of dimethyl dichloro-

5) J. Coops and K. Van Nes, *Rec. trav. chim.*, **T66**, 146 (1947).
6) H. M. Huffmann and E. L. Ellis, *J. Am. Chem. Soc.*, **57**, 41 (1935).
7) H. C. Dickinson, *Bull. Bureau of Standards*, **11**, 189 (1914).
8) Calculated from the result of Prosen and Rossini, *J. Research NBS.*, **33**, 439 (1944).
9) G. E. Moore, M. L. Renguist and G. E. Parks, *J. Am. Chem. Soc.*, **62**, 1505 (1940).
10) M. Kumada, *J. Inst. Polytech. Osaka City Univ.*, **2**, 11 (1951).
11) M. Kumada and T. Tarama, *J. Chem. Soc. Japan, Ind. Sec.*, **54**, 213 (1951), (in Japanese).
12) W. Patnode and D. F. Wilcock, *J. Am. Chem. Soc.*, **68**, 358 (1946).
13) C. A. Burkhard, ibid., **67**, 2173 (1945).

silane and diphenyl dichlorosilane, respectively. Another was prepared according to the method of Digiorgio et. al.[14] The physical constants of these samples used for the measurements are shown in Table I.

TABLE I

PHYSICAL CONSTANTS OF THE SAMPLES USED FOR COMBUSTION MEASUREMENTS

| Sample | b.p. °C/mm Hg | m.p. °C | $d_4^{20}$ | $n_D^{20}$ | $MR_D$ found | $MR_D$ calcd. |
|---|---|---|---|---|---|---|
| $(CH_3)_2Si(OC_2H_5)_2$ | 113/760 | — | 0.8410 | 1.3815 | 41.10 | 41.00 |
| $(n\text{-}C_3H_7)_2Si(OC_2H_5)_2$[a] | 85/20 | — | 0.8558 | 1.4100 | 59.10 | 59.26 |
| $(C_2H_5)_2Si(OH)_2$[b] | — | 96 | 1.134 | — | — | — |
| $[(CH_3)_2SiO]_3$ | 134/760 | 64 | — | — | — | — |
| $[(C_6H_5)_2SiO]_3$[c] | 290-300/1 | 190 | — | — | — | — |

Anal. a) Si % found 13.5, calcd. 13.7 b) C % found 39.86, calcd. 39.97; H % found 10.12, calcd. 10.07. c) Si % found 14.20, calcd 14.16.

## Results and Discussion

By complete burning, gaseous carbon dioxide, liquid water and silicon dioxide evolved as the end products. The completeness of combustion was ascertained by visual inspection of the bomb contents for traces of black or yellow materials[15], and sometimes by chemical analysis. The experimental data for the combustion of dimethyl diethoxysilane are presented in Table II.

TABLE II

THE EXPERIMENTAL DATA FOR DIMETHYL DIETHOXYSILANE AT 20°C

| Wt. of sample g. | Total heat evolved cal. | $\Sigma$ cal. | $\Sigma'$ cal. | $-\Delta U_B$ cal./g. | $\Delta$ cal./g. |
|---|---|---|---|---|---|
| 0.2530 | 2177.1 | 26.5 | 245.9 | 7528 | − 8 |
| .2650 | 2406.9 | 18.0 | 389.0 | 7547 | +11 |
| .2848 | 2461.4 | 20.3 | 297.7 | 7526 | −10 |
| .2945 | 2652.2 | 18.3 | 412.9 | 7542 | + 6 |
| .3271 | 2726.5 | 19.1 | 240.3 | 7542 | + 6 |
| .3316 | 2904.7 | 20.6 | 386.8 | 7531 | − 5 |
| | | | mean.....7536 (±0.1%) | | |

The energy evolved per gram at 20°C is represented by $-\Delta U_B$ and the deviations of the individual runs from the mean by $\Delta$. $\Sigma$ is the sum of the calorific values from nitric acid, iron wire used as the ignition medium, and Joule's energy due to the electric current. $\Sigma'$ is the sum of the heats of combustion of the promoter and the cotton string. The detailed experimental data for the remaining four samples have been omitted here, involving an overall uncertainty of not more than ±0.1% in relative mean deviation.

Table III contains the summary of the experimental data for the heats of combustion of five substances together with some important thermal data calculated therefrom. The number of satisfied combustion measurements in each case are given in the third column. The values of the bomb process were then recalculated per mole and corrected to the standard constant-volume process where the reactants are at 1 atm. pressure by means of Washburn's equation[16]. The energy evolved in this hypothetical standard process was denoted in Table III by the symbol $-\Delta U_R$. From this quantity the heat evolved in the isobaric process at 1 atm., $-\Delta H_c$, was obtained by the addition of the proper work term. Finally, the heats of formation, $-\Delta H_f°$ (obs.), of these five substances from the standard

TABLE III

HEATS OF COMBUSTION AND DERIVED DATA FOR FIVE COMPOUNDS

| Compounds | Mol. wt. | No. of satisfied combustion | $-\Delta U_B$ cal./g. | $-\Delta U_R$ kcal./mol. | $-\Delta H_C$ kcal./mol. | $-\Delta H_f°$ kcal./mol. obs. | calcd. from Pauling's data | calcd. by Gilman and Dunn | calcd. by Thompson |
|---|---|---|---|---|---|---|---|---|---|
| $(CH_3)_2Si(OC_2H_5)_2$ | 148.25 | 6 | 7536 | 1117 | 1119 | 200 | 180 | 198.3 | 214 |
| $(n\text{-}C_3H_7)_2Si(OC_2H_5)_2$ | 204.35 | 6 | 8552 | 1747 | 1751 | 217 | 205 | 226.7 | 233 |
| $(C_2H_5)_2Si(OH)_2$ | 120.20 | 3 | 6495 | 781 | 782 | 212 | 193 | 228.2 | 228 |
| $[(CH_3)_2SiO]_3$ | 222.38 | 5 | 6314 | 1404 | 1407 | 396 | 357 | 421.9 | 463 |
| $[(C_6H_5)_2SiO]_3$ | 594.78 | 4 | 8086 | 4805 | 4810 | 225 | 151 | — | 216 |

14) P. A. Digiorgio, L. H. Sommer and F. C. Whitemore, ibid., **68**, 344 (1946).

15) L. H. Long and R. G. W. Norrish, *Proc. Farad. Soc.*, **A241**, 587 (1949).

16) E. W. Washburn, *Bur. Standards J. Research*, **10**, 525 (1933).

elements (gaseous $H_2$ and $O_2$, graphitic C, and metallic Si) were calculated from $-\Delta H_c$ by using -68.32[17], -94.05[17] and -208.14[3] kcal./mole for the heats of formation of water, carbon dioxide and amorphous silica, respectively.

Then, we calculated $-\Delta H_f°$ (calcd.) in Table III by using the following data in accordance with the pressumption mentioned below: Data—Heats of atomization of elements; 85.0, 59.1, 51.7, and 124.3 kcal./g.-atom[18] for Si, O, H and C. Bond energies; 87.3, 57.6, 89.3, 58.6, 100 and 110.2 kcal./mole[18] for C-H, Si-C, Si-O, C-C, C=C and O-H, respectively. Resonance energy for benzene nucleus; 39 kcal./mole[18]. The heat of sublimation for hexamethyl-cyclotrisiloxane was found to be 13.2 kcal./mole by Osthoff, et. al.[19] The heats of vaporization for other compounds were presume from Trouton's Rule, and the heats of fusions were assumed to be one-tenth of those of vaporization.

As is shown in Table III the differences between the observed and calculated values of the heats of formation are not small. Uncertainty in the Si-O and Si-C bond energies proposed by Pauling may be the most probable reason for such disagreement.

The values of 52.0 and 59.2 kcal./g.-atom are now generally accepted for the heats of atomization of hydrogen and oxygen, respectively[20]. The corresponding value for carbon is controversial. Direct and various indirect measurements give varying values which fall into three main groups centering around 124,[21] 140[22] and 170[23] kcal./g.-atom. The value of silicon is in even greater doubt. Gilman and Dunn[24] calculated the Si-C and Si-O bond energies using the values 170 and 102 kcal./g.-atom for the heats of atomization of carbon and silicon, respectively, from the heats of formation of carborundum and silica. The resulting values are as follows: Si-C, 75.0; Si-O, 106 kcal./mole. Thompson[3] measured the heats of combustion of some polydimethyl siloxane, and calculated as 64 and 117 kcal./mole for the Si-C and Si-O bond energies from his results. (These values correspond to the following heats of atomization: C, 171.7; Si, 88.04 kcal./g.-atom). They also calculated the heats of formation of dimethyl diethoxysilane etc. These results are shown in Table III and comparatively near to the observed values except those of cyclic compounds.

However, the bond energies obtained by Gilman and Dunn were those derived from the heats of formation of silica and carborundum. It is also very desirable to derive these corresponding bond energies from the organosilicon compounds. The combustion measurements carried out by Thompson[3] contain considerable deviations, so we are not satisfied with bond energies derived from his measurements.

The compounds used here in our measurements, except hexamethyl cyclotrisiloxane, have such a large number of C-C and C-H bond etc. that Si-O and Si-C bond energies calculated from them turn out to be small differences between large quantities, so that they may be unreliable.

Recently we have measured the heats of combustion of some methoxy-polysilane and -polysiloxane, and calculated their heats of formation. The details will soon be published.

## Summary

1. A bomb calorimeter has been used for the measurements of the heats of combustion of the following five compounds at 20°C and at constant volume: dimethyl diethoxysilane, di-*n*-propyl diethoxy silane, diethyl silanediol, hexamethyl cyclotrisiloxane and hexaphenyl cyclotrisiloxane.

2. From these experimental results the corresponding heats of combustion and formation at constant pressure have been calculated, and the latter values were compared with the calculated values of the heats of formation derived from the data of the bond energies.

The authors wish to express their sincere thanks to Mr. Kumada, Osaka City University, and Mr. Nozakura, Osaka University, for the preparation of these samples.

*Department of Applied Chemistry, Faculty of Engineering, Osaka University, Higashinoda, Osaka*

17) Wagman, Kilpatrick, Taylor, Pitzer and Rossini, *J. Research NBS.*, **34**, 143 (1945).
18) L. Pauling, "The Nature of the Chemical Bond" Cornell Univ. Press, Ithaca, New York, 1940.
19) R. C. Osthoff, W. T. Grubb and C. A. Burkhard, *J. Am. Chem. Soc.*, **75**, 2227 (1953).
20) "Selected Values of Chemical Thermodynamic Properties" (*Natl. Bur. Stand.*, Washington, 1950).
21) G. Herzberg, *J. Chem. Phys.*, **10**, 306 (1942). L. H. Long and R. G. W. Norrish, *Proc. Roy. Soc.*, (*London*) **A187**, 337 (1946).
22) F. H. Field, *J. Chem. Phys.*, **19**, 793 (1951).
23) G. Glockler, ibid., **19**, 124 (1951).
24) H. Gilman and G. E. Dunn, *Chem. Revs.*, **52**, 77 (1953).

# *Studies on Molecular Structure by the Measurement of the Dielectric Constants of Gases and Vapors. I. Construction of an Apparatus and the Dipole Moment and the Molecular Structure of 1, 1-Dichloroacetone*

By Takehiko CHIBA

(Received June 5, 1954)

The measurement of dipole moment is one of the most powerful tools for the study of molecular structure. However by the dilute solution method usually employed it is difficult to obtain the true dipole moment of free molecules. The determination of atomic polarization and the measurement of the moment for the substances which are insoluble in nonpolar solvents as well as those which have a moment of small magnitude can only be made by a gas method. In spite of its importance, gas measurements reported so far are very scarce, because a very high precision is required in this method compared with the solution method. The purpose of this research is to study many interesting problems on molecular structure by precise determination of the dielectric constants in the gaseous state.

The present paper deals with the details of the construction of the apparatus and the result of the measurement of the dipole moment of 1,1-dichloroacetone.

## I. Apparatus

The measuring apparatus is shown in Fig. 1,

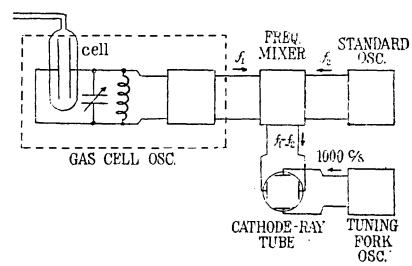



Fig. 1. Block-diagram of the measuring system.

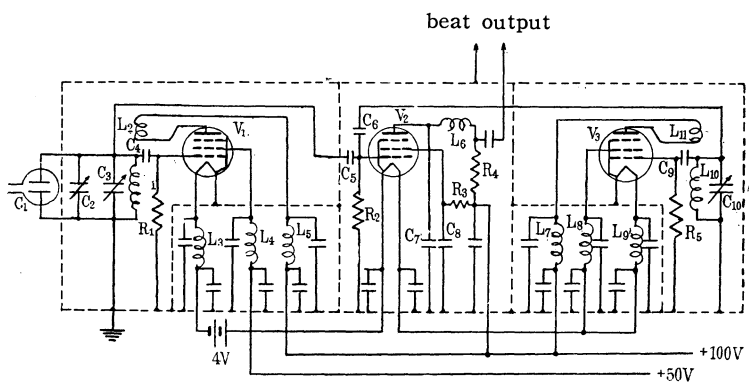



Fig. 2. Oscillators and mixer circuit.

$C_1$ Gas cell
$C_2$ Precision condenser
$C_3$ Variable air condenser (max. capacity, ca. 90$\mu\mu$F)
$C_4$, $C_9$ 100$\mu\mu$F
$C_5$, $C_6$ ~1$\mu\mu$F
$C_7$ 250$\mu\mu$F
$C_8$ 0.01$\mu$F
$C_{10}$ Variable air condenser (max. capacity, ca. 860$\mu\mu$F)
All the other capacitors have values of 0.1$\mu$F.

$R_1$, $R_5$ 200k$\Omega$
$R_2$ 1M$\Omega$
$R_3$ 100k$\Omega$
$R_4$ 50k$\Omega$

$L_1$ 41 turns of 0.4mm diameter enamel wire space-wound on 60 mm. diameter "steatite" bobbin.
$L_2$ 10 turns of 0.32 mm. diameter silk-covered wire close-wound on the same bobbin as $L_1$, with $L_2$ spaced 7 mm. from $L_1$.
$L_{10}$ and $L_{11}$ same as $L_1$ and $L_2$
$L_3$, $L_9$ 200$\mu$H
$L_4$, $L_5$, $L_6$, $L_7$, $L_8$ 4mH
$V_1$, $V_2$, $V_3$ 1N5-GT

which is similar to that employed by Groves[1]. A beat output from two oscillators, one of which is a standard oscillator and the other one which has a gas cell and a precision condenser in its tank circuit, is fed to one deflection plate of a cathode-ray tube, and 1000-cycle output from a tuning fork oscillator to the other plate to form a Lissajous figure on the screen. The change in the cell capacity by the introduction into the cell of a vapor of a sample is measured by the decrease of the capacity of the precision condenser until the figure takes the original form.

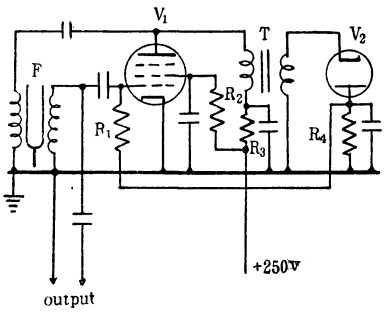
**1. Oscillators and Mixer.**—The circuit connexion of the oscillators and the mixer is shown in Fig. 2. The gas cell oscillator and the standard one are constructed as similarly as possible, their operating frequency being about one megacycle. The outputs of the two oscillators are fed to the mixer, where a beat frequency is formed.

In the course of the construction of the oscillators, several points are found to be important for maintaining the oscillation frequency in extremely high stability which is necessary for the measurement of a dielectric constant in the gaseous state.

These are as follows: Air condensers exclusively are used for the tank circuit capacity because a mica or titanate condenser gives time drift to the frequency. The tank circuit is designed so as to give the least loss, and, accordingly, both the grid leak and the plate resistance of the vacuum tube circuit are made high (electron coupling circuit is used). The fluctuation of the plate resistance is minimized by not inserting a carbon resistor in the screen grid circuit for potential drop. In order to avoid heat emission from the tube a dry cell tube 1N5-GT is empolyed. The oscillators and the mixer are all battery-operated. They are placed in a wooden box lined with brass plates. The high frequency filters of both high tension and filament supplies for the oscillators are placed in a shielded chassis to avoid inter-oscillator coupling. The earth line is made of a stout brass pipe well soldered to water piping.

The circuit thus constructed proved to be very stable: the drift of the beat frequency was found to be less than one cycle per hour, which corresponds to $2\times10^{-4}$ per cent per hour in the cell capacity change.

The circuit of the tuning fork oscillator is shown in Fig. 3. A slight change in the frequency is noticed by an occasional change




$R_1$ 1MΩ T A.F. transformer
$R_2$ 150kΩ F Tuning fork
$R_3$ 30kΩ $V_1$ 6SK7
$R_4$ 500kΩ $V_2$ 6H6
Capacitors are all 0.01μF.

Fig. 3. Tuning fork oscillator circuit.

in the amplitude of oscillation, a diode amplitude limiter being attached to it.

**2. Precision Condenser.**—The precision condenser is a micrometer variable condenser[2] shown in Fig. 4. The capacity change

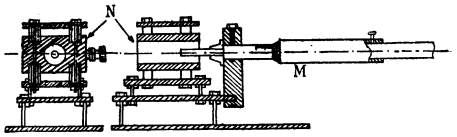



Fig. 4. Precision micrometer condenser.

produced by 1-mm. step of the micrometer condenser is about 0.06μμF, so that a change of capacity can be read to the order of $6\times10^{-4}$μμF.

**3. Gas Cell.**—The gas cell is the most important part of the apparatus since the plate surface inevitably comes into contact with various kinds of vapors at high temperatures, and a change in its state affects sensitively the observed value. The cell must be fixed rigidly in order to keep the capacity constant over a long period of time and over a wide range of temperatures. Thus, four kinds of cells shown in Table I are tested. Cell A is that used by Watanabe[3]: the small distance between the plates seems to make serious the capacity instability which occurs in the case of adsorption or condensation of a sample onto the plates. Cell B is constructed with wide gaps but it has mica spacers which were proved to be the cause of an abnormally large increase in the capacity recorded even with far less filling of a sample vapor below its saturation pressure. Cells C and D are constructed so as to eliminate these shortcomings. The

1) L. G. Groves, *J. Chem. Soc.*, **1939**, 1144.

2) H. E. Watson et al., *Proc. Roy. Soc.*, **143**, 558 (1934).

3) I. Watanabe, *Bull. Inst. Phys. Chem. Research (Tokyo)*, **20**, 681 (1941).

TABLE I

DATA OF THE GAS CELLS USED

| | Plate material | Diam. (mm.) | Length (mm.) | No. of plates | Gaps (mm.) | Spacing insulator | Capacity ($\mu\mu$f) |
|---|---|---|---|---|---|---|---|
| A | Nickel | 45 | 130 | 4 | approx. 1 | Mica | approx. 540 |
| B | Brass (gold plated) | 46 | 130 | 5 | „ 1.5 | Mica | „ 450 |
| C | Nickel | 35 | 120 | 3 | „ 1.3 | Glass | „ 160 |
| D | Nickel (gold Plated) | 46 | 137 | 3 | „ 1.3 | Glass | „ 200 |

spacing of these cells is as follows. Short nickel wires are silver-soldered at three points, each 120° apart at both ends of each cylinder plate, these three plates are placed in a coaxial position, and glass beads are melted on three nickel wires at each corner (Fig. 5b). The cell is designed to have a capacity of 150 to 200$\mu\mu$F, since, on account of the high stability of the oscillation, it is unnecessary to use a cell of so large a capacity as was previously thought requisite. The middle plate of Cell D is made 2 mm. shorter than the two other plates and the nickel wires are shielded by small guard pieces to reduce stray capacity. Cell D was found to be the most satisfactory.

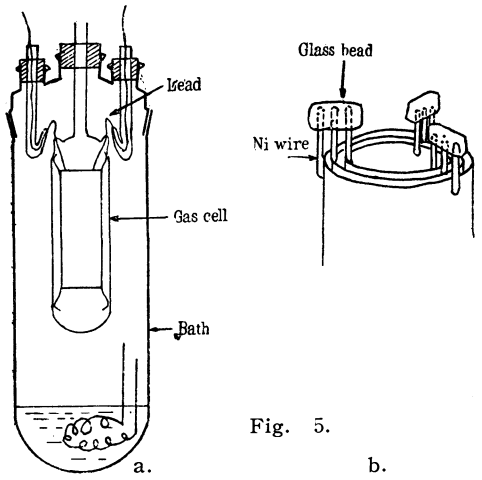



Fig. 5.

a. Gas cell in the vapor bath

b. Spacing of the plates

**4. Gas Filling Apparatus and Manometer.**—The equipment of gas filling as shown in Fig. 6 is constructed as a modification of Groves' method[1]. A sample in gaseous state is introduced from the cock $C_2$, while that in a liquid state is first poured into S, cooled from outside, and the whole system is evacuated. Then the cock $C_4$ is closed and $C_5$ opened to admit air through the cock $C_6$ so that the liquid goes up slowly to the capillary U-tube. The path from the cell to the point P is heated with a nichrome wire

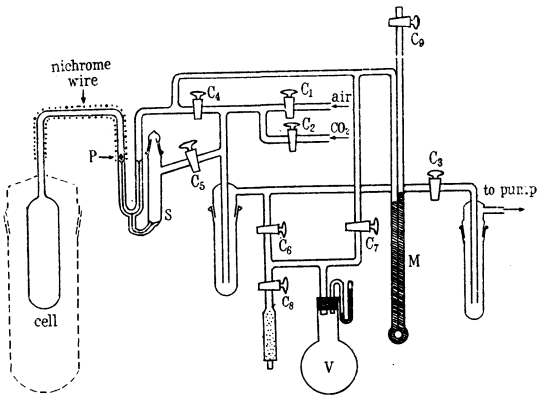



Fig. 6. Apparatus for gas filling and manometer.

to nearly the same temperature as that of the cell. The liquid evaporates at the point P, where a small piece of gold is placed to prevent bumping. Air is admitted from the flow controllable leak-cock $C_6$ and $C_7$ so as to keep the liquid in contact with the gold piece, whereby the velocity of the air flow is so adjusted that the liquid meniscus in the manometer side of the U-tube remains at about the middle. Fine pneumatic control is facilitated by connecting cocks, $C_6$ and $C_7$, to an air reservoir, V, the pressure in which is kept at about 15 to 30 cmHg. When a desired amount of the vapor is introduced, the two cocks are closed after bringing the liquid menisci of both arms to an equal level; the pressure of the vapor is then directly read by the manometer. The measurement is repeated by evacuating the whole system, condensing the vapor at S, and then carrying out the same operation as stated above. For a sample having a rather high vapor pressure at room temperature, the measurement becomes difficult since it readily condenses on the manometer wall.

**5. Vapor Bath.**—The cell is maintained at a constant temperature by the use of a vapor bath thermostat (Fig. 5a). Since the lead-wires to the cell are stretched in the vapor of the bath, dew-drops condense on them, followed by a rapid change in stray

capacity disturbing a stationary Lissajous figure at a balancing point. This difficulty is eliminated by covering the lead with glass tubes so that dew does not touch the leads directly (Fig. 5a).

Methanol, benzene, heptane, toluene, xylene, bromobenzene, and decaline are employed for the bath at 65°, 80°, 98°, 111°, 140°, 156° and 192°, respectively.

**II. Calibration and Measuring Procedures**

**1. Calibration of the Micrometer condenser.**—It is not necessary to know the absolute capacity of the micrometer condenser accurately, but its linearity must be checked. This is done by observing at each point of the micrometer the difference of the two micrometer readings which occur when the oscillation frequency shifts from a constant frequency to one higher by a given frequency (for instance, 100 cycles). The actual procedure is conveniently carried out by employing two tuning fork oscillators of 1000 and 700 cycles, respectively, and adjusting the beat frequency first to the first overtone of 1000 cycles and then to the second one of 700 cycles. By this procedure it is found that the deviation of capacity from linearity is less than 0.2 percent in the region of 8 to 23 mm. of its readings.

**2. Measuring Procedure.**—A sample is first introduced to a few mmHg, $p_1$, by the method described above, and the micrometer reading of the condenser is taken, $l_1$. The vapor is again filled to the pressure $p_2$, and the micrometer reading $l_2$ is taken. The polarization, $P$, is then given by

$$P=\frac{1}{3}\times\frac{\Delta l}{l_0}\times\frac{RT}{\Delta p}=20790\times\frac{\Delta l}{\Delta p}\times\frac{T}{l_0},$$

where $\Delta l=l_2-l_1$, $\Delta p=p_2-p_1$, $T$ is the absolute temperature of the vapor, and $l_0$ is the cell constant in the unit of capacity of 1 mm. of the micrometer condenser. $l_0$ is determined by known substances. Air and carbon dioxide are convenient for this purpose, but these substances have such small polarizations that measurements at several hundred mm. filling have to be carried out. Usually, however, gradual capacity change is observed in such cases, resulting in large fluctuation of $l_0$ values observed. Therefore mesitylene, on account of its moderate vapor pressure, is used for this purpose and $l_0$ is measured at three temperatures, 111°, 141°, and 192°. The measured values are constant within experimental errors, $l_0$ is taken to be their mean value, i. e. 3545 mm. in Cell D.[4] The additional check of the cell constant is made at room temperature using carbon dioxide with a large number of observations of different $\Delta p$'s. The resultant $l_0$ is in good accord with the value mentioned above.

The same frequency is used in every measurement, since otherwise a change of the cell constant cannot be avoided if there exists non-negligible inductance between the cell and the other part of the tank circuit.

Samples are filled to about 5 to 15 cmHg. The pressure should not exceed about two-thirds of its saturation pressure, because otherwise abnormally large values are often observed.

In all measurements gas is assumed to be ideal, for the correction of gas imperfection is 0.3 per cent at most and is usually far less than experimental errors. A mean value of $\Delta l/\Delta p$ is used instead of the value extrapolated to zero pressure, since, though it is more rigorous to use the latter, the observed value is always proved to be approximately the same within experimental errors throughout all the values of $\Delta p$. In most cases, the error in the observed polarization is 1 to 2 percent in each observation, and the error originates from the pressure readings as well as from the capacity measurement. By several runs of observation, however, it is easy to reduce the error to less than 0.5 per cent.

**III. The Dipole Moment and the Molecular Structure of 1.1-Dichloroacetone**

**1. Experimental and the Result of the Measurement.**—1.1-Dichloroacetone was prepared by passing chlorine gas into a mixture of acetone, granulated marble, and water. One volume of the raw product was washed with ten volumes of water to separate monochloroacetone, dried over calcium chloride, and fractionally distilled; b.p. 118–120°C. The main contamination in this product is monochloroacetone, whose absence was confirmed by the observation of the infrared spectrum.

The results of the measurement are given in Table II. The plot of the molecular polarisation, $P$, against $1/T$ is found to be almost a straight line. If the dipole moment is assumed to be independent of temperature, the inclination of this straight line gives the moment of 1.52 D, and the intercept of this line with the axis of $P$ affords the atomic polarization $P_A$ of 29 cc. It is impossible, however, to allow such a large value to the atomic polarization, since it is well known that in most cases the atomic polarization dose not exceed 10 percent of the electronic polarization, and $MR_D$ of this compound is

4) The polarization of mesitylene is taken to be 41.5 cc.

only 25.8 cc. Thus, by the usual assumption that $P_E+P_A=1.05MR_D=27.1$ cc., it must be concluded that the moment of this molecule increases with the temperature as listed in Table II.

TABLE II

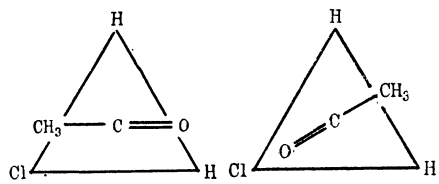
THE OBSERVED POLARIZATION AND DIPOLE MOMENT OF 1, 1-DICHLOROACETONE

$MR_D=25.8$ cc. $P_E+P_A=1.05MR_D$ (assumed)=27.1 cc.

| $T°$ | $p$ | $n$ | $P$ | $\Delta P$ | $\mu$ |
|---|---|---|---|---|---|
| K | mmHg | | cc. | cc. | D |
| 338.3 | 65–90 | 7 | 92.6 | 0.5 | 1.91 |
| 371.1 | 66–117 | 7 | 89.0 | 0.2 | 1.94 |
| 413.3 | 72–120 | 7 | 85.2 | 0.3 | 1.99 |
| 467.5 | 85–113 | 9 | 81.5 | 0.4 | 2.05 |

$p$: pressure range of the observations.
$n$: number of the observations.
$\Delta P$: mean deviation of $P$.

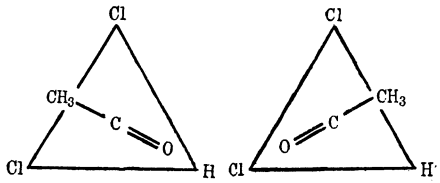
**2. Discussion.**—It is found that the dipole moment increases with the temperature, which shows clearly that the molecules are distributed over a range of positions with small moment to that with larger moment, and that the former position is more stable than the latter. In the case of monochloroacetone, a small dependence of its moment on temperature was observed by Zahn.[5] The molecular structure of the compounds with a carbonyl group at one end of the axis of internal rotation has been studied extensively through molecular spectra[6] and electron diffraction.[7] According to a spectroscopic study[8] of monochloroacetone, it was concluded, taking Zahn's data into account, that there are two forms of rotational isomers corresponding to the internal rotational angle of 150° and 0°, respectively, taking the *trans*-posistion of the chlorine atom with respect to the methyl group as 0° (Fig. 7a, 7b). It was further




a (more stable) b (less stable)

Fig. 7. Rotational isomers of monochloro acetone.

concluded that in the gaseous state the former is more stable than the latter, the energy difference being estimated as 1 to 2 kcal./mole.[9] The recent molecular spectroscopic study of dichloroacetone[10] revealed that there exist also two rotational isomers in this case. In analogy to the case of monochloroacetone, it may safely be assumed that these isomers take the forms shown in Fig. 2a (the angle $\theta$ is taken as 0° at this position) and b ($\theta=120°$). These two forms are considered as well-defined isomers, since they may be separated by a potential barrier of a considerable height due to the steric repulsion between the chlorine atoms and the methyl group.




a (more stable) b (less stable)

Fig. 8. Rotational isomers of 1.1-dichloroacetone.

The dipole moment of this molecule is estimated as follows. The bond moments and the bond angles are taken to be $\mu_{C-Cl}=1.86$ D, $\mu_{C=O}=2.50$ D, $\angle CCCl=\angle ClCCl=$ tetrahedral, and $\angle CCO=123°$. For the correction of the induction effect, the rule suggested by Miyagawa and Morino[11] is used, whereby the amount of induction moment by C=O dipole is taken as being equal to the amount of induction by C-Cl bond dipole multiplied by a factor $\mu_{C=O}/\mu_{C-Cl}=2.50/1.86$. The moments calculated are shown in Table III. As described above, the more stable form

TABLE III

THE CALCULATED MOMENT OF 1, 1-DICHLOROACETONE AT VARIOUS POSITIONS OF INTERNAL ROTATION

| $\theta$ | 0° | 30° | 60° | 90° | 120° | 150° | 180° |
|---|---|---|---|---|---|---|---|
| $\mu$ | 1.30 | 1.53 | 2.01 | 2.54 | 2.96 | 3.24 | 3.34 |

is the one with the smallest moment. Therefore, it should be form (a), corresponding to $\theta=0°$. By assuming the moment of this form to be 1.30 D it is found from the observed temperature dependence of the moment that the difference in energy between the two isomers, $\Delta E$, is about 800 cal./mole., together with the moment of the less stable form of 2.7 D, a value close to the calculated moment for the 120°-form. It should be pointed out that this value of $\Delta E$ is smaller than that of mo-

5) C. T. Zahn, *Phys. Rev.*, **33**, 686 (1932).
6) (a) S. Mizushima, et. al., *J. Chem. Phys.*, **20**, 1720 (1952); (b) S. Mizushima, et al., *J. Chem. Phys.*, **21**, 815 (1953).
7) Y. Morino, et al., *J. Chem. Soc. Japan (Pure Chem. Sect.)*, **75**, 647, 721 (1954).
8) Ref. 6(b).
9) T. Miyazawa, private communication.
10) T. Miyazawa, private communication.
11) Y. Morino, I. Miyagawa, and T. Oiwa, *Bochu-Kagaku*, **15**, 181 (1950).

nochloroacetone (1-2 kcal./mole). It may easily be understood from the comparison of Figs. 1 and 2 that the difference in the steric energy between the two forms of dichloroacetone is not so far from that between the corresponding two forms of monochloroacetone. The difference in the dipole interaction energy would also be nearly the same in both cases, if the moment of C-Cl and C=O bonds in the former is equal to those in the latter. Actually, however, the two chlorine atoms in dichloroacetone are attached to the same carbon atom so that the C-Cl bond moments must be reduced considerably by the mutual induction, and consequently the energy difference between the two isomers would also be diminished.

Now the dipole interaction energy in these molecules will be computed in the following way by simple assumptions. The bond dipoles are assumed to converge to dipoles at the contact points of the atomic radii in each bond, their magnitudes being taken to be equal to the corrected bond moments. The assumed dimensions of the molecules are such that $R_{cc}=1.54$ Å, the radius of $-C=0.77$ Å, and of $=C=0.67$ Å, and the bond angles are the same as described above. The calculation shows that the energy difernce of the two isomers is 1.3 kcal./mole in dichloroacetone and 2.2 kcal./mole in monochloroacetone. Because of the approximation of the assumptions used here, it might be too much to expect a quantitative agreement between the calculated and the observed values of $\Delta E$, but it is very interesting to note that the calculated values are parallel to the observed $\Delta E$'s. It may, therefore, be concluded from this that the greater part of the energy difference in these molecules is due to the electrostatic energy of dipole interaction, and the lowering of $\Delta E$ in dichloroacetone is the result of the reduced moment of the C-Cl bonds by mutual induction. This result is in accord with the conclusion obtained by Mizushima, Morino, and Shimanouchi[13] and that by Miyagawa[14] in the case of haloethanes.

The author expresses his sincere thanks to Professor Y. Morino for his kind guidance in this study and to Dr. I. Miyagawa for his valuable advice.

## Summary

An apparatus for the measurement of dielectric constant in the gaseous state is constructed. The electrical circuit is a heterodyne double-beat type, the oscillators with a remarkably high frequency stability are constrcuted. By testing several types of gas cell, it was found that one of them (cell D) can be used satisfactorily for the present purpose. For the gas filling system, a modification of Groves' method is employed. Using this apparatus dielectric constant measurement with an error of less than 0.5 per cent can be obtained.

The dipole moment of 1,1-dichloroacetone was measured in this apparatus. The moment was found to increase with temperature. This increase is attributed to the increase of the more polar isomer (b), which coexists with the form (a). The energy difference of the two isomers was found to be about 800 cal./mole. This value is smaller than that of monochloroacetone, and the lowering of $\Delta E$ was considered to be due mainly to the reduced moment of the C-Cl bonds by mutual induction. It was thereby concluded that the energy difference in these molecules is electrostatic in nature rather than steric.

*Department of Chemistry, Faculty of Science, Tokyo University, Tokyo*

12) As for the method of determining $\Delta E$ from the temperature dependence of the moment, see I. Miyagawa, *J. Chem. Soc. Japan (Pure Chem. Sect.)*, 75, 970 (1954).

13) S. Mizushima, Y. Morino and T. Shimanouchi, *J. Phys. Chem.*, 56, 324 (1952).

14) I. Miyagawa, *J. Chem. Soc. Japan (Pure Chem. Sect.)*, 75, 1169, 1173, 1177 (1954).

# *Studies on A.C. Polarography. I. Theoretical Treatment*

By Isamu TACHI and Tomihito KAMBARA

(Received June 12, 1954)

## Introduction

Application of the square wave voltage in the polarographic electrolysis originates from Kemula[1], who employed the rotating switch for the abrupt change of electrode potential. Recently, the polarographic electrolysis, in which the conventional sine wave a.c. voltage is superimposed upon the ordinary d.c. voltage has been elaborated by Breyer and his co-workers[2], and also by Randles[3] and Fournier[4], and their works teem with many interesting findings. Therefore the present authors will discuss this problem mathematically from the general viewpoint.

## General Aspects of the Problem

The diffusion processes of the oxidised form (suffix O) and the reduced from (suffix R) are given by Fick's second law of diffusion; i.e.

$$\frac{\partial C_o}{\partial t}=D_o\frac{\partial^2 C_o}{\partial x^2}\ ;\ \frac{\partial C_R}{\partial t}=D_R\frac{\partial^2 C_R}{\partial x^2}. \qquad (1)$$

Here $C$ represents the concentration, $D$ the diffusion coefficient, $x$ the distance from the electrode surface, and $t$ the time. Let ${}^*C_o$ and ${}^*C_R$, respectively, be the uniform initial concentrations of the oxidised and reduced forms, then the initial condition is given by

$$t=0,\ 0\leq x\leq\infty,\ C_o={}^*C_o,\ C_R={}^*C_R. \qquad (2)$$

Upon employing the Laplace-transformation defined by

$$\mathfrak{L}C=p\int_0^\infty e^{-pt}\cdot C(x,t)\cdot dt=u(x,p)$$

we obtain from Eqs. (1) and (2)

$$p(u-{}^*C)=D\cdot\partial^2 u/\partial x^2,$$

which yields the following general integral.

$$u={}^*C+B\cdot\exp\left[-\sqrt{\frac{p}{D}}\,x\right]$$

It follows further that

$$D(\partial u/\partial x)_{x=0}=-\sqrt{pD}\,B.$$

The integral constants $B_o$ and $B_R$ are functions of $p$, and are determined by the boundary condition. Next, it is quite clear that

$$t>0,\ x=0,\ \phi(t)=\frac{I}{nFq}=D_o\frac{\partial C_o}{\partial x}=-D_R\frac{\partial C_R}{\partial x} \qquad (3)$$

where $I$, $q$, $F$ and $n$ represent current intensity, area of the electrode surface, Faraday's constant and the number of electrons associated with the reaction of one molecule of oxidant. Writing

$$\mathfrak{L}\phi(t)=\Phi(t)\ ;\ \mathfrak{L}Z_o(t)=B_o(p)\ ;\ \mathfrak{L}Z_R(t)=B_R(p),$$

it is seen that

$$-\sqrt{D_o}B_o=\sqrt{D_R}B_R=\frac{\sqrt{p}\,\Phi(p)}{p},$$

which is inversely transformed into

$$-\sqrt{D_o}Z_o=\sqrt{D_R}Z_R=\int_0^t\frac{\phi(\xi)}{\sqrt{\pi(t-\xi)}}d\xi.$$

Thus it follows that the interfacial concentrations of both forms are shown by

$$\left.\begin{aligned}{}^\circ C_o&={}^*C_o-\frac{1}{\sqrt{\pi D_o}}\int_0^t\frac{\phi(\xi)}{\sqrt{t-\xi}}\cdot d\xi\ ;\\ {}^\circ C_R&={}^*C_R+\frac{1}{\sqrt{\pi D_R}}\int_0^t\frac{\phi(\xi)}{\sqrt{t-\xi}}\cdot d\xi.\end{aligned}\right\} \qquad (4)$$

On the other hand, the current intensity is also governed by the rate constants of the electrode processes; thus

$$\phi(t)=\frac{I}{nFq}=\vec{k}f_o{}^\circ C_o-\overleftarrow{k}f_R{}^\circ C_R, \qquad (5)$$

where $\vec{k}$ and $\overleftarrow{k}$ are the rate constants of the cathodic reduction and anodic oxidation, respectively, and $f_o$ and $f_R$ are the respective activity coefficients at the electrode surface.

According to the theory of absolute reaction rate, $\vec{k}$ and $\overleftarrow{k}$ are given by

$$\left.\begin{aligned}\vec{k}&=\vec{k}_S\exp\frac{-\alpha nFV}{RT}\ ;\\ \overleftarrow{k}&=\overleftarrow{k}_S\exp\frac{(1-\alpha)nFV}{RT}.\end{aligned}\right\} \qquad (6)$$

where $V$ denotes the potential of the observation electrode, $\vec{k}_S$ and $\overleftarrow{k}_S$ are the respective rate constants at $V=0$, and other symbols $\alpha$, $R$ and $T$ are employed in their usual significances. In a.c. polarography, to the dropping mercury electrode is applied the usual constant voltage $E$ and further a sine-

1) W. Kemula, *Collection Czech. Chem. Communs.*, **2**, 502 (1930).

2) B. Breyer and F. Gutman, *Discuss. Faraday Soc.*, **1**, 19 (1947); B. Breyer, F. Gutman and S. Hacobian, *Austral. J. Sci. Research*, **A3**, 558, 567 (1950), **A4**, 595 (1951); B. Breyer and S. Hacobian, ibid., **A4**, 604, 610 (1951).

3) J. E. B. Randles, *Discuss. Faraday Soc.*, **1**, 11 (1947).

4) M. Fournier, *Compt. rend.*, **232**, 1673 (1951).

wave a.c. voltage is superimposed thereupon. Thus it is seen that

$$V=E-A\sin\omega t. \tag{7}$$

Namely, both rate constants are also functions of time. The combination of Eqs. (3)... (7) gives the following relationship:

$$\phi(t)=g_1(t)+g_2(t)\int_0^t \frac{\phi(\xi)}{\sqrt{\pi(t-\xi)}}d\xi. \tag{8}$$

In this equation the functions $g_1(t)$ and $g_2(t)$ are shown by

$$\left.\begin{aligned} g_1(t)&=k_f{}^*C_O f_1(t)-k_b{}^*C_R f_2(t);\\ g_2(t)&=-\frac{k_f}{\sqrt{D_O}}\cdot f_1(t)-\frac{k_b}{\sqrt{D_R}}f_2(t);\\ k_f&=\vec{k}_S f_O\cdot\exp\frac{-\alpha nFE}{RT};\\ k_b&=\vec{k}_S f_R\cdot\exp\frac{(1-\alpha)nFE}{RT};\\ f_1(t)&=\exp\frac{\alpha nFA\cdot\sin\omega t}{RT};\\ f_2(t)&=\exp\frac{-(1-\alpha)nFA\cdot\sin\omega t}{RT}; \end{aligned}\right\} \tag{9}$$

Thus it is seen that in the case that the electrode potential is a function of time, the resulting diffusion current $I$ is, as shown by Eq. (8), in general demonstrated by Volterra's integral equation of the second kind; this has been already shown in the mathematical treatment of oscillographic polarography of Sevcik-Randles type by Matsuda[5], who has taken the rates of forward and backward reactions into account. The equation of the same form has been discussed also by Delahay[6] dealing with the perfectly irreversible process. Although the solution of Eq. (8) has been mathematically known, the result thereof is too complicated for any practical application.

We will next consider the problem with assumption that both the rate constants $\vec{k}_S$ and $\overleftarrow{k}_S$ are extraordinarily great. Under such a condition, we can legitimately apply the Nernst formula, since the interfacial concentrations of both forms may be then regarded to be always at equilibrium. Therefore we have the following boundary condition.

$t>0,\ x=0,\ K={}^\circ C_R/{}^\circ C_O=({}^*C_R+Z_R)/({}^*C_O-Z_O)$

$$=\exp\frac{-nF(V-E_o)}{RT}$$

$$=\exp\frac{-nF(E-E_o-A\cdot\sin\omega t)}{RT}. \tag{10}$$

In this equation $E_O$ denotes the normal potential of the concerned redox system. Then, upon utilizing the relationship:

$$-\sqrt{D_O}Z_O=\sqrt{D_R}Z_R$$

we can easily obtain the following expression.

$$Z_O=\frac{{}^*C_R-K{}^*C_O}{K+\sqrt{\frac{D_O}{D_R}}}=\mathfrak{L}^{-1}B_O(p).$$

Then it is seen that

$$\phi(t)=\mathfrak{L}^{-1}[-\sqrt{pD_O}\cdot B_O(p)]=$$

$$=-\sqrt{D_O}\frac{d}{dt}\int_0^t\frac{Z_O(\xi)}{\sqrt{\pi(t-\xi)}}\cdot d\xi.$$

Namely, we have

$$\left.\begin{aligned} \phi(t)=&-\frac{d}{dt}\int_0^t\sqrt{\frac{D_O}{\pi\xi}}X\\ &\times\left\{{}^*C_R-{}^*C_O\beta\exp\frac{nFA\cdot\sin\omega(t-\xi)}{RT}\right\}\times\\ &\times\left\{\sqrt{\frac{D_O}{D_R}}+\beta\exp\frac{nFA\cdot\sin\omega(t-\xi)}{RT}\right\}^{-1}\cdot d\xi;\\ \beta=&\exp\frac{-nF(E-E_O)}{RT}, \end{aligned}\right\} \tag{11}$$

which is the fundamental equation for the instantaneous current intensity due to the a.c. voltage polarization of a reversible electrode.

The above stated theoretical treatment is based on the sound basis, and although the conclusion is mathematically complicated, it may be noteworthy to compare the present theory with the earlier works performed by Randles[3], Breyer with colleagues[2] and others.

Let us at first call to mind the Helmholz theory of electric double layer. For a long time, the electrode surface has been regarded as behaving like an electrostatic condenser. As is well known, the electrolysis with an a.c. voltage is intimately connected with the experimental measurement of the conductivity of electrolytic solution; and in the course of development of the investigations, the terms "polarization resistance" and "polarization capacitance" have been introduced, which indicate the essential rôle of the electrode-solution interface in the electrolysis with a.c. voltage. On the other hand, the electrochemists, who have been studying the "ideal polarized electrode", i.e. the electrode, across the surface of which no charged particle moves, have recently begun to treat the present problem; and especially the works performed by Grahame[7] are decidedly of importance. His opinion may be summarised qualitatively from the a.c. polarographic viewpoint as follows. At a reversible electrode, at which

5) H. Matsuda, Reported at the Discussion Meeting at Nagoya held in November 1952 by the Electrochemical Society of Japan.

6) P. Delahay, *J. Am. Chem. Soc.*, **75**, 1190 (1953).

7) D. C. Grahame, *Chem. Revs.*, **41**, 441 (1947).

the two rate constants of the electrode processes in forward and reverse directions, i.e. the rate constants of reduction and oxidation, are sufficiently great, by the superposition of an a.c. voltage, the electrode potential is made more negative in a half-period resulting in the predominance of the reduction process of oxidised form at the interface, and thus the reduction product is accumulated considerably at the surface, although some portion of the product may diffuse away. And in the next half-period, the electrode potential becomes so positive that the reductant accumulated at the surface is readily to be oxidised. Hence, corresponding to the periodic change of the electrode potential, the cathodic reduction and anodic oxidation happen alternatively at the electrode surface. Therefore in such a case, a prominant alternating current flows through the surface, so that the electrode surface behaves like a condenser of great capacity. Grahame called such an apparent capacity of electrolytic nature at first "pseudo-capacity"[7] and later introduced a more adequate term "faradayic admittance"[8] in which not only the pseudo-capacity but also the polarization resistance of the electrode surface are taken into consideration.

The above quoted conceptions are to be rationally elucidated by the aid of the integral equation (8) and the Duhamel's integral shown by Eq. (11). Unfortunately these expressions are too complicated to be employed without further modifications; however, the oscillatory character of the electrolytic current is easily to be predicted, since we can legitimately judge that the function $\phi(t)$ may be composed of the periodic functions from the forms of the above equations. This has been really performed in our laboratory by Senda and Tachi[9]; they have transformed the Eq. (8) and (11) into more convenient forms, and thus it is found that the resulting a.c. current is composed of non-alternating d.c. component and a.c. component consisting of many higher harmonic waves.

It must next be mentioned here that Randles' theory[3] concerning such a phenomenon gives a prominent result; i.e. upon assuming the periodic changes of interfacial concentrations, he has derived the equations, by which the rate constant of the electrode reaction can be calculated from the experimental data of a.c. voltage electrolysis. It must however, be pointed out that a weak a.c. voltage of the amplitude of a few millivolts should be employed, owing to the approximate mathematical treatment. Breyer and others[2] have also elaborated the same problem, but is seems that they have not considered the structural change of the diffusion layer with time and regarded the instantaneous current intensity as governed by the value corresponding to the mean diffusion current in the classical polarogram. It may be safe to say that the ordinary polarogram does not show behaviour similar to the characteristic curve of the triode vacuum tube. Nevertheless, their works provide us much experimental information most lavishly and the term "a.c. polarography" has actually originated from them. On the other hand, the articles of Fournier[4] and Kalousek[10] are of special interest, and a more advanced systematic theory for the a.c. polarography will be fully discussed in the succeeding chapter.

## Simplified Theory for the A.C. and D.C. Components of Electrolytic Current

(1) **Reversible Electrode.**—The electrode potential in the a.c. polarographic electrolysis is composed of the d.c. voltage $E$ and the sine-wave a.c. voltage $A \sin wt$, as illustrated in Fig. 1(a). Now, let us suppose that the sine-wave a.c. voltage is equivalent to a square-wave voltage, then the electrode potential $V$ shows a change with time as shown in Fig. 1(b); namely,

$$\left.\begin{aligned} E=&\begin{cases} E_1 & \text{for } 0<t<T \\ E_2 & \text{for } T<t<2T; \end{cases} \\ &V(t)=V(t+2T); \\ &2T=1/f=2\pi/\omega. \end{aligned}\right\} \qquad (12)$$

In this case, the suitable amplitude of the hypothetical squarewave voltage may be equal to the effective value of amplitude of the original sinusoidal voltage; i.e.

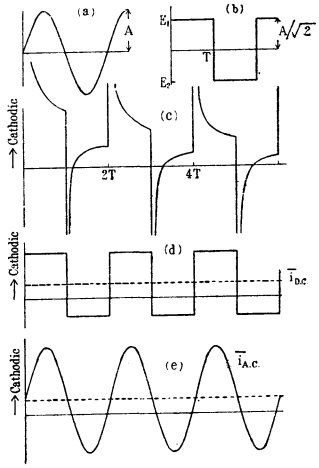



Fig. 1.

8) D. C. Grahame, *J. Electrochem. Soc.*, **99**, 370C (1952).

9) M. Senda and I. Tachi, Reported at the 7th Annual Meeting of the Chemical Society of Japan, held on the 3rd April 1954 in Tokyo.

10) M. Kalousek, *Collection Czech. Chem. Communs.*, **13**, 105 (1948).

$$\frac{1}{2}(E_2-E_1)=\frac{A}{\sqrt{2}} \tag{13}$$

The course of the current-time curve due to the application of a rectangular voltage has been elaborated theoretically by Kambara[11], and an example thereof is given in Fig. 1(c). Further it has been manifested that upon evaluating the respective mean current flowing in each half-period shown by $V=E_1$ and $V=E_2$, we may approximately regard the whole electrolytic current to be the algebraic sum of the constant current $\bar{i}_{D.C.}$, and the square-wave-current $\bar{i}_{A.C.}$, as illustrated in Fig. 1(d); and the current is possessed of the same period $2T$ as the applied square-wave voltage. Let $\bar{i}_1$ be the mean current, that is to be observed when the constant potential $E_1$ is applied, and let $\bar{i}_2$ be that observed with the constant voltage $E_2$. Then it can be demonstrated from Kambara's theoretical treatment that

$$\bar{i}_{D.C.}=(\bar{i}_1+\bar{i}_2); \tag{14}$$

$$\bar{i}_{A.C.}=2\left(s\sqrt{f}-\frac{1}{4}\right)(\bar{i}_1-\bar{i}_2)\cdot M(t,\ T) \tag{15}$$

where $S=1.195$ and the meander function $M(t,\ T)$ is defined by

$$M(t,\ T)=\left\{\begin{matrix}+1 \text{ for } 0<t<T \\ -1 \text{ for } T<t<2T\end{matrix}\right\}; \tag{16}$$

$$M(t,\ T)=M(t+2T,\ T)$$

Next, we will regard the square wave current, that is shown by Eq. (15) and in Fig. 1(d), as equivalent to a sine-wave alternating current; in order to keep the integrated amount of electricity flowing in each half-period constant, upon employing the familiar factor $\pi/2$, we may be able to describe

$$\bar{i}_{A.C.}=\pi\left(s\sqrt{f}-\frac{1}{4}\right)\cdot(\bar{i}_1-\bar{i}_2)\cdot\sin\omega t. \tag{17}$$

From the above cited somewhat conventional consideration, it may be concluded that when the polarographic electrolysis is carried out under the superposition of sine-wave voltage, the resulting electrolytic current, which is to be represented by a complicated function of time, may be regarded as the sum of two components, i.e. the d.c. component given by Eq. (14) and the a.c. component given by Eq. (17). It follows immediately therefrom that Fournier's polarogram[4] is the register of the d.c. component, and Breyer's current-voltage curve[2] is the recording of the a.c. component. The essential validity of the above conclusion concerning the Fournier's polarogram, has been already reported[11] (see Fig. 2); and further it is expected from the above theory that when we register $\bar{i}_{A.C.}$ against the usual d.c.

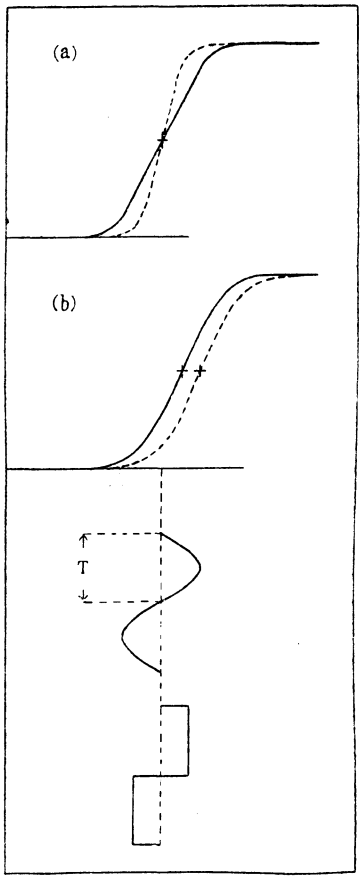



Fig. 2. Fournier's polarogram (a, reversible; b, irreversible).

voltage $E$, the derivative curve of the reversible polarogram is to be obtained according to Eq. (17), provided that the amplitude of the superimposed a.c. voltage remains constant. This conclusion is quite in harmony with the observations of Breyer's school as well as with the experimental results obtained with the I-F apparatus[12]. It must be, however, pointed out that Breyer and others, although their experimental work is prominent, have shown an irrational consideration in regard to the a.c. component of the irreversible wave; the fast that the irreversible system shows no peak in a.c. polarogram is not due to the less steep inclination at the half-wave point, but it should be essentially ascribed to the irreversible character of the system concerned.

(2) **Fournier's Polarogram in the Case of Irreversible Wave.**—It has been pointed out that what governs the whole course of polarogram of irreversible redox system is not the interfacial equilibrium concentration of the

11) T. Kambara, This Bulletin, **27**, 527, 529 (1954).
12) M. Ishibashi and T. Fujinaga, This Bulletin, **23**, 261 (1950), **25**, 68, 238 (1952).

depolarizer, but the rate constant at that electrode potential[13]. Now, let us again suppose that the superimposed sine-wave voltage $A \sin wt$ is equivalent to the square-wave voltage of the same frequency, the amplitude of which is shown by $\Delta E = A/\sqrt{2}$ (Fig. 3). Then the rate constant of the cathodic reduction is given by

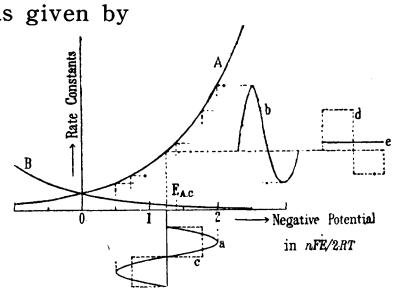



Fig. 3.

$$\vec{k}_{A.C.} = \begin{cases} \vec{k}_E \exp\dfrac{\alpha nF\Delta E}{RT} \\ \quad \text{for } 2nT<t<(2n+1)T\,; \\ \vec{k}_E \exp\dfrac{-\alpha nF\Delta E}{RT} \\ \quad \text{for } (2n+1)T<t<(2n+2)T\,; \end{cases} \tag{18}$$

where $n$ denotes the integer, and $\vec{k}_E$ is shown by

$$\vec{k}_E = \vec{k}_S \exp\frac{-\alpha nFE}{RT} \tag{19}$$

where $\vec{k}_S$ shows the rate constant for $E=0$ [cf. Eq. (6)]. Next writing

$$\Delta\xi = \frac{\alpha nF}{RT}\cdot\Delta E, \tag{20}$$

we can find that

$$\text{Mean value of } \vec{k}_{A.C.} = \vec{k}_E \cdot \frac{1}{2}\left(e^{+\Delta\xi} + e^{-\Delta\xi}\right)$$

$$= \vec{k}_E \cosh\Delta\xi =$$

$$= \vec{k}_S \exp\left\{\frac{-\alpha nF}{RT}\left(E - \frac{RT}{\alpha nF}\ln\cosh\Delta\xi\right)\right\} \tag{21}$$

It has been derived[14] that when a constant potential $E$ is applied to a stationary plane electrode, at which the cathodic reduction proceeds irreversibly, then the resulting rate constant $\vec{k}_E$ determines the instantaneous current intensity $i$; viz.

$$i = nFq\vec{k}_E{}^* C_O \exp\left(\frac{\vec{k}_E{}^2 t}{D_O}\right)\operatorname{erfc}\left(\frac{\vec{k}_E\sqrt{t}}{\sqrt{D_O}}\right) \tag{22}$$

13) H. Eyring, L. Marker and T. C. Kwoh, *J. Phys. Coll. Chem.*, 53, 1453 (1949); N. Tanaka and R. Tamamushi, This Bulletin, 22, 187 (1949); R. Tamamushi and N. Tanaka, ibid., 227, 23, 110 (1950); R. Goto and I. Tachi, *Proc. I. Inter. Polarogr. Congr. in Prague*, Part 1, 69 (1951); N. Tanaka and R. Tamamushi, ibid., 486; M. Kalousek and A. Tockstein, ibid., 563.

14) T. Kambara and I. Tachi, This Bulletin, 25, 135 (1952).

Further it is known that the polarogram, in which the mean current $I$ is plotted against $E$, is shown by

$$I = \frac{I_d}{2}\left\{1 + \tanh\frac{-\alpha nF(E-E_{1/2})}{2RT}\right\},$$

which is transformed into

$$E = E_{1/2} + \frac{RT}{\alpha nF}\ln\frac{I_d - I}{I} \tag{23}$$

where $I_d$ denotes, as usual, the mean value of the limiting cathodic diffusion current, and $E_{1/2}$ the half-wave potential of the irreversible wave[13]. It follows from Eq. (21) that the superposition of the a.c. voltage on the constant voltage $E$ is effectively equivalent to the application of the constant voltage $E_{A.C.}$, which is more negative than $E$ as shown in Fig. 3 and is given by

$$E_{A.C.} = E - \frac{RT}{\alpha nF}\ln\cosh\Delta\xi. \tag{24}$$

Therefore, the Fournier's polarogram is the case of irreversible wave is represented by

$$E = E_{1/2} + \frac{RT}{\alpha nF}\ln\cosh\frac{\alpha nF\Delta E}{RT}$$

$$+ \frac{RT}{\alpha nF}\ln\frac{I_d - I}{I}. \tag{25}$$

Namely, by the superposition, the resulting polarogram should be shifted positively (see Fig. 2 and 3); and the half-wave potential of Fournier's polarogram $E_{1/2\text{-Fournier}}$ is more positive than that of the classical polarogram. And the difference between the two half-wave potential is shown by

$$(\Delta E_{1/2})_{A.C.} = E_{1/2\text{-Fournier}} - E_{1/2} =$$

$$\frac{RT}{\alpha nF}\ln\cosh\frac{\alpha nF\Delta E}{RT}. \tag{26}$$

In a case when the amplitude of the superimposed a.c. voltage is of the order of hundred millivolts or more, i.e., $\alpha nF\Delta E/RT \gg 1$, it can be derived approximately that

$$(\Delta E_{1/2})_{A.C.} \simeq \Delta E + \frac{RT}{\alpha nF}\ln\frac{1}{2}. \tag{27}$$

Thus at the room temperature, the shift of half-wave potential is given by

$$(\Delta E_{1/2})_{A.C.} \simeq \Delta E - \frac{0.301}{\alpha n}\times 58\,mV.$$

Hence it is found that there is a linear relationship between the shift of half-wave potential and the amplitude of the superimposed a.c. voltage. On the other hand, for the smaller value of $\Delta E$, it can be readily seen that

$$\ln\cosh\Delta\xi \simeq \ln\left(1 + \frac{1}{2}\Delta\xi^2\right) \simeq \frac{1}{2}\Delta\xi^2;$$

therefore it is found that

$$(\Delta E_{1/2})_{A.C.} \simeq \frac{\alpha nF}{RT} \cdot \Delta E^2.$$

There is no doubt that $(\Delta E_{1/2})_{A.C.}$ becomes zero for $\Delta E=0$, which is a quite rational conclusion. The above developed theoretical consideration has been amply confirmed experimentally and will be reported in our succeeding paper.

## Fundamental Theory of A.C. Polarography

It may be concluded from the above stated theory that the essential principle of a.c. polarography is as follows. I.e., when we superimpose an a.c. voltage, the wave form of which may be sinusoidal or rectangular, on the usual polarographic d.c. voltage, then the resulting electrolytic current is an extraordinarily complicated function of time; it is, however, possible to separate the current into the a.c. component and the d.c. component and to observe and record both the components individually. The former is to be called Breyer's polarogram and the latter Fournier's current-voltage curve, and the essential features of Breyer's and Fournier's polarograms are easily comprehensible from the present theory. Thus, from the practical standpoint of polarographic application, the methodology of a.c. polarography is expected to be very important. In the case of the irreversible redox system the a.c. component will show no appreciable peak, which would be advantageous for the elimination of disturbing irreversible waves; and as for the d.c. component, the superposition of the a.c. voltage will surely shift the anodic wave negatively as well as shifting the cathodic one positively, so that at last the separated two waves of the irreversible redox system would unite together, as illustrated in Fig. 4 Although such an example has not yet been reported, it may be safe to say that the superposition of a.c. voltage shows the behaviour of catalyst, since in a half-period it accelerates the cathodic reduction and in

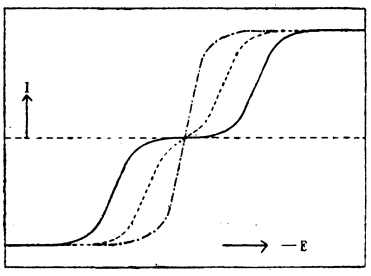



Fig. 4.

another half-period it promotes the anodic oxidation. Next, in the case of the reversible wave, the a.c. component shows a peak, which is to be regarded as the derivative polarogram; and in the case of decreased reversibility, the peak height depends on the degree of reversibility concerned as well as the concentration of the depolarizer; it is well known that the peak height is remarkably dependent of the nature of supporting electrolyte, as reported by Breyer and others.[2] If we record the d.c. component together with the a.c. component and the classical polarogram, then the half-wave potential is to be indicated by the summit potential of the peak and also by the intersection of Fournier's polarogram with the classical one.

So far the a.c. polarography with the a.c. voltage of the constant amplitude has been discussed. It is further possible to make the amplitude vary with time as the d.c. voltage in the ordinary polarography. Then it may be possible with the sine-wave voltage to attain the polarogram of increased sensitivity, which has been shown by I-F apparatus[12] with the aid of rotating switch and current alternator. Further some attractive and characteristic findings obtained with Kalousek's apparatus,[8] which have been cleared up theoretically by Kambara[11], may also be developed by the a.c. polarography, in which the amplitude of a.c. voltage is made to change linearly with time as well as the d.c. voltage.

## Addendum[15]

Recently Breyer and Hacobian[16] have published a new theoretical treatment of the present problem, in which the essential role of diffusion in a.c. polarography is legitimately taken into account. The theory deals with the complete reversible electrode reaction. The present authors wish to publish our opinion on the paper later.

## Summary

At first the rigorous and orthodox treatment of the polarographic electrolytic current due to the superposition of an alternating voltage upon a constant voltage is shown and the earlier polarographic studies, in which an alternating voltage is employed, are discussed. Next it is shown that in order to treat the a.c. polarography theoretically, we can profitably assume that the superimposed sinusoidal a.c. voltage is equivalent

15) At the request of the editor the present paper was rewritten in a new form. Consequently the new paper by Breyer and Hacobian can be cited here.

16) B. Breyer and S. Hacobian, *Austral. J. Chem.*, 7, 225 (1954).

to the square-wave voltage of the same frequency. In a case when an a.c. voltage, is superimposed upon the usual d.c. voltage, the resulting current becomes a very complicated function of time. It can be shown, however, that the current is the algebraic sum of a.c. component and d.c. component, the latter of which is Fournier's polarogram and the former Breyer's polarogram. Some outstanding characteristics of both components are satisfactorily cleared up, and it demonstrated that in such a manner a rational and systematic explanation of a.c. polarography is given.

The authors wish to express their hearty thanks to Prof. B. Breyer, who has communicated to them the progress of studies carried out in the University of Sydney.

*Department of Agricultural Chemistry, Faculty of Agriculture, Kyoto University, Kyoto*

# *Studies on A.C. Polarogroaphy. II. Fundamental Circuit and Some Experimental Results**)

By Mitsugi SENDA, Mitsuko OKUDA and Isamu TACHI

(Received June 12, 1954)

## Introduction

A design of a.c. polarographic circuit, where a small alternating potential is superimposed on the usual direct potential applied to the dropping mercury electrode, has been proposed by Breyer and his coworkers[1]. In the circuit designed by them, the a.c. component of the electrolytic current flowing is measured by means of a vacum-tube voltmeter after amplifying the potential drop across a resistor inserted in the electrolytic circuit and the readings of the voltmeter are plotted against the direct potential, giving a.c. polarogram with peak currents at the potentials characteristic to the discharging depolarizers. Recently Ishidate and his coworkers[2] have also showed a new design of a.c. polarograph, in which the amplifier circuit was mainly improved.

In another type of a.c. polarograph, which was first proposed by Kalousek[3], a rectangular alternating potential is superimposed on the usual direct potential with the aid of a rotating switch and the electrolytic current is measured by means of a usual galvanometer by connecting the galvanometer circuit with the switch in a proper way. A similar circuit was also devised by Ishibashi and Fujinaga[4] independently.

In the present paper a design of a.c. polarograph will be given, in which an alternating potential with not only constant but also varying amplitude is superimposed on the direct potential applied to the dropping mercury electrode and the a.c. component of the electrolytic current flowing is recorded against the direct potential automatically on photographic paper. The mean value of the total electrolytic current, which was first observed by Fournier[5] and should be called Fournier's current, is easily obtained by inserting a galvanometer directly in the electrolytic circuit. A brief discussion on the experimental results is also given. All the experiments were carried out at room temperature.

## Fundamental Circuit

A schematic diagram of a.c. polarograph designed is shown in Fig. 1. The circuit is composed of three main parts, i.e. an applied voltage source, A, a cell circuit, B, and a device for measuring the resulting current, C. In this figure, $A_1B_1$ is a potentiometric bridge wound upon an insulating drum, upon which a contact, $P_1$, slides from $B_1$ to $A_1$ with rotation of the drum as in the ordinary polarograph. $A_2B_2$ is a rheostat and $L_1$ is a transformer, through which a sinusoidal

* Read at the monthly meeting of the Agric. Chemical Society of Japan held at Kyoto University on 18. July 1953.

1) B. Breyer and F. Gutmann, *Discussion Faraday Soc.* No. 1, 19 (1947). B. Breyer, F. Gutmann and S. Hacobian, *Australian J. Sci. Research* **A3** 558, 567, 595 (1951). B. Breyer and S. Hacobian, Ibid. 604, 610 (1951). We are indebted to Prof. Dr. B. Breyer for sending us reprints of the papers on a.c. polarography.

2) M. Ishidate, T. Isshiki and Y. Masuko, *Japanese Patent*, Application No. 5561/1953.

3) M. Kalousek, *Collection Czech. Chem. Communs.*, **13**, 105 (1948).

4) M. Ishibashi and T. Fujinaga. This Bulletin, **25**, 68, (1952).

5) M. Fournier, *Compt. rend.*, **232**, 1673 (1951).

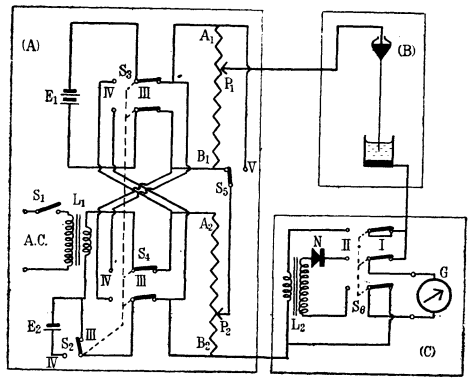



Fig. 1. A.C. Polarographic circuit.

alternating voltage of a definite amplitude is supplied from a 100 v., 60 cycle, A.C. line. Current supplied from a storage battery, $E_2$, is adjusted so that the direct potential drop across $A_1B_1$ is equal to the amplitude of the alternating potential drop across it. $L_2$ is a step-up transformer, N is a crystal rectifier, and G is a moving mirror galvanometer with a conventional shunt. The cell circuit is composed of a dropping mercury electrode inserted into an electrolytic solution and a mercury pool serving as a nonpolarizable reference electrode. Photographic recording of the polarogram is carried out by means of proper mechanical connection between photographic paper and rotation of the drum, as in the Heyrovský-Shikata polarograph.

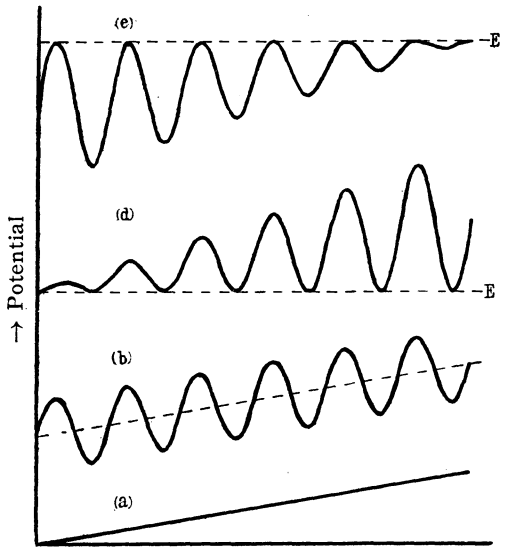



Fig. 2. The change of applied potential with time.
Curve (a): ordinary polarograph.
Curve (b): Fournier's and Breyer's polarograph.
Curve (d): Polarograph with increasing amplitude.
Curve (e): polarograph with decreasing amplitude.
E is the constant applied potential.

The circuit connection illustrated in Fig. 1 represents (a) a circuit operating as an ordinary polarograph. (b) When the switch $S_1$ is closed, the alternating potential drop of amplitude, $\Delta V$, is produced across the rheostat, i.e.

$$\Delta E = \frac{P_2B_2}{A_2B_2}\Delta V$$

is superimposed upon the d.c. voltage, which, increasing gradually with time or rotation of the potentiometric drum, is applied to the electrolytic cell (Fig. 2-(b)) and the Fournier's polarogram is obtained. Furthermore, (c) connecting the switch $S_6$ to (II), the Breyer's polarogram, that is a.c. polarogram with constant amplitude, is registered. (d) Connecting the switches $S_2$, $S_3$ and $S_4$ to (IV) and the other switches as in (c), the amplitude of the applied alternating voltage increases gradually with time as is shown in Fig. 2-(d). The constant applied potential, E, is chosen to take the potential value, at which the residual current in ordinary polarogram is obtained, by adjusting the contact of the rheostat. In this case the a.c. component of the electrolytic current has the similar waveform as in the usual polarography[6] and should be called a.c. polarogram with increasing amplitude. (e) Connecting the switch $S_5$ to (V), the other switches as in (d), and adjusting $P_2$ so as to produce the applied direct potential at which the limiting current in ordinary polarography is obtained, the amplitude of the applied alternating voltage decreases gradually with time as is shown in Fig. 2-(e) and the a.c. polarogram with decreasing amplitude is obtained[6].

In the latter two cases the so-called base current, i.e. a.c. polarogram of empty solution changes considerably with the amplitude of the applied alternating potential but this change of the base current is easily compensated by connecting $P_2$ and $B_2$ to the galvanometer circuit by a resistor of large value, because the base current changes linearly with the amplitude, if the differential capacity of electrical double layer at the mercury-solution interface remains almost constant in the potential range, over which the polarograms are taken. All of the polarograms shown in Fig. 4 were taken using this method. Near the electrocapillary maximum potential, however, this condition is not

6) I. Tachi and T. Kambara, This Bulletin, 28, 25 (1955).

fulfilled (Fig. 4-(b) and (d)) and a current eliminator of differential type[7] will be necessary for getting well-defined waves. Polarograms recorded by the present circuit are shown in Fig. 3 and Fig. 4. The sudden change of current intensity in the polarograms (e) and (f) in Fig. 4 (marked by arrows) is due to the sudden decrease of drop time, which occurs at a certain potential governed by the amplitude of the applied alternating potential[8]. In such a case artificial control of drop time is needed.

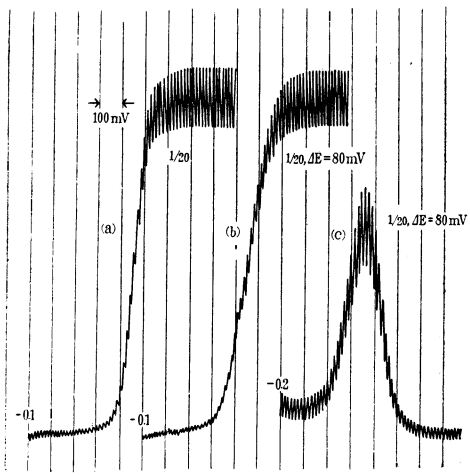



Fig. 3. Ordinary and a.c. polarograms of $10^{-3}$ M $Tl^{+}$ ion in 0.1 N. KCl solution.
Curve (a): ordinary polarogram.
Curve (b): Fournier's polarogram.
Curve (c): Breyer's polarogram.

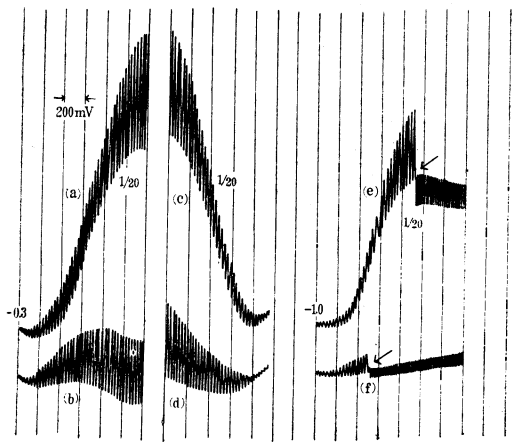



Fig. 4. A.C. Polarogram with varing amplitude.
Curve (a): $1.2\times10^{-3}$ M $Tl^{+}$ ion in 0.1 N KCl soln., with increasing amplitude.
Curve (b): base current of 0.1 N KCl soln., with increasing amplitude.
Curve (c): $1.2\times10^{-3}$ M $Tl^{+}$ ion in 0.1 N KCl soln., with decreasing amplitude.
Curve (d): base current of 0.1 N KCl soln., with decreasing amplitude.
Curve (e): $10^{-3}$ M $Zn^{++}$ ion in N KCl soln., with increasing amplitude.
Curve (f): base current of N KCl soln., with increasing amplitude.

7) G. Semerano and L. Riccoboni, *Gazz. chim. ital.*, 72, 297 (1942).

## Effect of Circuit Characteristics on A.C. Polarogram

Because a.c. polarography is a sort of potential-conditioned electrolysis, the total impedance of the electrolytic circuit must be kept as small as possible, so that it is negligible compared with the equivalent impedance of the observed electrode interface. Though the latter is a function of the direct potential, the amplitude of alternating potential, concentration of depolarizer discharging and other factors concerning the electrode reaction, it is usually far less than it is in ordinary polarography. Accordingly this condition must be carefully fulfilled. In the present experiment the total impedance of the electrolytic circuit except the cell circuit was kept at about 500 ohms, which is not small enough when we carry out the experimental study of a.c. polarography, e.g. in a wide range of concentration of depolarizer. In a.c. polarography the resistance of the electrolytic solution can not be neglected, when the electrode impedance is vanishingly small, e.g. the concentration of depolarizer is high. Fig. 5 shows the effect of concentration of supporting electrolyte on the magnitude of a.c. polarographic current. This effect of supporting electrolyte might be partially due to the change of reversibility of electrode

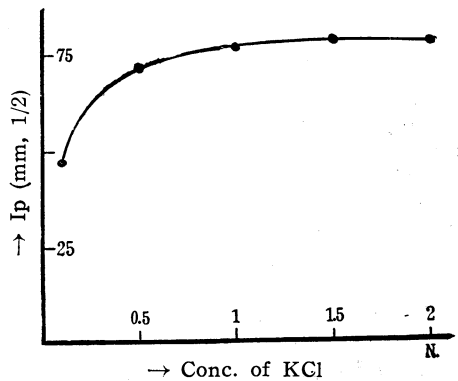



Fig. 5. Effect of concentration of supporting electrolyte on the peak height of a.c. polarographic current of $10^{-3}$ M $Cd^{++}$ ion in KCl solution.

8) I. Tachi and M. Okuda, This Bulletin, 27, 310 (1954).

reaction (see below) but, in a large part, due to the resistance of electrolytic solution.

The relation between galvanometer deflection and alternating current flowing across the primary coil of the transformer $L_2$, is shown in Fig. 6. When the alternating

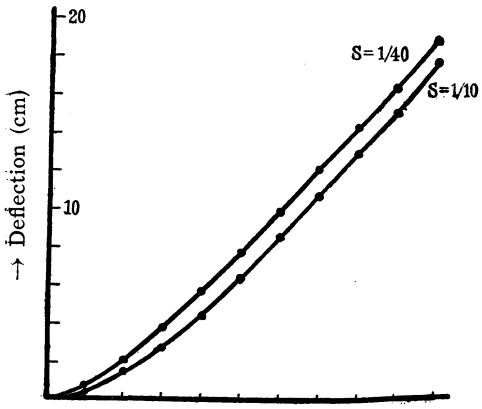



Fig. 6. Characteristics of alternating current detector.

current flowing is negligibly small, the crystal rectifier loses its function. A high gain electronic amplifier is now being constructed in this laboratory.

## Effect of Reversibility of Electrode Reaction

In a.c. polarography the reversibility of electrode reaction plays a far more important rôle than it does in the ordinary polarography. Detailed experimental study on the a.c. polarographic behaviour of sufficiently reversible electrode reaction will be reported in the succeeding paper of this series. In the present paper preliminary experimental study on the effect of reversibility will be given.

When the electrode reaction is irreversible, the half-wave potential of Fournier's polarogram is shifted to more positive potential with increasing amplitude of the applied alternating potential. According to the theory developed in the previous paper[6], the difference $(\Delta E_{1/2})_{A\cdot\sigma}$. of half-wave potentials between ordinary polarogram and Fournier's is given by the equation

$$(\Delta E_{1/2})_{A\cdot\sigma.}=\frac{RT}{\alpha nF}\ln\cosh\frac{\alpha nF}{RT}\Delta E$$

where $\Delta E$ is the amplitude of the alternating potential, $n$ the number of electrons required for reduction of one molecule of depolarizer, $\alpha$ the transfer coefficient of reduction process at the electrode and $F$, $R$ and $T$ are Faraday constant, gas constant and absolute temperature, respectively. When $\Delta E$ is larger than a hundred millivolts, $(\Delta E_{1/2})_{A\cdot\sigma.}-\Delta E$ curve becomes a straight line and the tangent of the straight line must be unity. Moreover $\alpha$ could be calculated from the ordinate of the intersection of the straight line and $(\Delta E_{1/2})_{A\cdot\sigma.}$-axis. Experimental results with nickel ion in 0.1 N KCl solution, which is known to be reduced irreversibly at the dropping mercury electrode[9], are given in Fig. 7, where $\Delta E$ is plotted in effective value.

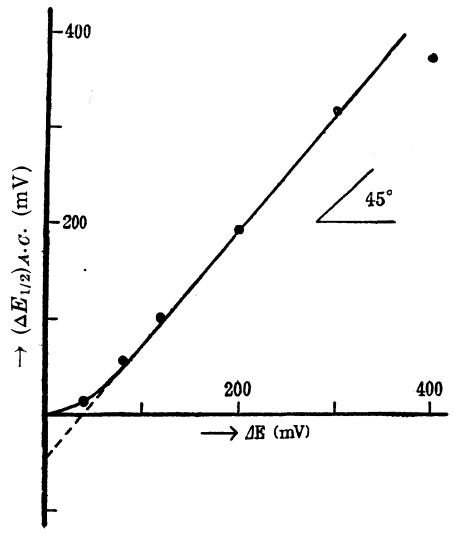



Fig. 7. Shift of the half-wave potential of Fournier's polarogarm with the amplitude of applied alternating potential.

By the graphical extrapolation of the experimental curve, the transfer coefficient was determined to be about 0.3. However, the slope of the experimental curve is slightly steeper than the slope of the theoretical one. This might be attributed to the assumption that the sinusoidal wave was supposed to be equivalent to the square wave.

Randles[10] and others[11,12] have shown that when the amplitude of the applied alternating potential is sufficiently small i.e.

$$\Delta E\frac{\alpha nF}{RT}\ll 1,$$

the electrode interface at equilibrium potential is at the stationary state electrically equivalent to the circuit shown in Fig. 8, where

9) J. Heyrovský, *Discussion Faraday Soc.* No. 1, 121 (1947).
10) J.E.B. Randles, ibid., No. 1, 11 (1947).
11) H. Ershler, ibid., No. 1, 269 (1947).
12) H. Gerisher, *Z. physik. Chem.*, **198**, 286 (1951).

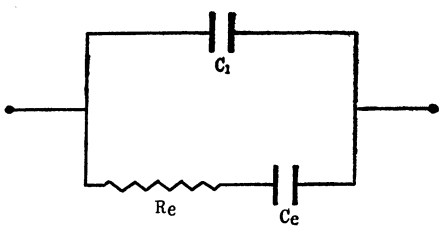



Fig. 8. Equivalent circuit of electrode surface at equilibrium potential at the stationary state.

$C_l$ is the differential capacity of the electrical double layer and $C_e$ and $R_e$ are the capacity and resistance equivalent to the electrode reaction and given by

$$1/\omega C_e = \frac{RT}{n^2F^2} \cdot \frac{1}{qC} \cdot \sqrt{\frac{2}{\omega D}}$$

and

$$R_e = \frac{RT}{n^2F^2} \cdot \frac{1}{qC} \cdot \left(\sqrt{\frac{2}{\omega D}} + \frac{1}{k}\right)$$

respectively, where $D$ is the diffusion coefficient of oxidized and reduced forms, assumed to have the same diffusion coefficient, $\omega$ is angular velocity of the alternating potential, $k$ the rate constant of electrode reaction at the equilibrium potential, $q$ surface area of electrode and $C$ is concentration of the depolarizer. From this theory, it is easily recognised that the current intensity of the a.c. component is closely related to the reversibility of electrode reaction. Recently Grahame[13] has developed a more comprehensive theory of a.c. electrolysis and, assuming Ilkovič equation for the diffusion process of depolarizer, he showed that the current intensity at peak potential decreases with decreasing value of $k$. Fig. 9 shows the Breyer's polarogram and ordinary polarogram of $Cd^{++}$ ion and $Z_n^{++}$ ion in 0.1 N KCl solution; it is known that the reversibility of the former is higher than the latter. In Table I relative values of peak heights of a.c. polarograms of $Zn^{++}$ ions in various supporting electrolytes are given. The experimental results confirm the above theoretical conclusion. $Ni^{++}$ ion in 0.1 N KCl solution shows no appreciable a.c. polarographic wave, which corresponds to its characteristic behaviour in Fournier's polarogram.

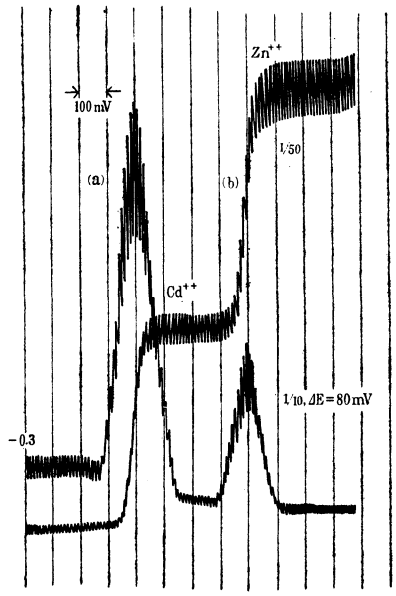



Fig. 9. Breyer's polarogram (Curve-(a)) and ordinary polarogram (curve-(b)) of $10^{-3}$ M $Cd(SO_4)+10^{-3}$ M $Zn(NO_3)_2$ in 0.2 N KCl solution.

TABLE I
CHANGE OF PEAK HEIGHT OF $10^{-3}$ M $Z^{++}$ ION WITH THE REVERSIBILITY OF ELECTRODE REACTION

| Supporting electrolyte (1 N.) | $KNO_3$ | KCl | KBr | KI |
|---|---|---|---|---|
| k*) (cm/sec) | $3.5\times10^{-3}$ | $4\times10^{-3}$ | $8\times10^{-3}$ | $7\times10^{-3}$ |
| peak height (%) | 71 | 100 | 201 | 570 |

*) B.E. Conway: Electrochemical data, Elsevier Pub. Co. (1952); see also reference (14).

## Applications of A.C. Polarography

The high utility of a.c. polarography in analytical applications has been discussed by Breyer and his coworkers[1], i.e. (a) there is no need to remove dissolved oxygen from the electrolytic solution, (b) small amounts of less noble ions can be determined in the presence of a large excess of noble ions, (c) reduction potentials only 40 mV apart are separable using small alternating voltage, (d) the a.c. polarographic current is greater than the ordinary polarographic current, and the limit of sensitivity is at about $10^{-5}$ N.

The considerable effect of reversibility of electrode reaction on a.c. polarography leads to another interesting applicability of a.c. polarography as is shown in the following model experiment. In Fig. 10, a-I and II are

13) D. C. Grahame, *J. Electrochem. Soc.*, **99**, 370c. (1952).

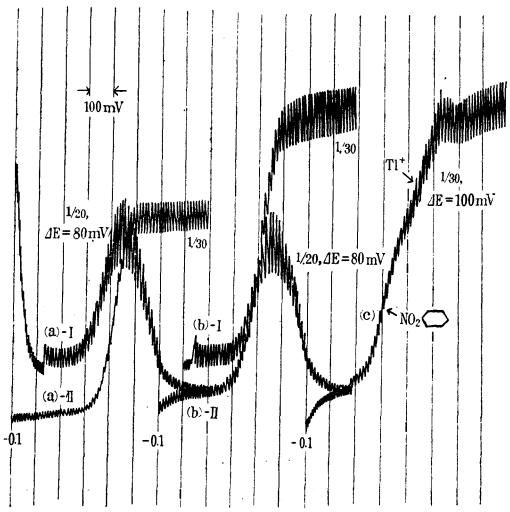



Fig. 10.
Curve (a)-I: Breyer's polarogram of $10^{-3}$ M $TlNO_3$ in 0.5 N KCl soln. pH=6.
Curve (a)-II: ordinary polarogram of the same solution as (a)-I.
Curve (b)-I: Breyer's polarogram of $10^{-3}$ M $TlNO_3$+nitrobenzen in 0.5 N KCl soln. pH=6.
Curve (b)-II: ordinary polarogram of the same solution as (b)-I.
Curve (c): Fournier's polarogram of the same solution as (b)-I.

a.c. polarogram and ordinary polarogram of $Tl^+$ ion, respectively, and b-I and II are the same polarograms, after addition of certain amounts of nitrobenzen to the same solution as (a). Curve (c) is Fournier's polarogram of the same solution as (b). Because the reversibility of electrode reaction of $Tl^+$ ion is sufficiently high but that of nitrobenzene is considerably low, the magnitude of a.c. polarographic current of the latter is negligible compared with that of the former. Also, because of the positive shift of Fournier's polarogram of nitrobenzene, the completely overlapped wave in b-II has a tendency to separate into two waves in (c). The above experimental results predicate that, when two depolarizers have half-wave potentials lying very close together, or lying even at the same potential, the separate determination is possible, if the degree of reversibility of them is considerably different. Using a.c. polarography for analytical purpose, the effect of the ionic species of supporting electrolytes on the reversibility must be also taken into account. The effect of change of reversibility caused by a minor contamination of surface active substances, which might come into electrolytic solution during sampling, could be avoided by addition of certain amounts of gelatine to the electrolytic solution. Reversibility of electrode reaction, though it decreases by the addition of gelatine, stays almost constant after the concentration of gelatine added attains to a certain range[14]. More detailed experimental as well as theoretical studies on a.c. polarography are now in progress in our laboratory.

## Summary

Fundamental circuit for a.c. polarography, in which a.c. polarogram with varying as well as constant amplitude is automatically registered, was shown. And the close relation between reversibility of electrode reaction and a.c. polarographic behaviour of depolarizers was experimentally verified and another applicability of this method was pointed out.

The authors are indebted to Yanagimoto Co. Ltd. for the support of this investigation.

*Department of Agricultural Chemistry, Faculty of Agriculture, Kyoto University, Kyoto*

14) J. E. B. Randles and K. W. Somerton, *Trans. Faraday* Soc., 48, 951 (1952).

# *Studies on A. C. Polarography. III. Reversible Wave**)

By Mitsuko OKUDA and Isamu TACHI

(Received June 12, 1954)

## Introduction

In Part I[1] and II[2] of this study the theoretical treatment of the Alternating Current-Polarography (a. c. polarography) was reported, and in Part III[3] the fundamental circuits together with the results of several basic experiments were communicated. In this article, the experiments concerning the d. c. and a. c. components of electrolytic current due to the reversible electrode reaction observed with the a. c. polarographic equipment, in which a sinusoidal alternating voltage of a constant amplitude is superimposed on the constant d. c. voltage used in the ordinary polarography, will be given and compared with the theoretical conclusion.

As is well known, the mean current $\bar{i}$, which is observed in the ordinary polarography using a dropping mercury electrode, is a function of the electrode potential $V$, and is given by

$$\bar{i}=\frac{\bar{i}_d}{2}\left\{1+\tanh\frac{nF}{2RT}(E_{1/2}-V)\right\}, \qquad (1)$$

where $\bar{i}_d$ is the mean limiting diffusion current, $n$ the number of electrons associated with the electrolytic reduction, $E_{1/2}$ the half-wave potential, and the other symbols have their usual significances. According to the theoretical treatment given in Part II of this study, in the case that the electrode reaction proceeds reversibly, the mean value, $\bar{i}_F$, of the d. c. component of the a. c. polarographic electrolytic current, i. e. Fournier's polarogram, is shown by

$$\bar{i}_F=\frac{1}{2}(\bar{i}_1+\bar{i}_2), \qquad (2)$$

whereas the mean value of the amplitude of a. c. component, i. e. Breyer's polarogram, is given by

$$i_{A.C.}=K(\bar{i}_1-\bar{i}_2). \qquad (3)$$

Let $E$ be the constant d. c. voltage applied to the dropping mercury electrode, and $\Delta E$ the amplitude of the superimposed a. c. voltage, then $\bar{i}_1$ and $\bar{i}_2$, respectively, are given by

$$\left.\begin{aligned}\bar{i}_1&=(\bar{i})_{V=(E-\Delta E)};\\ \bar{i}_2&=(\bar{i})_{V=(E+\Delta E)}.\end{aligned}\right\} \qquad (4)$$

$K$ in Eq. (3) is given by $(s\sqrt{f}-1/4)$, in which $f$ is the frequency of the a. c. voltage, and $S=1.192$ is a constant. Because we use a. c. voltage of 60 c/s, $K$ is nearly equal to 9.04. The above theoretical treatment has been based on the assumption that the superimposed sinusoidal alternating voltage is equivalent to the square wave voltage of a suitable amplitude; we employ here the a. c. voltage of sinusoidal wave form. Thus, in the present experiment, the effective value of the superimposed a. c. voltage is regarded to be equivalent to the amplitude of the square wave voltage, and the results are discussed. As the depolarising cation, thallous ion in 0.1 N KCl solution is chiefly employed, since it is well known that the ion shows nearly a perfect reversible behaviour[4,5]; and further cadmium ion is often, according to the necessity, employed, which also shows a high degree of reversibility[4]. Circuit for a. c. polarography, as already reported in Part III of this study, is used. The superimposed a. c. voltage is obtained by lowering the 100 v., 60 cycle a. c. line by means of a transformer and a suitable rheostat divider; the electrolysis is carried out in room temperature at 25°C and the bottom mercury layer was used as the anode, against which the cathode potential is measured. The sensitivity of galvanometer used is $4\times10^{-9}$ Amp./mm./m.

## Experimental Results and the Theoretical Consideration

**(1) Wave Form of the A. C. Polarogram.** —Fig. 1 shows the theoretical a. c. polarograms together with the ordinary polaro-

*) Read at the monthly meeting of the Agric. Chemical Society of Japan held in Kyoto University on the 18th July 1953.

1) I. Tachi and T. Kambara, This Bulletin, 28, 25 (1955).

2) T. Kambara and I. Tachi, ibid., **28** 25 (1955).

3) M. Senda, M. Okuda and I. Tachi, ibid., **28** 31 (1955)

4) J. Heyrovský, *Discus. Farad. Society*, No. 1, 121 (1947).

5) J.E. Randless, ibid., 11.

gram; and in Fig. 2 and 3 are illustrated the a. c. polarograms observed experimentally. In Fig. 1 curves d and e represent the

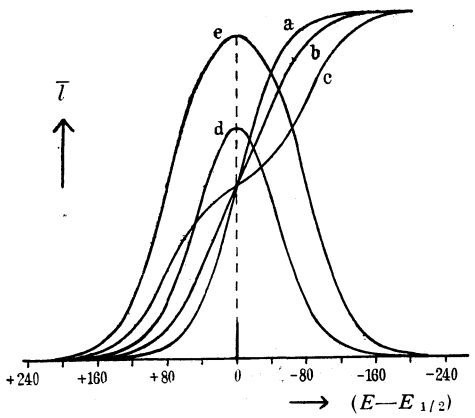



Fig. 1. Theoretical polarograms.
($n=1$, $t=25$°C)
a: ordinary polarogram, $\Delta E=0$mV
b: Fournier's polarogram, $\Delta E=40$mV
c: Fournier's polarogram, $\Delta E=80$mV
d: Breyer's polarogram, $\Delta E=40$mV
e: Breyer's polarogram, $\Delta E=80$mV

a. c. components, where the currents are plotted in $1/K$ unit of the calculated values. As required by the theoretical conclusion shown by the Eqs. (1) and (2), the d. c. component of a. c. polarogram (namely, the Fournier's polarogram) shows the less steep slope than the classical polarogram with the increasing amplitude of the superimposed a. c. voltage, until it begins to split into two steps; and the classical and Fournier's polarograms intersect with each other always at the half-wave point. The experimental results shown in Fig. 2 are in good harmony

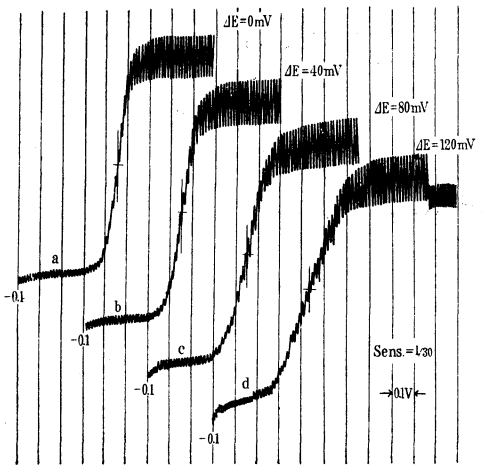



Fig. 2. Observed Fournier's polarogram due to the depolarization of $Tl^+$. Solution: $10^{-3}$ M $TlNO_3$ in 0.1 N KCl

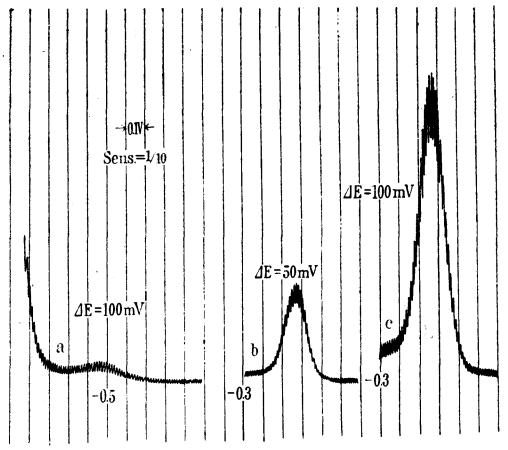



Fig. 3. Observed Breyer's polarogram due to the depolarization of $Tl^+$.
a: 0.1 N KCl solution
b and c: $2\times10^{-3}$ M $TlNO_3$ in 0.1 N KCl solution

with the theoretical prediction. On the other hand, the a. c. component of the a. c. polarogram (namely, the Breyer's polarogram) is found to show a peak at the half-wave potential, as shown obviously by Eq. (3) and also in Fig. 3. In the case of the Breyer's polarogram, owing to the differential capacity[6] of the electric double layer at the electrode-solution interface, an alternating current governed by the product of the differential capacity and surface area flows, even when there is no depolarizer in the solution (Fig. 3 (a) ); thus the recorded alternating current is the vector sum of the alternating current, $\bar{i}_B$, due to the differential capacity, which is to flow in the empty solution, and the electrolytic alternating current, $\bar{i}_{A.C.}$. It is clear that when we observe the Fournier's polarogram, the current due to the differential capacity is not observable by the galvanometer, since the mean value thereof is obviously zero.

It must be mentioned here that the anodic dissolution of mercury affects the a. c. polarogram considerably. Namely, in Fig. 2 (d) the Fournier's polarogram due to the anodic reaction of mercury is observable in the more negative potential than in the case of classical polarogram. Also in Fig. 3 (a) the Breyer's polarogram increases suddenly at the positive potential, where the oscillatory current due to the reversible deposition and dissolution of mercury is of special importance.

It is seen further that the drop time often becomes abruptly short resulting in the sud-

6) D.C. Grahame, *Chem. Revs.*, **41**, 441 (1947).

den decrease in the current intensity; this is found in the ascending parts of the waves shown in Fig. 2 (c) and (d) and in the final part of the wave shown in Fig. 2 (d). This finding seems to be due to the effective decrease in the interfacial tension caused by the superposition of a. c. voltage. The critical potentials, at which such a sudden decrease occurs, lie in both sides of the potential corresponding to the electrocapillary maximum, and furthermore the two critical potentials shift nearly symmetrically with the varying amplitude of the superimposed a. c. voltage, as has been already reported by us[7].

According to the above cited theoretical equation, the half-wave potential of the Fournier's polarogram, denoted by $E_F$, and the peak potential of the Breyer's polarogram, denoted by $Ep$, are expected to be identical with the half-wave potential of the ordinary polarogram, independently of the concentration of depolarizer and the amplitude of the superimposed a. c. voltage. Table I gives the experimental results obtained with thallous ion. We can find a fairly good accordance thereof. However, it is found experimentally, that $Ep$ is by ca. 20mV more negative than $E_{1/2}$ and $E_F$ is shifted positively with the increasing amplitude. The reason of such phenomena will be perfectly clarified, when a more exact theoretical treatment, in which the velocity constants of the electrode processes and the transfer coefficient, usually denoted by $\alpha$, are taken into consideration.

Also the limiting current in the Fournier's polarogram coincides with that of the classical polarogram at a *sufficiently* negative potential. The experimental results shown in Fig. 2 are in harmony with the theoretical prediction. On the other hand the observed peak height in Breyer's polarogram is far less than the theoretical value. This will be discussed in the succeeding section of this report.

TABLE I

COMPARISON OF THE HALF-WAVE POTENTIAL OF FOURNIER'S POLAROGRAM AND THE PEAK POTENTIAL OF BREYER'S POLAROGRAM

Solution: $10^{-3}$ M $TlNO_3$ in 0.1 N KCL

| $\Delta E$ (mv.) | $E_F$ (v.) | $E_p$ (v.) |
|---|---|---|
| 0 | $-0.55_0$ | |
| 40 | $-0.54_8$ | $-0.57_0$ |
| 80 | $-0.54_5$ | $-0.57_0$ |
| 120 | $-0.54_0$ | $-0.57_0$ |

**(2) Effects due to the Amplitude of the Superimposed A. C. Voltage.**—Fournier has verified experimentally the influence of the frequency of the superimposed a. c. voltage on the d. c. component of the polarographic current, and found that in the case of the reversible electrode reaction the wave form remains nearly unchanged independently of the frequency, provided that the amplitude thereof is kept constant[8]. This is theoretically predicted by Eq. (2). Thus we have investigated the behaviour of d. c. component in the case that the amplitude is varied, while the frequency of 60 c/s is unchanged. As stated above, the d. c. component is at last splitted into two waves with the increasing amplitude employed, while the half-wave point lies unchanged at the original half-wave potential. This can be far more distinctly observed when the wave analysis is carried out concerning the Fournier's polarogram. Fig. 4 gives an example of thallous ion. A small deviation of the experimental observation from the theoretical equation is found, which may be due to the simplified supposition that the applied sinusoidal alternating potential is equivalent to a square wave voltage. The course of the observed current-potential curve, however, runs quite in the same manner to the theoretical curve, indicating the essential legitimacy of the theory.

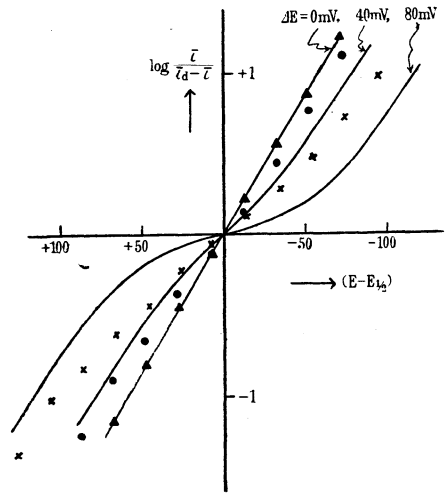



Fig. 4. Wave analysis of the Fournier's polarograms of $Tl^+$ (for a, b and c in Fig. 1 and 2) by means of the logarithmic plott.
——: theoretical curves
▲ ($\Delta E$=0mV)
● ($\Delta E$=40mV) : experimental values
× ($\Delta E$=80mV)

7) I. Tachi and M. Okuda, This Bulletin, 27, 310 (1954).

8) M. Fournier, *Comp. rend.*, 237, 1673 (1951).

In Fig. 5 is given the dependency of the

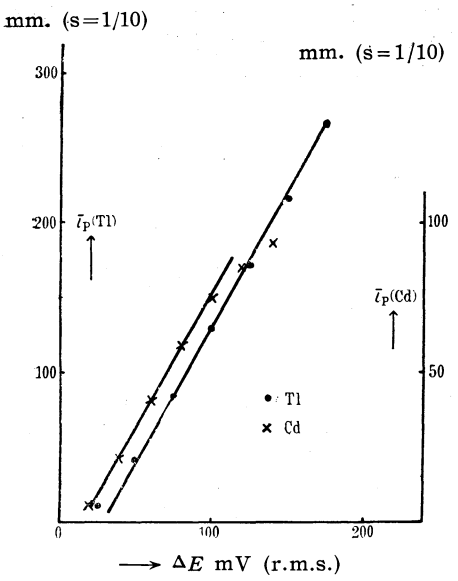



Fig. 5. Peak current vs. $\Delta E$ curve.
●: $2\times10^{-3}$ M $TlNO_3$ in 0.1 N KCl
×: $5\times10^{-4}$ M $Cd(SO_4)$ in 0.1 N KCl

peak current intensity of the Breyer's polarogram on the amplitude of the employed a. c. voltage. Ih this diagram each current intensity has been calibrated for the capacity current, which is also observable with the blank solution. From Eq. (3), it follows that

$$\bar{i}_p=[\bar{i}_{A\cdot C\cdot}]_{V=E_p=}A\cdot K\cdot \bar{i}_d\cdot \tanh\frac{nF}{2RT}\cdot \Delta E \quad (5)$$

where $A$ is a constant given experimentally and depends on some characteristic constants of circuit and equipment employed. In the present experiment this constant is about 1/40. This exhibits the relationship between the peak current and amplitude. It is expected therefrom that the slope of $\bar{i}_p$ vs. $\Delta E$ curve becomes gradually less steep with the increasing value of $\Delta E$, until $\bar{i}_p$ approaches to a constant value given by $A\cdot K\cdot \bar{i}_d$. The experimentally obtained value with cadmium ion, shows such a tendency, however, not in such a remarkable manner as expected from Eq. (5), and a linear relationship between $\bar{i}_p$ and $\Delta E$ is observable in an appreciably wide range. In the case of thallous ion, such a linearity persists even with the amplitude greater than 170 mV. Such a difference between $Cd^{++}$ and $Tl^{+}$ seems to be ascribed to the difference of the reversibility as well as to the difference of number of electrons of the two redox-systems.

(3) **Effect due to the Height of Mercury Reservoir.**—Variations of the d. c. and a. c. component due to the change of the height of mercury reservoir are illustrated in Fig. 6.

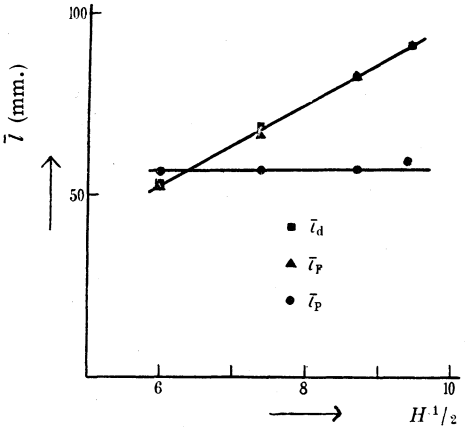



Fig. 6. Effect due to the height of mercury reservoir.
Solution: $10^{-3}$ M $TlNO_3$ in 0.1 N KCl
$\Delta E$=100mV. Sensitivity of galvanometer is 1/30 for $\bar{i}_d$ and $\bar{i}_F$, and 1/10 for $\bar{i}_q$.

It is clear that the limiting diffusion current of the ordinary polarogram and also that of the Fournier's polarogram are nearly proportional to the square root of the reservoir height. That these two limiting currents must coincide at a sufficiently negative potential, is predicted theoretically by Eqs. (1) and (2). On the contrary, the peak current intensity of Breyer's polarogram remains *constant* independently of the reservoir height. This finding suggests that the a. c. component ought to be proportional to the mean value of the drop surface, as in the case of *kinetic current* investigated by Koutecky and Brdička[9]. This result seems to be comprehensible from the fact that the change of the a. c. component of the electrolytic current is much faster than that of the mercury drop surface.

(4) **Dependency of Current Intensity on the Concentration of Depolarizer.**—The limiting current in the Fournier's polarogram coincides with that of the classical polarogram at a sufficiently negative potential, provided that the drop time remains unchanged, so that it is proportional to the concentration of depolarizing matter. Also it can be derived from Eq. (5) that the peak current intensity of the Breyer's polarogram must be proportional to the concentration. Experimental results with thallous ion are shown

9) J. Koutecky and R. Brdička, *Collection Czech. Chem. Communs.*, 12, 337 (1947).

in Fig. 7, and it is obvious that when the

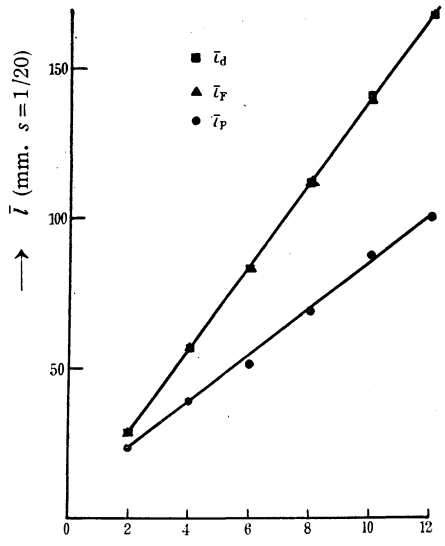



Fig. 7. Dependency of each current intensity on the concentration.
Solution: $TlNO_3$ in 0.1 N KCl. $\Delta E$ =80mV.

concentration lies in the concentration range varying from $10^{-4}$ to $10^{-3}$ mol. per liter, the satisfactory result is found. Quite the same results are also obtained with cadmium ion. Fig. 8 gives an experimental $\bar{i}_p$-$^*C$ curve, in which the bulk concentration $^*C$ of depolarizer is of the order of $10^{-3}$ molar, and it is found that the peak current approaches to a certain limiting value with the increasing concentration, the phenomenon of which will be discussed later elsewhere.

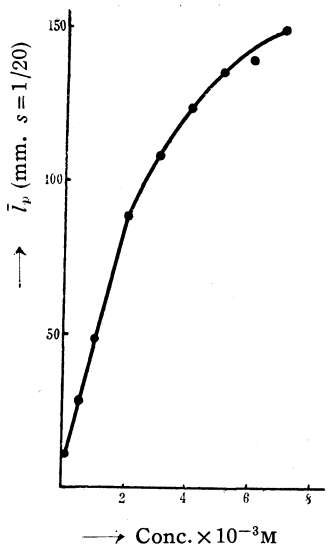



Fig. 8. Dependency of peak current on the concentration.
Solution: $Cd(SO_4)$ in 0.5 N KCl. $\Delta E$ =100mV.

## Summary

The d. c. and a. c. components of the electrolytic current observed a. c. polarographically, i. e. the Fournier's and Breyer's polarograms, are investigated experimentally for the reversible electro- reductions of cadmium and thallous ions. The result of the experiment shows convincingly the essential legitimacy of our theoretical conclusion.

*Department of Agricultural Chemistry,*
*Faculty of Agriculture,*
*Kyoto University, Kyoto*

# *Reactions of Bis-alkylsulfonylmethanes and Their Halogen-substituted Derivatives**)

By Shigeru OAE

(Received June 19, 1954)

Bis-alkylsulfonylmethane is a fairly interesting compound in many respects.[1] Its central methylene group is active like that of dialkyl malonate and behaves quite similarly. For example, methyl iodide reacts with sodium salt of bis-alkylsulfonylmethane according to the following equation.[1,2]

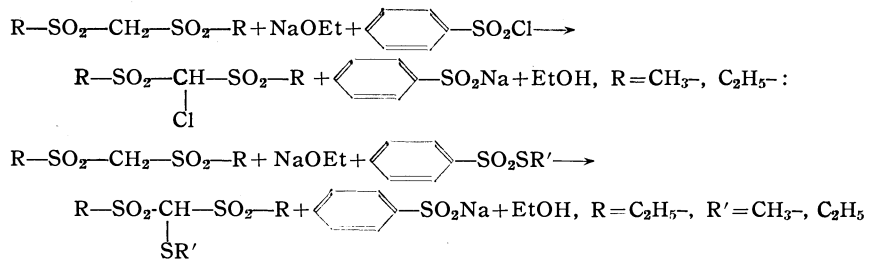
$$R—SO_2—CH_2—SO_2—R + NaOEt + CH_3I \longrightarrow R—SO_2CH(CH_3)—SO_2—R + NaI + EtOH$$

This active methylene group readily undergoes electrophilic substitution. A few typical reactions of this type are as follows:

* A part of this study was made at the Department of Chemistry, University of Kansas, Lawrence, Kansas, U.S.A.

1) C.M. Suter, "The Organic Chemistry of Sulfur", pp. 739

2) (a) E. Fromm, *Ann.*, **253**, 141 (1889).
E. Fromm et al., ibid., **394** 344 (1912).



The former reaction presumably takes place by the attack of chlorine cation, while the latter does by that of SR'. However, no similar reaction was observed between ethyl benzenesulfonate and bis-alkylsulfonylmethane. This mixture eventually did not react under the same condition as for the sulfur analog.

A reaction was carried out between sodium salt of bis-alkylsulfonylmethane and methyl nitrate under the speculation that it might give bis-alkylsulfonyl-methoxymethane. However, the resulting compound was found to be bis-alkylsulfonyl-methylmethane; namely, it would be a simple nucleophilic substitution.

$$R{-}SO_2{-}CH_2{-}SO_2{-}R + NaOEt + CH_3ONO_3 \longrightarrow R{-}SO_2{-}\underset{\displaystyle CH_3}{\underset{|}{CH}}{-}SO_2{-}R + NaONO_2 + EtOH$$

Bis-alkylsulfonylmethane is readily halogenated and forms dihalides.[1,2,3] Both dihalide and monohalide of bis-alkylsulfonylmethane show interesting chemical behaviour. Their halogens are easily replaced by hydrogen giving original bis-alkylsulfonylmethane when attacked by nucleophilic reagents. Bis-alkylsulfonyl-dibromomethane reacts with potassium iodide liberating iodine,[2b] while it reacts with thiophenol giving diphenyldisulfide.[1a] Aqueous ammonia, sodium acetate and potassium thiocyanate also replace bromine by hydrogen. These reactions with bis-alkylsulfonyldibromomethane can be explained when one assumes that it gives a bromocation which readily oxidizes nucleophilic reagents. This assumption is probably valid, because halogens attached to the central methylene group having two adjacent strong electron-attractive sulfonyl groups, do not readily split as halogen anions but do so as cations rather easily.

In this investigation, a few more similar reactions were observed. Bis-ethylsulfonylchloromethane gave bis-ethylsulfonylmethane in the reaction with sodium methylate. Sodium methylate converted bis-alkylsulfonyldichloromethane also to its original bis-alkylsulfonylmethane. Aluminum ethylate caused practically the same reaction with bis-methylsulfonydibromomethane.

A somewhat peculiar reaction of bis-ethylsulfonyldibromomethane was one with silver nitrate in methanol. The reaction took place almost spontaneously, one bromine being lost, and gave bis-ethylsulfonylbromomethane, which did not undergo any further reaction with excess silver nitrate. On the other hand, its chloro-analog, bis-ethylsulfonyldichloromethane, reacted very little, even though it was boiled for ten hours with silver nitrate in ethanol. The very much higher reactivity of the dibromo compound over the dichloro-analog can not be ascribed only to the difference in the polarizability of the relevant bond. Moreover, the cleavage of bromine as anion would be greatly suppressed by the inductive effect of the two strongly electron-attractiing sulfonyl groups. The failure of explanation by the electrical effect led us to seek the alternative one by the steric effect. As was reported previously[4], the steric requirement of the sulfonylmethyl group is of similar bulkiness to that of the neopentyl group. According to the current concept of "Strained Homomorph" by H. C. Brown[5], di-(*tert*-butyl)-methane is sterically strained by ca. 5 kcal.; therefore, its 'Strained Homomorph', bis-alkylsulfonylmethane should also be sterically strained by as much as about 5 kcal. When one bromine is substituted for its methylene, the resulting monobromo-compound will have more strain, but the inductive effect of the two strong electron-attractive sulfonyl groups might still overwhelm the steric strain energy, thus rendering the net result the retardation of reactivity. However, when another bromine is introduced, the steric strain of the resulting bis-alkylsulfonyldibromomethane would suddenly jump up to such an extent that the second bromine atom would no longer be held stably at the methylene carbon, in spite of the strong inductive effect of three other

(b) R.E. Stutz and R.L. Shriner, *J. Am. Chem. Soc.*, 55, 1242 (1933).
R.L. Shriner et al., ibid., 52, 2068 (1930).

3) D.T. Gibson, *J. Chem. Soc.*, **1931**, 2637.

4) S. Oae, *Waseda Applied Chem. Bull.*, 21, No. 1, 7 (1952); ibid., No. 2, 8 (1953).

5) H.C. Brown, *J. Am. Chem. Soc.*, 75, 1, (1953).

electron-attractive substituents attached to it. Since the chlorine atom is smaller than bromine, even the second chlorine atom might possibly be held with quite enough stability at the methylene carbon, thus showing its inertness in the reaction with silver nitrate.

The reaction of bis-alkylsulfonyldibromomethane with aniline and with toluene were investigated under the speculation that it might be used as a mild brominating agent. However, aniline did not react readily while toluene did, giving benzyl bromide in the presence of a small amount of benzoyl peroxide.

## Experimental

**Bis-ethylsulfonylmethylmercaptomethane and Bis-ethylsulfonylethylmercaptomethane.**—1 g. of methyl *p*-toluenethiosulfonate of m.p. 53–4°, which was prepared by the reaction of methyl iodide upon sodium *p*-toluenethiosulfonate, was reacted with 1 g. of bis-ethylsulfonylmethane in 15 ml. of ethanol dissolving 0.1 g. of metalic sodium. The reaction mixtur was boiled on a water bath for seven hours and then was kept at room temperature overnight. After removing ethanol and allowing the residue to soak in hydrochloric acid until it became acidic, colorless crystalline needles were formed which were collected and recrystalized from ethanol-petroleum ether. 0.7 g. of bis-ethylsulfonyl-methylmercaptomethane of m.p. 119–20° was thus obtained in 57% yield. (Found: S, 39.0. Calcd. for $C_6H_{14}S_3O_4$: S, 39.2%).

Bis-ethylsulfonyl-ethylmercaptomethane of m.p. 103–4° was obtained in 62% yield, starting from ethyl *p*-toluenethiosulfonate of m.p. 50–3° with bis-ethylsulfonylmethane as in the previous case and then recrystallization was performed from benzene-petroleum ether. (Found: S. 36.6; Calcd. for $C_7H_{16}S_3O_4$: S, 36.9%).

**The Reaction between Bis-methylsulfonylmethane and Ethyl *p*-toluenesulfonate.**—0.5 g. of bis-methylsulfonylmethane was dissolved in 10 ml. of ethanol which dissolved 0.05 g. of metallic sodium. Into this solution, 0.6 g. of freshly prepared ethyl *p*-toluenesulfonate of m.p. 29–30° was added and the whole mixture was boiled on a water bath for an hour. After treating the mixture similarly to the case of thio-analog, only the original substances were isolated. Longer heating was found not to be effective in bringing the reaction any further.

**The Reaction between Bis-alkylsulfonylmethane and Methyl Nitrate.**—1 g. of bis-methylsulfonylmethane was dissolved in 15 ml. of methanol which dissolved 0.05 g. of metallic sodium. Into this solution 0.5 g. of methyl nitrate was added and the mixture was boiled on a water bath for an hour and a half; then crystals formed. These crystals were collected and were found to be sodium nitrate which was identified by the appearance of blue-violet color when treated with a mixture of diphenylamine and sulfuric acid. The residue was diluted with water and the crystals precipitated were collected. Well-dried crystals were recrystallized from benzene and 0.7 g. of colorless crystals of m.p. 120–122° were obtained. This compound was found to be identical to bis-methylsulfonylmethane of m.p. 124° which was authentically prepared from bis-methylsulfonylmethane and methyl iodide. 0.65 g. of bis-ethylsulfonylmethane and 0.25 g. of methyl nitrate were dissolved in 10 ml. of methanol which contained 0.25 g. of potassium hydroxide, and the mixture was treated as in the previous case, and then bis-ethylsulfonyl-methylmethane of m.p. 75° was obtained. This was identified as bis-ethylsulfonyl-methylmethane by the mixed melting point with the authentic sample prepared from bis-ethylsulfonylmethane and methyl iodide.

**The Reaction of Sodium Methylate upon Bis-ethylsulfonyldibromomethane.**—4 g. of bis-ethylsulfonyl-dibromomethane was added in 40 ml. of methanol which dissolved 0.65 g. of metallic sodium and the whole mixture was boiled for an hour, and then methanol was removed. The residue was diluted with water and the crystals formed were washed with ether, then 2 g. of bis-ethylsulfonylmethane of m.p. 102–3° were obtained. Sodium bromide was obtained from the mother liquor.

**The Reaction of Sodium Ethylate upon Bis-methylsulfonyl-dibromomethane.**—0.5 g. of bis-methylsulfonyl-dibromomethane was reacted in 5 ml. of ethanol with sodium ethylate made from 0.08 g. of metallic sodium, and then 0.2 g. of bis-methylsulfonylmethane were obtained.

**The Reaction of Aluminum Ethylate upon Bis-methylsulfonyl-dibromomethane.**—1 g. of bis-methylsulfonyl-dibromomethane was mixed with 0.5 g. of freshly prepared aluminum ethylate, the mixture was sealed in a tube, and the tube was heated at 200° for twenty minutes. After the tube was cooled, the contents were poured into water and then 0.3 g. of crystal melting at 140–45° was obtained. This was identical with bis-methylsulfonylmethane.

**The Reaction between Bis-ethylsulfonyl-dibromomethane and Silver Nitrate.**—When 1 g. of bis-ethylsulfonyl-dibromomethane was placed into 50 ml. of methanol dissolving 0.5 g. of silver nitrate, the whole solution became milky white and the reaction was over in ten minutes. Then it was further heated up to the boiling point and then was cooled. The silver bromide which formed was filtered off and methanol was removed, and then crystals appeared. These crystals were recrystallized and 0.5 g. of colorless compound of m.p. 121° was obtained. This was found to be monobromo compound. The reaction with large excess of silver nitrate also gave the same compound, though it was heated for a longer period. (Found: Br, 30.0; Calcd. for $C_5H_{11}O_4Br$: Br, 30.4%).

When 0.5 g. of this compound was reacted with 0.3 g. of bromine, the dibromo compound of m.p. 131° was obtained almost quantitatively.

**The Reaction between Bis-ethylsulfonyl-dichloromethane and Silver Nitrate.**—0.5 g. of bis-ethylsulfonyl-dichloromethane and 0.35 g. of silver nitrate were dissolved in 50 ml. of methanol and the solution was boiled for ten hours, but the solution did not become turbid and the starting material was recovered.

**The Reaction between Bis-ethylsulfonyl-dibromomethane and Aniline.**—1.5 g. of bis-ethylsulfonyl-dibromomethane and 0.5 g. of aniline were dissolved in 40 ml. of benzene and the solution was boiled for 30 minutes. A small portion of crystal was observed at the end of thirty minutes. Heating was continued for additional four hours and benzene was removed, but no crystalline substance was successfully obtained after a serious attempt.

The same amounts of the starting materials were heated in 50% acetic acid for three hours but only the starting materials were isolated.

**The Reaction of Bis-ethylsulfonyl-dibromomethane upon Toluene.**—5 g. of bis-ethylsulfonyl-dibromomethane was added to 10 ml. of toluene which dissolved 1 g. of benzoyl peroxide and the whole solution was boiled for five hours. Gradually the solution became lachrymatory. After cooling at the end of five hours, a small portion of benzoic acid of m.p. 120–2° formed in the solution. The remaining oil was distilled in vacuo and 1.5 g. of an oil was obtained which boiled at 70–80°/10 mm. This oil was found to be benzyl bromide which was identified by leading it to S-benzylthiouronium bromide.

## Summary

Bis-alkylsulfonylmethane did react with alkyl *p*-toluenethiosulfonate giving bis-alkylsulfonyl-alkylmercaptomethane. Bis-alkylsulfonyl-halogenomethane was found to react with metal alkoxide giving original bis-alkylsulfonylmethane. It was also found that bis-alkylsulfonyl-dibromomethane readily reacts with silver nitrate giving the monobromo-compound while its dichloro-analog resists in the same condition.

The mechanisms of these reactions were discussed.

The author is deeply grateful to both Professor M. Murakami at Osaka University and Professor Calvin A. Van der Werf at the University of Kansas who encouraged him all through this study.

*The Institute of Scientific and Industrial Research, Osaka University, Sakai City, Osaka*

# *Studies on Unsaturated Organosilicon Compounds. II.* Reactions and Properties of Vinyltrimethylsilane*

By Motonori KANAZASHI

(Received June 22, 1954)

In a previous paper,[1] the syntheses of organovinylsilanes and addition of trichlorosilane to the double bond of these compounds were discussed. The present paper reports three types of reactions of vinyltrimethylsilane, that is, addition, cleavage, and polymerization. Vinyltrimethylsilane is of much theoretical interest because it is one of the simplest unsaturated organosilicon compounds and it has a silicon atom directly bonded to the C=C double bond.

**Addition Reactions to the Double Bond.**[2]— Vinyltrimethylsilane is thought to be one of the monosubstituted ethylenes; thus to this ethylenic double bond many compounds may be added as to ordinary unsaturated organic compounds.

The hydrogenation of unsaturated organosilicon compounds was first reported by Sommer and his coworkers on allyltrimethylsilane[3] and recently on β-styryltrimethylsilane[4] by the same author. These reactions were carried out under hydrogen pressure with Raney nickel catalyst. In the present study vinyltrimethylsilane was found to be easily hydrogenated under normal conditions with platinum oxide as catalyst in glacial acetic acid solution. The catalytic hydrogenation under normal conditions with platinum or palladium catalyst seems to be useful for the analytical determination of the number of unsaturated

*) This work was presented in the 7th. annual meeting of the Chemical Society of Japan in April, 1954, at Tokyo.

1) M. Kanazashi, This Bulletin, **26**, 493 (1953).

2) Most of the experimental results of this section were presented in the 6th. annual meeting of the Chemical Society of Japan in April, 1953.

3) L.H. Sommer, L.J. Tyler and F.C. Whitmore, *J. Am. Chem. Soc.*, **70**, 2872 (1948).

4) L.H. Sommer, D.L. Bailey, G.M. Goldberg, C.E. Buck, T.S. Bye, F.J. Evans and F.C. Whitmore, *J. Am. Chem. Soc.*, **76**, 1613 (1954).

bonds in organosilicon compounds within an error of about 2%.

The addition of halogen to the double bond of vinyltrimethylsilane was reported by the author[2] and very recently by Sommer and his coworkers[4]. It was found that chlorine and bromine easily add to the double bond of vinyltrimethylsilane, as they do in the case of vinyltrichlorosilane,[5,6,7,8] giving $\alpha$, $\beta$-dihalogenoethyltrimethylsilane as reported by Sommer and his coworkers[4]. Especially the addition of bromine was found also to be useful for the analytical determination of the number of unsaturated bonds of organosilicon compounds by normal methods, i.e. reaction of a sample with carbon tetrachloride solution of bromine followed by a back titration with standard solution of sodium thiosulfate.

The addition of hydrogen halides to the double bond of vinylsilanes was first reported by Larsson[9] on vinyltriethylsilane with hydrogen chloride and bromide in the presence of hydroquinone or benzoyl peroxide. In all cases $\beta$-halogenoethyltriethylsilanes were obtained contrary to the well known Markownikoff rule. A similar result was obtained by Wagner and his coworkers[8] in the aluminum chloride catalyzed addition of hydrogen chloride to vinyltrichlorosilane. The present author also found this non-Markownikoff addition to vinyltrimethylsilane of hydrogen bromide and of hydrogen iodide in the presence and absence of a peroxide or an antioxidant, and independently from the above two reports. These results were reported orally in April 1953[2] but it was decided to postpone the publication in a journal until more detailed data for discussion of the reaction mechanism had been obtained.

Recently Sommer and others[4] reported the same results on vinyltrimethylsilane with hydrogen bromide in the presence of benzoyl peroxide and with hydrogen iodide. They found that hydrogen bromide did not add to vinyltrimethylsilane in the absence of a peroxide catalyst during a reasonable time. Contrary to this result, in the present study hydrogen bromide added easily to vinyltrimethylsilane in the absence of a peroxide catalyst or in the presence of catechol as an antioxidant, by a slight warming for ten minutes followed by cooling to $-70°$ and saturating with hydrogen bromide.

The $\beta$-halogenoethyltrimethylsilanes obtained by these addition reactions were found to be very unstable. $\beta$-Iodoethyltrimethylsilane fumed in air and slowly decomposed to give free iodine, and $\beta$-bromoethyltrimethylsilane decomposed even at room temperature by a catalytic action of the surface of unglazed porcelain or ground glass, giving trimethylbromosilane and ethylene.

$$(CH_3)_3SiCH_2CH_2Br \longrightarrow (CH_3)_3SiBr+CH_2=CH_2$$

This $\beta$-halogen in $\alpha$, $\beta$-dihalogeno-or $\beta$-halogeno-ethyltrimethylsilane could be titrated by dilute alkali solution as reported by Sommer and his coworkers[10].

$$(CH_3)_3SiCH_2CH_2X \xrightarrow{OH^-} (CH_3)_3SiOH+CH_2=CH_2+X^-$$

$$(CH_3)_3SiCHXCH_2X \xrightarrow{OH^-} (CH_3)_3SiOH+CH_2=CHX+X^-$$

**Cleavage Reaction of Vinyl-Silicon Bond.**—The vinyl-silicon bond in vinyltrimethylsilane was cloven by concentrated sulfuric acid giving ethylene and trimethylsilyl sulfate similarly to the allyl-silicon bond in allyltrimethylsilane[3]. But the reaction was slow compared with that of allyltrimethylsilane. In these reactions a proton seems to add to $\alpha$-carbon leaving a $\beta$-carbonium cation, which undergoes cleavage involving electron-release from silicon to the electronically deficient $\beta$-carbon. The resulting trimethylsilyl cation unites with sulfate anion.

$$H_2SO_4 \longrightarrow H^+ + HSO_4^-$$

$$(CH_3)_3SiCH=CH_2+H^+ \longrightarrow (CH_3)_3Si-CH_2-CH_2^+$$

$$(CH_3)_3Si\text{-}CH_2-CH_2^+ \longrightarrow (CH_3)_3Si^+ + CH_2=CH_2$$

$$2(CH_3)_3Si^+ + SO_4^{--} \longrightarrow [(CH_3)_3Si]_2SO_4.$$

Cleavage of the vinyl-silicon bond was also attempted by methanolic potassium hydroxide. But contrary to allyltrimethylsilane[3], the expected evolution of ethylene as a reaction product was hardly detected, and starting materials were recovered, indicating that almost no reaction had occurred. In this case, the nucleophilic attack on the electropositive silicon is prevented by the mutual action between the trimethylsilyl and the directly bonded C=C double bond as will be discussed later.

**Consideration on the Reaction Mechanisms.**—At present it is postulated[11] for the mechanism of the ionic addition to the C=C

5) L.H. Sommer, *U.S.P.*, 2,605,273 (1952).
6) C. Tamborski and H.W. Post, *J. Org. Chem.*, **17**, 1397 (1952).
7) C.L. Agre and W. Hilling, *J. Am. Chem. Soc.*, **74**, 3895, 3899 (1952).
8) G. H. Wagner, D. L. Bailey, A. N. Pines, M. L. Dunham and D. B. McIntire, *Ind. Eng. Chem.*, **45**, 367 (1953).
9) E. Larsson, *Trans. Chalmers Univ. Technol.*, No. 115, 25 (1951).
10) L.H. Sommer, E.H. Dorfman, G.M. Goldberg and F.C. Whitmore, *J. Am. Chem. Soc.*, **68**, 488 (1946); ibid., **68**, 1083 (1946).
11) Dewar, "The Electronic Theory of Organic Chemistry", (1949), p. 143.

double bond that a positive part of the reagent makes a complex with $\pi$-electron pair and then combines to electron-rich carbon, forming a carbonium cation which unites with a negative part of the reagent. Both these results of the non-Markownikoff addition of hydrogen halides to vinyltrimethylsilane and cleavage reactions of this compound by concentrated sulfuric acid described above, provide clear evidence for the addition of a proton to $\alpha$-carbon forming a $\beta$-carbonium cation intermediately. This addition of proton to $\alpha$-carbon is thought to result from electronic polarization of vinyltrimethylsilane as follows.

$$(CH_3)_3Si-\overset{\delta-}{C}H=\overset{\delta+}{C}H_2$$

But such an electronic polarization is inconsistent with an established inductive effect of electron-release, relative to alkyl for trimethylsilyl, $Me_3Si$[12,13].

Larsson[9] pointed out the similarity between vinyltriethylsilane and acrylic acid toward hydrogen chloride or bromide. Hydrogen halide adds to $\alpha$, $\beta$-unsaturated carbonyl compounds such as acrylic acid to give $\beta$-halogeno-compounds in the absence or presence of a peroxide catalyst. And this is explained by the limit formula of resonance hybrids of these compounds as follows.

$$-CH=CH-C=O \longleftrightarrow -\overset{+}{C}H-CH=C-\overline{\underline{O}}|^-$$

For the resonance hybrids of vinyl and allyl silicon compounds, the following limit formulae may be considered (left for vinyl and right for allyl compounds).

| | | |
|---|---|---|
| I | $CH_2=CH-Si$ | $CH_2=CH-CH_2-Si$ |
| II | $\dot{C}H_2-\dot{C}H-Si$ | $\dot{C}H_2-\dot{C}H-CH_2-Si$ |
| III | $CH_2^+-CH^--Si$ | $CH_2^+-CH^--CH_2-Si$ |
| IV | $CH_2^--CH^+-Si$ | $CH_2^--CH^+-CH_2-Si$ |
| V | $CH_2=CH^-\ Si^+$ | $CH_2=CH-CH_2^-\ Si^+$ |
| VI | $CH_2=CH^+\ Si^-$ | $CH_2=CH-CH_2^+\ Si^-$ |
| VII | $CH_2^+-CH-Si^-$ | $CH_2=CH^+\ CH_2=Si^-$ |

Among the last three formulae involving the interaction with silicon atom, V is considered to make a larger contribution to the structures of the compounds than VI, due to the smaller electro-negativity of silicon relative to carbon[14], and a possibility of hyperconjugation of three methyl groups in the resulting trimethylsilyl cation as follows[15].

$$\begin{array}{ccc} CH_3 & & CH_2H^+ \\ | & & \| \\ {}^+Si-CH_3 & \longrightarrow & Si-CH_3 \\ | & & | \\ CH_3 & & CH_3 \end{array}$$

Further, V seems to make a larger contribution to the structures of allyl compounds than to those of vinyl compounds for its allylic resonance as shown below.

$$CH_2=CH-CH_2^- \longleftrightarrow CH_2^--CH=CH_2$$

VII corresponds to the structures of $\alpha$, $\beta$-unsaturated carbonyl compounds and it is considered that the silicon has the tendency to expand its valence shell by the interaction of the $3d$ orbitals of silicon with $\pi$-electrons of C=C double bond and to place ten electrons around it. But this interaction is prevented by the shielding effect of a methylene group between silicon and C=C double bond in allyl silicon compounds, and contribution of VII to the structures of allyl silicon compounds seems therefore to be small.

It is explained by these two structures, i.e. V and VII, that a proton adds to $\alpha$-or $\gamma$-carbon for vinyl or allyl compounds respectively and give $\beta$-carbonium cation. It unites with a halogen anion to give $\beta$-halogeno-compound as an addition product, or it undergoes cleavage involving electron-release from silicon to electronically deficient $\beta$-carbon by the stronger action of the sulfate anion than the halogen anion, then the resulting trimethylsilyl cation unites with sulfate anion to give trimethylsilyl sulfate and ethylene as cleavage products.

In the case of the reaction with potassium hydroxide, the nucleophilic attack on electropositive silicon having a tendency to expand its valence shell is postulated[3]. This nucleophilic attack on silicon is accelerated by structure V, but prevented by structure VII because of the electronegative silicon whose valence shell is already expanded in this structure. It seems to be the reason why vinyltrimethylsilane did not react with methanolic potassium hydroxide contrary to allyltrimethylsilane, because the contribution of V is smaller and that of VII is larger in vinyl than allyl compounds.

Sommer and his coworkers reported that hydrogen chloride added to isopropenyltrimethylsilane to give $\alpha$-chloroisopropyltrimethylsilane as an addition product[4], and isopropenyltrimethylsilane reacted with concentrated sulfuric acid to give *tert*-butyldimethylsilanol hemi-hydrate after treatment with water, as an intramolecular rearrangement product[16], both indicating addition of

12) H. Gilman and G. E. Dunn, *Chem. Res.*, 52, 77 (1953).

13) (a) L.H. Sommer, J.R. Gold, C.M. Goldberg and N.S. Marans, *J. Am. Chem. Soc.*, 71, 1509 (1949); (b) L.H. Sommer and J. Rockett, ibid., 73, 5130 (1951).

14) Pauling, "The Nature of the Chemical Bond", (1940), p. 58—70.

15) A similar hyperconjugation was proposed by Yakubovich, et. al., (*Uspekhi Khim. S.S.S.R.*, 18, 46 (1949)) to explain the C—Si bond distance in methylchlorosilanes.

16) L.H. Sommer and F.J. Evans, *J. Am. Chem. Soc.*, 76 1030 (1954).

a proton to the terminal methylene group of the olefinic grouping to give $\alpha$-carbonium cation intermediately. These reactions are explained by considering that a resonance structure such as V or VII is overcome by introduction of a single $\alpha$-methyl having a possibility of hyperconjugation as follows.

$$CH_2=C(CH_3)-Si \longleftrightarrow {}^{-}CH_2-C(=CH_2H^{+})-Si$$

They reported also that $\beta$-chlorovinyltrimethylsilane gave no $\beta$-elimination on titration with dilute alkali, in contrast with saturated $\beta$-halogenoalkyl compounds[4]. This evidence is explained by considering the resonance structure similar to VII as shown below.

$$Cl-CH=CH-Si \longleftrightarrow {}^{+}Cl=CH-CH=Si^{-}$$

Petrov[17] reported that hydrogen bromide added to isobutenyltrimethylsilane to give $\beta$-bromoisobutyltrimethylsilane. This is also explained by considering resonance structrures such as V or VII, and VII is further conjugated with the two methyl groups bonded to $\beta$-carbon as follows.

$$(CH_3)_2C=CH-Si \longleftrightarrow (CH_3)_2C=CH\ Si \longleftrightarrow H^{+}CH_2-C(CH_3)_2-CH=Si$$

Many reactions of vinyl, allyl and other related organosilicon compounds are able to be explained by the two resonance structures discussed above. These two structures were postulated by several authors[18,19], but Gilman and Dunn[11] considered it unlikely that organosilicon compounds received significant contributions from resonance structures involving silicon-carbon double bond as VII.

Recently the resonance structures involving a silicon-carbon double bond as VII was postulated for nitration of trimethylsilylbenzene by Speier[20] and for Hammett's $\sigma$-values of p-trimethylsilyl-phenol, aniline and dimethylaniline by Benkeser and Krysiak[21]. Sommer and his coworkers pointed out this limited non-inductive effect of trimethylsilyl in vinyltrimethylsilane similarly to the consideration in this paper.

Further evidence for this resonance structure was obtained from infrared and Raman spectra of these compounds. Petrov and Nikishin[17] reported on a characteristic absorption band due to the $\nu_{C=C}$ vibrational mode at 1620 cm.$^{-1}$ in the infrared absorption spectra of isobutenyltrimethylsilane, and Egorov and Bazhulin[22] reported on a similar band at 1591 cm.$^{-1}$ for vinyltriethylsilane. In a previous paper[1] it was reported that the characteristic absorption band due to the $\nu_{C=C}$ vibrational mode was found at 6.29–6.30 $\mu$ (1590–1587 cm.$^{-1}$) in the infrared spectra of four vinylsilanes, i.e. vinyltrimethylsilane, divinyldimethylsilane, vinyltriethylsilane and vinyldimethylphenylsilane[23]. In the present study, the same band at 1590 cm.$^{-1}$ was also observed with Raman spectrum of vinyltrimethylsilane.

It is postulated that $\nu_{C=C}$ is primarily dependent upon the C=C streching force constant and is therefore lowered by conjugation, showing a shift of $\nu_{C=C}$ from the standard position, ca. 1650 cm.$^{-1}$, to longer wave length[24].

The observed shift of $\nu_{C=C}$ in these vinyl or isobutenyl silanes, provides a clear evidence of the presence of conjugation such as in structure VII in these compounds, as in the case of conjugated nitriles[25], ketones and esters of $\alpha$, $\beta$-unsaturated acids[26]. Studies of the conjugation of vinyltrimethylsilane by electron diffraction and dipole moment measurement are under way.

**Polymerization Reactions.**—The four vinylsilanes synthesized in a previous study[1] did not seem to be polymerized by heating for twenty four hours at 150° in the presence of benzoyl or acetyl peroxide[2]. (For details see the experimental part of the present paper). It was already reported by Ushakov and Itenberg[27] that vinyltriethylsilane was not polymerized by heating in the presence of a peroxide catalyst.

Recently Wagner and his coworkers[8] reported polymerization of vinyltrichlorosilane and vinyl triethoxysilane at high temperature in the presence and absence of a peroxide

17) A.D. Petrov and G.I. Nikishin, *Doklady Akad. Nauk, S.S.S.R.*, **93**, 1049 (1953).
18) J.D. Roberts, E.A. McElhill and R. Armstrong, *J. Am. Chem. Soc.*, **71**, 2923 (1949).
19) H. Soffer and T. De Vries, ibid., **73**, 5817 (1951).
20) J.S. Speier, ibid., **75**, 2930 (1953).
21) R.A. Benkeser and H.R. Krysiak, ibid., **75**, 2421 (1953).
22) Yu. P. Egorov and P.A. Bazhulin, *Doklady Akad. Nauk S.S.S.R.*, **88**, 647 (1953).
23) The characteristic bands at 9.94—9.99 $\mu$, and 10.50—10.54 $\mu$ in the spectra of the four vinylsilanes reported in a previous paper[1], are considered to be assigned to the out-of-plane bending vibrational mode of H in the ethylene group according to the results of Davison and Bates[24].
24) W.H.T. Davison and G.R. Bates, *J. Chem. Soc.*, **1953**, 2607.
25) Sheppard and Sutherland, ibid., **1947**, 453; Kitson and Griffith, *Anal Chem.*, **24**, 334 (1952).
26) Hartwell, Richards and Thompson, *J. Chem. Soc.*, **1948**, 1436.
27) S.N. Uschakow and A.M. Itenberg *Zhr. Obshchei Khim. S.S.S.R.*, **7**, 2495 (1937).

catalyst or a Friedel-Crafts type catalyst such as aluminum chloride. There was obtained a low molecular weight polymer consisting mainly of tetramers, by heating at 290° without a catalyst or by heating 50–90° with a Friedel-Crafts type catalyst. But with a peroxide catalyst the formation of polymer was very small. And a high molecular weight polymer was not obtained in all cases.

In view of the conflicting evidence as to the ability of vinylsilanes to polymerize, it seemed of importance to reinvestigate the subject. In the present study, therefore, the radical polymerization of vinyltrimethylsilane with peroxide or $\alpha$, $\alpha'$-azodiisobutyronitrile as a catalyst and the cationoid polymerization of the same compound with a Friedel-Crafts type catalyst were investigated. Contrary to vinyltrichlorosilane, vinyltrimethylsilane gave no polymer by the cationoid polymerization and gave a small amount of low molecular weight polymer by the radical polymerization. No high molecular weight polymer was obtained from vinyltrimethylsilane.

The absence of high molecular weight polymers in the product from vinyltrichloro- or vinyltrimethyl-silane seems to result from the steric hindrance of the large trisubstituted silyl group in the structural unit of the polymer, $-CH_2CH_2-$ (X=Cl, Me, Et), as

$$\begin{array}{c} \\ | \\ SiX_3 \end{array}$$

shown in Fig. 1. The presence of a polymer of relatively high molecular weight in the product from vinyltriethoxysilane seems to be explained by the free rotation of the ethoxy group around Si—O bond as shown in Fig. 2.[28]

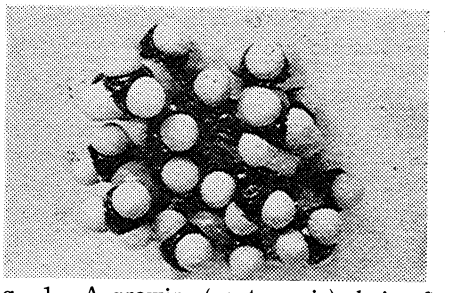


Fig. 1. A growing (pentameric) chain of polymerizing vinyltrimethylsilane. Further addition seems to be very difficult.

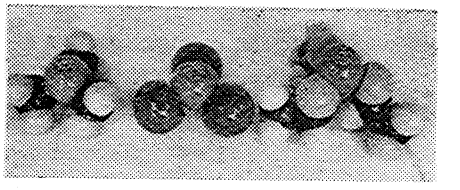


Fig. 2. Comparison of steric effect of tri-substituted silyl group. (left to right: trimethylsilyl, trichlorosilyl and triethoxysilyl group).

The extent of a group bonded to silicon in the neighboring space around silicon is able to be made the smallest in triethoxysilyl by the free rotation of the ethoxy group around Si-O bond.

Further studies on polymerization and other reactions of vinylsilanes are being continued now in this laboratory.

## Experimental

**Addition Reactions.**—Products of addition reactions to the double bond of vinyltrimethylsilane are listed in Table I.

TABLE I

| Reagent | Catal. | Product $Me_3Si-$ | Yield % | m.p. °C | b.p. °C | b.p. mm. | $d_4^{20}$ | $n_D^{20}$ | Mol. ref. Calcd. | Mol. ref. Found | Titratable halogen % Calcd. | Titratable halogen % Found |
|---|---|---|---|---|---|---|---|---|---|---|---|---|
| $H_2$ | Pt | $CH_2CH_3$ a) | 70 | | 62–4 | 760 | 0.6839 | 1.3821 | 34.91 | 34.80 | | |
| $Cl_2$ | | $CHClCH_2Cl$ b) | 76 | −16 | 67–9 | 20 | 1.0586 | 1.4608 | 44.59 | 44.37 | 20.72 | 21.2 j) |
| $Br_2$ | | $CHBrCH_2Br$ c) | 90 | −7 | 62–3 | 4 | 1.5321 | 1.5062 | 50.27 | 50.45 | 30.73 | 33.5 j) |
| $HSiCl_3$ | $Ac_2O_2$ | $CH_2CH_2SiCl_3$ d) | 90 | −18 | 94–6 | 50 | 1.1062 | 1.4473 | 57.32 | 56.96 | 45.13 | 45.0 |
| HBr | | $CH_2CH_2Br$ e) | 65 | | 50–2 | 21 | 1.1481 | 1.4562 | 42.59 | 42.91 | 44.11 | 44.1 |
| HBr | $Ac_2O_2$ | $CH_2CH_2Br$ e) | 72 | | 49 | 19 | 1.1489 | 1.4556 | 42.59 | 42.86 | 44.11 | 44.6 j) |
| HBr | $Bz_2O_2$ | $CH_2CH_2Br$ e) | | | 35–45 g) | 20 | 1.1483 | 1.4560 | 42.59 | 42.89 | 44.11 | 45.4 j) |
| HBr | Catechol | $CH_2CH_2Br$ e) | | | 33–47 g) | 20 | 1.150 | 1.4568 | 42.59 | 42.88 | 44.11 | 44.5 j) |
| HI | | $CH_2CH_2I$ f) | | | 53–5 | 10 | 1.3976 | 1.4950 | 47.77 | 47.61 | 55.62 | 57.3 j) |

(a) b.p. 62°C (760 mm.), $d_4^{20}$ 0.6849, $n_D^{20}$ 1.3820.[29] (b) b.p. 61°C (14 mm.), $d_4^{20}$ 1.0537, $n_D^{20}$ 1.4617, m.p. −15°C.[4,30] (c) b.p. 74–5°C (8 mm.), $d_4^{20}$ 1.5497, $n_D^{20}$ 1.5095, m.p. −9–11°C.[4] (d) Reported in a previous paper.[1] (e) b.p. 64–5°C (39 mm.), $d_4^{20}$ 1.1499, $n_D^{20}$ 1.4575.[4] (f) b.p. 76–76.5°C (27 mm.), $d_4^{20}$ 1.3862, $n_D^{20}$ 1.5008.[4] (g) Decomposition occurred. (h) To a solution of the sample in methanol, there was added N/5 NaOH aq. solution and back titrated by N/10 HCl with phenol phthalein as an indicator. (i) Calculated for a halogen bonded to $\beta$-carbon or silicon. (j) This high halogen value seems to result from decomposition during distillation or preservation.

28) B.A. Arbuzov and T.G. Shavsha, *Doklady Akad. Nauk S.S.S.R.*, 68, 859 (1949); C. A., 44, 886 (1950).
29) F.C. Whitmore, L.H. Sommer, et. al., *J. Am. Chem. Soc.*, 68, 475 (1946).
30) L.H. Sommer, U.S.P., 2,605,273 (1952).

**1. Hydrogenation.**—A solution of 6.84 g. of vinyltrimethylsilane in 150 cc. of glacial acetic acid was shaken with hydrogen for two hours in the presence of 0.1 g. of platinum oxide catalyst. The absorption of hydrogen took about two hours, being very fast during the middle period of twenty minutes. At the end the volume of absorbed hydrogen was 1444 cc. (including 18 cc. used for reduction of the catalyst), corresponding to 1.013 mole per mole of vinyltrimethylsilane. The reaction product was separated from the catalyst by filtration, then a fraction boiling up to 90° was collected upon fractionation. Twenty grams of toluene was added to the fraction and washed with 10% sodium bicarbonate solution and water. After drying over calcium chloride, the fractionation of the product gave ethyltrimethylsilane as shown in Table I.

**2. Halogenation.**—Ten grams (0.1 mol.) of vinyltrimethylsilane was cooled to −70° in a bath of dry ice and acetone, then a theoretical amount of bromine was added drop by drop or a theoretical amount (from weight increase) of chlorine was bubbled with shaking. Toward the end of the reaction white crystals of the product were observed. Upon warming to room temperature, the product was fractionated and α, β-dibromo- or dichloro-ethyltrimethylsilane was obtained as shown in Table I.

**3. Addition of Hydrogen Bromide.**—In a test-tube equipped with gas inlet and outlet tubes, there was placed 10 g. (0.1 mol.) of vinyltrimethylsilane. Hydrogen bromide gas dried with phosphorus pentoxide was introduced in the first experiment, but 0.1 g. of peroxide or catechol was added prior to the introduction of HBr in the other three experiments. The reaction mixture was warmed slightly for ten minutes to initiate the reaction and cooled to −70° in a bath of dry ice and acetone, then saturated with a theoretical amount of HBr. Standing overnight up to room temperature, the reaction mixture was fractionated giving β-bromoethyltrimethylsilane as shown in Table I.

**Decomposition of β-Bromoethyltrimethylsilane.**—The β-bromoethyltrimethylsilane thus obtained was very unstable and decomposed by slight heating in distillation or other treatment, and with a catalytic action of a surface of unglazed porcelain or ground glass it decomposed even at room temperature. In a flask fitted with a reflux condenser and a gas outlet tube at the top, containing a few small pieces of unglazed porcelain such as boiling chips, there was added β-bromoethyltrimethylsilane. At once a vigorous reaction occurred and almost half of the sample was lost. Then the remaining liquid was heated slowly on a water bath, a reaction occurred at 40–45°, and ethylene gas was evolved. Ethylene was identified by convertion to ethylene dibromide, $n_D^{15}$ 1.5392. The residue was fractionated and trimethylbromosilane boiling at 80.5–81.0° was obtained, this was converted to disiloxane, $n_D^{17}$ 1.3784.

**4. Addition of Hydrogen Iodide.**—In a test-tube equipped with gas inlet and outlet tubes, there was placed 10 g. (0.1 mol.) of vinyltrimethylsilane. Hydrogen iodide gas dried with phosphorus pentoxide was introduced in the test-tube cooled to −30° in a bath of dry ice and acetone. After a theoretical increase in weight had taken place, the reaction mixture was allowed to be warmed slowly to room temperature and it was fractionated, giving β-iodoethyltrimethylsilane as shown in Table I.

**Cleavage Reactions 1. With Concentrated Sulfuric Acid.**—In a test-tube equipped with a gas outlet tube, there was placed 3 g. of vinyltrimethylsilane and 1.5 g. of conc. $H_2SO_4$ and cooled to −20° in a bath of dry ice and acetone. But almost no reaction occurred at this temperature. Then the reaction mixture was warmed to room temperature (15–20°) with shaking, the reaction proceeding slowly with the evolution of ethylene gas. The ethylene was absorbed by carbon tetrachloride solution of bromine. The reaction became rapid gradually, and the upper layer of vinyltrimethylsilane decreased, while the lower layer of sulfuric acid increased conversely. The reaction became more and more vigorous and the temperature rose to about 40° in the course of four hours, toward the end of which the reaction mixture became homogeneous. It was cooled to 10° and gradually warmed up to 20°. After about six hours the reaction came to the end and no more ethylene was evolved. The carbon tetrachloride solution was fractionated and 3 g. of ethylene dibromide was obtained, $n_D^{15}$ 1.5410 (after washing with $H_2O$ and drying with $CaCl_2$), about 50% yield. The residue was solidified by cooling and melted at 46–51°; it therefore seems to be crude trimethylsilyl sulfate, of which the melting point of a pure specimen is reported to be 56–58°[31].

**2. With Methanolic Potassium Hydroxide.**—In a 50 cc. flask equipped with a reflux condenser and a gas outlet tube at the top, there were placed 10 g. (0.1 mol.) of vinyltrimethylsilane, 12 g. (ca. 0.2 mol.) of KOH and 10 g. of methanol. The mixture was heated at the reflux temperature for 15 hrs., but the evolution of a gaseous product was hardly detected. The reaction mixture was distilled rapidly at a reduced pressure. Upon fractionation of the distillate, 9.5 g. of an azeotrope of methanol and vinyltrimethylsilane, b.p. 44.3° $n_D^{20}$ 1.3865, and a mixture of methanol and vinyltrimethylsilane, b.p. 46–60°, $n_D^{20}$ 1.3350, were obtained. Neither trimethylmethoxysilane (in an azeotrope with methanol) nor trimethylsilanol was obtained. The azeotrope was further characterized by an independent preparation as follows. A mixture of 5 g. of vinyltrimethylsilane and 5 g. of methanol was distilled through a distillation column of about 10 theoretical plates. A fraction boiling at 44.3°, $n_D^{20}$ 1.3860 was obtained, but the ratio of

31) L.H. Sommer, et. al., *J. Am. Chem. Soc.*, 68, 156 (1946). Sommer, et. al.[3] reported m.p. 49—52° for a crude one.

two components was not determined.

**Polymerization Reactions 1. Polymerization of vinylsilanes on a small scale.**—A half gram of each three vinylsilanes, i.e. trimethylvinylsilane, dimethyldivinylsilane, and dimethylphenylvinylsilane, was heated at 100° or 150° for 24 hours in a sealed glass tube in the presence of 10 mg. of acetyl or benzoyl peroxide. But neither solidification nor increase of viscosity was found even in the case of divinyldimethylsilane, indicating that no polymerization occurred.

**2. Polymerization of Vinyltrimethylsilane.**—The conditions of polymerization of vinyltrimethylsilane and properties of the polymers are shown in Table II.

TABLE II

POLYMERIZATION OF VINYLTRIMETHYLSILANE

| Catalyst | Yield % | Polymer Fraction | B.p. °C. | B.p. mm. | $n_D^{20}$ | Mol.[c] Weight | Analytical Data C% Calcd.[d] | C% Found | H% Calcd.[d] | H% Found |
|---|---|---|---|---|---|---|---|---|---|---|
| $Bz_2O_2$-$Ac_2O_2$ | 15 | I. | 100–104 | 8–9 | 1.4593 | 360 | 59.91 | 61.20 | 12.07 | 11.86 |
| | | II. | 120–140 | 3 | 1.4698 | 460 | 59.91 | 61.12 | 12.07 | 11.69 |
| | | residue | | | 1.4780 | 550 | 59.91 | 60.25 | 12.07 | 11.76 |
| Azonitrile[a] | 10 | I. | 80–100 | 3–10 | 1.4474 | 400 | 59.91 | 61.01 | 12.07 | 11.73 |
| | | II. | 100–130 | 2 | 1.4568 | 350 | 59.91 | 63.63 | 12.07 | 12.07 |
| | | residue | | | 1.4763 | 1000 | | | | |
| $AlCl_3$ | 2 | | | | | | | | | |
| $BF_3$[b] | 0 | | | | | | | | | |

a) α, α'-Azodiisobutyronitrile $CH_3(CH_3)C(CN)-N=N-C(CN)(CH_3)CH_3$ was used. b) used as an addition compound with diethylether. c) obtained by Rast method, but these values are very rough. d) calculated for $(C_5H_{12}Si)n$

**With Acetyl Peroxide and Benzoyl Peroxide Mixture.**—In a sealed glass tube there were placed 20 g. (0.2 mol.) of vinyltrimethylsilane, 0.12 g. (0.5 mol.%) of diacetyl peroxide, and 0.24 g. (0.5 mol.%) of dibenzoyl peroxide. The tube heated at 150–5° for 24 hours. Unreacted vinyltrimethylsilane was recovered at atmospheric pressure. The precipitated crystals of benzoic acid were filtered, recrystalized, m.p. 117–8°, mixed m.p. to be 117.5–9.0°. The filtrate was fractionated under reduced pressure to give fractions as shown in Table II.

**With Other Catalysts.**—Similarly to the case with the peroxide catalyst, all catalyst were used in amount of 1 mole % to vinylsilanes. But heating at 150° for boron trifluoride and 120° for α, α'-azodiisobutyronitrile and aluminum chloride was employed. As in the case of azonitrile, tetramethylsuccinonitrile was isolated as a decomposition product of the catalyst, m.p. 165.5–6.5°, mixed m.p. 165.5–7.0°. In the case with boron trifluoride and aluminum chloride almost no polymer was obtained.

## Summary

1) Addition reactions to the double bond of vinyltrimethylsilane were studied with hydrogen, bromine, chlorine, hydrogen bromide and iodide, and the properties of the products were given.

2) Vinyl-silicon bond was cloven by concentrated sulfuric acid but no reaction occurred with methanolic potassium hydroxide.

3) Reaction mechanisms of the above two reactions of vinyl, allyl or related unsaturated organosilicon compounds were discussed. A conjugated structure involving silicon-carbon double bond in which the silicon atom has an expanded valence shell was postulated for some of these reactions. Such a structure was further confirmed by the shift of $\nu_{C=C}$ in the absorption spectra of vinyltrimethylsilane.

4) Polymerization reactions of this compound were studied and the steric hindrance by a large trimethylsilyl group in the structural unit of the polymer was discussed, particularly concerning the absence of a high molecular weight polymer in the reaction product.

The author wishes to express his sincere thanks to Dr. O. Simamura and Dr. T. Yamada for their kind advice and encouragement during this work. The author is also indebted to Mr. I. Tsuchiya for the Raman spectra reported in this paper and to Mr. M. Takakusa for his assistance during this work.

*Electrotechnical Laboratory, Agency of Industrial Science and Technology, Nagata-cho, Chiyoda-ku, Tokyo*

# *Influence of the Addition of High Molecular Electrolyte upon the Absorption Spectra and Fluorescence of Organic Dyestuffs. IV.**

By Noboru MATAGA and Masao KOIZUMI

(Received July 19, 1954)

## Introduction

In the earlier papers[1,2,3] of this series, the present authors have investigated the influence of the addition of high molecular electrolyte upon the absorption spectra and fluorescence of basic dyes. The conclusion then reached was that for the interpretation of metachromasy, the change of aggregation of dye ions caused by the addition of high molecular electrolyte is of primary importance rather than the direct interaction between dye and high molecular electrolyte.

Now, an investigation has been made with acidic dyes which, in contrast to basic dyes, have little tendency to associate in the aqueous solution and accordingly obey Beer's law quite well. The influence upon absorption spectra and fluorescence of such dyes caused by the addition of basic electrolytes of various molecular weights was examined in order to confirm our previous conclusion more definitely.

The acidic dyes examined were uranine, eosine and erythrosine, and the following basic electrolytes were used: a) chitosan hydrochloride b) glucosamine hydrochloride and c) several aliphatic amines of different chain length.

As the result of the investigation using various combinations of dyes and electrolytes, it was found that the data can be interpreted along the same reasoning as before, and the phenomenological interrelation has now become more comprehensive.

The present paper reports in a rather abbreviated form some experimental results and the discussions based upon them. The details will be published in J. Inst. Polytech. Osaka City Univ.

## Experimental Results

Beckman spectrophotometer model D.U. was used for the measurement of absorption spectra and the relative intensities of the fluorescence.

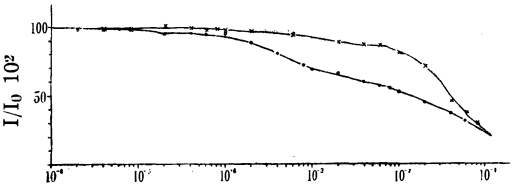
**Sample.**—Uranine (Merck) was purified by recrystallisation.

Glubler's eosine and erythrosine were used without further purification.

Chitosan hydrochloride and glucosamine hydrochloride were kindly supplied by Mr Kanji Okawa of the Institute of Cellulose Research of Osaka University.

Methylamine hydrochloride is of commercial supply, *n*-propylamine and *n*-dodecylamine hydrochloride were kindly supplied respectively by Mr. Shiro Morimoto and Shuji Saito of Osaka University.

**1) Uranine** *a) Chitosan hydrochloride.*— The absorption spectra and the relative intensity of fluorescence of the aqueous uranine solution containing various quantities of chitosan hydrochloride, are shown in Figs. 1 a and 2, respectively.




a. Chitosane hydrochloride (mol./*l.*) (log scale)
b. Glucosamine hydrochloride (mol./*l.*) (log scale)

Fig. 1. Change of relative fluorescence intensity of aqueous uranine solution by added chitosan hydrochloride, and glucosamine hydrochloride. Dye conc., $2\times10^{-5}$mol./*l*; temperature, 27°C.
○ a
× b

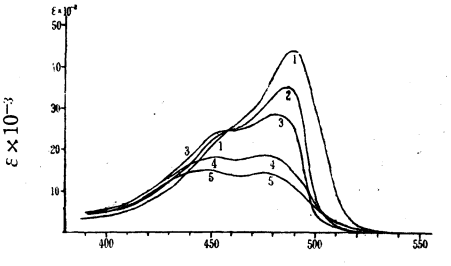



Fig. 2. Change of absorption spectrum of aqueous uranine solution by chitosane hydrochloride.
Dye conc. $2\times10^{-5}$mol./*l*. Temperature, 27°C. Quantity of added chitosane hydrochloride: (1) $0\text{–}4\times10^{-5}$mol./*l*. (2) $6\times10^{-5}$ mol./*l* (3) $8\times10^{-5}$mol./*l*. (4) $6\times10^{-4}$mol./*l*. (5) $2\times10^{-3}$mol./*l*.

* Physicochemical Studies of Organic Dyestuffs in Relation to Photochemistry. VI.

1) M. Koizumi and N. Mataga, This Bulletin, **26**, 115 (1952).
2) M. Koizumi and N. Mataga, ibid., **27**, 194 (1954).
3) N. Mataga and M. Koizumi, ibid., **27**, 197 (1954).

Up to $10^{-5}$ mol./*l*. (referred to a unit group with one amino group) of the added chitosan hydrochloride, no change is observed.

In the range between $-10^{-5}$ and $-10^{-4}$ mol./*l*., the intensity of fluorescence slightly decreases, while the absorption spectra change conspicuously in such a manner as to suggest the existence of an association equilibrium of some kind between chitosan hydrochloride and uranine.

Beyond $10^{-4}$ mol./*l*., quenching of fluorescence gradually increases and at the same time the intensity of absorption wholly decreases.

There is observed no phenomenon of recovery either in fluorescence or absorption, however much chitosan hydrochloride is added.

*b*) *Glucosamine hydrochloride*.—The variations of the relative fluorescence intensity and the change of absorption spectra when various quantities of glucosamine hydrochloride (a structural unit of chitosan hydrochloride) are added to the uranine solution, are shown in Figs. 1 b and 3.

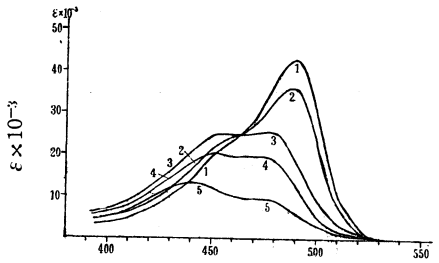



Fig. 3. Change of absorption spectrum of aqueous uranine solution by glucosamine hydrochloride.
Dye conc. $2\times10^{-5}$mol./*l*. Temperature 27°C. Quantity of added glucosamine hydrochloride (1) $0\sim10^{-4}$mol./*l*. (2) $6\times10^{-4}$mol./*l*. (3) $6\times10^{-3}$mol./*l*. (4) $2\times10^{-2}$ mol./*l*. (5) $6\times10^{-2}$mol/l.

Up to $10^{-4}$ mol./*l*., there scarcely exists any change either in fluorescence intensity or absorption spectra.

Between ca. $2\times10^{-4}$ mol./*l*. and ca. $10^{-2}$ mol./*l*., a slight decrease of fluorescence intensity is observed and quite similar changes of absorption spectra as those observed in the case of chitosan hydrochloride take place.

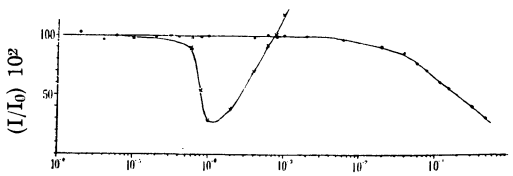
Beyond $10^{-2}$ mol./*l*., the intensity of fluorescence falls conspicuously and at the same time, the absorption spectra decline in the whole range of visible region. No phenomenon of recovery exists either in fluorescence or absorption.

*c*) *Aliphatic amino compounds*.—Only the result of methylamine will be described as a representative.

As small an addition as $2\times10^{-5}$ mol./*l*. causes a rapid increase in the intensity of absorption and from this region up to $10^{-1}$ mol./*l*. There exists a change of absorption spectra suggestive of an association equilibrium of some kind. No change of fluorescence intensity is observed.

Above $10^{-1}$ mol./*l*. both the intensity of fluorescence and absorption decreases quite remarkably, and the feature of this decrease is somwhat similar to the case of glucosamine hydrochloride.

**2) Eosine and Erythrosine** *a*) *Chitosan hydrochloride*.—The relative intensities of fluorescence and the absorption spectra when various quantities of chitosan hydrochloride are added to the aqueous solution of eosine, are shown in Figs. 4 b and 5.




a. Glucosamine hydrochloride (mol./*l*.) (log scale).
b. Chitosan hydrochloride (mol./*l*.) (log scale).

Fig. 4. Change of relative fluorescence intensity of aqueous eosine solution by added chitosane hydrochloride and glucosamine hydrochloride. Dye conc. $10^{-5}$mol./*l*. Temperature, 27°C.
○ a
× b

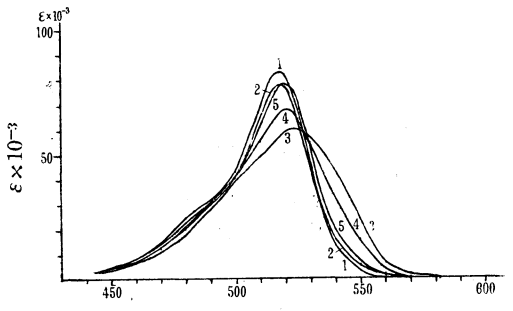



Fig. 5. Change of absorption spectrum of aqueous eosine solution by chitosane hydrochloride.
Dye conc. $10^{-5}$mol./*l*. Temperature, 27°C. Quantity of added chitosane hydrochloride. (1) $0\sim10^{-5}$mol./*l*. (2) $6\times10^{-5}$mol./*l*. (3) $10^{-4}$mol./*l*. (4) $4\times10^{-4}$mol./*l*. (5) $10^{-3}$ mol./*l*.

There occurs no change either in absorption or fluorescence untill the concentration of chitosan hydrochloride reaches about $10^{-5}$ mol./*l*.

Beyond this concentration, the fluorescence is quenched gradually and the absorption spectrum shifts toward red and somewhat broadens accompanied with the decrease of extinction.

Such a change becomes most prominent near $10^{-4}$ mol./*l*., but over this point a marked phenomenon of recovery comes to be observed both in absorption and fluorescence and when the concentration reaches $10^{-3}$ mol./*l*., the shape of the absorption curve becomes quite similar to that in the pure aqueous solution and the intensity of fluorescence exceeds to some extent, that of the pure aqueous solution.

In the case of erythrosine, the main features

of change of absorption spectra caused by the addition of chitosan hydrochloride, are quite similar as in the case of eosine.

*b) Glucosamine hydrochloride.*—The effects of glucosamine hydrochloride upon the relative intensity of fluorescence and absorption spectra of the aqueous eosine solution are shown in Figs. 4 a and 6.

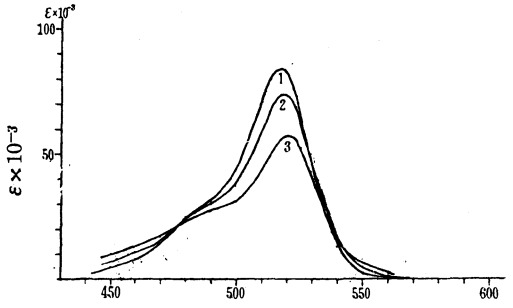



Fig. 6. Change of absorption spectrum of aqueous eosine solution by glucosamine hydrochloride.
Dye conc. $10^{-5}$mol./*l.*, Temp, 27°C. Quantity of added glucosaminehydrochloride.
(1) $0\text{–}6\times10^{-3}$mol./*l.*, (2) $8\times10^{-2}$mol./*l.*, (3) $3.36\times10^{-1}$mol./*l.*

No marked change is observed either in fluorescence or absorption below $10^{-2}$ mol./*l.*, but over this point the intensity of fluorescence gradually falls and the absorption also declines in the whole range.

Quite similar results were obtained for the absorption spectra of erythrosine.

*c) Aliphatic amino compounds.*—When methylamino hydrochloride is added to the aqueous eosine solution, there is no marked change either in fluorescence or absorption until the concentration reaches as much as ca. $4\times10^{-1}$ mol./*l.*, beyond which the intensity of fluorescence gradually falls accompanied with the decline of extinction in the entire region. The state of affairs for erythrosine is quite similar to eosine.

But in the case of dodecylamine hydrochloride, which is capable of forming micelle[4], quite different phenomena were observed, the changes both in fluorescence intensity and absorption curve are analogous to the case in which alkyl sulfate of long chain is added to basic dyes.

## Discussion

It can safely be concluded from the above results, that in the case of uranine there exists no action specific to high molecular electrolyte and the effects of the added electrolyte upon fluorescence and absorption are mainly due to the direct interaction between amino group and dye ion, most probably the ionic association.

Indeed, there is some difference between the effect of aliphatic amine and glucosamine or chitosan hydrochloride, but this is quite natural in view of the fact that aliphatic and ring compounds generally differ much in the property.

It may be worth adding here that in the case of uranine, the fluorescing power is not affected much by its association with amino group, since there is no marked change of intensity in the region where absorption spectra conspicuously change.

Now the state of affairs is quite different in the case of eosine and erythrosine; when the amino compounds of low molecular weight such as methylamine and glucosamine hydrochloride are added to the solution, no change suggestive of strong interaction between amino group and dye ion is perceived at all. Therefore, only a weak interaction due to ionic interaction or van der Waals' force will exist in this case. The conspicuous change of absorption and fluorescence intensity observed in the case of chitosan hydrochloride must accordingly be attributed to the specificity of high molecular substance. The intense quenching of fluorescence by dodecylamine and the phenomenon of recovery occurring prior to micelle formation must also be due to the same reason.

For the interpretation of these phenomena, it is quite natural to adopt the same reasoning as that used in the case of basic dyes; thus they are ascribed to the accumulation of dye ions around high molecular ions by virtue of the weak interaction between them. For example, quenching is produced by the increase of concentration of dye ions around high molecular electrolyte, while the recovery takes place because the accumulation of dye ions around high molecular electrolyte becomes less marked as the latter is increased. In fact, the concentration quenching of the pure aqueous solution of eosine was examined and found to be quite remarkable. The above explanation as it runs, is completely analogous to that applied to the similar phenomena observed when high molecular acidic electrolytes are added to basic dyes. It is an interesting problem to be settled why the interaction of amino group and dye ion is so strong in case of uranine while it is rather weak in eosine and erythrosine; perhaps steric hindrance due to Br and I would be an important factor for it, though the question must of course await further investigations.

Another important result obtained, which shows a sharp contrast to basic dyes, is that no such band as deserves to be called a metachromasy band appears in eosine-chitosan

4) M.L. Corrin and W.D. Harkins, *J. Chem. Phys.*, 14, 641 (1946).

hydrochloride, in spite of the marked accumulation of dye ions around high molecular electrolyte.

One cannot but attribute this difference to the fact that acidic dyes have scarcely any tendency to associate while basic dyes easily dimerise or polymerise. Thus our previous conclusion[1,2,3] that the phenomenon of metachromasy is mainly due to the change of aggregation of dye, conforms quite well with the present results. One may rather say that metachromasy is the conspicuous change of absorption spectra produced by the change of aggregation of dye ions accumulated around high molecular electrolyte when the interaction between dye and functional group of electrolyte is moderate.

## Summary

The relative intensity of fluorescence and the change of absorption spectra were examined when chitosan hydrochloride and other amine hydrochloride were added to the aqueous solution of uranine, eosine and erythrosine, which are all acidic and have no tendency to associate.

It was found that in the case of uranine, the interaction between amino group and the dye ion is so strong that it directly influences the absorption band remarkably, and thence the interaction is commonly observed irrespective of whether the molecular weight of electrolyte is high or low. In the case of eosine and erythrosine there exists no such strong interaction between amino group and dye ion because the amino compound of low molecular weight produces no marked change in either fluorescence or absorption; a quite notable change is observed in the case of the amino compounds of high molecular weight; thus for example, the fluorescence at first drops and then recovers as the concentration is increased. The phenomena were interpreted as due to the concentration effect of dye ions gathered around the electrolyte ion by weak attraction. This interpretation is quite analogous to that already applied for basic dyes.

There appeared, however, no metachromasy band and this was ascribed to the fact that the acidic dyes have scarcely any tendency to associate; thus our opinion put forth for the case of basic dyes, that the change of aggregation of dye ions is mainly responsible for metachromasy, was confirmed once more in the case of acidic dyes.

The authors express their hearty thanks to Mr. Okawa, Mr. Morimoto, and Mr. Saito, who gave them the valuable sample. A part of the experiment was done by Mr. S. Oi to whom the authors' thanks are also due.

A part of the expense has been defrayed from a grant by the Ministry of Education.

*Institute of Polytechnics, Osaka City University, Osaka*

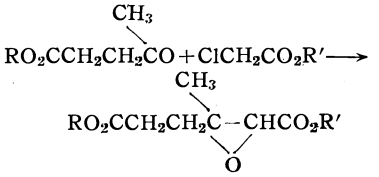
# *New Derivatives of Levulinic Acid. I.*[1] *Synthesis of 2,3-Epoxy-3-Methyladipic Esters*

By Eturô MAEKAWA, Masako MIZOGUCHI* and Yoshio ISHII

(Received August 21, 1954)

Glycidic esters, namely 2, 3-epoxy esters, are easily obtained by the condensation of carbonyl compounds with $\alpha$-halo esters[2]. Many types of ketones have been reported to give good yields smoothly. Nevertheless, previous investigations of analogous reactions of keto-esters have not been extended beyond the synthesis of $\gamma$-lactones by zinc from ethyl levulinate[3] and 3, 3-dimethyllevulinate[4] with ethyl monobromoacetate.

This investigation was undertaken to synthesize glycidic esters, viz. 2, 3-epoxy-3-methyladipic esters, from levulinic and monochloroacetic esters as represented in the following equation:



1) Presented at the 7th Annual Meeting of the Chemical Society of Japan, Tokyo, April 2, 1954.

2) M. S. Newman, *Org. Reactions*, **5**, 413 (1949), a review.

3) H. E. Baumgarten, *J. Am. Chem. Soc.*, **75**, 979 (1953).

4) H. E. Baumgarten and W. P. Schneider, *J. Org. Chem.*, **16**, 1658 (1951).

*n*-Butyl (I), 2-ethylhexyl and lauryl levulinates were used as a carbonyl component, *n*-butyl (I′), 2-ethylhexyl and lauryl monochloroacetates as halo ester, and sodium methoxide, sodium ethoxide, potassium *tert.*-butoxide[5] and sodium amide as a condensing agent. The synthesis of these glycidic esters was conducted by a slightly modified procedure of the standard Darzens glycidic synthesis.

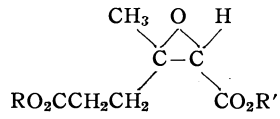
The results are presented in Table I. On the basis of the saponification value and quantitative elemental analysis, it seems reasonable to assume that the products, obtained by the use of potassium *tert.*-butoxide and sodium amide as the condensing agent, are the desired 2, 3-epoxy-3-methyladipic esters, which have not yet been reported in literature. In the case of these two di-*n*-butyl esters, the observed values of molecular refraction are higher by about 0.7 than the calculated value. From consideration of the case of cyclopropane (exaltation is known as +0.7) this exaltation seems to be attributed to the existence of a three-membered oxirane ring neighbouring a carboxyl group.

The epoxy contents of these glycidic esters were determined by Swern's method[6]. The observed epoxy contents of these epoxy esters, however, were about one third of the calculated values, while the observed epoxy content of 2, 3-epoxylauric acid[7] and the observed iodine values for 2, 3-unsaturated acids show also similar results. Therefore the low observed values are probably due to some effect of the neighbouring carboxyl group.

Slight differences are observed between the properties of the two di-*n*-butyl esters, obtained by potassium *tert.*-butoxide and sodium amide respectively, while the esters obtained by sodium amide have a tendency to turn yellow if kept. Therefore these differences may be due to some impurities.

TABLE I

2, 3-Epoxy-3-methyladipates




| R | R′ | Condensing agent | Yield % | b. p. | S. V. Calcd. | S. V. Found | $n_D^{20}$ | Analytical C% Calcd. | C% Found | H% Calcd. | H% Found |
|---|---|---|---|---|---|---|---|---|---|---|---|
| *n*-Butyl | *n*-Butyl | $NaNH_2$ | 17 | 148-149°/1.5 mmHg | 391.8 | 395.9 | 1.4478 | 62.91 | 62.80 | 9.15 | 9.20 |
| „ | „ | *tert.*-BuOK | 48 | 189-191°/15 mmHg | „ | 389.1 | 1.4458 | „ | 62.56 | „ | 9.25 |
| „ | 2-Ethyl-hexyl | $NaNH_2$ | (11) | 163-165°/1 mmHg | 327.6 | 322.2 | 1.4537 | 66.63 | 66.50 | 10.01 | 10.10 |
| 2-Ethyl-hexyl | *n*-Butyl | „ | (10) | 159°/1 mmHg | 327.6 | 322.5 | 1.4532 | 66.63 | 66.80 | 10.01 | 10.15 |
| „ | 2-Ethyl-hexyl | „ | ( 8) | ca. 160°/0.1 mmHg | 281.5 | 285.0 | 1.4599 | 69.31 | 69.01 | 10.62 | 10.66 |
| *n*-Butyl | Lauryl | „ | (24) | ca. 190°/0.1 mmHg | 281.5 | 288.2 | 1.4602 | 69.31 | 69.27 | 10.62 | 10.73 |
| Lauryl | *n*-Butyl | „ | (23) | ca. 195°/0.1 mmHg | 281.5 | 273.1 | 1.4595 | 69.31 | 69.20 | 10.62 | 10.55 |
| 2-Ethyl-hexyl | Lauryl | „ | (25) | ca. 200°/0.1 mmHg | 246.8 | 246.2 | 1.4650 | 71.32 | 71.09 | 11.09 | 11.25 |
| Lauryl | 2-Ethyl-hexyl | „ | (23) | ca. 200°/0.1 mmHg | 246.8 | 243.0 | 1.4642 | 71.32 | 71.38 | 11.09 | 11.30 |
| „ | Lauryl | „ | (28) | ca. 220°/0.1 mmHg | 219.5 | 225.0 | 1.4708 | 72.89 | 72.75 | 11.45 | 11.68 |
| „ | „ | *tert.*-BuOK | (34) | ca. 220°/0.1 mmHg | „ | 221.5 | 1.4695 | „ | 72.70 | „ | 11.58 |

Yields in parentheses show those of the crude ester.

5) W. S. Johnson, J. S. Beloew, L. J. Chinn and R. H. Hunt, *J. Am. Chem. Soc.*, **75**, 4995 (1953).

*) Present address, Nagoya University, Faculty of Engineering.

6) D. Swern, T. W. Findley, G. N. Billen and J. T. Scanlan, *Anal. Chem.*, **19**, 414 (1947).

7) Unpublished data, 2,3-epoxylauric acid was obtained by epoxidation of *trans*-2-dodecenoic acid with hydrogen peroxide and acetic acid, m.p. 48—48.5°C.

which must be included in the esters by sodium amide[8].

Only a few drops of the pure esters were obtained from the combinations of the higher starting esters, because of their higher boiling points and greater tendency to decompose at elevated temperatures. Also, as commercial sodium amide from different stock was used in each reaction, it is impossible to compare the reactions in regard to yield. But combinations of the lower starting esters gave generally lower yields, which is perhaps due to hydrolysis of the keto-esters. While it was reported that cyclohexanone and monochloroacetic esters gave as high as 90% of the desired products by the use of potassium *tert.*-butoxide[5], only 48% of the desired di-*n*-butyl 2, 3-epoxy-3-methyladipate was obtained from (I) and (I′) under similar conditions. But this yield is still higher than those obtained in the case when sodium amide was used. Sodium ethoxide and methoxide were not suitable as condensing agent, because they probably caused transesterification and gave no desired results. Calculated saponification values are 391.8 for di-*n*-butyl 2, 3-epoxy-3-methyladipate, 488 for the diethyl ester and 555 for the dimethyl ester, while the observed values were 554 for the ester obtained by sodium ethoxide and 585 for the ester obtained by sodium methoxide. Therefore it is deduced that these fractions suffered transesterification and some hydrolysis, and that they were also contaminated by some by-products.

As they are the esters of a dibasic acid and have an epoxy ring, these esters would be able to be utilized as a plasticizer and simultaneously as a stabilizer for polyvinyl chloride (PVC). In fact they showed more excellent results than dioctyl phthalate in our preliminary examinations. For example, the testing sheets, obtained by adding 30, 40 and 50 parts of di-*n*-butyl 2, 3-epoxy-3-methyladipate to 100 parts of polyvinyl chloride, were put to the Shopper tensile strength test at 25°C, and the values of tensile strength, elongation, elongation at 100 kg./cm² load, 100% modulus, tear resistance and permanent set are listed in Table II. Also it was shown that they were heat-proof stabilizers.

TABLE II

SHOPPER TENSILE STRENGTH TEST (at 25°C)

| Proportion of the di-*n*-butyl ester (Parts to 100 parts of PVC) | 30 | 40 | 50 |
|---|---|---|---|
| Elongation % | 175 | 245 | 283 |
| Tensile strength kg./cm² | 324 | 209 | 206 |
| Elongation at 100 kg./cm² load | 5 | 105 | 165 |
| 100 % Modulus kg./cm² | 246 | 98 | 68 |
| Tear resistance kg./cm² | 161 | 100 | 70 |
| Permanent set % | 65 | 12.5 | 10 |

## Experimental

**Reagents.** *Levulinic acid.*—This material was obtained by courtesy of the Aji-no-moto Co. Ltd., and was used without purification.

*Monochloroacetic acid and sodium amide.*—Commercial products were used without purification.

*2-Ethylhexyl alcohol.*—A commercial product, obtained by courtesy of the Shin-Nihon-Chisso-Hiryo K. K., was distilled under diminished pressure, b. p. 94°C/27 mm Hg.

*Lauryl alcohol.*—Commercial fatty alcohol, obtained by hydrogenation of coconut oil, was rectified repeatedly in vacuo, b. p. 140–141°C/15mm Hg, hydroxyl value 296.5 (calcd. for $C_{12}H_{25}OH$ 301.1), S. V. 2.5.

*tert-Butyl alcohol.*—Commercial *tert.*-butyl alcohol was dried by refluxing with sodium and then by distilling in the presence of the free metal[9].

*Sodium alcoholates.*—Eighteen grams (0.8 mol.) of fresh sodium was dissolved in 450 ml. of anhydrous ethyl or methyl alcohol. Upon removal of the excess alcohol under diminished pressure on a water bath the alcoholate was obtained in the form of yellow or white powder.

*Potassium tert-butoxide.*—Fresh potassium (5.88 g., 0.15 mol.) was dissolved in 125 ml. of dry *tert.*-butyl alcohol by refluxing in an atmosphere of dry nitrogen[9].

*Monochloroacetic and levulinic esters.*—*n*-Butyl, 2-ethylhexyl and lauryl esters of these two acids were prepared by refluxing a mixture of an appropriate alcohol, acid and concentrated sulfuric acid with azeotropic removal of water. For the preparation of both the lauryl esters and 2-ethylhexyl levulinate benzene was added to the refluxing mixture. Some properties of these six esters are listed in Table III.

TABLE III

STARTING ESTERS

| Ester | b. p. | $n_D^{25}$ | S. V. Calcd. | S. V. Found |
|---|---|---|---|---|
| Butyl levulinate | 125–126°/20 mmHg | 1.4257 | 327.9 | 325.8 |
| 2-Ethylhexyl levulinate | 157–159°/15 mmHg | 1.4372 | 245.8 | 247.6 |
| Lauryl levulinate | 190–195°/18 mmHg | 1.4437 | 204.8 | 201.9 |
| Butyl monochloroactate | 178–180° | 1.4271 | 745.4 | 749.8 |
| 2-Ethylhexyl monochloroacetate | 123–124°/16 mmHg | 1.4395 | 542.9 | 545.1 |
| Lauryl monochloroacetate | 158–160°/5 mmHg | 1.4468 | 443.9 | 445.0 |

8) C. F. H. Allen and J. Van Allan, *Org. Synth.*, **24**, 82.

9) W. S. Johnson and W. P. Schneider, *Org. Synth.*, **30**, 20.

**Syhntheses of 2, 3-epoxy-3-methyladipic esters. Synthesis of the di-*n*-butyl esters** (*a*) *Use of sodium amide as condensing agent.*—To a mixture of 86 g. (0.5 mol.) of *n*-butyl levulinate, 75 g. (0.5 mol.) of *n*-butyl monochloroacetate and 100 ml. of dry benzene in a 500-ml. three-necked round-bottomed flask was added 25 g. (0.6 mol.) of pulverized sodium amide over a period of 2 hrs. with mechanical stirring. The temperature was kept at 15–20°C in a water bath. After addition had been completed, the mixture was stirred for 2 hrs. more at room temperature. The mixture was poured upon 350 g. of cracked ice with hand stirring. The organic layer was separated and the aqueous layer was extracted with 100 ml. of benzene. The combined benzene solution was washed with three 100-ml. portions of water, dried with anhydrous sodium sulfate, and benzene was removed under diminished pressure. The product (90 g.) was distilled in vacuo to give 25 g. of the desired ester, b. p. 148–149°C/1.5 mm Hg, $n_D^{20}$ 1.4478, $d_4^{20}$1.023, S. V. 395.9 (calcd.for the dibutyl ester 391.8).

Found: C 62.80%; H 9.20%. Calcd. for $C_{15}H_{23}O_5$: C 62.91%; H9.15%.

Other experiments were conducted in exactly the same way as the above, but the temperature was kept at 5°C. Only a few grams of the di-*n*-butyl ester were obtained.

(*b*) *Use of potassium tert-butoxide as condensing agent.*—A mixture of 25.5 g. (0.15 mol.) of *n*-butyl levulinate, 22.5 g. (0.15 mol.) of *n*-butyl monochloroacetate was placed in a 500-ml. four-necked round-bottomed flask, fitted with a stirrer, thermometer and dropping funnel containing *tert.*-butyl alcohol solution of potassium *tert.*-butoxide (from 5.88 g. of the metal). The reaction was carried out with mechanical stirring in an atmosphere of dry nitrogen. The alcoholate was added during one hour, and then the mixture was stirred for one hour. The temperature was kept at 25–30°C. From the reaction mixture *tert.*-butyl alcohol was removed as much as possible under diminished pressure on a steam bath. After addition of water the product was extracted successively with three 100-ml. portions of ether. The combined ether solution was washed with 50 ml. of water and dried with anhydrous sodium sulfate. The product (35.8 g.) was distilled in vacuo to give 20.5 g. (48% yield) of colorless fraction, b.p. 189–191°C/15 mm Hg, $n_D^{20}$ 1.4458, $d_4^{20}$ 1.021, S. V. 389.1 (calcd. for the dibutyl ester 391.8).

Found: C 62.56%; H 9.25%. Calcd. for $C_{15}H_{26}O_5$: C 62.91%; 9.15%.

Other experiments were conducted in exactly the same way as the above, but the temperature was kept at 5–10°C, and 30–38% yields were procured.

(*c*) *Attempted use of sodium ethoxide as condensing agent.*—To a mixture of 86 g. (0.5 mol.) of *n*-butyl levulinate and 75 g. (0.5 mol.) of *n*-monochloroacetate, cooled in an ice-salt bath, 40 g. (about 0.5 mol.) of freshly prepared sodium ethoxide was added over a period of 4 hrs. The mixture was then stirred for 9 hrs. with cooling, 2 hrs. at room temperature, and finally 6 hrs. with warming on a water bath, and then poured on ice water. The mixture was acidified with acetic acid, and the product was extracted with ether. The ether layer was dried with anhydrous sodium sulfate, and the ether was removed under diminished pressure. The product (60 g.) was distilled in vacuo, b.p 150°C/2.5 mm Hg, $n_D^{20}$ 1.4688, S. V. 554.1 (calcd. for the dibutyl ester 391.8).

(*d*) *Attempted use of sodium methoxide as condensing agent.*—The synthesis was conducted similarly to the above. To a mixture of *n*-butyl monochloroacetate (0.5 mol.), *n*-butyl levulinate (0.5 mol.) and 200 ml. of dry benzene was added 54 g. (0.8 mol.) of sodium methoxide. The product (60 g.) was distilled in vacuo to give 24 g. of yellow fraction, b.p. 128–130°C/3 mmHg, $n_D^{20}$ 1.4701, S. V. 584.6 (calcd. for the dibutyl ester 391.8).

**Syntheses of the 2-ethylhexyl-(1)-*n*-butyl-(6), *n*-Butyl-(1)-2-ethylhexyl-(6), Di-2-ethylhexyl, Lauryl-(1)-*n*-butyl-(6), *n*-Butyl-(1)-lauryl-(6), Lauryl-(1)-2-ethylhexyl-(6), and 2-Ethylhexyl-(1)-lauryl-(6) esters.**—These seven 2, 3-epoxy-3-methyladipates were synthesized from 0.5 mol. of the monochloroacetate and 0.5 mol. of the levulinate by 0.6 mol. of sodium amide in a way exactly similar to the method of synthesis of the di-*n*-butyl ester using sodium amide, and are represented in Table I.

**Synthesis of the Di-lauryl ester** (*a*) *Use of sodium amide as condensing agent.*—A mixture of 137 g. (0.5 mol.) of lauryl levulinate, 126 g. (0.5 mol.)of lauryl monochloroacetate and 100 ml. of dry benzene was used with 25 g. (0.6 mol.) of sodium amide. The properties of the ester are recorded in Table I.

(*b*) *Use of potassium tert-butoxide as condensing agent.*—To a mixture of 41.0 g. (0.15 mol.) of lauryl levulinate and 37.8 g. (0.15 mol.) of lauryl monochloroacetate was added potassium *tert.*-butoxide prepared from 5.88 g. (0.15 mol.) of potassium. The method of synthesis was exactly similar to that of the di-*n*-butylester. As a residue of the first vacuum distillation (over 150°C/i2 mm Hg), the crude desired ester was obtained n 34% yield, S. V. 221.5 (calcd. for the dilauryl ester 219.7).

## Summary

Levulinic and monochloroacetic esters are condensed by sodium amide or potassium *tert.*-butoxide to give the corresponding 2, 3-epoxy-3-methyladipic esters. *n*-Butyl (B), 2-ethylhexyl (O), and lauryl (L) alcohols were used as alcoholic components of these starting esters. Although the yields were poor, nine new esters, namely the B-B, B-O, O-B, B-L, L-B, O-O, O-L, L-O,and L-L 2, 3-epoxy-3-methyladipates were obtained.

As for condensing agents, potassium *tert.*-

butoxide was the most excellent, and sodium amide gave also good results, while sodium ethoxide and methoxide gave no desired ester.

These new esters would be able to be utilized as a stabilizing plasticizer for polyvinyl chloride.

*Department of Chemistry, Nagoya Institute of Technology and Department of Industrial Organic Chemistry, Faculty of Engineering, Nagoya University*

# *Molecular Structures of Propylene Oxide and Epichlorohydrin by Electron Diffraction*

By Masato IGARASHI

(Received August 6, 1954)

In the previous report[1], it was stated that the molecular structure of ethylene oxide was reinvestigated by electron diffraction and the results coincided better with those of the microwave investigation[2] than those of the early electron diffraction study[3].

In the present paper electron diffraction studies about the structures of propylene oxide and epichlorohydrin are reported.

Propylene oxide and epichlorohydrin have a ring of ethylene oxide and the chief aim of these studies is to know the configuration of $-CH_3$ in propylene oxide and $-CH_2Cl$ in epichlorohydrin with respect to the ring.

## Procedure

Propylene oxide was prepared from lime and propylenechlorohydrin which had been obtained from propyleneglycol and hydrogen chloride gas (b. p. 35–36°C). Epichlorohydrin was purified by distillation of the commercial product (b. p. 115°C).

Electron diffraction photographs were prepared by the apparatus described in the previous report[1]; the camera distance at that time was about 9 and 10 cm., and the wave length of the electron beam was about 0.055 Å. Visual intensity curves $V_1$ (propylene oxide) and $V_2$ (epichlorohydrin) were drawn from measurements of the photographs (Figs. 1 and 2). The $q$ values of maxima and minima are shown in Tables III and IV.

TABLE I

STRUCTURE OF ETHYLENE OXIDE BY MICROWAVE INVESTIGATION[2]

| | | | |
|---|---|---|---|
| C–C | 1.472Å | C–O | 1.436Å |
| C–H | 1.082Å | | |
| ∠H–C–H | 116°41' | ∠$H_2$–C–C | 159°25' |

1) M. Igarashi, This Bulletin, 26, 330 (1953).
2) G.L. Cunningham, A.W. Boyd, R.J. Myer, W.D. Gwinn and W.I. Le Van, *J. Chem. Phys.*, 19, 676 (1951).
3) P.C. Ackermann and J.E. Mayer, *J. Chem. Phys.*, 4, 377 (1936).

TABLE II

MODELS FOR PROPYLENE OXIDE (A, B, C, D) AND EPICHLOROHYDRIN (E, F, G, H, I, J, K)

| Model | $C_2-C_3$ Å | Angle between $C_2-C_3$ and $C_1C_2O$ plane | Configuration of Cl atom in epichlorohydrin |
|---|---|---|---|
| A | 1.54 | 58° | |
| B | 1.50 | 58° | |
| C | 1.54 | 50° | |
| D | 1.54 | 65° | |
| E | 1.54 | 58° | *trans* against the midpoint of $C_1-O$ |
| F | 1.50 | 58° | |
| G | 1.54 | 50° | |
| H | 1.54 | 65° | |
| I | 1.54 | 58° | *cis* against the midpoint of $C_1-O$ |
| J | 1.54 | 58° | *trans* against $C_1$ |
| K | 1.54 | 58° | *trans* against O |

Triangle $C_1C_2O$, $C_1-H$ and $C_2-H$ are equal to those of ethylene oxide (Table I). $C_3-H=1.09$Å, $C_3-Cl=1.76$Å. Angles in $-CH_3$ and $-CH_2Cl$ are all equal to tetrahedral angle.

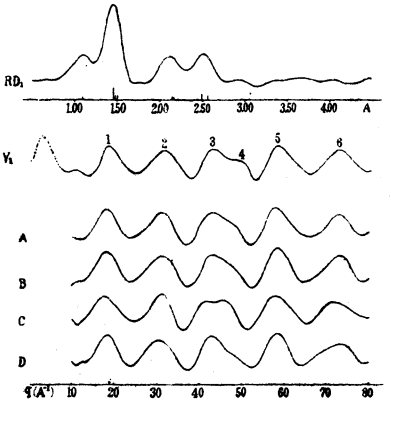



Fig. 1. Propylene oxide

TABLE III

PROPYLENE OXIDE

| Max. | Min. | $q_{obs}$ | $q_{calc}/q_{obs}$ A | B | C | D |
|---|---|---|---|---|---|---|
| 1 | | 18.3 | 0.983 | 0.988 | 0.972 | 1.004 |
| | 2 | 25.05 | 0.943 | 0.947 | 1.003 | 0.947 |
| 2 | | 31.45 | 0.982 | 0.992 | 0.982 | 0.970 |
| | 3 | 37.25 | 0.988 | 1.001 | 0.974 | 1.001 |
| 3 | | 42.1 | 1.014 | 1.016 | 0.998 | 1.012 |
| | 4 | 45.85 | (0.992) | (1.012) | (0.949) | (1.025) |
| 4 | | 49.4 | (0.042) | (1.042) | (0.929) | (0.982) |
| | 5 | 52.4 | 0.992 | 0.998 | 0.982 | 1.001 |
| 5 | | 57.8 | 1.000 | 1.007 | 1.000 | 1.000 |
| | 6 | 65.4 | 1.025 | 0.987 | 1.006 | 0.983 |
| 6 | | 72.2 | 1.004 | 1.007 | 0.991 | 1.015 |
| | 7 | 78.75 | 0.992 | 0.977 | 1.013 | 1.001 |
| 7 | | (84.0) | | | | |
| Average, 10 features | | | 0.994 | 0.994 | 0.991 | 0.994 |
| Average deviation | | | 0.015 | 0.012 | 0.012 | 0.017 |

TABLE IV

EPICHLOROHYDRIN

| Max. | Min. | $q_{obs}$ | $q_{calc}/q_{obs}$ E | F | G | H |
|---|---|---|---|---|---|---|
| 1 | | 11.9 | (0.908) | (0.950) | (0.908) | (0.915) |
| | 2 | 14.45 | (0 920) | (0.920) | (0.906) | (0.934) |
| 2 | | 17.1 | 0.977 | 0.954 | 0.971 | 0.983 |
| | 3 | 20.05 | 1.006 | (1.021) | 1.001 | 1.011 |
| 3 | | 21.3 | 0.994 | (1.008) | 1.008 | 1.008 |
| | 4 | 23.25 | 1.002 | 1.006 | 0.998 | 1.024 |
| 4 | | 26.25 | **1.002** | **1.006** | **0.998** | **1.014** |
| | 5 | 29.05 | 0.992 | 0.999 | 0.978 | 1.024 |
| 5 | | 31.9 | **0.991** | **0.998** | **0.982** | **0.994** |
| | 6 | 34.7 | 0.994 | 1.008 | 0.988 | 1.000 |
| 6 | | 37.05 | 1.007 | 1.001 | 1.001 | 1.001 |
| | 7 | 39.35 | 0.973 | 0.986 | 0.970 | 1.001 |
| 7 | | 41.6 | 0.993 | 1.003 | 0.979 | 1.017 |
| | 8 | 44.0 | 0.991 | 0.998 | 0.984 | 1.000 |
| 8 | | 46.95 | **0.991** | **1.003** | **0.986** | **0.995** |
| | 9 | 49.65 | 0.984 | (1.016) | 0.982 | 1.013 |
| 9 | | 51.05 | 1.005 | (1.019) | 0.999 | 1.027 |
| | 10 | 53.2 | 1.004 | (1.006) | 0.996 | 1.021 |
| 10 | | 56.8 | **1.011** | **1.014** | **0.998** | **1.026** |
| | 11 | 58.95 | 0.997 | 1.011 | 0.984 | (1.017) |
| 11 | | 60.8 | **0.995** | **0.998** | **0.998** | **1.003** |
| | 12 | 64.7 | 0.998 | 1.003 | 0.998 | 1.003 |
| 12 | | 70.0 | 1.023 | 1.024 | 1.011 | .... |
| | 13 | 77.25 | 1.019 | 1.022 | 1.020 | .... |
| 13 | | (82.25) | | | | |
| Average | | | 0.998 | 1.002 | 0.992 | 1.008 |
| Average deviation | | | 0.009 | 0.009 | 0.010 | 0.010 |

Values in Gothics were doubly weighted in computing averages.

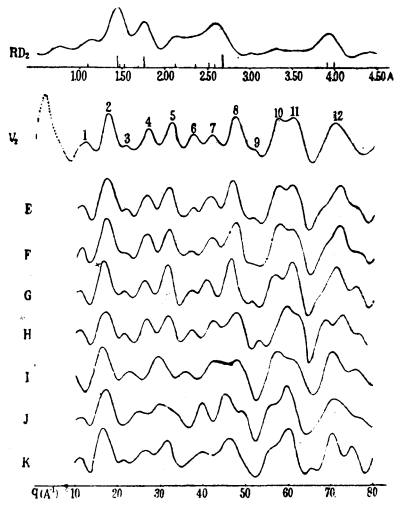



Fig. 2. Epichlorohydrin

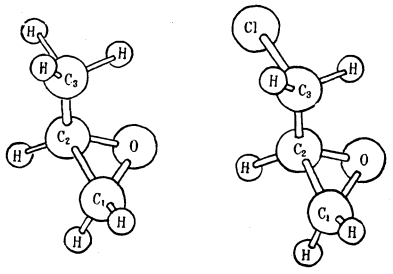



Fig. 3. Perspective picture of propylene oxide and epichlorohydrin molecules.

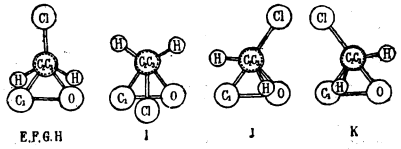



Fig. 4. Various configurations of epichlorohydrin.
H-atoms of $C_1H$ and $C_2H$ are omitted for convenience.

## Analysis and Results

From the visual intensity curves $V_1$ and $V_2$, radial distribution curves $RD_1$ (propylene oxide) and $RD_2$ (epichlorohydrin) were drawn by using the formula,

$$rD(r)=\sum_{q=1,2,\cdots}^{q=80} V(q)\exp(-aq^2)\sin(\pi qr/10)$$

where $q=10s/\pi=(40/\lambda)\sin\phi/2$, $\phi$ the scattering angle, and $a$ was determined such that $\exp(-aq^2)=0.1$ at $q=80$.

In $RD_1$ main peaks are at 1.10, 1.44, 2.11, 2.51 and 2.92 Å, which seem to correspond to the distances C−H, ($C_1-C_2$, C−O, $C_2-C_3$), ($C_1\cdots$H, O $\cdots$ H), ($C_1\cdots C_3$, $C_3\cdots$O) and long range (C $\cdots$ H, O $\cdots$ H), respectively.

In $RD_2$ main peaks are at 1.14, 1.45, 1.76, 2.13, 2.60 and 3.93 Å, which seem to correspond to the distances C−H, ($C_1-C_2$, C−O, $C_2-C_3$), $C_3$−Cl, (C $\cdots$ H, O $\cdots$ H), ($C_1\cdots C_3$, $C_3\cdots$O, $C_2\cdots$Cl) and ($C_1\cdots$Cl, O $\cdots$ Cl), respectively.

Making reference to the radial distribution curves and the results of ethylene oxide, molecular models for the correlation method were constructed in the ranges as follows, $C_1-C_2$; 1.44–1.56 Å, $C_1-O=C_2-O$; 1.43–1.45 Å, $C_2-C_3$; 1.50–1.58 Å, angle between $C_2-C_3$ and $C_1C_2O$ plane; 50°–70°.

Among them models A, B, C, D (propylene oxide) and E, F, G, H, I, J, K (epichlorohydrin) are described here (Table II and Figs. 3 and 4).

In models E, F, G and H, Cl atom is *trans* against the midpoint of $C_1$–O. Models I, J, K for epichlorohydrin in which Cl atom is in different configuration from those of E, F, G and H, are also used for comparison.

Theoretical intensity curves for these models were calculated from the equation,

$$I(q)=\sum_{i,j}(Z_iZ_j/r_{ij})\exp(-b_{ij}q^2)\sin(\pi qr_{ij}/10)$$

where $r_{ij}$ is the distance between atoms $i$ and $j$, and $Z_i$ is the atomic number of atom $i$, apart from the value 1.25 for the hydrogen atom. The coefficient $b_{ij}$ was assumed to be 0.00016 for bonded hydrogen terms, 0.0004 for unbonded hydrogen terms, and zero for all the others.

**Propylene Oxide.**—From the correlation between visual and theoretical intensity curves and the values $q_{calc}/q_{obs}$ (Table III), model B seems to be the best among them.

The main results are as follows; $C_2-C_3=1.52\pm0.03$ Å, the angle between $C_2-C_3$ and $C_1C_2O$ plane is equal to 58°±5°. This angle is almost equal to that between C−H and $C_1C_2O$ plane of ethylene oxide studied by microwave spectrum[2].

**Epichlorohydrin.** — Theoretical intensity curves of models E, F, G and H which are *trans* in reference to Cl atom and the midpoint of $C_1-O$, are in good accordance with the visual intensity curve, though the max. 6 is a little weaker than visual. Among them E and F are better than the others according to the value $q_{calc}/q_{obs}$ (Table IV). As the curves of H, I and J are very different from the visual, these configurations would scarcely be worthy of further consideration.

The main results are as follows; $C_2-C_3=1.52\pm0.03$ Å, the angle between $C_2-C_3$ and $C_1C_2O$ plane is equal to 58°±5°. They are

equal to those of propylene oxide. The configuration of Cl atom is almost *trans* against the midpoint of $C_1-O$.

The author wishes to express his gratitude to the late Professor H. Oosaka and Professor A. Kotera for their kind guidance during the course of this research. He also owes much to Mr. M. Yamaha to whom his thanks are due.

*Department of Chemistry, Faculty of Science, Tokyo University of Education, Tokyo*

# *The Role of Ethylene Glycol and Polyethylene Glycol in the Freeze-Thaw Stability of Synthetic Latex*

By Seizo OKAMURA and Takuhiko MOTOYAMA

(Received August 9, 1954)

## Introduction

One of the most important properties of synthetic latex is its freeze-thaw stability, and it is necessary to study this property for industrial application. In the paint industry it is usual to employ the freeze-thaw test in order to determine the stability. Recently Digioia and Nelson[1] have reported freeze-thaw cycles of certain commercial synthetic latices. However, they have not mentioned either the sources or the conditions of the freezing stability. The freeze-thaw test is widely used for the checking of the commerciability of the emulsion, but there is lack of reliable data in quantitative studies concerning it. In the present work the adsorption of ethyleneglycol and of polyethyleneglycol by the emulsion particles of various polyvinyl compounds was studied with reference to the conditions under which freeze stability was attainable.

## Experimental

The monomers used are styrene (St.), methylmethacrylate (MMA.), methylacrylate (MA.), vinylacetate (VAc.) and acrylonitrile (AN.). These are purified by vacuum distillation. The polymerization catalyst used is ammonium persulfate, commercial c.p. grade; and the emulsifier mainly employed is sodium-dodecylsulfate, recrystallized twice in ethanol solution. The emulsion polymerization of MMA., MA., VAc. and AN. is carried out at 60°C in still-stand, and that of St. at 80°C in agitation, both for 5 hrs. The concentration of catalyst is 0.1%, and the ratio of monomer to aqueous solution is 0.08.

The freezing process of the emulsion obtained is accomplished by cooling it at $-17.5\pm2.5$°C for 24 hrs. If the latex prepared by the addition of glycols is stable enough after its thawing at room temperature, its second freezing is conducted at the same temperature for as many hours, and further its third, if stable, like the second, for 45 hrs. In almost all these cases stability is observed in the second and the third process of the test only when the first process of the test has been satisfactory.

## Results and Discussion

**1. Preliminary Experiments on the Addition of Ethyleneglycol.**—The experiments are shown in Table I. In this table X-marks represent the unstable cases and 0-marks the stable.

TABLE I

EXAMPLES OF THE LATICES OF PVAc. AND PMMA.

| Kind of Monomer | Kind (& Amount) of Emulsifier used in Polymerisation | Kind (& Amount) of Stabilizer | Freezing 1st. | 2nd. | 3rd. |
|---|---|---|---|---|---|
| VAc. | None | None | x | | |
| „ | N. (0.5%) | „ | x | | |
| „ | A. ( „ ) | „ | x | | |
| „ | K. (1.0%) | „ | x | | |
| „ | PVA. (0.5%) | „ | x | Slightly | |
| „ | None | Ethyleneglycol (5%) | 0 | x | |
| „ | „ | „ (10%) | 0 | 0 | 0 |
| „ | N. (0.5%) | „ (3%) | 0 | 0 | 0 |
| MMA. | A. (0.1%) | „ (3%) | x | | |
| „ | „ (0.2%) | „ ( „ ) | 0 | 0 | 0 |
| „ | „ (0.5%) | „ ( „ ) | 0 | 0 | 0 |
| „ | „ (0.5%) | None | x | | |
| „ | K. (1.0%) | Ethyleneglycol (10%) | x | | |

N. Polyethyleneoxide-dodecylether having $\bar{P}$=45
A. Sodium dodecylsulfate
K. Cetyltrimethylammoniumbromide
PVA. Polyvinylalcohol having $\bar{P}$=ca. 1000

1) F.A. Digioia and R.E. Nelson, *Ind. Eng. Chem.*, 45, 745 (1953).

**2. The Minimum Amount of Ethyleneglycol Required for Stabilization.**—The freeze-thaw stability can be measured by the determination of the minimum amount of glycol required for the stabilization of the latex. The curves indicating the concentrations of ethyleneglycol versus that of emulsifier are given in Figure 1.

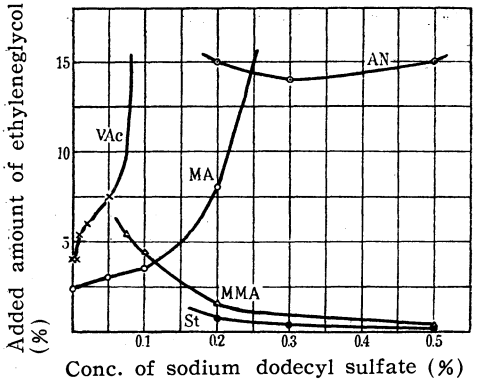



Fig. 1. The minimum amount of glycol required in various types of emulsions polymerized with sodium-dodecylsulfate.

As shown in Fig. 1, these curves are classified into three groups, the first is the case of St. and MMA., the second MA. and VAc., and the third AN. The amount of glycol required decreases in the first groups and increases in the second, and finally is constant in the third, as the concentration of emulsifier increases. In the range of this work, the monomers of the first group are more hydrophobic and those of the second more hydrophilic. An. is most hydrophilic in the monomer state but relatively hydrophobic in the polymer. It may, therefore, be concluded that the facility of stabilization attained by the addition of glycol increases as the hydrophobic property of the monomers or the polymers increases.

From Figure 2 it will be noticed that the amount of glycol required for stabilization is small in the case of using relatively high molecular weight compds, such as polyethyleneglycol as emulsifiers. As shown in the comparison of Fig. 1 and Fig. 2, the freeze-thaw stability is attained more easily in the nonionic than in the anionic detergents. Also in Fig. 2 the order of hydrophobic nature, (St.>MA.>VAc.) is shown as parallel to the order of properties for stabilization.

In all the five monomers the latices obtained with cetyltrimethylammoniumbromide (concentration range 0.7–2.0%) could not be stabilized by the addition of ethyleneglycol (to 20%).

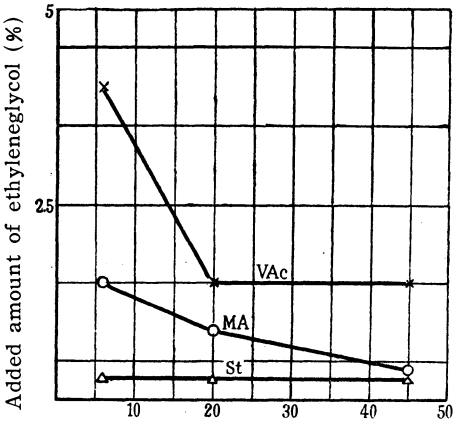



Fig. 2. The minimum amount of glycol required in three types of emulsions polymerized with polyethyleneoxidedodecylether having various degrees of polymerization.

**3. The Properties of Stabilized Latices for Freeze-thaw A) Depression of the Freezing Point of Latices.**—The value of the freezing point of emulsion must be equal to that of its aqueous solution because the size of its molecules is much larger than of those of the dispersing medium. The depression measurement indicates therefore the decrease of the concentration of glycol in the aqueous solution. Table II represents the comparison of the value of freezing point depression in the aqueous solution of ethyleneglycol and that in the stabilized latices.

TABLE II
THE FREEZING DEPRESSION OF STABILIZED LATICES

| Concentration of glycol (g./l.) | 15 | 45 | 75 |
|---|---|---|---|
| Depression in aqueous solution (°C) | 0.46 | 1.46 | 2.54 |
| Depression in stabilized AN.-latices (°C) | 0.46 | 1.40 | 2.33 |
| Depression in stabilized St.-latices (°C) | 0.36 | 1.22 | 2.12 |

Table II shows that the St.-latex which is most easily stabilized has the lowest depression value and that the adsorption of glycol on emulsion particles has occurred in the St.-latices.

**B) The Electrophoretic Mobility of Stabilized Latices.**—The electrophoretic mobility of emulsion has been determined by the present researchers. As previously reported, it has been shown to alter by the adsorption of detergents. It is also suggested that the electrophoretic mobility changes by the adsorption of different solvents having different

dielectric constants[2]. The partition of additives between the solution and the particles may be sensitive to the mobility. Thus the changes of mobility by stabilization are measured by the usual U-type assembly previously reported[3]. The results of the experiment are plotted in Figures 3 and 4.

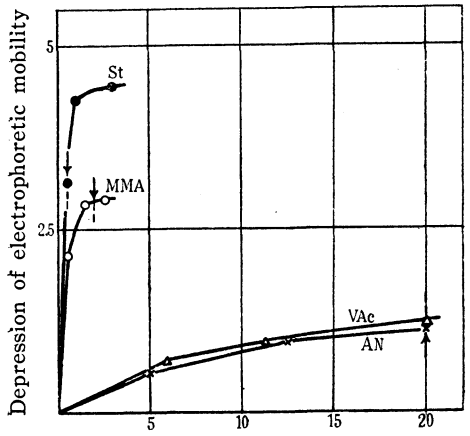



Fig. 3. The decrease of the electrophoretic mobility after the addition of ethyleneglycol (Emulsifier used was sodium dodecylsulfate 0.2%.).

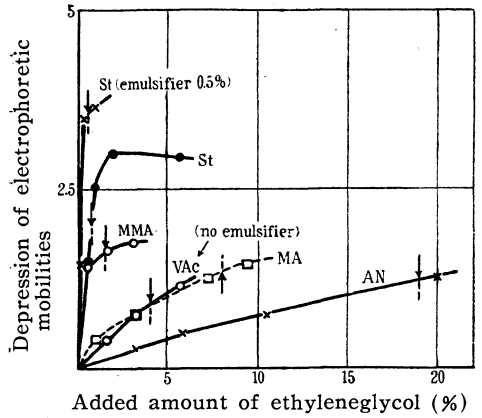



Fig. 4. The decrease of the electrophoretic mobility after the addition of polyethyleneglycol 300 (U.C.C. Ltd.) (Emulsifier used was sodium dodecylsulfate 0.2%).

As shown in Figs. 3 and 4, the order of the change of mobility is in good agreement with the order of the facility of stabilization. The stabilized points in each latex are marked with arrows which are in the neighbourhood of the saturation. The ratios of the mobilities of the stabilized latices to those of the originals are tabulated in Table III.

It is of interest to note that the average value of these ratios agrees with the ratio of dielectric constants of ethylene glycol and that of water, 41.2 (d.c. of glycol)/81.0 (d.c. of water)=0.508.

**C) The Adsorption of Additives on Emulsion Particles.**—It is necessary to determine directly the amount of adsorption of additives for the investigation of freeze-thaw stability. Fortunately the concentration of ethyleneglycol and polyethyleneglycol in aqueous medium can be measured quantitatively by the periodic acid (volumetric) method[5], and by the Shaffer (gravimetric) method[4] respectively. Figure 5 gives the case of ethyleneglycol and Figure 6 that of polyethyleneglycol.

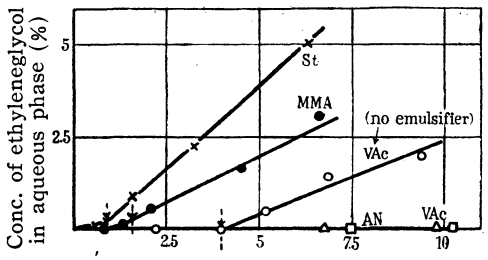



Fig. 5. The adsorption of ethyleneglycol on the emulsion particles (Arrows show points which have attained stability.). (emulsifier: Sodium dodecylsulfate 0.2%)

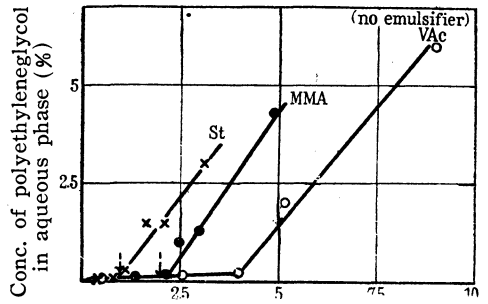



Fig. 6. The adsorption of polyethyleneglycol on the emulsion particles (Arrows show points which have attained stability.). (emulsifier: Sodium dodecylsulfate 0.2%)

TABLE III

RATIOS OF THE MOBILITIES OF THE STABILIZED AND UNSTABILIZED LATICES

| Kind of Emulsion | St. | St. | MMA. | MA. | VAc. | AN | Average |
|---|---|---|---|---|---|---|---|
| Kind of Emulsifier | A | A | A | A | None | A | — |
| Conc. of Emulsifier | 0.5 | 0.2 | 0.2 | 0.2 | — | 0.2 | — |
| Ratio of Mobilities | 0.49 | 0.67 | 0.58 | 0.57 | 0.59 | 0.48 | 0.56 |

2) E.K. Rideal, "An Introduction to Surface Chemistry," Camb., p. 406.

3) T. Motoyama and S. Okamura, *Mem. Fac. Eng. Kyoto Univ.*, 15, 242 (1653).

4) C.B. Shaffer and F.H. Critchfield, *Ind. Eng. Chem.*, 19, 32 (1947).

5) G.O. Curme and F. Johnston, "Glycols," Reinhold, (1952).

As represented in Figs. 5 and 6, the points of saturated adsorption coincide with the stabilizing points (shown as arrows in figures). Also the Figures indicate that the facility of saturated adsorption agrees with that of stabilization, (St.>MMA.>VAc.>AN.)

## Summary

The freeze-thaw stability of synthetic latices obtained by the emulsion polymerisation of styrene, methyl methacrylate, methyl acrylate, vinyl acetate and acrylonitrile has been measured at the freeze-thaw cycles of −17.5°C and room temperature. It is found that the addition of ethyleneglycol and polyethyleneglycol into the latices increases the stability. The freezing point depression and the electrophoretic mobility of stabilized latices indicate the adsorption of stabilizing additives on the emulsion particles. Finally the adsorption of ethylene glycol and polyethylene glycol on the emulsion particles is determined directly. In consideration of these experimental results the freeze-thaw stability seems to be attained by the adsorption of additives on the emulsion particles.

The authors are grateful to Professor Ichiro Sakurada for his interest in this work.

*Department of Textile Chemistry, Faculty of Engineering, Kyoto University, Kyoto*

# *Surface Chemistry of High Polymers. VI. The Monolayer of Polyethylene Terephthalate and Poly-N-vinyl Pyrrolidone*

By Hiroshi HOTTA

(Received August 10, 1954)

Although we studied the monolayer of various linear polymers up to the preceding paper, these polymers consist of chains alone either in the main chain or in the side chain.[1-5] In order to obtain some information in respect to the contribution of the ring group in the side chain as well as in the main chain to the behavior of surface film, we studied the monolayer of polyethylene terephthalate and poly-N-vinyl pyrrolidone by the measurements of interfacial pressure and potential at the air/water and oil/water interfaces. It was found as the results of the present investigation that the ring groups in the main chain make the polymer molecule rigid even at the oil/water interface, while that in the side chain is not essentially different from the chain groups. Further more the study of the hydrolysis of poly-N-vinyl pyrrolidone by the monolayer technique provides a useful inference concerning it.

## Experimental

Polyethylene terephthalate was spread from the solution of the mixture of benzene and cresol (1: 1) at the air/water and benzene/water interfaces using a micrometer syringe. The distilled water was used as the water phase.

Poly-N-vinyl pyrrolidone, whose molecular weight is 13,400, was spread from the aqueous solution containing 20% pyridine at the air/water and petroleum ether/water interfaces. The pH of the substrate was adjusted with hydrochloric acid or sodium hydroxide as in the previous papers[4,5] to investigate the effect of hydrolysis.

Both materials were kindly supplied from Prof. S. Murahashi of our Institute.

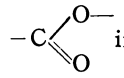
The interfacial pressures at the air/water and oil/water interfaces were measured by the hanging plate method[1] and ring method[2], respectively, as in the previous papers. The interfacial potential at both interfaces was measured by the vibrating electrode method.[1,5] The detailed descriptions of spreading technique and of measurements were already given in the previous papers. The only different technique adopted in the present investigation is that the area at the air/water interface was changed by the successive injection method for poly-N-vinyl pyrrolidone, which was already reported in the first paper.[1] The surface moment-area curve, shown by dotted lines and denoted with prime in Figs. 1 and 4, was calculated from observed surface potential using the Helmholtz's formula as usual.[1]

## Results and Discussion

**A. Polyethylene Terephthalate.**—The surface potential and moment at the air/water interface (15°C) plotted against area per residue are shown in Fig. 1. The reliable value of surface potential was obtained at a smaller area than 115 Å$^2$ per residue, and became

1) T. Isemura, H. Hotta and T. Miwa, This Bulletin, 26, 380 (1953).
2) H. Hotta, ibid., 26, 386 (1953).
3) H. Hotta, ibid., 27, 80 (1954).
4) T. Isemura, H. Hotta and S. Otsuka, ibid., 27, 93 (1954).
5) H. Hotta, ibid. 27, 412 (1954).

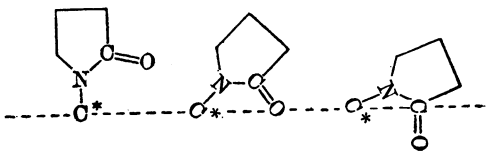
constant at 62 $A^2$ per residue. The corresponding surface moment was kept constant to 350 mD. up to about 72 $Å^2$ per residue Therefore, the surface moment of 175 mD. might be attributed to a single group of

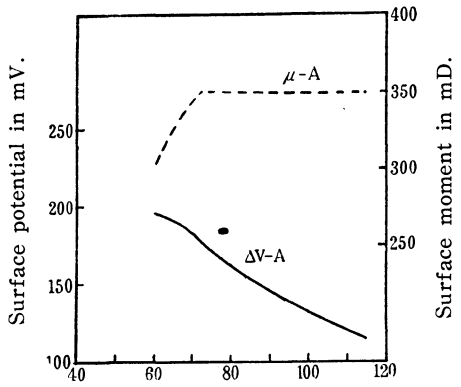


in this constant range. When we consider the magnitude and direction of each polar bond in this group,[6] the model proposed in Fig. 2 is entirely consistent with Table I in the third paper[3] showing the relationship between the value of surface moment and the inclination of C=O bond at the surface. Thus, this table would be useful for estimating the inclination of C=O bond at the surface for an unknown polymer.

TABLE I

THE STATE OF POLY-N-VINYL PYRROLIDONE AT THE OIL/WATER INTERFACE

| Model | | | | |
|---|---|---|---|---|
| | Oil |  | | |
| | Water | | | |
| Most compact area estimated from Fig. 4 in $Å^2$ per residue | | 18 | 25 | 35 |
| Surface moment in mD. | | 210 | 290 | 350 |




Area in $Å^2$ per residue

Fig. 1. The surface potential ($\Delta V$) (or moment ($\mu$))-area curve of polyethylene terephthalate at the air/water interface.

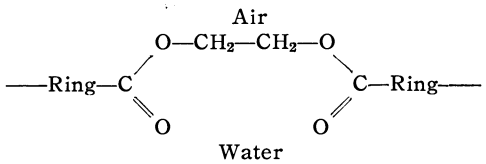
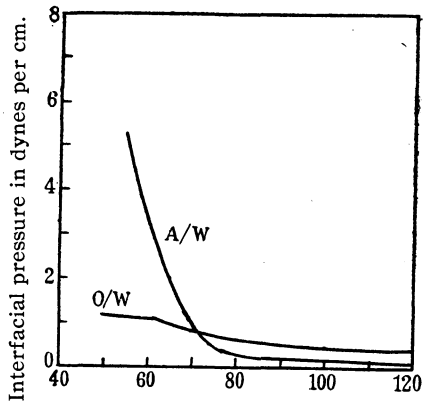



Fig 2

Although the surface pressure at the air/water interface was measured by the hanging plate method using a glass barrier for compression, the film was so gelatinous that a hanging plate, which was once raised with compression, did not return to an equilibrium position during moderate experimental time. Especially, it was recognized that the plate was considerably displaced horizontally as the area of the film was decreased to less than about 72 $Å^2$ per residue, from which the surface moment begins to decrease. Therefore, since the true surface pressure could not be obtained, a tentative curve for it is shown in Fig. 3 (15°C).




Area in $Å^2$ per residue

Fig. 3. The interfacial pressure of polyethylene terephthalate at the air/water (A/W) and benzene/water (O/W) interfaces.

Although the attempt was made at first the interfacial pressure to measure at the petroleum ether/water interface, we failed to measure it due to the slow desorption of cresol in the spreading solution from the surface. Then, it was measured at the benzene/water interface (15°C) as shown in Fig. 3. The kink point of this curve (62 $Å^2$ per residue) corresponds to the area where the surface potential at the air/water interface attained a constant value. This area may be very plausible as the area occupied by the model proposed in Fig. 2. By using the extrapolated value of the product of interfacial pressure and area to infinite area as

6) C.P. Smyth, *J. Am. Chem. Soc.*, 60, 183 (1938).

already reported,[2,3] the degree of polymerization for the segment as a statistical kinetic unit at the oil/water interface is estimated to be 13. Although the detailed interpretation for this value will be given elsewhere with other polymers,[7] it is concluded that the ring groups in the main chain make the polymer molecule rigid and should be interpreted in the light of a different base from the chain groups.

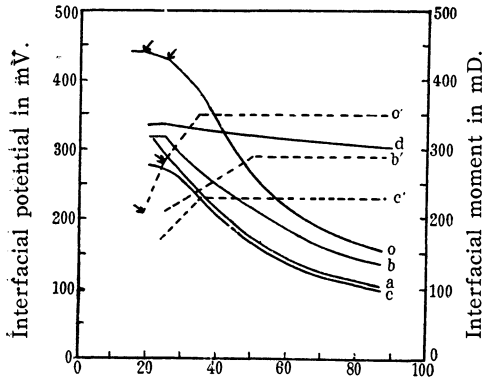



Fig. 4. The interfacial potential (—) (or moment (...))-area curve of poly-N-vinyl pyrrolidone (curve a, pH 0.3, 0.8, curve b, pH 1.4, 3.8, 4.5, and curve c, pH 5.6 –11.4) by successive injection method, (curve d, pH 3.8, 5.6) by compression of glass barrier at the air/water interface, and (curve o, pH 0.4–9.0) at the petroleum ether/water interface.

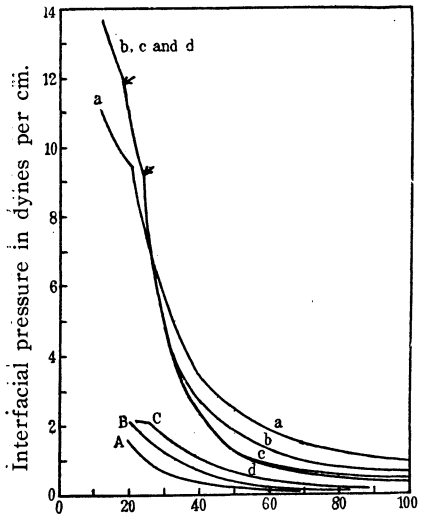



Fig. 5. The interfacial pressure of poly-N-vinyl pyrrolidone at the air/water interface (curve A, pH<0.8, curve B, pH 1.4—7.4 and curve C, pH 11.0) and at the petroleum ether/water interface (curve a, pH 0, curve b, pH 0.4, 1.4, 3.6, 4.6, curve c, pH 5.7, 7.5, 11.0, and curve d, pH 11.6).

7) H. Hotta, *J. Colloid Sci.* 9, 504 (1954).

**B. Poly-N-vinyl Pyrrolidone.**—When the film was compressed, for the measurement at the air/water interface, by using a glass barrier as usual, the obtained surface potential was very abnormal as shown as curve d in Fig. 4. It is presumably because the molecules are not spread or compressed uniformly all over the surface. Therefore, the successive injection method using a micrometer syringe was adopted instead of compression by barrier, for, in this case, the film is spread in a small place so as to avoid to some extent the lack of uniformity as mentioned above. The obtained results of surface potential (or moment) and pressure (19±1°C) were grouped as shown in Figs. 4 and 5, respectively.

The interfacial potential (or moment) (20±1°C) and pressure (8±1°C) at the petroleum ether/water interface were also shown in Figs. 4 and 5, respectively. The interfacial potential at the pH between 0.4 and 9.0 lay on a single curve o in Fig. 4. Those at pH 10.0 and 11.0 were somewhat lower than that shown by this curve at the larger area than about 70 Å² per residue. That on pH 11.8 was furthermore lower at the larger area than about 50 Å² per residue, but identical at the smaller area. However, we had to wait for a long time to obtain the equilibrium value at the higher pH than 9. This fact and the trend of some fluctuation for observed value show that there may be some lack of uniformity even at the oil/water interface. The values of the product of interfacial pressure and area per residue extrapolated to infinite area are shown in Fig. 6 as the function of the pH of substrate.

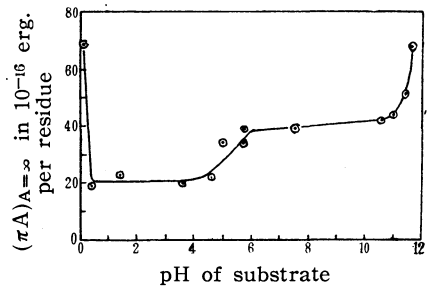



Fig. 6. The product of interfacial pressure ($\pi$) and area per residue (A) of poly-N-vinyl pyrrolidone extrapolated to infinite area plotted against the pH of substrate.

From these facts, it is concluded that the behavior of this film is different according to the acidity or alkalinity of the substrate, and affected more sensitively by alkali than acid. However, the evidence of this difference is somewhat obscured by the non-uniformity of compression as mentioned above.

This non-uniformity is so considerable in the pH range to show the effect of the substrate that we could not confirm the extent of change with the pH sufficiently accurately. On the other hand, Frank had found on studying the lactam-amino acid equilibrium at 100°C that this polymer is more labile in the alkaline solution in contrast with the acidified solution[8]. His result is also qualitatively consistent to the present result.

The trend shown in Fig. 6 gives another evidence of the above conclusion. The value on the acidified substrate is almost identical to that of polyvinyl acetate[2], which has the massive side chains lying at the interface similar to this polymer. The value on the alkaline substrate does not show any serious change of structure, but only a small change such as hydration. Such a hydration is conceivable when we consider the instability in the alkaline solution mentioned above[8]. The high value at both the extremes of pH in Fig. 6 is presumably owing to the partial hydrolysis, but its extent in the pH range shown in Fig. 6 should be very small in the light of the value of interfacial potential at these pH especially at the smaller area. Such a fact was previously reported in the case of polymethacrylic acid[4].

The interfacial moment at the oil/water interface in Fig. 4 is kept constant to 350 mD. up to 35 Å$^2$, decreases rapidly to 290 mD. at 25 Å$^2$ and furthermore to 210 mD. at 18 Å$^2$ per residue, namely, at the collapse point. The latter two kink points shown by arrows in Fig 4 appear also in the interfacial pressure curve at the same areas as shown by arrows in Fig. 5, respectively. Therefore, the film is considered to be transformed at these areas with the fair change of hydrophility of polar groups. Furthermore, since the bond moment of C−N bond as well as C−O bond in vacuo is small compared with C=O bond[6], the inclination of C=O bond for each state of this polymer at the oil/water interface can be estimated from Table I of the third paper[3]. The models proposed in Table I in the present paper are considered to be consistent with the previous table[3] and also with the corresponding area shown in this table taking into account the behaviour of other polymers previously investigated[1-5]. In this table carbon atom of main chain is represented by C*.

Although the surface moment at the air/water interface is somewhat uncertain due to the non-uniformity as mentioned above, the valus of curves b′ and c′ in the constant moment range at the larger area in Fig. 4 are almost identical with those at the areas of the first and second kink points of curve o, respectively. Furthermore, the largest area of maximum surface potential is also identical with the area at the first kink point of curve o. It is considered from these facts that the configuration under the above respective condition corresponds to that for the same value of surface moment in Table I. That is, as mentioned above, the difference between their respective condition is not caused by the serious change of structure, but by the small change of hydration of polar groups as shown in Table I. The model of most condensed type corresponding to curve c′ is consistent with the trend of observed value already mentioned, but apparently inconsistent with the lability of the film on alkaline substrate. Such an inconsistency is not clarified at present.

## Summary

As the result of the measurements of the interfacial pressure and potential of polyethylene terephthalate and poly-N-vinyl pyrrolidone at the air/water and oil/water interfaces, it is concluded that the ring groups in the main chain make the polymer molecule rigid even at the oil/water interface, while that in the side chain is not essentially different from the chain groups. The film of poly-N-vinyl pyrrolidone is relatively labile on the alkaline substrate.

In conclusion, the author expresses his hearty thanks to Prof. T. Isemura for his kind guidance throughout the present work and to Prof. S. Murahashi of our Institute who kindly supplied valuable samples to him. The cost of this research has partly defrayed from the Scientific Research Encouragement Grant from the Ministry of Education, to which the author's thanks are due.

*The Institute of Scientific and Industrial Research, Osaka University, Sakai, Osaka*

8) H. P. Frank, *J. Polymer Sci.*, **12**, 565 (1954).

# *Studies on Fused Iron Catalyst for Alcohol Synthesis by Hydrogenation of Carbon Monoxide. III. Function of Copper in the Catalyst*

By Hiroshi UCHIDA, Hideo ICHINOKAWA and Kiyoshi OGAWA

(Received August 16, 1954)

## Introduction

Though the fused iron catalyst had been used in the I. G. Farbenindustrie A. G.,[1] and thereafter by R. B. Anderson,[2-4] et al. for the Fischer-Tropsch- as well as Synol-synthesis, it had never been a special catalyst for the synthesis in high yield of alcohols, but the ordinary catalyst for ammonia synthesis.

In this respect, we have been conducting a series of experiments in order to shed some light upon the fused iron catalyst for alcohol synthesis. Our preceeding experiment[5,6] revealed that the fused iron catalysts could be divided into two groups. The catalysts in one group contained $Al_2O_3$ and $K_2O$ as principal promoters, and those in another group had $SiO_2$, MgO and $K_2O$ as such. The catalysts of the first group could sometimes be found highly active, and gave alcohol-rich products when the synthesis was conducted at low temperatures. In the facility of producing alcohol-rich products, the catalysts in the second group, however, stood behind those of the first group, even though the synthesis could be undertaken at a considerably low temperature.

A consideration of this result has led us to expect that a catalyst suitable for alcohol synthesis may be obtained if it contains other promoters together with those found in the highly active catalyst of the first group.

The present paper deals with the experiments of the expectation, and shows the effect of the addition of copper ont he behaviour of the catalyst. The effect is to make the catalyst favorable for the production in high yield of oxygenated compounds, but to cause a decrease in the activity in water-gas synthesis.

1) P.B.R. 98, 165.
2) R.B. Anderson, and J.F. Shultz et al., *J. Am. Chem. Soc.*, 72, 3503 (1950).
3) R.B. Anderson, and B. Seligman et al., *Ind. Eng. Chem.*, 44, 391 (1952).
4) R.B. Anderson, and J. Feldman et al., ibid., 44, 2418 (1952).
5) H. Uchida, and N. Todo et al., *J. Chem. Soc. Japan, (Ind. Sect.)*, 56, 487 (1953) (in Japanese).
6) H. Uchida, and K. Ogawa et al., ibid., 57, 100 (1954).

## Experimental Procedure

The contribution of promoters in the fused iron catalyst was examined both by the activity measurement and by the analysis of synthesis products obtained with the catalyst.

Surface properties of the catalyst were simultaneously studied, in order that a better knowledge of the effect and role of the promoter might be obtained.

**Preparation of Catalyst and the Synthesis.**—The catalyst was prepared according to the method previously reported,[7] and was subsequently crushed to granules of 1–2 mm. diameter. Figs. 1, 2, 3, and Table I illustrate the composition of the promoters. The numerals listed in the row for promoter-composition indicate the weight percentages of the promoters which might be present in the catalyst when iron could be exactly oxidized to $Fe_3O_4$.

The synthesis was carried out in an electrically heated 15 mm. I. D. catalyst testing reactor into which was inserted a 7 mm. O. D. thermocouple well. Before the synthesis, the catalyst (60 cc.) was reduced in a hydrogen stream under a pressure of between 20 to 40 kg. per $cm^2$ at a space velocity of between 3,000 to 5,000 per hour. The temperature was in the range of 470–500°C. The reaction was made under a pressure kept at 25 kg. per $cm^2$ and at a space velocity for the synthesis gas ($H_2$ : CO = 1 : 1) of 500 per hour. It was started from a temperature where the gas contraction* could be kept below 20% for the initial 2 or 3 days, and was continued with a gradually rising temperature, until a gas contraction of 50% was attained. The temperature required for maintaining this contraction in the continued operation was taken as a measure of the relative activity.

The oily products were distilled into fractions** of a temperature difference of 20°C and subsequently analysed for alcohols, esters and carbonyl compounds by the method previously reported[5]. At the same time, the contents of carbon monoxide, hydrogen, methane, and of gaseous olefins in the exit gas were determined.

**Microscopic Observation.**—A preparation of a catalyst was observed under a microscope, after having been thoroughly polished and subsequently

7) G. Shima and H. Uchida, *Rep. Chem. Ind. Res. Inst. Tokyo*, 45, 369 (1950) (in Japanese).

* Defined as $(1-E/F)\times 100\%$, where $E$ is the volume of exit gas containing $CO_2$ at S.T.P. and $F$ is the volume of feed gas at S.T.P. (30l./hr.).

* The fractional distillation was continued first under the atmospheric pressure, and then under a reduced pressure of 5 mm Hg, until the final distillation temperature attained to 200°C and 190°C respectively.

etched by hydrochloric acid. Observations were made at a definite time interval on the same region of the specimen throughout the reduction. In addition, a replica stripped from the etched surface was subjected to the electron microscopic observation.

**Determination of Surface Properties of the Catalyst.**—The speciments having been used for the activity measurement in the ammonia synthesis at 100 kg./cm², were employed for the surface area determination by means of B E T method from the physical adsorption isotherms of $CO_2$ at −78°C. The surface concentration of $K_2O$ (+CaO)* was also estimated according to the procedure by P. H. Emmett.[8] After the measurements with $CO_2$, the chemisorption of CO was undertaken at −78°C according to S. Brunauer[9] in order to estimate the surface concentration of iron. The pore volumes were measured by water- and mercury-displacement method[10] to calculate the average pore radius.

## Experimental Results

**Activity and Oxygenated Compounds.**—Cat. 101 was highly active, as shown in Fig. 1. The addition of CuO to the Cat. 101, producing Cat. 301, reduced the activity markedly, but, in turn, increased the quantity of the oxygenates in the products. The detailed measurement of the activity in relation to varying amounts of CuO and $K_2O$, showed that the activity tended to decrease

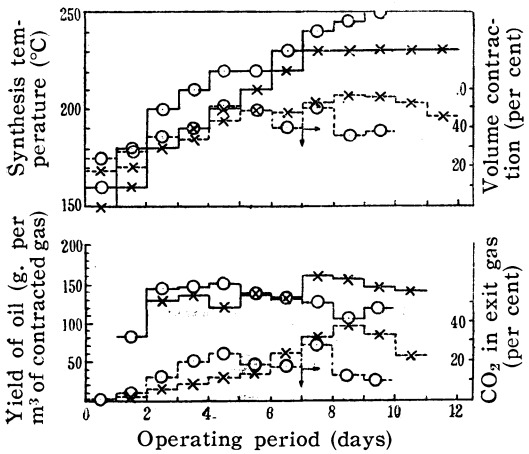



Fig. 1–3 Above; Temperatures of operations required to maintain constant contraction.
Below; Yields of oil products, g./m³ of contracted gas and $CO_2$ in exit gas.
×; Cat. 101 ($2Al_2O_3$, 1CaO, 1MgO, $1WO_3$, $1K_2O$)
○; Cat. 301 ($3Al_2O_3$, 1CaO, 1MgO, $1WO_3$, 1CuO, $1K_2O$)

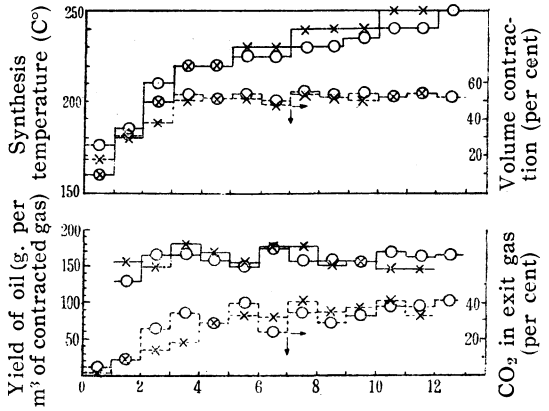



Fig. 2.
×; Cat. 302 ($3Al_2O_3$, 1CaO, 1MgO, $1WO_3$, 0.5CuO, $1K_2O$)
○; Cat. 304 ($3Al_2O_3$, 1CaO, 1MgO, $1WO_3$, 0.25CuO, $0.5K_2O$)

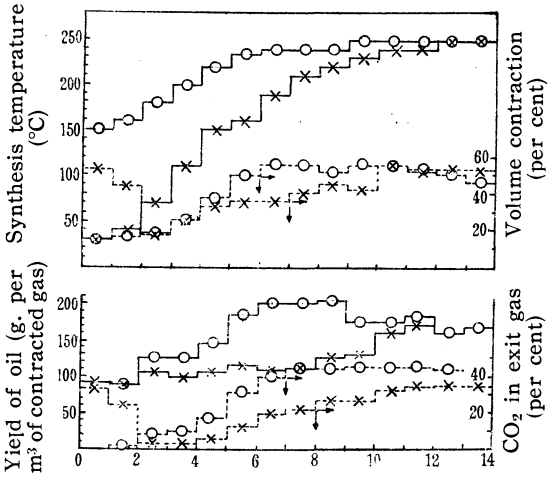



Fig. 3.
×; Cat. 330 ($3Al_2O_3$, $2SiO_2$, 1CaO, 1MgO, $2.5K_2O$)
○; Cat. 331 ($3Al_2O_3$, $2SiO_2$, 1CaO, 1MgO, 1CuO, $2K_2O$)
The ordinates below in Figs. 1–3 indicate $a \times 1000/(F-E)$; a, oil per $F$ litres of feed gas, $E$, volume of exit gas containing $CO_2$.

with the increasing amount of CuO (0.25–0.5–1.0%) but remained unaffected by the varying amount of $K_2O$ (0.5–1.0%). A small amount of 0.25% of CuO was sufficient to increase the content of oxygenates. Among the catalysts of the first group, Cat. 302 (CuO, 0.5%) seemed to produce a maximum of oxygenates which attained to one half of the products (Fig. 5). Therefore it follows by no means that the products obtained with the catalysts of high activity are necessarily rich in the oxygenates. More oxygenates, however, were

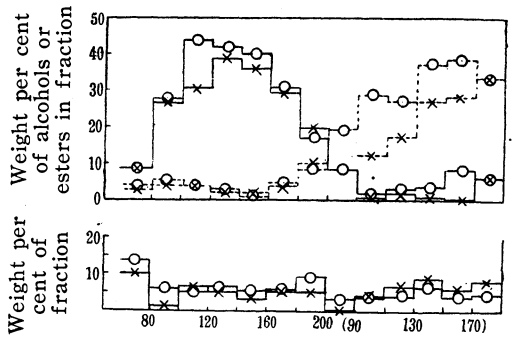
* CaO behaves similarly with $K_2O$ in the physical and chemical adsorption of $CO_2$. (H. Uchida and T. Sato, ibid., **46**, 103 (1951)).

8) P. H. Emmett and S. Brunauer, *J. Am. Chem. Soc.*, **59**, 310 (1937).

9) S. Brunauer and P.H. Emmett, ibid., **62**, 1732 (1940).

10) A. Juhola and E.O. Wiig, ibid., 71, 2078 (1949).

produced with Cat. 304 (Fig. 5). at lower reaction temperatures than at higher temperatures. The results may be interpreted to




Figs. 4–6 Above; Contents of alcohols and esters in oil products. Full line, alcohols; dotted line, esters.
Below; Weight per cent of fractions.
×; Cat. 101 ($2Al_2O_3$. 1CaO, 1MgO, $1WO_3$, $1K_2O$)
(React. temperat., 180–230°C)
○; Cat. 301 ($3Al_2O_3$, 1CaO, 1MgO, $1WO_3$, 1CuO, $1K_2O$)
( ,, ,, ,180-230°C)

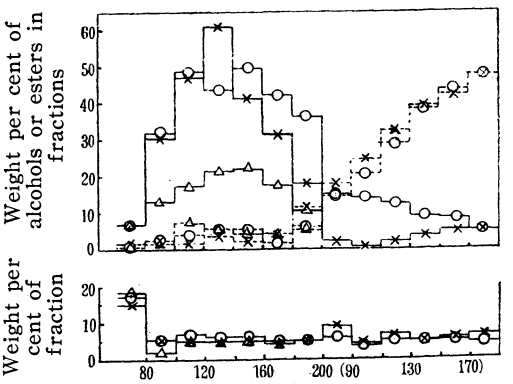



Fig. 5.
×; Cat. 304 ($3Al_2O_3$, 1CaO, 1MgO, $1WO_3$, 0.25CuO, $0.5K_2O$) (180–230°C)
△; ,, ( ,, ) (240–250°C)
○; Cat. 302 ($3Al_2O_3$, 1CaO, 1MgO, $1WO_3$, 0.5CuO, $1K_2O$) (170–250°C)

mean that in the case of a given catalyst, the lower the operation temperature is, the higher the yield in oxygenates is. The carbonyl compounds increased with the increasing amount of alcohols plus esters and amounted to an extent of from 4 to 7% in the fractions of between 100–200°C. Throughout the syntheses, with the catalysts of the first group, $CO_2$ in the exit gases remained small in amount at low operation temperatures and increased up to 40% with rising temperature. The higher temperature was favourable for the formation of gaseous olefins and methane, each attaining in amount to 2–3% and 7–9% respectively in the exit gas at 240–250°C. Aqueous products were usually about one half of the oily products in weight and contained 7–12% of alcohols*, and acids equivalent in amount to 2–2.7% acetic acid.

Among the catalysts of the second group, a particular catalyst (2.5 $SiO_2$, 2MgO, 1CaO, $1WO_3$, $1K_2O$) was active at low temperatures of 70–100°C.[6] A catalyst containing $Al_2O_3$ together with $SiO_2$, MgO, CaO, and $K_2O$ (Cat. 330) was again highly active producing the oil at 30–50°C with 50% of the gas contraction (Fig. 3). The activity lasted only for 2 days, and the temperature of 170–180°C was required to maintain the contraction at 40% in the continued operation. With this catalyst, the product below 120°C contained very small amounts of alcohol (Fractions; 120–140°C, 4.4%, 140–160°C, 4.1%, 160–180°C, 6.0%), while that at higher temperatures (130–250°C) the somewhat greater amount (14.0%, 10.6%, 3.9%, of the respective fractions). The catalyst seemed rather less suitable for the alcohol synthesis than those of the first group. In this connection, H. Tramm[11] had already avoided a large quantity of diatomite earth in the precipitated iron catalyst for the alcohol synthesis. By the addition of CuO to Cat. 330 (Cat. 331), the activity was lowered (Fig. 3), while the somewhat higher yield of alcohols was obtained (Fig. 6), yet not very significantly. Similar behaviour was also found with the catalysts containing $SiO_2$, MgO, CaO, and $K_2O$ with (Cat. 320) and without CuO (Cat. 209).

Among the precipitated iron catalysts, a catalyst promoted by MgO, CaO, CuO, and $K_2O$, but by neither $Al_2O_3$ nor $SiO_2$ was frequently used in the Fischer-Tropsch synthesis by H. Koelbel[12]. A fused catalyst of the similar promoter-composition (Cat. 311) was employed in the present experiment. It was found to be of a low activity, and produced a very small amount of oxygenates (Fig. 6) with a large quantity of high boiling fraction (Table I).

**Microscopic Structure.**—Large grains develop on the etched surface of Cat. 101 containing $Al_2O_3$, CaO, $K_2O$ etc. and no CuO. The grains are divided into finer sub-grains by regular orientations of narrow grain boundaries (Photo. 1). These grains appeared as fine crystallites with sharp facets in the electron microscope (Photo. 2), their dimen-

* The water-soluble alcohols obtained with Cat. 301, comprised 0.4%-$C_1$, 7.0%-$C_2$, 1.2%-$C_3$, 0.4%-$C_4$.

11) H. Tramm, *Brennstoff Chem.*, **33**, 21 (1952).

12) H. Koelbel, and P. Ackermann et al., *Chem. Ing. Tech.*, **23**, 183 (1951).

TABLE I

PROMOTER-COMPOSITION AND FRACTION OF THE PRODUCT DISTILLED BELOW 200°C

| Catalyst | 101 | 301 | 302 | 303 |
|---|---|---|---|---|
| Promoter-composition | $2Al_2O_3$, 1CaO $1WO_3$, 1MgO, $1K_2O$ | $3Al_2O_3$, 1CaO, 1MgO, $1WO_3$, 1CuO, $1K_2O$ | $3Al_2O_3$, 1CaO, 1MgO, $1WO_3$, 0.5CuO, $1K_2O$ | $3Al_2O_3$, 1CaO, 1MgO, $1WO_3$, 1CuO, $0.5K_2O$ |
| Fraction below 200°C wt. % | 37.3 | 51.3 | 52.0 | 53.2 (180–230) 56.5 (240–250) |
| (Reaction temperature °C) | (180–230) | (180–250) | (170–250) | |
| Catalyst | 304 | 311 | 209 | 210 |
| Promoter-composition | $3Al_2O_3$, 1CaO, 1MgO, $1WO_3$, $0.25CuO$, $0.5K_2O$ | 3MgO, 1Cao, $1WO_3$, 1CuO, $1K_2O$ | $2.5SiO_2$, 2MgO, 2CaO, $1K_2O$ | $2.5SiO_2$, 2MgO, 2CaO, $1K_2O$, 0.5CuO |
| Fraction below 200°C wt. % | 43.2 (180–230) | 27.0 | 45.7 | 40.5 |
| (Reaction temperature °C) | 48.1 (235–250) | (180–270) | (180–250) | (180–250) |
| Catalyst | 330 | | | |
| Promoter-composition | $3Al_2O_3$, $2SiO_2$, 1CaO, 1MgO, $2.5K_2O$ | | | |
| Fraction below 200°C wt. % | 67.8 (30–110) | | | |
| (Reaction temperature °C) | 47.0 (130–250) | | | |

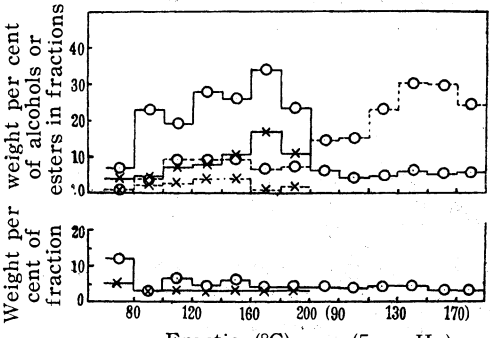



Fig. 6.

×; Cat. 311 (3MgO, 1CaO, $1WO_5$, 1CuO, $1K_2O$) (180–270°C)

○; Cat. 331 ($3Al_2O_3$, $2SiO_2$, 1CaO, 1MgO, 1CuO, $2K_2O$) (150–250°C)

sions being a few microns in the smallest. By the addition of a small amount of CuO (0.25%), the narrow grain boundaries disappeared (Photo. 3, 4). Increasing amounts of CuO caused the gradual appearance of intergranular inclusions (Photo. 5), which revealed the metallic lustre of copper before the etching (Cat. 303). Copper added in excess of the quantity which permitted the copper to dissolve into the grains, thus segregated along the grain boundaries. Quite different from those of the first group were the catalysts of the second group, containing glassy inclusions between the grains as previously reported[13,14] (Photo. 7), and not possessing well-developed cleavage surfaces (Photo. 8). This is a significant feature of the catalyst of the second group. The addition of copper gave no remarkable change in the microscopic structures of these catalysts. After the reduction in hydrogen, cracks wider than those of the catalysts of the first group appeared, probably because of stronger shrinkage of the grains. Cat. 330 which contained $SiO_2$ and $Al_2O_3$ with a large amount of $K_2O$, showed the regular orientations of narrower boundaries as well as the crystalline inclusions (Photo. 9 and 10).

**Determination of Surface Properties of the Catalyst.**—The results are summarised in Table II. The addition of copper seemed to bring about increase in the surface area. With respect to the surface concentration of $K_2O$, the data were not sufficient to give any definite effect of copper. The adsorption of CO by copper might prevent the S. Brunauer's[9] procedure for the estimation of the surface concentration of iron from the direct use of the method for the catalysts containing copper. Preliminary measurements of adsorption of CO at −78°C were, therefore, carried out with copper supported on $Al_2O_3$. Nearly the same amount of CO

13) Z.W. Wilchinsky, *Anal. Chem.*, **21**, 1188 (1949).
14) H. Uchida, N. Todo et al., *Rep. Chem. Ind. Res. Inst. Tokyo*, **46**, 11 (1951) (in Japanese).

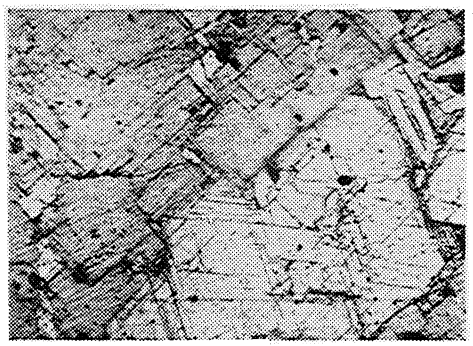


Photo. 1. Cat. 101 ($2Al_2O_3$, 1CaO, 1MgO, $1WO_3$, $1K_2O$) ×100



Photo. 2. Cat. 101 Replica ×5.000

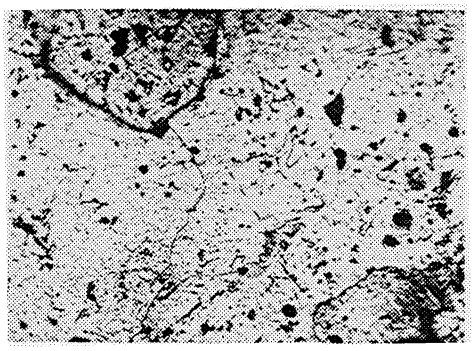


Photo. 3. Cat. 304 ($3Al_2O_3$, 1CaO, 1MgO, $1WO_3$, 0.25CuO, $0.5K_2O$)

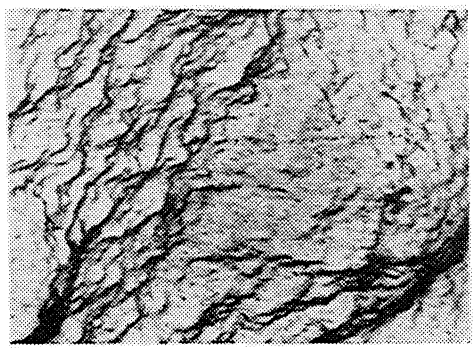


Photo. 4. Cat. 304 Replica

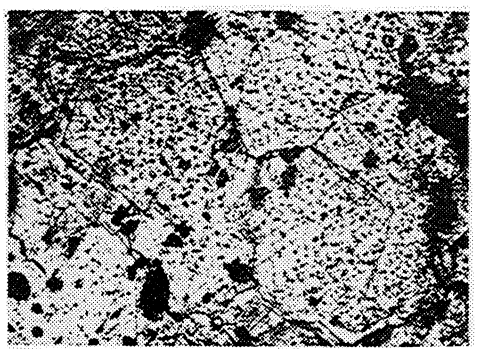


Photo. 5. Cat. 302 ($3Al_2O_3$, 1CaO, 1MgO, $1WO_3$, 0.5CuO $1K_2O$)

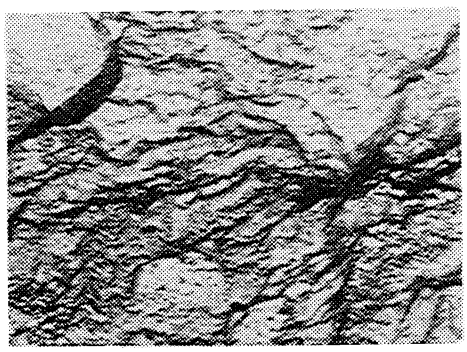


Photo. 6. Cat. 302 Replica

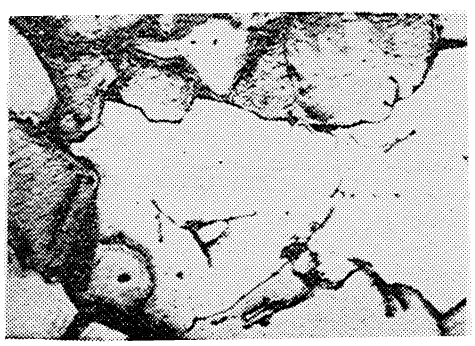


Photo. 7. Cat. 209 (2.5$SiO_2$, 2MgO, 2CaO, $1K_2O$)

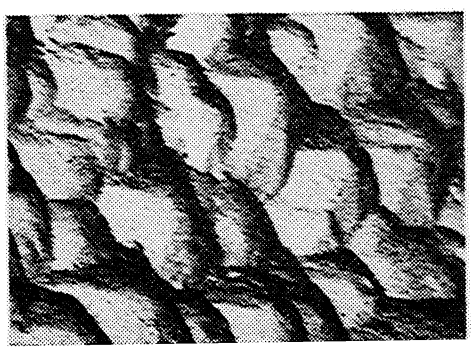


Photo. 8. Cat. 209 Replica

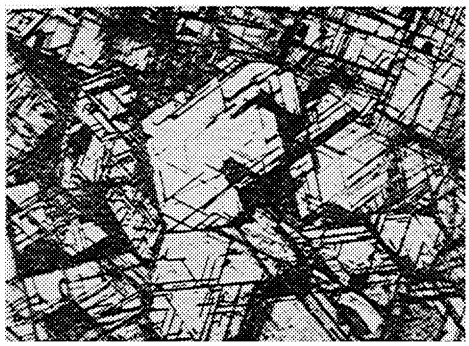


Photo. 9. Cat. 330 ($3Al_2O_3$, $2SiO_2$, ICaO, 1MgO, $2.5K_2O$) ×100

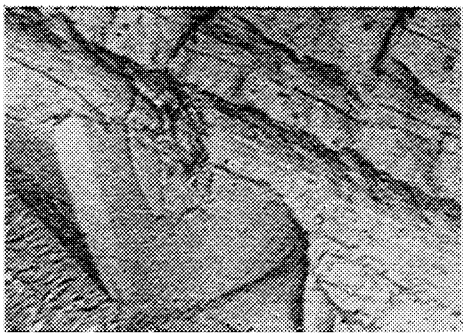


Photo. 10. Cat. 330 Replica ×5.000

was adsorbed at the following successive adsorptions; the one immediately after a degassing at 500°C and the one succeeding after an evacuation at 0°C for one hour (8.2 cc./g.Cu at the first and 7.9 cc./g.Cu at the second at 50 mm Hg). In contrast to the above, the major part of CO adsorbed at −78°C remained adsorbed through the evacuation at 0°C with Cat. 101. The difference between the first and the second measurements ($V_{CO} - V'_{CO}$) might be assumed, for convenience, to represent the surface concentration of iron with respect to the catalysts containing copper. The values of ($V_{CO} - V'_{CO}$) for the catalysts of the second group (Cat. 209, 320) were smaller than those for the first group, while the values of $V_{CO}$ per unit area for the former were larger than those of the latter. The values of 1-A in Table II might express the surface concentration of the promoters, as of $Al_2O_3$, Cu, exclusive of both iron and $K_2O$ (+CaO). In the case of the catalysts of the first group (with an exception of Cat. 302), the values increased with the addition of copper. This fact suggested that copper might concentrate on the surface.

## Discussion

According to the study by H. Koelbel,[12] the addition of 0.05% of copper to iron caused a complete activation during the induction (or the formation) of the precipitated catalysts as well as a marked change in character of the products. On the other hand, according to S. Kodama,[15] 25% of copper to iron was needed for a sufficiently high yield of the oil. The present experiments have shown that a small amount of CuO was enough to bring about a considerable increase of the oxygenates. The microscopic structure, the surface area, and the chemisorption of CO changed also appreciably at the addition of this amount. These results were more like those of H. Koelbel. Since an excess addition of copper causes the segregation along the grain boundaries, it may be right that the further tendency for alcohols to increase considerably, should not be predicted.

TABLE II

SURFACE PRORERTIES

| Catalyst | 101 | 301 | 302 | 303 | 304 | 311 | 209 | 210 | 330 |
|---|---|---|---|---|---|---|---|---|---|
| Surface area $m^2/g.$ | 3.3 | 8.9 | 7.5 | 12.5 | 13.5 | 1.6 | 4.3 | 3.7 | 6.0 |
| $V_{cCO_2}/V_{mCO_2}$ | 0.59 | 0.32 | 0.61 | 0.36 | 0.37 | 0.57 | 0.45 | 0.28 | 0.74 |
| Pore volume cc./g. | 0.120 | 0.112 | 0.122 | 0.112 | 0.124 | 0.123 | 0.136 | 0.102 | 0.138 |
| Average pore radius Å | 1385 | 465 | 600 | 355 | 325 | 2710 | 1100 | 1215 | 720 |
| $V_{CO}$ (at −78°C) | 0.29 | 0.69 | 0.61 | 1.09 | 0.88 | | 0.63 | 0.55 | 0.53 |
| $V'_{CO}$ (at −78°C) | 0.096 | 0.24 | 0.24 | 0.39 | 0.36 | | 0.43 | 0.28 | 0.12 |
| 1-A* | 0.13 | 0.45 | 0.16 | 0.39 | 0.45 | | 0.24 | 0.38 | 0.04 |

* $A=(V_{CO} - V'_{CO} + V_{cCO_2})/V_{mCO_2}$, $V_{mCO_2}$; volume of $CO_2$ forming the monolayer on the surface, $V_{cCO_2}$; volume of $CO_2$ chemisorbed at −78°C.

In the case of the precipitated iron catalysts for the hydrocarbon synthesis, the promoting action of copper was ascribed by H. Koelbel[12] to an easier formation of iron-carbon com-

15) S. Kodama, and H. Tawara et al., *J. Chem. Soc. Japan, (Ind. Sec.)* **45**, 1268 (1942) (in Japanese).

pounds. In this connection, S. Kodama[16] attributed it to an increase in number of the active centers at which iron carbides were formed. D. Gall,[17] and E. J. Gibson[18] assumed the synthesis mechanism to involve step-wise addition of methylene radicals to one end of a growing chain terminated by a hydroxymethylene radical or methylene radical to produce alcohols or alcohols and olefins as the initial, desorbed products. Therefore, primarily, the surface structures which may increase or favour the survival of hydroxymethylene radicals, and secondarily, those on which alcohols are not easily adsorbed to be converted to hydrocarbons, may be expected to increase the yield in alcohols. Since the alcohols have been shown to be increased by copper on the surface, copper may contribute to an easier formation of these structures. The structures might be ascribed to the carbides of iron, so far as the considerations by H. Koelbel and by S. Kodama were adopted. The assumption may be also consistent with the fact that the products obtained with Cat. 330 at low temperatures contain an extremely small amount of alcohols, while rather more abundant alcohol has been produced with increasing temperatures in the additional continued operation, during which the formation of the carbides may be achieved.

The low activity of Cat. 311 containing neither $Al_2O_3$ nor $SiO_2$ is expected, to a certain extent, due to its extremely small surface area. Since the catalyst has produced a large amount of high molecular fraction, $Al_2O_3$ together with $SiO_2$ are also effective in the shortening of carbon chains. On the other hand, $Al_2O_3$ and $SiO_2$ showed the promoting actions different from each other in the synthesis. Their microscopic structure as well as their behaviour for the chemisorption of CO differed also greatly between $Al_2O_3$ and $SiO_2$. Consequently, some structural difference of the surface may be supposed between the catalysts promoted by either $Al_2O_3$ or $SiO_2$.

16) S. Kodama, and S. Matsumura et al., ibid., **47**, 3 (1944).
17) D. Gall, and E.J. Gibson et al., *J. Appl. Chem.*, 2, 371 (1952).
18) E.J. Gibson and C.C. Gall, ibid., **4**, 49 (1954).

## Summary

Among the fused iron catalysts for the syntheses from water-gas, those containing $Al_2O_3$ and $K_2O$ as principal promoters behaved differently from those containing $SiO_2$, MgO, and $K_2O$ as such. With the former, it was well known that the products rich in oxygenates were obtained when the synthesis could be carried out at low temperatures. In the present study, an addition of copper has proved to bring about an increase in oxygenates with a simultaneous decrease of the activity. A marked effect of copper on the yield of alcohols has already been realized at the addition of 0.25% of CuO into the catalyst, while no further remarkable effect has been easily observed with its increasing amounts. The observations of microscopic structures, such as the area, the chemisorption of $CO_2$, and CO showed also considerable changes at this amount of addition. An excess amount of copper is liable to segregate along the grain boundaries and hence seems to contribute little for the promotion.

By the addition of $Al_2O_3$ together with $SiO_2$ besides the usual promoters such as CaO, $K_2O$ etc., a catalyst of the high activity, though of short durability, was obtained. In the product obtained with this catalyst at low temperatures, oxygenates have been extremely small, while those obtained by the additional operation at higher temperature are greater in amount.

A particular promoting action, quite different from that of $Al_2O_3$, has been ascribed to $SiO_2$.

## Acknowledgment

The authors' thanks are due to Mr. Tadasuke Hosoya for his cooperation. He has been carrying out a part of this experiment.

*Government Chemical Industrial Research Institute, Tokyo*
*Meguro*

# *Raman Spectrum of Tropolone*

By Sunao IMANISHI and Mitsuo ITO

(Received August 18, 1954)

## Introduction

Infra-red absorption of tropolone (cycloheptatrienolone) has been reported by several authors,[1,2,3] while its Raman data are not published yet. Just as with any other compound these two sets of information are indispensably needed in attempting to analyze and interpret the vibrational structure in the near ultra-violet absorption spectrum of tropolone vapor, which we also are investigating. In this paper are reported the results of our observation on the Raman spectrum of tropolone, one of the prototypes of seven-membered ring hydrocarbons.

## Experimental

The spectrograph used is one constructed in this laboratory having three dense flint glass prisms of side lengths 6 cm. or more, and heights 4.5 cm. or more. The camera lens is a photographic objective of 21 cm. focal length and $F/2.6$ relative aperture, while the collimator lens is an achromat of 45 cm. focus and $F/5$ relative aperture. The spectrum is photographed on a strongly curved film strip placed at the focal surface of the instrument. The reciprocal dispersion of this spectrograph in the vicinity of Hg 4359 Å line is 39 Å per mm.

The scatterer was a solution of 5 g. tropolone in white crystalline powder form prepared in Prof. Nozoe's laboratory at Tohoku University, Sendai, dissolved in pure benzene, the concentration being about 1.6 mol. per litre. The solution was put into a Wood's tube of 1 cm. bore and 15 cm. length, and was irradiated sidewise with two glass mercury lamps, each consuming about 10 amp. current. Kodak "Super XX" panchromatic film was used and the time of exposure was 10 hr. For the calibration of wave-lengths iron arc spectrum was photographed in juxtaposition on the scattered spectrum.

Nine Raman scattered lines in all were observed, all being excited by the Hg 4359 Å and no line originating from the Hg 4047 Å was recorded. This is due to the strong absorption of tropolone lying in the region expected for the appearance of the latter lines. The measured wave-number shifts of the nine Raman lines are given in the 1st. column of Table I, along with their estimated intensities in brackets, the highest of which is assigned to grade number 5.

The tropolone solution was colorless at the start of the exposure, but soon began to turn yellow on irradiation, and the whole sample ultimately became a reddish-brown viscous fluid. This photo-chemical change accompanied by strong coloration made further continuation of the exposure almost meaningless, and a rather premature termination of the experiment was inevitable, although it was not favorable for satisfactorily recording weaker lines. The same photo-chemical coloration was experienced by us in photographing the vapor absorption spectrum of tropolone, but in that case the colored product remained in the liquid phase, not affecting the vapor phase absorption, provided pure tropolone still remained.

## Discussion

Comparing our results with those of infra-red absorption reported by Shimanouchi et al., and given in the 2nd. column of our Table*, the agreement of wave-numbers is generally good, and the intensities go parallel. As we see in the Table three new low frequencies are found in Raman effect which were not measured in infra-red absorption, while counterparts of the two strong infra-red peaks at 1480 $cm.^{-1}$ and 1560 $cm.^{-1}$ could not be clearly confirmed on our film, owing to the approximate coincidence of positions of these lines with the strong scattered lines due to benzene.

In a Raman spectrum shifted lines with overtone or combination frequencies are not normally observed, so that our nine frequencies observed with not insignificant intensities, even under the unfavorable condition stated above, are to be considered all of fundamentals. From this standpoint the reported infra-red frequencies 770 $cm.^{-1}$, 880 $cm.^{-1}$, and 1050 $cm.^{-1}$ may very probably be interpreted as combinations and an overtone, $357+436$ $cm.^{-1}$, $2\times436$ $cm.^{-1}$, and $357+679$ $cm.^{-1}$, respectively, for which, naturally, Raman lines are not observed.

In the 3rd. column of the Table are given some of the fundamental vibration frequencies of tropolone in its electronically unexcited state, which are determined in the vibrational analysis of the near ultra-violet absorption bands of the vapor.[4] The agree-

* Shimanouchi et al. (ref. 3) have not reported the numerical value of frequencies and the intensities of the infra-red absorption peaks. The values given in our Table are those estimated from their published absorption curve.

1) Scott and Tarbell, *J. Am. Chem. Soc.*, 72, 240 (1950).

2) Doering and Knox, *J. Am. Chem. Soc.*, 73, 828 (1951).

3) K. Kuratani, M. Tuboi and T. Shimanouchi, This Bulletin 25, 250 (1952).

4) MS. in preparation.

ment between these and the corresponding Raman values is very satisfactory. The largest discrepancy, 6 cm.$^{-1}$ between the 1262 cm.$^{-1}$ Raman and the 1256 cm.$^{-1}$ ultra-violet frequencies is probably due to change of bond forces concerned in the respective phases of aggregation, revealed specifically pronouncedly in this particular mode of vibration, even though the magnitude itself is quite small. In the near ultra-violet absorption spectrum we have found that the wave-number difference 643 cm.$^{-1}$ constitutes the key frequency, solely giving rise to many long band progressions, meaning that it is the excited state value of a totally symmetrical vibration frequency in the tropolone molecule with respect to its symmetry. In its spectral behaviour this frequency is entirely analogous to the 923 cm.$^{-1}$ excited state frequency of the benzene molecule. Now, the strong Raman shift 743 cm.$^{-1}$ in tropolone can plausibly be identified with the ground state value of the above 643 cm.$^{-1}$ Accordingly, we interpret 743 cm.$^{-1}$ as belonging to the totally symmetrical breathing vibration of the heptatriene ring, analogous to the 992 cm.$^{-1}$ frequency in benzene.

The three frequencies 1262, 1418 and 1610 cm.$^{-1}$, strongly observed in Raman and infra-red, and partly confirmed in ultra-violet absorption, may collectively be assigned to the stretching vibrations of the C—O bonds in the molecule. If these bonds were normal single and double bonds as a conventional non-resonating structure formula would indicate, their stretching vibration frequencies should be much more differentiated (1030 cm.$^{-1}$ in methanol and 1760 cm.$^{-1}$ in acetone). Then, the actual values of these frequencies, being concentrated in a comparatively narrow intermediate frequency region, suggest that the carbon-oxygen bonds in tropolone are of a somewhat different nature from either of the ordinary single or double bond. From electron diffraction measurements the two C—O distances are reported to be 1.34 Å and 1.26 Å,[5] values intermediate between Pauling's covalent radii sums 1.43 Å and 1.22 Å for the normal single and double C—O bonds. This may be understood as due mainly to the effect of resonance, and partly also to the influence of an intramolecular hydrogen bond bridging the two oxygen atoms in the molecule, an inference entirely compatible with the above-reported findings in the Raman spectrum.

By analogy to the benzen spectrum the frequencies 357, 436, 679, 743, 959 and 1208 cm.$^{-1}$ very probably belong to skeleton vibrations of the molecule, in which mainly the seven C atoms move. As we were not able to determine depolarization factors, the symmetry assignments of these fundamentals cannot be directly given now. However, we can at least see that the close parallelism thus found to exist between the skeleton vibration frequencies in benzene and tropolone simply reflects the close similarity of the ring forming valence forces, and hence of the electron structures of the two kinds of aromatic compounds.

The authors thank Professor T. Nozoe for the supply of samples of tropolone and related compounds.

TABLE I

VIBRATION FREQUENCIES IN TROPOLONE (cm.$^{-1}$)

| Raman (present work) $C_6H_6$ solution | Infra-red absorption[3]** $CS_2$ and $CCl_4$ solutions | Ultra-violet absorption vapor |
|---|---|---|
| 357 (2) | | 356 |
| 436 (1) | | |
| 679 (2) | | 678 |
| 743 (3) | 735 (3) | 741 |
| | 770 (2) | |
| | 880 (2) | |
| | 910 (1) | |
| 959 (1) | 950 (2) | |
| | 1050 (2) | |
| 1208 (2) | 1200 (3) | |
| | 1230 (4) | |
| 1262 (4) | 1260 (5) | 1256 |
| | 1300 (4) | |
| 1418 (5) | 1415 (4) | |
| | 1480 (4) | |
| | 1560 (4) | |
| 1610 (5) | 1610 (4) | |

*Chemical Laboratory, Faculty of Science, Kyushu University, Fukuoka*

5) M. Kimura and M. Kubo, This Bulletin, **26**, 250 (1953).

** Regarding the frequency and intensity values for the infra-red absorption peaks see foot note * on p. 75.

# *Vat Dyes of Benzanthrone Series. XXIX.*[1] *Chlorination of 16, 17-Dihydroxy-violanthrone with Phosphorus Pentachloride*

By Toshio MAKI and Mamoru MAEZAWA

(Received August 23, 1954)

A new attempt, a study of the reaction between 16, 17-dihydroxy-violanthrone(I) and phosphorus pentachloride, was carried out by us and certain new 16, 17-derivatives of violanthrone were obtained. They are highly interesting in the chemistry of this polynuclear system. A non aqueous colloidal suspension of 16,17-dihydroxy-violanthrone in *o*-dichlorobenzene was prepared and heated with an excess (2.5 times of the theory) of $PCl_5$ in a nitrogen atmosphere in order to prevent the oxidation of the two hydroxyls. The crude reaction product was a mixture of certain substances of distinctly different solubilities, which were very useful for the separation of the constituents with nitrobenzene and *o*-dichlorobenzene (see Table I).

TABLE I

SOLUBILITY RELATIONS

| | Nitrobenzene | | *o*-Dichlorobenzene | |
|---|---|---|---|---|
| Sbst. | 210° | 15° | 180° | 15° |
| (I) | Hardly sol. | Insol. | Practically insol. | Insol. |
| (II)-A,B | Insol. | Insol. | Insol. | Insol. |
| (III)-A,B | Sol. | Insol. | Hardly sol. | Insol. |
| (IV) | Sol. | Hardly sol. | Sol. | Hardly sol. |
| (V) | Sol. | Sol. | Sol. | Sol. |

The presence of the hydroxyl in either or both of the 16,17-positions was conveniently detected by the sensitive color change of the cotton dyeings with acids and alkalis. We have found also that the absence of the hydroxyl is indicated by a water drop sensitiveness of the dyed fabrics, whereby a temporary reddish spot is produced by wetting with a water drop. Thus, for example, the initial 16,17-dihydroxy-violanthrone dyes cotton from a blue vat in clear yellowish green, which is quite indifferent against a water drop but becomes clear blue by dilute mineral acids and yellow green by dilute caustic alkalis (see Table II).

The part perfectly insoluble in boiling nitrobenzene is concluded as a monochloro-16,17-violanthrone-oxide (II-A of Table III), associated with a small amount of a dichloro compound (II-B). The 16,17-violanthrone-oxide is quite a new type of compound hitherto unknown in this series. The conlstitution is determined by us from the folowing facts: (1) Its blue violet color is entirely different from the yellowish green of the original 16,17-dihydroxy compound. The color change is remarkably hypsochromic. (2) It is extremely insoluble in organic solvents. Such insolubility is not found among the known blue-violet compounds of violanthrone series. (3) The hydroxyl group is absent. (4) It is sensitive to a water drop. (5) Its chlorine content is distinctly lower (found Cl, 8.68%) than that of the chlorine replacement of the 16,17-dihydroxyls to (IV) (calcd. Cl, 13.50%). (6) It is easily soluble

TABLE II

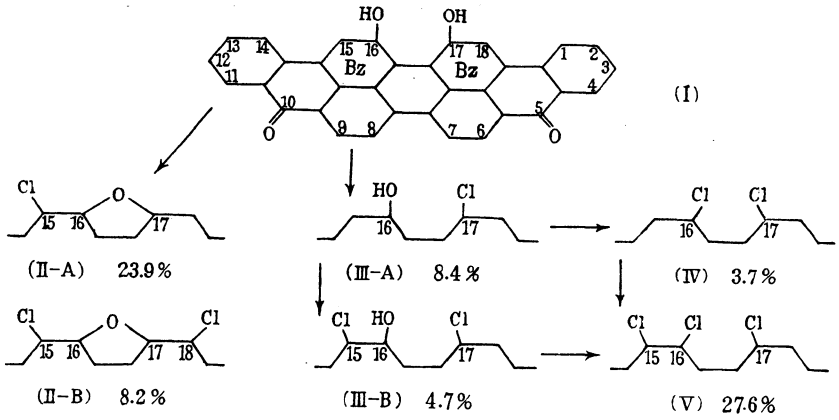
COLOR REACTIONS OF COTTON DYEINGS (1%)

| Sbst. | Original shade | Dil. HCl | Dil.NaOH | Water drop | OH in 16.17-position |
|---|---|---|---|---|---|
| (I) | Yellowish green | Clear blue | Yellow green | Indifferent | 2 |
| (II)-A,B | Blue violet | Indifferent | Indifferent | Reddish | None |
| (III)-A,B | Greenish gray blue | Dark blue | Gray green | Almost indifferent | 1 |
| (IV) | Violet blue | Indifferent | Indifferent | Reddish | None |
| (V) | Grayish blue | Indifferent | Indifferent | Reddish | None |

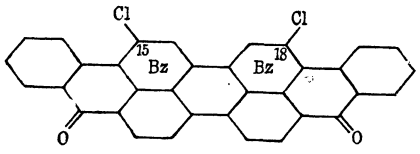
1) Read before the 6th Annual Meeting of the Chemical Society of Japan on April 5, 1953. Cf. the preceding report XXVIII, T. Maki, *J. Chem. Soc. Ind. Japan*, 50, 142 (1947).

TABLE III

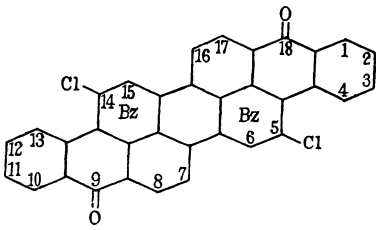
CONSTITUTION AND YIELD (% OF THE THEORY)




in alkaline hydrosulfite giving a blue vat, which proves the presence of the unchanged 5,10-dicarbonyls. (7) Considering the steric relation of 15-chloro or 15,18-dichloro group the monomolecular formula (II-A, B) is preferred by us rather than the bimolecular structure. The position of the chlorine atoms is most probably suggested as 15,18- for two reasons. One of the reasons is the ortho-orienting power of the hydroxyls and the other is our former studies on dichloro-violanthrone[2] and dichloro-isoviolanthrone[3]. Thus, when chlorination was carried out in organic solvents such as nitrobenzene, *o*-dichlorobenzene or acetic acid with free chlorine or sulfuryl chloride the chlorine atoms predominantly entered into 15,18-position



(VI)



(VII)

of violanthrone molecule giving a clear violet vat dye (VI), and also giving the equivalent 5,14-dichloro-isoviolanthrone (VII), which is the chief constituent of Indanthrene Brilliant Violet 2R and 4R.

Any traces of the starting material, 16,17-dihydroxy compound, were no longer found in the reaction product. The part soluble in boiling nitrobenzene but insoluble in hot *o*-dichlorobenzene is mainly 17-chloro-16-hydroxy-violanthrone (III-A), greenish gray blue dye, associated with 15,17-dichloro-16-hydroxy-violanthrone (III-B).

16,17-Dichloro-violanthrone (IV), a new, theoretically very important, violet blue substance, was obtained in minor quantity from the part soluble in hot *o*-dichlorobenzene by cooling. After chromatographic purification its yield was only 3.7% of the theory. The solubilities in organic solvents remarkably increased by the replacement of the 16,17-dihydroxyls with chlorine atoms. It is important that the color of 16,17-dichloro-violanthrone (IV) is found to be more bluish than that of violanthrone, while the 15,18-dichloro isomer (VI) is much redder than the latter.

Both 16,17-and 15,18-dichloro-violanthrone give dyeings of more clear shades than those of the mother substance, violanthrone. The part easily soluble in cold nitrobenzene and cold *o*-dichlorobenzene is mainly 15,16,17-trichloro-violanthrone (V), a grayish blue vat dye.

All the above substances (I—V), which are actually substituted in Bz-rings, have blue vats and Maki's discovery [2,3] on the relation between the blue vat and Bz-substitution in violanthrone derivatives was again confirmed.

2) T. Maki and T. Aoyama, *J. Chem. Soc. Ind. Japan, Suppl.*, 38, 636B (1935).
3) T. Maki and Y. Nagai, *Ber.*, 70, 1867 (1937).

Formerly, one of us studied the reaction between phosphorus pentachloride and 4,4'-dihydroxy-indanthrone, when the chief final product was 3,4,3',4'-tetrachloro-indanthrone[4] and 4,4'-dichloro compound was practically not obtained. It may be, therefore, a behaviour of $PCl_5$ that in the reactions with polynuclear anthraquinone derivatives nuclear chlorination predominates to a greater extent than the simple hydroxyl substitution. In the present case, also, trichloro-violanthrone (V) was obtained in comparatively higher yield.

The formation of the oxide ring (II-A,B), apparently by a dehydration of the two hydroxyls, is quite a special reaction between 16,17-dihydroxy-violanthrone and $PCl_5$. We tried to obtain a substance of the oxide type by fusing 1 part of 16,17-dihydroxy-violanthrone with 15 parts of anhydrous zinc chloride at 290°, but the result was negative. When a colloidal suspension of 1 mol. ratio of 16,17-dihydroxy-violanthrone in *o*-dichlorobenzene was boiled with 20 mol. ratio (large excess) of thionyl chloride for 12 hours the replacement of the hydroxyls with chlorine did not take place at all and only yellow green 15-chloro-16,17-dihydroxy-violanthrone (79%) was obtained together with some unchanged dihydroxy compound (21%).

## Experimental Part

**(1) Treatment of 16,17-Dihydroxy-violanthrone[5] with Phosphorus Pentachloride.**—16,17-Dihydroxy-violanthrone (3.00 g.) was vatted with 24 g. of 25% sodium hydroxide, 5.0 g. of hydrosulfite conc. powder and 600 cc. of water by keeping at 55° for 20 minutes. The filtered vat was oxidized by a current of air and the collected precipitate, after thoroughly washed with water, was treated on the filter 3 times with methanol (20 cc., 10 cc. and 10 cc. resp.) in order to replace the water with methanol. The paste was then mixed with 150 g. of *o*-dichlorobenzene and the remaining methanol, together with about 1/3 the volume of the *o*-dichlorobenzene, was distilled off in a nitrogen atmosphere and thus a colloidal suspension of 16,17-dihydroxy-violanthrone in about 100 g. of *o*-dichlorobenzene was obtained. Phosphorus pentachloride (6.40 g., 5 mol. ratio) was added and also in a nitrogen atmosphere agitated 1 hour at room temperature, 4 hours on a boiling water bath and at last 1 hour at the boiling point of *o*-dichlorobenzene. After neutralizing with anhydrous sodium carbonate, the solvent was distilled off with steam and the collected precipitate, as a dry powder, was heated with 20 times of conc. sulfuric acid at 80° for 1 hour and then poured into water in order to hydrolyze the unstable chlorine such as $>CCl_2$ to $>C=O$. The weight of the reaction product was 3.17 g.

**(2) The Part Insoluble in Boiling Nitrobenzene (II-A,B).**—The crude reaction product (3.17 g.) was finely powdered and boiled with 317 g. of nitrobenzene under reflux and stirring for 1 hour and the insoluble (1.11 g.) was once more boiled with 111 g. of nitrobenzene. The yield of the final insoluble substance was 1.01 g. or 31.9% of the crude product. It is a violet black powder, entirely insoluble in boiling nitrobenzene and *o*-dichlorobenzene, soluble in conc. sulfuric acid with red violet color and dark reddish blue precipitate is formed by the addition of water. From a blue hydrosulfite vat (IN) it dyes cotton blue violet and the obtained dyeings are indifferent against acids and alkalis, but are sensitive to a water drop giving a temporary reddish spot, which disappears with the natural evaporation of water. Found: Cl, 8.68; calcd. for $C_{34}H_{13}O_3Cl$ (II-A): Cl, 7.02%; calcd. for $C_{34}H_{12}O_3Cl_2$ (II-B): Cl, 13.15%. So the substance corresponds mainly (73%) to 15-chloro-16,17-violanthrone oxide (II-A), associated with 27% of the dichloro oxide (II-B). The actual yield of (II-A) is therefore 23.9% and that of (II-B) is 8.2% of the theory.

**(3) The Part Soluble in Boiling, but Insoluble in Cold Nitrobenzene.**—By standing over night 0.76 g. and 0.05 g. of precipitates were obtained from the above first and second nitrobenzene filtrate respectively.

**A) The Part Insoluble in Boiling *o*-Dichlorobenzene (III-A,B).**—Both precipitates were combined (0.81 g. or 25.6% of the crude reaction product) and as a dry powder boiled with 81 g. of *o*-dichlorobenzene for 1 hour and the insoluble substance (0.50 g.) was once more boiled with 50 g. of the same solvent, whereby 0.41 g. (15% of the crude reaction product) of an insoluble matter was obtained. This is a violet black powder of dark blue streak and soluble in conc. sulfuric acid with red violet color. Hydrosulfite vat (IN) is blue with weak violet fluorescence and dyes cotton in greenish gray blue, which is changed by acids into dark blue and by alkalis into gray green, but is almost indifferent against a water drop. Found: Cl, 9.22, calcd. for $C_{34}H_{15}O_3Cl$ (III-A): Cl, 7.00%; calcd. for $C_{34}H_{14}O_3Cl_2$ (III-B): Cl, 13.10%. This substance is therefore composed of 64% of 17-chloro-16-hydroxy-violanthrone (III-A)

4) Dark violet needles from o-dichlorobenzene, in conc. sulfuric acid brown and with water blue violet precipitate. It was hardly soluble in alkaline hydrosulfite. T. Maki and T. Mine, *J. Chem. Soc. Ind. Japan*, **51**, 15 (1948).

5) Benzanthrone (20 g.) was fused with 50 g. of KOH and 48.5 g. of isobutanol in presence of anhydr. sodium acetate (6 g.) at 110—2° for 3 hours. The crude product, as a dry powder, was boiled with 10 parts of *o*-dichlorobenzene to remove certain soluble impurities. The obtained 2, 2'-dibenzanthronyl was an olive gray powder, but of high purity, melting at 330—3° (corr.) and dissolving in conc. $H_2SO_4$ orange red without fluorescence. The yield was 15.8 g. (79.4% o. th.). Dibenzanthronyl (10 g.) was then dissolved in 300 g. of 84% $H_2SO_4$ and oxidized with 19 g. of 66% $MnO_2$ at 25—30° for 3 hours. The insoluble part was filtered through asbestos, thrown into water, and the obtained paste was heated with 15 g. of sodium bisulfite in 300 cc. of water and after acidification 16, 17-dihydroxy-violanthrone was collected. The yield was 8.0 g. (75.1% o. th.). The operations given in FIAT **1313**, II, 83—5 should be somewhat modified.

and 36% of 15,17-dichloro-16-hydroxy compound (III-B). The actual yield of (III-A) is 8.4% and that of (III-B) is 4.7% of the theory.

**B) The Part Soluble in Boiling, but Insoluble in Cold *o*-Dichlorobenzene (IV).**—When the above *o*-dichlorobenzene filtrates (3A) were allowed to stand over night 0.27 g. (8% of the crude reaction product) of a violet black precipitate was obtained. In order to make it completely free from the trace of the associated chlorohydroxyl compounds (III-A,B) it was dissolved in 54 g. of boiling *o*-dichlorobenzene, chromatographed on alumina, developed with 32.4 g. of boiling nitrobenzene, washed with 10 cc. of alcohol and the upper dark blue gray layer was eluted 5 times with each 50 g. of boiling *o*-dichlorobenzene. After steam distillation of the solvent 0.12 g. (3.6% of the crude reaction product) of a purified substance was obtained, which is a violet black crystalline powder with metallic lustre. Found: Cl, 14.53%; calcd. for $C_{34}H_{14}O_2Cl_2$ (IV): Cl, 13.50%.

The hydrosulfite vat of this substance is blue with weak violet fluorescence and dyes cotton (IN) violet blue, more bluish than violanthrone and 15,18-dichloro-violanthrone (VI). Its dyeings are quite indifferent against acids and alkalis, but are sensitive to a water drop giving a temporary reddish spot. The substance has no connection with the hydroxyl group and corresponds to 16,17-dichloro-violanthrone (IV). Contrary to the hydroxylated compounds it is soluble in hot *o*-dichlorobenzene with intense violet blue color with strong red fluorescence. Conc. sulfuric acid solution is red violet without flourescence and blue precipitate is produced from the acid solution by water. The actual yield of 16,17-dichloro-violanthrone is about 3.7% of the theory.

**(4) The Part Soluble in Cold Nitrobenzene and Cold *o*-Dichlorobenzene (V).**—The above cold nitrobenzene filtrates (2) were combined (ca. 428 g.) and nearly 5/6 of this solvent was distilled off. After cooling 0.27 g. of an impure precipitate was removed and the clear filtrate was distilled with steam, when 0.89 g. of a violet black powder was obtained. Found: Cl, 19.72%; calcd. for $C_{34}H_{13}O_2Cl_3$ (V): Cl, 19.01%. It dyes cotton grayish blue from a blue hydrosulfite vat (IN) and the dyed fabrics are quite indifferent against acids and alkalis, but are sensitive to a water drop. The substance is found to be 15,16,17-trichloro-violanthrone (V), free from any hydroxyl groups. It is very easily soluble in *o*-dichlorobenzene in red violet color with strong red fluorescence and is soluble in conc. sulfuric acid red violet without fluorescence. A small quantity (0.06 g.) of the same substance was also obtained from the cold *o*-dichlorobenzene filtrates of (3B) after steam distillation of the solvent. The total yield of the trichloro-violanthrone (V) is therefore 0.95 g. or 27.6% of the theory.

*Dyestuffs Ressearch Laboratory, Department of Applied Chemistry, Tokyo University, Tokyo*

# *The Preparation of 4-Methoxy-2-butenal, a New Dienophile, and Notes on Related Compounds*

By Iwao ICHIKIZAKI, Ching-Chun YAO, Yutaka FUJITA and Yoshihiko HASEBE

(Received August 26, 1954)

It is thought that the 2-butenals containing a functional substituent in the 4-position may be valuable as new type dienophiles for the practical use of the Diels-Alder reaction. No work on the synthesis of such $\gamma$-substituted crotonaldehydes had been found in the literature of the subject, till the formation of 4-dimethylamino-2-butenal was first reported by the authors,[1] who were unable to isolate the free aldehyde, but succeeded in isolating the 2,4-dinitrophenylhydrazone ethylsulfate. In this paper we wish to describe a synthesis of 4-methoxy-2-butenal, which was proved to be a dienophile, and to make several notes on new compounds obtained during the course of investigation on 4-dialkylamino- and 4-hydroxy-2-butenals.

Both attempts to prepare 4-bromo-2-butenal by hydrolysing its diacetate[2] (I) and to prepare 4-diethylamino-2-butenal by hydrolysing the diacetate (II), which had been derived from the bromo-compound through the action of diethylamine, were in vain. The two acetates cited here seemed to be extremely labile in the hydrolysis process.

$$BrCH_2CH:CHCH(OCOCH_3)_2 \longrightarrow$$
(I)
$$(C_2H_5)_2NCH_2CH:CHCH(OCOCH_3)_2$$
(II)

The second attempt to prepare amino-

1) I. Ichikizaki and Yao, the 6th annual meeting of the Chemical Society of Japan at Kyoto University on April 2, 1953.

2) H. Schmid and E. Crob, *Helv. Chim. Acta*, 32, 77 (1949).

butenals was carried out by hydrolysing 4-dialkylamino-2-butenal diethyl acetals. 4-Dimethylamino-2-butynal diethyl acetal (III), prepared in a fairly good yield by the interaction of 3-dimethylamino-1-propynylmagnesium bromide and ethyl orthoformate in a benzene-ether solution, was hydrogenated to 4-diethylamino-2-butenal diethyl acetal (IV) in the presence of a catalyst such as palladium-barium sulfate. 4-Dimethylamino-2-butenal diethyl acetal (VI) was obtained from diethylpropargylamine via 4-dimethylamino-2-butynal diethyl acetal (V) through a similar process as above.

$$R_2NCH_2C:CMgBr \longrightarrow R_2NCH_2C:CCH(OC_2H_5)_2$$
(III) R=$C_2H_5$; (V) R=$CH_3$

$$\longrightarrow R_2NCH_2CH:CHCH(OC_2H_5)_2$$
(IV) R=$C_2H_5$; (VI) R=$CH_3$

These olefinic acetals were easily hydrolysed with mineral or organic acids, but repeated attempts to isolate the corresponding free aldehydes were all unsuccessful, because they were readily resinified on standing even for short times. Only when 4-dimethylamino-2-butenal diethyl acetal was hydrolysed with an equivalent amount of concentrated hydrochloric acid and immediately treated with Brady's reagent, the formation of 4-dimethylamino-2-butenal was confirmed by charachterizing it as the 2,4-dinitrophenylhydrazone ethylsulfate (VII).

$$\text{(VI)} \xrightarrow{\text{HCl, Brady reagent}} (CH_3)_2N^+HCH_2CH:CHCH:NNHC_6H_3(NO_2)_2\ C_2H_5SO_4^- \quad \text{(VII)}$$

Another investigation was made to prepare 4-hydroxy-2-butenal. By the action of ethyl orthoformate on propargyl alcohol dimagnesiumbromide, 4-hydroxy-2-butynal acetal (VIII) was obtained; however on catalytic reduction it did not yield 4-hydroxy-2-butenal acetal but a low-boiling oil which apparently contained 2-ethoxydihydrofurane (IX).[3]

$$BrMgOCH_2C:CMgBr \longrightarrow HOCH_2C:CCH(OC_2H_5)_2 \quad \text{(VIII)}$$
$$\longrightarrow CH_2CH:CHCHOC_2H_5 \quad \text{(IX)}$$
(with a bridging O)

The last attempt to prepare a free aldehyde of the class was made in a way to oxidize 4-methoxy-2-butenol to the corresponding aldehyde and resulted in success.

3) I.M. Heilbron, E.R.H. Jones and H.P. Koch, *J. Chem. Soc.*, (1942) 735.
Fernand Quennehen and Henn Normant, *Compt. rend.*, 228, 1301 (1949).

4-Methoxy-2-butynol (X) was prepared through a partial methylation of butynediol with dimethyl sulfate in an aqueous alkali, followed by a partial reduction to 4-methoxy-2-butenol (XI) in the presence of palladium-calcium carbonate in ethyl acetate. This was oxidized successfully according to either the method of Oppenauer[4] or that of Attenburrow et al.,[5] into 4-methoxy-2-butenal (XII) which was heated at 140°C with an equivalent amount of 2,3-dimethylbutadiene in a sealed tube to yield an adduct, 4,5-dimethyl-2-methoxymethyl-4-cyclohexene-1-carboxaldehyde (XIII).

$$(:CCH_2OH)_2 \longrightarrow CH_3OCH_2C:CCH_2OH \quad \text{(X)}$$
$$\longrightarrow CH_3OCH_2CH:CHCH_2OH \quad \text{(XI)}$$
$$\longrightarrow CH_3OCH_2CH:CHCHO \quad \text{(XII)}$$

$CH_2:C(CH_3)-C(CH_3):CH_2$ + $CH_3-C(CH_3)-CH_2-CHCHO$ $\longrightarrow$ $CH_3-C(CH_3)-CH_2-CH(CHO)CH_2OCH_3$ (XIII)

## Experimental

**4-Diethylamino-2-butenal Diacetate.**—Diethylamine (3.2 g.) was dissolved in dry ether (25 cc.), and 4-bromo-2-butenal diacetate (5 g.) was added slowly with stirring and cooling. The mixture was allowed to stand over-night, then filtered. The filtrate was evaporated and the residue distilled to give 4-diethylamino-2-butenal diacetate (1.9 g.), a colorless oil, b.p. 108-109°/3 mm. On standing in air this became dark red. The iodomethylate, m.p. 125° (Found: N, 3.3%. $C_{13}H_{24}O_4NI$ requires 3.6%).

**4-Diethylamino-2-butynal Diethyl Acetal and 4-Dimethylamino-2-butynal Diethyl Acetal.**—After the most part of ether had been distilled off from an ethereal solution of ethylmagnesium bromide (from 2.5 g. of magnesium, 10.9 g. of ethyl bromide and 80 cc. of ether), dry benzene (100 cc.) was added. Then a solution of diethylpropargylamine[6] (11.1 g.) in benzene (10 cc.) was added dropwise with stirring. After the addition had been completed the solution was stirred for 30 minutes, and ethyl orthoformate (14.8 g.) was added. The reaction mixture thus obtained was heated to 65° and stirred vigorously for 3 hours, cooled and decomposed with a saturated solution of ammonium chloride. The organic layer was separated and the aqueous layer extracted with benzene. The combined extracts were washed, dried and distilled, giving 4-diethylamino-2-butynal diethyl acetal (10.5 g.), b.p. 90°/3.5 mm., $n_D^{16.5}$ 1.4492 (Found: N, 6.7%. $C_{12}H_{25}O_2N$ requires 6.5%).

Following a quite similar procedure, 4-dimethylamino-2-butynal diethyl acetal (10.5 g.) was pre-

4) A. Lauchenauer and H. Schins, *Helv. Chim. Acta*, 32, 1265 (1949).
5) J. Attenburrow, A.F.B. Cameron, I.H. Chapman, R.M. Evans, B.A. Hem, A.B.A. Jansen and T. Walker, *J. Chem. Soc.*, (1952) 1094.
6) John W. Copenhaver and Maurice H. Bigelow, "Acetylene and Carbon Monoxide Chemistry," (1949), p. 110.

pared by the action of ethyl orthoformate (18 g.) on 3-dimethylamino-1-propynylmagnesium bromide (from 2.6 g. of magnesium and 9 g. of dimethylpropargylamine[6]), b.p. 84-86°/6 mm., $n_D^{16.5}$ 1.4419. The iodomethylate, m.p. 139-140° (Found: N, 4.1%. $C_{11}H_{24}O_2NI$ requires 4.2%).

**4-Diethylamino-2-butenal Diethyl Acetal and 4-Dimethylamino-2-butenal Diethyl Acetal.**—4-Diethylamino-2-butynal diethyl acetal (15.6 g.) was dissolved in ethanol (25 cc.) and hydrogenated in the presence of 3% palladium-barium sulfate (0.5 g.). After 140 minutes one equivalent of hydrogen (1565 cc.) had been absorbed, the catalyst was then separated and the filtrate was distilled, giving 4-diethylamino-2-butenal diethyl acetal, b.p. 80-81°/4 mm., $n_D^{15}$ 1.4402 (Found: N, 58.1%. $C_{12}H_{25}O_4N$ requires 58.2%). The iodomethylate, m.p. 130°.

4-Dimethylamino-2-butynal diethyl acetal was analogously hydrogenated (in 20 cc. of ethanol, 0.2 g. of the catalyst) to 4-dimethylamino-2-butenal diethyl acetal (4.0 g.), b. p. 62-62.5°/3 mm., $n_D^{18}$ 1.4353. The iodomethylate, m.p. 115° (Found: N, 4.0%. $C_{11}H_{24}O_2NI$ requires 4.2%).

**2,4-Dinitrophenylhydrazone Ethylsulfate of 4-Dimethylamino-2-butenal.**—Concentrated hydrochloric acid (3 drops) was added to 4-dimethylamino-2-butenal diethyl acetal (0.1 g.). With an evolution of heat the mixture became dark red. Brady's reagent (3 cc.) was added to the solution. After 12 hours the reaction mixture was filtered, and the orange reddish needles were recrystallysed from alcohol, m.p. 185-186° (Found: C, 40.3%; H, 4.8%; N, 16.8%. $C_{14}H_{21}O_8N_5S$ requires C, 40.2%; H, 5.0%; N, 17.2%).

**4-Hydroxy-2-butynal Diethyl Acetal.**—An ethereal solution of ethylmagnesium bromide (from 15 g. of magnesium and 200 cc. of ether) was partly evaporated, 150 cc. of ether being removed. After benzene (200 cc.) had been added, a solution of propargyl alcohol[7] (12.5 g.) in benzene (120 cc.) was added dropwise to the mixture during 1 hour with stirring and heating on a water-bath. After a solution of ethyl orthoformate (49.5 g.) in benzene (50 cc.) had been added in small portions, stirring and heating were continued for 2 hours; then the reaction mixture was cooled and decomposed by adding a saturated aqueous solution of ammonium chloride. The organic layer was dried and fractionated to yield 4-hydroxy-2-butynal diethyl acetal (23.4 g.), b.p. 118-119°/3 mm. (Found: C, 59.8; H, 9.1%. $C_8H_{14}O_3$ requires C, 60.9; H, 8.8%).*

The acetal (18 g.) and a solution of tartaric acid (25 g. in 18 cc. of water) were agitated with a small amount of hydroquinone in an atmosphere of nitrogen, neutralized and then extracted with ether. A part of the extracts was treated with Brady's reagent to yield the 2,4-dinitrophenylhydrazone, orange needles from alcohol, m.p. 119° (Found: N, 27.5%. $C_{10}H_7O_5N_4$ requires 27.5%).

**4-Methoxy-2-butynol.**—Butynediol[8] (40 g.) was dissolved in an aqueous solution of sodium hydroxide (24 g. in 100 cc. of water). Dimethyl sulfate (31 g.) was added dropwise with agitating at the temperature not higher than 70°. After stirring had been continued at 80° for a further 2 hours, the reaction mixture was extracted continuously with ether over 12 hours. The extract was washed, dried and evaporated. The residue was fractionated cautiously to give dimethoxybutyne (4.1 g.), b.p. 54-55°/15 mm., and 4-methoxy-2-butynol (18.8 g.),[9] b. p. 96-97°/15 mm., 81-82°/5 mm., $n_D^{20}$ 1.4593, $d_4^{20}$ 1.0462 (Found: C, 58.0%; H, 8.2%. $C_5H_8O_2$ requires C, 59.9%; H, 8.0%).

**4-Methoxy-2-butenol.**—4-Methoxy-2-butynol (28.9 g.) was hydrogenated, in ethyl acetate (30 cc.), in the presence of 3% palladium-calcium carbonate (2.5 g). One equivalent of hydrogen (7065 cc.) was absorbed within 5 hours. 4-Methoxy-2-butenol, b.p. 87-88°/20 mm., $n_D^{20}$ 1.4485, $d_4^{20}$ 0.9910 (Found: C, 58.3; H, 9.6%. $C_5H_{10}O_3$ requires C, 58.8; H, 9.9%).

**4-Methoxy-2-butenol.**—*A. By the Method of Attenburrow et. al.*—4-Methoxy-2-butenol (16.9 g.) was stirred for 30 minutes with a suspension of manganese dioxide (98.9 g.) in carbon tetrachloride (290 cc.). The mixture was filtered and evaporated at room temperature under a reduced pressure. The residue, with a small amount of hydroquinone, was distilled to give 4-methoxy-2-butenal (2.1 g.), a colorless oil with irritating odor, b.p. 72-75/26 mm. (Found: C, 59.5; H, 8.2%. $C_5H_8O_2$ requires C, 59.9; H, 8.0%). The 2,4-dinitrophenylhydrazone, m. p. 139-140° (Found: N, 19.8%. $C_{11}H_{12}N_2O_5$ requires 18.9%). The final residue (7.9 g.), an odorless oil, has not been investigated,

*B. By the Method of Oppenauer (Modified).*—Aluminium isopropoxide (9.9 g.) and 4-methoxy-2-butenol (15 g.) were heated gradually to 70-100° at 12 mm., the replaced isopropyl alcohol being distilled off through a Vigreux column (1.2×20 cm.). After 50 minutes, cinnamic aldehyde (23.9 g.) was added dropwise and the temperature of the oil-bath was kept at 130-150°. The distillate, b.p. 70-88° at 25-27 mm., amounted to 10.4 g. On rectification 4-methoxy-2-butenal (7.1 g.) was obtained. The analytical data was identical with that of the sample in A.

**4,5-Dimethyl-2-methoxymethyl-4-cyclohexene-1-carboxaldehyde.**—2,3-Dimethylbutadiene[10] (0.77 g.), 4-methoxy-2-butenal (0.61 g.) and petroleum ether (1 cc.) were heated at 140° in a sealed glass tube for 8 hours. The light yellow reaction mixture was fractionated to yield the adduct, a colorless oil with citral-like odor (0.66 g.), b.p. 82-84°/2.5 mm. (Found: C, 72.5%; H, 9.9. $C_{11}H_{18}O_2$ requires C, 72.1; H, 10.0%). The thiosemicarbazone, m.p. 152° (Found: C, 56.1;

7) ibid., p. 105.

* All the acetylenic compounds reported in this paper gave too low analytical values of carbon; these values were reproduced identically on repeated combustions. This analytical problem is serious, but has not been solved by the authors.

8) ibid., p. 98.

9) Hans J. Pistor, *Gem. Pantent*, 804, 569 (April 26, 1951).

10) Louis F. Fieser, "Experiments in Organic Chemistry." D.C. Health and Company. (1941). p. 383.

H, 8.2; N, 16.1%. $C_{12}H_{25}ON_3S$ requires C, 56.5; H, 8.2; N, 16.4%).

The authors wish to express their thanks to Professor Toshio Hoshino for encouragement during the course of research and to Mr. Asaji Kondo for the microanalysis.

*Laboratory of Organic Chemistry,*
*Tokyo Institute of Technology,*
*Ookayama Meguro-ku, Tokyo*

# *Practical Method for Estimating Surface Tensions of Solutions*

By Mikio TAMURA, Michio KURATA and Hisashi ODANI

(Received September 20, 1954)

## Introduction

The surface tension of solutions has a great effect on the efficiency of gas-liquid contact in unit operations such as distillation, absorption and extraction, so it is desired to establish a simple and practical method for calculating the surface tension of solutions. Recently, Meissner and Michaels[1] presented a method of calculating surface tension of mixtures of organic liquids, which is based on the additivity of Sugden's parachor, but this method is not available for solutions composed of organic solute and a highly polar solvent such as water.

Prigogine and Marechal[2] and one of the present authors[3] developed independently a statistical mechanical theory of the surface tension of a solution of rod-like molecules and derived a relationship between the concentration of the solute in the surface layer and that in the bulk phase. Although the statistical mechanical method gives the most rigorous approach to the present problem, the expression for the surface tension obtained by this method takes a somewhat complicated form which is undesirable for practical purposes.

In this paper, we propose a simple semi-empirical method for calculating the surface tension of solutions, and this method is based on the assumption of the additivity of the parachor in the *surface layer*, not in the *bulk*, and is available for the solutions composed of liquids differing widely in polarity.

## Additivity of Sugden's Parachor

Sugden's parachor, $(P)$, can be practically written as follows:

$$(P)=V\cdot\gamma^{1/4}, \qquad (1)$$

where $V$ is the molecular volume and $\gamma$ is the surface tension of liquids. The parachor is independent of temperature and shows an additivity with respect to atoms or atomic groups constituting the molecule, in spite of a wide variety of intramolecular or intermolecular forces; the strength of the intermolecular force decreases, in general, with increasing temperature or with decreasing density, even in the same liquid. These facts suggest that the parachor will practically depend only on the atomic or molecular composition of the system. We may, therefore, write the parachor, $(P)$, of the mixture of liquids A and B in the following form:

$$(P)=V\cdot\gamma^{1/4}=(1-x_b)(P)_A+x_b(P)_B, \qquad (2)$$

with

$$(P)_A=V_A\cdot\gamma_A^{1/4} \text{ and } (P)_B=V_B\cdot\gamma_B^{1/4}. \qquad (3)$$

Here $(P)_A$ and $(P)_B$ are the parachors, $V_A$ and $V_B$ the molecular volumes, and $\gamma_A$ and $\gamma_B$ the surface tensions of liquids A and B, respectively. $x_b$ is the molar fraction of B in the bulk phase, and $V$ is the mean molecular volume of the mixture. These relationships are essentially equivalent to those of Hammick and Andrew,[4] and of Meissner and Michaels.[1]

However in the case of the solutions showing an appreciable effect of adsorption such as aqueous solutions of organic substances, it seems to be more reasonable to assume the additivity of the parachor in the surface, for the parachor is essentially a quantity concerning the surface. The defect of M.-M.'s method mentioned already originates in the neglect of the effect of adsorption of the solute molecules on the surface, as has been pointed out by M. and M. themselves.[5]

According to the assumption mentioned above we obtain at once

1) H.P. Meissner and A.S. Michaels, *Ind. Eng. Chem.*, **41**, 2782 (1949).

2) I. Prigogine and J. Marechal, *J. Colloid Sci.*, **7**, 122 (1952).

3) M. Kurata, *Busseiron Kenkyu Researches on Chem. Phys.*), No. 56, 60 (1952), (in Japanese). This paper will be published in English in near future.

4) D.L. Hammick and L.W. Andrew, *J. Chem. Soc.*, (London) 1929, 754.

5) M.-M. proposed another empirical method for calculating the surface tension of aqueous solutions, but it is not adequate for practical purposes.

$$V_s \cdot \gamma^{1/4} = (1-x_s)(P)_A + x_s(P)_B, \quad (4)$$

instead of Eq. (2). Here $V_s$ is the mean molecular volume and $x_s$ the molar fraction of B, both in the surface layer. If the volume change on mixing is ignored, we can put

$$V_s = (1-x_s)V_A + x_s \cdot V_B. \quad (5)$$

Combining Eq. (4) with Eq. (5), and using the volume fraction of B-molecule in the surface, $v_s$, we obtain

$$\gamma = \{(1-v_s)\gamma_A^{1/4} + v_s \cdot \gamma_B^{1/4}\}^4. \quad (6)$$

This equation enables us to calculate the surface tension of the mixture in terms of the bulk concentration, $x_b$, provided that the relation of $v_s$ to $x_b$ is known.

## Method for Calculating the Concentration of Solute in the Surface of a Solution

For the solutions of rod-like molecule B consisting of $P$ segments, Prigogine[2] and one of the authors[3] derived statistically the following relation between the volume fraction of the solute molecule B in the bulk, $v_b$, and that in surface, $v_s$ ; i.e.

$$\{(1-v_b)^P \cdot v_s\}/\{(1-v_s)^P \cdot v_b\} = \exp\{P(\gamma_A - \gamma_B)/NkT\} \quad (7)$$

where $N$ is the number of lattice points, or the number of the solvent molecule A, per unit area, $k$ is the Boltzmann constant and $T$ is the absolute temperature.

This relation can also be derived by considering a kind of chemical equilibrium between two states of the molecular arrangements ; one of which is composed of $P$ solvent molecules located in the surface layer and a solute molecule located in the bulk, and the other of which is composed of $P$ solvent molecules in the bulk and a solute molecule in the surface, i.e.

$$P \cdot A_{surface} + B_{bulk} \rightleftarrows P \cdot A_{bulk} + B_{surface}. \quad (8)$$

The surface tension is the increase of the free energy per unit area due to shifting molecules from the bulk phase to the surface layer; then, $\gamma_A/N$ or $\gamma_B/N$ represents this increase of the free energy per molecule A or segment of B. As a molecule of B has $P$ segments, $P(\gamma_B - \gamma_A)/N$ represents the increase of the free energy with the change in Eq. (8), from left to right, and we have for the equilibrium condition Eq. (7), which enables us to estimate the surface composition of the solution $v_s$ in terms of $v_b$.[6]

## Comparison with Experimental Data

If we denote by $n_A$ and $n_B$ the numbers of molecules per unit area of liquids A and B, respectively, the number of lattice points $N$ is given by

$$N = n_A = Pn_B \quad (9)$$

according to the definition. Using this relation, we can write Eq. (7) as follows:

$$\log_{10}\left(\frac{1-v_s}{v_s}\right) + (P-1)\cdot\log_{10}(1-v_s) = \log_{10}\left(\frac{1-v_b}{v_b}\right) + (P-1)\cdot\log_{10}(1-v_b) + Q$$

with (10a)

$$Q \equiv \frac{P}{2.303\,kT}\left(\frac{\gamma_B}{Pn_B} - \frac{\gamma_A}{n_A}\right). \quad (10b)$$

In the estimation of $Q$, we adopt for $n_A$ and $n_B$ the values

$$n_A = (N/V_A)^{2/3} \text{ and } n_B = (N/V_B)^{2/3} \quad (11)$$

where $N$ is the Avogadro number. For the value of $P$ the following assumptions were made:

1) Aqueous solutions of fatty acids and alcohols,

$P$=Carbon Number. (12a)

2) Aqueous solutions of ketones,[7]

$P$=(Carbon Number)−1. (12b)

3) Aqueous solutions of halogen derivatives of fatty acids, e.g. homologue of monochloro acetic acid,

$$P = \begin{pmatrix}\text{Carbon}\\ \text{Number}\end{pmatrix} \cdot \left\{\frac{\text{Mol. Vol. of the Substance}}{\text{Mol. Vol. of the Corresponding Fatty Acid}}\right\}. \quad (12c)$$

4) Solutions composed of organic solute

6) We assume in this paper that B molecules orientate parallel to the surface (the parallel type), then all of $P$ segments of an adsorbed B molecule occupy the lattice points located in the surface layer. On the other hand, if B molecules do not orientate parallel to the surface (the vertical type), only one end-segment of an adsorbed B molecule occupies the lattice point located in the surface layer, and we obtain

$$\{(1-v_b)\cdot v_s\}/\{(1-v_s)\cdot v_b\} = \exp\{(\gamma_A - \gamma_B)/NkT\} \quad (7')$$

instead of Eq. (7). When $(\gamma_A - \gamma_B)$ is so large in comparison with $NkT$ that $v_s$ becomes much larger than $v_b$ and the adsorption of B molecules contributes an appreciable effect on surface tension, we can safely ignore the adsorption of the vertical type in comparison with that of the parallel type at high dilutions. At high concentrations, both of the Eqs. (7) and (7′) reduce to a common expression,

$$(1-v_b)/(1-v_s) = \exp\{(\gamma_A - \gamma_B)/NkT\} \quad (7'')$$

so we can again ignore the effect of the vertical type adsorption.

7) Cf. Ref. (1), p. 2787. M.-M. have pointed out that the ketones tend to affect the surface tension in a manner characteristic of the acid or alchol containing one less carbon atoms.

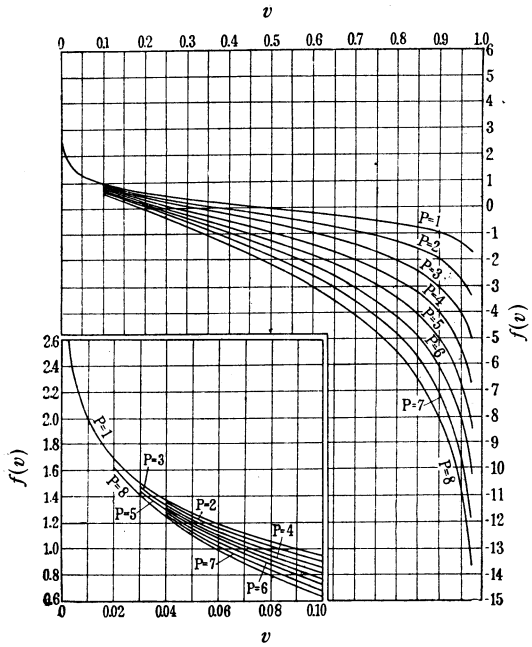



Fig. 1. Curves of $f(v)=\log_{10}(1-v)/v+(P-1)\times\log_{10}(1-v)$ vs. $v$ for some value of $P$.

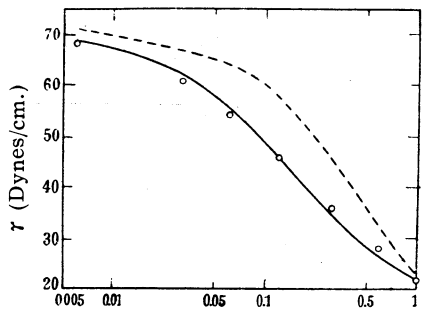



Fig. 2. Comparison between $\gamma_{calc}$ and $\gamma_{obs}$ of aqueous solution of $CH_3OH$ at 30°C.
O $\gamma_{obs}$,
—— $\gamma_{calc}$ (Present method),
– – – $\gamma_{calc}$ (M.-M. method).

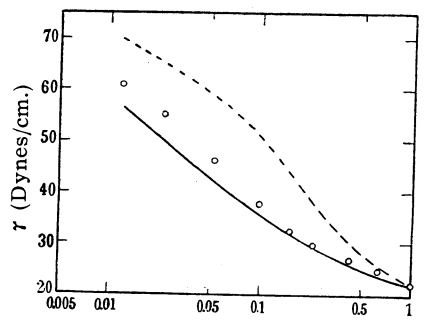



Fig. 3. Comparison between $\gamma_{calc}$ and $\gamma_{obs}$ of aqueous solution of $C_2H_5OH$ at 25°C.

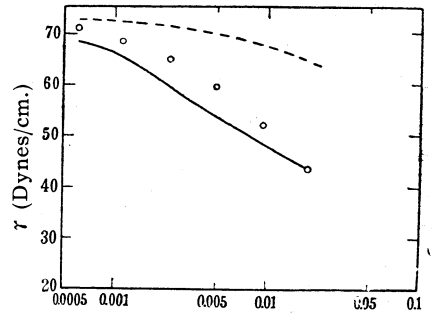



Fig. 4. Comparison between $\gamma_{calc}$ and $\gamma_{obs}$ of aqueous solution of $n$-$C_3H_7OH$ at 15°C.

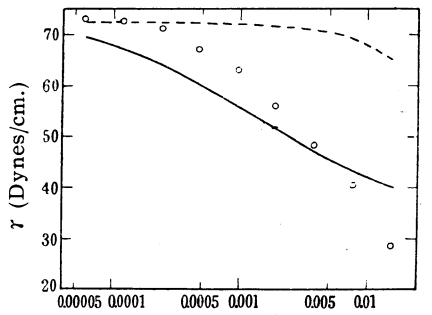



Fig. 5. Comparison between $\gamma_{calc}$ and $\gamma_{obs}$ of aqueous solution of $n$-$C_4H_9OH$ at 15°C.

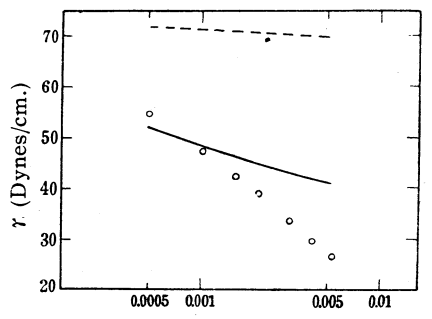



Fig. 6. Comparison between $\gamma_{calc}$ and $\gamma_{obs}$ of aqueous solution of $iso$-$C_5H_{11}OH$ at 30°C.

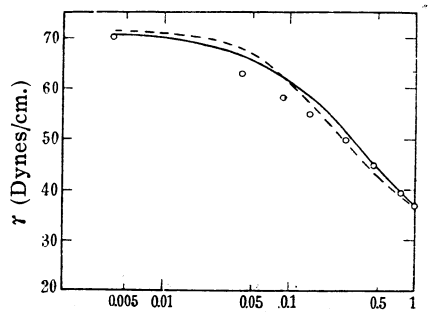
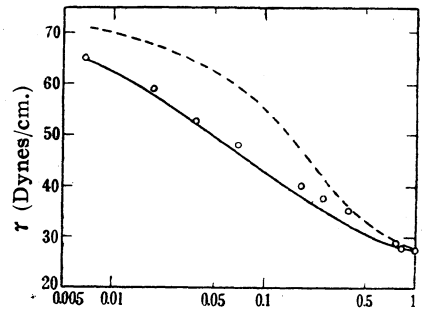
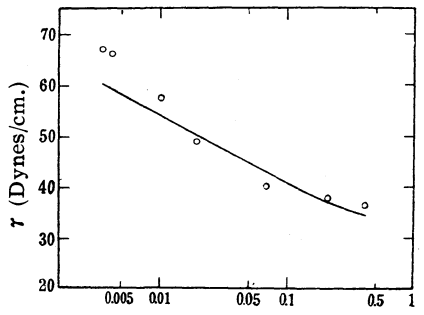



Fig. 7. Comparison between $\gamma_{calc}$ and $\gamma_{obs}$ of aqueous solution of HCOOH at 30°C.



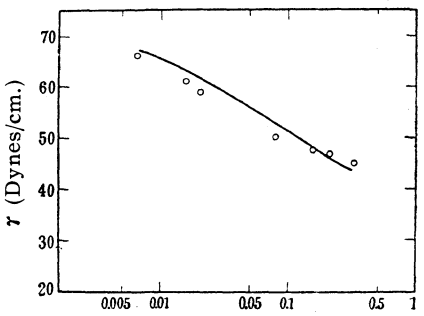

Mole fraction $CH_3COOH$

Fig. 8. Comparison between $\gamma_{calc}$ and $\gamma_{obs}$ of aqueous solution of $CH_3COOH$ at 25°C.



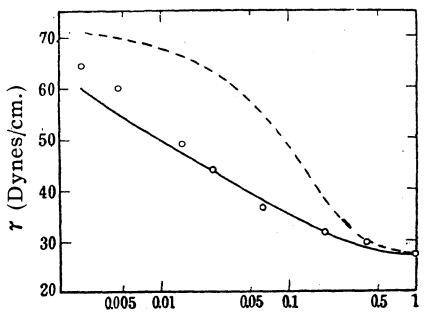

Mole fraction $CCl_3COOH$

Fig. 9. Comparison between $\gamma_{calc}$ and $\gamma_{obs}$ of aqueous solution of $CCl_3COOH$ at 25°C.



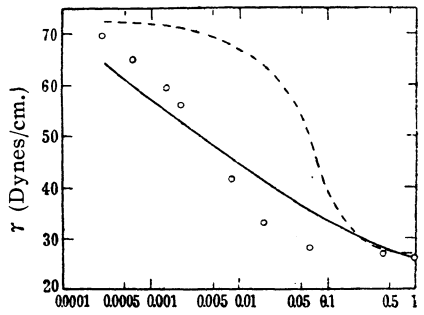

Mole fraction $CH_2ClCOOH$

Fig. 10. Comparison between $\gamma_{calc}$ and $\gamma_{obs}$ of aqueous solution of $CH_2ClCOOH$ at 25°C.



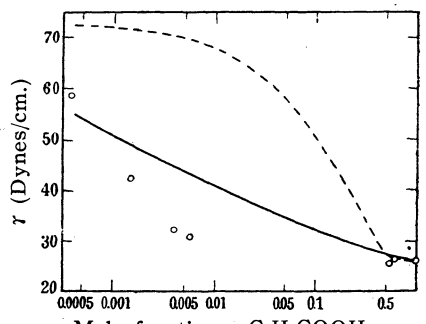

Mole fraction $C_2H_5COOH$

Fig. 11. Comparison between $\gamma_{calc}$ and $\gamma_{obs}$ of aqueous solution of $C_2H_5COOH$ at 25°C.



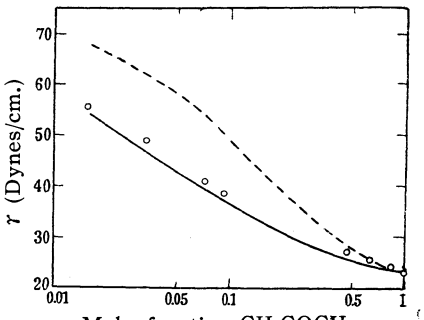

Mole fraction $n$-$C_3H_7COOH$

Fig. 12. Comparison between $\gamma_{calc}$ and $\gamma_{obs}$ of aqueous solution of $n$-$C_3H_7COOH$ at 25°C.



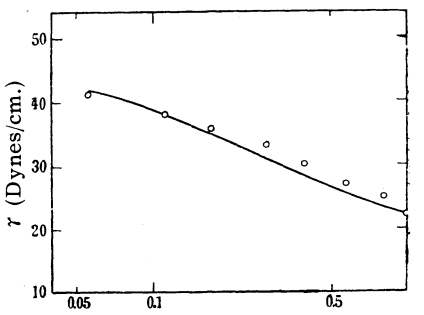

Mole fraction $n$-$C_4H_9COOH$

Fig. 13. Comparison between $\gamma_{calc}$ and $\gamma_{obs}$ of aqueous solution of $n$-$C_4H_9COOH$ at 25°C.




Mole fraction $CH_3COCH_3$

Fig. 14. Comparison between $\gamma_{calc}$ and $\gamma_{obs}$ of aqueous solution of $CH_3COCH_3$ at 25°C.




Mole fraction $C_2H_5OH$

Fig. 15. Comparison between $\gamma_{calc}$ and $\gamma_{obs}$ of ethylene glycol solution of $C_2H_5OH$ at 20°C.

and organic polar solvent,[8,9]

$P$=(Mol. Vol. of Solute)/(Mol. Vol. of Solvent) (12d)

The values of $Q$ thus obtained are listed in Table I.

Fig. 1 shows the curves of $f(v)[\equiv\log_{10}\{(1-v)/v\}+(P-1)\cdot\log_{10}(1-v)]$vers. $v$ for some values of $P$. Using this figure, we can easily solve Eq. (10a) graphically. For example, in the case of aqueous solution of $CH_3OH$ at 30°C, $P=1$ and $Q=-0.338$ are obtained from

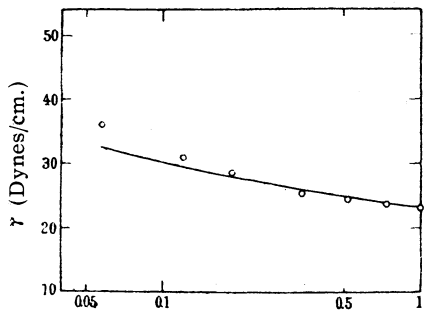



Fig. 16. Comparison between $\gamma_{calc}$ and $\gamma_{obs}$ of ethylene glycol solution of $n$-$C_4H_9OH$ at 20°C.

TABLE I

LIST OF $Q$ OF VARIOUS SYSTEMS

| system A | system B | °C | $Q$ |
|---|---|---|---|
| $H_2O$ | $CH_3OH$ | 30 | −0.338 |
| $H_2O$ | $C_2H_5OH$ | 25 | −0.983 |
| $H_2O$ | $n$-$C_3H_7OH$ | 15 | −1.662 |
| $H_2O$ | $n$-$C_4H_9OH$ | 20 | −2.265 |
| $H_2O$ | $i$-$C_5H_{11}OH$ | 30 | −2.801 |
| $H_2O$ | $HCOOH$ | 30 | −0.111 |
| $H_2O$ | $CH_3COOH$ | 25 | −0.857 |
| $H_2O$ | $CCl_3COOH$ | 25 | −1.497 |
| $H_2O$ | $CHCl_2COOH$ | 25 | −1.054 |
| $H_2O$ | $CH_2ClCOOH$ | 25 | −0.758 |
| $H_2O$ | $C_2H_5COOH$ | 25 | −1.532 |
| $H_2O$ | $n$-$C_3H_7COOH$ | 25 | −2.157 |
| $H_2O$ | $n$-$C_4H_9COOH$ | 25 | −2.801 |
| $H_2O$ | $CH_3COCH_3$ | 25 | −0.868 |
| $CH_2OH$ \| $CH_2OH$ | $C_2H_5OH$ | 20 | −0.549 |
| $CH_2OH$ \| $CH_2OH$ | $n$-$C_4H_9OH$ | 20 | −1.396 |

8) For the sake of convenience we use

$P$=(Carbon Number of Solute)/(Carbon Number of Solvent) (12d′)

instead of Eq. (12d) in the calculations given below. The difference between two values of $P$ obtained by Eqs. (12d) and (12d′) seems to be not appreciable in the examples adopted in this paper.

9) For mixtures of organic liquids, Meissner and Michaels' method can be used with sufficient accuracy, provided that the difference in the polarity of the liquids is not large.

TABLE II

COMPARISON BETWEEN $\gamma_{calc}$ AND $\gamma_{obs}$ OF AQUEOUS SOLUTION OF $CH_3OH$ AT 30°C.

| $v_b$ | $v_s$ | $\gamma_{calc}$ (Dynes/cm.) | $\gamma_{obs}$ (Dynes/cm.) |
|---|---|---|---|
| 0.013 | 0.028 | 69.2 | 68.4 |
| 0.063 | 0.126 | 62.4 | 61.0 |
| 0.124 | 0.232 | 55.7 | 54.6 |
| 0.241 | 0.406 | 45.9 | 46.1 |
| 0.460 | 0.651 | 34.3 | 36.1 |
| 0.749 | 0.865 | 26.1 | 28.2 |

Eqs. (12a) and (10b). If $v_b=0.241$, we get $f(0.241)=0.500$, $f(v_s)=f(0.241)+Q=0.162$, and then $v_s=0.406$ from Fig. 1. The substitution of this value of $v_s$ into Eq. (6) gives us $\gamma=$ 45.9 dynes/cm, while the observed value of $\gamma$ is 46.1 dynes/cm. $v_s$ and $\gamma_{calc}$ of this example are given in Table II with $v_b$ and $\gamma_{obs}$.

The values of $\gamma$ obtained by the present method, Eq. (6) with Eqs. (10) and (11), are shown in Figures 2 to 16 by solid lines,[10] where the observed values[11,12,13] are plotted by circles and also the calculated values of M.—M. are given by dotted lines for the sake of comparison. Although the agreement of the solid lines with observed data is not entirely excellent, the present method seems to be adequate for most practical purposes, if we take into consideration that the surface tention of the solution given here decreases extremely rapidly with increasing concentration of the solute. In the present method, the values necessary to calculate the surface tension are only four quantities, $\gamma_A$, $\gamma_B$, $V_A$ and $V_B$.[14] $\gamma_A$ and $\gamma_B$ can be easily calculated, with good accuracy, by using the additivity of the atomic parachor; therefore we can use the present method even when the observed values of these two quantities are absent. This will be one of the merits of our method.

In the case of the mixtures of organic liquids, the difference between $\gamma_A$ and $\gamma_B$ are commonly small so that the effect of adsorption can be safely ignored, and then Eq. (2) or the method of M.—M. can be used with sufficient accuracy.

10) On performing calculation, we ignore the volume change on mixting; i.e.

$$V=(1-x_b)V_A+x_bV_B.$$

11) "International Critical Tables", Vol. 4, p. 467 (New York, McGraw-Hill Book Co., Inc., 1926).

12) H. Landolt and R. Börnstein, "Physikalisch-chemische Tabellen", 5th ed., (Berlin, J. Springer, 1928).

13) I. Yamakita and H. Aida, private communication.

14) When the pure solute is in solid state at the temperature in question (e.g. in the case of aqueous solution of $CCl_3COOH$), we can use the extrapolated values of $\gamma_B$ and $V_B$ from its liquid state.

## Conclusion

We have presented a method for estimating the surface tension of the solutions composed of liquids differing widely in polarity, for which Meissner and Michael's method can not be applied, and have obtained good consistency of the calculated values with observed data. The percentage error, $\{(\gamma_{calc}-\gamma_{obs})/\gamma_{obs}\}\times 100$, is within 10% when $P<5$, and within 20% for large $P$.

In conclusion, the authors are indebted to Dr. I. Yamakita and Mr. H. Aida of Kyoto University for offering some unpublished data of the surface tension, and also to the Ministry of Education of the Japanese Government for a grant-in-aid.

*Department of Industrial Chemistry, Faculty of Engineering, Kyoto University, Kyoto*

# SHORT COMMUNICATIONS

## *Ultraviolet Spectrophotometric Determination of Iron with Ethylenediaminetetraacetic Acid*

By Yasumitsu UZUMASA and Masakichi NISHIMURA

(Received September 6, 1954)

It was found that in acid medium ferric iron together with ethylenediaminetetraacetic acid (EDTA) develops an intense absorption in the ultraviolet region due to the formation of a complex which may be successfully utilized to a spectrophotometric determination of iron.

The procedure used in this study is as follows: an excess EDTA is added to a hydrochloric acid solution containing ferric iron, and the solution diluted to a definite volume. The resulting solution is 0.1N as to hydrochloric acid and 0.001M as to EDTA. The transmittancy measurements are made with a Beckman Model DU spectrophotometer equipped with 1 cm. silica cells, a blank of distilled water being referred to.

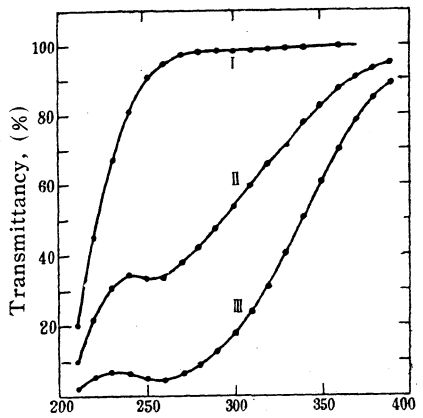



Fig. 1. Absorption spectra of ferric-ethylenediaminetetraacetic acid.
I: without iron, II: $5.0\times10^{-4}$ M and III: $1.5\times10^{-4}$ M ferric iron solution.

In Fig. 1, curve I shows the absorption spectrum of EDTA itself obtained by the said procedure; curves II and III represent the absorption spectra of ferric-EDTA complex solutions which contain $5\times10^{-5}$ mol. and $1.5\times10^{-4}$ mol. ferric iron per litre respectively. The latter solutions are characterized by a transmittancy minimum at 260 mμ.

Fig. 2 gives the calibration curve for iron at 260 mμ. The ferric-EDTA complex is stable and its molar absorbancy index at the absorption peak is somewhat larger than

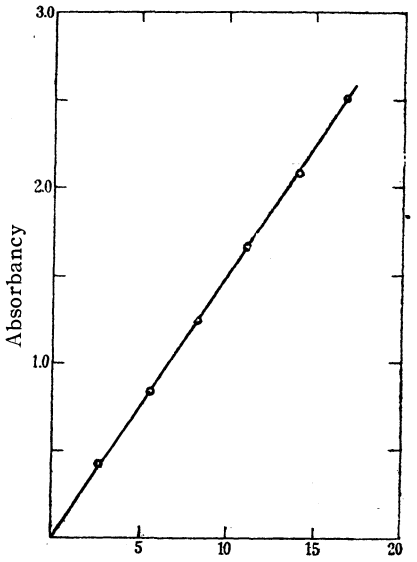



Fig. 2. Calibration curve for iron.

that of ferric-thiocyanate complex in the visible region.

The application of Job's continuous variations method reveals that one mole of ferric iron combines with one mole of EDTA.

Sulfuric acid as well as hydrochloric acid can be used in this determination, and the absorbancy remains constant over the range of 0.001 to 0.3N acid concentrations.

The work is being continued and its results will be reported in detail later.

*Department of Chemistry, Faculty of Science, Hokkaido University, Sapporo*

## *Separation of Sixth B Group Elements (S, Se, Te, Po) with Anion Exchange Resin*

Yukiyoshi SASAKI

(Received September 27, 1954)

Selenium (IV), tellurium (IV) and polonium are known to form chloride complex anions of the type $MCl_5^-$ or $MCl_6^{--}$ in conc. hydrochloric acid solutions. This communication reports the complete separation of sulfur, selenium, tellurium and polonium by anion exchange chromatography of these chloride complexes.

The resin used was Dowex 1 X-4, porous strongly-basic type resin, ground less than 180 mesh, and was settled in a cylindrical bed 0.6 $cm^2 \times 3.8$ cm. Weighed quantities of 4 mg. of selenium, 6 mg. of tellurium and ca. $5 \times 10^{-3} \mu$C. of polonium were mixed and oxidized with fuming nitric acid. The mixture solution was evaporated to dryness, and dissolved in 1 cc. of 12 N hydrochloric acid. Besides them, the amount of 3 mg. of sulfur was added to the mixture in the form of sulfuric acid, as sulfur is volatile in its quadrivalent oxidation state in strong acidic solution.

The solution was placed at the top of the bed and the liquid level was allowed to fall to the resin, which was previously conditioned with 12 N hydrochloric acid. When the mixture solution was passing through the column, yellowish-green and yellow sharp adsorption bands due to selenium and tellurium respectively were clearly observed and distinguished from each other.

Elution was performed with 12 N hydrochloric acid at flow rate of about 0.2 cc./$cm^2$/min. at room temperature, and every 0.5 cc. fraction of effluent was collected and analyzed.

Sulfate was effectively not adsorbed to the resin and immediately appeared in the effluent, whereas the adsorption band of selenium moved only 1.5 cm. after the addition of 2.6 cc. of eluent (elution constant $E=0.3$),[1] and in the effluent the latter was not detected by the thiourea test.

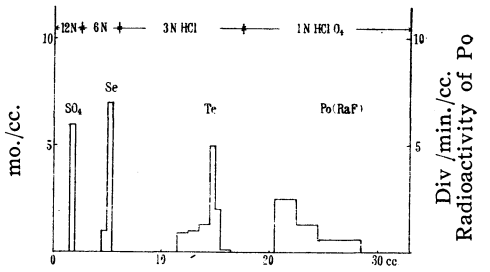



Fig. 1. Elution curve

Succeedingly, selenium was eluted completely with 3.5 cc. of 6 N hydrochloric acid, and then tellurium with 12 cc. of 2 N acid. Finally, polonium was desorbed with 1 N perchloric acid or 1N nitric acid.[2]

Sulfuric acid was determined as barium sulfate. Selenium and tellurium were reduced to their elementary states with sulfur dioxide and determined gravimetrically. Radioactivity of polonium was measured with the use of the Lauritsen electroscope. As shown in the figure, a nearly complete separation was obtained.

Within several hours after the adsorption of the sample, perchloric acid was effective to elute polonium. But after fifty hours, 3 N perchloric acid could elute only 10% of the total quantity of polonium; on the other hand, 3 N nitric acid was still effective. It was very likely that polonium was reduced in the bed or reacted irreversibly with ion exchange resin.

1) K.A. Kraus, G.E. Moore, *J. Am. Chem. Soc.*, **73**, 9 (1951), ibid., **75**, 1460 (1953).

2) T. Ishimori, : Abstracts of the Second Annual Meeting of The Japan Society for Analytical Chemistry., Oct. 1953 at Tokyo.

*Department of Chemistry, Faculty of Science, The University of Tokyo*

## *Magnetic Resonance Absorption of Protons in Water Adsorbed on Carbon and Cellulose*

By Kōji TANAKA and Kyōzō YAMAGATA

(Received December 4, 1954)

The line shapes of the proton magnetic resonance absorption in water adsorbed on carbon and cellulose was studied by an autodyne oscillator circuit[1]. We report here the derivatives of the absorption lines obtained with these substances at 20°C. The proton magnetic resonance absorption was observed by the variation of the resistance part of the oscillator coil, in which the sample was inserted. This phenomenon occurred as a resonance between the frequency of the oscillator and the transition frequency, a function of the static magnetic field ap-

plied to the sample. The derivatives of the absorption lines were recorded on photographic paper. The second moment was calculated from the curves of the recorded derivative and then the line width of the absorption curves was graphically determined.

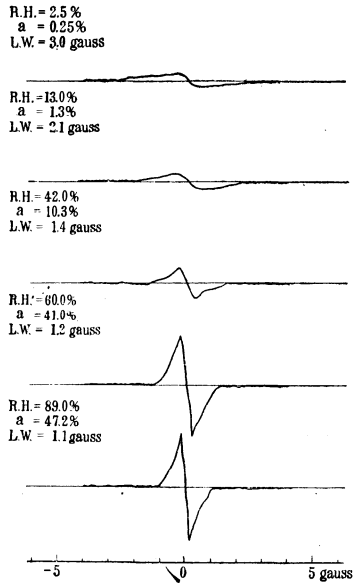



Fig. 1 Resonance line derivatives for carbon.
R.H. =Relative humidity (%)
a =Amount of adsorbed water vapor (%)
L.W.=Line width (gauss)

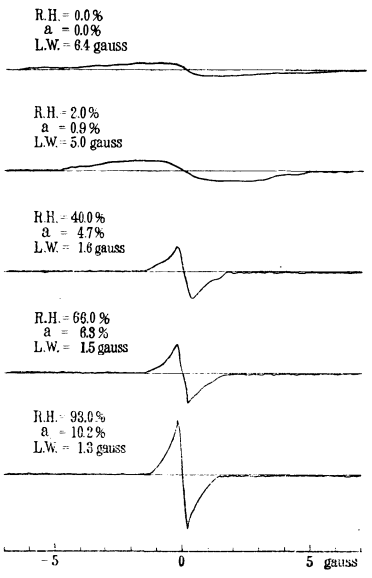



Fig. 2 Resonance line derivatives for cellulose.

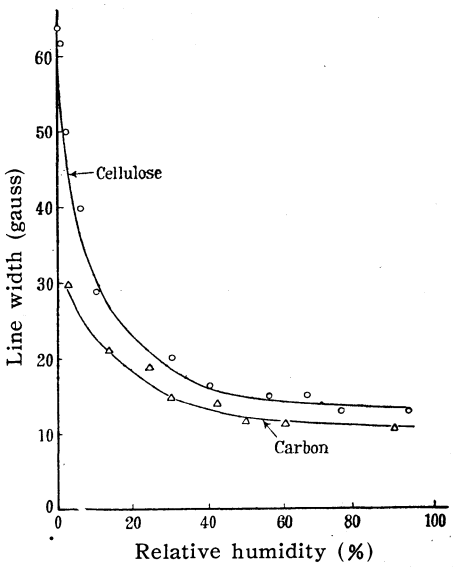



Fig. 3 The variation of line width of resonance absorption with relative humidity.

**Carbon.**—We used a vegetable active carbon (Takeda Co.) and freshly prepared conductivity water. The water vapor was adsorbed on the sample at 20°C for a period of 3 days in a desiccator of constant relative humidity. The curve of the magnetic resonance absorption of protons in water adsorbed on carbon at 20°C and the line width vs. relative humidity are shown in Fig. 1 and Fig. 3 respectively.

As shown in Fig. 1 the line shape becomes gradually sharp with the increase of relative humidity. In the higher relative humidity, the part of broad line shape practically disappears by the

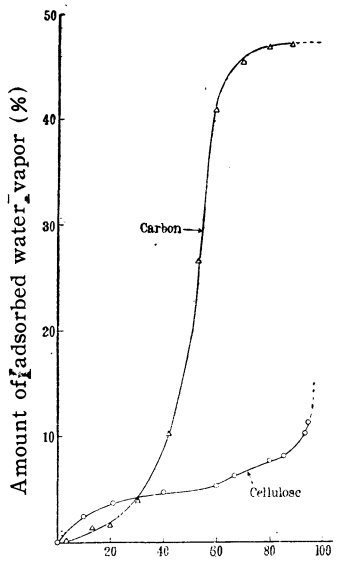



Fig. 4 Adsorption isotherms of water vapor on carbon and cellulose at 20°C.

influence of a large quantity of adsorbed water, although it should theoretically be observed.

The adsorption isotherm of water vapor on the active carbon measured at 20°C by spring balance method is shown in Fig. 4. By using the method of Brunauer, Emmett and Teller[2] it has been found that water is adsorbed on this sample with a mono-molecular layer, where the relative humidity is about 20%, so that we may conclude that the adsorbed water vapor of this monolayer is firmly held on the active carbon.

It is a remarkable fact that the line width (Fig. 3) rapidly decreases with the increase of relative humidity in the region of about 20% and that the sharp line shape (Fig. 1) overlaps gradually on the broad line shape. This is probably due to the considerable difference between the Brownian motion of protons in the water adsorbed in and above the mono-molecular layer. Thus it is demonstrated that the protons above the mono-molecular layer are movable, while the protons in the mono-molecular layer are rigid.

**Cellulose.**—A quantitative filter paper of best quality (Toyo Filter Paper No. 7) was used as cellulose material. Water vapor was adsorbed on the filter paper, previously dried in vacuo at 100°C, for a period of one day in a desiccator of constant relative humidity. In Figs. 2 and 3 are shown respectively the curves of the proton magnetic resonance absorption in water adsorbed on the cellulose at 20°C and the line width determined graphically vs. relative humidity.

The adsorption isotherm of water vapor on the filter paper measured at 20°C by spring balance method is of the usual sigmoid type as shown in Fig. 4. Resonance absorption of protons was found with cellulose even in the neighborhood of zero relative humidity, in contrast to carbon, and the line width was found to be about several gausses. This resonance absorption may be due to the protons in the cellulose molecule itself, but not to the adsorbed water. The line width both of cellulose and carbon decreases rapidly in the neighborhood of the relative humidity of 20%. When the relative humidity is above 40%, a sharper line shape appears in the case of cellulose, overlapping on the broad curve, and above 90% the line shape becomes strikingly sharp, quite in contrast to corbon. This is attributable to the known fact that the adsorption of water on cellulose suddenly increases in the neighborhood of saturated vapor pressure. It is a remarkable fact that the line shape of cellulose changes more rapidly than that of carbon, suggesting that the adsorption layer of water on cellulose has a character of a multiple layer, in contrast to that on the carbon.

The authors wish to express their appreciation to Professor M. Takeda and S. Kittaka for their interest in this work.

1) K. Sano, *Proc. J. Phys. Soc. Japan*, **6**, 228 (1951).
2) S. Brunauer, S.H. Emmett and E. Teller, *J. Am. Chem. Soc.*, **60**, 309 (1938); ibid., **62**, 1723(1940).

*The Departments of Chemistry and Physics, Tokyo College of Science, Kagurazaka, Tokyo*

# *Reduction of Acetophenone by an Electrolytic Method Using Raney Nickel as Catalyst*

By Buhei SAKURAI and Toshio ARAI

(Received May 31, 1954)

The electrolytic reduction of ketones has been studied with many compounds, and its reduction proceeds to the formation of hydrocarbon, alcohol, and pinacol or a mixture of both alcohol and pinacol. These reductions depend upon the electrode materials, electrolyte, temperature, and the concentration of ketones. Concerning acetophenone, Elbs and Brand[1] found that in alkaline or acid solution at lead cathode, it was reduced to a mixture of acetophenonepinacol and methylphenylcarbinol. Swann[2], Kauffler[3], and Müller[4] prepared acetophenonepinacol by using many electrode materials in alkaline or acid solution. Futaki[5] prepared methylphenylcarbinol with a better yield in the solution of sodium sulfate at mercury cathode and lead anode. By the chemical method, acetophenone[6] was hydrogenated to methylphenylcarbinol at room temperature under the pressure of 15 to 45 lb./sq.in. using Raney nickel as catalyst.

Raney nickel, however, has not been used for electrolytic reduction. The author tried to prepare methylphenylcarbinol from acetophenone by the electrolytic method with Raney nickel and found a way to produce it with a satisfactory result by using lead cathode in weak alkaline electrolyte with Raney nickel suspended.

## Experiment and Discussion

In acid or alkaline solutions using lead, copper, and zinc amalgam electrode, the reduction of acetophenone by electrolytic method was not suitable for the synthesis of methylphenylcarbinol.

Then Raney nickel was suspended in cathodic solution,—Wako Pure Chemical Industries Ltd.'s Raney nickel was used. By this method, in acid solution the resinous material formed in electrolysis mixed with nickel, adhered to the cathode plate, and in consequence the electrolysis was not conducted well. In alkaline electrolyte with Raney nickel which corresponded from about 5 to 10% by weight of the ketone, the reduction was confirmed to be the most favorable for the purpose. The electrolysis was conducted under following conditions;

*Cathode:* lead plate 100 $cm^2$; Cathodic solution: 25 g. of acetophenone and 2 g. of Raney nickel suspended in a mixture of 70 ml. of 5% sodium hydroxide and 70 ml. of alcohol was placed in a porous pot;

*Anode:* carbon plate; Anodic solution: 5% sodium hydroxide;

*Temperature:* 25°C average; Time of electrolysis: 17 hours.

The electrolysis was carried out by cooling the electrolytic bath in cold water and by vigorously stirring the cathodic solution to which 2 g. of Raney nickel was added at the same time.

The completion of electrolysis is recognized when a small quantity of cathodic solution, after acidifying, gave a negative ketone test with sensitive 2,4-dinitrophenylhydrazine reagent.

After the finishing of electrolysis, the alcohol was evaporated on a water bath and the residue was made slightly acidic by addition of diluted sulfuric acid and had the nickel therein filtered off after cooling. Then it was extracted repeatedly with ether, and the combined ether extracts were dried over anhydrous potassium carbonate.

The ether was removed and the residue distilled. The fraction distilling at 98°–100°C/18 mm Hg was collected. Its yield was about 18.5 g., corresponding to 74% of the theoretical amount. This substance was colorless, and gave a negative test with 2,4-dinitrophenylhydrazine reagent, but it smelled like acetophenone when oxidized with potassium chromate and sulfuric acid, and formed 2,4-dinitrophenylhydrazone melting at 246°–247°C (uncorr).

Moreover, the reduced material was mixed with phenyl isocyanate and then the crystal formed was recrystallized from alcohol, m.p. 92°–93°C. This corresponds to the reported value of 94°C for methylphenylcarbinol.

The average yield of reduction was calculated to correspond to 73% of the theoretical amount. The yield was not affected by ketone concentration from 1 to 3 molar, but in higher concentrations the yield was decreased, and it resulted in the formation of tarry materials. Sodium acetate in cathodic solution which was used for a pinacol formation was not favorable in this experiment.

1) K. Elbs and K. Brand, *Z. Electrochem.*, 8, 784 (1902).
2) S. Swann and C. Herson, *Electrochem., Spec.*, reprint, 67, 49 (1935).
3) F. Kauffler, *Z. Electrochem.*, 13, 633 (1907).
4) E. Müller, *Z. Electrochem.*, 16, 236 (1910).
5) Zenji Futaki (present address: Shiono Chemical Industrial Co.), *Japan. P.* 174, 272 Dec. 10 (1946).
6) H. Adkins and H. Billica, *J. Am. Chem. Soc.*, 70, 659 (1948).

The temperature was found not to influence the reduction result from 20°C to 50°C, but the yield was lowered above 80°C in a water bath.

It was also found that the current density had no effect between 4 and 7 amps./cm$^2$.

In this method, it was thought that the electrode material was of little significance as Raney nickel was suspended in electrolyte, therefore copper cathode was used instead of lead, and the electrolysis was conducted under the same condition as before.

Consequently, the same reduction product and similar yield was obtained.

This was regarded as a catalytic reduction by electrolysis, that is, the electrolysis was used only for the evolution of hydrogen.

Up to the present, the electrolysis using the catalyst has been attempted in different methods, but these have not been carried out well, because the catalyst reacted on the acid of electrolyte generally, except that platinum electrode was used.

In our experiment, however, as electrolysis was conducted in alkaline solution, the catalyst was not changed, so that this case was thought to be very favorable.

In the experiments related above, ethylbenzene was not prepared from acetophenone, and therefore the reduction of methylphenylcarbinol obtained was carried out in acid electrolyte. The electrolysis was conducted by using zinc amalgam cathode in the mixture of 50% sulfuric acid and ethyl alcohol, and it seemed that only benzene ring was partially hydrogenated, but the identification of the reduction product was not investigated further.

## Summary

The catalytic reduction of acetophenone by electrolysis using Raney nickel in weak alkaline solution with lead or copper cathode was studied and methylphenylcarbinol was prepared.

*Institute of Chemistry, Faculty of Liberal Arts and Science,*
*Shinshu University,*
*Matsumoto, Japan*

# *Studies on Polymerization and Depolymerization of ε-Caprolactam. I. The Formulation of Amide-Interchange Reaction, the Heat of Reaction and the Activation Energy**)

By Hirosuke YUMOTO

(Received May 20, 1954)

## Introduction

Considering possible reactions in ε-caprolactam polymerization, they are a sort of reaction expressed by the amide-interchange formula. The equations capable of treating the reaction rate are introduced under such a consideration, and simplified by the approximation peculiar to the super high polymeric system. The main object of this study is to elucidate the reality of the supposed reaction formulas, experimentally.

From the results of this study, polymerization reaction of ε-caprolactam is considered to be the equilibration process by amide-interchange reactions, in which two series of polymerizates, namely chain- and ring-molecules, such as supposed by Jacobson and Stockmayer.[1] are expected to exist. Herein a series of chain-molecules should be the series of condensation polymerizate which had been primarily introduced by Flory.[2]

Furthermore the heat of polymerization and the activation energies of amide-interchange reactions are estimated under these suppositions. The former is apparently coincident with the value determined calorimetrically by S. M. Skurator et al.[3]

## The Formulas of the Reactions

As the catalyst of ε-caprolactam polymerization, water, acids, bases, alkali metals, etc. have been reported. Now for the sake of argument, it is assumed that benzoic acid is alone used as the catalyst and the lactam is completely free of water. In the poly-

* Presented at the Symposium of Polymer Science at Nagoya November 9, 1953.

1) H. Jacobson and W. H. Stockmayer, *J. Chem. Phys.*, **18**, 1600 (1950).

2) P. J. Flory, *J. Am. Chem. Soc.*, 58, 1877 (1938).

3) S. M. Skuratov, A. A. Stepikheev and E. N. Kanarskaya, *Kolloid Zhur.*, **14**, 185—91 (1952); *C. A.*, **46**, 8506c (1952); *Faserforschung und Textiltechnik*, **4**, 390 (1953).

merizing reaction from such ε-caprolactam and benzoic acid, the monomer, dimer, trimer, ....., $m$-mer, .....in the series of chain- and ring (lactam)-molecules are designated by the notations of $M_1$, $M_2$, $M_3$, ....., $M_m$. ..... and $L_1$, $L_2$, $L_3$, .....$L_m$, ....., respectively. Two end-groups of chain-molecules must always be benzoyl and carboxylic acid groups. $M_1$ corresponds to the benzoylaminocaproic acid, and $L_1$ corresponds to the ε-caprolactam. Besides the molecule of free benzoic acid is designated by the notation B.

1. Reactions between ring- and chain-molecules
   (i) About lactam-monomer
   $L_1+B \rightleftarrows M_1$, $L_1+M_n \rightleftarrows M_{n+1}$
   (ii) About lactam-dimer
   $L_2+B \rightleftarrows M_2$, $L_2+M_n \rightleftarrows M_{n+2}$
   (iii) Generally about lactam-$m$-mer
   $L_m+B \rightleftarrows M_m$ (1)
   $L_m+M_n \rightleftarrows M_{m+n}$ (2)
2. Reactions between two chain-molecules
   $M_n+M_m \rightleftarrows M_{n+m}+B$ (3)
   $M_{n+i}+M_m \rightleftarrows M_{n+m}+M_i$ (4)

Formula (3) represents the condensation reaction and formula (4) represents what is called amide-interchange reaction.

It was already found by K. Hoshino[4] that the completely dried pure ε-caprolactam cannot be polymerized merely by means of heating it. The lactam-dimer or -trimer should be similar in such behavior. These chemical properties make it possible to suppose that the reaction between two lactam-molecules should not arise; e.g. the reaction $L_1+L_1 \rightleftarrows L_2$ does not occur. When amide linkage and the carboxylic acid group collide, the amide-interchange reaction is expected to ensue; but when two amide linkages collide, the amide-interchange reaction is not expected to ensue for the same reason. Consequently

$M_{n+m}+M_{i+j} \rightleftarrows M_{n+j}+M_{m+i}$ is not conceivable.

All of the reactions which arise from caprolactam and benzoic acid can be represented by any of the above formulas (1), (2), (3), and (4). Those reactions can be regarded as the amide-interchange reaction which is indicated by the following formula.

$R_1CONHR_2+R_2COOH \rightleftarrows R_3CONHR_2+R_1COOH$

In the case of ring-molecule, two radicals R in one molecule are linked together. Carboxyl group in chain-molecule can react with the amide linkage in the lactam-molecule, in the own chain-molecule or in the other chain-molecule. As the result of such reaction, polymerization, depolymerization or what is called amide-interchange reaction is expected to arise respectively.

Now consider the reaction where only lactam-monomer ($L_1$) is related. Hereafter, notations of $L$, $M$, $B$ shall represent the mol. no. of each molecule. In this case it is sufficient to consider the following equations,

$$L_1+\sum M_i \rightleftarrows \sum M_{i+1}, \quad (5)$$

$$L_1+B \rightleftarrows M_1. \quad (6)$$

(In this paper $\sum$ represents $\sum_{i=1}^{\infty}$,)

As for the super high polymeric system where the degree of polymerization is about 100, $B \ll \sum M_i$[a] and $M_1 \ll \sum M_i$[b]. Therefore the following equations are approximately applicable to the super high polymeric system,

$$\left.\begin{aligned} L_1+\sum M_i &\rightleftarrows \sum M_{i+1} \\ \sum M_i &\approx \sum M_{i+1}. \end{aligned}\right\} \quad (7)$$

Generally, insofar as $B$, $M_1 \ll \sum M_i$ is effective, the equilibrium and the rate[c] of reaction can be discussed with Eq. (7) in approximation.

a) As for the super high polymeric system where the degree of polymerization $P$ is about 100, $B$ is too small to make quantitative analysis by extraction, and also from equilibrium between amide linkages and carboxyl groups, i.e. [–CO–NH–]+⟨⟩–COOH $\rightleftarrows$ [–COOH]+[–NH–CO–⟨⟩, $B$ will be about one hundredth of $\sum M_i$, because the equilibrium constant will be the magnitude of nearly 1.

b) As for the super high polymeric system where $P$ is about 100, $M_1$ is too small to make quantitive analysis by extraction and also according to Flory's molecular weight distribution[2] $M_1=(1-p)\sum M_i$ derived from the probability law, $M_1$ will be about one hundredth of $\sum M_i$, if $p=0.99$.

c) The applicability of eq. (7) for rate process depends on the constancy of $\sum M_i$ in reaction. Considering the general reaction formulas (1), (2), (3), (4), there is no change of $\sum M_i$ in (1), (2), (4), and no change of $\sum M_i+B$ in (3). Accordingly, insofar as $B \ll \sum M_i$ is effective, the change of $\sum M_i$ resulting from reaction (3) will be negligible, and therefore Eq. (7) can be applied to the rate process.

## Depolymerizing Process

Polycapramide filament of about 3 denier, which was completely free of water soluble components, i.e. lactam-monomer, -dimer, -trimer, through scouring in boiling water, was dried to be used for experiments. It was sealed in a glass tube and melted by heat for a definite time in a salt bath. Thereafter the content was analysed. The temperature of the salt bath was maintained constant (±1°C) by means of a mercury re-

4) K. Hoshino, *J. Chem. Soc. Japan* (in Japanese), **64**, 628 (1943).

gulator. Analytical procedures were as follows. The sample was chipped and water soluble components were throughly extracted into boiling water. Then the nitrogen content in this extract-solution was estimated by micro-Kjeldahl's method. Besides this analysis, part of this extract-solution was evaporated and dried up completely until the weight of the residue became constant. The nitrogen content of this residue was determined as decribed above.

The filament yarn used for experiments was super high polymer whose degree of polymerization was seemingly about 110[d] estimated from the intrinsic viscosity, i.e. $[\eta]$ (25°C cresol)≈1.1. Those polymers which have such high degree of polymerization contain negligibly small quantities of low molecular weight chainmolecules soluble in water. Therefore one may practically consider the water soluble substances to be only low molecular weight ring-molecules, i.e. monomer, dimer and trimer of lactam. As the lactam-monomer is much more volatile than the two others the quantity of lactam-monomer can be estimated from the above mentioned two nitrogen contents.[5]

The temperatures of reaction were 230, 257, 280, 295 and 310°C. For the purpose of comparison caprolactam was heated to polymerize with ε-aminocaproic acid[e] at the same temperatures. Polymeric systems which had been equilibrated through such a polymerization process were similarly analysed as the polymeric systems obtained by the above mentioned depolymerizing process.

The results of these experiments are shown in Tables I and II, and by dots in Fig. 1.

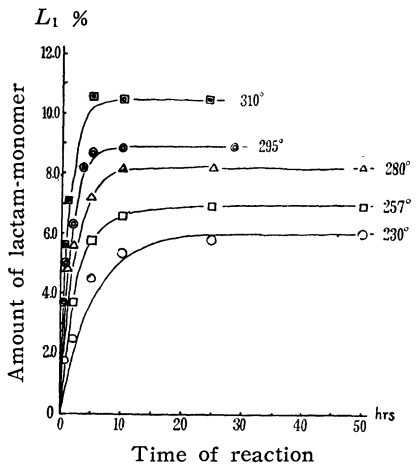



Fig. 1. Amounts of lactam-monomer in depolymerizing process at varying temperatures (Dots represent experimental values, and real lines represent deduced lines from the supposed equation.).

TABLE I
AMOUNTS OF LACTAM-MONOMER IN DEPOLYMERIZING PROCESS AT VARYING TEMPERATURES

| Temp. °C | hrs. | $L_1$ (%) weight/weight |
|---|---|---|
| 230 | 1 | 1.9 |
| | 2 | 2.5 |
| | 5 | 4.5 |
| | 10 | 5.3 |
| | 25 | 5.8 |
| | 50 | 6.0 |
| 257 | 1 | 2.5 |
| | 2 | 3.7 |
| | 5 | 5.8 |
| | 10 | 6.6 |
| | 25 | 6.9 |
| | 50 | 6.9 |
| 280 | 1 | 4.9 |
| | 2 | 5.6 |
| | 5 | 7.2 |
| | 10 | 8.2 |
| | 25 | 8.2 |
| | 50 | 8.3 |
| 295 | 0.5 | 3.7 |
| | 1 | 5.0 |
| | 2 | 6.3 |
| | 3.5 | 8.2 |
| | 5 | 8.7 |
| | 10 | 8.8 |
| | 27 | 8.9 |
| 310 | 1 | 5.6 |
| | 2 | 7.1 |
| | 5 | 10.6 |
| | 10 | 10.5 |
| | 24 | 10.5 |

TABLE II
AMOUNTS OF LACTAM-MONOMER AND -DIMER PLUS -TRIMER AT EQUILIBRIUM STATE IN HIGH POLYMERIC SYSTEMS

| Temp. °C | $L_1°$ (%) | $L_2°+L_3°$ (%) |
|---|---|---|
| 230 | 6.2 | 2.0 |
| 257 | 7.0 | 2.2 |
| 280 | 8.3 | 2.3 |
| 295 | 8.9 | 2.4 |
| 310 | 10.6 | 2.5 |

The rate of reaction in such high polymers can be discussed by Eq. (7). From Eq. (7) following equation may be supposed.

$$\frac{d(L_1/A)}{dt}=\kappa\sum M_i/A-kL_1\sum M_i/A^2, \qquad (8)$$

where $L_1$=mol. no. of lactam monomers, $M_i$=mol. no. of the end groups in $i$-mer chain

5) W. E. Hanford and R. M. Joyce, *J. Polym. Sci.*, 3, 167 (1948). Independently O. Fukumoto in Research Laboratory of Toyo Rayon Co. had established the analysis of lactam-monomer discriminating lactam -dimer and -trimer.

molecules relating to amide-interchange reaction,[1] $A$=mol. no. of the Brownian motion unit in whole reaction phase. $\kappa$= the rate constant of lactam-monomer appearing from chain molecule (depolymerization), $k$=the rate constant of lactam-monomer disappearing into chain molecule (polymerization). At equilibrium, $d\left(\frac{L_1}{A}\right)/dt=0$; therefore

$$\kappa\sum M_i/A - kL_1^\circ\sum M_i/A^2=0$$
$$k=\kappa A/L_1^\circ, \qquad (9)$$

where $L_1^\circ$ represents $L_1$ at equilibrium. Substituting Eq. (9) into Eq. (8),

$$d(L_1/A)/dt=(\kappa/A)\sum M_i\left(1-\frac{L_1}{L_1^\circ}\right)$$
$$=(\kappa/L_1^\circ)\ (\sum M_i/A)\ (L_1^\circ-L_1). \qquad (10)$$

It is necessary to give an explanation about $A$, the mol. no. of average unit of the Brownian motion in the whole reaction phase. For the kinetics of polymerization in the melt phase or in the particularly concentrated solution one cannot simply take "(the number of mol.)/(the volume of whole reaction phase)" as the concentration of the reaction component. It is more reasonable to take "the molar fraction"; the "molar fraction" in this case shall be "(the number of mol.)/(the number of mol. of average unit of the Brownian motion in whole reaction phase)". For the polymer molecule the unit of flow or segment must be taken into consideration; it is apparently doubtful to consider this unit to be a structural unit of the chemical formula.[7] The unit of flow in linear polyamide had not been estimated by melt viscosity measurements. Nevertheless, the assumption that $A$ does not change in reaction is approximately allowable in the case of these depolymerizing processes, because the fairly high polymerized molecules always hold more than 90 percent of the system during the course of the reaction. The particular studies of the value of $A$ shall be reported in next paper.

Integrating Eq. (10) under assumption that $A$ and $\sum M_i$ are invariable with time and the initial condition that $L_1^\circ=0$ at $t=0$,

$$(L_1^\circ/\kappa\sum M_i)\{\ln L_1^\circ-\ln(L_1^\circ-L_1)\}=t \qquad (11)$$

i.e.

$$(2.303\,L_1^\circ/\kappa\sum M_i)\{\log L_1^\circ-\log(L_1^\circ-L_1)\}=t. \qquad (11')$$

If $L_1^\circ\{\ln L_1^\circ-\ln(L_1^\circ-L_1)\}$ are plotted against $t$, a straight line through the origin is expected to be obtained in case that Eq. (11) is suitable. Values of $\kappa\sum M_i/2.303$ of Table III were estimated from the slope of these lines which were roughly found from the experimental data of Table I and II. The curve $L_1$ vers. $t$, recalculated from $L_1^\circ$ and these values of $\kappa\sum M_i/2.303$ by means of Eq. (11) is the real line in Fig. 1. The experimental data fall on this real line within the limit of experimental error. This is evidence to confirm the supposed reaction formulas.

Furthermore, because the values of $\sum M_i/A$ may be approximately assumed hardly to change with temperature, the activation energy $\Delta E_{act.}$ of depolymerization reaction, i.e.

$$\sum M_{i+1}\rightarrow\sum M_i+L_1$$

can be obtained from these values of $\kappa\sum M_i/2.303$ and $\kappa\propto\exp\left(-\frac{\Delta E_{act.}}{RT}\right)$. Logarithms of $\kappa\sum M_i/2.303$ are plotted against reciprocals of the absolute temperature in Fig. II which is linear and then leads to $\Delta E_{act.}$ of 12.5 kcal./mol.

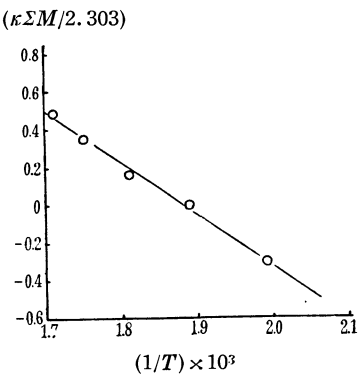



Fig. 2. Ratio of depolymerizing rate plotted against the reciprocal of absolute temperature.

Eq. (9) takes the form,

$$\kappa/k=K=L_1^\circ/A. \qquad (12)$$

The ratios of equilibrium constants $K$ of varing temperatures, relating to the amide-interchange reaction about lactam monomer, can be found from values of $L_1^\circ$. Therefore one could determine the energy difference $\Delta E$ between a lactam-monomer and a structural unit of chain-molecule, because no change of $A$ with temperature may be assumed for the first approximation. $\Delta E$ of 3.8 kcal./mol. was estimated from Fig. 3 where log $KA$ is plotted against reciprocals of the absolute temperature.

In conclusion. the thermochemical equation

$$\underset{\text{|}\qquad\qquad\text{|}}{CO-(CH_2)_5-NH}+3.8\text{ kcal.}$$
$$=[-CO-(CH_2)_5-NH-]$$

6) K. Hoshino and M. Watanabe, *Scientific Reports of Toyo Rayon Co.* (in Japanese) Vol. 3, No. 4, 110 (1948).

7) A. Matthes, *Makromol. Chem.*, 5, 197 (1951).

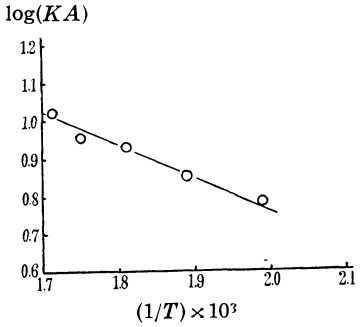



Fig. 3. Ratio of equilibrium constant plotted against the reciprocal of absolute temperature.

and Fig. 4 which illustrate energy levels in such reaction can be obtained.

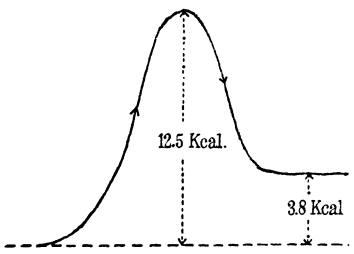



Fig. 4. Illustraction of energy levels in polymerizing and depolymerizing reaction.

The values of $\kappa\sum M_i$ and $(\kappa/k)A$ afford the ratio of rate constant $k$ in Table IV by means of equation

$$\kappa\sum M_i/(\kappa/k)A=k\sum M_i/A. \quad (13)$$

As the absolute values in Table IV should be changed by units of concentration and time, only their ratio can be criticized here.

TABLE III
THE RATE OF DEPOLYMERIZING AT VARYING TEMPERATURES FROM EXPERIMENTS

| Temp. °C | $L_1°$ (mol. no.) | $\kappa\sum M_i/2.303$ (mol. no./hr.) |
|---|---|---|
| 230 | 6.0 | 0.50 |
| 257 | 7.0 | 0.98 |
| 280 | 7.8 | 1.46 |
| 295 | 8.9 | 2.25 |
| 310 | 10.6 | 3.10 |

d) $\overline{M}_n=10400[\eta]^{1.51}$ [6], where $\overline{M}_n$ denotes number-average molecular weight. Molecular weight was estimated by this relation.

e) 5% aminocaproic acid was added to caprolactam for the purpose of accelerating the reaction.

f) A linear chain molecule can have two groups affecting amide-interchange reaction. Accordingly it is reasonable to consider the mol. no. of groups capable of affecting amide-interchange reaction rather than the number of chain-molecules. In the case of lactam and benzoic acid reaction, $M_i$ coincides with mol. no. of chain-molecules.

## Polymerizing Process

20 g. of $\epsilon$-caprolactam and 100 g. of polycapramide filament from which water soluble components are removed by extraction, were sealed in a tube and heated at 257°C. The decrease of caprolactam was analysed. The methods of heating and analyses were identical with the above mentioned experiments. The results are shown by circles in Fig. 5.

Eliminating $\kappa$ from Eqs. (8) and (9)

$$d(L_1/A)/dt=(k\sum M_i/A^2)(L_1°-L_1). \quad (14)$$

Integrating eq. (14) under the initial condition that $L_1=L_1^*$ at $t=0$,

$$\frac{A}{k\sum M_i}\ln\{(L_1°-L_1^*)/(L_1°-L_1)\}=t. \quad (15)$$

$L_1$ plotted against $t$, calculated from Eq. (15) using values that $L_1^*=16.7$, $L_1°=7.0$, and $2.303A/k\sum M_i=1/0.14$ shown in Table IV, is represented by a real line in Fig. 5.

TABLE VI
THE RATE OF POLYMERIZING AT VARYING TEMPERATURES

| Temp. °C | $\kappa\sum M_i\frac{1}{2,303}$ (mol. no./hr.) | $\frac{\kappa}{k}A$ (mol. no.) | $k\frac{\sum M_i}{A}\frac{1}{2.303}$ (mol. no./mol. no. hrs.) |
|---|---|---|---|
| 230 | 0.50 | 6.0 | 0.083 |
| 257 | 0.98 | 7.0 | 0.14 |
| 280 | 1.46 | 7.8 | 0.19 |
| 295 | 2.25 | 8.9 | 0.25 |
| 310 | 3.10 | 10.6 | 0.29 |

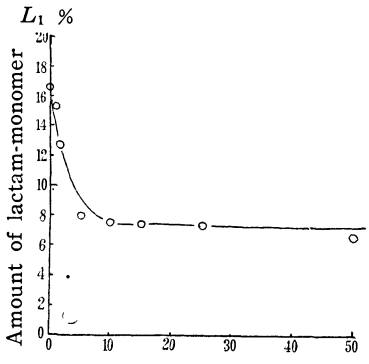



Fig. 5. Amounts of lactam-monomer in polymerizing process at 257°C (Circles represent experimental values and the real line represents deduced line from supposition.)

Experimental data are in accordance with the calculated curve within the limit of ex-

perimental error. This accordance assures the reality of assumed reaction formulas. For this means that two equilibrium constants, derived from the ratio of rate constants of polymerization and depolymerization and directly obtained from the amount of lactam-monomer at equilibrium state, are coincident.

## Discussion

One of the results of this study is that the difference of energy ($\Delta E$) between the lactam-monomer (closed ring) and the structural unit in chain-molecule (opened chain) is 3.8 kcal./mol. and the reaction is exothermic in ring-opening. Recently a calorimetric measurement on polymerization heat of caprolactam under the existence of water has been reported.[3] According to this report, the reaction is exothermic and the heat of polymerization is 28.5–29.0 cal./g. independent to the amount of water. This value corresponds to 3.28 kcal./mol. lactam. As the polymeric system contains ca. 10% of low molecular weight lactam-molecules, the reaction heat of the ring-opening of caprolactam,

$$CO-(CH_2)_5-NH \rightarrow [-OC-(CH_2)_5-NH-],$$

becomes to 3.6 kcal./mol. and this value apparently agrees to the value of $\Delta E$ deduced from this equilibrium experiments.

However this value seems to be too small as a heat of chemical reaction, but because the difference of entropy of reaction with temperature change is considered to be negligibly small, this heat of reaction is probably due to the potential which restricts the intramolecular bond rotation. In chain-molecules all of the paraffine bonds can take the *trans* or the *gauche* configurations.[8] But in the comparatively small numbered ring each of these bonds cannot take the *trans* nor even the correct *gauche* configurations: only in cyclohexane can the correct *gauche* configurations be taken. ε-Caprolactam ring contains five methylene- and one amide-linkages. For the present we cannot calculate quantitatively the configuration of these linkages. Suppose that cycloheptane ring can be taken as the substitute of caprolactam ring. The potential energy of this ring is $V_r(=\alpha+\beta)$ higher than the minimum energy belonging to the configuration that all of bonds take the *trans*, namely $\alpha$ and $\beta$ components are respectively the energy difference between *trans* and *gauche* configurations and the additional energy due to the deviation of the correct *gauche* configuration. Being 0.8 kcal./mol. (butane)[9] or 0.5 kcal./mol. (from pentane to cetane)[10,11,12] the energy difference between *trans* and *gauche* configurations in normal paraffin, the value of the latter will be applied here: then $\alpha$ is $(0.5\times7=)3.5$ kcal./mol. Above 500°K even a chain molecule contains a considerable ratio of the *gauche* configurations; the corresponding increment ($V_c$) of potential energy from the level of all *trans* configurations can be presumed to be 1.9 kcal./mol.[8] ($V_r-V_c$) shall be compared with the heat of reaction ($\Delta E=3.6$ kcal./mol.). Neglecting the differences of the oscillation and the molecular rotation energies, $V_r-V_c=\Delta E$. Then $\beta=2.0$ kcal./mol. is obtained; this value is considered to be conceivable. For the interpretation of the heat of reaction the idea above described is fairly probable. An analogous treatment of data for the sum of lactam-dimer (14-membered ring) and -trimer (21-membered ring) leads to the energy difference between chain and ring whose value was about 1/2–1/3 of the value for monomer. As the large numbered ring contains a large ratio of the *trans* configuration or small deviation from the correct *trans* and *gauche* configurations, it seems reasonable in accordance with the above opinion. The larger the ring is, the smaller these effects are, and the ring becomes more stable.

Activation energies, 12.5 kcal./mol. for the depolymerization where a lactam-monomer appears from the chain-molecule, and 8.7 kcal./mol. for the polymerization where a lactam-monomer is converted to the chain-molecule were estimated. But there have been no results of studies directly referable for discussing these values of activation energies. Nevertheless, because these are comparatively small (about 10 kcal./mol.) and effective catalysts have tendencies to ionize easily, the amide-interchange reaction is seemingly the reaction where the ionization occurs. As the rate or the activation energy of the pure amide-interchange reaction is being further investigated, such discussions will be treated in detail in subsequent reports.

The view that the lactam-polymerization is an amide-interchange reaction, may be conjectured from the early patent.[13] D'Alelio imaginatively explained it through the carbonium ion under similar consideration.[14]

8) "Physical Chemistry I" Ed. S. Mizushima (in Japanese) Kyoritsu Publisher, Tokyo (1948), pp. 272—6.

9) K. S. Pitzer, *J. Chem. Phys.*, 8, 711 (1940).

10) S. Mizushima, Y. Morino and M. Takeda, *J. Chem. Phys.*, 9, 826 (1941).

11) S. Mizushima and H. Okazaki, *J. Am. Chem. Soc.*, 71, 3411 (1949).

12) N. Sheppard and J. G. Szasz, *J. Chem. Phys.*, 17, 86, 93 (1949).

13) P. Schlack, *U.S.P.*, 2,241,321 (1941).

14) G. E. D'Alelio, "Fundamental Principles of Polymerization" New York, John Wiley & Sons. Inc. pp. 441—6 (1952).

Mark and Tobolsky[15] also considered this interchange reaction.

But recently it was reported by Wiloth[16] that caprolactam-polymerization is a bimolecular condensation reaction; i.e. any caprolactam is always hydrolyzed into ε-aminocaproic acid

"$HN(CH_2)_5CO + H_2O \rightarrow H_2N(CH_2)_5COOH$"

and it is polymerized by the dehydration with other chain molecule "$H_2N(CH_2)_5COOH + H[HN(CH_2)_5CO]_nOH \rightarrow H[HN(CH_2)_5CO]_{n+1}OH + H_2O$" therefore the lactam-monomer is equilibrated with the aminocaproic acid only. And also Wiloth has taken the position that for the completely dried lactam benzoic acid cannot act as a catalyst: water is necessary for benzoic acid to be a catalyst. The experimental bases of these descriptions are seemingly doubtful and the kinetics on his consideration was not investigated. If water is coexistent with benzoic acid both may be catalysts. By Matthes[7] comprehensive research was accomplished and the addition-theory about the radical $-NH(CH_2)_5CO-$ was represented. His experimental data are very useful, but his theory is questionable. The author, like D'Alelio, has considered the amide-interchange reaction and revealed its reality: the "amide-interchange reaction" shall probably be "an ionic reaction".

g) If $N_{C2h}$ and $N_{C2}$ represent the number of *trans* and *gauche* configurations in chain molecule respectively,

$K_p = N_{C2}/N_{C2h} = \text{constant} \cdot e^{-\Delta E/RT}$, where $\Delta E$ is the energy difference between both configurations. From values at various temperatures about dichloroethane[17] the value of this constant is roughly presumed to be about 2. Substituting $\Delta E = 0.5$ kcal./mol. and $T = 530°K$ (257°C) into the above equation, $K_p = 1.24$. Then the ratio of the *gauche* configurations in chain molecule is obtained and the increment of the potential energy is 1.9 kcal./mol. (0.5 kcal × 7 × 1.24/2.24).

15) H. Mark, A. V. Tobolsky, "Physical Chemistry of High Polymeric Systems", Interscience Publishers, Inc., New York p. 382 (1950).
16) F. Wiloth, *Angew. Chem.*, **65**, 351 (1953).
17) H. A. Stuart, "Die Struktur des freien Moleküls," Springer Verlag (1952) pp. 219—21.

## Conclusion

All possible reactions in lactam-polymerization are brought to reactions of a sort, i.e. amide-interchange reaction, and the equation enabling us to discuss the reaction rate by measurable value is derived by the approximation peculiar to super high polymeric system. The experimental results on polymerizing and depolymerizing processes show the reality of this reaction formula. All reactions relating to the lactam-monomer can be indicated by the amide-interchange equation,

$$L_1 + M_n \rightleftarrows M_{n+1}$$

where $L_1$, $M_n$ are the lactam-monomer and $n$-mer-chain molecules respectively. The heat of polymerization of caprolactam was 3.8 kcal./mol. exothermically, which coincides with the calorimetrically measured value. The ratios of the reaction rates were derived. Activation energy of depolymerizing is 12.5 kcal./mol. and that of polymerizing is 8.7 kcal./mol., which suggest that the ionization will participate in these reactions. The unit of Brownian motion in the molten linear high polymer presented in this paper was not determined but will be deduced from experiments about dilution in a subsequent paper.

The author wishes to thank Dr. K. Hoshino and Dr. H. Kobayashi who instructed him in these studies and permitted this publication.

*Research Laboratory of Toyo Rayon Co. Ltd.*

# *Studies on Polymerization and Depolymerization of ε-Caprolactam. II.* The Effects of the Diluent and an Estimation of the Size of the "Segment"*

By Hirosuke YUMOTO

(Received July 13, 1954)

## Introduction

The polycapramide ordinarily manufactured from ε-caprolactam contains the caprolactam-monomer, -dimer and -trimer which are soluble in water. Even if these lactams (ring-molecule oligomers) are completely removed from the polymer on scouring in hot water, they are always regenerated on melting. It has been found by the author that if the diluent is coexistent on melting, the quantities of the regenerated lactams increase exceedingly. Besides, if ε-caprolactam is polymerized in the presence of a diluent, such prepared polymer contains greater quantities of the lactam oligomers than that prepared from ε-caprolactam only. The diluent has little effect on the polymerization-degree of the chain molecules, but makes the quantities of lactams, especially lactam-monomer, notably increase. These phenomena suggest that the reaction-orders of the lactam-formation (depolymerization) and the lactam-disappearing (polymerization) are different.

Generally when the two reaction-orders of the direct and the reversal reaction are different, the effect of the concentration or the pressure is an important factor for the composition at equilibrium state.

The polymer prepared from the pure caprolactam without the diluent contains still considerable quantities of lactams. This fact should be interpreted as showing that in this case there is also a sort of reaction in the solution, and the problem of how to determine the concentration of the component must be subjected to consideration above everything else.

Usual methods of determining the concentration on the chemical kinetics are suitable to the reaction of gases or in the dilute solutions, but cannot be directly applied to the reactions of liquid especially to those of the molten high polymer-systems. At the reaction in dilute solution the concentration of the component is usually represented by means of the number of mols in unit volume. Polymerization makes little change of volume of system. Then when such a method is applied to the molten polymer system, if only the number of mol. of any component is invariable, the concentration is constant in the whole course of reaction whether polymerization occurs or not: e.g. carboxylic acid group component in this case. But polymerization occurring, even if the number of mol. is invariable, the functional concentration should be truly variable. If the direct and reverse reactions are in the same order, such a complicated problem should not arise.

In view of the classical interpretation, the "molar fraction" is the most adequate expression of the concentration to consider the probability of the molecular collision, and in order to determine the molar fraction, the number of mol. of whole reaction phase must be prescribed. But as it has not yet been known, how to determine the number of mols of the molten high polymer, the author, as the first step, assumed the average unit of macro-Brownian motion for the linear high polymeric molecule, and prescribed the number of mol. of the whole reaction phase according to this unit. As for the viscosity of liquid, Eyring has already considered the "segment" to be the unit of flow in the high molecular weight substance, and this idea has been experimentally approved to be real. Therefore, such a consideration may be seemingly applied to the chemical reaction, namely collisions of molecules, and the author had derived the equation of kinetics on the polymerization and depolymerization of caprolactam in view of the "segment" and the "amide-interchange reaction".[1]

In this study the polymerizations of ε-caprolactam in coexistence of the various amounts of thymol at the various temperature were subjected to the experiments. The experimental data were applied to the deduced equation; the result is that the reaction formulas about the amide-interchange reaction are proved again to be true and also the size of the unit of macro-Brownian motion of the linear polycapramide molecules can be determined. The size of unit determined by such method was of nearly the same magni-

* Presented at the 7th Annual Meeting of the Chemical Society of Japan in Tokyo, April 1, 1954.

1) H. Yumoto, This Bulletin, 28, 94 (1955).

tude as the segments of hydrocarbon[2] and polyester[3] determined by the measurement of the melt viscosities.

As the results of determing the size of such a unit, the equilibrium constants at various temperatures, concerning with the transforming reactions between lactam-monomer [CO$-(CH_2)_5-$NH] and the structural unit of the polycapramide chain-molecule [$-$CO$-(CH_2)_5-$NH$-$], can be estimated; from these equilibrium constants the energy difference between both the above states can be obtained more accurately than that estimated previously[1] for the first approximation, its value giving better coincidence to the value determined calorimetrically by S. M. Skurator et al.[4]

## Experiments

10 g. of pure ε-caprolactam, 0.5 g. of ε-aminocaproic acid, and purified thymol were mixed and heated to polymerize in a glass tube at the atmospheric pressure preventing oxidation. The amounts of the mixed thymol were changed from 3/100 to 70/100 by the molar ratio to the sum of mol. of caprolactam and aminocaproic acid. The temperatures of polymerization-reactions were 257, 230 and 200°C. The time of reaction is 50 hrs. at 257 or 230°C and is 100 hrs. at 200°C. The boiling point of thymol being 232°C, the temperature of the system containing a large quantity of thymol cannot rise to 257°C under the atmospheric pressure; the melting point of polycapramide being 215–220°C, a small quantity of thymol could not be used at 200°C because of solidification. ε-Aminocaproic acid is used as the catalyst for the purpose of shortening the time to reach the equilibrium state but also can convert to a structural unit of the polycapramide molecule as the polymerizible component.

The obtained polymer contains the lactam oligomers. The amounts of lactam-monomer and the sum[a] of lactam-dimer and -trimer were found through the micro-Kjeldahl's nitrogen contents of the water-extracted components: the quantities of

TABLE I

THE AMOUNTS OF LACTAM-MONOMER, AND SUM OF LALTAM-DIMER AND -TRIMER

| Polymerization temp. °C | The number of mol. of (ε-caprolactam+ε-aminocaproic acid) for polymerization | The number of mol. of thymol as the diluent $S$ | The number of mol. of lactam-monomer in polymer $L_1^\circ$ | The number of mol. of (lactam-dimer +-trimer) in polymer[a] $L_2^\circ+L_3^\circ$ |
|---|---|---|---|---|
| 257 | 1.00 | 0 | 0.070 | 0.010 |
| | | 0.036 | 0.079 | 0.009 |
| | | 0.072 | 0.084 | 0.010 |
| | | 0.107 | 0.092 | 0.010 |
| | | 0.143 | 0.096 | 0.010 |
| 230 | 1.00 | 0 | 0.060 | 0.006 |
| | | 0.036 | 0.069 | 0.006 |
| | | 0.072 | 0.068 | 0.007 |
| | | 0.107 | 0.075 | 0.007 |
| | | 0.143 | 0.081 | 0.007 |
| | | 0.286 | 0.106 | 0.007 |
| | | 0.572 | 0.151 | 0.007 |
| 200 | 1.00 | 0.072 | 0.058 | 0.004 |
| | | 0.178 | 0.071 | 0.006 |
| | | 0.356 | 0.098 | 0.007 |
| | | 0.572 | 0.125 | 0.007 |
| | | 0.678 | 0.145 | 0.007 |

2) W. Kauzmann and H. Eyring, *J. Am. Chem. Soc.*, **62**, 3113 (1940).

3) P. J. Flory, ibid., **62**, 1057 (1940).

4) S. M. Skuratov, A. A. Stepikheev, and E. N. Kanarskaya, *Kolloid. Zhur.*, **14**, 185 (1952); *Faserforschung u. Textiltechnik* **4**, 390 (1953); *Chem. Abstr.*, **46**, 8506 (1952).

a) The weight of the sum of lactam-dimer and -trimer can be found through the analytical value, but the number of moles of the sum of them cannot be determined unless the weight-ratio of them is estimated. The polymeric system of polycapramide contains two series of chain and ring molecules. Such polymeric system being in equilibrium, the ratio of the numbers of the ring molecules in their series will be presumed from the probability. The order of apporoximation for the value of the ratio calculated from the probability may increase for the large rings, e.g. the 14-membered ring of lactam-dimer or the 21-membered ring of lactam-trimer. Therefore, by means of this presumption,[7] the ratios of numbers of moles of lactam-dimer to that of -trimer were determined as follows;

$$L_n^\circ \approx A(7n)^{-3/2}n^{-1},\quad L_n^\circ \propto n^{-5/2}$$
$$\therefore\ L_2^\circ/L_3^\circ \approx 1.5^{5/2}=2.8$$

where $L_n^\circ$=the number of moles of the $n$-mer ring (lactam) molecule at the equilibrium state, $A$=a constant. Using this relation the values of $(L_2^\circ+L_3^\circ)$ were obtained.

5) P. J. Flory, *J. Am. Chem. Soc.*, 58, 1877 (1938).

6) K. Hoshino and M. Watanabe, *Scientific Reports of Toyo Rayon Co.* (In Japanese) Vol. 3, No. 4, 110 (1948).

7) H. Jacobson and W. H. Stockmayer, *J. Chem. Phys.*, **18**, 1600 (1950).

the water-soluble chain oligomers are negligibly small.[b)8)] These analytical procedures were similar to that described in the preceding paper.[1)] The results of the experiments are shown in Table I.

The degree of polymerization of the chain molecules were estimated from the intrinsic viscosity of the cresol solution about the polymer prepared at the temperature of 230°C. The results is presented in Table II.

Table II

The degree of polymerizaton of the chain molecule in the polymer, prepared at 230°C in coexistence of thymol

| The no. of mol. of thymol for 1 mol. of (ε-caprolactam+ε-aminocaproic acid) | 0 | 0.075 | 0.188 | 0.376 | 0.603 |
|---|---|---|---|---|---|
| $[\eta]$ 25°C cresol | 1.13 | 1.10 | 1.08 | 0.87 | 0.94 |
| The number-average[c)] degree of polymerization (P) | 112 | 107 | 102 | 73 | 94 |

## Discussions

Assuming the number of mol. of the unit of macro-Brownian motion in the whole reaction phase to be $A$, the equilibration about lactam-monomer in the case of the super-high polymeric system was represented by Eq. (9) in the previous paper.[1)] The reactions about lactam-monomer are

$$M_n+L_1 \underset{\kappa}{\overset{k}{\rightleftarrows}} M_{n+1},\ B+L_1 \rightleftarrows M_1 \qquad (1)$$

where $L_1$=lactam-monomer, $M_n=n-$mer chain molecule, $B$=the catalyst unbound. For the super-high polymeric system, $B \ll \sum_{n=1}^{\infty} M_n$, $M_1 \ll \sum_{n=1}^{\infty} M_n$,[1)] so that approximately $\sum_{n=1}^{\infty} M_n + L_1 \rightleftarrows \sum_{n=1}^{\infty} M_{n+1}$, $\sum_{n=1}^{\infty} M_n \approx \sum_{n=1}^{\infty} M_{n+1}$. Consequently polymerizing 1 mol. of ε-caprolactam, in equilibrium

$$L_1^\circ = A\kappa/k \qquad (2)$$

where $L_1^\circ$=the number of mol. of lactam-monomer at the equilibrium state, $\kappa$=the rate constant of lactam-monomer to be formed from the chain-molecule, $k$=the rate constant of lactam-monomer to transform into a structural unit of the chain-molecule. In the previous paper $A$ in Eq. (2) was treated approximately as a constant, but in this study on the reactions in coexistence of the diluent $A$ is the most important function.

The larger the value of $A$ is, namely the reaction which arises in the more dilute state, the more lactam-monomer in equilibrium is. Even if the diluent increases, the degree of polymerization of the chain-molecules could hardly change; for it is only directly affected by the quantity of the reagent that possibly reacts to the amide-linkage.

It is experimentally required as the diluent to choose a substance which is a solvent of polycapramide and also chemically stable at the temperature of about 250°C. Thymol (m. wt. 150) was chosen among the usually obtainable substances. The reactiveness of thymol to the amide-linkage is shown by $P$ (the degree of polymerization of the chain-molecules) which is represented in Table II. The larger the dilution was, the smaller $P$ was. The dilution brought increase of the lactam (ring)-molecules so that the chain-molecules were decreased. Considering this effect, however, the observed $P$ is still smaller than the calculated value on the assumption that thymol is a pure diluent. Nevertheless the decrease of the value of $P$ is too slight to assume that thymol reacts on the amide-linkage, considering that the experimental error of intrinsic viscosity measuring is about 5%. Although 0.6 mol. of thymol was used to 1 mol. of lactam, $P$ was about 90; if 0.6 mol. of benzoic acid was used to 1 mol. of lactam, $P$ would be less than 2.[d)] Consequently the main effect of thymol must be the dilution. If $P$ is about 80, Eq.(2) may be enough applied approximately because $M_1 \ll \sum_{n=1}^{\infty} M_n$, $B \ll \sum_{n=1}^{\infty} M_n$: so that Eq. (2) is able to be used in the case of discussing the equilibrium about lactam-monomer, assuming thymol as merely

(b) As for the super-high polymeric system where the degree of polymerization $P$ is about 100, the amounts of water-soluble chain oligomers are too small to make quantitative analysis by extraction. Besides, according to Flory's molecular weight distribution,[5)] they are negligibly little.

8) P. H. Hermans, *Rec. trav. chim. Pay-Bas*, 72, 798 (1953).

(c) The number-average molecular weight $\bar{M}$ was estimated by the following relation;[6)]

$$\bar{M}_n = 10400[\mu]^{1.61}$$

where $[\eta]$ is the instrinsic viscosity on the cresol solution at 25°C. It is enough to make a rough estimation.

(d) Polymerizing 1 mol. of ε-caprolactam with 0.5 mol. of benzoic acid at the temperature of 257°C, the number-average degree of polymerization about the chain-molecules was 2.4 and the number of moles of lactam-monomer remaining in the system was 0.11. Benzoic acid effects the reaction not only as the diluent but also as the component that possibly reacts to the amide-linkage.

the diluent.

The size of the unit of macro-Browian motion of the polycapramide molecule has not yet been known. Then it was assumed as follows;

" if 1 mol. of caprolactam were to be entirely polymerized into the polycapramide chain-molecule, the number of mols of the average unit of macro-Browian motion would be $\alpha$."

In the high polymeric system the quantities of the chain-oligomers are negligibly small[6)8)] and so only the ring-oligomers are well considered quantitatively as the oligomers. Assume that 1 mol. of caprolactam is polymerized together with $S$ mol. of the diluent, and in equilibrium $L_1^\circ$, $L_2^\circ$ and $L_3^\circ$ mol. of lactam-monomer,-dimer and-trimer, respectively, are of existence in the polymer. Consequently

$$A=S+L_1^\circ+(1-L_1^\circ)\alpha \tag{3}$$

or

$$A=S+L_1^\circ+L_2^\circ+L_3^\circ+(1-\overline{L_1^\circ+2L_2^\circ+3L_3^\circ})\alpha \tag{4}$$

Eq. (3) is the case that only lactam-monomer besides the diluent is taken into account as the molecule of the low molecular weight in the phase of reaction; Eq. (4) is the case that also lactam-dimer and -trimer are considered. $L_2^\circ+L_3^\circ$ is far less than $L_1^\circ$ as is shown in Table I, so that also Eq. (3) is approximately applicable. Substituting Eq. (3) or Eq. (4) into Eq. (2),

$$L_1^\circ/(1-L_1^\circ)=(\kappa/k)\{(S+L_1^\circ)/(1-L_1^\circ)\}+(\kappa/k)\alpha \tag{5}$$

or

$$L_1^\circ/(1-\overline{L_1^\circ+2L_2^\circ+3L_3^\circ})=(\kappa/k)\{(S+L_1^\circ+L_2^\circ+L_3^\circ)/(1-\overline{L_1^\circ+2L_2^\circ+3L_3^\circ})\}+(\kappa/k)\alpha \tag{6}$$

Plotting $L_1^\circ/(1-L_1^\circ)$ or $L_1^\circ/(1-\overline{L_1^\circ+2L_2^\circ+3L_3^\circ})$ against $(S+L_1^\circ)/(1-L_1^\circ)$ or $(S+L_1^\circ+L_2^\circ+L_3^\circ)/(1-\overline{L_1^\circ+2L_2^\circ+3L_3^\circ})$ about the experimental values of Table I, Fig. 1 or Fig. 2 resulted. As a straight line through the dots is obtainable, these experimental data seemingly satisfy the Eq. (5) or Eq. (6). The values of $\kappa/k$ and $\alpha$ can be found from the gradient of this straight line and from the coordinate at the point of this straight line to cut across the horizontal axis, respectively. Three straight lines at the temperatures of 200, 230 and 257°C seem apparently to converge to a point on the horizontal axis in the limit of experimental error. The difference between Fig. 1 and Fig. 2 is very small: but Fig. 2 shall be preferred in spite of the assumption to determine $L_2^\circ+L_3^\circ$. The values of $\alpha$ and $\kappa/k$ from Fig. 2 are shown in Table III.

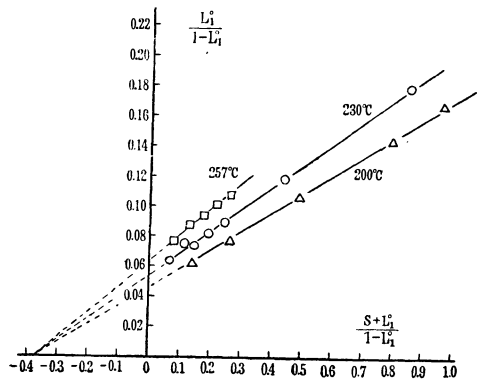



Fig. 1. Application of the experimental data (Table I) to Eq. (3).

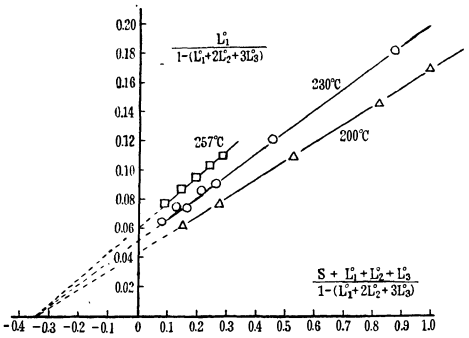



Fig. 2. Application of the experimental data (Table I) to Eq. (4).

TABLE III
THE EXPERIMENTAL VALUES OF $\alpha$ AND $\kappa/k$ FROM FIG. 2

| Temp. °C | 257 | 230 | 200 |
|---|---|---|---|
| $\alpha$ | 0.36 | 0.36 | 0.36 |
| $\kappa/k$ | 0.170 | 0.147 | 0.125 |

(i) **The Size of the "Segment".**—According to the experimentally obtained value of $\alpha$ and the above assumption about $\alpha$, if 1 mol. of caprolactam were to be entirely polymerized into the polycapramide chain-molecule, 0.36 mol. of the average unit of macro-Browian motion would be presented in the phase. And so the magnitude of the average unit of macro-Browian motion is of ($1/0.36\approx$) 2.8 mol. of the structural unit. Expressing the magnitude by the number of atoms of the skeleton, because the structural unit is a 7-atoms member, it is ($7\times2.8\approx$) 19.5 atoms.

The unit of macro-Brownian motion should be equivalent to the unit of flow discussed on the liquid-viscosity; so it is also equivalent to the "segment" which Eyring put forward about the motion of macromolecule. The magnitude of the "segment" has been hitherto exclusively presumed from the activation energy of flow, and two examples are

known. Kauzmann and Eyring[2] measured the activation energies of flow about the various normal hydrocarbons and so estimated the size of the unit of flow by extrapolation to be about 20-25 atoms for the macromolecule. Flory[3] also measured the activation energies of flow on the polyesters and presumed under some suppositions the unit of flow to be 28-34 atoms.

The value here estimated of about 20 atoms on the polycapramide is somewhat smaller than these values on the hydrocarbon and the polyesters, but is roughly equal to them. The method described here to presume the size of a segment is more direct and less hypothetical than the method from the viscosity measurement. As far as these three linear macromolecules are concerned, it is almost approved that the size of the "segment" in molten state has no intimate relation to the intermolecular strength of cohesion.

(ii) **Equilibrium Constant.**—$\kappa/k$ is the constant which governs whether the structural unit close into ε-caprolactam or open into chain through the amide-interchange reaction.

The value of $\alpha$ is not changed between 200 and 257°C and then it will be possibly applied to 310°C. When ε-caprolactam is polymerized without dilution at the temperatures of 230, 257, 280, 295 and 310°C, the amounts of lactam-monomer and (-dimer+-trimer) at the equilibrium state are analysed; these values were presented in Table II of the previous paper.[1] The values of $L_1^\circ$ and $(L_2^\circ+L_3^\circ)$ to denote the numbers of mols of each molecules are deduced by calculation.[a] The value of $A$ in the case of no diluent ($S=0$) at each temperature can be calculated by Eq. (4), and substituting it into Eq. (2), the value of $\kappa/k$ is obtained. The results of such calculations are Table IV. Plotting the logarithms of $\kappa/k$ against the reciprocals of the absolute temperature, Fig. 3 is obtained. The energy difference between the ring and

TABLE IV

THE VALUES OF THE EQUILIBRIUM CONSTANT $\kappa/k$ AT THE VARIOUS TEMPERATURES

$\left(\kappa/k=L_1^\circ/A,\ A=S+L_1^\circ+L_2^\circ+L_3^\circ \atop +(1-\overline{L_1^\circ+2L_2^\circ+3L_3^\circ})\alpha,\ S=0,\ \alpha=0.36\right)$

| Temp. °C | $L_1^\circ$ mol. | $L_2^\circ+L_3^\circ$ | $A$ mol. | $\kappa/k$ |
|---|---|---|---|---|
| 200 | — | — | 0.400 | 0.125 |
| 230 | 0.062 | 0.009 | 0.406 | 0.153 |
| 257 | 0.070 | 0.010 | 0.411 | 0.170 |
| 280 | 0.083 | 0.010 | 0.420 | 0.197 |
| 295 | 0.089 | 0.011 | 0.424 | 0.210 |
| 310 | 0.106 | 0.011 | 0.435 | 0.244 |

the chain states, i.e.

$$\underset{\lfloor_____\rfloor}{CO-(CH_2)_5-NH} \rightleftarrows [-CO-(CH_2)_5-NH-],$$

may be estimated through Fig. 3; its value is

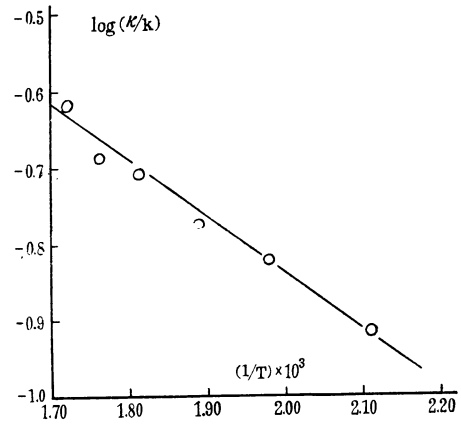



Fig. 3. Logarithms of the equilibrium constants vers. reciprocals of the absolute temperatures.

3.4-3.6 kcal./mol. In the previous paper[1] the values of $A$ could not be determined, so $A$ was treated as a constant under the first approximation. Therefore, there is nothing for estimation of the energy difference but to use $A(\kappa/k)$ instead of $\kappa/k$. Practically the values of $A$ at the various temperatures are slightly different as are shown in Table IV. Considering this effect for the second approximation, slightly smaller value is obtained; this value coincids better with the heat of polymerization calorimetrically measured by Skurator et al. [4,1]

## Conclusion

In the previous paper the author deduced the equation of kinetics about polymerization and depolymerization of ε-caprolactam in the super-high polymeric system through the amide-interchange reaction, and investigated the formulas experimentally. In succession, the experiments about the polymerization of ε-caprolactam with thymol as the diluent were carried out at 200, 230 and 257°C and their results were discussed in view of the deduced equations. The quantities of lactam oligomers in the polymeric systems containing the diluent were larger than those containing no diluent. Such inclination shows the reaction-orders of polymerization and depolymerization to be different. The increase of lactam-monomer satisfied the deduced equation quantitatively. Then from this relation the size of unit of macro-Browian motion, i.e. a "segment", about the polycapramide chain-molecules could be estimated to be ca. 20 atoms. The method described here to

estimate unit of macromolecule's macro-Brownian motion contains less assumption than the method from the melt viscosity measurement. The number of mol. of the unit of macro-Brownian motion in the whole reaction phase, $A$, being assumed in the derived equation, was calculated. Consequently the equilibrium constants, concerned with the transforming reactions between a structural unit (opened state) and a lactam monomer (closed state), could be found at the various temperatures, and so the heat of the above reactions can be estimated to be 3.4–3.6 kcal./mol.

The author wishes to thank Dr. K. Hoshino and Dr. H. Kobayashi who instructed studies and permitted the publication.

*Research Laboratory of Toyo Rayon Co., Ltd.*

# *Reaction Rates in the Synthesis of Ammonia. I. Dependence upon Reaction Pressure and Hydrogen-Nitrogen Ratio*

By Hiroshi UCHIDA and Michio KURAISHI

(Received June 16, 1954)

## Introduction

Many workers[1-6] have measured the rate of the reaction of ammonia synthesis. P. H. Emmett[3] and R. M. Adams[5] measured the ammonia concentration in exit gases over a wide range of space velocities, pressures, and temperatures using mixtures of different ratios of hydrogen to nitrogen of 3, 1, and 1/3. However, they confined the measurements to one kind of catalyst. H. Kobayashi[4] recently made extensive measurements with four kinds of catalysts under varying conditions of pressure, flow rate, and temperature, but used only a mixture of the ratio of 3 throughout the experiments. As for the ammonia concentration relating to hydrogen-nitrogen ratio, A. Nielsen[6] carried out the measurements with a triply promoted catalyst, but only at a pressure of 330 atm., at a space velocity of $15\times10^3$ and a temperature of 450°C.

No one, so far as we are aware, has ever published results sufficient to estimate the rate of the ammonia synthesis varying the ratio of hydrogen to nitrogen as well as the kind of catalyst. The authors have conducted the measurements with both of a singly and a triply promoted catalyst over an extended range of these conditions.

Our results have been to test the practical utility of the rate equations proposed by M. I. Temkin[2] and by M. Shindo[7], each based on different concepts as to the rate determining step. We have also attempted to modify the Temkin's equation to represent the experimental results more adequately, though not completely.

## Experimental

A mixture of hydrogen and nitrogen was obtained in ratio of 3 by introducing ammonia gas over an ammonia catalyst at 500°C and in order to obtain the mixtures of different composition either hydrogen or nitrogen was added from a cylinder. After having been compressed, the mixtures were purified by passing over palladium-asbestos at 200°C followed by cooling and subsequent drying through solid caustic potash. Fig. 1 is a diagram of the reactor. The catalyst chamber is made of copper tube, 27 mm. in outer dia. and 15 mm. in inner dia., inserted with an iron thermo-couple of 7 mm. in dia. The gas feed was directed downward on an electric heating nichrome coil wound on the copper tube, then upwards first into the preheating zone where copper granules of 2 mm. dia. were packed and finally through the catalyst bed.

Measurements of the rate of the ammonia synthesis were carried out with both a singly and a triply promoted catalyst, i.e. $Fe_3O_4$ containing 5% $Al_2O_3$ (Cat. No. 1) and 4% $Al_2O_3$, 1% CaO, 1% $K_2O$ (Cat. No. 2). The catalysts were prepared according to a procedure previously reported by G. Shima and one of the authors.[8] The latter catalyst is in current industrial use in this country. The catalysts were screened to obtain par-

1) A. T. Larson and R. S. Tour, *Chem. Met. Eng.*, **26**, 683 (1922).
2) M. I. Temkin and V. Pyzhev, *Acta Physicochim.*, (U.S.S.R.) **12**, 327 (1940).
3) P. H. Emmett and J. T. Kummer, *Ind. Eng. Chem.*, **35**, 677 (1943).
4) H. Kobayashi and H. Kubota, *Bull. Faculty Eng.* Hokkaido Univ., **5**, 118 (1951).
5) R. M. Adams and E. W. Comings, *Chem. Eng. Progr.*, **49**, 359 (1953).
6) A. Nielsen, "Advances in Catalysis and Related Subjects," Academic Press Inc., **5**, 1 (1953).
7) M. Shindo, *Bull. Faculty Eng., Hokkaido Univ.*, **3**, 136 (1949), *Mem. Muroran Univ. Eng.*, **1**, 75 (1950).
8) G. Shima and H. Uchida, *Rept. Chem. Ind. Res. Inst.*, Tokyo, **45**, 369 (1950).

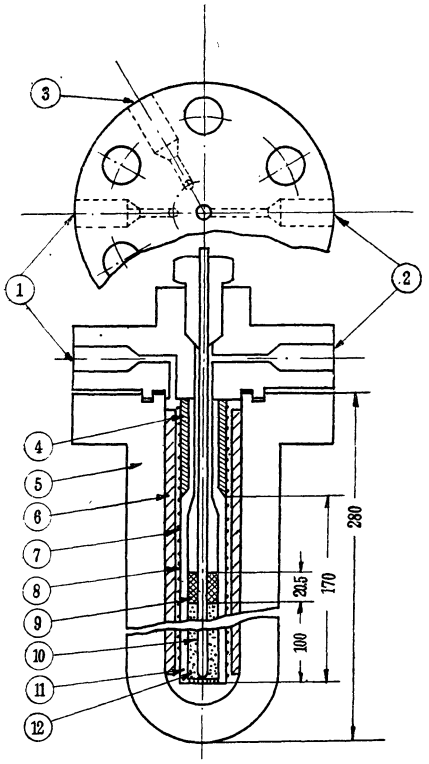



Fig. 1. Reactor.

1. Gas inlet
2. Gas outlet
3. Furnace lead
4. Asbestos
5. Steel shell, 100$\phi$/50$\phi$
6. Silica tube
7. Nichrome heater
8. Mica
9. Catalyst
10. Preheating zone
11. Catalyst chamber, 27$\phi$/15$\phi$
12. Thermocouple well 7$\phi$/5$\phi$

ticles which passed a 1.5 mm. mesh sieve, but were retained on the 1 mm. mesh. About 3 cc. of these specimens, weighing 7.25 g., was placed in the catalyst chamber just to fill 20.5 mm. at the height of the catalyst bed.

The catalysts were reduced in a current of the gas mixture of the ratio of 3 under 50–100 kg./cm$^2$ at space velocities of $3\sim5\times10^4$ and the reduction was continued until no more increase of ammonia concentration at 425°C under 100 kg./cm$^2$ was observed after further six hours reduction.

Temperature was measured both at the higher place near the inlet of the catalyst bed and at the lower place near the outlet. During the synthesis, the temperature difference through the catalyst bed remained usually less than 1°C, however it was not successful in retaining a difference less than 7°C, when the reaction temperature was higher than 500°C and the space velocity higher than $10^5$. The gaseous products were reduced to an atomospheric pressure and their volumes were measured after ammonia was absorbed in sulfuric acid which was determined as usual.

The measurements were made with both of the two catalysts at 6 to 7 different temperatures from 350°C to 525°C and at space velocities from $5\times10^3$ to $5\times10^5$ hr$^{-1}$., (1) using a mixture whose ratio of hydrogen to nitrogen was 3, under the pressure of 50, 100 and 150 kg./cm$^2$, and (2) using other mixtures of the ratio of 7, 5, 2, 1 and 1/3 under a constant pressure of 100 kg./cm$^2$.

## Results

Some of the experimental results* are shown in Figs. 2–9 presenting the ammonia concentration or the conversion efficiency as functions of the space velocity, the reaction pressure, and the initial gas composition.

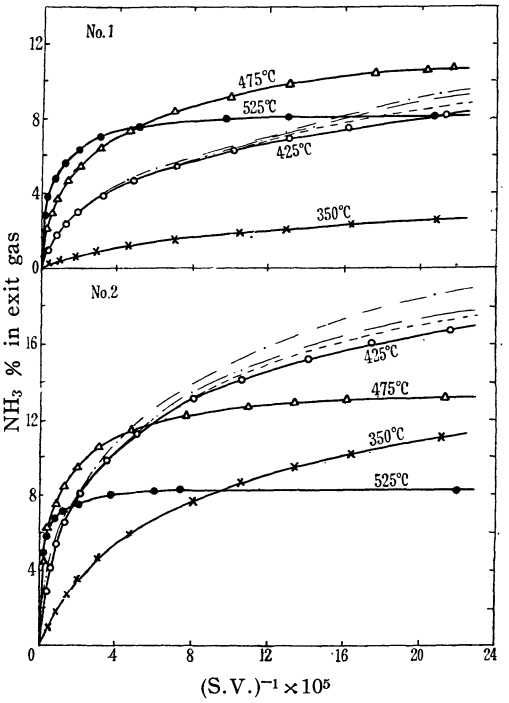



Fig. 2. Relation between reciprocal space velocity and ammonia %.
—○— Experimentally determined
----- Estimated from Eq. (5)
—·—·— Estimated from Temkin's Eq.
— — — Estimated from Shindo's Eq.

When the results concern the use of a mixture of a constant ratio of hydrogen-nitrogen ratio of 3, the ammonia concentration increases, as is well known, with the increasing pressures, but differently according to the kind of catalyst.[1,4,9] A greater increase of conversion percentage and a smaller decrease of efficiency with the increasing pressure are observed with Cat. No. 2 than with Cat. No. 1 (Fig. 3). To the extent that the space velocity is sufficiently high and at the same time the temperature low, the ammonia

9) H. Uchida and K. Ogawa, *Rept. Chem. Ind. Res. Inst.*, Tokyo, **46**, 114 (1951).

* A paper providing the results described in full will be published in *Rept. Chem. Ind. Inst.* Tokyo.

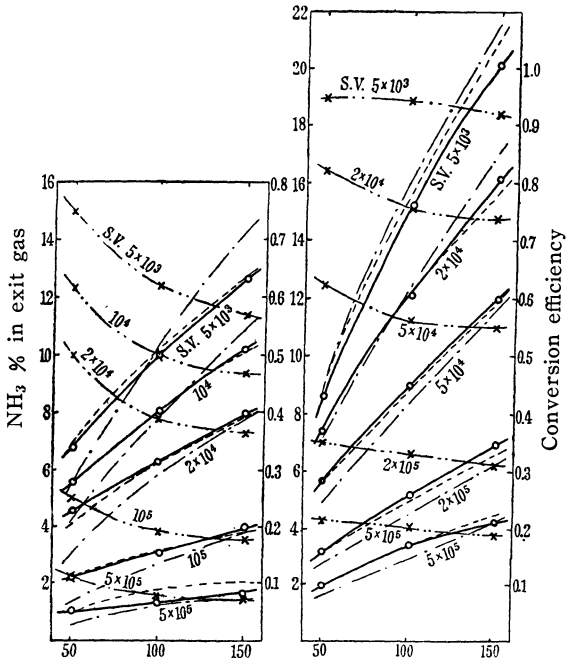



Fig. 3. Effect of pressure on ammonia % and conversion efficiency with catalyst No. 1 and No. 2. $N_2/H_2=1/3$, 450°C; left, No. 1, right, No. 2.

—○— %$NH_3$ determined experimentally

----- %$NH_3$ estimated from Eq. (5)

— — — %$NH_3$ estimated from Temkin's Eg.

———— Conversion efficiency

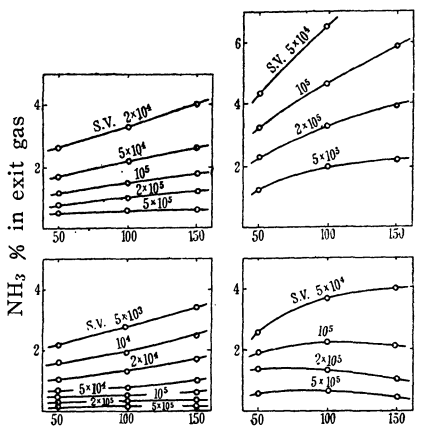


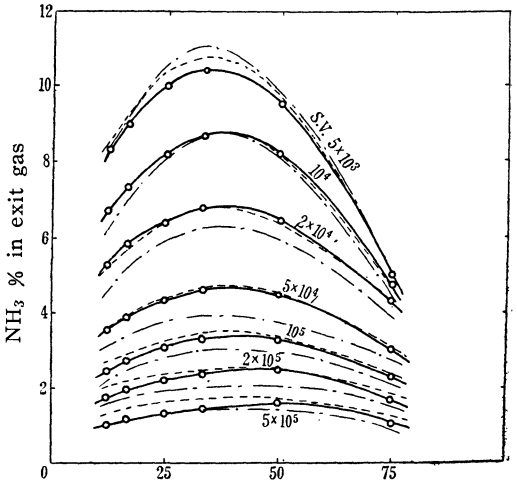

Fig. 4. Effect of pressure on ammonia % at low temperature and high space velocity. $N_2/H_2=1/3$.
above, left; No. 1, 400°C. above, right; No. 2, 400°C. below, left; No. 1, 350°C. below, right; No. 2, 350°C.

concentration remains, however, almost constant, irrespective of the different pressure. Ranges of the space velocity and the temperature in which this constancy holds are different between the two catalysts.**

A. Nielsen has shown an evidence of a maximum of the ammonia concentration together with a minimum of the conversion efficiency with respect to the initial nitrogen percentage, at limited pressure, space velocity, and temperature. In a wider range of space velocity and temperature, as shown in Figs. 5-8, the ammonia concentration and the conversion efficiency are expressed as functions of the initial nitrogen percentage at a pressure of 100 kg./cm² with each of the two catalysts. The maximum ammonia percentage tends to shift with increasing space velocities towards higher nitrogen percentages from 25%, in the neighbourhood of which the maximum is observed at high temperature and low space velocities, say, at the conditions closely approaching equilibrium. The maximum also tends to shift alike with lower temperatures, even at low space velocities.

** The space velocity below which the concentration begins to increase with the pressure is $5\times10^5$ at 400°C, $1\times10^5$ at 350°C with Cat. No. 1, while $2\times10^5$ at 350°C with Cat. No. 2.

(Fig. 5a)




(Fig. 5b)

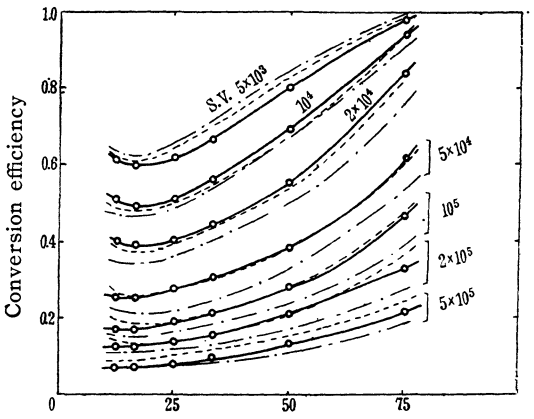
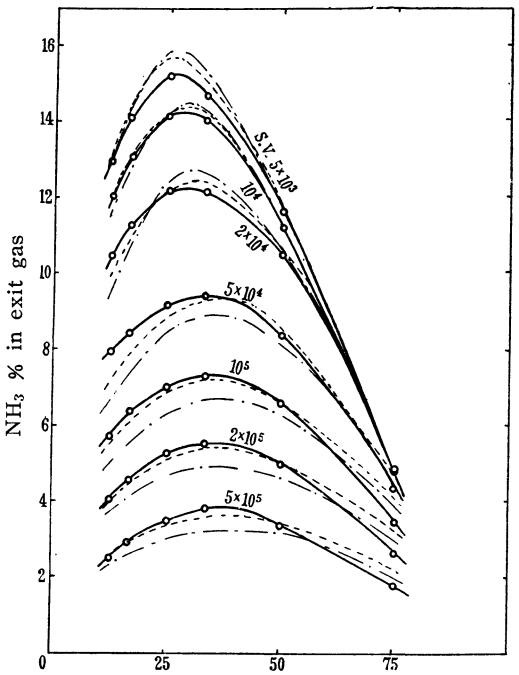
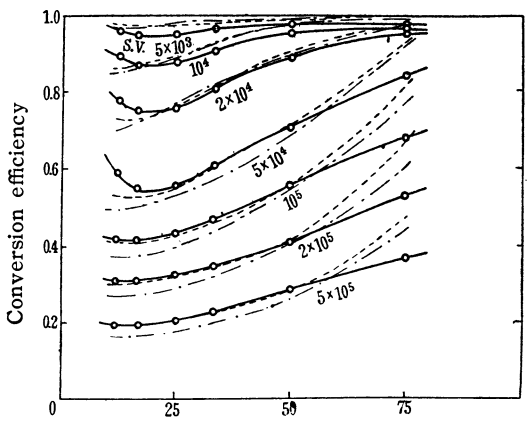


Fig. 5. Dependence of ammonia % and conversion efficiency upon initial gas composition, 100 kg./cm², 450°C, Catalyst No. 1.
—○— Experimentally determined
----- Estimated from Eq. (5)
——— Estimated from Temkin's Eq.

(Fig. 6a)

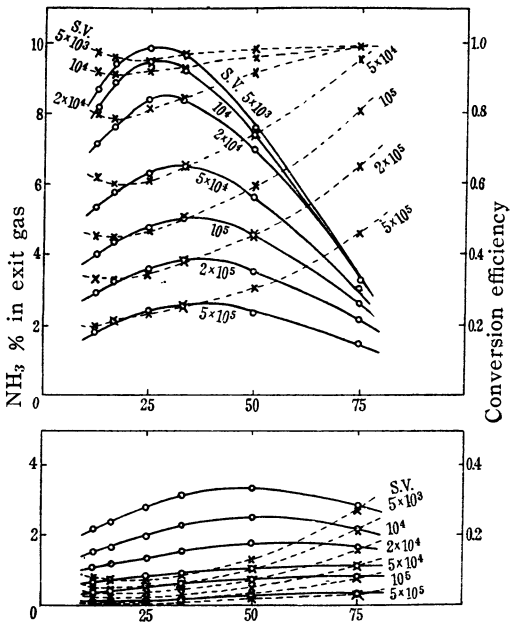



(Fig. 6b)




N₂ % in initial gas mixture

Fig. 6. Dependence of ammonia % and conversion efficiency upon initial gas composition, 100 kg./cm², 450°C, Catalyst No. 2.
—○— Experimentally determined.
----- Estimated from Eq. (5).
——— Estimated from Temkin's Eq.




N₂ % in initial gas mixture

Fig. 7. Depenence of ammonia % and conversion efficiency upon initial gas composition, 100 kg./cm², catalyst No. 1. above, 500°C. below, 350°C.
—○— $NH_3$ %.
--x-- Conversion efficiency,

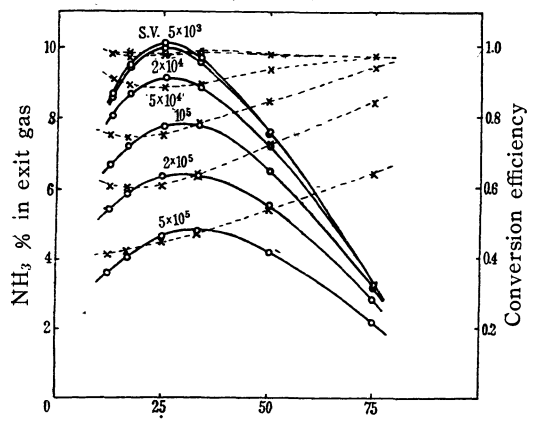
The shifting is observed to be more rapid with Cat. No. 1.* At a low temperature and at a high space velocity such as 350°C and $5\times10^5$, it shifts further through 75% with Cat. No. 1 and 54% with Cat. No. 2. At lower space velocities, the minimum of the conversion efficiency appears at 20–25% nitrogen percentage independent of the temperature. With increasing space velocity, it tends to shift towards a lower nitrogen percentage, and more rapidly at a higher temperature. When a comparison is made between the two catalysts at a constant temperature, the minimum lies at a lower percentage of nitrogen with Cat. No. 2.

S. L. Kiperman[10] pointed out that the ammonia concentration $z$ was in the relation of a straight line with space velocity at a normal pressure, when space velocity is very high. As shown in Figs. 2 and 9, this relation is found also valid at the high pressure in the range of extremely small values of 1/S.V. According to the present observations,

* The maximum is obtained at 25—26% nitrogen percentage at 500°C, $5\times10^3$ S.V. with both of the catalysts, and shifts to 48% with Cat. No. 1 and 33% with Cat. No. 2 at 350°C, $5\times10^3$ S.V., to 40% and 32% at 500°C, $5\times10^5$ S.V., respectively.

10) S. L. Kiperman and V. S. Granovskaya, *Chem. Abstr.*, **45**, 9346 (1952), **47**, 6749 (1953).

(Fig. 8a)




(Fig. 8b)

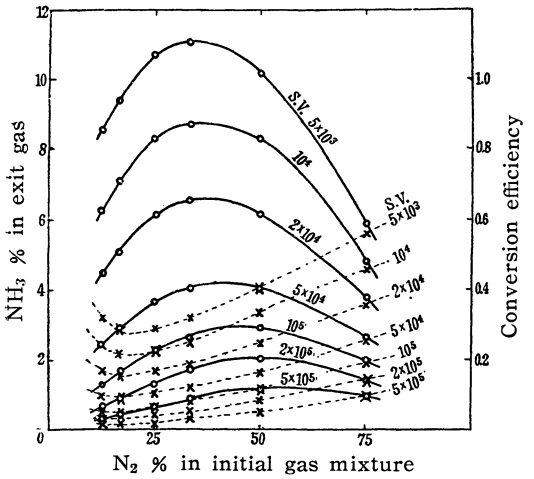



Fig. 8. Dependence of ammonia % and conversion efficiency upon initial gas composition, 100 kg./cm², catalyst No. 2. above, 500°C. below, 350°C.
—○— $NH_3$ %.
--×-- Conversion efficiency.

it extends towards lower space velocities with lower temperatures, with increasing pressure, and with higher hydrogen percentage. The results may be expressed in terms of the conversion efficiency as follows: the lower the efficiency becomes, the wider is the range at which the linear relation holds.

The proportionality factor between $z$ and 1/S.V. increases with the increasing nitrogen pressure in the mixtures of different hydrogen-nitrogen ratios at a constant total pressure, though it remains constant independent of the different total pressure when a mixture of the ratio of 3 is used.

## Discussion

A number of the rate equations for the ammonia synthesis have been proposed.[2,3,4,7,10,11]

11) H. de Bruijn. *Disc. Faraday Soc.*, 8, 69 (1950).

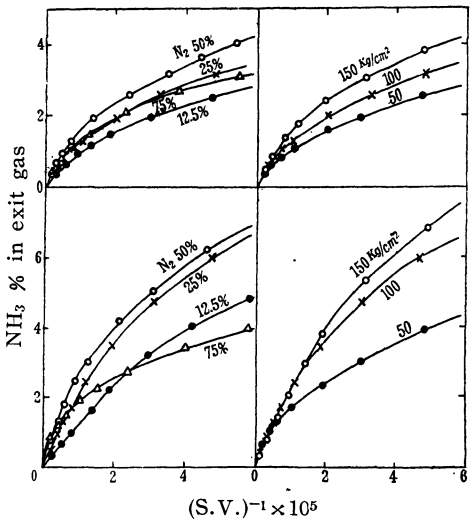



Fig. 9. Relation between ammonia % and reciprocal space velocity at earlier stage of the reaction.
above left, No. 1, 100 kg./cm², 400°C;
above right, No. 1, $N_2/H_2=1/3$, 400°C
below left, No. 2, 100 kg./cm² 350°C;
below right, No. 2, $N_2/H_2=1/3$, 350°C

Among them, the equations by P. H. Emmett,[3] H. de Bruijn,[11] and S. L. Kiperman[10] were in accordance with M. I. Temkin's[2] on the basic assumption that the adsorption rate of nitrogen determines the rate of the synthesis. Likewise H. Kobayashi's[4] agrees with M. Shindo's[7] on assuming the rate of formation of ammonia from NH or $NH_2$ on the catalyst surface as the rate determining step. The equations by M. I. Temkin and by M. Shindo are here taken as the representatives and their conformity with the experimental results will be checked.

For a flow reactor at a constant temperature and pressure, the reaction rate is in general given by Equation (1)

$$U=dN/A\cdot dl. \tag{1}$$

On rearranging

$$U=dz/273\cdot R\cdot c_m(1+z)^2d(1/S_0), \tag{2}$$

where $U$ is reaction rate, moles $NH_3$/hr. m³ catalyst, $N$ is flow rate of ammonia, moles $NH_3$/hr, $A$ is cross sectional area of catalyst bed, m², $l$ is bed length, m, $z$ is mole fraction of ammonia, $R$ is gas constant, $c_m$ is mean compressibility factor of gas mixture at N. T. P., and $S_0$ is space velocity based on influent gas, 1/hr.

According to M. I. Temkin and M. Shindo, the rate of the ammonia synthesis is given in terms of activity by Eqs. (3) and (4) respectively.

$$U=k_1\frac{a_{N_2}\cdot a_{H_2}^{3/2}}{a_{NH_3}}-k_2\frac{a_{NH_3}}{a_{H_2}^{3/2}}, \tag{3}$$

$$U=k_1\frac{a_{N_2}^{1/2}\cdot a_{H_2}^{3/2}}{a_{NH_3}}-k_2, \qquad (4)$$

where $k_1$ and $k_2$ are respective rate constants for a forward and a reverse reaction, and $a_i$, activity of the $i$ th component. Combining (2) with (3) or (4), rate constant $k_T$* from Eq. (3) and $k_S$ from Eq. (4) are expressed respectively by:

$$k_T=\left(\frac{\nu_{H_2}^{3/2}}{c_m\cdot\nu_{NH_3}}\right)\frac{P^{1/2}\cdot S_0}{2^{3/2}\cdot 273\cdot R}\int_0^z\frac{z[2-z-2\alpha(1+z)]^{3/2}\cdot dz}{(1+z)^2\left\{\left(\frac{K_P\cdot P}{4}\right)^2[2\alpha(1+z)-z][2-z-2\alpha(1+z)]^3-z^2\right\}}$$

$$k_S=\left(\frac{\nu_{NH_3}}{c_m\cdot\nu_{N_2}^{1/2}\cdot\nu_{H_2}^{3/2}}\right)\frac{S_0}{273\cdot R}\int_0^z\frac{K_P\cdot z\cdot dz}{(1+z)^2\left\{\left(\frac{K_P\cdot P}{4}\right)[2\alpha(1+z)-z]^{1/2}[2-z-2\alpha(1+z)]^{3/2}-z\right\}}$$

where $P$, total pressure in atm., $K_P$, equilibrium constant, $\nu_i$, fugacity coefficient of the $i$th component, $\alpha$, mole fraction of nitrogen in the initial gas. Using either of the equations, $k_T$ and $k_S$ are evaluated by means of numerical integration. The obtained values of $k_T$'s and $k_S$'s are not always equal over the measured range of space velocity. For the sake of convenient comparison of the calculated value with the experimental, one value of $k$ is chosen among many values so that $z$ evaluated in use of the $k$ may best approximate to the experimental data over the measured range of space velocity. The values of $z$ thus obtained from Temkin's are illustrated in Fig. 2 together with those from Shindo's, in a dotted and dashed, and a double dotted and dashed line respectively, at 100 kg./cm², 425°C. Temkin's equation gives a good approximation at low $z$ to the experimental data while Shindo's equation rather a better one at higher $z$.

The pressure being varied, the rate of the forward reaction is proportional to 1.5 power of the total pressure by Temkin's while it is proportional to one power by Shindo's. In this respect, the former equation agrees better with Cat. No. 2, while the latter agrees better with Cat. No. 1.

With respect to Temkin's equation, S. Kodama[12] has come to the conclusion that the nitrogen percentage at which a maximum ammonia concentration is obtained shifts towards the higher percentage with increasing space velocity; from the value of 25% (where S.V.=0) asymptotically to a critical value of 40%. Shindo's equation leads us, however, to the conclusion that the nitrogen percentage remains always at 25% independent of the value of space velocity. The experimental data are in agreement with what was expected from Temkin's equation, the percentage shifting towards the higher with increasing space velocity, but are not exactly so because of the further shifting through the critical value of 40%.

Taking into account the varying dependence of the conversion upon the pressure with respect to the kind of catalyst, the authors propose a modification on Temkin's equation as follows:

$$U=k\frac{1}{(1+k_{NH_3}\cdot a_{NH_3})^{1/2}}\left[\frac{a_{N_2}\cdot a_{H_2}^{3/2}}{a_{NH_3}}-\frac{a_{NH_3}}{K^2\cdot a_{H_2}^{3/2}}\right], \qquad (5)$$

where $k_{NH_3}$ is a constant characteristic of the catalyst in use.* The modification suggests different degrees of covering of ammonia, depending on the kind of catalyst. It is derived from M. Shindo's fundamental concept on resistivity caused by covering of ammonia on the catalyst surface as well as H. Kobayashi's by which a characteristic degree of the covering dependent on the kind of the catalysts is assumed. Shindo's equation has been improved by H. Kobayashi by means of the above concept and has attained to a better agreement with the latter's experiments with respect to change of pressure.

The values of $z$ or conversion efficiency calculated in the use of Equation (5) are shown in Figs. 2, 3, 5, and 6. being compared with the experimental as well as the calculated by Equations (3) and (4) respectively. In Fig. 2, the deviation from the experimental data (full line) becomes less on Equation (5) (dashed line) than in the case of both Equation (3) (dotted and dashed line) and Equation (4) (double dotted and dashed line), though it remains yet in the region of extremely low as well as extremely high space velocity. With respect to $z$ dependent upon the pressure, the values evaluated by Equation (5) agree well with the observed on both catalysts, except for those observed at higher space velocities

* M. I. Temkin (*Chem. Abstr.*, **45**, 3699 (1951)) improved recently his equation to make it more applicable on varying pressures by introducing another factor. The correction has a less important effect as compared with that due to fugacity.

12) S. Kodama and K. Fukui et al., *J. Chem. Soc., Japan (Ind. Sect.)* **54**, 157 (1951).

* The values of $k_{NH_3}$ were calculated by means of trial and error to agree most to the observed data at different temperatures and found to be 0.76 and 0.11 with Cat. No. 1 and No. 2 respectively.

and at the same time at lower temperatures, at which $z$ remains constant independent of the pressure. As for the representation of $z$ as a function of the hydrogen-nitrogen ratios of the gas mixtures, Equation (5) is no more satisfactory than Equation (3). It deviates somewhat from the experimental data with Cat. No. 2, though it approximates closer to those with Cat. No.1 (Figs. 5 and 6).

Temkin's equation together with Equation (5) is thus often in disagreement with the experimental results, pronouncedly at higher space velosities. From the basic concept of M. I. Temkin, S. L. Kiperman proposed the following equation:

$$U=k'\cdot a_{N_2}-k''\frac{a_{NH_3}^2}{a_{H_2}^3} \qquad (6)$$

and interpreted his experimental results at a normal pressure in an earlier stage of the reaction i.e. at low $z$ situated far from the equilibrium.

Combining Equations (2) and (6), it can be readily shown that $z$ should be nearly proportional to 1/S.V.,* and the proportionality factor between them should also be proportional to the nitrogen pressure. This prediction is confirmed as shown in Fig. 9 left (at a space velocity of $5\times10^5$) as well as Fig. 7 below (at space velocities higher than $1\times10^5$), in both of which the mixtures of varying hydrogen-nitrogen ratio are used at a constant pressure. However, the fact that the factor remains constant irrespective of the varying total pressures when a mixture of the constant ratio is used, seems unable to be interpreted in any way.

Equation (6) calls for the shift of the nitrogen percentage, at which the maximum $z$ is obtained, towards the higher percentages through the critical value of 40% nitrogen at extremely high space velocities, i.e. at low values of $z$.

## Summary

This series of experiments presents the well known fact about the different concentration increases as well as the different decreases of the conversion efficiency with the increasing pressure depending upon the kinds of catalysts in greater detail. At extremely high space velocities, the ammonia concentration remains constant independent of the change of the total pressure when the mixture of a constant gas ratio ($H_2$: $N_2$=3: 1) is used; however, it increases with increasing nitrogen pressure when the mixtures of different initial compositions are used at a constant pressure.

As predicted by Temkin's equation, the nitrogen percentage or hydrogen percentage, at which a maximum ammonia concentration or a minimum conversion efficiency is observed, shifts towards the higher percentage with the increasing space velocity; however, the nitrogen percentage corresponding to the maximum shifts further through the critical value predicted by Temkin. The shifting is more or less rapid depending on the kind of catalyst. To the extent that the space velocity is very high and the total pressure remains constant the equation by S. L. Kiperman can represent the shifting in a better agreement together with the observed proportionality between the ammonia concentration and the reciprocal space velocity.

The rate equations of M. I. Temkin and M. Shindo, which are based on different concepts, have been compared with the present results, and neither M. I. Temkin's nor M. Shindo's (unimproved) is in satisfactory agreement with the results. An equation based on the concept by M. I. Temkin and provided with another factor characteristic of the kind of catalyst has been proposed. The equation is in better agreement with the experimental results concerning the ammonia concentration expressed as functions of the space velocity and the pressure. The maximum of the ammonia concentration or the minimum of the conversion efficiency related to the ratio of hydrogen to nitrogen is represented in a somewhat better agreement with the singly promoted catalyst, while yet unsatisfactorily with the triply promoted.

*Government Chemical Industrial Research Institute, Tokyo*

* A. Nielsen has found that $z^2\times(S.V)$ approaches a limiting value when S.V. is increased higher than $1\times10^5$, as a consequence of Temkin's equation. According to our observations, $z\times(S.V.)$, instead of $z^2\times(S.V.)$, approaches that value.

# *Polarographic Studies on Heterocyclic Compounds. II. Saponification of Isonicotinic Acid Methyl Ester*

by Yoshinosuke NAGATA and Isamu TACHI

(Received June 30, 1954)

## Introduction

In the previous paper[1], polarographic investigations on isonicotinic acid have been carried out and it has been clarified that the limiting current has a character of the kinetic current which is due to the recombination of the dissociated anion of isonicotinic acid with proton. However, if behaviour similar to this acid should be observed also in isonicotinic acid methyl ester, the kinetic current might have to be attributed to some other cause. In this paper, the discussion in the previous paper was confirmed on the basis of the fact that the methyl ester shows behaviour different from the acid. On the other hand, the fact that the methyl ester is saponified in the alkaline medium was found. Since the limiting current of the methyl ester is controlled by diffusion process, the velocity constant of the saponification was determined polarographically from the decrease in the limiting current of the methyl ester. Further, the effects of the temperature and the neutral salt concentration on the velocity constant were estimated by means of the polarographic method.

## Experimental Part

Isonicotinic acid methyl ester is provided by Tanabe Pharmaceutical Co. Ltd. It is redistilled at 120°C under reduced pressure (in 25 mm Hg), since it is comparatively unstable in atmosphere and under light.

The buffer solutions used are as follows:

McIlvain's buffer solutions (0.1 M Citric acid—0.2 M Sodium phosphate), Kolthoff's buffer solutions (0.1 M Potassium biphosphate—0.05 M Sodium Borate) and Sörensen's buffer solutions (0.05 M Sodium borate—0.1 N Sodium hydroxide).

Capillary constants are $m=1.55$ mg/sec. and $t=3.24$ sec. ($m^{2/3}t^{1/6}=1.63$) in 0.2 N KCl solution at -1.8 v. *vs.* N.C.E., where $m$ and $t$ are the rate of flow of mercury and drop time, respectively. Electrode potentials are referred to the normal calomel electrode and the temperature of the electrolytic solution is maintained at 25±0.5°C.

## Experimental Results and Discussion

### (1) Effects of pH

A well-defined reduction wave is observed in the acidic and neutral pH range as shown in Fig. 1 (Curve 1). Table I indicates the relationship between pH of the electrolytic solution, the limiting current and the half-wave potential. The half-wave potential shifts to more negative potential with increasing pH value, and the limiting current has a nearly constant value in the acidic and neutral pH range, while in the alkaline side the current gradually decreases with increasing pH value and also with time, and a new second reduction wave appears at the more negative potential than the first one. The second wave is so drawn out (Fig. 1, Curve 2) that the half-wave potential is hardly determinable. At pH 13 (in 0.1 N NaOH), the first wave disappears completely and only the second wave is observed (Fig. 1 Curve 3). Therefore, it is seen that isonicotinic acid methyl ester is decomposed in the alkaline medium and the second wave corresponds to the reduction of decomposition product. Because the second wave is not well-defined, its qualitative estimation is difficult. However, it seems probable that isonicotinic acid methyl ester is hydrolysed by alkali hydroxide as well as general esters. After

TABLE I

RELATIONSHIP BETWEEN pH, THE HALF-WAVE POTENTIAL ($E^{1/2}$) AND THE LIMITING CURRENT ($i$). $1.06\times10^{-3}$ M ISONICOTINIC ACID METHYL ESTER IN 0.2 N KCl

| pH | $E^{1/2}$ (v. *vs.* N.C.E.) | $i$ ($\mu$A) |
|---|---|---|
| 1 (0.1 N HCl) | −0.840 | 8.77 |
| 2.6 | −0.885 | 8.17 |
| 3.4 | −0.957 | 8.17 |
| 4.4 | −0.995 | 8.10 |
| 5.4 | −1.055 | 8.17 |
| 6.4 | −1.110 | 8.17 |
| 7.5 | −1.185 | 7.97 |
| 8.2 | −1.230 | 7.57 |
| 9.0 | −1.275 | 7.27 |
| 10.1 | −1.290 | 6.60 |
| 10.7 | −1.290 | 5.85 |
| 13 (0.1 N NaOH) | −1.800* | 5.70* |

(*); The second wave

All values are measured standing for 30 minutes after prepareation of the electrolytic solutions.

1) Y. Nagata and I. Tachi, This Bulletin, 27, 290 (1954).

the hydrolysis of the ester by the action of sodium hydroxide and then neutralization with hydrochloric acid, pH of solution is adjusted to the appointed value. By comparing the half-wave potential of the hydrolysis product with that of isonicotinic acid, a good agreement between these two values is observed as shown in Table II. Therefore, the

TABLE II

THE HALF-WAVE POTENTIAL ($E_{1/2}$) OF THE HYDROLYSIS PRODUCT OF ISONICOTINIC ACID METHYL ESTER IS COMPARED WITH THAT OF THE ACID. (1) FIRST WAVE, (2) SECOND WAVE

| | Hydrolysis Product | | Acid | |
|---|---|---|---|---|
| pH | $E_{1/2}(1)$ | $E_{1/2}(2)$ | $E_{1/2}(1)$ | $E_{1/2}(2)$ |
| 9.0 | −1.38 | — | −1.38 | — |
| 10.1 | −1.47 | −1.80 | −1.47 | −1.80 |
| 10.7 | −1.48 | −1.81 | −1.47 | −1.80 |

second wave is due to the reduction of isonicotinic acid. In other words, methyl ester is saponified by alkali hydroxide. At pH 13, it corresponds to the reduction of the dissociated anion of the acid. Hence the second wave in the alkaline pH range is drawn out in consequence of the overlap of the wave of the acid molecule with that of the dissociated anion.

### (2) Dependence of the Limiting Current on the Height of Mercury Reservoir

When the limiting current in the acidic and neutral pH range increases linearly with the square root of $h$ ($h$ is the height of mercury reservoir), it is controlled by diffusion process (Table III)[2]. However, as in the case of the alkaline pH range the saponification reaction takes place at the same time, it is necessary to take the reaction into account. Now, if the approximate correction for the decrease in the limiting current of the first wave caused by the saponification is made, the limiting current has a linear realtionship with $\sqrt{h}$ and the slope (of the line that $i$ is) plotted *vs.* $\sqrt{h}$ agrees with that at pH44. Hence the limiting current of the first wave at pH 10.7 is also controlled by diffusion process as well as at pH 4.4. On the other hand, the second wave height, which can be calculated as the difference between the total wave height and the corrected first wave height, since during the measurements the total wave height, which corresponds to the sum of ester and acid, is hardly changed by saponification, changes linearly with $\sqrt{h}$, so that it has been concluded that the limiting current of second wave (the mixed wave of the acid molecule and dissociated anion of isonicotinic acid) is controlled by the diffusion process. However, in the polarogram after the saponification, the limiting current of the saponification product wave is nearly independent of the height of the mercury reservoir (Table IV), so that it has the

TABLE IV

INFLUENCE OF THE HEIGHT OF EHE MERCURY RESERVIOR ON THE FIRST WAVE HEIGHT OF THE SAPONIFICATION PRODUCT OF ISONICOTINIC ACID METHYL ESTER AT pH 10.1

| $h$ | $i$ |
|---|---|
| 60 | 0.570 |
| 55 | 0.555 |
| 50 | 0.570 |
| 45 | 0.555 |
| 40 | 0.540 |
| 35 | 0.555 |
| 30 | 0.540 |

TABLE III

DEPENDENCE OF THE LIMITING CURRENT INTENSITY ON THE HEIGHT OF THE MERCURY RESERVOIR. $1.06\times10^{-3}$ M ISONICOTINIC ACID METHYL ESTER IN 0.2 N KCl

| pH | | 4.4 | | 10.7 | | | |
|---|---|---|---|---|---|---|---|
| $h$ | $\sqrt{h}$ | $i$ | $i/\sqrt{h}$ | $i_1$ | $i_2$ | $i_1/\sqrt{h}$ | $i_2/\sqrt{h}$ |
| 60 | 7.74 | 9.30 | 1.20 | 4.86 | 1.44 | 0.628 | 0.186 |
| 55 | 7.42 | 8.70 | 1.17 | 4.65 | 1.38 | 0.626 | 0.186 |
| 50 | 7.07 | 8.40 | 1.19 | 4.53 | 1.14 | 0.645 | 0.161 |
| 45 | 6.71 | 7.95 | 1.17 | 4.21 | 1.29 | 0.627 | 0.192 |
| 40 | 6.32 | 7.42 | 1.16 | 3.99 | 1.17 | 0.631 | 0.185 |
| 35 | 5.91 | 6.97 | 1.18 | 3.84 | 1.11 | 0.649 | 0.187 |
| 30 | 5.48 | 6.45 | 1.18 | 3.54 | 1.08 | 0.646 | 0.197 |
| | | av. | 1.18 | | av. | 0.636 | 0.185 |
| | | $i/\sqrt{h}C$ | 1.11 | | $i/\sqrt{h}C$ | 1.15 | 1.13 |

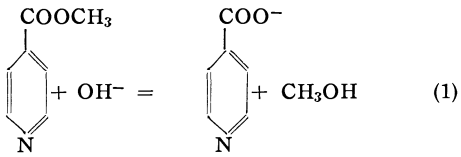
C denotes the concentration (millimol/litre) of the depolarizer.

2) D. Ilkovič, *Collection Czech. Chem. Communs.*, 6, 498 (1934). I. M. Kolthoff and J. J. Lingane, "Polarography", Interscience Publishers, Inc. New York, N. Y., 1952, p. 44, 85. I. Tachi, "Polarography", Iwanami Book Co. Ltd., Tokyo, 1954, p. 82.

character of the kinetic current[3]. Therefore, the idea that the kinetic current of isonicotinic acid is due to the recombination of the dissociated anion of acid with proton is supported.

**(3) Saponification of Isonicotinic Acid Methyl Ester**

**(a) Measurement of the velocity constant.**—Assuming that isonicotinic acid methyl ester is saponified by alkali hydroxide in the same way as in general saponification of ester, we may consider that



(1)

Since the saponification reaction takes place in the second order, the reaction velocity of saponification, $dx/dt$, and the velocity constant, $k$, are given by

$$\frac{dx}{dt}=k(a-x)(b-x) \tag{2}$$

and

$$k=\frac{2.303}{(b-a)t}\log\frac{a(b-x)}{b(a-x)} \tag{3}$$

respectively, where $a$ and $b$ denote the initial concentrations of isonicotinic acid methyl ester and sodium hydroxide, respectively, and $x$ represents the decrease of each component after time $t$.

In order to determine the velocity constant, the unreacted amount of each substance at time $t$, $(a-x)$ and $(b-x)$, must be measured. The concentration of methyl ester can be determined polarographically, while that of sodium hydroxide is impossible. However, since the reaction between ester and sodium hydroxide proceeds one to one, $(b-x)$ value can be calculated from $b$ and $(a-x)$ values. The concentration of the ester is determined by means of the calibration curve which is drawn beforehand in 0.2 N KCl solution. Futhermore, since the values of $(a-x)$ and $(b-x)$ are given as the molar concentration, it is unnecessary to take the kinetic current into account.

J. Heyrovský[4] and others[5,6,7], in the case of the determination of the hydrolysis velocity constant, have measured the wave height at a certain time interval, in order to follow the change in the concentration of the reactant with time. In our case, since the reaction velocity is considerably great, the method which has been examined by R. Pasternak[8] is adopted: i. e., the potentiometer drum is used as a timer, and the applied voltage is kept by the aid of another potentiometer at a constant value, where the limiting diffusion current of the ester is oberved.

The electrolytic solution ($1.09\times10^{-3}$ M ester in 0.2 N KCl and $2\times10^{-3}$ M NaOH) is prepared rapidly and after hydrogen gas is bubbled through the solution for one minute for the sake of removal of dissolved oxygen in the solution, it is then polarographed immediately. Fig. 2 shows the current-time diagram obtained in this way. The slit lamp line indicates the time interval (the potentiometer drum is rotated in the rate of 28±0.5 sec. per round), hence the wave height at an arbitrary time can be measured from the base line which is obtained in the current-voltage curve of the ester.

Table V gives the velocity constant calculated by inserting the experimental values, which are obtained from Fig. 2, into Eq. (3). In the same way, the velocity constants in the case of the various concentrations of sodium hydroxide are determined (Table VI). When the concentration of sodium

TABLE V

VELOCITY CONSTANT CALCULATED BY THE DATA OF FIG. 2

| $t$ (sec.) | $(a-x)\times10^4$ M | $(b-x)\times10^4$ M | $k$(M/L)$^{-1}$ sec$^{-1}$ |
|---|---|---|---|
| 0 | 6.77 | 15.87 | |
| 50 | 5.82 | 14.92 | 1.951 |
| 100 | 5.02 | 14.12 | 2.001 |
| 150 | 4.47 | 13.57 | 1.892 |
| 200 | 3.94 | 13.04 | 1.893 |
| 250 | 3.43 | 12.53 | 1.945 |
| 300 | 3.10 | 12.20 | 1.894 |
| 350 | 2.76 | 11.86 | 1.900 |
| 400 | 2.48 | 11.58 | 1.891 |
| 450 | 2.16 | 11.26 | 1.949 |
| | | av. | 1.924±0.037 |

TABLE VI

DEPENDENCE OF THE VELOCITY CONSTANT ON THE CONCENTRATION OF SODIUM HYDROXIDE

| Conc. of NaOH | $k$ (M/L)$^{-1}$sec.$^{-1}$ |
|---|---|
| $2\times10^{-3}$ M | 1.924±0.037 |
| 3 〃 | 2.023±0.066 |
| 4 〃 | 2.086±0.086 |
| 5 〃 | 2.013±0.060 |
| 7.5 〃 | 1.957±0.063 |

3) R. Brdička and K. Wiesner, *Collection Czech. Chem. Communs.*, **12**, 138 (1947). I. Tachi, "Polarography" Iwanami Book Co. Ltd., Tokyo, 1954, p. 107.
4) J. Heyrovsky and I. Smoler, *Collection Czech. Chem. Communs.*, **4**, 521 (1932).
5) R. Brdička, *J. Gen. Physiol.*, **19**, 899 (1936).
6) R. Pasternak and H. v Halban, *Helv. Chim. Acta*, **29**, 190 (1946).
7) H. H. G. Jellinek and A Gordon, *J. Phys. and Colloid Chem.*, **53**, 986 (1949).
8) R. Pasternak, *Helv. Chim. Acta*, **30**, 1984 (1947).

hydroxide is higher than $10^{-2}$ M, the reaction rate is so great that we can not follow the decrease of the ester polarographically. It is concluded from the data in Tables V and VI that the saponification of the ester proceeds in the second order, and the average velocity constant is equal to 1.924 $(M/L)^{-1}$ $sec^{-1}$.

**(b) Effect of the Concentration of the Neutral Salt on the Velocity Constant.**—In general, the reaction rate in the solution is influenced by the presence of neutral salt. The neutral salt effect is caused by the fact that, by addition of neutral salt, in the case of ionic reaction the ionic strength is varied (primary salt effect), or when one of reaction substances is a weak electrolyte the dissociation equilibrium is effected (secondary salt effect). As shown in Table VII, though the

TABLE VII

EFFECT OF THE NATURE AND CONCENTRATION OF THE NEUTRAL SALT ADDED $1.09\times10^{-3}$ M ESTER IN 0.002 M NaOH

| Conc. of salt | $k$ $(M/L)^{-1}$ $sec.^{-1}$ |
|---|---|
| 0.2 N KCl | 1.924±0.037 |
| 0.5 N 〃 | 1.987±0.096 |
| 1 N 〃 | 1.991±0.076 |
| 0.5 N NaCl | 2.027±0.054 |
| 〃 +0.5 N KCl | 1.819±0.070 |

velocity constant can not be determined polarographically under the condition without neutral salt, it seems probable that the velocity constant is not affected by the nature and concentration of neutral salt. It may be due to the fact that the saponification reaction takes place between molecule and ion.

**(c) Effect of the Temperature on the Velocity Constant.**—It is clear by the data in Table VIII that the velocity constant increases considerably with rising temperature. The influence of the temperature on the velocity constant is expressed by Arrhenius equation.

$$k = Ae^{-E/RT} \qquad (4)$$

where $E$, $R$, $T$ and $A$ are the energy of activation, gas constant, absolute temperature and frequency factor, respectively.

TABLE VIII

INFLUENCE OF THE TEMPERATURE ON THE VELOCITY CONSTANT $1.06\times10^{-3}$ M ESTER IN 0.2 N KCl AND $2\times10^{-3}$ M NaOH

| $t°$ C | $k$ $(M/L)^{-1}$ $shc^{-1}$. |
|---|---|
| 25 | 1.924±0.037 |
| 35 | 3.433±0.120 |
| 44 | 6.690±0.514 |
| 53 | 11.230±1.303 |

From Eq. (4), it follows that

$$\log k = -\frac{E}{2.303\,RT} + \text{const.} \qquad (5)$$

This indicates that the plot of $\log k$ against $1/T$ should be a straight line, whose tangent gives the energy of activation. From the tangent of the straight line in Fig. 3 which is plotted by means of the data in Table VIII, it is found that the energy of activation is equal to 12 kcal.

## Summary

(1) Isonicotinic acid methyl ester gives a single reduction wave and the half-wave potential shifts to more negative potential with increasing pH.

(2) Isonicotinic acid methyl ester is saponified in the alkaline medium and the velocity constant of saponification is determined polarographically on the basis of the second order reaction equation.

(3) The velocity constant is scarcely influenced by the addition of neutral salts, but increases with rising temperature. The activation energy of saponification is calculated according to the Arrhenius equation.

The authors wish to express their thanks to Tanabe Pharmaceutical Co. Ltd., which furnished the specimen, and also to the polarographic group, to which they belong, for their helpful discussion.

*Department of Agricultural Chemistry, Faculty of Agriculture, Kyoto University, Kyoto*

# *Irreversible Photobleaching of the Solution of Fluorescent Dyes. I. Kinetic Studies on the Primary Process*

By Masashi IMAMURA and Masao KOIZUMI

(Received July 19, 1954)

## Introduction

Although our information about the photochemical behaviour of excited dye molecules has been much increased through many investigations on the photosensitized reactions induced by fluorescent dyes, there are rather few cases in which the primary processes of the reactions are definitely established.

In addition, few investigations have been made for the settlement of the problem whether the excited state of dye participating in the reaction is singlet or triplet, though the problem has become quite important since the confirmation of the triplet state as phosphorescent state by Lewis *et al*[1].

Now, the following three types of primary process have been presented for the photosensitized oxidation in general[2]:

1) Energy transference from an excited dye molecule to the molecular oxygen.
2) Direct combination of oxygen with an excited dye molecule.
3) Univalent oxidation or reduction process.

The latter two seem at present to be most favorable for many cases.

For example, the second scheme has recently been applied by Schenck[3] to photosensitized oxidation of various organic substances, while the third scheme has long been claimed by Weiss, Franck, Livingston and others[4] for many reactions.

It seems to be quite essential to decide, on the one hand, whether the excited dye molecule (or ion) produced in the solution primarily interacts with the molecular oxygen or alternatively with solvent molecules, and, on the other hand, to make clear whether the excited state of dye in question is singlet or triplet. The objective of the present series of investigations is to elucidate these questions through kinetic studies on the irreversible photobleaching of dyes by oxygen.

Now, there exist rather few investigations published in this field, among which the work of Blum and Spealman[5] seems to be most prominent. They studied the photobleaching of the aqueous eosine solution under the atmospheric oxygen and proposed such a scheme as is abbreviated in the following way:

1) $D^* + O_2 \longrightarrow D + O_2^*$
2) $O_2^* + H_2O \longrightarrow HO + HO_2$
3) Oxidation reaction induced by $HO_2$, formation of $H_2O_2$, etc.

The experimental facts which led them to the above conclusion were mainly the recognition of the induction period and the detection of hydrogen peroxide.

It must, however, be noted that they used a relatively concentrated solution of dye in which the interaction of excited dye molecules and those of the ground state is so great[6] that it is liable to make the features of the reaction rather complicated. The employment of more dilute solutions seems to be demanded and from such a view point the present authors have investigated the photobleaching of eosine, erythrosine and uranine in the aqueous solutions or in the mixed solutions of water and ethyl alcohol, the concentration of dyes being chosen as $10^{-5}$ mol./l. in most cases.

Though the definite answers to the above questions have not yet been attained, some remarkable results have been obtained and from them certain deductions have been derived, which we believe to be valuable for the further attack of the problem. The present paper reports the essential points of the experimental results and some discussions about them; the details of the experimental procedure and full data obtained will be published in the *J. Inst. Polytech. Osaka City University*.

## Experimental

**A. Procedure.**—The following method was employed to measure the quantity of bleaching

1) G. N. Lewis and M. Kasha, *J. Am. Chem. Soc.*, 66, 2100 (1944), etc.
2) For example, see Th. Förster, *Z. Elektrochem.*, 56, 716 (1952).
3) G. O. Schenck, *Naturwiss.*, 40, 205, 229 (1953).
4) For example, J. Weiss, *J. Soc. Dyers and Colourists*, 65, 719 (1949).
5) H. F. Blum and C. R. Spealman, *J. Phys. Chem.*, 37, 1123 (1933).
6) N. Mataga and M. Koizumi, This Bulletin, 28, 51 (1955).

successively for one sample. The solution was put into A (diameter 25 mm., thickness 16 mm.) of the reaction cell, Fig. 1, and was irradiated in the thermostat for a certain time with the light of constant intensity. The cell was taken out of the bath occasionally, and after the sample was poured into part B (inner diameter 15 mm., length 25–30 mm.), the quantity of bleaching was measured colorimetrically by use of RCA 931A photomultiplier.

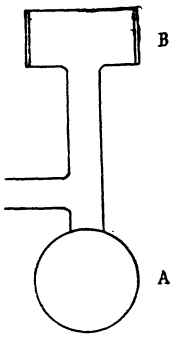


Fig. 1. Reaction cell

As a light source a tungsten projection lamp (100v.–500w.) was employed and the range of wave length was adequately chosen by means of Matsuda color filters. The intensity was controlled with blackened metallic nets.

**B. Results.**—*1. Features of the photobleaching under atmospheric pressure.*—The degrees of photobleaching in the aqueous solutions of eosine, erythrosine and uranine, the concentrations of which were all $10^{-5}$ mol./l., were measured at first under the atmospheric pressure. The concentration-time relations, Fig. 2, which show only the results for eosine, are all simple and monotonous without any slight indication of the induction phenomenon which was observed by Blum and Spealman. The percentage depicted along each line concerns the relative intensity of the light source. The results for erythrosine and uranine are similar to those of eosine.

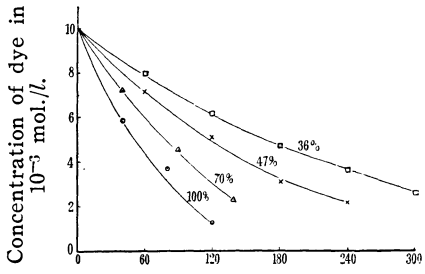


Fig. 2. Photobleaching of eosine in aqueous solution under various relative light intensities from 100 to 36% at 30°C.

As regards the formation of hydrogen peroxide reported by Blum and Spealman, it could not be detected by the iodometry in the nitrogen atmosphere, by $TiCl_3$-method and also by the polarographic method. The possibility of the intermediate formation of hydrogen peroxide in a very small quantity below the sensitivities of the above methods was scrutinized by the test of the addition of sodium pyruvate or sodium thiosulfate which ought to decrease the rate, if this be the case. The result was that the addition of the reagents each in several millimol./l. did not affect the rate at all. Thus one can deny even the slight formation of hydrogen peroxide in the present conditions.

The difference of the present result as compared with that of Blum and Spealman may plausibly be due to a different concentration of dye. In fact we could detect hydrogen peroxide by iodmetry when the concentration of $2\times10^{-4}$ mol./l. of dye was employed.

As for the reaction products, we have not yet undertaken the analysis, and only the absorption spectra after irradiation were examined. Similar changes were observed for erythrosine, eosine and uranine; thus the main adsorption in the visible region and the neighboring one declined monotonously with the irradiation while a slight increase of extinction was observed in the region of 360–440 m$\mu$.

*2. Rate formula.*—In view of the relatively simple form of the bleaching curves, the following simplest rate formula was tested at first.

If the rate of reaction only depends on and is proportional to the quantity of absorbed light, then

$$-\frac{dc}{dt}=kI_0(1-e^{-\alpha cd}). \qquad (1)$$

where $c$ is the concentration of dye, $\alpha$ the average molar absorption coefficient, $d$ the thickness of the solution, $I_0$ the intensity of light, and $k$ is the overall rate constant. Integrating eq. (1) one gets

$$\ln(1-e^{-\alpha c\ d})-\ln(1-e^{-\alpha cd})+\alpha d(c_0-c)=\alpha dkI_0t \qquad (2)$$

where $c_0$ is the initial concentration of dye. The intensity of light was measured by a thermopile previously calibrated with the standard lamp and was expressed as a number of photons per unit time. For example, $I_0$ was $10^{16}$ photons/sec. cm.$^2$ when 90 v. was applied on the lamp. $\alpha$ was also determined with the same thermopile. The values of $\alpha$ were $6.0\times10^4$, $5.6\times10^4$ and $4.2\times10^4$ for eosine, erythrosine and uranine, respectively. When the rate of bleaching is expressed as a number of dye molecules decomposed per sec., then the rate constant $k$ obtained from eq. (2) is nothing but a quantum yield of the reaction.

Now it was proved that the eq. (2) can express the experimental results quite well from the beginning up to 70–80% bleaching, when the dye concentration lies in the region from $5\times10^{-6}$ to $1\times10^{-4}$ mol./l. It must be noted, however that in the case of $1\times10^{-4}$ mol./l. the deviation is somewhat large, sug-

gesting the non-applicability of eq. (2) in more concentrated regions. The value of $k$ was not affected by the intensity of light, which was varied from 100% (full light) down to 25%. Some of the results are tabulated in Table I.

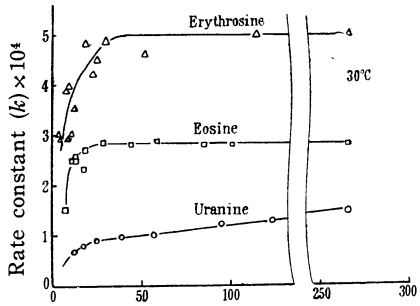
TABLE I
RATE CONSTANTS* (QUANTUM YIELDS) AT 30°C

| Relative intensity (%) | $k_1 \times 10^4$ | $k_2 \times 10^4$ | $k_3 \times 10^4$ | |
|---|---|---|---|---|
| | Eosine | | | |
| 100 | 3.1 | 2.9 | 3.3 | |
| | 2.9 | 2.9 | 3.2 | |
| 70 | 2.9 | 3.1 | 3.9 | |
| | 2.7 | 2.7 | 3.2 | |
| 47 | 2.4 | 2.6 | 3.0 | |
| | 2.8 | 2.8 | 2.9 | |
| 36 | 2.6 | 2.6 | 2.8 | |
| | 2.7 | 2.5 | — | ±0.2 |
| | Erythrosine | | | |
| 78 | 4.9 | 4.9 | 5.2 | |
| | 4.7 | 5.0 | 5.0 | |
| 54 | 5.1 | 5.3 | 5.6 | |
| | 5.1 | 5.1 | 5.3 | |
| 36 | 4.1 | 4.4 | 4.9 | |
| | 4.5 | 5.2 | 5.4 | |
| 28 | 4.7 | 5.2 | 5.7 | |
| | 4.4 | 4.8 | 5.2 | ±0.3 |
| | Uranine | | | |
| 100 | 1.4 | 1.3 | 1.2 | |
| | 1.4 | 1.4 | 1.5 | |
| 70 | 1.2 | 1.2 | 1.4 | |
| | 1.4 | 1.3 | 1.3 | |
| 47 | 1.1 | 1.2 | 1.3 | |
| | 1.2 | 1.2 | 1.2 | |
| 36 | 0.9 | 1.0 | 1.2 | |
| | 1.5 | 1.2 | 1.3 | ±0.2 |

*$k_1$, $k_2$ and $k_3$ are calculated from time required for 25, 50 and 75% bleaching, respectively

*3. The effect of the quantity of the dissolved oxygen.*—Eq. (2) can express the experimental results equally well, when the dye solution of $10^{-5}$ mol./1. is completely evacuated and a certain amount of oxygen is added to the sample. The values of $k$ are plotted against the concentrations of the dissolved oxygen in Fig. 3. Here the concentration of the dissolved oxygen was provisionally calculated from the quantity of added oxygen on the basis of the solubility data for pure water.

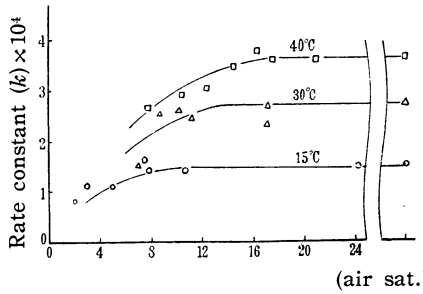
It is evident from this figure that in the cases of eosine and erythrosine, the rate rapidly declines when the concentration of dissolved oxygen is decreased below ca. $1 \sim 2 \times 10^{-5}$ mol./1., while above this critical




Concentration of dissolved oxigen in $10^{-6}$ mol./$l$.

Fig. 3. Influence of the concentration of oxygen on the rate constants.

concentration the rate remains constant and the $k$-value under atmospheric pressure coincides with it quite satisfactorily, showing no effect of the coexistent nitrogen on the rate. In the case of uranine, $k$ increases gradually with the increase of the oxygen concentration. For eosine, the effect of the concentration of dissolved oxygen was particularly examined at three different temperatures. As shown in Fig.4, the critical concentration of the dissolved oxygen at which $k$ reaches its maximum value, slightly increases when the temperature is raised.




Concentration of dissolved oxygen in $10^{-6}$mol./$l$.

Fig. 4. Influence of temperature on the oxygen effect.

*4. The effect of temperature on the rate.*—The rate of photobleaching of the aqueous solution of uranine, eosine and erythrosine under atmospheric pressure was measured at several temperatures between 13 and 40°C. The $k$-values obtained are tabulated in Table II.

TABLE II
AVERAGE RATE CONSTANTS AT VARIOUS TEMPERATURES $k \times 10^4$

| | 40 | 34 | 30 | 27 | 22 | 20 | 13°C. |
|---|---|---|---|---|---|---|---|
| Eosine | 3.6 | 2.9 | — | 2.5 | 2.0 | 1.8 | — |
| Erythrosine | 5.6 | — | 5.2 | — | — | 3.7 | 2.9 |
| Uranine | 1.8 | — | 1.3 | — | — | 1.1 | 1.0 |

These results can approximately be expressed by the following Arrhenius equations:

eosine: $k=5.3\ \exp(-6000/RT)$ (3)
erythrosine: $k=2\ \exp(-5000/RT)$ (4)
uranine: $k=0.3\ \exp(-4000/RT)$ (5)

It may be necessary to remember here that for eosine and erythrosine, the $k$-value under atmospheric pressure is constant, irrespctive of the quantity of dissolved oxygen, hence eqs. (3) and (4) express the direct influence of the temperature on the reaction rate itself, while for uranine, the $k$-value in the region of atmospheric oxygen is still affected by the quantity of oxygen and so the effect of temperature on the solubility of oxygen participates in eq. (5).

*5. The photobleaching of eosine in the water-ethyl alcohol mixtures.*—With the hope of seeing how the water molecule takes part in the reaction, the effect of addition of ethyl alcohol to the aqueous eosine solution was examined. At first, the pure alcoholic solution of eosine of $10^{-5}$ mol./1. was irradiated under atmospheric pressure and it was found that not even slight photobleaching occurred even after two or three hours of irradiation by the light of the strongest intensity employed. On the contrary, when the dissolved oxygen was eliminated, a quite rapid photobleaching did take place. As to this unexpected and astonishing result, investigation is now going on. When a small quantity of alcohol was added to the aqueous eosine solution dissolving atmospheric oxygen, the rate of photobleaching decreased quite remarkably. The rate formula (2) still holds in this case at least up to 30 vol. % alcohol at which the rate is quite small.

The values of $k$ are plotted against the concentration of alcohol in Fig. 5. The experiments were done at 20, 27, 34 and 40°C., but in this figure only two curves at 27 and 40°C. are given.

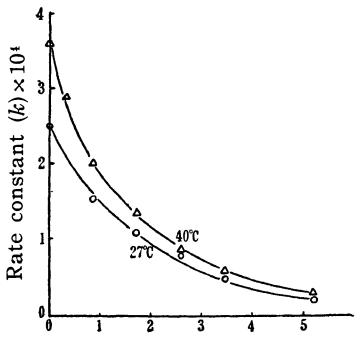



Fig. 5. Effect of EtOH concentration on the rate constant.

Now, it was found that the following formula can express the relation between $k$ and the composition of the solvent quite satisfactorily in the low concentration region of alcohol (see the section of discussion).

$$\frac{1}{k}=\frac{1}{k^\circ}+K\frac{[\mathrm{EtOH}]}{[\mathrm{H_2O}]}, \qquad (6)$$

were $k^\circ$ is the rate constant of the pure aqueous solution, $K$ a certain constant experimentally determined, and [EtOH] and $[H_2O]$ are the molar concentrations of alcohol and water, respectively.

As is evident from eq. (6), $1/k$ when plotted against $[EtOH]/[H_2O]$ ought to be linear. In fact, the relations between $1/k$ and $[EtOH]/[H_2O]$ at various temperatures are just as shown in Fig. 6. This figure shows that at least up to 15–20 vol. % the formula (6) holds, but near 20 vol. % of alcohol, marked breaks appear at all temperatures, which lie at the lower value of $[EtOH]/[H_2O]$, as the temperature is higher.

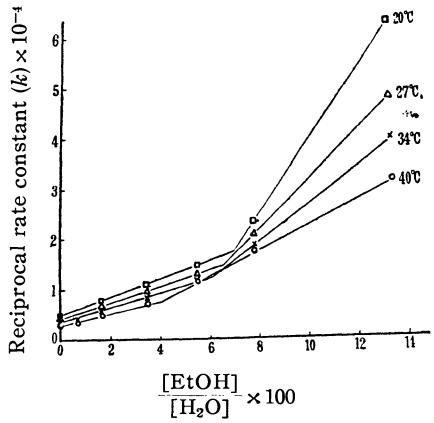



Fig. 6. Relation between $1/k$ and $[EtOH]/[H_2O]$ at several temperatures.

As to these discontinuous breaks, one may plausibly attribute them to the specific nature of the alcohol-water system. Because, it is well known that the partial molar volume of alcohol in this system, for example, begins to deviate from the linear relation at about the same composition[7].

Moreover, we measured the absorption spectra and the relative intensities of fluorescence of eosine in these solutions and found that both the displacements of the absorption maximum and the relative intensity as poltted against [EtOH] are almost linear up to this region, but from here upward the deviation comes to be notable.

In view of these results, it is quite natural that the applicability of the eq. (6) is limited up to 15–20 vol. %, and one may say

7) G. N. Lewis and M. Randall, "Thermodynamics", p. 40.

that the results shown in Fig. 6 confirm the relation (6) rather definitely.

The values of $k$ and $K$ at various concentrations of alcohol and at several temperatures are tabulated in Table III.

TABLE III

$k$- AND $K$-VALUES AT VARIOUS CONDITIONS

| [EtOH] vol. % | $k\times10^{t}$ 40°C. | 34°C. | 27°C. | 20°C. | [EtOH]/[$H_2O$] $\times100$ |
|---|---|---|---|---|---|
| 0 | 3.6 | 2.9 | 2.5 | 1.9 | 0 |
| 2 | 2.9 | 2.7 | — | — | 0.64 |
| 5 | 2.0 | 1.8 | 1.5 | 1.3 | 1.65 |
| 10 | 1.4 | 1.2 | 1.1 | $0.9_0$ | 3.47 |
| 15 | $0.9_5$ | $0.8_0$ | $0.7_7$ | $0.6_7$ | 5.52 |
| 20 | $0.5_7$ | $0.5_4$ | $0.4_3$ | $0.4_3$ | 7.82 |
| 30 | $0.3_2$ | $0.2_6$ | $0.2_1$ | $0.1_5$ | 13.4 |
| $K\times10^{-5}$··· | 1.33 | 1.45 | 1.62 | 1.73 | |

Applying the Arrhenius equation to $1/K$ one gets

$$1/K=41\times10^{-5}\cdot\exp(-2500/RT) \qquad (7)$$

Combining eqs. (3), (6) and (7), $1/k$ at various temperatures and at various concentrations of alcohol the result can be expressed as

$$\frac{1}{k}=\frac{1}{5.3\exp(-6000/RT)}+\frac{1}{41\times10^{-5}\cdot\exp(-2500/RT)}\frac{[\mathrm{EtOH}]}{[\mathrm{H_2O}]} \qquad (8)$$

The coincidence of the calculated values of $k$ with the observed ones is quite satisfactory at least up to 15 vol. % of alcohol.

## Discussion

From the fact that the stationary state is reached at once just with the commencement of irradiation and that the rate is proportional to the quantity of absorbed photons, it can safely be concluded that the reaction proceeds as it is of the first order in respect to the excited dye, so far as the rate determining processes are concerned. The mechanism presented by Blum and Spealman which consists of the attack of hydrogen peroxide upon excited dye, the former being produced by the interaction of water with excited dye, is definitely denied in the present case on the ground of the above kinetic results as well as from non-existence of hydrogen peroxide.

Now, since the presence of oxygen and water is indispensable for the occurrence of the reaction the first attack on the excited dye molecule must be made either by oxygen or water, and as to the excited state of dye which participates in the reaction, on the other hand, two alternatives are considered, singlet and triplet states. Hence the following four schemes are conceivable, if one assumes that the reaction proceeds successively and further if one neglects the possibility of direct transference of energy from excited dye to oxygen, which is improbable from the above results as well as from our knowledge of the photosensitized reactions in general.

I. First attack by $O_2$.

a) Singlet state:

$$D \xrightarrow{h\nu} D^* \xrightarrow{O_2} D^*\cdots O_2 \xrightarrow{H_2O} \cdots \mathrm{Prod.}$$

b) Triplet state:

$$D \xrightarrow{h\nu} D^* \rightarrow D^t \xrightarrow{O_2} D^t\cdots O_2 \rightarrow \cdots \mathrm{Prod.}$$

II. First attack by $H_2O$.

a) Singlet state:

$$D \xrightarrow{h\nu} D^* \xrightarrow{H_2O} D^*\cdots H\cdots OH \xrightarrow{O_2} \cdots \mathrm{Prod.}$$

b) Triplet state:

$$D \xrightarrow{h\nu} D^* \rightarrow D^t \xrightarrow{H_2O} D^t\cdots H\cdots OH \xrightarrow{O_2} \cdots \mathrm{Prod.}$$

It must be noted here, that all the formulas of the intermediates involved in the above schemes are only conventional without any specification of their real structures and, that $D^t$ is to be taken as a representative of any metastable states of dye taking part in the reaction which comes from singlet excited state $D^*$ directly produced by irradiation.

Let us consider in succession, which of the above four possible schenes conforms best with the experimental result, particularly on the basis of rate formula (section A) and the oxygen effect (section B).

(A)

### Ia) First Attack of Oxygen on Singlet State of Dye

The rate constant in water-alcohol mixture for the reaction scheme, Ia, can be expressed as follows:

$$k_{Ia}=\frac{k_{O_2}}{k_e+k_{qt}+h_1[\mathrm{H_2O}]+k_2[\mathrm{EtOH}]+k_{O_2}}\times\frac{k'_1[\mathrm{H_2O}]}{k'_{-1}+k'_1[\mathrm{H_2O}]+k'_2[\mathrm{EtOH}]} \qquad (9)$$

where

$k_e$: specific rate of fluorescence,

$k_{qt}$: specific rate of inner quenching of fluorescence,

$k_1$, $k_2$: rate constants of the dissipation of excitation energy by the interaction with water and alcohol,

$k_{O_2}$: rate of the reaction between oxygen and $D^*$ expressed as a constant, since it does not depend on oxygen pressure under ordinary condition.

* Deactivation of $D^*\cdots O_2$ by water is omitted for the sake of simplicity, since the ultimate result is not essentially affected.

* The ultimate formula is not essentially altered even if the deactivation of $D^*\cdots H_2O$ by oxygen is taken into account not only in this case but also in all other cases in II.

$k'_{-1}$: rate constant for the spontaneous deactivation of the intermediate $D^*\cdots O_2$,

$k'_1$: rate constant for the reaction between $D^*\cdots O_2$ and water,*

$k'_2$: rate constant for the deactivation of $D^*\cdots O_2$ by alcohol.

Since the intensity of fluorescence should decrease just to the same degree as that which is $D^*\cdots O_2$ produced, $k_{O2}$ ought to be equal to the rate of quenching of fluorescence due to oxygen. In fact, however, there is no quenching action of oxygen observed and so the magnitude of $k_{O2}$ must be 1/1000 or less of the denominator of the first factor if one provisionally assumes that the quantum yield of fluorescence is about 10% and that the sensitivity of the intensity measurement of fluorescence is about 1/100.

Thus the first factor of eq. (9) should be a very small value, which will plausibly be put approximately constant in the small concentration region of alcohol.

Putting the first factor as $\varphi_{O_2}$ and making the probable assumption that $k'_{-1}$ is much smaller than $k'_1[H_2O]$, one gets the following rate formula, which has just the same form as Eq. (6).

$$\frac{1}{k_{Ia}}=\frac{1}{\varphi_{O2}}\left\{\frac{k'_1[H_2O]+k'_{-1}}{k'_1[H_2O]}+\frac{k'_2[EtOH]}{k'_1[H_2O]}\right\}$$

$$\fallingdotseq\frac{1}{k^\circ_{Ia}}+\frac{1}{\varphi_{O2}}\frac{k'_2[EtOH]}{k'_1[H_2O]},$$

where $k^\circ_{Ia}$ is the overall rate constant in the pure aqueous solution. Then the constant $K$ in eq. (6) is given as follows:

$$K=\frac{1}{\varphi_{O2}}\frac{k'_2}{k'_1}$$

Using the $K$-values in Table III and assuming the upper limit of $\varphi_{O_2}$ as $10^{-3}$, one can estimate that $k'_2/k'_1$ must be about 100 or so. Thus when $D^*\cdots O_2$ is deactivated by alcohol about 100 times more frequently than it reacts with water, then this scheme conforms quite well with the experimental results. **(deduction a)**

**Ib) First Attack of Oxygen on Triplet State of Dye**

Introducing the transition probability $\varphi_{S\to T}$ for $D^*\to D^t$, one can write the overall rate constant $k_{Ib}$ as follows:

$$k_{Ib}=\varphi_{S\to T}\times\frac{k_{O2}}{k_{qt}+k_1[H_2O]+k_2[EtOH]+k_{O2}}$$

$$\times\frac{k'_1[H_2O]}{k'_{-1}+k'_1[H_2O]+k'_2[EtOH]}$$

where the constants in the second factor all refer to the triplet state.

If the product of the first and second factors is quite small and is approximately constant irrespective of alcohol concentration, that is, when $k_1\fallingdotseq k_2$ or when $k_{O2}\gg k_{qt}+k_1[H_2O]+k_2[EtOH]$, then this scheme can give the experimental rate formula just in the same way as in the case of Ia, and the *deduction* (*a*) can be applied for this case too.

At this point one must note that there is another scheme conceivable in which the first attack on dye is by oxygen; it is the one in which the overall rate is determined by the rate with which oxygen attacks the hydrated dye ion of excited state. This mechanism, however, can be rejected quite conclusively in the following way.

Using the similar notations as above, one gets

$$k_{Ia}=k^\circ_{Ia}\frac{[D^*\cdot H_2O]}{[D^*\cdot EtOH]+[D^*H_2O]}$$

where $[D^*\ H_2O]$ and $[D^*\ EtOH]$ are the concentrations of the excited dye ions associated with water and alcohol. They may be put, in the low concentration region of alcohol, as $k'_1[H_2O]$ and $k'_2[EtOH]$, hence the following formula corresponding to eq. (6) can be derived.

$$\frac{1}{k_{Ia}}=\frac{1}{k^\circ_{Ia}}+K\frac{[EtOH]}{[H_2O]}, \tag{11}$$

where

$$K=\frac{1}{k^\circ_{Ia}}\frac{k'_2}{k'_1}. \tag{12}$$

But the calculated values of $k'_2/k'_1$, which should be interpreted as the ratio of tendency of alcoholation to that of hydration, proved to be very unreasonable since they are too large and, moreover, increase with the rise of temperature (33 (20°C.), 40 (27°C.), 41(34°C.), 47 (40°C.)).

Thus it may be concluded that if the dye ion is first attacked by oxygen, then the reaction must be successive and the intermediate $D^*\cdots O_2$ or $D^t\cdots O_2$ must be deactivated by alcohol very much more frequently than it reacts with water, the ratio of the rate constants for both the reactions being about 100 or so (**deduction a**).

**IIa) First Attack of Water on Singlet State of Dye**

If all the colliding water molecules which quench the fluorescence produce the intermediates of the reaction, then the overall rate constant should be given as follows:

$$k_{IIa}=\frac{k_1[H_2O]}{k_e+k_{qt}+k_1[H_2O]+k_2[EtOH]}$$

$$\times\frac{k'_{O2}}{k'_{-2}+k'_1[H_2O]+k'_2[EtOH]+k'_{O_2}} \tag{13}$$

where all the rate constants involved are analogous to those in the case Ia. The magnitude of the first factor should be moderate since the quenching action of water is not expected to be so little. Hence the second factor must be very small in order to interpret the quantum yield experimentally obtained. Since the first factor can not be expected to be much affected by the composition of the solvent, the remarkable decrease of the rate caused by the added alcohol must be attributed mainly to the second factor and so the relation $k'_2[EtOH]>k_{-2}+k'_1[H_2O]$ must hold. If one takes these relations into account, the present scheme can never lead to the rate formula experimentally obtained.

But in the case when the process producing the intermediate of the reaction is only one of the various quenching processes caused by water molecule simultaneously occurring, there is a possibility, though quite improbable, that the present scheme conforms with the experiment. Thus if the following conditions are fulfilled,

1) the ratio of the intermediate-producing pro-

cess to the whole quenching processes due to water, is moderately small,

2) the denominator of the first factor can be considered approximately constant irrespective of the concentration of alcohol,

3) $k'_1[H_2O] \gg k'_{-2}+k'_{o2}$, and

4) $k'_2 \gg k'_1$,

then eq. (13) can be written approximately

$$k_{IIa}=\frac{k_1[H_2O]}{\text{const.}}\times\frac{k'_{o2}}{k'_1[H_2O]+k'_2[EtOH]}$$

which has the same form as eq. (6).

The scheme is quite improbable in view of the above conditions, but if it supposedly holds, then the most noteworthy condition to be fulfilled is that the intermediate produced from the excited dye and water, must be deactivated by alcohol at a much faster rate than those of the competing processes. (**deduction b**)

**IIb) First Attack of Water on Triplet State of Dye**

Formally it is only necessary to add a factor $\varphi_{S\to T}$ to the above case (IIa).

In case the triplet state loses its energy spontaneously or it interacts with water or alcohol, forming the intermediate of the bleaching reaction in the second case, while deprived of its energy in the last case, then the rate formula will be

$$k_{IIb}=\varphi_{S\to T}\times\frac{k_1[H_2O]}{k_{qi}+k_1[H_2O]+k_2[EtOH]}\times\frac{k'_{o2}}{k'_{-2}+k'_1[H_2O]+k'_2[EtOH]+k'_{o_2}} \quad (14)$$

Now, if the product of the first and second factors is moderately small and if in addition, conditions analogous to those related to *deduction b* hold, then the above rate formula is approximated by the experimental one (6) just as in the case of the above speciallized case of IIa.

There is another possibility, however, that the above eq. (14) may lead to eq. (6).

Thus if in eq. (14)

1) the product of the first and second factors is very small,

2) $k_{qi}$ is negligible compared with $k_1[H_2O]$ or $k_2[EtOH]$ in the second fator, and

3) $k'_1[H_2O]$ and $k'_2[EtOH]$ are far less than the other $k'$-terms in the denominator of the third factor,

then

$$k_{IIb}\fallingdotseq\varphi_{S\to T}\times\frac{k_1[H_2O]}{k_1[H_2O]+k_2[EtOH]}\times\frac{k'_{O_2}}{k_{-2}'+k'_{O_2}}.$$

Hence

$$\frac{1}{k_{IIb}}\fallingdotseq\frac{1}{\varphi_{S\to T}}\cdot\frac{k_{-2}'+k'_{o2}}{k'_{o2}}+\frac{1}{\varphi_{S\to T}}\cdot\frac{k_{-2}'+k'_{O_2}}{k'_{O_2}}\cdot\frac{k_2[EtOH]}{k_1[H_2O]}.*$$

Thus in this case the triplet state of dye must be deactivated by alcohol far more frequently than it interacts with water producing the reaction intermediate in order to interpret a large effect of the added alcohol. (**deduction c**)

In case the interaction of the triplet state and water only partially produces the intermediate for bleaching reaction, the discussion is essentially analogous to that above. Thus *deduction c* is applicable when most of the dye molecules in the triplet state attacked by water lose their energies in vain producing very little of the reaction-intermediate, while *deduction b* must hold in the opposite situation.

Among these three favorable cases mentioned above, the one corresponding to *deduction b* is quite improbable in view of many unreasonable conditions; for example the condition that the deactivation of water-dye intermediate by alcohol takes place more frequently than other competitive processes, seems quite improbable from the usual chemical reasoning. The case Ia or Ib corresponding to *deduction a* is most probable, but it is impossible to deny conclusively scheme IIb corresponding to *deduction c* on the basis of the above kinetic results. On the contrary there are some facts which seem to be favorable for the latter scheme. Thus in view of the fact that eosine in pure alcohol is photochemically bleached quite easily *in vacuo*, there is no doubt that the interaction of excited dye with alcohol can be of such a nature as to cause a genuine chemical reaction, and this fact appears to conform better to the scheme IIb.

(B)

As to the question whether oxygen attacks on singlet or triplet state of dye, one may judge the matter to some extent on the basis of the observed oxygen pressure effect on the rate. Thus the fact that the rate becomes independent of the oxygen pressure above a certain critical point requires that in this region the intermediate molecular species to be attacked by oxygen, in whatever scheme considered in section (A), must at least have enough chances of the attack during its life.

The number of collisions between oxygen and the intermediate in question during its life at the above critical pressure can easily be estimated if one assumes that the molecules of oxygen are distributed at random in the solution without any specific interaction with dye ion, and, that oxygen must reach the position of dye ion by diffusion.

Now in the case of eosine at 20°C., the rate becomes constant at ca. $10^{-5}$ mol./l. of the dissolved oxygen when calculated on the assumption that the solubility of oxygen in the dilute dye solution is the same as that in pure water. It follows that the mean distance of neighboring oxygen and dye ion is about $10^{-6}$ cm., and the time interval required for oxygen molecule to move this distance is roughly estimated to be about $10^{-7}$–$10^{-8}$ sec. on the basis of the usual formula for diffusion process and by use of the diffusion constant of oxygen in the aqueous solution, which is $2\times10^{-5}$ cm.$^2$/sec. at 20°C.[8] The time interval thus obtained is quite great compared with the lifetime of singlet state of eosine, which is about

8) "International Critical Table", Vol. V, p. 64.

$1.9\times10^{-3}$ sec.[9] or so. Of course the above estimation is approximate in nature but it will be correct at least in the order of magnitude, hence one can safely conclude that the state of dye attacked by oxygen is not the singlet excited state directly produced by light absorption, as long as the assumption of random distribution of oxygen in the solution is correct. In other words, the life of the intermediate to be attacked by oxygen must be at least $10^{-6}$ sec. or longer for the experimentally observed oxygen saturation effect to be interpreted. It must, however, be added that Evans[10] has recently reported that certain organic substances can form molecular complexes with oxygen, which produce new absorption spectra. In case of eosine we examined the effect of the coexistence of oxygen upon the absorption spectra but could not find such a phenomenon.

Therefore it seems permissible to deny scheme Ia in which singlet excited state is attacked by oxygen if the possibility is neglected that a molecular complex, which can not be detected spectroscopically, is formed between oxygen and dye. The decisive conclusion may perhaps be obtained from the effect of dye on the solubility of oxygen in water.

## Summary and General Conclusion

The irreversible photobleaching of eosine in the aqueous solution and in alcohol-water mixtures was studied and it was found that the rate of photobleaching depends only on and is proportional to the quantity of absorbed light when the dye concentration is $10^{-5}$ mol./l.

The overall unimolecular rate constant $k$ or the quantum yield, when the quantity of dissolved oxygen is varied, does not change over a wide region but begins to decrease below a certain critical point.

The values of $k$ in water-alcohol mixtures were found to be expressed by the following equation in the low concentration region of alcohol.

$$\frac{1}{k}=\frac{1}{k^{\circ}}+K\frac{[\mathrm{EtOH}]}{[\mathrm{H_2O}]}, \qquad (6)$$

where $k^{\circ}$ is the rate constant of the pure aqueous solution and $K$ is a certain constant.

The possible schemes were given particularly on the bases of the rate formula (6) and of the effect of the quantity of dissolved oxygen.

It is most probable that the irreversible photobleaching of eosine by oxygen is a successive reaction as represented by the following scheme

$$\text{Ib)}\quad D \xrightarrow{h\nu} D^{*} \rightarrow D^{t} \xrightarrow{O_2} D^{t}\cdots O_2 \xrightarrow{H_2O} \cdots \text{Product.}$$

In this case, the probability with which $D^{t}\cdots O_2$ is deactivated by alcohol is about 100 times greater than that of $D^{t}\cdots O_2$ being attacked by water.

There is some possibility that the reaction may proceed in the following way.

$$\text{IIb)}\quad D \xrightarrow{h\nu} D^{*} \rightarrow D^{t} \xrightarrow{H_2O} D^{t}\cdots H_2O \xrightarrow{O_2} \cdots \text{Product}$$

Two cases corresponding to this scheme are possible. When a moderate fraction of $D^{t}$ contributes to the reaction, the intermediate $D^{t}\cdots H_2O$ must be deactivated by alcohol far more frequently than it reacts with oxygen, while when a very small fraction of $D^{t}$ participates in the reaction, the probability with which $D^{t}$ is deactivated by alcohol is much larger than that of the reaction with water. The former case is rather improbable, while, the latter one seems to conform to a newly discovered fact that eosine in alcoholic solution is photobleached quite easily under evacuated conditions.

The kinetic studies of the vacuum-state-photobleaching of eosine in alcohol, the comparison of the effects of various alcohols upon the rate of oxygen-water-bleaching and the measurement of the rate of the possible vacuum-bleaching in various alcohols, all these investigations now in progress will give a more definite conclusion.

The cost of the present research has been partly defrayed from the Scientific Research Grant from the Ministry of Education.

*Institute of Polytechnics, Osaka City University, Osaka*

9) E. Gaviola, *Z. Physik*, **42**, 853 (1927).
10) D. F. Evans, *J. Chem. Soc.*, **1953**, 345.

# *Spectroscopic Investigations of the Interaction Between Simple Salt Anions and Transition Metal Cations. Part I. The Absorption Spectra of Hexammine Cobalt (III) and Chromium (III) Complexes in Aqueous Solutions of Salts of Weak Acid*

By Hayami YONEDA

(Received July 28, 1954)

The solubility of the luteo complex in various concentrated aqueous salt solutions varies to a large extent with the kinds of salt. The present author assumed that this fact has a close relation to the formation of "zweischalige" complexes resulting from the association of anions around complex cations. On the association between complex cations and halogen ions, Linhard[1] reported the spectroscopic investigations and, especially in the case of the iodide, he succeeded in obtaining the equilibrium constants from his analysis of the absorption band appearing newly in association. The present author expected that such "association bands" would appear not only in the iodide solution, but also in other salt solutions. He confirmed this expectation by measuring absorption spectra and also obtained some knowledge on the association by analysing the results.

## Experimental

The complexes used were $[Co(NH_3)_6]Cl_3$, $[Co\ en_3]Cl_3$, $[Cr(NH_3)_5]Cl_3$ and $[Cr\ en_3]Cl_3$, and the salts used were KNCS, $Na_2SO_3$, $Na_2S_2O_3$ and $Na_2CO_3$. Each salt was dissolved to make solutions of 1, 0.1, 0.01 mol./l. concentrations. In each solution, the complex was dissolved to 0.005 mol./l. concentration. This solution of the complex was used in the absorption measurement. In order to cancel the absorption due to the unassociated free anions, the corresponding salt solution was used as a standard for the measurement. The measurement of absorption was made using a quartz spectrograph by the rotating sector method. As internal change of the complex may be possible during measurement, the whole procedure was completed in 20 minutes after the preparation of the complex solution. The measurement was done at room temperature between 18–20°C.

## Results

The experimental results are shown in Fig. 1–10. In these figures full lines 1, 2, 3 correspond to the absorption curves for 1, 0.1, 0.01 mol./l. salt solutions respectively, one broken line 4 to that of the complex itself, and the other broken line 5 to that of the corresponding monoacidopentammine complex having the same anion as the salt solution in its complex radical.

In the Cr complex, the end absorption lies in the far ultraviolet region. Consequently, if the absorption band due to association should appear at the same position as in the Co complex, we could easily find its maximum exactly, and from such values we could calculate an exact value of the degree of association. But the experimental result did not fulfil this expectation. The association band

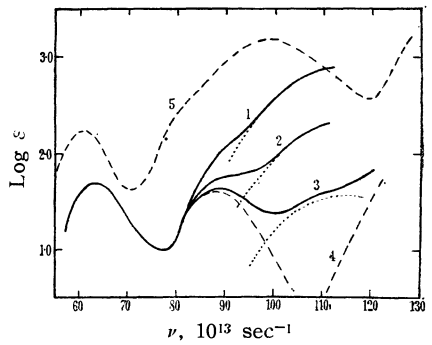



Fig. 1. $[Co(NH_3)_5]\ Cl_3$ in KNCS solutions.

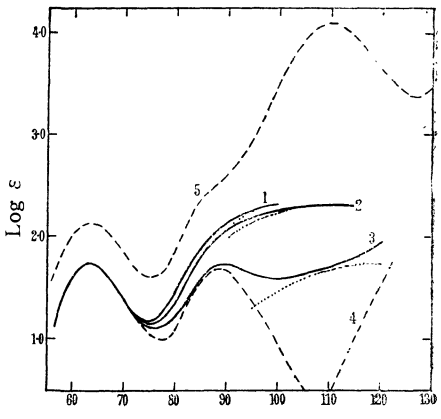



Fig. 2. $[Co(NH_3)_5]\ Cl_3$ in $Na_2SO_3$ solutions.

1) M. Linhard, *Z. Elektrochem.*, **50**, 224 (1944), M. Linhard and M. Weigel, *Z. anorg. u. allgen. Chem.*, 266, 49 (1951).

appeared farther in the ultraviolet than in the Co complex and its maximum position could not be ascertained. However, in this case the similar characteristics of the association were also recognized.

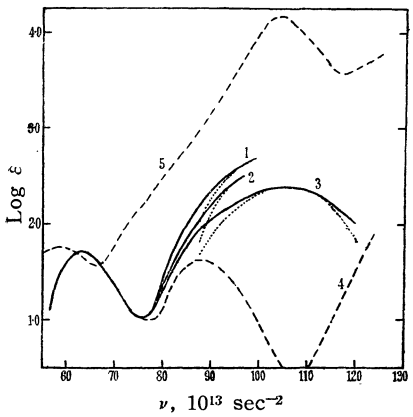



Fig. 3. $[Co(NH_3)_6]Cl_3$ in $Na_2S_2O_3$ solutions.

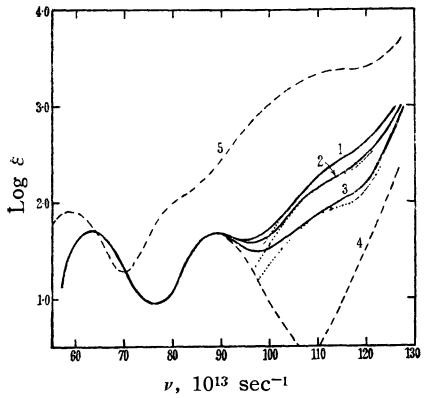



Fig. 4. $[Co(NH_3)_6]Cl_3$ in $Na_2CO_3$ solutions.

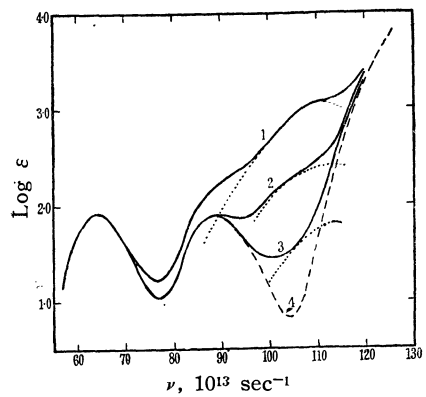



Fig. 5. $[Co\ en_3]Cl_3$ in KNCS solutions.

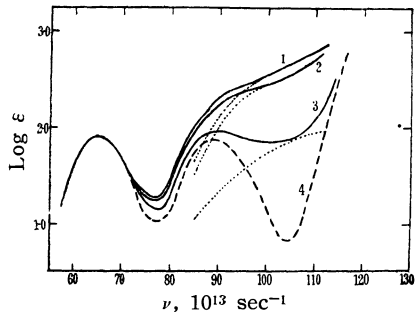



Fig. 6. $[Co\ en_3]Cl_3$ in $Na_2SO_3$ solutions.

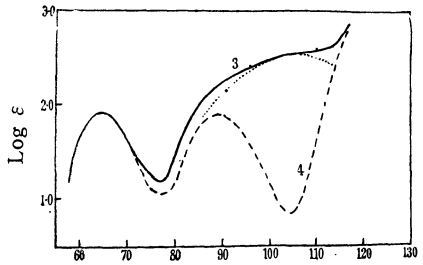



Fig. 7. $[Co\ en_3]Cl_3$ in a $Na_2S_2O_3$ solution.

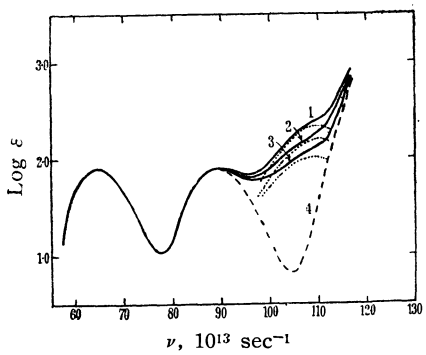



Fig. 8. $[Co\ en_3]Cl_3$ in $Na_2CO_3$ solutions.

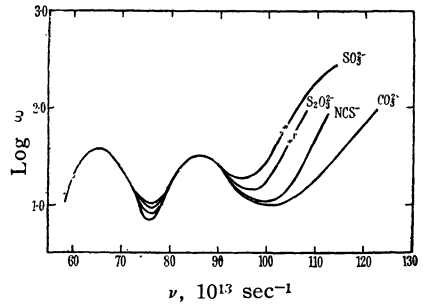



Fig. 9. $[Cr(NH_3)_6]Cl_3$ in 1 mol./l. salt solutions.

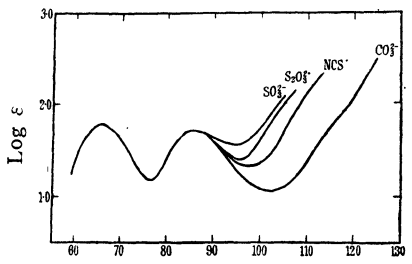



Fig. 10. [Cr en$_3$] Cl$_3$ in 1 mol./l. salt solutions.

The inspection of these figures shows the following facts.

(1) As expected, in every case there exists in the ultraviolet a new broad band probably due to the association between anions and complex cations.

(2) The first band proper to the complex always has a constant maximum, irrespective of kind and concentration of the salt solution, that is, it coincides with that of the complex itself in its position and height. The second band also has a constant maximum, coinciding with that of the complex itself in its position and height within the experimental errors. In some cases, however, where a new broad band covers them more or less completely, their maximum positions cannot be recognized.

TABLE I

THE MAXIMA OF THE FIRST AND SECOND BANDS

| | First Bands | | Second Bands | |
|---|---|---|---|---|
| | $\nu \cdot 10^{13}$sec.$^{-1}$ | log $\varepsilon$ | $\nu \cdot 10^{13}$sec.$^{-1}$ | log $\varepsilon$ |
| [Co(NH$_3$)$_5$]Cl$_3$ | 63.5 | 1.70 | 88.5 | 1.63 |
| [Co en$_3$]Cl$_3$ | 65.5 | 1.92 | 89.5 | 1.89 |
| [Cr(NH$_3$)$_5$]Cl$_3$ | 65.0 | 1.60 | 86.0 | 1.52 |
| [Cr en$_3$]Cl$_3$ | 66.0 | 1.78 | 86.0 | 1.75 |

## Discussion

**Separation of "Association Bands".**—As the association band appears in every case as a very broad band spreading between the second and the end absorption, the recognition of its maximum position and height is very difficult. But as mentioned above, the first and second bands of the complex in salt solutions are the same as those of the complex itself, so it may be justified as an approximation to assume that absorption due to the association, remains when the absorption of the complex itself is subtracted from the whole absorption of the complex in the salt solution. On this assumption, the absorption curves were calculated, and were drawn in the figures with the dotted lines affixed to the corresponding full lines. By these calculations the association band is separated from the second band distinctly and, at the same time, from the end absorption.

TABLE II

THE PROBABLE MAXIMUM POSITIONS OF THE ASSOCIATION BANDS IN THE Co COMPLEXES

(Faequency $10^{13}$sec$^{-1}$. units)

NCS$^-$: 115, $SO_3^{2-}$: 110, $S_2O_3^{2-}$: 105, $CO_3^{2-}$: ca.115

But as the end absorption is affected easily by the experimental conditions, there is almost no meaning in discussing the difference of such calculated maximum positions. Thus except in the case of $S_2O_3^{2-}$, where the maximum lies far from the end absorption, we can derive no more than a generalisation that there exist maxima at about $115 \sim 110 \times 10^{13}$sec$^{-1}$. In each figure the absorption curve of the corresponding monoacidopentammine complex is drawn by the broken line 5 for comparison. Comparing this with it, we can easily find that the maximum position of the association band, in the cases of $SO_3^{2-}$, $S_2O_3^{2-}$ and $CO_3^{2-}$, is almost identical with the special band of the corresponding monoacido complex. In contrast to this, in the case of NCS$^-$, the two maxima do not coincide in their position, and the maximum of the association band lies much farther in the shorter wave-lengths compared with the special band of the corresponding monoacido complex. Here it should be noted that the maximum positions of the association bands are almost identical in the cases both of the ammonia complexes and the ethylenediamine complexes.

**Equilibrium of Association.**—In order to treat the equilibrium of association from the value of the optical density, it is assumed that though there exist several kinds of association products i.e. those having 1, 2, 3, etc. anions per one complex cation, their absorptions appear as that of the same deformed anions. Accordingly, their optical densities are determined only by the number of the anions associating around the complex cations. Linhard assumed that in the association between complex cations and halogen ions, the association products in a concentrated KI solution exist in electrically neutral ion-pairs. Under this assumption he succeeded in the calculation of the equilibrium constants. In his case the association bands were so sharply separated that the use of the optical densities at their maximum position was possible. In the present case, the association bands are so broad and, in addition, no maximum positions are available in most cases, that the calculation of the equilibrium constants after Lihard's method will produce greater errors. Besides, the solubility of the

complex in the salt solutions is very large in the present case. This fact makes a marked contrast to the case of the alkali iodide solution in which the solubility of the complex is exceedingly small. Thus the author considered that it was not proper to assume the association product as an electrically neutral ion-pair, and that it should be regarded as a "zweischalige" complex containing excessive anions, e.g. $[Co(NH_3)_6](NCS)_{4-6}$, $[Co\ en_3](SO_3)_{2-3}$ etc.

On the basis of the above consideration, the author must be content with the rough estimation of the degree of association. Here the degree of association is defined as follows: The "zweischalige" complex in a 1 mol./l. salt solution is regarded as saturated with anions and taken as a standard. (This assumption does not hold in the association of $NCS^-$. From the inspection of the curves of the association bands in the 1, 0.1 and 0.01 mol./l. $NCS^-$ solutions, we can presume that the complex is not yet saturated even in the 1 mol./l. solution. (See Fig. 1 and Fig. 5.) The degree of association in a 0.1 or 0.01 mol./l. salt solution is obtained as the ratio of the optical densities of the association band of the solution to that of the corresponding 1 mol./l. solution. As the optical densities the author used those at frequencies as near as possible to the maximum position. The calculated results are shown in Table III.

The results of calculation are rather satisfactory, considering the accuracy of the experiment and the roughness of the calculation procedure. It is very suggestive to find that a more voluminous trisethylenediamine complex shows almost the same degree of association as that of a less voluminous hexa-ammonia complex. As already noted, the maximum positions of the association bands in the two complexes are almost identical to each other. These facts suggest that the main origin of the association lies not in the mere electrostatic attraction but in some localized force acting between the anion and the complex radical. As one of the probable origins of such localized force we may consider the hydrogen bridge between the $NH_2$ radical and the anion. But as the appearence of the marked association band cannot be explained merely by the hydrogen bridge, the main origin of the association should be searched for in the special interaction between the anion and the central metal ion of the complex radical.

**Origin of the Association Band.**—According to the present author's opinion, the appearence of the association band may be considered as occurring in the following way.

An anion in an aqueous solution forms with water molecules the hydrogen bridge. In this state it has an absorption maximum at about 2000Å, corresponding to the energy difference of the ground and excited states of the anion concerned. But when the complex is dissolved, the anion enters into the special field of the complex and associates with it. In this case it is quite natural for the anion to alter its electronic states and

TABLE III
DEGREES OF ASSOCIATION

| $\nu \cdot 10^{13}sec^{-1}$. | 1 mol./l soln. Opt. | Dens. | 0.1 mol./l soln. Opt. | Dens. | Degr. As. (%) | 0.01 mol./soln. Opt. | Dens. | Degr. As. (%) |
|---|---|---|---|---|---|---|---|---|
| $[Co(NH_3)_6]Cl_3$ | | | | | | | | |
| $SO_3^{2-}$: 100 | 211 | | 174 | | 82.5 | 29 | | 11.3 |
| 95 | 178 | | 141 | | 79.2 | 20 | | 11.2 |
| | | | | mean | 81 | | mean | 11 |
| $S_2O_3^{2-}$: 95 | 327 | | 282 | | 75.8 | 145 | | 38.9 |
| 90 | 190 | | 133 | | 70.0 | 75 | | 39.5 |
| | | | | mean | 73 | | mean | 39 |
| $CO_3^{2-}$: 115 | 282 | | 200 | | 71.0 | 89 | | 31.2 |
| 110 | 182 | | 139 | | 76.5 | 72 | | 39.6 |
| | | | | mean | 74 | | mean | 35 |
| $[Co\ en_3]Cl_3$ | | | | | | | | |
| $SO_3^{2-}$: 105 | 473 | | 376 | | 79.5 | 71 | | 15 |
| 100 | 355 | | 282 | | 79.5 | 56 | | 15.8 |
| | | | | mean | 80 | | mean | 15 |
| $CO_3^{2-}$: 110 | 214 | | 160 | | 74.8 | 99 | | 46.3 |
| 107.5 | 207 | | 143 | | 69.1 | 100 | | 48.3 |
| | | | | mean | 72 | | mean | 47 |

In the case of $[Co\ en_3]Cl_3$, the thiosulphate solutions of 0.1 and 1 mol./l. concentrations cannot dissolve the complex to make a 0.005 mol./l. complex solution.

as a result the energy difference between the ground and excited states is diminished. This diminishing effect appears as the bathochromic shift of the absorption band. When an anion enters into the complex radical, that is, it contacts with the central metal ion to form an acidopentammine complex, this tendency is strengthened and in general induces a more bathochromic special band. This interpretation is exceedingly probable, when the absorption curves of $NCS^-$, $[Co(NH_3)_6](NCS)_n$ and $[Co(NH_3)_5NCS]^{2+}$ are compared with each other. In the Cr complex the same tendency is observed. But in the Co complex and the bivalent anions $SO_3^{2-}$, $S_2O_3^{2-}$ and $CO_3^{2-}$, the association bands and the special bands of the corresponding monoacido complexes have almost the same maximum positions. In these cases the anions are greatly affected in their electronic states and are considered to have almost the same state with as of the anions of the monoacido complex. This interpretation suggests that even in the association product, the anion comes very near to the central metal ion owing to the strong attraction, and forms a structure like that of the hepta-coordinated complex. However, it is not yet decided from the present data, whether such strong interaction is originated merely from the strong electrostatic attraction between the bivalent anions and the trivalent cations. In connection with this, it is interesting to notice the fact that the cation of a typical element can produce neither association nor special band with anions. For example, an aluminum cation forms the rhodanato complex in a concentrated rhodanate solution, but even in a very concentrated rhodanate solution, we can find no special band in the ordinary measurable regions. From this fact we may conclude that the deforming power of the transition metal ion is not merely due to its strong positive field, but chiefly originated in its special electronic state, namely in its *d*-electron configuration. The great difference of the maximum positions of the association bands between Co and Cr complexes is explained by the difference of their electronic configurations.

## Conclusion

The association of anions $NCS^-$, $SO_3^{2-}$, $S_2O_3^{2-}$ and $CO_3^{2-}$ around hexa-ammonia and trisethylenediamine Co and Cr complexes was studied by the spectroscopic method. As the results, the following facts were revealed:

1) The association bands of the ammonia complex have almost the same maximum positions as those of the ethylenediamine complex.

2) The degrees of association in the ammonia complex are almost identical with those in the ethylenediamine complex.

From these facts the main origin of the association was discussed.

The author wishes to express his heartfelt thanks to Prof. R. Tsuchida and Prof. M. Kobayashi, Osaka University, for their kind advice and encouragement.

*Chemistry Department, Wakayama University, Wakayama*

# *Studies on the Oxy-acid Phosphors. III. Aluminate Phosphors (Part I)**

By Yoshihide KOTERA and Tadao SEKINE

(Received August 19, 1954)

## Introduction

The aluminate phosphors were investigated for the first time by Lecoq de Boisbaudran who reported the emission of magnesium aluminate activated by manganese or chromium[1], and several other researchers[2-7] studied also about aluminate phosphors, but the full details of their preparations, charac-

* Read before the Fourth Annual Meeting of the Chemical Society of Japan, 1951. Report II was published in this Bulletin, **27**, 13 (1954).

1) Lecoq de Boisbaudran, *Compt. rend.* **105** 261 1887).

2) D. T. Wilber, *Phys. Rev.*, **20**, 101 (1922).

3) O. Deutchbein, *Ann. Physik*, **14**, 712, 729 (1932): *Z. Physik*, **77**, 489 (1938): *Physik. Z.*, **33**, 874 (1932).

4) E. Iwase, *Sci. Papers Inst. Phys. Chem. Research* (Tokyo), **34**, 487 (1938).

5) H. W. Leverenz, *Proc. I. R. E.*, **32**, 256 (1944).

6) J. W. Strange and S. T. Henderson, *Proc. Phys. Soc.*, **58**, 369 (1946).

7) R. H. Clapp and R. J. Ginther, *J. Optical Soc. Am.*, **37**, 355 (1947).

teristics etc. are yet unknown. H. C. Froelich reported recently on the strontium aluminate which emits red light when excited by 3650 Å or cathode rays[8]. We have prepared various aluminate phosphors and found some remarkable results.

## Experimental and its Results

**(1) Purification of Sodium Aluminate and Metallic Salts.**—In the preparation of aluminate phosphors, aluminum metal was used as one of the starting materials.

Aluminum metal, which is prepared by electrolysis and contains 99.81% Al, 0.10% Si, 0.07% Fe, 0.01% Ti and 0.01% Cu was dissolved in caustic soda solution and, after filtration, the filtrate was decomposed by pure carbon dioxide. Thus, the crystalline aluminum hydroxide was obtained, and its purity was established spectroscopically.

As for the other starting materials, respective metallic salts were used, which were purified by the process described in a previous paper[9].

**(2) Mixing and Firing.**—The purified aluminum hydroxide was mixed with the purified metallic salts, flux and activators.

When sodium fluoride was used for flux, its solution was purified by the addition of ammonium sulfide and, after filtration, the filtrate was added to the batch. After being mixed in the wet state, the product was dried and fired. Aluminum fluoride, which was used more frequently than sodium fluoride solution, was prepared from purified fluoride solution and aluminum salt solution, both being purified by the processes analogous to those described in a previous paper. It was precipitated by mixing the fluoride and aluminum salt solutions, washed, dried, and then mixed in the dry state in an agate mortar with the body materials and activators.

As for activators, commercial "chemical pure" grade of manganese sulfate, cerric oxide or lead oxide was used. When the activator was added in a considerably large amount, for example, in a case when lead was used as an activator, it was purified by processes similar to those described in a previous paper.

The batch was fired by the electric furnace. When the atmosphere had to be controlled, the tube furnace was employed, through the tube of which the gas purified by the method of Smith[10] was streamed.

TABLE II

THE OPTIMUM MIXING RATIO OF ALUMINATE PHOSPHORS

| | $Al_2O_3 \cdot 3H_2O$ : (MO or $MC_2O_4$ or $M(NO_3)_2$) | Flux($AlF_3$'s case) (mol.) |
|---|---|---|
| Mg aluminate | 1 : 2 mol(MgO was used) | 0.2 |
| Ca aluminate | 1 : 0.95 mol($CaC_2O_4$) | 0.3 |
| Sr aluminate | 1 : 0.9 mol($SrC_2O_4$) | 0.24 |
| Ba aluminate | 1 : 1.5 mol($Ba(NO_3)_2$) | 0.048 |
| Zn aluminate | 1 : 2 mol(ZnO) | 0.27 |
| Cd aluminate | Wet process | 0.27 |
| Pb aluminate | 1 : 1.2–1.3 mol($PbCO_3$) | 0.25 |

**(3) Properties.**—The properties of some aluminate phosphors and their optimum mixing ratio were shown in Tables I and II respectively. The spectral curves measured by means of a quartz spectrograph, are shown in Fig. 1, no corrections

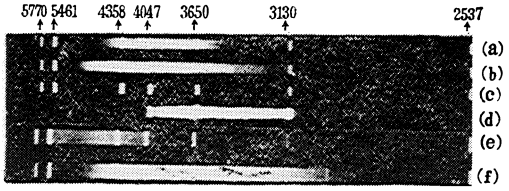
8) H. C. Froelich, *U. S. Pat.* Spec., 2392814.
9) Y. Kotera and T. Sekine, This Bulletin, 27, 13 (1954).
10) A. L. Smith, *Trans. Electrochem. Soc.*, 93, 324 (1948).

TABLE I

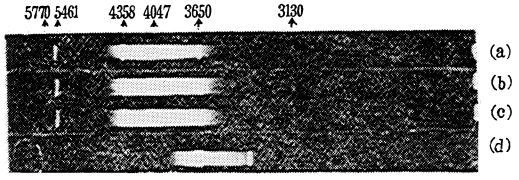
THE COLORS OF EMISSIONS OF ALUMINATE PHOSPHORS

| Host lattice | Activators | 3650 Å | 2537 Å | X-rays | Cathode rays |
|---|---|---|---|---|---|
| Mg aluminate | none | orange f | none | none | none |
| ,, | Mn (0.002) | orange m | orange f | green f | orange |
| ,, | Pb (0.001) | yellowish green f | blue m | none | none |
| Ca aluminate | none | violet f | none | none | none |
| ,, | Mn (0.0002) | orange m | orange f | yellow f | orange |
| ,, | Pb (0.105) | none | blue m | none | none |
| ,, | Ce (0.0008) | violet m | violet f | none | none |
| Sr aluminate | none | orange f | none | none | none |
| ,, | Mn (0.002) | orange m | red f | green f | green |
| ,, | Pb (0.1) | blue f | blue m | none | none |
| ,, | Mn (0.001) Pb (0.02) | orange m | pink m | none | green |
| Ba aluminate | Pb (0.066) | none | blue | violet | violet |
| Zn aluminate | Mn (0.0015) | green f | green f | green m | green |
| Cd aluminate | Mn (0.0015) | orange f | orange f | orange f | orange |
| Pb aluminate | none | none | white | white | white |
| | | | blue m | blue | blue |

The concentration of activator was expressed by mol ratio to the host lattice.
f=faint, m=medium.




(a) Ba aluminate Pb (2537Å)
(b) Ca aluminate Pb (2537Å)
(c) Mg aluminate Pb (2537Å)
(d) Sr aluminate Mn (3650Å)
(e) Pb aluminate (2537Å)
(f) Ca aluminate Pb (2537Å)




(a) Activated by Mn and Pb (Pb in large amount, 2537Å)
(b) Activated by Pb (2537Å)
(c) Activated by Mn and Pb (Pb in small amount, 2537Å)
(d) Activated by Mn and Pb (Pb in small amount, 3650Å)

Fig. 1.

being made on the spectral sensitivity of the photographic plate. The ranges of emission for aluminate phosphors activated by lead and lead aluminate were shown in Table III.

Table III

The ranges of the emission for aluminate phosphors activated by lead and lead aluminate (2537 Å excitation)

| | |
|---|---|
| Mg aluminate Pb | 3700–4200 Å |
| Ca aluminate Pb | 2900–4700 Å |
| Sr aluminate Pb | 3200–4900 Å |
| Ba aluminate Pb | 3300–4600 Å |
| Pb aluminate | 4000–4700 Å |

We have taken an interest in the preparation of doubly activated phosphors and continued the studies on the preparation of strontium aluminate phosphors.

**(4) The preparation of Strontium Aluminate Phosphors.**—According to Froelich strontium aluminate activated by manganese shows red luminescence when excited by long wavelength ultraviolet light, or cathode rays. We prepared it after his description and obtained a product which emits red light under the ultraviolet excitation, but all the products, emit green light when excited by cathode rays, although the conditions of preparation were varied as shown in Table IV.

We tried to decide whether this phosphor emits light even by the excitation of short wavelength ultraviolet light or not. We thought that the sensitization of this phosphor by secondary activator—or "sensitizer"—makes it possible, and added lead salt to the batch before firing. In this way we got strontium aluminate phosphor, which is activated by manganese and lead, and emits luminescence shown in Fig. 2, when excited by

Table IV

The conditions of prerearation of strontium aluminate phosphors

| | |
|---|---|
| Molar ratio($Al_2O_3$ : SrO) | 1 : 0.8–2.0 |
| Flux($AlF_3$) | 0–0.5 mol/1mol. $SrAl_2O_4$ |
| Center(Mn) | 0–6 mol.%/1mol. $SrAl_2O_4$ |
| ,, (Pb) | 0–20 mol.%/1mol. $SrAl_2O_4$ |
| Firing temperature | 1100–1200°C |
| Firing time | 2–6 hours |
| Atmosphere | $H_2$, $N_2$, $O_2$, Air and Steam |

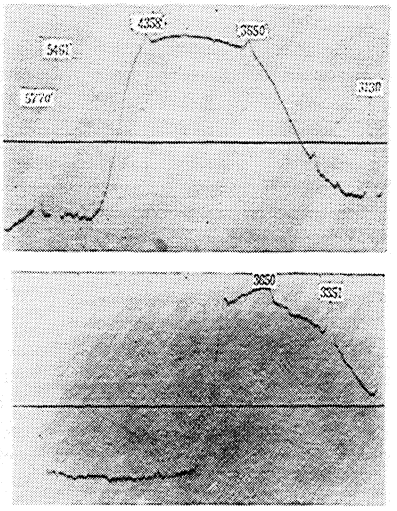



Fig. 2.

ultraviolet light. Its preparation was done under the conditions described in Table V. Though the

Table V

The conditions of preparation of strontium aluminate phosphor activated by manganese and lead

| | |
|---|---|
| Molar ratio($Al_2O_3$ : SrO) | 1 : 0.9 |
| Flux($AlF_3$) | 0.24 mol./1 mol. $SrAl_2O_4$ |
| Center(Mn) | 0.1 mol.%/1 mol. $SrAl_2O_4$ |
| ,, (Pb) | 2.0 mol.%/1 mol. $SrAl_2O_4$ |
| Firing conditions | 1200°C, 4 hours, in air |

emission curve did not show the red band, owing possibly to the poor spectral sensitivity of the photographic plate in this region, this phosphor emits weak red light also by short wavelength ultraviolet light. It emits red light by long ultraviolet, but green light by cathode rays. The observations of its properties will be made later.

## Discussion

Many reports were published on the aluminate phosphors, but all of these reports treated them as singly-activated ones. We tried to prepare the "doubly-activated" alu-

minate phosphors, and chose manganese as an emitting activator, because its emission is rather independent of the host crystal. At first, we prepared some aluminate phosphors, which were activated by manganese, lead and cerium, and confirmed that the manganese-activated phosphors show almost the same characteristics as those reported previously, except that strontium aluminate activated by manganese emits green light under cathode rays, although the conditions for its preparation were varied as shown in Table IV. As for the phosphors, which were activated by lead or cerium, we found that they have their characteristic emissions, which was not yet reported. Tables I and III show their characteristics. In Table II, it is interesting to note that the optimum mixing ratio is comparatively great in magnesium and zinc aluminates, the cause of which might be attributed to their spinel structure[1-3].

In the aluminate phosphors, which were prepared by us, strontium aluminate activated by both manganese and lead is the only one which might be considered as activated by double activators. It might be necessary to measure the absorption and excitation spectra in order to determine whether the red emission by 2537 Å is due to sensitization or not, and the facts that the lead-activated strontium aluminate emits blue light under shorter wavelength ultraviolet light and the manganese-activated one has no emission when excited by 2537 Å, but shows strong emission under 3650 Å, may be considered as a rather firm basis for the double activation. Calcium aluminate activated by manganese and lead or cerium was prepared by us, but in this case we could not obtain any doubly-activated phosphor.

## Summary

Various aluminate phosphors were prepared and some of their emissions were measured. When activated by manganese, aluminate phosphors emit green, orange, or red light, while those activated by lead show blue or violet emission. Cerium acts as an activator only for calcium aluminate and emits violet light under ultraviolet excitation Strontium aluminate activated by manganese and lead shows a weak emission under short wavelength ultraviolet excitation. This may be caused by the double activation due to manganese and lead.

The authors wish to thank Mr. Shigeo Shionoya for the measurements of spectral distribution of emission, and Dr. Hiromi Nishida and Dr. Shoji Makishima for the general discussion on the subject and the experimental work they have done.

*Government Chemical Industrial Research Institute, Tokyo*
*Hatagaya, Tokyo*

# *Studies on the Oxy-acid Phosphors. IV. Application of Polarography to the Analysis of Activators, Especially, in Calcium Silicate Phosphors**)

By Yoshihide KOTERA, Michiko YONEMURA and Tadao SEKINE

(Received August 19, 1954)

## Introduction

In the preparation of the phosphors, the amount of activators is one of the most important factors for determining their characteristics, and it is usually calculated by the mixing ratio for the batch before firing. As certain activators may be dissipated during the firing, it is necessary to determine the residual amount for discussing properties of resulting phosphors in connection with the amount of activators. We have determined this amount for several phosphors by means of polarography.

Especially, for calcium silicate phosphors activated by manganese and lead, whose characteristics depend upon the atmosphere during the firing, it is proved that the atmosphere during firing gives remarkable changes in the residual amount of activators and that the brightness of phosphors is affected by this amount.

## Experimental and its Results

**(1) Analysis of Activators in Phosphors by Polarography.**—We tried to analyse activators in various phosphors by means of polarography.

*) Read before the Fifth Annual Meeting of the Chemical Society of Japan, 1952. Report III will be published in this Bulletin.

The procedures are described as follows.

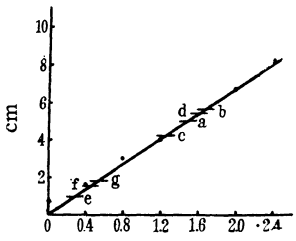
(*a*) *Manganese in $Zn_2SiO_4$: Mn and $(Zn, Be)_2SiO_4$: Mn.*—Manganese was analysed by the procedure which was reported by Spalenka[1].

1.5–2.0 g. of the unfired and fired sample were dissolved in conc. HCl. This solution was evaporated up to dryness, to which warm distilled water was added. After silica was removed by filtration, 20–40 ml. of 6N HCl were added to the filtrate. 1 ml. of this solution was taken as a sample for polarography, and, after addition of one to two drops of $H_2O_2$, 2.5 ml. of the mixed solution of saturated sodium sulfite solution (solution No. 3 in the Spalenka's receipt) and methol solution (solution No. 4), 5 ml. of ammonia solution (solution No. 5), and 10 ml. of the mixed solution of cyanide solution (solution No. 6) and caustic soda solution (solution No. 7), it was analysed by polarography. The solutions used in this procedure were prepared by the method of Spalenka's.

In order to detect manganese in the silica obtained by filtration, it was fused with $Na_2CO_3$ and NaOH in a platinum crucible, but manganese was not found in its polarogramm.

$Zn_2SiO_4$: Mn was prepared by firing the batch for 3 hours at 1150°C, the batch containing 1 g. ZnO, 0.4 g. $SiO_2$, 0.003 g. NaF and 0.01 g. Mn. As for $(Zn, Be)_2SiO_4$: Mn, the batch used contained 1 g. ZnO, 0.5 g. $SiO_2$, 0.03 g. BeO, 0.05 g. Mn and 0.03 g. $(NH_4)_2S_2O_8$.

The results are shown in Table I and Fig. 1.




mgMn in 20 ml

Fig. 1. Determination of Mn in $Zn_2SiO_4$: Mn, $(Zn, Be)_2SiO_4$: Mn and the mixed white phosphors.
a: $Zn_2SiO_4$: Mn (unfired)
b: $Zn_2SiO_4$: Mn (fired)
(a, b: 0.2 g. sample in 20 ml)
c: $(Zn, Be)_2SiO_4$: Mn (unfired)
d: $(Zn, Be)_2SiO_4$: Mn (fired)
(c, d: 0.05 g. sample in 20 ml)
e: 3500°K white f: 4500°K white
g: warm white
(e, f, g: 0.05 g. sample in 45 ml)

TABLE I

CONTENT OF MANGANESE IN $Zn_2SiO_4$: Mn and $(Zn, Be)_2SiO_4$: Mn

| | unfired | fired |
|---|---|---|
| $Zn_2SiO_4$: Mn | 0.0075 g. Mn/g. | 0.0084 g. Mn/g. |
| $(Zn, Be)_2SiO_4$: Mn | 0.025 g. Mn/g. | 0.033 g. Mn/g. |

(*b*) *Manganese and antimony in the mixed white phosphors.*—"3500°K white", "4500°K white" and "warm white", which were prepared in U.S.A. and expected to be the mixture of calcium halophosphate phosphor activated by manganes and antimony and other phosphors, were used as samples. 0.2 g. of sample were fused with 1.6 g. of $Na_2CO_3$, the fused mass was dissolved in HCl, and the volume of solution thus obtained was adjusted to 40 ml., the acidity of which was found to be that of 3N HCl.

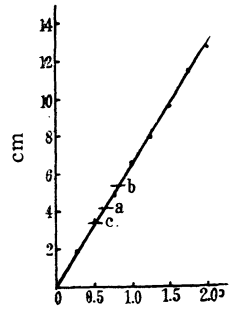
The antimony in this solution was analysed directly by the method of Page and Robinson[2], while manganese was analysed by the procedure described above. The standard solution of antimony was prepared by dissolving $Sb_2O_3$ in $CaCl_2$ solution, which was previously made acidic by the addition of HCl.

The results obtained are shown in Table II and Fig. 2.

TABLE II

CONTENT OF MANGANESE AND ANTIMONY IN THE MIXED WHITE PHOSPHORS

| | manganese | antimony |
|---|---|---|
| 3500°K white | 0.015 g./g. | 0.0065 g./g. |
| 4500°K white | 0.021 | 0.0085 |
| warm white | 0.024 | 0.0053 |




mg. Sb in 20 ml.

Fig. 2. Determination of Sb in the mixed white phosphors
a: 3500°K white
b: 4500°K white
c: warm white
(a, b, c: 0.1 g. sample in 20 ml.)

(*c*) *Copper in ZnS: Cu.*—Being dissolved in HCl, ZnS: Cu was analysed by the usual polarographic procedure, and it is confirmed that the copper content remained unchanged during the usual firing.

**(2) Analysis of Activators in Calcium Silicate Phosphors and the Measurement of Their Brightness.**

(*a*) *Preparation of calcium silicate phosphors.*—The batch containing 1.0 g. $SiO_2$, 2.0 g. $CaCO_3$, 0.08 g. $MnSO_4$, 0.02 g. $PbF_2$ and 0.8 g. $(NH_4)_2S_2O_8$, was fired at 1120°C for 2 to 6 hours in various atmospheres. Two kinds of silica were used for the batch, one being prepared from ethyl silicate, the other from sodium silicate. The atmosphere during firing was controlled by the precedure described in a previous paper[3].

(*b*) *Analysis of activators in the phosphors and the measurements of their brightness.*—The fired products were dissolved in HCl and

1) M. Spalenka, *Z. anal. Chem.*, **128**, 42 (1948).

2) J. E. Page and F. A. Robinson, *J. Soc. Chem. Ind.* (London), **61**, 93 (1942).

3) Y. Kotera and T. Sekine, This Bulletin, **28**, 129(1955),

the solution evaporated up to dryness repeatedly, and then, after filtration, it was adjusted to 30 ml., which had acidity of 3 N HCl. The lead in this solution was analysed directly according to Terui[4]. Manganese was analysed according to Hohn[5], after the solution of 50 g. of $NH_4Cl$ and 50 ml. of conc. $NH_3$ in 500 ml. of water was added to the solution of the sample and the total volume was expected to be 20 ml. The standard solution of lead was prepared by dissolving $PbCl_2$ in HCl.

The measurement of brightness under the excitation by 2537 Å was carried out by the procedure described in a previous paper[6].

(*c*) *The effects of atmosphere and firing time on the residual amount of activators and the brightness.*—The results obtained are shown in Table III and Fig. 3. These results were analysed by the completely randomized block designs for the residual amount of lead and manganese and the brightness, the atmosphere and the firing time which the divided portions were taken and fired in the same furnace. The effects of the atmosphere and the time are significant at the 1% and 5% levels respectively. As the brightness would be changed with the residual amount of lead or manganese, the correlation coefficients between one of these residual amounts and the brightness were calculated. Multiple correlation coefficient was 0.926 (significant at the 1% level), and partial correlation coefficient was 0.850 (signif. at the 1% level) in the case of lead, while it was −0.408 (not signif.) in the case of manganese. From these values, it is concluded that

(i) The amount of lead has a more important effect upon the brightness than manganese.

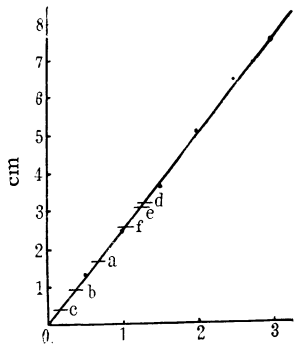
(ii) These effects go by contrary, viz., the brightness is increased either with the increase being taken as factorial effects. Care concerning randomization was taken, for example, a large quantity of the batch was prepared by mixing, of of the amount of lead, or with the decrease of that of manganese.

In order to verify these results, the analysis of covariance was carried out and the effects of atmosphere and firing time on the brightness were investigated, the amount of manganese or lead being taken as additional factorial effects. These results are listed in Table IV, from which it is concluded that

TABLE III

THE RESIDUAL AMOUNTS OF ACTIVATORS AND THE BRIGHTNESS OF CALCIUM SILICATE PHOSPHORS

| | Firing time (hr.) | Atmosphere | | | | |
|---|---|---|---|---|---|---|
| | | air | $H_2O$ | $O_2$ | $H_2$ | $N_2$ |
| Lead content | 2 | 0.0021 | 0.0013 | 0.0014 | 0.0007 | 0.0013 |
| | 4 | 0.0019 | 0.0015 | 0.0011 | 0.0004 | 0.0013 |
| | 6 | 0.0017 | 0.0013 | 0.0011 | 0.0002 | 0.0011 |
| Manganese content | 2 | 0.0039 | 0.0039 | 0.0036 | 0.0057 | 0.0056 |
| | 4 | 0.0040 | 0.0043 | 000037 | 0.0057 | 0.0057 |
| | 6 | 0.0040 | 0.0043 | 0.0039 | 0.0057 | 0.0057 |
| Brightness | 2 | 9.5 | 7.0 | 8.2 | 1.6 | 6.9 |
| | 4 | 9.1 | 6.5 | 7.4 | 1.6 | 7.2 |
| | 6 | 9.0 | 5.1 | 7.5 | 1.4 | 5.9 |




mg. Pb in 20 ml.

Fig. 3 Determination of Pb in calcium silicate phosphors. a, b, c: fired in $H_2$ d, e, f: fired in $N_2$ (1 gr sample in 20 ml.)

In order to verify these results, the analysis of covariance was carried out and the effects of atmosphere and firing time on the brightness were investigated, the amount of manganese or lead being taken as additional factorial effects. These results are listed in Table IV, from which it is concluded that

TABLE IV

TABLE OF THE ANALYSIS OF COVARIANCE

(a) When the amount of lead is taken as addditional effects

| Source of variation | Degree of freedom | Sum of squares | Mean squares | F |
|---|---|---|---|---|
| firing time | 2 | 119.58 | 59.79 | 2.98 |
| atmosphere | 4 | 1601.79 | 400.45 | 19.95## |
| average·linear response | 1 | 8447.76 | 8447.76 | 420.91## |
| error | 7 | 140.47 | 20.07 | |

4) Y. Terui, *Bull. Inst. Phys. Chem. Research* (Tokyo), **17**, 644 (1938).
5) N. Hohn, *Z. Electrochem.*, **43**, 127 (1939).
6) Y. Kotera and T. Sekine, This Bulletin, **27**, 13 (1954).

(b) When the amount of manganese is taken as additional effects

| Source of variation | Degree of freedom | Sum of squares | Mean squares | F |
|---|---|---|---|---|
| firing time | 2 | 76.90 | 38.45 | 1.72 |
| atmosphere | 4 | 4946.15 | 1236.53 | 63.80## |
| average linear response | 1 | 5150.88 | 5150.88 | 265.78## |
| error | 7 | 135.67 | 19.38 | |

## significant at the 1% level, #, signif. at the 5%.

(i) The F-ratio for the atmosphere variation is significant at the 1% level while that for the firing time variation is not significant.

(ii) As the linear response is separated, the analysis of covariance gives clarified results, and as for the selection of additional factorial effects, the amount of lead is preferable to that of manganese, which would be expected from the values of the correlation coefficients and from Table IV.

From the results of the randomized block design, the effect of firing time on the brightness is significant at the 5% level, but, this effect on the residual amounts of both lead and manganese is also significant at the 5% level, and it is verified from the analysis of covariance, that the changes of brightness are almost always caused by the changes of residual amounts of activators.

The significance of the effects difiers between five kinds of atmosphere, as is listed in Table V. It is to be noted that better results were not obtained for hydrogen, which has hitherto been considered to be an adequate atmosphere for the preparation of this phosphor[7].

TABLE V

THE SIGNIFICANCE OF EFFECTS OF THE ATMOSPHERES

| | |
|---|---|
| amount of lead | $air > H_2O,\ N_2,\ O_2 > H_2$ (## ##) |
| amount of manganese | $H_2,\ N_2 > H_2O > air > O_2$ (## # #) |
| brightness | $air > O_2 > N_2,\ H_2O > H_2$ (## # ##) |

(d) *Effect of the source of silica on the residual amounts of manganese and lead.*—The results described above were obtained for the silica, which was prepared from ethyl silicate, and they were compared with those for the silica prepared from sodium silicate. These results are shown in Table VI, in which the values are expressed by percentage of the residual amounts of activators remaining after firing to those present before firing. The values above 100 may be caused by the fact that, although activators were not dissipated, the decrease in weiget was brought out by the evolution of gas produced during the raction for formation of the host lattice. From these results, it is shown that, if the silica from sodium silicate is used instead of one from ethyl silicate, lead is decreased remarkably, and manganese decreases only a little, so the decrease in brightness might be expected.

TABLE VI

EFFECTS OF THE SOURCE OF SILICA ON THE RESIDUAL AMOUNT OF MANGANESE AND LEAD

| | Source of silica | Atmosphere: air | $H_2O$ | $O_2$ | $H_2$ | $N_2$ |
|---|---|---|---|---|---|---|
| Amount of lead | Ethyl silicate | 50 | 31 | 33 | 17 | 31 |
| | Sodium silicate | 16 | 16 | 23 | — | 7 |
| Amount of manganese | Ethyl silicate | 74 | 74 | 68 | 107 | 106 |
| | Sodium silicate | 107 | 104 | 111 | 106 | 122 |

## Discussion

The amount of activators was determined for various phosphors before and after firing by means of polarography. These procedures were considered to be one of the most effective methods to control the production of phosphors. Almost all of the activators, which are now used for the present phosphors, could be analysed by employing polarographic methods. We found it, however, difficult to detect some of impurities in the raw materials of phosphors, for example, iron in purified ammonium diphosphate.

Manganese or copper was not dissipated during firing, while antimony or lead seemed to be lost in that period. The fact that the amount of manganese in $Zn_2SiO_4$ : Mn or $(Zn, Be)_2SiO_4$ : Mn was increased during firing, may be explained by the assumption that the water contained in these batches, probably as silicic acid, was lost during firing. The reason why antimony content differs between 3 samples of white phosphors might be found in their different contents of one kind of calcium halophosphate phosphors.

The factorial design of experiment, which is used for the determination of effects of atmosphere and firing time on the brightness, seems to be one of the most powerful methods for the control of the phosphor production and gives a good result for the case of calcium silicate phosphor. In this case, the residual amounts of activators were analysed by polarography and used as the additional factorial effects for the analysis of covariance of the brightness. The results obtained from this analysis could clarify the effects of atmosphere and firing time on the residual amounts of activators and the brightness separately. From these results, it is shown in the calcium silicate phosphors, that lead

7) H. C. Froelich, *Trans. Electrochem. Soc.*, 93, 101 (1948).

has a more significant effect upon the brightness than manganese and the change of atmosphere causes that of the amount of activators and the brightness. The fact, that, with the increase of the amount of lead the brightness is increased, while manganese has an opposite effect, is in accord with the previous results[7], but we could not obtain such a decisive results when hydrogen was employed as an atmosphere, as reported previously. As to the source of silica, it will be preferable to use one from ethyl silicate, because the increase of the brightness may be expected.

## Summary

The amount of activators, which are now used for the present phosphors, was determined by means of polarography. The results obtained shows that manganese or copper is not dissipated during firing, while antimony or lead is dissipated in that period.

As for calcium silicate phosphors activated by manganese and lead, the residual amounts of activators were analysed by polarography and, these amount being taken as the additional factorial effects, the analysis of covariance was carried out to see the effects of atmosphere and firing time on the brightness. The results obtained show that the amount of lead has a more significant effect upon the brightness than manganese and the change of atmosphere causes that of the amount of activators and the brightness.

The authors wish to thank Dr. Hiromi Nishida and Dr. Shoji Makishima for the general discussion on the subject and the experimental work they had done.

*Government Chemical Industrial Research Institute, Tokyo*
*Hatagaya, Tokyo*

# *Dye-sensitized Photopolymerization of Vinyl Compounds. Polymerization of Styrene by Cyanine Dyes. I.*

By Masao KOIZUMI and Ai WATANABE

(Received August 19, 1954)

## Introduction

Quite recently two interesting investigations were published about the photopolymerization of vinyl compounds by means of organic dyestuffs.

One is the paper of Ueberreiter and Sorge[1] concerning polymerization of styrene induced by neutral red, quinoline yellow and other dyestuffs. and the chain initiation was attributed to the transference of energy from excited dye to vinyl monomer.

The other paper is a brief communication by Oster,[2] which reported rather preliminarily the polymerization of various vinyl compounds by using the proper combination of organic dye and suitable reducing agent in the presence of oxygen; the polymerization was interpreted to be initiated by OH or other simple radicals produced during the reoxidation of reduced dye by oxygen.

Now since our preliminary report[3] on the photosensitized polymerization of styrene. published in 1951, the work has been continued and especially the investigations using cyanine dyestuffs have been successfully extended and it has become quite clear that suitable dyestuffs, when excited, directly react with vinyl monomer to induce the polymerization quite efficiently. Thus, it was established that, when the mixture of styrene and *n*-butanol, 15 : 1 in volume, containing about $6\times10^{-5}$ mol./l. of various cyanine dye is irradiated by visible light at 60°C in vacuo, the decomposition of dye molecules occurs and at the same time the polymerization of styrene is greatly accelerated, and the number of initiations of the latter produced by one decomposed dye molecule was found to be one or two. The quantum yields for the photobleaching of dye and for the initiation of polymerization were also measured. The present paper will present a brief account of our results; the details of the practical implications and full data will be published in Journ. Inst. of Polytech. Osaka City University.

1) K. Ueberriter and G. Sorge, *Z. Elektrochem.*, 57, 795 (1953).
2) G. Oster, *Nature*, 173, 300 (1954).
3) M. Koizumi, J. Kuroda and A. Watanabe, *J. Inst. Polytech. Osaka City Univ.*, Series C, 2, 1 (1951).

## Experimental

**Sample.**—Cautiously purified styrene was once more distilled in vacuo prior to the experiment. All the cyanine dyes except pinacyanol chloride, which was provided by the Japan Research Institute for Photosensitizing Dyes. Co., Ltd. in Okayama, were kindly supplied by Dr. T. Ogata of the Institute of Science in Tokyo.

**Apparatus and Experimental Procedure.**—The main part of the apparatus is shown in Fig. 1.

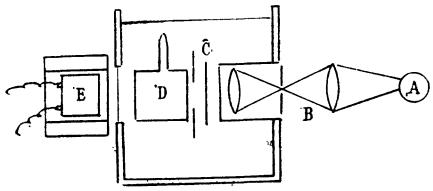



Fig. 1. Apparatus.

A, A 750 W tungsten lamp used as a light source.
B, Lens system.
C, Filter.
D, Drum-shaped reaction vessel of about 5 cc.
E, Kipp thermopile.

The quantity of absorbed light was measured by the use of a potentiometer during the experiment, and the calibration of the thermopile was done with a Hefner lamp. The number of photons entering the reaction cell was about $10^{16}$ per sec.·cm.$^2$ in most cases.

The experimental procedure is as follows.

One part of *n*-butanol solution of dye and 15 parts of styrene are mixed and, after thorough out-gassing, each 5 cc. of the sample are poured into two reaction vessels in vacuo and fused off separately; one is for the dark reaction and the other for the photo-reaction, and these two reactions are carried out at the same time so that they may be compared with each other. Of course, the whole procedure is performed in the dark. The two cells are kept in a thermostat of 60°C and one is irradiated by the light suitably selected by Matsuda color filter. After a certain time, an interval of one to more than ten hours, the absorption spectrum of each sample is examined by a Beckman spectrophotometer in order to determine the quantity of bleaching of dye. Next each is disstilled in vacuo to separate the produced polymer, then the latter is dissolved in benzene and after eliminating the benzene by sublimation in vacuo, the remaining polymer is weighed. Lastly the viscosity of the benzene solution of polymer is measured, and from the intrinsic viscosity the average molecular weight of the polymer is calculated by the formula proposed by Pepper.[4]

## Experimental Results

**1. Main Features of the Bleaching and Polymerization Reactions.**—The absorption spectra of five cyanine dyes employed for the experiment are shown in Fig. 2, the concentrations of dyes being all $6.3\times10^{-5}$ mol./1.

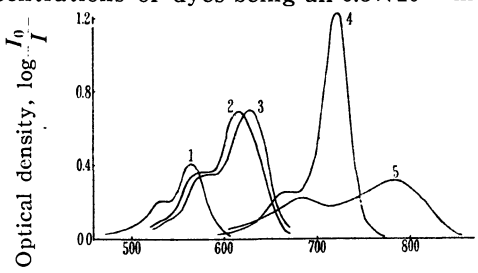
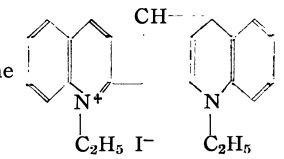
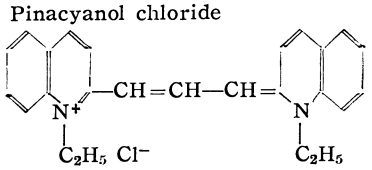



Fig. 2. Absorption spectra of cyanine dyes in styrene and butanol (15 : 1), thickness of the cell; 1 cm.

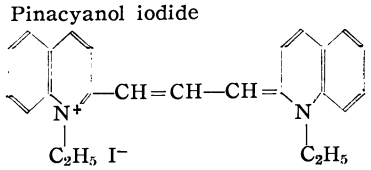
(1) Isocyanine



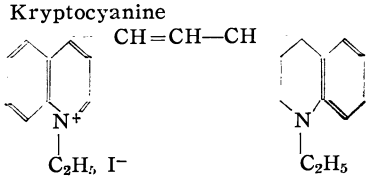

(2) Pinacyanol chloride



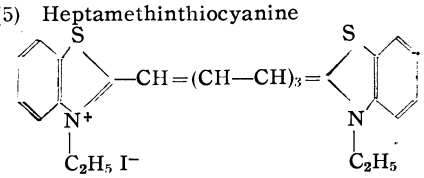

(3) Pinacyanol iodide




(4) Kryptocyanine




(5) Heptamethinthiocyanine




All the dyes have two absorption maxima, and in most experiments the incident light of the wave lengths covering these two maxima was used. When the solutions of dye in *n*-butanol were irradiated at 60°C in vacuo, no bleaching was observed within the experimental error.

Bleaching of dye took place only when the dye solution in styrene-butanol mixture was irradiated, and in accordance with it, the rate of polymerization was accelerated.

4) D. C. Pepper, *J. Polymer Sci.*, 7, 347 (1951).

Some typical bleaching curves are shown in Fig. 3, in which the percentage of decomposed dye calculated from the observed drop of the higher maximum of absorption are plotted against time.

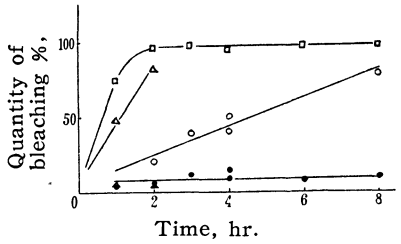



Fig. 3. Bleaching of dye.

Filter
Pinacyanol iodide { □ V-O2, ○ V-R2, ● Dark
Isocyanine { △ V-Y1, ▲ Dark

As is evident from the figure, the bleaching occurs slightly even in the dark, but its quantity being very small and independent of time, one may safely conclude that it is due to some impurity or to a minute quantity of oxygen remaining in the sample.

As for the photobleaching, the absorption curves as a whole decline in the region of visible wave lengths in case of pinacyanol chloride, kryptocyanine, heptamethinthiocyanine, but in case of isocyanine and pinacyanol iodide a new absorption band, though small in shape, seems to appear in the shorter wave length side of the original maxima. For a group of experiments on one kind of dye, the constancy of the light intensity being assured as much as possible the quantities of absorbed light are almost the same, but for different kinds of dye, the extinction not being the same, the curves do not necessarily represent the ease of photobleaching. It can be said, however, that under the present conditions all the dyes except pinacyanol chloride are decomposed almost completely within a few to more than ten hours.

The quantity of polymerization as represented by the percentage of the original monomer are plotted against time in Fig. 4.

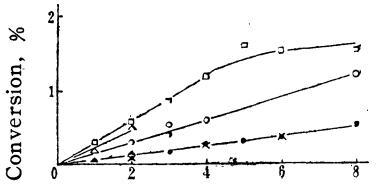



Fig. 4. The relation between the quantity of polymerization and time in various conditions.

Pinacyanol iodide { □ V-O2, ○ V-R2, ● Dark
Isocyanine { △ V-Y1, ▲ Dark
No dye ×

TABLE I
THE AVERAGE POLYMERIZATION DEGREE

| Dye | Time (hr.) | Dark | | Light | | Filter |
|---|---|---|---|---|---|---|
| | | % of conversion | $\bar{P}$ ($10^3$) | % of conversion | $\bar{P}$ ($10^3$) | |
| | 2 | 0.09 | | | | |
| | 4 | 0.24 | 9.5 | | | |
| | 6 | 0.42 | 11 | | | |
| Isocyanine | 1 | 0.06 | | 0.17 | 4.8 | V—Y1 |
| | 2 | 0.15 | | 0.51 | 4.7 | V—Y1 |
| Pinacyanol chloride | 6 | 0.59 | 10 | 0.87 | 9.2 | V—R2 |
| | 18 | 1.46 | 9.2 | 1.58 | 8.8 | V—R2 |
| Pinacyanol iodide | 2 | 0.09 | 10 | 0.33 | 5.6 | V—R2 |
| | 3 | 0.16 | 13 | 0.55 | 7.1 | V—R2 |
| | 4 | 0.21 | 12 | 1.19 | 5.5 | V—O2 |
| | 5 | 0.31 | 12 | 1.62 | 5.7 | V—O2 |
| Krypto-cyanine | 3 | 0.20 | 11 | 0.46 | 8.0 | V—O2 |
| | 6 | 0.46 | 11 | 1.06 | 7.0 | V—O2 |
| | 6 | 0.46 | 11 | 0.83 | 6.9 | V—C1 |
| Heptamethin-thiocyanine | 2 | 0.10 | 10 | 0.35 | 7.2 | V—R2 |
| | 3 | 0.12 | | 0.47 | 8.4 | V—R2 |
| | 4 | 0.23 | 9.2 | 0.54 | 7.2 | V—R2 |

It is clear from this figure that the polymerization in the dark or the thermal polymerization in the system containing dye takes place at just the same rate as that in the simple mixture of butanol and styrene.

The enhancement of the magnitude of polymerization when illuminated is marked in all the cases, though the quantity differs to some extent for each dye. After a certain time of illumination the curves for the polymerization in light* run parallel to that for dark polymerization, which assures the non-existence of the effect of the decomposed dye upon the polymerization rate.

From the comparison of Fig. 3 and Fig. 4, it is clear that bleaching and photopolymerization, broadly speaking, are closely related with each other and it seems that the two processes proceed side by side, but in case of pinacyanol iodide the photopolymerization seems to survive the disappearance of dye a little longer. The details of this phenomenon will be stated in the next paper. The photobleaching of pinacyanol chloride and the accompanying photopolymerization, which are not shown in Fig. 3 and Fig. 4, are very small compared with other dyes.

**2. The Average Polymerization Degree.**— Some of the main results for the degree of polymerization are tabulated in Table I.

These values, of course, concern the whole reaction including those in the dark and the photopolymerizations and are rather conventional in nature. The proper treatment of the data will be given in the following paper, and it will be found there that the discussion, if qualitative in nature, is not affected much. Here one will not go further than to say that the larger the quantity of photopolymerization, the smaller is the polymerization degree.

**3. The Number of Kinetic Chain for Polymerization Produced per one Dye Molecule Decomposed ($\alpha$). Quantum Yields for Bleaching and for the Initiation Process in the Polymerization.**

Using the degree of polymerization tabulated above, one can easily get the value of $\alpha$, the number of initiation for polymerization per one dye molecule decomposed, from the quantity of decomposed dye and that of photopolymerization, which in the present case will be tentatively put as equal to the difference between the quantity of polymerization in the light and the dark. The assumption involved is of course open to question, but the precise treatment which will be given in the next paper will show that the above simple treatment is not greatly in error.

Some of the values of $\alpha$ thus obtained are tabulated in Table II. They are all close to

TABLE II

THE VALUE OF $\alpha$

| Dye | Time (hr.) | $\alpha$ | Filter |
|---|---|---|---|
| Isocyanine | 1 | 0.78 | V—Y1 |
| | 2 | 1.4 | V—Y1 |
| | 6 | 3.1 | V—R2 |
| Pinacyanol | 18 | 0.6 | V—R2 |
| chloride | 18 | 3.1 | V—O2 |
| | 2 | 3.5 | V—R2 |
| Pinacyanol | 3 | 2.5 | V—R2 |
| iodide | 4 | 1.5 | V—R2 |
| | 3 | 1.6 | V—O2 |
| Kryptocyanine | 6 | 2.3 | V—O2 |
| | 6 | 1.9 | V—C1 |
| | 2 | 0.79 | V—R2 |
| Heptamethin- | 3 | 0.97 | V—R2 |
| thiocyanine | 4 | 1.3 | V—R2 |

1 or 2. In case of pinacyanol iodide the value of $\alpha$ seems to be somewhat large when the filter V—R2 transmitting only the maximum of the longer wave length was employed, but it will be shown in the next paper that the corrected value is perhaps two. The values for pinacyanol chloride are unreliable, since the quantities of bleaching and of the photopolymerization are so small in this case that the accurate measurements are quite difficult.

The quantum yields for photobleaching and for the initiation process in the polymerization are tabulated in Table III.

The latter statistics are approximate in nature since the degrees of polymerization in Table I concern the complete polymerization in the light. As is evident from the table, the values are nearly equal for pinacyanol iodide, heptamethinthiocyanine and isocyanine; next comes kryptocyanine and the value for pinacyanol chloride is much less.

## Discussion

From the fact that the dye in the mixture of *n*-butanol and styrene neither decomposes in the dark nor affects the thermal poly-

* To avoid confusion the following terminology will be used in the present research. The polymerization in the whole, when illuminated, will be referred as "the polymerization in light", while the term "photopolymerization" will only be adopted for the part left when the polymerization in the dark is subtracted from the polymerization in the light.

TABLE III

QUANTUM YIELD

| Dye | Time (hr.) | Quantum yield for bleaching ($10^{-4}$) | Quantum yield for initiation process of polymerization ($10^{-4}$) | Filter |
|---|---|---|---|---|
| Isocyanine | 1 | 7.8 | 6.0 | V—Y1 |
| | 2 | 6.9 | 9.4 | V—Y1 |
| Pinacyanol chloride | | 0.10 | 0.30 | V—R2 |
| | | 0.08 | 0.05 | V—R2 |
| | | 0.04 | 0.12 | V—O2 |
| Pynacyanol iodide | 2 | 0.7 | 2.4 | V—R2 |
| | 3 | 1.0 | 2.5 | V—R2 |
| | 4 | 1.9 | 2.8 | V—R2 |
| | 3 | 0.36 | 0.58 | V—O2 |
| Kryptocyanine | 6 | 0.40 | 0.94 | V—O2 |
| | 6 | 0.54 | 1.0 | V—C1 |
| Heptamethin-thiocyanine | 2 | 5.2 | 4.1 | V—R2 |
| | 3 | 2.4 | 2.3 | V—R2 |
| | 4 | 6.6 | 8.4 | V—R2 |

merization, it can be concluded that there is no interaction between the dye molecule in the ground state on the one hand and the monomer molecule or polymer radical on the other hand. Most probably the dye molecules when excited will not decompose of themselves, since they are stable in the illuminated solution of *n*-butanol. The decomposition of dye only takes place when the excited dye molecule interacts with styrene to initiate the polymerization. Thus one may presumably conclude that the present photopolymerization is due to the direct interaction between the excited dye and the monomer.

In view of the small quantum yield both for photobleaching and for the initiation process in the polymerization, most of the excited dyes release the excess energy, but only a small fraction of them is available for the polymerization. Perhaps the interaction between dye and monomer will produce two radicals, both of which initiate the polymerization more or less effectively. The iodine atom seems to play an important role in the present photopolymerization, since all the dyes containing iodine show the same order of effectiveness, while pinacyanol chloride, the absorption of which is quite similar to pinacyanol iodide, is far less effective. It will be worth adding that the quantum yield for the initiation process in the polymerization is of the same order of magnitude as that reported by Oster, and hence cyanine dyes may be equally valuable for the practical purpose as the combination of some dye and reducing agent used by Oster.

## Summary

The photopolymerization induced by the excited cyanine dyes was investigated, and it was established that the direct interaction between excited dye and monomer initiates the polymerization. The quantum yields for photobleaching and for the initiation process in the polymerization were both found to be of the order of $10^{-4}$. It was further found that one dye molecule produces one or two kinetic chains of polymerization.

The authors express their hearty thanks to Dr. T. Ogata and Dr. M. Banno who gave them valuable samples of dye and to Dr. B. Kanatsuka who supplied them with β-phenyl-ethyl alcohol. The cost of the research has been partly defrayed from the Scientific Research Grant from the Ministry of Education.

*Institute of Polytechnics, Osaka City University, Osaka*

# *Dye-sensitized Photopolymerization of Vinyl Compounds. Polymerization of Styrene by Cyanine Dyes. II.*

By Ai WATANABE and Masao KOIZUMI

(Received August 19, 1954)

## Introduction

As reported in the preceding paper[1], the photosensitized polymerization occurs when the solution of cyanine dye in a mixture of styrene and *n*-butanol is irradiated at 60°C. In this reaction, the dye molecule is decomposed most probably by its interaction with styrene, when the former is in the excited state, producing one or two kinetic chains of polymerization per one dye molecule decomposed. Now in order to know the features of the reaction in more detail, the effects of various factors upon the reaction such as temperature, the wave lengths of the incident light, and the concentrations of dye, have been examined, chiefly employing pinacyanol iodide as a sensitizer.

Further, the probable scheme of the reaction has been proposed and on its basis suitable corrections have been given to the $\alpha$-values reported in the previous paper.

The apparatus and the experimental procedures are the same as in the previous paper.

## Experimental Results

**1. Effect of Temperature.**—Two series of experiments were performed at 40°C and 60°C, using a $6\times10^{-6}$ mol./l. solution of pinacyanol iodide in a mixture of 15 parts styrene and 1 part of *n*-butanol. A Matsuda color filter VO-2, which transmits the wave lengths of the two absorption maxima of dye, was used, and the number of photons entering the reaction cell was measured to be about $10^{16}$ per sec.·cm$^2$.

The bleaching curves and the polymerization curves both in light and dark at 40°C are given in Figs. 1 and 2, respectively. The results at

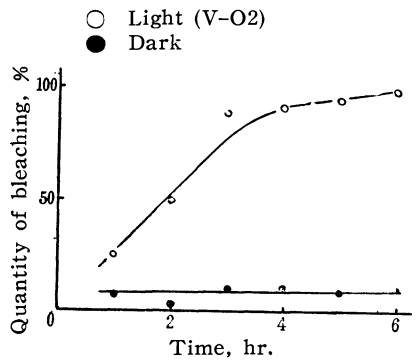



Fig. 1. Bleaching of pinacyanol iodide at 40°C.

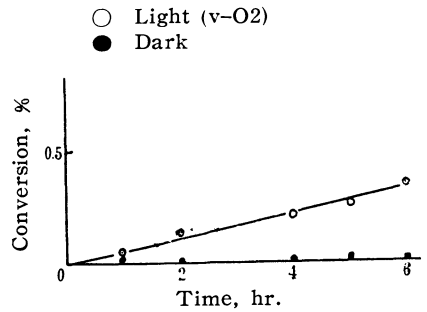



Fig. 2. Polymerization of styrene at 40°C.

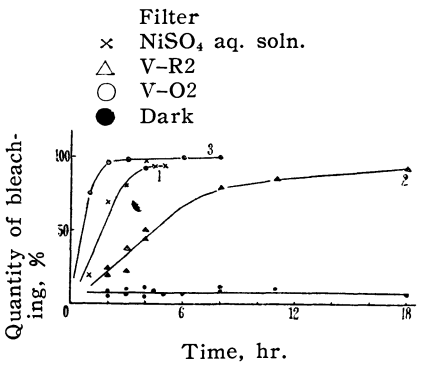



Fig. 3. Bleaching of pinacyanol iodide at 60°C.

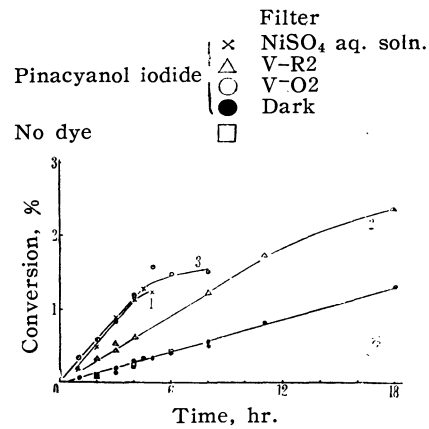



Fig. 4. Polymerization of styrene at 60°C.

1) M. Koizumi and A. Watanabe, This Bulletin, 28, 136 (1955).

60°C are shown by the curves, (3) in Figs. 3 and 4, which include the other results obtained when the different filters were used.

As seen from Figs. 1 and 3, the bleaching of dye occurs even in the dark both at 40°C and 60°C, but its quantity is small and independent of time, and moreover in the same order of magnitude in both cases. The photobleaching is much faster at 60°C than at 40°C.

As for the polymerization, thermal polymerization scarcely occurs, and only photopolymerization proceeds at 40°C; the latter seems to continue even after the completion of photobleaching. At 60°C, thermal polymerization takes place, but its rate is not affected by the addition of dye as already reported in the previous paper. A remarkable fact is that a new band, which will be shown later, appears in the region of shorter wave lengths, and this is more marked at 40°C than at 60°C.

The influence of temperature upon the polymerization degree, $\alpha$-value and upon the quantum yield will be given later.

**2. Effect of the Dye Concentration.**—The polymerization curves at 60°C for three different concentrations of dye are given in Fig. 5. It is

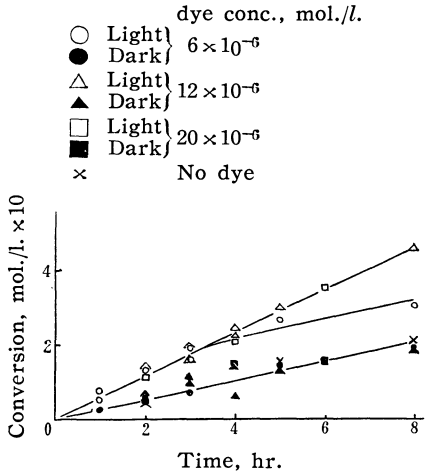



Fig. 5. The effect of dye concentration on the quantity of polymerization.

to be noted that styrene in this case was not distilled directly before the experiment and that the thermal polymerization proceeded faster than in the other cases. In spite of this fact, it is certain that the photopolymerization continues longer in the more concentrated solution, and that at least in the initial stage the reaction goes on at almost the same rate at three different concentrations of dye. Judging from the molar extinction coefficient of dye, the effective light is absorbed almost completely in the initial stage of the reaction so that it is very probable that the rate depends only on the number of excited dye molecules rather than on the total concentration of dye.

**3. Effect of the Wave Lengths of Incident Light.**—Pinacyanol iodide has two maxima at 580 m$\mu$ and at 630 m$\mu$. In order to investigate the effect of different wave lengths, the three series of experiments were done using the following filters; 1) 200 g./l. aqueous solution of $NiSO_4$ 2.5 cm. in thickness, which transmits only the maximum of shorter wave length, 2) Matsuda color filter V-R2 which selects the light longer than about 600 m$\mu$ and 3) Matsuda color filter V-O2 which transmits the wave lengths at the two absorption maxima. The results are shown in Figs. 3 and 4.

It is remarkable that the rate of photobleaching in (2) is much slower than in (1) and (3), though the exact comparison can not be given on account of the difference of the light intensity in the three cases. The number of photons absorbed in the initial stage of the reaction are approximately $1\times10^{15}$, $2\times10^{15}$ and $6\times10^{15}$ quanta per sec.·cc. for the above three cases, respectively.

In addition, it is observed that in case 3) the photopolymerization continues even after the almost complete destruction of the dye. In cases 1) and 2), the photobleaching and photopolymerization proceed seemingly in a parallel manner. Now the appearance of a new absorption band mentioned in section 1 and the survival of the photopolymerization after the completion of photobleaching in case 3) could be successfully correlated in the following way.

In case (1) the absorption curve of the sample after the reaction declines throughout the whole visible region as the bleaching proceeds, while in case (2) a new absorption band appears accompanied by the fall of the two original maxima. A typical example is shown in Fig. 6. In case

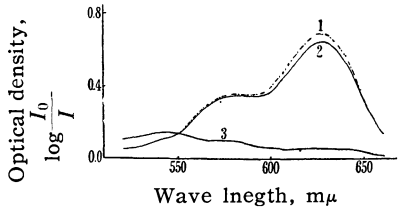



Fig. 6. Absorption spectra of $6\times10^{-5}$ mol./l. pinacyanol iodide in styrene and butanol (15: 1) in 1 cm. silica cell.
(2) After the reaction in dark for 18 hrs. at 60°C.
(3) After the reaction in light for 18 hrs. at 60°C.

3), this new absorption band, which appears in the proper stage of reaction though less markedly than in case 2), gradually drops as time goes on. It was ascertained by another experiment that this new absorption band does not decline when the sample is maintained in the dark at 60°C for a long time. Thus it becomes quite clear that the reaction product which produces this new absorption band is decomposed only by irradiation.

Further, it was found in case (2) that, when the polymer is dissolved in benzene and reprecipitated by use of methanol, the polymer still has a tint of pink, while the polymer obtained in the dark reaction, when treated in the same way, becomes completely colorless. The analogous and still more marked results were obtained at 40°C;

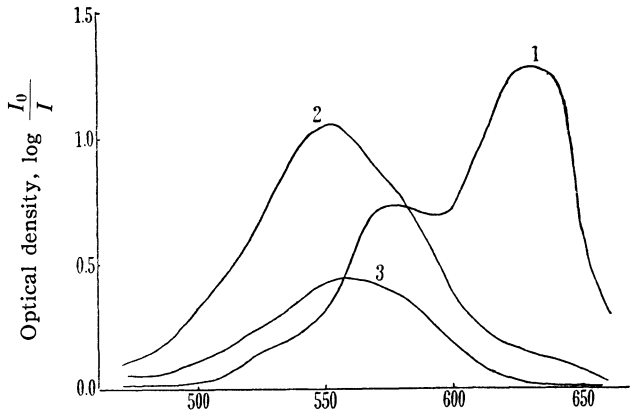



Fig. 7. Absorption spectra of the sample and the polymer.
(1) $1.2\times10^{-5}$ mol./l. pinacyanol iodide in styrene and butanol (15: 1) in 1 cm. silica cell.
(2) After light reaction (filter V-O2) for 16 hrs. at 40° C.
(3) The polymer separated from the sample in (2).

thus when the concentration of dye is made two fold and the illuminated portion of the cell is increased, the polymer obtained has a marked pink color which can never be eliminated by the above treatment. In Fig. 7, the absorption curve of the sample after 16 hours irradiation through V-O2 at 40°C and that of the polymer separated and dissolved in a mixture of styrene and butanol (15: 1) are compared with the original curve. All these facts demonstrate quite strongly that a fragment of decomposed dye molecule is attached to the polymer.

An experiment similar to the above was tried for pinacyanol chloride, but in this case it was not possible to recognize the same phenomenon.

**4. The Average Polymerization Degree.**— The average polymerization degree under various experimental conditions is tabulated in Table I. It is about 12000 for the thermal reaction at 60°C. and for the reaction in light it seems that the value, approximately half of that in the dark, becomes less the faster the reaction.

**5. Quantum Yields for Photobleaching and for the Initiation Process in Polymerization. The Value of $\alpha$.**—Quantum yields for photo-

Table I
The Average Polymerization Degree

| Temperature (°C) | Time (hr.) | Dark $\bar{P}$ ($10^3$) | Light $\bar{P}$ ($10^3$) | Filter |
|---|---|---|---|---|
| 60 | 1 | | 6.9 | $NiSO_4$aq. soln. |
| | 2 | | 5.0 | |
| | 3 | 12 | 5.4 | |
| | 4 | 10 | 6.7 | |
| | 1 | | 5.0 | V-O2 |
| | 2 | 14 | 5.3 | |
| | 3 | 14 | 5.2 | |
| | 4 | 12 | 5.5 | |
| | 5 | 12 | 5.7 | |
| | 2 | 10 | 5.6 | V-R2 |
| | 3 | 13 | 7.1 | |
| | 4 | 11 | 6.7 | |
| | 8 | | 6.5 | |
| 40 | 2 | | 5.4 | V-O2 |
| | 4 | | 5.6 | |
| | 4.7 | | 5.6 | |
| | 5 | | 4.3 | |

Table II
Quantum Yield

| Time (hr.) | Quantum yield for bleaching ($10^{-4}$) | | | | Quantum yield for initiation process in polymerization ($10^{-4}$) | | | |
|---|---|---|---|---|---|---|---|---|
| | 40°C. V-O2 | 60°C. | | | 40°C. V-O2 | 60°C. | | |
| | | $NiSO_4$ aq.soln. | V-O2 | V-R2 | | $NiSO_4$ aq.soln. | V-O2 | V-R2 |
| 1 | 0.78 | 4.7 | 4.8 | | 0.40 | 10 | 4.3 | |
| 2 | 1.5 | 12 | 5.5 | 0.7 | 1.2 | 15 | 6.8 | 2.4 |
| 3 | | 11 | 4.5 | 1.0 | | 21 | 8.4 | 2.5 |
| 4 | 1.5 | 8.7 | 2.9 | 1.9 | 0.91 | 18 | 8.2 | 2.8 |
| 5 | 1.1 | 10 | | | 0.85 | 23 | | |
| 6 | 1.2 | | 4.2 | | 0.90 | | 12 | |
| 8 | | | 4.2 | 2.0 | | | 12 | 3.5 |

TABLE III
THE VALUE OF $\alpha$

| Time (hr.) | $\alpha$ | | | | $\alpha'$ | | | $\alpha_0$ | | |
|---|---|---|---|---|---|---|---|---|---|---|
| | 40°C. | 60°C. | | | 60°C. | | | 60°C. | | |
| | V-02 | $NiSO_4$ aq.soln. | V-O2 | V-R2 | $NiSO_4$ aq.soln. | V-O2 | V-R2 | $NiSO_4$ aq.soln. | V-O2 | V-R2 |
| 1 | 0.52 | 2.0 | 0.91 | | 2.4 | 1.1 | | 1.8 | 0.93 | |
| 2 | 0.79 | 1.3 | 1.2 | 3.5 | 2.0 | 1.5 | 4.4 | 1.6 | 1.2 | 3.2 |
| 2 | | 1.0 | 0.86 | 2.3 | 1.7 | 1.3 | | 1.4 | 1.0 | |
| 3 | 0.70 | 2.0 | 1.9 | 2.7 | 2.8 | 2.3 | 3.3 | 2.3 | | 2.4 |
| 3 | | | | 2.4 | | | 2.5 | | | 1.7 |
| 4 | 0.60 | 2.0 | 2.8 | 1.5 | 2.3 | 3.2 | 2.3 | | | 1.7 |
| 4.5 | | 2.5 | | | 3.6 | | | | | |
| 4.7 | 1.0 | | | | | | | | | |
| 5 | 0.77 | 2.3 | 3.8 | | 2.7 | 4.4 | | | | |
| 6 | 0.77 | | 2.8 | | | 3.3 | | | | |
| 8 | | | 2.8 | 1.8 | | 2.7 | 2.9 | | | |
| 11 | | | | 2.5 | | | 3.6 | | | |
| 18 | | | | 2.4 | | | | | | |

bleaching and for the initiation process in polymerization under various conditions are shown in Table II, and the values of $\alpha$ in Table III. $\alpha$ was calculated by using the $P$-value averaged for each filter. This procedure is of course not exact and the rigorous treatment will be given below. It is further to be added that $\alpha$-value in the later stage of reaction in case of V-O2 can not be adopted, since the decomposed fragment of dye attached to the polymer still accelerates the reaction photochemically even after the complete fall of the original maximum of absorption utilized for determining the dye concentration. The order of the quantum yields is 1)>3)>2) both for the photobleaching and the photopolymerization.

## Discussion

At first, let us consider how to obtain the correct value for $\alpha$ or the number of initiation processes per one dye molecule decomposed. The values hitherto tabulated were calculated according to the following formula and must be corrected accordingly.

$$\frac{\left(\begin{matrix}\text{Quantity of polymer}\\ \text{in light reaction}\end{matrix}\right)-\left(\begin{matrix}\text{Quantity of polymer}\\ \text{in dark reaction}\end{matrix}\right)}{\text{(The average polymerization degree in light)}}\Bigg/\left(\begin{matrix}\text{Quantity of}\\ \text{photobleaching}\end{matrix}\right) \tag{1}$$

For this correction, there are two facts to be taken into consideration. One concerns the experimental condition and the other is related to the reaction mechanism.

Now, scrutinizing the experimental condition, it was found that only 1.6/5 of the sample is irradiated. Hence one must consider that the polymerization in light takes place only in this part, while in the remaining part only the pure dark polymerization proceeds at the same time. It may, therefore, be plausible to admit that the whole reaction is a mere superposition of the two, and the average polymerization degree $\bar{P}$, which was hitherto tabulated, is a weighted mean of the two separate reactions occuring in the different parts of the cell.

Thus if one puts the quantities of polymerizations in dark and in light respectively as $D$ and $L$, then $\bar{P}$ will be expressed as follows:

$$P=\frac{L}{L-\dfrac{\dfrac{3.4D}{5}}{\bar{P}_L}+\dfrac{\dfrac{3.4D}{5}}{\bar{P}_D}} \tag{2}$$

where $\bar{P}_D$ and $\bar{P}_L$ are respectively the degree of polymerization in dark and in light space. If one uses $\bar{P}_L$ value calculated from (2) the more plausible values of $\alpha$ would be obtained, which are tabulated as $\alpha'$ in Table III.

Another fact to be criticized in equation (1) is the assumption that the polymerization in light is a simple sum of the dark-and photo-polymerization. This assumption will perhaps be wrong, and in order to treat the problem it is necessary to put forth a correct mechanism for the reaction, which will require a more detailed kinetic investigation. All that can be done in the present stage of research is to propose a plausible mechanism and develop a deduction on the basis of it.

In view of the facts that the dye molecules in the ground state do not affect the

dark polymerization and that the number of excited dye molecules in the stationary state is very small, the most plausible scheme of the polymerization in light will be just the one in which only the initiation process is the sum of the dark and light processes. Thus,

1. Initiation $V_{id}+V_{il}$
2. Propagation $k_p[R][M]$
3. Monomer transfer $k_{tr\cdot M}[R][M]$
4. Solvent transfer $k_{tr\cdot s}[R][S]$
5. Termination $k_t[R]^2$ ,

where $V_{id}$ and $V_{il}$ are respectively the rates of thermal- and photochemical-initiation, and $k_p$, $k_{tr\cdot M}$, $k_{tr\cdot s}$ and $k_t$ are the rate constants respectively for propagation, monomer transfer, solvent transfer and termination. All the other notations have the usual meaning.

Now, it is worthy to state that the above mechanism can be supported to some extent on the basis of the data already obtained as follows.

Thus if the above mechanism is correct, the average polymerization degree in light is easily given by the following formula

$$P_L=\frac{k_p[R][M]}{k_t[R]^2+k_{tr\cdot M}[R][M]+k_{tr\cdot s}[R][S]} . \quad (3)$$

Combining (3) with the overall rate

$$V=k_p[R][M] , \quad (4)$$

one gets

$$\frac{1}{\bar{P}_L}=\frac{k_tV}{k_p^2[M]^2}+\frac{1}{k_p[M]}\left[k_{tr\cdot M}[M]+k_{tr\cdot s}[S]\right] . \quad (5)$$

Thus $\frac{1}{\bar{P}_L}$, when plotted against $V$, must give a straight line. If one takes $V$, as a quantity of the polymer produced in 1.6/5 of the cell per one hour, one can test the above relation with the data for the various dyes described in the previous paper and with those in various conditions including the dark reaction.

The result is satisfactory to some degrees, as shown in Fig. 8.

Having thus shown the above scheme to be quite probable, one can, on the basis of it, obtain the more reliable values of $\alpha$ in the following way. Combining the relation

$$V_{id}+V_{il}=k_t[R]^2 \quad (6)$$

with (4), one can rewrite the formula (5) in the following way,

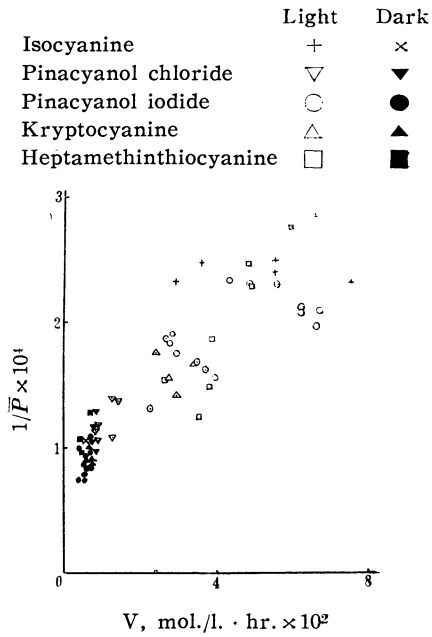



Fig. 8. Variation of the average polymerization degree with the overall rate.

$$\frac{V}{\bar{P}_L}=(V_{id}+V_{il})+\left[\frac{k_{tr\cdot M}}{k_t^{1/2}}[M]+\frac{k_{tr\cdot s}}{k_t^{1/2}}[S]\right](V_{id}+V_{il})^{1/2} . \quad (7)$$

In this equation $V$, $\bar{P}_L$, $[M]$ and $[S]$ are the known quantities. Hence if the values of $k_{tr\cdot s}$, $k_{tr\cdot M}$ and $k_t$ are given, one can easily calculate $(V_{il}+V_{id})$. $V_{id}$ can also be calculated if one employs the data for $V$ and $\bar{P}_D$ in the thermal polymerization. Thus one gets $V_{il}$ which is just the quantity necessary to obtain the correct $\alpha$-values.

Now it is fortunate that the necessary constants for our system were already given in previous literature. They are

$C_m=\frac{k_{tr\cdot M}}{k_p}=6\times10^{-5}$ [2] at 60°C

$C_s=\frac{k_{tr\cdot s}}{k_p}=0.6\times10^{-5}$ [3] at 60°C for *n*-butanol

$k_p=60$ l. mol.$^{-1}$ sec.$^{-1}$ [4]

$k_t=4.6\times10^7$ l. mol.$^{-1}$ sec.$^{-1}$ [4]

In most cases, the value of $V_{id}$ is a few percent or less compared with that of $V_{il}$. Using the values of $V_{il}$ obtained by the above

2) F. R. Mayo, R. A. Gregg and M. S. Matheson, *J. Am. Chem. Soc.*, 73, 1691 (1951).
3) R. A. Gregg and F. R. Mayo, *J. Am. Chem. Soc.*, 75, 3530 (1953).
4) C. H. Bamford and M. J. S. Dewar, *Proc. Roy. Soc.*, **A192**, 309 (1948).

procedure, one can get the most reliable $\alpha$-values, which are given in Table III and denoted as $\alpha_0$. It is quite probable that $\alpha_0$ does not exceed 2.

In order to discuss the mechanism of the reaction one must make further investigations, particularly kinetic in nature, but, from the results already obtained, one may give the following outline of the reaction.

The excited dye molecule interacts with the monomer molecule and initiates the polymerization, and at the same time it decomposes partially. Broadly speaking, the two reactions run parallel, but the process of decomposition of the dye molecule and that of initiation of polymerization are not necessarily an identical process in view of the fact that $\alpha_0$ value is smaller than 1 at 40°C while it is approximately 2 at 60°C. Activation seems to be necessary for the both reactions.

## Summary

Choosing pinacyanol iodide as a sensitizer, the authors studied the effects of temperature, concentration of dye and the wave lengths of incident light upon the photopolymerization of styrene in a mixture of styrene and butanol (15 : 1). It was found that the number of initiation processes as for polymerization produced by one decomposed dye molecule is decidedly less than 1 at 40°C, while it is about 2 at 60°C, and, from this result and other facts, it was concluded that the initiation of polymerization and the photobleaching are not necessarily an identical process though the two processes are related quite closely. As for the probable scheme of the polymerization in light, it was proposed that the addition of dye and illumination only increases the initiation process without any effects upon the remaining processes in the polymerization.

It was further found that, in favorable conditions, the fragment of decomposed dye molecule is attached to the polymer, which can also initiate the polymerization photochemically.

A more detailed account of the experiments will be reported in Journ. Instit. of Polytech., Osaka City Univ.

The cost of the research has been partly defrayed from the Scientific Research Grant from the Ministry of Education.

*Institute of Polytechnics,*
*Osaka City University, Osaka*

# SHORT COMMUNICATIONS

## *The Ionization Potentials of Aliphatic Alcohols*

By Itiro OMURA, Hiroaki BABA and Keniti HIGASI

(Received December 20, 1954)

Although there is ample information about the ionization potentials of homologous series, little attention has been directed towards the effect of branched chain. The present investigation was undertaken to study the variations of the appearance potentials due to the structure change of this particular sort.

The apparatus employed is a mass spectrometer of Hagstrum type.[1,2] The first appearance potentials were obtained by use of Honig's critical slope method,[3] argon being used as the standard gas.

The values obtained for methyl, ethyl and *n*-propyl alcohols are in good agreement with those of the previous investigators. It will be seen from the data of the table that the observed ionization potentials decrease in magnitude as the alkyl groups become either larger or more highly branched. Further it will be noted that the potentials are strongly affected by the structure changes

FIRST IONIZATION POTENTIALS, (ev.)

| Substance | Present authors (Electron impact) | Values in literature | |
|---|---|---|---|
| | | (Electron impact) | (Spectroscopic) |
| Methyl alcohol | 10.97±0.05 | 10.95[a] | 10.80[b] |
| Ethyl alcohol | 10.65±0.05 | 10.60[a] | 10.70[b] |
| *n*-Propyl alcohol | 10.42±0.1 | 10.46[a] | 10.70[b] |
| Isopropyl alcohol | 10.27±0.1 | | |
| *n*-Butyl alcohol | 10.30±0.1 | | |
| Isobutyl alcohol | 10.17±0.1 | | |
| *t*-Butyl alcohol | 9.92±0.1 | | |

in the immediate neighbourhood of the OH group.

Grateful acknowledgement is made to Prof. K. Hirota, for initiating the present work. Thanks are also due to the Education Ministry for a grant-in-aid.

1) H. D. Hagstrum, *Rev. Mod. Phys.*, **23**, 185 (1951).
2) I. Omura, *Bull. Res. Inst. Appl. Elec.*, **6**, 15 (1954).
3) R. E. Honig, *J. Chem. Phys.*, **16**, 105 (1948).
a) J. D. Morrison and A. J. C. Nicholson, *J. Chem. Phys.*, **20**, 1021 (1952).
b) W. C. Price, *Chem. Rev.*, **41**, 257 (1947).

*The Research Institute of Applied Electricity, Hokkaido University, Sapporo*

agent are added to each tube, shaken for a few seconds and set for the same space of time strictly—e.g. for 1 hr.—at room temperature. (If more rapid determination is desired, it is possible to shorten this space of time.) Filter off the lake by filter paper (for quantitative use), and the colors of filtrates (being deeper according to $F^-$ contents) are compared with each other, or the absorbancies of them are determined and compared, using a photoelectric colorimeter, spectrophotometer, or Duboscq colorimeter. The colored solution has an absorption maximum at 500 m$\mu$. As the Beer's law conforms to these dye solutions in the above conditions (0—1 p.p.m. of $F^-$) it is easy and accurate to evaluate the $F^-$ concentration of the sample solution using only three standard solutions when the colorimeter is used. The colored filtrates are so stable even when exposed to diffused sunlight for a long time that the absorbancy measurement need not be hasty.

Interfering substances which give $\pm$0.05 p.p.m. error refering to 0—1 p.p.m. of $F^-$ are: 2 p.p.m. of thiosulfate, sulfide, 5 p.p.m. of nitrite, cyanide, chromate, 10 p.p.m. of sulfite, permanganate, aluminum, 50 p.p.m. of sulfate, borate, antimony, tin, cadmium and iron. The other common substances do not interfere when their conc. are below 50 p.p.m. A large amount of organic substance interferes also considerably.

It is unnecessary to consider these substances in rain water, river water and ground water as usual. When a large amount of these substances is present, the separation of them from $F^-$ is necessary.

**Results.**—The lowest concentration of the standard solution, whose color can be easily distinguished from that of the blank test using photoelectric colorimeter, is 0.01 p.p.m. of $F^-$.

Accuracy and reproducibility are satisfactory as follows: [Results obtained by using photoelectric colorimeter with 500 m$\mu$. filter.]

| | $F^-$(p.p.m.) | |
|---|---|---|
| | Present | Found |
| NaF solution | 0.00 | $-0.00_5$, $-0.00_5$, 0.01, 0.00, $0.00_5$, |
| | 0.50 | 0.49, 0.50, 0.50, 0.51, $0.50_5$, |
| | 1.00 | $1.00_5$, 0.99, 1.00, $0.98_5$, 1.02, |
| Sample A (rain water) | | $0.05_5$, 0.06, $0.05_5$, 0.06, 0.06, |
| Sample B (river water) | | $0.11_5$, $0.11_5$, 0.12, $0.11_5$, $0.12_5$, |
| Sample C (distillate of hot spring water distilled as $H_2SiF_6$) | | $0.89_5$, $0.90_5$, $0.89_5$, $0.88_5$, $0.90_5$, |

This rapid and simple method for the determination of the low concentration of fluoride can be widely applied to the determination of fluoride in natural waters.

* This report was presented at the Symposium on Geochemistry of the Chem. Soc. Japan, October, 1954.

** Abbreviation: "Azodye".....*p*-dimethylaminoazophenylarsonic acid.

1) F. Feigl, and E. Rajmann, *Mikrochemie*, 12, 133 (1933).

*Laboratory of Analytical Chemistry,*
*Faculty of Liberal Arts,*
*Kagoshima University,*
*Kagoshima*

# *Studies on A. C. Polarography. IV. Reversible Behaviour of Anions*

By Yoshio TAKEMORI and Isamu TACHI

(Received July 21, 1954)

## Introduction

A comprehensive polarographic investigation of various anions was carried out by Revenda,[1] and Kolthoff and Miller,[2] who introduced the polarographic equations of those anions depolarizing the dropping mercury anode. Recently, Breyer et al.[3] have communicated many investigations on a. c. polarography of anions, using an a. c. polarographic equipment, and have shown that the summit-potential of an a. c. polarogram does not agree with the half-wave potential of the ordinary polarogram and also that the shape of Breyer's polarogram is unsymmetrical, which is different from the fact found in the case of cations.

In the previous paper, the theoretical equation representing the a. c. electrolytic current in a. c. polarography was introduced by Tachi and others[4] and it has been confirmed that Breyer's polarogram is a derivative curve of the ordinary polarogram, provided that the depolarizing process is reversible. And now, the authors will show the results of the experiments in which they attempted to discover whether Breyer's polarogram of anions would agree with the derivative curve led from the equation of the polarographic diagram introduced by Kolthoff and Miller. And also, the experimental results of the behaviour of d. c. component in a. c. polarography, i. e. Fournier's current, and the relationship between the concentration of the depolarizer and the polarographic current intensity of Breyer's polarograms will be reported.

## Experimental

The anions used here as the depolarizer were $Cl^-$, $Br^-$, $I^-$, $S_2O_3^=$ and $CN^-$, which are in the form of KCl, KBr, KI, $Na_2S_2O_3$ and KCN respectively. They were polarographed in the concentration range from $10^{-4}$ N to $10^{-3}$ N for the ease of comparing Breyer's polarogram with the ordinary polarogram, since the ordinary polarograms of anions, especially halogen ions, in the concentration higher than $10^{-3}$ N are not well-defined in general.

The concentration of $KNO_3$ aq. solution as the supporting electrolyte was made 0.2 N to keep the low impedance of the solution in the polarographic cell. But in the case of polarographic electrolysis of $CN^-$, 0.2 N NaOH aq. solution was used instead of 0.2 N $KNO_3$ aq. solution.

The circuit of a. c. polarography used was the same one as described in the previous papers. A pool condenser (50$\mu$F electrolytic condenser) was always connected between the bottom mercury and reference electrode in order to decrease the impedance of the liquid junction. In the case of polarographing Breyer's polarogram, the amplitude of a. c. voltage superimposed upon d. c. voltage was kept always 50 mv (60 c/s), and in registering Fournier's polarogram, it was changed from 0 to 100 or 120 mv (60 c/s).

The drop time of mercury electrode was 4.6 sec. and the rate of mercury flow was 2.2 mg/sec. (at O v *vs.* N.C.E.). The normal calomel electrode was employed as the reference electrode. All measurements were carried out at room temperature (about 17°C). The sensibility of the galvanometer was $2.87\times10^{-9}$ amp./mm/m.

## Experimental Results and Discussion

### (1) The Shape of Breyer's Polarogram

(i) ***Cl⁻, Br⁻, I⁻.***—Kolthoff and Miller gave the following equation for the polarographic wave of the depolarizers which form slightly soluble mercurous compounds at the dropping mercury electrode

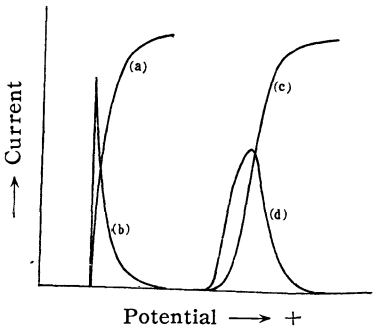
$$i=\begin{cases} i_d-\exp\dfrac{-F(E-E_o')}{RT} & \text{for } E\geqq E_{st} \\ O & \text{for } E\leqq E_{st} \end{cases} \quad (1)$$

where $E_{st}$ represents the starting potential of the ordinary polarogram, and $E_o'$ is determined by the solubility product of the mercurous compound formed at the anode, and $i_d$ is the limiting current of the polarographic wave and the positive sign of $i$ means the anodic current. Thus the derivative curve of the ordinary polarogram is given by

$$\frac{di}{dE}=\begin{cases} \dfrac{F}{RT}\exp\dfrac{-F(E-E_o')}{RT} & \text{for } E\geqq E_{st}, \\ O & \text{for } E\leqq E_{st}. \end{cases} \quad (1a)$$

1) J. Revenda, *Collection Czech. Chem. Communs.*, 6, 453 (1934).
2) I. M. Kolthoff and C. S. Miller, *J. Am. Chem. Soc.*, 63, 1405 (1941).
3) B. Breyer, F. Gutman and S. Hacobian, *Aust. J. Sci. Res.* **A3**, 558, 567, 595 (1950), **A4**, 611 (1951).
4) I. Tachi, et al., This Bulletin 28, 25, 31, 37, (1955).

The curves represented by the equations (1) and (1a) are illustrated in Fig. 1 (a) and (b).




(a) and (c); $i$—E curve
(b) and (d); $di/dE$—$E$ curve.

Fig. 1. The model curves of the ordinary polarographic wave and the derivative polarographic wave.
(a) $i$—$E$ curve in the case of $Cl^-$, $Br^-$ and $I^-$.
(b) $di/dE$—$E$ curve of the upper.
(c) $i$—$E$ curve in the case of $S_2O_3^=$ and $CN^-$.
(d) $di/dE$—$E$ curve of the upper.

Now, assuming that Breyer's polarogram would be given by the derivative curve of the ordinary polarogram as stated in the introduction, Breyer's polarographic wave is supposed to be the curve whose peak potential agrees with the starting potential of the ordinary polarographic wave.

The experimental results are shown in Table I and Fig. 2 (a), (b) and (c), and it is recognized that the summit potentials of Breyer's polarograms ($E_s$) generally coincide with the starting potentials of the ordinary polarograms ($E_{st}$) except in the case of $Br^-$, whose $E_s$ always agrees with the potential at which a kink appears on the ordinary polarogram. Further, this kink suggests that the ordinary polarogram of $Br^-$ consists of two steps, of which the first step may be due to the adsorption of $Br^-$ at the electrode. The reasons are as follows.

The fact that the shape of Breyer's polarogram of $Br^-$ is different from those of $Cl^-$ and $I^-$ in the point of having a prewave adjoining the main wave (Fig. 3), shows that another increase of the admittance at the dropping mercury electrode occurs at more negative potentials than $E_s$ of Breyer's

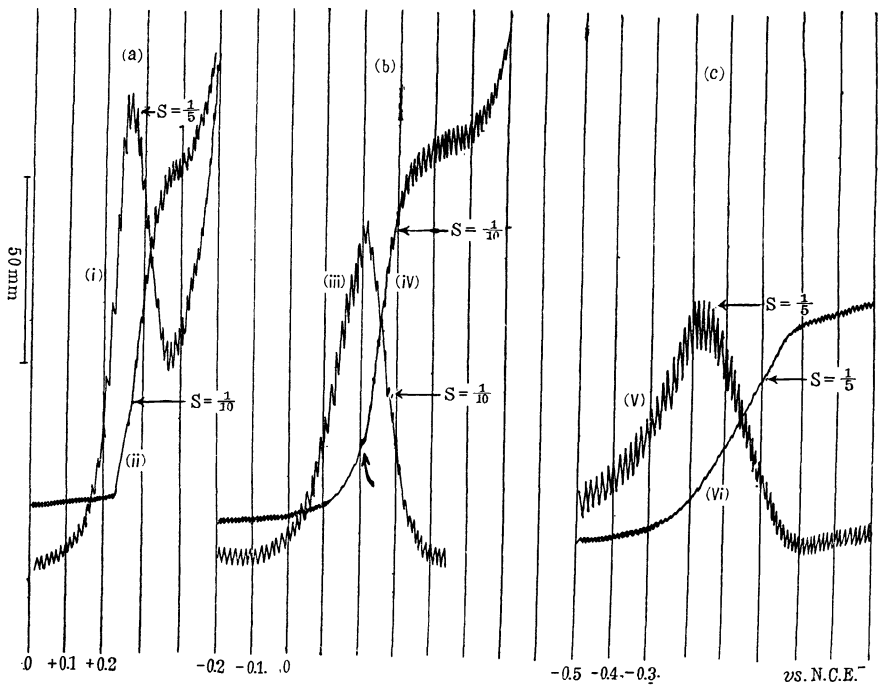



Fig. 2. Breyer's and the ordinary polarogram of $Cl^-$, $Br^-$ and $I^-$.
(i) Breyer's polarogram of $6\times10^{-4}$N $Cl^-$.
(ii) Ordinary polarogram of (i).
(iii) Breyer's polarogram of $8\times10^{-4}$N $Br^-$.
(iv) Ordinary polarogram of (iii).
The arrow points the kink on the ordinary polarogram of $Br^-$.
(v) Breyer's polarogram of $1\times10^{-3}$N $I^-$.
(vi) Ordinary polarogram of (v).

TABLE I

| Depolarizer | Potential *vs.* N. C. E. | Conc. ×10⁴ N 2 | 4 | 6 | 8 | 10 |
|---|---|---|---|---|---|---|
| | | (V) | (V) | (V) | (V) | (V) |
| | $E_s$ | 0.270 | 0.260 | 0.240 | 0.230 | 0.230 |
| $Cl^-$ | $E_{1/2}$ | 0.275 | 0.275 | 0.275 | 0.280 | 0.280 |
| | $E_{st}$ | 0.250 | 0.240 | 0.230 | 0.220 | 0.210 |
| | $E_s$ | 0.160 | 0.140 | 0.120 | 0.110 | 0.100 |
| $Br^-$ | $E_{1/2}$ | 0.150 | 0.140 | 0.160 | 0.150 | 0.150 |
| | $E_{st}$ | 0.100 | 0.090 | 0.050 | 0.090 | |
| | $E_s$ | −0.170 | −0.170 | −0.160 | −0.170 | −0.180 |
| $I^-$ | $E_{1/2}$ | | | −0.025 | −0.030 | −0.060 |
| | $E_{st}$ | | | −0.210 | −0.210 | −0.200 |
| | $E_s$ | −0.140 | −0.165 | −0.180 | −0.200 | −0.220 |
| $S_2O_3^=$ | $E_{1/2}$ | −0.100 | −0.110 | −0.120 | −0.120 | −0.120 |
| | $E_{(\sqrt{2}-1)id}$ | −0.130 | −0.135 | −0.145 | −0.150 | −0.150 |
| | $E_s$ | −0.320 | −0.330 | −0.330 | −0.335 | −0.335 |
| $CN^-$ | $E_{1/2}$ | −0.335 | −0.340 | −0.340 | −0.340 | −0.350 |
| | $E_{(\sqrt{2}-1)id}$ | −0.340 | −0.350 | −0.355 | −0.355 | −0.355 |

$E_s$: Peak potential of Breyer's polarogram.
$E_{1/2}$: Half-wave potential of the ordinary polarogram.
$E_{st}$: Starting potential of the ordinary polarogram.
$E_{(\sqrt{2}-1)id}$: Potential of the inflection point of the ordinary polarogram, namely the potential at which $i=(\sqrt{2}-1)i_d$.

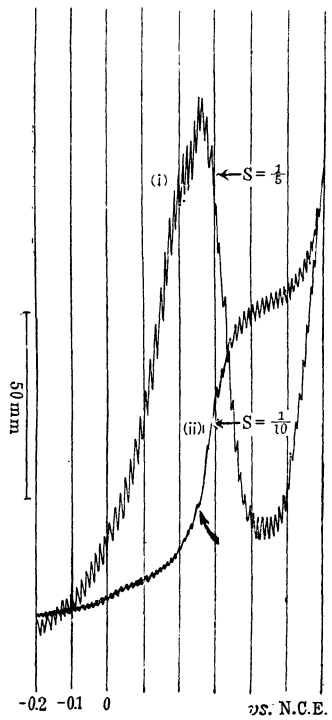



Fig. 3. Breyer's and the ordinary polarogram of $Br^-$ with gelatine.
(i) Breyer's polarogram of $5\times10^{-4}$N $Br^-$ with gelatine.
(ii) Ordinary polarogram of (i). The arrow points the kink on the ordinary polarogram of $Br^-$.

polarographic wave of $Br^-$, owing to the adsorption of the surface-active bromide ion. And the fact that the height of the prewave in the ordinary polarogram does not vary with the change of the concentration of the depolarizer suggests that the prewave may be due to the electro-oxidation of bromide ions oriented at the surface of the dropping mercury electrode.

**(ii) *$S_2O_3^=$ and $CN^-$*.**—Kolthoff and Miller introduced the following equation for the polarographic wave of depolarizers, which form slightly dissociated mercuric compounds or stable complex ions with mercuric ion; it can be written in the form

$$i=i_d+\frac{1}{2}\exp\frac{-2F(E-E_o')}{RT}-\frac{1}{2}\sqrt{4i_d\exp\frac{-2F(E-E_o')}{RT}+\exp\frac{-4F(E-E_o')}{RT}} \quad (2)$$

It follows therefore that

$$\frac{di}{dE}=\frac{F}{RT}\left\{\frac{2i_d+\exp\frac{-2F(E-E_o')}{RT}}{\sqrt{4i_d\exp\frac{2F(E-E_o')}{RT}+1}}-\exp\frac{-2F(E-E_o')}{RT}\right\} \quad (2a)$$

From these equations, it will be shown that the potential ($E_s$), where $di/dE$ becomes maximum, namely the inflection point of the equation (2), is to be the potential ($E_{(\sqrt{2}-1)id}$) given by $i=(\sqrt{2}-1)i_d$. Therefore, it is seen that the model curve of Breyer's polarogram of these anions is to be the curve which is unsymmetrical and have the peak potential ($E_s$) at the potential ($E_{(\sqrt{2}-1)id}$) of the ordinary polarogram as shown in Fig. 1 (d).

The experimental results obtained with $S_2O_3^=$, $CN^-$ are shown in Tabe I and Fig. 4 (a)

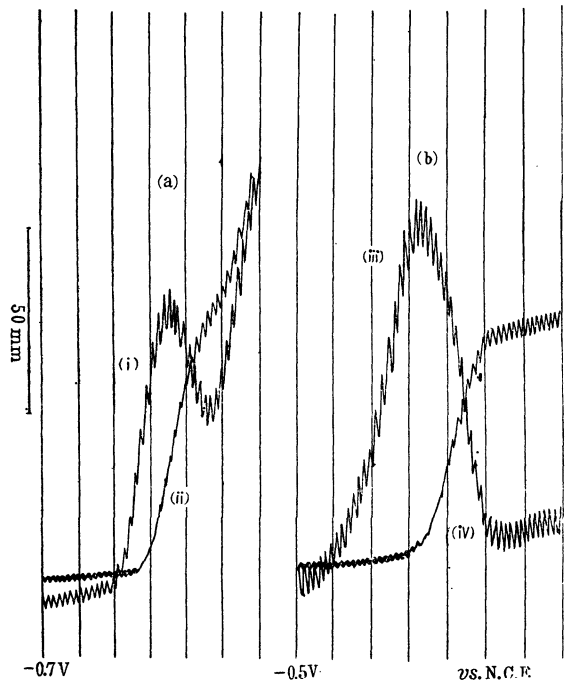



Fig. 4. Breyer's and the ordinary polarogram of $S_2O_3^=$ and $CN^-$.
(i) Breyer's polarogram of $6\times10^{-4}$N $CN^-$.
(ii) Ordinary polarogram of (i).
(iii) Breyer's polarogram of $6\times10^{-4}$N $S_2O_3^=$.
(iv) Ordinary polarogram of (iii).

and (b). It was found that $E_s$ was near to $E(\sqrt{2}-1)id$, though the sharp agreements of these two potentials were not obtained, in the case of $CN^-$. But $E_s$ of $S_2O_3^=$ shifts remarkably to more negative potential than $E(\sqrt{2}-1)id$ of the ordinary polarogram, for which the reason is not clear and a further study is necessary.

**(2) Fournier's Polarogram.**—In this section, it will be reported that the experimental results as to the d. c. component in the a. c. polarography, i. e. Fournier's current, $i_{Four}$, generally agree with the theoretical consideration that Fournier's current observed by a galvanometer would be the mean value of the ordinary polarographic currents at both extreme potentials given by the superposition of small a. c. voltage ($\Delta E$) on the d. c. potential, namely; $i_{Four}=\frac{1}{2}(i_{E-\Delta E}+i_{E+\Delta E})$.

Then the curves of Fournier's polarograms of $Cl^-$, $Br^-$ and $I^-$ are given by

$$i_{Four}=i_d-\exp\frac{-F(E-E_o')}{RT}\cdot\cosh\frac{E}{RT}\Delta E \quad (3)$$

Thus from equations (1) and (3), it follows that

$$i-i_{Four}=\exp\frac{-F(E-E_o')}{RT}\cdot\left(\cosh\frac{F}{RT}\Delta E.-1\right)\geqq 0. \quad (4)$$

Whence it follows that

$$i\geqq i_{Four}. \quad (5)$$

Namely, Fournier's current increases more slowly than the ordinary polarographic current with increasing positive potential.

Next, in the case of $S_2O_3^=$ and $CN^-$, the equation representing Fournier's theoretical polarogram is comparatively complicated so that we merely assume that Fournier's polarogram would be less steep than the ordinary polarogram and the former would cross the latter at the inflection point of the ordinary polarogram.

The experimental results shown in Fig. 5 agree with the theoretical consideration. The fact that Fournier's polarogram of $S_2O_3^=$ crosses the ordinary polarogram at a more negative potential than that of the inflection point is not theoretically clear as well as the above mentioned discrepancy between $E_s$ and $E_{(\sqrt{2}-1)id}$, and a further investigation will be necessary for the complete explanation of it.

**(3) The Dependency of Breyer's Polarographic Current and the Ordinary Polarographic Current on the Concentration of Depolarizers.**—The relationship between Breyer's polarographic current and the concentration of depolarizer is shown in Fig. 6. The relationship between the ordinary polarographic current and the concentration of the depolarizer is shown in Fig. 7.

5) M. Fournier, *Comp. Rend.*, **237**, 1673 (1951).

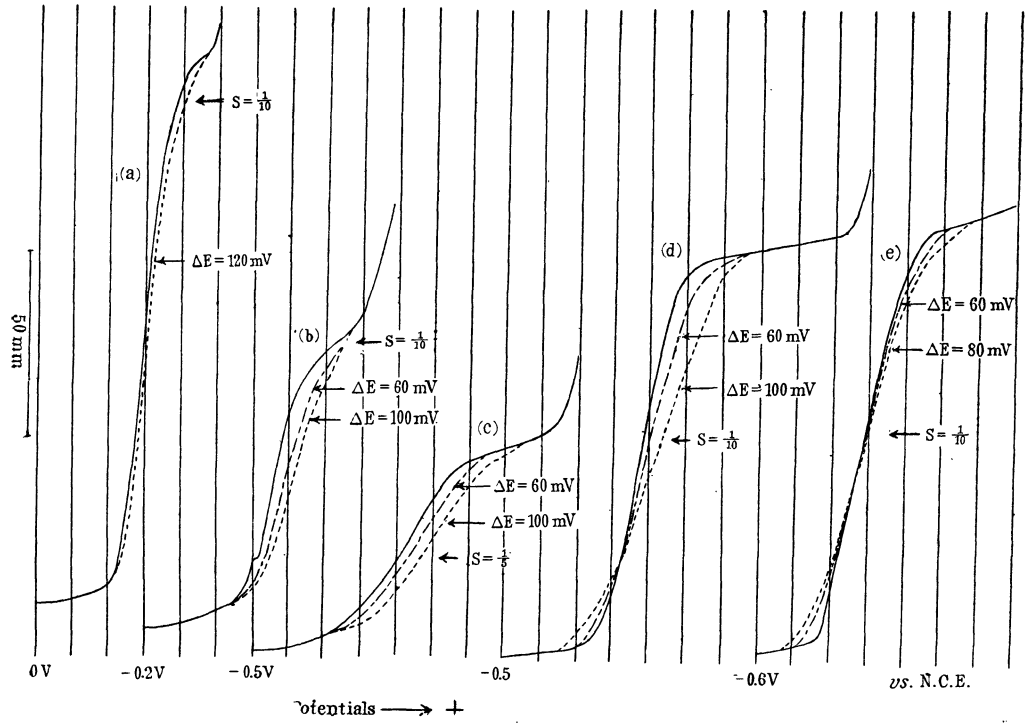



Fig. 5. Fournier's polarogram indicating the reversible electrode reactions of the named anions.
(a) $1\times10^{-3}$N $Cl^-$. (b) $6\times10^{-4}$N $Br^-$. (c) $1\times10^{-3}$N $I^-$. (d) $1\times10^{-3}$N $S_2O_3^=$. (e) $1\times10^{-3}$N $CN^-$.
The ordinary poralogram is demonstrated by full lines, and Fournier's polarograms are indicated by dotted lines.

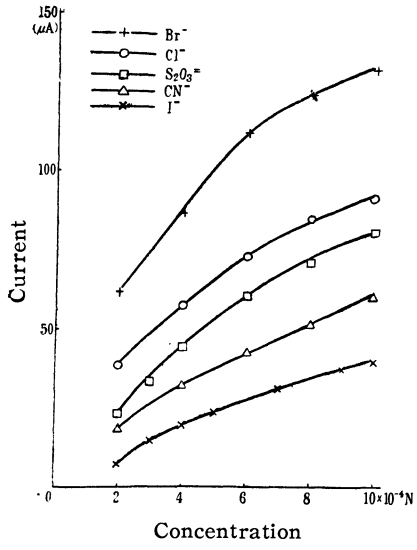



Fig. 6. The relationship between Breyer's polarographic current intensity and the concentration of depolarizer.

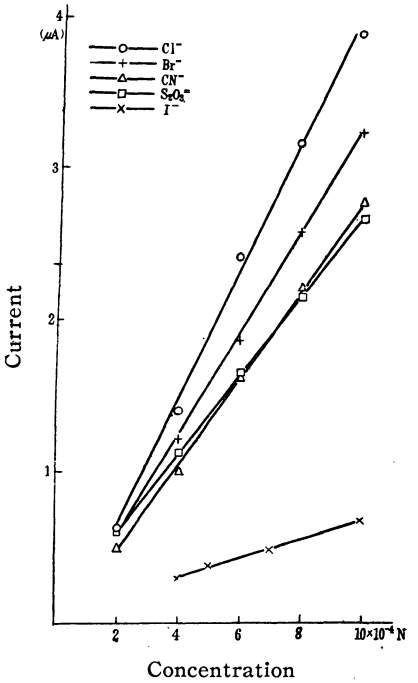



Fig. 7. The relationship between the ordinary polarographic current intensity and the concentration of the depolarizer.

The experimental results show that the linearity of the former holds generally over the concentration range from $2\times10^{-4}$ N to $8\times10^{-4}$ N, while the latter is linear over a tenfold concentration range. The non-linearity in a. c. polarography is probably due to the external impedance caused in the circuit. And the application of a. c. polarographic method to the quantitative determination of the anions is considered to be available, and for that purpose it must be cautioned that the external impedance in the circuit should be kept negligibly small.

## Summary

A train of a. c. polarographic investigations on several anions, which depolarize the dropping mercury anode, was carried out. The experimental results of a. c. polarography of $Cl^-$, $Br^-$, $I^-$ and $CN^-$ generally agreed with the theoretical consideration based on the reversible electrode process. Namely, it can be concluded that Breyer's polarogram shows the derivative curve of the ordinary polarogram and Fournier's current of these anions is regarded as the mean of two current intensities at both the extreme potentials of the pulsing potential produced by the superposition of a small a. c. voltage on the ordinary d. c. potential. Thus the electrode processes of these anions are found to be reversible. And the possibility of the application to the quantitative determination of these anions was found in the proper concentration range.

The authors are indebted to the polarographic group to which we belong for their advice during the course of the research.

*Department of Agricultural Chemistry*
*Faculty of Agriculture, Kyoto*
*University, Kyoto*

# *Microscopic Studies on Fused Catalysts for Ammonia Synthesis. IV. Decomposition of Ammonia over Two Different Constituents*

By Yoshio ŌSUMI

(Received August 25, 1954)

## Introduction

Many works on the iron catalyst for ammonia synthesis have been reported by many authors for these forty years. Many interesting results have been obtained about the role of potash added to the catalyst. But, so far as I am aware, no one has ever noticed the microscopic heterogeneity of the fused oxide, both before and after reduction.[1)]

As reported in our previous papers[2)], the optical, the surface-electron and the surface-ion microscopy revealed that the polished surface of some mixed catalysts in the unreduced state consists of two different sorts of grains. Of twelve catalysts investigated only those with potash or potash-alumina addition belong to this class.

Grains of the one sort (B) are found mainly along the boundaries of grains of the other sort (A), and the total quantity of B is very much less than that of A. B grains were found incidentally to be much less ferromagnetic than A grains. This fact furnished us with a convenient magnetic method of separating B grains from A grains. Chemical analysis showed that B powder was richer in $K_2O$ than A powder. X-ray examination[3)] showed that A powders separated from different sorts of catalysts always possessed the pattern of spinel lattice of magnetite, and B powders, on the other hand, highly complicated patterns which differed slightly from each other and probably belonged to slightly modified lattices of magnetite with reduced degrees of symmetry. It was suggested that magnetite would not contain more than about 0.5 per cent of potash in its lattice, so that during solidification B crystals would segregate to take over its

1) In one of our previous papers[3)] B grains have been considered to be formed only in fused oxides rich in alumina and potash. Later experiments, however, showed that potash exess alone was sufficient for their formation.

2) N. Sasaki and Y. Ōsumi, *J. Chem. Soc. Japan (Pure Chemistry Section, Japanese)*, **73**, 808 (1952); Y. Ōsumi, ibid., **74**, 308 (1953). More details of the results of optical-, electron- and ion-microscopy are found in: a) Y. Ōsumi, "*Ammonium sulfate Engineering*" (*in Japanese*) **16**, 13 (1952). b) Y. Ōsumi, ibid., **17**, 8 (1953). c) Y. Ōsumi, ibid., **18**, 11 (1953).

3) Y. Ōsumi, This Bulletin, **26**, 519, (1953). Y. Ōsumi, "*Ammonium Sulphate Engineering*" (*in Japanese*) **18**, 14 (1953).

exess[4]).

The present paper deals with the activities for the decomposition of ammonia at about one atmospheric pressure of A and B powders separated from an ordinary doubly promoted catalyst.

**Apparatus, Procedure and Preliminary Test.**—Since the separation of B powder is tedious work a very small quantity of it (0.5 g.) was taken for the experiment and accordingly a very low flow rate (3.8 cc. per minute) had to be chosen, so that an unusual type of gas analysis was employed (Fig. 1).

e. a ⟶ b ⟶ c,·····c ⟶ b ⟶ a.

Catalyst powders were placed in the lower halves of horizontal reaction tubes, which were of terex glass, 4.3 mm. in inner diameter and 60 mm. long (Fig. 1c). Each was inserted in one of three tunnels bored through a copper block which could be heated electrically (Fig. 1b). The size of capillary tube 17 is such that while the largest part of the gas coming from the reaction tubes is sucked into the absorber where high vacuum prevails at the beginning, a certain small fraction of it still flows through stop cocks 18 and 19 into the atmosphere. This can be ascertained by means of flowmeter 16 by closing stop cock 18

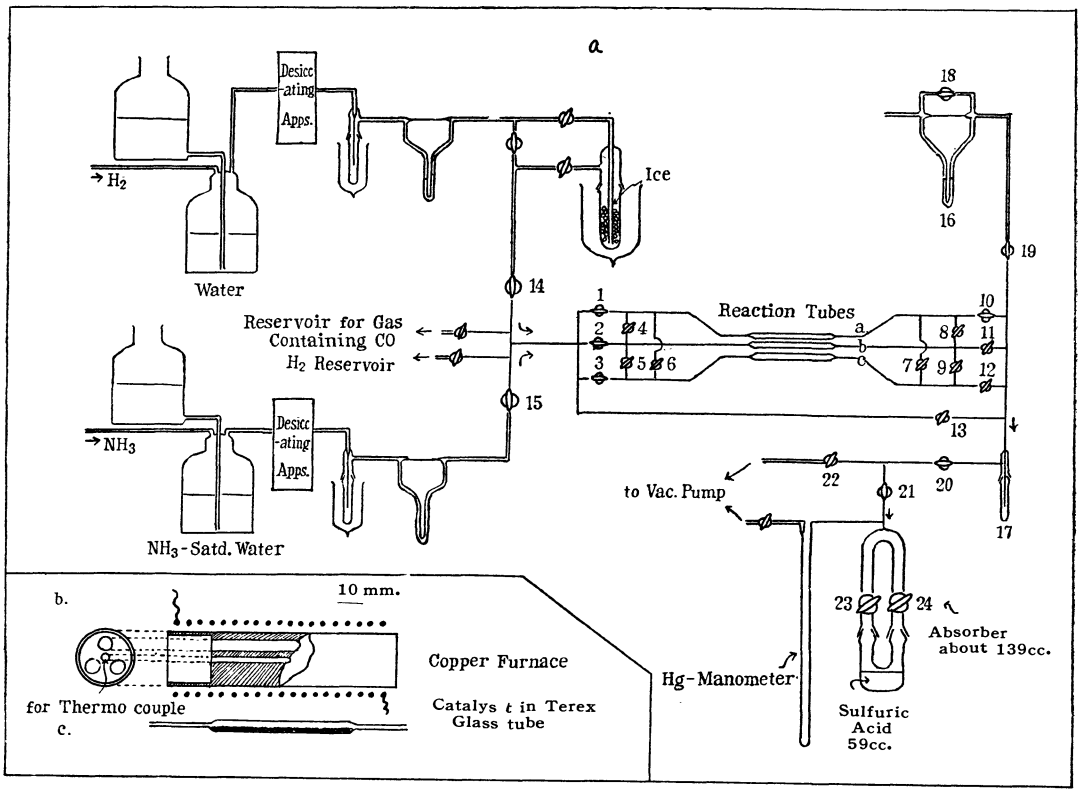



Fig. 1.

Electrolytic hydrogen gas was purified by passing through the solutions of potassium permanganate and potassium hydroxide, and over red hot copper, potassium hydroxide, and phosphorus pentoxide. Synthetic ammonia gas was dried over solid potassium hydroxide. The flow rate of each gas was kept nearly constant by inserting a buffer gas holder with large liquid levels before a capillary tube maintained at 25°C. In Fig. 1 straight lines beginning at stop cocks 14 and 15 show a system of capillary tubes, 1.5mm. in inner diameter. The gas can flow through three reaction tubes a, b and c in six different orders, i.

for a short time. Thus the pressure inside the reaction tubes can always be kept slightly higher than one atmosphere.

The analysis of the gas from the reaction tubes is carried out in the following way: after evacuating the absorber (with stop cocks 21–24 open and 20 closed), the gas is sucked into the upper part of the absorber (with stop cocks 22–24 closed and 20–21 open) up to the pressure of about 400 mm Hg, and stop cock 21 is closed. Cock 23 is then opened as slowly as possible and then 24 is opened. The gas now begins to circulate in the absorber and ammonia is absorbed rapidly.

A certain amount of unreduced catalyst powder was divided into three parts. Each was placed in one of the reaction tubes connected in series and reduced at the same time. Our purpose was

4) From thermomagnetic measurements the possible existence of more than one magnetic phase in highly promoted catalysts has been concluded by L. R. Maxwell, J. S. Smart and S. Brunauer, *J. Chem. Phys.*, **19**, 303 (1951).

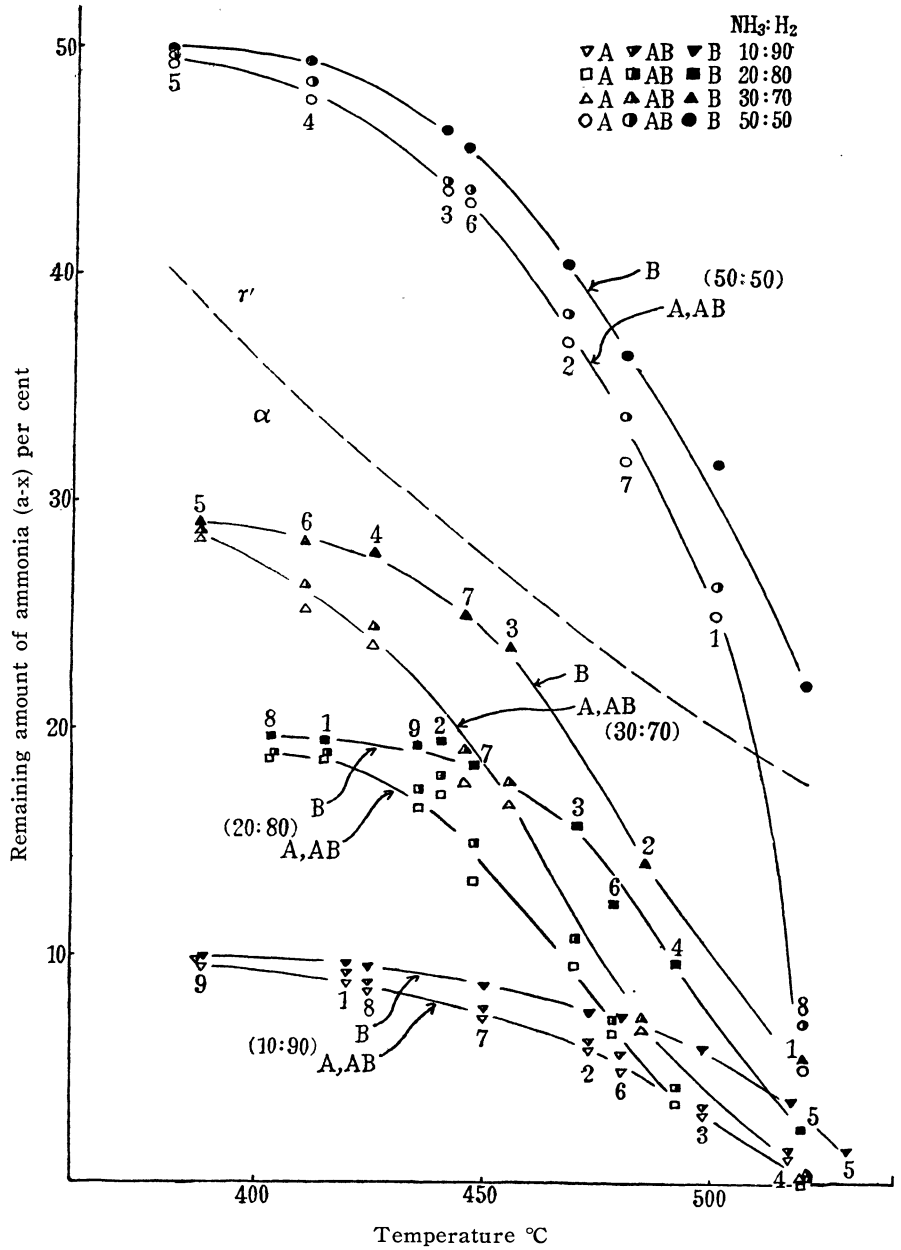



Fig. 2. Activities of A, B and AB powders for decomposing ammonia in $NH_3$-$H_2$ mixtures of various compositions.

(1, 2, 3,.....and a, b, c.....in the figure indicate the chronological order of data.)

From the ammonia per cent in original gas mixture (a) and that in decomposed gas mixture (b), the decomposed or remaining amount ($x$ or $a$-$x$) was calculated as following:

$$H_2+NH_3 \longrightarrow H_2 + NH_3+N_2$$
$$100-a \quad a \quad 100a-+3/2x \quad a-x \quad 1/2x$$

therefore $b/100=(a-x)/(100+x)$, $x=100\ (a-b)$.

to see whether the catalysts so prepared were equally active toward ammonia decompositions. Hydrogen gas was passed through the tubes in the order a ⟶ b ⟶ c for seven hours each at 350°C, 400°C, 450°C, 500°C successively and then for fourteen hours at 530°C, the flow rate being 2.7 cc. per minute. After the reduction the activity of the catalyst at several temperatures between 400°C and 500°C was measured separately for each tube by passing a mixture of ammonia and hydrogen gas (3: 7 in volume) at the rate of 3.7 cc. per minute through it. It was found that the activity decreased in the order a ⟶ b ⟶ c.

The reduction was then further continued by

passing hydrogen gas at 2.7 cc. per minute in the order c ⟶ b ⟶ a for seventeen hours and then in the order b ⟶ c ⟶ a for twenty-eight hours at 530°C. The three reaction tubes showed almost no difference in activity. The same was also the case when hydrogen gas at the rate of as high as 40 cc. per minute, was passed over the fresh oxide powder in one direction a ⟶ b ⟶ c only, the time and temperature schedule being the same as in the first instance. It may be inferred that the existence of a small amount of water vapour in hydrogen gas has a detrimental action.

Between runs the cold catalysts stood in hydrogen at about 800 mm Hg in order to prevent the intrusion of air.

**Activity of A and B Powders toward Decomposition of Ammonia in Ammonia-Hydrogen Mixtures of Various Composition.**—B powder amounting to about 3 per cent was separated from catalyst No. 4[5]. 0.5 g.[6] of each powder A, B and the original unseparated powder AB of the same mesh size (under about 300) was placed in three different tubes and reduced at the flow rate of 40 cc. per minute for 6 hours each at 300°C, 350°C, 400°C, 450°C, 470°C, 500°C and 520°C. In order to make the condition of reduction in each tube as equal as possible, the order of gas flow was altered every hour from one to another of the six ways. The ammonia-hydrogen gas mixtures for the decomposition test had the mixing ratios in volume, namely, 10: 90, 20: 80, 25: 75, 30: 70 and 50: 50. The results are shown in Fig. 2, the remaining amount of ammonia being expressed in % of the undecomposed original mixture. For all gas mixtures A and AB powders showed similar activity which was higher than that of B powder. The decomposed amount of the gas mixture 50: 50 is smaller than that of the mixture 30: 70 below about 500°C, but the situation is reversed above that temperature. This fact can be related to the work of Lehrer[7], who showed that four sorts of nitrides are formed by the action of mixtures of ammonia and hydrogen when the gas composition and temperature are suitably varied. It is significant that the broken line in Fig. 2 showing the boundary of $\alpha$ and $\gamma'$ nitrides crosses the curve for the 50: 50 mixture at about 500°C. The apparent energy of activation roughly calculated from the curves for the mixture 30: 70, was found to be 30 kcal. for B powder and 25 kcal. for A powder.

**The Poisoning Effect of Water Vapour and Carbon Monoxide.**—The influence of water vapour upon the activity was tested with three sorts of powders A, B and AB of catalyst No. 4. Hydrogen was passed through a bottle filled with crushed ice and placed in a bath kept at −7°C and then mixed with ammonia to the composition $NH_3$: $H_2$=1: 3 (Fig. 1a, Water vapour pressure over ice at

5) An iron catalyst including $Al_2O_3$ (5%), and $K_2O$ (1%).

6) For the scientific purpose activity per unit area of catalyst would be more significant than activity per unit mass. The measurement of the surface area is planned.

7) E. Lehrer, *Z. Elektrochem.*, **36**, 383 (1930).

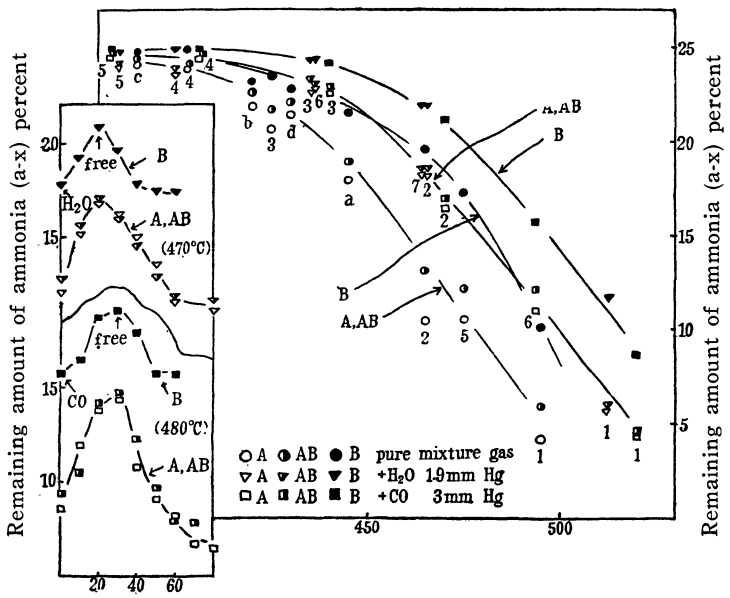



Fig. 3b.

Fig. 3a. Poisoning effects of water vapour and carbon monoxide.

−7°C is 2.54 mm Hg). The results are shown in Fig. 3a. A (AB) and B powders all show similar decreases in activity.

Carbon monoxide affected the activity to nearly the same extent, when the gas mixture was led to the reaction tubes from a gas holder in which 3 mm Hg of carbon monoxide had been diluted to the atmospheric pressure with the ammonia-hydrogen mixture 1: 3 (stop cocks 14, 15 and 19 being held closed).

The progress of poisoning and recovering were also studied by measuring the decomposition rate every ten minutes. These processes went on also similary on both powders (Fig. 3b). It is to be noted that the activity of A (and AB) powder is somewhat greater after recovering than before poisoning.

**The Effect of Thermal Treatment.**—After the activities of new samples of catalyst No. 4 were determined at temperatures between about 400 and 500°C using the gas mixture 30:70 (Fig. 4), the temperature was raised to about 740°C and kept for one hour in the hydrogen stream. No change in activity was observed on the next day. The catalysts were further heated at about 830°C for one hour. The powder now showed a lower activity at the beginning of the measurement, but later recovered the activity to the value before the heat treatment. B showed, however, less activity throughout the whole measurement.

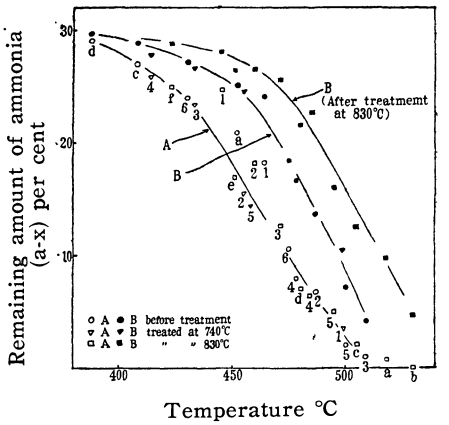



Fig. 4. Effect of heat treatment.

It seems that reduction at temperatures ranging from 300 to 520°C has caused a considerable grain growth of iron, and the heating at 740°C after the reduction does not effect any further change in the surface structure. The decrease in activity of B powder heated at 830°C may be considered, apart from the effect of simple sintering, in conjunction with our previous ion-microscopical observation that potassium in B powder above 800°C migrates through grain boundaries and evaporates from the surface.

**The Effect of Mixing B Powder to the Catalyst Singly Promoted with Alumina.**—As reported previously A and B powders

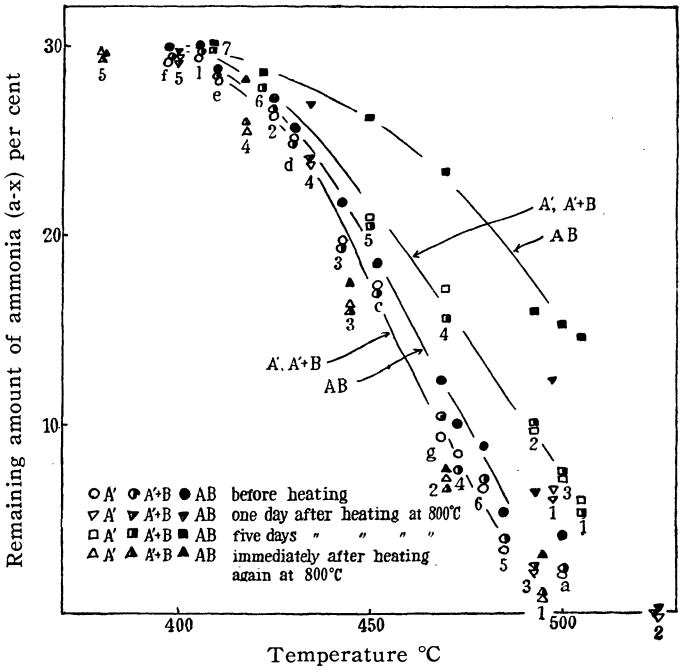



Fig. 5. Effects of adding B powder to alumina-promoted catalyst.

contain about 0.4 and 4 per cent of potash respectively. If potassium at the temperature of ammonia synthesis could now migrate from B powder to A powder, which has in some way lost potassium, B powder could play the role of potash source and contribute to the maintenance of activity of the catalyst. The idea was tested by the possible change in activity toward the ammonia decomposition of an alumina-promoted catalyst (A'), in which a small amount of B powder had been added before reduction.

The samples filled in the three tubes were respectively

(A') catalyst No. 2 (promoter: 5% $Al_2O_3$)

(A'+B) mixture of 97 parts of catalyst No. 2 and 3 parts of B powder from catalyst No. 4

(AB) catalyst No. 4 (promoters: 5% $Al_2O_3$ and 1% $K_2O$)

The result is that A' and A'+B are almost equally and AB somewhat less active (Fig. 5). They were then heated for one hour at 800°C. On the following day A' and A'+B were found to be as active as before the heating (though they showed lower activities at the beginning of measurement), while AB showed somewhat less active (Fig. 5). If left for five days after reduction both A' and A'+B showed similar decreases in activity, and AB a greater decrease. These catalysts were again subjected to the same heat treatment and their activities were immediately measured. They were found to be rather greater than before the first heat treatment. As to the mechanisms of the recovery of activity during the decomposition tests and the diminution of activity during preservation at room temperature, various explanations are possible, but none of them has yet been tested experimentally.

In any case we may conclude that potassium in B grains probably does not play any important role in the commercial synthesis of ammonia.

## Summary

An unreduced iron synthetic ammonia catalyst promoted with potash or potash and alumina was separated into two different sorts of powders (A and B). Some of their properties were mentioned in the previous reports. Their catalytic activities for decomposing ammonia mixed with hydrogen were studied at atmospheric pressure by a specially devised flow method. The results are:

1. Between about 400°C and 500°C and for the gas mixtures of several compositions, A powder is more active than B.
2. The actions of the gas mixture laden with water vapour over ice kept in a −7°C bath and of that with 0.4% carbon monoxide are much the same in the rate and extent of poisoning as well as in the rate of recovering when the admixing of the poisoning gases is discontinued. As to the liability to the effects, one sort of powder scarcely differs from another.
3. Heating at 740°C for one hour has no effect. Heating at 830°C for one hour makes B powder less active and A powder also less active at first, but its activity before heating is soon recovered in the course of a run.
4. The activity of a potash-free alumina-promoted catalyst is not affected by adding before reduction a small amount of potash-rich B powder.

I should like to express my sincere thanks to Professor Nobuji Sasaki for his kind guidance throughout this work.

*Department of Chemistry, Faculty of Science, Kyōto University, Kyōto, and Mitsubishi Kasei Co.*

# *A Physico-chemical Study on the Hydrolysis of Thorium Nitrate*

By Kuan PAN and Tong Ming HSEU

(Received July 14, 1954)

It has been known that all tetrapositive ions exhibit strong tendencies toward polymerization accompanied by hydrolysis. The hydrolysis and polymerization of zirconium in perchloric acid solution has been investigated by Connick and his coworkers[1,2] and it has been shown that in 2 M perchloric acid at 25°C the average zirconium species at low zirconium concentration has a charge somewhere between +3 and +4, corresponding to a mixture of $Zr^{+4}$ and $ZrOH^{+3}$ or possibly $ZrO^{2+}$. It has also been known that thorium salts produce acidic solution and that gelatinous thorium hydroxide is precipitated from an old aqueous solution of thorium nitrate. Qualitatively, however, thorium salts exhibit a less marked tendency to hydrolyze in aqueous solution than zirconium, and little quantitative investigation has been found in previous literatures*[3]. The purpose of the present work is to study the hydrolysis of thorium nitrate in a very dilute solution and in the presence of sodium perchlorate which has been used for maintaining the solution at constant ionic strength by means of the pH measurement with glass electrode. The assumption is that in the presence of sodium perchlorate, there is no complicating effect such as polymerization and colloid formation except in the case of hydrolytic behavior. For purposes of calculation, the data are treated as though the activity coefficients of all ion species are equal to unity in a very dilute solution, or remain constant at constant ionic strength. The equilibrium constants of thorium ion species are calculated stoichiometrically from the data of hydronium ion concentration observed and the total concentration of thorium nitrate.

## Experimental

A) **Materials.** — Conductivity water with a specific conductivity of 1.6 to $2.4\times10^{-6}$ mho was used throughout this experiment.

Thorium nitrate of C. P. grade was purified by the hydrogen peroxide method[4] and then by the hexamine method[5]. The washed hydroxide was digested in sufficient nitric acid, and evaporated to dryness after each of repeated additions of water to remove the excess of acid. The hydrate of thorium nitrate was obtained by recrystallization. The stock solution of thorium nitrate was prepared directly by dissolving the salt in conductivity water free from carbon dioxide. The concentration of the stock solution was checked by the gravimetric method before use.

B) **Procedure and Apparatus.**—Solutions with the initial concentration of $10^{-2}$ mol. of thorium nitrate were made to be 0.05, 0.1, 0.3 and 0.5 M with respect to sodium perchlorate, respectively. Each solution was diluted successively with an equal volume of the sodium perchlorate solution of the specified concentration, so that the concentration of thorium nitrate was diluted to one half while the solution was kept practically at constant ionic strength.

The change in pH during the dilution was followed with a vacuum tube potentiometer, constructed in our laboratory as shown in one of the previous papers[6]. The glass electrode made by Beckman Instrument Inc., in U. S. A., and a vacuum tube, UX-54 A, made by Matsuda Co. in Japan were used in the potentiometer circuit.

The glass electrode was frequently calibrated against a series of pH buffer solutions. The pH measurement was carried out in an oil thermostat controlled at 25°±0.1°C. Approximately ten-minute intervals were allowed for the attainment of equilibrium in each measurement.

## Result and Discussion

When thorium nitrate dissolves in a dilute solution and in the presence of sodium perchlorate which is used for maintaining the solution at constant ionic strength, it may be assumed that the pH value of the solution is governed by no complicating effect, but the hydrolytic behavior for which the following reactions involving thorium ion species may be supposed:

$$Th^{+4}+H_2O \rightleftarrows Th(OH)^{+3}+H^+,\ K_1 \quad (1)$$

$$Th^{+4}+2H_2O \rightleftarrows Th(OH)_2^{+2}+2H^+,\ K_2 \quad (2)$$

$$\cdots\cdots\cdots\cdots$$

$$Th^{+4}+nH_2O \rightleftarrows Th(OH)_n^{4-n}+nH^+,\ K_n \quad (3)$$

* There are some reports on this problem, e.g., K. A. Kraus and R. W. Holmberg, U.S. Atomic Energy Commission Report (1950), which are not available to us.

1) Robert E. Connick and William H. McVey, *J. Am. Chem. Soc.*, **71**, 3182 (1949).

2) Robert E. Connick and William H. Reas, ibid., 73, 1171 (1951).

3) R. Schaal and J. Faucherre, *Bull. soc. chim. France*, **1947**, 927.

4) Arthur C. Neish, *J. Am. Chem. Soc.*, **26**, 781, (1904).

5) H. H. Willard and L. Gordon, *Anal. Chem.*, 26, 165 (1948).

6) K. Pan and T. M. Hseu, This Bulletin, **26**, 126 (1953).

Then if the most possible type of reaction among them is the $n$-th type, the hydrolysis constant, $K_n$, may be given by the following equation:

$$K_n=\frac{a_X\cdot a_H}{a_{Th}}=\frac{f_X f_H{}^n}{f_{Th}}\cdot\frac{C_X\cdot C_H{}^n}{C_{Th}}, \quad (4)$$

where $a_{Th}$, $a_X$, $a_H$; $f_{Th}$, $f_X$, $f_H$ and $C_{Th}$, $C_X$, $C_H$ are the activities, activity coefficients and concentrations of ion species, $Th^{+4}$, $Th(OH)_n{}^{+4-n}$ and $H^+$, respectively.

Then if the degree of hydrolysis is small, as a first approximation, equation (4) may be expressed as follows:

$$K_n\fallingdotseq\frac{f_X\cdot f_H{}^n}{f_{Th}}\frac{C_H{}^{n+1}}{nC} \quad (5)$$

$$\fallingdotseq K_f\frac{a_H{}^{n+1}}{nC}, \quad (6)$$

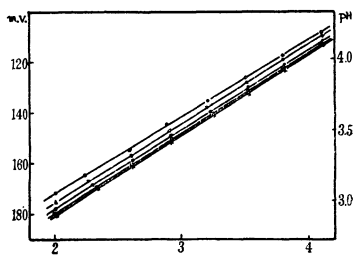
where $C$ is the total concentration of the salt and $K_f=\frac{f_X}{f_{Th}\cdot f_H}$ is a constant at a constant ionic strength, consequently,

$$pH=\frac{1}{n+1}[pK_n-pK_f-\log n]-\frac{1}{n+1}\log C \quad (7)$$

$$=K-\frac{1}{n+1}\log C, \quad (8)$$

that is to say, a linear relation may be held between pH and $-\log C$, and the differential quotient of pH with respect to $-\log C$ is $\frac{1}{n+1}$.

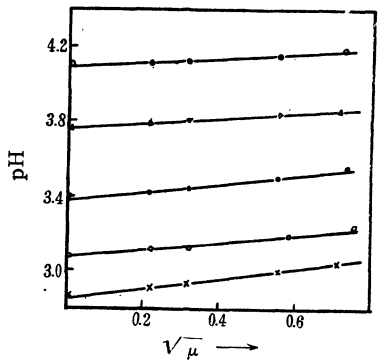
As shown in Fig. 1, the curves plotting pH vs. $-\log C$ from 0.01 to 0.0001 M of thorium nitrate in sodium perchlorate solution as well as in pure water run parallel with each other and the slope is nearly equal to 1/2, that is, $n=1$, one may pressume that the existence of the ion, $Th(OH)^{+3}$ is highly probable. The linear relationship between the square root of ionic strength and pH at each concentration is indicated in Fig. 2.




⟶ $-\log C$.

×: in pure water
○: in 0.05M $NaClO_4$ soln.
●: in 0.1M $NaClO_4$ soln.
△: in 0.3M $NaClO_4$ soln.
○: in 0.5M $NaClO_4$ soln.

Fig. 1.




○: C $7.8\times10^{-5}$ △: C $=3.125\times10^{-4}$
●: $1.25\times10^{-3}$ □: $5.00\times10^{-3}$
×: $1.00\times10^{-2}$

Fig. 2.

In fact, since the hydrogen ion concentration in thorium nitrate solution is not so low as to be negligible against the total concentration of the salt, the above calculation is nothing but an approximate estimation. It suggests, however, that the average thorium ion species at this concentration range has a charge between +4 and +3 or even possibly +2, corresponding to a mixture of $Th^{+4}$, $Th(OH)^{+3}$ and $Th(OH)_2{}^{+2}$ or possibly $ThO^{+2}$.

For the purposes of calculating the equilibrium constants the data are treated as though the activity coefficients of all species in solution remain strictly constant at constant ionic strength and the general equilibrium constant is stoichiometrically expressed as

$$K_n=\frac{[Th(OH)_n{}^{4-n}]\ [H^+]^n}{[Th^{+4}]}. \quad (9)$$

Thus by expressing the total concentration of thorium and hydronium ion in a solution as a function of the equilibrium constants of all ion species as shown by the following stoichiometric relations,

$$[Th]_t=[Th^{+4}]+[Th(OH)^{+3}]+[Th(OH)_2{}^{+2}]\cdots\cdots$$

$$=[Th^{+4}]\left\{1+\frac{K_1}{[H^+]}+\frac{K_2}{[H^+]^2}\cdots\cdots\right\}$$

$$=[Th^{+4}]\left\{1+\sum_n\frac{K_n}{[H^+]^n}\right\} \quad (10)$$

and

$$[H^+]=[Th(OH)^{+3}+2[Th(OH)_2{}^{+2}]$$

$$+3[Th(OH)_3{}^{+1}]\cdots\cdots=[Th^{+4}]\left\{\frac{K_1}{(H^+)}+\right.$$

$$\left.\frac{K_2}{[H^+]^2}+\cdots\cdots\right\}=[Th^{+4}]\sum_n n\frac{K_n}{[H^+]^n}. \quad (11)$$

The stoichiometric ratio, $r$, of the hydronium ion concentration and the total concentration of thorium in the solution is expressed as follows:

$$r=\frac{[H^+]}{[Th]_t}=\frac{\sum_n K_n/[H^+]^n}{1+\sum K_n/[H^+]^n}, \qquad (12)$$

where $[Th]_t$ is the total concentration of thorium.

An attempt has been made to apply the experimental data to equation (12) for calculating the equilibrium constants of four ion species of $Th(OH)_n^{4-n}$, where $n$ takes all the values of 1. 2, 3 and 4, using the least square method, but two negative values are obtained for two of the four constants which indicates the inadequacy of the application.

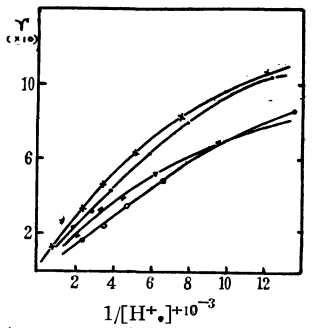
On the other hand, by assuming the existence of the ion species of $Th^{+4}$, $Th(OH)^{+3}$ and $Th(OH)_2^{+2}$ in the same solution of the specified condition as suggested by the above approximate estimation, and applying the same data to equation (12) to calculate the equilibrium constants, reasonable values of $K_1$ and $K_2$ for reactions (1) and (2) are obtained by the same method, as shown in Table I. Experimental values of $r$ are plotted against $\frac{1}{[H^+]}$ at varying ionic strengths in Fig. 3.

TABLE I

CONCENTRATION EQUILIBRIUM CONSTANTS AT VARYING IONIC STRENGTHS AT 25°C

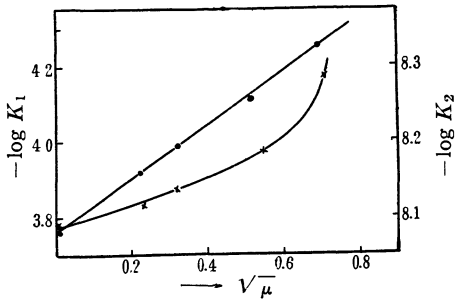
| Ionic strength (In $NaClO_4$ solutions) | $K_1(\times 10^4)$ | $K_2(\times 10^9)$ |
|---|---|---|
| 0.5 M | 0.55 | 5.2 |
| 0.3 M | 0.76 | 6.5 |
| 0.1 M | 1.0 | 7.3 |
| 0.05 M | 1.2 | 7.7 |
| 0 | 1.3 | 8.2 |
| In pure water | 1.7 | 8.2 |

The dissociation constants expressed as concentration equilibrium constants are strictly valid, however, only for solutions at constant ionic strength. The limiting values of $K_1$ and $K_2$ obtained by plotting $K_1$ and $K_2$ against $\sqrt{\mu}$ in Fig. 4, and extrapolating to zero ionic strength are $1.3\times10^{-4}$ and $8.2\times10^{-9}$, respectively.




×: in pure water
●: in 0.1M $NaClO_4$ soln.
△: in 0.3M $NaClO_4$ soln.
○: in 0.5M $NaClO_4$ soln.

Fig. 3.




●: $K_1$ ×: $K_2$

Fig. 4.

## Summary

1) The dilution effect on the pH change in a dilute solution and in the presence of sodium perchlorate was followed by a glass electrode.

2) A linear relationship is held between pH and $-\log C$. The curves plotting pH vs. $-\log C$ run parallel with each other at varying ionic strengths, and the slope is nearly equal to 1/2 by which the most possible existence of $Th(OH)^{+3}$ is pressumed.

3) The equilibrium constants for ion species, $ThOH^{+3}$ and $Th(OH)_2^{+2}$, are calculated stoichiometrically from the data of hydronium ion concentration observed and the total concentration of thorium nitrate.

*Department of Chemistry,*
*College of Science,*
*National Taiwan University*

# *Dipole Moments of 2,3-Dihalogeno-2,3-dimethylbutanes*

By Yonezo MORINO, Ichiro MIYAGAWA, Toshio HAGA, and San-ichiro MIZUSHIMA

(Received September 8, 1954)

## Introduction

It has been shown by the measurements of the Raman effect, infrared spectra, dipole moment, etc., that 1,2-dihalogenoethanes[1,2] and simple hydrocarbons[2] are the equilibrium mixtures of the rotational isomers. However, 2,3-dibromo-2,3-dimethylbutane has been concluded by the spectoscopic investigation by Cleveland and Lamport[3] to have only one isomer (the *trans* isomer with center of symmetry in benzene and in carbon tetrachloride solutions). On the other hand van Arkel and Snoeck[4] reported a fairly large value 1.35 D of the dipole moment of 2,3-dichloro-2,3-dimethylbutane in benzene solution in spite of the vanishing moment in carbon tetrachloride solution. According to this result we have to assume the existence of both the *trans* and gauche forms in benzene solution, whereas we assume only the *trans* form with no moment in carbon tetrachloride solution. This does not seem to be compatible with our conclusions on rotational isomerism. At least, such a large solvent effect as that found by van Arkel and Snoeck will not be expected. In view of this situation it is desirable to measure the dipole moments of these substances more accurately in various solvents and at different temperatures.

## Experimental

**$Cl(CH_3)_2C$-$C(CH_3)_2Cl$.**—Pinacon was treated with aqueous solution of hydrochloric acid saturated at −20°C, and the reaction product was allowed to stand for several days. The precipitate was recrystalized with ethyl ether and purified by sublimation: m.p. 155–156°C.

**$Br(CH_3)_2C$-$C(CH_3)_2$.**—The sample was supplied by Professor Cleveland, Illinois Institute of Technology. It is the same sample as that used by him and Lamport for the measurement of the Raman and infrared spectra. It was recrystalized from the solution and purified by sublimation: m.p. 157.4–158.5°C.

**Benzene.**—The commercial product was boiled with aluminium chloride for one hour, treated with concentrated sulphuric acid several times, dried over sodium, and then fractionally distilled: b.p. 80.0–80.5°C.

**Carbon Tetrachloride.**—The commercial product was dried over calcium chloride and then fractionally distilled: b.p. 75.6–75.9°C.

The apparatus and the method of the measurement of dielectric constant were already described in a previous paper[5]. The density of the solution at 25°C was measured with a pycnometer, and those at other temperatures were obtained by measuring the volume change of the solutions by use of a dilatometer.

## Results

The observed values of dielectric constant $\epsilon$ and the density $d$ of these substances in carbon tetrachloride and benzene solutions are shown in Tables I and II, where $w$ is the

TABLE I

DIELECTRIC CONSTANT, DENSITY, AND MOLECULAR POLARISATION OF 2,3-DICHLORO-2,3-DIMETHYLBUTANE

($P_E+P_A=MR_D=39.66$ cc.).

Benzene Solution (25°C).

| $w$ | $\varepsilon$ | $d$ |
|---|---|---|
| 0.00000 | 2.2720 | 0.8721 |
| 0.01439 | 2.3023 | 0.8755 |
| 0.02365 | 2.3198 | 0.8767 |
| 0.04225 | 2.3561 | 0.8797 |
| 0.06983 | 2.4089 | 0.8835 |
| 0.09048 | 2.4512 | 0.8865 |

$\varepsilon_\infty=2.2740$, $d_\infty=0.8734$,

$a=1.945$, $b=0.145$, $P_{2\infty}=101.0\pm0.4$ cc.

Carbon Tetrachloride Solution (−20°C).

| $w$ | $\varepsilon$ | $d$ |
|---|---|---|
| 0.00000 | 2.3109 | 1.6770 |
| 0.01053 | 2.3344 | 1.6677 |
| 0.01428 | 2.3426 | 1.6644 |
| 0.02134 | 2.3584 | 1.6582 |
| 0.02650 | 2.3700 | 1.6537 |

$\varepsilon_\infty=2.3111$, $d_\infty=1.6771$,

$a=2.23$, $b=0.880$, $P_{2\infty}=76.4$ cc.

1) S. Mizushima, Y. Morino, I. Watanabe, T. Shimanouchi, and S. Yamaguchi, *J. Chem. Phys.*, **17**, 591 (1949).

2) S. Mizushima, "Structure of Molecules and Internal Rotation", Academic Press Inc., New York (1954).

3) F. F. Cleveland and J. E. Lamport, *J. Chem. Phys.*, **18**, 1320 (1950).

4) A. E. van Arkel and J. L. Snoeck, *Z. Physik. Chem.*, **B18**, 159 (1932).

5) Y. Morino, I. Miyagawa, and T. Oiwa, *Botyu-Kagaku*, **15**, 181 (1950).

(0°C).

| | | |
|---|---|---|
| 0.00000 | 2.2722 | 1.6346 |
| 0.01053 | 2.2954 | 1.6257 |
| 0.01428 | 2.3037 | 1.6226 |
| 0.02134 | 2.3192 | 1.6167 |
| 0.02650 | 2.3301 | 1.6123 |

$\varepsilon_\infty=2.2720$, $d_\infty=1.6346$,
$a=2.20$, $b=0.840$, $P_{2\infty}=77.2$ cc.

(25°C).

| | | |
|---|---|---|
| 0.00000 | 2.2254 | 1.5840 |
| 0.01053 | 2.2480 | 1.5757 |
| 0.01428 | 2.2557 | 1.5727 |
| 0.02134 | 2.2710 | 1.5671 |
| 0.02650 | 2.2821 | 1.5630 |

$\varepsilon_\infty=2.2252$, $d_\infty=1.5840$,
$a=2.14$, $b=0.791$, $P_{2\infty}=77.8$ cc.

(55°C).

| | | |
|---|---|---|
| 0.00000 | 2.1651 | 1.5270 |
| 0.01053 | 2.1872 | 1.5189 |
| 0.01428 | 2.1954 | 1.5160 |
| 0.02134 | 2.2098 | 1.5105 |
| 0.02650 | 2.2206 | 1.5066 |

$\varepsilon_\infty=2.1653$, $d_\infty=1.5270$,
$a=2.10$, $b=0.771$, $P_{2\infty}=79.8$ cc.

TABLE II

DIELECTRIC CONSTANT, DENSITY, AND MOLECULAR POLARISATION OF 2,3-DIBROMO-2,3-DIMETHYLBUTANE

($P_E+P_A=MR_D=45.46$ cc.).

Benzene Solution (25°C).

| | | |
|---|---|---|
| 0.00000 | 2.2720 | 0.8721 |
| 0.01529 | 2.2830 | 0.8785 |
| 0.01929 | 2.2858 | 0.8801 |
| 0.02903 | 2.2926 | 0.8841 |
| 0.03837 | 2.2987 | 0.8876 |

$\varepsilon_\infty=2.2729$, $d_\infty=0.8725$,
$a=0.679$, $b=0.454$, $P_{2\infty}=76.6\pm0.4$ cc.

Carbon Tetrachloride Solution (−15°C).

| | | |
|---|---|---|
| 0.00000 | 2.3032 | 1.6662 |
| 0.00828 | 2.3102 | 1.6659 |
| 0.01100 | 2.3124 | 1.6664 |
| 0.01591 | 2.3170 | 1.6658 |
| 0.02046 | 2.3202 | 1.6665 |

$\varepsilon_\infty=2.3032$, $d_\infty=1.6662$,
$a=0.84$, $b=0$, $P_{2\infty}=63.7$ cc.

(+6°C).

| | | |
|---|---|---|
| 0.00000 | 2.2622 | 1.6224 |
| 0.00828 | 2.2692 | 1.6221 |
| 0.01100 | 2.2716 | 1.6225 |
| 0.01591 | 2.2762 | 1.6220 |
| 0.02046 | 2.2800 | 1.6224 |

$\varepsilon_\infty=2.2620$, $d_\infty=1.6223$,
$a=0.86$, $b=0$, $P_{2\infty}=65.9$ cc.

(25°C).

| | | |
|---|---|---|
| 0.00000 | 2.2259 | 1.5849 |
| 0.00828 | 2.2332 | 1.5847 |
| 0.01100 | 2.2354 | 1.5851 |
| 0.01591 | 2.2398 | 1.5845 |
| 0.02046 | 2.2450 | 1.5851 |

$\varepsilon_\infty=2.2261$, $d_\infty=1.5849$,
$a=0.86$, $b=0$, $P_{2\infty}=67.1$ cc.

(55°C).

| | | |
|---|---|---|
| 0.00000 | 2.1640 | 1.5259 |
| 0.00828 | 2.1714 | 1.5255 |
| 0.01100 | 2.1740 | 1.5259 |
| 0.01591 | 2.1788 | 1.5257 |
| 0.02046 | 2.1831 | 1.5261 |

$\varepsilon_\infty=2.1640$, $d_\infty=1,5258$,
$a=0.91$, $b=0$, $P_{2\infty}=69.8$ cc.

concentration of the solute in weight fraction. The molecular polarisation $p_{2\infty}$ of the solute extrapolated to infinite dilution was calculated by use of the Halverstadt and Kumler equation[6]:

$$p_{2\infty}=(\varepsilon_0-1)/(\varepsilon_0+2)\cdot M_2/d_0\cdot \{1+3a/(\varepsilon_0-1)(\varepsilon_0+2)-b/d_0\}, \quad (1)$$

where $M_2$ denotes the molecular weight of the solute, $\varepsilon_0$ and $d_0$ the dielectric constant and the density extrapolated to zero concentration, and $a$ and $b$ the inclination of the lines of $\varepsilon$ vs. w and $d$ vs. w respectively. The dipole moment was calculated by the Debye equation:

$$\mu=0.0128\{p_{2\infty}-(p_E+p_A)\}^{1/2}T^{1/2} \quad (2)$$

where $p_E$ and $p_A$ are the electronic and atomic polarisations. $p_E+p_A$ was assumed to be equal to $MR_D$, which was calculated from the atomic refractions of the constituent atoms. It is easily seen that this approximation does not affect our conclusion on the temperature dependence of dipole moment.

## Discussion of Results

**1. Rotational Isomers.**—In the present experiment finite moments were observed for 2,3-dichloro-2,3-dimethylbutane in carbon tetrachloride solution as well as in benzene solution, in contrast to the result obtained by van Arkel and Snoek. This was also shown to be the case for 2,3-dibromo-2,3-dimethylbutane. Our results are shown in Table III, in which the experimental data in heptane solution obtained previously by one of us[7] are also included.

6) I. F. Halverstadt and W. D. Kumler, *J. Am. Chem Soc.*, **64**, 2988 (1942).
7) I. Miyagawa, *J. Chem, Soc. Japan*, **75**, 1162 (1954).

TABLE III

DIPOLE MOMENTS OF 2,3-DICHLORO- AND 2, 3-DIBROMO-2, 3-DIMETHYLBUTANE IN VARIOUS SOLUTIONS (D)

| °C | Chloro-compound | | | Bromo-compound | | |
|---|---|---|---|---|---|---|
| | B[a] | CT[b] | Hp[c] | B[a] | CT[b] | Hp[c] |
| −20 | | 1.24 | 1.14 | | | 0.77 |
| −15 | | | | | 0.88 | |
| 0 | | 1.30 | | | | |
| 1 | | | 1.23 | | | 0.84 |
| 6 | | | | | 0.97 | |
| 25 | 1.74 | 1.37 | 1.31 | 1.24* | 1.03* | 0.96 |
| 50 | | | 1.41 | | | 1.02 |
| 55 | | 1.47 | | | 1.15 | |

a) Benzene solution,
b) Carbon tetrachloride solution,
c) Heptane solution[7].
* The values referred to by Cleveland and Lamport[3], 1.20 and 1.01 D, in B and CT solution respectively, should be corrected as shown in the Table. The difference between the values of Cleveland and Lamport and of us comes from whether $P_E+P_A$ is taken as $MR_D$ or as 1.05 $MR_D$ (the former).

The result obtained by Cleveland and Lamport on the Raman and infrared spectra of dibromodimethylbutane was explained by the existence of the *trans* form only, and therefore, was in apparent agreement with van Arkel's result of vanishing moment of dichlorodimethylbutane in carbon tetrachloride solution. Actually, however, there is a difficulty in this explanation, since the finite moment was observed in benzene solution and no difference in Raman spectra have been detected between benzene and carbon tetrachloride solutions. Thus van Arkel's result is not consistent with that obtaind by Cleveland and Lamport.

The dipole moment of the rigid *trans* form is evidently zero, and even if the rotational vibration about the trans position is taken into account, the moment value will not exceed 0.3 *D* (see Appendix). Therefore, we have to conclude the existence of a rotational isomer with a finite moment. This should be the less stable isomer, since the apparent moments of these compounds increase with temperature. From the analogy to 1,2-dihalogenoethanes this isomer can reasonably be assumed to be the gauche form, which is obtained from the *trans* form by an internal rotation by about 120°C.

The values of the dipole moment observed at a fixed temperature depend considerably upon the solvent as shown in Table III. In particular, the values observed in benzene solutions are much higher than those in other solutions. This result is quite analogous to that obtained for 1,2-dihalogenoethanes and many other compounds showing rotational isomerism[2] and is a further evidence of the existence of rotational isomers for dichloro- and dibromo-dimethylbutanes.

Let the number of the *trans* molecules be $N_t$ and that of the gauche molecules be $N_g$. Then we have:

$$N_g/N_t=2(\Omega_V{}^g\Omega_R{}^g\Omega_{int}{}^g)/(\Omega_V{}^t\Omega_R{}^t\Omega_{int}{}^t)\cdot \exp(-\Delta E/kT), \quad (3)$$

where $\Omega_{int}$ is the partition function for the internal rotation about the C−C axis, $\Omega_V$ and $\Omega_R$ the vibrational and rotational partition functions (excluding the internal rotation), and $\Delta E$ the energy difference of the two isomers. For the vibrational and rotational partition functions Gwinn and Pitzer[8] have shown the approximate relation:

$$\Omega_V{}^g\Omega_R{}^g/\Omega_V{}^t\Omega_R{}^t=1. \quad (4)$$

Therefore, we may assume the same relation for dichloro- and dibromo-dimethylbutane and can avoid the difficulty arising from the ambiguity of the assignment of the normal frequencies. If we assume further that $\Omega_{int}{}^g/\Omega_{int}{}^t=1$, eq. (3) is reduced to:

$$N_g/N_t=2\exp(-\Delta E/kT), \quad (5)$$

and the mean dipole moment is calculated as:

$$\bar{\mu}^2=(N_t\mu_t{}^2+N_g\mu_g{}^2)/(N_t+N_g) =\{\mu_t{}^2+2\mu_g{}^2\exp(-\Delta E/kT)\}/\{1+2\exp(-\Delta E/kT)\}, \quad (6)$$

or

$$\bar{\mu}^2-\mu_t{}^2=(\mu_g{}^2-\mu_t{}^2)G(x), \quad (7)$$

where

$$G(x)=2\exp(-x)/\{1+2\exp(-x)\}, \quad (8)$$

and

$$x=\Delta E/kT. \quad (9)$$

The calculation of the energy difference $\Delta E$ and the moment $\mu_g$ of the gauche form from the mean moments observed at different temperatures is made according to the method proposed by Lennard-Jones and Pike[9].

First $G(x)$ is calculated for various values of $x=0\sim\infty$, and a curve is drawn for log $G(x)$ against log $x$. The experimental curve representing log $(\mu_{obs}{}^2-\mu_t{}^2)$plotted against log $1/T$ should be superposable on some part of the theoretical curve log $G(x)$ *vs.* log $x$. Hence, by shifting the experimental curve along $x$- and $y$-axes so as to superpose it on the $G(x)\sim$log $(x)$ curve as much as possible, $\Delta E$ and $(\mu_g{}^2-\mu_t{}^2)$ are obtained from the displacements in $x$- and $y$-directions. In this treatment the value of $\mu_t$ should be known

8) W. D. Gwinn and K. S. Pitzer, *J. Chem. Phys.*, **16**, 303 (1948).
9) J. E. Lennard-Jones and H. H. M. Pike, *Trans. Faraday Soc.*, **30**, 830 (1934).

in advance. We have used two extreme values of $\mu_t$, 0.0D and 0.3D, since as referred to above $\mu_t$ should be less than 0.3D.*

The results thus obtained are shown in Table IV, the estimated error in the value

TABLE IV

THE ENERGY DIFFERENCE BETWEEN THE ROTATIONAL ISOMERS OF DIHALOGENODIMETHYLBUTANE

| Compound | Solvent | $\Delta E$ (kcal./mol.) | $\mu_t$ (D) | $\mu_g^{obs}$ (D) | $\mu_g^{calc}$ (D) |
|---|---|---|---|---|---|
| DCl | CT | 1.10 | 0 | 2.8 | 3.33 |
| | | 1.10 | 0.3 | 2.8 | |
| | Hp | 1.30 | 0 | 3.1 | |
| | | 1.30 | 0.3 | 3.2 | |
| DBr | CT | 1.45 | 0 | 2.6 | 3.30 |
| | | 1.60 | 0.3 | 2.6 | |
| | Hp | 1.50 | 0 | 2.6 | |
| | | 1.50 | 0.3 | 2.6 | |

of the energy difference being ±0.15 kcal/mol. It makes almost no difference, whether the value of $\mu_t$ be taken as 0.0D or as 0.3D. We see that there is dependence upon the solvent of the energy difference of dichlorodimethylbutane, although this is less pronounced than that observed for 1,2-dihalogenoethanes[10]. An explanation of the change of $\Delta E$ with solvent has been given in the case of 1,2-dihalogenoethanes[11,12]. In a medium of dielectric constant $\varepsilon$ the gauche isomer is stabilized by an amount of energy $(\varepsilon-1)/(2\varepsilon+1)\cdot\mu^2/a^3$ as compared with the trans isomer, where $a$ is the radius of the solute molecule. In other words the energy difference between the rotational isomers of dichloroethane decreases with the increasing polarity of the solvent. The same consideration would apply for dichlorodimethylbutane.

In contrast to the case of dichlorodimethylbutane, $\Delta E$ of the corresponding dibromo-compound was found to be almost independent of the solvent and, accordingly, $\Delta E$ in vacuum will also be 1.5 kcal./mol. In connection with this it may be noted that the change of $\Delta E$ of 1,2-dibromoethane with solvent was found by the earlier measurements[13,14,15] to be small as compared with dichloroethane. The accuracy of these measurements is not so high as in the case of those made recently, but they can be considered as experimental evidence in support of our conclusion on dichloro- and dibromo-dimethylbutanes.

In the earlier investigations on the internal rotation[2,13], the temperature dependence of dipole moment was explained on the assumption that the molecules exert rotatory vibration about the *trans* position which corresponds to the single minimum of the potential curve. The mean dipole moment was calculated by Lennard-Jones and Pike[9] as:

$$\bar{\mu}^2=2\mu_{2\perp}{}^2F(x), \tag{11}$$

where

$$F(x)=\int_0^{2\pi}(1-\cos\theta)\exp\{-x(1-\cos\theta)\}d\theta/\int_0^{2\pi}\exp\{-x(1-\cos\theta)\}d\theta, \tag{12}$$

and

$$x=V_0/2kT, \tag{13}$$

and

$$V=1/2\cdot V_0(1-\cos\theta). \tag{14}$$

Here $\mu_\perp$ is the component of the dipole moment of the rotating group perpendicular to the rotation axis. As shown by curve **a** of Fig. 1, the observed values of 1,2-dichloro

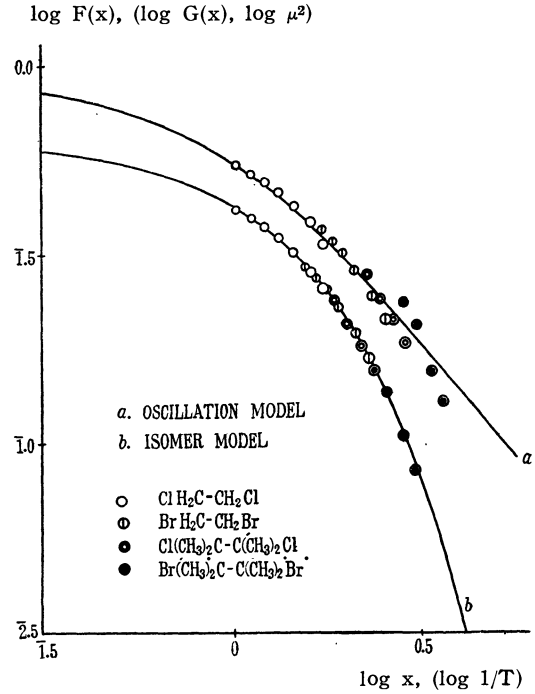



Fig. 1. The observed values of dipole moments and the computed values obtained on the assumption of the rotatory vibration about the *trans* position and on the assumption of the coexistence of two rotational isomers.

* Strictly speaking, the value of $\mu_t$ depends on temperature. However, as the temperature dependence can be shown to be small, we can safely use a constant value for $\mu_t$.

10) Y. Morino, S. Mizushima, K. Kuratani, and M. Katayama, *J. Chem. Phys.*, 18, 754 (1959).

11) I. Watanabe, S. Mizushima, and Y. Masiko, *Sci. Papers Inst. Phys. Chem. Research* (Tokyo), 40, 425 (1943): cf. P. J. Powling and H. J. Bernstein, *J. Am. Chem. Soc.*, 73, 1815 (1951).

12) A. Wada, *J. Chem. Phys.*, 22, 198 (1954).

13) S. Mizushima, Y. Morino, and K. Higasi, *Sci. Papers Inst. Phys. Chem. Research* (Tokyo), 25, 159 (1934).

14) C. P. Smyth, R. W. Dornte, and E. B. Wilson, Jr., *J. Am. Chem. Soc.*, 53, 4242 (1931).

15) G. I. M. Bloom and L. E. Sutton, *J. Chem. Soc.*, 727 (1941).

and 1,2-dibromo-ethane are in agreement with the computed values. Yet the observed values can also be brought into agreement with the theoretical curve computed from eq. (7) which was derived on the assumption of the coexistance of two rotational isomers (curve **b** in Fig. 1). Therefore, so far as the dipole moments of 1,2-dihalogenoethanes are concerned, we can not tell which of the two explanations is preferable, the vibration of two halves of molecules against each other in one potential trough or the coexistence of two rotational isomers.

However, in the case of 2,3-dibromo-2,3-dimethylbutane no displacement enables us to superpose the observed values on the theoretical curve **a** obtained on the assumption of the rotatory vibration about the *trans* position. Even in the chloro-compound there is a small but definite discrepancy between the experimental and theoretical curves. The difference in the two cases can be explained as a result of the lower potential barrier for 1,2-dichloro- and -dibromo-ethane and of the higher potential barrier for 2,3-dichloro- and -dibromo-2,3-dimethylbutane. It is quite reasonable to assume that dihalogenodimethylbutanes have barriers higher than dihalogenoethane since the van der Waals radius of methyl group is much larger than that of the hydrogen atom.

**2. The Origin of the Energy Difference between the Rotational Isomers.** — The nature of the hindering potential to internal rotation has been discussed by several investigators[16–19]. From the comparison of the many experimental data we have come to the conclusion that the stable positions of the internal rotation are determined mainly by the steric repulsion between the atoms of the rotating groups including hydrogen atoms, whereas in the energy difference between rotational isomers there are contributions of other intramolecular forces besides the steric repulsion[19].

As referred to above, the energy difference of 2,3-dibromo-2,3-dimethylbutane was found to be almost the same as that of 1,2-dibromo-ethane. This fact can not be understood, if the hindering potential arises only from the steric repulsion, since the repulsion arising from the $CH_3$ group may be considered to be almost the same as that from Br-atom. (As referred to above, the van der Waals radius of the bromine atom is of the same magnitude as that of the $CH_3$-group). In other words, if the energy difference would arise only from the steric repulsion, we should find the vanishing value of $\Delta E$ for dibromodimethylbutane, which is inconsistent with the experimental result. Therefore, we have to conclude that electrostatic forces should play an important part in $\Delta E$. This is compatible with the fact that we have found almost the same value of $\Delta E$ for 2,3-dibromo-2,3-dimethylbutane and 1,2-dibromo-ethane, both of which are expected to have nearly the same electrostatic potential, since the dipole moments of the rotating groups are almost the same for both cases.

The same conclusion is derived for 2,3-dichloro-2,3-dimethyl-butane by comparing the value of $\Delta E$ (1.6kcal)** with that of 1,2-dichloroethane (1.2kcal). There is a small difference between these two values, but all we can say is that $\Delta E$ of the former substance is not smaller than that of the latter. We go too far, if we discuss this difference quantitatively.

We should like to refer to a recent paper by one of us (I. M.)[20], in which the configurations of the rotational isomers and the energy difference were discussed on the assumption that the steric repulsion between the rotating groups could approximately be calculated from the interatomic potentials obtainable from the experimental data on the second virial coefficients and the electrostatic energy from the interactions between the point dipoles located at each bond.

**3. The Dipole Moment of the Gauche Form.**—The dipole moment of the gauche form $\mu_g$ was found to be 3.1D for 2,3-dichloro-2,3-dimethylbutane and 2.6D for 2,3-dibromo-2,3-dimethylbutane (in heptane solution). These values are greater than those of 1,2-dichloro-(2.62D)[21] and 1,2-dibromo-ethane (2.23D)[21]. The greater values of the former two substances are considered to arise from the induction effect in the methyl radicals by the C-X dipoles. If the induction effect is calculated according to the empirical rule derived by two of us[22] the resultant moments of the gauche forms of 2,3-dichloro- and 2,3-dibromo-2,3-dimethylbutanes are found to be 3.33D and 3.30D respectively. The corresponding

16) E. N. Lassettre and L. B. Dean, *J. Chem. Phys.*, **17**, 317 (1949).
17) H. J. Bernstein, *J. Chem. Phys.*, **17**, 262 (1949).
18) L. J. Oesterhoff, *Discussion of the Faraday Soc.*, **10**, 79 (1951).
19) S. Mizushima, Y. Morino, and T. Shimanouchi, *J. Phys. Chem.*, **56**, 324 (1952).

** $\Delta E$ of 2,3-dichloro-2,3-dimethylbutane, 1.6 kcal., has been obtained by extrapolation to $\varepsilon=1$.
20) I. Miyagawa, *J. Chem. Soc. Japan*, **75**, 1169, 1173, 1177 (1954).
21) I. Miyagawa, *J. Chem. Soc. Japan*, **75**, 1057 (1954).
22) Y. Morino, I. Miyagawa and T. Oiwa, *Botyu-Kagaku*, **15**, 181 (1950); I. Miyagawa, *J. Chem. Soc., Japan* **75**, 1061 (1954).

experimental values 3.1D and 2.6D are somewhat less than the computed values. However, it should be noted that the experimental values of $\mu_g$ are obtained on the assumption that $S=Q_{in}{}^g/Q_{in}{}^t=1$. If different values are assigned to $S$, the values of $\mu_g$ become quite different from the above ones. If, for instance, $S$ is taken as 1/2, $\mu_g$ will be 3.5D for dichloro- and 3.2D for dibromo-dimethylbutanes. It will be shown from the discussion of partition functions that $S$ may be taken to be less than 1[23].

On the other hand the observed value of $\Delta E$ does not depend appreciably on the value of $S$ and, therefore, as the experimental molecular constant of rotational isomers the energy difference $\Delta E$ is more reliable than $\mu_g$.

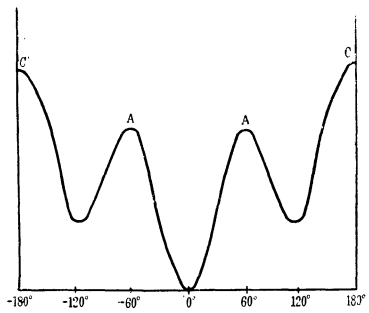
**4. Molecular Spectra and Dipole Moments.**—Let us now discuss the experimental result of Cleveland and Lamport. According to the Raman and infrared spectra observed by them in benzene and carbon tetrachloride solutions the molecules of 2,3-dibromo-2,3-dimethylbutane have been concluded to be in the *trans* form in both solutions. This seems at first sight to be inconsistent with the results of our dipole measurement. However, as the concentration of 2,3-dibromo-2,3-dimethylbutane in their measurement was considered to be less than 0.1 molar fraction and, as $\Delta E$ can reasonably be assumed to be 1.5 kcal./mol., the concentration of the gauche form is at most 0.014 in molar fraction. Even if the energy difference is reduced to half ($\Delta E=700$ cal./mol.) the concentration of the gauche form would not exceed 0.02 in molar fraction. Therefore, it is no wonder that the bands arising from the gauche form were not observed.

In connection with this we should like to refer to the Raman spectra of 1,2-dibromoethane. The Raman line at 551 $cm^{-1}$ assigned to the stretching frequency of the gauche form has a fairly strong intensity in the spectra of the pure liquid, but, when it is diluted with *n*-heptane, the intensity decreases more quickly than the line arising from the *trans* form, and finally at the molar fraction of 0.1 the line becomes too weak to be detectable[13]. The most intense line in the spectra of 2,3-dibromo-2,3-dimethylbutane would be the line arising from the corresponding C-Br stretching frequency, which will behave in the same manner as the 551 $cm^{-1}$ line referred to above. Therefore, as the molar fraction of the dibromodimethylbutane solution in the experiment of Cleveland and Lamport was about 0.1 or less, it is quite possible that all the lines of the gauche form of dibromo-dimethylbutane escaped detection.

23) I. Miyagawa, *J. Chem. Soc. Japan*, **75**, 970 (1954).

## Appendix

The hindering potential to internal rotation about the central C-C bond as axis is considered to have a form such as shown in Fig. 2. The




gauche trans gauche

Fig. 2.

more stable position corresponds to the *trans* form, and the less stable positions to the gauche forms which are obtained from the *trans* form by an internal rotation by about ±120°. There are two lower barriers $A$ and $A'$ and one higher barrier C in one complete internal rotation. Therefore, in order to obtain the moment of the *trans* isomer, $\mu_t$, or, exactly speaking, the mean moment of all the molecules in the *trans* trough, we must make an integration:

$$\bar{\mu}_t{}^2=2\mu_\perp{}^2\int_{A'}^{A}(1-\cos\theta)\exp(-V(\theta)/kT)d\theta/\int_{A'}^{A}\exp(-V(\theta)/kT)d\theta, \quad \text{(A1)}$$

where $\mu_\perp$ is the perpendicular component of the moment of the rotating group. The potential function $V(\theta)$ in this expression may reasonably be approximated as:

$$V(\theta)=1/2\cdot V_0(1-\cos 3\theta), \quad \text{(A2)}$$

and, furthermore, the limit of integration $A$ and $A'$ in terms of azimuthal angle may be taken as ±60°. Then we have

$$\mu_t{}^2=2\mu_\perp{}^2F(x), \quad \text{(A3)}$$

where

$$F(x)=3\sqrt{3}/(2\pi I_0(x))\cdot\left[I_0(x)+2\sum_{\Delta=1}^{\infty}(-1)^s/(9\Delta^2-1)\cdot I_s(x)\right], \quad \text{(A4)}$$

and

$$x=V_0/2kT. \quad \text{(A5)}$$

Here $I_s(x)$ denotes the modified Bessel function of the first kind. If the bond moment of C-Cl is

TABLE V

THE TABLE OF $F(x)$

| $x$ | $F(x)$ |
|---|---|
| 0 | 0.1730 |
| 0.5 | 0.1243 |
| 1 | 0.0812 |
| 2 | 0.0413 |
| 5 | 0.0125 |
| 10 | 0.0064 |

taken as 1.86D, and the induction effect of C-Cl moment upon the $C-CH_3$ bonds is calculated according to our empirical rule, the perpendicular component $\mu_\perp$ is obtained as 2.15D. Using this value, $\mu_t$ at 300°K is calculated as shown in Table VI. As the value of $V_0$ for hexachloroethane was

TABLE VI

THE CALCULATED MOMENT OF THE TRANS FORM AT 300°K

| $V_o$ (kcal./mol.) | $\mu$(D) |
|---|---|
| 0 | 1.14 |
| 0.5 | 1.00 |
| 1 | 0.83 |
| 2 | 0.62 |
| 3 | 0.50 |
| 5 | 0.36 |
| 10 | 0.23 |

found to be about 10 kcal./mol., that of dichlorodimethylbutane must be greater than 10 kcal./mol., since the potential barrier arises mainly from the steric repulsion between the atoms of the rotating groups and is much higher in dichlorodimethylbutane than in hexachloroethane. (As referred to above the van der Waals radius of the methyl group is much larger than that of a Cl atom. In fact, the hindering potential barrier of 1,1,1-trichloroethane was found to be 2.7 kcal./mol.[24], while that of neopentane is 4.3 kcal./mol.[25], the latter being obtained by the replacement of chlorine atoms of the former by methyl radicals. Therefore, from Table V, we can surely conclude that $\mu_t$ is smaller than 0.3D.

The value of $\mu_t$ of 2,3-dibromo-2,3-dimethylbutane will be still smaller, since the steric repulsion in dibromo-compound should be much larger than that in dichloro-compound.

24) J. R. Lubin, B. H. Lebedahl, and D. M. Yost, *J. Am. Chem. Soc.*, **66**, 279 (1944).
25) K. S. Pitzer, *Discussion of the Faraday Soc.*, **10**, 66 (1951).


## Summary

The dipole moments of 2,3-dichloro- and 2,3-dibromo-dimethylbutane were measured in carbon tetrachloride solution in the temperature range from −25° to +55°C, and in benzene solutions at 25°C. The moment was found to increase with temperature in carbon tetrachloride solution. Much higher values of moment were observed in benzene solutions. It was concluded from these experimental results that there exist two rotational isomers, the *trans* isomer with vanishing or a small moment, and the gauche isomer with a finite moment. The experimental result could be explained satisfactorily by the rotational isomer theory, but not on the assumption of only one potential trough at the *trans* position.

By comparing the energy difference between the rotational isomers of these compounds with those of 1,2-dichloro- and 1,2-dibromoethane it was concluded that the electrostatic force plays an important role in the energy difference between the rotational isomers, whereas the potential barrier is mainly determined by steric repulsion.

An explanation was presented to reconcile the result of our dipole measurement with that of Raman and infrared measurement, the two results being in apparent contradiction with each other.


The authors wish to thank Professor Forrest F. Cleveland, Illinois Institute of Technology, for sending us a sample of 2,3-dibromo-2,3-dimethylbutane and for his interest in our measurement.

*Department of Chemistry, Faculty of Science, Tokyo University, Tokyo*

# *A Rapid Determination of Oxidation Values of Non-Volatile Organic Compounds by the Iodic Acid Decomposition Method*

By Shigeru OHASHI

(Received September 27, 1954)

In the course of preparing organic compounds, on many occasions, it is only necessary to determine the percentages of carbon or other elements to serve as a check on the purity. For this purpose, however, it is not always necessary to determine the content of an element such as carbon, hydrogen, or nitrogen, but instead the "oxidation value" of the compound, named by the author, can also be useful. The oxidation value of a compound is defined as the number of oxygen atoms required to completely oxidize one molecule of the compound.

A survey of the literature reveals that Strebinger[1] and Christensen, Facer, and

1) R. Strebinger, *Z. analyt. Chem.*, 58, 97 (1919).

Wong[2,3] determined the "oxygen consumed" of an organic compound, which is defined as oxygen requirement in gram per hundred grams of the sample, by means of iodic acid in concentrated sulfuric acid. In spite of all these developments there is still need for wider applicability, simpler techniques, less expensive equipment, and methods by which the occasional determination can be made easily.

For the complete wet combustion of organic compounds a powerful oxidizing agent is required and, furthermore, to determine the oxidation values of the compounds, the reduced part of the oxidant must be measured readily and exactly after the oxidation reaction. Iodic acid in strong phosphoric acid is a very suitable reagent for this purpose. The strong oxidizing action of this reagent was already used by the author and his co-workers[4] for the determination of elementary carbon, such as charcoal, graphite, and others, which are completely oxidized by it to form carbon dioxide.

$$5C + 4HIO_3 = 5CO_2 + 2I_2 + 2H_2O$$

The amount of the reduced part of iodic acid can be known by means of a volumetric determination of the iodine produced.

Now one may suppose in general an organic compound composed of carbon, hydrogen, and oxygen, and indicate it as $C_kH_mO_n$. Then the oxidation of the organic compound with iodic acid is shown by the following equation (3), which is derived from equations (1) and (2).

$$C_kH_mO_n + (2k + m/2 - n)\,O = k\,CO_2 + m/2H_2O \quad (1)$$

$$2HIO_3 = H_2O + I_2 + 5O \quad (2)$$

$$5C_kH_mO_n + 2(2k + m/2 - n)HIO_3 = 5kCO_2 + (2k + 3m - n)H_2O + (2k + m/2 - n)I_2 . \quad (3)$$

Namely, 5 mol. of the organic compound $C_kH_mO_n$ is oxidized completely with $2(2k+3m-n)$ mol. of iodic acid under the production of $(2k+m/2-n)$ mol. of iodine. Therefore, if the organic compound is completely oxidized with the reagent according to the above equation, its oxidation value may be obtained by the determination of the iodine produced.

In this study the method of determining the oxidation values based on the above-mentioned principle was investigated and the oxidation values were determined for several non-volatile organic compounds, which are composed of carbon, hydrogen, and oxygen.

### Apparatus

The apparatus used in this study is illustrated in Fig. 1. It is mainly composed of two parts, a

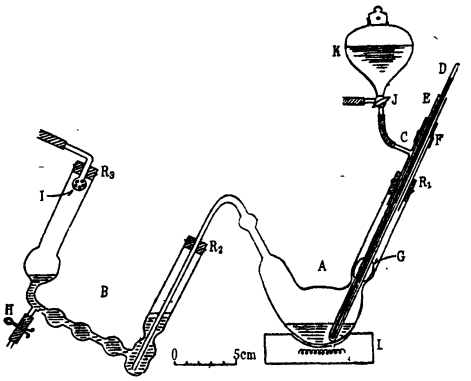



Fig. 1 Apparatus

A: Reaction vessel
B: Absorption vessel
C: Gas-introducing tube
D: Thermometer
E: Thermometer-protecting tube
F: Rubber tube
G: Glass lock
H: Pinch cock
I: Glass bulb
J: Three-way stopcock
K: Water-addition funnel
L: Electric heater
$R_1$-$R_3$: Rubber stopper



Fig. 2 Glass lock.



Fig. 3. Weighing tube.

reaction vessel A and an absorption vessel B. The right tube of the vessel A is closed at the top by means of a rubber stopper $R_1$, through which a gas-introducing tube and a thermometer are inserted. The thermometer is protected by a glass tube. If the thermometer-protecting tube is not used, the very thin bottom glass of the thermometer may easily be destroyed by heating with strong phosphoric acid. In the right arm of the vessel A, there is a constricted part above which a small glass lock shown in Fig. 2 is set for the sake of protecting it against the backward stream of gas. The left arm of the vessel A is inserted deeply into the absorption vessel B through a rubber stopper $R_2$. In order to prevent the liberated iodine from going upward to the rubber stopper $R_2$, the right arm of the vessel B is constricted at the position as shown in Fig. 1. On the left arm of the vessel B, there is an outlet, having a short rubber tube and a pinch cock, for convenience to pour out the solution in the vessel. The top of the left arm is closed by

2) B. E. Christensen and J. F. Facer, *J. Am. Chem. Soc.*, **61**, 3001 (1939).
3) B. E. Christensen and R. Wong, *Ind. Eng. Chem., Anal. Ed.*, **13**, 444 (1941).
4) T. Kiba, S. Ohashi, T. Takagi, and Y. Hirose, *Japan Analyst*, **2**, 446 (1953).

means of a rubber stopper $R_3$, through which a glass tube with a small glass bulb, having some pinholes, is inserted to prevent loss from a splash.

After passing through the solutions of sodium carbonate, potassium permanganate, and mercuric chloride in turn, the air is introduced by means of a suction pump into the vessel A through the three-way stopcock of a water-addition funnel, which is used to add water to the vessel A after the decomposition of a sample.

The vessel A is heated at the bottom with an electric heater, the temperature of which can be regulated with a transformer.

## Reagents

**Potassium Iodate.**—Standard reagent grade (The Osaka Industrial Research Institute) or extra pure grade potassium iodate was used.

**Strong Phosphoric Acid.**—Commercial extra pure grade orthophosphoric acid ($d$=1.7) was dehydrated by heating until the temperature of the liquid reached 300°C. The very viscous liquid thus obtained is called strong phosphoric acid[5], which is a mixture of ortho-, pyro-, and triphosphoric acid.

**Standard Solution of Sodium Arsenite.**—A 0.1 N solution of sodium arsenite was used. Dissolve 4.95 g. of standard reagent grade (The Osaka Industrial Research Institute) arsenic trioxide in 150 ml. of 10% sodium carbonate solution, add 25 ml. of normal sulfuric acid, and dilute to 1000 ml.

**Standard Solution of Iodine.**—A 0.05 N solution of iodine was used. It was standardized with the above sodium arsenite solution.

## Procedure

Weigh accurately a 15 to 100 mg. sample, depending upon its oxidation value, into a small weighing tube shown in Fig. 3; choose the sample weight so that the iodine formed will not consume more than 50% of the sodium arsenite used. From a buret, pour about 3 to 5 ml. of strong phosphoric acid into a reaction vessel A through its upper inlet, and add a suitable amount of powdered potassium iodate. The optimum amount of potassium iodate will be discussed later. Next, let fall the weighing tube containing the sample along the inside wall of the vessel carefully. Add 10 or 20 ml. of sodium arsenite solution into an absorption vessel B. If only 10 ml. of sodium arsenite solution is used, add further about 10 ml. of water. Then connect all of the vessel A, B and so on.

While a slow stream of washed air is flowing through the vessel A and B by a suction pump, gently heat the bottom of the vessel A on a small electric heater. With increase of temperature, viscosity of the reaction medium decreases and a decomposition reaction begins at the appearance of a violet vapor of iodine. During the decomposition reaction shake the vessel A in order to get a complete reaction.

The reaction temperatures are varied from 80° to 240°C in accordance with species of samples. However, the temperature of the reactants must be kept carefully under 260°C, because at any higher temperature than this limit iodic acid is decomposed with the evolution of iodine[6].

The end of the decomposition reaction is easily recognized by the ceasing of the production of iodine. After the end of the decomposition reaction, stand the vessel A aloof from the electric heater until the temperature of the reaction medium falls to about 140°C, while air is flowing through the vessel.

After the cooling, open the three-way stopcock and introduce 10 to 15 ml. of water into the vessel A. Then heat once more the aqueous solution in the vessel A on the electric heater, until all of the iodine dissolved in the reaction solution is removed and absorbed into the sodium arsenite solution.

Remove the absorption vessel B from the rubber stoppers, let the solution flow into a beaker, and wash out the vessel B and the small glass bulb with water. Add some sodium bicarbonate to the solution in the beaker and titrate the excess sodium arsenite with 0.05 N iodine solution using starch solution as indicator.

## Results and Discussion

In order to estimate the indispensable quantity of potassium iodate for the complete oxidation of an organic compound, the following experiment was carried out in the case of oxalic acid as an example.

About 50 mg. of oxalic acid weighed accurately was oxidized with various amounts of potassium iodate and the iodine produced was measured by the procedure described above. Results obtained are given in Table I. Nos. 4 and 5 in this experiment have

TABLE I

AMOUNT OF POTASSIUM IODATE REQUIRED FOR COMPLETE OXIDATION OF OXALIC ACID

| No. | Sample Weight mg. | Potassium Iodate Used mg. | Potassium Iodate Ratio: mg. used to mg. equiv. | Iodine Produced Found mg. | Iodine Produced Ratio: mg. found to mg. calc. |
|---|---|---|---|---|---|
| 1 | 51.5 | 20.5 | 0.58 | 11.6 | 0.56 |
| 2 | 50.0 | 30.5 | 0.98 | 18.7 | 0.92 |
| 3 | 50.7 | 32.7 | 0.95 | 17.9 | 0.88 |
| 4 | 49.2 | 34.0 | 1.02 | 18.2 | 0.92 |
| 5 | 50.6 | 40.0 | 1.16 | 19.8 | 0.90 |
| 6 | 51.1 | 52.2 | 1.50 | 20.4 | 0.99 |
| 7 | 50.0 | 65.3 | 1.91 | 20.1 | 0.99 |
| 8 | 49.8 | 100.5 | 2.97 | 20.1 | 1.00 |

indicated obviously that an amount of potassium iodate slightly in excess of that required theoretically can not oxidize the sample completely. For this purpose an excess of at least half as much again as the theoretical

5) L. F. Audrieth, "Inorganic Syntheses, Volume III", McGraw-Hill Book Company, Inc., New York, (1950), p. 89.

6) T. Kiba et al., loc. cit.

quantity should be used.

In the first course of this investigation the reactions were carried out in the stream of carbon dioxide, but if a sample and sodium arsenite solution can not be oxidized with air, air may be used instead of carbon dioxide. With regard to this presumption the following tests were performed.

At first in order to investigate the stability of sodium arsenite solution against aeration, the washed hot air accompanied with aqueous vapor was introduced into a certain amount of sodium arsenite solution at the rate of about 5 bubbles of air per second. After the aeration titrating the arsenite solution with the standard solution of iodine, the data shown in Table II were obtained. This result

TABLE II

EFFECT OF AERATION ON STABILITY OF SODIUM ARSENITE SOLUTION

| Quantity of 0.05 N Iodine Solution Consumed | |
|---|---|
| Before Aeration ml. | After 1 hr. of Aeration ml. |
| 34.43 | 34.44 |
| 34.43 | 34.44 |
| 8.89 | 8.88 |
| 8.89 | 8.88 |

shows that the sodium arsenite solution can not be oxidized by one hour's aeration. Since the period of aeration in the practical procedure is shorter than thirty minutes, the oxidation of the arsenite solution with air may be out of the question.

Next, for the determination of the oxidation value of sodium oxalate, for example, the air flowing method was compared with the carbon dioxide flowing method. As shown in Table III there is no difference between the two methods.

TABLE III

COMPARISON OF CARBON DIOXIDE FLOWING METHOD AND AIR FLOWING METHOD

Sample: Sodium Oxalate

| Gas Used | Sample Weight mg. | Iodine Produced | | Deviation mg. |
|---|---|---|---|---|
| | | Calc. mg. | Found mg. | |
| $CO_2$ | 33.2 | $12.5_8$ | $12.5_2$ | $-0.0_6$ |
| 〃 | 50.0 | $18.9_4$ | $18.9_2$ | $-0.0_2$ |
| 〃 | 82.5 | $31.2_5$ | $31.1_5$ | $-0.1_0$ |
| 〃 | 87.5 | $33.1_5$ | $33.0_6$ | $-0.0_9$ |
| Air | 30.5 | $11.5_5$ | $11.5_1$ | $-0.0_4$ |
| 〃 | 57.0 | $21.5_9$ | $21.5_5$ | $-0.0_4$ |
| 〃 | 45.3 | $17.1_6$ | $17.1_1$ | $-0.0_5$ |
| 〃 | 80.9 | $30.6_4$ | $30.3_9$ | $-0.2_5$ |

Analyses of some known organic compounds were carried out by this method. These results are summarized in Table IV. Purest

TABLE IV

DETERMINATION OF OXIDATION VALUES OF SOME COMPOUNDS BY THIS METHOD

| Substance | Oxidation Value Calc. | Reaction Temperature °C | Sample Weight mg. | Iodine Produced | | Oxidation Value | |
|---|---|---|---|---|---|---|---|
| | | | | Calc. mg. | Found mg. | Found | Deviation from Average |
| Oxalic acid | 1 | 90–120 | 34.6 | $13.9_3$ | $13.9_4$ | $1.00_1$ | $-0.00_1$ |
| $H_2C_2O_4 \cdot 2H_2O$ | | | 42.8 | $17.2_4$ | $17.3_3$ | $1.00_5$ | $+0.00_3$ |
| | | | 53.2 | $21.4_2$ | $21.4_4$ | $1.00_1$ | $-0.00_1$ |
| | | | 60.4 | $24.3_2$ | $24.3_3$ | $1.00_0$ | $-0.00_2$ |
| | | | 73.2 | $29.4_8$ | $29.6_1$ | $1.00_4$ | $+0.00_2$ |
| | | | | | Av. | $1.00_2$ | |
| Sodium oxalate | 1 | 80–150 | 34.7 | $13.1_4$ | $13.2_1$ | $1.00_5$ | $-0.00_1$ |
| $Na_2C_2O_4$ | | | 41.6 | $15.7_6$ | $15.7_6$ | $1.00_4$ | $-0.00_2$ |
| | | | 55.9 | $21.1_7$ | $21.3_2$ | $1.00_7$ | $+0.00_1$ |
| | | | 78.4 | $29.7_0$ | $29.9_0$ | $1.00_7$ | $+0.00_1$ |
| | | | | | Av. | $1.00_6$ | |
| Tartaric acid | 5 | 80–150 | 25.4 | $42.9_5$ | $42.9_7$ | $5.00_5$ | $+0.01_1$ |
| $C_4H_6O_6$ | | | 26.5 | $44.8_0$ | $45.0_7$ | $5.01_5$ | $+0.02_1$ |
| | | | 33.9 | $57.3_2$ | $57.2_1$ | $4.99_0$ | $-0.00_4$ |
| | | | 35.9 | $60.7_1$ | $60.0_0$ | $4.94_0$ | $-0.05_4$ |
| | | | 40.4 | $68.3_4$ | $68.3_7$ | $5.00_5$ | $+0.01_1$ |
| | | | 45.3 | $76.6_0$ | $76.5_6$ | $4.99_5$ | $+0.00_1$ |
| | | | 55.7 | $94.1_9$ | $94.4_2$ | $5.01_0$ | $+0.01_6$ |
| | | | 64.9 | $109.8$ | $109.5$ | $4.98_5$ | $-0.00_9$ |
| | | | 75.0 | $126.8$ | $126.8$ | $5.00_0$ | $+0.00_6$ |
| | | | | | Av. | $4.99_4$ | |

TABLE IV (Contd.)

| Substance | Oxidation Value Calc. | Reaction Temperature °C | Sample Weight mg. | Iodine Produced | | Oxidation Value | |
|---|---|---|---|---|---|---|---|
| | | | | Calc. mg. | Found mg. | Found | Deviation from Average |
| Sodium potassium tartrate | 5 | 90–150 | 25.4 | $22.8_4$ | $22.7_9$ | $4.99_0$ | $+0.00_5$ |
| $C_4H_4O_6NaK \cdot 4H_2O$ | | | 32.0 | $28.7_8$ | $28.6_4$ | $4.97_5$ | $-0.01_0$ |
| | | | 35.3 | $31.7_5$ | $31.6_5$ | $4.98_5$ | $0.00_0$ |
| | | | 47.1 | $42.3_6$ | $42.1_9$ | $4.98_0$ | $-0.00_5$ |
| | | | 50.4 | $45.3_2$ | $45.2_6$ | $4.99_5$ | $+0.01_0$ |
| | | | 65.3 | $58.7_2$ | $58.5_4$ | $4.98_5$ | $0.00_0$ |
| | | | | | Av. | $4.98_5$ | |
| Citric acid | 9 | 80–150 | 23.5 | $41.0_9$ | $41.4_9$ | $9.08_1$ | $+0.00_3$ |
| $C_6H_8O_7 \cdot H_2O$ | | | 26.8 | $58.2_6$ | $58.5_8$ | $9.05_4$ | $-0.02_4$ |
| | | | 39.5 | $85.8_7$ | $86.7_1$ | $9.09_0$ | $+0.01_2$ |
| | | | 39.8 | $86.2_3$ | $86.9_3$ | $9.07_2$ | $-0.00_6$ |
| | | | 40.7 | $88.4_8$ | $89.2_8$ | $9.08_1$ | $+0.00_3$ |
| | | | 48.1 | $104.6$ | $105.6$ | $9.09_0$ | $+0.01_2$ |
| | | | | | Av. | $9.07_8$ | |
| Sodium citrate | 9 | 90–150 | 24.1 | $30.8_2$ | $30.9_2$ | $9.03_6$ | $+0.04_7$ |
| $C_6H_5O_7Na_3 \cdot 5.5H_2O$ | | | 32.2 | $41.1_8$ | $41.2_6$ | $9.01_8$ | $+0.02_9$ |
| | | | 39.9 | $51.0_3$ | $50.8_1$ | $8.96_4$ | $-0.02_5$ |
| | | | 54.8 | $70.0_8$ | $69.7_2$ | $8.95_5$ | $-0.03_4$ |
| | | | 62.0 | $79.3_0$ | $79.1_2$ | $8.98_8$ | $-0.00_1$ |
| | | | 75.7 | $96.8_2$ | $96.5_7$ | $8.97_3$ | $-0.01_6$ |
| | | | | | Av. | $8.98_9$ | |
| Succinic acid | 7 | 160–230 | 19.4 | $58.3_7$ | $57.9_3$ | $6.94_4$ | $-0.01_4$ |
| $C_4H_6O_4$ | | | 20.9 | $62.8_9$ | $62.4_5$ | $6.95_1$ | $-0.00_7$ |
| | | | 22.0 | $66.2_0$ | $65.9_9$ | $6.97_9$ | $+0.02_1$ |
| | | | 29.1 | $87.5_6$ | $87.0_1$ | $6.95_8$ | $0.00_0$ |
| | | | 44.2 | $133.0$ | $132.1$ | $6.95_1$ | $-0.00_7$ |
| | | | 54.3 | $163.4$ | $162.6$ | $6.96_5$ | $+0.00_7$ |
| | | | | | Av. | $6.95_8$ | |
| Arabinose | 10 | 90–230 | 19.8 | $66.1_9$ | $66.3_5$ | $10.0_2$ | $+0.0_2$ |
| $C_5H_{10}O_5$ | | | 30.0 | $100.3$ | $100.3$ | $10.0_0$ | $0.0_0$ |
| | | | 33.4 | $111.7$ | $111.2$ | $9.9_5$ | $-0.0_5$ |
| | | | 47.1 | $157.5$ | $156.7$ | $9.9_5$ | $-0.0_5$ |
| | | | 50.5 | $168.8$ | $169.8$ | $10.0_6$ | $+0.0_6$ |
| | | | | | Av. | $10.0_0$ | |
| Glucose | 12 | 80–250 | 26.6 | $88.9_2$ | $88.9_1$ | $12.0_0$ | $+0.0_6$ |
| $C_6H_{12}O_6$ | | | 35.9 | $110.6$ | $110.0$ | $11.9_4$ | $0.0_0$ |
| | | | 36.6 | $122.4$ | $121.2$ | $11.8_8$ | $-0.0_6$ |
| | | | 41.1 | $134.2$ | $133.8$ | $11.9_6$ | $+0.0_2$ |
| | | | 44.4 | $136.9$ | $136.3$ | $11.9_5$ | $+0.0_1$ |
| | | | 62.8 | $193.4$ | $192.5$ | $11.9_4$ | $0.0_0$ |
| | | | | | Av. | $11.9_4$ | |
| Galactose | 12 | 80–230 | 25.2 | $85.1_9$ | $84.9_9$ | $11.9_8$ | $+0.0_2$ |
| $C_6H_{12}O_6$ | | | 26.5 | $89.5_8$ | $88.9_8$ | $11.9_2$ | $-0.0_4$ |
| | | | 35.9 | $121.4$ | $120.9$ | $11.9_5$ | $-0.0_1$ |
| | | | 46.3 | $156.5$ | $156.4$ | $11.9_9$ | $+0.0_3$ |
| | | | 50.6 | $171.1$ | $170.7$ | $11.9_8$ | $+0.0_2$ |
| | | | | | Av. | $11.9_6$ | |
| Dulcitol | 13 | 90–200 | 25.6 | $92.7_4$ | $92.3_0$ | $12.9_3$ | $-0.0_3$ |
| $C_6H_{14}C_6$ | | | 30.5 | $110.5$ | $110.2$ | $12.9_5$ | $-0.0_1$ |
| | | | 39.0 | $141.3$ | $141.3$ | $13.0_0$ | $+0.0_4$ |
| | | | 41.9 | $151.8$ | $151.4$ | $12.9_5$ | $-0.0_1$ |
| | | | 45.1 | $163.4$ | $162.8$ | $12.9_5$ | $-0.0_1$ |
| | | | 52.6 | $190.6$ | $190.4$ | $12.9_9$ | $+0.0_3$ |
| | | | | | Av. | $12.9_6$ | |

TABLE IV (Contd.)

| Substance | Oxidation Value Cale. | Reaction Temperature C° | Sample Weight mg. | Iodine Produced | | Oxidation Value | |
|---|---|---|---|---|---|---|---|
| | | | | Cale. mg. | Found mg. | Found | Deviation from Average |
| Saccharose | 24 | 100–230 | 16.9 | 60.$1_6$ | 59.$5_0$ | 23.$7_8$ | $-0.0_3$ |
| $C_{12}H_{22}O_{11}$ | | | 20.7 | 73.$6_9$ | 73.$0_7$ | 23.$8_1$ | $0.0_0$ |
| | | | 29.0 | 103.$_2$ | 102.$_4$ | 23.$8_1$ | $0.0_0$ |
| | | | 33.8 | 120.$_3$ | 119.$_5$ | 23.$8_3$ | $+0.0_2$ |
| | | | 37.1 | 132.$_1$ | 130.$_9$ | 23.$7_8$ | $-0.0_3$ |
| | | | 40.0 | 142.$_4$ | 141.$_4$ | 23.$8_3$ | $+0.0_2$ |
| | | | | | Av. | 23.$8_1$ | |
| Treharose | 24 | 90–230 | 12.4 | 44.$1_3$ | 44.$0_3$ | 23.$9_5$ | $+0.0_1$ |
| $C_{12}H_{22}O_{11}$ | | | 14.7 | 52.$3_2$ | 52.$0_7$ | 23.$8_8$ | $-0.0_6$ |
| | | | 15.3 | 54.$4_5$ | 54.$2_6$ | 23.$9_3$ | $-0.0_1$ |
| | | | 16.1 | 57.$3_0$ | 57.$2_2$ | 23.$9_8$ | $+0.0_4$ |
| | | | | | Av. | 23.$9_4$ | |

grade organic compounds were selected or prepared and dried in the calcium chloride or sulfuric acid desiccator before analysis.

The results listed for the various organic compounds in Table IV indicate that the precision of the data is within ±1%.

The constantly high value obtained for citric acid might be due to the loss of a part of the crystallization water. The slightly low values for succinic acid and saccharose led to the belief that these substances had not been completely dried prior to analysis.

Most of the analyses reported in Table IV were conducted according to the procedure described above and required only twenty to thirty minutes for one estimation.

This method can not be applied to volatile samples such as benzoic acid. For the development of this method to the volatile compounds the apparatus would have to be improved. The investigation of this point is a future problem.

## Summary

A new method has been developed to permit accurate and rapid determination of oxidation values of organic compounds. The oxidation value of a compound can be readily obtained by determining the iodine produced from the reaction of the organic compound and potassium iodate in strong phosphoric acid. The iodine produced is absorbed into the sodium arsenite solution and the excess arsenite is titrated with the standard solution of iodine.

The apparatus and procedures for this method have been investigated. According to the data obtained on some pure non-volatile organic compounds, utilizing sample weights of 10 to 80 mg., it is indicated that this method is very accurate and an analysis can be accomplished as rapidly as in twenty to thirty minutes.

The author is grateful to Prof. T. Kiba for his encouragement and valuable advice during the course of this investigation, to Prof. Y. Kurata for supplying some of the samples used in this study, and to Mr. T. Takagi and Mr. K. Tanaka for their helpful assistance. A part of the expense for the experiment has been defrayed from a grant given by the Ministry of Education, to which the author's thanks are due.

*Department of Chemistry, Faculty of Science, Kanazawa, University, Kanazawa*

# *A Rapid Determination of Nitrogen in Organic Compounds by the Iodic Acid Decomposition Method*

By Shigeru OHASHI

(Received September 27, 1954)

The applications of the characteristic behavior of iodic acid in strong phosphoric acid to chemical analysis have been investigated, and the volumetric methods of determining elementary carbon[1] such as charcoal, graphite etc. and determining oxidation values[2] of organic compounds have been already reported by the author and his coworkers. In the course of these studies it was found that nitrogen contained in organic substances can be easily determined by the iodic acid-strong phosphoric acid reagent. If an organic compound containing nitrogen is heated with iodic acid in strong phosphoric acid, the compound is decomposed and the nitrogen in it is liberated. Consequently, after the decomposition mentioned above, sending this nitrogen with carbon dioxide into an azotometer, which is filled with potassium hydroxide solution, the nitrogen can be determined gas-volumetrically. This method is, so to speak, the wet Dumas method; namely, the combustion tube in the case of the Dumas method is replaced by the special reaction vessel in which samples are decomposed.

**Apparatus.**—The apparatus necessary in this method is shown in Fig. 1. It is mainly composed of three parts, reaction vessel A, azotometer B, and carbon dioxide generator C. All of these are hand-made in addition to a Kipp's apparatus for production of carbon dioxide.

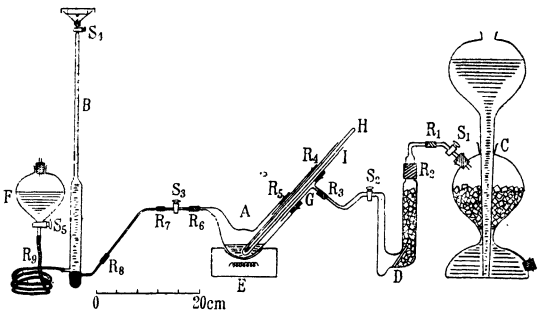



Fig. 1. Apparatus.

A: Reaction vessel.
B: Azotometer.
C: $CO_2$ generator.
D: $CaCO_3$-filled guard tube.
E: Electric heater.
F: Leveling vessel.
G: Gas-introducing tube.
H: Thermometer.
I: Thermometer-protecting tube.
$R_1$-$R_9$: Rubber tube.
$S_1$-$S_5$: Stopcock.

Into the reaction vessel a gas-introducing tube G and a thermometer H, which is covered with a thermometer-protecting tube I, are inserted. These tubes are attached to the reaction vessel with suitable rubber tubes as shown in Fig. 1.

The measuring-tube of the azotometer is made of a commercial buret, which is graduated at intervals of 0.02 ml. and has a graduated capacity of 5 ml. It is connected at the bottom by means of a rubber tube with a leveling vessel F.

Between the reaction vessel and the Kipp's apparatus there is a calcium carbonate-filled guard tube D for catching particles of hydrochloric acid.

The reaction vessel is heated with an electric heater, the temperature of which is regulated with a transformer.

**Reagents.** — *Strong phosphoric acid.* Strong phosphoric acid prepared by heating and evaporating commercial extra pure grade orthophosphoric acid ($d$=1.7) until its temperature reached 300°C was used.

*Potassium iodate.*—Extra pure grade potassium iodate was used.

*Carbon dioxide.* This was produced from calcium carbonate (marble) and hydrochloric acid (1: 1) in a Kipp's apparatus. To obtain the carbon dioxide in the purest condition the operation of putting these substances into a Kipp's apparatus should be carried out in the same manner as that used in the case of the micro-Dumas method.

*Potassium hydroxide.* A 30% solution of potassium hydroxide was used.

**Procedure.**—Weigh accurately a 10 to 50 mg. sample, depending upon its nitrogen content, into a small weighing tube; choose the sample weight so that the volume of the nitrogen formed will be 1 to 5 ml. Previously heat gently in a reaction vessel a mixture of 3 to 5 ml. of strong phosphoric acid and two or three times as much of the theoretically required amount of potassium iodate until the added potassium iodate disperses into the acid homogeneously. After cooling the contents of vessel, put the weighing tube containing the sample into the vessel along the inside wall of it.

Insert a gas-introducing tube, a thermometer, and a thermometer-protecting tube into the reaction vessel, and connect the reaction vessel with a carbon dioxide generator and a guard tube. Connect a rubber tube $R_7$ with a suction pump, open the stopcock $S_3$, and suck up the air present

1) T. Kiba, S. Ohashi, T. Takagi and Y. Hirose, *Japan Analyst*, 2, 446 (1953).
2) S. Ohashi, This Bulletin, 28, 171 (1955).

between $S_2$ and $S_3$. Now, close the stopcock $S_3$ and open the stopcock $S_2$ to fill the container with carbon dioxide. Repeat these operations several times to make sure that no air remains in the container. Finally fill it with carbon dioxide. Next, connect the rubber tube $R_7$ with an azotometer and open the stopcock $S_2$, $S_3$ and $S_4$ to let carbon dioxide flow through it for two or three minutes. Close the stopcock $S_3$ and immediately raise the leveling vessel F to fill the azotometer with the potassium hydroxide solution. Then close the stopcock $S_4$.

Heat the liquid in the reaction vessel A on a small electric heater. During the decomposition reaction shake well the reaction vessel to decompose the sample completely, and keep the temperature of the reactants below 260°C, above which iodic acid is decomposed, liberating oxygen, and leading to a serious error. The end of the decomposition reaction can be easily recognized by the ceasing of the liberation of iodine. Remove the electric heater and transfer the gas in the reaction vessel into the azotometer by carefully opening the stopcock $S_2$. A part of the iodine liberated is sent into the azotometer and absorbed into the potassium hydroxide solution. Drive the gas in the vessel by letting the carbon dioxide flow, until the gas introduced into the azotometer becomes so-called micro-bubbles.

After standing fifteen minutes, raise the leveling vessel until the solution in it stands at exactly the same height as that in the azotometer. Read the volume of nitrogen, the thermometer, and the barometer.

The percentage of the nitrogen present is computed according to the following equation:

$$\log N\% = \log v + \log g + (1 - \log w).$$

In this equation, $N\%$ represents the percentage of the nitrogen, $v$ the volume (ml.) of the nitrogen measured at $t$°C and $p$ mm Hg, and $g$ the weight (mg.) of 1 ml. of the nitrogen at $t$°C and $p$ mm Hg, and $w$ the weight (mg.) of the sample used for the analysis. The value of $p$ mm Hg is obtained by subtracting the aqueous vapor pressure of the 30% potassium hydroxide solution at $t$°C from the atmospheric pressure measured by means of the barometer.

## Results and Discussion

Analyses of various known organic compounds containing nitrogen were made with this method. These results are summarized in Table I.

TABLE I

DETERMINATION OF NITROGEN IN VARIOUS KNOWN ORGANIC COMPOUNDS

| Substance | Nitrogen Content % | Sample Weight mg. | Nitrogen Content: Found % | Nitrogen Content: Deviation % |
|---|---|---|---|---|
| Ammonium chloride $NH_4Cl$ | 26.18 | 15.2 | $26.6_8$ | $+0.5_0$ |
| | | 12.8 | $26.5_9$ | $+0.4_1$ |
| | | 17.8 | $25.6_3$ | $-0.5_5$ |
| | | 16.6 | $25.6_2$ | $-0.5_6$ |
| | | 10.8 | $26.1_8$ | $0.0_0$ |
| Ammonium oxalate $(COONH_4)_2 \cdot H_2O$ | 19.71 | 25.7 | $19.4_6$ | $-0.2_5$ |
| | | 21.5 | $19.4_4$ | $-0.2_7$ |
| | | 24.9 | $19.0_6$ | $-0.6_2$ |
| | | 10.4 | $19.5_3$ | $-0.1_8$ |
| | | 15.9 | $19.5_6$ | $-.01_5$ |
| Acetanilide $C_6H_5NHCOCH_3$ | 10.36 | 34.3 | $10.3_4$ | $-0.0_2$ |
| | | 27.6 | $10.1_7$ | $-0.1_9$ |
| | | 19.5 | $10.4_0$ | $+0.0_4$ |
| | | 19.7 | $10.3_6$ | $0.0_0$ |
| | | 26.5 | $10.0_3$ | $-0.3_3$ |
| Phthalimide $C_6H_4(CO)_2NH$ | 9.52 | 18.0 | 9.23 | −0.29 |
| | | 18.7 | 9.22 | −0.30 |
| Phenacetin $C_2H_5OC_6H_5NHCOCH_3$ | 7.82 | 26.1 | 7.74 | −0.08 |
| | | 44.6 | 7.76 | −0.06 |
| | | 39.6 | 7.79 | −0.03 |
| | | 34.4 | 7.74 | −0.08 |
| | | 32.8 | 7.91 | +0.09 |
| Thionalide $C_{10}H_7NHCOCH_2SH$ | 6.45 | 23.2 | 6.33 | −0.12 |
| | | 11.9 | 6.28 | −0.18 |
| | | 18.5 | 6.34 | −0.11 |
| | | 24.1 | 6.53 | +0.08 |

TABLE I (Contd.)

| Substance | Nitrogen Content % | Sample Weight mg. | Nitrogen Content Found % | Nitrogen Content Deviation % |
|---|---|---|---|---|
| Urea | 46.63 | 9.5 | $46.0_5$ | $-0.5_8$ |
| $NH_2CONH_2$ | | 9.2 | $47.2_5$ | $+0.6_2$ |
| | | 10.6 | $46.5_4$ | $-0.0_9$ |
| | | 10.0 | $46.2_7$ | $-0.3_6$ |
| | | 10.6 | $45.8_7$ | $-0.7_4$ |
| Thiourea | 36.81 | 13.4 | $36.4_3$ | $-0.3_5$ |
| $NH_2CSNH_2$ | | 23.3 | $36.2_6$ | $-0.5_5$ |
| | | 10.9 | $36.2_7$ | $-0.5_4$ |
| | | 14.8 | $36.8_8$ | $+0.0_7$ |
| | | 12.3 | $36.0_8$ | $-0.7_3$ |
| Methyl orange | 12.84 | 16.5 | $12.7_8$ | $-0.0_6$ |
| $(CH_3)_2NC_6H_4NNC_6H_4SO_3Na$ | | 14.0 | $12.7_2$ | $-0.1_2$ |
| | | 24.7 | $12.8_5$ | $+0.0_1$ |
| | | 14.0 | $12.9_3$ | $+0.0_9$ |
| | | 23.2 | $12.5_3$ | $-0.2_8$ |
| Methyl red | 15.61 | 23.8 | $15.9_9$ | $+0.3_8$ |
| $(CH_3)_2NC_6H_4NNC_6H_4COOH$ | | 17.8 | $15.5_8$ | $-0.0_3$ |
| | | 17.8 | $15.5_3$ | $-0.0_8$ |
| | | 15.4 | $15.8_2$ | $+0.2_1$ |
| | | 21.0 | $15.6_5$ | $+0.0_4$ |
| Dithizone | 21.85 | 23.6 | $21.2_3$ | $-0.6_2$ |
| $C_6H_5NHCSNNC_6H_5$ | | 23.2 | $21.0_2$ | $-0.8_3$ |
| | | 15.5 | $21.8_8$ | $+0.0_3$ |
| | | 14.0 | $21.7_8$ | $-0.0_7$ |
| | | 15.0 | $21.7_7$ | $-0.0_8$ |
| DL-Tryptophane | 13.72 | 15.5 | $13.1_4$ | $-0.5_8$ |
| $C_8H_6N \cdot CH_2CH(NH_2)COOH$ | | 23.8 | $13.5_6$ | $-0.1_6$ |
| | | 10.6 | $13.3_0$ | $-0.4_2$ |
| L-Histidine hydrochloride | 20.05 | 17.4 | $19.8_7$ | $-0.1_8$ |
| $C_3H_3N_2 \cdot CH_2CH(NH_2HCl)COOH \cdot H_2O$ | | 20.7 | $20.2_7$ | $+0.2_2$ |
| | | 27.2 | $19.7_5$ | $-0.3_0$ |
| | | 20.8 | $19.5_9$ | $-0.4_6$ |
| 1-Phenyl-3-methyl- | 16.08 | 36.50 | 16.31 | +0.23 |
| pyrazolone-(5) | | 32.94 | 16.35 | +0.27 |
| $CH_3C_3H_2ON_2 \cdot C_6H_5$ | | 99.86 | 15.86 | −0.22 |
| | | 26.93 | 16.08 | 0.00 |
| | | 33.36 | 16.39 | +0.31 |
| 2-Aminobenzothiazole | 18.65 | 9.82 | 18.39 | −0.26 |
| $C_7H_4NS \cdot NH_2$ | | 16.76 | 18.58 | −0.07 |
| | | 22.19 | 18.24 | −0.41 |
| | | 21.31 | 18.17 | −0.48 |
| Nitron | 17.94 | 19.0 | $18.1_3$ | $+0.1_9$ |
| $C_{20}H_{16}N_4$ | | 22.4 | $18.1_7$ | $+0.2_3$ |
| | | 19.0 | $17.7_9$ | $-0.1_5$ |

Two ammonium salts were also analyzed. As pure samples as possible were selected or prepared and dried in the calcium chloride or sulfuric acid desiccator.

Not only the nitrogen in ammonium salts (ammonium chloride and ammonium oxalate) and amines (acetanilide, phthalimide, phenacetin, thionalide, urea, and thiourea), but also in azo-compounds (methyl orange, methyl red, and dithizone), a pyrrole (DL-tryptophane), pyrazols (L-histidine hydrochloride and 1-phenyl-3-methyl-pyrazolone-(5)), and a thiazole (2-aminobenzothiazole) were determined by means of this method. The nitrogen in the complicated compound such as nitron was also quantitatively determined. The precision and accuracy of the data are within ±3%.

Since it was assumed that the nitrogen in amino acids might be accurately estimated with this method, several amino acids (glycocoll, DL-α-alanine, DL-α-amino-n-valeric acid, L-leucine, DL-isoleucine, L-cystine, and arginine hydrochloride) were analyzed. Analyses for these compounds gave satisfactory results as shown in Table II.

For the compounds containing the already oxidized-form nitrogen such as nitro- or nitroso- radicals this method can not be used.

Uric acid and theobromine, which are derivatives of purine, atropine and lacto-flavine, which have complicated rings containing nitrogen, and antipyrine gave very low results for nitrogen with this method. The reason why this method can be applied to 1-phenyl-3-methyl-pyrazolone-(5), but not to antipirine, although these compounds have similar pyrazol rings, has not yet been determined.

TABLE II

DETERMINATION OF NITROGEN IN SOME AMINO ACIDS

| Substance | Nitrogen Content % | Sample Weight mg. | Nitrogen Content Found % | Nitrogen Content Deviation % |
|---|---|---|---|---|
| Glycocoll $NH_2CH_2COOH$ | 18.66 | 15.3 | $18.8_5$ | $+0.1_9$ |
| | | 24.0 | $18.1_4$ | $-0.4_2$ |
| | | 21.9 | $18.3_9$ | $-0.2_7$ |
| | | 19.1 | $18.8_6$ | $+0.2_0$ |
| | | 25.6 | $18.3_8$ | $-0.2_8$ |
| DL-α-Alanine $CH_3CH(NH_2)COOH$ | 15.76 | 25.5 | $15.6_3$ | $-0.1_3$ |
| | | 22.1 | $15.9_0$ | $+0.1_4$ |
| | | 18.1 | $15.5_6$ | $-0.2_0$ |
| | | 26.2 | $15.7_6$ | $0.0_0$ |
| | | 25.6 | $15.3_6$ | $-0.4_0$ |
| DL-α-Amino-n-valeric acid $CH_3CH_2CH_2CH(NH_2)COOH$ | 11.96 | 30.9 | $11.6_8$ | $-0.2_8$ |
| | | 20.3 | $11.8_1$ | $-0.1_5$ |
| | | 18.6 | $11.5_4$ | $-0.4_2$ |
| | | 35.6 | $11.7_6$ | $-0.2_0$ |
| | | 16.3 | $12.0_4$ | $+0.0_8$ |
| L-Leucine $(CH_3)_2CHCH_2CH(NH_2)COOH$ | 10.68 | 21.1 | $10.6_0$ | $-0.0_8$ |
| | | 18.3 | $10.5_9$ | $-0.0_9$ |
| | | 21.2 | $10.9_9$ | $+0.3_1$ |
| | | 13.3 | $10.6_7$ | $-0.0_1$ |
| | | 31.1 | $10.5_3$ | $-0.1_5$ |
| DL-Isoleucine $CH_3CH_2CH(CH_3)CH(NH_2)COOH$ | 10.68 | 23.1 | $10.9_0$ | $+0.2_2$ |
| | | 18.3 | $10.9_7$ | $+0.2_9$ |
| | | 19.2 | $10.6_5$ | $-0.0_3$ |
| | | 15.7 | $10.2_8$ | $-0.4_0$ |
| L-Cystine $(-SCH_2CH(NH_2)COOH)_2$ | 11.66 | 20.9 | $11.3_7$ | $-0.2_9$ |
| | | 20.9 | $11.4_7$ | $-0.1_9$ |
| | | 28.1 | $11.6_3$ | $-0.0_3$ |
| Arginine hydrochloride $NH_2C(NH)NHCH_2CH_2CH_2-CH(NH_2HCl)COOH$ | 26.60 | 14.3 | $26.4_1$ | $-0.1_9$ |
| | | 14.4 | $26.8_5$ | $+0.2_5$ |
| | | 12.3 | $25.8_9$ | $-0.7_1$ |
| | | 13.7 | $26.6_9$ | $+0.0_9$ |
| | | 18.5 | $25.8_0$ | $-0.8_0$ |

As has been indicated above this iodic acid decomposition method can be applied to many species of organic compounds containing nitrogen, but not to all species.

The compounds having relatively low melting points such as diphenylamine, p-dimethylaminobenzaldehyde, and azobenzene, the melting points of which are 54, 74, and 68°C, respectively, can not be analyzed with this method, because these compounds are partially volatilized during the decomposition reaction.

It was shown by means of experiments for nicotinic acid and oxine that the nitrogen in pyridine and quinoline ring can not be liberated with this reagent at all. Since the nitrogen in amino-form can be determined with this method as mentioned above, it was presumed that for the two nitrogens of nicotinic amide only the nitrogen in amino-form

TABLE III
DETERMINATION OF NITROGEN IN NICOTINIC AMIDE

| Substance | Half the Nitrogen Content % | Sample Weight mg. | Nitrogen Content Found % | Nitrogen Content Deviation % |
|---|---|---|---|---|
| Nicotinic amide $C_5H_4N \cdot CONH_2$ | 11.57 | 14.8 | $11.9_3$ | $+0.3_6$ |
| | | 21.2 | $11.6_9$ | $+0.1_2$ |
| | | 19.5 | $11.6_8$ | $+0.1_1$ |
| | | 13.8 | $11.9_4$ | $+0.3_7$ |

might be measured. As might have been expected half the total nitrogen could be determined as indicated in Table III.

The advantages of this method are as follows: (1) Since the iodic acid decomposition of organic compounds in strong phosphoric acid is a wet reaction, the velocity of the decomposition in this method is much more rapid than in the micro-Dumas method. The time required for one analysis is about thirty to forty minutes. If this method is modified from semi-micro to micro method in the future, the analysis time will be more shortened. (2) The progress of the decomposition reaction can be watched through the glass and the end of its reaction can be easily recognized. Namely, it is indicated by means of the ceasing of the bubble formation and clearing of the liquid. (3) The apparatus is very cheap and all of it can be made by oneself.

The defects of this method are the following: (1) Similarly to the case of the Kjeldahl method, not all types of compounds containing nitrogen can be analyzed with this method as mentioned above. (2) The precision and accuracy of the data in this method are slightly worse than the micro-Dumas or Kjeldahl method. This is probably owing to the imperfection of the apparatus. The improvements of these defects for this method and the modification of this method to the micro scale are the remaining problems for the future.

**Summary**

A new method has been developed to permit the rapid determination of nitrogen in organic compounds. The sample is decomposed with iodic acid-strong phosphoric acid reagent in a glass reaction vessel, and the liberated nitrogen is collected in an azotometer filled with potassium hydroxide solution by the flow of pure carbon dioxide. From the volume of the nitrogen thus collected the percentage of the nitrogen in the sample can be readily determined. This method is, so to speak, the wet modification of the Dumas method.

For various types of compounds containing nitrogen, ammonium salts, amine, azo-compound, pyrrol, thiazole, etc., satisfactory results were obtained by means of this method. The nitrogen in a 10 to 50 mg. sample can be determined for thirty to forty minutes with a simple and inexpensive apparatus.

But volatile compounds, nitro- or nitroso-compounds, compounds having purine, pyridine, quinoline, and other complicated rings, etc., can not give good results.

The author wishes to thank Prof. T. Kiba for his encouragement and valuable advice during the course of this investigation, Prof. Y. Kurata for suppling some of the samples used in this study, and Mr. T. Takagi and H. Higashidani for their helpful assistance. The cost of this research has been partly defrayed from the Scientific Research Grant from the Ministry of Education.

*Department of Chemistry, Faculty of Science, Kanazawa University, Kanazawa*

# *Decrease of the Surface Area of Raney-type Catalysts in the Aluminium-dissolution Process*

By Masaki SATO and Nobuto OHTA

(Received October 4, 1954)

## Introduction

Some authors have shown[1-5] that the surface areas or the catalytic activities of Raney nickel catalysts decrease on reserving. The present authors suggested in the studies on Raney copper catalyst for the dehydrogenation of cyclohexanol to cyclohexanone,[6] that the similar, but much more rapid decrease of the surface area might occur in the process of dissolving aluminium with alkali.

It has been confirmed that this suggestion was right and applicable also to the usual Raney nickel catalyst.

## Experimental Procedure

**(1) Preparation of the Catalysts.**

*a) Starting alloy.*—The starting alloy for the catalyst No. 16* was obtained as follows.

Firstly, 40 parts of aluminium were melted in an electrically heated furnace or Tammann furnace and then 5 parts of zinc, 50 parts of copper, and 5 parts of nickel were put into it in the above order.

The fused solution was stirred with a silica tube to be homogenized, the temperature being raised to about 900°C. After cooling the alloy was powdered and 200 mesh powders were used as the sample. The content of aluminium was 40.6%.

As Raney nickel, a commercial one containing 48.9% of aluminium was used.

*b) Dissolving of aluminium.*—The dissolution of aluminium was carried out using 30% NaOH aqueous solution in an open vessel. After dissolution, the remaining catalyst was taken out of the alkali solution and washed with cold water till the washed water became neutral to litmus-paper. The time required for this treatment was always 3 to 4 hrs.

As soon as the washing was finished the sample was put into a vessel for the measurement of the surface area and dried at 20° to 30°C under the reduced pressure until the pressure of the system reached about $10^{-4}$ mm Hg.

**(2) Measurement of the Surface Area.**—The surface area was determined by using the usual method of low temperature adsorption of carbon-dioxide and making use of the B. E. T. equation. Nitrogen gas was used to the measurement of the dead space of the apparatus.

The carbondioxide that we used was a commercial one stored in an iron cylinder. It was purified by the usual cleaning up system, consisting of a copper sulfate bottle for scrubbing out hydrogen-sulfide, a concentrated sulfuric acid bottle for drying and a phosphorus pentoxide tube for removing the trace of moisture.

After the system was pumped out to high vacuum (about $10^{-4}$ mm Hg), the first adsorption test of carbon dioxide was carried out at −78.5°C. To avoid errors based on the probable presence of a trace of alkali on the surface of the catalyst, the system was degassed by a diffusion pump for an hour at 0°C after the first test and the adsorption test was repeated again at −78.5°C.

The surface area was calculated from the $V_m$ value (the volume of gas required to form a monomolecular layer all over the surface) obtained from the second isotherm, where the cross-sectional area of carbondioxide molecule was assumed to be 17.0 Å$^2$.

## Results

The experimental results are shown in Fig. 1, Fig. 2, Table I-a and Table I-b.

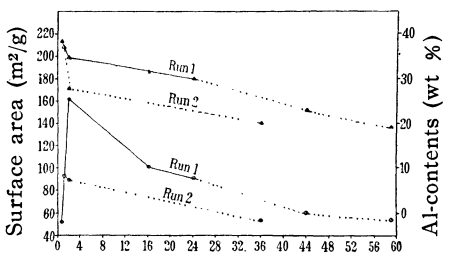



Fig. 1. The relationship between the surface area and the condition of aluminium-dissolution, on the catalyst "No. 16".
⊙ Surface area. ◬ Content of aluminium. (Temperature of dissolution are 10°to 15°C at solid lines and 70° to 80°C at dotted lines.)

* One of the best catalysts for the dehydrogenation of cyclohexanol to cyclohexanone which was discovered by the present authors.[7]

1) J. Aubry, *Bull. soc. chim.* (France), 5, 1333 (1938).
2) R. Schröter, *Angew. Chem.*, 54, 229, 252 (1941).
3) A. A. Pavlic and H. Adkins, *J. Am. Chem. Soc.*, 68, 1471 (1946).
4) H. A. Smith, W. C. Bedoit and J. F. Fuzek, *J. Am. Chem. Soc.*, 71, 3769 (1949).
5) J. H. Pattison and F. Degering, *J. Am. Chem. Soc.*, 73, 486 (1951).
6) This suggestion was presented at the 6th Annual Meeting of the Chemical Society of Japan held at Kyoto, April, 1953.

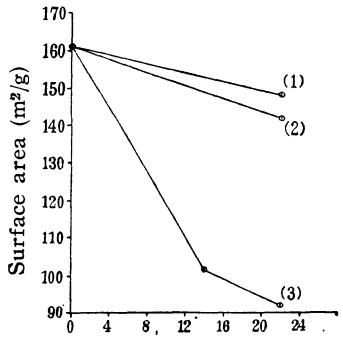



Fig. 2. Variations of the surface area of the catalyst "No. 16" on standing.
Note: Dissolution of aluminium was carried out at 10° to 15°C. for 2 hrs. Each sample was reserved in a following condition.
(1) 70° to 80° C, in vacuum.
(2) room temperature (20°C), in water.
(3) 10° to 15°C, in 30% NaOH aq. solution.

TABLE I-a
VARIATION OF THE SURFACE AREA IN THE ALUMINIUM DISSOLUTION PROCESS ON RANEY NICKEL CATALYST

| Condition of the solution | | Surface area ($m^2$/g.) | Al-content (wt%) |
|---|---|---|---|
| 1 hr. | 10° to 15°C | 48.2 | 33.0 |
| 2 hrs. | 10° to 15°C | 58.8 | 31.0 |
| 24 hrs. | 10° to 15°C | 47.0 | |
| 1 hr. +1 hr. | 10° to 15°C 70° to 80°C | 43.0 | 24.8 |
| 1 hr. | 70° to 80°C | 46.5 | 29.5 |

TABLE I-b
THERMOSTABILITY OF CATALYST "NO. 16" OBTAINED BY A SEVERE DISSOLUTION PROCESS
(24 hrs., 10° to 15°C+35 hrs., 70° to 80°C)

| | Surface area ($m^2$/g.) | Al-content (wt%) |
|---|---|---|
| Original | 55.5 | 19.8 |
| After heating at 400°C for 3 hrs. in vacuum | 55.5 | 19.8 |

## Discussion

From the experimental results above mentioned the following is obvious.

1) At an initial step of the dissolution-process, the content of aluminium becomes lower on the surface of the catalyst and bare copper or nickel atoms, active centers for catalysis, increase in number to form abnormally uneven surfaces having a large area.

At the next step of this process, where the velocity of dissolution of aluminium is rather small and the internal aluminium may be dissolved out, the surface area decreases in spite of successive dissolution of aluminium. It surely leads to a conclusion that during this step nascent bare atoms of nickel or copper formed by dissolution of aluminium move so as to reconfigurate the surface-structure to a more stable one. This kind of reconfiguration (or decrease of surface area) may be sufficiently reasonable, but has not been reported on the Raney type catalyst. As anticipated, the rate of this decrease is higher as the temperature of the dissolution process is higher (Fig. 1 and Table I-a).

2) It is valid to say on the catalyst "No. 16" (Fig. 1 and Fig.2), that the decrease of surface area during the aluminium-dissolution process is more rapid when compared with that during reserving in dried state or in water. Smith,

Fig. 3 The catalyst "No. 16" prepared by an exhaustive dissolution-process (24 hrs. at 10° to 15°C and next 20 hrs., at 70° to 80°C).

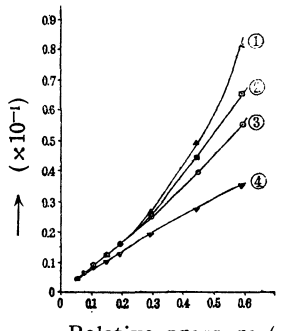



Fig. 3-A
(1) B. E. T.-line. (2) Hüttig-line.
(2) Anderson-line. (4) Langmuir-line.

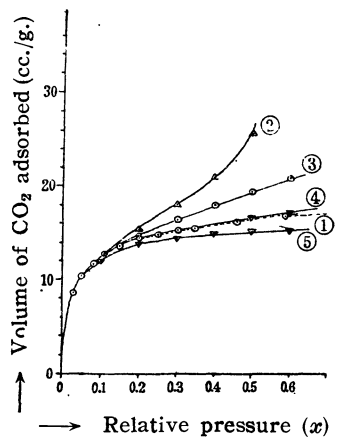



Fig. 3-B
(1) observed-curve. (4) modified B. E. T. -curve ($n$=2.0).
(2) B. E. T.-curve.
(3) Hüttig-curve. (5) Langmuir-curve.

Bedoit and Fuzek[4] reported the aging of the Raney nickel "W-2", of which the surface area originally was 38.0 $m^2/g$. and which, after ten or 40 days, decreased to 31.0 or 26.0 $m^2/g$. respectively. The rate of decrease of surface is merely less than one-tenth compared to that shown in Table I-a.

3) From Table I-b, it can be understood that the catalyst prepared by an exhaustive dissolution-process (24 hrs. at 10° to 15°C, and next 35 hrs. at 70° to 80°C) has a very heat-stable surface. This must be one of the causes that the catalyst maintained the most suitable activity for a long time[8].

4) In Fig. 3-A, the abscissa represents the relative pressure $x$ $(=p/p_0)$, the ordinate $x/v(1-x)$, $x/v(1-0.8x)$, $x(1+x)/x$ or $x/v$ in the case of the B. E. T.[9], Anderson[10], Hüttig[11] or Langmuir[12] equation, respectively (the $v$ is the volume of $CO_2$ adsorbed).

In each case, the rigid linearity exists at 0.05 to 0.25, 0.05 to 0.25, 0.05 to 0.35 or 0.15 to 0.15 of $x$, respectively; that is, the Hüttig line shows the linearity in the widest range. (Fig. 3-A)

In Fig. 3-B, solid lines were shown to represent the relations between the relative pressure and the volume of adsorbed carbon-dioxide, calculated by putting each $V_m$ found in Fig. 3-A into the corresponding Hüttig, Langmuir, B. E. T. and modified B. E. T. equation (1)[13] in which the maximum numbers of adsorbed molecules are assumed to be finite.

$$V=\frac{V_m\cdot C\cdot X}{1-x}\cdot\frac{1-(n+1)\cdot x+n\cdot x^{n+1}}{1+(C-1)\cdot x-n\cdot x^{n+1}}, \qquad (1)$$

where $C$ is a constant, and $n$ is the maximum numbers of adsorbed molecules.

A dotted line is the observed curve, which accords best with the modified B. E. T. line $(n=2)$.

5) In Fig. 4-5, calculated values of the adsorbed carbon-dioxide $(V_{cal})$~the relative pressure lines are shown as dotted lines. The $V_{cal}$ were obtained by putting various finite values in "$n$" of the modified B. E. T. equation (1), where the $V_m$ found from the B. E. T. line of $x/v(1-x)\sim x$ was always used. Observed curves of the same relation were shown as the solid lines.

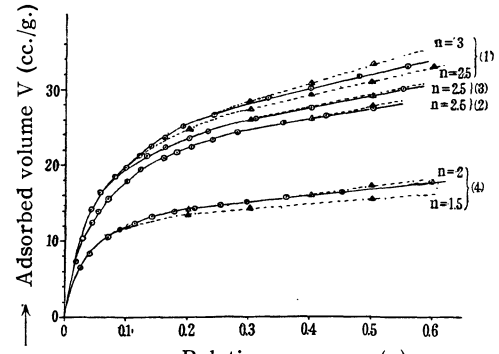



Fig. 4. Alloy-catalyst "No. 16"

| Run No. | Condition of aluminium dissolution | $n$ |
|---|---|---|
| (1) | 16 hrs., 10° to 15°C | 2.5–3 |
| (2) | 24 hrs., 10° to 15°C | 2.5 |
| (3) | 1 hr, 10° to 15°C, +1 hr, 70° to 80°C | 2.5 |
| (4) | 24 hrs, 10° to 15°C+20 hrs, 70° to 80°C | 2.0 |

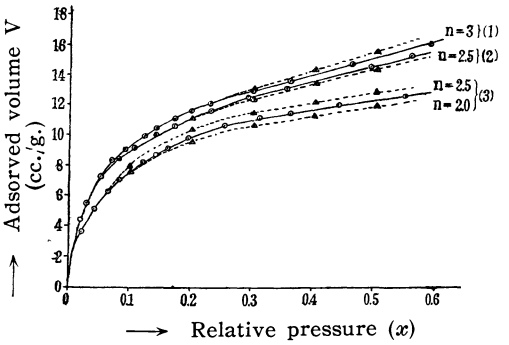



Fig. 5. Raney-nickel

| Run No. | Condition of aluminium dissolution | $n$ |
|---|---|---|
| (1) | 1 hr, 10° to 15°C | 3.0 |
| (2) | 24 hrs, 10° to 15°C | 2.5 |
| (3) | 1 hr, 10° to 15°C, +1 hr, 70° to 80°C | $2.0<n<2.5$ |

A comparison of the curves with the calculated ones shows that the severer the condition of dissolution is, the lower the reliable $n$-value is. As this value indicates the number of molecular layers adsorbed on the catalyst surface, it may be considered** as a factor indicating the adsorption affinity, which, in turn, probably is a variable having some relation with the catalytic activity.

On dehydrogenation of cyclohexanol to cyclohexanone at 275°C, the catalyst "No. 16" prepared by a mild dissolution process[6] (12°C, 75 hrs.) showed a very high activity in the initial period as compared with the same catalyst prepared by the above exhausive dissolution. But the activity of the former decreased rapidly to a degree lower than that of the latter catalyst, which

7) N. Ohta and M. Sato, *J. Chem. Soc. Japan* (Ind. Chem. Section), **56**, 153, 250 (1953).
8) N. Ohta, M. Sato and J. Imamura, *J. Chem. Soc. Japan*, (Ind. Chem. Section) **56**, 495 (1953).
9) S. Brunauer, P. H. Emmett and E. Teller, *J. Am. Chem. Soc.*, **60**, 309 (1938).
10) R. B. Anderson, *J. Am. Chem. Soc.*, **68**, 686 (1946).
11) G. F. Hüttig, *Kolloid-Z.*, **121**, 50 (1951).
12) I. Langmuir, *J. Am. Chem. Soc.*, **37**, 1139 (1915), **38**, 2221 (1916).
13) T. L. Hill, *J. Chem. Phys.*, **14**, 263 (1946).

maintained the initial activity for a long time.

It was concluded from these facts that a very active, but unstable surface is left at an initial step of dissolution process in dissolution at a low temperature, while a less active, but more stable surface appears in process of dissolution or the severe dissolution process.

Furthermore, the reconfiguration pointed out at 1) may be an important cause of this decrease of catalytic activity. Active centers on the Raney nickel "W-6"[14], which is the most active catalyst of this type particularly at low temperatures, may seem to be nascent bare nickel atoms formed at the low temperature dissolution.

## Summary

Variations of the surface area in the dissolution process were investigated on a Raney copper catalyst "No. 16" (for dehydrogenation of cyclohexanol) and a Raney nickel catalyst.

It has been found that nascent bare atoms of copper or nickel formed at the initial step move rapidly, perhaps particularly in alkali solution, to reconfigurate the surface-structure to a more stable one.

That is to say, the surface area reaches a maximum at an initial step, where only a small quantity of aluminium is dissolved out, then rapidly decreases to a stable value in spite of successive dissolution of aluminium. The rate of decrease is much greater than that recognized on reserving the catalyst in its dried state or in water.

By calculating reliable "$n$" values, the number of adsorbed molecular layers on the surface area from the modified B. E. T. equation, it has been deduced that the average catalytic activity per unit area of the surface may be decreased in process of dissolution of aluminium.

*The Government Chemical Industrial Research Institute, Tokyo*
*Hatagaya*

14) H. Adkins and H. R. Billica, *J. Am. Chem. Soc.*, 70, 695 (1948).

** The $n$-value may not be considered as a factor indicating the variation of pore- radius at the catalyst from the adsorption-desorption isotherm.

# *Surface Chemistry of Synthetic Protein Analogues. VI. The Interaction of Urea and Salt with Non-electrolytic Polypeptides*

By Toshizo ISEMURA, Kozo HAMAGUCHI and Hideyo KAWASATO

(Received September 27, 1954)

When protein is spread on the surface of water as a monolayer, it suffers in general surface denaturation. On the other hand, it is also denatured by the interaction with some reagent such as urea. Moreover, it is well known that urea forms adduct compounds[1] with most compounds having a relatively long, straight hydrocarbon chain. The behaviour of the synthetic polypeptides such as poly-DL-$\alpha$-aminolauric acid etc. which had been investigated as a protein model in the previous experiments,[2] has been studied on the substrate of urea solution by measuring surface pressure-area and surface viscosity-area relations. Meanwhile, the interaction of salt solution on these films of non-electrolytic polypeptides was also investigated. Urea affects the pressure-area relation profoundly, in spite of the absence of -S-S- or -SH groups in these polypeptides, as compared with the protein which contains such groups.

## Experimental

**The Method and Materials.** — The surface pressure was measured by the surface balance of Langmuir-Adam type. The torsion thread used was phosphorbronze wire, 0.12 mm. in diameter. The pressure was measured up to 5 dynes/cm. The surface viscosity was measured by the dumping of the oscillatory rotation of disc. The details of the measurements are essentially the same as those in the previous investigations.[3] The materials were poly-DL-$\alpha$-aminolauric acid, poly-DL-$\alpha$-aminocapric acid, poly-DL-$\alpha$-aminocaprylic acid and poly-$\gamma$-benzyl-L-glutamate. The urea used was a commercial product of Toyo Koatsu Kogyo Co., which was used after repeated recrystallization and adsorption by active carbon. Potassium chloride was used as an example of salt in this case. It was a chemical reagent grade and doubly recrystallized.

1) A.E. Smith, *J. Chem. Phys.*, **18**, 150 (1950).
2) T. Isemura and K. Hamaguchi, This Bulletin, **25**, 40 (1952).
3) T. Isemura and K. Hamaguchi, ibid., **27**, 125 (1954).

## Experimental Results

The measured surface pressure-area relations are shown in Fig. 1–4. The film expanded considerably on the substrate containing urea. The more urea existed in the substrate, the film the more expanded. The viscosity-area relations on the substrates with or without urea are shown in Fig. 5. The viscosity of the film on the urea containing substrate was rather irregular and the reproducibility of the results was relatively unsatisfactory. The products of pressure and area $FA$ were plotted against pressure $F$ in the low pressure region. Satisfactorily linear relations were obtained as shown in Fig. 6. In each figure, all straight lines intersect $FA$-axis at a single point.

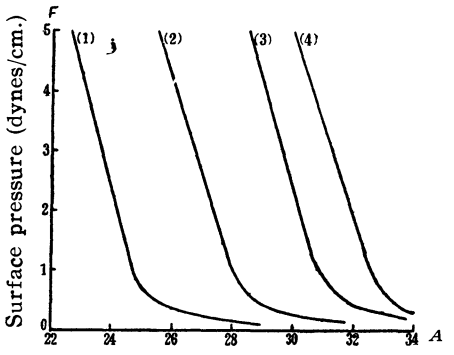



Fig. 1. Surface pressure-area curves of poly DL-$\alpha$-aminolauric acid. (1) on distilled water; (2) on 10 % urea solution; (3) on 20 % urea solution; (4) on 30 % urea solution.

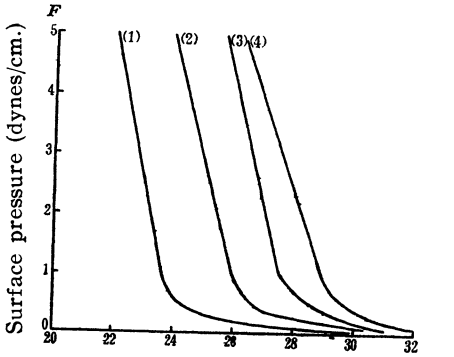



Fig. 2. Surface pressure-area curves of poly DL-$\alpha$-aminocapric acid. (1) on distilled water; (2) on 10 % urea solution; (3) on 20 % urea solution; (4) on 30 % urea solution.

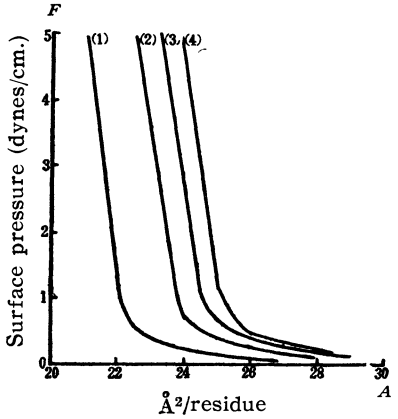



Fig. 3. Surface pressure-area curves of poly DL-$\alpha$-aminocaprylic acid. (1) on distilled water; (2) on 10 % urea solution; (3) on 20 % urea solution; (4) on 30 % urea solution.

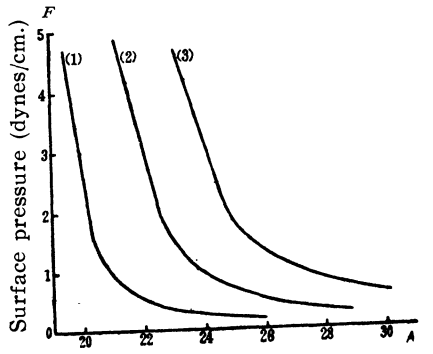



Fig. 4. Surface pressure-area curves of poly $\gamma$-benzyl-L-glutamate. (1) on distilled water; (2) on 10 % urea solution; (3) on 30 % urea solution.

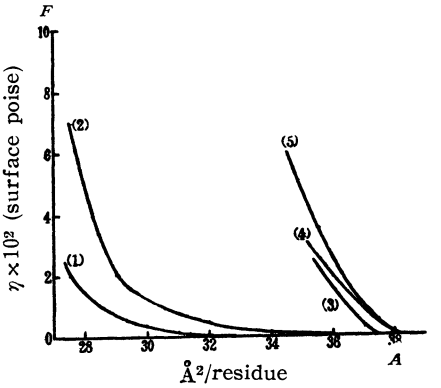



Fig. 5. Surface viscosity-area curves of poly-$\gamma$-benzyl-L-glutamate. (1) on distilled water or 0.1 % urea solution; (2) on 0.3 % urea solution; (3) on 0.5 % urea solution; (4) on 5 % urea solution; (5) on 10 % urea solution.

The effect of potassium chloride is shown in Fig. 7. While potassium chloride affects considerably the $F$–$A$ curve in the case of electrolytic polypeptide as reported in the preceding paper[4] in the concentration as low

4) K. Hamaguchi and T. Isemura, ibid., 28, 9 (1955).

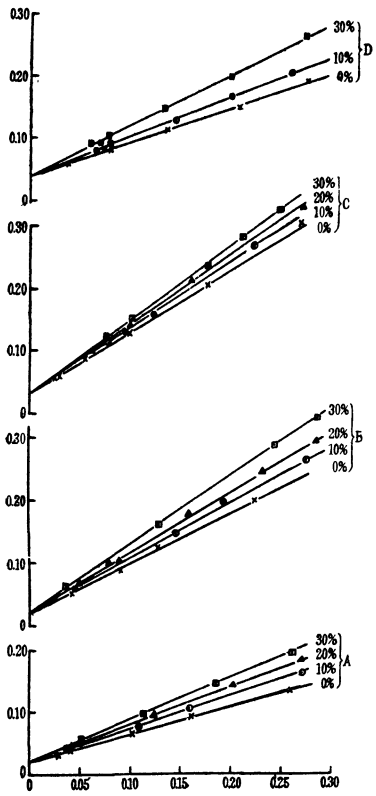



Fig. 6. Plot of $FA$ versus $F$ for poly DL-$\alpha$-aminolauric acid (A), poly DL-$\alpha$-aminocapric acid (B), poly DL-$\alpha$-aminocaprylic acid (C), and poly $\gamma$-benzyl-L-glutamate (D).

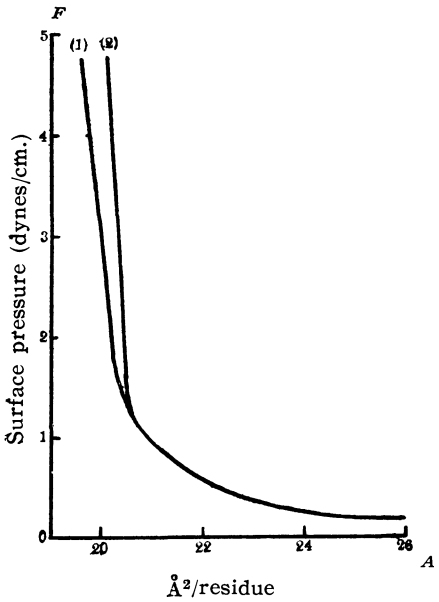



Fig. 7. Surface pressure-area curves of poly $\gamma$-benzyl-L-glutamate on distilled water (1) and on 10 % KCL solution (2).

as 0.5 %, it did not affect that of the non-electrolytic polypeptide in the concentration of 1 %. However, the film expanded slightly on 10 % potassium chloride solution.

## Discussion

From these experimental results, it might be concluded that the Guastalla's relation[5],

$$FA=\alpha F+\beta$$

holds for the polypeptide films on distilled water as well as on urea solutions. The estimated molecular weights of these polypeptides are shown in Table I.

TABIE I

MOLECULAR WEIGHT DETERMINED ON VARIOUS SUBSTRATES

| Substrate sample | Distilled water | 10% urea solution | 20% urea solution | 30% urea solution |
|---|---|---|---|---|
| Poly-DL-$\alpha$-amino caprylic acid | 74,500 | 73,500 | 74,000 | 74,000 |
| Poly-DL-$\alpha$-amino capric acid | 122,000 | 111,700 | 111,700 | 111,700 |
| Poly-DL-$\alpha$-amino lauric acid | 121,000 | 122,000 | 111,500 | 111,800 |

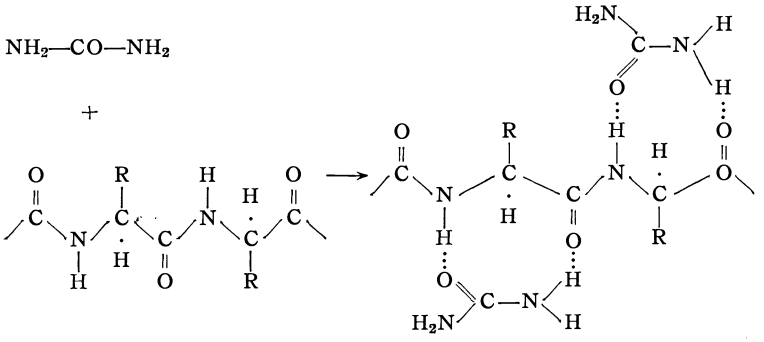
The coincidence of points of intersection made by the $FA$ axis and $FA$–$F$ lines indicates that the molecule of the polypeptide suffers neither association nor dissociation on the substrate of urea solution. The slopes of these $FA$–$F$ lines become steeper with the increase of the concentration of urea. As generally accepted, the slopes of these lines correspond to the co-area of the molecule.[5] Therefore, it is very probable that the polypeptide molecule interacts in some way with urea and forms a labile addition compound which occupies a larger area. The interaction was non-stoichiometric because the slope of $FA$–$F$ lines became steeper when the solution was more concentrated. It does not seem to be caused by the aduct formation, because the expansion of the film was observed on the dilute aqueous urea solution as low as 5 %. This concept is also valid in view of the fact that the film of poly-$\gamma$-benzyl-L-glutamate which should not form urea aduct, also expanded on the urea solution, and that the formation of aduct is generally agreed to be difficult with compounds of branched chain or those containing a large group such as benzene in the chain.

If the effect of urea found in the present experiments stands with the urea denaturation of protein, the view that the sulfhydryl groups play a special part in denaturation might be incorrect. Bonding of urea to the

5) J. Guastalla, *Compt. rend.*, 208, 1078 (1938); H.B. Bull, *J. Biol. Chem.*, 185, 27 (1950).

polypeptide linkage replaces the intramolecular hydrogen bondings in protein and leads to the cleavage of salt bridges causing the unfolding of the polypeptide. In our present experiment the polypeptide was unfolded by spreading it as a surface film. Hence, the urea solution as dilute as 5% in concentration will readily interact with polypeptide linkage. The appearance of -SH groups in the protein denatured by the interaction with urea rather means the removal of steric hindrance by neighbouring peptide chains against the reaction with the reagent such as nitroprusside.

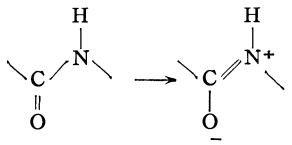
With a given polypeptide sample, all *FA–F* lines obtained with the substrate of different urea content intersect *FA*-axis at a single point as mentioned above. This is a very striking fact, which may be comprehended to be such that the number of polypeptide molecules does not change by the urea interaction. Nevertheless, the co-area of the molecule of film substance increased with the increase of urea concentration in the substrate. It is said that the denaturing action of solution of urea on protein is probably due to the formation of hydrogen bonds with the peptide linkages of the peptide chains[5]. Hence, the expansion of the film might be caused by the bonding of urea to the polypeptide linkage as follows:



Once this bonding was formed, it would be fairly strong. When the substrate water was partially replaced by dropping distilled water of equal volume to that of the through into it at a corner and overflowing the substrate water through syphone from it at its farthest corner without causing any disturbance on the film surface, the film area did not decrease.

A view may be expressed that the expanding effect of urea on the film of polypeptide would be caused by the breaking of the inter- and intrachain hydrogen bonds. However, if that were the case, the number of molecules on substrates of different urea concentrations would have changed and the *FA–A* lines should not intersect *FA* axis at a single point.

It was reported in the previous paper[4] that electrolyte such as potassium chloride exerts a profound influence on the nature of film of amphoteric copolypeptide. However, on the films of non-electrolytic polypeptide as in the present experiment was scarcely detected. On the highly concentrated solution the film non-electrolytic in nature was slightly affected as shown in Fig. 7. The reasons for this expansion of the film might be explained by the formation of rather looser network, by the interaction of polarized backbone as follows.



From the results of the viscosity measurements, the influence of urea was found to be predominant at the concentration more than 0.5% in the substrate. Although the *F–A* curve tends to shift to the larger area on the more concentrated urea solution, the *η–A* curves on the substrates of concentrated urea solution were independent of urea concentration.

## Summary

The interaction of urea and potassium chloride with non-electrolytic polypeptide monolayers was investigated. The film of polypeptide was expanded considerably in the presence of urea in the substrate. The number of molecules was, however, not changed by the interaction with urea. The molecular weights of polypeptides determined by surface pressure measurement on the substrates with

6) F. Haurowitz. "Chemistry and Biology of Proteins," Acad. Press, New York, (1950) p. 130.

or without urea were the same. Whereas the co-area of the molecule was increased by increase of urea concentration in the substrate. Urea might be bound to the peptide linkages in backbone by hydrogen bonding and the formation of aduct seems improbable.

Although potassium chloride affected the nature of electrolytic polypeptide film profoundly, it scarcely affected that of the non-electrolytic polypeptide film. The interaction with urea was discussed in relation to the protein denaturation.

The authors wish to express their sincere thanks to Dr. H. Tani and Mr. H. Yuki of the Faculty of Science of Osaka University and Dr. J. Noguchi of Kanazawa University who gave them the valuable samples of the synthetic polypeptides. A part of the expense for this experiment has been defrayed from grants given by the Ministry of Education and by the Asahi Press, to which the authors thanks are also due.

*The Institute of Scientific and Industrial Research,*
*Osaka University,*
*Sakai, Osaka*

# *A Note on Some Alkoxydisilanes*

By Rokuro Ōkawara, Toshio Tanaka and Keiichi Maruo

(Received November 8, 1954)

Many alkoxy-monosilane and -polysiloxanes have been studied, but on the alkoxydisilanes only a few reports[1,2,3] have been presented. The difficulty encountered on preparing the alkoxydisilanes from hexachlorodisilane and alcohol is the fission of Si-Si bond during the reaction. In the fission product, usually, alkoxy-monosilane and -polysiloxanes were found. Among them, disiloxane has a boiling point close to that of disilane and it is difficult to separate these two compounds by distillation. This paper will describe in as great detail as possible the preparation of alkoxydisilanes in the pure state. And the properties of hexamethoxydisilane (I), hexaethoxydisilane (II) and hexaisopropoxydisilane (III) will be described.

As previously reported[3], to prepare (I) from hexachlorodisilane and methanol, the dehydrochlorination by bubbling of nitrogen should be carried out under 30°C to prevent the fission of Si-Si bond also any trace of chlorine compound contaminated in the product should be precipitated by dry ammonia. In the light of this experiment, the preparation method to give pure (II) reported by Martin[1] and followed by Abrahamson et al,[2] appeared questionable. To drive off a trace of chlorine compound from the reaction product, Martin added ethanol and distilled it repeatedly and finally he obtained the chlorine free (II). In our experiment, it was found very difficult to purge off all the chlorine compound by repeated addition of ethanol and by followed aeration even at about 92°−95°C. And the product obtained after distillation still contained a trace of chlorine compound which makes the product slightly turbid and on prolonged standing there was a little precipitation of a white substance.

To assure whether the elevated temperature treatment of dehydrochlorination may give the completely chlorine free product or not the following incompletely dehydrochlorinated mixture of ethanol (6 mol.) and hexachlorodisilane (1 mol.) was refluxed. The chlorine content gradually decreased as in the case of partially alkolyzed alkylchlorosilanes[4,5]. And there was obtained a completely chlorine free product which was assured by Beilstein test. On fractional distillation, tetraethoxysilane, hexaethoxydisiloxane contaminated with a very small amount of (II) and octaethoxytrisiloxane were obtained. From this experiment, it may be concluded that by prolonged heating at the reflux temperature the incompletely dehydrochlorinated ethoxydisilane becomes chlorine free, but the ethoxydisilane is decomposed to form the mixture of the ethoxy-monosilane and -polysiloxanes.

Hexaisopropoxydisilane (III), a crystalline solid having the melting point 84.5° to 84.7°C,

1) G. Martin, *J. Chem. Soc.*, 105, 2860 (1914).
2) E.W. Abrahamson, I. Joffe and H.W. Post, *J. Org. Chem.*, 13, 275 (1948).
3) R. Ōkawara and T. Tanaka, This Bulletin, 27, 120 (1954).
4) R. Ōkawara, This Bulletin, 27, 428 (1954).
5) R. Ōkawara and I. Ishimaru, ibid., 27, 582 (1954).

was obtained after repeated recrystallizations from isopropanol. The relation of its melting point and the silicon content was determined after each recrystallization.

Analytical data of silicon of (I) and (II) were somewhat lower than the calculated value, but it may be seen within the experimental error. It may be possible that these two liquid alkoxy-disilanes are contaminated with a small amount of corresponding disiloxane, which has a boiling point close to that of the disilane. To determine the contamination of disiloxane in disilane, the volumetric method of determination of hydrogen evolved on the reaction with a basic reagent may be the suitable one, since with the determination of silicon content it is not easy to differentiate these two compounds. But the volumetric method which was described by Abrahamson[2] and Schumb[6] may not be useful for the time being, for the hydrogen evolved by the fission of Si-Si bond was not quantitative in general.

It was further found that the prevailing method of preparation of alkoxymonosilane using pyridine as an acid acceptor throughout the reaction could not be applied to the preparation of alkoxydisilane, because in pyridine medium, the fission of Si-Si bond takes place and alkoxymonosilane becomes the main product.

## Experimental

**Starting Materials.**—For the starting materials dehydrated methanol and ethanol, of which the water content was found by the Karl Fischer method to be 0.05% and 0.17% respectively, and isopropanol of Shell Chemicals (b.p. 82.2°C, $n_D^{20}$ 1.3776) were used. The hexachlorodisilane used in this experiment was prepared by the reaction of chlorine and powdered 75% ferrosilicon at the temperature of 160°–250°C. As the catalyst a small amount of potassium chloride[7] was mixed with the ferrosilicon. The liquid product obtained was rigorously fractionated through a Stedman column of about 30 theoretical plates. The fraction having the boiling point 147°C/760 mmHg and the melting point −1.2°—0.8°C was taken as the starting material. Analysis for the hydrolyzable chlorine was carried out by breaking 0.2–0.5 g. of the weighed sample in water-methanol solution in a sealed vessel, and titrating the liberated acid with 0.1 N-NaOH solution.

*Anal.* Found: Cl, 79.0. Calcd. for $Cl_6Si_2$: Cl, 79.1%.

**Preparation of Hexamethoxydisilane (I).**—The preparation and properties of this compound were already described.[3] Data on this substance are given in Table I.

**Preparation of Hexaethoxydisilane (II).**—In a 500 cc. three-necked flask equipped with an efficient stirrer, a dropping funnel and a reflux condenser hexachlorodisilane (32 g., 0.119 mol.) was placed. Ethanol (33 g., 0.72 mol.) was added with vigorous stirring for 1 hour. During the addition the temperature was kept below 5°C. After the addition the temperature was raised to 30°C for 30 minutes. The mixture (52 g.) was aerated with dry nitrogen for 2 hours during which the temperature was gradually raised to 50°C. The weight of the mixture lessened to 40 g., where the chlorine content was 9.7%. Aeration was further continued at the room temperature by adding 5 g. of ethanol. After 1.5 hours a product (37 g.) containing 2% chlorine was obtained. A slight excess of pyridine (3 g.) was added to precipitate any trace of chlorine compound. The filtrate (30 g.) was fractionated through a semi-micro Stedman column of about 20 theoretical plates. After a slight excess of pyridine and a small amount of tetraethoxysilane were distilled off, the product was fractionated under 0.8 mmHg. The constant boiling fraction (12 g., 31% of the theory) was obtained, the middle portion of which was analysed. The results are given in Table I.

**(i) Preparation of Hexaethoxydisilane (II) by Dehydrochlorination at 95°C.**—At the room temperature (10°C), 31 g. (0.115 mol.) of hexachloro-

TABLE I

ALKOXYDISILANES

| Formula | Boiling Point °C/mmHg | Melting Point °C | Refractive Index $n_D^{20}$ | Density $d_4^{20}$ | Molecular Weight Found** (Calcd.) | % Si Found (Calcd) |
|---|---|---|---|---|---|---|
| $(CH_3O)_6Si_2$ (I) | 100–1/20 | — | 1.4070 | 1.095 | 235 (242) | 23.00 (23.18) |
| $(C_2H_5O)_6Si_2$* (II) | 75–6/0.8 | — | 1.4102 | 0.9728 | 318 (327) | 17.18 (17.20) |
| $(i\text{-}C_3H_7O)_6Si_2$ (III) | 164–6/38 | 84.5–7 | — | — | 415 (411) | 13.68 (13.68) |

* G. Martin, loc. cit., B. P., 123/15, $n_D^{14.5}$ 1.4134, $d_4^{17}$ 0.9718

** Cryoscopic measurement in benzene

6) W.C. Schumb and R.A. Lefever, *J. Am. Chem. Soc.*, 75, 1513 (1953).

7) D.F. Stedman, U.S.P. 2, 621, 111; *Chem. Abstr.* 47, 3037 (1953).

disilane and 32 g. (0.7 mol.) of ethanol were mixed with vigorous stirring during the course of 40 minutes. The mixture was gradually heated to 60°C for 1.5 hours. At this temperature dehydrochlorination was carried out by bubbling a slow stream of dry nitrogen through the mixture. After 1 hour, the weight of the mixture amounted to 37 g., and the chlorine content was found to be 4.1%. To complete the dehydrochlorination, ethanol (2 g.) was added and nitrogen was bubbled for 3 hours at 70°–80°C. But the product (34 g.) which contains still 2.3% chlorine was obtained. Finally, the product (27 g.) of which chlorine content 0.7% was obtained after repeated addition of 2–3 g. of ethanol (the total amount was 7 g.) and by followed aeration for 8 hours with nitrogen at the temperature of 92°–5°C. After adding a small amount of ethanol, the product was rigorously fractionated through the semi-micro Stedman column under the reduced pressure. The following three fractions were obtained.

| Fraction | b.p. (°C/mmHg) | $n_D^{20}$ | %Si (Found) | Weight of the fraction (g.) |
|---|---|---|---|---|
| A′ | 79/32 | — | — | 0.5 |
| B′ | 75–6/0.8 | 1.4122 | 17.28 | 10 |
| C′ | 108–10/0.8 | 1.3963 | — | 2 |

The fractions A′, B′ and C′ may be considered tetraethoxysilane (reported[8] : b.p. 77/32, $n_D^{20}$ 1.3837), hexaethoxydisilane (II) and octaethoxytrisiloxane (reported[9] : b.p. 126/0.5, $n_D^{20}$ 1.3948; unpublished author's data: b.p. 107/0.8 mm, $n_D^{20}$ 1.3952). But the fraction B′ was contaminated by a small amount of chlorine compound, which was assured by the Beilstein test. Further the fraction B′ became turbid in moist air and it was difficult to weigh.

**(ii) Dehydrochlorination at the Refluxing Temperature.**—At the room temperature (10°C), 41 g. (0.15 mol.) of hexachlorodisilane and 42.5 g. (0.9 mol.) of ethanol were mixed with vigorous stirring during the course of 1.5 hours and the mixture was gradually heated to 60°C for 2 hours. Then the mixture (49 g.) of which chlorine content 6.6% was heated to its refluxing temperature in a small flask fitted with a condenser, the upper end of which was connected to a calcium chloride tube. As a volatile chlorine compound was gradually evolved from the mixture, the refluxing temperature rose gradually. After 50 hours of refluxing, the temperature attained to 187°C and the chlorine was not found in the mixture by the Beilstein test. The product (41 g.) was rigorously fractionated through the semi-micro Stedman column. The following three fractions were obtained.

| Fraction | b.p. (°C/mmHg) | $n_D^{20}$ | %Si (Found) | Volume of the fraction (cc.) |
|---|---|---|---|---|
| A | 57/10 | 1.3822 | — | 14 |
| B | 76–7/1 | 1.3928 | 16.26 | 4 |
| C | 105/1 | 1.3956 | 17.46 | 3 |

The fractions A, B and C may be considered tetraethoxysilane, hexaethoxydisiloxane (Anal. Calcd. Si, 16.40%. reported[9] : b.p. 94/0.5, $n_D^{20}$ 1.3914) and octaethoxytrisiloxane (Anal. Calcd. Si, 17.68%).

From the silicon content, hexaethoxydisilane (II) which may appear in the fraction B was not found in this experiment. A qualitative test of Si-Si bond in the fraction B and in the residue by the saturated potassium hydroxide solution, showed that the fraction B evolved a very small volume of hydrogen, while the residue evolved hydrogen violently, showing the presence of the compound having Si-Si bond.

From the result of the elevated temperature treatment described here, it was clearly shown that the preparation of alkoxydisilane should be carried out at as low a temperature as possible.

**Hexaisopropoxydisilane (III).**—In a 300 cc. three necked flask equipped with an efficient stirrer, a dropping funnel and a reflux condenser, hexachlorodisilane (40 g., 0.15 mol.) was placed. Isopropanol (54 g., 0.9 mol.) was added with vigorous stirring for 70 minutes. During the addition the temperature was kept below 5°C. After addition the temperature was gradually raised to 80°C for 2 hours and at this temperature, the mixture was dehydrochlorinated by bubbling dry nitrogen through the mixture until the chlorine content of the mixture became constant (the final value, 2.7%, was attained after bubbling for 4 hours). At this stage the weight of the mixture amounted to 47 g. When the mixture was cooled to the room temperature (10°C), there was a deposit of crystalline matters. The crystals were filtered and recrystallized from ethyl ether, but the crystals could not be completely separated from the fuming matter which may be chloroisopropoxydisilane. To prepare the pure hexaisopropoxydisilane, 3.5 g. of pyridine and 3 g. of isopropanol were added to the mixture (47 g.) and the mixture was maintained at 60°C for 2 hours. The deposited pyridine hydrochloride was filtered off at the temperature of 85°C. The pure hexaisopropoxydisilane could be prepared from recrystallization (a) or distillation (b) of this mixture (40 g.).

**(a) Recrystallization.**—The crystal was recrystallized four times from isopropanol, and its melting point and silicon content were determined. The results were as follows:

| Sample | | | Recrystallization times 1 | 2 | 3 | 4 |
|---|---|---|---|---|---|---|
| (a) | Filtered at 85°C | m.p. (°C) | 73–4 | 81–3 | 84.5–4.7 | 84.5–4.7 |
| | | % Si | 14.4 | 13.70 | 13.69 | 13.74 |
| (b) | (a) was simply distilled | m.p. (°C) | 84.5–4.7 | 84.5–4.7 | — | — |
| | | % Si | 13.63 | 13.65 | — | — |

8) D. F. Peppard, W.G. Brown and W.C. Johnson, *J. Am. Chem. Soc.*, **68**, 77 (1946).
9) T. Takatani, *J. Chem. Soc. Japan (Pure Chem. Section)*, **73**, 409 (1952), (in Japanese).

**(b) Distillation.**—The mixture (40 g.) was distilled under reduced pressure. The first fraction distilled at the temperature 90°–164°C/38 mmHg (5 g.) and the second constant boiling fraction 164°–6°C/38 mmHg (22 g., 36% theory) of hexaisopropoxydisilane (III) was obtained. The residue was composed of a gelatinous mass and amounted to 12 g. By the analyses of silicon (13.9%) and its melting point (72.5°–76°C), the second fraction may be considered as the crude (III). Pure hexaisopropoxydisilane (III) was obtained by the recrystallization from isopropanol. The properties of this substance are given in Table I. The relation between the melting point and the silicon content after each recrystallization is already shown above together with (a).

**Reaction of Hexachlorodisilane and Alcohol in Pyridine-Benzene Solution** (i) *In isopropanol.*—In the 500 cc. three-necked flask cooled with ice-bath and equipped as above, 38 g. (0.14 mol.) of hexachlorodisilane diluted with 125 g. of benzene was placed. To this mixture 51 g. (0.85 mol.) of isopropanol mixed with 67 g. (0.84 mol.) of pyridine was added with vigorous stirring. After pyridine hydrochloride was filtered off and benzene was distilled, the product with slight excess of pyridine amounted to 49 g. The product was distilled under reduced pressure. The distillate boiling at the temperature of 70°–110°C/13 mmHg (33 g.) was washed with water and dehydrated with sodium sulphate. From the refractive index $n_D^{20}$ 1.3850, and density $d_4^{20}$ 0.8770 (reported:[10] b.p. 93.4°C/28 mmHg, $n_D^{20}$ 1.3835 and $d_4^{20}$ 0.8744), the distillate was found to be tetraisopropoxysilane, which was produced by the fission of Si-Si bond. The oily residue 17 g. was not further examined.

(ii) *In ethanol.*—To the mixture of hexachlorodisilane (30 g., 0.11 mol.) and benzene was added the mixture of ethanol (32 g., 0.7 mol.) and pyridine (55 g., 0.7 mol.) and treated in the same way as above. After simple distillation the fraction boiling at 55°–65°C/10 mmHg and the residue (10 g.) were obtained. The slightly turbid distillate was thoroughly washed with water and dehydrated on sodium sulfate. From its density ($d_4^{20}$ 0.9330), the distillate may be considered to be tetraethoxysilane (reported[11] : $d_4^{20}$ 0.9356).

10) R. Ōkawara, T. Tanaka and I. Ishimaru, This Bulletin, 27, 45 (1954).
11) H. D. Cogan and C. A. Setterstrom. *Ind. Eng. Chem.*, 39, 1364 (1947).

## Analyses

**Silicon.**—Silicon was determined by decomposing the sample with concentrated sulfuric acid.

**Hydrogen.**—Only qualitative tests were carried out with the three disilanes by using the Zerewitinoff apparatus. Hexamethoxydisilane (I) evolved about 94% theory of hydrogen by mixing butanol saturated with sodium hydroxide at the room temperature (8°C), while hexaethoxydisilane (II) on the same condition became a gel and scarcely evolved hydrogen. By adding a saturated aqueous solution of potassium hydroxide, hexaethoxydisilane (II) easily evolved hydrogen (ca. 94% of the theory), but by 30% aqueous solution, it was difficult to evolve hydrogen. Since isopropoxydisilane (III) floats on the surface of saturated aqueous solution of potassium hydroxide, it was dissolved in dry piperidine and mixed with wet piperidine. Hydrogen evolved very slowly and the volume of it reached to ca. 90% of the theory after standing over night.

## Summary

1) Hexamethoxy-, hexaethoxy- and hexaisopropoxy-disilane were prepared and characterized.

2) Dehydrochlorination at an elevated temperature was not suitable for the preparation.

3) A trace of chlorine compound contaminated in the product could be completely taken off by dry ammonia or pyridine.

4) Alkoxydisilanes could not be prepared by using pyridine throughout the reaction as an acid acceptor.

5) The volume of hydrogen evolved by the fission of alkoxydisilanes varied with the reagents.

The authors wish to express their sincere thanks to Dr. Watase for his gracious encouragement and Miss Ukiko Takahashi for her aid during this experiment. Our thanks are also due to the Ministry of Education for aid in this research.

*Department of Applied Chemistry, Faculty of Engineering, Osaka University, Osaka*

# *The Dielectric Constant of 1,4-Dioxane*

By Masasi YASUMI and Michio SHIRAI

(Received November 24, 1954)

The possibility of a significant contribution of the atomic polarization to the dielectric constant of the polyatomic molecule was discussed by Van Vleck.[1] The experimental evidences were obtained by Sutton et al.[2], for the substances considered as nonpolar stereochemically. Their conclusions were based upon the following facts:

1) The molecular polarization of the gaseous substance was independent of the temperature over a wide range.

2) The value of the molecular polarization for the gaseous substances agreed with that obtained by the solution method.

3) The molecular polarization obtained by the solution method was independent of the solvent used.

In the present work we shall propose new criteria for determining whether the molecular polarization is due to the atomic polarization plus electronic polarization.

A) If the value of the molecular polarization in the pure liquid state does not depend upon the temperature.

B) If the molecular polarization in the solution states is dependent neither on concentration nor on the species of solvent.

C) If the molecular polarization in the solid state does not depend upon the temperature.

D) If the obtained values in the various states are consistent with each other.

Then we may conclude that the molecular polarization is simply the sum of the atomic polarization and electronic polarization except in very special cases.*

We shall apply these criteria to the 1,4-dioxane, and shall conclude that we cannot exclude the explanation that the dioxane molecule has only nonpolar form and the observed molecular polarization consists of the atomic and of the electronic polarizations.

The dielectric constant of dioxane in the gaseous state was measured by M. Kubo.[3] The molecular polarization was calculated in the usual way. The obtained value is about 5 cc. greater than the electronic polarization. It was concluded that the difference between the molecular polarization and the electronic polarization is due partly to the orientation polarization of the dioxane molecules in the polar form (or "boat" form) which exist in a small amount in the nonpolar form (or "chair" form). An alternative possibility that the difference is due entirely to atomic polarization of the molecule in the nonpolar form, was considered by the author to be less likely, for he believed that the atomic polarization is equal to about 10 % of the electronic polarization.

The statement that the atomic polarization is approximately equal to 10 % of the electronic polarization was not proved theoretically[1] but was merely guessed from analogy to the case of compounds,[4] which, however, have only one bond of an appreciable moment or have a rigid structure. If the vibrations of a molecule are harmonic and are not influenced by a neighbouring molecule, then the atomic polarization is independent of the temperature and of the states (gas, liquid, solution, solid). On the other hand, if we find that the molecular polarization of a substance depends neither upon the temperature over a wide range nor upon the state, we can conclude that the molecule of the concerned substance is nonpolar and the molecular polarization is due to the atomic and electronic polarizations. (It may happen that exceptions exist.)

To determine whether the molecular polarization of the dioxane is due to the atomic and electronic polarization, we have measured the dielectric constant of the substance in the liquid state and the solid state. Also the dielectric constants of the dioxane solutions of various concentrations in various solvents (hexane, heptane, cyclohexane and benzene) are measured.

The measurement of the dielectric constant in the solid state is very important to determine if the substance is polar or nonpolar. The dielectric constants of most of the polar substances suddenly decrease to lower values

1) J.H. Van Vleck, "Theory of Electric and Magnetic Susceptibilities", (1932) p. 51, 68. Oxford, Clarendon Press.

2) I.E. Coop and L.E. Sutton, *J. Chem. Soc.*, **1938**, 1269.

* It must be noted that the inverse statement is not always valid. It may happen that the atomic polarization is dependent upon the temperature and upon the states.

3) M. Kubo, *Sci. Pap. Inst. Phys. Chem. Res. (Tokyo)*, **30**, 238 (1936).

4) M. Kubo, *Sci. Pap. Inst. Phys. Chem. Res.*, **29**, 122 (1936).

when they go from the liquid state to the solid state. Some substances behave similarly at the transition point in the solid state[5]. Consequently, if we measure the dielectric constant of the substance concerned in the solid state from melting point to a much lower temperature, we can determine if the substance is polar or nonpolar.

Our plan is to measure the dielectric constant of dioxane in the liquid state and in the solid state, and to measure those of solutions, to calculate the molecular polarization using Clausius-Mosotti relation, and to see whether it is constant or not.

## Experimental

The dielectric constant was measured by a resonance method. (Fig. 1.) The replaceable capacity (liquid cell, C also used for solid) was incorporated into the circuit of a Hartley oscillator (A), the signal from which was picked up in an adjacent wave-meter (B). Each electrical component was enclosed in an earthened metal box.

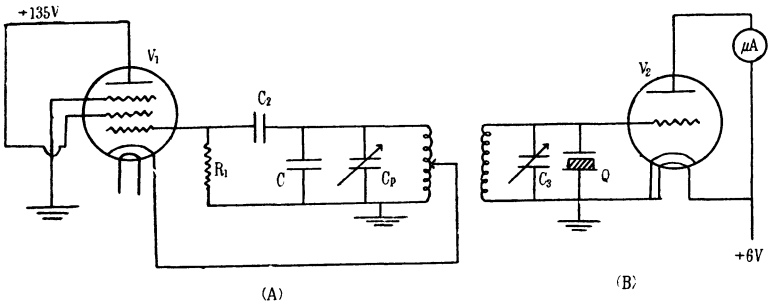



Fig. 1.

$V_1$: UZ-6C6
$V_2$: UY-76
$C_p$: Precision variable air condenser
$C_2$: Fixed condenser 60 pF
$C_3$: Air condenser 300 pF
Q : 2 Mc. Resonance quartz
$R_1$: Fixed resistance 30 kΩ
C : Liquid Cell

The resonance frequency of the wave-meter (B), when the quartz piece Q was not in the circuit, was arranged so that it would at the natural frequency of the quartz piece Q. When the frequency of the oscillator (A) was nearly the same as that of the wave-meter the anode current in the wave-meter humped, and when exactly the same it fell down. The resonance point thus indicated was very sharp.[6]

**Precision Condenser $C_p$.**—This was made by Yokogawa Electric Co. Ltd. The working range is 500 pF traversed in 25 turns. Each division (1/100 turn) corresponds to 0.2 pF. The limit of the reading is 1/10 of this division.

**Liquid Cell C.**—This was made up of two concentric nickel cylinders sealed into a glass vessel. This cell is similar to that used by Mizushima et al.[7] The cell constant did not change when the liquid froze. The capacity of the cell was about 24 pF.

The cell was immersed in a constant temperature bath filled with toluene, and was fixed at a definite position. Low temperatures were obtained by adding dry ice pieces to the bath. The low temperature was measured with an ether thermometer.

The densities of the liquid near room temperature were measured with an Ostwald's pycnometer. The densities of solid were measured with a dilatometer made of a glass tube having a capacity of ca. 5 cc.

The cell constant was determined using benzene as the standard whose dielectric constant was assumed to be 2.2423 at 20°C.

In order to determine the dielectric constant of a solid, it must be considered whether the thermal equilibrium was attained or not. In our experiment, however, it seems that the thermal equilibrium was attained. The reason is as follows: We have measured the dielectric constant of the solid after half an hour from the time when the temperature became constant. After two hours the dielectric constant was re-measured. (The constancy of the temperature was maintained in this time interval). The obtained values are consistent within experimental errors.

Materials used were as follows.

**Dioxane.**—Commercial dioxane was treated with potassium hydroxide. After distillation over potassium hydroxide, it was fractionally distilled over metallic sodium, a fraction of b. p. 101.5° C being taken.

5) S.O. Morgan, *Ann. New York Acad. Sci.*, XL, 357 (1940).

6) As to the detailed description of the apparatus and procedure of the measurement; see R.J.W. Le Fèvre, "Dipole moment", Methuen's monograph on physical subjects; Methuen Co. Ltd., London (1953), p. 36.

7) S. Mizushima, Y. Morino and K. Higasi, *Sci. Pap. Inst. Phys. Chem. Res.* (*Tokyo*), 25, 159 (1934).

**Benzene.**—Commercial benzene was washed with concentrated sulfuric acid, then with water, and was dried over calcium chloride. After drying over metallic sodium, it was fractionally distilled, b. p. 80°C.

***n*-Heptane.**—Commercial *n*-heptane was washed with sulfuric acid, then with water. After drying over calcium chloride, it was distilled, b. p. 97.5°C.

**Cyclohexane.**—Commercial cyclohexane was dried over calcium chloride, it was then distilled. After drying over metallic sodium, it was fractionally distilled, the fraction of b. p. 81°C being taken.

## Experimental Results and Discussions

In Table I are given the values of dielectric constants $\varepsilon$, densities $d$ and molecular polarizations ($P_M$)* for dioxane in the liquid and the solid state for various temperatures. The values of $P_M-P_E$ are also given in Table I. $P_E$ denotes the electronic polarization, the value of molecular refraction extrapolated to infinite wave-length and amounts to 20.8 cc.

TABLE I

DIELECTRIC CONSTANT OF DIOXANE IN THE LIQUID AND THE SOLID STATE

| $t$ | $\varepsilon$ | $d$ | $P_M$(cc.) | $P_M-P_E$(cc.) |
|---|---|---|---|---|
| 60 | 2.185 | 0.9911 | 25.2 | 4.4 |
| 50 | 2.194 | 1.0023 | 25.1 | 4.3 |
| 40 | 2.206 | 1.0126 | 25.0 | 4.2 |
| 30 | 2.220 | 1.0220 | 24.9 | 4.1 |
| 20 | 2.233 | 1.0321 | 24.9 | 4.1 |
| 15 | 2.248 | 1.0386 | 25.0 | 4.2 |
| 12 | 2.251 | 1.0416 | 24.9 | 4.1 |
| m.p. 11.7 | | | | |
| 11 | 2.329 | 1.0880 | 24.9 | 4.1 |
| 10 | 2.339 | | | |
| 0 | 2.329 | | | |
| −10 | 2.331 | | | |
| −20 | 2.331 | | | |
| −30 | 2.329 | | | |
| −40 | 2.329 | | | |
| −50 | 2.329 | | | |
| −60 | 2.329 | | | |
| −70 | 2.329 | | | |

The values of dielectric constanst $\varepsilon$ and of densities $d$ for dioxane-hexane solutions at the temperature of 20° C for various molecular fractions $x$ are tabulated in Table II. The molecular polarizations of dioxane are calculated in the usual way,[8] and are tabulated also in Table II, the values of $P_M-P_E$ are shown in Table II.

* $P_M=\frac{\varepsilon-1}{\varepsilon+2}\frac{M}{d}$; where $M$ is molecular weight of dioxane.

8) P. Debye, "Polare Molekeln", (1929), p. 46, Leipzig.

TABLE II

DIELECTRIC CONSTANT OF DIOXANE-*n*-HEPTANE SOLUTION AT 20°C

| $x$ | $\varepsilon$ | $d$ | $P_M$(cc.) | $P_M-P_E$(cc.) |
|---|---|---|---|---|
| 0.0000 | 1.9491 | 0.6870 | — | — |
| 0.2085 | 1.9780 | 0.7287 | 25.0 | 4.2 |
| 0.4359 | 2.0251 | 0.7884 | 25.0 | 4.2 |
| 0.6282 | 0.0786 | 0.8533 | 24.9 | 4.1 |
| 0.7488 | 2.1235 | 0.9026 | 24.9 | 4.1 |
| 1.0000 | 2.2326 | 1.0321 | 24.9 | 4.1 |

In Tables III and IV are given the above-mentioned values for dioxane-benzene and dioxane-cyclohexane solutions at the temperature of 20° C and 40° C respectively.

TABLE III

DIELECTRIC CONSTANT OF DIOXANE-BENZENE SOLUTION

$t=20°$ C

| $x$ | $\varepsilon$ | $d$ | $P_M$ | $P_M-P_E$ |
|---|---|---|---|---|
| 0.0000 | 2.2825 | 0.8770 | — | — |
| 0.1874 | 2.2751 | 0.9068 | 24.7 | 3.9 |
| 0.3498 | 2.2751 | 0.9315 | 24.7 | 3.9 |
| 0.5630 | 2.2635 | 0.9640 | 25.0 | 4.2 |
| 0.7128 | 2.2529 | 0.9880 | 24.9 | 4.1 |

$t=40°$ C

| $x$ | $\varepsilon$ | $d$ | $P_M$ | $P_M-P_E$ |
|---|---|---|---|---|
| 0.0000 | 2.2423 | 0.8583 | — | — |
| 0.1874 | 2.2423 | 0.8862 | 25.4 | 4.6 |
| 0.3498 | 2.2423 | 0.9106 | 25.4 | 4.6 |
| 0.5630 | 2.2266 | 0.9428 | 25.1 | 4.2 |
| 0.7128 | 2.2193 | 0.9663 | 25.0 | 4.2 |

TABLE IV

DIELECTRIC CONSTANT OF DIOXANE-CYCLOHEXANE SOLUTION

$t=20°$ C

| $x$ | $\varepsilon$ | $d$ | $P_M$ | $P_M-P_E$ |
|---|---|---|---|---|
| 0.0000 | 2.0483 | 0.7789 | — | — |
| 0.1715 | 2.0740 | 0.8093 | 25.9 | 5.1 |
| 0.3525 | 2.1066 | 0.8471 | 25.8 | 5.0 |
| 0.5476 | 2.1437 | 0.8951 | 25.5 | 4.7 |
| 0.7156 | 2.1872 | 0.9408 | 25.5 | 4.7 |

$t=40°$ C

| $x$ | $\varepsilon$ | $d$ | $P_M$ | $P_M-P_E$ |
|---|---|---|---|---|
| 0.0000 | 2.0059 | 0.7616 | — | — |
| 0.1715 | 2.0271 | 0.7902 | 25.6 | 4.8 |
| 0.3525 | 2 0579 | 0.8278 | 25.4 | 4.6 |
| 0.5476 | 2.0971 | 0.8749 | 25.3 | 4.5 |
| 0.7156 | 2.1310 | 0.9197 | 25.2 | 4.4 |

We see from Table I, that the value of molecular polarization of dioxane is constant over a wide temperature range, on solidification the value of molecular polarization does not change and maintains the same value down to −70° C. The fluctuation of the value is only about 1%, (mean value : 24.9 cc.).

From Tables II and IV, it is shown that the molecular polarization of dioxane in the

various solutions are consistent with each other and with that for pure dioxane in the liquid and the solid state. The deviations from the mean value (25.2 cc.) are slightly greater than that for pure dioxane but does not exceed 4%.

The values obtained by M. Kubo for dioxane in the gaseous state are tabulated in Table V.

TABLE V
DIELECTRIC POLARIZATION OF DIOXANE IN THE GASEOUS STATE

| $T$(K) | $P$(cc.) |
|---|---|
| 328.7 | 26.39 |
| 352.1 | 26.20 |
| 412.4 | 25.91 |
| 478.9 | 25.95 |

The difference between the values for the gaseous state and those for the solid and the liquid state is about 1 cc.

The structure of the 1,4-dioxane molecule has been investigated by various methods. X-ray data for the structure of the molecule seem to be lacking. The electron diffraction data[9,10] showed that the molecule exists predominantly in the nonpolar "chair" form[11,12].

The dielectric constants of dioxane in the gaseous state have been measured by M. Kubo[3]. It was concluded that the molecules of dioxane exists predominantly in the "chair" form, but a small amount of the molecule exists in the polar "boat" form. This conclusion was based upon the assumption that the atomic polarization is equal to 10% of the electronic polarization.

The value of the atomic polarization of $N$ one-dimensional oscilator is calculated[1] by the following equation, provided that the latter is harmonic.

$$ {}_AP_i = \frac{Ne_i^2}{4\pi m_i \nu_i^2} = \frac{4\pi N e_i^2}{9 f_i} \qquad (1) $$

where $m_i$ denotes the effective mass, $e_i$ effective charge, $\nu_i$ frequency and $f_i$ force constant, respectively.

For the bending vibration (replacing $e_i/f_i$ by $\mu_i^2/V_i$) equation (1) is reduced to

$$ {}_AP_i = \frac{4\pi \mu_i^2}{9 V_i} \qquad (1') $$

where $\mu_i$ is bond moment and $V_i$ is force constant for bending.

From equation (1) or (1') we see that the smaller the frequency (or the smaller the force constant) the greater the atomic polarization. In a complex polyatomic molecule, such as 1,4 dioxane, there exist many normal vibrations, some of which may have small frequencies. If they are infra-active, their contribution to the atomic polarization may be considerably significant.

The vibrational frequencies of the dioxane molecule have been observed[9,10], except for the infra-active vibrations of small frequencies. However, the calculation of the frequencies of skeletal vibrations has been made for the "chair" form of the molecule, and it is shown that the frequencies of infra-red active deformation vibrations are about 200 $cm^{-1}$.

It may be expected, that the atomic polarization of the dioxane molecule in the "chair" form exceeds 10% of the electronic polarization.

So there is no evidence that we cannot attribute the observed difference between the molecular polarization and the electronic polarization entirely to the atomic polarization of the dioxane molecule in the nonpolar "chair" form.

In the following paper the theoretical calculation of the value of the atomic polarization for the dioxane molecule in the nonpolar "chair" form will be given.

We are grateful to Prof. San-ichiro Mizushima for his kind advice and encouragement throughout this work. Our thanks are also due to the Ministry of Education for a grant in aid of this research.

## Summary

The dielectric constant of pure dioxane was measured in the liquid and the solid state.

The dielectric constants of dioxane solutions dissolved in various solvents were also measured.

Using Clausius-Mosotti relation, the molecular polarization of dioxane was computed. The computed value was dependent neither upon the state (solid liquid, solution) nor upon the temperature, and agreed almost exactly with the value obtained from the measurement for the gaseous substance.

The difference between the molecular polarization and the electronic polarization is ca. 4 cc. It seems natural to attribute this value to atomic polarization.

*Institute of Science and Technology, University of Tokyo*

9) L.E. Sutton and L.O. Brockway, *J. Am. Chem. Soc.*, 57, 473 (1935).
10) O. Hassel, *Fra. Fysik. Verden*, 7, 1648 (1947).
11) D. A. Ramsay, *Proc. Roy. Soc. S. A.* 190, 562 (1947).
12) S.C. Burket and R.M. Badger, *J. Am. Chem. Soc.*, 72, 4397 (1950).

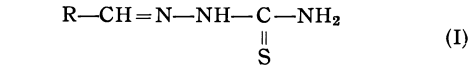
# *Antituberculous Compounds. V. 1-Thiocarbamyl-3-methyl-5-phenyl-2-pyrazoline, 1-thiocarbamyl-3-methyl-5-(4-nitrophenyl)-2-pyrazoline, and Related Compounds*

By Tamio NISHIMURA

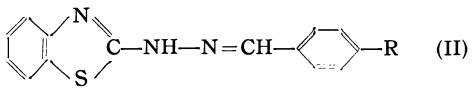
(Received December 4, 1954)

Considerable interest has been aroused by the publication of Domagk, Behnisch, Mietzsch, and Schmidt concerning the antituberculous activity *in vitro* of several thiosemicarbazones of aromatic aldehydes and ketones.[1] An excellent review of the investigation developed by the German workers in correlating structure with activity appeared in 1950.[2] Hoggarth, Martin, Storey, and Young[3] published in 1949 their excellent quantitative *in vivo* evaluation of a considerable number of thiosemicarbazones and compounds of related structure. Furthermore, the extensive synthesis[4] of thiosemicarbazones and related substances, and their *in vitro*[5] and *in vivo*[6] activities were reported by Bernstein et al.

L. Katz[7] prepared a series of the condensation products (II) closely related to the thiosemicarbazone (I), of 2-hydrazinobenzothiazoles with aromatic aldehydes and reported that most active compounds were obtained when the *p*-substituents (R) were carboxymethoxy and dimethylamino radicals.

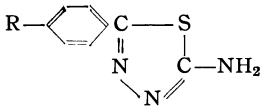


(I)

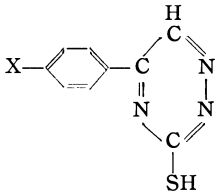


(II)

Bernstein et al.[4] mentioned the preparation of a number of heterocyclic compounds structurally related to I; 5-substituted-2-amino-1,3,4-thiadiazole derivatives (III), and N-(2-benzothiazolyl)-N′-(4-substituted benzal) hydrazone (II). R. Fusco et al.[8,8a] described the synthesis of 5-aryl-3-mercapto-1,2,4-triazines (IV) as new synthetic antitubercular agents.

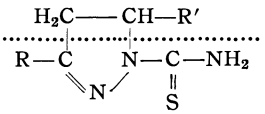


(III)



(IV)

However, the evaluation of 1-thiocarbamyl-2-pyrazolines (V) against *Mycobacterium tuberculosis* has not been reported. A study was therefore inaugurated in this Laboratory with the aim of preparing a number of 1-thiocarbamyl-2-pyrazolines and related substances. It is clear that the structure below the dotted line of (V) coincides with that of the thiosemicarbazone (I). Such a similarity between (V) and (I) was the basis for expecting antitubercular activity in this class of compounds.



(V)

The compounds prepared were 3-methyl-5-phenyl-2-pyrazoline, 3-methyl-5-(4-nitrophenyl)-2-pyrazoline, and their 1-substituted derivatives. The 1-substituents included the $-CS-NH_2$, $-CS-NHC_6H_5$, $-CS-NHCOC_6H_5$, $-CHO$, $-COCH_3$, and $-C_6H_5$ groups. The compounds described herein were prepared as indicated in the flow sheet.

1) G. Domagk, R. Behnish, F. Mietzch and H. Schmidt, *Naturw.*, **33**, 315 (1946); *Chem. Abstr.*, **43**, 3523e (1949).

2) R. Behnisch, F. Miezsch and H. Schmidt, *Am. Rev. Tuberc.*, **61**, 1 (1950).

3) E. Hoggart, A.E. Martin, N.E. Storey, and E.H.P. Young, *Brit. J. Pharm.*, **4**, 248 (1949).

4) J. Bernstein, H.L. Yale, K. Losee, M. Holsing, J. Martins, and W.A. Lott, *J. Am. Chem. Soc.*, **73**, 906 (1951).

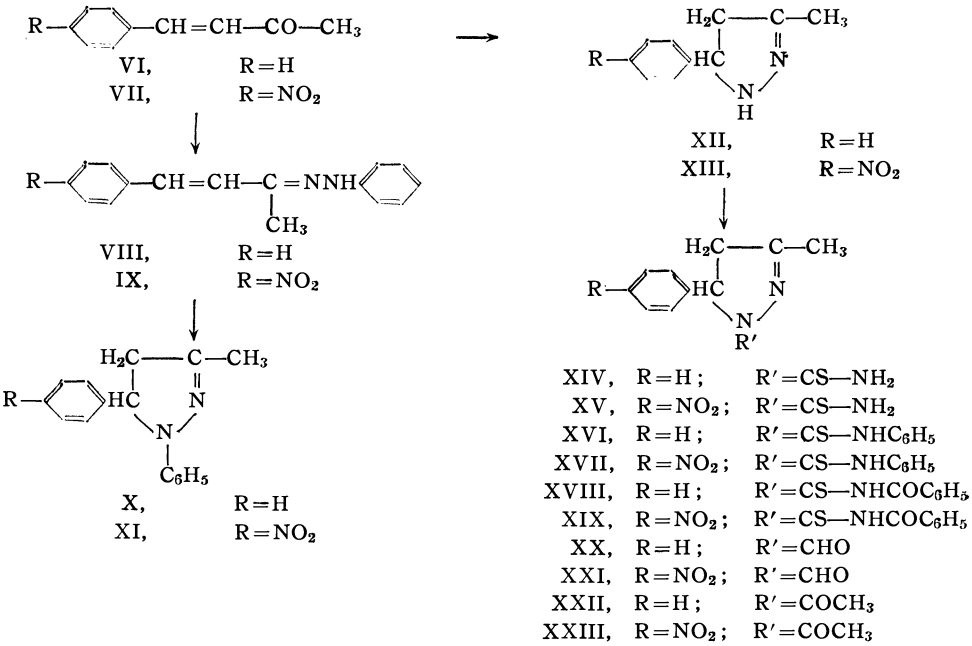
5) R. Donovick, F. Pansy, G. Stryker and J. Bernstein, *J. Bacteriol.*, **59**, 667 (1950).

6) D. Hamre, J. Bernstein and R. Donovick, ibid. 675.

7) Leon Katz, *J. Am, Chem. Soc.* **73**, 4007 (1951).

8) R. Fusco, P. Mantegazza, S. Rossi and R. Tommasini, *Boll. soc. ital. biol. sper.*, **27**, 1730-2 (1951); *Chemi. Abstr.*, **46**, 9199 (1952).

8*a*) R. Fusco, S. Rossi, G. Mantegazza and R. Tommasini, *Ann. chim.* (Rome), **42**, 94-104 (1952); *Chem. Abstr.*, **47**, 4301*c* 1953).




Benzalacetone (VI) was prepared according to the method described in Organic Syntheses,[9] and *p*-nitrobenzalacetone (VII) according to the procedure reported previously.[10] (VI) and (VII) were converted to the phenylhydrazones (VIII, IX) which were then cyclized to the pyrazolines (X, XI) by heating with glacial acetic acid. 3-Methyl-5-phenyl-2-pyrazoline (XII) was obtained in a 67% yield by the action of 80% hydrazine hydrate upon (VI) in ethanol according to the description of Beech et al.[11] (VII) and hydrazine hydrate in ethanol gave smoothly 3-methyl-5-(4-nitrophenyl)-2-pyrazoline (XIII) at room temperature. 1-Thiocarbamyl-3-methyl-5-(4-nitrophenyl)-2-pyrazoline (XV) was obtained in small yields when (XIII) and pottasium thiocyanate in water was acidified with glacial acetic acid and then heated on a water bath, a considerable amount of the 1-acetyl derivative being isolated from the reaction mixture, whereas in good yields when acidified with hydrochloric acid. On the basis of this finding, 1-thiocarbamyl-3-methyl-5-phenyl-2-pyrazoline (XIV) was easily obtained by the same procedure. The 1-(N-phenylthiocarbamyl)-derivatives (XVI, XVII) were prepared by the action of phenylisothiocyanate on (XII) and (XIII) in petroleum ether at room temperature. The 1-(N-benzoylthiocarbamyl)-derivatives (XVIII, XIX) were obtained by the action of ammonium thiocyanate plus benzoyl chloride on (XII) and (XIII). (XII) and (XIII) were easily converted to 1-formyl derivatives (XX, XXI) by heating with formic acid and to 1-acetyl derivatives (XXII, XXIII) by heating with glacial acetic acid.

9) N.L. Drake and P. Allen, Jr., "Organic Syntheses" Coll. Vol. I, p. 77 (1946).
10) Tamio Nishimura, This Bulletin, **26**, 253 (1953).
11) S.G. Beech, J.H. Turnbull and Walter Wilson, *J. Chem. Soc.* **1952**, 4689.

## Experimental

*Benzalacetone phenylhydrazone* (VIII).—Heating a mixture of benzalacetone (1.4 g.), phenylhydrazine hydrochloride (1.5 g.), sodium acetate trihydrate (1.6 g.), and methanol (20 cc.) gave 1.8 g. (76%) of the desired product melting at 152–158°. Recrystallization from methanol yielded yellow plates melting at 155–157°.[13]

*4-Nitrobenzalacetone phenylhydrazone* (IX).—By the foregoing procedure, an almost quantitative yield of the hydrazone was obtained in red microcrystals melting at 194–196°.[14]

*1-Phenyl-3-methyl-5-phenyl-2-pyrazoline* (X).—A mixture of benzalacetone phenylhydrazone (1 g.) and glacial acetic acid (3 cc.) was heated in an oil bath of 130° for 1 hour. Crystals (0.8 g.) separated on cooling were recrystallized from 13 cc. of methanol to give the desired product, yellow long prisms melting at 112–113°.[15]

*1-Phenyl-3-methyl-5-(4-nitrophenyl)-2-pyrazoline* (XI).—The crude product obtained similarly from 1 g. of the phenylhydrazone (IX) was three times recrystallized from ethanol, yielding 0.6 g. of apricot yellow needles, m. p. 113–113.5°.[16]

12) All temperatures are uncorrected.
13) Reported m.p. 157°. See E. Fischer, *Ber.*, 17, 576 (1884).
14) Reported m.p. 195-196°. See K. Auwers and H. Voss, *Ber.*, 42, 4425 (1909).
15) K. Auwers and H. Voss (loc. cit.) give m.p. 115-116°.
16) K. Auwers and H. Voss (loc. cit.) give m.p. 112-113°.

*3-Methyl-5-phenyl-2-pyrazoline* (XII).—Following the procedure of Beech et al.[11], 11 g. (67 %) of the desired pyrazoline, b. p. 140–142°/13 mm.[17] was obtained from benzalacetone (14.6 g.), 80 % hydrazine hydrate (11 g.), and ethanol (40 cc.).

*3-Methyl-5-(4-nitrophenyl)-2-pyrazoline* (XIII).—A mixture of 9.6 g. of 4-nitrobenzalacetone, 4 g. of 80 % hydrazine hydrate, and 20 cc. of ethanol was stirred at room temperature. As soon as the ketone dissolved, yellow precipitates[18] began to separate, but dissolved again to make a clear red solution, and then the whole slowly solidified on further stirring. The cake was filtered, washed with ethanol, suspended in 100 cc. of water and acidified with 10 % hydrochloric acid. The solution was filtered and neutralized partially with 10 % sodium hydroxide, forming a resinous orange substance which was filtered off. The filtered solution was made slightly alkaline to give cream yellow crystals, m. p. 98–100°. After a recrystallization from 20 cc. of ethanol, 6.6 g. (65 %) of the desired product, m. p. 97–102°, was obtained. Further recrystallization from ethanol gave an elevation of the melting point to 104–107° (Found: N, 20.60 %. Calcd. for $C_{10}H_{10}N_3O_2$: N, 20.58 %.). As this substance is likely to change to red resinous material, it is desirable to store it in sealed brown colored ampules.

*1-Thiocarbamyl-3-methyl-5-phenyl-2-pyrazoline* (XIV).—A mixture of 1.5 g. of benzalacetone, 1 g. of 80 % hydrazine hydrate, and 10 cc. of ethanol was refluxed gently on a water bath for 1 hour. After removing the ethanol under reduced pressure, the residue was mixed with ammonium thiocyanate (1.1 g.) and water (20 cc.). The whole was acidified with 10 % hydrochloric acid and the undissolved red oil was removed by filtration. The solution was then heated on a water bath for 5 hours to give yellow plates, m. p. 228–229° (decomp.), yield 0.5 g. (23 %). Recrystallization from ethanol changed the melting point to 230–231° (decomp.) (Found: N, 19.12 %. Calcd. for $C_{11}H_{13}N_3S$: N, 19.12 %).

*1-Thiocarbamyl-3-methyl-5-(4-nitrophenyl)-2-pyrazoline* (XV).—A mixture of 3-methyl-5-(4-nitrophenyl)-2-pyrazoline (2.1 g.), ammonium thiocyanate (1.1 g.), and water (40 cc.) was acidified with 10 % hydrochloric acid to pH 2.2 and an undissolved red tarry substance was removed by decantation. The solution was then heated on a water bath for 3 hours to form the desired product melting at 268–269° (decomp.), slightly orange yellow prisms (Found: N, 21.68 %. Calcd. for $C_{11}H_{12}N_4O_2S$: N, 21.20 %). Several recrystallizations from ethanol yielded faintly yellow prisms, m. p. 271° (decomp.).

*1-(N-Phenylthiocarbamyl)-3-methyl-5-phenyl-2-pyrazoline* (XVI).—Phenyl isothiocyanate[19] (1.4 g.) and 3-methyl-5-phenyl-2-pyrazoline (1.6 g.) were mixed and stirred at room temperature. The whole solidified immediately. The white solid was triturated with petroleum ether, filtered and washed with petroleum ether, to obtain the product, m. p. 166–167°, yield 2.8 g. On recrystallization from 200 cc. of methanol, there was obtained 2.1 g. (70 %) of colorless prisms, m. p. 160–161°. Further recrystallization from methanol did not change the melting point. (Found: N, 13.82 %. Calcd. for $C_{17}H_{17}N_3S$: N, 14.23 %).

*1-(N-Phenylthiocarbamyl)-3-methyl-5-(4-nitrophenyl)-2-pyrazoline* (XVII).—A solution of 3-methyl-5-(4-nitrophenyl)-2-pyrazoline (0.51 g.), and phenyl isothiocyanate (0.34 g.) in benzene (4 cc.) was allowed to stand at room temperature for several days. After removing benzene, reddish brown syrup was extracted with 25 cc. of ether and the ether extract was dried over anhydrous sodium sulfate. The ether was evaporated to form a red oil which changed to a glass-like solid after several days. The solid was extracted with 15 cc. of hot methanol and the methanol was removed to give crystalline residue. Recrystallization from methanol gave tiny slightly greenish-yellow needles melting at 141–142°, yield 0.33 g. (38 %). Further recrystallization elevated the melting point to 143–144° (Found: N, 16.41 %. Calcd. for $C_{17}H_{16}N_4O_2S$: N, 16.46 %).

*1-(N-Benzoylthiocarbamyl)-3-methyl-5-phenyl-2-pyrazoline* (XVIII).—Benzoyl chloride (4.2 g.) was added dropwise to a suspension of ammonium thiocyanate (2.4 g.) in acetone (24 cc.) and the whole refluxed gently for several minutes. To this reaction mixture was added dropwise a solution of 3-methyl-5-phenyl-2-pyrazoline (prepared from 1.5 g. of benzalacetone and 0.9 g. of 80 % hydrazine hydrate) in acetone. The content was refluxed for several minutes after the addition was completed and then poured into 200 cc. of water. Yellow crystals were collected, washed with water and recrystallized from ethanol. The yield was 2.2 g. (69 % based on benzalacetone), m.p. 185–185.5° (decomp.), greenish yellow plates (Found: N, 13.07 %. Calcd. for $C_{18}H_{17}N_3OS$: N, 13.00 %).

*1-(N-Benzoylthiocarbamyl)-3-methyl-5-(4-nitrophenyl)-2-pyrazoline* (XIX).—This compound was similarly prepared, yellow prisms (from acetone), yield 2.7 g. (73 %) from 2.2 g. of 3-methyl-5-(4-nitrophenyl)-2-pyrazoline, m. p. 199–200° (decomp.) Found: N, 15.41 %. Calcd. for $C_{18}H_{16}N_4O_3S$: N, 15.21 %).

*1-Formyl-3-methyl-5-phenyl-2-pyrazoline* (XX).—A solution of 1.7 g. of 3-methyl-5-phenyl-2-pyrazoline in 8 cc. of formic acid was heated for 1 hour on a water bath. Methanol was added to the reaction mixture and removed under reduced pressure. This procedure was repeated twice more to give a yellow oil. The oil was dissolved in 2 cc. of 25 % methanol and the methanol solution poured into 10 cc. of water. By rubbing the wall of the beaker a white precipitate was formed, which was filtered, and washed with water, m. p. 66–69°, colorless needles. This was recrystallized from 25 % methanol to yield 1.1 g. (55 %) of the desired product, m. p. 65–78° before drying, m. p. 88.5–89° after drying in a desiccator (Found: N, 14.75 %. Calcd. for $C_{11}H_{12}N_2O$: N, 14.89 %).

*1-Formyl-3-methyl-5-(4-nitrophenyl)-2-pyrazoline* (XXI).—3-Methyl-5-(4-nitrophenyl)-2-pyrazo-

17) S.G. Beech, et al. (loc. cit.) give b.p. 166°/35mm.

18) Intermediate formation of the precipitates was not observed when the reaction temperature was higher.

19) F. B. Dains, R. Q. Brewster and C. P. Olander, "Organic Syntheses", Col. Vol. I. p. 447 (1946).

line (1.1 g.) was dissolved in 5 cc. of formic acid and heated on a water bath for 1 hour. After removing the formic acid, methanol was added and removed under reduced pressure. This procedure was repeated once more to give dull orange yellow crystals. Recrystallizations from 25 % methanol gave a sample melting at 121–122°, yield 0.7 g. (60 %), pale yellow plates (Found: N, 18.05 %. Calcd. for $C_{11}H_{11}N_3O_3$: N, 18.02 %).

*1-Acetyl-3-methyl-5-phenyl-2-pyrazoline* (XXII).—A mixture of 1.7 g of 3-methyl-5-phenyl-2-pyrazoline, 2 cc. of acetic anhydride, and 10 cc. of water was stirred at room temperature. Colorless oil separated was extracted with ether (20 cc.) and the ether washed with water containing sodium hydroxide, with water containing hydrochloric acid and then with distilled water and dried over anhydrous sodium sulfate. Evaporation of ether at room temperature gave 1.1 g. of colorless crystals. On recrystallization from ether, there was obtained a sample melting at 77.5-78°.[20]

*1-Acetyl-3-methyl-5-(4-nitrophenyl)-2-pyrazoline* (XXIII).—

(a) A mixture of 0.5 g. of 3-methyl-5-(4-nitrophenyl)-2-pyrazoline and 2.5 cc. of glacial acetic acid was heated on a water bath. Duration of heating and yield were as follows: 1 hour, 0.17 g. (28 %); 3 hours, 0.21 g. (34 %); 5 hours, 0.28 g. (45 %); 8 hours, 0.25 g. (40 %). The crude product of m. p. 136–137° was dissolved in hot water and the filtered solution was allowed to stand for 1–2 weeks at room temperature, giving large yellow crystals melting at 138° (Found: C, 58.57; H, 5.67; N, 16.90 %. Calcd. for $C_{12}H_{13}N_3O_3$: C, 58.27; H, 5.30; N, 16.99 %).

(b) To a suspension of 3-methyl-5-(4-nitrophenyl)-2-pyrazoline (0.8 g.) in 5 cc. of water 0.8 cc. of acetic anhydride was added dropwise and with stirring. The precipitate was washed with water and with cold ether to remove the red gummy substance, giving yellow powder melting at 137–138°. Recrystallizations from ether gave the desired product of m. p. 137–139°.

20) Beech et al. (loc. cit.) give m.p. 77-79°.

## Summary

The preparation is described of 3-methyl-5-phenyl-2-pyrazoline, 3-methyl-5-(4-nitrophenyl)-2-pyrazoline and their 1-phenyl, thiocarbamyl, N-phenylthiocarbamyl, N-benzoylthiocarbamyl, formyl, and acetyl derivatives which were to be tested for antituberculous activity.

The author wishes to express his appreciation to the Ministry of Education for a Grant in Aid for the Miscellaneous Scientific Research, under which a portion of this work was carried out.

*Chemical Laboratory, The Kitasato Institute, Tokyo*

# *Radiometric Determination of Small Amounts of Antimony*

By Tomitaro ISHIMORI and Kaoru UENO

(Received April 26, 1954)

Dichlorobisethylenediamine cobaltic hexachlorostibinate, the insoluble precipitate obtained by adding *trans*-dichlorobisethylenediamine cobaltic chloride to a hydrochloric acid solution of quinquevalent antimony, was reported first by Pfeiffer and Tapauch[1] in 1906. The reaction can be written as

$$[Co(en)_2Cl_2]Cl+(Sb^vCl_6)^- \longrightarrow [Co(en)_2Cl_2](Sb^vCl_6)+Cl^-$$

*trans*-Dichlorobisethylenediamine cobaltic chloride → Dichlorobisetylenediamine cobaltic hexachlorostibinate

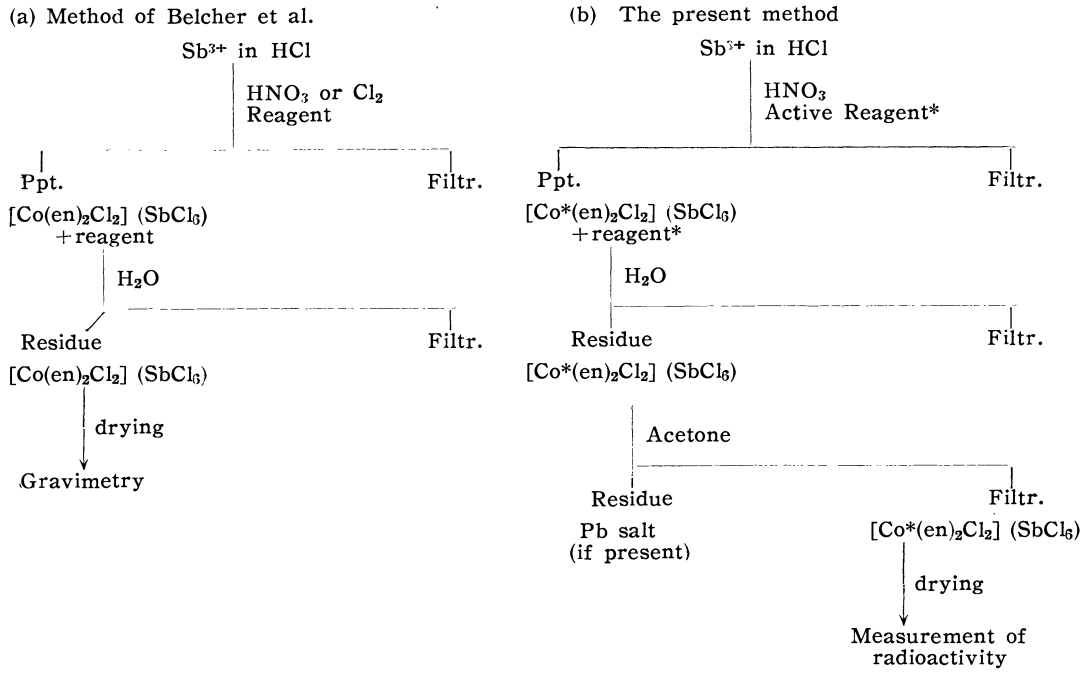
Recently Belcher and Gibbons[2] succeeded in gravimetric determination of antimony by means of the above-mentioned reaction. The scheme of the method is given in Table Ia. According to their paper, the lower limit of determinable amount is lmg. antimony, and the determination is interfered with seriously with a very small amount of lead.

In the present paper, a radiometric method of determination of $(1-0.06)$ mg. antimony by radioactive *trans*-dichlorobisethylenediamine cobaltic chloride labelled with cobalt-60 is described. The present method consists of the precipitation of antimony and the washing with water according to the procedure given by Belcher et al. and the dissolution of the precipitate into acetone followed by the measurement of radioactivity. (Table Ib). Owing to the treatment with acetone in which antimony and lead salts are separated, this method is not disturbed

1) P. Pfeiffer und M. Tapauch, *Z. anorg. Chem.*, **49**, 438 (1906).
2) R. Belcher and D. Gibbons, *J. Chem. Soc.*, **1952**, 4775.

TABLE I

SCHEMES OF DETERMINATION OF ANTIMONY




even in the presence of small amounts of lead.

(1) **Selection of Washing Solution and Solvent.**—Before beginning the radiometric study, nonactive dichlorobisethylenediamine cobaltic chloride,[3] antimony and lead salts[4] of the complex are prepared and their behaviors against some kinds of organic solvents or mineral acids are checked.

The results are summarized in Table II.

TABLE II

BEHAVIORS AGAINST ORGANIC SOLVENTS AND MINERAL ACIDS

| | Reagent | Sb salt | Pb salt |
|---|---|---|---|
| water | soluble | insoluble | partial decomposition |
| conc. HCl. | slightly soluble | insoluble | slightly soluble |
| hot dil. $HNO_3$ | — | — | soluble with decomposition |
| acetone | insoluble | soluble | insoluble |
| ethyl alcohol | insoluble | slightly soluble | insoluble |
| ethyl ether | insoluble | slightly soluble | insoluble |
| chloroform | insoluble | slightly soluble | insoluble |

3) W. C. Fernelius, "Inorganic Synthesis", Vol. II, McGraw-Hill Book Company, New York, N. Y. (1946), p. 222; Tupizina, dissertation, Zürich, 1912.

4) The antimony salt is prepared according to Belcher's method. The lead salt is prepared similarly from a saturated hydrochloric acid solution of lead nitrate. The composition of the lead salt is not known.

As can be seen from the table, the washing with water is suitable in separating precipitant and its antimony salt, and acetone is available to dissolve the antimony salt leaving the lead salt undissolved. These different behaviors against water and acetone are used as the basis of the following procedure.

(2) **Radiometric Determination of (1—0.06) mg. Antimony.**—Various amounts of antimony are taken and radioactive $[Co^*(en)_2Cl_2](SbCl_6)$ is precipitated; this is dissolved in acetone according to the following procedure. The relation between the relative intensity of the radioactivity of the residue of acetone extracts and the amounts of antimony taken is investigated.

(a) **Preparation of the Radioactive Reagent.**—Radioactive precipitant $[Co^*(en)_2Cl_2]Cl$ is prepared from radioactive cobalt chloride (about 0.2 milli curie $Co^{60}$/g. $CoCl_26H_2O$) according to the usual method[3], the heating to constant weight in an oven being omitted. This reagent is reserved in solid state to prevent the decomposition in an aqueous solution.

(b) **Procedure.**—1.5 cc. of the sample solution is taken in a microbeaker. The solution must be concentrated hydrochloric acid containing 1 to 0.06 mg. antimony. Three drops of concentrated nitric acid are added, and the solution is warmed for a few minutes and cooled quickly. In this treatment anti-

mony is oxidized to the quinquevalent state. 0.23 to 0.3 cc. Of a freshly prepared solution of the radioactive reagent (0.02 g. in 1 cc. of 2 N-hydrochloric acid) are added, and the mixture is set aside over night with occasional stirring. The precipitate is filtered off with a filter tube, washed with three or four portions of water until the washings become colorless, and dissolved in acetone. The acetone solution is transferred to a glass dish and evaporated under an infra-red lamp.

The radioactivity of the residue is measured by a Lauritsen electroscope, made by the

Table III
Results of (2)

| microg. Sb (taken) | Relative Intensity of Radioactivity, $(d/m)/(d/m)_s$ | $(d/m)/(d/m)_s$ / microg. Sb. | % Deviation |
|---|---|---|---|
| 0.0 | 0.000 | — | — |
| 67.0 | 0.180 | 2.69 | −2.53 |
| 136.0 | 0.369 | 2.71 | −1.81 |
| 199.9 | 0.527 | 2.64 | −4.35 |
| 268.0 | 0.756 | 2.82 | 2.17 |
| 334.5 | 0.935 | 2.80 | 1.45 |
| 342.5 | 0.973 | 2.84 | 2.80 |
| 469.0 | 1.340 | 2.86 | 3.62 |
| 670.0 | 1.780 | 2.66 | −3.62 |
| 682.0 | 1.910 | 2.80 | 1.45 |
| 945.0 | 2.660 | 2.81 | 1.81 |
| | Mean | 2.76 | ±2.57 |

The activity of the standard, $(d/m)_s$, is about $14d/m$. It shows slight variations according to the daily variation of the sensitivity of the Lauritsen electroscope.

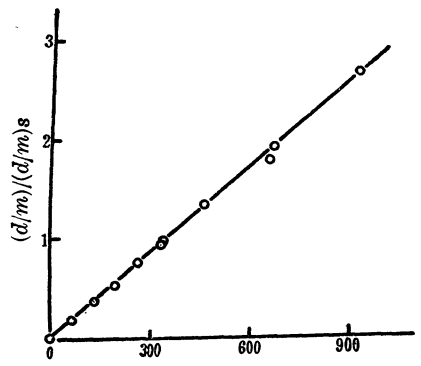



Fig. 1. Results of (2b).

Scientific Research Institute, Tokyo, and compared with that of a standard of cobalt-60.

(c) **Results Obtained.**—The results of experiments are shown in Table III and Fig. 1. The strictly linear relationship between the relative radioactivity and the amount of antimony taken is shown in Fig. 1, so we can conclude that 1 to 0.06 mg. antimony is determinable according to the above procedure.

If the reagent with much stronger specific activity is used, the determination of much smaller amounts of antimony may be successful. However it is so dangerous to handle the reagent of such high specific activity in solid state (as described above the reagent must be dissolved just before use). that we gave up such experiments.

(3) **Determination of Antimony in the Presence of Lead.**—Solutions which contain antimony as well as lead, are treated according to the procedure given in (2b). As can be seen from the results given in Table IV, the presence of a small amount of lead does not disturb the determination unless

Table IV
Determination of Antimony in the Presence of Lead

| microg. Pb (present) | microg. Sb (taken) | microg. Sb (found) | % Error |
|---|---|---|---|
| 22.9 | 201 | 198 | −1.5 |
| 22.9 | 201 | 199 | −1.0 |
| 34.4 | 201 | 193 | −3.9 |
| 114.5 | 397 | 394 | −0.8 |
| 114.5 | 268 | 258 | −3.7 |
| 114.5 | 130 | 95 | −26.7 |
| 229 | 271 | 263 | −2.9 |
| 229 | 268 | 261 | −2.7 |
| 229 | 131 | 80 | −39.1 |

the ratio of lead to antimony is much less than one. However the errors are always negative and tend to increase as the ratio increases. Finally in two determinations in which the ratios are about one or more than one, errors become seriously negative.

Negative errors will be caused by the coprecipitated lead salt which prevents complete dissolution of antimony salt in acetone.

Roughly speaking, the present radiometric method is available in determining antimony in the presence of an almost equal amount of lead, while Belcher's gravimetric method is disturbed by 0.1 mg. lead in the determination of 23.74 mg. antimony.

The authors wish to express their hearty thanks to Professor Jun Yoshimura who was kind enough to read through the manuscript.

*Department of Chemistry, Faculty of Science, Kyushu University, Hakozaki, Fukuoka*

# *Radiochemical Studies on Ultra-Micro Quantities of Organometallic Compounds. III. On Hydroxyquinolates of Promethium and Yttrium*

By Tomitaro ISHIMORI

(Received November 11, 1953)

Hydroxyquinolates of promethium and yttrium have been studied using radioactive isotopes, promethium-147 and yttrium-90.

The formation of the hydroxyquinolates is confirmed by the facts that both promethium and yttrium are extracted from an aqueous solution into a chloroform solution of 8-hydroxyquinoline while they are not extracted by pure chloroform.

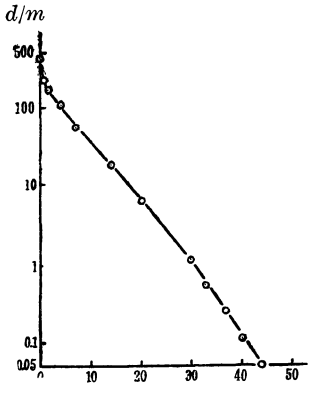
Further, some results are obtained on the composition of the complex compounds according to the method described in the first paper of these studies.[1]

## (I) Promethium Hydroxyquinolate

So far there is no report on promethium hydroxyquinolate. The formation and composition of the complex salt are studied using promethium-147.

**(A) The Solution of Promethium-147 Used.**—Promethium chloride which was imported from the Oak Ridge National Laboratory, U. S. A., is diluted with hydrochloric acid (10% vol.). The resultant solution containing about 1.3 microcurie promethium-147 per cc. is used in the following experiments.

*Radiochemical purity.*—1 cc. of the solution mentioned above is evaporated up to measure the radioactivity of the residue through aluminum absorber of known thickness. The results are shown in Fig. 1, in which logarithms of the intensities (measured with a Lauritsen electroscope, made by the Scientific Research Institute, Tokyo, and given in divisions per minute) are plotted against thickness of absorber. From the figure we can guess that this radioactivity consists of two components, namely an alpha and a beta activity.




Thickness of absorber (mgAl/cm²)

Fig. 1. Absorption curve of "Promethium-149" (Semilog plot).

As contamination of plutonium is described on the certificate sent in the package of the solution of promethium-147, this alpha activity is considered to be due to plutonium.

The beta rays seem to be absorbed entirely by 45–50 mg. Al/cm². Substitution of this value in Glendenin's diagram[2] gives about 0.2 Mev. as the energy of the observed beta rays. This value coincides with that given by Friedlander and Kennedy[3] for the energy of radiation of promethium-147. Therefore, the solution of promethium used is considered to contain promethium-147 and some isotopes of plutonium.

In the following experiments, however, the activity is measured by a Lauritsen electroscope through an aluminum foil (about 8 mg. Al/cm²), so the contamination does not disturb the measurements of the activity of promethium. For this reason the separation of promethium from plutonium has not been tried.

**(B) On the Formation of Promethium Hydroxyquinolate.** — An aqueous solution (about 8–9 cc.) which contains 1 cc. of the solution of promethium-147 and 5 cc. of the solution of sodium potassium tartrate (5g./30 cc.) or the saturated solution of ammonium acetate is prepared. To adjust pH, ammonium hydroxide is added dropwise to the solution. The solution is made up to 10 cc. with water, and pH of the solution is checked with a pH test paper.

5 cc. of chloroform solution of 8-hydroxyquinoline (61 mg./50 cc.) are added to the aqueous solution and the mixture is shaken vigorously for one minute in a small separating funnel. The chloroform layer is taken and evaporated up under an infra-red lamp. The radioactivity due to promethium in the

1) T. Ishimori, This Bulletin, 27, 139 (1954).

2) L.E. Glendenin, *Nučleonics*, 2, 16 (1948).
cf. G. Friedlander and J.W. Kennedy, "Introduction to Radiochemistry", John Wiley & Sons, New York, (1949) p. 164.

3) ibid., p. 358.

residue is measured by the Lauritsen electroscope. The extractability is calculated by comparing the activity with that of promethium-147 taken into the separating funnel.

This procedure is repeated for several known pH values of the aqueous solution. The results are shown in Table I, in which

TABLE I
FORMATION OF PROMETHIUM 8-HYDROXYQUINOLATE

| From the solution containing | pH | Extractability |
|---|---|---|
| Sodium potassium tartrate | 9.2 | 23 % |
| ,, | 7.4 | 0.5 |
| ,, | 3.4 | ...* |
| Ammonium acetate | 5.6 | 0.4 |
| ,, | 4.4 | 0.0 |

* tartaric acid is pptd.

we can see the remarkable transference of promethium into the phase of chloroform in the experiment at about pH 9. The similar procedure is repeated further with pure chloroform at about pH 9, but no promethium is extracted. So we may conclude that the formation of a new complex salt between promethium and 8-hydroxyquinoline at about pH 9 is proved by these experimental facts.

**(C) On the Composition of Promethium Hydroxyquinolate.**—The composition of the hydroxyquinolate is determined according to the method described in the first paper[1] of this series.

When a definite volume of an aqueous solution of promethium is shaken, at constant value of pH, with a known volume of a chloroform solution of 8-hydroxyquinoline until the equilibrium is established, the following equation is expected based on the theoretical consideration of the chemical system.

$$E^{-1}=A\,(HO_x)^{-n}+B.$$

$E$: Extractability, the ratio of the activities due to promethium extracted and total promethium taken into the system.
$(HO_x)$: The amount of 8-hydroxyquinoline added to the system.
$A$ and $B$: Constants.
$n$: The number of the anion of 8-hydroxyquinoline bound to one atom of promethium.

Therefore, if several experiments are repeated with chloroform solutions of 8-hydroxyquinoline in varying concentration (keeping the other conditions constant) and their results are plotted in the $E^{-1}$ $-(HO_x)^{-1,2,3\cdots\cdots}$ diagrams, $n$ is determined by finding out $(HO_x)^{-n}$ which is linear to $E^{-1}$.

**(1) The Absorption of the beta Rays of Promethium.**—In the experiments for the determination of the composition, precise measurement of the activity is earnestly desired. As promethium-147 is an emitter of considerably soft beta rays (0.20 MeV.), the absorption by 8-hydroxyquinoline which may come into the layer of chloroform must be considered.

Fortunately most 8-hydroxyquinoline seems to have been eliminated during the evaporation of chloroform solution under an infrared lamp. This is proved in two ways. The first is based on weighing the residue of chloroform solution of 8-hydroxyquinoline, namely the residue of 5 cc. solution (101 mg. 8-hydroxyquinoline/50 cc.) is less than 1 mg. Secondly, known volumes of the chloroform solution are evaporated in a glass dish containing the residue of 1 cc. of promethium solution and the radioactivity is measured. Table II shows the results in which we can

TABLE II
ABSORPTION OF BETA RAYS BY 8-HYDROXYQUINOLINE

| mg. 8-hydroxyquinoline (added) | 0.00 | 1.01 | 2.02 | 3.03 | 5.05 | 6.06 | 10.1 |
|---|---|---|---|---|---|---|---|
| % Radioactivity | 100 | 100 | 98 | 102 | 97 | 92 | 100 |

see that no serious error will occur by the absorption of the beta rays. The glass dishes used for measurements have a diameter of about 4 cm.

**(2) Experimental Procedure.**—A solution which contains 5 g. sodium potassium tartrate and 10 cc. of promethium-147 solution is made alkaline by adding ammonium hydroxide dropwise and finally made up to 100 or 50 cc. The pH value of the solution is checked by indicator paper. 10 cc. of the resultant solution is mixed with 5 cc. of a

TABLE III
RESULTS OF FIRST SERIES (pH=9.3)

| $(HO_x)$ | $(HO_x)^{-1}$ | $(HO_x)^{-2}$ | $(HO_x)^{-3}$ | $(HO_x)^{-4}$ | $(HO_x)^{-5}$ | $E^{-1}$ |
|---|---|---|---|---|---|---|
| 10 mg. | 0.10 | 0.01 | 0.001 | $10^{-4}$ | $10^{-5}$ | 1.35 |
| 4 | 0.25 | 0.06 | 0.016 | 0.004 | $10^{-4}$ | 3.78 |
| 3 | 0.33 | 0.11 | 0.037 | 0.012 | 0.004 | 6.88 |
| 2.7 | 0.37 | 0.14 | 0,051 | 0.019 | 0.007 | 11.6 |
| 2.4 | 0.42 | 0.17 | 0.073 | 0.030 | 0,013 | 16.4 |

TABLE IV
RESULT OF SECOND SERIES (pH=9.6)

| $(HO_x)$ | $(HO_x)^{-1}$ | $(HO_x)^{-2}$ | $(HO_x)^{-3}$ | $(HO_x)^{-4}$ | $(HO_x)^{-5}$ | $E^{-1}$ |
|---|---|---|---|---|---|---|
| 10 mg. | 0.10 | 0.01 | 0.001 | $10^{-4}$ | $10^{-5}$ | 1.23 |
| 4 | 0.25 | 0.06 | 0.016 | 0.004 | $10^{-3}$ | 2.00 |
| 3.12 | 0.33 | 0.10 | 0.033 | 0.011 | 0.0034 | 3.23 |
| 2.68 | 0.38 | 0.14 | 0.055 | 0.021 | 0.0078 | 5.64 |

chloroform solution of 8-hydroxyquinoline (known concentration) and treated as described in (B). The procedure is repeated for several varying concentrations of 8-hydroxyquinoline in chloroform. Two series of experiments are carried out; the first is done at about pH 9.3 and the second is done at about pH 9.6.

(3) **Results Obtained.**—The results of these experiments are shown in Tables III and IV.

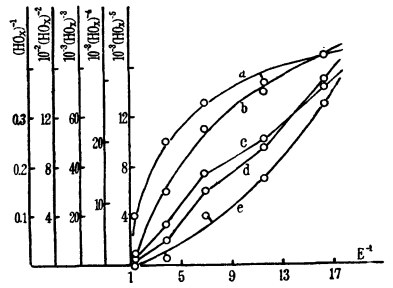


Fig. 2. Results of 1st series (pH=9.3).
a; $E^{-1}-(HO_x)^{-1}$, b; $E^{-1}-(HO_x)^{-2}$,
c; $E^{-1}-(HO_x)^{-3}$, d; $E^{-1}-(HO_x)^{-4}$,
e; $E^{-1}-(HO_x)^{-5}$,

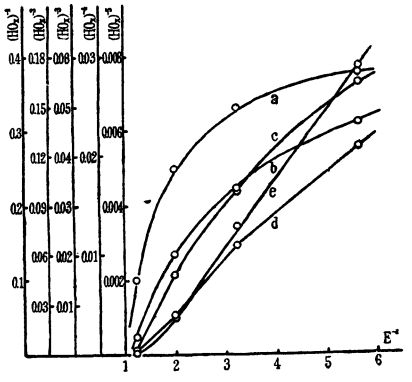


Fig. 3. Results of 2nd series (pH 9.6).
a; $E^{-1}-(HO_x)^{-1}$, b; $E^{-1}-(HO_x)^{-2}$,
c; $E^{-1}-(HO_x)^{-3}$, d; $E^{-1}-(HO_x)^{-4}$,
e; $E^{-1}-(HO_x)^{-5}$,

In Fig. 2 and 3 the diagrams of $E^{-1}-(HO_x)^{-1,2,3,4 \text{ and } 5}$ are given.

In these diagrams, figures of curve vary more slowly against the variation of $n$ than in the cases previously reported by the author where the best linearity is got for $n=2$. So the determination of $n$ becomes more difficult than the cases of lead dithizonate, lead hydroxyquinolate or polonium dithizonate.[1,4] Fig. 2a and b and Fig. 3a and b are clearly convex, and Fig. 2e and Fig. 3e are probably concave. So the best linearity is expected for $2<n<5$. However, we can not decide the value of $n$ which gives the best linearity in $E^{-1}$ vs. $(O_x)^{-n}$ diagram, because Fig. 2c and d and Fig. 3d are broken to a considerable extent. (We may assume that Fig. 3c is slightly convex.)

There is no generally accepted formula about the oxidation state of promethium in an aqueous solution, but according to its position in the periodic table, it belongs to the rare earth elements and it is most likely to assume trivalent cation of promethium. Based on this assumption, we can guess that the formula of the complex will probably be written as $Pm(O_x)_3$ or $Pm(O_x)_3(HO_x)$.[5] As the example of hydroxyquinolate of the latter type, thorium hydroxyquinolate, $Th(O_x)_4(HO_x)$, is known.[6]

## (II) Yttrium Hydroxyquinolate

There is no description on yttrium hydroxyquinolate, except a report on its formation in an acetic acid solution[7]. In the present paper, the formation and composition of the complex salt of yttrium and hydroxyquinoline in chloroform medium, are studied using yttrium-90 which is easily prepared from strontium-90.

**(A) Preparation of Solution of Yttrium-90.**—Solution of "strontium-89" imported from the Oak Ridge National Laboratory, U.S.A., contains strontium-90. In the solution of "strontium-89" which has been left to stand for about 20 days, yttrium-90, the daughter element of strontium-90, is formed in an amount which is in equilibrium with strontium-90. Therefore, yttrium-90 can be isolated by the common chemical methods. Although a method for preparation of yttrium-90 based on radiocolloid of yttrium-90 was reported by G.K. Schweitzer et al.[8] a

4) T. Ishimori, This Bulletin, 27, 520 (1954).
5) The concentration of undissociated 8-hydroxyquinoline in the aqueous solution is proportional to that of the anion of 8-hydroxyquinoline. Therefore, even in a case in which the complex salt is of the mentioned formula, the basis of the method is available.
6) F.J. Frere, *J. Am. Chem. Soc.*, 55, 4362 (1933).
7) K. Shiba, *Rep. Gov. Chem. Ind. Res. Inst., Tokyo*, 28, No. 8 (1932).

different method was used in the present research.

A solution of non-active strontium chloride (containing about 15 mg. strontium) is added to the solution which contains yttrium-90, strontium-90 and strontium-89 (about 0.5 milli curie strontium-90). After addition of ferric alum (0.1 g.), the resultant solution is made up to about 100 cc. and treated with ammonium chloride and ammonium hydroxide in order to coprecipitate yttrium-90 with ferric hydroxide. The precipitate is filtered off and reprecipitated according to the usual way.

Strontium goes to the filtrate and yttrium remains in the precipitate of ferric hydroxide. The precipitate is dissolved in hydrochloric acid (1 : 1) and iron is extracted into ether according to the Rothe's method. The aqueous solution which contains yttrium-90 is evaporated up and the residue is redissolved with water to obtain 25 cc. of the aqueous solution.

Ammonium chloride which is contained in the resultant solution does not disturb the result of the experiment.

Radioactivity of residue of the yttrium-90 solution thus prepared is strong enough (20–30 div./min. per cc.) for the following experiments and shows the decay as shown in Fig. 4. From the figure the half-life of the radio-

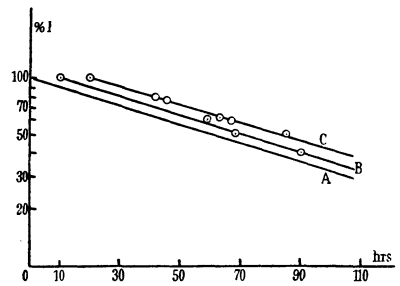



Fig. 4. Decay of Yttrium-90.
A : Theoretical decay for t=60 hrs.
B : Y-90 used in 1st series of experiments.
C : Y-90 used in 2nd series of experiments.

activity is calculated as about 60 hours, and this value almost coincides with that described by Friedlander and Kennedy[9].

As strontium has a long half-life (19.9 years), yttrium-90 is repeatedly prepared from the filtrate which contains strontium-90.

8) G.K. Schweitzer, B.R. Stein and Wm. M. Jackson, *J. Am. Chem. Soc.*, 75, 793 (1953).
9) G. Friedlander and J.W. Kennedy, "Introduction to Radiochemistry", John Wiley & Sons, New York, (1949) p. 327.

**(B) On the Formation of Yttrium Hydroxyquinolate.** — An aqueous solution which contains 1 cc. of the solution of yttrium-90 and 5 cc. of the solution of sodium potassium tartrate (20%) or 5 cc. of ammonium acetate (20%) is treated in the almost same way as described in I, (B) and the extractability is calculated. This procedure is repeated for several different pH values of the aqueous solution.

The results are shown in Table V, in which

Table V
Extraction of yttrium hydroxyquinoline

| Extraction of the complex from the solution containing | pH | Concentration of 8-hydroxyquinoline in $CHCl_3$ (mg./50 cc.) | Extractability |
|---|---|---|---|
| ammonium acetate | 3.5 | 10 | 0.05% |
| ,, | 4.5 | ,, | 0.1 |
| ,, | 6.8 | ,, | 0.15 |
| ,, | 8.6 | ,, | 3.6 |
| ,, | 8.6 | 1000 | 53 |
| sodium potassium tartrate | 3.5 | 111 | ...* |
| ,, | 5.8 | ,, | 0.0 |
| ,, | 8.8 | ,, | 28 |
| ,, | 8.6 | none | 0.1 |
| ,, | 8.8 | ,, | 0.0 |

* Tartaric acid is pptd.

we can see that remarkable amounts of yttrium-90 are extracted from weak alkaline solution. Further similar procedure is repeated with pure chloroform at pH 8.6 and 8.8, but no yttrium is extracted. Basing our ideas on these facts, we can conclude that yttrium forms a hydroxyquinolate in an alkaline solution.

**(C) On the Composition of Yttrium 8-Hydroxyquinolate.**—The composition of yttrium hydroxyquinolate is estimated in a similar way as that described in I, (C). Two series of experiments are carried out at about pH 8.6 and 8.8.

The results of experiments are shown in Tables VI and VII. The $E^{-1}-(HO_x)^{-1,2,3}$

Table VI
Results of first series (pH=8.6)

| $(HO_x)$ | $(HO_x)^{-1}$ | $(HO_x)^{-2}$ | $(HO_x)^{-3}$ | $E^{-1}$ |
|---|---|---|---|---|
| 1.0 | 1.0 | 1.0 | 1.0 | 1.78 |
| 0.4 | 2.5 | 6.3 | 15.6 | 11.9 |
| 0.2 | 5.0 | 25 | 125 | 40.3 |
| 0,12 | 8.3 | 69 | 578 | 100 |

$(HO_x)$: Amount of 8-hydroxyquinoline given in an arbitrary unit in which $(HO_x)=1$ corresponds to 8.3 mg. 8-hydroxyquinoline.
$E$: Extractability.

TBALE VIII

RESULTS OF SECOND SERIES (pH=8.8)

| $(HO_x)$ | $(HO_x)^{-1}$ | $(HO_x)^{-2}$ | $(HO_x)^{-3}$ | $E^{-1}$ |
|---|---|---|---|---|
| 11.1 | 0.09 | 0.008 | 0.0008 | 3.66 |
| 4.4 | 0.23 | 0.052 | 0.012 | 14.8 |
| 3.3 | 0.30 | 0.092 | 0.028 | 35.7 |
| 2.6 | 0.38 | 0.15 | 0.057 | 58.7 |
| 2.2 | 0.46 | 0.21 | 0.094 | 86.0 |

$(HO_x)$: Amount of 8-hydroxyquinoline given in mg.
$E$: Extractability.

diagrames are given in Figs. 5 and 6. As

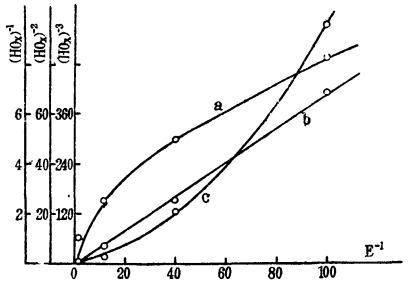



Fig. 5. Results of 1st series (pH=8.6).
a: $E^{-1}-(HO_x)^{-1}$, b: $E^{-1}-(HO_x)^{-2}$,
c: $E^{-1}-(HO_x)^{-3}$

can be seen in the figures, $(HO_x)^{-2}$ is linear to $E^{-1}$. So we can conclude that yttrium hydroxyquinolate contains 8-hydroxyquinoline anion in such a ratio as two anions are bound to one atom of yttrium. Consequently,

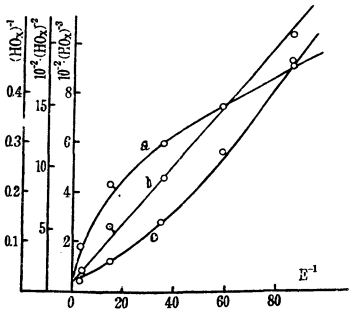



Fig. 6. Results of 2nd series (pH=8.6).
a: $E^{-1}-(HO_x)^{-1}$, b: $E^{-1}-(HO_x)^{-2}$,
c: $E^{-1}-(HO_x)^{-3}$

according to the results of the present study, we may guess that the composition of the complex salt will correspond to a formula such as $Y(O_x)_2\,X$, where $(O_x)$ represents $C_9H_6ON$ and X represents some monovalent anion other than $(O_x)^-$.

The studies of the complex in macro amounts is desired, because of possible differences between the composition of the complex compound formed from a concentrated solution and that formed from an extremly dilute solution.

*Department of Chemistry, Faculty of Science, Kyushu University*
*Hakozaki, Fukuoka*

# *Studies on Dimethylglyoximato-cobalt (III)* Complexes. II. Absorption Spectra of Bis-(dimethylglyoximato)-and Bis-(mono-O-methyl-dimethylglyoximato)-cobalt (III) Complexes*

By Akitsugu NAKAHARA

(Received October 21, 1954)

In the previous papers[1] the author discussed on the strong tendency of two dimethylglyoximate ions to form planar configuration about a cobalt atom, and attributed its origin to the formation of O–H–O hydrogen bonds in the complex radical. The successful synthesis of the tris-(dimethylglyoximato)-cobalt (III) reported in the same papers strongly supports the above conclusion. In order to confirm the conclusion, it might be suitable to compare properties of bis-(dimethylglyoximato)-cobalt (III) derivatives which have the O–H–O hydrogen bonds and bis-(mono-O-methyl - dimethylglyoximato) - cobalt (III) derivatives, in which the hydrogen bonds cannot be anticipated.

In this work, bis-(mono-O-methyl-dimethylglyoximato)-diammine-cobalt (III) chloride and hydrogen dinitro-bis-(mono-O-methyl-dimethylglyoximato)-cobaltate (III) were newly synthesized, and investigated spectrochemically. Absorption spectra of some bis-(dimethylglyoximato)-cobalt (III) complexes were

* The word "dimethylglyoximo-" was used in the former paper, but the above nomenclature seems to be better.

1) A. Nakahara, This Bulletin, **27**, 560 (1954); A. Nakahara and R. Tsuchida, *J. Am. Chem. Soc.*, **76**, 3103 (1954).

also investigated in relation to the above complexes of O-methyl-substituted dimethylglyoxime.

## Experimental

**Materials.- Bis-(mono-O-methyl-dimethylglyoximato)-diammine-cobalt (III) chloride, [Co$(NH_3)_2(DCH_3)_2$**] Cl·1.5 $H_2O$.**[2]—This compound was prepared as reddish brown plates or prisms by the following method: 5 g. of purpureo cobalt (III) chloride, 5.2 g. of dimethylglyoxime-mono-methylether and 0.5 g. of charcoal were added to a mixture of 60 ml. of alcohol and 30 ml. of water, boiled for 10–15 hours on a water-bath, and then filtered. Alcohol was distilled off from the filtrate. The residual aqueous solution was evaporated and dried on a water-bath. The residue was washed once with chloroform and dissolved in alcohol. In this procedure only the objective complex was dissolved, and ammonium chloride was removed by filtration. When this dark brown filtrate was condensed in a vacuum desiccator on calcium chloride, the compound crystallized gradually. Analyses and other experiments for identification were already reported.[2]

**Hydrogen dinitro-bis-(mono-O-methyl-dimethylglyoximato)-cobaltate (III), H [Co$(DCH_3)_2(NO_2)_2$].**—This new compound was quantitatively precipitated from a hot solution of sodium hexanitrito-cobaltate (III) by careful addition of dimethylglyoxime-mono-methylether. The precipitate was almost pure after having been washed several times with hot water and alcohol. The compound did not show any reaction characteristic of sodium ion contrary to that showed by the dimethylglyoximato-complex obtained in the same procedure.[3] Found: C, 29.19; H, 4.61; N, 20.59, Calculated for H [Co$(DCH_3)_2(NO_2)_2$]: C, 29.27; H, 4.66; N, 20.48%. In order to determine the valency of cobalt, the magnetic susceptibility of the compound in solid state was measured, and it was necessarily concluded that cobalt should be tervalent since the compound proved to be diamagnetic. The compound appeared as orange, rhombic crystals. It is almost insoluble in water and alcohol, but dissolves a little in concentrated acetic acid. It explodes suddenly and burns on action of concentrated sulfuric acid.

**Bis-(dimethylglyoximato)-diammine-cobalt (III) chloride, [Co$(NH_3)_2(DH)_2$] Cl·5$H_2O$.**—This yellowish brown compound was prepared according to the direction of Nakatsuka and Iinuma.[4] As was already reported,[5] the crystal is of special interest in relation to its peculiar habit and unusual optical property.

**Hydrogen dichloro-bis-(dimethylglyoximato)-cobaltate (III), H [Co$(DH)_2Cl_2$].**[6]—The method of Cambi et al.[7] was applied in preparing the compound. To a concentrated aqueous solution of cobaltous acetate was added a slight excess of dimethylglyoxime, and the solution was oxidized by passing air through it. On adding concentrated hydrochloric acid, the compound was precipitated in dark green rhombs. It was recrystallized from the aqueous solution by adding concentrated hydrochloric acid.

**Hydrogen dibromo-bis-(dimethylglyoximato)-cobaltate (III), H [Co$(DH)_2Br_2$].**—The compound was precipitated in a similar way as the above described procedure from the reaction mixture by adding concentrated hydrobromic acid.

**Chloro-bis-(dimethylglyoximato)-ammine-cobalt (III), [Co$(NH_3)(DH)_2Cl$]; Ammonium dinitro-bis-(dimethylglyoximato)-cobaltate(III), $NH_4$[Co$(DH)_2(NO_2)_2$]·$H_2O$; Nitro-bis-(dimethylglyoximato)-aquo-cobalt (III), [Co$(H_2O)(DH)_2(NO_2)$]; Nitro-bis-(dimethylglyoximato)-ammine-cobalt (III), [Co$(NH_3)(DH)_2(NO_2)$]; Hydrogen dinitro-bis-(dimethylglyoximato)-cobaltate(III), H [Co$(DH)_2(NO_2)_2$].**—These complexes were prepared according to the direction of Tschugaeff.[3,8]

**Dimethylglyoxime-mono-methylether.** — Although there are some established methods concerning the syntheses of the compound,[9,10,11] a new method was adopted in this work: 7 g. of caustic soda and 20 g. of dimethylglyoxime were added to a mixture of 100 ml. of water and 200 ml. of alcohol, stirred and dissolved entirely on a water-bath. Into the mixture 25 g. of methyliodide was poured drop by drop during about half an hour with continuous stirring. The reaction mixture was boiled on the water-bath for two hours. Then alcohol was distilled off. On cooling the residual solution a white crystalline powder was deposited, which was filtered by suction, and purified by steam distillation. Thus 8.3 g. of pure dimethylglyoxime-mono-methylether (m.p. 104°C) was yielded, and 8.7 g. of unreacted dimethylglyoxime was recovered. By adding a large quantity of water to the distilled alcohol, dimethylglyoxime-dimethylether (m.p. 44°C) was also isolated.

**Measurements.** — Absorption spectra of the above compounds in solution were measured in the region from 40 to $135\times10^{13}$/sec. by a Beckman DU quartz spectrophotometer. The formal extinction coefficient $\varepsilon$ is given by the equation $I=I_0\times10^{-\varepsilon cd}$, where $c$ is the concentration of the complex in mol. or gram-ion per liter and $d$ the thickness of the layer in cm. The concentrations used were $1/10^3-1/10^5$ and $1/10^2-1/10^4$ mol./l., in complexes and ligands, respectively. Absorption spectra of dichloro- and dibromo-complex were observed in water, as well as in methanol containing hydrochloric- and hydrobromic acid, respectively. Those of hydrogen dinitro-bis-(dimethylglyoximato)- and hydrogen dinitro-bis-(mono-

** $DCH_3=H_3CC(NOCH_3)C(NO)CH_3$; $DHCH_3=H_3CC(NOCH_3)C(NOH)CH_3$, $DH=H_3CC(NOH)C(NO)CH_3$; $DH_2=H_3CC(NOH)C(NOH)CH_3$.

2) A. Nakahara, Y. Yamamoto and R. Tsuchida, *J. Chem. Soc. Japan*, **74**, 1021 (1953).

3) L. Tschugaeff, *Ber.*, **41**, 2228 (1908).

4) Y. Nakatsuka and H. Iinuma, This Bulletin, **11**, 48 (1936).

5) Y. Saito, A. Nakahara and H. Kuroya, *J. Inst. Polytech.*, Osaka City Univ., **1**, No. 2, Ser. C, 15 (1950).

6) F. Feigl and H. Rubinstein, *Ann.*, **433**, 183 (1923).

7) L. Cambi and C. Coriselli, *Gazz. chim. ital.*, **66**, 81 (1936).

8) L. Tschugaeff, *Z. anorg. Chem.*, **46**, 144 (1905); *Ber.*, **39**, 2692 (1906); **40**, 3498 (1907); **41**, 2226 (1908).

9) G. Charrier, *Gazz. chim. ital.*, **37**, 145 (1907).

10) L. Avogadro and G. Tavola, ibid., **55**, 329 (1925).

11) E. Thilo, *Ber.*, **62**, 869 (1929).

O-methyl-dimethylglyoximato)-cobaltate (III) were also measured in 50% acetic acid, since they are almost insoluble in water as already mentioned. Absorption spectra of ligands, dimethylglyoxime and its methylether, were observed in alcohol. In cases other than the above, aqueous solutions were used.

## Results and Discussion

**Absorption Spectra of $[Co(NH_3)_2(DH)_2]Cl$, $[Co(NH_3)(DH)_2Cl]$ and $H[Co(DH)_2Cl_2]$.** — The results of the measurements are shown in Fig. 1 and Table I. The three absorption curves are quite similar to each other except for the isolated maximum in the longer wavelength region on the curve of dichloro-complex, (c). As far as the absorption spectra of cobalt (III) complexes are concerned, there are, in general, two absorption maxima in the visible and near ultraviolet region.[12] The one in the visible has been designated as the "first absorption band", and the other in the near ultraviolet as the "second absorption band". According to Tsuchida, the first band is due to the electronic transitions in the unsaturated transition shell of the central ion and the second band is attributed to the transitions of the coördination electrons.[12)13] In the above complexes, however, the second bands are completely concealed by large absorption bands presumed to be the "specific absorption bands" which are due mainly to the dimethylglyoximate ions in coördination. Only the vestiges of the first bands remain slightly as inflations at $60\sim70\times10^{13}$/sec. in (a) and (b). The origin of dark or brownish colors which is characteristic of all Tschugaeff's dimethylglyoximato-complexes is attributed to the above mentioned facts. From this standpoint Feigl-Rubinstein's compound, $H[Co(DH)_2Cl_2]$,[6)7] having green color is a quite rare type of cobaltic complexes with dimethylglyoxime. Namely, the first band of this complex, (c), is nearly isolated from the specific band, showing its maximum at $\nu = 53.9\times10^{13}$/sec. The difference between (a), (b) and (c), however, is quite natural, considering the "spectrochemical series", an empirical rule found by Tsuchida.[12)13] Since the chloride ion is by far a more bathochromic ligand than the ammonia molecule in the series, the first band should be shifted bathochromically by substitution of the ammonia molecules by the chloride ions. On the other hand, Yamada and Tsuchida[14] recently presented another empirical rule, the "hyperchromic series" which is concerned with the intensity of the absorption of complexes. In the series, the ammonia molecule precedes the chloride ion, i.e., ammonia is a more hyperchromic ligand than the chloride ion. According to this rule, therefore, the relation between the first absorption bands of the three complexes can be explained also

TABLE I

ABSORPTION MAXIMA OF BIS-(DIMETHYLGLYOXIMATO)-COBALT (III) COMPLEXES

| Notation | Complex radical | Solvent | First absorption band | | Specific absorption band | | Other bands | | |
|---|---|---|---|---|---|---|---|---|---|
| | | | $\nu$, $10^{13}$/sec. | log ε | $\nu$, $10^{13}$/sec. | log ε | $\nu$, $10^{13}$/sec. | log ε | assignment |
| (a) | $[Co(NH_3)_2(DH)_2]^+$ | water | — | — | 123.0 | 4.41 | — | — | — |
| (b) | $[Co(NH_3)(DH)_2Cl]$ | water | — | — | 122.0 | 4.38 | — | — | — |
| (c) | $[Co(DH)_2Cl_2]^-$ | $CH_3OH$-HCl | 53.9 | 1.65 | 116.5 | 4.49 | — | — | — |
| (d) | $[Co(DH)_2Cl_2]^-$ | water | — | — | 121.0 | 4.36 | — | — | — |
| (e) | $[Co(DH)_2(NO_2)_2]^-$ | water | — | — | 122.0 | 4.44 | 87.6 | 3.86 | nitro-groups |
| (f) | $[Co(NH_3)(DH)_2(NO_2)]$ | water | — | — | 123.0 | 4.40 | — | — | — |
| (g) | $[Co(H_2O)(DH)_2(NO_2)]$ | water | — | — | 121.5 | 4.41 | — | — | — |
| (h) | $[Co(DH)_2Br_2]^-$ | $CH_3OH$-HBr | 52.1 | 1.79 | 118.8 | 4.22 | 99.8 | 4.27 | third band |

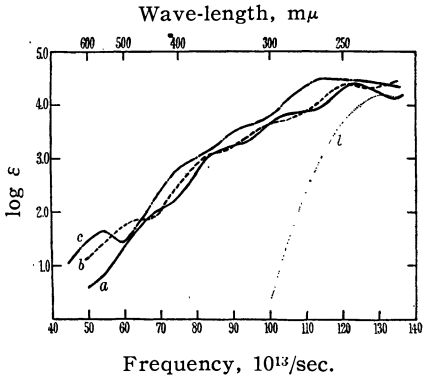



Fig. 1. Absorption spectra of: (a), $[Co(NH_3)_2(DH)_2]Cl$ in water; (b), $[Co(NH_3)(DH)_2Cl]$ in water; (c), $H[Co(DH)_2Cl_2]$ in 4% HCl-methanol.

12) See, for example, R. Tsuchida and M. Kobayashi, "The Colours and the Structures of Metallic Compounds" (in Japanese), (Zoshindo, Osaka, Japan, 1944).

13) R. Tsuchida, This Bulletin, **13**, 388 (1938).

14) S. Yamada and R. Tsuchida, This Bulletin, **26**, 15 (1953).

with respect to their intensities.

In the ultraviolet region, there can be recognized two inflations and one maximum. These may be considered to be the above mentioned specific absorption bands, since they are truly characteristic of dimethylglyoximato-complexes. Above all, in (a) and (b) the appearances of the absorption curves in the region are quite similar to each other, suggesting the same configuration of two dimethylglyoximate ions in each complex radical. As is clear from Table I, however, the maximum on the curve of dichloro-complex, (c), is shifted bathochromically, to a considerable degree. For this phenomenon some origins may be considered: (1) the effect of the two chloride ions coördinated in trans-positions*; (2) the solvent effect in methanol-hydrochloric-acid solution. It would probably be supposed that both the two effects are concerned in the above phenomenon. Further discussion will be given in the later section concerning the origins which contribute to the specific band.

**Absorption Spectra of $NH_4[Co(DH)_2(NO_2)_2]$, $[Co(NH_3)(DH)_2(NO_2)]$ and $[Co(H_2O)(DH)_2(NO_2)]$.**—The results of the measurements are shown in Fig. 2 and Table I. Absorption

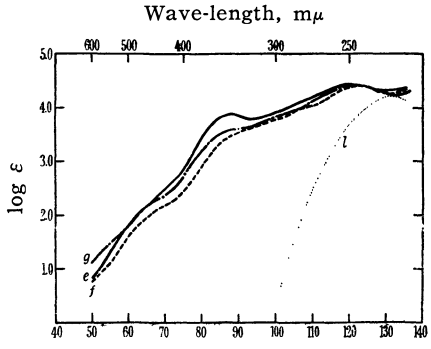



Fig. 2. Absorption spectra of aqueous solution of: $NH_4[Co(DH)_2(NO_2)_2]$, (e); $[Co(NH_3)(DH)_2(NO_2)]$, (f); $[Co(H_2O)(DH)_2(NO_2)]$, (g).

curves of these three complexes are quite similar to one another. Only the maximum at $\nu=87.6\times10^{13}$/sec. on the curve of dinitro-complex, (e), is conspicuous. This is the specific absorption band which is due to the nitro-groups in coördination.[15] Also on the curves, (f) and (g), the inflations higher than those of other complexes are recognized in this region. But they are not so remarkable as that of the dinitro-complex. This is due to the number of nitro-groups contained in the complex radical, since the specific absorption band usually changes hyperchromically with increasing number of the concerned ligands.[16] In the longer wave-length region, the vestiges of the first bands are almost unrecognized. But this may be understood by taking into consideration the above described intense specific band originating from the nitro-groups along with the hypsochromic shift of the first bands, which is also caused by the nitro-groups, one of the most hypsochromic ligand in the spectrochemical series. So far as the maxima in the shorter wave-length are concerned, there cannot be recognized any particular difference from the curves, (a) and (b), as is clear from Table I.

**Absorption Spectra of $H[Co(DH)_2Br_2]$ and $H[Co(DH)_2(OH)Cl]$.**—In Fig. 3 absorption

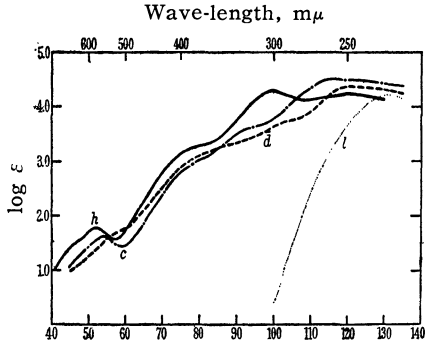



Fig. 3. Absorption spectra of: (d), H [Co $(DH)_2Cl_2$] in water; (h), H $[Co(DH)_2Br_2]$ in 5% HBr-methanol.

curves of the above two compounds are illustrated. In the measurement of the former, (h), methanol-hydrobromic-acid solution was used, while in the case of the latter, (d), was adopted aqueous solution of the Feigl-Rubinstein's dichloro-complex, $H[Co(DH)_2Cl_2]$. It is because the dichloro-complex has been known to change itself into the above described chloro-hydroxo-complex in aqueous solution.[17] Although the valency of cobalt in the Feigl-Rubinstein's complex was considered previously to be bivalent, it is quite sure, by the investigation of Cambi et al[17]., that it must be tervalent. Therefore, the above change should be elucidated according to the following scheme:

* It has been well-known that the third absorption band should appear readily when a central ion of a complex radical involves two anions in trans-positions. (Ref. 12). Consequently, there may be expected an overlapping of the third-and specific-band. In this case, such a bathochromic shift as above mentioned is very probable.

15) H. Kuroya and R. Tsuchida, *J. Chem. Soc. Japan*, **59**, 1142 (1938).

16) R. Tsuchida and M. Kobayashi, This Bulletin, **13**, 474 (1938).

17) "*Gmelins Handbuch d. anorg. Chem.*", 8 Aufl., **58 B**, p. 21 (1930).

$$H[Co(DH)_2Cl_2]+H_2O \rightleftarrows H[Co(DH)_2(OH)Cl]+HCl$$

As shown in Fig. 3 the curve, (d), is quite different from (c), suggesting the substitution of a ligand as presented in the above equation. Since the change is, however, in an equilibrium in aqueous solution, further discussion would be impossible without more detailed researches.

As for the absorption spectrum of the dibromo-complex, (h), all the explanations described in the case of the dichloro-complex, (c), can be applied. An important fact is that the bromide ion is a more bathochromic ligand than the chloride ion. In the present case, however, there can be recognized clearly a new maximum at $\nu=100\times10^{13}$/sec. This may be considered to be the third absorption band which is due to the two bromide ions coördinated in *trans*-positions, as is known in the absorption spectrum of *trans*-dibromo-bis-(ethylenediamine)-cobalt (III)-complex.[18]

**Absorption Spectra of $[Co(NH_3)_2(DCH_3)_2]Cl$ and $H[Co(DCH_3)_2(NO_2)_2]$ in Relation to Those of $[Co(NH_3)_2(DH)_2]Cl$ and $H[Co(DH_2)(NO_2)_2]$.**—The results of the measurements are shown in Fig. 4. The absorption curve of bis-

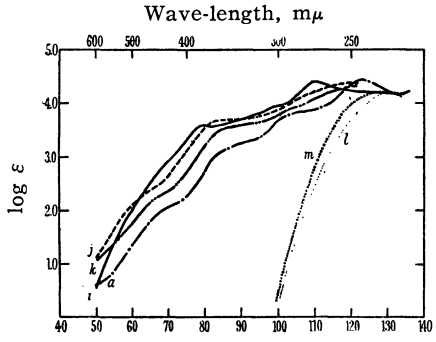



Fig. 4. Absorption spectra of: (i), [Co $(NH_3)_2(DCH_3)_2]$ Cl in water; (j), H [Co $(DCH_3)_2(NO_2)_2]$ in 50% acetic acid; (k), H $[Co(DH)_2(NO_2)_2]$ in 50% acetic acid; (l), dimethylglyoxime in alcohol; (m), dimethylglyoxime-mono-methylether in alcohol.

(mono-O-methyl-dimethylglyoximato)-diammine-cobalt (III) chloride, (i), resembles, as a whole, that of the corresponding dimethylglyoximato-complex, (a), but the former is considerably bathochromic to the latter.

Since dimethylglyoxime and its methylether are closely related in their electronic structures, it may be expected quite naturally that the curve, (i), would have a strong resemblance to the curve, (a). In fact, notwithstanding a little difference between the absorption maxima of the two ligands, (l) and (m), there is brought about a considerable difference when they are in coördination. (Table II). This can be understood by taking

TABLE II
SPECIFIC BANDS OF $[Co(NH_3)_2(DH)_2]Cl$ AND $[Co(NH_3)_2(DCH_3)_2]Cl$

| | $\nu$max, $10^{13}$/sec. | log ε | $\nu$ max(complex) ~ $\nu$ max(ligand) |
|---|---|---|---|
| $[Co(NH_3)_2(DH)_2]Cl$ | 123.0 | 4.41 | 7.4 |
| ligand, $DH_2$ | 130.4 | 4.20 | |
| $[Co(NH_3)_2(DCH_3)_2]Cl$ | 110.3 | 4.37 | 17.9 |
| ligand, $DHCH_3$ | 128.2 | 4.21 | |

the origin of the specific bands into consideration.

That is, the specific bands are the results of the polarizing deformation of the concerned ligands in the complex radical. While the two strong O-H-O hydrogen bonds are, as discussed in the previous paper,[1] expected in the bis-(dimethylglyoximato)-cobalt (III)-complexes, there could not be expected such hydrogen bonds in the corresponding bis-(mono-O-methyl-dimethylglyoximato)-complexes. Therefore, the degree of the polarizing deformation is anticipated to be larger in the latter than in the former. As for the reason of the above presumption, there may be supposed defying action of protons against the polarizing deformation of the concerned ligands under the effect of the cobalt (III) ion. In other words, the difference between the absorption spectra of $[Co(NH_3)_2(DCH_3)_2]Cl$ and $[Co(NH_3)_2(DH)_2]Cl$ supports the conclusion that the O-H-O hydrogen bonds play an important role in the determination of the electronic structure of bis-(dimethylglyoximato)-cobalt (III)-complex. The relation between the absorption curves of $H[Co(DCH_3)_2(NO_2)_2]$ and $H[Co(DH)_2(NO_2)_2]$ are similar to that between (a) and (i).

**The Stabilities of Bis-(dimethylglyoximato)-complexes.**—In the previous paper, it was concluded that the high stability of the bis-(dimethylglyoximato)-cobalt(III)-complexes, in which the two dimethylglyoximato ions coördinate to a cobalt atom with planar configuration, is attributed to the O-H-O hydrogen bonds in the complex radical. In this work, the above conclusion was confirmed by the other chemical evidence. Although bis-(mono-O-methyl-dimethylglyoximato)-diammine-cobalt (III) chloride can be prepared from purpureo cobalt (III) chloride according to the almost similar direction to that of the corresponding dimethylglyoximato-complex, the

18) M. Linhard and M. Weigel, *Z. anorg. Chem.*, **271**, 101 (1952).

reaction for preparing the former is caused by the aid of charcoal and is finished less rapidly than that for preparing the latter. This indicates the fact that the bis-(dimethylglyoximato)-complex is by far more stable than bis-(mono-O-methyldimethylglyoximato)-complex. With respect to many other reactions for preparing bis(mono-O-methyl-dimethylglyoximato)-derivatives and corresponding dimethylglyoximato-derivatives, the above described conclusion is also supported. Such a distinct difference, which is originated from the substitution of the hydrogen atom by the methylradical will verify a remarkable contribution of O-H-O hydrogen bonds in the bis-(dimethylglyoximato)-complex radical towards the stabilization of the compounds. *Being united through the two O-H-O hydrogen bonds, the two dimethylglyoximate ions in the complex must be considered as one quadridentate group.*

## Summary

Two new compounds, $[Co(NH_3)_2(DCH_3)_2]Cl$ and $H[Co(DCH_3)_2(NO_2)_2]$ have been synthesized as the first examples of tervalent-cobalt complexes of dimethylglyoxime-mono-methylether. Absorption spectra of the compounds and several bis-(dimethylglyoximato)-cobalt (III)-complexes in solution have been measured.

The absorption curves of bis-(dimethylglyoximato)-cobalt (III)-complexes, generally, consist of three inflations and one maximum. The inflation in the visible region is the vestige of the first absorption band, and the two other inflations and one maximum in the ultraviolet region are the specific absorption bands which are due mainly to the dimethylglyoximate ions in coördination.

As for the first absortion bands, the results of the measurements can successfully be elucidated on the basis of the spectrochemical- and hyperchromic-series found by Tsuchida et al. For $NH_4[Co(DH)_2(NO_2)_2]$, is also the specific band originated from the nitro-groups in coördination remarkable.

The isolated maxima on the curves of $H[Co(DH)_2Cl_2]$ and $H[Co(DH)_2Br_2]$ in the longer wave-length region are nothing but the first absorption bands which are shifted towards red owing to the bathochromic effect of the two halogenide ions.

In the dibromo-complex, the third absorption band is conspicuous. It has never been recognized clearly in the other complexes with dimethylglyoxime.

The absorption curves of bis-(mono-O-methyl-dimethylglyoximato)-complexes, as a whole, resemble those of corresponding dimethylglyoximato-complexes, but the bathochromic shift of the specific absorption bands from that of free ligand molecule amounts to a considerable degree in comparison with the cases of dimethylglyoximato-complexes. And this phenomenon is elucidated in connexion with the O-H-O hydrogen bonds.

From comparison of the reactions for preparing the bis-(mono-O-methyl-dimethylglyoximato)- and bis-(dimethylglyoximato)-complexes, the high stability of the latter was discussed.

The author wishes to express his sincere thanks to Professor R. Tsuchida and Dr. S. Yamada for their kind guidance and encouragement throughout this work. Appreciation is also expressed to Professor G. Hazato of the Tohoku University for the determination of magnetic susceptibilities. This study was supported in part by a grant from the Ministry of Education.

*Department of Chemistry, Faculty of Science, Osaka University, Nakanoshima, Osaka*

# *On the Specific Coloration of the Benzylamine Type Compounds in the Ninhydrin Color Reaction. I.**)

By Eiichi TAKAGI, Mitsuo MANGYO, Masanobu SAWAI and Isao ENSAKA

(Received September 10, 1954)

During the course of an investigation concerning reactions between aromatic aldehydes and $\alpha$-amino acids[1], the authors noticed the specific coloration of the benzylamine type compounds with ninhydrin in paper chromatography.

We thought that if the amines have the following constitution, Ar–CH(NH$_2$)–R (Ar = Aryl group; R = H or Ar–CH(OH)–), yellow coloration will appear and then after an interval change to purple. Satake[2] pointed out a similar phenomenon, but details were not mentioned.

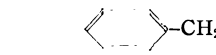
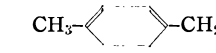
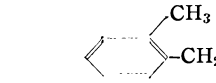
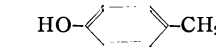
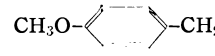
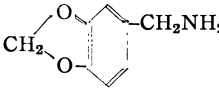
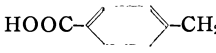
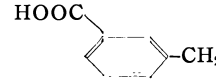
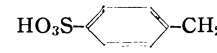
As the authors believed that this specific coloration could be a convenient and simple method for detecting a specific benzylamine-skeleton in a molecule, we studied several similar compounds and already published some of the results of the thesis[3].

Further studies were made on the same phenomenon using other substances and also using another reagent, alloxan. The present paper summarizes evidences obtained since the previous work.[1]

## Coloration with Ninhydrin

The results with ninhydrin and alloxan color reactions are summarized in Table I.

TABLE I

| No. | Ar-CH(NH)- type compounds | Specific ninhydrin color reaction | Specific alloxan color reaction | *Rf* value | Synthetic methods of the compounds* |
|---|---|---|---|---|---|
| 1 |  | + | + | 0.65 | E. Takagi et al[4] |
| 2 |  | + | + | 0.71 | F. Lustig[5] |
| 3 |  | + | + | 0.71 | H. Strassmann[6] |
| 4 |  | + | + | 0.55 | M. Tiffeneau[7] |
| 5 |  | + | + | 0.64 | E. Takagi[8] |
| 6 |  | + | + | 0.62 | E. Takagi[8] |
| 7 |  | + | + | 0.58 | F. F. Blicke et al[9] |
| 8 |  | + | + | 0.50 | A. Einhorn[10] |
| 9 |  | + | + | 0.09 | Sample No. 10 is hydrolysed with sulfuric acid. |

* Continuation of the paper: E. Takagi and M. Mangyo, *J. Pharm. Soc. Japan*, 72, 812-5 (1952).

1) loc. cit.

2) K. Satake, "Chromatography" (Kyoritsu Zensho) (1951), p. 88.

3) 6th Meeting of the Chemical Society of Japan, held at Kyoto on April 4, 1953.

4) E. Takagi, I. Ensaka, M. Mangyo and M. Sawai, *J. Pharm. Soc. Japan*, 73, 1086 (1953).

5) F. Lustig, *Ber.*, 28, 2988 (1895).

6) H. Strassmann, *Ber.*, 21, 577 (1888).

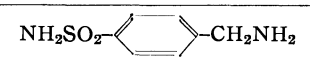
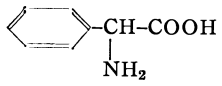
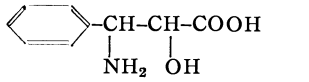
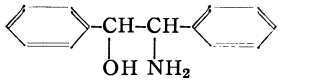
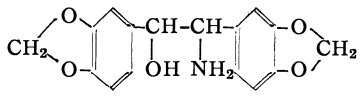
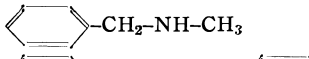
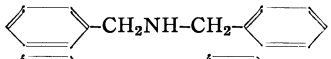
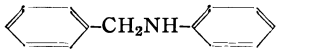
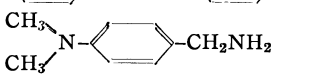
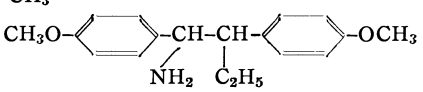
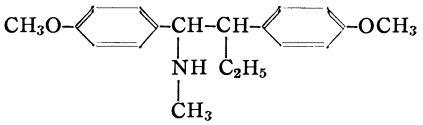
7) M. Tiffeneau, *Bull. soc. chim. France*, 9, 823 (1911).

8) E. Takagi, *J. Pharm. Soc. Japan*, 71, 656 (1951).

9) F. F. Blicke and W.M. Lilienfeld, *J. Am. Chem. Soc.*, 65, 2281 (1943).

10) A. Einhorn, *Ann.*, 343, 295 (1905).

TABLE I (Concluded)

| No. | Ar-CH(NH)- type compounds | Specifiic ninhydrin color reacton | Specific alloxan color reaction | *Rf* value | Synthetic methods of the compounds* |
|---|---|---|---|---|---|
| 10 |  | + | + | 0.37 | Commercial substance made by the Wako Pure Chemical Industries, Ltd. |
| 11 |  | + | + | 0.48 | C.S. Marvel et al[11] |
| 12 |  | + | + | 0.59 | M.O. Forster et al[12] |
| 13 |  | + | + | 0.81 | E. Takagi et al[4] |
| 14 |  | + | + | 0.74 | E. Takagi[8] |
| 15 |  | + | + | 0.70 | E. L. Holmes et al[13] |
| 16 |  | + | + | 0.67 | A. Galat et al[14] |
| 17 |  | − | − | ** | Org. Synth[15] |
| 18 |  | (+) | − | 0.65 | *** |
| 19 |  | + | − | 0.87 | *** |
| 20 |  | + | − | 0.88 | *** |

* Literature cited for the synthesis.

** Clear spot is not obtained.

*** We are indebted to Mr. T. Takahashi of the Department of Chemistry, Faculty of Science, Tokyo University, for these substances.

According to results obtained, with the exceptions of *p*-dimethylaminobenzylamine (18) and benzylaniline (17), all substances caused specific colorations on filter paper with ninhydrin, i.e., first yellow coloration which then changed to purple. *p*-Dimethylaminobenzylamine (18) developed at first an orange red color, but being comparatively stable, changed to purple very slowly. In the case of benzylaniline (17), we could not obtain a clear spot and moreover the color developed was purple-without passing the yellow stage, i.e., this substance resembled aniline in its behaviour.

In the samples of Table I, if the *p*-position of aminomethyl group is substituted with hydroxyl or methoxyl group, or 3,4-positions are substituted with methylenedihydroxyl group, the rate of color change was slow. This was especially so in the case of *p*-hydroxybenzylamine (4), which took a very long interval (few weeks) to change its color.

We can show other kinds of substances, too, which cause similar specific coloration with ninhydrins. The results with these other kinds of substance are summarized in Table II.

11) C.S. Marvel and W.A. Noyes, *J. Am. Chem. Soc.*, **42**, 2264 (1920).

12) M.O. Forster and K.A. RaO, *J. Chem. Soc.*, **1926**, 1947; K. Vogler, *Helv. Chim. Acta.* **33**, 2111 (1950).

13) E.L. Holmes and K. Ingold, *J. Chem. Soc.*, **127**, 1813 (1925).

14) A. Galat, and G. Elion, *J. Am. Chem. Soc.*, **61**, 3585 (1939).

15) Org. Synth., Vol. 8, 38 (1928).

TABLE II

| No. | Substances | Specific ninhydrin color reaction | Specific alloxan color reaction | *Rf* value | Synthetic methods of substances |
|---|---|---|---|---|---|
| 1 | $NH_2$–$CH_2CO$–$NHCH_2COOH$[2)20)] | + | – | 0.11 | Commercial substance made by Wako Pure Chemical Industries, Ltd. |
| 2 | $NH_2$–$CH_2$–$COOC_2H_5$[2)] | + | – | 0.52 | T. W. Curtius[16)] |
| 3 | $NH_2$–CH($CH_3$)–$COOC_2H_5$ | + | – | 0.64 | T. W. Curtius[16)] |
| 4 | $(CH_3)_2$CH–CH($NH_2$)–$COOC_2H_5$ | – | – | 0.85 | T. W. Curtius[16)] |
| 5 | $CH_3$–C($CH_3$)($NH_2$)–$COOC_2H_5$ | – | – | — | A. L. Barker et al[17)] |

Glycylglycine (1), glycine ethylester (2) and alanine ethyl ester (3) became yellow at first and then changed to purple.

Generally, the rates of the color changes of these substances in Table II are much greater than those of the substances in Table I.

Especially in the case of alanine ethyl ester (3), the color change occurred instantly. We could not find a yellow stage in the case of isoleucine ethyl ester (4) but it became purple directly, as normally occurs. Ethyl-$\alpha$-amino-isobutyrate (5) gave no color with ninhydrin, which resembled that of the *tert*-butylamine[18)] due probably to lack of hydrogen atom where carbon atom is linked to the amino group.

## Coloration with Alloxan*

As the intensity of coloration with alloxan was much weaker than that of the ninhydrin, we were obliged to change experimental conditions (cf. experimental). The results obtained are shown in the section of alloxan in Table I and II.

Generally, in the samples of Table I, the color first became yellow, then changed to orange in the middle stage and finally to a pink color. The relations between the rates of the color changes and the constitutions of the substances seemed to be similar to the tendency in the case of ninhydrin. However the yellow stage of $\alpha$-aminophenylacetic acid (11) and $\beta$-amino-$\beta$-phenyl-lactic acid (12) were relatively long (about one day), being different from that of ninhydrin.

Contrary to the case of ninhydrin, the substances (Nos. 1, 2, 3 and 4) in Table II developed an orange or pink color directly without first passing through the yellow stage. Ethyl $\alpha$-aminoisobutyrate (5) developed no color as in the case of ninhydrin.

## Factors Affecting Color Change

We sought the factor affecting color change to solve the problem, i.e., what causes color change.

The results were:

(1) After having removed the specimens to a dark place at the first color stage, further color change took place.

(2) When kept in a vacuum desiccator, they did not change color but when they were brought into contact with air, they began to change color.

(3) When kept in an atmosphere of nitrogen gas with some water vapour, normal color change occurred.

(4) If the specimens were exposed to steam, the color change occurred very rapidly.

Accordingly, the rate of the color change is dependent on the degree of the humidity of air and to the chemical structure of the substances at a given temperature*. The mechanism of the color change will be discussed later[19)].

16) T.W. Curtius, *J. prakt. Chem.*, (2) **37**, 159 (1888).
17) A.L. Barker and G.S. Skinner, *J. Am. Chem. Soc.*, **46**, 405 (1924).
18) R. Moubasher and A. M. Othman, *J. Am. Chem. Soc.*, **72**, 2666 (1950).
* We are indebted to Prof. K. Miyagi of the College of Pharmacy, Chiba University for this reagent.
19) Paper II. *J. Chem. Soc. Japan* (in press).
* When the samples were treated with water, the color change occurred comparatively slowly, showing that the rate of color change is affected by temperature.

## Experimental

**I. On the Paper Chromatography.**—The authors carried out the paper chromatography in the usual manner. Details are as follows.

Sample: 0.5% aqueous solutions of the amino-carboxylic acids or the amino sulfonic acid. In the case of amines, 0.5–1% aqueous solutions of their hydrochlorides.

1/1000 cc. of the samples are spotted on the filter paper at the point, 3 cm from the end.

Filter paper: Toyo Roshi No. 2, 2 cm×20 cm.

Developing method: One dimensional ascending method.

Developing solvent: Mixture of *n*-butanol, acetic acid and water (4:1:1).

Developing temperature and time: 15–18°C, 3–4 hrs.

Developing distance to the solvent front from the original point: 13–15 cm.

Reagent: 0.2% ninhydrin solution in *n*-butanol.

In the case of alloxan the coloration was very weak as mentioned before, so we examined the color reaction by spot tests on filter paper using 0.5% alloxan solution in *n*-butanol.

**II. On the Factor Affecting Color Change.**—We prepared five series of the same specimens of a substance to seek the factor affecting color change and examined their behaviours as follows.

Samples: The positive substances of the specific color reaction in the Tables I and II were used. The tests of the special substances, which took a very long time or a very short time for the color change, were excluded.

Filter paper: Toyo Roshi No. 2.

Reagents; 0.2% ninhydrin and 0.5% alloxan solutions in *n*-butanol.

Color tests:

*A*) *Ninhydrin test.*—0.01 cc. of a sample was spotted in the same manner on five filter papers, airdried, sprayed with the ninhydrin reagent, and heated on an electric heater to develop the yellow color.

The five yellow colored specimens were examined for five series of the following tests.*

The first series of the specimens was kept in room air for control. The second was kept in a desiccator at an atmospheric pressure filled with air on calcium chloride and the third in an evacuated desiccator on concentrated sulfuric acid.

The fourth series was kept under an atmospheric pressure filled with nitrogen gas on some water, using a vacuum desiccator as the vessel, and the fifth was enclosed in a piece of black paper and was kept in a dark place.

We observed that the color change of the first series took place relatively rapidly (in several minutes to several hours); the second series caused slight color change in 100 hours, yellow-brown to brown but not to purple; the third series maintained its yellow to yellow-brown color for 100 hours; the fourth and the fifth series were similar to the first series, changing their color rapidly.

We could not observe remarkable differences among the first, the fourth and the fifth series.

*B*) *Alloxan test.*—In the case of the alloxan reagent, although the color changes were not identical to that of the ninhydrin, being orange in the middle stage in general, results obtained were similar. In the cases of both the ninhydrin and alloxan tests, when the specimens of the second and the third series were brought out to room air, they began to change their color in the normal manner, i.e., in ninhydrin, the color stabilized to purple and in alloxan, the color stabilized to pink.

When the specimens of the first color stage or the middle color stage were exposed to steam, they changed their color very rapidly to the stabilizing color.

The authors wish to acknowledge the support of Dr. F. Nagasawa, The Director of the Laboratory.

## Summary

The specific coloration of the benzylamine type compounds in the ninhydrin color reaction is extended to other kinds of compounds. Alloxan resembles ninhydrin in its behaviour as reagent. The fact that the specific coloration reaction seems to be common to the benzylamine type compounds, is verified.

However a few exceptions are observed as in the case of benzylaniline (17) and *p*-dimethylaminobenzylamine (18). The fact that the color change of these compounds in the usual paper chromatography is due to moisture in the air, is confirmed.

*Research Laboratory, Mitsubishi Chemical Industries Ltd.*
*Kawasaki, Kanagawa*

20) Akabori and Narita, *Seni Kagaku Kenkyusho Nenpo*, 5, 76 (1950).

* The room temperature was about 26°C and the humidity of the air was about 70%.

# *Solvent Effects on Ion Exchange Equilibria. Part I.*

By Tomohiko SAKAKI

(Received September 27, 1954)

## Introduction

It has been found that the addition of non-electrolytes to the ion exchange system generally causes shifts in equilibrium, which depend on the composition of the solvent system, the ionic species, etc. These effects have been studied in detail from the physico-chemical point of view, and some noticeable regularities have been found, thus suggesting that simple and well-defined procedures may be added to the list of ion exchange techniques.

The fact that only a few papers on this subject have as yet been published indicates that this aspect has been somewhat overlooked in the past. Some decades ago Wiegner et al[1] studied the ion exchanges between a calcium zeolite and various alkali chlorides dissolved in aqueous ethanol, and observed that more alkali ions passed into the exchanger as the concentration of ethanol was increased and that the exchange became nearly equal for all ions at higher concentrations of alcohol. The problem remained untouched until a recent investigation by Kressman and Kitchener[2]; they studied the effect of the addition of an organic solvent on the exchange of alkali ion, using a phenol-sulfonate resin. It was found that with the calcium resin-alkali salt system in aqueous ethanol the logarithm of the equilibrium constant increased linearly with the ethanol percentage, whereas with the $NH_4^+-K^+$ system in aqueous acetone the equilibrium constant itself changed linearly with the acetone concentration. More recently Okuno, Honda and Ishimori[3] investigated the exchange of alkali ions by sulfonated styrene type resins (H-form) in aqueous solutions containing various quantities of methanol or ethanol. They observed that the difference in the equilibrium constants of various alkali ions became greater as the alcohol concentration was increased. Their results have been reconfirmed by the more detailed study of the same system carried out in our laboratory under the collaboration of Kakihana and his co-workers.

A short note on our results has already been published[4] and the application of these to analytical and preparative chemistry has been discussed elsewhere.[5] Therefore the present paper will be limited to the physico-chemical treatment of the problem.

## Experimentals and Results

**(i) Properties of the Resin Used.**—Amberlite IR-120 was used. Conventional techniques were employed for the conversion of the resin to the H-form, regeneration, determination of the exchange capacity per gram of dry resin, etc.

When the H-resin granules, which had been dried at 100°C under 15 mm Hg to constant weight, were allowed to absorb water vapor at 100 per cent relative humidity at room-temperature during ten days, it uptook 0.9 gram of water per gram of dry resin. To determine the exchange capacity of the resin, 0.1N solutions of potassium chloride in water, and 20, 40, 60, 80 and 100 per cent methanol or ethanol were used. This was found to be $5.10\pm0.02$ meq. per gram of dry resin, independent of the alcohol concentration of the solution used, that is, the total capacity was uninfluenced by the addition of alcohol.

**(ii) Experimental Procedures.**—The measurements were carried out under the following conditions. The alkali chloride was dissolved in the aqueous solution containing a known amount of alcohol, to yield 0.05, 0.1, or 0.2N salt/l. solutions. An adequate amount of the H-resin was added to 50 ml. of the salt solution, and subsequently the vessel containing the exchange system was kept shaken at $25\pm0.05$°C until the equilibrium had been attained. An aliquot portion of the solution was then analyzed for the hydrogen ion. The mole ratio of an alkali ion to hydrogen ion in the resinous phase at equilibrium was kept around unity by varying the quantity of the resin added. To avoid error due to the instability of the H-resin, the exchange capacity of the resin sample was simultaneously determined with each measurement of the exchange equilibrium.

**(iii) Apparent Equilibrium Constant.**—The exchange reaction involving metal ion $M^+$ and hydrogen ion $H^+$ is written as,

$$M^+ + HR = H^+ + MR.$$

The apparent exchange equilibrium constant, $K_H^M$, is given by

$$K_H^M = \frac{[H^+]\,[MR]}{[M^+]\,[HR]} \qquad (1.1)$$

1) G. Wiegner and H. Jenny, *Kolloid-Z.*, **42**, 268 (1927).

2) T. R. E. Kressman and J. A. Kitchener, *J. Chem. Soc.*, **1949**, 1211.

3) H. Okuno, M. Honda and K. Ishimori, *Bunseki-Kagaku* (*Japan Analyst*), **2**, 430.

4) T. Sakaki and H. Kakihana, *Kagaku* (*Science*), **23**, 471 (1953).

5) H. Kakihana, Chemical Industry (Kagaku Kogyo), Symposium Kogyo-Keisoku.

TABLE I
EFFECT OF ALCOHOL (25°C)

| Salt | Conc. (N) | Alkali chloride–H-resin (Amb. IR-120) | | | | |
|---|---|---|---|---|---|---|
| LiCl | 0.2 | Wt. % of methanol | 0 | 30.0 | 50.0 | |
| | | $K_H^{Li}$ | $0.84_4$ | 1.45 | 2.15 | |
| | 0.1 | Wt. % of ethanol | 0 | 21.8 | 36.7 | 40.5 |
| | | $K_H^{Li}$ | $0.80_3$ | 1.32 | 2.18 | 2.37 |
| NaCl | 0.05 | Wt. % of methanol | 0 | 13.5 | 29.5 | 47.0 |
| | | $K_H^{Na}$ | 1.70 | 2.86 | 5.07 | 10.7 |
| | 0.2 | Wt. % of ethanol | 0 | 14.0 | 32.0 | |
| | | $K_H^{Na}$ | 1.84 | 3.33 | 8.15 | |
| KCl | 0.1 | Wt. % of methanol | 0 | 13.5 | 21.5 | |
| | | $K_H^{K}$ | 3.61 | 4.74 | 6.65 | |
| | 0.2 | Wt. % of ethanol | 0 | 14.0 | 34.0 | |
| | | $K_H^{K}$ | 3.74 | 5.25 | 17.8 | |

The mole ratio, $[MR]/[HR]$, was kept at 0.85–1.10 for $Li^+$ and $Na^+$, and at 1.86–2.30 for $K^+$.

where the bracket [ ] represents the analytical concentration of each species in eq./l.

The equilibrium measurements were carried out with 0.2N, 0.1N and 0.05N alkali chloride solutions containing various amounts of alcohol. A part of the results is given in Table I as typical data illustrating the solvent effects. It is to be noted that the following features may be deduced from these results.* First, for the same metal ion and for the equal content of alcohol, $K_H^M$ is always greater in aqueous ethanol than in aqueous methanol; secondly, the value of $K_H^M$ becomes higher as the alcohol concentration is increased, and finally, the sequence of the magnitude of $K_H^M$ is $K^+ > Na^+ > Li^+$, provided that the alcoholic solutions are of identical concentration.

## Discussion

**(i) The Free Energy Change of Ion Exchange and the Dielectric Constant of Solution.**—In the system of aqueous alkali chloride solution and the sulfonic acid exchanger, it has been found by Boyd, Schubert and Adamson,[6] and ascertained by Kressman and Kitchener[7] that the apparent free energy change** accompanied by ion exchange is inversely proportional to the hydrated radius of the exchangeable ion. This regularity is conveniently represented by the following equation;

$$-\Delta F'_{MR} = RT \ln K_H^M, \qquad (1.2)$$

$$= B + \frac{C_m}{D_s \cdot a_M} \qquad (1.3)$$

where $-\Delta F'_{MR}$ represents the apparent free energy change, $B$ and $C_m$ are constants, and $D_s$ and $a_M$ are the dielectric constant of solution and the hydrated radius of $M^+$ ion, respectively.

Fig. 1-1. shows the graph of $-\Delta F'_{MR}$ against

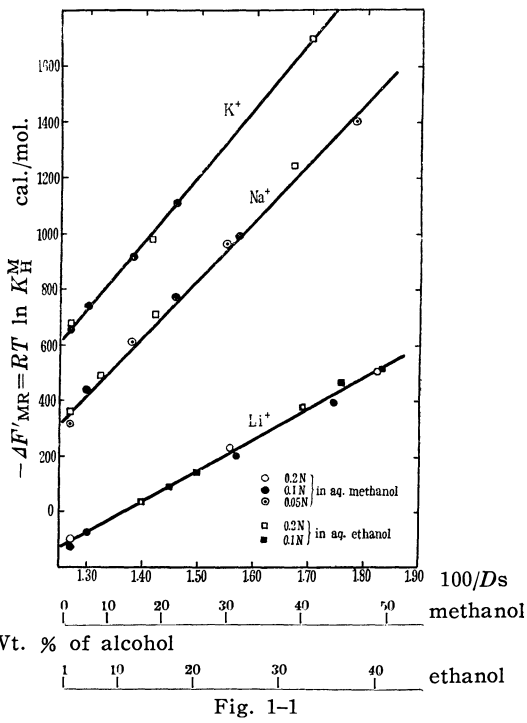



Fig. 1-1

$1/D_s$ for each ion. The values of $-\Delta F'_{MR}$ have been calculated from the data according to Eq. (1.2). Since the salt concentration is too low to give a notable influence on the values of $D_s$, they have been estimated from the alcohol concentrations of solutions, using results from macroscopic measurements.[8]

* See also the data given in reference 3).

6) G. E. Boyd, J. Schubert and A. W. Adamson, *J. Am. Chem. Soc.*, **69**, 2818 (1947).

7) T. R. E. Kressman and J. A. Kitchener, *J. Chem. Soc.*, **1949**, 1190.

** The free energy which these authors have used is nearly equal to the apparent free energy.

8) G. Åkerlöf, *J. Am. Chem. Soc.*, **54**, 4125 (1932).

This manner of plotting apparently gives a straight line for each ion in the range of $D_s > 55$. In order to let Eq. (1.3) represent the linear relationship between $-\Delta F'_{MR}$ and $1/D_s$, $a_M$ must be kept invariable through the region of $D_s$ in Fig. 1-1. It might be possible that owing to the preferential hydration of the ion the value of $a_M$ is essentially uninfluenced by the addition of alcohol up to a concentration of 40 or 50 per cent in weight. When the alcohol content is increased and consequently the reciprocal of $D_s$ exceeds the region shown in Fig. 1-1 the free energy vs. $-1/D_s$ curve, losing the linearity, reaches a maximum and falls sharply as $1/D_s$ approaches the value of absolute alcohol, as illustrated in Fig. 1-2.

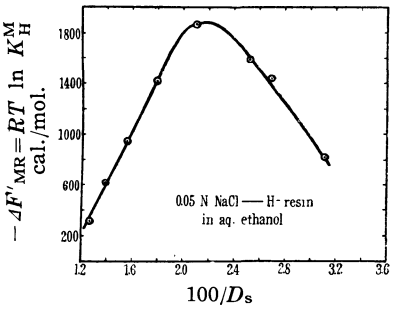



Fig. 1-2

This fact leads us, as the natural consequence, to the viewpoint that the ion may gradually lose its apparent affinity for water molecules in higher alcohol concentrations.

Furthermore it is to be noted that the slope of the line shown in Fig. 1-1 is characteristic to each ion and indifferent to the kind of coexisting alcohol, and that, as is expected from Eq. (1.3), the order of its magnitude is $K^+ > Na^+ > Li^+$, which is equal to the sequence of the value of $K^M_H$ or $-\Delta F'_{MR}$ in aqueous solution. It goes without saying that these results are consistent with the observations stated in section II (iii).

(ii) **The Effect of Urea.**—It is interesting to examine the effect caused by the addition of non-electrolytes, such as urea, which contrary to the case of alcohol, increase the dielectric constant of solution.

According to Eq. (1.3) the value of $K^M_H$ is expected to decrease with the addition of urea. This is supported by the results listed in Table II, which illustrates the data on the

TABLE II
EFFECT OF UREA (25°C)
0.1N NaCl—H-resin
(Amberlite IR-120)

| Conc. of urea (Wt. %) | $K^{Na}_H$ |
|---|---|
| 0 | 1.68 |
| 0.8 | 1.31 |
| 1.6 | 0.93 |
| 2.4 | 0.77 |
| 3.2 | 0.70 |
| 4.0 | 0.44 |
| 6.0 | 0.37 |

system of Amberlite IR-120 and urea in 0.1N sodium chloride at 25°C. Though Eq. (1.3) seem to coincide with the facts in this case as well, close examination reveals that the agreement of the equation with experiments is only qualitative. If the data on $D_s$ of aqueous urea solutions[9] are inserted into Eq. (1.3), the constants of which have beeen determined from Fig. 1-1, then, the value of $K^M_H$ is found to be by far greater than that observed, that is, $K^M_H$ appears to be more sensitive to the presence of urea than to that of alcohol. This discrepancy may be formally eliminated by admitting that the gradient $C_m$ in Eq. (1.3) is generally dependent on the species of the non-electrolyte added, so far as $a_M$ can not be assumed to decrease rapidly with the concentration of urea. But it must be taken into consideration that this simple empirical equation is inadequate for quantitative usage, since it lacks sufficient theoretical basis.

In conclusion, Eq. (1.3) represents semi-quantitatively the effect of the addition of non-electrolytes on ion exchange equilibria. However, this cannot correlate successfully the free energy change with the valency of the exchangeable ion. Hence, further work is necessary to establish a relationship, which is not only consistent with the mentioned facts but also more generally applicable; this will be attempted in the ensuing paper.

*Chemical Institute, Faculty of Science, Nagoya University*

9) J. Wyman Jr., *J. Am. Chem. Soc.*, 55, 4116 (1933).

# *Solvent Effects on Ion Exchange Equilibria. Part II.*

By Tomohiko SAKAKI

(Received September 27, 1954)

In the preceding paper[1] it was pointed out that a semi-quantitative relationship exists between the free energy change of univalent ion exchange and the dielectric constant of the solution. The present paper is concerned with a more general regularity which governs the solvent effects on the exchange of polyvalent ion.

## The Free Energy Change of Univalent Ion Exchange

The present discussions are limited, for simplicity, to the case in which the exchange groups of resin have the same ionization constant. Then, the free energy change, $\Delta F^\circ$, for the reaction of the type

$$M^+ + HR = H^+ + MR$$

is written

$$RT \ln K_a = -\Delta F^\circ, \qquad (2.\ 1)$$

where $K_a$ is the thermodynamic equilibrium constant and is expressed as

$$K_a = K_H^M \cdot \frac{f_H \cdot f_{MR}}{f_M \cdot f_{HR}} \qquad (2.\ 2)$$

where $f_i$ shows the activity coefficient of i species. Now let us specify by the symbol $(X)_o$ the value of the quantity $X$ to be measured in aqueous solution—resin system, and by $(X)_m$ that in the system of aqueous alcohol—resin; then, from Eqs. (2. 1) and (2. 2), we get

$$(\Delta F'_{MR})_o - (\Delta F'_{MR})_m = (\Delta F^\circ)_o - (F^\circ)_m - RT\left\{\ln\frac{(f_H)_m}{(f_H)_o} - \ln\frac{(f_M)_m}{(f_M)_o}\right\} - RT\left\{\ln\frac{(f_{MR})_m}{(f_{MR})_o} - \ln\frac{(f_{HR})_m}{(f_{HR})_o}\right\} \qquad (2.\ 3)$$

The second term on the right-hand side of the above equation is readily evaluated by the Debye-Hückel theory, assuming that the solvated radii are kept constant indifferently of the addition of alcohol. The result of the calculation shows that this term contributes only a little to the total value of the difference in $-\Delta F'_{MR}$ shown in Fig 1-1 of the preceding paper.

It is difficult to estimate, without any assumption, the value of the third term, but it does not seem to be so unreasonable to assume that under the present experimental conditions this term is not so great when compared with the preceding term.

Thus,

$$(\Delta F'_{MR})_o - (\Delta F'_{MR})_m \approx (\Delta F^\circ)_o - (\Delta F^\circ)_m, \qquad (2.\ 4)$$

or

$$RT \ln \frac{(K_H^M)_m}{(K_H^M)_o} \approx RT \ln \frac{(K_a)_m}{(K_a)_o} \qquad (2.\ 5)$$

## A Simple Model of Ion Exchange

Let us consider the free energy change of ion exchange, based upon a simple model. When an ion is brought into the resin phase and is fixed, either loosely or tightly, by one of the ionic groups, the solvent molecules attached to the ion may be more or less detached from it; the ion fixation may be accompanied by the desolvation process to a certain extent. This process can be analyzed into the three steps shown in Fig. 2-1. Step 1 represents the partial desol-

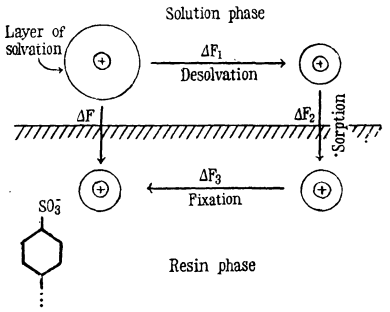



Fig. 2-1

vation of ion in the solution having Ds; the ion enters the resin phase through step 2; and in step 3 the charge of the ion is neutralized by an ionic group of the opposite sign. Each step is accompanied by the free energy change $\Delta F_1$, $\Delta F_2$ and $\Delta F_3$, respectively. It seems that among these free energy changes the second and the third do not vary with the species of exchangeable ion, that is, it is likely that the difference in the resultant free energy change between a pair of exchangeable ions is predominantly determined by that in the magnitude of $\Delta F_1$.

The work of step 1 may be essentially of an electrical nature, so that, as a rough ap-

1) This Bulletin, **28** 217 (1955).

proximation, it can be regarded as being proportional to the solvation number of the ion and inversely proportional to the dielectric constant of the medium.

If the solvation number is tentatively replaced by the hydration number in the case of the solution of the lower alcohol concentration, we obtain the following equation as the final result of the above considerations;

$$(\Delta F^\circ)_o-(\Delta F^\circ)_m=C_n\cdot(n_H-n_M)\cdot\left\{\frac{1}{(D_s)_m}-\frac{1}{(D_s)_o}\right\}, \quad (2.6)$$

where $n_H$ and $n_M$ are the hydration numbers of hydrogen ion and metal ion, and $C_n$ is a constant which depends upon the species of the solvent added and that of the resin used.

Combining Eqs. (1. 2), (2. 4) and (2. 6),

$$RT\ln\frac{(K_H^M)_m}{(K_H^M)_o}\approx C_n(n_H-n_M)\cdot\left\{\frac{1}{(D_s)_m}-\frac{1}{(D_s)_o}\right\}. \quad (2.6)$$

or, in general

$$RT\ln K_H^M\approx B+(n_H-n_M)\cdot\frac{C_n}{D_s}, \quad (2.8)$$

where $B=C_n(n_H-n_M)/(D_s)_o$.

Here the hydration numbers of exchangeable ions are adopted as parameters in place of their hydrated radii in Eq. (1. 3). When the values proposed by Stokes and Robinson[2] are introduced for $n_H$ and $n_M$, it is readily found that Eq. (2. 8) agrees with the experimental results, obtained in the case of univalent ion exchange.

**Polyvalent Ion Exchange**

The apparent equilibrium constant $K_H^M$ for the exchange reaction of the type

$$M^{z+}+zHR^+=zH^++MR_z$$

is written as

$$K_H^M=\frac{(H^+)(MR_z)^{1/z}}{(M^{z+})^{1/z}(HR)}\cdot\left\{\frac{v}{V}\right\}^{\frac{z-1}{z}} \quad (2.9)$$

where $z$ is the valency of metal ion, $V$ and $v$ are the volume of the solution and that of the solvent in the resin phase accessible to the ion in it, respectively, and ( ) represents the absolute quantity (equivalent) of each species found in each phase.

From Eq. (2. 9)

$$RT\ln K_H^M=RT\ln\frac{(H^+)\cdot(R_zM)^{1/z}}{(M^{z+})^{1/z}(RH)}+\left\{\frac{z-1}{z}\right\}RT\ln\left\{\frac{v}{V}\right\}. \quad (2.10)$$

If the same consideration as in the case of univalent ion exchange is applied to this case, it leads us to

$$RT\ln K_H^M\approx B+(n_H-n_{M/z})\frac{C_n}{D_s}. \quad (2.11)$$

The volume of free solvent in the resin phase, $v$, is a rather indefinite quantity, though $RT\ln K_H^M$ cannot be evaluated unless the value of $v$ is determined. But, fortunately, when $RT\ln K_H^M$ is plotted against $1/D_s$ with constant $v$, the slope of the curve is unaffected by the value of v. Thus, it is possible to check the validity of Eq (2. 11). The measurements were carried out on the resin-alkali earth chloride systems in aqueous ethanol under the same conditions as stated in the preceding paper, except that one gram of the resin (dry weight) was added to the solution in each measurement. This procedure may assure us of the constancy of $v$, since the value of $v$ is likely to be insensitive to the variation of alcohol concentration. But at the same time it follows that the mole ratio of the two species in the resin phase is no longer maintained at a constant value.

The plot of the data suggests in this case, too, the existence of the linear relationship between $RT\ln K_H^M$ and $1/D_s$ in the range of $D_s>55$. Moreover it is found that the relative value of $RT\ln K_H^M$ increases more rapidly for the heavier ion. By comparing the linear parts of the curves obtained for alkali and alkali earth ions, it is found that the order in the magnitude of the slope is $K^+>Na^+>\frac{1}{2}Ba^{++}>\frac{1}{2}Sr^{++}>\frac{1}{2}Ca^{++}Li^+>\frac{1}{2}Mg^{++}$, which comes into line with the sequence expected from Eq. (2. 11) and the values of $n_H$ and $n_M$ given by Stokes and Robinson.[2] These facts do not directly lead to the conclusion that the treatment given Section II is entirely adequate. Because of the complexities of the probem it is impossible at present to provide an exact quantitative expression of the phenomena associated with the solvent effects. The probem has been treated rather in a qualitative manner in Section II; a series of assumptions has been introduced either explicitly or implicitly, and several factors have been neglected for the sake of simplicity in the course of the computations. Therefore, Eq. (2. 8) or (2. 11) is to be regarded not as a theoretical formula but as a semi-empirical one. But it may be admitted that Eq. (2. 11) is a useful representation reflecting the general tendency of the solvent effects.

**The Value of "$v$"**

It was pointed out in the preceding report that the metal ion having the greater value

2) R. H. Stokes and R. A. Robinson, *J. Am. Chem. Soc.*, 70, 1870 (1948).

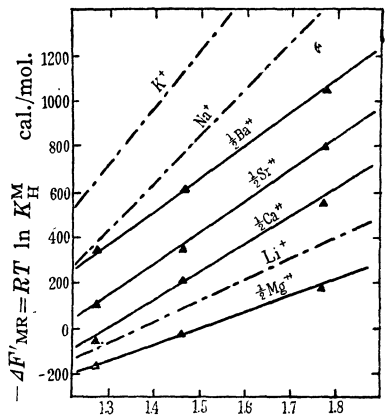



Fig. 2-2

of $RT\ln K_H^M$ in aqueous solution exhibits the more rapid increase of $RT\ln K_H^M$ with $1/D_s$. Consequently, in the graph of $RT\ln K_H^M$ plotted against $1/D_s$, the lines of barium, strontium and calcium ions should lie between those of sodium and lithium ions, and the line of magnesium ion should be found below that of lithium ion.

Since the first term of the right hand side of Eq. (2. 10) has been known from the experiment, the value of the second term must be determined so that the above requirements may be satisfied. By this procedure 0.20—0.25 ml. is found for the value of $v$ per one gram of dry resin.

This result shows nothing but the fact that the ion behaves as if it were surrounded by this volume of free water in the resin phase. Besides, the value of $v$ presumably depends upon the species of the ions in the resin and their quantities. But the found value seems to be not far from the real value of the free water in the resin.

Fig. 2-2 shows the results obtained by using this value for $v$.

## Summary

The effect of the addition of non-electrolytes to the ion exchange system has been studied. It has been found that the dielectric constant of the solution gives a profound effect on the ion exchange equilibrium and that in the case of lower concentrations of alcohol a linear relationship exists between the apparent free energy change and the reciprocal of the dielectric constant. A working equation has been proposed to account for the relationships between the free energy change, dielectric constant, ionic species and valency of exchangeable ion.

The author would like to express his thanks to Professor Isamu Sano and Professor Kazuo Yamasaki for their interest and encouragement; also to Dr. Hidetake Kakihana for his helpful advice. He is much indebted to Mr. Yoshihiro Mori for experimental assistance. The cost of the research has been defrayed from the Scientific Research Grant of the Ministry of Education.

*Chemical Institute, Faculty of Science, Nagoya University*

# *Spectrochemical Study of Microscopic Crystals. VII.*[1] *Absorption Spectra of Trans-dihalogeno-bis (ethylenediamine)-cobalt (III) Complexes*

By Shoichiro YAMADA, Akitsugu NAKAHARA, Yoichi SHIMURA and Ryutaro TSUCHIDA

(Received October 21, 1954)

In the former paper of this series[2] the present authors reported on the dichroism of the crystal of *trans*-dichloro-bis-(ethylenediamine) cobalt (III) salts. One of the conclusions therein, concerning the way of arrangement of the complex cations in the crystal of the hydrochloride dihydrate was found to be in disagreement with the result of X-ray investigation performed subsequently by one of the present authors.[3] The interpretation on the absorption bands of the praseo-salts in the previous paper was found to be in a dequate. We have, therefore, repeated the dichroism measurement of the hydrochloride and further measured the

1) Part VI, S. Yamada and R. Tsuchida, This Bulletin, 27, 436 (1954).
2) S. Yamada and R. Tsuchida, ibid., 25, 127 (1952).
3) A. Nakahara, Y. Saito and H. Kuroya, ibid., 25, 331 (1952).

dichroism with crystals of *trans*-dichloro-bis (ethylenediamine)-cobalt (III) perchlorate and the hydrobromide of *trans*-dibromo-bis (ethylenediamine)-cobalt (III) bromide. In this paper we present the results of the above measurements and discuss the results on the basis of the revised interpretation about the absorption bands.

## Experimental

**Materials.—Trans-dichloro-bis (ethylenediamine)-cobalt (III) perchlorate.**—Green crystals were prepared according to the direction of Linhard et al.[4] These crystallize in rhombic plates belonging to the monoclinic system. The external form and dichroism are closely similar to those of *trans*-$[Co(en)_2Cl_2]$ $Cl\cdot HCl\cdot 2H_2O$.[2,3,5] In the dominant (001)-plane, the crystal exhibits a remarkable dichroism; it appears greenish yellow with the electric vector along the b-axis and blue with that perpendicular to the b-axis. Dichroism measurements were made along these two directions.

**Trans-dibromo-bis (ethylenediamine)-cobalt (III) bromide hydrobromide dihydrate, $[Co(en)_2Br_2]Br\cdot HBr\cdot 2H_2O$.**[6]—Green crystals were prepared by the method of Jörgensen.[7] This compound crystallizes in forms similar to those of the above praseo-salts, that is, in monoclinic crystals with well-developed (001)-planes. On the c-plane the crystal shows a striking dichroism; that is, it appears brownish yellow with the electric vector along the b-axis, and green with the electric vector perpendicular to the above. Dichroism measurements were made with respect to these directions.

**Trans-dichloro-bis (ethylenediamine) cobalt (III) chloride hydrochloride dihydrate, $[Co(en)_2Cl_2]$ $Cl\cdot HCl\cdot 2H_2O$.**—The preparation and properties were reported in the former paper.[2]

**Measurements.**—Quantitative dichroism measurements were performed with a microcrystal by Tsuchida-Kobayashi's microscopic method[8] in the region covering 2400 to 7500 Å. $\alpha$ denotes absorption coefficient per mm. of a crystal. Molecular absorption coefficients, K, were estimated from the relation, $K=10\,M\alpha/\rho$, where $M$ and $\rho$ represent the formula weight of the compound and the density of the crystal, respectively.

## Results and Discussion

**Dichroism of $[Co(en)_2Cl_2]$ $Cl\cdot HCl\cdot 2H_2O$ and $[Co(en)_2Cl_2]$ $ClO_4$.**—Redetermined absorption spectra of a crystal of the hydrochloride, which differ slightly from those in the former paper,[2] are shown in Fig. 1, and data given in Table I. Results with the praseo-perchlorate are given in Fig. 2 and Table II.

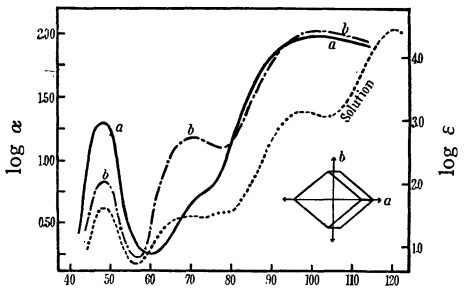



Fig. 1. Absorption spectra of $[Co(en)_2Cl_2]$ $Cl\cdot HCl\cdot 2H_2O$. The curve of the solution is taken from ref. 11.

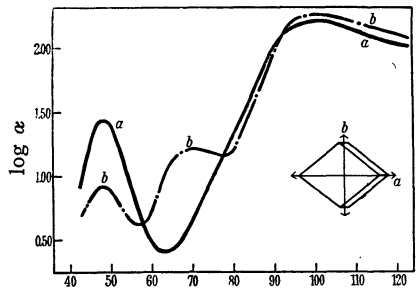



Fig. 2. Absorption spectra of $[Co(en)_2Cl_2]$ $ClO_4$.

TABLE I

ABSORPTION MAXIMA OF THE CRYSTALS OF $[Co(en)_2Cl_2]$ $Cl\cdot HCl\cdot 2H_2O$

| | $\nu$ $10^{13}$/sec. | log α | $\nu$ $10^{13}$/sec. | log α | $\nu$ $10^{13}$/sec. | log α |
|---|---|---|---|---|---|---|
| a-abs. | 48.2 | 1.29 | — | (0.65) | (100) | 1.97 |
| b-abs. | 48.3 | 0.82 | 70 | (1.18) | (102) | 2.02 |

TABLE II

ABSORPTION MAXIMA OF THE CRYSTALS OF $[Co(en)_2Cl_2]ClO_4$

| | $\nu$ $10^{13}$/sec. | log α | $\nu$ $10^{13}$/sec. | log α | $\nu$ $10^{13}$/sec. | log α |
|---|---|---|---|---|---|---|
| a-abs. | 48.0 | 1.44 | — | (0.7 ) | (100) | 2.20 |
| b-abs. | 48.1 | 0.91 | 70.8 | (1.22) | (102) | 2.25 |

In the former paper,[2] the authors presumed from the dichroism that the Cl-Co-Cl direction in the crystal of the hydrochloride should nearly conform with the b-axis.[9]

4) M. Linhard and G. Stirn, *Z. anorg. allg. Chem.*, 268, 105 (1952).

5) The notation, en, represents a molecule of ethylenediamine.

6) Two formulae have been proposed for this crystal, that is, one with two water molecules of crystallization and the other with one molecule of water. (Cf. "Gmelins Handb. anorg. Chem.", 8. Aufl., Teil 58 B, (1930) p. 252). In this paper we tentatively adopted the formula with two water molecules of crystallization, since the crystal shows a close similarity to that of $[Co(en)_2Cl_2]Cl\cdot HCl\cdot 2H_2O$.

7) S. M. Jörgensen, *J. prakt. Chem.*, (2) 41, 444 (1890).

8) R. Tsuchida and M. Kobayashi, "The Colours and the Structures of Metallic Compounds, (in Japanese)" Zoshindo, Osaka, Japan, (1944), p. 180. See also the previous papers of this series.

9) The a, b and c-axes adopted in the present paper and former paper (Ref. 2) correspond, respectively, to the c-, b- and a-axes in (Ref. 3).

This conclusion, however, was found to be incorrect. According to the X-ray crystal analysis with $[Co(en)_2Cl_2]Cl \cdot HCl \cdot 2H_2O$,[3] the Cl-Co-Cl direction in this crystal nearly conforms with the a-axis,[9] more exactly, inclined by about 18° to the a-axis, and by 76° to the b-axis. Using the data of the X-ray analysis, the components of the molecular absorption coefficients for the praseo-complex cation in the crystal of the hydrochloride dihydrate were calculated from the data in Table I, and shown in Table III.[10] As can be seen in Table III, the absorption band at $48\times10^{13}$/sec. is polarized in the Cl-Co-Cl direction, and the absorption band at $70\times10^{13}$/sec. is polarized in the plane formed by a cobalt and four nitrogen atoms. $K_{Cl\text{-}Co\text{-}Cl}/K_{Co\text{-}en}$ is found to be 5.9 for the former band and 1/5.5 for the latter band.

Linhard et al.[11] extensively studied absorption spectra of *trans*-dihalogeno-tetrammine- and bis (ethylenediamine)-cobalt (III) complexes in solution, and showed from comparison of absorption spectra of many complexes that in the dihalogeno-complexes the "first band,"[12] which usually appears with one band maximum, splitts itself into two bands. Thus the bands at 48 and $70\times10^{13}$/sec. of the praseo-salts correspond to the first band. The band at $100\times10^{13}$/sec. may be considered as the "specific band."[13] Its second band may be covered under the large specific band.

The present measurement shows that the praseo-perchlorate in the crystalline state displays absorption bands at 48, 71 and $100\times10^{13}$/sec., which correspond with those of the hydrochloride. Corresponding bands are also observed in the absorption spectra of the solution.

It is also found that the crystal of the perchlorate shows a quite similar dichroism to that of the hydrochloride. Comparison of the dichroism and absorption spectra of both the crystals indicates that in the crystal of the perchlorate, just as in the case of the crystal of the chloride, the Cl-Co-Cl direction in the complex cation is nearly coincident with the a-axis. The angle which the Cl-Co-Cl direction makes with the a-axis in this crystal is estimated to be even a little smaller than in the crystal of the hydrochloride dihydrate.

TABLE III

DICHROISM OF THE COMPLEX-ION, *trans*-$[Co(en)_2Cl_2]^+$

| | $\nu$, $10^{13}$/sec. | $K_a$ | $K_b$ | $K_{Cl\text{-}Co\text{-}Cl}$ | $K_{Co\text{-}en}$ |
|---|---|---|---|---|---|
| Band Ia | 48 | $431\times10^3$ | $136\times10^3$ | $470\times10^3$ | $80\times10^3$ |
| Band Ib | 71 | $98.8\times10^3$ | $346\times10^3$ | $68\times10^3$ | $375\times10^3$ |

TABLE IV

ABSORPTION MAXIMA OF THE CRYSTALS OF $[Co(en)_2Br_2]Br \cdot HBr \cdot 2H_2O$

| | $\nu$ | log $\alpha$ | $\nu$ | log $\alpha$ | $\nu$ | log $\alpha$ | $\nu$ | log $\alpha$ |
|---|---|---|---|---|---|---|---|---|
| a-abs. | 44.6 | 1.47 | —— | —— | 77 | 2.18 | 98.5 | 2.22 |
| b-abs. | 45.0 | 0.77 | 65 | 1.16 | 87 | 2.13 | 103 | 2.27 |
| | | log $\varepsilon$ | | log $\varepsilon$ | | log $\varepsilon$ | | log $\varepsilon$ |
| solution[a] | 45.6 | 1.73 | 65.0 | 1.49 | 84.3 | 3.35 | 103.8 | 4.34 |

a) These values are taken from ef. r12.

**Dichroism of the $[Co(en)_2Br_2]Br \cdot HBr \cdot 2H_2O$.** —Results are shown in Fig. 3 and given in Table IV. The crystal shows absorption bands at 45, 65, 86 and $103\times10^{13}$/sec. These bands find corresponding bands in the absorption spectra of the solution at almost identical wave-lengths, although the intensity relation among bands is not same as that

The band at $102\times10^{13}$/sec., which may be assigned to the "specific band,"[13] mainly due to the chlorine atoms in coordination, seems to be only slightly polarized. For this band, the Cl-Co-Cl absorption is found to be slightly bathochromic to the Co-en absorption.[14] It seems interesting enough that the hydrochloride and perchlorate crystallize in a closely similar form, in monoclinic plates with almost equal angles in the well-developed (001)-plane, showing also a quite similar dichroism, in spite of great difference in the size of the anions.

10) Some of the values in Ref. 2 were corrected after repeated measurements. $K_{Cl\text{-}Co\text{-}Cl}$ and $K_{Co\text{-}en}$ are molecular absorption coefficients with the electric vector along the Cl-Co-Cl direction and along the plane constructed from one cobalt and four nitrogen atoms, respectively.

11) M. Linhard and M. Weigel, *Z. anorg. allg. Chem.*, **271**, 101 (1952).

12) R. Tsuchida, This Bulletin, **13**, 388, 436 (1938).

13) R. Tsuchida, and M. Kobayashi, ibid., **13**, 471 (1938).

14) The X-Co-X-absorption, X being halogens, represents the absorption with the electric vector along the X-Co-X direction, and the Co-en-absorption the absorption with the electric vector along the plane formed by one cobalt and four nitrogen atoms.

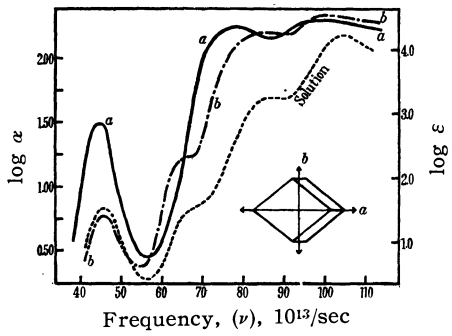



Fig. 3. Absorption spectra of $[Co(en)_2Br_2]Br \cdot HBr \cdot 2H_2O$. The curve of the solution is taken from ref. 11.

for the solution. The first band of this compound, as in the case of the corresponding dichloro-compound, may be considered to split into two band maxima. Thus the bands at 45 and $65\times10^{13}$/sec. of $[Co(en)_2Br_2]^+$ correspond to the bands at 48 and $70\times10^{13}$/sec. of $[Co(en)_2Cl_2]^+$. It is readily seen that the cations, $[Co(en)_2Br_2]^+$ and $[Co(en)_2Cl_2]^+$, show quite similar dichroism. It may be supposed that the band at $45\times10^{13}$/sec. is almost completely polarized in the Br-Co-Br direction and that the band at $65\times10^{13}$/sec. is polarized in the plane formed by one cobalt and four nitrogen atoms. It is seen that the difference in the absorption coefficient for the band at $45\times10^{13}$/sec. between the b- and a- absorptions is even larger than that for the corresponding band with the hydrochloride of the praseo-salt. It is, therefore, most probable that the Br-Co-Br direction of the complex cations in the crystal corresponds almost exactly with the a-axis.

For the band at $70—90\times10^{13}$/sec., which may tentatively be assigned to the "specific band,"[13] mainly due to the bromine atoms in co-ordination, the Br-Co-Br-absorption[14] is bathochromic to the Co-en absorption. This relation agrees with that induced for the specific band of other ligands.[15] For the band at about $100\times10^{13}$/sec., which is assumed to be the "third band,"[12] the Br-Co-Br-absorption is slightly bathochromic to the Co-en-absorption. The relation is also found to be in good agreement with that for the corresponding band of $[Co(en)_2Cl_2]^+$.

Further, it is to be noted that $[Co(en)_2Br_2]Br \cdot HBr \cdot 2H_2O$ appears to be isomorphous with $[Co(en)_2Cl_2]Cl \cdot HCl \cdot 2H_2O$, both crystallizing in a closely similar form, monoclinic plates with nearly equal angles. Thus it is probable that in the crystals of the above two compounds the complex cations take an isomorphous arrangement, and, in consequence, that in the crystal of the latter compounds, like in the former,[16] there might exist a network of hydrogen bonds involving bromine atoms. This being the case, the compound would afford one of the few examples that would involve bromine atoms forming hydrogen bonds. The crystal structure investigation of the compound is expected to yield interesting results.

**Absorption Spectra of *Trans*-dihalogeno-bis(ethylenediamine)-compounds in the Crystalline State.**—As stated in the above paragraph, Linhard et al. showed clearly that in the solution of *trans*-dihalogeno-complexes the first band, which in most complexes appears with one band maximum, shows two separate maxima. Thus the bands at 48 and $70\times10^{13}$/sec. for $[Co(en)_2Cl_2]ClO_4$ and the bands at 45 and $65\times10^{13}$/sec. for $[Co(en)_2Br_2]Br \cdot HBr \cdot 2H_2O$ are considered to correspond to the first band. For the first band of the *trans*-dihalogeno-complexes, the following relation can be induced. *The trans-dihalogeno-complexes show two separate absorption maxima corresponding to the first band. The absorption at the longer wave-length, polarized in the X-Co-X direction, takes place with the electric vector along the X-Co-X direction, and the absorption at the shorter wave-length occurs with the electric vector along the plane constructed from one cobalt and four nitrogen atoms.* The fact that the transition along the direction binding cobalt and halogen atoms requires much less energy much less than the transition in the plane formed by one cobalt and four nitrogen atoms may be understood qualitatively from the semi-empirical relation that halogen stands far behind ethylenediamine in the spectrochemical series;[12] the linkage between a metal and a nitrogen atom of an amine in a complex causes an electronic absorption in the shorter wave-length regions than the linkage between the metal and a halogen atom. Such a clear splitting of the first band as was observed in the above instances has not been found in many other complexes of a *trans*-configuration.[17] It may be assumed that, when two ligands in *trans*-positions stand much lower or higher in the spectrochemical series than the other four ligands, the complex would have its first band definitely split into two bands. In every *trans*-

15) To be submitted later.

16) In Ref. 3. on the crsytal structure of $[Co(en)_2Cl_2]Cl \cdot HCl \cdot 2H_2O$, only the word "N-Cl bond" was used, and not any word, "hydrogen bond between N and Cl." But since the distance between N and Cl atoms is so short, 2.9 Å, that the bond is surely expected, it is reasonable to suppose that the H- atom originally attached to N of the ethylenediamine molecule should be directed toward Cl, and that the bond between the N and Cl should be a kind of hydrogen bonds.

17) To be submitted later.

disubstituted-tetrammine complex, more or less marked splitting of its first absorption band might be expected from symmetry consideration. But when the ligands in *trans*-positions stand rather close to en or $NH_3$ in the spectrochemical series, the splitting may be less distinct. Besides, the electrostatic effect of ligand ions could not be overlooked. Thus the strongly ionic character of the linkage between cobalt and chlorine atoms might be another cause for the above splitting of the band.

For both the third band and the specific band, the X-Co-X absorption is found to be slightly bathochromic to the Co-en-absorption. The relation that for the above two bands the electronic transition along the X-Co-X direction requires less energy than that along the Co-en plane may readily be understood qualitatively on the basis of the idea about the origins of the absorption bands,[12,13] proposed by one of the present authors, that the third absorption band is due to charge transfer between the central ion and a ligand anion which is especially facilitated in the case of the existence of two anions in *trans*-positions, and that the specific band is due to the ligand concerned in co-ordination.

**Absorption Spectra of the *Trans*-dihalogeno-tetrammine-complexes in Solution.**— Absorption spectra of the praseo-salts in solution may be understood in the light of the dichroism. Earlier, Mathieu[18] and one of the present authors[19] pointed out the possibility that absorption bands of sexa-co-ordinated complexes having lower symmetry might consist of a set of component absorptions, which would appear as separate maxima in some cases. Later, Ilse et al.[20] treated the absorption spectra of octahedral complexes of titanium (III) in terms of the group theory, and showed that the hexa-co-ordinated complexes of tetragonal symmetry involve more energy levels, and therefore give rise to more electronic transitions than those of octahedral symmetry. Linhard et al. showed experimentally that the *trans*-dihalogeno-complexes should have their first absorption bands split into two components and ascribed this phenomenon to the tetragonal symmetry of the complex-cations. The present dichroism measurements seem to afford an evidence for the above idea that the praseo-salts should exhibit two separate maxima corresponding to the components of their first band. Thus, of the two maxima for the first band, the one at the longer wave-length has been shown to be due principally to the transition along the Cl-Co-Cl direction, and the other at the shorter wave-length may be due to the transition along the plane formed by one cobalt and four nitrogen atoms. A small inflation at $75\times10^{13}$/sec. in the absorption spectrum of the solution of the dichloro-bis(ethylenediamine)-cobalt (III)-compound may be considered as due to the second absorption band.

Similar explanation may be applied to the absorption spectrum of the solution of dichloro-tetrammine-cobalt (III)-ion. Since the complex cation, *trans*-$[Co(NH_3)_4Cl_2]$, is unstable in solution, the conventional method is not applicable in determining the absorption spectrum of the complex. By making spectrographic analysis of the aquotization reaction, one of the present authors[21] determined the absorption spectrum of this complex cation (Table V). As in the case of the corresponding ethylenediaminecompounds, it seems reasonable to suppose that the maxima at 48 and $62\times10^{13}$/sec. correspond to the first band. Thus the band at $48\times10^{13}$/sec. may be due to the transition along the Cl-Co-Cl direction, and the one at $62\times10^{13}$/sec. may be due to the transition along the plane formed by one cobalt and four nitrogen atoms. The slight inflation at $75\times10^{13}$/sec. may be assigned as the second absorption band. The bands at 100 and $120\times10^{13}$/sec. should be assigned to the specific band and the third band, respectively.

On the basis of the foregoing discussion,

18) J. P. Mathieu, *Bull. soc. chim. France*, [5], **3**, 463 (1936).
19) R. Tsuchida, *J. Chem. Soc. Japan*, **59**, 586 (1938).
20) F. E. Ilse and H. Hartmann, *Z. physik. Chem.*, **197**, 239 (1951).
21) R. Tsuchida, This Bulletin, **11**, 721 (1936).

TABLE V

ABSORPTION MAXIMA OF *trans*-DIHALOGENO-COBALT (III) COMPLEXES IN SOLUTION

| | | 1st Band | | | | 2nd Band | | Specif. Band | | 3rd Band | |
|---|---|---|---|---|---|---|---|---|---|---|---|
| | | $\nu$ | log $\varepsilon$ | $\nu$ | log $\varepsilon$ | $\nu$ | log $\varepsilon$ | $\nu$ | log $\varepsilon$ | $\nu$ | log $\varepsilon$ |
| $[Co(NH_3)_4Cl_2]Cl$ | (a) | 50 | 1.21 | 62.3 | 1.41 | 77.0 | 1.40 | 100 | 3.16 | | |
| | (b) | 47.7 | 1.63 | 63.0 | 1.38 | 74.8 | 1.54 | 98.9 | 2.86 | 118.4 | 4.39 |
| $[Co(en)_2Cl_2]Cl$ | (b) | 48.4 | 1.61 | 67.5 | 1.46 | 77.8 | 1.49 | 97.5 | 3.12 | 120.8 | 4.43 |
| | (c) | 48.0 | 1.54 | 66.7 | 1.41 | 78.9 | 1.64 | — | — | 119.0 | 4.31 |
| $[CO(en)_2Br_2]Br$ | (b) | 45.6 | 1.73 | 65.1 | 1.49 | — | — | 84.3 | 3.35 | 103.8 | 4.34 |

(a) ref. 22. (b) ref. 11. (c) F. Basolo, *J. Am. Chem. Soc.*, **72**, 4393 (1950).

the absorption bands of the above *trans*-dihalogeno-complexes in solution may be designated as given in Table V.

The dichroism measurements should be expected to throw light upon the origins of the absorption bands of metallic complexes. Unfortunately, the second band has not been found as a separate maximum in the three compounds investigated. The investigation of the data obtained by Linhard et al.[11] indicates that the second band of the *trans*-dihalogeno-complexes appears to show no splitting, at least, none so distinct as the first band. On the other hand, the above measurements have shown that the first band splits itself into two bands. It seems, therefore, evident that the two bands, the first and second bands, should be ascribed to two transitions of different electrons. Although the decisive discussion on the origins of the first and second bands must be postponed until other materials are accumulated, the idea that the first band originates from *d*-electrons of a cobalt atom and the second band from co-ordination electrons seems to be one of the most probable.

**Summary**

Dichroism of the crystals of *trans*-$[Co(en)_2Cl_2]ClO_4$, $[Co(en)_2Cl_2]Cl \cdot HCl \cdot 2H_2O$ and $[Co(en)_2Br_2]Br \cdot HBr \cdot 2H_2O$ have been quantitatively determined by Tsuchida-Kobayashi's microscopic method in the visible and ultraviolet regions.

As to the dichroism of the *trans*-dihalogeno-complexes, the following relations have been induced. The first band splits itself into two component absorptions. One at the longer wave-length is polarized in the X-Co-X direction, and the other at the shorter wave-length is polarized in the Co-en plane. For the third and specific bands, the X-Co-X-absorption is bathochromic to the Co-en-absorption.

On the basis of the above results, absorption spectra of several praseo-complexes in solution have been discussed.

The authors wish to express their thanks to the Ministry of Education for a grant.

*Department of Chemistry, Faculty of Science, Osaka University, Nakanoshima, Osaka*

# *Conductivity of Aqueous Potassium Dodecyl Sulfonate at Various Temperatures and with Solubilized Benzene*

By Wei-chuwan Lin

(Received October 26, 1954)

## Introduction

The somewhat abrupt change with concentration of many physical properties of solution of long-chain electrolytes has been attributed to the formation of micelles, and the concentration at which this change occurs has been termed " the critical concentration for the formation of micelles ".[1)]

Electrical conductivity is one of the properties which may be utilized for the determination of the critical concentration. It has been pointed out[2,3)], that if the specific conductivity be plotted against the concentration the critical concentration is given by the intersection of the resulting two straight lines.

We have determined the specific conductivity of aqueous solutions of potassium dodecyl sulfonate as a function of the concentration of the salt at temperatures ranging from 25 to 60°C and in the presence of varying amounts of solubilized benzene.

In this manner we have determined the critical concentration of potassium dodecyl sulfonate at several different temperatures and at several different concentrations of solubilized benzene. We also could obtain data for the effect of solubilized benzene on the relation between equivalent conductivity and concentration at constant temperature.

## Experimental

Potassium dodecyl sulfonate was prepared by the reaction between dodecyl bromide and aqueous potassium sulfite. The salt was washed sev-

1) See references quoted by M. L. Corrin, H. B. Klevens, and W. D. Harkins, *J. Chem. Phys.*, **14**, 480 (1946).

2) K. A. Wright, A. D. Abbott, V. Sivertz and H. V. Tartar, *J. Am. Chem. Soc.*, **61**, 549 (1939).

3) A. P. Brady and H. Huff, *J. Colloid Sci.*, **3**, 511 (1948).

eral times with petroleum ether, recrystallized twice from ethanol and twice from conductivity water and dried in vacuo. Benzene was of reagent grade and used without further purification.

Solutions containing solubilized benzene were prepared by adding weighed amounts of the salt to solutions of benzene in water. These solutions were made up by weight-volume.

Conductivity measurements were made in a Leeds-Northrup pyrex conductivity cell at 1000 cycles. A Leeds-Northrup Jones bridge and electronic amplifier and oscillator were used and the null points determined on an oscilloscope. An oil bath constant to 0.01°C was used for temperature control; cell constants were determined for each temperature. The electrodes were platinized.

Critical concentrations were determined graphically as the point of intersection of two straight lines in the plot of specific conductivity against concentration.

## Results and Discussion

Plots of specific conductivity versus concentration at temperatures five degrees apart in the range of 25 to 60°C are given in Fig. 1. These are characteristic of solutions

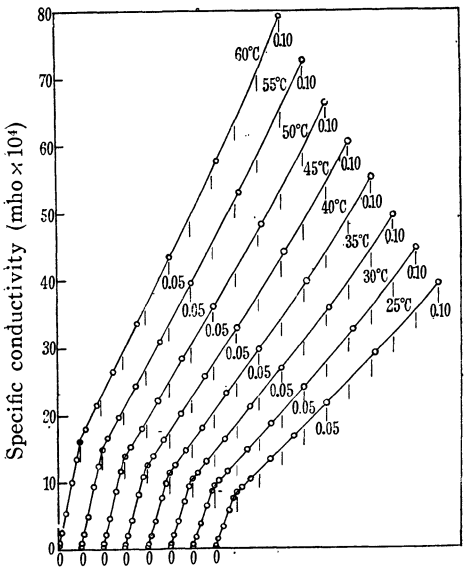



Fig. 1. Specific conductivity plotted against volume normality for aqueous solution of potassium dodecyl sulfonate

of long-chain electrolytes. Similar plots of the equivalent conductivity as a function of the square root of the concentration are given in Fig. 2. The form of these curves has been discussed by Wright, Abbott, Sivertz and Tartar[2], by Wright and Tartar[4], and by

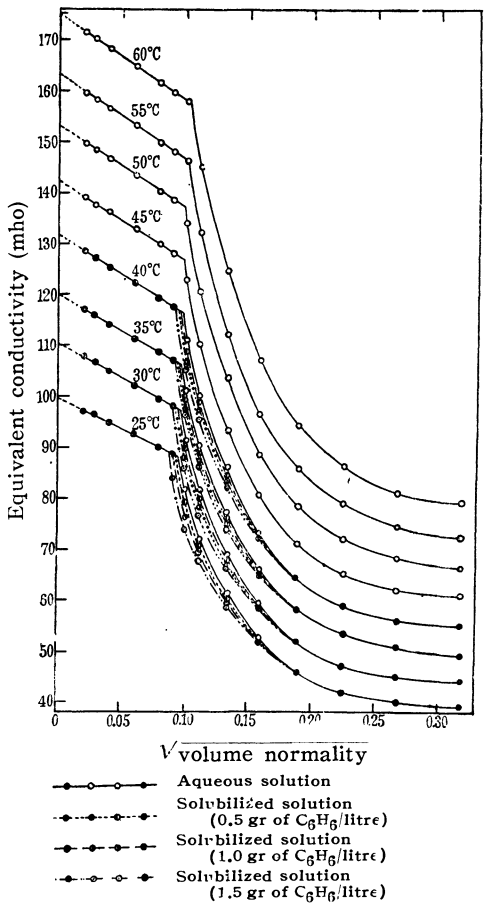



Fig. 2. Equivalent conductivity plotted as a function of the square root of potassium dodecyl sulfonate concentration in the presence of varying amounts of solubilized benzene

Ralston and Hoerr[5]. The rapid increase in equivalent conductivity at the higher salt concentrations has been attributed to "retrograde dissociation".

Plots of the specific conductivity versus salt concentration at several temperatures in the presence of varying amounts of solubilized benzene are given in Fig. 3. Similar plots of the equivalent conductivity as a function of the square root of the salt concentration at several temperatures in the presence of varying amounts of solubilized benzene are also given in Fig. 2. It is evident that (a) the solubilized benzene does not affect the conductivity at concentrations below the critical concentration, (In this range the salt is supposedly completely ionized and the Debye-Hückel-Onsager limiting law may be applied.), (b) the critical concentration is lowered by

4) K. A. Wright and H. V. Tartar, *J. Am. Chem. Soc.*, **61**, 544 (1939).

5) A. W. Ralston and C. W. Hoerr, *J. Am. Chem. Soc.*, **64**, 772 (1942).

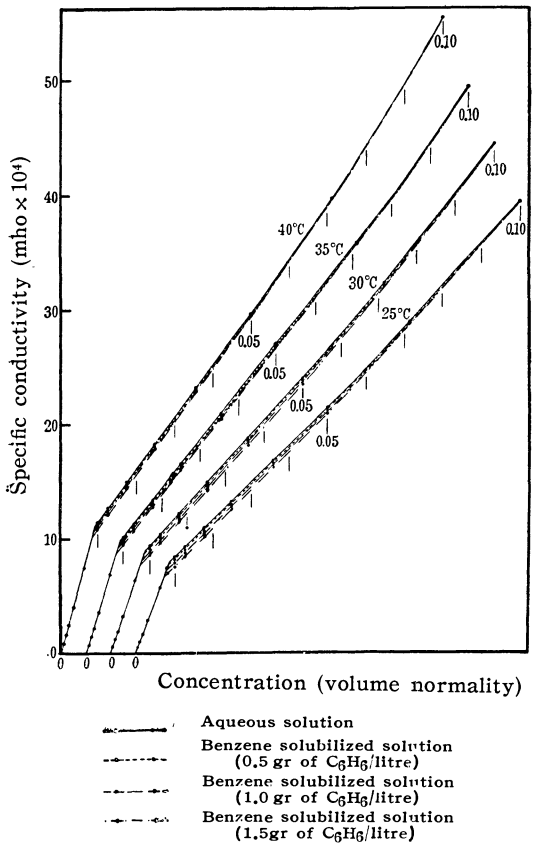



Fig. 3. Specific conductivity plotted against concentration of potassium dodecyl sulfonate in the presence of varying amounts of solubilized benzene

the solubilized benzene with the amount of lowering increasing with the increase of benzene concentration, and (c) the effect of added benzene becomes increasingly less as the salt concentration becomes greater.

**Change of Critical Concentration with Temperature.**—The variation in critical concentration with temperature has been discussed by several authors. Tartar and his coworkers have reported that with long-chain sulfonates in the range of 40 to 80°C the critical concentration increases with temperature[2]. Brady and Huff[3] found a decrease with temperature for lauryl sulfonic acid and potassium laurate in the range of 0 to 90°C. A similar decrease was noted by Scott and Tartar[6] for quaternary ammonium salts between 25 and 60°C. The above estimates were made from conductivity data. Using the dye method Herzfeld observed a minimum in the critical concentration as the temperature was varied from 0 to 80°C[7]. The results obtained in this study as shown in Table I and Fig. 4 are in agreement with

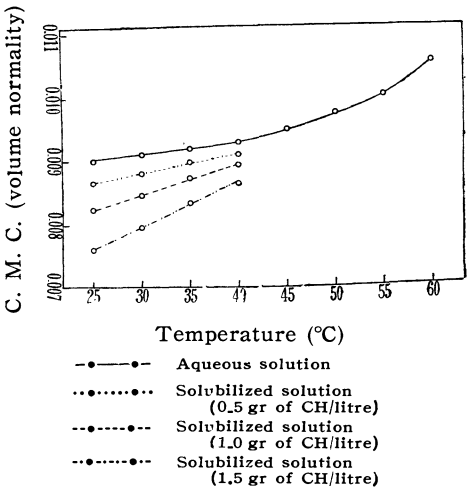



Fig. 4. Change of C. M. C. with temperature

those noted for the sulfonates by Tartar et al[2,6]; namely, that the critical concentration increases with temperature.

TABLE I

CHANGES OF C. M. C. FOR AQUEOUS SOLUTIONS OF POTASSIUM DODECYL SULFONATE WITH CHANGE IN TEMPERATURE AND CONCENTRATION OF SOLUBILIZED BENZENE

| Temperature (°C) | Amount of benzene solubilized (grams of $C_6H_6$/litre of aqueous solution) 0 | 0.5 | 1.0 | 1.5 |
|---|---|---|---|---|
| 25 | 0.0090 | 0.0086 | 0.0082 | 0.0076 |
| 30 | 0.0091 | 0.0088 | 0.0084 | 0.0079 |
| 35 | 0.0092 | 0.0090 | 0.0087 | 0.0083 |
| 40 | 0.0093 | 0.0091 | 0.0089 | 0.0086 |
| 45 | 0.0095 | — | — | — |
| 50 | 0.0097 | — | — | — |
| 55 | 0.0100 | — | — | — |
| 60 | 0.0104 | — | — | — |

**The Effect of Benzene on the Critical Concentration.**—The effects of various concentrations of solubilized benzene on the critical concentration of potassium dodecyl sulfonate are given in Table I and plotted in Fig. 5. At constant temperature the lowering of the critical concentration increases with the increase of benzene concentration. The lowering becomes less marked with increasing temperature.

These results are in essential agreement with those obtained by Lingafelter, Wheeler

6) A. B. Scott and H. V. Tartar, *J. Am. Chem. Soc.*, 65, 692 (1943).

7) S. H. Herzfeld, Unpublished work

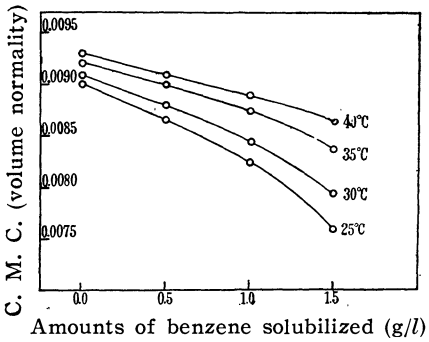



Fig. 5. C. M. C. plotted against amount of solubilized benzene

and Tartar[8] for benzene and several sodium alkylsulfonates by an interfacial tension method.

An interpretation of this work must rest upon the analysis of the various energy terms involved in micellization. Herzfeld, Corrin and Harkins[9] have suggested two such energy terms of major importance. First a decrease in free energy is brought about by removal of the long-chain ion from its aqueous environment into the interior of the micelle (environmental term). This term will be maximal when the removal of the non-polar chain from the water is as complete as possible. Second, short range repulsive terms come into play as the polar head groups are brought together in the micelle and this repulsive energy term must be taken into account. On the basis of this analysis the micelle would contain fewer ions than the limit set by steric factors.

In the presence of relatively non-polar additives such as benzene it might be expected that the environmental terms might be increased in magnitude and that the repulsive term might be decreased by the inclusion of benzene in the micelle. This would lead to (a) a decrease in critical concentration and (b) a change in the size or the number of long-chain ions per micelle or both. It would seem from the conductivity measurements reported here that the change in micelle size in the presence of benzene cannot be very great since at concentrations exceeding the critical concentration there is little difference between the conductivity terms in the presence and absence of benzene. It is possible, although unlikely, that a change in micelle size is exactly balanced by a change in micelle ionization.

We do not propose to discuss the conductivity curves completely at this time.

8) F. C. Lingafelter, O. L. Wheeler and H. V. Tartar, *J. Am. Chem. Soc.*, 68, 1490 (1946).
9) S. H. Herzfeld, M. L. Corrin and W. D. Harkins, *J. Phys. & Colloid Chem.*, 54, 271 (1950).

## Summary

The specific conductivity of aqueous solutions of potassium dodecyl sulfonate has been measured as a function of concentration in the presence and absence of solubilized benzene in the temperature range between 25 and 60°C.

Below the critical concentration for the formation of micelles solubilized benzene has no effect on the conductivity. In the critical concentration range there is a marked effect which decreases with salt concentration and finally becomes negligible.

The critical concentration decreases in the presence of solubilized benzene; this effect becomes more marked as the benzene concentration is increased. The critical concentration increases with increasing temperature both in the presence and absence of benzene.

The experimental part of this work was done at George Herbert Jones Laboratory, University of Chicago, Ill., U. S. A. The author would like to express his hearty gratitude to Dr. M. L. Corrin for many fruitful discussions during his stay at the University of Chicago, and for personal communications after his return to Formosa.

The author is also indebted to the China Foundation for the Promotion of Education and Culture for the fellowship grant which made this research possible.

*Department of Chemistry, National Taiwan University, Taipei Formosa, China*

## *On the Role of a Cytochrome in the Thiosulfate Reduction by Sulfate-Reducing Bacterium*

By Makoto Ishimoto and Jiro Koyama

(Received January 22, 1955)

In a previous report (1) we have shown that a cell-free extract which was obtained from ground cells of sulfate-reducing bacterium displaved a marked activity of reducing thiosulfate to hydrogen sulfide in the presence of molecular hydrogen. From the extract we could separate hydrogenase and thiosulfate reductase (2) both of which are conceivably involved in the process in question. The mixture of these separated enzymes, however, were found to be totally inactive in cataysing the said reaction. A marked enhancement of the reaction rate was observed when methyl viologen was added to the enzyme mixture, indicating that the dye-stuff acted as an intermediary carrier filling the missing link between the enzyme systems. The course of events occurring in this case was supposed to be as follows:

$$H_2 \cdots \underset{\text{genase}}{\text{Hydro-}} \cdots \underset{\text{carrier}}{\text{Intermediary}} \cdots \underset{\text{reductase}}{\text{Thiosulfate}} \cdots S_2O_3^{--}$$
(Methyl viologen)

Recently we found (3), in confirmation of the report by Postgate (4), that a certain cytochrome (showing absorption maxima at 419 m$\mu$ and 553 m$\mu$ in reduced state, and at 410 m$\mu$ in oxidized state) is contained in the cells of sulfate-reducing bacterium. The present paper deals with the isolation of this cytochrome from bacterial cells and the elucidation of its role as an intermediary carrier, similar to that assigned to methyl viologen in the above scheme, in the mechanism of thiosulfate reduction.

The procedure of isolation of the cytochrome was similar to that for cytochrome *c* (5). Acetone-dried cells of the bacterium were extracted with M/15 phosphate buffer of pH 6.4. On adding acetone to the extract in concentration of 33–66%, there appeared a precipitate which was dissolved in M/150 phosphate buffer of pH 7.0, dialyzed against the same buffer overnight and then passed through the column of ammonium salt of cation-exchange resin, Amberlite IRC-50. While the cytochrome was absor bed on the top

of the column, thiosulfate reductase, hydrogenase and a green pigment (3) as well as the greater part of porteins ran through it without being adsorbed. By elution with a mixture of ammonium chloride and hydroxide, the cytochrome absorbed could be separated in two fractions. Absorption spectra of these two fractions were hardly distinguishable from each other, both showing a maximum at 410 mμ, the Soret band of oxidized form. Compared with the strong absorption at 410 mμ, there was only insignificant absorption at 280 mμ, indicating that the solution of cytochrome contained, if any, only a small amount of proteinous impurities.

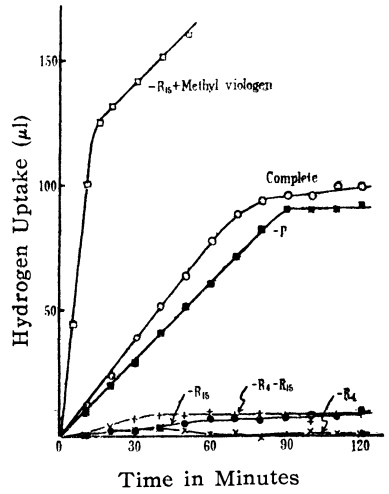



Fig. 1. Reaction between $H_2$ and thiosulfate (measured by $H_2$-uptake) caused by reconstructed system of various combinations.

$H_2$-uptake was measured with Warburg's manometer. Volume of each reaction mixture: 2.25 ml.; temperature: 30° C.; atmosphere: $H_2$. The center well contained 0.2 ml. of alkali.

The "complete" system was composed of:

(i) 0.5 ml. of suspension of particulate hydrogenase preparation (P) (800 hydrogenase units (2)),

(ii) 0.4 ml. of crude thiosulfate reductase preparation (R4) which was almost free from the cytochrome (70 reductase units (2)),

(iii) 0.75 ml. of the cytochrome preparation (R15) (0.55 cytochrome units (2)),

(iv) 0.2 ml. of 0.2 M phosphate buffer of pH 7.0, containing 6 mg. of egg albumin and 5 μM of $Na_2S_2O_3$.

No hydrogen uptake occurred in the absence of thiosulfate.

The non-absorbed solution containing thiosulfate reductase and hydrogenase showed no activity of reducing thiosulfate in the presence of hydrogen. The same was true when the solution was supplied with an additional quantity of hydrogenase.* A striking increase in the activity of the mixture was observed when the second fraction of the cytochrome was added to the mixture of non-adsorbed solution and hydrogenase preparation. (Fig. 1). Of interest is to note that the first fraction of cytochrome was quite ineffective in accelerating the reaction rate. The effectiveness (as well as the absorption spectrum) of the cytochrome in the second fraction was not modified by boiling the fraction for 3 minutes. This fact the accelerating effect of the fraction is not due to some thermolabile proteinous substances which might have been admixed with the cytochrome in the fraction.

The evidence presented here makes it quite plausible to assumed that the cytochrome obtained in the second fraction is an intermediary carrier, intrinsic to bacterial cells, which functions as a link between the systems of thiosulfate reductase and hydrogenase, just as did methyl viologen in the experiment reported previously. It should be added that the cytochrome in question could not be substituted in its carrier-function by cytochrome *c* from bovine heart muscle (6) or diphosphopyridine nucleotide.

*Department of Chemistry,*
*Faculty of Science,*
*Tokyo University*

* Although the original non-adsorbed solution contained a certained amount of hydrogenase, its activity was found to be comparatively less than that of co-existing thiosulfate reductase. The preparation of hydrogenase added was the centrifugate (at 16000×g) from the extract which was obtained from finely ground bacterial cells.

1) M. Ishimoto, J. Koyama, Y. Nagai, *J. Biochem. Japan.* **42**, 41 (1955).
2) M. Ishimoto, J. Koyama, Symposium on Enzyme Chemistry, **10**, 77 (1954).
3) M. Ishimoto, J. Koyama, Y. Nagai, *J. Biochem. Japan*, **41**, 763 (1954).
4) J. Postgate, *Biochem. J.*, **56**, xi (1954).
5) E. Margoliash, *Biochem. J.*, **56**. 535 (1954).
6) D. Keilin, E. F. Hartree, Proc. Roy. Soc. London, **B122**, 289 (1937).

precipitate appeared gradually and was complete in about 20–30 minutes. It was kept aside for six hours, filtered through Whatman 40, washed initially with cold alcohol and then repeatedly with hot 50% alcohol. The precipitate was dissolved in a minimum quantity of dilute 2N-HCl, the solution diluted further to about 50 ml. and thorium reprecipitated. This was washed finally with alcohol, dried and ignited to constant weight as $ThO_2$.

award of a research fellowship to one of us (G. S. D.) during the course of the above work

## Summary

Quantitative estimation of thorium by precipitating it from aqueous thorium chloride (or nitrate) solution by *o*-tolidine, dianisidine, *p*-phenylenediamine, *o*-anisidine and *o*-phenetidine has been studied. The precipitated complex is ignited to constant weight and determined gravimetrically as $ThO_2$.

TABLE II

| Expt No. | Wt. of $ThO_2$ (g.) *m*-nitrobenzoic acid (a) | Wt. of $X_2O_3$ (g.) added | Wt. of $ThO_2$ (g.) *o*-phenetidine (b) | Wt. of $ThO_2$ (g.) *o*-anisidine (c) | Difference a~b | Difference a~c |
|---|---|---|---|---|---|---|
| 1 | 0.0640 | 0.0580 | 0.0642 | 0.0644 | 0.0002 | 0.0004 |
| 2 | 0.0922 | 0.0886 | 0.0926 | 0.0924 | 0.0004 | 0.0002 |
| 3 | 0.1152 | 0.1022 | 0.1150 | 0.1154 | 0.0002 | 0.0004 |
| 4 | 0.1164 | 0.1162 | 0.1166 | 0.1166 | 0.0002 | 0.0002 |
| 5 | 0.1378 | 0.1162 | 0.1376 | 0.1380 | 0.0002 | 0.0002 |
| 6 | 0.1390 | 0.1228 | 0.1394 | 0.1390 | 0.0004 | . . |

X=Ce, La, Y or Er

Results in Table II show that the double precipitation effects a quantitative separation of thorium from the trivalent rare earths used in the present investigation. The interference of other familiar congeners of thorium in its determination by the above precipitants is under investigation.

Grateful thanks of the authors are due to Professor S. S. Joshi for facilities and to the National Institute of Sciences of India for

The use of *o*-anisidine and *o*-phenetidine for the separation of thorium from trivalent cerium has been suggested.

*Chemical Laboratories Benaras Hindu University*
&
*The Indian Association for the Cultivation of Science Calcutta*

# *Micelle Formation and Solubilization in Benzene by Fatty Acid Salts of Higher Amines*

By Ayao KITAHARA

(Received September 20, 1954)

## Introduction

Whilst numerous investigations have been made on the micelle formation as well as the solubilization both of which take place in *aqueous solutions* of detergents, little is known about the similar phenomena in *non-aqueous solutions*.

Some investigators[1,2] have assumed the micelle formation of detergents in non-polar solvents. However,it is not necessarily certain that detergent molecules can aggregate to micelles spontaneously when they are dissolved in non-polar solvents, because the present theories regarding the micelle formation in aqueous solutions of detergents can not be applied to a case when a solvent is a non-polar one. Hence, the more experimental

1) M. van der Waarden, *J. Colloid Sci.*, 5, 448 (1950). S. Kaufmann and C. R. Singleterry, *J. Colloid Sci.*, 7, 453 (1952). M.B. Mathews and E. Hirschhorn, *J. Colloid Sci.*, 8, 86 (1953).

2) Recently, Palit et al. have observed the enhancement in dissolving power for water into non-polar solvent with the presence of detergent such as fatty acid salts of higher amines, and this apparent solubilization was assumed to be parallel phenomena with micelle formation. See: S. R. Ralit and V. Venkateswarlu, *Proc. Roy. Soc.*, A208, 542 (1951); *J. Chem. Soc.*, 1954, 2129.

evidences are desired concerning the micelle formation as well as the solubilization which may take place in non-aqueous solutions of detergents, especially when the solvents are non-polar ones.

## Experimental

**Preparation of Detergents.**—It was presumed that fatty acid salts of higher aliphatic amines are the most favourable materials as detergents for the present purpose. A series of compounds were prepared in possibly purified states in the following way.

Commercial dodecylamine and octadecylamine were purified by distillation under reduced pressure. The fraction having b.p. 131–133°C under 15 mmHg and those having b.p. 188–190°C under 4 mmHg were collected. Commercial propionic and butylic acid were dried by means of anhydrous copper sulfate and purified by distillation. For the other fatty acids, the products of Nihon Yushi Co. were used. The neutralization of amines with acids was carried out at room temperature. The solvents used in the preparation and the melting points of the products are summarized in Table I.

All the purified compounds were white and crystalline. The fluctuation of their melting points was ±1°C. Butylate and caproate of dodecylamine were strongly hygroscopic.

When the reaction of amines and acids was carried out at about 150°C instead of room temperature, substances having different melting points were obtained. The infra-red absorption spectra of reaction products from dodecylamine and propionic acid or capric acid were taken in nujol on a Perkin-Elmer 112 instrument. The products (1) obtained at high temperature showed absorptions at 1630 and 3300 $cm^{-1}$. The former absorption is attributed to the carbonyl group of

TABLE I

PREPARATION AND MELTING POINTS OF DETERGENTS

| Detergent | Solvent used in neutralization | Solvent used in recrystallization | m.p. °C |
|---|---|---|---|
| Dodecylamine propionate | Benzene and *n*-Hexane | — | 54–56 |
| „ butylate | *n*-Hexane | *n*-Hexane | 39–41 |
| „ caproate | „ | „ | 31–33 |
| „ caprylate | „ | — | 43–45 |
| „ capriate | Benzine | *n*-Hexane | 60–61 |
| „ laurate | „ | „ | 62–64 |
| „ myristate | „ | „ | 64 |
| „ palmitate | „ | „ | 70–71 |
| Octadecylamine propionate | Acetone | Benzine+Acetone | 69–72 |
| „ butylate | „ | Benzine | 56–58 |
| „ caproate | „ | „ | 46–47 |
| „ caprylate | „ | Acetone | 52–54 |
| „ capriate | „ | „ | 59–61 |
| „ laurate | „ | „ | 62–64 |
| „ myristate | „ | — | 71–72 |
| „ palmitate | „ | — | 78–79 |

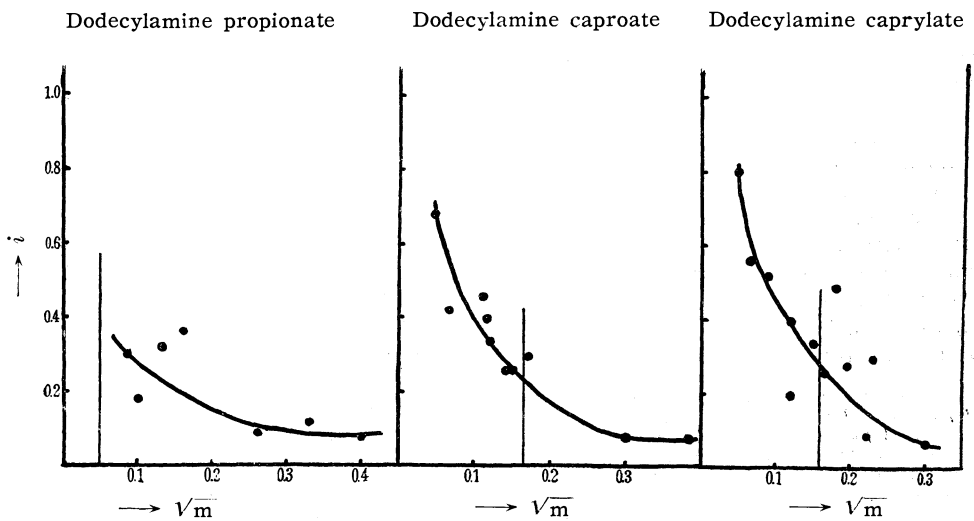



Fig. 1. Change of van't Hoff factor ($i$) with molality ($m$).

acid amide and the latter to its amide group. On the other hand, the corresponding products (2) obtained at room temperature had absorptions at 1400 and 1600 $cm^{-1}$. These two absorption peaks are attributed to carboxylic ions. Therefore, compounds (1) are acid amides, and (2) are fatty acid salts of higher amines having the structure of $[RCOO^-]$ $[H^+_3NR']$[3].

**Determination of van't Hoff Factors.**—For the purpose of ascertaining micelle formation, the van't Hoff factors ($i$) for dodecylamine propionate, caproate and caprylate in benzene were determined at various concentrations by means of cryoscopy (Fig. 1). The measurement was carried out with the usual Beckmann's apparatus.

**Measurements of Solubilization.**—The limiting amount of solubilized water into a benzene solution of a detergent was determined by the following simple method. Five cc. of solution was put into a test tube. By means of a micro-burette, water was added in portions of 0.002–0.003 cc. After addition of each portion the solution was vigorously shaken 50–250 times, and then put to stand for half an hour. The occurrence of turbidity was detected by means of Tyndall light. Near the limit of solubilization, Tyndall light was observed one or two days after water had been added in order to ascertain the attainment of equilibrium. The limit of solubilization was confirmed by the occurrence of faint turbidity. The measurements were carried out at 26°C.

## Results and Discussion

**Formation of Micelle.**—The relation between the van't Hoff factor ($i$) and the root of molality was given in Fig. 1. At these concentrations the depression of temperature was insufficient to be observed accurately by a Beckmann's thermometer. Accordingly the data are not so accurate and show fluctuation. But these are adequate for qualitative discussion.

In aqueous solutions the critical concentration of micelle formation of ionic detergents has been discussed from the relation between an osmotic coefficient and a concentration.[4] In non-polar solvents micelle formation may be discussed with van't Hoff factor in place of an osmotic coefficient, because an ionic dissociation in non-polar solvent is doubtful. Therefore, Fig. 1 will be useful for the discussion of micelle formation in benzene.

In the cases of dodecylamine caproate and caprylate, the van't Hoff factors show a remarkable decrease at a range of the concentration in the manner similar to the well-known cases of osmotic coefficients in aqueous solutions. It is thought that this remarkable decrease shows the initiation of micelle formation at this range. In the case of dodecylamine propionate, the remarkable decrease was not observed within the concentration range of this experiment. Its range of the initiation of micelle formation seems to be in the left side of the obtained curve, but in this range no measurement was accurately carried out because of the slight depression of temperature. In any case the values of $i$ at higher concentration are sufficient to show that micelles have been formed. It will be, therefore, concluded that micelle formation begins to take place at a certain concentration for these detergents. The phenomenon of solubilization should take place as the result of micelle formation.

On the other hand, the van't Hoff factors of acid amides in benzene have shown only slight decreases at comparable concentrations. For example, van't Hoff factors of dodecyl amide of caproic acid was 1.0 and 0.55 at 0.20 and 0.32 of $\sqrt{m}$, respectively. It is, therefore, assumed that micelles have not been formed at these concentrations in the case of acid amides.

**Solubilization of Water.**—The amount of solubilized water was plotted against the concentration of detergents, correction being made with respect to the solubility of water in benzene (Figs. 2 and 3). The salts of

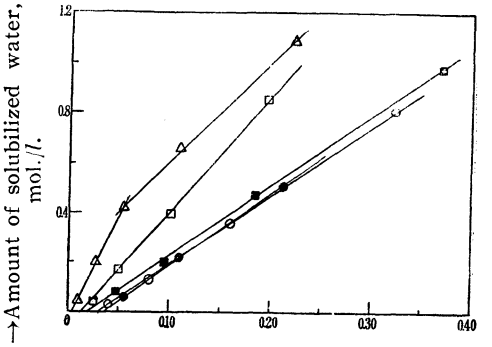



Fig. 2. The relation between solubilized water and concentration of salts of dodecylamine.

△ dodecylamine propionate
□ „ butylate
■ „ caproate
○ „ caprylate
● „ capriate

3) Fatty acid salts of amines and acid amides were prepared, (a) keeping $R'=12$ and changing R from 3, 4, 6, 8, ...., 16, and (b) keeping $R'=18$ and R in the same way. It was found that the caproates ($R=6$) both of (a) and (b) have the lowest melting points in the case of fatty acid salts of amines.

4) J. W. McBain, "Colloid Science", D. C. Heath & Co., Boston, (1950), p. 242.

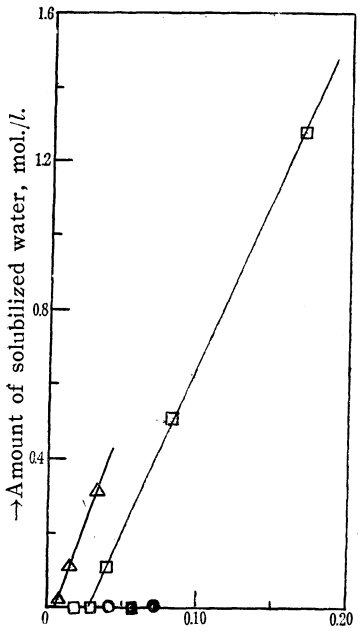



Fig. 3. The relation between solubilized water and concentration of salts of octadecylamine.

△ octadecylamine propionate
□ „ butylate
■ „ caproate
○ „ caprylate
● „ capriate

octadecylamine had less solubility as compared with those of dodecylamine. It was, therefore, hardly possible to carry out the measurement at higher concentrations similar to the later case. In octadecylamine caproate, caprylate and capriate, no solubilization was observed even at the concentrations 0.055, 0.040 and 0.077 mol./l., respectively. The measurements on laurate, myristate and palmitate of dodecylamine as well as on those of octadecylamine were impossible because of their limited solubility in benzene. The acid amides, i.e. the reaction products at higher temperature, showed no solubilization at comparable concentrations, corresponding to the slight variance of the van't Hoff factor.

The amount of solubilized water was found to be proportional to the concentration of detergents except for the higher concentration range of dodecylamine propionate. In the concentration range 0.005−0.4 mol./l. the relation can be expressed by the formula

$$S=\alpha(C-\beta)$$

where, $S$=amount of solubilized water, mol./l.,
$C$=concentration of detergents, mol./l.,
$\alpha$, $\beta$=constants.

The values of $\alpha$ and $\beta$ are given in Table II.

TABLE II
VALUES OF $\alpha$ AND $\beta$

| Detergent | $\alpha$ | $\beta$(mol./l.) |
|---|---|---|
| Dodecylamine propionate | 7.2 | 0.002 |
| „ butylate | 4.6 | 0.012 |
| „ caproate | 2.9 | 0.020 |
| „ caprylate | 2.8 | 0.030 |
| „ capriate | 2.9 | 0.035 |
| Octadecylamine propionate | 12 | 0.005 |
| „ butylate | 9.0 | 0.028 |
| „ caproate | — | >0.055 |
| „ caprylate | — | >0.040 |
| „ capriate | — | >0.070 |

The value of $\alpha$ is taken as a measure of solubilizing power, i.e. the number of moles of water which is solubilized per one mole of a detergent. The value of $\beta$ gives the critical micelle concentration which is obtained from the measurement of the solubilization of water.

From the curve of Fig. 1 a critical concentration of micelle formation cannot be sharply recognized. But it is seen from the comparison between the values of $\beta$ and Fig. 1 that the value of the critical micelle concentration from the data of solubilization (the value of $\beta$) is within the steep range of decreasing in the curve. The vertical lines of Fig. 1 show the values of $\beta$, the unit of concentration being corrected. It will be, therefore, concluded that the idea of micelle formation which is suggested from the cryoscopical experiment is not in conflict with that of micelle formation from solubilization.

It is seen from Table II that the critical micelle concentration increases with the chain length of the acid part as well as of the amine part and that the small critical micelle concentration corresponds to the great solubilizing power. The relation between the critical micelle concentration and the chain length is entirely different from the cases of aqueous solutions. Accordingly, the mechanism of the micelle formation in the benzene solution seems to be quite different from that in the aqueous solution.

The author wishes to express his thanks to Prof. H. Akamatsu for his suggestions.

## Summary

Fatty acid salts of higher aliphatic amines were prepared and used as detergents. The micelle formation in the benzene solution was verified from the relation between the van't Hoff factor and the concentration. It was shown that the amount of solubilized

water is proportional to the concentration of the detergent. The value of the critical micelle concentration was determined from the extraporation of the proportionality. This value is within the region of the remarkable decrease in the curve between the van't Hoff factor and the concentration. With the increases of the carbon number of the amine or the acid part, the critical micelle concentration increases and the solubilizing power decreases. This result is quite different from that of aqueous solutions.

*Department of Chemistry, Faculty of Science, Tōhō University, Chiba*

# *Lower Electronic States of the Free* $NH_2$ *Radical*[1]

By Jiro HIGUCHI

(Received October 20, 1954)

## Introduction

Free radicals like $CH_2$, $CH_3$, $NH_2$ and others have been assumed to be intermediates in many chemical reactions, but their existence has not definitely been identified. Recently, the flash technique was applied to the spectroscopy by Porter[2], and the existence of some free radicals has been identified. For such polyatomic free radicals, however, only limited information should be expected about the electronic states and the structures, because at present many levels have not yet been identified experimentally even for stable molecules. Thus, it is very difficult to determine the course of such reactions as photolysis or electric discharge, in which the role of electronic excited states is of great significance. The theoretical interpretation is, therefore, very important not only as a supplement to observation but as the discussion of chemical reaction, in which such a radical is assumed to exist as an intermediate.

The so-called $\alpha$ band of ammonia has long been known from emission spectra of oxy-ammonia flames and electric discharges through ammonia,[3] and has long been suspected of being due to the free $NH_2$ radical. Recently, Herzberg and Ramsay[4] observed the $\alpha$ bands in absorption in photodecomposed ammonia by using a flash technique and confirmed the fact that the free $NH_2$ radical is responsible for the $\alpha$ band. Little, has, however, been done on the theoretical interpretation.

Thus, the lower electronic states and the structure of the free $NH_2$ radical are theoretically investigated in the present work. The method used is the LCAO-SCF one developed by Roothaan[5] and the SCF calculation is performed for the ground state only. The energy levels of the lower excited states are computed by use of the ground state MO's without configuration interaction, because some reasonable results have been obtained on the CH radical in a similar way[6] and such reliable results may also be expected here if reasonable values of energy integrals can be used.

## Outline of Calculation

The calculation was performed by assuming the spatial configuration of the $NH_2$ radical as an isosceles triangle, and taking the $x$ and $y$ axes in the molecular plane and the $z$ axis being perpendicular to the plane as shown in Fig. 1. The internuclear distance between the nitrogen and the hydrogen was

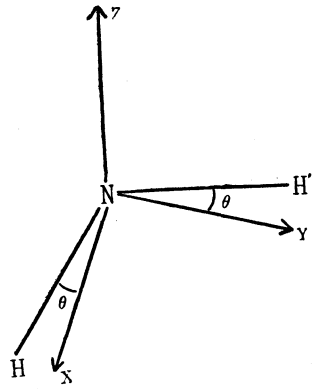



Fig. 1. Axes for the $NH_2$ radical.

1) A preliminary account of the present paper was given in *J. Chem. Phys.*, 22, 1467 (1954).
2) G. Porter, *Proc. Roy. Soc.* (*London*), A200, 284 (1950).
3) W. B. Rimmer, *Proc. Roy. Soc.* (*London*), A103, 696 (1923); F. Fowler and J.S. Badami, *Proc. Roy. Soc.* (*London*), A133, 325 (1931); A. G. Gaydon, *Proc. Roy. Soc.* (*London*), A181, 197 (1942).
4) G. Herzberg and D.A. Ramsay, *J. Chem. Phys.*, 20, 347 (1952); *Discussion Faraday Soc.*, No. 14, 11 (1952).
5) C.C.J. Roothaan, *Rev. Mod. Phys.*, 23, 69 (1951).
6) J. Higuchi, *J. Chem. Phys.*, 22, 1339 (1954).

taken as 1.01 Å as in the equilibrium distance of the ammonia molecule[7].

$NH_2$ is a nine-electron radical, and the LCAO-SCF calculation was carried out by taking the seven atomic orbitals $n$, $s$, $x$, $y$, $z$, $h$ and $h'$ into consideration, which mean 1s, 2s, 2px, 2py, 2pz orbitals of nitrogen atom, 1s of one hydrogen (the side of the $x$ axis) and 1s of the other hydrogen, respectively. The interactions between all electrons were explicitly included but the orthogonality between $n$ and $h$ or $h'$ was assumed, because its overlap integral is fairly small in comparison with the others[8].

The atomic orbitals used were the Hartree-Fock SCF AO's in the $^4S$ state of nitrogen[9] and in the $^2S$ state of hydrogen. The majority of the two-center integrals is, however, very difficult to calculate, and it was, therefore, assumed that the use of Slater AO's[10] instead of the SCF AO's gives satisfactory approximations of the two-center integrals, and they were taken from the table by Kotani and Amemiya.[11] The core-field energies were, however, obtained from the Fock equations of the $^4S$ state of nitrogen atom as in the case of the CH radical[5]. The one-electron three-center integrals for the nitrogen-hydrogen type were calculated by following Oohata's method[12], but for the hydrogen-hydrogen type were taken from the table by Hirschfelder and Weygandt[13], while the two-electron integrals were approximately obtained by modifying Mulliken's approximation[14].

7) H. Sponer, "Molekülspektren I. Tabellen", Verlag Julius Springer Berlin, (1935) p. 80.

8) $S_{nh}=0.0678$, while $S_{sh}=0.5601$ and $S_{\sigma h}=0.4187$.

9) D. R. Hartree and W. Hartree, *Proc. Roy. Soc. (London)*, **A193**, 299 (1948).

10) $n=(\delta'^8/\pi)^{1/2}r\exp(-\delta' r)$, $s=(\xi^5/3\pi)^{1/2}r\exp(-\delta r)$. $\sigma=(\delta^5/\pi)^{1/2}r\exp(-\delta r)\cos\theta$, $\pi=(\delta^5/\pi)^{1/2}r\exp(-\delta r)\sin\theta\begin{Bmatrix}\cos\phi\\ \sin\phi\end{Bmatrix}$ and $h=(1/\pi)^{1/2}\exp(-r)$. In the present paper, $\delta$ and $\delta'$ are chosen as 1.90 and 6.757, respectively.

11) M. Kotani and A. Amemiya, *Proc. Phys. Math. Soc. Japan*, **22**, Extra No. 1 (1940).

12) K. Oohata, *Busseiron Kenkyu*, **50**, 38 (1952).

13) J.O. Hirschfelder and C.N. Weygandt, *J. Chem. Phys.*, **6**, 806 (1938).

14) R. S. Mulliken, *J. chim. phys.*, **46**, 500 and 521 (1949).

Some values calculated by Mulliken's approximation are rather small as compared with the exact values, for example in the case of the one-electron integrals for the hydrogen-hydrogen type. In the present work, therefore, the two-electron three-center integrals were obtained from the exact value of one-electron three-center integrals as follows:

$(\alpha\beta:\gamma\delta)=(1/4)T_{\alpha\beta}T_{\gamma\delta}[(\alpha\alpha:\gamma\gamma)+(\beta\beta:\gamma\gamma)+(\alpha\alpha:\delta\delta)+(\beta\beta:\delta\delta)]$, where

$T_{\alpha\beta}=2(P_{\gamma\delta}:\alpha\beta)/[(P_{\gamma\delta}:\alpha\alpha)+(P_{\gamma\delta}:\beta\beta)]$.

Here the $P_{\gamma\delta}$ is the point which was found by maximizing the overlapping charge $\chi_\gamma\chi_\delta d\tau$ along the internuclear axis. This approximation gives fairly good results in two-center integrals but somewhat doubtful results from the point of view of physical meaning. It is, therefore, more desirable to use the higher order expansion of atomic orbitals.

LACO MO's $\phi$'s which are formed by these seven atomic orbitals $\chi_p$'s were chosen so that they belong in sets to irreducible representations of the symmetry $C_{2v}$ of $NH_2$, and they are reduced to[15]

$$\begin{aligned}
K(a_1)&=n\\
1a_1&=a_{11}(s)+a_{12}(x+y)+a_{13}(h+h')\\
2a_1&=a_{21}(s)+a_{22}(x+y)+a_{23}(h+h')\\
3a_1&=a_{31}(s)+a_{32}(x+y)+a_{33}(h+h')\\
1b_1&=z\\
1b_2&=a_{44}(x-y)+a_{45}(h-h')\\
2b_2&=a_{54}(x-y)+a_{55}(h-h')
\end{aligned}\qquad(1)$$

Here the order of increasing number for the MO's within each symmetry species is the order of increasing energy. The coefficients $a_{ip}$'s of atomic orbitals $\chi_p$'s were chosen to satisfy the orthonormality conditions:

$$\int\bar{\phi}_i{}^\nu\phi_j{}^\nu d\tau^\nu=\sum_{p,q}\bar{a}_{ip}s_{pq}a_{jq}=\delta_{ij},\qquad(2)$$

where the overlap integrals $S_{pq}$'s are defined by

$$S_{pq}=\bar{S}_{qp}=\int\bar{\chi}_p\chi_q d\tau.\qquad(3)$$

The electronic structure of the $^2B_1$ state, which has been considered to be the ground state of the $NH_2$ radical, is given as resulting from configuration $(1a_1)^2(1b_2)^2(2a_1)^2(1b_1)^1$, and the total nine electron normalized wave function $\Phi$ for this state is then built up as an antisymmetrized product of these LCAO MO's and the energy of this state is given by

$$E=\int\bar{\Phi}\mathfrak{H}\Phi d\tau.\qquad(4)$$

where

$$\mathfrak{H}=\sum_{\mu=1}^{9}\left(-\frac{1}{2}\Delta_\nu-\frac{7}{r_{N\nu}}-\frac{1}{r_{H\nu}}-\frac{1}{r_{H'\nu}}\right)+\frac{1}{2}\sum_{(\mu,\nu=1)\atop(\mu\neq\nu)}^{9}\frac{1}{r^{\mu\nu}}\qquad(5)$$

Introducing the notations

$$H_i=\int\bar{\phi}_i{}^\nu\left(-\frac{1}{2}\Delta_\nu-\frac{7}{r_{N\nu}}-\frac{1}{r_{H\nu}}-\frac{1}{r_{H'\nu}}\right)\psi_i{}^\nu d\tau^\nu\qquad(6)$$

$$J_{ij}=\int\bar{\phi}_i{}^\mu\bar{\phi}_j{}^\nu\frac{1}{r^{\mu\nu}}\phi_i{}^\mu\phi_j{}^\nu d\tau^{\mu\nu}\qquad(7)$$

$$K_{ij}=\int\bar{\phi}_i{}^\mu\bar{\phi}_j{}^\nu\frac{1}{r^{\mu\nu}}\varphi_j{}^\mu\phi_i{}^\nu d\tau^{\mu\nu}\qquad(8)$$

and

$$H'_i=H_i+2J_{ni}-K_{ni},\qquad(6')$$

one obtains

$$\begin{aligned}
E=&2H_n+J_{nn}+2H'_{1a_1}+2H'_{1b_2}+2H'_{2a_1}\\
&+H'_{1b_1}+J_{1a_11a_1}+4J_{1a_11b_2}-2K_{1a_11b_2}\\
&+4J_{1a_12a_1}-2K_{1a_12a_1}+2J_{1a_11b_1}-K_{1a_11b_1}\\
&+J_{1b_21b_2}+4J_{1b_22a_1}-2K_{1b_22a_1}+2J_{1b_21b_1}\\
&-K_{1b_21b_1}+J_{2a_12a_1}+2J_{2a_11b_1}-K_{2a_11b_1}.
\end{aligned}\qquad(9)$$

15) In the present work, the choice of the symmetry axis is made according to Mulliken.

To obtain the $1a_1$, $1b_2$ and $2a_1$ orbitals, a variational procedure was carried out for the energy of state (4), subject to the orthonormality conditions of the MO's (1). It can be shown that this variational process leads to the following equation

$$(\boldsymbol{H}'+\boldsymbol{G})\boldsymbol{a}_i=\epsilon_{ii}\boldsymbol{S}\boldsymbol{a}_i. \tag{10}$$

Here the column vectors $\boldsymbol{a}_i$'s give the coefficients of the AO's in the $ia_1$ and $ib_2$ orbitals. $\boldsymbol{S}$ is a hermitian matrix with elements given by (3); $\boldsymbol{H}'$ is the core-field energy matrix with elements

$$H'_{pq}=\overline{H}'_{qp}=\int\overline{\chi}_p^{\nu}\left(-\frac{1}{2}\Delta_v-\frac{7}{r_{Nv}}-\frac{1}{r_{Hv}}-\frac{1}{r_{H'v}}\right)\chi_q^{\nu}d\tau^{\nu}+2(pq:nn)-(pn:nq), \tag{11}$$

where

$$(pq:rt)=\int\overline{\varphi}_p^{\mu}\overline{\varphi}_r^{\nu}\frac{1}{r^{\mu\nu}}\varphi_q^{\mu}\varphi_t^{\nu}d\tau^{\mu\nu}.^{16)} \tag{12}$$

$\boldsymbol{G}$ is the electronic interaction matrix with elements

$$\begin{aligned}G_{pq}=\overline{G}_{qp}=&2(pq:1a_11a_1)-(p1a_1:1a_1q)\\&+2(pq:1b_21b_2)-(p1b_2:1b_2q)\\&+2(pq:2a_12a_1)-(p2a_1:2a_1q)\\&+(pq:1b_11b_1)-(1/2)(p1b_1:1b_1q).\end{aligned} \tag{13}$$

The procedure followed in the calculation is to assume values of $\boldsymbol{a}_i$'s in (1) consistent with the orthonormality conditions (2), compute the $G_{pq}$'s by (13), solve Eq. (10) for $\epsilon_{ii}$ and a new set $\boldsymbol{a}_i$'s and repeat until self-consistency is attained.

## LCAO MO's

The LCAO MO's of the lowest energy of the $^2B_1$ state by the SCF procedure are given in Table I, and the orbital energies are

TABLE I

LCAO-SCF MO'S FOR THE $^2B_1$ STATE

$K(a_1)=n$

$$1a_1=\begin{Bmatrix}0.762\\0.759\\0.753\\0.742\\0.737\end{Bmatrix}(s)+\begin{Bmatrix}0.151\\0.132\\0.112\\0.067\\0.000\end{Bmatrix}(x+y)+\begin{Bmatrix}0.156\\0.166\\0.179\\0.200\\0.211\end{Bmatrix}(h+h')$$

$$2a_1=-\begin{Bmatrix}0.618\\0.578\\0.531\\0.355\\0.000\end{Bmatrix}(s)+\begin{Bmatrix}0.533\\0.561\\0.590\\0.661\\0.707\end{Bmatrix}(x+y)+\begin{Bmatrix}0.245\\0.237\\0.227\\0.159\\0.000\end{Bmatrix}(h+h')$$

$$3a_1=\begin{Bmatrix}1.031\\1.075\\1.111\\1.183\\1.235\end{Bmatrix}(s)+\begin{Bmatrix}0.580\\0.527\\0.464\\0.281\\0.000\end{Bmatrix}(x+y)-\begin{Bmatrix}0.856\\0.875\\0.883\\0.891\\0.898\end{Bmatrix}(h+h')$$

$1b_1=z$

$$1b_2=\begin{Bmatrix}0.397\\0.389\\0.386\\0.385\\0.392\end{Bmatrix}(x-y)+\begin{Bmatrix}0.532\\0.503\\0.479\\0.449\\0.431\end{Bmatrix}(h-h')$$

$$2b_2=\begin{Bmatrix}0.746\\0.777\\0.805\\0.851\\0.866\end{Bmatrix}(x-y)+\begin{Bmatrix}0.968\\0.949\\0.948\\0.967\\0.983\end{Bmatrix}(h-h')$$

at the bond angle of $\begin{Bmatrix}90^\circ\\115^\circ\\120^\circ\\150^\circ\\180^\circ\end{Bmatrix}$, respectively.

plotted in Fig. 2. These LCAO MO's are

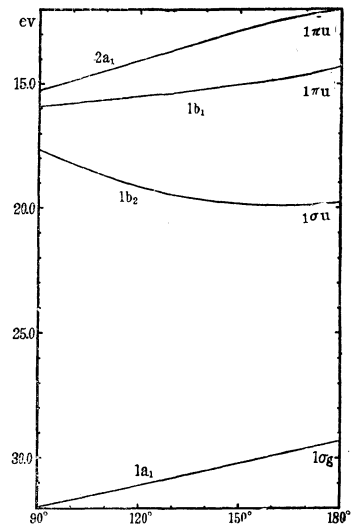



Fig. 2. Ionization energies for the $^2B_1$ state of the $NH_2$ radical. The value for the linear form are given as the extrapolated one from the non-linear form.

considered to be reasonable for that state, and their electronic properties can be regarded as corresponding to those of $H_2O$ by Ellison and Shull[17] and by Maeda[18], which are also calculated by the LCAO-SCF method, because the $NH_2$ and $H_2O$ are molecules belonging to the same symmetry group $C_{2v}$. That is, the $1a_1$ orbital indicates strong bonding property, for the coefficient of $s$ is much larger than the others, but $2a_1$ orbital is weakly bonding due to strong $s$-$p$ mixing in the nitrogen orbitals of the MO at the bond angle near the equilibrium point. Such natures of the $\sigma$ orbitals discussed in the case of the CH radical[6] are considered to be quite similar to those of the $a_1$ orbitals in

16) Orbitals $\varphi_p$'s mean either AO's $\chi_p$'s or MO's $\phi_p$'s.

17) F. O. Ellison and H. Shull, *J. Chem. Phys.*, **21**, 1420 (1953).

18) S. Maeda, *Busseiron Kenkyu*, **70**, 101 (1954).

this case. That is, the $a_1$ (or $\sigma$) orbital of the lowest energy except the inner shell is strongly bonding but the $a_1$ (or $\sigma$) orbitals of higher energies are weakly bonding.

It is seen that the coefficients of $x-y$ in the $1b_2$ orbitals are almost independent of the bond angle, while others are not. On the other hand, the hybridized orbitals used in the electron pair bond theory[19] are written as follows:

$$\begin{aligned}\Psi_1&=(1/2)^{1/2}(s)\cos\alpha-(1/2)(x+y)\sin\alpha\\&\quad+(1/2)(x-y)\\\psi_2&=(1/2)^{1/2}(s)\cos\alpha-(1/2)(x+y)\sin\alpha\\&\quad-(1/2)(x-y)\\\psi_3&=(s)\sin\alpha+(1/2)^{1/2}(x+y)\cos\alpha\end{aligned}\qquad(14)$$

where

$$\sin\alpha=(1-\tan\theta')/(1+\tan\theta')\qquad(15)$$

and $\psi_1$ and $\psi_2$ are equivalent orbitals with their charge clouds extending along two straight lines which make an angle $\theta'$ with the $x$- and $y$-axis, respectively. In these orbitals (14), the coefficients of $x-y$ are also independent of the bond angle or the angle between the directions of their charge clouds. It is of interest to see that the LCAO-SCF calculation comes to the same conclusion for the coefficient of $x-y$ as the electron pair bond theory.

The localized symmetry orbitals of the $NH_2$ radical can be obtained by a unitary transformation of the two of the $a_1$ orbitals as shown by Pople[20] in the case of $H_2O$, and they are given in Table II. In these orbitals, $1a_1'$

TABLE II

LOCALIZED SYMMETRY ORBITALS FOR THE $^2B_1$ STATE

$K(a_1)=n$

$$1a_1'=\begin{matrix}0.975\\0.953\\0.920\\0.740\\0.000\end{matrix}(s)-\begin{matrix}0.159\\0.214\\0.277\\0.476\\0.707\end{matrix}(x+y)$$

$$2a_1'=\begin{matrix}-0.113\\-0.038\\+0.049\\+0.360\\+0.737\end{matrix}(s)+\begin{matrix}0.531\\0.535\\0.533\\0.464\\0.000\end{matrix}(x+y)+\begin{matrix}0.290\\0.290\\0.289\\0.256\\0.211\end{matrix}(h+h')$$

$1b_1=z$

$$1b_2=\begin{matrix}0.397\\0.389\\0.386\\0.385\\0.392\end{matrix}(x-y)+\begin{matrix}0.532\\0.503\\0.479\\0.449\\0.431\end{matrix}(h-h')$$

at the bond angle of $\begin{matrix}90^\circ\\115^\circ\\120^\circ\\150^\circ\\180^\circ\end{matrix}$, respectively.

and $2a_1'$ may be said to represent the $a_1$ lone pair and the $a_1$ bonding orbital, respectively. It is evident that the lone pair orbital $1a_1'$ has mainly $s$ character, especially at the bond angle of 90°, but has not a perfect $s$ character as it has in the electron pair bond theory, and the relationship between the coefficients of $s$ and $x+y$ is also complicated. This may be due to the influence of ionic character.

The "LCAO orbital energies" represent good approximation to the ionization energies of corresponding electron shells. In the present work, the calculated value of $2a_1$ orbital is 14.4 ev which is the minimum ionization energy at the equilibrium bond angle for the $^2B_1$ state. This value approximately corresponds to the removal of an electron from $2a_1$ orbital, but it is somewhat higher than the observed one of 11.05 ev.[21]

In spite of the fact that both the $2a_1$ and $1b_1$ orbitals turn into the $1\pi_u$ orbital in the linear form, the ionization energy of $2a_1$ is lower than that of $1b_1$, and neither value shows the same value at the bond angle of 180° in Fig. 2. This is due to the fact that the $NH_2$ radical has an unpaired electron: the $2a_1$ orbital is filled by two electrons with paired spins while the $1b_1$ has only one electron, and further the electronic repulsion in the former is stronger than in the latter. In view of these facts, the ground state of the $CH_2$ radical is probably the $^3B_1$ state, for the energy of the $^1A_1$ state $(1a_1)^2(1b_2)^2(2a_1)^2$ is considered to be higher than that of the $B_1$ states $(1a_1)^2(1b_2)^2(2a_1)^1(1b_1)^1$ and also the $^3B_1$ state may be the most stable.

Using the LCAO MO's in Table I without configuration interaction, the dipole moment for the corresponding bond angle can be calculated and is shown in Table III. These

TABLE III

DIPOLE MOMENT

| Bond angle | 90° | 105° | 120° | 150° | 180° |
|---|---|---|---|---|---|
| Dipole moment D. ($N^-H_2^+$) | 1.75 | 1.32 | 0.83 | −0.14 | 0.00 |

values may be rather small but not considered to be unreasonable as compared with the value of the ammonia molecule of 1.40 D.[22] This correspondence may be due to the similarity of electronic structures between the $NH_2$ radical and the ammonia molecule. But such correspondence does not exist in the relationship between the CH radical and the methane molecule, for there is a consi-

19) For example, see T. Inui and S. Yanagawa, "Group Representation and Atoms and Molecules", Shokabo, Tokyo, (1950) p. 253.

20) J.A. Pople, *J. Chem. Phys.*, **21**, 2234 (1953).

21) J.C. Devins and M. Burton *J. Am. Chem. Soc.*, **76**, 2618 (1954).

22) L.G. Wesson, "Table of Electric Dipole Moments", The Technology Press. Massachusetts Institute of Technology, (1948) p. 2.

derable difference in the electronic structure, that is, the former has lone pair electrons but the electrons in the latter are all bonding[5], and the lone pair electrons make a substantial contribution to the dipole moments[23].

**Electronic States and Structures**

By using the LCAO MO's given in Table I, the energies of the lower electronic states were calculated without configuration interaction, and are shown in Fig. 3. They may

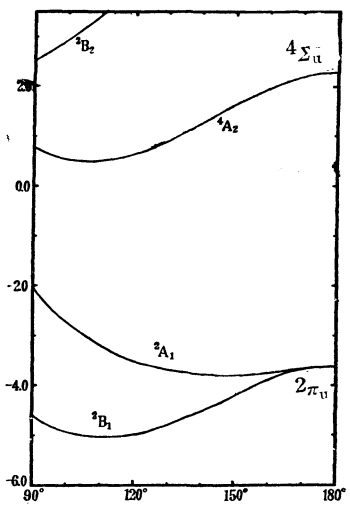



Fig. 3. Lower electronic states of the free $NH_2$ radical (without configuration interaction). The origin of energy is chosen to be $N(^4S)+2H(^2S)$.

be considered to be fairly reasonable, if the good result of the CH radical[5] obtained by the similar procedure is referred to. The electronic configurations of these states are as follows:

$^2B_1$: $K(1a_1)^2(1b_2)^2(2a_1)^2(1b_1)^1$
$^2A_1$: $K(1a_1)^2(1b_2)^2(2a_1)^1(1b_1)^2$
$^4A_2$: $K(1a_1)^2(1b_2)^2(2a_1)^1(1b_1)^1(2b_2)^1$
$^2B_2$: $K(1a_1)^2(1b_2)^1(2a_1)^2(1b_1)^2$.

Herzberg[24] showed that, in the upper state of the $\alpha$ bands, the bond angle is fairly large and possibly 180° while, in the lower state, it has an intermediate value. According to Luft's estimation,[25] the equilibrium bond angles of the lower and the upper state are 110° and 135–160°, respectively. These results are very close to the values of the present calculation for the $^2B_1$ and the $^2A_1$ state. The calculated value of a $^2B_1 \rightarrow {}^2A_1$ transition (1.8 ev) is also in fairly good agreement with the experimental result, which was observed in absorption spectrum in the region of 4500–7400 Å. In view of these facts, the present calculation may be said to give the theoretical interpretation of the $\alpha$ bands as follows: this spectrum is due to the free $NH_2$ radical, and the upper and the lower states are the $^2A_1$ and the $^2B_1$ state, respectively.

The calculated $^2B_2$ state was, however, higher than that predicted by Mulliken[4]. This is mainly due to the facts that the present calculation ignores configuration interaction and that the variational procedure is carried out for the $^2B_1$ state only. Especially, the second $^2B_2$ state $K(1a_1)^2(1b_2)^2(2a_1)^2(2b_2)^1$ is very close to the lowest $^2B_2$ state, and then the effect of configuration interaction may not be disregarded.

In the previous section, the similarity of electronic structures for the nitrogen atoms in the $NH_2$ radical and in the ammonia molecule has been discussed from the point of view of dipole moment. Besides this, such similarity can be deduced from their structures, that is, the tetrahedral structure of bond angle is almost perfectly preserved in the ground state of the $NH_2$ radical as in the ammonia molecule. On the other hand, the HCO angle of the HCO radical is also scarcely changed from that of the formaldehyde molecule in the photochemical reaction,[26] and this may be also due to the preservation of the electronic structure for the carbon atom. In view of these facts, the bond angle of the ground state may scarcely be changed in such reactions due to the preservation of electronic structure for the atom whose bond is ruptured. In the excited states, however, such property is not preserved in the case of the $NH_2$ radical and of the HCO radical. The analogous relationship between the ground and the excited state can be seen in molecules such as HCN[27], $C_2H_2$[28] and others, in which the linear form is not preserved in the excitation of an electron from the bonding orbital to the non- or anti-bonding orbital.

The results in the present work are, however, qualitatively satisfying, but can not be conclusive because of the method used, the approximate values in the many-center integrals and the ignorance of configuration interaction. It may be desiable to investigate these points more accurately, though they, in part, have been discussed by the present author in his calculation of CH[5].

23) A. B. F. Duncan and J. A. Pople, *Trans. Faraday Soc.*, **49**, 217 (1953).
24) G. Herzberg, private communication.
25) N.W. Luft, *Discussion Faraday Soc.*, No. 14, 114 (1952).
26) D.A. Ramsay, *J. Chem. Phys.*, **21**, 960 (1953).
27) G. Herzberg and K.K. Innes, to be published.
28) C. W. King and C. K. Ingold, *Nature*, **169**, 1101 (1952); K. K. Innes, *J. Chem. Phys.*, **22**, 863 (1954).

**Summary**

LCAO MO's and ionization potentials have been calculated for the $^2B_1$ state of the free $NH_2$ radical by using the LCAO-SCF method. The interactions of all electrons have been explicitly considered, but the orthogonal relationship between the 1*s* orbitals of nitrogen and hydrogen was assumed. Using these MO's the lower electronic states have also been investigated without configuration interaction. The calculated value of a $^2B_1 \rightarrow {}^2A_1$ transition is 1.8 ev in fairly good agreement with the observed one of the $\alpha$ bands of ammonia in the region of 4500 to 7400 Å. The calculated bond angles of the $^2B_1$ and the $^2A_1$ state are about 110° and 150°, respectively. These results are in good agreement with the observation and the opinion by Herzberg and Ramsay and the estimation by Luft.

The author wishes to thank Dr. S. Shida for his helpful advice and encouragement, Dr. K. Niira for his useful suggestions and Mr. S. Maeda and Mr. K. Oohata for their kind discussion and permission to use the unpublished data on the auxiliary function of the three-center integrals. He also expresses his thanks to Dr. G. Herzberg for his kind communication.

*Laboratory of Physical Chemistry,*
*Tokyo Institute of Technology,*
*Tokyo*

# *Grain Growth of Silver Chloride Suspensions in Polyvinyl Alcohol*

By Yasushi OHYAMA and Kiyoshi FUTAKI

(Received December 6, 1954)

## Introduction

Aqueous suspensions of silver chloride in the presence of protective colloid such as gelatin are usually called emulsion in photography. It is well known that grains of silver halide formed by mixing silver nitrate solution with alkali halide solution quickly coagulate and precipitate when the protective colloid is absent. In the aqueous solution of gelatin, not only is this coagulation or precipitation inhibited, but the grain growth is also retarded. The grain-growth, however, is not so completely inhibited as in polyvinyl alcohol described later, but is smooth enough to fulfil the requirements of emulsion-making in the photographic industry.

On the contrary silver halide emulsions prepared with polyvinyl alcohol as protective colloid consist of very fine grains not exceeding 0.1 $\mu$ and 0.05 $\mu$ in diameter for bromide and chloride respectively. They scarcely grow by the prolonged ripening at rather high temperature, because the grain-growth is inhibited by its extraordinarily strong adsorption to the silver halide grain and the lack of active substances ordinarily found in gelatin. The function of these active substances is to accelerate the grain-growth. In the following, the role of these substances is disscussed.

The author reported previously[1] that it becomes very turbid as soon as traces of some sulfur-containing substances are added to the suspension, and this increase in turbidity is the evidence of grain growth in the suspension. This was confirmed by the electron micrograph. The amount of addition necessary to produce the increase of turbidity (i.e. the growth of grains) differs very widely from one to another. This grain-growth can easily be traced by the nephelometric method, and can be described as functions of time and temperature of ripening and amounts of active substances added. Substances tested and reported in the previous paper are limited only in some sorts of sulfur-containing compounds known as chemical sensitizers in photography, e.g. thiosinamine, thiosulphates, rhodanine, the N-alkyl-thiones of Kendall[2] and their derivatives. These substances, however, with few exceptions, produce heavy fog during ripening from lack of stability of the complex compounds with silver halide.

In this paper the author will present some other types of active substances, much more important for the investigation of physical

1) Y. Ohyama, Royal Photographic Society Centenary Conference, London, Sept. (1953) (Proceeding is now in press).

2) J. D. Kendall, 9th Internat. Congress of Phot., Paris, 235 (1935).

ripening of photographic emulsion and for the understanding of the role of gelatine. They do not produce fog but increase stability of the emulsion in many cases. Compounds now investigated include a large number of substances not containing active sulfur, e.g. N-alkyl homologues of guanidine, pyrrolidone, pyridone, quinolone, 2-iminobenzothiazoline, etc. High molecular compounds such as polyvinyl pyrrolidone or albumin have also been tested and their activities are confirmed.

## Experimental

The grain-growth can be traced by the nephelometric method as was previously reported[1], because in the region of the sizes in question (between 0.05 $\mu$ and 0.25 $\mu$ in diameter) it was confirmed by Evva[3] and Ammann-Brass[4] that the increase of turbidity of the suspension is in linear proportion to the mean graindiameter. To 42 ml. of aqueous solutions of active substances with varying concentration (10 ml. of this solution may be replaced by alcohol if needed for substances sparingly soluble in water), 10 ml. of 6% solution of polyvinyl alcohol and 4 ml. of 0.6 M NaCl solution are added. The mixture is heated to 70°C, and 4 ml. of 0.2 M silver nitrate solution (70°C) is added in 15 seconds. After drawing out 2 ml. of this suspension of AgCl at 2, 4, 8 and 16 min. after the addition of silver ions, it is diluted with 20 ml. of cold water and the turbidity is measured. This is done by measuring the intensity of a parallel light beam which passes through a glass cuvette (1 cm. depth) containing the diluted suspension with the aid of a photocell at two points: just behind the cuvette and 20 cm away from it. Afterwards this rather complicated method was replaced by a simple measurement of optical absorption and this is designated as the transmission method.

In the previous report[1], dealing with sulfur-containing chemical sensitizers, the addition of active substances was effected after the emulsification (formation of fine suspension of silver chloride) was accomplished. In this report, however, the addition was effected before the emulsification except for the case specially cited. Usually this has no influence upon the turbidity obtained at the same period of ripening and also the activity of the substance used is identical. The new method is very convenient for the experiments at high concentration and particularly suitable for a thermally coagulating substance such as albumin.

3) F. Evva, *Z. wiss. Phot.* **47**, 39, (1952).

4) H. Ammann-Brass, *Sci. et Ind. Phot.*, [2], **23**, 249, (1952).

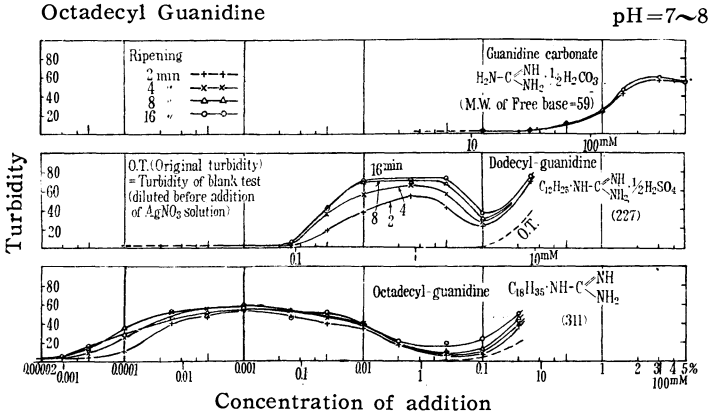



Fig. 1. Ripening characteristics of guanidine derivatives (Part. 1).

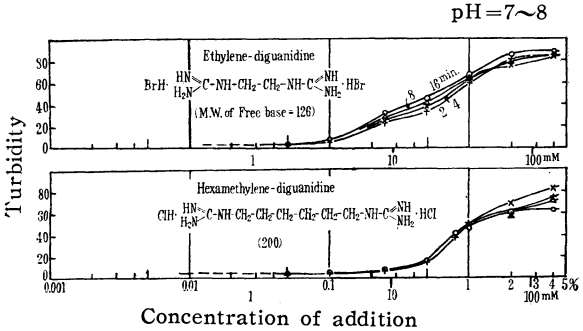



Fig. 2. Ripening characteristics of guanidine derivatives (Part. 2).

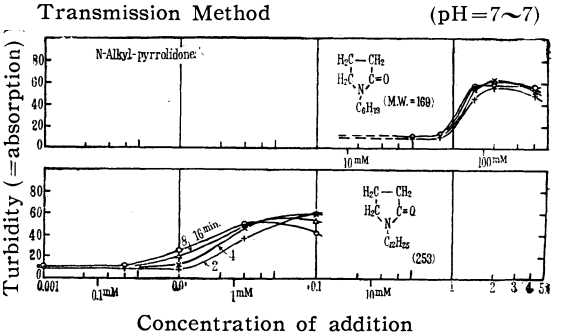



Fig. 3. Ripening characteristics of pyrrolidones.

pH=7～8

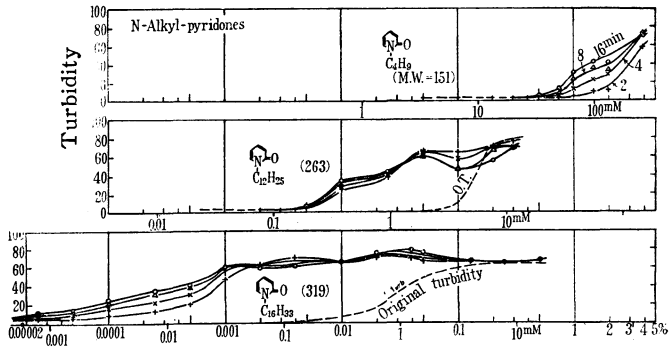



Fig. 4. Ripening characteristics of pyridones.

pH=7～8

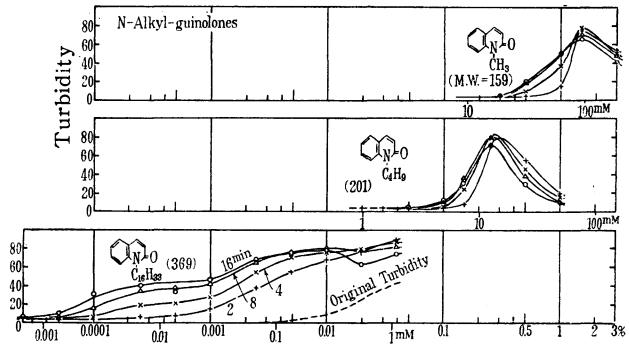



Fig. 5. Ripening characteristics of quinolones.

Transmission Method (pH=7～8)

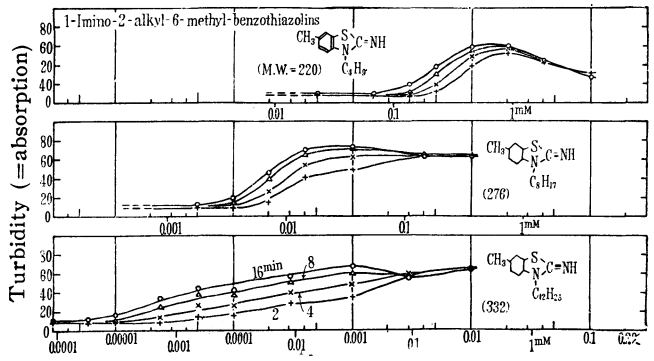



Fig. 6. Ripening characteristics of 2-imino-thiazolines.

## Results and Discussion

(a) **Ripening Characteristics.**—If turbidity is plotted against the concentration (on logarithmic scale) of added substance in the emulsion, taking ripening (or heating) time as parameter, characteristic curves of many substances are obtained. Using these diagrams, comparisons of their activities and also ripening characteristics at various concentrations are easily recognizable at a glance. Fig. 1, and Fig. 2 show some examples of these characteristic curves of the guanidine series. Fig. 3, 4, 5 and 6 are those of pyrrolidone, pyridone, quinolone and 2-imino-thiazoline series respectively.

(b) **Activity and its Dependance on Molecular Weight.**—Activity defined as the reciprocal of the minimum addition concentration (in milli mol.) which causes definite

turbidity-increase is valuable for the comparison of the activities of many substances and can also be used for the determination of the relation between activity and the molecular weight or the chemical constitution of active substances. The choice of the comparison point may be optional, turbidity increase of 2, 10, 20 or 40 units (or absorption of 15, 20, 30 or 40% for transmission method) are convenient and usually 10 unit increase (or absorption of 20%) was preferred.

Fig. 7, 8 and 9 show the relation between activities and molecular weights of N-alkyl homologues of the above mentioned substances. Symbols of G, PQ and IT represent guanidine, pyridone (and also pyrrolidone) quinolone and 2-imino-thiazoline series respectively. It is very astonishing to know that activities in these several series of

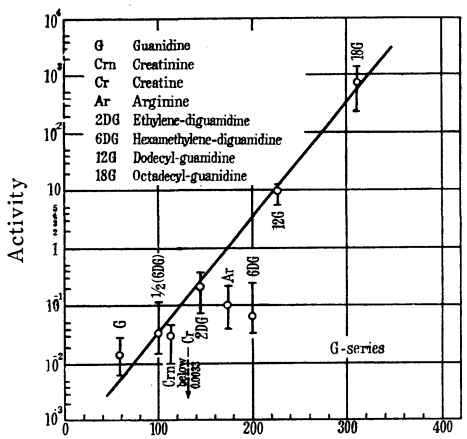



Fig. 7. Relation between activities and molecular weight of guanidine series.

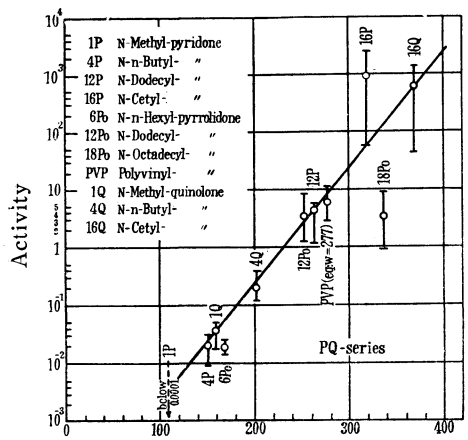



Fig. 8. Relation between activities and molecular weight of pyrrolidone, pyridone and quinolone series.

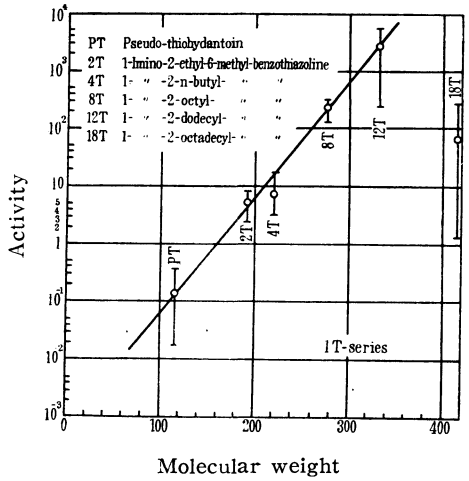


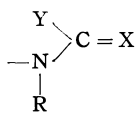

Fig. 9. Relation between activities and molecular weight of imino-thiazoline series.

substances increase markedly with increasing molecular weight by introducing alkyl radicals of increasing numbers of carbon atoms. The relation between activity ($A$) and molecular weight ($M$) can be expressed approximately in the following equation,

$$\log_{10}A = \frac{M}{50} - \alpha$$

where $\alpha$ is constant in each series. The equation states that the increase in molecular weight by 50 enhances the activity 10 times in each series of substances. It is varied as far as the molecular weight reaches 300–400.

(c) **General Constitution of Active Substances.**—The above mentioned active substances have the following general chemical constitution,



where X is O or NH and Y is $-NH_2$, $-NH-$, $-N=$, $-CH=CH-$, $-CH_2-CH_2-$, $-O-$, $-S-$, or radicals constituting heterocyclic ring with N atom adjacent to central carbon atom. R is alkyl, aryl or aralkyl radical usually up to 20 carbon atoms. It is interesting to recall here that sulfur containing active substances previously reported by the author[1], with few exceptions have chemical constitution in accord with this general structure if X is taken as S, for example thioacetanilide, isothiocyanates, thiourea derivatives, rhodanines or the N-alkyl thiones of Kendall[2].

Of course, there are many active substances which do not coincide with the above mentioned general constitution such as thiosulphates, xanthates, alkylamines, heterocyclic amines or many thiol compounds. Some of them were reported already[1] and others will be reported in another paper.

**(d) Polyfunctional Derivatives and Effective Molecular Weight.**—As is shown in Fig. 7, the activity and molecular weight relation for hexamethylene-diguanidine is irregular whereas ethylene-diguanidine is regular, and if the molecular weight of hexamethylene-diguanidine is divided by 2, the position of the substance falls just on the line and we are able to conclude that the effective equivalent weight of hexamethylene-diguanidine is one half of its real molecular weight.

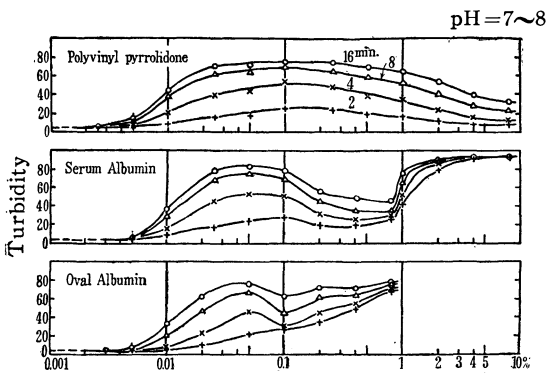



Fig. 10. Ripening characteristics of albumins and polyvinyl-pyrrolidone.

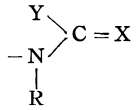
It supports the assumption that hexamethylene-diguanidine adsorbs, on the surface of silver chloride particles, by both active functional ends, whereas ethylene-diguanidine cannot bend enough, because of the shorter chain length. Polyvinyl-pyrrolidone is also active and is almost 10 times as powerful as ordinary active gelatine, and the grain-growth of silver chloride suspension in the mixture with polyvinyl-alcohol is very smooth and rapid as in a gelatinous solution (usual photographic emulsion). The ripening characteristic curve is shown in Fig. 10 and it is possible to estimate the effective equivalent weight of polyvinyl-pyrrolidone from the relation between activity and molecular weight of pyrrolidone derivatives (Fig. 8). The figure obtained is about 277* and it means that every one, two or three pyrrolidone radicals in this long chain molecule** adsorb to the surface of silver chloride. It is interesting to notice that ripening characteristic curves of oval and serumalbumin (also shown in Fig. 10) closely resemble that of polyvinyl-pyrrolidone, considering that their chemical constitutions differ so far and the latter may also be used as an artificial substitute for the former in medical application.

**(e) Influence of Carboxyl Group and Amide Linkage.**—Also in Fig. 7 data on some amino acids having guanyl group, such as arginine, creatine and creatinine are shown. Arginine is not so active as is expected from its molecular weight, and creatine is practically inactive (if active, its activity is below 0.003), whereas creatinine is fairly active (a little below the line). This means that the carboxyl group hinder the activity to a great extent and the amide linkage has scarcely any influence on the activity.

## Conclusions

(1) Many substances which accelerate the grain growth of silver chloride suspension in polyvinyl-alcohol were found. Most of them are organic compounds having in their molecule at least one sulfur atom or one nitrogen atom. The most simple compounds are mercaptans or amines of the aliphatic or aromatic series.

(2) Many of them are, however, more complicated compounds having general chemical constitutions as follows,



where X is O, NH, or S, and Y is $NH_2$; $-NH-$, $-N=$, $-CH=CH-$, $-CH_2-CH_2-$, $-O-$, $-S-$ or radicals constituting the heterocyclic ring with N atom adjacent to central C atom. R is alkyl, aryl or aralkyl radical usually up to 20 C atoms (or vinyl radical for polyvinyl compounds).

(3) Their activities, difined as the reciprocal of the minimum added concentration (in milli mol.) which causes definite turbidity increase, differ very widely from one to another, and increase with increasing numbers of C atoms in R of above general constitutions up to about 16–20 atoms.

(4) The relation between activity ($A$) and molecular-weight ($M$) can be expressed in the equation.

$$\log_{10}A=\frac{M}{50}-\alpha$$

(5) Activities of polyfunctional compounds fit more reasonably to the above equation

* The sum of atomic weight of one unit vinyl-pyrrolidone is 111 and $277=1/2(2\times111+3\times111)$

** The sample used in this experiment is Albigen, which have a molecular weight of about 25,000.

in which molecular weight is replaced by the effective equivalent weight, which is defined as the molecular weight divided by the number of effective functional groups. And from this effective equivalent weight the mode of adsorption of the active substance can be estimated.

(6) Usually at about a molecular weight of 300–400, the activity for acceleration of the grain-growth reaches its maximum, where the grain-growth of AgCl suspension in polyvinyl-alcohol will take place at very low concentration (about 0.0003 mM≒0.00001%) of an active substance.

(7) From these and other evidences, it may be concluded that in most cases acceleration of the grain-growth is optimum when only the surface of grain is partially covered (at least a few %) with active substances, and the remainder of the surface is occupied by the adsorbed layer of polyvinyl-alcohol.

*Research Section, Kyoto Factory,*
*Mitsubishi Paper Mills Co.,*
*Kyoto*

# *Acetylation of Holocellulose in Fibrous State*

By Toshikazu FUJIMURA*

(Received December 27, 1954)

When wood pulp is used as raw-material for cellulose acetate, the effect of pentosan comes into question. In a previous paper, it was reported that pentosan hindered acetylation of holocellulose with acetic anhydride —acetic acid—sulfuric acid system[1]. Because the product is gradually dispersed in that case, acetylation process in acetic anhydride —benzene—sulfuric acid system, which keeps its fibrous state and proceeds layer by layer, seems suitable to be used to disclose the hindering effect of pentosan and the structure of holocellulose. In this paper, the change of acetic acid content with the time of acetylation was compared with the equation, the rate-determining step of which is internal diffusion or surface resistance. The process of acetylation of single fiber was also observed by birefringence, based on the small little birefringence of the acetate. Then, the effect of alkaline refining on acetylation was studied and compared with beech sulfite rayon pulp and Bemberg rayon, which have circular section.

## Derivation of Theoretical Rate Equation

The equation which was suggested for the combustion of spherical pyrite particle, was modified for a cylinder of infinite length[2]. It was assumed as follows:

(1) The reaction is so fast that the progress of acetylated layer is controlled by the migration rate of the reagent.

(2) The migration velocity at the surface is proportional to the difference of concentration.

(3) Diffusion in the acetylated layer follows Fick's law.

(4) Steady state is attained in a short time.

(5) The concentration of reagent in the surrounding medium is constant.

From the assumption (4), (2) and (3) respectively, the following relations are established per unit length,

$$2\pi R dm'/dt = 2\pi r dm/dt = 2\pi r'' dm''/dt = -2\pi r'' a(dr''/dt) \quad (1)$$

$$dm'/dt = k(C^* - C') \quad (2)$$

$$dm/dt = D dc/dr \quad (3)$$

where:

$a$: mass of reagent to react with unit volume of fiber.

$R$, $r''$: outer radius, unreacted radius of fiber.

$C^*$, $C'$, $C''$: Concentration of reagent in the surrounding medium, at the surface and at the interface of unreacted layer.

$m'$, $m''$, $m$: Migrated mass of reagent at the surface, at the interface of unreacted layer and in acetylated layer of radius $r$.

Rearranging (3) and combining (1) gives

$$Ddc = (dm/dt)dr = -ar''(dr''/dt)dr/r$$

Integrating from $r''$ to $R$

$$D(C' - C'') = -\ln(R/r'')ar''(dr''/dt) \quad (4)$$

Combining (2) and (1) yields

$$C' = C^* + ar''(dr''/dt)/kR \quad (5)$$

Combining (5) and (4)

$$(C^* - C'')dt = a\{1/kr + \ln(R/r'')/D\}(r''dr'')$$

Integrating between zero and $t$

$$(C^* - C'')t = a[(1/2k + R/4D)R - r''/2kR + \{r''\ln(R/r'')/2D + r''/4D\}r'']$$

$r''$ becomes zero when $t$ is $T$

$$(C^* - C'')T = a(1/2k + R/4D)R$$

i) When surface resistance is rate-determining, $k \ll D$, $t/T = 1 - (r''/R)^2$

* Present addres: Kokoku Rayon and Pulp Co. Ltd., Yatsushiro Mill, Kumamoto.

1) T. Fujimura, *J. Chem. Soc. Japan (Ind. Chem. Sec.)*, **56**, 99 (1953).

2) S. Yagi and D. Kunii, *J. Chem. Soc. Japan (Ind. Chem. Sec.)*, **56**, 131 (1953).

ii) When internal diffusion is rate-determining,

$k \gg D$, $t/T=1-(r''/R)^2\{1-2\ln(r''/R)\}$

When it is converted into acetic acid content,

i) $t/T=9A/(10-7A)$

ii) $t/T=1-(10-16A)\{1-\ln(10-16A)+\ln(10-7A)\}/(10-7A)$

Because acetic acid content $A$ is calculated, assuming no volume change by acetylation,

$A=180\{1-(r''/R)^2\}/[162(r''/R)^2+288\{1-(r''/R)^2\}]$

Then,

$(r''/R)^2=(10-16A)/(10-7A)$

## Materials and Methods

As material, beech wood fiber was selected because of its nearly cylindrical form. Holocellulose was prepared by treating five times with sodium chlorite[3]. Its yield was 81.6% and it contained 33.3% pentosan and 3.45% lignin. The rayon pulp was commercial beech sulfite pulp. Bemberg rayon of 40 denier/30 was used.

Acetylating reagent was prepared by heating acetic anhydride—benzene—sulfuric acid mixture on water bath for two hours to convert into sulfoacetic acid[4]. After the separate samples of material were treated with acetylating reagent in separate flasks dipped in thermostat for various times respectively, they were filtered, washed successively with ethanol, water and again ethanol, and finally air dried.

The alkaline-refining time was five hours and the liquid ratio was 1:40. The refined product was filtered and washed first by aq. alkali of the same concentration and temperature as the treating alkali, then water, 10% acetic acid and again water, and finally air dried.

Acetic acid content was determined by alkaline saponification method. Retardation was measured by quartz-wedge.

## Results

**1. Holocellulose.**—Acetylating conditions and the results are given in Tables I, II, III, IV and V. In the initial stage readily reacting portion is observed. Pretreatment, boiling with acetic acid as well as replacing successively with water and acetic acid, accelerates the reaction. Lowering liquid ratio to 1:50 has no remarkable effect, but in the final stage the acetic acid content is a little decreased. By reducing acetic anhydride or sulfuric acid content, as well as by lowering the temperature, the reaction is retarded. The yield first decreases abruptly

TABLE I

CONDITIONS OF ACETYLATION

| Expt. No. | Pre-treating | Temp. °C | $Ac_2O$ | $C_5H_5$ | $H_2SO_4$ | Liquid ratio |
|---|---|---|---|---|---|---|
| F-11 | Air drying | 30 | 100 | 300 | 1.8 | 100 |
| F-12 | Replacing | 30 | 100 | 300 | 1.8 | 100 |
| F-13 | Boiling | 30 | 100 | 300 | 1.8 | 100 |
| F-21 | Air drying | 30 | 100 | 300 | 1.8 | 50 |
| F-22 | Air drying | 30 | 50 | 300 | 0.9 | 100 |
| F-23 | Air drying | 30 | 100 | 300 | 0.9 | 100 |
| F-31 | Air drying | 45 | 100 | 300 | 1.8 | 100 |
| F-32 | Air drying | 15 | 100 | 300 | 1.8 | 100 |

TABLE II

CHANGE OF ACETIC ACID CONTENT WITH TIME

| Expt. No. | Acetic acid content (%) at time (hr.) | | | | | | | | |
|---|---|---|---|---|---|---|---|---|---|
| | ½ | 1 | 2 | 4 | 6 | 8 | 15 | 20 | 25 |
| F-11 | 14.4 | 16.6 | 20.1 | 25.4 | 30.6 | 34.7 | 47.7 | 57.4 | 62.6 |
| F-12 | 42.9 | 44.9 | 46.8 | 50.7 | 55.1 | 56.5 | 61.5 | — | 65.6 |
| F-13 | 44.5 | 45.5 | 47.6 | 50.6 | 53.5 | 57.4 | 61.6 | — | 65.2 |
| F-21 | 13.5 | 18.3 | 21.1 | — | 31.9 | 36.7 | 49.0 | — | 59.1 |
| F-22 | 14.4 | 15.5 | 16.1 | 20.2 | 23.1 | 26.1 | 33.2 | — | 43.8 |
| F-23 | 15.7 | 17.4 | 19.7 | 22.6 | 27.0 | 30.2 | 42.7 | 47.3 | 48.9 |
| F-31 | 21.7 | 26.2 | 38.7 | 43.2 | 54.2 | 58.6 | 64.0 | 67.2 | 68.2 |
| F-32 | 13.4 | 14.9 | 15.9 | 16.6 | 18.7 | 19.1 | 22.5 | 26.0 | 29.1 |

TABLE III

CHANGE OF BIREFRINGENCE WITH TIME

| Expt. No. | Birefringence (×1000) at time (hr.) | | | | | | | | |
|---|---|---|---|---|---|---|---|---|---|
| | ½ | 1 | 2 | 4 | 6 | 8 | 15 | 20 | 25 |
| F-11 | 13.4 | 14.9 | 17.9 | 17.9 | — | 12.8 | 8.5 | 5.4 | 4.1 |
| F-12 | 9.5 | 8.3 | 5.5 | 5.4 | 6.0 | 5.0 | 7.3 | — | 4.7 |
| F-13 | 4.3 | 9.0 | 6.1 | 6.3 | 5.5 | 4.7 | 3.8 | — | 3.2 |
| F-21 | 12.6 | 14.2 | 8.2 | 10.2 | 7.9 | 6.3 | 4.4 | — | 3.4 |
| F-22 | 9.6 | 7.2 | 7.7 | 10.2 | 12.1 | 8.4 | 8.8 | — | 6.0 |
| F-23 | 13.4 | 9.1 | 9.5 | 9.7 | 13.7 | 10.1 | 7.0 | 5.7 | 11.3 |
| F-31 | 9.7 | 5.3 | 7.7 | 9.4 | 5.6 | 4.7 | — | — | 4.2 |
| F-32 | 14.1 | 13.4 | 10.8 | 8.2 | 15.2 | 13.2 | 11.3 | 9.5 | 9.6 |

TABLE IV

CHANGE OF YIELD WITH TIME

| Expt. No. | Yield (%) at time (hr.) | | | | | | | | |
|---|---|---|---|---|---|---|---|---|---|
| | ½ | 1 | 2 | 4 | 6 | 8 | 15 | 20 | 25 |
| F-11 | 91.7 | 90.1 | 90.4 | 85.7 | 90.0 | 87.7 | 85.2 | 80.2 | 79.9 |
| F-12 | 97.9 | 92.8 | 92.3 | 87.2 | 78.1 | 77.2 | 89.9 | — | 69.4 |
| F-13 | 90.9 | 96.6 | 94.9 | 81.4 | 78.2 | 76.3 | 90.8 | — | 90.7 |
| F-21 | 91.2 | 94.4 | 89.2 | — | 87.7 | 90.6 | 84.8 | — | 79.4 |
| F-22 | 89.4 | 90.8 | 87.8 | 88.6 | 88.0 | 82.4 | 86.3 | — | 83.5 |
| F-23 | 88.4 | 88.7 | 89.3 | 91.3 | 88.7 | 87.4 | 88.6 | 82.6 | 85.1 |
| F-31 | 90.7 | 89.8 | 87.6 | 84.3 | 84.5 | 86.9 | 71.9 | 67.6 | 59.7 |
| F-32 | 90.4 | 89.3 | 90.9 | 87.8 | 85.9 | — | 90.1 | 87.1 | 82.1 |

TABLE V

CHANGE OF PENTOSAN CONTENT WITH TIME

| Expt. No. | Content (%) at time (hr.) | | | | |
|---|---|---|---|---|---|
| | ½ | 2 | 6 | 15 | 25 |
| F-11 | 37.7 | 39.4 | 41.1 | 40.0 | 43.5 |
| F-12 | 40.6 | 41.2 | 44.2 | 39.3 | — |
| F-13 | 40.3 | 40.0 | 41.3 | 34.4 | 34.5 |
| F-21 | 34.1 | 39.7 | 37.7 | 26.3 | 24.0 |
| F-22 | 36.7 | 37.7 | 37.9 | 26.1 | 41.1 |
| F-23 | 37.1 | 37.8 | 39.7 | 41.2 | 55.4 |
| F-31 | 47.9 | 37.0 | — | 35.2 | 42.3 |
| F-32 | 45.6 | 37.2 | 47.3 | 47.8 | 35.8 |

3) L. E. Wise, M. Murphy and A. A. D'Addieco, *Paper Trade J.*, **122**, No. 2, 35 (1946).

4) I. Sakurada et al., *J. Chem. Soc. Japan (Ind. Chem. Sec.)*, **37**, 127, 1339 (1934).

and then stays constant. Pentosan is not entirely lost. Birefringence decreases at first abruptly, then increases and finally gradually again decreases, but its value is scattered.

**2. Alkali Refined Holocellulose.**—The refined products shown in Table VI were

TABLE VI
REFINING CONDITIONS AND RESULTS

| Expt. No. | Refining Temp. °C | Refining NaOH % | Total Yield % | α-Cellulose Cont. % | α-Cellulose Yield % | Pentosan Cont. % | Pentosan Yield % |
|---|---|---|---|---|---|---|---|
| C-41 | 15 | 1 | 63.0 | 80.9 | 90.7 | 27.6 | 52.1 |
| C-43 | 15 | 4 | 55.9 | 92.0 | 91.5 | 14.8 | 24.8 |
| C-44 | 15 | 8 | 52.2 | 94.8 | 88.0 | 12.3 | 19.3 |
| C-42 | 15 | 17.5 | 49.9 | 96.6 | 85.9 | 10.6 | 16.0 |
| W-62 | 60 | 1 | 66.5 | 76.8 | 90.9 | 29.7 | 59.4 |
| W-61 | 60 | 4 | 55.9 | 88.5 | 88.0 | 17.3 | 29.0 |
| H-52 | 95 | 1 | 64.7 | 77.3 | 89.0 | 31.2 | 60.5 |
| H-51 | 95 | 0.2 | 67.7 | 75.2 | 93.4 | 31.3 | 65.2 |
| Raw material | | | 100 | 56.2 | 100 | 33.3 | 100 |
| RP | | | 100 | 90.9 | 100 | 5.1 | 100 |

acetylated at 30°C. The acetylating mixture was composed of 100 parts acetic anhydride, 300 parts benzene and 1.8 parts sulfuric acid, and the liquid ratio used was 1 : 100. The results are shown in Tables VII, VIII, IX and X.

TABTE VII
CHANGE OF ACETIC ACID CONTENT WITH TIME

| Expt. No. | Acetic acid content (%) at time (hr) ½ | 1 | 2 | 4 | 6 | 8 | 15 | 20 | 25 |
|---|---|---|---|---|---|---|---|---|---|
| C-41 | 5.6 | 6.1 | 7.3 | 9.4 | 11.5 | 13.5 | 21.2 | 25.5 | 29.2 |
| C-43 | 4.3 | 6.4 | 8.1 | 8.5 | 11.9 | 13.5 | 18.4 | 22.3 | — |
| C-44 | 3.7 | 4.9 | 5.1 | 7.9 | 8.6 | 10.4 | 10.3 | 13.0 | — |
| C-42 | 2.0 | 2.1 | 2.2 | 2.3 | 3.0 | 3.8 | 3.7 | 4.4 | 6.2 |
| W-62 | 6.8 | 8.2 | 9.4 | 13.5 | 15.5 | 17.6 | 22.7 | 26.7 | 31.6 |
| W-61 | 3.2 | 4.9 | 6.3 | 8.7 | 9.9 | 12.8 | 19.9 | 24.1 | 29.8 |
| H-52 | 5.5 | 6.8 | 7.6 | 8.9 | 11.2 | 13.9 | 22.6 | 26.0 | 30.6 |
| H-51 | 5.4 | 5.8 | 6.8 | 8.9 | 12.5 | 14.4 | 20.3 | 25.5 | 30.2 |
| P-72 | 1.5 | 2.8 | 2.8 | 3.9 | 5.3 | 5.8 | 10.6 | 11.9 | 13.7 |

TABLE IX
CHANGE OF BIREFRINGENCE WITH TIME

| Expt. No. | Birefringence (×1000) at time (hr) ½ | 1 | 2 | 4 | 6 | 8 | 15 | 20 | 25 |
|---|---|---|---|---|---|---|---|---|---|
| C-41 | 21.8 | 17.7 | 18.3 | 17.0 | 13.4 | 17.8 | 14.6 | 16.1 | 13.2 |
| C-43 | 18.1 | 21.6 | 14.9 | 18.4 | 12.9 | 17.2 | 15.6 | 15.3 | 4.5 |
| C-44 | 19.2 | 21.1 | 24.1 | 15.0 | 20.7 | 18.5 | 13.6 | 24.3 | 16.3 |
| C-42 | 25.1 | 29.6 | 28.5 | 28.9 | 28.2 | 30.1 | 29.6 | 27.1 | 20.7 |
| W-62 | 16.7 | 24.3 | 20.5 | 25.1 | 17.7 | 18.2 | 17.6 | 17.6 | 16.9 |
| W-61 | 17.9 | 18.4 | 15.1 | 19.9 | 16.7 | 15.9 | 17.3 | 11.9 | 14.9 |
| H-52 | 15.4 | 16.2 | 16.1 | 20.4 | 18.1 | 18.3 | 16.6 | 15.6 | 14.3 |
| H-51 | 15.4 | 12.3 | 15.5 | 15.7 | 18.4 | 14.5 | 17.6 | 17.1 | 14.1 |
| P-72 | 11.8 | 11.5 | 12.0 | 9.7 | 13.0 | 12.5 | 11.8 | 11.7 | 11.3 |

TABLE X
CHANGE OF PENTOSAN WITH TIME

| Expt. No. | Content (%) ½ | 6 | 25 |
|---|---|---|---|
| C-41 | 33.2 | 37.8 | 33.2 |
| C-43 | 13.5 | 14.2 | 14.8 |
| C-44 | 14.7 | 15.2 | 15.1 |
| C-42 | 16.1 | 11.4 | 11.4 |
| W-62 | 33.6 | 32.4 | 28.8 |
| W-61 | 16.8 | 16.5 | 19.4 |
| H-52 | 31.5 | 32.9 | 26.0 |
| H-51 | 34.0 | 32.0 | 32.9 |
| P-72 | 7.1 | 7.7 | 6.4 |

The product refined with concentrated cold alkaline education reacted with difficulty. Refining temperature affects little on the reaction rate, but product refined at 60°C seems to be a little superior. The further refined products exhibit less initial decrease of yield, less abrupt change of acetic acid content and more diffused loss of birefringence. Pentosan is apparently little changed.

**3. Bemberg Rayon and Pulp.**—As shown in Table XI, the reaction is slow. Soaping has no effect. Birefringence decreases naturally.

TABLE VIII
CHANGE OF YIELD WITH TIME

| Expt. No. | Yield (%) at time (hr.) ½ | 1 | 2 | 4 | 6 | 8 | 15 | 20 | 25 |
|---|---|---|---|---|---|---|---|---|---|
| C-41 | 92.8 | 94.4 | 95.9 | — | 95.7 | 95.9 | 94.4 | 93.6 | 92.0 |
| C-43 | 96.4 | 95.2 | 88.2 | 93.7 | 95.8 | 94.6 | 96.4 | 96.0 | — |
| C-44 | 97.4 | 97.6 | 98.4 | 95.7 | 95.8 | 93.5 | 94.7 | 92.3 | — |
| C-42 | 94.8 | 95.0 | 95.8 | 98.2 | 98.6 | 95.5 | 96.4 | 96.2 | 97.7 |
| W-62 | 93.6 | 90.4 | 91.4 | 91.8 | 89.9 | 92.4 | 91.8 | 92.4 | 103.2 |
| W-61 | 96.3 | 95.0 | 95.9 | 95.6 | 95.2 | 95.8 | 93.6 | 93.5 | 92.1 |
| H-52 | 102.0 | 101.4 | 100.7 | 101.8 | 101.4 | 100.7 | 99.0 | 99.3 | 94.6 |
| H-51 | 92.8 | 95.1 | 94.1 | 93.3 | 93.5 | 92.2 | 93.2 | 93.2 | 86.2 |
| P-72 | 105.0 | 106.1 | 100.3 | 106.9 | 100.1 | 101.3 | 95.2 | 100.0 | 100.4 |

TABLE XI
ACETYLATION OF BEMBERG RAYON

| Expt. No. | Change with time (hr.) ½ | 1 | 2 | 4 | 6 | 8 | 15 | 20 | 25 | 50 | 100 | 200 |
|---|---|---|---|---|---|---|---|---|---|---|---|---|
| | Acetic acid content (%) | | | | | | | | | | | |
| B-81 | 2.2 | 3.1 | 3.2 | 3.1 | 3.4 | 4.2 | 4.6 | 4.6 | 4.5 | | | |
| B-82 | 1.4 | 1.7 | 3.1 | 2.8 | 3.5 | 3.7 | 4.8 | 5.0 | 5.3 | 7.6 | 11.7 | 13.1 |
| B-83 | 14.2 | 22.7 | 24.1 | 24.7 | 27.6 | 27.6 | 32.9 | 34.5 | | 48.7 | 51.1 | 54.5 |
| | Yield (%) | | | | | | | | | | | |
| B-81 | 94.6 | 97.0 | 97.6 | 98.1 | 97.3 | 97.0 | 95.3 | 96.4 | 96.0 | | | |
| B-82 | 98.8 | 99.8 | 98.1 | 98.5 | 98.4 | 97.7 | 97.7 | 96.4 | 97.6 | 94.8 | 94.2 | 96.7 |
| B-83 | 97.1 | 96.9 | 92.9 | 93.6 | 94.2 | 93.5 | 93.4 | 98.5 | 86.4 | 82.2 | 85.9 | 89.4 |
| | Birefringence (×1000) | | | | | | | | | | | |
| B-81 | 22.9 | 21.7 | 24.8 | 21.7 | 20.5 | 21.3 | 22.3 | 21.5 | 21.1 | | | |
| B-82 | 26.8 | 26.4 | 25.0 | 22.2 | 24.1 | 22.1 | 21.6 | 22.9 | 20.3 | 21.3 | 20.2 | 19.5 |
| B-83 | 25.6 | 21.3 | 22.1 | 20.8 | 20.0 | 20.1 | 18.0 | 18.7 | 19.1 | 19.0 | 16.1 | 9.1 |

## Discussion

**1. Unreacted Radius.**—Assuming that pentosan is concentrated at outer layer and preferentially acetylated,

$$A=-\frac{180(1-x^2/y)/162+120(x^2-1)/132}{x^2/y+288(1-x^2/y)/162+216(x^2-1)/132}$$

where $x$: unreacted radius/radius excluding pentosan.
$X=1/(1-P)$: total radius/radius excluding pentosan
$P$: content of pentosan in product
$y$: yield of product, fraction of theoretical value.

Then, $x^2=(10-16A)y/(10-7A)(1-P)-2yP/(1-P)$

$x$ is plotted against time fraction, which is arranged so as to lay the last experimental point on the calculated line of reaction controlled by surface-resistance, which is given as a full line in the figure. The broken line shows the case controlled by internal diffusion. As shown in Figs. 1, 2, 3 and 4, air-dried holocellulose tends to follow the reaction controlled by surface resistance regardless of the composition of acetylating mixture, acetylating temperature and degree of refin-

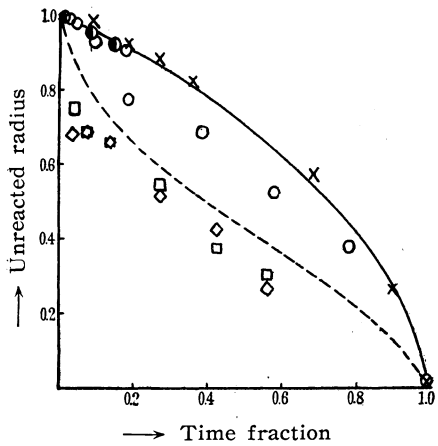



Fig. 1. Effect of pretreatment and temperature on acetylation rate of holocellulose.
(○, at 45°C; ×, at 30°C; ◐, at 15°C (air-dried); □, ◇: replacing or boiling with acetic acid)

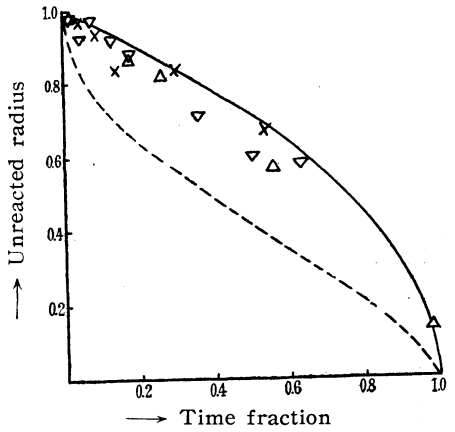



Fig. 2. Effect of composition of reagent on acetylation rate of holocellulose.
(△, +, ▽: low liquid ratio, low acetic anhydride or low sulfuric acid)

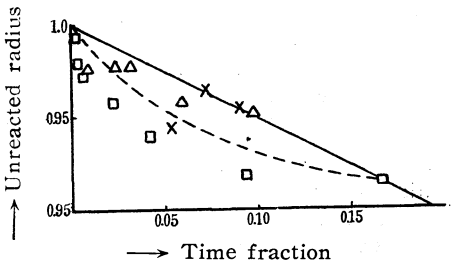



Fig. 3. Effect of cold alkali concentration on acetylation rate of refined holocellulose.
(×, △, □: 1%, 4%, 8% NaOH)

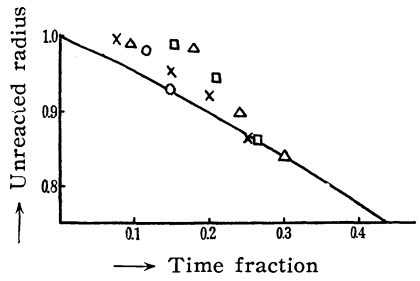



Fig. 4. Effect of warm and hot alkali concentration on acetylation rate of refined holocellulose.
(×, △, ○, □: 1%, 4% at 60°C; 1%, 0.2% at 95°C)

ing. Pretreated sample follows close by the curve controlled by internal diffusion. Hence pentosan layer may hinder the acetylation in air-dried state, but pretreatment would remove the hindrance. Figs. 5 and 6 shows

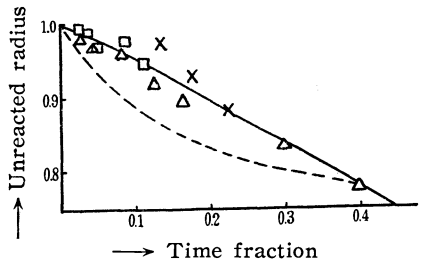



Fig. 5. Acetylation rate of air-dried rayon pulp and bemberg rayon.
(△, □, × : rayon, soaped, rayon, pulp)

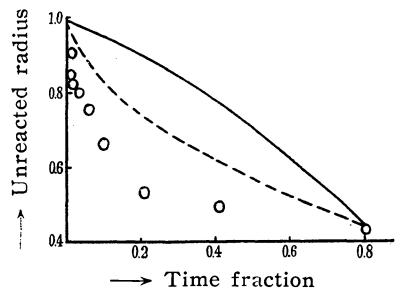



Fig. 6. Acetylation rate of pretreated bemberg rayon.

that not only pretreated Bemberg rayon but also air-dried rayon is likely counted as the type controlled by internal diffusion.

**2. Relation to Structure.**—Steep increase of acetic acid content and loss of yield in initial stage may be derived from the readily reacting and dispersing amorphous portion, for its magnitude is almost independent of acetylating conditions. The behavior of birefringence is elucidated by considering that initially it is reduced by acetylation of the accessible part, secondly it is raised by loss of amorphous portion, both bringing about the increase of residual crystallinity, and thirdly it is reduced again gradually by acetylation of crystalline region. Since the final acetic acid content is higher than the value corresponding to the birefringence and the yield is low, so acetolysis might have occurred.

**3. Effect of Refining.**—Slower reaction resulting from cold concentrated alkali refining is likely due to hornification, the loss of accessible portion or transformation into cellulose hydrate. The low reactivity of the sample refined with more dilute alkali than 4% is explained probably by the incomplete removal of the acetylation hindering layer and its gelatinization. The slow reaction of pulp and Bemberg rayon may be ascribed to more compact structure.

**4. Behavior of Pentosan.**—The content of pentosan in the product is apparently rather higher. Slight solubility of acetate and the easy production of oxymethylfurfural may be responsible for this. If all pentosan in holocellulose is preferentially acetylated, its acetic acid content should amount to 24.8%, but the value of only 12% observed in its initial stage suggests that pentosan is not exclusively accessible.

## Summary

Acetylation in fibrous state of holocellulose, its alkali-refined product, rayon pulp and Bemberg rayon was undertaken to disclose the effect of pentosan and the structure of holocellulose.

1) Acetylation of air-dried holocellulose is roughly controlled by surface resistance, regardless of various ratios depending on conditions of acetylation and degree of refining. The rate of pretreated sample seems to be determined by internal diffusion.

2) The birefringence decreases at first abruptly and then increases and finally decreases again. The final higher birefringence compared to acetic acid content may be ascribed to acetolysis. Definite amorphous portion is acetylated easily at the initial stage and lost, so that residual crystallinity, and also birefringence, increase.

3) By alkali-refining, acetylation is retarded and initial abrupt change, which is caused by the amorphous portion is diffused. There is optimum point in the concentration of refining alkali, probably relating to hornification, loss of amorphous portion, transformation of crystal form and hindrance by residual pentosan layer. The refining temperature affects the acetylation slightly.

4) Pentosan in product is not reduced apparently, probably due to oxymethylfurfural yielding and poor solubility of acetate. Also pentosan may not be entirely accessible at initial stage.

The author wishes to thank Prof. H. Sobue for his guidance and inspiration.

*Department of Applied Chemistry,*
*Faculty of Engineering,*
*Yamanashi University, Kofu*

# *On the Thermal Dissociation of Organic Compounds. VII. The Urea Linkage (1,3-Dibenzylurea and 1-isopropyl-3,3-diethylurea in Alcohols)*

By Teruaki MUKAIYAMA

(Received, July 26, 1954)

## Introduction

As described in the previous reports[1-4], ureas thermally dissociate into isocyanates and amines:

$$RHNCONHR \rightleftarrows R-N=C=O+H_2NR.$$

The kinetics of the thermal dissociation of ureas in various fatty acids have been studied and the results show that the rate of dissociation increases as the acidity of the solvent acid increases. A general acid catalysis for the thermal dissociation of urea in fatty acids can be shown as,

$$RHNCONHR+R'COOH \rightleftarrows R'COO^-+RNH_2+RNH_2CO^+ \xrightarrow{-H^+} R-N=C=O$$

In this experiment, the kinetic data on the thermal dissociation of ureas in alcohols have been determined in order to gain an understanding of the dissociation of ureas in a very weak acid, as in alcohols.

By the present experiment, benzyl N-phenylcarbamate, m.p. 78°, was obtained on heating 1,3-diphenylurea in a large excess of benzyl alcohol at 170° for 3 hrs. In this case, the mechanism shown by equation (1) and (2) can be considered.

$$C_6H_5HNCONHC_6H_5 \rightleftarrows C_6H_5N=C=O+H_2NC_6H_5 \quad (1)$$

$$C_6H_5N=C=O+HOCH_2C_6H_5 \rightleftarrows C_6H_5HNCOOCH_2C_6H_5 \quad (2)$$

The dissociation reaction of urea is a reversal of the formation reaction and the addition of isocyanate and amine to form urea proceeds very rapidly, when accompanied by a liberation of heat. In eq. (1), the equilibrium between urea and isocyanate—amine is in favor of the left side of the reaction. When urea is heated in alcohol, isocyanate dissociated forms urethane according to eq. (2) which removes a considerable part of isocyanate, the equilibrium will be disturbed and a readjustment must take place. Thereupon an additional amount of urea will dissociate, forming isocyanate and amine until the equilibrium is again established.

Thus, when urea is reacted in a large excess of alcohol, if the reaction (1) is the rate-determining step, the rate of dissociation of urea becomes measurable if one determines the amount of amine formed according to eq. (1).

As has been previously mentioned, 1,3-diphenylurea dissociates more readily than 1,3-dibenzylurea used in the present experiment and the use of the former urea seemed to be convenient for the kinetic study because it dissociates at a lower temperature than the latter. In the titration of aniline formed from the former urea, however, the change in pH at the equivalence point is small, which makes the experiment difficult. Therefore 1,3-dibenzylurea and 1-isopropyl-3,3-diethylurea which form strong bases were used.

## Experimental

**Materials.**—1,3-Dibenzylurea was prepared from benzyl isocyanate[5] and water, m.p. 167°C, recrystallized from ethanol.

1-Isopropyl-3,3-diethylurea was prepared from isopropyl isocyanate[6] and diethylamine, m.p. 66°C,

1) T. Hoshino, T. Mukaiyama and H. Hoshino, *J. Am. Chem. Soc.*, **74**, 3097 (1952).
2) T. Hoshino, T. Mukaiyama and H. Hoshino, This Bulletin, **25**, 392 (1952).
3) T. Mukaiyama and T. Matsunaga, *J. Am. Chem. Soc.*, **75**, 6209 (1953).
4) T. Mukaiyama, S. Ozaki and T. Hoshino, This Bulletin, **27**, 578 (1954).
5) T. Curtius and E. Boetzlen, *J. prakt. Chem.*, **64**, 316 (1901).
6) O. Hambsch, *J. prakt. Chem.*, **125**, 182 (1930).

recrystallized from petroleum ether.

The following alcohols were used: benzyl alcohol, b.p. 112°C at 20 mm.; anisyl alcohol, b.p. 147°C at 20 mm.; 1,2-propanediol b.p. 91°C at 16 mm.; ethylene glycol, b.p. 120°C at 20 mm.; diethylene glycol, b.p. 137°C at 15 mm.; triethylene glycol, b.p. 166°C at 15 mm.; 1,4-butanediol, b.p. 136°C at 24mm.; glycerol, b.p. 185°C at 23 mm.:

**Procedure and Analysis.**—In carrying out the dissociation reaction, a definite quantity of alcohol was measured into a 20 ml. reaction tube having a ground stopper. The reaction tubes were then placed in a thermostat for 20 min. in order to allow them to attain the constant temperature. Thereupon a small glass tube containing a weighed amount of urea was put into the alcohol and shaken hard to dissolve out the urea. At appropriate intervals of time the tubes were removed from the thermostat and the reaction was stopped by rapid cooling with cold water. The temperature control of the reaction thermostat was accurate to ±0.05°C within the temperature range 165—190°C using a tetraline-mercury regulator. The amounts of amine produced were determined by titration with 0.1 normal hydrochloric acid, back-titration being carried out with 0.1 normal sodium hydroxide, using methyl red as indicator.

## Results and Discussion

The steps in the thermal dissociation of urea in alcohol are believed to proceed *via* equations (3) and (4)

$$\mathrm{RHNCONHR} \underset{k_2}{\overset{k_1}{\rightleftarrows}} \mathrm{RNCO}+\mathrm{H_2NR} \qquad (3)$$

$$\mathrm{RNCO}+\mathrm{HOR'} \underset{k_4}{\overset{k_3}{\rightleftarrows}} \mathrm{RHNCOOR'} \qquad (4)$$

The first step is a reversible reaction for which the differential equation is

$$-\frac{d(\mathrm{A})}{dt}=\frac{d(\mathrm{C})}{dt}=k_1(\mathrm{A})-k_2(\mathrm{B})\,(\mathrm{C}) \qquad (5)$$

The symbols *A*, *B* and *C* are used for urea, isocyanate and amine, respectively. The rate of change of the concentration of the isocyanate is the difference between the rates of its formation from urea (3) and urethane (4) and the rates of its reaction to form both urethane (4) and urea (3).

$$\frac{d(\mathrm{B})}{dt}=k_1(\mathrm{A})-k_2(\mathrm{B})\,(\mathrm{C})-k_3(\mathrm{B})\,(\mathrm{D})+k_4(\mathrm{E}) \qquad (6)$$

The symbols *D* and *E* are used for alcohol and urethane.

The rate of reaction of alcohol and isocyanate and that of amine and isocyanate are very fast in comparison with that of dissociation of urea and of urethane. Thus, the concentration of isocyanate remains small and the rate of change of its concentration $\frac{d(\mathrm{B})}{dt}$ is small, compared with the rate $k_1(\mathrm{A})$ at which it is formed from urea. This means in view of eq. (6) that $\frac{d(\mathrm{B})}{dt}$ is a small difference between relatively large quantities so that it may be neglected in comparison with them. Consequently, eq. (6) approximates closely to

$$0=k_1(\mathrm{A})-k_2(\mathrm{B})\,(\mathrm{C})-k_3(\mathrm{B})\,(\mathrm{D})+k_4(\mathrm{E})$$

and $$(\mathrm{B})=\frac{k_1(\mathrm{A})+k_4(\mathrm{E})}{k_2(\mathrm{C})+k_3(\mathrm{D})}$$

Introduction of the values of (B) into eq. (5) leads to

$$-\frac{d(\mathrm{A})}{dt}=\frac{d(\mathrm{C})}{dt}=k_1(\mathrm{A})-k_2\left\{\frac{k_1(\mathrm{A})+k_4(\mathrm{E})}{k_2(\mathrm{C})+k_3(\mathrm{D})}\right\}\cdot(\mathrm{C}) \qquad (7)$$

If *D* is in great excess compared with *A*, the second term in eq. (7) becomes negligible and the amount of amine formed in the reaction directly gives the amount of urea dissociated.

The amount of amine formed according to eq. (3) was determined by the titration. On plotting the logarithm of the amount of amine formed at regular intervals of time a linear relationship was obtained. This indicates that the reaction was of a first order. The rate constant is given by the gradient of such a plot[7], as show in Fig. 1.

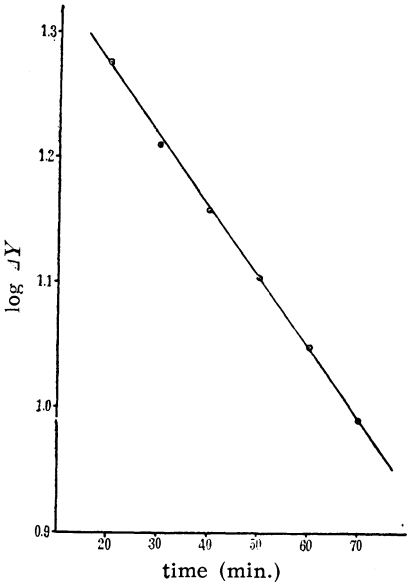



Fig. 1.—The thermal dissociation of 1,3-dibenzylurea in benzyl alcohol at 179.8°C: the plot of log ΔY against time.

7) E. A. Guggenheim, *Phil. Mag.*, 2, 538 (1926).

**(a) 1,3-Dibenzylurea (1 mole) in Alcohol (100 moles*).**—The alcohols were benzyl alcohol, anisyl alcohol, 1,2-propanediol, ethylene glycol, diethylene glycol, triethylene glycol, 1,4-butanediol and glycerol. The results are shown in Table I. The rates were of the first order with respect to 1,3-dibenzylurea. As an example of a typical run, the thermal dissociation of 1,3-dibenzylurea in benzyl alcohol at 179.8°C is shown in Fig. 1.

TABLE I

THE RATE CONSTANTS OF THE THERMAL DISSOCIATION OF 1,3-DIBENZYLUREA IN ALCOHOLS

| Alcohols | $t$°(C) | $k_1 \times 10^2$ (min.$^{-1}$) |
|---|---|---|
| Benzyl Alcohol | 190.5 | 2.86 |
| | 185.7 | 2.00 |
| | 179.8 | 1.25 |
| | 175.3 | 0.80 |
| | 166.7 | 0.46 |
| Ethylene Glycol | 185.2 | 2.63 |
| | 179.1 | 1.73 |
| | 176.0 | 1.32 |
| | 173.5 | 1.12 |
| | 166.4 | 0.56 |
| Glycerol | 186.3 | 2.61 |
| | 184.5 | 2.28 |
| | 180.2 | 1.70 |
| | 177.5 | 1.34 |
| | 173.3 | 0.95 |
| Anisyl Alcohol | 184.5 | 2.38 |
| Triethylene Glycol | 184.5 | 1.66 |
| Diethylene Glycol | 184.5 | 1.37 |
| 1,2-Propanediol | 180.4 | 1.14 |
| 1,4-Butanediol | 184.7 | 0.967 |

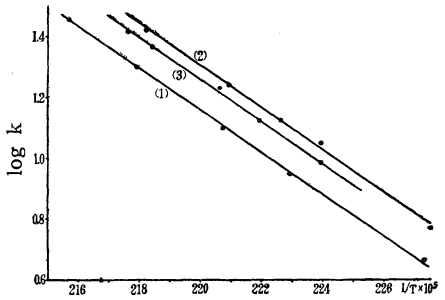



Fig. 2. The thermal dissociation of 1,3-dibenzylurea in benzyl alcohol (1), ethylene glycol (2) and glycerol (3): the plot of 1/T against log K.

The kinetic data were further analyzed by means of the Arrhenius equation

$$\ln k = \ln A - (E/RT)$$

and by the absolute rate equation

$$\ln (k/T) = \ln R\kappa/Nh + \Delta S^{\neq}/R - \Delta H^{\neq}/RT$$

The transmission coefficient, $\kappa$, was set equal to unity. The calculated kinetic and thermodynamic functions are collected in Table II.

In Table III, the percentage of dissociated urea in the thermal dissociation of 1,3-dibenzylurea (1 mole) in benzyl alcohol, ethylene glycol and glycerol (each alcohols 100 moles) are shown against time.

As is seen from Table III, the amount of dissociated urea in ethylene glycol is nearly twice that in benzyl alcohol and that in glycerol is nearly 2.5 times that in benzyl alcohol, while the rate constants, as measured by the amount of benzylamine produced, of dissociation in these three alcohols are nearly equal. This suggests that the velocities of dissociation of urea in alcohols are dependent on the concentration of the hydroxylic group in the solvent alcohols.

The result can be explained by postulating

TABLE II

KINETIC AND THERMODYNAMIC FUNCTIONS FOR THE THERMAL DISSOCIATION OF 1,3-DIBENZYLUREA IN ALCOHOLS

| Alcohol | $T$° | $A \times 10^{11}$ (sec.$^{-1}$) | $E$(kcal.) | $\Delta H^{\neq}$(kcal.) | $\Delta S^{\neq}$(cal. mol.$^{-1}$ deg.$^{-1}$) | $\Delta E^{\neq}$(kcal.) |
|---|---|---|---|---|---|---|
| Benzyl alcohol | 458.9 | 4.62 | 31.8 | 32.2 | −6.02 | 34.4 |
| Ethylene glycol | 458.4 | 1.69 | 30.6 | 30.6 | −8.01 | 34.3 |
| Glycerol | 457.7 | 2.42 | 31.0 | 30.7 | −7.30 | 34.3 |

TABLE III

THE PERCENTAGE OF DISSOCIATED 1,3-DIBENZYLUREA (1 MOLE) IN ALCOHOLS (100 moles) *vs.* TIME

| Solvent | Temperature (°C) | Time (min.) 20 | 40 | 60 | 80 | 100 | Rate constant ($k_1 \times 10^2$) (min.$^{-1}$) |
|---|---|---|---|---|---|---|---|
| Benzyl alcohol | 185.7 | 10.4 | 19.2 | 25.5 | 30.1 | 33.0 | 2.00 |
| Ethylene glycol | 185.2 | 17.1 | 38.2 | 49.9 | 56.7 | 61.2 | 2.63 |
| Glycerol | 184.5 | 26.9 | 48.3 | 63.0 | 72.9 | 80.8 | 2.28 |

the formation of an intermediate complex in equilibrium with urea and alcohol as shown in eq. (8), which dissociates into an isocyanate, an amine and alcohols *via* the rate-determing step according to eq. (9)

$$\text{urea}+\text{alcohols} \rightleftarrows (\text{urea-alcohols}) \quad (8)$$

$$(\text{urea-alcohols}) \overset{k_1}{\rightleftarrows} \text{isocyanate}+\text{amine}+\text{alcohols} \quad (9)$$

$$\text{isocyanate}+\text{alcohol} \rightleftarrows \text{urethane} \quad (10)$$

$$\text{urethane}+\text{alcohols} \rightleftarrows (\text{urethane-alcohols}) \quad (11)$$

The concentration of the complex is given by the following equation,

$$(C_{\text{complex}})=K\cdot(C_{\text{urea}})\cdot(C_{\text{alcohol}})$$

and the velocity of dissociation is therefore expressed as,

$$v=k_1\cdot K\cdot(C_{\text{urea}})\cdot(C_{\text{alcohol}})$$

**(b) 1-Isopropyl-3,3-diethylurea (1 mole) in Alcohols (100 moles).**—The alcohols were benzyl alcohol, anisyl alcohol, diethylene glycol, triethylene glycol and glycerol. The results are shown in Table IV. The rates

TABLE IV
THE RATE CONSTANTS OF THE THERMAL DISSOCIATION OF 1-ISOPROPYL-3,3-DIETHYLUREA IN ALCOHOLS

| Alcohols | $t$(°C) | $k\times10^2$ (min.$^{-1}$) |
|---|---|---|
| Benzyl alcohol | 169.7 | 0.99 |
| Anisyl alcohol | 169.7 | 1.20 |
| Ethylene glycol | 184.5 | fast |
| Glycerol | 169.7 | 1.53 |
| Triethylene glycol | 184.5 | 1.04 |
| Diethylene glycol | 184.5 | 2.00 |

were of the first order with respect to 1-isopropyl-3,3-diethylurea.

In the process of dissociation of ureas, the one nitrogen atom of urea accepts a proton to form an amine and the other nitrogen atom donates a proton to form an isocyanate.[4] The consideration leads to the conclusion that there are two roles of the solvents which control the dissociation.

(a) Ability of solvents to accept a proton from a urea molecule, namely basicity.

(b) Ability of solvents to donate a proton to a urea molecule, namely acidity.

As to the effect of the solvents, it is shown by the present experiment that the rate of dissociation increases in the series,

ethylene glycol>glycerol>anisyl alcohol>benzyl alcohol>1,2-propanediol>diethylene glycol, triethylene glycol>1,4-butanediol.

The rates of dissociation in these eight alcohols differ slightly; however, the rates of dissociation in ethylene glycol and in glycerol are faster than in anisyl alcohol and that in anisyl alcohol is faster than in benzyl alcohol. The basicities of these four alcohols are expected to increase in the following order, which coincides with that of the rates of dissociation.

ethylene glycol>glycerol>anisyl alcohol>benzyl alcohol.

This will lead to the consideration that the stronger the basicities of alcohols the faster the rates of dissociation.

Also, the fact that the rate of dissociation in ethylene glycol is faster than in all other dihydric alcohols (i.e., 1,2-propanediol, diethylene glycol, triethylene glycol and 1,4-butanediol) will show that the larger the molecular size the slower the rates of dissociation.

In order to compare the solvent effects of fatty acids and of alcohols on the thermal dissociation of ureas, the rate constants of the dissociation of 1,3-dibenzylurea and 1-isopropyl-3,3-diethylurea in fatty acids described in the previous report[4] are listed in Table. V.

TABLE V
THE RATE CONSTANTS OF THE THERMAL DISSOCIATION OF 1,3-DIBENZYLUREA AND 1-ISOPROPYL-3,3-DIETHYLUREA IN FATTY ACIDS
$k\times10^2$ (min.$^{-1}$), $t$(°C).

| Fatty acid \ Urea | 1.3-Dibenzylurea | 1-Isopropyl-3,3-diethylurea |
|---|---|---|
| $n$-Butyric acid | 1.27 (139.6) | 3.15 (139.45) |
| $n$-Caproic acid | 2.68 (155.0) | 6.2 (155.0) |
| $n$-Capric acid | 2.70 (155.0) | 3.19 (155.0) |
| Phenylacetic acid | 3.85 (154.9) | very fast (I54.9) |
| Benzoic acid | 0.418 (155.0) | 1.60 (155.1) |

It can be said that these two ureas dissociate more easily in fatty acids than in alcohols. Even in benzoic acid, in which the rates of dissociation of ureas are one-third or one-fourth of those in the other acids, the dissociation proceeds more easily than in alcohols.

This shows that in the process of dissociation of urea the ability of solvents to donate a proton to a urea molecule is an important factor. As the alcohol is a very weak acid, the ability to donate a proton to a urea molecule is so small that the rates in alcohols are slower than in fatty acids.

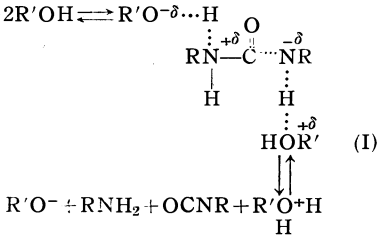
As the basicities of alcohols are nearly the same as those of ureas, in the case of dissociation in alcohols, alcohols would act as a base to accept a proton. Together with the facts above mentioned that the stronger the

basicity of alcohol the faster the dissociation, it can be said that in the process of dissociation of ureas in alcohols the deprotonation by the solvent alcohols plays an important role in determining reaction rate.

As to the effect of substituents, it is shown by the present experiment that 1-isopropyl-3,3-diethylurea dissociates more readily than 1,3-dibenzylurea in all alcohols used. Similar results were also found in the case of dissociation in fatty acids.

The facts show that the ability of one nitrogen atom in urea to accept a proton and that of the other to donate a proton are important factors of the dissociation. In these two ureas, the basicities of the nitrogen atoms in 1-isopropyl-3,3-diethylurea are stronger than those in 1,3-dibenzylurea. If the solvent alcohol acts only as a base, the order of the reactivities of the two ureas must be reversed. The experimental fact means that the process of protonation of urea by solvent alcohol also controls the rate of dissociation.

These facts will be explained by considering the intermediate complex containing two alcohol and one urea molecules as has been mentioned above. The mechanism is identical with that proposed in the dissociation of ureas in fatty acids[4]. One alcohol in the complex (I) acts as a base to accept a proton and the other alcohol acts as an acid to donate a proton at the same time.




(I)

The consideration on the experimental results of the thermal dissociation of ureas in fatty acids and in alcohols leads to the conclusion that the dissociation proceeds very rapidly in a solvent which can acts as a base and as a strong acid at the same time. The basicity of the solvent may be suitable when it is a slightly stronger base than urea and the acidity of it may be favorable when it is a very strong acid. Thus, when the dissociation of ureas in such a solvent as aminophenylacetic acid is measured, the rate of dissociation would be very fast.

## Summary

The rate constants of the thermal dissociation of 1,3-dibenzylurea and 1-isopropyl-3,3-diethylurea in alcohols were determined.

The rates of dissociation in fatty acids are faster than those in alcohols and it can be said that the process of protonation of ureas by solvents plays an important role in the dissociation.

In the case of dissociation in alcohols, the reaction seems to proceed by a base catalysis. And the intermediate complex containing two alcohol and one urea molecules was considered. The experimental results were reasonably explained by the proposed mechanism.

The author is indebted to Dr. T. Hoshino for his helpful discussion and Mr. Y. Fujita, Mr. T. Kurachi and Mr. H. Yoshizawa for their help during the course of this experiment.

*Department of Physics and Chemistry,*
*Gakushuin University,*
*Tokyo*

# *Heats of Combustion and Formation of Some Methoxy-polysilanes and -polysiloxanes*: Si-O *Bond Energy**

By Toshio TANAKA and Takeo WATASE

(Received December 15, 1954)

In the preceding paper[1], data on the heats of combustion and formation of some organosilicon compounds, containing alkyl or phenyl group, were presented. The compounds measured therein have such a large number of C-C and C-H bonds, etc., that the bond energies between silicon and other elements calculated from the results turn out to be small differences between large quantities, and may be unreliable. In order to derive the bond energies between silicon and other elements, it is desirable to measure the heat of combustion of organosilicon compounds having the least possible number of C-C and C-H bonds, etc., in the molecule. In the present work the heats of combustion of some methoxy-polysilanes and -polysiloxanes have been measured, and the heats of formations of them and Si-O bond energy have been calculated therefrom.

## Experimental

**Materials.** — Hexamethoxy disilane $(CH_3O)_3Si\cdot Si(OCH_3)_3$ was synthesized by methanolysis of hexachlorodisilane.[2] Tetramethoxysilane $Si(OCH_3)_4$, hexamethoxydisiloxane $(CH_3O)_3Si\cdot O\cdot Si(OCH_3)_3$ and octamethoxytrisiloxane $(CH_3O)_3Si\cdot O\cdot Si(OCH_3)_2\cdot O\cdot Si(OCH_3)_3$ were prepared by methanolysis of the corresponding polychloro-silane and -siloxanes, respectively. These hexachlorodisiloxane and octachlorotrisiloxane were obtained from the distillation residue of industrial tetrachlorosilane with careful fractionation through a helices packed-column of about 20 plates. ($Si_2OCl_6$ b.p. 137°C, Cl % calcd. 74.7, found 74.6; $Si_3O_2Cl_8$ b.p. 73°C/13 mm, Cl % calcd. 70.9, found 70.8.). These compounds prepared by methanolysis could not be freed from a trace of chlorine by the fractional distillation, so careful dehydrochlorination using dry ammonia[2] or sodium carbonate[3] was carried out. After that these products were carefully distilled through a Stedman column of about 30 theoretical plates. Physical constants and analytical data on these samples are shown in Table I.

TABLE I

DATA ON THE SAMPLES USED FOR COMBUSTION MEASUREMENTS

| Formula | b.p. °C/mm Hg | $d_4^{20}$ | $n_D^{20}$ | Si % Found | Si % Calcd. |
|---|---|---|---|---|---|
| $Si(OCH_3)_4$ | 122/760 | 1.034 | 1.3688 | 18.48 | 18.45 |
| $Si_2O(OCH_3)_6$ | 118.5/30 | 1.122 | 1.3818 | 21.77 | 21.74 |
| $Si_3O_2(OCH_3)_8$ | 95–6/2 | — | — | 23.17 | 23.12 |
| $Si_2(OCH_3)_6$ | 98/20 | 1.095 | 1.4070 | 22.99 | 23.18 |

**Calorimetry.**—The apparatus was the Nenken-type adiabatic bomb calorimeter, incorporating a 300 ml. stainless steel-made bomb and Beckmann thermometers. The temperatures in the calorimeter vessel and water jacket were observed with an accuracy of 0.001°C as described previously[1].

For the complete burning of liquid organosilicon compounds containing alkyl or phenyl group, we previously described the technique using a glass ampoule and promotor.[1] However, the poly-silanes and -siloxanes containing only methoxy group are readily burnt completely by themselves without ampoule, by the ignition of the liquid pool in the crucible.

The procedure used in the combustion experiments was the same as previously described.[1] The calibration experiments of the calorimeter were carried out at a temperature of 20°C. (based on the heat of combustion of benzoic acid at 20°C=6319.0 cal./g.[4], and its water equivalent value was determined to be 2494 cal./degree (relative mean deviation ±0.1%).

By the complete burning of the organosilicon compounds, gaseous carbon dioxide, liquid water and silicon dioxide were involved as the end products. The completeness of combustion was ascertained by visual inspection of the bomb contents for traces of black or yellow materials, and sometimes by the chemical analysis. Four to six combustion measurements were made with each liquid sample, the results of which are recorded in Table II.

TABLE II

| Formula | Heat of combustion at constant volume, cal./g. | | | | | | Mean |
|---|---|---|---|---|---|---|---|
| $Si(OCH_3)_4$ | 4548 | 4560 | 4556 | 4548 | 4553 | 4554 | 4553 |
| $Si_2O(OCH_3)_6$ | 4086 | 4084 | 4086 | 4085 | — | — | 4085 |
| $Si_3O_2(OCH_3)_8$ | 3836 | 3832 | 3840 | 3838 | 3833 | — | 3836 |
| $Si_2(OCH_3)_6$ | 4731 | 4743 | 4738 | 4735 | 4740 | — | 4737 |

Each deviation from the mean is somewhat high compared with modern precision techniques, but

* A part of this paper was published in Letter section of *J. Chem. Phys.*, 22, 1268 (1954).

1) T. Tanaka U. Takahashi, R. Ōkawara and T. Watase, This Bulletin, 28, 15 (1954).

2) R. Ōkawara and T. Tanaka, This Bulletin, 27, 119 (1954).

3) R. Ōkawara, T. Tanaka and I. Ishimaru, This Bulletin, 27, 45 (1954).

4) Calculated from the results of Prosen and Rossini, *J. Research NBS.*, 33, 439 (1944).

of sufficient precision for bond energy term purpose in view of the other uncertainties involved.

## Results and Discussion

Table III contains the summary of the data for the heats of combustion of four organosilicon compounds with some important thermal data calculated therefrom.

The value of the bomb process was calculated per mole and corrected to the standard constant-volume process where the reactants were at 1 atm. pressure by means of Washburn's equation.[5] The energies evolved in this hypothetical standard process were denoted in Table III by the symbol $-\Delta U_R$. From this quantity the heat evolved in the isobaric process at 1 atm. pressure, $-\Delta H_c$, was obtained by addition of the proper work term. The heats of formation, $-\Delta H_f$, of these compounds from the standard elements (gaseous $H_2$ and $O_2$, graphitic C and metallic Si) were calculated from $-\Delta H_c$ by using data $-68.32$,[6] $-94.05$[6] and $-208.14$[7] kcal./mol. for the heats of formation of water, carbon dioxide and amorphous silica, respectively.

Values of 52.1 and 59.2 kcal./g. atom are now generally accepted for the heats of atomization of hydrogen and oxygen, respectively.[8] The corresponding value for carbon may still be regarded as a matter of some controversy. Direct and various indirect measurements give varying values which fall into three main groups centering around 124,[9] 140[10] and 170[11,12] kcal./g. atom, later evidence tending strongly toward the latter two values rather than the former. Here the actual value 171.7 kcal./g. atom[8,12] was adopted. The heat of atomization of silicon is more dubious. In the present work the value 89.9 kcal./g. atom presented by Baughan[13] was adopted. The heats of formation in the gaseous state from monoatomic gases, $\Delta E$, were obtained from $\Delta H_f$ of these compounds of formula $Si_aC_bH_cO_d$ by use of the formula:

$$\Delta E = \Delta H_f - 89.9a - 171.7b - 52.1c - 59.2d - H_v$$

The heats of vaporization of these compounds, $H_v$, were estimated from Trouton's rule. The values $\Delta E$ of the four compounds are listed in Table III.

**Si-O bond energy.**—The value $\Delta E$ may be shown by the following formula:

$$\Delta E = pE_{si-o} + qE_{si-si} + rE_{c-o} + sE_{c-H}$$

In this equation $E$ represents the energy value of bond corresponding to each suffix and the factors $p$, $q$, $r$ and $s$ the number of bonds in the molecules coming into question. As the energy terms of C-O and C-H bonds are well known, Si-O bond energy can be evaluated. In the case of hexamethoxydisilane, Si-Si bond energy was considered as equal to the negative value of half of atomization heat for silicon. The Si-O bond energy computed in this manner is shown in Table III, using 98.9[14] and 84.1[15] kcal./mol. for C-H and C-O bond energies, respectively.

The earlier energy term value for the Si-O bond, derived from the heat of formation of silica, was given by Pauling as 89.3[16], by Syrkin and Dyatkina as 89[17], by Paul as 104[18] and by Gilman and Dunn as 104[19] kcal./mol. From the consideration of repulsive interactions of the bonding orbital of one with the inner shell of the other, Pitzer[20] estimated for Si-O bond energy to be 106 kcal./mol., using the value 90 kcal./g.

TABLE III

HEAT OF COMBUSTION AND FORMATION AND Si-O BOND ENERGY (kcal./mol.)

| Formula | Mole. wt. | $-\Delta U_R$ | $-\Delta H_c$ | $-\Delta H_f$ | $-\Delta E$ | $-E_{si-o}$ |
|---|---|---|---|---|---|---|
| $Si(OCH_3)_4$ | 152.23 | 693 | 694 | 300 | 1929 | 102 |
| $Si_2O(OCH_3)_3$ | 258.38 | 1054 | 1056 | 539 | 3090 | 101 |
| $Si_3O_2(OCH_3)_8$ | 364.54 | 1397 | 1399 | 798 | 4271 | 102 |
| $Si_2(OCH_3)_6$ | 242.38 | 1148 | 1150 | 445 | 2937 | 101 |

5) E. W. Washburn, *Bur. Standards J. Research*, **10**, 525 (1933).
6) Wagman, Kilpatrick, Taylor, Pitzer and Rossini, *J. Research NBS.*, **34**, 143 (1945).
7) R. Thompson, *J. Chem. Soc.*, **1953**, 1908.
8) "Selected Values of Chemical Thermodynamics Properties", Nat. Bur. Stand., Washington, (1950).
9) G. Herzberg, *J. Chem. Phys.*, **10**, 306 (1942); L.H. Long and R.G.W. Norrish, *Proc. Roy. Soc.* (*London*), **A187**, 337 (1951).
10) F.H. Field, *J. Chem. Phys.*, **19**, 793 (1951); Th. Doehard, P. Goldfinger and F. Waelbroeck, ibid., **20**, 757 (1952).
11) G. Glockler, ibid., **19**, 124 (1951).
12) Brewer, Gilles and Jenkins, ibid., **16**, 797 (1948).
13) E.C. Baughan, *Quart. Rev.*, **7**, 103 (1953).
14) Calculated by the method of least squares from the heats of for mation of lower members (from thanee to hexane) in paraffin series, other than methane; E. J. Prosen, W. E. Johnson and F. D. Rossini, *J. Research NBS.*, **37**, 51 (1946), and their preceding papers.
15) Calculated from the heat of formation of dimethyl ether (H.A. Skinner, *Trans. Farad. Soc.*, **41**, 645 (1945).) using above C-H bond energy.
16) L. Pauling, "The Nature of the Chemical Bonds", Cornell Univ. Press, Ithaca, New York, (1940).
17) J. K. Syrkin and M. E. Dyatkina, "Structure of Molecules", Butterworth, (1950).
18) Paul, "Principle of Chemical Thermodynamics", McGraw-Hill, (1951).
19) H. Gilman and G.E. Dunn, *Chem. Revs.*, **52**, 77 (1953).
20) K.S. Pitzer, *J. Am. Chem. Soc.*, **70**, 2140 (1948).

atom for the heat of atomization of silicon and Pauling's electronegativity formula. The value 104 kcal./mol. was also calculated by Thompson[7] from $\Delta H_f$ for amorphous silica. The only Si-O bond energy derived from the heats of formation of organosilicon compounds was proposed by Thompson[7] as 117 kcal./mol. However, his combustion experiments contain considerable deviations, so we are not satisfied with that energy value. Also, from the molecular orbital calculation of ionic resonance energy the energy value of 118 kcal./mol. was obtained by Pearson.[21]

The Si-O bond energy term derived here from four organosilicon compounds is in good agreement and slightly lower than the value of 104 kcal./mol. for that bond energy in amorphous silica, calculated from the following data: $\Delta H_{atom.}$ for Si=89.9, $\Delta H_{atom.}$ for O=59.2 and $\Delta H_f$ for amorphous silica= −208.14 kcal./mol. There is also such an example between the C—C bond energies for diamond structure and paraffin series compounds.[16]

21) P.G. Pearson, *J. Chem. Phys.*, **17**, 969 (1949).

**Summary**

1. The heats of combustion of the following four compounds have been measured at 20°C and at constant volume: Tetramethoxysilane, hexamethoxydisiloxane, octamethoxytrisiloxane and hexamethoxydisilane.

2. From these combustion results the corresponding heats of combustion and formation at constant pressure and Si-O bond energy have been calculated, and it has been found that the Si-O bond energy in methoxy-polysilanes and -polysiloxanes was slightly lower than that in amorphous silica.

The authors wish to express their sincere thanks to Mr. R. Ōkawara for his helpful advice in the preparation of samples. The cost of this research was partly defrayed from the Ministry of Education, to which the authors' thanks are due.

*Department of Applied Chemistry,*
*Faculty of Engineering,*
*Osaka University, Osaka*

# *The Ultra-violet Absorption Spectrum of Pyridine N-oxide*

By Mitsuo ITO and Norisuke HATA*

(Received December 21, 1954)

## Introduction

Organo-chemical properties of pyridine N-oxide have been investigated by Ochiai and his coworkers[1]. Recently, the ultra-violet absorption spectra of these compounds in solutions have been measured by Hirayama and Kubota[2,3]. Generally, in the absorption spectra of $\pi$-conjugated compounds containing the heteroatoms, e.g., pyridine and diazines etc., there occur $n$-$\pi^*$ electronic transitions as well as $\pi$-$\pi^*$ transitions[4,5]. In the present investigation, the absorption bands due to these two electronic transitions are observed with pyridine N-oxide both in solution of non-polar solvent and in vapor, and the effects of proton donors on these absorption bands are discussed.

## Experimental

**Solution Spectrum.**—The spectrum of pyridine N-oxide in various solutions was measured with a Beckman quartz spectrophotometer model DU, using a fused quartz cell of 1 cm. path. N-hexane, ethyl alcohol and water were used as solvents. Measurements were limited to the region of wavelength shorter than 350 m$\mu$.

**Vapor Spectrum.**—Ultra-violet absorption spectra of pure pyridine N-oxide vapor and of a mixture with ethyl alcohol in the vapor phase were photographed with a medium quartz spectrograph having a linear dispersion of about 16 Å per mm. at 3,100 Å. The absorption cell was a quartz tube 40 cm. in length, and 3 cm. in diameter, to which a side recess was attached at the middle part. The sample sealed in a thin-walled glass ampoule was inserted in the side recess, and then the cell was evacuated to the pressure of about $10^{-3}$ mm Hg. After sealing off the cell, the ampoule was broken, the vapor filling the cell at pressures corresponding to the temperatures of the sample.

* Present address: Department of Pharmacy, Nagasaki University, Nagasaki.

1) E. Ochiai, *J. Org. Chem.*, **18**, 534 (1953).
2) H. Hirayama and T. Kubota, *Annual Reports of* Shionogi *Research Laboratory*, **2**, 47 (1952).
3) T. Kubota, *J. Pharm. Soc. Japan*, **74**, 831 (1954).
4) M. Kasha, *Discus. Farad. Soc.*, **9**, 14 (1951).
5) F. Halverson and R.C. Hirt, *J. Chem. Phys.*, **19**, 711 (1951).

In the case of mixed vapor, conc. alcohol solution of pyridine N-oxide (mole fraction, about 0.25) was used as the sample. Exposures were made against the hydrogen continium, varying the temperature of the sample from 0° to 110°C for the pure vapor, and from 10° to 120°C for the vapor mixture.

## Results and Discussion

**Solution Spectrum.**—The absorption curves for various solutions are shown in Fig. 1.

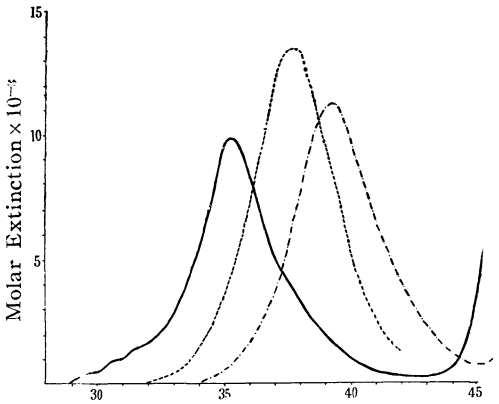



Fig. 1. Absorption spectrum of pyridine N-oxide.
——— *n*-hexane solution
------ ethyl alcohol solution
—·—·— water solution

As to the absorption of *n*-hexane solution, it appears that there are two absorption regions between 28,000 and 44,000 $cm^{-1}$; one of which is weak, accompanying a fine structure on longer wave-length end, and the other stronger having the maximum at 35,200 $cm^{-1}$ (280 $m\mu$).

When either alcohol or water is used as the solvent, the absorption in the long wave-length region is not observed and the maximum shifts toward shorter wave-length side. Such a spectral behavior in pyridine N-oxide, supporting the assignment that weak long wave-length absorption is an $n$-$\pi^*$ transition and the strong shorter wave-length absorption a $\pi$-$\pi^*$ transition, may be explained as follows.

Pyridine N-oxide molecule has two pairs of 2p non-bonding electrons on the oxygen atom, one of which is considered to be in conjugation with the $\pi$-electron system of pyridine ring and the other to remain as a non-bonding pair. Generally, since the energy level of the non-bonding orbital lies above the highest $\pi$-level in the ground state, the $n$-$\pi^*$ transition appears weakly in a longer wave-length region than the $\pi$-$\pi^*$ transition. When proton donor such as alcohol or water is used as the solvent, the oxygen non-bonding orbital is largely stabilized in energy as a result of the formation of hydrogen bond[3]. Consequently, the $n$-$\pi^*$ absorption disappears completely. At the same time, since the $\pi$-electron configuration will be perturbed by the formation of such a hydrogen bond, the $\pi$-$\pi^*$ absorption shifts considerably to shorter wave-length, which is in agreement with our observation.

In order to estimate each absorption contribution from the $n$-$\pi^*$ or $\pi$-$\pi^*$ transition the peak analysis was made for the absorption of *n*-hexane solution according to the procedure given by Stephenson[6]. According to the well known equation,

$$f = 4.32 \times 10^9 \int \epsilon d\nu,$$

the oscillator strengths of the $n$-$\pi^*$ and $\pi$-$\pi^*$ transitions are calculated from the areas under the curves (a) and (b) in Fig. 2 respectively, their values being shown in Table I together with those for the other compounds[3,7]. As found from the table, while

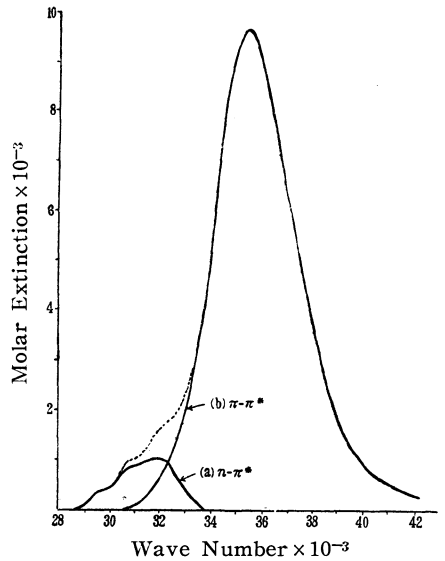



Fig. 2. Peak analysis of the absorption of *n*-hexane solution.

TABLE I
OSCILLATOR STRENGTH OF $n$-$\pi^*$ AND $\pi$-$\pi^*$ TRANSITIONS

| Compound | $f(n\text{-}\pi^*)$ | $f(\pi\text{-}\pi^*)$ | $\frac{f(n\text{-}\pi^*)}{f(\pi\text{-}\pi^*)}$ |
|---|---|---|---|
| Pyridine N-oxide | 0.012 | 0.173 | 0.079 |
| Pyridine[6] | 0.003 | 0.041 | 0.073 |
| Benzaldehyde[7] | 0.0006 | 0.02 | 0.030 |
| Acetophenone[7] | 0.0006 | 0.014 | 0.043 |
| P-benzoquinone[7] | 0.0003 | 0.008 | 0.038 |

the $f$ values for the $n$-$\pi^*$ and $\pi$-$\pi^*$ transitions are of considerably different orders for the

6) H.P. Stephenson, *J. Chem. Phys.*, 22, 1077 (1954).
7) H.L. McMurry, *J. Chem. Phys.*, 9, 241 (1941).

different compounds, their ratio is in the same order of $10^{-2}$ for pyridine N-oxide as for the other compounds. This also gives supporting evidence for the assignment with respect to the $n$-$\pi^*$ and $\pi$-$\pi^*$ transitions mentioned above.

**Vapor Spectrum.**—The absorption spectra at different temperatures for pure and mixed vapors are sketched in Fig. 3 and Fig. 4, respectively. In the figures the lines show the main absorption bands and their heights the relative intensities, the shaded portions indicating regions of continuous absorption. The calculated vapor pressure values of pyridine N-oxide are given for the various temperatures in the last columns of Fig. 3 and Fig. 4.

In the region 29,000 $cm^{-1}$~48,000 $cm^{-1}$ there are four absorption regions (I, II, III and IV regions in Fig. 3 or Fig. 4). The longest

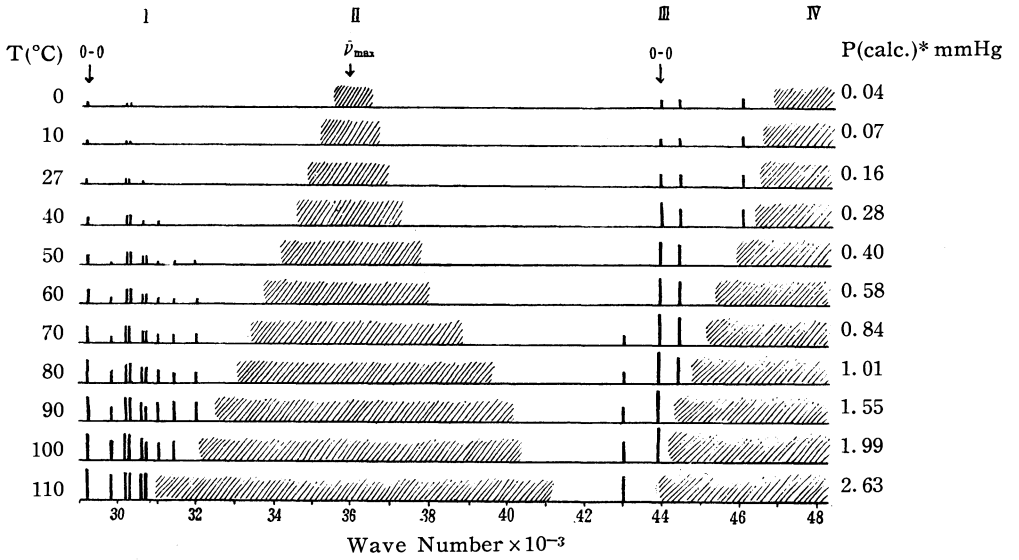



Fig. 3. Schematic absorption spectrum of pyridine N-oxide in pure vapor.
* Calculated by using the relation log $P \propto 1/T$ and the boiling points of pyridine N-oxide (135° at 5 mm Hg, 113°C at 3mm Hg).

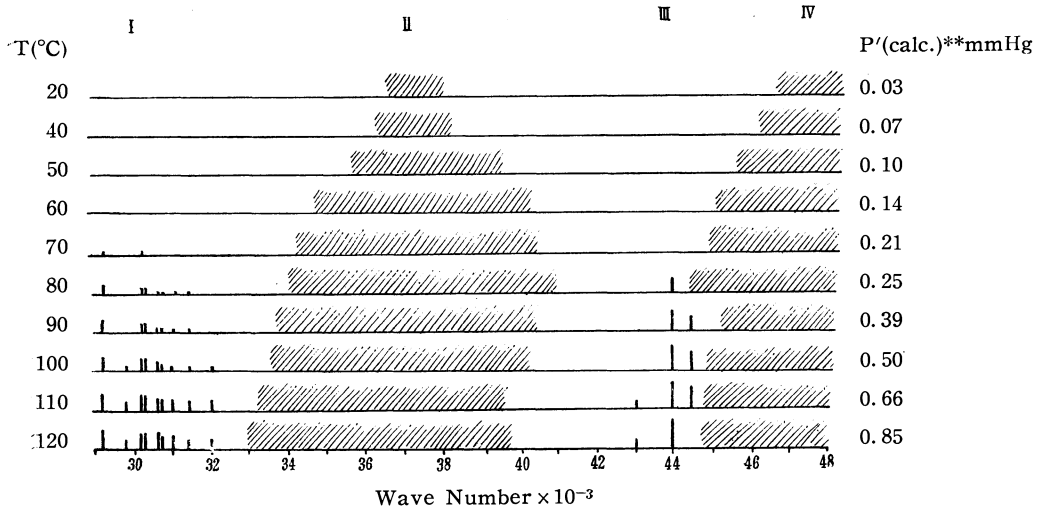



Fig. 4. Schematic absorption spectrum of pyridine N-oxide in vapor mixture with alcohol.
** The partial vapor pressure of pyridine N-oxide P′ is approximately given by $P' = G \times P$, where G is the mol fraction of pyridine N-oxide in alcohol solution and P the vapor pressure of pyridine N-oxide.

wave-length region I is of a very sharp vibrational structure having the O-O band at 29,291 $cm^{-1}$ [8], corresponding to the $n$-$\pi^*$ absorption of $n$-hexane solution. The next, region II is continuous having its absorption maximum at about 35,960 $cm^{-1}$, corresponding to the $\pi$-$\pi^*$ absorption of $n$-hexane solution. These spectral features fit in with Kasha's distinguishing criteria[4] that in vapor spectrum $n$-$\pi^*$ absorption generally consists of very sharp bands and $\pi$-$\pi^*$ absorption moderately broad or continuous bands. Thus, in accordance with the assignment for the solution spectrum, we confirm that the region I is an $n$-$\pi^*$ transition and the region II a $\pi$-$\pi^*$ transition.

Similarly, the region III is accompained by an extremely sharp vibrational structure having the O-O band at 43,884 $cm^{-1}$ [8] and the region IV is continuous. These spectral appearances suggest that the former is an $n$-$\pi^{**}$ transition and the latter is a $\pi$-$\pi^{**}$ transition, where $\pi^{**}$ is a $\pi$-level lying above the $\pi^*$-level related to the regions I and II.

Comparing the spectra of the pure vapor and the vapor mixture, we may notice that: (1) at low temperatures the $n$-$\pi^*$ and $n$-$\pi^{**}$ absorptions appear evidently in the former, but they are not observed in the latter, and (2) the $\pi$-$\pi^*$ absorption in vapor mixture, lying at a little shorter wave-length than that for pure vapor at low temperatures, approaches to the position for pure vapor with increasing temperature. This spectral behavior is almost the same as in the case of solution spectrum and shows that, even in the state of vapor, pyridine N-oxide molecule forms hydrogen bond with alcohol molecule at low temperatures[3]. With increasing temperature, the hydrogen bond is broken due to thermal motion, and then the spectral feature of vapor mixture becomes identical with that of pure vapor.

8) The detailed virbrational analysis is to be reported shortly.

## Summary

The near ultra-violet absorption spectrum of pyridine N-oxide was measured in solution and vapor, and we concluded from the considerations of solvent effect, oscillator strength and the feature of vapor spectrum that the two of the four absorption regions are due to the excitation of the non-bonding electron, the others due to the excitation of $\pi$-electron. From the spectral behavior of pyridine N-oxide, it is also concluded that the pyridine N-oxide molecule forms hydrogen bond with alcohol or water molecule in vapor and solution state.

The authors wish to express their hearty thanks to Prof. S. Imanishi for his kind guidance and valuable suggestions in this research. They are also indebted to Prof. G. Kobayashi of Nagasaki University for his helpful advice and to Mr. H. Umezu for his assistance in the experimental part of this research.

*Department of Chemistry, Faculty of Science, Kyushu University, Fukuoka*

# *On the Electro-Osmotic Water Transport Through Cation—Exchange Resin Membranes*

By Yoshio ODA and Tadashi YAWATAYA

(Received December 13, 1954)

## Introduction

When ion-exchange resin membranes are used as the ionic permselective diaphragms of electrochemical operations, the movement of water takes place through the membranes simultaneously with the ionic migration. This phenomenon seems important from the practical point of view, since it governs the maximum concentration of the electrolyte solution attainable by means of electrolysis, using the membrane. Also, as it concerns the transport number and electric conductivity of the membrane, the study of the phenomenon is expected to supply valuable clues for clarifying the fundamental properties of the ion-exchange resins.

There are three ways of transference of a solvent through a membrane, according to the driving forces which cause it. They are classified as follows.

(a) Transference due to osmotic pressure.

(b) Transference due to the electric potential difference between the two surfaces of the membrane.

(c) Transference due to the difference of hydrostatic pressure, if present.

The item (a), which takes place in the case where the solutions of both sides of the membrane differ in concentration, was previously studied by the authors and reported elsewhere[1].

As the item (b) seems to be especially important in the ordinary applications, the present work is devoted to its study.

The water transference through a membrane caused by electric potential difference has been known as the electro-osmotic phenomenon and already explored to a considerable extent[2]. These previous works were, however, undertaken using mostly very dilute solutions, and lack the data for the range of comparatively high concentration, up to several normals, despite the fact that the range is expected to be the most prosperous field of applying ion-exchange resin membranes.

Although the electro-osmosis in the case where a membrane is inserted between solutions of different concentrations is important for practical purposes, the present study deals with, as the most simple ones, the cation-exchange resin membranes placed between solutions of the same kind and equal concentration.

## Experimental

**Ion-exchange Resin Membranes.**—The cation-exchange resin membranes used in the experiments are mainly of sulfonated phenol resin type and prepared by Dr. M. Sekino and K. Kōno in the Research Laboratory of Asahi Glass Co. In addition to these a cation-exchange resin membrane of a similar type, Nepton CR-51, which had been furnished by Ionics Inc., U.S.A., was used.

The thickness of the membranes varied from 0.9 to 1.2 mm when swollen.

These membranes were thoroughly equilibrated with the solutions, to be used for measurements at least for 24 hours by repeatedly changing the solution.

**Apparatus.**—A glass cell composed of two half cells as shown in Fig. 1 was used, and a sample membrane was mounted between the flanges, the effective area of the membrane being 5.0 $cm^2$. The half cell at the right hand side was provided with a capillary tube which served to indicate

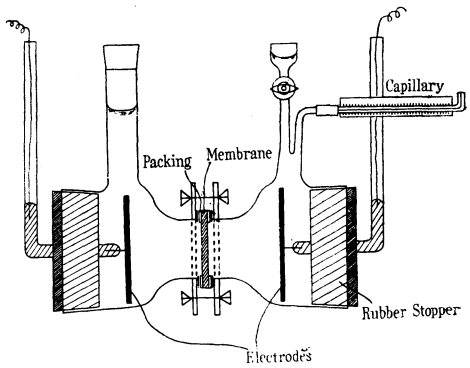



Fig. 1. Apparatus for measurement of electro-osmosis.

the movement of the meniscus due to the liquid transportation from the left half cell to the right one. The inner diameter of the capillary was chosen so as to indicate the volume change as sensitively as possible, and it was calibrated with mercury.

The electrodes were Ag and Ag-AgCl for the measurements in chloride solutions, and Pb and Pb-$PbSO_4$ for sulfate solution. Special care was taken for the use of electrodes of ample capacity in order to ensure reversibility of the electrodes.

During the experiments the main part of the cell was dipped into a water thermostat, and the temperature was kept at 25±0.2°C.

## Results

It has been known[3] that the volume of electro-osmosis is proportional to the quantity of electricity flowed, namely the product of current intensity, $I$, and time, $t$.

$$v=\beta \cdot I \cdot t \qquad (1)$$

In the above equation $\beta$ is the amount of electro-osmosis caused by the flowing of the unit quantity of electricity.

The present work was started by examining the above relation when using the cation-exchange resin membranes.

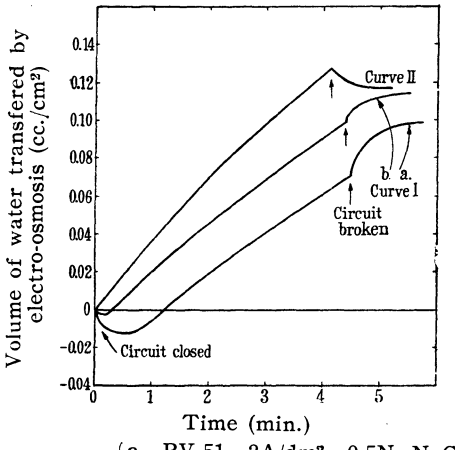
**(1) Liquid Transference in Relation to Time of Electrolysis.**—When the electrical circuit was closed in the apparatus shown in Fig. 1, it was observed that the meniscus in the capillary begins to move, and afterwards showed various tendencies as seen in Fig. 2. In the cases of curve I (Fig. 2) the meniscus retreats at first to the left for a little while and then turns to proceed to the right. On the contrary, in the case of the curve II the meniscus begins to proceed from the start.

Circuit breaking after the current has flowed for some duration causes in the former case a somewhat rapid shift of the

1) Reports of the Research Laboratory, Asahi Glass Co., Vol. III, No. 2, 180 (1953).

2) G. Schmid, *Z. Elektrochem.*, **55**, 229 (1951). K.S. Spiegler, *J. Electrochem.*, **100**, 303C (1953).

3) E. Manegold and K. Solf, *Kolloid Z.*, **55**, 273 (1931).




Curve I { a. PV-51, 2A/dm², 0.5N NaCl-soln.
b. Nepton CR-51, 2A/dm², 1N NaCl-soln.
Curve II Nepton CR-51, 2A/dm², 0.5 N $MgCl_2$-soln.

Fig. 2.

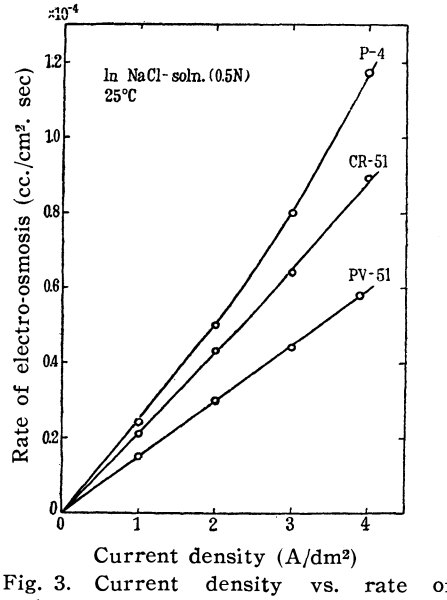



Fig. 3. Current density vs. rate of electro-osmosis.

meniscus toward the right to come to a standstill. In the latter case it causes the retreat of the meniscus toward the left for a short time.

The mode of the initial meniscus movement, the type of curve I being more frequently met and curve II rather rarely, appeared to vary according to the stiffness of the membrane, kind and concentration of the equilibrating solution, and other unknown factors. The main cause of this initial anomaly seemed to be attributed to the bending of the membrane due to the applied electric field. But further study will be necessary to explain it in detail.

For the present purpose, however, it is sufficient to find the inclination of the linear part of the curves showing water transference.

**(2) Current Density and Rate of Electro-osmosis.**—The rate of electro-osmosis was calculated from the inclination of the linear part of the curves such as shown in Fig. 2, for several typical cation-exchange resin membranes in sodium chloride solution. The samples employed are of sulfonated phenol resin type, P-4, PV-51, and CR-51, the thickness being 0.10, 0.12 and 0.09 cm. respectively. The latter two are backed by a plastic screen to increase mechanical strength.

As shown in Fig. 3, the rate of electro-osmosis appears to be approximately proportional to the current density except within the region of high current density in case of P-4 membrane.

Since the equation (1) has thus been confirmed to be applicable for the cation-exchange resin membranes, $\beta$ in the equation will be employed hereafter to compare the characteristics of the membranes.

**(3) Electro-osmosis in Relation to the Concentration of the Solution.**—The relations between $\beta$ and the concentration of the equilibrating sodium chloride solution were derived for the three sorts of membrane as shown in Fig. 4.

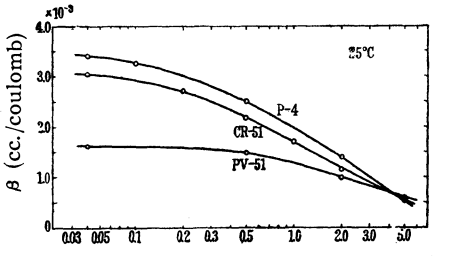



Fig. 4.

In the part of low concentration $\beta$ rises gradually with the decrease in the concentration and approaches a characteristic value, $\beta_0$. There are remarkable differences among $\beta_0$ of the three membranes. As the concentration increases $\beta$ for three membranes converge gradually to come to a nearly equal value at about 5 N.

**(4) $\beta$ and pH of the Solution.**—The change of $\beta$ with varying pH of the sodium chloride solution was measured, keeping the concen-

tration of chlorine ion constant at 0.5 N. The sample employed is PV-51. The result is plotted in Fig. 5.

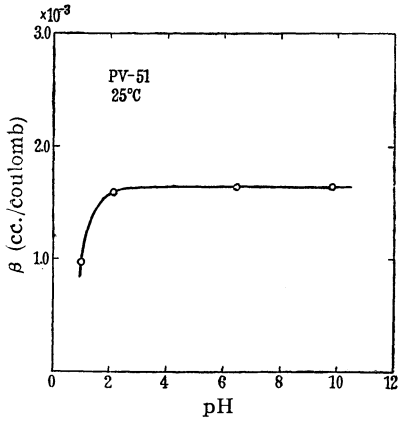



Fig. 5.

From pH 10 to pH 2, $\beta$ remains approximately constant. The influence of pH seems to become remarkable as the concentration of hydrogen ion comes near that of sodium ion.

(5) **Species of Electrolyte and $\beta$.**—Although the present experiments have been carried out using mainly sodium chloride solution, and the cases in other electrolyte solutions will be dealt with in the future, the measurement of $\beta$ in two other electrolyte solutions, i.e., magnesium chloride and sodium sulfate solution, are shown in Fig. 6

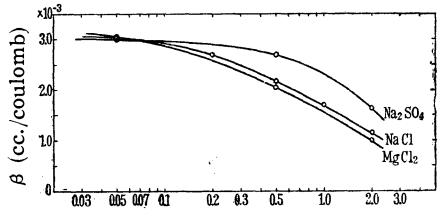



Fig. 6.

in comparison with those in sodium chloride solution. The two electrolytes were chosen in view of the fact that they possess anion or cation in common with sodium chloride.

As shown in the figures, the curves for NaCl- and $MgCl_2$- solution which have a common anion lie very close to each other, while the curve for $Na_2SO_4$ is separated.

## Discussion

Although experimental data are not yet sufficient to allow fully quantitative discussion for the membrane equilibrated with the concentrated solution like those employed in this study, some analyses will be made to interpret the results obtained.

The cation-exchange resins as used in this experiment have as the active groups $-SO_3H$ and -OH radicals fixed on the matrix of hydrocarbon, and the former alone is considered to display cation-exchange action in the neutral solutions. The resin equilibrated with a salt solution, swollen to a degree depending on the concentration of the solution and the degree of cross-linkage of the resin matrix, contains cations (exchangeable ions or counter ions), equivalent to the exchangeable polyanionic groups and an equivalent number of cations and anions (non-exchangeable ions). As the concentration of outside solution increases, more salt molecules penetrate into the resin and non-exchangeable ions increase, and at the same time more water within the resin goes out.

Although the cations corresponding to the penetrating neutral salt are called non-exchangeable cations, apparently discriminating them from the exchangeable ones, it will be assumed in the following discussion that there is essentially no distinction between these two kinds of cation in the resin. This assumption does not appear unreasonable, because the cations mix thoroughly with each other due to the thermal motion in such narrow pores[4] as are found within an ordinary ion-exchange resins.

If an electric field is applied to these ion-exchange resin membranes, all the mobile ions migrate to transport electricity in the direction determined by their charges. Water surrounding these ions seems to accompany the migrating ions.

**Transport Number of the Membrane and Electroosmosis.**—If the cationic transport number of a cation-exchange resin membrane is denoted by $n_+$, the volume of the water which moves with a mol of a cation $v_+$ (including the volume of the cations), and the respective values for the anions in the same membrane by $n_-$ and $v_-$, then the volume of the water flow caused by electricity of one Faraday is,

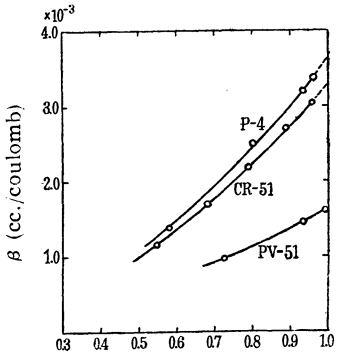
$$v = F\cdot\beta = n_+\cdot v_+ - n_-\cdot v_- = (v_+ + v_-)n_+ - v_- \qquad (2)^*$$

From the equation (2), $\beta$ would change linearly with the cationic transport number $n_+$, if $v_+$ and $v_-$ are assumed constant.

In order to compare the equation with the experimental results, the data of $\beta$ in the preceding chapter are plotted in Fig. 7 against the transport number in the membranes cal-

4) R. Griessbach, *Z. Elektrochem.*, 57, 147 (1953).

* $n_+ + n_- = 1$.



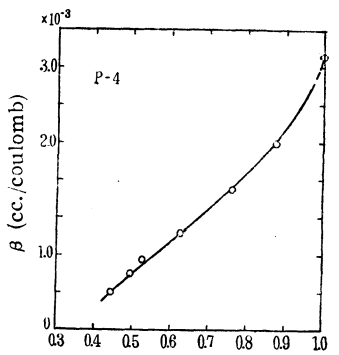

Cationic transport number ($n_+$).
Fig. 7.

culated** from the data reported elsewhere[1].

As shown in the figure, the linear relationship between $\beta$ and $n_+$ appears to hold approximately. But as for the value of $\beta$ corresponding to $n_+=1$, namely $\beta_0$, there is a remarkable discrepancy between the experiment and the theory. Although it is required from the equation (2) that $\beta$ comes to have a constant value, $\beta_0$, regardless of the species of the membrane when $n_+$ approaches 1, the experimental result reveals a very different situation. Also, a constant inclination of the lines which is suggested by the equation (2) is not realized.

The reason for these discrepancies seems to be attributed to the incorrectness of the assumption that $v_+$ as well as $v_-$ is constant.

As a matter of fact, from the experimental results the values of $(v_++v_-)$ for the membranes, P-4, CR-51 and PV-51 are found to be 480, 415 and 230 cc./mol. NaCl respectively in the sodium chloride solution (1 N). It is noteworthy that these amounts of water accompanied with the ionic migration through the membrane are decidedly greater than the hydration water of sodium chloride.

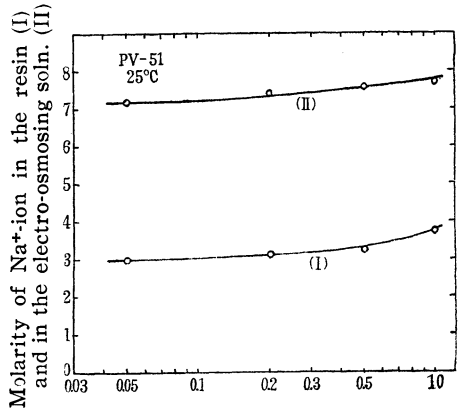



water content of the resin (Na-type) in NaCl-soln.
water content of the resin (Na-type) in distilled water
Fig. 8.

The electro-osmosis seems to depend on the water content of the resin rather than on the hydration water of the migrating ions. The situation can be shown in Fig. 8 in which $\beta$ is plotted against the water content of the resin (P-4).

Therefore in order to discuss the phenomenon further, it will be helpful to compare the concentrations of cation in the solution within the resin and of that in the membrane-permeating solution.

**Concentrations of Cation in the Solution within Cation-exchange Resine Membranes and of that in the Membrane-permeating Solution.**—Molarities of sodium ion in the solution within the cation-exchange resin membrane PV-51, and of that in the solution which passes through the membrane due to electro-osmosis were calculated from the experimental data and compared in Fig. 9.




Concentration of NaCl-soln. ($N$)
Fig. 9.

The former is plotted on the curve (I) and the latter on the curve (II).

Here the procedures of the measurement and the calculation are as follows.

First, in order to measure the water content, small pieces of the cation-exchange resin membrane which have been equilibrated with the solutions of various concentrations are wiped out with filter paper, weighed, dried by means of an Abderhalden's dryer under reduced pressure for 3 hours at 100°C and then weighed again. Second, the cation content of the membranes is determined by

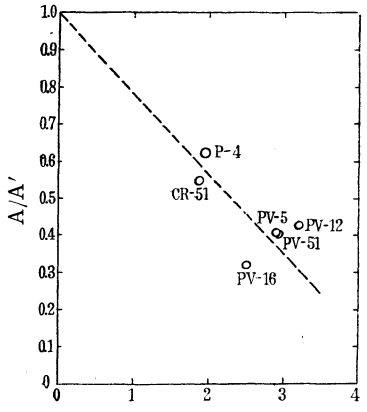
** Generally the transport numbers in an ion-exchange membrane are measured by inserting the membrane between the two solutions of different concentrations. The data of transport number plotted in Fig. 7 were obtained by extrapolating such data to the case where the concentrations of the two sides are made equal.

*** It is assumed that the transport number is not affected by the electro-osmosis.
The membrane-permeating solution due to electro-osmosis contains an unbalanced number of cation and anion, dependent on the transport number of the membrane, and is neutralized with the anion coming from the cathode.

measuring the cation-exchange capacity and the amount of non-exchangeable cation which may be taken out by leaching the membrane with a large volume of distilled water. Combining the above measurements, the molarity of the cation based on the water in the resin can be calculated.

On the other hand, the molarity of cation in the membrane-permeating solution can be calculated from the volume of electro-osmosis and the transport numbers of the membrane***.

As shown in Fig. 9, two curves, (I) and




Molarity of fixed charge (A).
Fig. 10.

(II), are alike in the tendency that they decrease gradually with the lowering of the equilibrating concentration, and approach constant values respectively. There are, however, always a distinct difference between them, namely the electro-osmosing solution appears to be more concentrated in cation than that in the resin.

To explain the result, an idea of mobile water and fixed water in the resin membrane will be introduced.

**Mobile Water and Fixed Water in the Resin Membrane.**—As described in the early part of this chapter, there are fixed polyanions, exchangeable cations and non-exchangeable cations and anions in the pores of cation-exchange resin, and all of these ions are supposed to be hydrated. Besides those occupied by these hydrated ions, the pores of the resin have still remaining rooms which is to be filled with water. And its amount depends on the characteristics of the resin and concentration of the equilibrating solution.

Then it will be reasonable to assume that the hydration water of the fixed polyanionic group and the water at the immediate neighborhood of it are fixed and other water moves with ions when an electric field is applied. The former may be called fixed water and the latter mobile water.

Thus considered, the difference between the two curves (I) and (II) in Fig. 9 is readily explained. Since the electro-osmosing solution comes out from the membrane leaving the fixed water in the resin structure, it must necessarily be more concentrated in cation than the solution within the resin.

Now, as the most simple case, the electro-osmosis through a cation-exchange resin membrane containing no non-exchangeable ions will be considered. Such a state can be attained by equilibrating the membrane with a salt solution and then leaching it with a large volume of distilled water.

If we denote the amount of the fixed water in the resin membrane by $\alpha$ (g./meq. fixed ion), the molarity of the fixed charge by $A$, and the molarity of the cation in the membrane-permeating solution by $A'$, the following relationship must exist among them.

$$A=\frac{1}{F\cdot\beta_0+\alpha}=\frac{1}{1/A'+\alpha} \tag{3}$$

Therefore,

$$A/A'=1-\alpha\cdot A \tag{4}$$

It is seen in the equation (4) that $A/A'$ plotted against $A$ should be linear, if $\alpha$ is independent of the structure of the resin and the concentration of the equilibrating solution.

The $A/A'$ derived by extrapolation of the curves like those in Fig. 7 to zero concentration are plotted in Fig. 10 for the several membranes of similar type. The results are not yet enough to prove satisfactorily the constancy of $\alpha$, but if we admit the linear relationship in the figure, the amount of the fixed water in the membrane can readily be estimated from the inclination of the line.

In this way $\alpha$ is found to be 10~15 mol./(eq. fixed ion) in the case of sulfonated phenol resin type in distilled water.

Thus considered, it becomes evident that neither $v_+$ or $v_-$ in equation (2) is constant and is dependent on the properties of the resins.

## Summary

The water transference due to electro-osmosis was studied for several cation-exchange resin membranes of sulfonated phenol resin type, mainly in sodium chloride solution. It was shown that (1) the electro-osmosis depended on the transport number of the membrane and the amount of water

contained in the resin, and (2) the experimental results could be explained by introducing the idea of fixed water and mobile water in the membrane. The fixed water is supposed to be composed mainly of the hydration water attached to the polar groups of the resin.

The writers would like to thank Dr. M. Sekino and Mr. K. Kōno for their kind supply of the cation-exchange resin membranes employed in this study. Also they are indebted to Dr. S. Uemura and Mr. M. Funaoka for helpful suggestions.

*Research Laboratory,*
*Asahi Glass Co. Ltd.,*
*Benten-cho, Tsurumi-ku,*
*Yokohama*

# *Studies on Hydration by Ultrasonic Interferometer. V. The Change of Hydration of Inorganic Electrolytes with Temperature*

By Tunetaka SASAKI* and Tatuya YASUNAGA

(Received January 17, 1955)

## Introduction

We have already calculated the amount of hydration of ions from the compressibility of their solution, on the assumption that the hydration shells together with the ions themselves are incompressible under the pressure of an ultrasonic wave[1], and confirmed that the results obtained were satisfactory, since they were in accord with the other known facts on hydration[2].

As the reaction of ionic hydration is exothermic, temperature rise is supposed to cause the dehydration of ions. This is always true for a salt crystal having water of crystalization and we can expect that this also applies for the ionic hydration in the aqueous solution. The present study was undertaken to confirm this for several simple electrolytes in solution, using an ultrasonic interferometer for the measurement of the hydration.

## Experimental Method

The ultrasonic interferometer used to measure the sound velocity and the method of calculation of hydration from the sound velocity was the same as in the first report[1]. The ultrasonic frequency used was 406.927 kc./sec.

## Experimental Results and Discussions

The samples used were the aqueous solutions of 1N NaCl. The sound velocity was measured at the temperature ranging from 0°C to 60°C for water and the aqueous solution of NaCl. The curves obtained for water and NaCl solution ran parallel to each other as shown in Fig. 1.

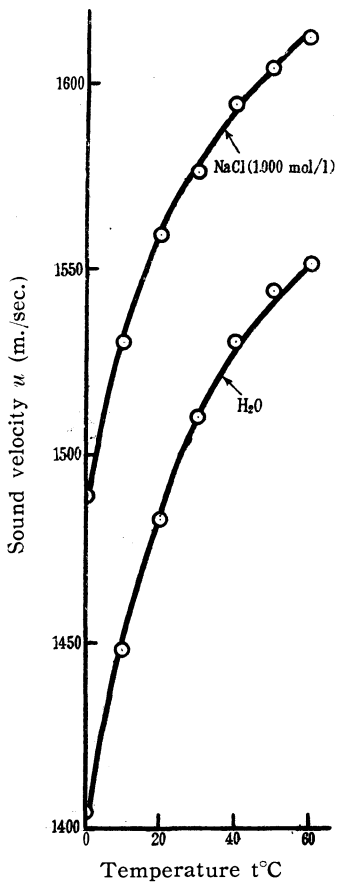



Fig. 1. Change of sound velocity with temperature.

* Present address: Department of Chemistry, Faculty of Science, Tokyo Metropolitan University, Setagayaku, Tokyo.

1) T. Yasunaga and T. Sasaki, *J. Chem. Soc. Japan*, **72**, 87 (1951).

2) T. Yasunaga and T. Sasaki, *J. Chem. Soc. Japan*, **72**, 89, 366 (1951); T. Sasaki, T. Yasunaga and H. Hujiwara, *J. Chem. Soc. Japan*, **73**, 181 (1952).

TABLE I

| Temperature °C | 0 | 10 | 20 | 30 | 40 | 50 | 60 |
|---|---|---|---|---|---|---|---|
| $U$ (m./sec.) | 1489.9 | 1528.0 | 1558.5 | 1576.6 | 1594.3 | 1604.0 | 1613.3 |
| $d$ (g./cc.) | 1.0458 | 1.0441 | 1.0413 | 1.0396 | 1.0378 | 1.0338 | 1.0292 |
| $\beta$ ($10^{-7}$ cgs) | 43.08 | 41.02 | 39.54 | 38.70 | 37.91 | 37.60 | 37.33 |
| $V$ (cc./mol.) | 137.8 | 125.9 | 116.7 | 106.6 | 106.5 | 99.6 | 103.5 |

We then calculated the compressibility from the sound velocity and density, and computed the amount of hydration of ions as the volume of incompressible water which was shown in Table I.

The amount of hydration decreases with increasing temperature as shown in Fig. 2.

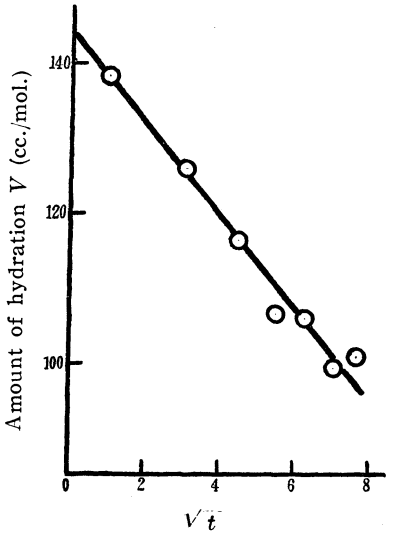



Fig. 2. Change of amount of hydration with temperature (1 N NaCl solution).

As the hydration reaction is exothermic, being caused by the mutual interaction between the ion and water dipoles, this temperature dependence is just what we expect. The relation is best expressed by

$$V_t = V_o - 6\sqrt{t}, \qquad (1)$$

where $V_t$ is the volume of hydration water per mole solute at $t$°C and $V_o$, the value of $V$ at 0°C. In this connection, we have already obtained a similar empirical formula for the change of the amount of hydration with concentration in a previous report[3], namely,

$$V_c = V_o - 36\sqrt{C}, \qquad (2)$$

where $V_c$ denotes the volume of hydration water per mole solute at the concentration $C$ and $V_o$, the value of $V_c$ at the infinite dilution. We can see that temperature and concentration affect the hydration in exactly the same manner. Further, we calculated so called electrostriction, namely, the volume change due to the dissolution of salt in water at various temperatures as we did in a previous paper[4]. Fig. 3 shows the result.

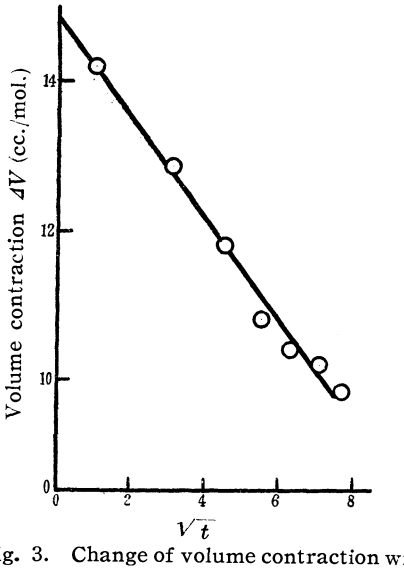



Fig. 3. Change of volume contraction with temperature (1 N NaCl solution).

In a previous paper[5] we have already confirmed a proportionality between the amount of hydration and the volume change at constant temperature and concentration for various electrolytes. From Figs. 2 and 3 we

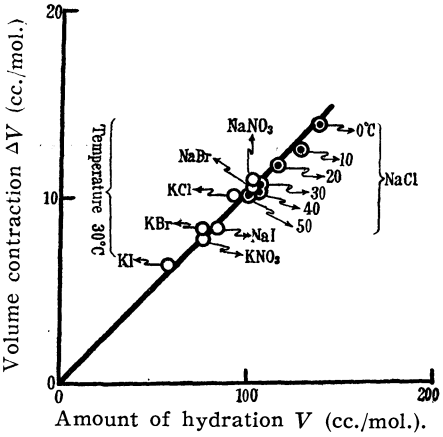



Fig. 4. Relation between amount of hydration and volume contraction.

3) T. Yasunaga and T. Sasaki, *J. Chem. Soc. Japan*, 72, 89 (1951).

4) T. Yasunaga and T. Sasaki, *J. Chem. Soc. Japan*, 70, 379 (1949).

5) T. Sasaki, T. Yasunaga and H. Hujiwara, *J. Chem. Soc. Japan*, 73, 181 (1952).

can also obtain a proportionality between them even for the change of temperature at constant concentration. They are shown in Fig. 4.

It is confirmed that these two straight lines coincide with each other. In other words, the amounts of hydration and volume contraction show a unique proportionality irrespective of whether it is produced by the change of the temperature or the nature of electrolyte, and is expressed by

$$\Delta V/V=0.10.$$

Again, this fact shows, as reported in a previous paper[3], that $\Delta V$ and $V$ are closely related to each other and are reasonably assumed to be the measure of hydration. If we assume that water of volume $V$ is compressed by $\Delta V$ due to hydration, the mean pressure of hydration of about 4000 atmospheres is obtained, which is necessary to produce this volume contraction. The theoretical calculation for the relation between $V$ and $\Delta V$ will be given in the next paper.

**Summary**

Sound velocity was measured at the temperature ranging from 0° to 60°C for water and the aqueous solutions of NaCl.

The amount of hydration was calculated from the sound velocity data for NaCl, which was shown to change linearly with the square root of temperature.

Volume contraction due to the dissolution of NaCl was also calculated at various temperatures which was found to change proportionally with the amount of hydration. The proportionality constant (0.10) was the same as obtained when the nature of the salt was changed. The mean hydration pressure was estimated to be about 4000 atmospheres.

A part of the cost of this study has been defrayed from the Scientific Research Expenditure of the Ministry of Education, given to one of the authors.

*Department of Chemistry, Faculty of Science, Kyushu University, Fukuoka*

# *Studies on the Electronic Structures of 2,5-Dichloroaniline and 2,5-Dichloronitrobenzene by Their Pure Quadrupole Spectra*

By Hisao NEGITA, Hitoshi YAMAMURA and Haruo SHIBA

(Received January 27, 1955)

Since Dehmelt and Krüger[1] succeeded in observing the pure quadrupole spectrum due to $Cl^{35}$ and $Cl^{37}$ of *trans*-1,2-dichloroethylene, many workers have reported spectra of various chlorine compounds, a few of them, however, from chemical viewpoints.

Among them, Meal[2] has pointed out that there is a rough linearity between Hammett's $\sigma$[3] of substituents and the resonance absorption frequencies in the spectra of several monosubstituted chlorobenzenes. But, as the absorption frequencies of *p*-nitrochlorobenzene and *o*- and *m*-chloroaniline have not so far been observed, i. e., data of the corresponding isomers of the two series have been missed, the electronic behaviors of amino- and nitro-groups in the benzene ring can not be compared with each other by the spectra of monosubstituted chlorobenzenes.

So we studied those of 2,5-dichloroaniline and 2,5-dichloronitrobenzene, each of which was observed at 77°K independently by Weatherly et al.[4], and by Bray et al.[5], and both of which were observed at 292°K by us.

## Experimental

As pointed out by several workers,[1,6] the absorption frequency $\nu$ of chlorine compounds is expressed as follows, provided that the electronic distribution around the chlorine nucleus is axially symmetric:

$$\nu = |eqQ|/2h,$$

where $e$ is the proton charge, $q$ the electric field gradient at the nucleus, $Q$ the nuclear quadrupole moment of the atom, which is negative,[7] and $h$ Planck's constant. As the moment $Q$ is regarded as constant in each compound, $\nu$ may be con-

1) H. G. Dehmelt and H. Krüger, *Z. f. Physik*, **129**, 401 (1951).
2) H. C. Meal, *J. Am. Chem. Soc.*, **74**, 6121 (1952).
3) L. P. Hammett, "Physical Organic Chemistry", McGraw-Hill Book Co. Inc., New York, N. Y. (1940), p. 188.
4) T. L. Weatherly and Q. Williams, *J. Chem. Phys.*, **21**, 2073 (1953).
5) P. J. Bray and P. J. Ring, *J. Chem. Phys.*, **21**, 2226 (1953).
6) H. C. Allen, *J. Phys. Chem.*, **57**, 501 (1953).
7) C. H. Townes and S. Geschwind, *Phys. Rev.*, **74**, 626 (1948).

sidered to be proportional to $q$, which, by its definition, has a maximum value in the pure covalent bond and is zero in the pure ionic. Accordingly, it is only necessary to determine $\nu$ in order to have an insight into the electronic structures of the chlorine compounds.

**Apparatus.**—To find the absorption frequencies, we used the frequency-modulated superregenerative spectrometer,[1] its main oscillator being shown in Fig. 1. The frequencies generated were between about 25 Mc. and 38 Mc., for the absorption frequencies of the most organic chlorine compounds are known to lie in this range.

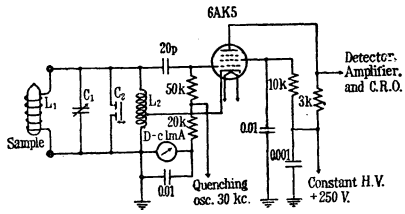



Fig. 1. Main oscillator of the spectrometer.
$L_1$; removable. ca. 1$\mu$H., $L_2$; fixed, ca. 1$\mu$H., tap being variable, $C_1$; variable, max. 50 pF., $C_2$; vibrating for freq. modulation.

For the frequency measurement, both the heterodyne frequency meter and the crystal oscillator of 1 Mc. were used. The experimental error was several kc., which was not serious in the following considerations.

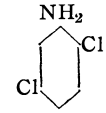
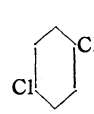
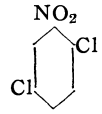
**Samples.**—2,5-Dichloronitrobenzene and 2,5-dichloroaniline were prepared by nitration and successive reduction of $p$-dichlorobenzene[8]. These compounds were recrystallized to the constant melting points, 54°–55° and 50°C respectively.

The $p$-dichlorobenzene used as the reference material was commercial pure grade.

## Results and Considerations

Results obtained are shown in Table I. The absorption lines of the two $p$-dichlorobenzene derivatives are more feeble than that of $p$-dichlorobenzene itself, the reason for which is not evident.

TABLE I
RESONANCE ABSORPTION FREQUENCIES DUE TO $Cl^{35}$ OF $p$-DICHLOROBENZENE AND ITS DERIVATIVES (292°K)

| Compounds |  |  |  |
|---|---|---|---|
| Resonance freq. (Mc.) | 33. 927 (2)<br>34. 044 (5) | 34. 286 (1,4) | 35. 545 (5)<br>37. 290 (2) |

In this Table, the numbers in the brackets stand for ordinal numbers of chlorine atoms in the benzene ring. These numbers were assigned in reference to the data of absorption frequencis of $Cl^{35}$ in $o$- and $m$-nitrochlorobenzene (37.260 and 35.457 Mc. respectively[2]) and $Br^{81}$ in $o$- and $m$-bromoaniline (220.255 and 222.614 Mc. respectively[9]) at 77°K; there were no available data of $o$- and $m$-chloroaniline to identify the lines of 2,5-dichloroaniline.

The lower values of frequencies of 2,5-dichloroaniline compared with that of $p$-dichlorobenzene indicate that the amino-group in the benzene ring releases elctrons, and more powerfully towards the $o$-position than towards the $m$-position. On the contrary, the greater values of 2,5-dichloronitrobenzene indicate that the nitro-group attracts electrons, and preferentially from the $o$-position; while the unique value of $p$-dichlorobenzene results from the fact that the state of the two chlorine atoms in this compound are equivalent, which is different from the cases of the other two derivatives.

These facts are in good agreement with the views of the "Electronic Theory of Organic Chemistry" by Robinson and Ingold and the results obtained from data of the dipole moments of amino- and nitro-groups[10]. Though the former is rather qualitative and the latter indirect, the quadrupole data show explicitly the state of electron shift.

Meal[3] suggested that there was a linear relation between resonance absorption frequency $\nu$ due to $Cl^{35}$ and Hammett's $\sigma$ of a substituent in monosubstituted chlorobenzene. We examined whether this relation existed or not in the $p$-dichlorobenzene derivatives, and found that there was a more excellent linearity between them, although the value of Hammett's $\sigma$ for Cl (2) in the 2,5-dichloroaniline was not seen. These results are shown in Table II and Fig. 2.

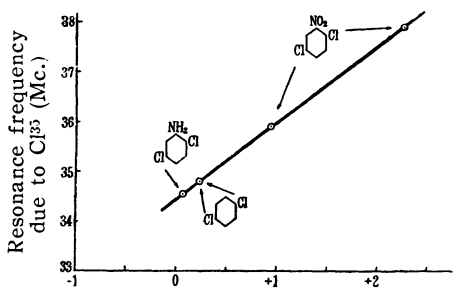



Fig. 2. Relation between the resonance absorption frequencies due to $Cl^{35}$ and Hammett's $\sigma$ of the substituents in $p$-dichlorobenzene and its derivatives.

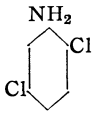
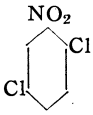
8) E. Jungfleisch, *Ann. chim.*, [4], **15**, 257, 259 (1868).

9) P. J. Bray, *J. Chem. Phys.*, **22**, 950 (1954).

10) L. F. Fieser and M. Fieser, "Textbook of Organic Chemistry", Maruzen Publishing Co. Ltd., Tokyo, (1952), p. 449.

TABLE II

RESONANCE ABSORPTION FREQUENCIES AT 0°K AND HAMMETT'S $\sigma$ OF $p$-DICHLOROBENZENE AND ITS DERIVATIVES

| Compounds |  |  |  | |
|---|---|---|---|---|
| Positon of Cl | Cl (2) | Cl (5) | Cl (1, 4) | Cl (2) | Cl (5) |
| Hammett's $\sigma$ | $o$-$NH_2$ ? <br> $p$-Cl +0.227 <br> ? | $m$-$NH_2$ −0.161 <br> $p$-Cl +0.227 <br> +0.066 | $p$-Cl +0.227 <br> +0.227 | $o$-$NO_2$ +2.03 <br> $p$-Cl +0.227 <br> +2.257 | $m$-$NO_2$ +0.710 <br> $p$-Cl +0.227 <br> +0.937 |
| Resonance freq. at 0°K (Mc.) | 34.42 | 34.55 | 34.80 | 37.92 | 35.92 |

In Table II, the value of Hammett's $\sigma$ of $o$-nitro-group was taken from Meal's data and the resonance absorption frequencies at 0°K were obtained to ignore effects of lattice vibrations, by extrapolating the data[4,5] at 77°K and our data at 292°K, referring to the curve of $p$-dichlorobenzene. Assuming the linearity between $\nu$ and $\sigma$, we may compute $\sigma$ of $o$-amino-group as −0.26 from Fig. 2.

## Summary

The pure quadrupole spectra of 2,5-dichloroaniline and 2,5-dichloronitrobenzene were observed at room temperature (292°K), and the effects of electron releasing or attracting power of amino- and nitro-group in the benzene ring were compared with each other. On the other hand, a linear relation between resonance absorption frequencies due to $Cl^{35}$ and Hammett's $\sigma$ of the substituents in these compounds was found, and Hammett's $\sigma$ of $o$-amino-group was assumed to be −0.26.

We are indebted to Prof. T. Ichikawa and Prof. D. Nakae for their generarity in granting us the use of their facilities, and to Prof. T. Kawano for the loan of the frequency meter.

*Chemical Department, Faculty of Science, and Chemical Laboratory, Faculty of Engineering, Hiroshima University, Hiroshima*

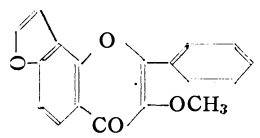
# *Synthetic Studies on the Benzofuran Derivatives. Part I. A New Synthesis of Karanjin*

By Yoshiyuki KAWASE, Takashi MATSUMOTO and Kenji FUKUI

(Received February 4, 1955)

Karanjin, a kind of flavonol, was isolated in colorless needle crystals, $C_{18}H_{12}O_4$, m.p. 158.5°C as an unsaponifiable matter from the seed oil of a leguminous plant *Pongamia glabra Vent.* karanjia by Limaye[1] and by Beal and Katti[2].

The chemical structure of this substance was studied by Limaye[3] and Manjunath, Seetharamiah and Siddappa[4], and was proved to have a constitutional formula (I). The




(I)

total synthesis of this karanjin (I) was reported by Seshadri and Venkateswarlu[5] and Row and Seshadri[6], but the yields were not so good. We also have been studying the synthesis of this substance independently and have obtained karanjin more easily and in higher yield.

Starting from 7-hydroxy-3-methoxyflavone-

1) D.B. Limaye, *Proc. Indian Sci. Congr.*, **1925**, 118; **1926**, 151.
2) Beal and Katti, *J. Am. Pharm. Assoc.*, **14**, 1086 (1926).
3) D.B. Limaye, *Rasayanam*, I, 1 (1936); I, 119 (1937).
4) B.L. Manjunath, A. Seetharamiah and S. Siddappa, *Ber.*, **72B**, 93 (1939).
5) T.R. Seshadri and V. Venkateswarlu, *Proc. Indian Acad. Sci.*, **13A**, 404 (1941).
6) L.R. Row and T.R. Seshadri, ibid, **33**, 168 (1951).

8-aldehyde (II) as Seshadri[7] and Limaye[8] did, 3-methoxyflavone-7,8-furan-$\alpha$-carboxylic acid (IV) was synthesised in a good yield by the method of Tanaka[9] for benzofuran synthesis;—that is, the aldehyde (II) and ethyl bromomalonate were made to react in acetone in the presence of potassium carbonate, and the condensation product was hydrolysed to the acid (IV), m.p. 283°C (decomp.), yield 88.2%. As the intermediate product of this reaction, the colorless needle crystals, m.p. 183°C, were obtained and were found to be identical with the ethyl ester (IIIa) of the above mentioned acid (IV); therefore, it is clear that the ethyl ester of furan-$\alpha$-carboxylic acid was produced in this reaction as the intermediate product.

Then, this acid (IV) was decarboxylated in quinoline in a stream of nitrogen gas with copper powder into colorless needle crystals, m.p. 159°C, yield 26.5%, the melting point of which was not depressed by admixture with natural karanjin (I). Further, this synthetic karanjin was derived to 3-hydroxy and 3-acetoxy derivatives and was decomposed into benzoic acid, methoxymethylkaranjketone (VI) and karanjic acid (VII) by alkaline hydrolysis. The melting points of these substances (I, Va, Vb, VI and VII) coincided well with those of the natural products, as shown in the following Table.

We are grateful to the Institute of Organic Chemistry, Osaka City University for carrying out microanalyses and to Prof. T. R. Seshadri for giving us the sample of natural Karanjin.

## Experimental[10]

**7-Hydroxy-3-methoxyflavone-8-aldehyde (II).**—This aldehyde (II) was prepared from 7-hydroxy-3-methoxyflavone by the methods of Seshadri[7] and Limaye[8].

**3-Methoxyflavone-7,8-furan-$\alpha$-carboxylic acid (IV).**—A Mixture of 7.5 g. of 7-hydroxy-3-methoxyflavone-8-aldehyde (II), 8 g. of ethyl bromomalonate, 30 g. of anhydrous potassium carbonate in 620 cc. of absolute acetone was refluxed under stirring for 10.5 hours on a steambath. After distilling off the acetone, the residue was mixed with a solution of 5 g. of potassium hydroxide in 50 cc. of water and heated on a steambath for one hour, then diluted with water, decolorised, filtered and acidified with dilute sulfuric acid. The precipitate was collected and dissolved in sodium bicarbonate solution, followed by filtering and acidifying with dilute sulfuric acid. The precipitates were collected, washed with water and recrystallised from alcohol in colorless plates of

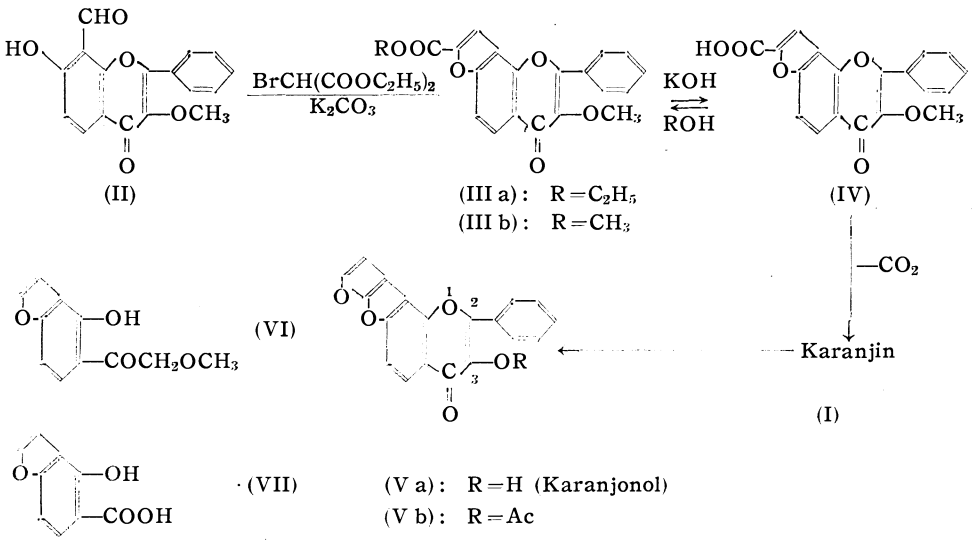



TABLE
THE MELTING POINTS OF KARANJIN AND ITS DERIVATIVES (°C)

| Products | Karanjin (I) | 3-OH (Va) | 3-OAc (Vb) | Alkaline dec. prod. (VI) | Alkaline dec. prod. (VII) |
|---|---|---|---|---|---|
| Natural products[4] | 158.5 | 199–200 | 177 | 96 | 218 (dec.) |
| Synthetic products | 159 | 200 | 177 | 95.5 | 215–6 (dec.) |

7) S. Rangaswami and T.R. Seshadri, *Proc. Indian Acad. Sci.*, 9A, 7, 259 (1939).
8) S.D. Limaye and Limaye, *Rasayanam*, I, 161 (1939).
9) S. Tanaka, *J. Am. Chem. Soc.*, 73, 872 (1951).
10) All melting points were not corrected.

m.p. 283°C (decomp.); yield 7.5 g. (88.2%). Found: C, 67.40; H, 3.83. Calculated for $C_{19}H_{12}O_6$: C, 67.86; H, 3.57%.

**Esters (IIIa, IIIb) of the Acid (IV) and the Intermediate Substance of the above Reaction.**—This acid (IV) was esterified with methanol or ethanol and sulfuric acid by the usual method. These esters were recrystallised from methanol or ethanol in colorless needles. *Methyl ester*, m.p. 194.5°C (IIIb). Found: C, 68.58; H, 3.96. Calculated for $C_{20}H_{14}O_6$: C, 68.57; H, 4.00%. *Ethyl ester*, m.p. 182°C (IIIa). Found: C, 69.38; H, 4.53. Calculated for $C_{21}H_{16}O_6$: C, 69.23; H, 4.39%.

A part of the residue after distilling off the acetone in the above procedure was recrystallised from alcohol in colorless needles, m.p. 183°C. Found: C, 69.22; H, 4.53. Calculated for $C_{21}H_{16}O_6$: C, 69.23; H, 4.39%. The melting point of this intermediate substance was not depressed by admixture with the ethyl ester (IIIa), m.p. 182°C.

**Karanjin (I).**—A mixture of 10 g. of 3-methoxyflavone-7,8-furan-α-carboxylic acid (IV), 4 g. of copper powder in 140 cc. of quinoline was heated under stirring in an atomosphere of nitrogen gas for about 40 minutes at 180–190°C until evolution of carbon dioxide ceased. It seems to be important that attention be paid to duration of time and temperature in this decarboxylation. After cooling, a little alcohol was added and the mixture was filtered from copper and was acidified with dilute hydrochloric acid. The brown precipitates thus formed were collected. The mother liquid was made alkaline with sodium hydroxyde and quinoline was distilled off by means of steam distillation. The residue was acidified after cooling and crude precipitates were collected. The crude karanjin thus obtained was recrystallised three times from ethyl acetate with the aid of charcoal in colorless needles, m.p. 159°C; yield 2.3 g. (26.5%). The melting point of this substance was not depressed by admixture with the natural karanjin. Found: C, 74.01; H, 4.04. Calculated for $C_{18}H_{12}O_4$: C, 73.97; H, 4.11%.

**3-Hydroxyflavone-7,8-furan (Va) and 3-acetoxyflavone-7,8-furan (Vb).**—These compounds (Va and Vb) were prepared according to the directions of Seshadri et al.[11].

A mixture of karanjin and anhydrous aluminium chloride in nitrobenzene was heated for one hour. After the product was worked up in the usual manner, the substance was recrystallised from dilute alcohol in colorless crystals, m.p. 200°C, which gave violet reaction with ferric chloride. This compound (Va) was acetylated to the 3-acetoxy derivate (Vb), m.p. 177°C with acetic anhydride in pyridine.

**Alkaline Decomposition of Synthetic Karanjin.**—According to the directions of Manjunath et al.,[4] a mixture of 1 g. of synthetic karanjin in alcohol and saturated methanolic potash was refluxed four hours. After distilling off the solvent, the residual solution was acidified and extracted with ether. The ethereal solution was first extracted with aqueous sodium bicarbonate solution and then with aqueous potassium hydroxide solution. Benzoic acid (0.2 g.) m.p. 121°C, and karanjic acid (0.02 g.) (VII), m.p. 215–6°C (decomp.) were obtained from bicarbonate solution; and methoxymethylkaranjketone (0.35 g.) (VI), m.p. 95.5°C, was obtained from potassium hydroxide solution.

## Summary

Starting from 7-hydroxy-3-methoxyflavone-8-aldehyde (II), 3-methoxyflavone-7,8-furan-α-carboxylic acid (IV) was synthesised in good yield by the method of Tanaka for benzofuran synthesis and was decarboxylated in quinoline with copper powder into karanjin (I).

*Faculty of Liberal Arts and Science,*
*Toyama University, Toyama*

11) T. R. Seshadri and V. Venkateswarlu, *Proc. Indian Acad. Sci.*, 17A, 16 (1943).

# *A Semi-empirical Approach to the SCF Molecular Orbitals*

By Hideo KON

(Received January 27, 1955)

## Introduction

The semi-empirical ASMO method recently proposed by Pariser and Parr[1] presents a way to calculate the transition energies and oscillator strengths of a variety of $\pi$-electron systems without much labour, in such a quantitative conformity with experiments as is rarely found in this kind of calculation. One of the essential points of their method is to alter the values of Coulomb repulsion integrals over atomic orbitals by introducing semi-empirical elements on a similar ground as in the method of "atoms in molecules" of Moffit[2]. The reasonable nature of such revision of integral values is illustrated by

1) R. Pariser and R.G. Parr, *J. Chem. Phys.*, **21**, 466, 767 (1953).

2) W. Moffit, *Proc. Roy. Soc.*, A210, 245 (1951).

the improvements in the results of their calculations. Nothing is known, however, of the improvements in the form of MO's which might be brought about by introducing the revised integrals, and one has to be content with the naive Hückel method or to resort to the elaborate, laborious, self-consistent field method of Roothaan[3].

In this preparatory note, a trial is given to incorporate the Pariser and Parr's semi-empirical method into the iterative procedure of Roothaan in order to reflect their reasonable revision of the integral values on the form of molecular orbitals. In the course of this calculation, the author found that Pople's treatment of unsaturated hydrocarbon[4] was based on a similar idea, but there, the Coulomb repulsion integrals were approximated by the Coulomb energy between two point charges instead of the charged sphere model of Pariser and Parr, and the details were somewhat different from the present treatment.

## Modification of Roothaan's SCF Equation

A molecular orbital ($\phi_i$) of a $\pi$-electron system is expressed as a linear combination of atomic orbitals ($\chi_p$),

$$\phi_i=\sum_p c_{ip}\chi_p.$$

The coefficients $c_{ip}$ are determined by a homogeneous set of equations derived by Roothaan.

$$\sum_q c_{ip}(L_{pq}-S_{pq}\varepsilon_i=0,$$

$$L_{pq}=G_{pq}+I_{pq},$$

$$G_{pq}=\sum_i^{occ}[2J_{i,pq}-K_{i,pq}],$$

$$I_{pq}=\int\chi_p(\nu)H_{core}\chi_q(\nu)d\tau_\nu$$
$$=\int\chi_p(\nu)[T(\nu)+\sum_r U_r(\nu)]\chi_q(\nu)d\tau_\nu .$$

$U_r(\nu)$ is the potential on the electron $\nu$ due to the atom $r$ stripped of its $\pi$-electron. $J_{i,pq}$ and $K_{i,pq}$ are defined as follows:

$$J_{i,pq}=\int\int\phi_i^*(\mu)\phi_i(\mu)[e^2/r_{\mu\nu}]\chi_p^*(\nu)\chi_q(\nu)d\tau_\nu\, d\tau_\mu,$$
$$K_{i,pq}=\int\int\phi_i^*(\mu)\phi_i(\nu)[e^2/r_{\mu\nu}]\chi_q^*(\mu)\chi_q(\nu)d\tau_\mu d\tau_\nu .$$

The simplifying assumptions of Pariser and Parr such as; 1) zero differential overlap, $\chi_p\chi_q=0$, 2) neglect of non-neighbour core integral $I_{pq}$, are taken into account here, so that $J_{i,pq}$ and $K_{i,pq}$ are rewritten in terms only of atomic Coulomb repulsion integrals as follows,

$$J_{i,pq}=0,\quad p\neq q,$$
$$J_{i,pp}=\sum_q c^2_{iq}\int\chi_q^*(\mu)\chi_q(\mu)[e^2/r_{\mu\nu}]\chi_p^*(\nu)\chi_p(\nu)d\tau_\mu d\tau_\nu=\sum_q c^2_{iq}(qq\,|\,pp)$$
$$=c^2_{ip}\,(pp\,|\,pp)+\sum_{q\neq p}c^2_{iq}(qq\,|\,pp),$$
$$K_{i,pq}=c_{ip}c_{iq}\,(pp\,|\,qq).$$

Similarly, the core integrals reduce to two integrals:

$$I_{pq}=\alpha_p,\quad p=q,$$
$$=\beta_{pq},\quad p\neq q,\ \text{atom } p \text{ being linked directly to atom } q,$$
$$=0,\quad \text{otherwise.}$$

Thus the expression for the quantity $L_{pq}$ is replaced by

$$L_{pp}=\alpha_p+\sum_i 2c^2_{ip}(pp\,|\,pp)+\sum_i\sum_{q\neq p}2c^2_{iq}(pp\,|\,qq)-\sum_i c^2_{ip}\,(pp\,|\,pp)$$
$$=\alpha_p+\frac{1}{2}Q_p(pp\,|\,pp)+\sum_{q\neq p}Q_q(qq\,|\,pp),$$
$$L_{pq}=\beta_{pq}-\sum_i c_{ip}c_{iq}(pp\,|\,qq)$$
$$=\beta_{pq}-\frac{1}{2}P_{pq}(pp\,|\,qq),\quad p\neq q.$$

Here $Q_p$ is the $\pi$-electron density on $p$-atom and $P_{pq}$ reduces to the mobile bond order, if atoms $p$ and $q$ are the neighbouring atoms, but if not, it has not any definite physical meaning. In addition to these simplifications, the following assumptions are made in this paper in dealing with the core integrals $\alpha_p$ and $\beta_{pq}$.

1) The Coulomb integral $\alpha_p$ can be approximated as the valence state ionization potential ($W_{2p}$) of a $2p$ electron on a free atom, less the sum only of the Coulomb repulsion integrals ($pp\,|\,qq$), summation being carried out over all the other atoms $q$ involved in the $\pi$-electron system. This neglect of Coulomb penetration integrals is found to reduce the labour without having a significant influence on the good numerical performance of Pariser and Parr's original work. 2) The resonance integral $\beta_{pq}$ which as in ref. 1, is one of the empirical parameters and is carried from molecule to molecule, is assumed, apart from Pariser and Parr, to be proportional to the inverse sixth-power of the bond distance $r_{pq}$ and the proportionality constants are so chosen as to reproduce the observed first transition energy of a particular molecule as closely as possible. As the reference molecule, ethylene, formaldehyde and pyrazine

3) C.C.J. Roothaan, *Rev. Mod. Phys.*, **23**, 69 (1951); R. G. Parr and R.S. Mulliken, *J. Chem. Phys.*, **18**, 1338 (1950).
4) J.A. Pople, *Trans. Farad. Soc.*, **49**, 1375 (1953).

are chosen for the bond C=C, C=O and C=N, respectively. In ref. 1, it is postulated that $\beta_{pq}$ can be expressed as, $\beta_{pq}=a\exp(-br_{pq})$. Two experimental data being needed to fix the parameters $a$ and $b$, it is not easy to extend it to other cases than C=C bonds. Whether or not the inverse sixth-power equation is appropriate will be tested by applying it to a variety of compounds and by comparing the results with observations. Taking these assumptions into account, the matrix element $L_{pp}$ can be written down as,

$$L_{pp}=W_{2p}+\frac{1}{2}Q_p(pp\,|\,pp)+\sum_{q\neq p}(Q_q-1)(qq\,|\,pp).$$

If we put, $Q_p=Q_q=1$, then $L_{pp}$ becomes a constant. As $L_{pp}$ in the present treatment plays an analogous role to the Coulomb integral in the simple molecular orbital method, the constant $L_{pp}$ will bring about a uniform distribution of $\pi$-electrons as in the alternant hydrocarbons treated by the simple molecular orbital method. For non-alternant hydrocarbons and hetero-molecules, $Q_p$, $Q_q\neq1$ and $L_{pp}$ depends in a complicated manner on the geometrical configuration of the molecule, that is $L_{pp}$ is a function not only of the charge density of $p$-atom and $q$-atoms. In Wheland and Mann's iterative method, the Coulomb integral on an atom $p$ is dependent only on $Q_p$[5]. The above mentioned functional relation, however, is a more satisfactory one and is in harmony with the Coulson and Longuet-Higgins' theory[6], where the charge density on an atom and the Coulomb integral of other atoms are connected to each other by their mutual polarizability ($\pi_{pq}$).

Roothaan's iterative procedure to find the self-consistent set of $c_{ip}$'s is then followed, making at each step a guess at a better set of $c_{ip}$ values to attain a rapid convergence. The symmetry coordinates are fully made use of in order to reduce the order of secular equations. Of the molecules calculated in this paper, ethylene and benzene have geometrical symmetry sufficient for finding the self-consistent set of $c_{ip}$'s only through the symmetry requirements, and so the iteration is unnecessary.

## Numerical Values of the Basic Quantities

Following Pariser and Parr, the Coulomb repulsion integrals $(pp\,|\,qq)$ are computed by making use of their uniformly charged sphere model for bond distances longer than 2.80 Å and proper quadratic extrapolation formulae are used for bonds shorter than 2.80 Å. The resonance integral $\beta_{pq}$ is computed as mentioned above from the formula, $\beta_{pq}=k/r^6_{pq}$, $k$ being the proportionality constant, to which numerical values $-17.464$, $-13.983$ and $-8.8086$ are assigned for C=C, C=N and C=O bond, respectively. In Fig. 1 are shown the geometricals and designations for the calculated eight molecules. Except for $s$-triazine, geometricals are all based on the experimental data.

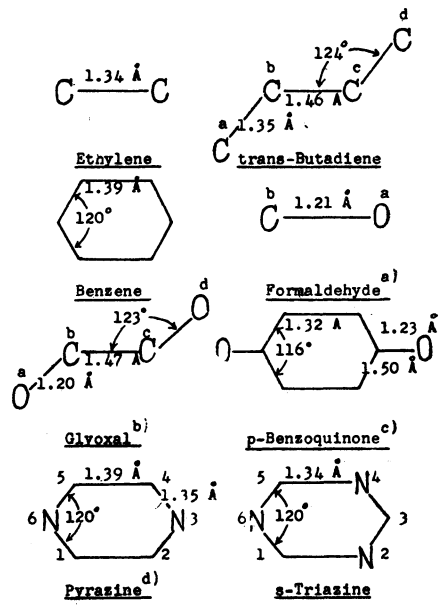



Fig. 1. Geometricals and designations of the calculated molecules.

a) D. P. Stevenson, J. E. LuValle and V. Schomaker, *J. Am. Chem. Soc.*, **61**, 2508 (1939).
b) J. E. LuValle and V. Schomaker, ibid., **61**, 3520 (1939).
c) S.M. Swingle, ibid., **76**, 1409 (1954).
d) V. Schomaker and L. Pauling, ibid., **61**, 1769 (1939).

## Results of Calculation

After the iterative processes have come to convergence, the electronic transition energies are calculated by use of the following formula, no configuration interaction being allowed for, except in the symmetry degenerate cases of benzene and $s$-triazine.

$$\left.\begin{matrix}E_{Vij}\\E_{Tij}\end{matrix}\right\}-E_N=(\epsilon_j-\epsilon_i)-(J_{ij}-K_{ij})\pm K_{ij}.$$

Here, $E_N$, $E_V$ and $E_T$ designate the energy of the ground, excited singlet and excited triplet configuration, respectively, electronic excitation being from orbital $i$ to $j$. $J$ and $K$ are the Coulomb repulsion and exchange

5) G.W. Wheland and D.E. Mann, *J. Chem. Phys.*, **17**, 264 (1949).
6) C. A. Coulson and H. C. Longuet-Higgins, *Proc. Roy. Soc.*, **A191**, 39; **A192**, 16 (1947).

repulsion integrals in terms of molecular orbitals.

$$J_{ij}=\iint\phi^*_i(\mu)\phi_i(\mu)[e^2/r]\phi^*_j(\nu)\phi_i(\nu)d\tau_\mu d\tau_\nu ,$$
$$K_{ij}=\iint\phi^*_i(\mu)\phi^*_j(\mu)[e^2/r]\phi_i(\nu)\phi_j(\nu)d\tau_\mu d\tau_\nu .$$

The calculated results are compared in Tables I-III with the observed values and with those by Pariser and Parr.

TABLE I
CALCULATED TRANSITION ENERGIES VS. EXPERIMENTAL VALUES OF HYDROCARBONS

| Molecule | State | Calculated energy above the ground state (ev) This paper | Calculated energy above the ground state (ev) Pariser-Parr | Obs.*) (ev) |
|---|---|---|---|---|
| Ethylene | $^1B_{1u}$ | (7.60) | (7.60) | 7.60 |
| | $^3B_{1u}$ | 4.47 | 4.5 | 3.1—5.6 |
| *trans*- | $^1B_u$ | 6.19 | 6.21 | 6.0 |
| Butadiene | $^1A_g$ | 7.72 | 7.87 | 7.2(?) |
| | $^3B_u$ | 4.10 | 3.92 | — |
| | $^3A_g$ | 6.17 | 4.61 | — |
| Benzene | $^1B_{2u}$ | 4.96 | 4.9 | 4.9 |
| | $^1B_{1u}$ | 5.37 | 5.3 | 6.0 |
| | $^1E_{1u}$ | 7.01 | 7.0 | 7.0 |
| | $^3B_{1u}$ | 3.62 | 4.0 | 3.8 |
| | $^3E_{1u}$ | 4.52 | 4.45 | — |
| | $^3B_{2u}$ | 4.96 | 4.9 | — |

*) See ref. 1 and those cited there.

It can be seen there that, in spite of the neglect of the Coulomb penetration integrals, the calculated values agree well with those observed, almost to the same extent as do the Pariser and Parr's values. It must, also, be noted that these agreements are obtained without taking account of the configuration interactions, except in benzene and triazine. This may be accepted as a good reason for neglecting the Coulomb penetration integrals and for the availability of the simple inverse sixth-power formula to compute $\beta_{pq}$, at least in hydrocarbons.

TABLE II
CALCULATED TRANSITION ENERGIES VS. EXPERIMENTAL VALUES FOR PYRAZINE AND *s*-TRIAZINE

| Molecule | State | Calculated energy above the ground state (ev) This paper | Calculated energy above the ground state (ev) Pariser-Parr | Obs. (ev) |
|---|---|---|---|---|
| Pyrazine | $^1B_{3u}$ | 4.74 | 4.71 | 4.77 |
| | $^3B_{3u}$ | 3.03 | 3.85 | 3.35 |
| *s*-Triazine | $^1A'_2$, $^3A'_2$ | 5.43 | 5.29 | 5.62*) |
| | $^1A'_1$ | 6.17 | — | — |
| | $^1E'_1$ | 7.41 | — | — |
| | $^3A'_1$ | 4.97 | 4.26 | — |

* R.C. Hirt, F. Halverson and R.G. Schmitt, *J. Chem. Phys.*, 22, 1148 (1954).

The calculation of *s*-triazine is based on the assumed bond length shown in Fig. 1, because it was non-existent. A slightly shorter C=N bond distance (1.34 Å) than in pyrazine is presumed for *s*-triazine, taking into account that the C=N bond in cyanuric triazide is shorter than 1.35 Å. As shown in Table II, the calculated result for N→V transition in *s*-triazine is improved, compared with Pariser-Parr's value. Recently it is reported that the existence of this molecule was shown by Grundmann and Kreutzberger. The experimental data of ultraviolet and infrared absorption spectra are published, and the detailed x-ray analysis is reported in progress, by which the present calculation might be revised so as to allow for the experimentally determined bond lengths.

TABLE III
CALCULATED TRANSITION ENERGIES VS. EXPERIMENTAL VALUES FOR OXYGEN CONTAINING MOLECULES

| Molecule | State | Calculated energy above the ground state (ev) | Obs. (ev) |
|---|---|---|---|
| Form- | $^1A_1$ | 7.80 | 7.95 |
| aldehyde*) | $^3A_1$ | 4.49 | — |
| Glyoxal | $^1B_u$ | 7.47 | 7.51**) |
| | $^3B_u$ | 5.09 | — |
| *p*-Benzo- | $^1B_{2u}$ | 6.08 | 5.21***) |
| quinone | $^3B_{2u}$ | 4.37 | — |

* Slight differences in calculated results between the present and the previous communication (This Bulletin, 27, 565 (1954).) are due to the different bond lengths adopted.

** Estimated value; see the previous communication (This Bulletin, loc. cit.)

*** G. Scheibe et al., *Ber.*, 59, 2617 (1926).

A comment on the calculated results of *p*-benzoquinone will be given in Sec. V.

The self-consistent molecular orbitals finally obtained are tabulated in Tables IV-V. Unfortunately, none of the molecules treated in this paper has definite dipole moment and there seems to be no means of crucial test for the quality of the molecular orbitals obtained. A few points are still to be noted. 1) The bond lengths $r_{ab}$ and $r_{bc}$ of *trans*-butadiene calculated from the theoretical bond orders through the bond order-bond length relation of Coulson are 1.35 Å and 1.49 Å, while the assumed values are 1.35 Å and 1.46 Å, respectively, a situation satisfactorily self-consistent. For other molecules containing hetero-atoms, the existence of excess charge prevents one from setting up a simple relation between bond orders and bond lengths. However, the bond length $r_{12}$ of pyrazine, where the net positive charge on carbon atoms is comparatively small, the

computed and assumed (experimental) bond lengths are in complete agreement, 1.39 Å.

2) The $\pi$-electron density on nitrogen atoms of pyrazine is computed by the simple molecular orbital method using the set of correction parameter for nitrogen atom which was found by Lowdin[7] to result in satisfactory agreements between the computed and observed values of dipole moment in diazines. It is 1.155 in units of electronic charge, while the present method gives only a little higher value, 1. 238.

These together with the fact that the present method applied to fulvene[8], yields the value of dipole moment in satisfactory agreement with the estimated value, might be helpful for judging the quality of the molecular orbitals obtained here.

TABLE IV

SELF-CONSISTENT MOLECULAR ORBITALS*)

| Molecule | $\varepsilon$ (ev) | Molecular Orbital | |
|---|---|---|---|
| *trans*-Butadiene | − 2.480 | $\phi_1=0.4397\ (\chi_a+\chi_d)+0.5538\ (\chi_b+\chi_c)$ | $q_a=1$ |
| | − 0.296 | $\phi_2=0.5538\ (\chi_a-\chi_d)+0.4397\ (\chi_b-\chi_c)$ | $q_b=1$ |
| | 10.826 | $\phi_3=0.5538\ (\chi_a+\chi_d)-0.4397\ (\chi_b+\chi_c)$ | $p_{ab}=0.974$ |
| | 13.010 | $\phi_4=0.4397\ (\chi_a-\chi_d)-0.5538\ (\chi_b-\chi_c)$ | $p_{bc}=0.227$ |
| Formaldehyde | − 3.701 | $\phi_1=0.5472\ \chi_a+0.8370\ \chi_b$ | $q_a=1.401$ |
| | 10.916 | $\phi_2=0.8370\ \chi_a-0.5472\ \chi_b$, $q_b=0.599$ | $p_{ab}=0.916$ |
| Glyoxal | − 5.140 | $\phi_1=0.5541\ (\chi_a+\chi_d)+0.4393\ (\chi_b+\chi_c)$ | $q_a=1.384$ |
| | − 3.853 | $\phi_2=0.6205\ (\chi_a-\chi_d)+0.3390\ (\chi_b-\chi_c)$ | $q_b=0.616$ |
| | 9.202 | $\phi_3=0.4393\ (\chi_a+\chi_d)-0.5541\ (\chi_b+\chi_c)$ | $p_{ab}=0.908$ |
| | 11.847 | $\phi_4=0.3390\ (\chi_a-\chi_d)-0.6205\ (\chi_b-\chi_c)$ | $p_{bc}=0.156$ |

*) $q$: $\pi$-electron density in units of $e$; $p$: mobile bond order

## Criticism of the Assumption-1

Now it seems necessary to make a remark on the validity of assumption-1, made in sec. II. According to the approximation of zero-differential overlap adopted throughout the present calculation, the Coulomb integral ($\alpha_p$) of an electron in the potential field due to the atomic cores in a molecule is expressed in terms of the Coulomb repulsion integrals as well as of the Coulomb penetration integrals as follows:

$$\alpha_p=W_{2p}-\sum_q[(pp\,|\,qq)+(q:\,pp)]\,,$$

Of the integrals in this equation, the Coulomb penetration integrals $(q:\,pp)$ can not be computed easily, in cases where the atoms $p$ and $q$ are of different species. As, in addition, the order of magnitude of $(q:\,pp)$ is supposed to be relatively small, they are left out, as a first approximation, in the calculations in the preceding sections. In order to see how much the results would be affected by this simplification, *trans*-butadiene is treated by use of the Coulomb integrals computed without leaving out the Coulomb penetration integrals. Instead of computing $(q:\,pp)$ exactly, corrections are made for $L$'s by subtracting 1.0 and 1.5 ev, respectively, from the $L_{pp}$(atom $p$ being a methylene carbon)

TABLE V

SELF-CONSISTENT MOLECULAR ORBITALS

| Molecule | $\varepsilon$ (ev) | Molecular Orbital | |
|---|---|---|---|
| Pyrazine | − 4.507 | $\phi_1=0.3646\ (\chi_1+\chi_2+\chi_4+\chi_5)+0.4838\ (\chi_3+\chi_6)$ | $q_1=0.881$ |
| | − 2.107 | $\phi_2=0.2397\ (\chi_1-\chi_2-\chi_4+\chi_5)-0.6205\ (\chi_3-\chi_6)$ | $q_3=1.238$ |
| | − 0.316 | $\phi_3=0.5000\ (\chi_1+\chi_2-\chi_4-\chi_5)$ | $p_{12}=0.651$ |
| | 9.572 | $\phi_4=0.3421\ (\chi_1+\chi_2+\chi_4+\chi_5)-0.5157\ (\chi_3+\chi_6)$ | $p_{23}=0.650$ |
| | 11.013 | $\phi_5=0.5000\ (\chi_1-\chi_2+\chi_4-\chi_5)$ | |
| | 13.506 | $\phi_6=0.4388\ (\chi_1-\chi_2-\chi_4+\chi_5)+0.3390\ (\chi_3-\chi_6)$ | |
| s-Triazine | − 4.965 | $\phi_1=0.3569\ (\chi_1+\chi_3+\chi_5)+0.4538\ (\chi_2+\chi_4+\chi_1)$ | $q_1=0.620$ |
| | − 1.940 | $\phi_2=0.2138\ (\chi_1-2\chi_3+\chi_5)-0.3478\ (\chi_2+\chi_4-2\chi_6)$ | $q_2=1.380$ |
| | − 1.940 | $\phi_3=0.3703\ (\chi_1-\chi_5)\quad+0.6024\ (\chi_2-\chi_4)$ | $p_{12}=0.621$ |
| | 10.402 | $\phi_4=0.6024\ (\chi_1-\chi_5)\quad-0.3703\ (\chi_2-\chi_4)$ | |
| | 10.402 | $\phi_5=0.3478\ (\chi_1-2\chi_3+\chi_5)+0.2138\ (\chi_2+\chi_4-2\chi_6)$ | |
| | 13.448 | $\phi_6=0.4538\ (\chi_1+\chi_3+\chi_5)-0.3569\ (\chi_2+\chi_4+\chi_6)$ | |

7) P.O. Lowdin, *J. Chem. Phys.*, **19**, 1323 (1951).
8) H. Kon, to be published soon.
9) R.G. Parr and B.L. Crawford, Jr., *J. Chem. Phys.*, **16**, 1049 (1948).

and $L_{qq}$ (atom $q$ being a methine carbon). This manner of correction comes from the following consideration: The values of Coulomb penetration integrals $(p:qq)$, where atom $p$ and $q$ are both carbon, can be obtained through the formula derived by Parr and Crawford[9] using the Slater type atomic orbitals. They are 0.91 and 0.58 ev for the interatomic distances 1.35 Å and 1.46 Å, respectively. The methylene carbon atoms in butadiene have one formal double bond (1.35 Å), while the methine carbons have one formal single (1.46 Å) and double bond. Assuming the contributions from the other atoms than those linked together directly to be small, the corrections to be made for $L$'s of a methylene and methine carbon atoms are 0.91 and 1.49 ev, respectively, which are rounded to 1.0 and 1.50 ev as given above. This correction, though it is only approximate because of ignoring the effect of the hydrogen atom and the non-neighbouring carbon atoms, would be sufficient for the qualitative purpose.

TABLE VI
COMPARISON OF CALCULATED RESULTS WITH AND WITHOUT CORRECTION

| | Correction | |
|---|---|---|
| | with | without |
| Orbital energy (ev) | − 2.730 | − 2.480 |
| | − 0.434 | − 0.296 |
| | 10.689 | 10.826 |
| | 12.777 | 13.010 |
| Excit. energy (ev) | | |
| $^1B_u$ | 6.20 | 6.19 |
| $^3B_u$ | 4.10 | 4.10 |
| Coeff. of AO | | |
| $c_{1a}$ | 0.4258 | 0.4397 |
| $c_{2a}$ | 0.5645 | 0.5538 |
| $\pi$-elec. density | | |
| $q_a$ | 0.953 | 1.000 |
| $q_b$ | 1.046 | 1.000 |
| Bond order | | |
| $p_{ab}$ | 0.972 | 0.974 |
| $p_{bc}$ | 0.228 | 0.227 |

The calculated results of transition energy, coefficients of AO, $\pi$-electron densities and mobile bond orders, with and without correction are compared in Table VI. As can be seen there, the overall alteration brought about by introducing the correction is a minor one. And though the orbital energies are changed a little after correction, the transition energies are almost unchanged. The same holds for the relation between the AO coefficients and the bond orders derived from the former.

Conspicuous among the results may be the fact that the uniformity of $\pi$-electron distribution in butadiene (or, the hydrocarbons in general), which is assured in the Hückel method is broken down by the correction. At any rate the results in Table VI, together with the good agreements between the calculated and the observed transition energies show that one can safely dispense with Coulomb penetration integrals at least in computing the transition energies of hydrocarbons (and those hetero-molecules where the perturbation due to the hetero-atoms are not so serious), and that the wave functions so obtained would be fairly good approximations to the best possible ones.

The numerical agreement between the computed and experimental transition energy of $p$-benzoquinone is shown to be inferior to other cases. (Table III) The situation may probably be improved by making such a correction as mentioned above, especially for the tertiary carbon atoms $(p)$ where, owing to the adjacent electronegative oxygen atoms, the amount to be subtracted from $L_{pp}$ is considered too great to be ignored. It can also be understood from the similar point of view that the $\pi$-electron densities on nitrogen atoms listed in Table V appear a little higher than desirable.

The author expresses his deep thanks to Professor H. Tominaga for his interest and encouragement throughout the course of this work.

*Department of Chemistry, Faculty of Science, Tôhoku University, Sendai*

# *Sorption of Gases on Evaporated Nickel Films. II. Adsorption and Decomposition of Carbon Monoxide at Low Pressures. Part 1*

By Zenjirō ODA

(Received October 19, 1954)

## Introduction

The adsorption of carbon monoxide by evaporated metallic films has already been investigated by several authors[1,2,3] it being known that carbon monoxide is chemisorbed without dissociation. However, some discrepancies are found among their views on the mechanism of adsorption. On the other hand, while a number of works[4,5,6,7] have been reported on the decomposition of this gas by reduced nickel catalysts, no attempt has been made on an evaporated nickel film. Since previous works have been carried out at higher pressures and on reduced nickel, elementary processes involved in the reaction have not yet been clarified.

The present work was undertaken to investigate the behavior of carbon monoxide molecules on a clean nickel surface at room temperature as well as at high temperatures above 100°C, which permitted one to discuss the special features of evaporated nickel film in catalytic activity. Part 1 of this series is confined to the adsorption at room temperature and the decomposition at high temperatures will be described in part 2.

## Experimental

The apparatus and procedures used were essentially the same as in the previous papers[8,9], except that the films deposited on the wall of a glass bulb at 0°C were pre-sintered at 90°C for about ten minutes.

Carbon monoxide, made by dropping 85% formic acid on concentrated sulfuric acid in a flask which was heated at about 110°C and well evacuated before the generation of the gas, was purified by passing it through the following train; (1) 55% potassium hydroxide solution, (2) the same solution containing 4% pyrogallol, (3) concentrated sulfuric acid, (4) phosphoric acid anhydride, and (5) a liquid-oxygen trap.

## Results and Considerations

1) **Adsorption Rate.**—Admitting the gas to the nickel film within the temperature range of −78 to 100°C, it is taken up in a similar way irrespective of the film temperature, and these uptakes shall be called *room-temperature-adsorption* and distinguished from *high-temperature-decomposition* which will be mentioned in part 2 of this series.

As shown in Fig. 1, the adsorption of carbon monoxide comprises two stages, i.e., an initial rapid stage and a later slow one. At the initial stage, the pressure change was too rapid to be followed by the Pirani gauge in the first one minute after admission of gas, but the rate appeared to be substantially constant irrespective of the adsorbed amount. At the later stage, on the other hand, the rate becomes slow with the amount of successive adsorption.

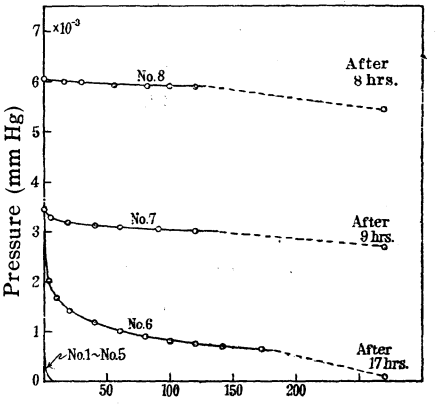



Fig. 1. Rate curves of adsorption at 0°C.

Setting the apparent rate of pressure decrease in the later stage $-\frac{dp}{dt}$ equal to the rate of adsorption $r_a$, we can plot $\log r_a$ against the adsorbed amount $v$ for curve 6 in Fig. 1, in which the rate begins to decrease with $v$ appreciably. Then a linear

1) (a) O. Beeck, A. E. Smith and A. Wheeler, *Proc. Roy. Soc.* (*London*), *A*, **177**, 62 (1940); (b) O. Beeck, "Advances in Catalysis" Vol II, Academic Press Inc. New York, 1950, p. 151.
2) E. K. Rideal and B. M. W. Trapnell, *Proc. Roy. Soc.* (*London*), *A*, **205**, 409 (1951).
3) A. S. Porter and F. C. Tompkins, ibid., A, **217**, 529, 544 (1953).
4) H. A. Bahr and Th. Bahr. *Ber.*, **61**, 2177 (1928).
5) S. Horiba and T. Ri, *Rev. Phys. Chem. Japan*, **4**, 73 (1930); T. Ri, ibid., **5**, 41 (1931).
6) H. Tsuchiya, *Bull. Inst. Phys and Chem. Research*, **10**, 951 (1931).
7) T. Kwan and T. Izu, *Catalyst*, no. 6, 43 (1949).
8) Z. Oda, *Oyobutsuri* (*J. Appl. Phys. Japan*), **22**, 142 (1953).
9) Z. Oda, This Bulletin, **27**, 467 (1954).

relation is obtained as shown in Fig. 2, from which the rate is represented as a function of $v$ by

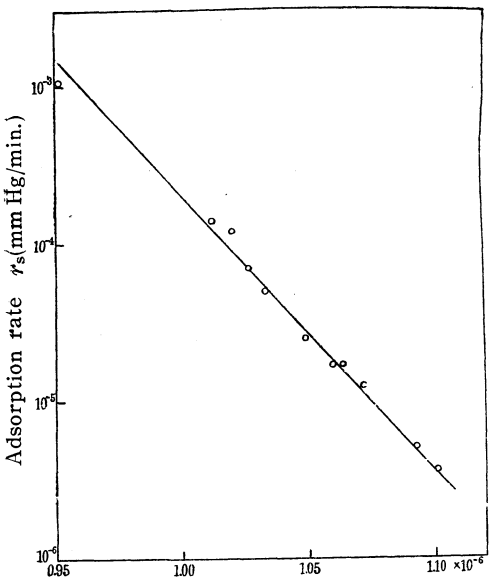



Fig. 2. The rate of adsorption as a function of adsorbed amount.

$$\ln r_a = \ln a - \alpha v, \tag{1}$$

The Elovich equation[10] is thus derived.

$$r_a = a e^{-\alpha v}. \tag{2}$$

As $r_a = \frac{dv}{dt}$, integration of Eq. (2) gives

$$v = 1/\alpha\{\ln(t+k) - \ln t_0\}, \tag{3}$$

where $k = \exp(av_0)/a\alpha$, $t_0 = 1/a\alpha$ and $v_0$ is the amount already taken up before $t=0$. Using $p$ instead of $v$ and plotting $p$ against

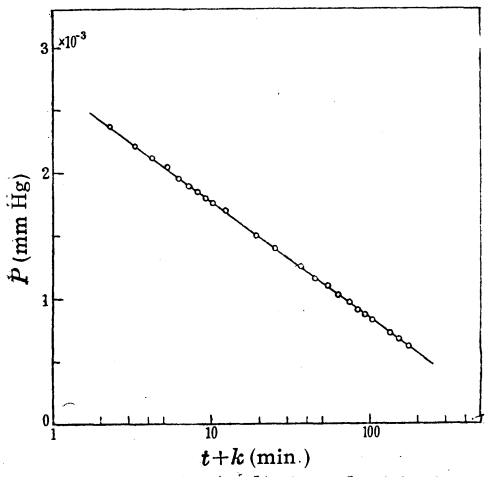



Fig. 3. $p - \log(t+k)$ plot $k = 1.3$ min.

10) S. Yu. Elovich and G. M. Zhabrova, *Zhur. fiz Khim.*, **13**, 1761, 1775 (1939).

$\log(t+k)$ for the result shown in Fig. 2, the validity of Eq. (3) is tested in Fig. 3, where the value of $k$ is selected to smooth the plot. The slope of this line gives $2.3/\alpha$. Values of $\alpha$ thus calculated from Figs. 2 and 3 are $4.09\times10^{7}$ mol.$^{-1}$ and $4.42\times10^{7}$ mol.$^{-1}$, respectively, showing a good agreement with each other. Furthermore, if one assumes $v_0=0$ at $t=0$, it is given from Eq. (3) that $t_0=k=1.3$ min. and so the initial rate $a$ is calculated to be about $1.8\times10^{-8}$ mol./min. from the relation $t_0=1/a\alpha$. This value shows a good coincidence with the observed one $5.6\times10^{-8}$ mol./min. obtained from Fig. 2. This fact indicates the assumption $v_0=0$ at $t_0=0$ to be probable, i. e., the rapid adsorption preceding the slow one is not included in Eq. (2).

When the adsorption increases still more, the rate is expressed by

$$r_a = \beta(p - p_e), \tag{4}$$

where $\beta$ is a rate constant and $p_e$ is an equilibrium pressure.

**2) Adsorption Equilibrium.** — The initial stage where the adsorption rate was very rapid gave equilibrium pressures of $10^{-6}$ to $10^{-5}$ mmHg, but at the later stage, the equilibrium was not readily attained. After measuring a rough adsorption isotherm up to a pressure of about $5\times10^{-2}$ mmHg, the system was evacuated to high vacuum. On admitting a dose of gas again, the rapid uptake was not observed but the slow one alone took place. Therefore, it is reasonable to consider that the initial stage is an irreversible adsorption and the later stage includes a reversible one; hence the calculation of isothermal heat of adsorption is not possible at the initial stage.

Now the Langmuir adsorption isotherm may be written in the form

$$p/v = 1/v_m b + p/v_m, \tag{5}$$

where $b$ is an adsorption coefficient and $v_m$ the amount adsorbed at saturation. Thus, as shown in Fig. 4a, plotting $p/v$ against $p$ for an isotherm, two straight lines intersecting at about $1\times10^{-4}$ mm Hg are obtained. Fig. 4b shows the data below this pressure on enlarged scales. From the slopes and intercepts at $p/v$ -axes in Figs. 4a and 4b, $v_m$ and $b$ can be calculated for both pressure ranges. For lower pressure range $v_{m_1}=1.15\times10^{-6}$ mol. and $b_1=4.97\times10^{5}$ mm Hg$^{-1}$; for higher range $v_{m_2}=1.29\times10^{-6}$ mol. and $b_2=3.87\times10^{3}$ mm Hg$^{-1}$. These results suggest that there exist two sites with different adsorption coefficients on the surface of the nickel film. In such a case, the adsorption isotherm is generally expressed by[11]

11) S. Brunauer, "Adsorption of Gases and Vapors, Physical Adsorption", Princeton Univ. Press, Princeton, 1945, p. 74.

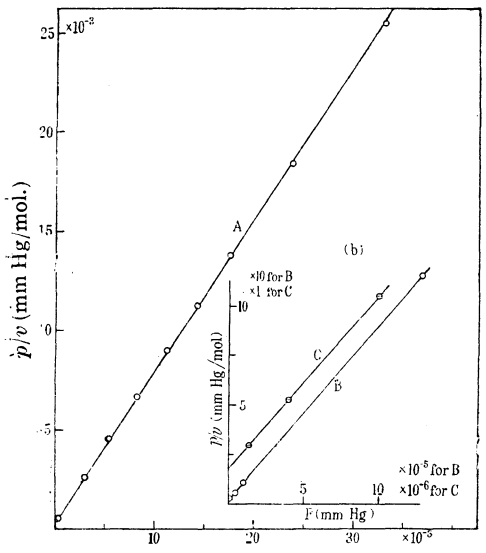



Fig. 4. Adsorption isotherms at 0°C plotted according to the Langmuir equation
(a) high-pressure range.
(b) low pressure range.

$$v=\frac{v_1b_1p}{1+b_1p}+\frac{v_2b_2p}{1+b_2p} \qquad (6)$$

In the present case, we can set $v_1=v_{m1}$, $v_2=v_{m2}-v_{m1}$ and $b_1\gg b_2$. If $p$ is small, the second term of the right-hand becomes negligible compared with the first term. So that

$$v\simeq\frac{v_1b_1p}{1+b_1p}, \qquad (7)$$

which indicates that the adsorption takes place exclusively on the sites with larger adsorption coefficient. On the other hand, if $p$ becomes large, it follows $b_1p\gg1$, so that

$$v\simeq v_1+\frac{v_2b_2p}{1+b_2p} \qquad (8)$$

which shows that the subsequent adsorption occurs on the remaining sites with smaller adsorption coefficient.

The amounts of rapid adsorption and the total one measured with several films at 0°C are summarized in Table I. The ratio of the rapid adsorption to the total one is about 80% and the average value of the latter is $3.92\times10^{-6}$ mol./10 mg. Ni.

## Discussions

Porter and Tompkins[3] have found the Elovich equation to be applicable to the rate of uptake of hydrogen and of carbon monoxide by evaporated iron films between 78 and 140°K. In order to interpret these results they have considered the total process involving the initial rapid process to be a united process, by assuming that the iron film has a heterogeneous surface with sites of different adsorption potential and activation energy required for adsorbed molecules to migrate, so that the sticking of gas molecules must proceed from sites of lower activation energy to sites of higher. However, as mentioned above, in the adsorption of carbon monoxide as well as in the case of oxygen[9], the rate of uptake in the initial stage is very rapid and substantially constant, independent of the adsorbed amount; in the case of the former this rapid adsorption amounts to about 80% of the total adsorption, after which the rate falls with the increase in adsorption. Furthermore, Eq. (2) has been proved to be applicable to the beginning of the later stage only.

From these facts, another interpretation for Eq. (2) than that of the above authors is desirable. Davis[12] has shown that in the chemisorption of nitrogen on tungsten the activation energy $E$ increases with surface coverage $\theta$. Recently Zwietering and Roukens[13] have also observed the same relation in the chemisorption of nitrogen on iron. If such a relation is assumed to exist in the present system, we may write

$$E(\theta)=E_0+r\theta, \qquad (9)$$

12) R. Davis, *J. Am. Chem. Soc.*, 68, 1395 (1946).
13) P. Zwietering and J. J. Roukens, *Trans. Farad. Soc.*, 50, 178 (1954).

Table I
Initial adsorption and total adsorption of CO at 0°C

| Equil. pressure | Evaporated amount | Rapid adsorption | Total adsorption (obs.) | Total adsorption (per 10mg. Ni) | Rapid adsorption / Total adsorption |
|---|---|---|---|---|---|
| $\times10^{-2}$ mm Hg | mg. | $\times10^{-6}$ mol. | $\times10^{-6}$ mol. | $\times10^{-6}$ mol. | % |
| 3.5 | 3.3 | 1.12 | 1.38 | 4.18 | 81.3 |
| 3.5 | 3.3 | 1.10 | 1.34 | 4.06 | 82.1 |
| 4.3 | 3.2 | 0.99 | 1.21 | 3.78 | 81.8 |
| 8.5 | 3.4 | 1.00 | 1.25 | 3.68 | 79.9 |
| | | | (average) | 3.92 | 81.3 |

where $E_0$ is the activation energy at the initial stage.

It is well known that carbon monoxide is adsorbed on evaporated metallic films as molecules[1,2,3]. Hence, the rate is generally given by the following equation

$$r_a = kp(1-\theta)e^{-E(\theta)/RT}. \quad (10)$$

Substituting for $E(\theta)$ from Eq. (9),

$$r_a = kp\, e^{-E_0/RT}(1-\theta)\, e^{-(\gamma/RT)\theta}. \quad (11)$$

In the isothermal adsorption, if $p$ is constant or its change is small, it is possible to set $kp\, e^{-E_0/RT} = a_0$ and $\gamma/RT = \alpha_0$. Then Eq. (11) reduces to

$$r_a = a_0(1-\theta)\, e^{-\alpha_0\theta}. \quad (12)$$

When $\alpha_0$ is so large that the change of $(1-\theta)$ can be negligible compared with that of $e^{-\alpha_0\theta}$, Eq. (12) may be approximately represented by the expression

$$r_a = a\, e^{-\alpha_0\theta}, \quad (13)$$

which is formally identical with Eq. (2).

In terms convenient for application to the data shown in Fig. 2, Eq. (9) can be written in the form

$$E(v) = E_0 + \gamma' v.$$

Since $\alpha = 4\times10^7$ mol.$^{-1}$ and $RT = 2\times273 = 546$ cal./mol., we obtain $\gamma' = \alpha RT = 2.2\times10^{10}$ cal./mol.[2] In addition, since the amount adsorbed in this run is $v = 1.5\times10^{-7}$ mol., the activation energy for the final part of this run is given by

$$E = E_0 + 3.3 \text{ kcal./mol.},$$

i.e., the activation energy increases by 3.3 kcal./mol. during this adsorption.

On the other hand, it is found from the adsorption isotherms that the surface of nickel film comprises two areas with sites differing in their adsorption coefficients and these areas correspond to the rapid and slow adsorption, respectively. According to Beeck[1], the heat of adsorption of carbon monoxide on nickel film is 35 kcal./mol. and constant over 85% of the surface coverage, after which it falls abruptly to a very low value. Hence, it is reasonable to consider the heat of adsorption at the initial stage equal to 35 kcal./mol. and that at the later stage corresponding to a very low value.

For the explanation of the over-all process of adsorption in connection with the surface character of the films, we assume the surface to comprise two areas A and B. Area A has sites of high heat of adsorption $Q_A$ and the adsorption on these requires a small activation energy $E_A$; area B has sites of low heat of adsorption $Q_B$ and for these the corresponding energy $E_B$ is large: between these quantities we have the relation $Q_A > Q_B$ and $E_A < E_B$. On admitting an amount of gas to a fresh film, gas molecules colliding at random against the surface will be adsorbed exclusively by A at the initial stage. After A has been completely covered with gas molecules, the adsorption on B will begin. However, $E_B$ is so large compared with $E_A$, that this process can be expected to be slow. These deductions would lead to a view that the initial and later stages correspond to A and B, respectively, i.e., the ratio of A to the total area is about 80% and the remainder corresponds to area B. However, it may be assumed that there exist some adsorption sites with various intermediate values of $Q$ and $E$ between those for A and B. Hence Eq. (2) is interpreted to represent the adsorption rate on these sites. On the other hand, when the remaining area becomes B alone, it is possible to set $\gamma = 0$, $E_0 = E_B$ and $\theta = \theta_B$ the coverage fraction of B. Then Eq. (11) becomes

$$r_a = kp(1-\theta_B)\, e^{-E_B/RT}. \quad (14)$$

At constant temperature and if $p$ is nearly constant or its change is small, Eq. (14) reduces to

$$r_a = \beta_0(1-\theta_B), \quad (15)$$

with $\beta_0 = kp\, e^{-E_B/RT}$. This equation is equivalent to Eq. (4). Thus the adsorption of carbon monoxide on nickel films may be satisfactorily interpreted in terms of the non-uniformity of the surface throughout its over-all process.

In conclusion, the auther wishes to thank Mr. Y. Mizushima for valuable discussion and Mr. T. Ichimiya for his interest and encouragement.

*The Electrical Communication Laboratory, Nippon Telegraph and Telephone Public Corporation, Musashino-shi, Tokyo*

# *Sorption of Gases on Evaporated Nickel Films. III. Adsorption and Decomposition of Carbon Monoxide at Low Pressures. Part 2*

By Zenjirō ODA

(Received October 29, 1954)

## Introduction

As mentioned in part 1[1] of this series, carbon monoxide was merely chemisorbed by nickel films under 100°C. However, with the rise of temperature above 130°C., carbon monoxide was found to be decomposed to carbon dioxide and atomic carbon which reacted with nickel atoms to give nickel carbide. In this report the kinetics of decomposition is discussed on the basis of the non-uniformity of the surface.

## Experimental

In order to determine the quantity of carbon dioxide produced by the decomposition of carbon monoxide, the apparatus used was partially modified as shown in Fig. 1. The reaction bulb

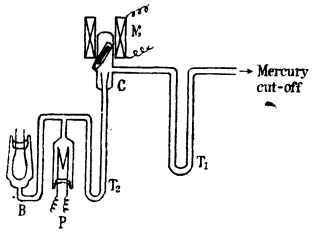



Fig. 1. The reaction apparatus.
B. Evaporation bulb; $T_1$, $T_2$. Cold traps
P. Pirani gange; C. Greaseless cock;
M. Electro-magnet.

was connected to the gas handling system through two cold traps $T_1$, $T_2$ and a "greaseless cock" C. During the reaction these traps were cooled with liquid-oxygen. The carbon dioxide produced was condensed onto the inside wall of $T_2$. Closing the "greaseless cock" C by means of an electro-magnet and removing the liquid-oxygen from $T_2$, the increase in pressure in the volume of $BPT_2$ could be measured by the Pirani gauge P. As will be mentioned below, since carbon dioxide was not adsorbed by nickel films covered with the carbon monoxide layer of rapid adsorption, the amount of carbon dioxide liberated was evaluated[2] from the rise in pressure.

In order to study the changes of the film structure after reaction, a small piece of cover glass for the microscope slide was previously set in the bulb, on which the nickel film was also deposited. When the reaction was finished, this piece was taken out as a sample for electron diffraction study. The films used in this experiment were pre-sintered for about thirty minutes at the same temperatures as those of the reaction.

## Results and Considerations

**1) Production of Carbon Dioxide.** — Changing the reaction temperature in turn from 100 to 250°C for each gas admission, the pressure change was followed. Fig. 2

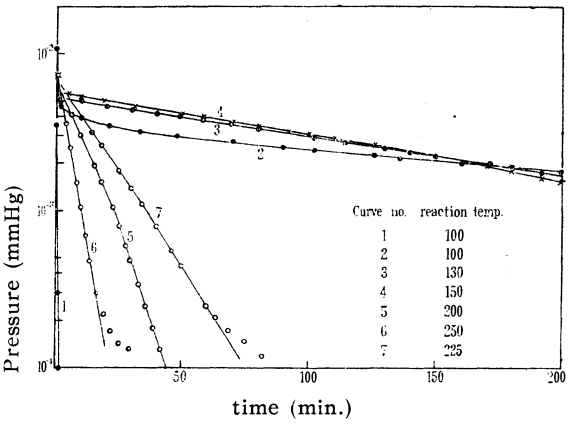



Fig. 2. Reaction rate curves at various temperatures.

shows the rate curves in log $P$ vs $t$ plots. We see that at the later stage the plots at 100°C are slightly convex, linear at 130°C and slightly concave towards $t$-axis at 150[3] and 200°C, whereas at 250°C the plot yields a straight line except below the pressure of $3\times10^{-4}$ mmHg. With the "greaseless cock" closed and liquid-oxygen removed from $T_2$, a remarkable rise in pressure was observed above 130°C. Even if the trap was cooled again by dry ice, pressure change was hardly observed. Furthermore, mass-spectrometric analysis[4] proved this condensable gas to be carbon dioxide. Hence, it became evident

1) Z. Oda, This Bulletin, 28, 281 (1955).

2) Allowance were made for the difference in temperature of each part and the leak of the "greaseless cock". The accuracy was about ±5%.

3) In this case, since the amount of carbon produced before this run was very small, it was considered that the diffusion of carbon took place readily, and the behavior was similar to that at 200°C.

4) A small gas reservoir with a "magnetic-slug-break-off" was previously inserted ahead of trap $T_2$. After reaction the gases condensed in trap $T_2$ were collected in this reservoir by transferring liquid-oxygen from $T_2$ to it, and then it was sealed off and analysed.

that carbon monoxide was decomposed on nickel film above 130°C.

On admitting the gas to a fresh film at a constant temperature, the rate of pressure change and the amount of carbon dioxide produced in each run was measured. These results obtained at 200 and 150°C are given in Figs. 3a, 3b, 4a and 4b. As shown in Figs. 3a and 3b, at the initial stage, carbon dioxide was not observed immediately after the reaction had ceased. This was also the case, even if the film was kept for several hours.

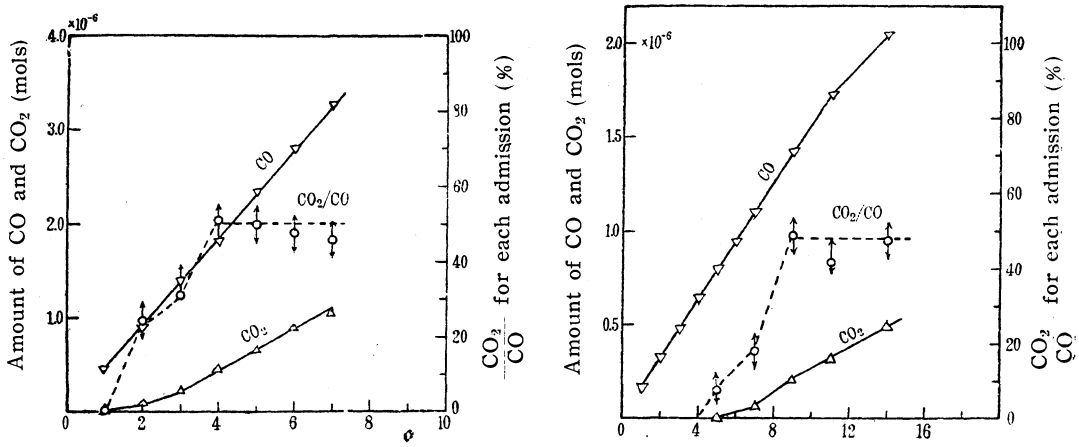



Fig. 3. The ratio of the amount of $CO_2$ produced to that of CO consumed.

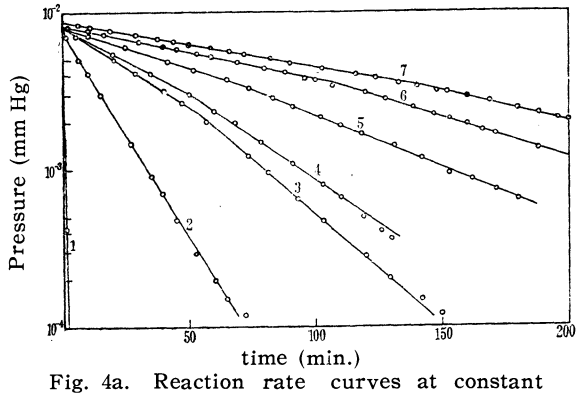



Fig. 4a. Reaction rate curves at constant temperature. ($T$=200°C)

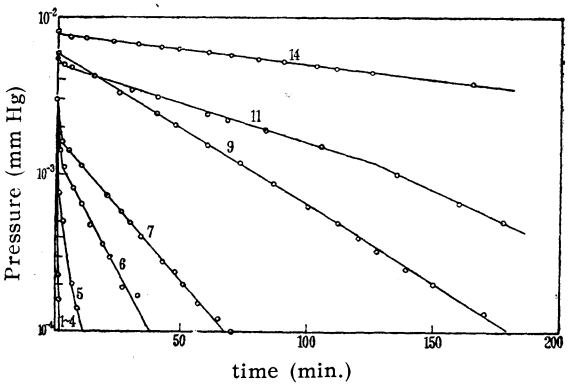



Fig. 4b. Reaction rate curves at constant temperature. ($T$=150°C)

at that temperature. With repetitions of reaction, the ratio of the amount of carbon dioxide to that of carbon monoxide consumed in one run (denoted by $CO_2$/CO) increases to 40~50%, which suggests that the reaction $2CO=CO_2+C$ occurs quantitatively on nickel films. Comparing these behaviors with the rate curves at 200°C shown in Fig. 4a, it is seen that run 1 represents the curve of adsorption, runs 2 and 3 the rate curves comprising the adsorption and decomposition, and the runs after 4 are regarded as being of decomposition itself. In a example at 150°C shown in Fig. 4b, a similar state of affairs occurs, i.e., the runs after 9 are the rate curves of decomposition. However, the log $P$ vs $t$ plots show linear relation at pressures above $10^{-4}$ mm Hg in order. At 250°C, on the other hand, while the ratio $CO_2$/CO changes in a manner similar to that at 200°C, the rate curves are linear between $1\times10^{-2}$ and $3\times10^{-4}$ mm Hg and slightly concave towards $t$-axis in higher pressure range than $1\times10^{-2}$ mm Hg.

**2) The Initial Stage.**—Prior to considerations of the rate of decomposition, we shall first compare the initial rapid adsorption with the total adsorption at high temperatures. The total adsorption[5] $3.92\times10^{-6}$ mol./10 mg

5) This is defined as the amount taken up at 0°C and $P$=$5\times10^{-2}$ mm Hg as mentioned in part 1.

Ni shown in part 1 of this series is the average value for several films pre-sintered at 90°C for ten minutes. In the present case, however, since the films have been pre-sintered at higher temperatures, their available areas should be decreased. Fig. 5

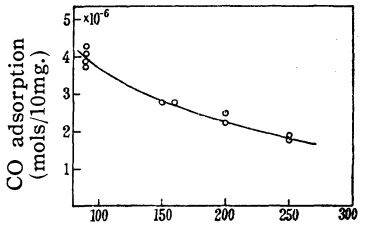



Fig. 5. Variation of total adsorption with pre-sintering temperature.

shows the variation of the total adsorption with pre-sintering temperature when the films have suffered pre-sintering for thirty minutes. These results are listed in Table 1, from which the initial adsorption is found to occupy 70~80% of the available area and to be almost independent of the reaction temperature.

However, it was not evident whether carbon monoxide was adsorbed with or without decomposition at the initial stage. While it was noted by previous authors that at high temperatures carbon dioxide was hardly adsorbed[5,7] on a nickel surface or slightly adsorbed[8] with dissociation even at 30°C, their experimental conditions differed substantially from the present author's. Hence, an attempt was made to make sure whether carbon dioxide was adsorbed on nickel film or not. After cooling only the trap $T_2$ with dry ice instead of liquid-oxygen, a dose of carbon dioxide was admitted to the film at 150 and/or 250°C. When the surface was clean or partially covered with carbon monoxide, rapid adsorption was observed. However, no adsorption was found after the rapid adsorption of carbon monoxide had been completed. This fact suggests that in the initial stage, if any carbon dioxide is formed, it is also adsorbed on nickel film and does not condense in the trap cooled with liquid-oxygen. Hence, it is impossible to decide the adsorbed state of carbon monoxide on nickel film. However, it may be possible to conclude that carbon monoxide and or its degradation products are strongly bounded by film surface and not readily desorbed until the surface is covered to 70~80% of its available area.

TABLE I

INITIAL RAPID ADSORPTION OF CO AT HIGH TEMPERATURES BEFORE DFCOMPOSITION

| React. temp. | Evaporated amount | Rapid adsorption (obs.) (per 10 mg. Ni) | | Total adsorption* (per 10 mg. Ni) | (Rapid adsorption)/(Total adsorption) |
|---|---|---|---|---|---|
| °C | mg. | $10^{-3}$ mol. | $10^{-6}$ mol. | $10^{-6}$ mol. | % |
| 150 | 3.3 | 0.65 | 1.97 | | |
| | 3.5 | 0.71 | 2.03 | | |
| | 2.8 | 0.78 | 2.78 | | |
| (average) | | | 2.33 | 2.9 | 80.3 |
| 200 | 3.2 | 0.52 | 1.62 | | |
| | 2.3 | 0.39 | 1.69 | | |
| | 3.0 | 0.49 | 1.65 | | |
| | 3.6 | 0.56 | 1.56 | | |
| | 2.8 | 0.46 | 1.64 | | |
| | 3.6 | 0.57 | 1.58 | | |
| (average) | | | 1.62 | 2.25 | 73.2 |
| 250 | 3.0 | 0.41 | 1.37 | | |
| | 3.5 | 0.48 | 1.37 | | |
| (average) | | | 1.37 | 1.8 | 76.1 |

*) Average values obtained from Fig. 5.

3) **The Later Stage.**—As mentioned above, the amount of carbon monoxide consumed in one run is wholly converted to carbon dioxide after the reaction has been repeated many times, and thus considerations will be made in such a case.

Now we start on the assumption that the decomposition of carbon monoxide on the

6) N. Nikitin, *Z. anorg. Chem.*, **154**, 130 (1926).

7) S. Horiba and T. Ri, *Rev. Phys. Chem. Japan*, **4**, 41 (1930).

8) J. A. Dillon and H. E. Farnsworth, *Phys. Rev.*, **94**, 753 (1954) ; *J. Chem. Phys.*, **22**, 1601 (1954).

surface of nickel film proceeds through the following elementary processes:

1) $CO\ (g) \rightleftarrows CO\ (ads)$,
2) $CO\ (ads) \rightarrow (C-O)^*$,
3) $CO\ (g)+(C-O)^* \rightarrow CO_2(g)+C\ (atom)$,
4) $C\ (atom)+Ni \rightarrow Ni_3C$,

where $(C-O)^*$ represents the activated state of a carbon monoxide molecule. Assuming the reaction 2) to be the rate-determining step, the reaction will be of the first order with respect to the adsorbed amount of carbon monoxide $v$. Hence the rate is given by

$$-dP/dt=k_1v \qquad (1)$$

Let $\theta_{co}$ and $\theta_c$ denote the fraction of the adsorption sites covered by carbon monoxide and carbon[9], respectively, then $(1-\theta_{co}-\theta_c)$ gives the fraction still bare at a given time. The corresponding adsorption isotherm is given by

$$\frac{\theta_{co}}{1-\theta_{co}-\theta_c}=bP. \qquad (2)$$

Hence

$$\theta_{co}=\frac{(1-\theta_c)\,bP}{1+bP},$$

or, using $v$ instead of $\theta_{co}$,

$$v=\frac{(1-\theta_c)v_m bP}{1+bP}, \qquad (3)$$

where $v_m$ is the amount of carbon monoxide corresponding to the total adsorption sites. Upon substituting this value for $v$ in Eq. (1), we obtain

$$-dP/dt=k_1(1-\theta_c)v_m bP/1+bP. \qquad (4)$$

Since the rate curves obtained is apparently of different form depending on temperature, we shall consider each case.

i) 200°C.

In this case, since carbon formed on the surface is considered to diffuse rapidly to interior, the rates of its production and disappearance from the surface balance with each other at a given $\theta_c$. Hence, $\theta_c$ may be taken as nearly constant during the reaction period of one admission, and thus Eq. (4) can be reduced to

$$-dP/dt=k_2P/1+bP, \qquad (5)$$

where

$$k_2=k_1(1-\theta_c)bv_m. \qquad (6)$$

Intergation of Eq. (5) gives

$$\ln P+bP=C-k_2t, \qquad (7)$$

or

$$\log P+(b/2,3)P=C'-(k_2/2,3)t. \qquad (8)$$

This means that if $b$ is sufficiently large the log $P$ vs $t$ plot should be concave towards $t$-axis (cf. Fig, 4a). In order to apply Eq. (8) to the experimental data, it is necessary to obtain the value of $b$. By assuming that as the reaction time increases the term $(b/2.3)P$ becomes negligible compared with the absolute value of log $P$ in the pressure range studied, Eq. (8) will be reduced to

$$\log P=C'-(k_2/2,3)t. \qquad (9)$$

Therefore, in Fig. 4a, by extrapolating the curve at large $t$ towards a smaller one and setting the extrapolated value at any time $t$ to be $G$, a plot of $G-\log P$ vs $P$ is obtained as shown in Fig. 6. The slope of this line

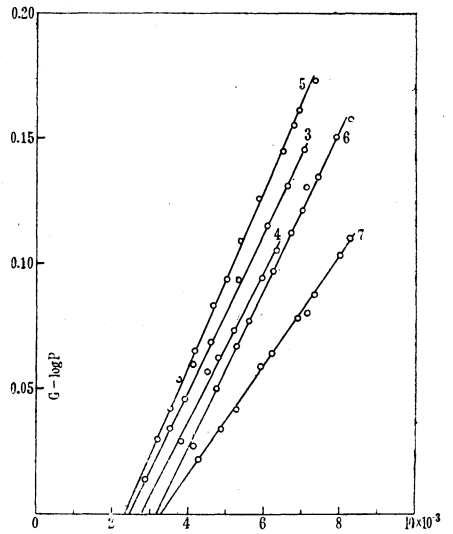



Fig. 6. $G-\log P$ vs $P$ plots.

gives $b/2.3$. Thus, plotting $\log P+(b/2.3)P$ against $t$ for the data shown in Fig. 4a, good straight lines are obtained as shown in Fig. 7. Although the value of $b$ is nearly constant, independent of the repetition of reaction, the slope of lines, i.e., $k_2$ decreases with reaction. According to the relation (6) this is attributed to the increase of $\theta_c$, i.e., a blocking effect by the carbon produced.

ii) 150°C.

From the definition of $b$ it is anticipated that the bends in the log $P$ vs $t$ plots at this temperature must appear in a lower pressure range than at 200°C. This is evident by comparing Fig. 4b with Fig. 4a.

On the other hand, since the diffusion of carbon seems to be slower than at 200°C $k_2$ should not be constant but should decrease with time even in one run. Therefore, it is probable that the tendency to become concave towards $t$-axis due to the neglet of $(b/2.3)P$ term is just compensated by the decrease of $k_2$, and thus the plots yield straight lines

9) This includes atomic carbon and nickel carbide ($Ni_3C$) remaining on the surface.

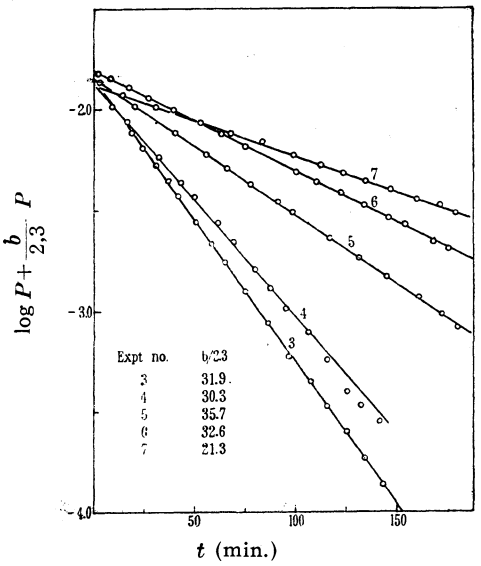



Fig. 7. $\log P+\frac{b}{2,3}P$ vs $t$ plots.

above $1\times10^{-3}$ mm Hg pressure. Consequently the plots of $G-\log P$ vs $P$ are not represented by straight lines giving the value of $b/2.3$. Although it is impossible to analyse the reaction rate more precisely, Eq. (4) seems to hold for this case also.

ii) 250°C.

In this case, $v$ is so small that the bend due to $(b/2.3)P$ term is not observed below $1\times10^{-2}$ mm Hg. For example, a value of $b$ derived from a rate curve above this pressure is 15 $(\text{mm Hg})^{-1}$, from which it follows $bP=0.075$ at $P=5\times10^{-3}$ mm Hg. Thus neglecting $bP$ compared to 1 in Eq. (5), we find

$$-dP/dt=k_2P, \qquad (10)$$

i.e., the reaction becomes of the first order type in agreement with experimental results.

4) **Heat of Adsorption and Activation Energy of Decomposition.**—Let $Q$ and $E_2$ be the heat of adsorption and the apparent activation energy of the reaction, respectively, the temperature dependencies of $b$ and $k_2$ are given by

$$b=b_0e^{Q/RT} \quad \text{and} \quad k_2=k_{20}e^{-E_2/RT}. \qquad (11)$$

Therefore, at two temperatures, for example 200 and 225°C, the rates of decomposition were measured on the same film and $b$ was evaluated by the procedure noted above. From plots of $\log b$ vs $1/T$ and $\log k_2$ vs $1/T$ for two films, the average values of $Q$ and $E_2$ were found to be about $20.5\pm1.4$ and $14.6\pm0.7$ kcal/mol., respectively.

In addition, the temperature dependency of $k_1$ is given by

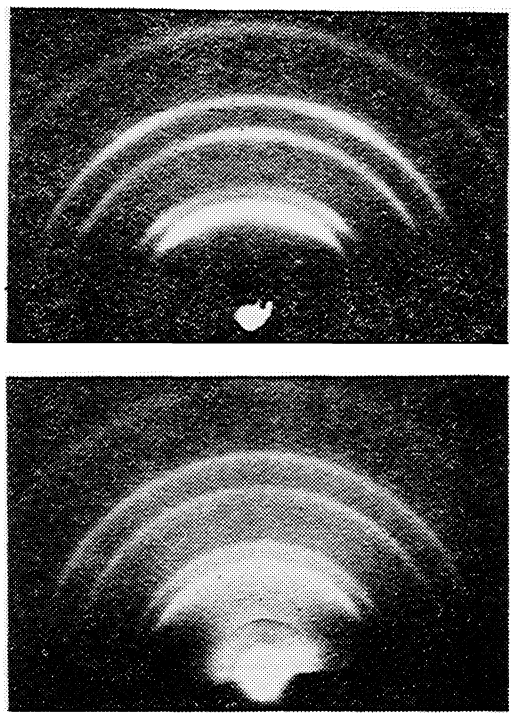
$$k_1=k_{10}e^{-E_1/RT}. \qquad (12)$$

Hence, from Eqs. (6), (11) and (12) we can obtain a relation

$$E_2=E_1-Q. \qquad (13)$$

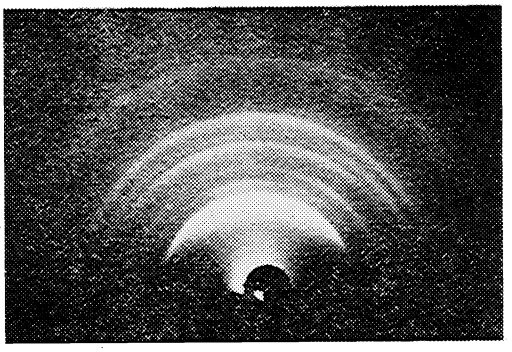
With the values of $Q$ and $E_2$ obtained above, it follows $E_1=35.1\pm2.1$ kcal/mol., which may be regarded as the potential energy difference between the activated state and the adsorbed state of the reactant. It is interesting to note that this energy is nearly equal to the heat of adsorption[10] at the initial stage where the decomposition cannot be detected.

5) **Electron Diffraction Study.**—After the reaction had been carried out under various conditions, electron diffraction photographs were taken with six films. If the ratio of the number of reactant molecules consumed to that of nickel atoms deposited was less than about 20%, the nickel pattern alone was observed, but if this ratio reached to about 40%, nickel carbide ($Ni_3C$) pattern[11] was also revealed in addition to that of nickel. The electron diffraction photographs before and after reaction are shown in Fig. 8.




10) See part 1.

11) This was analysed by X-ray diffraction data given by A. Cimino and G. Parravano, *J. Phys. Chem.*, **56**, 706 (1952).



(c)

Fig. 8. Electron diffraction patterns of evaporated nickel films before and after reaction. (a) Pre-sintered at 100°C. for 1 hr. (b) After reaction at 200°C.; CO molecules consumed $=1.98\times10^{18}$, Ni atoms of film $=2.9\times10^{19}$. (c) After reaction at 250°C.; CO molecules consumed $=1.29\times10^{19}$, Ni atoms of film $=3\times10^{19}$.

It has been pointed out by several authors[12,13,14] that in the carburization of nickel by carbon monoxide, carbide is initially formed and then graphitic carbon is produced, which increases with the rise in reaction temperature[15]. When the extent of decomposition is small no pattern of nickel carbide is detected. This fact may be interpreted as the insufficient intensity of diffraction by carbide of a small amount, even though it exists. We can conclude, therefore, that carbon monoxide is converted to carbon dioxide and nickel carbide instead of graphitic carbon on the surface of evaporated nickel films under our experimental conditions.

## Discussion

As has been mentioned in part 1, the surface is assumed to be non-uniform and consisted of two areas A and B with different activity. From the fact that the decomposition at high temperatures occurs after the initial rapid adsorption which covers a fraction of surface similar to that at *room-temperature-adsorption*, it is surely expected that carbon monoxide molecules adsorbed on B would participate in the reaction. Furthermore, the fact that the heat of adsorption obtained from the temperature dependency of $b$ is smaller than that on A (=35 kcal/mol.) also suggests that the molecules adsorbed on B with lower heat of adsorption would be activated and undergo decomposition. That is, in the decomposition of carbon monoxide, sites with high heat of adsorption are not active but those with low heat are rather active because of the ease of desorption. Similar observation has been made by Beeck[16] in the catalytic hydrogenation of ethylene with various evaporated metallic films. He has pointed out that the metals with higher activity possess lower heat of adsorption for ethylene and explained this finding by the reasoning that metals with higher heat of adsorption for ethylene are poisoned more seriously by adsorbed ethylene and its degradation products because of the difficulty of desorption.

In the previous investigations[7,17] on the decomposition of carbon monoxide by reduced nickel catalysts, such a phenomenon as that rapid adsorption precedes decomposition has not been observed. This difference may be attributed to the difference in the cleanliness of the surface. That is, under any conditions for the preparation of reduced catalysts generally adopted, it seems to be very difficult or impossible to drive out some impure gases which adhere firmly to the surface and produce such a clean surface as evaporated film. The catalytic reactions on these reduced catalysts have been well interpreted in terms of the intrinsic heterogeneity of the surface. In this work also, to explain the results obtained, it has been necessary to assume the surface heterogeneity on the evaporated nickel films, in spite of their cleanliness. However, it is uncertain whether this heterogeneity is due to the intrinsic difference in surface energy or the interaction of adsorbed molecules or both.

In conclusion, the author wishes to express his thanks to Messrs. Y. Mizushima and T. Ichimiya for their interest in this investigation and for valuable discussion; to Mr. K. Ono for the electron diffraction study, and to Mr. K. Nakagawa for mass-spectrometric analysis.

*The Electrical Communication Laboratory, Nippon Telegraph and Telephone Public Corporation, Musashino-shi, Tokyo*

12) H. A. Bahr and Th. Bahr, *Ber.*, **61**, 2177 (1928).
13) H. Tsuchiya, *Bull. Inst. Phys. and Chem. Research*, **10**, 951 (1931).
14) S. Oketani, S. Nagakura and K. Tsuchiya, *J. Japan Inst. Metals*, **18**, 325, 329 (1954).
15) The critical temperature where the process $Ni_3C \rightarrow C+Ni$ (or $Ni_xC$) begins to occur has been variously reported, for example 270,[12] 420 [13] or 500°C[14].
16) O. Beeck, *Disc. Farad. Soc.*, No 8, 118 (1950).
17) T. Kwan and T. Izu, *Catalyst*, No 6, 43 (1949).

# *On the Electronic Structures of Butadiene*

By Yuji MORI

(Received December 20, 1954)

## Introduction

The interpretation of the ultraviolet absorption spectra of molecules is approached by two methods in principle. The first is the molecular orbital[1] method, and the second is the valence bond method[2]. The hybridized method between these two, which was developed by London and was used in the calculation of the ultraviolet absorption spectra of diphenyl[3], has been employed in the present study. The outline of this method is as follows*. The molecule under consideration is divided into some parts in such a way that they have simple forms of molecular orbitals. Then the wave function of the entire molecule is approximated by the products of antisymmetrized molecular orbitals of these parts. For instance, styrene is divided into two parts, i. e., the phenyl radical and the vinyl radical. Then the wave functions of the $\pi$-electron system of styrene are expressed by the antisymmetrized products of molecular orbitals of the benzene ring and of the vinyl radical.

The important character of this treatment is that the electronic states of the entire molecule are expressed by those of the simple parts included in it. So this method may be thought of as the valence bond method which has the local molecular orbitals taking the place of the atomic orbitals.

In this treatment, polar structure which means charge transfer from one part to another is important for the excited state. Previously the absorption spectra[4] of styrene was studied by this treatment including polar structures, and it was shown that polar structures are important for excited states.

In the present paper, polar and bonding structures between $\pi$-electron systems of the two vinyl radicals of butadiene are introduced, and for convenience the semi-empirical treatment investigated by Parizer and Parr[5] is applied in the later section.

## Wave Functions and Computations

The "*trans*-form" model is chosen for butadiene in the present calculation, and the bond distances and the bond angle of skeleton are equal to those of the model in the calculation of Parr and Mulliken[6] (Fig. 1).

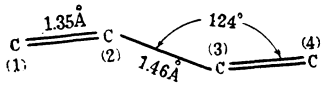



Fig. 1.

The wave functions of the $\pi$-electron system of butadiene are expressed by the $\pi$-electron wave functions of two vinyl radicals having the molecular orbitals as

$$\varphi_1=\frac{1}{\sqrt{2\sigma_1}}(\chi_1+\chi_2),\quad \varphi_3=\frac{1}{\sqrt{2\sigma_3}}(\chi_3+\chi_4),$$

$$\varphi_2=\frac{-1}{\sqrt{2\sigma_2}}(\chi_1-\chi_2),\quad \varphi_4=\frac{1}{\sqrt{2\sigma^4}}(\chi_3-\chi_4),$$

where $\chi_i$ is the atomic orbital, and $\sigma_i$ is the normalization factor.

Thus the unperturbed wave functions of butadiene are

$$(^1A_g),\ \psi_1=\frac{1}{\sqrt{4!}\sqrt{N_1}}\sum_P(-1)^P P\varphi_1(1)\bar{\varphi}_1(2)\varphi_3(3)\bar{\varphi}_3(4),$$

$$(^1A_g),\ \psi_2=\frac{1}{\sqrt{4!}\sqrt{N_2}}\sum_P(-1)^P P\frac{1}{2}\{\varphi_1(1)\bar{\varphi}_2(2)\varphi_3(3)\bar{\varphi}_3(4)$$
$$-\bar{\varphi}_1(1)\varphi_2(2)\varphi_3(3)\bar{\varphi}_3(4)+\varphi_1(1)\bar{\varphi}_1(2)\varphi_3(3)\bar{\varphi}_4(4)$$
$$-\varphi_1(1)\bar{\varphi}_1(2)\bar{\varphi}_3(3)\varphi_4(4)\},$$

$$(^1B_u),\ \psi_3=\frac{1}{\sqrt{4!}\sqrt{N_3}}\sum_P(-1)^P P\frac{1}{2}\{\varphi_1(1)\bar{\varphi}_2(2)\varphi_3(3)\bar{\varphi}_3(4)$$
$$-\bar{\varphi}_1(1)\varphi_2(2)\varphi_3(3)\bar{\varphi}_3(4)-\varphi_1(1)\bar{\varphi}_1(2)\varphi_3(3)\bar{\varphi}_4(4)$$
$$+\varphi_1(1)\bar{\varphi}_1(2)\bar{\varphi}_3(3)\varphi_4(4)\},$$

$$(^1A_g),\ \psi_4=\frac{1}{\sqrt{4!}\sqrt{N_4}}\sum_P(-1)^P P\frac{1}{2}\{\varphi_1(1)\bar{\varphi}_4(2)\varphi_3(3)\bar{\varphi}_3(4)$$
$$-\bar{\varphi}_1(1)\varphi_4(2)\varphi_3(3)\bar{\varphi}_3(4)+\varphi_1(1)\bar{\varphi}_1(2)\varphi_3(3)\bar{\varphi}_2(4)$$
$$-\varphi_1(1)\bar{\varphi}_1(2)\bar{\varphi}_3(3)\varphi_2(4)\},$$

1) Concerning the simple MO method, Eyring, "Quantum Chemistry", (1949), p. 192, 254. Concerning the ASMO method, M. Goeppert-Mayer and A. L. Sklar, *J. Chem. Phys.*, 6, 645 (1938); D. P. Craig, *Proc. Roy. Soc.*, A200, 474 (1950). Concerning the LCAOSCF method, C. C. J. Roothaan, *Rev. Mod. Phys.*, 23, 69 (1951).

2) L. Pauling, *J. Chem. Phys.*, 1, 280 (1933); Eyring "Quantum Chemistry," (1949) p 243.

3) A. London, *J. Chem. Phys.*, 13, 364 (1945).

* Reference 3).

4) Unpublished, presented at the Annual Meeting of the Chemical Society of Japan, Tokyo, April, 1951.

5) R. Pariser and R. G. Parr, *J. Chem. Phys.*, 21, 466, 767 (1953).

6) R. G. Parr and R. S. Mulliken, *J. Chem. Phys.*, 18, 1338 (1950).

$$(^1B_u),\quad \psi_5=\frac{1}{\sqrt{4!}\sqrt{N_5}}\sum_P(-1)^P P\frac{1}{2}\{\varphi_1(1)\bar{\varphi}_4(2)\varphi_3(3)\bar{\varphi}_3(4)$$
$$-\bar{\varphi}_1(1)\varphi_4(2)\varphi_3(3)\bar{\varphi}_3(4)-\varphi_1(1)\bar{\varphi}_1(2)\varphi_3(3)\bar{\varphi}_2(4)$$
$$+\varphi_1(1)\bar{\varphi}_1(2)\bar{\varphi}_3(3)\varphi_2(4)\},$$

$$(^1A_g),\quad \psi_6=\frac{1}{\sqrt{4!}\sqrt{N_6}}\sum_P(-1)^P P\frac{1}{2}\{\varphi_1(1)\bar{\varphi}_2(2)\varphi_3(3)\bar{\varphi}_4(4)$$
$$-\bar{\varphi}_1(1)\varphi_2(2)\varphi_3(3)\bar{\varphi}_4(4)-\varphi_1(1)\bar{\varphi}_2(2)\bar{\varphi}_3(3)\varphi_4(4)$$
$$+\bar{\varphi}_1(1)\varphi_2(2)\bar{\varphi}_3(3)\varphi_4(4)\},$$

$$(^1A_g),\quad \psi_7=\frac{1}{\sqrt{4!}\sqrt{N_7}}\sum_P(-1)^P P\frac{1}{2}\{\varphi_1(1)\bar{\varphi}_2(2)\varphi_3(3)\bar{\varphi}_4(4)$$
$$-\bar{\varphi}_1(1)\bar{\varphi}_2(2)\varphi_3(3)\varphi_4(4)-\varphi_1(1)\varphi_2(2)\bar{\varphi}_3(3)\bar{\varphi}_4(4)$$
$$+\bar{\varphi}_1(1)\varphi_2(2)\bar{\varphi}_3(3)\varphi_4(4)\},$$

where $P$ means the permutation of electrons, and $(-1)^P$ takes $+1$ or $-1$ according to even or odd permutation respectively, and $N_i$ is the normalization factor. The wave functions $\psi_1$, $\psi_2$, $\psi_3$ are non-polar, and $\psi_4$, $\psi_5$ are polar. $\psi_6$, $\psi_7$ represent bonding structures.

The perturbed wave function of butadiene $\Phi_i$ is

$$\Phi_i=\sum_j a_{ij}\psi_j.$$

The secular determinant is thus

$$\det|H_{ij}-N_{ij}W|=0,$$

where

$$H_{ij}=\int\psi_i H\psi_j d\tau,\quad N_{ij}=\int\psi_i\psi_j d\tau.$$

The matrix elements are expanded into the integrals over the molecular orbitals $\varphi_i$ of vinyl radicals. Further these integrals are expanded with the integrals over atomic orbitals $\chi_i$ which have already been given by Parr and Mulliken[5]. The numerical values of integrals necessary for the present calculation are listed in Tables I and II.

TABLE I

| | |
|---|---|
| $s_{12}=0.27854$ | (11 : 12)=3.60741 |
| $s_{13}=0.03371$ | (22 : 23)=2.93264 |
| $s_{14}=0.00218$ | (22 : 34)=1.93346 |
| $s_{23}=0.23281$ | (11 : 23)=1.66096 |
| | (11 : 34)=1.25870 |
| (1 : 12)=2.27950 e.v. | (11 : 13)=0.29845 |
| (2 : 23)=1.63069 | (11 : 24)=0.18599 |
| (1 : 22)=0.98620 | (22 : 13)=0.46282 |
| (2 : 33)=0.67476 | (11 : 14)=0.01730 |
| (1 : 13)=0.30278 | (22 : 14)=0.03027 |
| (1 : 23)=0.03460 | (12 : 12)=1.09000 |
| (2 : 34)=0.03027 | (23 : 23)=0.73099 |
| (2 : 14)=0.01730 | (12 : 23)=0.63583 |
| (1 : 33)=0.00865 | (12 : 34)=0.46282 |
| (1 : 14)=0.00000 | (12 : 13)=0.12543 |
| (1 : 24)=0.00000 | (12 : 24)=0.06920 |
| (1 : 34)=0.00000 | (13 : 23)=0.10813 |
| (1 : 44)=0.00000 | (12 : 14)=0.00432 |
| | (14 : 23)=0.00865 |
| (11 : 11)=16.92975 | (13 : 13)=0.01730 |
| (11 : 22)=9.23913 | (13 : 24)=0.00865 |
| (22 : 33)=8.69412 | (13 : 14)=0.00000 |
| (11 : 33)=5.52358 | (14 : 14)=0.00000 |
| (11 : 44)=3.82801 | |

TABLE II

| | |
|---|---|
| $\sigma_1=1.27854$ | $E_1=2W_{2p}-12.11931$ |
| $\sigma_2=0.72146$ | $E_2=2W_{2p}-1.44338$ |
| $S_{13}=0.11826$ | |
| $S_{14}=0.12007$ | [11 : 13]=1.15565 |
| $S_{24}=0.11613$ | [11 : 14]=1.26194 |
| $\varepsilon_1=W_{2p}-12.60205$ e.v. | [11 : 23]=1.10343 |
| $\varepsilon_2=W_{2p}-6.01337$ | [11 : 24]=1.16176 |
| $\lambda_1=-12.00831$ | [11 : 34]=1.26546 |
| $\lambda_2=-12.34752$ | [22 : 13]=1.14301 |
| $\lambda_{12}=-2.88461$ | [22 : 14]=1.24381 |
| $\omega_{13}=-5.50703$ | [22 : 23]=1.12520 |
| $\omega_{14}=-5.43695$ | [22 : 24]=1.20289 |
| $\omega_{24}=-5.09605$ | [22 : 34]=1.26878 |
| $K_{11}=13.08479$ | [12 : 13]=0.31791 |
| $K_{12}=13.00330$ | [12 : 14]=0.35521 |
| $K_{22}=13.37096$ | [12 : 23]=0.32708 |
| $K_{13}=5.84053$ | [12 : 24]=0.36362 |
| $K_{14}=5.88618$ | [12 : 34]=0.39976 |
| $K_{24}=6.07678$ | [13 : 14]=0.19285 |
| $J_{12}=4.16874$ | [13 : 24]=0.18874 |
| $J_{13}=0.18853$ | [14 : 23]=0.18874 |
| $J_{14}=0.19812$ | [14 : 24]=0.18571 |
| $J_{24}=0.17659$ | |
| $H_{11}=-93.69588$ | $N_1=0.97210$ |
| $H_{22}=-82.05927$ | $N_2=0.95815$ |
| $H_{33}=-84.14202$ | $N_3=0.98605$ |
| $H_{44}=-85.31311$ | $N_4=1.01395$ |
| $H_{55}=-84.44434$ | $N_5=0.98605$ |
| $H_{66}=-72.54143$ | $N_6=0.97210$ |
| $H_{77}=-85.96205$ | $N_7=1.01395$ |
| $H_{12}=+2.24563$ | $N_{12}=-0.02890$ |
| $H_{14}=-24.01682$ | $N_{14}=+0.24188$ |
| $H_{16}=+2.24209$ | $N_{16}=-0.01435$ |
| $H_{17}=+3.48230$ | $N_{17}=-0.02810$ |
| $H_{24}=+0.00508$ | $N_{24}=-0.00216$ |
| $H_{26}=+2.00350$ | $N_{26}=-0.02890$ |
| $H_{27}=+1.04476$ | $N_{27}=-0.01415$ |
| $H_{46}=+10.77883$ | $N_{46}=-0.12094$ |
| $H_{47}=+22.75146$ | $N_{47}=-0.23684$ |
| $H_{67}=-35.53348$ | $N_{67}=+0.48956$ |
| $H_{35}=-22.08459$ | $N_{35}=+0.23770$ |

In these tables $E_1$ and $E_2$ are the energy levels of the vinyl radical whose wave functions are

$$E_1;\ \sum_P(-1)^P P\varphi_1(1)\bar{\varphi}_1(2),$$

$$E_2;\ \sum_P(-1)^P P\frac{1}{\sqrt{2}}\{\varphi_1(1)\bar{\varphi}_2(2)-\bar{\varphi}_1(1)\varphi_2(2)\},$$

The integral $I_i$ is the core energy of the molecular orbital of vinyl radical and $\lambda_i$ is the energy of perturbation from another vinyl radical core. Then the next relation is

$$\int\varphi_i(\nu)H_{core}(\nu)\varphi_i(\nu)d\tau_\nu=I_i+\lambda_i.$$

The other integrals in these tables are

$$\lambda_{12}=\int\varphi_1(\nu)H_{core}(\nu)\varphi_2(\nu)d\tau_\nu,$$
$$\omega_{ij}=\int\varphi_i(\nu)H_{core}(\nu)\varphi_j(\nu)d\tau_\nu (i=1 \text{ or } 2,\ j=3 \text{ or } 4),$$
$$S_{ij}=\int\varphi_i(\nu)\varphi_j(\nu)d\tau_\nu,$$

$$K_{ij}=\int\int|\varphi_i(\nu)|^2\frac{e^2}{r_{\nu\mu}}|\varphi_j(\mu)|^2d\tau_\nu d\tau_\mu,$$

$$J_{ij}=\int\int\varphi_i(\nu)\varphi_j(\nu)\frac{e^2}{r_{\nu\mu}}\varphi_j(\mu)\varphi_i(\mu)d\tau_\nu d\tau_\mu,$$

$$[jk:lm]=\int\int\varphi_j(\nu)\varphi_k(\nu)\frac{e^2}{r_{\nu\mu}}\varphi_l(\mu)\varphi_m(\mu)d\tau_\nu d\tau_\mu,$$

$$(r:st)=\int\chi_s(\nu)\boldsymbol{H}_r(\nu)\chi_t(\nu)d\tau_\nu,\quad s_{rs}=\int\chi_r(\nu)\chi_s(\nu)d\tau_\nu,$$

$$(rs:tu)=\int\int\chi_r(\nu)\chi_s(\nu)\frac{e^2}{r_{\nu\mu}}\chi_t(\mu)\chi_u(\mu)d\tau_\nu d\tau_\mu,$$

where

$$H_{core}(\nu)=\sum_{r=1}^{4}H_r(\nu),$$

$$H_r(\nu)=\boldsymbol{H}_r(\nu)-\int\left(\frac{e^2}{r_{\nu\mu}}\right)|\chi_r(\mu)|^2d\tau_\mu,$$

and $\boldsymbol{H}_r(\nu)$ is the potential due to the neutral carbon atom.

The energy levels of butadiene obtained by the present calculation are shown in Fig. 2 (left column), and those of ASMO SCF CI calculation using the SCF wave functions by Parr and Mulliken[6], and including the same configurations as in Coulson's calculation[7] are also shown in Fig. 2 (second column).

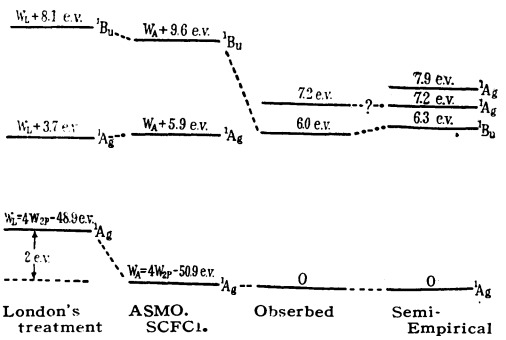



Fig. 2.

The wave functions of the ground state and the lowest $^1B_u$ state are

($^1A_g$)(ground state);

$$\psi_1=0.9326\phi_1+0.0381\phi_2+0.1500\phi_4+0.0491\phi_6-0.1688\phi_7,$$

($^1B_u$); $\psi_3=0.6062\phi_3+0.6641\phi_5$,

## Discussion

The absorption spectra of butadiene[8] show the strong absorption bands about 2000 Å and 1700 Å. No absorption band has been observed in the wave length region longer than 2000 Å.

The selection rule shows that the $^1A_g$—$^1B_u$ transition is allowed and the $^1A_g$—$^1A_g$ transition is forbidden. Then, the strong bands of 2000 Å and 1700 Å may correspond to the $^1A_g$—$^1B_u$ transitions*.

By this calculation the lowest $^1B_u$ state exceeds 8.1 e.v. over the ground state and the lowest $^1A_g$—$^1A_g$ transition is about 3.7 e.v. The ASMO SCF CI calculation predicts that the lowest $^1A_g$—$^1B_u$ excitation energy is about 9.6 e.v. and the lowest $^1A_g$—$^1A_g$ excitation energy is about 5.6 e.v. These two calculations agree qualitatively in the next point. The lowest excited $^1A_g$ state is lower than the lowest $^1B_u$ state. If this is true there may be a weak absorption band in the wave length longer than 2000 Å, while this weak band has not been observed. The cause of discrepancy may be interpreted as follows. In general the detailed ASMO calculation gives the high excitation energy for the excited singlet state and low excitation energy for the triplet state. This is mainly due to the overestimation of one center repulsion energy as Moffitt[9] mentioned it. This energy integral is important to determine the energies of polar structures. The ASMO wave functions of excited singlet states include more polar structures than that of ground state in most cases, and the contributions of polar structures for the triplet states are less than for the singlet ground state. In the case of ethylene the triplet state includes no polar structure, and the singlet excited $^1B_{1u}$ state is given by the linear combination of the polar structures only in usual estimation. Thus the overestimation of one centre repulsion energy results in the high excitation energy for singlet—singlet transition and results in the low energy for the triplet state. In the case of the lowest excited $^1A_g$ state of butadiene, however, the contributions of polar structures are slight, as the important configuration of this state is $\psi_7$, which is the product of the two triplet states of vinyl radicals. So the excitation energy for this $^1A_g$ state may be low in the non-empirical calculation. Therefore the excitation energy (5.9 e. v.) by ASMO SCF CI calculation may coincide with the experimental value better than that (3.7 e. v.) by this hybridized treatment, because the contributions of polar structures to the ground state are greater in this hybridized calculation than in ASMO SCF CI calculation owing to the neglect of the high energy structures as

$$\frac{1}{\sqrt{4!}}\sum_{P}(-1)^P P\frac{1}{\sqrt{2}}\{\varphi_2(1)\bar{\varphi}_2(1)\varphi_3(3)\varphi_3(4)+\varphi_1(1)\bar{\varphi}_1(1)\varphi_4(3)\bar{\varphi}_4(3)\},\cdots\cdots.$$

7) C. A. Coulson and J. Jacobs, *Proc. Roy. Soc.*, A206, 287 (1951).

8) E. P. Carr, L. W. Pickett and H. Stücklen, *Rev. Mod. Phys.*, **14**, 260 (1942).

* For *cis*-butadiene, the $^1A_1$—$^1A_1$ transition ( $A_g$—$A_g$ transition in *trans*-butadiene) is allowed but the intensity of the lowest $^1A_1$—$^1A_1$ transition may not be so strong.

9) W. Moffitt, *Proc. Roy. Soc.*, A210, 224, 245 (1951).

Then the weak forbidden band may not be observed, owing to the superposition with the strong allowed transition band.

The electron affinity of carbon atom is negative when the $2p$ and $2s$ orbitals with the usual screening constant for the neutral carbon atom are also used in the calculation of the energy of the negative carbon ion. Further, the electron affinity of vinyl radical which is calculated by the ASMO method is negative. This is an example of the error by the overestimation of the one center repulsion energy. In the negative carbon ion the electron cloud becomes larger on account of the increased electrostatic repulsion. So the consideration for the expansion of the electron cloud will be needed in the calculation of the energy of the negative carbon ion. Then in the valence bond method the variation of the screening constant of the negative carbon ion in polar structures will be the one approach to the energy levels of molecules avoiding this error. More directly the use of semi-empirical value of the one center repulsion integral which is determined by the consideration of the energy of the negative carbon ion was proposed by Moffitt[9] and by Parizer and Parr[5].

In the molecular orbital method the perfect non-empirical treatment may be given by the inclusion of the higher excited Rydberg orbitals and the effect of the $\sigma$-electrons. But this treatment will be too complicated to be useful or calculating the energy levels of the complex molecule. For London's treatment in this paper the use of semi-empirical values from the energy levels of the vinyl radical (or ethylene molecule) is interesting.

The energy of the ground state by this calculation exceeds 2 e. v. over the result of ASMO SCF CI calculation. This discrepancy is due to the neglect of the higher energy configurations, for instance the inclusion of the structure mentioned before,

$$\frac{1}{\sqrt{4!}}\cdot\sum_P(-1)^P P\frac{1}{\sqrt{2}}\{\varphi_2(1)\bar{\varphi}_2(2)\varphi_3(3)\bar{\varphi}_3(4)$$

$$+\varphi_1(1)\bar{\varphi}_1(1)\varphi_4(3)\bar{\varphi}_4(4)\},$$

depresses the ground state by about 2 e. v.. If the energy depression of the ground state by the interaction with the neglected high energy structures is assumed to be 2 e. v. and the depressions of the other states are assumed to be zero, the energy levels by this treatment of London's will be close to those by the ASMO SCF CI calculation. But in order to obtain the same result as that by the ASMO SCF CI calculation one needs more complicated computations by this treatment for the large molecule.

The energy depression of the ground state by the interaction between the two vinyl radicals is about 0.3 e.v. and is mainly contributed by polar structure and by bonding structures. By this result one can expect the small resonance energy of butadiene.

From the wave function of the lowest $^1B_u$ state, it can be seen that the weight of polar structure is great, and that in London's treatment polar structures can not be ignored.

## Semi-Empirical Calculation

Parizer and Parr[5] presented the semi-empirical method and obtained good results for the lower excited states of conjugated molecules by a simple procedure. They omitted many integrals except the Coulomb repulsion and resonance integrals, and simplified the procedure of calculation. Using their method the energy levels of butadiene are calculated in order to compare them with the results of the last section. The procedure of calculation is the same as that in the second section. The penetration integrals (11 : 3), (11 : 4) and (22 : 3)are assumed to be $-$(11 : 33), $-$(11 :44) and $-$(22 :33) respectively. The values of the integrals used in this calculation are shown in Table III, and the

TABLE III

| | |
|---|---|
| (11 : 11)=10.53 | $H_{11}=W_1$ |
| (11 : 22)=7.38 | $H_{22}=W_1+7.46$ |
| (11 : 33)=5.35 | $H_{33}=W_1+7.36$ |
| (11 : 44)=3.75 | $H_{44}=W_1+7.82$ |
| (22 : 33)=7.16 | $H_{55}=W_1+7.82$ |
| | $H_{66}=W_1+14.82$ |
| $\beta_{12}=-2.92$ | $H_{77}=W_1+10.11$ |
| $\beta_{23}=-1.68$ | $H_{12}=-0.68$ |
| | $H_{14}=-1.68$ |
| $\varepsilon_1=W_{2p}+\alpha-2.92$ | $H_{16}=+0.10$ |
| $\varepsilon_2=W_{2p}+\alpha+2.92$ | $H_{17}=+0.05$ |
| | $H_{24}=0$ |
| $\lambda_{12}=-2.04$ | $H_{25}=-0.68$ |
| $\lambda_i=\alpha'$ | $H_{27}=-0.34$ |
| | $H_{46}=+0.84$ |
| $K_{11}=K_{12}=8.95$ | $H_{47}=+1.68$ |
| $K_{13}=K_{14}=K_{24}=5.40$ | $H_{67}=\frac{1}{2}W_1+7.41$ |
| $J_{12}=1.57$ | $H_{35}=-1.68$ |
| [11 : 34]=0.85 | |
| [12 : 34]=0.05 | |
| | $N_i=1$ |
| $\omega_{ij}=-0.84$ | $N_{ij}=0$ (except $N_{67}$) |
| $E_1=2W_{2p}+2\alpha+3.11$<br>$E_2=E_1+7.41$ | $N_{67}=\frac{1}{2}$ |

other integrals are omitted. Then the matrix elements are easily computed. The result is shown in Fig. 2 (right column).

The calculation by this treatment predicts the absorption bands at 1950 Å, 1700 Å and 1500 Å. The 1950 Å band is an allowed transition $^1A_g$—$^1B_u$ and corresponds to the 2000 Å strong absorption band observed experimentally. The 1700 Å and 1500 Å bands by this calculation are forbidden transitions and may have weak intensities. The important result of this calculation is that the lowest $^1A_g$—$^1A_g$ transition is higher than the lowest $^1A_g$—$^1B_u$ transition. Then this result supports the possibility that the lowest $^1A_g$—$^1A_g$ transition band might overlap with the strong absorption band and be impossible to observe.

The energy depression of the ground state by the interaction between the vinyl radicals is about 0.4 e. v., and is mainly contributed by the polar structures.

## Conclusion

The energy levels of butadiene were calculated by London's treatment and by the semi-empirical treatment including polar structurs, and compared to the results by the ASMO SCF CI calculation and to the experimental data. According to this comparison, the non-empirical treatment which is described in this paper shows the same results as those by the ASMO SCF CI method. But for the experimental results, the non-empirical treatment does not show agreement. Most of the error in the excitation energy of the non-empirical treatment is due to the overestimation of the one centre repulsion energy, and this will be clear by the comparison to the result of the semi-empirical treatment. The result of the semi-empirical treatment is fairly good approximation to the experimental data. The effect of polar structures for the excited states is important and can not be ignored.

The author wishes to thank Dr. I. Tanaka and Prof. S. Shida of this laboratory for their kind discussion and encouragement. This research is supported in part by the grant in aid for the miscellaneous scientific researches of the Ministry of Education.

*Laboratory of Physical Chemistry,*
*Tokyo Institute of Technology,*
*Tokyo*

# *Studies on Molecular Structure by the Measurement of the Dielectric Constant of Gases. II. Dipole Moment and the Molecular Structure of Mono- and sym-Dihalogenomethyl ether*

By Takehiko CHIBA

(Received January 24, 1955)

In halogenomethyl ether, $CH_3OCH_2X$, the two groups $CH_3O$–and $CH_2X$–have the possibility of rotating around the central C–O bond. The rotation around C–C bond has been extensively studied hitherto, but the rotation about C–O bond has not been so often subjected to examination. In addition, the group $CH_3O$– has a dipole moment opposite in its direction to that of the group $-CH_2X$, i.e. the dipole of the former group points towards the oxygen atom, while that of the latter points outward from the central carbon to the halogen atom. This situation is not encountered in the case of dihalogenoethanes. The problem has already been investigated by the measurement of dipole moment in non-polar solution[1], Raman effect[2], and infrared absorption spectrum[3]. The conclusion obtained is that the molecule has a shallow minimum about the equilibrium position so that there exists a wide distribution of molecules from the equilibrium position. The present work is carried out on mono and di-halogenomethyl ethers to investigate the molecular structure in the gaseous state from the standpoint of the dipole moment at various temperatures, for a slight change in the molecular configuration may sensibly be detected by the dipole moment measurement.

## Preparation of the Materials

**Monochloromethyl Ether** $CH_2ClOCH_3$ was synthesized[4] from methanol, formalin, and hydro-

1) Y. Morino, H. Shiio and I. Miyagawa, *Repts. Radiation Chem. Research Inst.* (Tokyo Univ.), 5, 6 (1950).
2) M. Katayama and Y. Morino, ibid., 4, 1, (1949).
3) S. Mizushima, T. Shimanouchi, T. Miyazawa and M. Hayashi, unpublished.
4) *Org. Synthesis*, vol. 9, p. 59.

gen chloride. Dry air was passed through the crude distilate to exile the dissolved hydrogen chloride and then redistilled, b.p. 55–57°C.

***sym*-Dichloromethyl Ether** $CH_2ClOCH_2Cl$ was synthesized[5] by the reaction of chlorosulfonic acid on polyoxymethylene in conc. sulfuric acid. It was purified as above, b.p. 103°C.

**Monobromomethyl Ether** $CH_2BrOCH_3$ was synthesized[6] from polyoxymethylene, methanol, and hydrogen bromide. It was purified as above, and redistilled, b.p. 86–88°C.

***sym*-Dibromomethyl Ether** $CH_2BrOCH_2Br$ was synthesized[7] from polyoxymethylene, red phosphorus, and bromine, b.p. 148–150°C.

## Experimental Procedure and Results

The apparatus for the measurement of dielectric constant was reported in the preceding paper[8]. The compounds are all reactive, and particularly, decompose readily in moist air. For monochloro- and monobromo-methyl ether, the usual gas filling method cannot be used on account of their low boiling point. The sample is first introduced in a trap which is connected to the cell, cooled with dry ice during the evacuation of the apparatus, and then evaporated to fill the gas cell by bringing the trap to room temperature. This operation has the disadvantage that the vapor contacts the grease of the cocks.

In the case of monobromoether, the observed polarization increases gradually with the runs of observation, so that the temperature dependence of the moment of this substance is also measured in heptane solution. For dibromoether, the measurement is carried out only in heptane solution because of the instability of this compound. The results of the measurements are summarized in Table I[9].

TABLE I

OBSERVED POLARIZATIONS AND DIPOLE MOMENTS OF MONOCHLORO-, DICHLORO-, MONOBROMO-, AND DIBROMO-METHYL ETHERS

Monochloromethyl ether

$MR_D$ =18.0 cc. $P_E+P_A$ =18.9 cc.

| $T$(°K) | $n$ | $p$(mm Hg) | $P$(cc.) | $\Delta P$(cc.) | $\mu$(D) |
|---|---|---|---|---|---|
| 296.3 | 6 | 70–102 | 82.5 | 0.6 | 1.76 |
| 337.8 | 5 | 83–120 | 75.1 | 0.3 | 1.77 |
| 370.4 | 7 | 70–103 | 73.3 | 0.5 | 1.82 |
| 412.3 | 7 | 92–113 | 68.3 | 0.4 | 1.83 |
| 467.2 | 7 | 81–110 | 66.2 | 0.4 | 1.90 |

$n$: number of the observations.

$p$: pressure range of the observations.

$\Delta P$: average deviations of $P$.

*sym*-Dichloromethyl ether

$MR_D$ =22.9 cc. $P_E+P_A$ =24.0 cc.

| $T$ | $n$ | $p$ | $P$ | $\Delta P$ | $\mu$ |
|---|---|---|---|---|---|
| 338.3 | 8 | 48–82 | 41.4 | 0.5 | 0.98 |
| 353.0 | 8 | 59–76 | 40.2 | 0.5 | 0.97 |
| 371.0 | 7 | 54–79 | 40.7 | 0.4 | 1.01 |
| 412.2 | 6 | 62–83 | 41.6 | 0.3 | 1.09 |
| 412.5 | 5 | 60–82 | 41.8 | 0.6 | 1.10 |

Monobromomethyl ether*

$MR_D$ =20.8 cc. $P_E+P_A$ =21.8 cc.

| $T$ | $n$ | $p$ | $P$ | $\mu$ |
|---|---|---|---|---|
| 301.0 | 7 | 49–68 | 106.3–106.5 | 2.04 |
| 338.4 | 5 | 51–61 | 95.2– 98.0 | 2.03–2.07 |
| 338.4 | 8 | 61–70 | 93.5– 94.2 | 2.00 |
| 371.0 | 6 | 50–60 | 89.2– 94.0 | 2.03–2.10 |
| 371.1 | 6 | 63–74 | 89.2– 92.5 | 2.03–2.08 |
| 412.0 | 9 | 51–67 | 82.6– 83.4 | 2.03–2.08 |

* Observed polarization changes considerably with the runs of observation, so $\Delta P$ is not given in this case.

In heptane solution

| $T$ | $\varepsilon_1$ | $d_1$(g./cc.) | $\alpha$ | $\beta$ | $P_{2\infty}$(cc.) | $\mu$ |
|---|---|---|---|---|---|---|
| 267 | 1.9574 | 0.7076 | 3.38 | 0.477 | 128.2 | 2.16 |
| 298 | 1.9111 | 0.6810 | 2.92 | 0.458 | 119.1 | 2.18 |
| 330 | 1.8648 | 0.6530 | 2.43 | 0.399 | 109.8 | 2.18 |

*sym*-Dibromomethyl ether

$MR_D$ =28.6 cc. $P_E+P_A$ =30.0 cc.

| $T$ | $\varepsilon_1$'** | $d_1$'** | $\alpha$ | $\beta$ | $P_{2\infty}$ | $\mu$ |
|---|---|---|---|---|---|---|
| 261 | 1.971 | 0.707 | 5.58 | 0.506 | 50.5 | 0.94 |
| 274 | 1.944 | 0.697 | 5.45 | 0.507 | 50.9 | 0.97 |
| 297 | 1.909 | 0.678 | 5.16 | 0.487 | 50.2 | 0.99 |
| 323 | 1.874 | 0.656 | 4.87 | 0.460 | 51.2 | 1.06 |

** The prime indicates that these values are extrapolated ones, which differ a little from the values of the pure solvent.

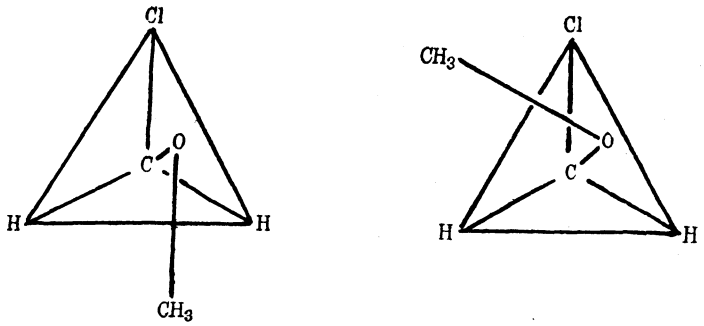
The observed moments of the monochloroether are in good agreement with the values previously reported by Morino, Shiio and Miyagawa in carbon tetrachloride solution[1]. Whereas for dichloroether the discrepancy between the present data and theirs seems fairly large. In the solution method some doubts may exist in the extrapolation to infinite dilution. Indeed, from their data polarization of about 44 cc. is estimated by a more reasonable extrapolation. This is close to the value obtained in the present observation.

## Discussion of Results

**I) Monochloromethyl Ether.**—The result shows a great increase in the moment with temperature. This means that these molecules are a mixture of molecular form of stable, less polar ones and less stable, more polar ones[10]. From the appropriate bond

5) H. Stephen, et al., *J. Chem. Soc.*, **117**, 514 (1920).
6) Karvonen, *Chem. Zentl.*, **1912** II, 1268.
7) W. Tischtschenko, et al., *Chem. Zentl.*, **1915** I, 837.
8) T. Chiba, This Bulletin, **28**, 19 (1955).
9) In the calculation of the moment all the $P_E+P_A$'s are assumed to be 1.05 $MR_D$.
10) If a single form is assumed for this molecule, from the observed $P$ *vs.* $1/T$ curve, the moment and the atomic polarization of 1.46 D and 20 cc. is obtained. The latter value is unreasonably high for the molecule of this kind, consequently the assumption of one rigid form is completely denied.

moments and bond angles, the moment of the molecule corresponding to the form in which the $CH_3$ group and Cl atom are in the *cis* position is calculated to be 0.65D, that of the form in which Cl atom is turned from the *cis* position through 60° (*gauche*) is 1.48D and that of the form in which the two are in the *trans* is 2.74D[11] (Fig. 1). The *cis* position is regarded as quite unstable, since at this position the distance between the Cl atom and the $CH_3$ group is very short. So we can safely ignore the *cis* form.




*trans* *gauche*

Fig. 1. The *trans* and *gauche* forms of monochloromethyl ether

From the results of the infrared and Raman effect spectroscopy[2,3], the existence of definite isomers is not concluded but rather the molecule should be distributed over a wide range of the angle of internal rotation. On the other hand, from the numerical calculation of the potential energy of these molecules as a function of the internal rotational angle by the use of appropriate interatomic potential[12], it was found that the molecule has a shallow potential minimum about the *gauche* position in good accord with the results of the spectra. From the temperature dependence of the dipole moment it cannot be decided whether the potential curve, as a function of the internal rotation angle, has minima at the *trans* and the *gauche* position, or whether it increases monotonously from the *gauche* position to the *trans* one: in other words, in such a curve as *a* or *b* in Fig. 2, the polarization vs. $1/T$ curve may be nearly the same in the temperature range of the present experiment. This means that, even if the potential be of the type *b*, the mean dipole moment may be treated by assuming the potential *a*[13]. Therefore, if we assume tentatively that the molecule is composed of the two isomers, *trans* and *gauche*, then from the observed change of the moment with temperature the energy difference of the two forms, $\Delta E$, that is, the energy of the *trans* form minus the energy of the *gauche* one, is found to be approximately 700 cal./mol.[14].

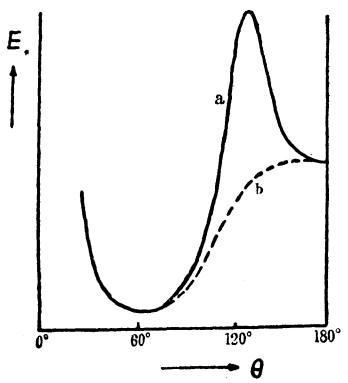



Fig. 2. Two types of intramolecular potential giving, respectively, (a) two separated isomers, and (b) continuous distribution.

With the model in which bond dipoles are located at the middle point of bond radius, the electrostatic energy between the two bond dipoles $OCH_3$ and CCl which stabilized the *gauche* position against the *trans* is calculated to be 1.3 kcal./mol.[15], so the observed result suggests that the *trans* position is stabilized by 1.3-0.7=0.6 kcal. due to the steric repul-

11) In the calculation the following values of bond moments are assumed: $\mu_{CCl}=1.8$ D, $\mu_{CO}=1.0$ D, $\mu_{CH_3O}=1.1$ D.

12) H. Shiio, unpublished.

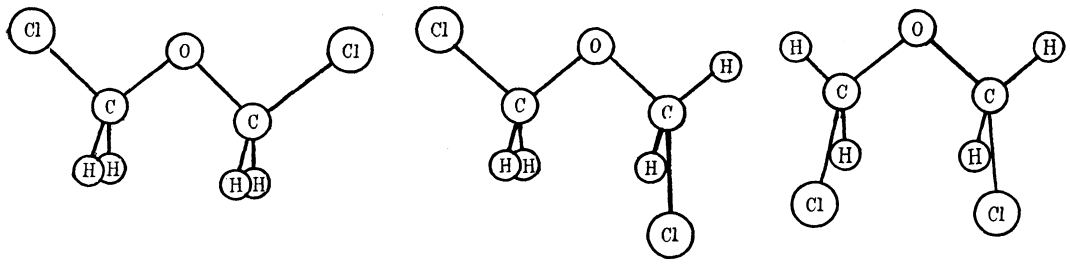
13) Strictly speaking, this is not true, but the above consideration may be allowed by taking average moment values in the neighborhood of the *trans* and the *gauche* as $\mu_t$ and $\mu_g$. To discuss whether the potential be *a* or *b*, needs more precise molecular parameters, which in this case are unfortunately not known.

14) For the method of estimating $\Delta E$ from the observed temperature dependence of the moment, see I. Miyagawa, *J. Chem. Soc. Japan, (Pure Chem. Sect.)* 75, 970 (1954).

15) Assumed bond distances and the bond radii are as follows:
$r_{CCl}=1.76$Å, $r_{CO}=1.42$Å, $r_{C\cdot}=0.77$Å, $r_{O\cdot}=0.65$Å.

sion between $CH_3$ group and Cl atom. Of course, we cannot put too much significance on the individual figures, because the approximation used here is rather crude, but this is a reasonable magnitude when compared with those of haloethane derivatives. It must now be added that if we assume a mixture of *cis* and *trans* or of *cis*, *gauche* and *trans*, instead of *gauche* and *trans*, the moment of the *trans* form must be considerably higher than the calculated one in order to explain the observed data. This account confirms the validity of the neglection of the *cis* form.

**II) *sym*-Dichloromethyl Ether.**—Extending the consideration I), the following three forms are assumed: *t,t*-form in which the two chlorine atoms are in the *trans* to the opposite $-CH_2Cl$ group, *t,g*-form in which the one is in the *trans* and the other in the *gauche*, and *g,g*-form in which both are in the *gauche* position[16] (Fig. 3). Using the




*t,t*-form *t,g*-form *g,g*-form

Fig. 3. The three forms considered for dichloromethyl ether

observed energy difference between the *trans* and the *gauche* forms of monochloro ether in I), the following relations can be obtained, provided that the interatomic distance and valence angles are the same in the two compounds.

$$E_{tt}-E_{gg}=0.7\text{ kcal.}\times 2+E_{tt}(\mu)-E_{gg}(\mu)$$
$$E_{tg}-E_{gg}=0.7\text{ kcal.}+E_{tg}(\mu)-E_{gg}(\mu)$$

where $E$'s are the energies corresponding to the individual forms, $E(\mu)$'s are the energies of the dipole interaction of two CCl bond dipoles. Calculating in the same way as in I), $E(\mu)$'s are as follows: $E_{tg}(\mu)-E_{gg}(\mu)=0.5$ kcal., and $E_{tt}(\mu)-E_{gg}(\mu)=1.3$ kcal., leading to the total energy difference of $E_{tg}-E_{gg}=1.2$ kcal. and $E_{tt}-E_{gg}=2.7$ kcal. Therefore, if these arguments are valid, the contribution of *t,t*-form to the observed moment may be neglected. Further, the moment value of *g,g*-form is definitely small, so if it is tentatively assumed to be zero, the observed temperature dependence of the moment gives the values of $E_{tg}-E_{gg}=1.3$ kcal., and $\mu_{tg}=2.02$D (calculated moment of $\mu_{tg}=2.37$D).

Thus in view of the order of approximation the agreement between the calculated and the observed values are fairly good, which lead to the conclusion that the energy relation discussed above is essentially correct. It is noted that in this case, too, *t,t*-, *t,g*- and *g, g*-forms need not be definite isomers, but represent mean values about their positions

**III) Monobromomethyl Ether.**—There is a small difference in the moment value in the gaseous state (average moment 2.04D) and in solution (2.18D), but no temperature dependence of the moment in either case[17]. The same discussion as in I) leads to the energy difference between the *trans* form and the *gauche* one or zero or $\pm\infty$[18]. The moment value of this compound must be nearly the same or at least slightly less than that of the corresponding form of monochloroether. From the assumption of $\Delta E=0$, the calculated average moment is 2.2D, but from the assumption of $\Delta E=\pm\infty$ the calculated moment is 2.7 or 1.5D using the moment of monochloroether. Therefore, $\Delta E$ is considered to be equal to zero.

The comparison of this result with the case of monochloroether is interesting. In I) it is seen that the difference in the electrostatic energy between the *trans* and the *gauche* form is partly reduced by the steric energy difference of Cl and $CH_3$, but in this case $\Delta E$ from the steric energy of Br and $CH_3$ is so great that the electrostatic one is completely

16) The *g,g*-form denotes the configuration in which each CCl bond rotates 120° in opposite direction from the *t,t*-form. The one in which both groups rotate in the same direction is excluded because of the shortness of the Cl, Cl distance: ca. 2.3Å.

17) We have found that in halogenoethane derivatives when the temperature dependence of the moment is measured both in heptane solution and in gaseous state, $\Delta E$ derived from both methods are usually in good agreement, although the moment value itself may differ to some extent. (cf. I. Miyagawa, *J. Chem. Soc. Japan (Pure Chem. Sect.)*, 75, 1166 (1954)).

18) The possibility of free rotation is completely ruled out because of the short distance between Br and $CH_3$ at *cis* position as mentioned in (I).

cancelled leaving $\Delta E$ zero. Since $\Delta E$, originated from electrostatic force, does not differ seriously in these two compounds, the steric one is several hundred calories higher in Br.....$CH_3$ than in Cl.....$CH_3$. This difference in steric energy is estimated to be 1.3 kcal. according to the Lenard-Jones type intermolecular potential used by Miyagawa for the case of halogenoethane derivatives[19]. As this figure depends greatly upon the molecular parameter, especially upon the valence angle, the agreement between the observed and the calculated figure seems fairly good.

**IV) *sym*-Dibromomethyl Ether.**—Temperature range of the measurement is narrow because the solution method has to be used. But the tendency of the temperature dependence of the moment is the same as in dichloroether. The same argument as that used in the dichloroether being applied, it is found from the observed value that the energy difference between the *t, g*- and *g, g*-forms is 0.9 kcal./mol. and $\mu_{tg}=1.9$D. Putting the dipole energy of dibromoether equal to that of dichloroether, then it is easily seen from the same discussion as in (II), that the difference in $\Delta E$ between dibromo- and dichloro-ether, is the same as that between monobromo- and monochloro-ether, i.e., 0.7 kcal. This value is compared to the observed one, that is, 1.3—0.9=0.4 kcal./mol.. In taking account of the errors in the experiment and the approximate nature of the treatment it can be said that the agreement is rather good.

Concluding the above discussion, the assumption that the dipole-dipole interaction and the steric repulsion are the main factors of the hindering potential of this kind of molecules holds approximately in the mono- and di-halogenomethyl ethers.

19) I. Miyagawa, *J. Chem. Soc. Japan (Pure Chem. Sect.)*, **75**, 1177 (1954).

## Summary

The temperature dependence of the dipole moment was investigated on monochloromethyl ether (I), *sym*-dichloromethyl ether (II) and monobromomethyl ether (III) in the gaseous state, and (III) and *sym*-dibromomethyl ether (IV) in heptane solution. The moment of (I), (II) and (IV) increases with temperature, while that of (III) does not.

From the observed data the energy difference between the *gauche* and the *trans* position is 0.7 kcal./mol. in (I), and zero in (III). Similarly $\Delta E$'s between *t,g*- and *g,g*-form of (II) and (IV) are estimated to be 1.3 kcal. and obtained to be 0.9 kcal./mol. respeetively from the observed results.

These energy values are explained satisfactorily by the electrostatic energy of dipole interaction and the steric energy between non-adjacent groups, which are of reasonable order of magnitudes as compared to the case of haloethane derivatives. The author wishes to express his sincere thanks to Prof. Y. Morino for his kind guidance through this study and to Dr. I. Miyagawa for much valuable advice. The cost of this research has been defrayed from the Grant in Aid for Fundamental Scientific Research from the Ministry of Education, to which the author's thanks are also due.

*Department of Chemistry, Faculty of Science, The University of Tokyo, Tokyo*

# *Reactions of Chloromethylpolysiloxanes with Thiourea*[1]

By Shunichi NOZAKURA

(Received January 31, 1955)

Concerning the reaction of halogenomethylsilicon compound with thiourea, the synthesis of thiuronium salts from bromomethyltrimethylsilane has been reported.[2] Recently, Noller and Post also carried out the reaction of chloromethyltrimethylsilane[3] with thiourea, and thereby synthesized trimethylsilylmethylmercaptan.

I have reported in a previous paper[4] that the silicon-containing thiuronium salts were obtained from the reaction of the various chloromethylsilicon compounds, $ClCH_2Si(CH_3)_2R$, ($R=CH_3$—, $CH_3(CH_2)_3$—, $CH_3(CH_2)_7$—, $C_6H_5$— and $ClCH_2(CH_3)_2SiO$—) with thiourea and

1) Paper III in a series on the study of organosilicon compound.

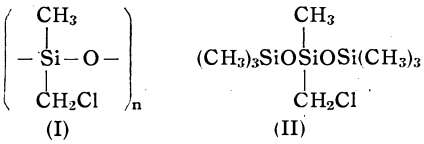
2) D.C. Noller and H.W. Post, *J. Org. Chem.*, **17**, 1393 (1952).

3) G.D. Cooper, *J. Am. Chem. Soc.*, **76**, 2500 (1954).

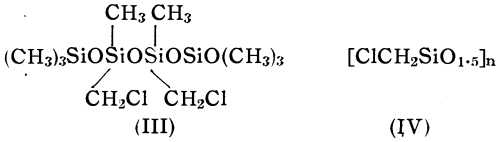
4) S. Nozakura, *J. Chem. Soc. Japan* (*Pure Chem. Sect.*), **75**, 958 (1954).

that no fission of silicon-carbon bonds took place. It was of great interest that the difunctional bischloromethyltetramethyldisiloxane gave only the corresponding dithiuronium salt even when an excess of disiloxane was used.

The present study has been undertaken in order to clarify the nature of the above reaction. Thus we have studied the reactions between the chloromethylpolysiloxanes (I, II, III and IV) and thiourea and the decomposition of thiuronium salts by an aqueous solution of alkali.

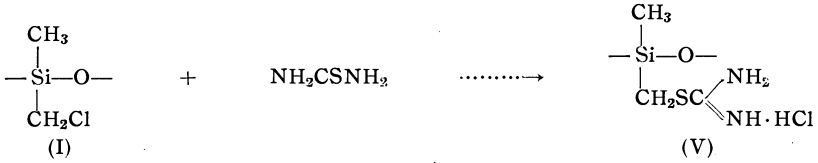


(I) (II)



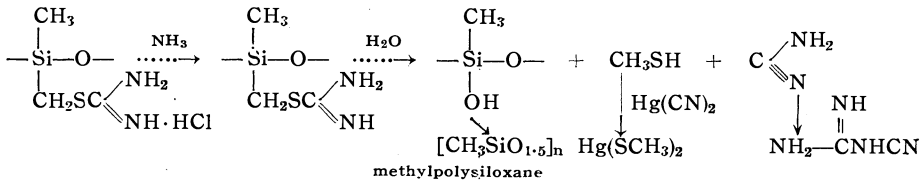
(III) (IV)

**Chloromethylmethylpolysiloxanes and Thiourea.**—Because of the low solubility of the compound (I) in hot alcohol, the reaction apparently was found to be heterogeneous in the first stage and gradually became homogeneous as the reaction proceeded. The water-soluble polythiuronium chloride (V) was obtained quantitatively as a glassy solid after refluxing for several hours.



(I) (V)

The addition of an excess of aqueous ammonia to an aqueous solution of the compound (V) gave a white amorphous precipitate, methylpolysiloxane, with an evolution of methylmercaptan. Probably the fission of silicon-carbon linkage would take place in the first place, followed by the usual fission of sulfur-carbon bond[5] and the immediate condensation of the newly formed silanol to give a new siloxane linkage, as shown below;



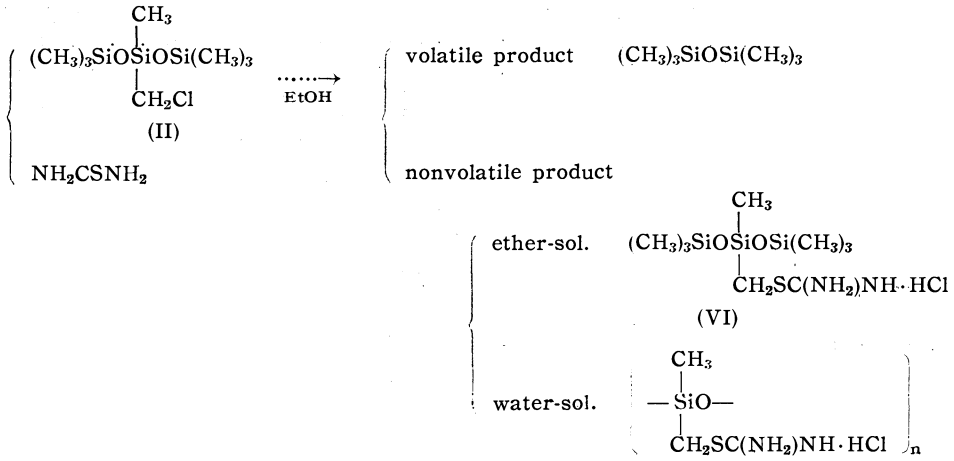
methylpolysiloxane

The chlorine content of the methylpolysiloxane was found to be very low (0.25%). This would suggest that the chlorine of chloromethylpolysiloxane (I) might be quite active in the reaction with thiourea.

When the compound (I) has been used in quantities double that calculated for thiourea, it was found that the ether-soluble part of the reaction product contained the compound (I), the unreacted substance. The decomposition of the water-soluble part by aqueous ammonia gave the precipitation of impure methylpolysiloxane, which contained a small amount of unreacted chloromethyl groups (Cl, 3.35%). These results indicate that nearly one half of the starting polysiloxane (I) reacted with thiourea and the other half remained unreacted. This may be interpreted to be due to the fission and recombination of siloxane bonds. Such an interpretation is confirmed experimentally by the reaction of trimethylsilyl-end-blocked simple chlormethylmethylpolysiloxanes (II) and (III) with thiourea as described below.

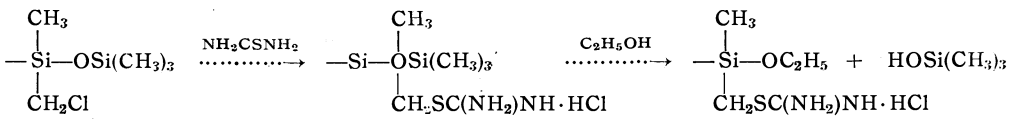
When a mixture of an alcoholic solution of the compound (II) and thiourea in equimolecular weight was heated under reflux for five hours, hexamethyldisiloxane was obtained as a volatile product. The ether-soluble part of the nonvolatile product contained thiuroniumchloride (VI) corresponding to the compound (II). The water-soluble part of the nonvolatile product gave methylpolysiloxane when treated with aqueous ammonia. Therefore, it is concluded that the reaction between 3-chloromethylheptamethyltrisiloxane (II) and thiourea gives the corresponding thiuronium chloride (VI) in the first stage and then the fission and recombination of siloxane bonds will take place, as shown below;

5) F. Arndt, *Ber.*, **54**, 2236 (1921).



The reaction of 3.5-di(chloromethyl)octamethyltetrasiloxane (III) with thiourea also showed the same type of fission of siloxane bonds and gave polythiuroniumchloride. However in this case no appreciable amount of corresponding thiuroniumchloride was detected.

On the contrary the fission of siloxane bonds did not take place in the case of decamethyltetrasiloxane, which has no chloromethyl group, under the similar condition. Therefore the decrease in electron density on the silicon atom might facilitate the nucleophilic attack of the solvent molecule, as shown in following scheme;



Consequently, the failure in obtaining the partially-reacted molecule in the case of bis(chloromethyl)tetramethyldisiloxane[4] and chloromethylmethylpolysiloxane (I) may be due to the fission of siloxane bonds.

Chloromethylpolysiloxane, which has the three dimensional structure, similarly gave the corresponding water-soluble thiuroniumchloride. Silicic acid was obtained by the treatment of the latter with aqueous ammonia. This is probably an additional evidence for the fission of siloxane bonds.

**The Effect of Various Alkalies on the Precipitation Phenomenon of Methylpolysiloxane from the Aqueous Polythiuroniumchloride (V).**—The comparison of the reaction time required for the precipitation of methylpolysiloxane in the alkaline decomposition of polythiuronium salt (V) is shown in Table I. The rate of precipitation of methylpolysiloxane became slower in the order of ammonia, sodium carbonate, and sodium bicarbonate, and became faster as their concentration increased. However in the case of sodium hydroxide the higher the alkaline concentration in the region below the equivalent concentration, the faster the rate of

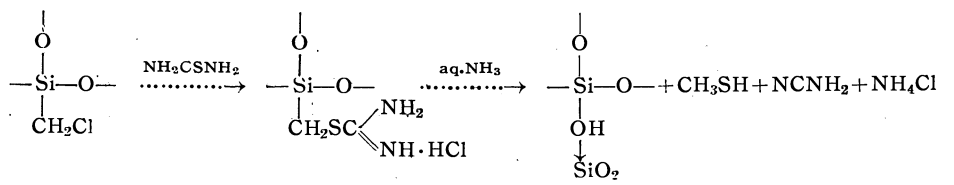
TABLE I

THE EFFECT OF VARIOUS ALKALIES ON THE PRECIPITATION OF METHYLPOLYSILOXANE FROM THE AQUEOUS POLYTHIURONIUM CHLORIDE (V) SOLUTION*

| Conc.** | Alkali | | | |
|---|---|---|---|---|
| | NaOH | $Na_2CO_3$ | $NaHCO_3$ | $NH_4OH$ |
| 6 N | no ppt. | 0.2 min. | | 0.5 min. |
| 1 N | 7.0 min. | 0.7 ,, | 8.5 min. | 0.6 ,, |
| 0.1 N | 3.2 ,, | 10.0 ,, | 30.0 ,, | 3.3 ,, |
| 0.05 N | 10.0 ,, | 24.0 ,, | | 6.5 ,, |

* 1 ml. of 10% aq. (V) was quickly mixed with 1 ml. of aq. alkali and the time required till ppt. or turbidity began to appear was measured.

** The equivalent quantity of alkali is about 1 ml. of about 0.5 N.



precipitation; on the contrary the higher the concentration in the region above the equivalent concentration, the slower the rate. Finally no precipitate was obtained. This means that sodium methylsilanolate would be produced in high alkaline concentration. In fact, the clear alkaline solution gave precipitation of methylpolysiloxane when neutralized with a dilute aqueous solution of hydrochloric acid.

**The Fission of Silicon-Carbon Bonds in Various Silicon-containing Thiuronium Chloride.**—The alkaline fission of silicon-carbon bonds in silicon-containing thiuronium chloride seemed to be a type of reaction analogous to the one which was found by Krieble and Elliott[6] in the reaction of chloromethylpolysiloxanes with an aqueous solution of alkali. They observed there the evolution of methylchloride. The effect of various substituents of the silicon atom on the fission of silicon-carbon bonds was compared qualitatively by titrating immediately the amount of methylmercaptan evolved on the decomposition of silicoalkylisothiourea at 100°C, as shown in Fig. 1. The polythiuronium salts of disiloxane and polysiloxane, in which the electron attracting oxygen atom is attached to the silicon atom, was decomposed much faster than the silicoalkylthiuronium salts in which the electron releasing *n*-butyl or *n*-octyl group is attached to the silicon atom. Phenyldimethylsilylmethylthiuronium chloride is situated between these two groups.

Trimethylsilylmethylthiuronium chloride showed an abnormal curve (C) as compared to those of other homologues. However unusual behaviour of this compound was observed by titrating amounts of volatile trimethylsilylmethylmercaptan which distilled over prior to the decomposition to methylmercaptan. Trimethylsilylmethylmercaptan is considered to be rather stable under this condition, because the methyl group has an electron releasing effect.

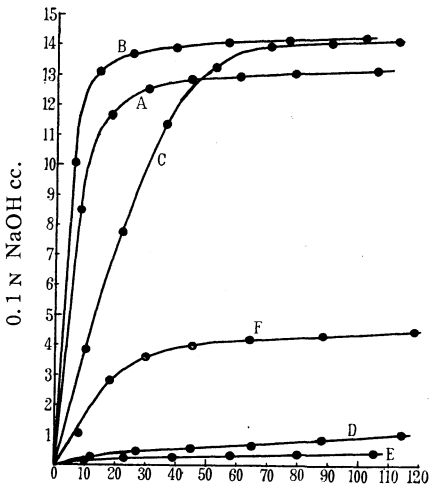



Fig. 1. Rate of alkaline decomposition of silicon-containing thiuronium chlorides.

A, $\left[-\mathrm{SiCH_2SC(NH_2)NH\ HCl}\right]$ (Me, O);

B, $\mathrm{O}\left[\mathrm{SiCH_2SC(NH_2)NH\ HCl}\right]_2$ (Me);

C, R=$CH_3$; D, R=$n$-$C_4H_9$;

E, R=$n$-$C_8H_{17}$; F, R=$C_6H_5$ in $RSi(Me)_2CH_2SC(NH_2)NH\cdot HCl$

The theoretical value of 0.1 N NaOH is 15.08 ml.

## Experimental

**Methylchloromethylpolysiloxane (I).** — One hundred and sixty-three grams of dimethyldichlorosilane was chlorinated by the usual vapor phase method,[7] until the temperature of the boiling mixture reached 114°C. The fractional distillation of the reaction mixture gave 161 g. (78%) of chlormethylmethyldichlorosilane, b.p. 120–2°C.

One hundred and seventy grams of chloromethylmethyldichlorosilane in 200 ml. of ether was added to 400 ml. of water cooled in an ice-bath under vigorous stirring at a temperature below 10°C during a period of one and a half hours. The ethereal layer was separated, washed with water, and dried over calcium chloride. When the solvent was removed in vacuo, 110 g. of (I) was obtained as a fairly viscous oil. Molecular weight, determined cryoscopically in benzene, was found to be 1810. Found: Cl, 32.1. Calculated for $C_2H_5OSiCl$: Cl, 32.6

**3-Chloromethylheptamethyltrisiloxane (II) and 3,5-Di(chloromethyl)octamethyltetrasiloxane (III).**—A mixture of 39.8 g. (0.367 mol.) of trimethylchlorosilane and 30.0 g. (0.184 mol.) of chloromethylmethyldichlorosilane in 30 ml. of dry ether was added gradually to 100 ml. of water cooled in an ice bath under vigorous stirring below 5°C, and then the ethereal layer was separated, washed with water and dried over calcium chloride. The ether solution was filtered, and after shaking with 4 ml. of concentrated sulfuric acid for one half hour, washed again with water, and dried over calcium chloride. Fractional distillation was carried out through a Stedman type column (about 30 theoretical plates) and the yields of various fractions were as follows; 100°/760 mm., 5.0 g. of hexamethyldisiloxane; 94–95°/30 mm. 10.1 g. of (II), $d_4^{25}$ 0.9183, $n_D^{25}$ 1.4042; 95°/30 mm.–126.5°/10 mm. 0.7 g.; 126.5–128°/10 mm., 7.0 g. of (III), $d_4^{25}$ 1.0053, $n_D^{25}$ 1.4199.

6) R. H. Krieble and J. R. Elliott, *J. Am. Chem. Soc.*, 68, 2291 (1946).

7) S. Nozakura, *J. Chem. Soc. Japan (Pure Chem. Sect.)*, 75, 427 (1954).

(II). *Anal.* Found: Si, 30.7; Cl, 12.5; Mol. wt. (in benzene), 279; $MR_D$, 72.06. Calculated for $C_8H_{23}O_2Si_3Cl$: Si, 31.0; Cl, 13.1; Mol. wt., 271; $MR_D$, 72.40.

(III), *Anal.* Found: Si, 29.6; Cl, 18.4; Mol. wt. (in benzene), 387; $MR_D$, 95.38. Calculated for $C_{10}H_{28}O_3Si_4Cl$: Si, 29.5; Cl, 18.7; Mol.wt., 379; $MR_D$, 95.88.

**Chloromethylmethylpolysiloxane (I) with Thiourea (1 : 1 mol.).**—A mixture of 10.88 g. (0.100 eq.) of (I), 7.62 g. (0.100 mol.) of thiourea, and 25 ml. of absolute alcohol was refluxed on a water bath for seven hours with a reflux condenser equipped with a calcium chloride tube. At the beginning of the refluxing (I) did not dissolve but settled down to the bottom of the flask; however, it gradually came into a homogeneous solution. Removal of the solvent in vacuo gave 22.4 g. of glass-like crude polythiuronium chloride. On dissolving this product in 50 ml. of water a slightly turbid solution was obtained, due to the presence of a minor amount of unreacted (I), and so this aqueous solution was extracted with a small amount of ether and again concentrated to dryness in vacuo to yield 18.27 g. of polythiuronium chloride (V) which contained a small amount of thiourea.

When 3 ml. of 6 N aqueous ammonia was added to a solution of 0.88 g. of (V) in 5 ml. of water a white amorphous precipitate was formed and mercaptan was evolved. The precipitate was centrifuged, washed thoroughly with water, and dried at 100° to give 0.32 g. of crude methylpolysiloxane.

*Anal.* Found: Si, 39.4; C, 17.8; H, 4.21; Cl, 0.25. Calculated for $CH_3OSi$: Si, 41.7; C, 17.8; H, 4.48; Cl, 0.0.

In order to identify the methylmercaptan evolved 2.7 ml. of 6 N aqueous sodium hydroxide was added to 0.4 g. of (V) in 10 ml. of water and the mixture was heated on the water bath, and the evolved gas was introduced into a solution of 1.0 g. of mercuric cyanide in 15 ml. of water. The resulted mercaptide (0.4 g.) was recrystallised from alcohol, m.p. 171. The mixed melting point with the known sample did not show any depression. The reaction mixture was filtered to remove the precipitated methylpolysiloxane and the filtrate was evaporated to a few milliliters on a water bath. After cooling 0.4 g. of crude dicyandiamide was obtained in colorless needles and showed the m.p. of 207.5–8° after a recrystallization from water. (207° in literature[5]).

**Chloromethylmethylpolysiloxane (I) and Thiourea (2 : 1 mol.).**—A mixture of 10.7 g. (0.098 eq.) of (I), 3.8 g. (0.050 mol.) of thiourea, and 25 ml. of absolute alcohol was refluxed for four and a half hours. At the end of the reaction the unreacted (I) remained insoluble. After removing the solvent in vacuo, the residual semisolid was dissolved in 50 ml. of water and the aqueous solutions was extracted with ether. Four and a half grams of the unreacted (I) was recovered as an oil (qualitative test for N and S was negative.) from the ethereal layer and 10.1 g. of crude (V) was obtained as a glass-like solid from the water layer. This product gave an impure methylpolysiloxane on the decomposition with ammonia, the analysis of which was as follows: Qualitative test for N and S was negative; Si, 37.0; Cl, 3.35.

**3-Chloromethylheptamethyltrisiloxane (II) with Thiourea.**—A mixture of 6.0 g. (0.022 mol.) of (II), 1.68 g. (0.022 mol.) of thiourea, and 10 ml. of absolute alcohol was refluxed for six hours. When the reaction mixture was distilled under reduced pressure, the distilate was caught in a trap cooled in an ice-salt bath and was added into 25 ml. of water to separate 0.8 g. of an insoluble oil, which boiled mostly at 98–101° and had the camphor-like odor, characteristic of hexamethyldisiloxane. The residue which remained was dissolved in 25 ml. of water and extracted with 20 ml. of ether. After drying the ether solution over calcium chloride and evaporating the solvent on a water bath, a crystalline mass of thiuronium chloride (VI) corresponding to (II) was obtained. After repeated washing with petroleum ether it gave colorless needles which amounted to 2.12 g., m.p. 111–2°. Found: Si, 23.8. Calculated for $C_9H_{27}N_2O_2SSi_3Cl$: Si, 24.2.

Its picrate decomposed at 180–1°. Found: Si, 15.5; N, 12.8. Calculated for $C_{15}H_{29}O_9N_5SSi_3$: Si, 15.5; N, 12.9.

One fifth of the water-soluble part of the product was decomposed with 5 ml. of 6 N aqueous ammonia and on standing over night 0.11 g. of methylpolysiloxane was obtained as a precipitate. Found: Si, 41.4; C, 18.3; H, 4.47. Calculated for $CH_3O_{1.5}Si$: Si, 41.4; C, 17.8; H, 4.48.

Another one-fifth gave 0.31 g. of picrate. Found: Si, 6.75; N, 17.58; N/Si atomic ratio= 5.21.

**3,5-Di (chlormethyl) octamethyltetrasiloxane (III) and Thiourea.**—A mixture of 1.75 g. (0.0046 mol.) of (III), 0.36 g. (0.0048 mol.) of thiourea, and 6 ml. of absolute alcohol was refluxed for five hours. Removing the solvent in vacuo there remained a semisolid and an oil. This was dissolved in 15 ml. of water and extracted with 20 ml. of ether. The ethereal layer gave 0.66 g. of oil. Four-fifths of the water layer, when treated with 6 ml. of 6 N aqueous ammonia, gave 0.133 g. of crude methylpolysiloxane. Found: Si, 40.4; C, 17.9; H, 3.91. Calculated for $CH_3O_{1.5}Si$, 41.7; C, 17.8; H, 4.48.

The residual one-fifth of the water layer gave 0.29 g. of picrate. Found: Si, 7.31; N, 17.74; N/Si atomic ratio=4.84.

**Decamethyltetrasiloxane (VII) and Thiourea.**—A mixture of 7.0 g. of (VII), 5.1 g. of thiourea, and 20 ml. of absolute alcohol was refluxed for eight and a half hours. An oil separated on pouring the reaction mixture onto 50 ml. of water. This was washed with a small quantity of water and distilled. Only 5.6 g. of the unreacted starting material was recovered, b.p. 188–193°.

**Chlormethylpolysiloxane (IV) and Thiourea.**—A mixture of 2.0 g. (0.020 eq.) of (IV), 1.6 g. (0.021 mol.) of thiourea, and 20 ml. of absolute alcohol was refluxed for four hours. The white powder of (IV) gradually became a transparent semisolid and stuck to the bottom of the flask.

After cooling, the upper alcoholic layer was decanted and the residual semisolid was washed several times with alcohol by decantation and dried in vacuo, yielding 2.8 g. of a glassy solid. Found: Si, 17.2; N, 12.8; N/Si atomic ratio=1.5.

Five-tenths of a gram of this product was treated with 10 ml. of water. The insoluble part (about 0.06 g.) was filtered off and the filtrate gave 0.1 g. of an impure amorphous silica on decomposition with 5 ml. of 6 N aqueous ammonia, Found: Si, 44.7; Cl, 0.22. Calculated for $SiO_2$: Si, 46.6; Cl, 0.0.

**The Fission of Silicon-Carbon Bonds in Various Silicon Containing Thiuronium Salts.**—The method of the preparation of chlormethyldimethylalkylsilanes where alkyls are methyl. *n*-butyl, *n*-octyl, and chloromethyldimethylsiloxy group and of their corresponding thiuronium chloride has been described in the previous paper.[4]

The general procedure is as follows: A three necked flask of 30 ml. capacity was equipped through ground joints with a side flask of about 5 ml. capacity, a vertical air condenser 30 cm. long, and a nitrogen gas inlet tube, the tip of which reached to the bottom of the main flask. Four mililiters of 0.377 N aqueous sodium hydroxide was placed in the main flask and was heated on a water bath, and a stream of nitrogen gas with a constant flow (23–4 ml./min.) was introduced into it, and then the solution of the sample in the side flask was quickly poured into the main flask. The samples used were in a slight excess over an equivalent amount of sodium hydroxide (0.001508 eq.) and dissolved in 3–5 ml. of water. The evolved methylmercaptan was removed along with the stream of nitrogen gas and led into a two percent aqueous solution of mercuric chloride through the air condencer. The liberated hydrochloric acid was titrated with 0.1 N aqueous sodium hydroxide using methyl orange as the indicator under vigorous shaking. The results are given in Fig. 1. After the reaction, in the case of A a white precipitate was obtained. In B, the reaction mixture was trans-parent and gave an oil, on addition of aqueous dilute hydrochloric acid. In C, the reaction mixture was transparent. No silicon-containing fragment was found in it nor in the flask of the mercuric solution, except for the precipitate of mercaptide which was not analysed quantitatively but showed distinctly the existence of silicon on ignition with sulfuric acid.

In the cases of D, E, and F there remained oils which were insoluble in dilute aqueous hydrochloric acid.

## Summary

Chloromethylmethylpolysiloxane (I), 3-chloromethylheptamethyltrisiloxane (II) 3,5-di(chloromethyl)octamethyltetrasiloxane (III), and chloromethylpolysiloxane (IV) were reacted with thiourea in absolute alcohol to give silicon-containing thiuronium chlorides.

Although in the case of (II) the corresponding thiuronium chloride was isolated, an extensive fission and recombination of siloxane bonds took place in every case.

Silicon-carbon bond in the thiuronium chloride derived from (I) was easily cleft by the treatment with an aqueous alkali to give three-dimensional methylpolysiloxane. In a similar manner the thiuronium chloride derived from (IV) gave silicic acid with aqueous alkali.

The fission of silicon-carbon bonds in the silicon-containing thiuronium salts was facilitated by the electron-attracting substituents on the silicon atom.

The author is much indebted to Shinetsu Chem. Ind. Co. for generous supplies of the materials used, to Profs. S. Murahashi and H. Tani for their many helpful suggestions, and to Mr. Konotsune for his help in some of the experiments.

*Department of Chemistry,*
*Faculty of Science,*
*Osaka University,*
*Osaka*

# *Formation and Aging of Precipitates. III. Electron Microscopic Studies on Barium Sulfate Precipitates in Aqueous Alcohol*

By Eiji SUITO and Kazuyoshi TAKIYAMA

(Received February 7, 1955)

## Introduction

It is interesting to examine the precipitates that are formed not only in water but also in other media. Many investigations have been made about precipitates which are produced in more soluble media than water to study their analytical conditions, and those which are produced in less soluble media to prepare the colloidal solutions. The authors reported about the morphology and aging of barium sulfate precipitates in water previously[1], and also examined the change of the shape and size of the precipitates produced by changing the solubility of barium sulfate. This paper is a report on barium sulfate precipitates produced in aqueous alcohol in the relations of the shape and size, the total concentration, the concentration of alcohol and the solubility of barium sulfate.

## Solubility of Barium Sulfate in Aqueous Alcohol

As there have been practically no investigations reported about the solubilities of barium sulfate in aqueous alcohol, the authors have measured them by the electric conductivity method, which will be explained by an example as follows.

The electric conductivity was measured by the method of the Wheatstone bridge. The specific conductivity of distilled water was $2.23\times10^{-6}$ mho and that of the saturated aqueous barium sulfate was $5.1\times10^{-6}$ mho. Then the solubility of barium sulfate in water was calculated as $1.2\times10^{-5}$ M. The specific conductivity of 45% alcohol was $5.3\times10^{-6}$ mho and that of the saturated barium sulfate solution in 45% alcohol was $6.6\times10^{-6}$ mho. Then to 15 ml. of 45% alcohol the saturated aqueous barium sulfate was added drop by drop from a micro-burette and the conductivities of these mixed solutions were measured. After 0.11 ml. of the saturated aqueous barium sulfate was added to the aqueous alcohol, the specific conductivity became $6.6\times10^{-6}$ mho. From these results the solubility of barium sulfate in 45% alcohol was calculated as follows:

$$\frac{1.2\times10^{-5}\times0.11}{15.11}=8\times10^{-8}\ (\mathrm{M})$$

The solubilities of barium sulfate in alcohol of various concentrations were measured by the same method and the results are shown in Table I and Fig. 1. As the concentration of the alcohol in which barium sulfate was saturated was somewhat different from that of the alcohol to which the saturated aqueous barium sulfate was added, the percentage of alcohol shown in Table I contains some errors, but they are negligible.

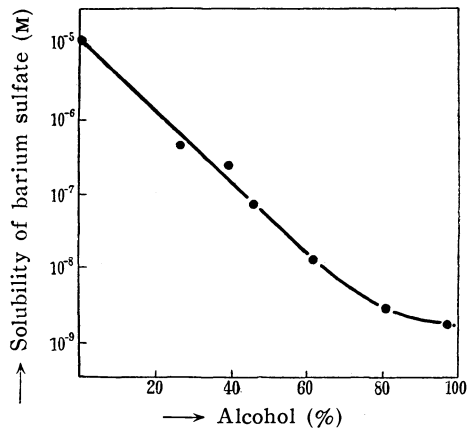



Fig. 1. The solubility of barium sulfate in aqueous alcohol.

TABLE I

SOLUBILITIES OF BARIUM SULFATE IN AQUEOUS ALCOHOL

| Concentration of Alcohol % | Solubility of Barium Sulfate M |
|---|---|
| 0 | $1.2\times10^{-5}$ |
| 30 | $3\times10^{-6}$ |
| 39 | $4\times10^{-7}$ |
| 45 | $8\times10^{-8}$ |
| 62 | $2\times10^{-8}$ |
| 80 | $4\times10^{-9}$ |
| 99 | $2\times10^{-9}$ |

## Morphology of Barium Sulfate Precipitates in Aqueous Alcohol

The barium sulfate precipitates in aqueous alcohol were prepared as follows. To 10 ml. of alcohol of a certain concentration were added simultaneously 5 ml. of barium hydroxide solution and sulfuric acid which were of the same concentration. The reaction temperature was 18°C. The precipitates produced were observed by an electron microscope.

The conditions of the precipitation and the properties of the precipitated particles are collectively

1) E. Suito and K. Takiyama, This Bulletin, 27, 121, 123 (1954).

shown in Table II. A, B and C groups in Table II are the cases in which the total concentrations of barium sulfate were kept constant and the concentrations of alcohol were changed. In these groups the precipitates produced in water, that is 0 % alcohol, are to be compared with the condition of the precipitation reported previously[1]. In D group the concentration of alcohol was kept definite; that is to say, the solubility of barium sulfate was definite, and the total concentration of barium sulfate was changed.

At the total concentration of 0.05 M (A group) the particles precipitated in water were spindle-shaped, as shown in Photo 1, but in aqueous alcohol the shapes of the particles were thin hexagonal plates, and their size became smaller with the increase of the concentration of alcohol as shown in Photos 2, 3 and 4. The hexagonal particles of barium sulfate were found only under these conditions and were not found in the precipitates formed in water nor at the other total concentrations in aqueous alcohol. As the particles of the specimen of No. 4 were very small, namely, the size was below 10 mμ, the shape was not clear.

At the other total concentrations the particles precipitated in the aqueous alcohol were practically diamond-shaped and their size became smaller with the increasing percentage of alcohol in the aqueous alcohol as shown in Table II.

change at the definite solubility was similar to the change of the size of the precipitated particles produced in water medium[1].

At the total concentrations higher than 0.05 M the size of the precipitated particles became extremely small with the addition of alcohol. None of the precipitated particles produced in the aqueous alcohol have changed their shape and size for 2 years on standing in the media.

In these precipitates the similar shaped particles were formed after the same induced period. Namely, the precipitates of diamond shape began to deposit immediately after mixing the reagents and completed their crystallization after 10 to 20 seconds. The precipitates of spindle shape were completly formed directly after mixing the reagents. Such phenomena have been observed both in cases of water and aqueous alcohol media. It seems that the mechanism of the growth of the crystals was similar, when the induced period of the formation of the crystals was identical.

### Identification of Crystals by the Electron Micro-Diffraction Method

The electron micro-diffraction method by means of the three stage electron microscope, SM-C3, was applied to analyze the crystal structure of the precipitated particles mentioned above. A few examples of the electron diffraction patterns obtained are shown in Photos 9 (a), (b) and (c).

TABLE II

THE PROPERTIES OF BARIUM SULFATE PRECIPITATES IN AQUEOUS ALCOHOL

| Group | No. | Total concentration $C_0$ (M) | Alcohol concentration (%) | Solubility S (M) | Particle size (mean) (mμ) | Particle shape |
|---|---|---|---|---|---|---|
| A | 1 | $5\times10^{-2}$ | 0 | $1\times10^{-5}$ | 470 | Spindle |
| " | 2 | " | 2.5 | $9\times10^{-6}$ | 90 | Thin hexagonal plate |
| " | 3 | " | 10 | $5\times10^{-6}$ | 70 | " |
| " | 4 | " | 50 | $7\times10^{-8}$ | <10 | —— |
| B | 5 | $5\times10^{-3}$ | 0 | $1\times10^{-5}$ | 3200 | Diamond (rugged) |
| " | 6 | " | 2.5 | $9\times10^{-6}$ | 3000 | " |
| " | 7 | " | 5 | $8\times10^{-6}$ | 2500 | " |
| " | 8 | " | 7.5 | $7\times10^{-6}$ | 2000 | " |
| " | 9 | " | 10 | $5\times10^{-6}$ | 1100 | Diamond (smooth) |
| " | 10 | " | 15 | $3\times10^{-6}$ | 400 | " |
| " | 11 | " | 50 | $7\times10^{-8}$ | <10 | —— |
| C | 12 | $5\times10^{-4}$ | 0 | $1\times10^{-5}$ | 3500 | Ellipse |
| " | 13 | " | 2.5 | $9\times10^{-6}$ | 3100 | Diamond (rugged) |
| " | 14 | " | 10 | $5\times10^{-6}$ | 3000 | Diamond (smooth) |
| " | 15 | " | 25 | $6\times10^{-7}$ | 2000 | Spindle (thin rugged) |
| " | 16 | " | 35 | $3\times10^{-7}$ | 70 | Sphere (rugged) |
| " | 17 | " | 50 | $7\times10^{-8}$ | <10 | —— |
| D | 18 | $5\times10^{-2}$ | 10 | $5\times10^{-6}$ | 70 | Hexagon |
| " | 19 | $4\times10^{-2}$ | " | " | 710 | Diamond (rugged) |
| " | 20 | $3\times10^{-2}$ | " | " | 820 | " |
| " | 21 | $1\times10^{-2}$ | " | " | 830 | " |
| " | 22 | $5\times10^{-3}$ | " | " | 1600 | " |
| " | 23 | $5\times10^{-4}$ | " | " | 3000 | Diamond (smooth) |

In D group the precipitated particles became larger with the decreasing total concentration of m sulfate as shown in Photos 5~8. This

Photo 9 (a) obtained from the diamond-shaped particles shown in Photo 7 (No. 21) is of coarse Debye-Scherrer rings, because there are not

Electron micrographs of various barium sulfate precipitates

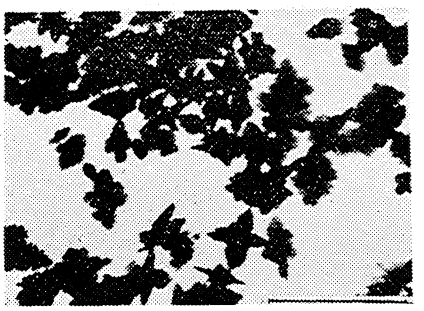


Photo. 1. No. 1. $C_0=5\times10^{-2}$ м, $S=1\times10^{-5}$ м (×20,000)

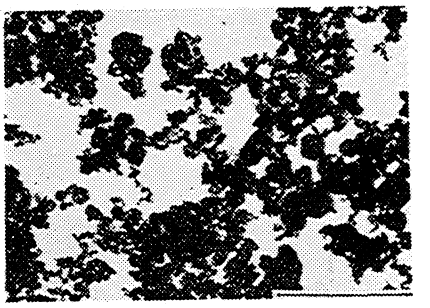


Photo. 2. No. 2. $C_0=5\times10^{-2}$ м, $S=9\times10^{-6}$ м (×20,000)

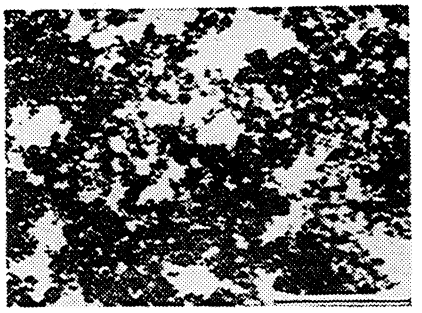


Photo. 3. No. 3. $C_0=5\times10^{-2}$ м, $S=5\times10^{-6}$ м (×20,000)

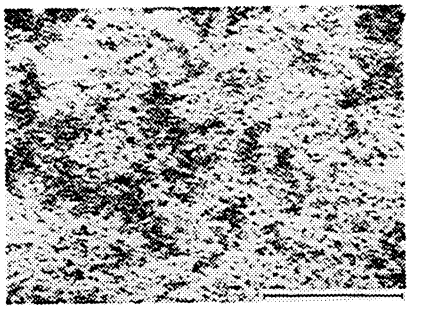


Photo. 4. No. 4. $C_0=5\times10^{-2}$ м, $S=7\times10^{-8}$ м (×20,000)

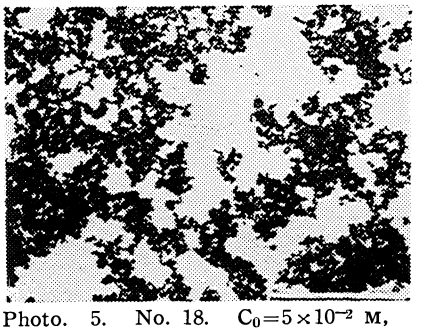


Photo. 5. No. 18. $C_0=5\times10^{-2}$ м, $S=5\times10^{-6}$ м (×20,000)

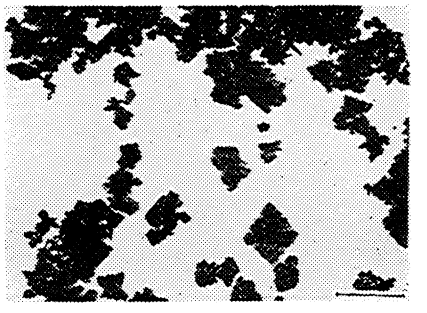


Photo. 6. No. 20. $C_0=3\times10^{-2}$ м, $S=5\times10^{-6}$ м (×10,000)

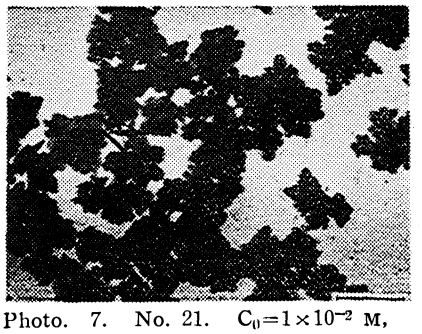


Photo. 7. No. 21. $C_0=1\times10^{-2}$ м, $S=5\times10^{-6}$ м (×10,000)

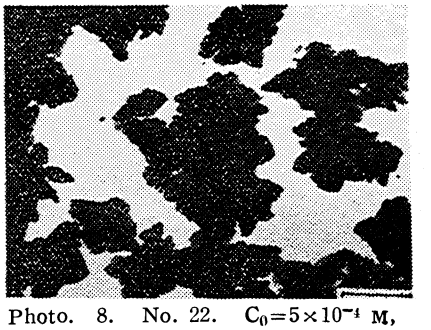


Photo. 8. No. 22. $C_0=5\times10^{-4}$ м, $S=5\times10^{-6}$ м (×10,000)

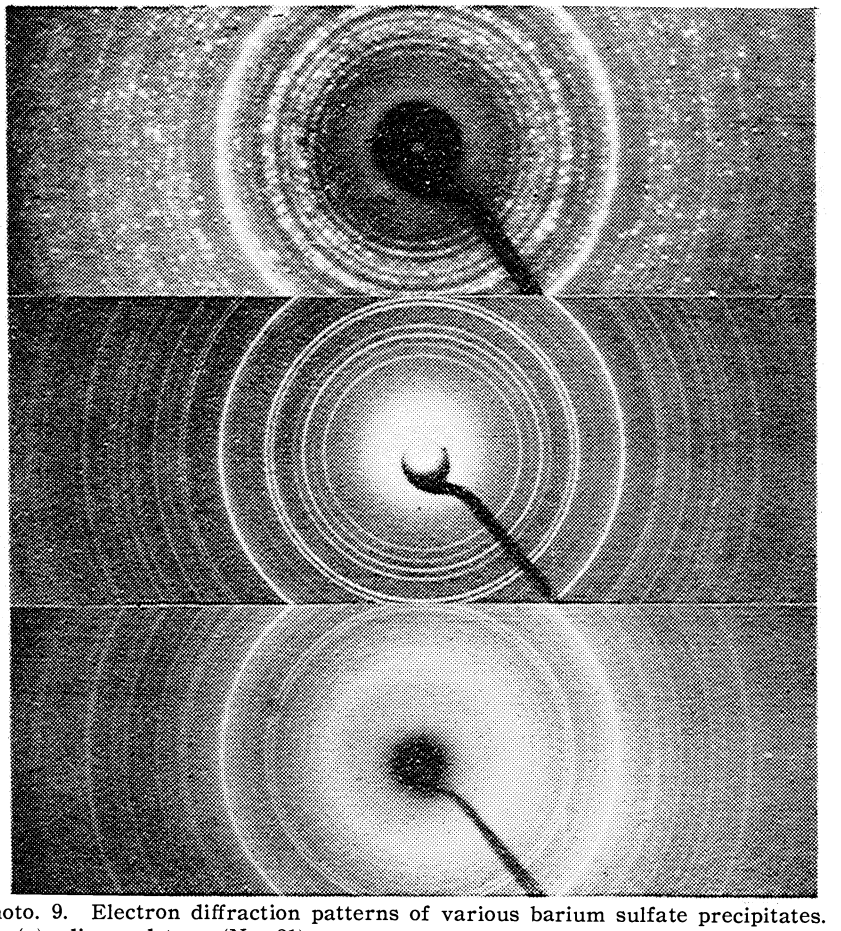


Photo. 9. Electron diffraction patterns of various barium sulfate precipitates.
(a) diamond type (No. 21)
(b) hexagonal type (No. 3)
(c) small particle (No. 4)

many crystalline particles in the selected area (5 μ) of the electron microscope. The patterns obtained from the particles of the hexagonal plates and the small particles shown in Photo 3 (No. 3) and Photo 4 (No. 4) were obtained by the ordinary electron diffraction technique for many crystalline particles, and are very fine as shown in Photos 9 (b) and (c). It is interesting that the pattern obtained from the small particles which are observed as "amorphous" by the electron microscope (<10 mμ) is very sharp, and the particles are obviously crystalline.

The arrangements of the rings of every diffraction pattern are the same as observed with barium sulfate crystals obtained by X-ray diffraction as shown in Fig. 2.

Differences in the intensity of each line in the electron and X-ray diffraction diagrams intimate the orientation of the flat particles on the film of the specimen holder of the electron microscope, though the difference in technique between the electron and X-ray diffractions have to be taken into consideration.

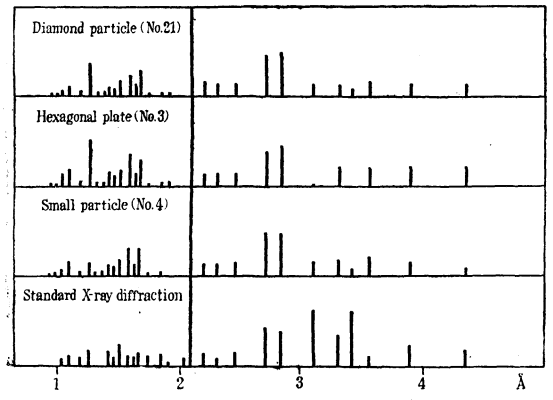



Fig. 2. Electron diffraction diagrams of various barium sulfate precipitates.

## Summary

1. The solubilities of barium sulfate in aqueous alcohol were measured.

2. The barium sulfate particles precipitated in aqueous alcohol became smaller with the increasing concentration of alcohol; namely, with the decreasing solubility of barium sulfate.

3. In the case of the aqueous alcohol of the certain percentage (for a definite solubility of barium sulfate) the precipitated particles became larger with the decreasing total concentration of barium sulfate.

4. The barium sulfate precipitates prepared in the aqueous alcohol were practically diamond shaped; and spindle, hexagonal and sphere particles were also found. The shape of the precipitated particles seemed to depend on the induced period of the precipitation.

5. The electron micro-diffraction method was applied to analyze the crystal structure and, of course, the patterns obtained from various types of crystals agreed with those of barium sulfate.

*The Institute for Chemical Research, Kyoto University, Takatsuki-Shi, Osaka-Fu*

and Maurice[7] reported the complex formation of thorium oxalate from the standpoint of the phase rule. In the present investigation the existence of these complex ions in dilute aqueous solution at 25°C was confirmed by means of potentiometric titration with glass electrode. It is found that the precipitation of thorium dioxalate is completed at pH 4.3 and the precipitate is then dissolved gradually with the addition of oxalate.

The pH value increases with the addition of oxalate after one type of complex formation is completely in equilibrium with the other, and it is kept constant when another type of complex begins to be formed. The milky suspension was dissolved gradually and a clear solution was obtained when the mole ratio exceeded 6 : 1.

It is evident, therefore, that when an excess precipitant is added, and when the pH value exceeds 4.5, the precipitate of thorium oxalate will be partially redissolved. Consquently a negative error will be found in the analytical result from the standpoint of analytical chemistry.

As shown in Fig. 1, in titrating a dilute solution of thorium nitrate with sodium or ammonium oxalate solution, four inflections are found in each titration curve of the thorium-oxalate system. The first sharp inflection, corresponding to the complete precipitation of thorium oxalate which is expected to have the mole ratio of oxalate ion to thorium ion, viz., the "$R$" value in brief, of 2 is found at the $R$ value of 1.9, and at pH ranging from 4.24 to 4.31 in each curve. The second, the third and the fourth inflections, which correspond to the formation of thoroxatale complexes, are found stepwisely in each curve at the approximate $R$ values of 3, 4 and 6 respectively.

In Fig. 1, curves (A) and (B) indicate the potentiometric titrations of 50 ml. of 0.001 M $Th(NO_3)_4$ with 0.01 M $Na_2C_2O_4$ and with 0.01 M $(NH_4)_2C_2O_4$ in pure aqueous solutions, and curve (C) and (D) indicate the corresponding titrations in 0.5 M $NaClO_4$ solutions, respectively. The $R$ value and pH observed at each point of inflection in these titration curves are summarized in Table I.

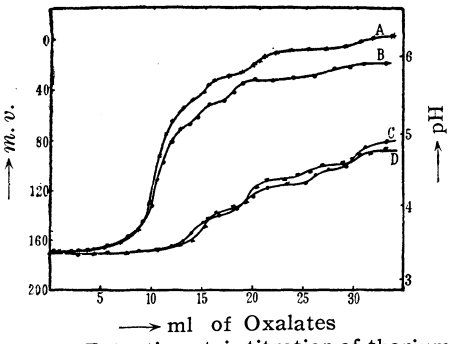



Fig. 1. Potentiometric titration of thorium nitrate with oxalates.

**B) Potentiometric Titration of Thorium and Cerium Nitrates with Sodium Hydroxide Solution.**—The difference between the basicities of thorium and cerium ions or between those of ceric and cerous ions has been used in the separation of the former from the latter by several investigators[8]. Britton and Maurice[9] and Bowles and Partrige[10] reported the potentiometric titration of thorium and

7) H. T. S. Britton and Maurice, *J. Chem. Soc.*, **1936**, 1419.

8) Therald Moeller, George K. Schweitzer and Donald D. Star, *Chem. Rev.*, **42**, 64 (1938).

9) H. T. S. Britton, *J. Chem. Soc.*, **127**, 2142 (1925).

10) T. A. C. Bowles and H. M. Partridge, *Ind. Eng. Chem. Anal. Ed.*, **9**, 124 (1937).

TABLE I

THE MOLE RATIO AND pH AT EACH MAXIMUM INFLECTION IN THE TITRATION CURVES OF THORIUM-OXALATE SYSTEM

| Curve | Thorium Nitrate | Oxalate (M) | | Inflect found at I | II | III | IV | V |
|---|---|---|---|---|---|---|---|---|
| (A) | 0.001 M ($f$=1.070) in pure water | 0.01 ($f$=1.009) $Na_2C_2O_4$ | $R$ value | 1.89 | 2.89 | 3.87 | | 5.85 |
| | | | pH | 4.24 | 5.56 | 5.92 | | 6.19 |
| (B) | ,, | 0.01 M ($f$=1.003) $(NH_4)_2C_2O_4$ | $R$ value | 1.91 | 2.72 | 3.38 | | 5.53 |
| | | | pH | 4.31 | 5.22 | 5.56 | | 5.86 |
| (C) | 0.001 M ($f$=1.070) in 0.5 M $NaClO_4$ | 0.01 M ($f$=1.009) $Na_2C_2O_4$ | $R$ value | | 2.89 | 3.68 | 4.91 | 5.66 |
| | | | pH | | 3.76 | 4.14 | 4.39 | 4.66 |
| (D) | ,, | 0.01 M ($f$=1.003) $(NH_4)_2C_2O_4$ | $R$ value | | 2.63 | 3.67 | 4.69 | 5.72 |
| | | | pH | | 3.64 | 4.17 | 4.44 | 4.66 |

TABLE II

POTENTIOMETRIC TITRATION OF THORIUM AND CEROUS NITRATES WITH SODIUM HYDROXIDE SOLUTION

| Curve | Initial concentration $Th(NO_3)_4$ $Ce(NO_3)$ or the mixture | pH at which the solution becomes opaque | Maximum inflection occurs at pH | mole ratio |
|---|---|---|---|---|
| (A) | 0.001 M $Th(NO_3)_4$ in aq. solution | 4.34 | 6.71 | 3.69 : 1 |
| (B) | 0.001 M $Th(NO_3)_4$ in 0.5 M $NaClO_4$ | 4.78 | 6.61 | 3.94 : 1 |
| (C) | 0.001 M $Ce(NO_3)_3$ in 0.0005 M $HNO_3$ | 7.32 | 8.39 | 2.92 : 1 |
| (D) | 0.001 M $Ce(NO_3)_3$ in 0.0005 M $HNO_3$ and 0.5 M $NaClO_4$ | 6.51 | 7.73 | 2.97 : 1 |
| (E) | 0.001 M $Th(NO_3)_4$ and 0.001 M $Ce(NO_3)_3$ in 0.0005 M $HNO_3$ | 7.62 | 5.59 and 8.76 | 3.70 : 1 and 2.92 : 1 |
| (F) | 0.001 M $Th(NO_3)_4$ and 0.001 M $Ce(NO_3)_3$ in 0.0005 M $HNO_3$ and 0.5 M $NaClO_4$ | 5.86 | 5.08 and 8.22 | 3.60 : 1 and 2.97 : 1 |

some rare earth ions to find the pH at ranges at which these hydroxides began to precipitate. In the present investigation, the potentiometric titration was extended to extreme dilute solutions having the final concentration of 0.001 molar with respect to cerous or thorium ions. Furthermore, by reducing ceric to cerous ions in a dilute solution containing thorium ion and titrating the resulting solution with sodium hydroxide solution, thorium and cerous ions could be determined in the presence of each other.

On account of the complicating effects of polymerization and the colloidal adsorption of these hydrous oxides in the basic solution, the coagulation points that are in coincidence with the maximum inflections of the titration curve occur before the attainment of the stoichiometric points which have the $R$ values of 4 for thorium and 3 for cerous hydroxide.

Inasmuch as the acid solution of cerous nitrate is used in the present investigation, the first inflection in the titration curve is attributed to the neutralization of the free acid and is subtracted from the total amount of the base added. The steep inflections are found at the $R$ values of 3.7 and 2.9 and at pH 6.7 and 8.4 in the titration curves for thorium and cerous salts respectively. The presence of sodium perchlorate represses the complicating effects of polymerization and colloidal adsorption of these hydrous oxides and draws the $R$ values in close proximity to the stoichiometric points at the $R$ values of 4 and 3, respectively.

In titration of a mixture of thorium and cerous nitrates with sodium hydroxide solution, the pH value at the coagulation point of cerous hydroxide is little influenced by the presence of thorium hydroxide, but that of the latter is remarkably lowered by the presence of the former. This fact facilitates the separation of the one from the other and the determination of the one in the presence of the other. In applying the above method to the determination of thorium and cerous ions individually or in the presence of another one however, the experimental results obtained

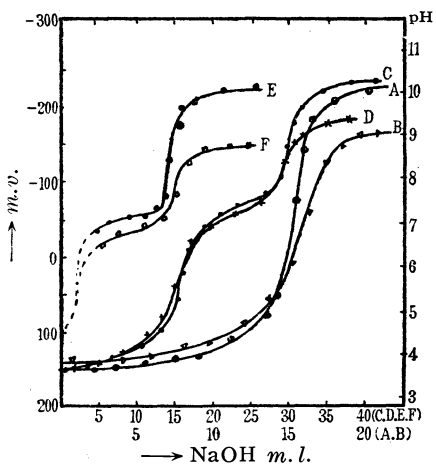



Fig. 2. Titration curves of thorium and cerous nitrates with sodium hydroxide.

from the potentiometric titration must be multiplied by experimental factors which are both greater than unity for correction, that is, 4.0/3.7 for the former and 3.0/2.9 for the latter.

## Summary

1) Thorium nitrate was potentiometrically titrated with sodium and ammonium oxalates by using glass electrode as an indicator electode. Four inflections were found in the titration curves of the thorium-oxalate system. The first steep inflection, corresponding to the precipitation of thorium dioxide, was found at the mole ratio of $C_2O_4^{2-}$ to $Th^{4+}$, viz., the "$R$" value, 1.9 and at pH 4.3. The second the third and the fourth inflections, corresponding to the formation of thoroxalate complexes were found at the approximate $R$ value of 3.4, and 6, and at pH values ranging from 5.4 to 6.3.

2) Thorium and cerium nitrates were potentiometrically titrated by sodium hydroxide in dilute solutions with glass electrode. By reducing ceric to cerous ions in a solution containing thorium ion, and by titrating the resulting solution with sodium hydroxide solution, two steps of inflection, corresponding to the precipitation of thorium and cerous hydroxides, were found respectively, in the titration curve. In applying this method to the determination of thorium and cerous ions in the presence of one another, however, the experimental results obtained from the titration curve must be multiplied by the experimental factors which are both greater than unity for accuracy.

*Department of Chemistry, College of Science, National Taiwan University, Taiwan*

# *Determination of Dielectric Constant and Loss Factor by Free Wave Method. III. Measurement on Aliphatic Alcohols at the Wavelength of 1.38 cm.*

By Hideo OKABAYASHI

(Received January 19, 1955)

The theory of determining the dielectric constant and the loss factor of liquids by the free wave method has been developed by M. Yasumi.[1] The dielectric properties of various liquids have been investigated in the microwave region (wavelength = 9.8, 4.5 and 3.24 cm.) in our laboratory[2,3,4], and several interesting results have been obtained.

Debye was the first who succeeded to explain theoretically the anomalous dispersion and the absorption of electric wave by polar substances[5]. The basic idea for the assumption of the internal field seems not to be entirely satisfactory. Nevertheless the assumption of the single relaxation time seems to be valid from the experimental point of view[4,6–10]. The validity of this assumption is being kept under consideration in our laboratory and is justified when we adopt a suitable internal field[11,12]. Assuming the single relaxation time, the following equations are shown to be valid irrespective of the relaxation mechanism.

$$\varepsilon' = \varepsilon_\infty + \frac{\varepsilon_0 - \varepsilon_\infty}{1+x^2}, \tag{1}$$

$$\varepsilon'' = \frac{(\varepsilon_0 - \varepsilon_\infty)}{1+x^2} x, \tag{2}$$

$$x = \omega\tau, \tag{3}$$

1) M. Yasumi, This Bulletin, **24**, 53 (1951).
2) M. Yasumi, K. Nukazawa and S. Mizushima, This Bulletin, **24**, 60 (1951).
3) M. Yasumi, H. Okabayashi, M. Shirai and S. Mizushima, *J. Chem. Phys.*, **19**, 978 (1951).
4) M. Yasumi, M. Shirai and S. Mizushima, This Bulletin, **25**, 133 (1952).
5) P. Debye, "Polare Molekeln", Leipzig: Hirzel (1929).
6) A. Schallachmach, *Trans. Faraday Soc.*, **42A**, 180 (1946).
7) C. H. Collie, J. B. Hasted and D. M. Ritson, *Proc. Phys. Soc.*, (London), **60**, 145 (1948).
8) J. B. Hasted, G. H. Haggis and P. Hutton, *Trans. Faraday Soc.*, **47**, 577 (1951).
9) G. H. Haggis, J. B. Hasted and T. J. Buchanan, *J. Chem. Phys.*, **20**, 1452 (1952).
10) J. A. Saxton, *Proc. Roy. Soc.*, A, **213**, 473 (1952).
11) J. Wyman, *J. Am. Chem. Soc.*, **58**, 1482 (1936).
12) M. Yasumi and H. Komooka (to be published).

where $\varepsilon'$ is the dielectric constant, $\varepsilon''$ the loss factor and $\omega$ the angular frequency. $\varepsilon_0$ and $\varepsilon_\infty$ are the values of the dielectric constant at $x=0$ and $x=\infty$ respectively. $\tau$ is called the relaxation time and is related to the characteristic frequency $\lambda_s$ as follows.

$$\lambda_s = 2\pi c\tau, \qquad (4)$$

where $c$ denotes the velocity of light.

Much of our interest is concerned with the values of $\varepsilon_\infty$ for the liquids. In the earlier works,[13] the value of $\varepsilon_\infty$ was assumed to be identical with the value of the square of the refractive index $(n_{opt})^2$ at optical regions. If the liquids show marked absorption spectra in infra-red region, the $(n_{opt})^2$ is not identical with $\varepsilon_\infty$. The origin of the difference is due partly to the infra-red-active interatomic vibrations in a molecule and partly to the intermolecular vibrations in the liquid structure.

In our preliminary work[4], the dielectric constant and the loss factor were measured at the wavelength of 3.24 cm., and the values of $\varepsilon_\infty$ were calculated, assuming the validity of Eqs. (1) and (2). It was concluded there that the atomic polarizations due to the liquid structure are almost constant for various aliphatic alcohols investigated. The obtained result was concerned, however, only with the data at the wavelength of 3.24 cm. The result must be confirmed for the other frequencies.

In the present work, the dielectric constant and the loss factor were measured at the wavelength of 1.38 cm. The method of determining the dielectric constant and the loss factor of the liquids was described by M. Yasumi.[1] The important points will be repeated here. The linearly polarized plane wave of the wavelength $\lambda$ is emitted vertically into the free space. When the wave comes to the mercury surface, the perfect standing-wave pattern may appear in the space above the mercury surface. If the liquid layer is placed on mercury, the amplitudes of the incident and reflected waves will be generally different. Also the crystal detector shows the imperfect standing-wave when the position of the detector is shifted vertically from the liquid surface to the free space. If the crystal detector obeys the square law, the ratio of the maximum-to the minimum-current induced in the detector, $I_M/I_m$, is expressed by the following equation,

$$I_M/I_m = (1+R)^2/(1-R)^2. \qquad (5)$$

where $R^2$ is the reflection coefficient of the system consisting of the liquid layer of the thickness $d$ and the mercury layer. Such measurements are made at different thicknesses of the liquid layer.

$$R^2 = \frac{\sin h^2\left(\frac{2\pi kd}{\lambda} + \frac{1}{2}\ln R_{12}\right) + \cos^2\left(\frac{2\pi nd}{\lambda} - \frac{\gamma}{2}\right)}{\sin h^2\left(\frac{2\pi kd}{\lambda} - \frac{1}{2}\ln R_{12}\right) + \cos^2\left(\frac{2\pi nd}{\lambda} + \frac{\gamma}{2}\right)}, \qquad (6)$$

The reflection coefficient $R^2$ is expressed as follows:

where $n$ and $k$ are the refractive index and the absorption coefficient of liquid respectively, and further $R_{12}$ and $\gamma$ are expressed as

$$R_{12}^2 = \frac{(n-1)^2+k^2}{(n+1)^2+k^2}, \quad \tan\gamma = \frac{2k}{n^2-1+k^2}. \qquad (7)$$

The real part $\varepsilon'$ and the imaginary part $\varepsilon''$ of the complex dielectric constant are related to $n$ and $k$ in the following manner,

$$\varepsilon' = n^2-k^2, \quad \varepsilon'' = 2nk. \qquad (8)$$

It is more convenient to choose as parameters in Eq. (2) $n$ and $k$ than $\varepsilon'$ and $\varepsilon''$, as easily seen from Eqs. (6) and (7).

Given $n$ and $k$, we can use Eqs. (6) and (7) to calculate the reflection coefficient $R^2$ for the various thickness $d$ and draw the curve of $R$ *versus* $d$. Here, it is convenient to take $d/\lambda$ as the abscissa instead of $d$ because in Eq. (6) the thickness $d$ appears always in the form of $d/\lambda$.

The method of obtaining the value of $n$ and $k$ for the liquid concerned is as follows. First we obtain the values of $I_M/I_m$ for various thicknesses experimentally. Secondly we calculate the value of $R$ for each value of $d/\lambda$. Then we draw the curve of $R$ *versus* $d/\lambda$. This experimentally obtained curve is compared with those calculated by Eqs. (6) and (7) for various $n$ and $k$. The values of $n$ and $k$ assumed in the theoretical curve which fit most satisfactorily the experimental curve, will be taken as values for the liquid investigated. In practice, the interpolation method is used. To confirm whether the values of $n$ and $k$ thus determined are the fittest or not, we make the curve $R$ *versus* $d/\lambda$ for the values of $n$ and $k$ thus obtained, and compare it with the experimental curve.

13) S. Mizushima, *Sci. Papers Inst. Phys. Chem. Res.*, (Tokyo), **9**, 109 (1928).

## Apparatus

The apparatus constructed is shown as a block diagram in Fig. 1.

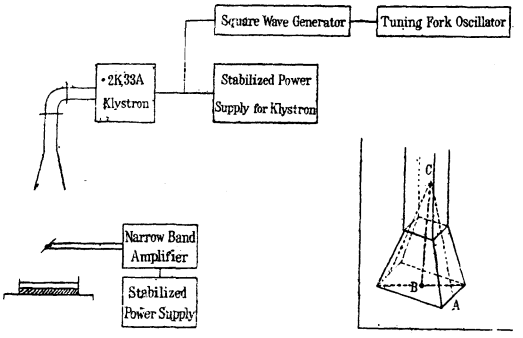



Fig. 1. The block diagram of our apparatus.

A type 2K33A reflex klystron is used as a source of the radiation. The high voltage power supply for the klystron must be highly stabilized by an electronic device because the output power and the frequency of the reflex klystron are extremely sensitive to the beam voltage and the reflector voltage. Our circuit diagram of the voltage stabilizer is shown in Fig. 2.

tions, and the rise- and fall-times are extremely short[14].

The electromagnetic horn is connected with the cavity of the klystron through an $E$-bend waveguide. In order that the wavefront at the aperture may approximate a plane, the difference between the distances from the point C to the center B and to the point A on the edge of the aperture (refer to Fig. 1) is designed to be smaller than $\lambda/8$. The dimension of the aperture is $7.5\times7.5\,cm^2$. The waveguide connected with the cavity of the klystron has a section of $1.07\times0.43\,cm^2$ and is operated in a mode $H_{01}$ when the wavelength is 1.38 cm. The electric field in the waveguide makes a right angle to its larger side. Therefore if the waveguide is enlarged gradually to the aperture of the horn, the electric field in the free space is kept in a fixed direction. Thus the radiated wave from the horn is linearly polarized.

The distance between the aperture of the horn and the surface of mercury is about 75 cm., so that the obtained radiation behaves like the plane wave near the liquid surface.

The vessel is made of wood and lacquered, and its dimension is $20\times20\,cm^2$. This area is sufficiently large to remove the effect of the edges The thickness of the liquid layer is determined from the volume of the liquid poured in.

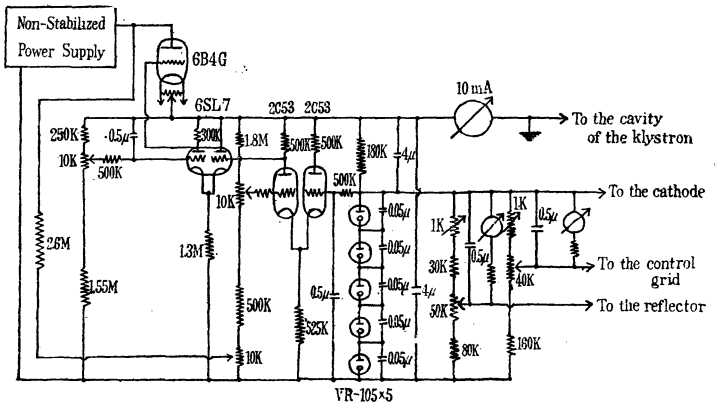



Fig. 2. The high voltage stabilizer for the klystron.

Modulation of the microwave source makes it possible to use a. c. amplification of the signal from the crystal detector and to shorten the time required for each measurement more than to use a galvanometer. For the standing-wave measurement, the percentage of the amplitude modulation should be large, but the frequency modulation must be avoided. Therefore, the "on-off" modulation, with a square modulation envelope, is preferred. Modulation is introduced in the reflector circuit by a square-wave voltage superposed on the steady-state reflector voltage. The square-wave generator is synchronized with the tuning fork oscillator of 1000 c/s., and is constructed so that on- and off-states have almost equal dura-

The crystal detector is made of a tungsten wire and a small pellet of silicon crystal picked out from a commercial crystal detector, 1N23B. Two leads of phosphor bronze which support the crystal and the wire are bound by a rubber ring to adjust the pressure of the tungsten wire against the silicon crystal. The crystal detector so constructed is stably fixed except in the case of a great mechanical shock. The detector system is arranged so that the direction from the tungsten wire to the crystal is parallel to the electric field of the linearly polarized wave. This

14) C. G. Montgomery, "Technique of Microwave Measurements", McGraw-Hill Book Company, Inc., New York and London (1947).

detector is shifted vertically to the liquid surface by the micrometer.

The signal of the square-wave from the crystal detector is amplified and introduced in an indicating ammeter of 1 m amp. Because some frequency modulation may occur during the rise- and fall-times of the modulating square-wave, the tuning amplifier is used in order to prevent a spurious signal. The frequency sensitivity of the amplifier is provided by a twin-T feedback network tuned in the 1000 c/s[14].

On adjusting the whole apparatus, the important points to be kept in mind are to determine the region in which the electric field may be measured by the crystal detector, and to construct a sufficiently small crystal detector, so that it might not disturb the radiation field except so slightly as to be negligible, and further to adjust the contact between the wire and the pellet of silicon crystal in order to give a high sensitivity to the microwave field.

Near the aperture of the horn, the radiation pattern is complicated, and far from the plane wave. Also because we cannot place a liquid layer in the infinite and empty space, we must choose the region near the liquid surface in order to avoid the effects of other bodies, for example, of the walls and of the supporter of the vessel, etc. On the other hand, the disturbance of the detector may be detected as a departure from the (sine)$^2$ law for the standing-wave pattern which appears on the mercury layer.

By trial and error, we adjusted the whole system in order that it may be operated under the best conditions, changing the frequency of the radiation source slightly. As the result we knew that the detector may be shifted in the region near the height 6 cm. from the liquid layer. The dimension of the crystal detector which was used is shown in Fig. 3. The resulting standing-wave

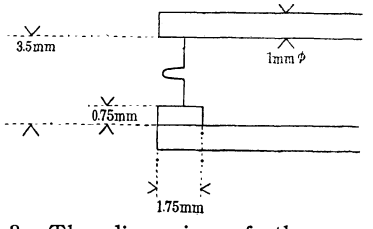



Fig. 3. The dimension of the crystal detector.

pattern on the mercury layer showed that near the above-mentioned height the maximum values of the induced current fluctuated within ±1 percent, and that the minimum values were recognized as zero as far as we used the ammeter of 1 m amp. as an indicating meter. The maximum point shifted about 0.15 mm from the middle point of two successive minimum points towards the radiation source. The induced currents showed the square law except in the region where the current was very small. We can determine the wavelength within the accuracy of ±0.2 percent from this perfect standing-wave pattern. In many cases the wavelength was 1.378 cm.

## Materials

Methyl alcohol: Commercial methyl alcohol is boiled with freshly burnt lime under reflux and distilled. Then the distillate is refluxed with silver nitrate and distilled. The distillate is dried over magnesium activated with iodine, b. p. 67.0–67.4°C.

Ethyl alcohol is purified by the same procedure as methyl alcohol, b. p. 77.8–78.3°C.

Purified *n*-butyl alcohol is obtained by means of the efficient fractionating column constructed by T. Tamura[15], b. p. 117.0–117.2°C.

Isobutyl alcohol is treated with freshly burnt lime, and then the distillate is dried over anhydrous copper sulphate, b. p. 107.5–108.2°C.

Tertiary butyl alcohol is dried over sodium hydroxide and then fractionated by means of the above-mentioned column, b. p. 83.5–83.8°C.

## Measurements

Each measurement is operated half an hour later, after the whole apparatus was switched on. At first we measure the standing-wave pattern when the vessel contains only mercury. The wavelength is determined from it. Thereafter a certain amount of liquid is poured in, and we measure the standing-wave ratio by shifting the crystal detector vertically to the liquid surface. These operations are repeated. Finally we can draw the curve $R$ *versus* $d/\lambda$ using the table of the standing-wave ratio *versus* the square root of the reflection coefficient, $R$.

For $n \gg k$, the maximum and minimum values of the square root of the reflection coefficient and the corresponding values of $d/\lambda$ are expressed approximately by simple equations derived from Eq. (2).[1] Therefore we can determine roughly $n$ and $k$ from the experimental curve, even if the condition $n \gg k$ is not satisfied. However, we have

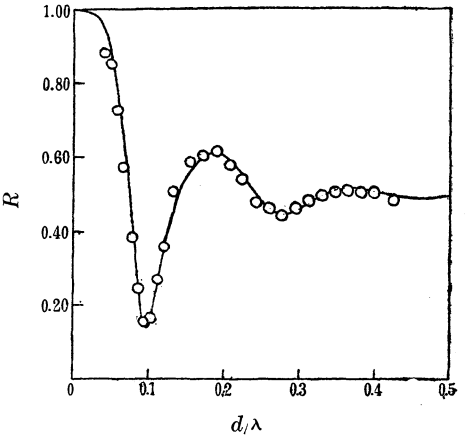



Fig. 4. The square root of the reflection coefficient of the methyl Alcohol layer of the thickness $d/\lambda$ measured at 9°C and the calculated curve corresponding to $n=2.72$ and $k=0.78$.

15) Cf. T. Tamura, *Reports of the Radiation Chemistry Research Institute* (Tokyo Univ; in Japanese), **5**, 49 (1950).

prepared many calculated curves for values of $n$ between 7.00 and 1.50 and of $k$ between 2.00 and 0.10, and we compared the experimental curve with the calculated ones. Two examples of the calculated curves are shown in Figs. 4 and 5.

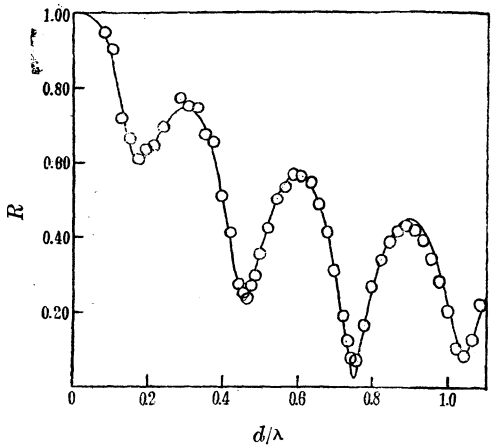



Fig. 5. The square root of the reflection coefficient of the *tert*-Butyl alcohol layer of the thickness $d/\lambda$ measured at 26°C and the calculated curve corresponding to $n=1.685$ and $k=0.135$.

But the number of such calculated curves are not sufficient to determine the values of $n$ and $k$ accurately. We can choose the two nearest curves among the calculated ones. Now we choose a more suitable set of values of $n$ and $k$, taking into account that the interval of $d/\lambda$ corresponding to the two neighboring minimum points depends mainly upon the value of $n$ and that the maximum and minimum values of $R$ depend mainly on the value of $k$. By means of the interpolation method, we can determine more accurately the values of $n$ and $k$ respectively. Then we draw a curve with this set of $n$ and $k$, and compare it once more with the experimental curve. If the experimental curve shows a deviation from the calculated one, we repeat the above-mentioned procedure once more. Thus we can determine a more and more suitable set of $n$ and $k$, and therefore $\varepsilon'$ and $\varepsilon''$. In this experiment, we measured in many cases the standing-wave ratio until the thickness of the liquid layer became greater than the wavelength used. Therefore we could measure several maximum and minimum positions of $R$, as seen from Fig. 5.

Evaporation gives rise to an error in determining the thickness of liquid. To remove this effect, first we increase the volume of the liquid concerned in order to know the behaviour of the square root of the reflection coefficient, and then decreasing the thickness, we measure the standing-wave ratio very rapidly and accurately.

In a case when liquid shows the medium absorption in this microwave region as *tert*-butyl alcohol does, it is fairly easy to determine the maximum and minimum points of the square root of the reflection coefficient. Taking into account that the feature of the curve $R$ *versus* $d/\lambda$ depends markedly on a given set of $n$ and $k$, we can compare the experimental curve with the calculated ones and determine accurately the set of $n$ and $k$. The errors in determining the values

TABLE I

THE SQUARE ROOT OF THE REFLECTION COEFFICIENT $R_e$ OF THE ETHYL ALCOHOL LAYER OF THE THICKNESS $d/\lambda$ MEASURED AT 9°C AND THE CALCULATED ONE $R_c$ CORRESPONDING TO $n=2.09$ AND $k=0.34$.

| $d/\lambda$ | $R_e$ | $R_c$ | $d/\lambda$ | $R_e$ | $R_c$ |
|---|---|---|---|---|---|
| 0.088 | 0.773 | 0.722 | 0.288 | 0.536 | 0.557 |
| 0.099 | 0.623 | 0.583 | 0.310 | 0.433 | 0.451 |
| 0.110 | 0.448 | 0.429 | 0.332 | 0.307 | 0.311 |
| 0.122 | 0.324 | 0.296 | 0.343 | 0.206 | 0.241 |
| 0.133 | 0.246 | 0.257 | 0.354 | 0.159 | 0.188 |
| 0.144 | 0.287 | 0.299 | 0.365 | 0.164 | 0.170 |
| 0.155 | 0.366 | 0.372 | 0.377 | 0.179 | 0.195 |
| 0.177 | 0.506 | 0.499 | 0.388 | 0.232 | 0.241 |
| 0.199 | 0.594 | 0.582 | 0.399 | 0.285 | 0.290 |
| 0.221 | 0.634 | 0.627 | 0.421 | 0.375 | 0.377 |
| 0.243 | 0.635 | 0.640 | 0.443 | 0.429 | 0.435 |
| 0.266 | 0.617 | 0.618 | 0.465 | 0.473 | 0.466 |

TABLE II

THE SQUARE ROOT OF THE REFLECTION COEFFICIENT $R_e$ OF THE $n$ BUTYL ALCOHOL LAYER OF THE THICKNESS $d/\lambda$ MEASURED AT 18°C AND THE CALCULATED ONE $R_c$ CORRESPONDING TO $n=1.72$ AND $k=0.165$

| $d/\lambda$ | $R_e$ | $R_c$ | $d/\lambda$ | $R_e$ | $R_c$ |
|---|---|---|---|---|---|
| 0.077 | 0.932 | 0.943 | 0.612 | 0.514 | 0.508 |
| 0.099 | 0.862 | 0.863 | 0.634 | 0.468 | 0.467 |
| 0.121 | 0.735 | 0.738 | 0.656 | 0.402 | 0.401 |
| 0.143 | 0.610 | 0.604 | 0.678 | 0.311 | 0.308 |
| 0.155 | 0.554 | 0.554 | 0.690 | 0.252 | 0.250 |
| 0.166 | 0.550 | 0.536 | 0.701 | 0.195 | 0.192 |
| 0.188 | 0.582 | 0.555 | 0.712 | 0.136 | 0.134 |
| 0.210 | 0.621 | 0.605 | 0.723 | 0.091 | 0.082 |
| 0.233 | 0.648 | 0.654 | 0.734 | 0.057 | 0.056 |
| 0.255 | 0.693 | 0.689 | 0.745 | 0.078 | 0.084 |
| 0.277 | 0.735 | 0.708 | 0.756 | 0.122 | 0.132 |
| 0.299 | 0.736 | 0.711 | 0.768 | 0.170 | 0.185 |
| 0.322 | 0.721 | 0.695 | 0.779 | 0.218 | 0.228 |
| 0.344 | 0.667 | 0.650 | 0.790 | 0.264 | 0.271 |
| 0.366 | 0.594 | 0.578 | 0.812 | 0.330 | 0.337 |
| 0.389 | 0.464 | 0.460 | 0.834 | 0.374 | 0.383 |
| 0.411 | 0.328 | 0.316 | 0.857 | 0.403 | 0.409 |
| 0.422 | 0.248 | 0.240 | 0.879 | 0.419 | 0.415 |
| 0.433 | 0.179 | 0.176 | 0.901 | 0.409 | 0.403 |
| 0.444 | 0.157 | 0.142 | 0.924 | 0.382 | 0.371 |
| 0.456 | 0.162 | 0.159 | 0.946 | 0.334 | 0.324 |
| 0.467 | 0.220 | 0.208 | 0.968 | 0.274 | 0.265 |
| 0.478 | 0.267 | 0.263 | 0.990 | 0.220 | 0.205 |
| 0.500 | 0.369 | 0.364 | 1.013 | 0.166 | 0.161 |
| 0.522 | 0.450 | 0.435 | 1.035 | 0.168 | 0.167 |
| 0.545 | 0.499 | 0.493 | 1.057 | 0.199 | 0.201 |
| 0.567 | 0.523 | 0.520 | 1.080 | 0.257 | 0.252 |
| 0.589 | 0.533 | 0.525 | | | |

of $n$ and $k$ by comparison are 0.2 percent for $n$ and 2.0 percent for $k$. On the other hand, in a case when the liquid shows high absorption in this microwave region, as methyl alcohol does, the maximum and minimum points except for the first minimum point cannot be accurately recognized from the experimental curve and the large part of the curve is in the high reflection region as easily seen from Fig. 4. Further we must take into account that the standing-wave ratio measurement has the disadvantage of being unable to show the high reflection coefficient accurately. In this case the accuracy of determining the value of $n$ is one percent.

Taking into account the errors due to the determination of the liquid thickness and of the wavelength, the accuracy in $n$ is 0.8 percent for $n$-butyl- and isobutyl-alcohol. For methyl alcohol, ethyl alcohol and *tert*-butyl alcohol, showing the high vapour pressure, the accuracies may be 2.5, 1.6, and 1.6 percent, respectively.

The measured square roots of the reflection coefficients for various thicknesses of the liquid layer are plotted in Figs. 4 and 5 for methyl alcohol and *tert*-butyl alcohol, respectively. For ethyl, $n$-butyl and isobutyl alcohol, the experimental square roots of the reflection coefficients are listed in Table I, II, and III, together with the calculated ones for the experimentally determind values of $n$ and $k$.

TABLE III

THE SQUARE ROOT OF THE REFLECTION COEFFICIENT $R_e$ OF THE *iso*-BUTYL ALCOHOL LAYER OF THE THICKNESS $d/\lambda$ MEASURED AT 23°C AND THE CALCULATED ONE $R_c$ CORRESPONDING TO $n=1.70$ AND $k=0.160$.

| $d/\lambda$ | $R_e$ | $R_c$ | $d/\lambda$ | $R_e$ | $R_c$ |
|---|---|---|---|---|---|
| 0.072 | 0.930 | 0.959 | 0.585 | 0.524 | 0.527 |
| 0.095 | 0.880 | 0.889 | 0.608 | 0.515 | 0.522 |
| 0.117 | 0.797 | 0.776 | 0.630 | 0.494 | 0.493 |
| 0.139 | 0.613 | 0.641 | 0.652 | 0.438 | 0.440 |
| 0.162 | 0.570 | 0.552 | 0.675 | 0.351 | 0.357 |
| 0.173 | 0.550 | 0.543 | 0.697 | 0.256 | 0.256 |
| 0.184 | 0.554 | 0.551 | 0.719 | 0.144 | 0.139 |
| 0.195 | 0.585 | 0.570 | 0.730 | 0.093 | 0.083 |
| 0.217 | 0.635 | 0.619 | 0.741 | 0.064 | 0.045 |
| 0.240 | 0.685 | 0.665 | 0.753 | 0.074 | 0.072 |
| 0.262 | 0.696 | 0.692 | 0.764 | 0.123 | 0.122 |
| 0.284 | 0.686 | 0.711 | 0.775 | 0.167 | 0.173 |
| 0.307 | 0.705 | 0.711 | 0.797 | 0.245 | 0.261 |
| 0.329 | 0.678 | 0.691 | 0.820 | 0.308 | 0.333 |
| 0.351 | 0.631 | 0.647 | 0.842 | 0.357 | 0.380 |
| 0.373 | 0.543 | 0.570 | 0.864 | 0.389 | 0.407 |
| 0.396 | 0.451 | 0.451 | 0.886 | 0.404 | 0.416 |
| 0.418 | 0.310 | 0.309 | 0.909 | 0.408 | 0.406 |
| 0.429 | 0.233 | 0.238 | 0.931 | 0.359 | 0.380 |
| 0.440 | 0.181 | 0.180 | 0.953 | 0.340 | 0.333 |
| 0.452 | 0.148 | 0.154 | 0.976 | 0.248 | 0.272 |
| 0.463 | 0.176 | 0.175 | 0.998 | 0.188 | 0.209 |
| 0.474 | 0.209 | 0.221 | 1.020 | 0.147 | 0.158 |
| 0.496 | 0.317 | 0.330 | 1.043 | 0.145 | 0.150 |
| 0.518 | 0.405 | 0.410 | 1.065 | 0.185 | 0.185 |
| 0.541 | 0.462 | 0.474 | 1.087 | 0.220 | 0.234 |
| 0.563 | 0.501 | 0.511 | 1.110 | 0.277 | 0.283 |

The dielectric constant and the related quantities of some aliphatic alcohols are shown in Table IV.

TABLE IV

DIELECTRIC PROPERTIES OF SOME ALIPHATIC ALCOHOLS

| Substance | Temp. | $n$ | $k$ | $\varepsilon'$ | $\varepsilon''$ |
|---|---|---|---|---|---|
| Methyl alcohol | 9°C | 2.72 | 0.78 | 6.79 | 4.24 |
| Ethyl alcohol | 8°C | 2.09 | 0.34 | 4.25 | 1.42 |
| $n$-Butyl alcohol | 18°C | 1.72 | 0.165 | 2.93 | 0.57 |
| *iso*-Butyl alcohol | 23°C | 1.70 | 0.160 | 2.86 | 0.54 |
| *tert*-Butyl alcohol | 26°C | $1.68_5$ | 0.135 | 2.82 | 0.45 |

## Conclusions

The dielectric constant and the loss factor of some aliphatic alcohols were measured by means of the free wave method developed by M. Yasumi. For liquids showing high boiling points, such as n-butyl and isobutyl alcohol, the accuracies of $n$ and $k$ are 0.8 and 2.0 percent, respectively. We should like to improve further the apparatus in the following points.

1) The accuracy in determining the thickness of the liquid layer must be increased.

2) Because we place the liquid layer on mercury in the free space, we can control the temperature within a limited range. But in order to study the dielectric properties of liquids, we must extend the temperature range. Also if the accuracy of measurement is further increased, the slight fall of temperature due to evaporation is a source of error. In the case of hygroscopic liquids, this effect may give rise to serious error.

3) It is necessary to make the radiation pattern more like the plane wave. By doing so, the error in fitting the experimental curve in the calculated curves will be decreased.

According to the plan described above, we are now improving the apparatus in order to increase the accuracy of measurement. We will postpone the detailed discussion of experimental results till later.

In conclusion, thanks are especially due to Dr. Masasi Yasumi for his guidance and to Prof. San-ichiro Mizushima for his kind advice and encouragement. The author also wishes to thank Mr. Yoshio Tsubahara who assisted him in constructing the electronic part of this apparatus, and to Mr. Tsurahide Cho and Mr. Takaaki Tamura who prepared the samples used in these experiments. The present work has been supported partly by the Scientific Research Grant from the Ministry of Educations.

*The Institute of Science and Technology,*
*Tokyo University,*
*Tokyo*

# *Reaction Rate of Water-Gas Shift Reaction*[1]

By Shinjiro KODAMA, Akira MAZUME, Kōsō FUKUBA and Kenichi FUKUI

(Received February 2, 1955)

The rate equation plays the most fundamental role in the industrial application of gas phase catalytic processes. It gives us the information which is necessary for the design of the catalytic reactor as well as for the operation of the plant. For example, the optimum temperature distribution in a catalyst layer can be calculated for a given inlet gas composition and a given space velocity when the rate constants and the equilibrium constants of the reaction are known at every temperature[2]. Other sorts of useful knowledge, such as the temperature distribution in an adiabatic type reactor[3] and in a self-heat-exchanger-type reactor[4] and the optimum space velocity which gives the maximum space time yield in an adiabatic reactor[5], may also be predicted from the rate equation.

Water-gas shift reaction is one of the most important methods for producing hydrogen on an industrial scale. Therefore, the kinetical study of the water-gas shift reaction is very significant.

Padovani and Lotteri[6] and also Laupichler[7] presented the following as a rate equation:

$$-\frac{dP_{CO}}{dt}=k_1\{P_{CO}P_{H_2O}-K_pP_{CO_2}P_{H_2}\} \quad (1)$$

In the process of an industrial-scale production of hydrogen, in which a large excess of water vapor is added to dry gas, the change in concentration of water vapor can be neglected during the course of reaction. Based on this fact, Laupichler derived the following equation as an approximation for Eq. (1).

$$-\frac{dP_{CO}}{dt}=k_1\{P_{CO}-P_{CO}^{\infty}\} \quad (2)$$

Kal'kova and Temkin[8] gave a different equation

$$-\frac{dP_{CO}}{dt}=k_1\left\{P_{CO}\left(\frac{P_{H_2O}}{P_{H_2}}\right)^{\beta}-K_pP_{CO_2}\left(\frac{P_{H_2}}{P_{H_2O}}\right)^{1-\beta}\right\} \quad (3)$$

where $\beta=0.45\sim0.55$.

This equation reproduces, according to the authors, the results of their experiments, which were made at relatively short contact times.

Reaction rates over a coprecipitated $Fe_2O_3-Cr_2O_3$ catalyst were followed in our laboratory[9] at also relatively short contact times and expressed by an equation different from Eq. (3), i.e.,

$$-\frac{dP_{CO}}{dt}=k_1\frac{P_{CO}P_{H_2O}-K_pP_{CO_2}P_{H_2}}{P_{CO_2}+KP_{H_2O}} \quad (4)$$

All of the above mentioned studies[5,7,8,9] are unsatisfactory for industrial purposes in the following points. First, in all of the experiments stated above the inlet gas compositions were limited in very narrow ranges. And, in the studies of Kal'kova and Temkin[8] and in our laboratory[9], the contact times were far shorter than those used in industrial reactors. Moreover, the experimental verifications of these equations have been tried for only a very limited range of initial gas composition and space velocity.

The kinetics of reverse shift reaction is also one of the most interesting problems not only from an academic viewpoint, but also because of its industrial importance. As the reverse shift reaction occurs during the gasification of coal in industry, kinetical studies at high temperatures have been made by many investigators. On the other hand at relatively low temperatures reaction proceeds so slowly that very little has been known concerning the rate of reaction. Recently Barkley, Corrigan, Wainwright and Sands[10] followed the reaction rate by passing 1:4 to 4:1 mixtures of $CO_2$ and $H_2$ at 1000°F over

1) Part of this paper was presented at the 7th Annual Meeting of the Chemical Society of Japan, April 2, 1954.

2) S. Kodama, K. Fukui, H. Tanaka and A. Mazume, *Chem. Eng.* (Japan), **15**, 85 (1951); P. H. Calderbank, *Chem. Eng. Progress*, **49**, 585 (1953); D. Annable, *Chem. Eng. Sci.*, **1**, 145 (1952).

3) S. Kodama and K. Fukui, *Chem. Eng.* (Japan), **15**, 145 (1951).

4) S. Kodama, K. Fukui and H. Tanaka, *J. Chem. Soc. Japan (Ind. Chem. Sec.)*, **54**, 303 (1951); C. van Heerden, *Ind. Eng. Chem.*, **45**, 1242 (1953).

5) S. Kodama, K. Fukui and A. Mazume, *Ind. Eng. Chem.*, **45**, 1644 (1953).

6) C. Padovani and A. Lotteri, *J. Soc. Chem. Ind.*, **56**, 391T (1937).

7) F.G. Laupichler *Ind. Eng. Chem.*, **30**, 578 (1938).

8) N. B. Kal'kova and M. I. Temkin, *Zhur. Fiz. Khim.*, **23**, 695 (1949); *Chem. Abstr.*, **43**, 7308 (1949).

9) S. Kodama, K. Fukui, T. Tame and M. Kinoshita, *Catalyst* (Japan), **8**, 50 (1952).

10) L. W. Barkley, T. E. Corrigan, H. W. Wainwright and A. E. Sands, *Ind. Eng. Chem.*, **44**, 1066 (1952).

$Fe_2O_3$—CuO catalyst at different flow rates and derived the following rate equation,

$$\frac{dP_{CO}}{dt}=k_2\frac{P_{CO_2}P_{H_2}-\frac{1}{K_p}P_{CO}P_{H_2O}}{1+K'P_{CO}+K''P_{CO_2}} \quad (5)$$

But they did not make sure if this equation holds also in the water-gas shift reaction.

Under the circumstances mentioned above, it may be significant to obtain a rate equation of water-gas shift reaction which would be at least both accurate and practically useful for designing reactors. At the same time, it is of interest to ascertain that the rate expression obtained for the water-gas shift reaction would also be fit for the reverse shift reaction with the opposite sign, as it should be theoretically. Both the reactions were kinetically studied over a wide range of space velocity and inlet gas composition.

## Experimental

Experiments were made by flow method at atmospheric pressure. Schematic flow diagrams of the apparatuses for the forward and the reverse reaction are shown in Figs. 1 and 2, respectively.

Carbon dioxide and hydrogen were taken from cylinders. Carbon monoxide was generated by dehydration of formic acid. These gases were purified by the usual methods.

The industrial catalyst used was of the composition shown below:

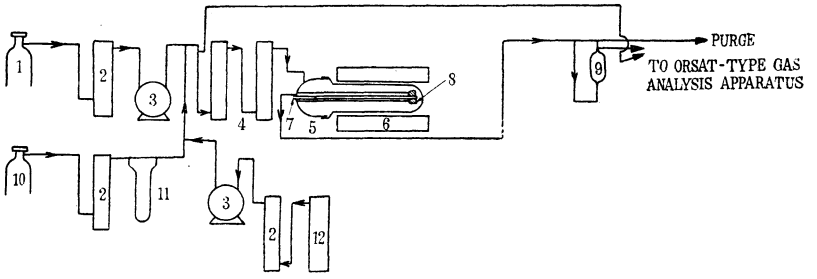
| | | | |
|---|---|---|---|
| $Fe_2O_3$ | 72.25 (wt. %) | MgO | 4.69 (wt. %) |
| $Al_2O_3$ | 12.55 ( „ ) | $K_2O$ | 1.53 ( „ ) |
| $Cr_2O_3$ | 7.46 ( „ ) | | |

The particle size of the catalyst was ranging in diameter from 10 to 20 Tyler mesh.

Flow rates of carbon monoxide and hydrogen were measured by a wet-type gas meter and that of carbon dioxide by an orifice-type flowmeter.

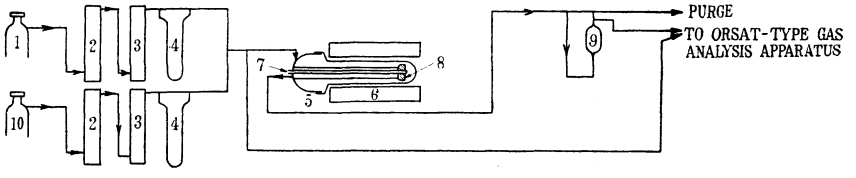
For water-gas shift reaction, inlet gas composition was determined from the analysis of dry gas and the saturation temperature with steam. For reverse shift reaction, inlet gas composition was calculated from the flow rates of carbon dioxide and hydrogen.

In the case of water-gas shift reaction dry gas was saturated with steam in a two-stage packed column kept at constant temperature. In order to prevent unsaturation, flow rates of dry gas were carefully kept at constant. The comple-




1. CYLINDER HYDROGEN
2. PURIFICATION TRAIN
3. WET-TYPE GAS METER
4. WATER SATURATOR (TWO-STAGE PACKED COLUMN)
5. SELF-HEAT-EXCHANGER-TYPE PYREX REACTOR
6. ELECTRIC FURNACE
7. THERMOCOUPLE WELL
8. CATALYST PACKED LAYER
9. GAS BURETTE
10. CYLINDER CARBON DIOXIDE
11. ORIFICE-TYPE FLOWMETER
12. CARBON MONOXIDE GENERATING APPARATUS

Fig. 1. Schematic flow diagram of the apparatus used for forward Reaction.




1. CYLINDER HYDROGEN
2. PURIFICATION TRAIN
3. DEHYDRATING TOWER
4. ORIFICE-TYPE FLOWMETER
5. SELF-HEAT-EXCHANGER-TYPE PYREX REACTOR
6. ELECTRIC FURNACE
7. THERMOCOUPLE WELL
8. CATALYST PACKED LAYER
9. GAS BURETTE
10. CYLINDER CARBON DIOXIDE

Fig. 2. Schematic flow diagram of the apparatus used for the reverse reaction.

teness of saturation was confirmed by preliminary experiments at each temperature.

In order to avoid the non-uniformity in the temperature distribution of the catalyst layer, a two-path-counter-current-type pyrex reactor[11] was used. Several reactors of different diameters were used for the experiments of different catalyst volumes, so that the packed length did not exceed 25 mm. and practically uniform temperature distribution was secured. The temperature of the catalyst layer was measured with a calibrated chromel-alumel thermocouple which was inserted in the bed.

Samples of both inlet and exit gas were analyzed with an Orsat-type gas analyzer. Most of the samples were analyzed for carbon dioxide, carbon monoxide and hydrogen.

## Experimental Results

In Figs. 3, 4, 5, 6, 7, and 8 are shown the results for the water-gas shift reaction, plotted as the fractional conversions of carbon monoxide ($Z$) against contact times ($t$) for each investigated temperature and inlet gas composition. Fig. 9 shows the results of the reverse shift reaction by the plot of the

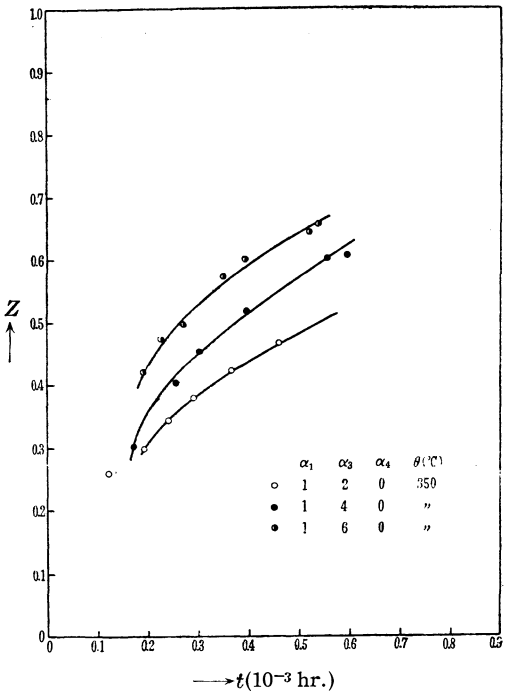



Fig. 4. Fractional conversion of carbon monoxide ($Z$) vs. contact time ($t$).

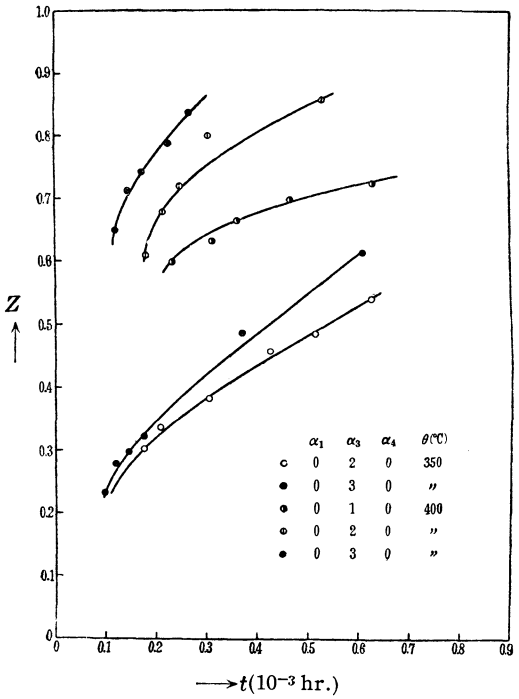



Fig. 3. Fractional conversion of carbon monoxide ($Z$) vs. contact time ($t$).

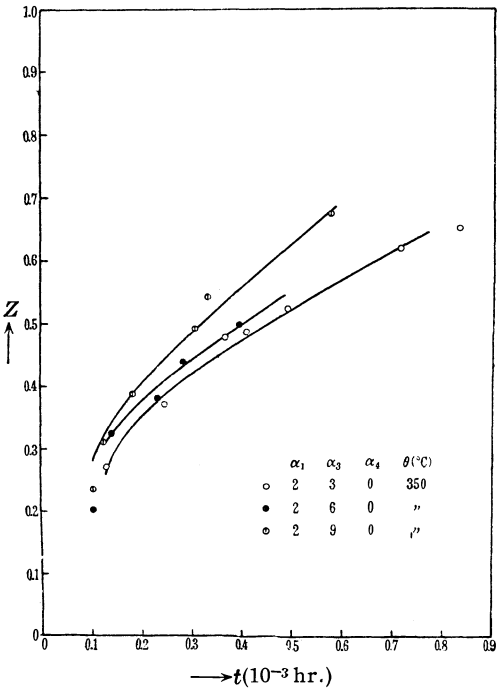



Fig. 5. Fractional conversion of carbon monoxide ($Z$) vs. contact time ($t$).

11) A. F. Farkas and H. W. Melville, "Experimental methods in gas reactions," Mac Millan and Co. Ltd., London, (1939) p. 305.

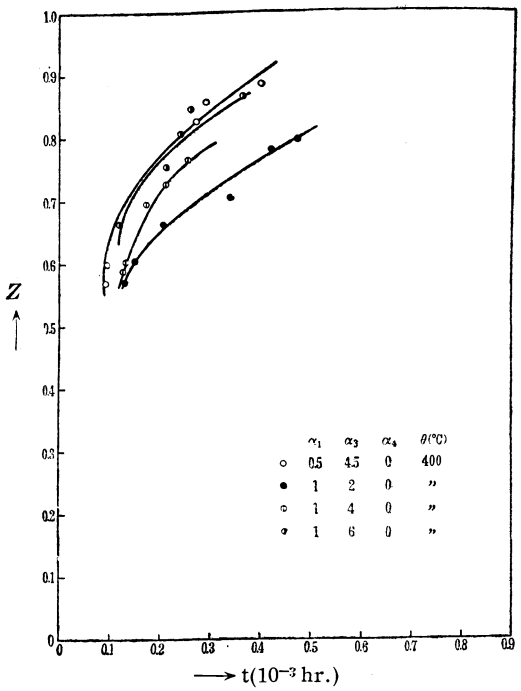



Fig. 6. Fractional conversion of carbon monoxide ($Z$) vs. contact time ($t$).

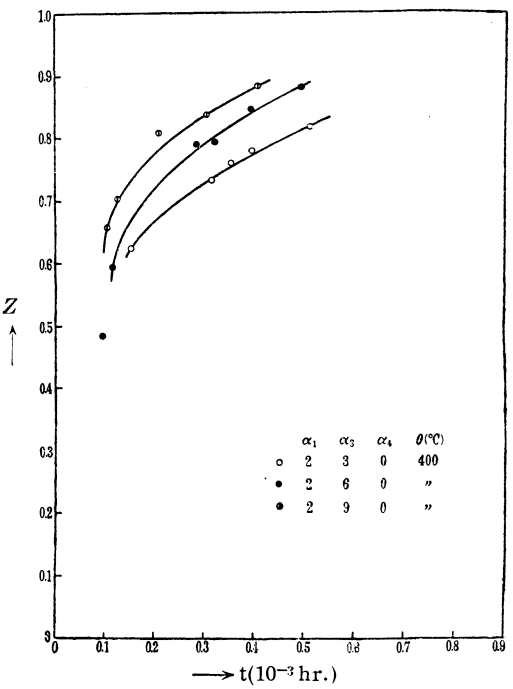



Fig. 7. Fractional conversion of carbon monoxide ($Z$) vs. contact time (t).

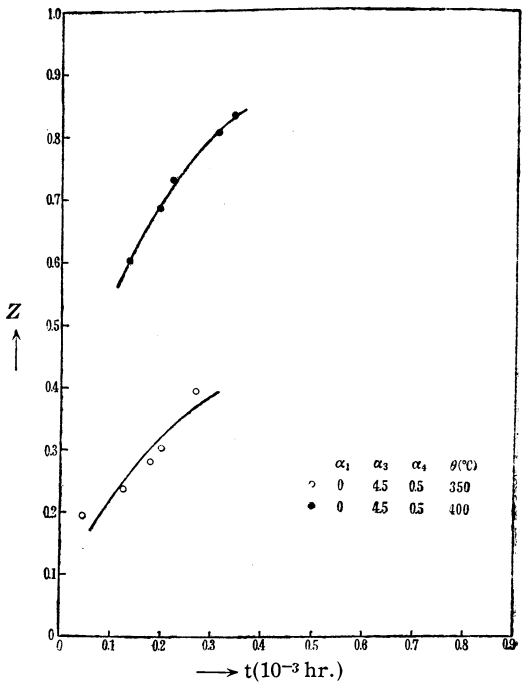



Fig. 8. Fractional conversion of carbon monoxide ($Z$) vs. contact time ($t$).

fractional conversions of carbon dioxide ($Z'$) vs. contact times ($t$). The values of $Z$ and $Z'$ were calculated from the carbon dioxide content in the exit gas and the inlet gas composition, neglecting the side reaction, and $t$ was calculated by the follwing equation.

$$t=\frac{\text{packed volume of catalyst (c.c.)}}{\text{total flow rate at each reaction temperature (c.c./hr.)}}$$

**a) Water-Gas Shift Reaction.**—In order to find the rate equation for the water-gas shift reaction which can reproduce the present results, many equations were put to the test, among which the following was proved to be most satisfactory.

$$-\frac{dP_{CO}}{dt}=k_1\frac{P_{CO}P_{H_2O}-K_pP_{CO_2}P_{H_2}}{1+KP_{CO}+K'P_{H_2O}+K''P_{H_2}+K'''P_{CO_2}} \quad (6)$$

The partial pressure of the component $i$, $P_i$ can be written in terms of fractional conversion and inlet gas composition, as

$$P_i=\frac{\alpha_i-\nu_iZ}{\sum_r\alpha_r}$$

where

$$\alpha_i=\frac{P^\circ_i}{P^\circ_{CO}} \quad (7)$$

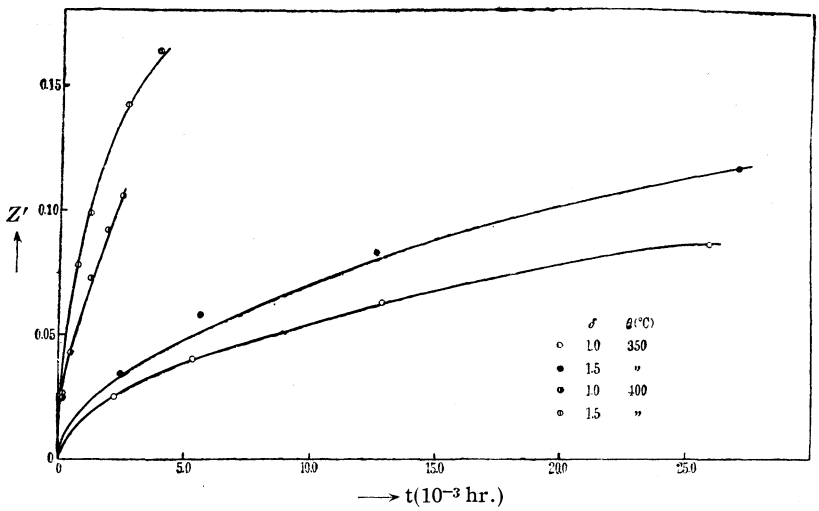



Fig. 9. Fractional conversion of carbon dioxide ($Z'$) vs. contact time ($t$).

and $\nu_i$ represents the stoichiometric ratio of the component $i$ in the forward reaction[8], i.e.,

$$\nu_{CO}=\nu_{H_2O}=1,\quad \nu_{CO_2}=\nu_{H_2}=-1$$

Using Eq. (7) the rate expression is represented as a function of $Z$ and $t$. On integrating Eq. (6), the relation of $Z$ and $t$ is derived as follows:

$$P\frac{k_1 t}{2.303}=\frac{1}{\beta-\gamma}\Big[\{1+KP+\alpha_3(1+K'P)+\alpha_1(1+K''P)+\alpha_4(1+K'''P)+(K'''+K''-K'-K)P\beta\}\times\log\frac{\beta-Z}{\beta}-\{1+KP+\alpha_3(1+K'P)+\alpha_1(1+K''P)+\alpha_4(1+K'''P)+(K'''+K''-K'-K)P\gamma\}\times\log\frac{\gamma-Z}{\gamma}\Big] \quad (8)$$

where $\beta$ and $\gamma$ are the positive and negative roots of the following equation, respectively.

$$(1-K_p)Z^2-\{K_p(\alpha_1+\alpha_4)+(\alpha_3+1)\}Z+(\alpha_3-K_p\alpha_1\alpha_4)=0 \quad (9)$$

Table I shows the values of $k_1$ calculated

TABLE I

VALUES FOR $k_1$ (atm.$^{-1}$ hr.$^{-1}$ Unit)

(I) $\theta=350$, $K=0.3$ (atm.$^{-1}$), $K'=1.5$ (atm.$^{-1}$), $K''=4$ (atm.$^{-1}$), $K'''=20$ (atm.$^{-1}$)

| $\alpha_1=0$, $\alpha_3=2$, $\alpha_4=0$ | | $\alpha_1=0$, $\alpha_3=3$, $\alpha_4=0$ | |
|---|---|---|---|
| $t$(10$^{-3}$ hr.) | $k_1$(10$^4$) | $t$(10$^{-3}$ hr.) | $k_1$(10$^4$) |
| 0.176 | 1.048 | 0.0982 | 1.016 |
| 0.207 | 0.890 | 0.113 | 1.039 |
| 0.308 | 0.970 | 0.144 | 1.036 |
| 0.424 | 0.949 | 0.175 | 1.022 |
| 0.515 | 0.881 | 0.373 | 0.936 |
| 0.626 | 0.972 | 0.611 | 0.974 |

| $\alpha_1=1$, $\alpha_3=2$, $\alpha_4=0$ | | $\alpha_1=1$, $\alpha_3=4$, $\alpha_4=0$ | |
|---|---|---|---|
| $t$(10$^{-3}$ hr.) | $k_1$(10$^4$) | $t$(10$^{-3}$ hr.) | $k_1$(10$^4$) |
| 0.145 | 1.745 | 0.171 | 1.050 |
| 0.191 | 1.679 | 0.258 | 1.078 |
| 0.239 | 1.673 | 0.300 | 1.135 |
| 0.289 | 1.441 | 0.395 | 1.091 |
| 0.365 | 1.649 | 0.555 | 1.070 |
| 0.457 | 1.516 | 0.595 | 0.977 |
| $\alpha_1=1$, $\alpha_3=6$, $\alpha_4=0$ | | $\alpha_1=2$, $\alpha_3=3$, $\alpha_4=0$ | |
| $t$(10$^{-3}$ hr.) | $k_1$(10$^4$) | $t$(10$^{-3}$ hr.) | $k_1$(10$^4$) |
| 0.189 | 1.191 | 0.130 | 0.972 |
| 0.226 | 1.186 | 0.246 | 1.391 |
| 0.269 | 1.062 | 0.364 | 1.530 |
| 0.348 | 1.062 | 0.407 | 1.404 |
| 0.389 | 1.011 | 0.491 | 1.366 |
| 0.520 | 0.909 | 0.713 | 1.355 |
| 0.537 | 0.914 | 0.831 | 1.294 |
| $\alpha_1=2$, $\alpha_3=6$, $\alpha_4=0$ | | $\alpha_1=2$, $\alpha_3=9$, $\alpha_4=0$ | |
| $t$(10$^{-3}$ hr.) | $k_1$(10$^4$) | $t$(10$^{-3}$ hr.) | $k_1$(10$^4$) |
| 0.105 | 0.920 | 0.106 | 1.025 |
| 0.140 | 1.224 | 0.151 | 1.049 |
| 0.228 | 0.959 | 0.183 | 1.159 |
| 0.282 | 0.909 | 0.308 | 0.996 |
| 0.392 | 0.864 | 0.331 | 1.080 |
| | | 0.574 | 0.985 |

| $\alpha_1=0$, $\alpha_3=4.5$, $\alpha_4=0.5$ | |
|---|---|
| $t$(10$^{-3}$ hr.) | $k_1$(10$^4$) |
| 0.044 | 1.149 |
| 0.126 | 1.220 |
| 0.178 | 1.079 |
| 0.200 | 1.065 |
| 0.268 | 1.168 |

(II) $\theta=400$, $K=0.1$ (atm.$^{-1}$), $K'=0.5$ (atm.$^{-1}$), $K''=2$ (atm.$^{-1}$), $K'''=10$ (atm.$^{-1}$)

| $\alpha_1=0$, $\alpha_3=1$, $\alpha_4=0$ | | $\alpha_1=0$, $\alpha_3=2$, $\alpha_4=0$ | |
|---|---|---|---|
| $t$(10$^{-3}$ hr.) | $k_1$(10$^4$) | $t$(10$^{-3}$ hr.) | $k_1$(10$^4$) |
| 0.233 | 4.450 | 0.181 | 4.132 |
| 0.311 | 4.258 | 0.215 | 4.187 |
| 0.360 | 4.453 | 0.249 | 3.713 |
| 0.466 | 4.442 | 0.305 | 4.432 |
| 0.630 | 3.635 | 0.527 | 3.358 |

| $\alpha_1=0$, $\alpha_3=3$, $\alpha_4=0$ | | $\alpha_1=0.5$, $\alpha_2=4.5$, $\alpha_4=0$ | |
|---|---|---|---|
| $t(10^{-3}$ hr.) | $k_1(10^4)$ | $t(10^{-3}$ hr.) | $k_1(10^4)$ |
| 0.120 | 3.162 | 0.0884 | 2.802 |
| 0.145 | 3.276 | 0.0921 | 2.932 |
| 0.172 | 3.126 | 0.272 | 2.471 |
| 0.224 | 3.002 | 0.290 | 2.551 |
| 0.313 | 2.788 | 0.400 | 2.217 |
| $\alpha_1=1$, $\alpha_3=2$, $\alpha_4=0$ | | $\alpha_1=1$, $\alpha_3=4$, $\alpha_4=0$ | |
| $t(10^{-3}$ hr.) | $k_1(10^4)$ | $t(10^{-3}$ hr.) | $k_1(10^4)$ |
| 0.130 | 4.000 | 0.125 | 2.552 |
| 0.149 | 4.215 | 0.131 | 2.578 |
| 0.205 | 4.028 | 0.173 | 2.583 |
| 0.342 | 2.907 | 0.209 | 2.590 |
| 0.414 | 3.622 | 0.255 | 2.358 |
| 0.470 | 4.132 | | |
| $\alpha_1=1$, $\alpha_3=6$, $\alpha_4=0$ | | $\alpha_1=2$, $\alpha_3=3$, $\alpha_4=0$ | |
| $t(10^{-3}$ hr.) | $k_1(10^4)$ | $t(10^{-3}$ hr.) | $k_1(10^4)$ |
| 0.117 | 2.702 | 0.150 | 2.780 |
| 0.216 | 1.966 | 0.315 | 3.045 |
| 0.239 | 2.342 | 0.353 | 3.080 |
| 0.259 | 2.553 | 0.394 | 3.062 |
| 0.368 | 2.000 | 0.510 | 2.976 |
| $\alpha_1=2$, $\alpha_3=6$, $\alpha_4=0$ | | $\alpha_1=2$, $\alpha_3=9$, $\alpha_4=0$ | |
| $t(10^{-3}$ hr.) | $k_1(10^4)$ | $t(10^{-3}$ hr.) | $k_1(10^4)$ |
| 0.095 | 2.156 | 0.107 | 2.323 |
| 0.116 | 2.480 | 0.126 | 2.758 |
| 0.284 | 1.970 | 0.211 | 2.614 |
| 0.319 | 1.924 | 0.304 | 1.860 |
| 0.392 | 1.970 | 0.407 | 1.740 |
| 0.496 | 2.047 | | |

| $\alpha_1=0$, $\alpha_3=4.5$, $\alpha_4=0.5$ | |
|---|---|
| $t(10^{-3}$ hr.) | $k_1(10^4)$ |
| 0.135 | 2.618 |
| 0.195 | 2.379 |
| 0.220 | 2.456 |
| 0.313 | 2.412 |
| 0.344 | 2.468 |

by Eq. (8). The numerical values of $K_p$ used were taken from Lewis and Randall's work[12] and $K$, $K'$, $K''$, and $K'''$ were chosen so that the value of $k_1$ becomes most satisfactorily constant at a given temperature.

Experiments were also made at 450°C for a wide range of inlet gas composition and contact time. But in this case Eq. (6) failed to reproduce the experimental results.

**b) Reverse Shift Reaction.**—If Eq. (6) reproduces the results of the water-gas shift reaction, the reaction rate of the reverse shift reaction must be given as:

$$\frac{dP_{CO}}{dt}=k_2\frac{P_{CO_2}P_{H_2}-\frac{1}{K_p}P_{CO}P_{H_2O}}{1+KP_{CO}+K'P_{H_2O}+K''P_{H_2}+K'''P_{CO_2}} \quad (10)$$

12) G. N. Lewis, and M. Randall, "Thermodynamics and free energy of chemical substances," Mc Graw Hill Book Co., New York, (1923) p. 574.

As in the case of the forward reaction, also, the relation of $Z'$ and $t$ is derived for the reverse shift reaction from Eq. (10), as

$$P\frac{k_2t}{2.303}=\frac{1}{-\beta'+\gamma'}\Big\{[1+K'''P+\delta(1+K''P)+(K+K'-K''-K''')\beta'P]\log\frac{\beta'-Z'}{\beta'}-[1+K'''P+\delta(1+K''P)+(K+K'-K''-K''')\gamma'P]\log\frac{\gamma'-Z'}{\gamma'}\Big\} \quad (11)$$

where $\delta$ represents the mole ratio of hydrogen to carbon dioxide at inlet, and $\beta'$ and $\gamma'$ are the positive and negative roots of the following equation, respectively.

$$(1-Z')(\delta-Z')-\frac{1}{K_p}Z'^2=0 \quad (12)$$

Calculated values of $k_2$ for all the experimental conditions are tabulated in Table II. The values of $K$, $K'$, $K''$, $K'''$ and $K_p$ used for computing are the same as those used in the calculation for $k_1$.

TABLE II

VALUES FOR $k_2$ (in atm.$^{-1}$ hr.$^{-1}$ Unit)

(I) $\theta=350$, $K=0.3$ (atm.$^{-1}$), $K'=1.5$ (atm.$^{-1}$) $K''=4$ (atm.$^{-1}$) $K'''=20$ (atm.$^{-1}$)

| $\delta=1.0$ | | $\delta=1.5$ | |
|---|---|---|---|
| $t(10^{-3}$ hr.) | $k_2(10^2)$ | $t(10^{-3}$ hr.) | $k_2(10^2)$ |
| 2.23 | 5.381 | 2.505 | 5.164 |
| 5.35 | 5.056 | 5.680 | 5.482 |
| 12.86 | 5.170 | 12.65 | 5.241 |
| 25.97 | 5.203 | 27.22 | 5.129 |

(II) $\theta=400$, $K=0.1$ (atm.$^{-1}$), $K'=0.5$ (atm.$^{-1}$), $K''=2$ (atm.$^{-1}$), $K'''=10$ (atm.$^{-1}$)

| $\delta=1.0$ | | $\delta=1.5$ | |
|---|---|---|---|
| $t(10^{-3}$ hr.) | $k_2(10^3)$ | $t(10^{-3}$ hr.) | $k_2(10^3)$ |
| 0.175 | 2.067 | 0.128 | 1.925 |
| 0.403 | 2.078 | 0.749 | 2.097 |
| 1.242 | 1.915 | 1.224 | 1.966 |
| 1.890 | 1.943 | 2.660 | 1.956 |
| 2.534 | 1.985 | 3.924 | 1.890 |

## Discussion

As seen from Tables I and II, the constancy of $k_1$ and $k_2$ is fairly good, which reveals the fact that the rate equations (6) as well as (10) are sufficiently accurate at least for the practical purpose.

Namely, the values of $k_1$ given in Table I are sufficiently constant over the contact time range $0.1$–$0.8\times10^{-3}$ hr. and various inlet gas compositions at 350°C. At 400°C, $k_1$ varies somewhat with $P^\circ_{CO}$. This change in $k_1$ may reasonably be attributed to the occurrence of the catalytic decomposition of carbon monoxide. However, at relatively small

$P°_{CO}$, as in the case of industrial reactors, the dependence of $k_1$ upon $P°_{CO}$ is negligibly small, so that Eq. (6) may be useful for the reactor design.

Eqs. (1), (2), and (4) may be derived through some simplifications from Eq. (6), but Kalkova and Temkin's equation may not. Eq. (6) is similar to that of Horiuchi[13], derived theoretically.

Within the range of experimental error, no systematic deviation of the rate constants $k_2$ can be found from Table II. As is seen from these data, it is evident that Eq. (10) reproduces the rate data well.

Equilibrium constants $K_p$ at 350°C and 400°C are calculated from $k_1$ and $k_2$. These values of $K_p$ are shown in Table III together

TABLE III
VALUES FOR $K_p$

| $\theta$(°c) | $K_p$ | |
|---|---|---|
| 350 | 0.041 | Neumann and Köhler[14] |
| | 0.0471 | Lewis and Randall[12] |
| | 0.0474 | Kodama, Mazume, Fukuba and Fukui |
| 400 | 0.0734 | Engels[a] |
| | 0.080 | Neumann and Köhler[14] |
| | 0.0824 | Lewis and Randall[12] |
| | 0.0796 | Kodama, Mazume, Fukuba and Fukui |

a) Engels, Dissertation, (1911) Karlsuhe (Cited in Reference 14).

with those previously presented. The values of $k_1$ at 400°C used in calculating $K_p$ are the average of $k_1$'s obtained at relatively small $P°_{CO}$. The present values of $K_p$ are in good agreement with previous publications, especially with values obtained by the direct method[14]. Eq. (6) may suggest something to us concerning the reaction mechanism, but no direct evidence for it has been given. It may rather be stressed that Eq. (6) serves as an empirical equation which is useful for industrial purposes.

## Conclusion

The conclusion is as follows:

A rate equation for the water-gas shift reaction as well as for the reverse shift reaction which can reproduce the experimental results at 350°C and 400°C for various inlet gas compositions and contact times is obtained.

The equation seems to be sufficiently accurate at least for industrial purposes.

The assistance of Mr. T. Okada and Mr. M. Okazaki are gratefully acknowledged. Also the authors are indebted to The Befu Chemical Co. Ltd., for liquefied carbon dioxide.

*Faculty of Engineering, Kyoto University, Kyoto*

13) J. Horiuti, *Catalyst* (Japan) 8, 58 (1952).

14) B. Neumann and G. Köhler, *Z. Elektrochem.*, 34, 218 (1928).

$k_1$, $k_2$, $K$, $K'$, $K''$, $K'''$=constants in the rate equation, which are function of temperature only.

$K_p$=equilibrium constant of the water-gas reaction

$$=\frac{P^{\infty}_{CO}\ P^{\infty}_{H_2O}}{P^{\infty}_{H_2}\ P^{\infty}_{CO_2}}$$

$P_i$=partial pressure of component i, atmospheres.

$P$=total pressure atmospheres.

$t$=contact time measured at reaction temperature, hours.

$Z$=fractional conversion of carbon monoxide for the forward reaction.

$Z'$=fractional conversion of carbon dioxide for the reverse reaction.

$a_i$=mole ratio of component i to carbon monoxide in feed of the forward reaction ($a_2$=1).

$\delta$=mole ratio of hydrogen to carbon dioxide in feed of the reverse reaction.

$\theta$=temperature, °C.

Subscripts 1, 2, 3 and 4 designate hydrogen, carbon monoxide, water and carbon dioxide, respectively.

Superscript $\infty$ designates equilibrium conditions.

Superscript 0 designates inlet conditions.

# *Polymorphic Phase Transition of Beryllium Oxyacetate* $Be_4O(CH_3CO_2)_6$*

By Masanobu MOMOTANI,** Syûzô SEKI, Hideaki CHIHARA and Hiroshi SUGA

(Received February, 16, 1955)

## Introduction

In 1943, by Preston and Trotter[1] as well as by Beevers[2] it was found that the symmetry of Laue photograph of the cubic modification of this crystal changes from $T_h$-m3 to $O_h$-m3m in the temperature interval of 30°~50°C. Beevers explained this phase transition as due to the change in the parameter values of the carboxyl oxygen atom from (−0.17, −0.06, −0.04) to (−0.17, −0.05, −0.05) when the temperature rises and passes the transition range, thus bringing all the oxygen atoms exactly onto (110) planes. On the other hand, in 1947, Jaffray[3] measured the specific heat of this crystal below and above the transition region and found that at 40.5±0.5°C there is an anomaly of typical λ-type in the heat capacity curve.

In 1949, Watanabé and Saito[4] observed that this crystal became waxy when it was heated above 160°C, though it melted very sharply at about 285°C. They studied the crystal structure of this high temperature modification as well as the above-mentioned phase transition at about 40°C by the X-ray method and in order to explain the results they put forward a mechanism of the order-disorder type. They also investigated the so-called γ-form of this crystal which was obtained by sublimation at ordinary pressure.

We have undertaken to study these phase transitions as a part of our thermochemical investigation on the nature of the so-called plastic crystals.

## Experimental

**a) Sample.**—Beryllium oxide was dissolved in acetic acid and by evaporating the excess acid in the evaporating dish we obtained the crude specimen. This was then recrystallized three times from chloroform and finally subjected to fractional sublimation under high vacuum ($10^{-5}$ mmHg), m.p. 286.7°C.

**b) Apparatas and Procedures.**—The apparata used for the differential thermal analysis,[5] dilatometry[6], vapor pressure measurement[7] and the conduction calorimetry[8] were all the same as those that have been used hitherto in our laboratory, so that their description may be omitted here.

## Experimental Results

**i) Differential thermal analysis.**—As mentioned above, by the observation of the change of appearance of the crystal above 160°C by Watanabé and Saito, it was strongly inferred that this crystal would undergo a phase transition around this temperature. To determine the accurate temperatures of transition and melting, we carried out the differential thermal analysis. One of the typical curves is given in Fig. 1. From

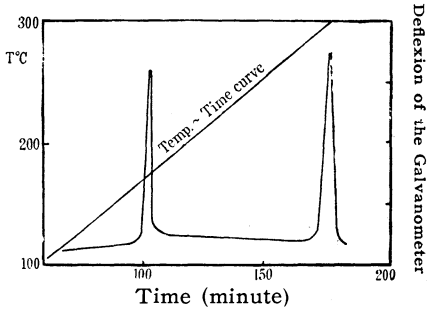



Fig. 1. Curves of differential thermal analysis of $Be_4O(CH_3CO_2)_6$.

this curve, it was found that the magnitude of the heat effects accompanying these two phase changes are comparable with each other. To examine the nature of the polymorphic phase transition further in detail, we then performed a series of thermal analyses under various conditions. All the experimental curves of the deflection of the galvanometer for measuring the temperature head are shown in Fig. 2.* We may enumerate some features of these curves as follows:

* A part of this research was already published in *Nature*, **163**, 226 (1949).

** Present address: Momotani Juntenkan Co., Ltd., Osaka.

1) G. D. Preston and T. Trotter, *Nature*, **151** 166 (1943).

2) C.A. Beevers, *Nature*, **152**, 447 (1943).

3) J. Jaffray, *Compt. rend.*, **225**, 106 (1947).

4) T. Watanabé and Y. Saito, *Nature*, **163**, 225 (1949), T. Watanabé, Y. Saito and H. Koyama, ibid., **164**, 1056 (1949).

5) H. Chihara and S. Seki, This Bulletin, **26**, 88 (1953).

6) I. Nitta, S. Seki and M. Momotani, *Proc. Japan Acad.*, **26**, (10) 11, (1950).

7) I. Nitta, S. Seki, M. Momotani and K. Sato, *J. Chem. Soc. Japan*, **71**, 378 (1950).

8) S. Seki, M. Momotani, K. Nakatsu and T. Oshima, This Bulletin, (in press).

* The figure attached at the highest temperature side of each curve means the temperature at which the heating was stopped.

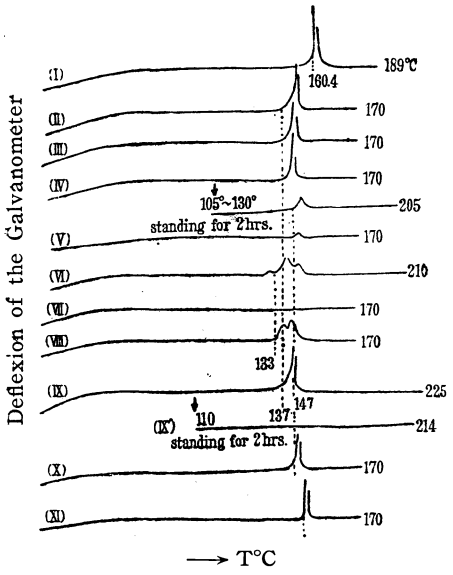



Fig. 2. Curves of differential thermal analyses of $Be_4O(CH_3CO_2)_6$ at various conditions.

(a) Curve (i) represents the result of the sample which has been stored for about half a year in a desiccator over calcium chloride. As shown in the figure this sample shows the highest transition point of 160.4°C (heating velocity is about 2~2.5°C/min.).

(b) When the sample was not heated above around 210°C, it always shows the transition point at about 140°~147°C (curves (ii), (iii), (iv)).

(c) If the sample was cooled down below 110°C, standing it at this temperature for about two hours and then heated again, it showed a small hump at about 147°C. However, if it was not cooled down below 110°C, no transition phenomenon could be observed.

(d) If the sample was heated above 210°C and then left to natural cooling down to the room temperature, there appeared no transition phenomenon in the heating curve which was measured again, even on the following day (two sets of curves (vi) and (vii), and (ix) and (ix)'). However, if the supercooled sample which showed no phase change was ground in an agate mortar at room temperature, it exhibited phase change of a rather complex nature (curves (vi) and (viii)).

(e) Freshly prepared sample by sublimation shows normal phase change at about 147°C (see Fig. 1 and curve (x)). But, when such sample was thoroughly ground to very fine powders, it showed a little higher temperature of phase change (curve (xi)).

A possible explanation of the somewhat complex characteristics of these curves may be given after the following description on the dilatometric investigation.

**ii) Dilatometric investigation.**—Since the method of differential thermal analysis was not sensitive enough to detect a phase change with small heat effect, we then measured the volume change very carefully using the freshly prepared specimen in order to find out some clues to explain the complex nature just mentioned above. As the results, we could find out that the expansion coefficient changes at four temperatures, namely, 32±0.5°C, 42±0.4°C, 77±0.4°C, and 124.5±0.5°C, and further that the volume itself increases abruptly at 148°C by a great amount which corresponds to about 5.6% of the volume at 25°C. Of these temperatures, the secound one, 42±0.4°C,

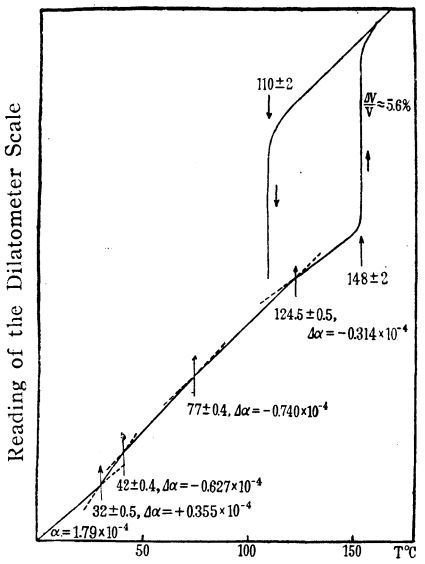



Fig. 3. Volume vs. temperature curve of $Be_4O(CH_3CO_2)_6$.

coincides with that determined by Jaffray, while the third and the fourth were discovered first by the present experiment. Moreover, it was revealed that the transition at 148°C shows a hysteresis phenomenon covering over a wide range of temperatures, the volume change in the cooling curve taking place at 110±2°C, far below the transition point observed in heating direction. Among these changes of expansion coefficient at four temperatures only the first one has the plus sign. It is to be added that after these results were published,**Jaffray[9] recently confirmed our experimental results.

**iii) Heat capacity measurement.**—As mentioned above, the transition at about 42°C seems to be of particular interest, since the crystal structures on each side of the transition temperature have been already known. Although Jaffray has measured the heat capacities at these temperatures, the temperature range was not wide enough to determine the heat of transition, so we measured anew the heat capacities extending our measurements over a much wider temperature range both in heating and cooling directions. Our

** See footnote (*) in page 325.

9) J. Jaffray, Compt. rend. de la deuxième Réunion Annuelle tenue en Commun avec la Commission de Thermodynamique de l'Union Internationale de Physique Changements de Phases. p. 267. (1952).

data are given in Table I and the heat capacity curves are shown in Fig. 4. In the figure, we can

TABLE I
HEAT CAPACITY OF $Be_4O(CH_3CO_2)_6$

| Heating direction | | Cooling direction | |
|---|---|---|---|
| $t$°C | $C_p$ cal./mole | $t$°C | $C_p$ cal./mole |
| 0.00 | 116.5 | 85.22 | 138.1 |
| 13.02 | 118.7 | 79.60 | 136.0 |
| 19.4 | 120.93 | 76.84 | 135.5 |
| 25.7 | 123.0 | 75.20 | 138.7 |
| 31.48 | 127.9 | 73.81 | 131.9 |
| 38.15 | 133.7 | 73.15 | 130.7 |
| 41.78 | 136.3 | 71.78 | 138.4 |
| 43.05 | 129.6 | 70.58 | 132.4 |
| 44.20 | 126.6 | 69.20 | 131.5 |
| 50.21 | 126.9 | 62.20 | 129.0 |
| 62.20 | 129.0 | 56.25 | 126.8 |
| 66.87 | 129.9 | 50.21 | 124.7 |
| 69.20 | 130.9 | 47.82 | 124.1 |
| 71.52 | 134.1 | 45.41 | 124.7 |
| 72.68 | 131.8 | 43.05 | 127.7 |
| 73.81 | 132.1 | 40.60 | 135.0 |
| 74.99 | 132.9 | 40.08 | 134.4 |
| 76.13 | 135.9 | 38.15 | 132.2 |
| 76.84 | 134.9 | 35.66 | 130.8 |
| 78.46 | 134.8 | 30.72 | 126.1 |
| 80.73 | 135.9 | 25.70 | 122.8 |
| 83.00 | 136.6 | | |
| 85.22 | 137.8 | | |
| 97.48 | 139.1 | | |

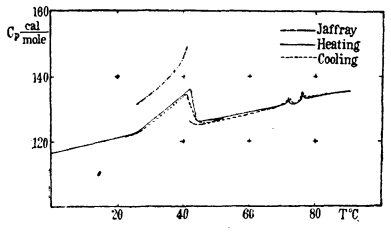



Fig. 4. Heat capacity vs. temperature curves of $Be_4O(CH_3CO_2)_6$.

realize that the heating curve almost completely coincides with the cooling one, showing no hysteresis. By this measurement, it was made clear that the temperature (32°C) where the expansion coefficient increases sharply, corresponds to the temperature where the heat capacity curve begins to increase.

**iv) Vapor pressure measurement.**—This material sublimes slowly even at room temperatures, so we attempted to measure the sublimation pressures below and above the transition point to determine the heat of sublimation as well as the heat of transition. The results are all given in Table II. The heat and entropy of fusion were estimated to be 6.5 kcal./mole and

TABLE II
VAPOR PRESSURES OF $Be_4O(CH_3CO_2)_6$

| $t$°C | $P$ mm Hg $\times 10^3$ | $t$°C | $P$ mm Hg $\times 10^3$ |
|---|---|---|---|
| 120.7 | 2.828 | 152.6 | 52.22 |
| 124.9 | 4.081 | 156.3 | 65.33 |
| 126.5 | 4.539 | 160.0 | 92.92 |
| 134.4 | 9.508 | 164.6 | 124.8 |
| 135.1 | 11.30 | 168.3 | 164.1 |
| 139.9 | 15.93 | 172.8 | 213.6 |
| 145.6 | 29.60 | | |
| 145.7 | 30.43 | | |
| 148.6 | 39.98 | | |

$\log P = 15.029_9 - 6934.8/T$
(below the transition point)
$\log P = 12.626_6 - 5922.8/T$
(above the transition point)

| | $\Delta H$ kcal./mole | $\Delta F$ cal./mole | $\Delta S$ e.u. |
|---|---|---|---|
| Sublimation (low-temp. phase) | 31.7 | $31734 - 60.170T$ | 60.2 |
| Sublimation (high-temp. phase) | 27.1 | $27102 - 44.598T$ | 44.6 |
| Transition | 4.6 | — | 15.6 |

11.6 e.u., respectively by comparison of the corresponding areas of the two peaks obtained by the thermal analysis (see Fig. 1).

## Discussion of Results

As pointed out by Watanabé and Saito, the fact that the melting point of this material is abnormally higher than those of other compounds of homologous series and also that the soft waxy appearance above the transition temperature of 148°C suggests that the high-temperature modification will belong to the so-called plastic crystal. By our measurements of the entropy changes at the transition and melting points, we can confirm the fact that their prediction is correct. They further investigated the X-ray diffraction effects of the high temperature modification at various temperatures of 160°, 170°, 220°, 270° and 280°C. According to them, the crystal structure gradually changes with the rise of temperature and approaches the final structure which belongs to a rhombohedral lattice with the cell dimensions of $a = 9.72$ kX and $\alpha_r = 54°20'$, containing one molecule in it.[10] They noticed, however, that the crystal structure just above the transition temperature may be of a little lower symmetry than the final rhombohedral lattice structure which is reached gradually between 220° and 280°C. In our thermal analysis study, we have noticed the curious fact that the sample which was

10) Y. Saito, *X-rays*, 7, 1 (1952).

previously heated above about 210°C did not exhibit the transition phenomenon in the repeated heating experiments carried out on the following day. This phenomenon and the above-mentioned results of the X-ray investigation seem to imply that the crystal structure in the temperature region between the transition point and about 210°~220°C will retain some characteristic feature of the structure below the transition point rather than that of the high temperature form above 220°C.

The transition at 148°C is of a typical 1-st order type, judging from the discontinuities of vapor pressure curves and of volume change. This transition point is, however, sensitive to the history of the crystal lattice and is displaced to higher temperatures when the crystal was stored for a long time after the preparation (see curve (i) in Fig. 2) or ground mechanically (curve (xi) in Fig. 2). The curves of the differerential thermal analysis sometimes show more or less complex structures which are observed in the temperature region about 130°~147°C (see curve (vi) and (viii) in Fig. 2). This process may also be explained as due to the relative degree of metastability of the phases which exist between 124°C and 148°C and of the high temperature phase above the transition point.[11] This result also reminds us of the fact that $Pb(C_2H_5)_4$ and $Sn(C_2H_5)_4$[12] show several melting points depending on the heating or cooling rate as well as on the previous histories. These phenomena suggest that for the molecular crystals composed of molecules which have methyl groups at their periphery, it is rather difficult to establish the real equilibrium state on account of the meshing-gear-like interaction between methyl groups belonging to one and the same molecule as well as to the neighbouring other molecules.

Now, we proceed to the discussion of the phase transition at about 40°C. As shown in Fig. 4, the heat capacity curve is of typical $\lambda$-type and the heat of transition is very small compared with that at 147°C. Nonexistence of the hysteresis phenomenon is in agreement with the prediction by Staveley from the stand point that the lattice strain energy is very small in the case of higher-order phase transition[13]. Thus, these facts reasonably indicate the higher order type of this transition.

As already mentioned, the crystal structures above and below this transition point are already investigated in detail by several authors. According to their results, it may be said that there may exist two kinds of molecules of *d*- and *l*- types, so to speak, below the transition temperature in reference to the two equivalent potential minima for the orientation of the oxygen pair of the carboxyl group.* Confining our study to the intramolecular interaction, no difference can exist between these two kinds of molecules. However, if we consider the intermolecular interaction, the interaction energy between two different types of molecule will be different from that between two of the same type of molecule and the former is probably larger than the latter. As a result, it may be assumed that the *d*- (or *l*-) type molecule is the more stable the larger the number of the neighbouring *l*- (or *d*-) type molecules. As the temperature rises, the rotational vibration of the carboxyl group about C–C axis becomes more and more violent and the distinction between these two types of molecule will disappear when two oxygen atoms of the carboxyl group surmount the potential barrier between the two potential minima. The difference of intermolecular energies between a pair of the same kind of molecules and a pair of different kinds just mentioned above also disappears at the same time. In such a way, we may understand this phase transition as a kind of order-disorder type. In the case of the ordinary order-disorder transition of an alloy system, the interchange of the atomic position between different kinds of atoms takes place, while in the present case only the transition of atoms from unequivalent potential minima to equivalent ones occurs within one and the same molecule. Thus, it may be said that this case is somewhat similar to the so-called Ising model designed for the ferromagnetic transition, etc.

Finally, we should like to propose a tentative theory on the rotational transition of the molecular crystal of this sort, although it may be of qualitative nature.

Following the theory of Fowler on the rotational phase transition[14], we assume all the libration and rotation to be classical. Then the total energy in Hamiltonian form is

$$H=T+V, \qquad \text{with } V=\frac{W}{2}\cos\theta,$$

where $T$ is the kinetic energy of rotation of the rigid rotator with axial symmetry, $V$

11) A.R. Ubbelohde, *Nature*, **169**, 832 (1952).
12) D.G. Thomas and L.A.K. Staveley, *J. Chem. Soc.*, (1951) 2572.
13) L.A.K. Staveley et al. *J. Chem. Soc.*, (1950) 2290.

* As to the possibility of two forms of this molecule, see reference 11).
14) Fowler: *Statistical Mechanics* (1936). p. 810.

the potential energy due to the surrounding field of force, $W$ the height of the hindering potential of the rotator, and $\theta$ the displacement of the axis of figure from a single preferred direction of equilibrium. The probability $P(\theta)d\theta$ of finding the rotator between $\theta$ and $\theta+d\theta$, is

$$P(\ )d\theta=\int_0^{2\pi}\int_{-\infty}^{+\infty}\int_{-\infty}^{+\infty}e^{-H/kT}dP_\theta dP_\varphi d\varphi d\ )$$

The partition function $f$ is then given by

$$f=\frac{2\pi IkT}{h^2}\cdot 2\pi\cdot\int_0^\pi e^{-V/kT}\sin\theta d\theta$$

$$=\frac{8\pi^2IkT}{h^2}\cdot\frac{kT}{W}\sin hW/kT \qquad (3)$$

where $I$ is the moment of inertia of the rotationg group of the molecule. As is well known, Fowler defined the degree of non-rotation $S$ by the next equation:

$$S=f_0/f$$

where

$$f_0=\int\int_{H<\beta V}e^{-H/kT}dP_\theta d\theta \qquad (4)$$

Here, the parameter $\beta$ is the measure of non-rotation in the sense that the molecule having less energy than $\beta V$ can not rotate anyhow. However, the physical meaning of $\beta$ is not very obvious, and this ambiguity may be removed in a slightly improved way by defining the order parameter by the following quantity,

$$S=\int_0^\pi P(\theta)(-\cos\theta)d\theta/f$$

$$=\int_0^\pi e^{-W/2kT\cos\theta}(-\cos\theta)\sin\theta d\theta$$

$$=\coth W/2kT-2kT/W \qquad (5)$$

At 0°K, $S=1$ and as temperature rises $S$ decreases gradually from 1. According to the Bragg-Williams approximation, we then assume

$$W=W_0S+W_0^\circ. \qquad (6)$$

In this equation, $W_0^\circ$ is the part of $W$ which does not depend on $S$. In other words, this means that even above the transition temperature the molecules are not necessarily to be looked upon as free rotators. $W_0^\circ$ is, therefore, a measure of hindering potential which is not affected by the long range cooperation. Thus, if the ratio of $W_0^\circ/W$ is not zero, the straight line representing the above equation does not start from the origin in the plot of $S$ against $\alpha$ $(=W/2kT)$ (see Fig. 5).

Now, on the assumption, in the case of the present substance, that for the potential energy $V$ for the rotation of carboxyl radical,

$$V=\frac{W}{2}\cos 2\theta,$$

the order parameter $S$ mentioned above becomes

$$S=I_1/I_0,$$

where $I_1$ and $I_0$ are the 1-st and 0-th order modified Bessel functions, respectively. The relation between $S$ and $\alpha$ is shown in Fig. 5,

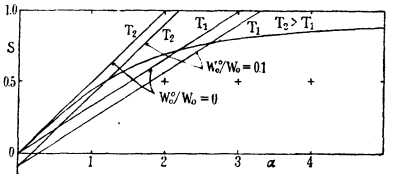



Fig. 5. Dependence of order parameter $S$ upon $\alpha$.

and that between $S$ and $T/T_c$ is given in Fig. 6. In these figures two cases of $W_0^\circ/W_0$

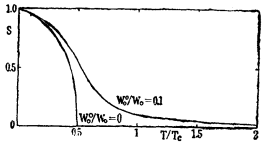



Fig. 6. Relation between order parameter $S$ and $T/T_c$.

$=0$ and $=0.1$ are represented. By the ordinary method we can then calculate the energy as a function of temperature as illustrated in Fig. 7. By differentiation we can finally

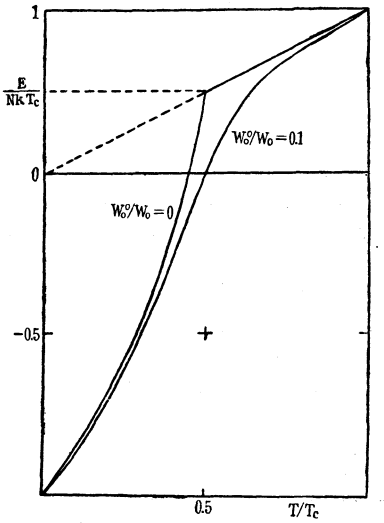



Fig. 7. Curves of $E/NkT_c$ vs. $T/T_c$.

find the heat capacity curve as shown in Fig. 8.

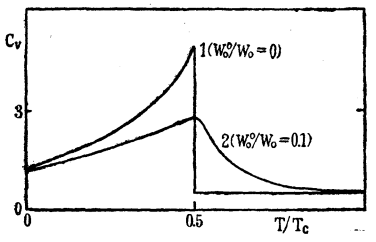



Fig. 8. Curves of $C_v$ (calculated) vs. $T/T_c$.

From the results of these curves, we can find out that when the ratio $W_0°/W_0$ is not zero, there occurs no phenomenon of the latent heat. The heat capacity curve (1) in Fig. 8 is similar in shape to the actual behavior found in this material at about 40°C. In this case the value of $W_0$ is calculated to be about 2.5 kcal./mole which seems to be not so unreasonable an order of magnitude for a molecular crystal like the present material.

Although these results are only of qualitative nature, it may be of some significance to understand the rotational phase transition in such a simple way.

In conclusion, the authors should like to express their hearty appreciation to Professor Nitta for his gracious interest during this work and to Dr. Y. Saito of Osaka City University and Dr. K. Motojima of Kyoto Ritsumeikan University for kindly giving the samples used. The cost of this research was defrayed from the funds of Taniguchi Kôgyô Shôreikai as well as from the Scientific Research Expenditure Grant from the Ministry of Education, to which the thanks of the present authors are due.

*Department of Chemistry, Faculty of Science, Osaka University, Osaka*

Note added in Proof: K.N. Semenenko, Yu.P. Simanov and A.V. Novoselova have recently raised an objection about the reality of the transition at 148°C. (Vestnik Moskov Univ., 9, No. 2, Ser. Fiz-Mat. i Est. Nauk No. 1, 61 (1954)). They, however, dealt only with the monoclinic γ-modification, even though prepared by three different methods, and did nothing with the cubic modification. Because they carried out neither the thermal analysis nor the dilatometric investigations of the cubic modification, it is quite natural that they did not observe the transition at 148°C. The determination as to which of the monoclinic or the rhombohedral modification is more stable at high temperatures requires measurements of the vapor pressures of the monoclinic form in addition to those of the rhombohedral form described in the present paper.

# *Internal Rotation in n-Propyl Chloride and Bromide*

By Chizuko KOMAKI, Isao ICHISHIMA, Kenji KURATANI, Tatsuo MIYAZAWA, Takehiko SHIMANOUCHI, and San-ichiro MIZUSHIMA

(Received February 19, 1955)

## Introduction

In a previous paper it was shown by the Raman measurement that *n*-propyl halides exist in two forms in the liquid state and in only one form in the crystalline state.[1] The same conclusion was drawn by Brown and Sheppard[2] from their infrared absorption measurement of *n*-propyl bromide. Goubeau and Pajenkamp have reported the energy difference between the rotational isomers of *n*-propyl chloride and *n*-propyl bromide[3]. However, as the stable molecular forms have not yet been determined, we have made further spectroscopic studies of these substances. The results will be reported in the present paper.

## Vibrational Spectra

The sample used in the measurement was prepared from *n*-propyl alcohol and phosphorous trihalide and purified by distillation under ordinary pressure using a column having 30 theoretical plates. The materials used were center fraction boiling over a range of ±0.1°C. Raman spectra were measured with the spectrograph of our own construction[4] and the infrared absorptions with the Baird spectrophotometer with the NaCl and KBr prisms. The results are listed in Tables I and II. In these tables are also shown

1) S. Mizushima, Y. Morino and S. Nakamura, *Sci. Pap. Inst. Phys. Chem. Res. Tokyo*, **37**, 205 (1940).

2) J. K. Brown and N. Sheppard, *Disc. Faraday Soc.*, **9**, 144 (1950).

3) J. Goubeau and H. Pajenkamp, *Acta Physica Austriaca*, **3**, 283 (1949).

4) S. Mizushima, "Structure of Molecules and Interna Rotation," Academic Press, New York (1954).

TABLE I

RAMAN AND INFRARED FREQUENCIES OF $CH_3CH_2CH_2Cl$

| Observed | | | | | | Calculated | | | |
|---|---|---|---|---|---|---|---|---|---|
| Gas | | Liquid | | Solid | | | | | |
| I. R. | | I. R. | R. | I. R. | R.[1] | *trans* | *gauche* | Type of Vibration | |
| | | | 144 (2b) | | | | | | |
| | | | 220 (0b) | | | | | | |
| | | | 249 (2b) | | 229 (1) | 252 | | $\delta$ | *trans* |
| | | | 292 (3) | | —— | | 267 | $\delta$ | *gauche* |
| | | | 368 (6) | | 363 (5) | 334 | | $\delta$ | *trans* |
| | | 426 (m) | 426 (4) | | —— | | 429 | $\delta$ | *gauche* |
| 660 | (s) | 648 (s) | 651 (8) | —— | —— | | 708 | $\nu$ (C-Cl) | *gauche* |
| | | | | 700 (w) | | | | | |
| 743 | (s) | 729 (s) | 728 (6b) | 717, 725 (s) | 716 (7) | 744 | | $\nu$ (C-Cl) | *trans* |
| | | 749 (m) | —— | 749 (s) | | | | $CH_2$ *rocking* | *trans* |
| 787, 793, 800 | (s) | 789 (s) | 788 (6) | —— | —— | | | $CH_2$ *rocking* | *gauche* |
| 852, 858, 864 | (s) | 856 (s) | 856 (4) | 863 (m) | | | | | |
| 894, 903 | (s) | 897 (s) | 896 (3) | 898 (s) | | | | | |
| 1038 | (m) | 1034 (s) | 1026 (6) | 1030 (m) | 1029 (5) | | | | |
| 1050 | (m) | 1067 (m) | 1064 (1) | 1065 (w) | | | | | |
| 1067 | (w) | 1081 (w) | 1088 (0) | 1083 (m) | | | | | |
| 1097 | (w) | 1094 (w) | | | | | | | |
| | | 1104 (w) | 1108 (1) | 1103 (w) | | | | | |
| | | 1158 (w) | | 1155 (vw) | | | | | |
| | | 1213 (w) | 1211 (1) | 1218 (vw) | | | | | |
| 1253, 1261 | (s) | 1258 (s) | 1255 (2) | 1257 (s) | | | | | |
| 1300, 1309 | (s) | 1304 (s) | 1297 (1) | 1287 (vw) | | | | | |
| 1331 | (m) | 1338 (m) | 1341 (3) | 1332 (m) | | | | | |
| 1390 | (m) | 1385 (s) | 1381 (0) | 1370 (m) | | | | | |
| 1456 | (s) | 1447 (s), 1460 (s) | 1441 (5), 1462 (2b) | 1460 (s) | 1441 (2) | | | | |
| | | | 2743 (4) | | | | | | |
| | | | 2854 (2) | | 2829 (0) | | | | |
| 2870 | (s) | | 2876 (6) | | 2870 (5) | | | | |
| | | 2900 (s) | 2900 (3b) | | 2894 (2) | | | | |
| | | | 2915 (3b) | | 2908 (2) | | | | |
| | | | 2936 (6) | | 2941 (6) | | | | |
| 2950 | (s) | 2960 (s) | 2957 (6) | | | | | | |
| | | | 2979 (3) | | 2975 (0) | | | | |
| | | | 3003 (3) | | 2997 (0) | | | | |

1. Frequencies reported in reference 1).

the infrared absorption spectra in the crystalline state observed in the frequency range 600 to 800 cm.$^{-1}$ with the use of a spectrophotometer of our own construction[4].

## Rotational Isomers

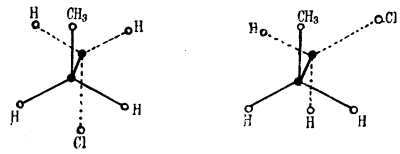
As has been shown in many of our previous papers on internal rotation, the absence of some of the liquid spectral lines in the solid state (Tables I and II) shows the presence of rotational isomers in the liquid state[1]. In the solid state, however, the presence of only one isomer is sufficient to account for the number of the observed lines.

TABLE II

INFRARED FREQUENCIES OF $CH_3CH_2CH_2Br$

| Gas | Liquid | Solid | Type of Vibration |
|---|---|---|---|
| | 406 | | |
| 561 (s) | 564 (s) | | $\nu$(C-Br) *gauche* |
| 658 (s) | 646 (s) | 638 (s) | $\nu$(C-Br) *trans* |
| 742 (w) | 741 (m) | 737 (s) | $CH_2$ *rocking trans* |
| 775, 780, 785 (s) | 777 (s) | —— | $CH_2$ *rocking gauche* |
| 837 (s) | 838 (s) | 849 (w) | |
| 892 (s) | 887, 893 (s) | 892 (s) | |
| 1033 (s) | 1030 (s) | 1025 (m) | |
| 1085 (m) | 1079 (m) | 1038 (s) | |
| | 1094 (w) | 1099 (m) | |
| | 1196 (m) | | |
| 1232 (s) | 1225 (s) | 1218 (s) | |
| 1290 (s) | 1284 (s) | —— | |
| 1339, 1351 (m) | 1326, 1340 (m) | 1321 (s) | |
| 1391 (s) | 1381 (s) | 1364 (s) | |
| 1456 (s) | 1437, 1460 (s) | 1445 (s) | |
| 2900 (s) | 2890 (s) | | |
| 2960 (s) | 2960 (s) | | |

We are now interested in determining the molecular configurations of the rotational isomers. The symmetry considerations cannot be applied conveniently for this molecule. However, from the nature of the hindering potential discussed in a previous paper[5], the stable configurations of this molecule can be considered to be the *trans* and *gauche* forms shown in Fig. 1. Accordingly the normal vibration calculation of the skeleton $(CH_3)\cdot(CH_2)\cdot(CH_2)\cdot Cl$ has been made for the *trans* and *gauche* forms according to the method described in a previous paper[6]. The force constants used in this calculation are those which yielded the computed frequency values in good agreement with those observed for other molecules with similar structure.



*Trans* form *Gauche* form

Fig. 1. Stable molecular configurations of *n*-propyl chloride.

The computed skeletal frequencies of *n*-propyl chloride are shown in Table I. Those for the *trans* form are close to the frequencies observed in the solid state. Accordingly we conclude the stable configuration in the solid state to be the *trans* form, in which the $CH_3$ group and the Cl atom are farthest apart. The fact that all the solid frequencies are also observed in the liquid state shows that the *trans* form is one of the stable configurations in this state. The other stable configuration can be considered to be the *gauche* form, since the Raman lines observed only in the liquid state have frequencies close to those calculated for the *gauche* form.

In order to confirm this conclusion, we have calculated the dependence of the skeletal deformation frequency on the azimuthal angle $\theta$ of internal rotation, because this frequency is very sensitive to the change of this angle[6] and accordingly we can determine fairly accurately the azimuthal angle from the observed frequency value. The result of this calculation is shown in Fig. 2, from

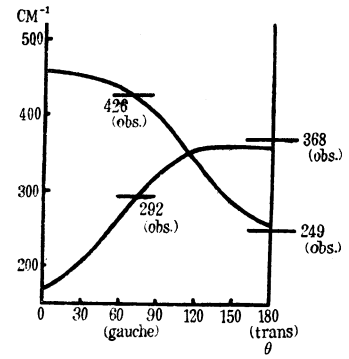



Fig. 2. Dependence of skeletal deformation frequencies on azimuthal angle.

which we see that the observed frequencies are close to those calculated for the *trans* ($\theta=180°$) and the *gauche* ($\theta=60°$) forms, respectively.

The conclusion was also checked by the product rule derived in our previous paper[6]. If we denote the kinetic energy matrices for the *trans* and *gauche* forms by $G_t$ and $G_g$, respectively, we have

$$(|G_g|/|G_t|)^{\frac{1}{2}}=\Pi\nu_g/\Pi\nu_t \qquad (1)$$

where $\nu_t$ and $\nu_g$ are the normal frequencies of the *trans* and the *gauche* molecules. The ratio on the left-hand side of this equation has been calculated as the function of $\theta$ as shown in Fig. 3, putting $\theta$ of the *trans* form as 180°. The experimental value $\Pi\nu_g/\Pi\nu_t$ is close to that calculated for the *gauche* form ($\theta=60°$).

5) S. Mizushima, Y. Morino and T. Shimanouchi, *J. Phys. Chem.*, **56**, 324 (1952).
6) S. Mizushima, T. Shimanouchi, I. Nakagawa and A. Miyake, *J. Chem. Phys.*, **21**, 215 (1953).

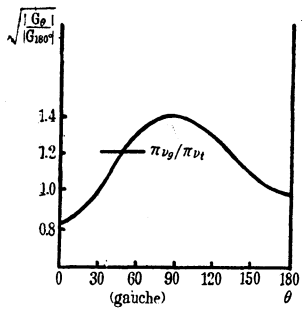



Fig. 3. The calculated values of $(|G\theta|/|G_{180°}|)^{1/2}$ and the observed value of $\Pi\nu_g/\Pi\nu_t$.

In addition to the confirmations made by these calculations we have an experimental evidence in support of the assignment of lines made above. *n*-Propyl chloride has a chain structure similar to that of ethylene chlorhydrin so that the skeletal frequencies of these two molecules will not be very different from each other. Actually these two substances show similar low frequency lines in the liquid and the gaseous states. However, there is a great difference between the spectra of these two substances in the solid state. Namely, the lines 292, 426, 651 cm.$^{-1}$ of liquid *n*-propyl chloride disappear on solidification, whereas the corresponding lines of ethylene chlorhydrin persist in the solid state. From this we can conclude that the configuration of *n*-propyl chloride in the solid state must be different from that of the crystalline ethylene chlorhydrin. Now that our previous measurement[7] has shown the *gauche* form to be present in the crystalline state of ethylene chlorhydrin, we can conclude that the molecule of *n*-propyl chloride in the solid state is the *trans* form in conformity with the conclusion drawn from the normal vibration calculation.

## Energy Difference between the Rotational Isomers

The energy difference between the rotational isomers has been determined by the measurement of the ratio of optical densities $D$ of the two infrared absorption bands, one assigned to the *trans* form and the other to the *gauche* form:

$$D_t/D_g = \frac{\kappa_t}{2\kappa_g} e^{-\frac{\Delta S}{R}} e^{\frac{\Delta E}{RT}},$$

where $\Delta S = S_g - S_t$ and $\Delta E = E_g - E_t$ denote the differences in entropy and energy, $\kappa$ the molecular absorption coefficient and suffices $t$ and $g$ refer to the *trans* and *gauche* molecules, respectively. In a narrow range of temperature $\Delta S$ and $\Delta E$ can be considered to be constant and accordingly the value of $\Delta E$ can be determined by measuring the temperature dependence of the ratio $D_t/D_g$ of the two bands. As these bands we have chosen one at 793 cm.$^{-1}$ or 660 cm.$^{-1}$ assigned to the *gauche* form and the other at 743 cm.$^{-1}$ assigned to the *trans* form.* From the measurement in the gaseous state made in the temperature range from 20°C to 150°C, the energy difference has been obtained as:

$$\Delta E = -0.05 \pm 0.15 \text{ kcal./mol.}$$

For the measurement in the liquid state in the temperature range from 10° to −60°C we have chosen two bands at 789 cm.$^{-1}$ (*gauche*) and at 729 cm.$^{-1}$ (*trans*). The energy difference has been found to be

$$\Delta E = +0.05 \pm 0.06 \text{ kcal./mol.}$$

This is in agreement with the value obtained by Goubeau and Pajenkamp from their Raman measurement[3], provided that the assignment of lines is made as referred to above.

It is to be noted that the energy difference found in the gaseous state is nearly equal to that in the liquid state. This is compatible with our explanation of the interaction of molecules in the liquid state[8]. It is seen that the *trans* and the *gauche* forms of *n*-propyl chloride will have almost the same value of the dipole moment which will result in the same change of energy in the liquid state. In other words, the energy difference between the *trans* and *gauche* molecules will have almost the same value in the liquid state as in the gaseous state.

The intensity measurement made for *n*-propyl bromide by use of two bands at 780 cm.$^{-1}$ (*gauche*) and 658 cm.$^{-1}$ (*trans*) in the temperature range from 20° to 150°C gave the value of enery difference $-0.1 \pm 0.2$ kcal./mol. in the gaseous state.

In our previous papers[4,5,7] we have discussed the energy difference between the *trans* and *gauche* forms of many disubstituted ethanes. The very small value of $\Delta E$

7) S. Mizushima, T. Shimanouchi, T. Miyazawa, K. Abe and M. Yasumi, *J. Chem. Phys.*, **19**, 1477 (1951).

* We are sure that no *trans* band (strong enough to disturb the energy difference measurement) overlaps the 793 and 660 cm.$^{-1}$ *gauche* bands, because these two bands disappear in the solid state. Nor is the 743 cm.$^{-1}$ *trans* band considered to be overlapped by any *gauche* band, because the only *gauche* frequency expected to appear in this range is the $CH_2$-rocking frequency assigned to the 793 cm.$^{-1}$ band. This assignment is made from comparisons with the spectra of *n*-propyl bromide, dichloroethane, etc. See I. Nakagawa and S. Mizushima, *J. Chem. Phys.*, 21, 2195 (1953).

8) I. Watanabe, S. Mizushima and Y. Mashiko, *Sci. Pap. Inst. Phys. Chem. Res. Tokyo*, **40**, 425 (1942). See also reference 4).

obtatined for *n*-propyl chloride and bromide is very interesting as compared with the large values found in the cases of 1,2-dichloro and 1,2-dibromoethane. This fact provides us data useful for the further development of our view[5] concerning the nature of the hindering potential to internal rotation**.

**Summary**

Infrared spectra of *n*-propyl chloride and bromide have been measured in the gaseous, liquid and solid states. The Raman measurement was also made in the liquid state. From the normal vibration calculation and by comparison with the spectra of ethylene chlorhydrin it has been concluded that in the liquid state both the *trans* and *gauche* forms are present and of these only the *trans* form persists in the solid state. The energy difference between the *trans* and the *gauche* forms has been determined by the absorption intensity measurement.

*Chemical Laboratory, Faculty of Science, Tokyo University, Tokyo*

** After our manuscript was finished, a paper by J. K. Brown and N. Sheppard, *Trans, Faraday. Soc.*, 50. 1164 (1954), became available to us. They reported a detailed infrared measurement of *n*-propyl halides in the solid state, the result of which supports our assignment of the bands used for the determination of the energy difference. Other conclusions reported in this paper are also in good agreement with ours.

# *Phototropy of New Photosensitive Complexes between a Fluorescent Pigment and SH-Compounds*

By Eiji FUJIMORI

(Received February 21, 1955)

## Introduction

Recently it has been recognized that the SH-group plays an important role not only in coenzyme-A and many enzymes, but also in the synthesis of the hormone and its activity, the coagulation of blood, the penetration of cellular membrane, the contraction of muscles, and cellular mitosis. It would be specially significant also in the reversibility of light energy conversion in vision and photosynthesis. On the other hand, there are many biological fluorescent pigments in the organism, such as porphyrin, carotenoids, flavin, and pteridine, which exhibit their physiological functions in close association with other biological substances such as protein and suitable oxidizing or reducing agents.

During the course of the investigation on the synthesis and preparation of organic fluorescent and photosensitive substances, their spectral structures, their abilities of emission, and their photosensitized and other photochemical reactions, the author noticed that the combination and interaction of these fluorescent pigments with some foreign substances possessing the SH-group responsible for the migration of excitation energy by molecular complex formation and electron transfer might be significant for their photosensitivity as light-sensitive substances. In confirmation of this point of view, it has been found in this laboratory that the complexes between a fluorescent pigment and SH-compounds selected as the reaction partner for the above mentioned reasons exhibit a specific photosensitivity.

It is well known that there are several photosensitive pigment-protein complexes in the retina of the eye[1]. One of them, visual purple or rhodopsin has the light absorption maximum at about 500 m$\mu$. The absorption of light by this rhodopsin activates the pigment molecules and stimulates rod vision. Rhodopsin is bleached by light to retinene$_1$ and protein opsin, and is then regenerated from them in the dark. Recently, the liberation of SH-groups in the photobleaching of rhodopsin has been discovered by Wald and Brown[2], who ascertained the important role of SH-groups in the synthesis and bleaching of rhodopsin. As the author succeeded in fitting a fluorescent pigment into the SH-group of SH-protein or other SH-compounds

1) G. Wald, *J. Opt. Soc. Am.*, **41**, 949 (1951); *Federation Proc.*, **12**, 606 (1953); *Ann. Rev. Biochem.*, **22** 497 (1953).

2) G. Wald and P. K. Brown, *J. Gen. Physiol.*, **35**, 797 (1952); **37**, 189 (1953).

and since these pigment-SH compound complexes showed a phototropy analogous to this rhodopsin, the experimental results are described in this paper.

## Experimental Methods

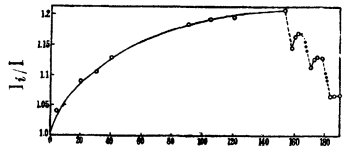
**Materials.**—The fluorescent pigment (I) used in this experiment was derived from fluorescein by the same method as described in the previous paper[3]. This yellow pigment showed a stable yellow fluorescence in a neutral aqueous solution. Hoffmann-La Roche reagent grade glutathione and Wako reagent grade egg albumin, cysteine, and thioglycolic acid were used.

On addition of this pigment solution to the alkaline solution of SH-compounds such as egg albumin, glutathione, cysteine, and thioglycolic acid, the yellow color disappeared with a slow appearance of an absorption in the longer wave length range, and its yellow fluorescence was partly quenched at the moment of the addition and then gradually deactivated as the reaction proceeded. These pigment-SH compound complexes were bleached by light and regenerated thermally in the dark. Since the experimental results were different in each complex, each case will be described separately below.

**Measurements.**—For the photobleaching reaction, the white light of a 1-KW projection lamp was allowed to fall upon a reaction cell of 2.5 cm. ×2.5 cm. ×3 cm. at a distance of 20 cm. from the light source. The variation of green light absorption during the formation reaction and regeneration reaction of the complexes was photoelectrically measured by the use of a 6-volt headlight lamp filtered through the Mazda glass filter V-G1 (maximum transmission at about 520 mμ) as a light source, at right angles to the irradiation source for photobleaching, and would be represented by the ratio of the initial value at the beginning of the reaction, $I_i$, to the respective measured value, I. The absorption spectra were measured by the Beckman spectrophotometer.

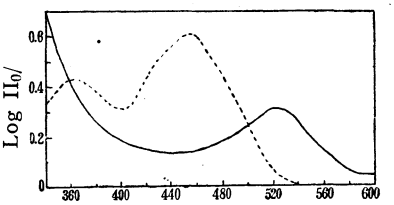
## Experimental Results

(1) **Egg Albumin.**—When $2.5\times10^{-4}$ M pigment (I) reacted with 1–7.5% egg albumin in 0.1–3 N NaOH solution, its yellow color disappeared and a red color of the reaction product appeared gradually as shown in Fig. 1. Fig. 2 shows the absorption spectra of this pigment and the reaction complex. The absorption maximum of the yellow pigment at 453 mμ shifted to the longer wave length of 520 mμ, together with the deactivation of its fluorescence, which occurred instantaneously at the beginning of the reaction and continued to complete disappearance as the reaction proceeded.




Time∼minutes

Fig. 1. Formation and phototropy of pigment-SH-protein complex. Dotted lines indicate bleaching during the illumination by light. $2.5\times10^{-4}$ M pigment and 7.5% egg albumin in 3 N NaOH.



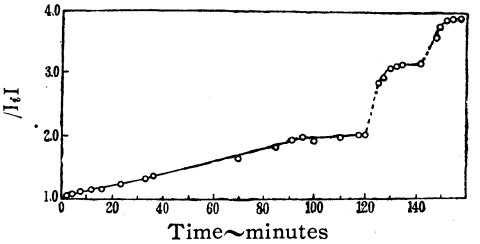

Wave legth∼mμ

Fig. 2. Absorption spectra of pigment (I) and its complex with egg albumin:....., $10^{-4}$ M pigment in phosphate buffer solution at pH 7.0;—, $10^{-4}$ M pigment and 1% egg albumin in 3 N NaOH.

This non-fluorescent red pigment-protein complex was bleached by light and regenerated rapidly within about two minutes at room temperature in darkness (Fig. 1). In this case, the more often the photobleaching was repeated, the lower the degree of regeneration became. The average initial regeneration degree was about 30, 15, and 8%, respectively, to 7.5, 5 and 2.5% of protein concentration; thus the regeneration degree was parallel to the protein concentration.

The addition of cysteine to this protein complex altered the color from red to orange. This fact seems to suggest the reversible formation of an orange pigment-cysteine complex; i, e., the exchange reaction of the SH-compound.

(2) **Glutathione.**—The absorption maximum of a complex produced by the reaction of glutathione with the pigment was at the same 520 mμ as in the csae of protein. In light this complex showed a deep color, in-




Time∼minutes

Fig. 3. Formation and phototropy of pigment-glutathione complex. $2.5\times10^{-4}$ M pigment and 0.05 M glutathione in 3 N NaOH.

3) E. Fujimori, *J. Chem. Soc. Japan (Pure Chem. Sect.)*, 75, 24 (1954); *J. Am. Chem. Soc.*, in the press.

stead of bleaching, which changed towards regeneration in darkness (Fig. 3). This strange regeneration reaction was completed within about ten minutes at room temperature. Such a photochemical change to a deep color took place even in the case of cysteine and thioglycolic acid, but on account of its slowness the ordinary photobleaching and regeneration were observed on short irradiation, as will be mentioned below. The light absorption maximum before and after irradiation was at the same wave length, namely 520 mμ (Fig. 4).

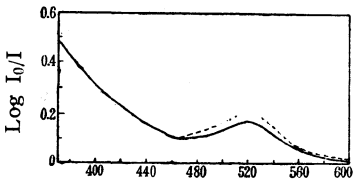



Fig. 4. Absorption spectra of pigment-glutathione complex:—, before irradiation of light;....., after irradiation and regeneration. $2.5 \times 10^{-4}$ M pigment and 0.02 M glutathione in 1.2 N NaOH.

(3) **Cysteine.**—The reaction between the pigment and cysteine of high concentration in alkaline solution produced an orange complex whose absorption maximum was at 505 mμ (Fig. 6). It was found that the phototropy is repeated many times as shown in Fig. 5. As long as the irradiation time was short, the bleached product showed a pale yellow color which returned to the original orange color in the dark, but on repeating the illumination many times or irradiating it for a long time it changed to a pale red and in the dark converted into a deep red color whose absorption maximum gradually approached 520 mμ (Fig. 6). In both cases the regeneration degree was almost 100 %. The initial orange complex fluoresced more weakly than the original pigment, while the red complex produced photochemically showed the almost complete disappearance of fluorescence as in protein complex. This color and phototropy remained unchanged by neutralization with hydrochloric acid.

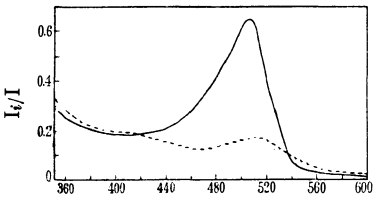



Fig. 6. Absorption spectra of pigment-cysteine complex:—, before irradiation of light;....., after irradiation and regeneration. $10^{-4}$ M pigment and 0.4 M cysteine-HCl in 1.2 N NaOH.

(4) **Thioglycolic Acid.**—Thioglycolic acid behaved in a manner analogous to that of

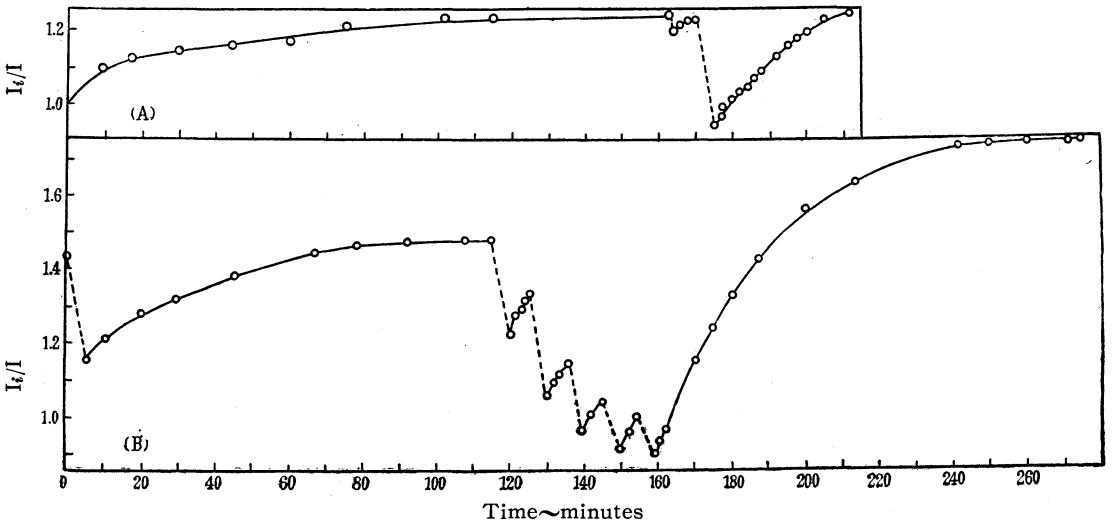



Fig. 5 (A) Formation and phototropy of pigment-cysteine complex. $2.5 \times 10^{-4}$ M pigment and 1 M cysteine-HCl in 3 N NaOH.
(B) Phototropy followed after standing for about 15 hours from the terminal of Fig. 5A.

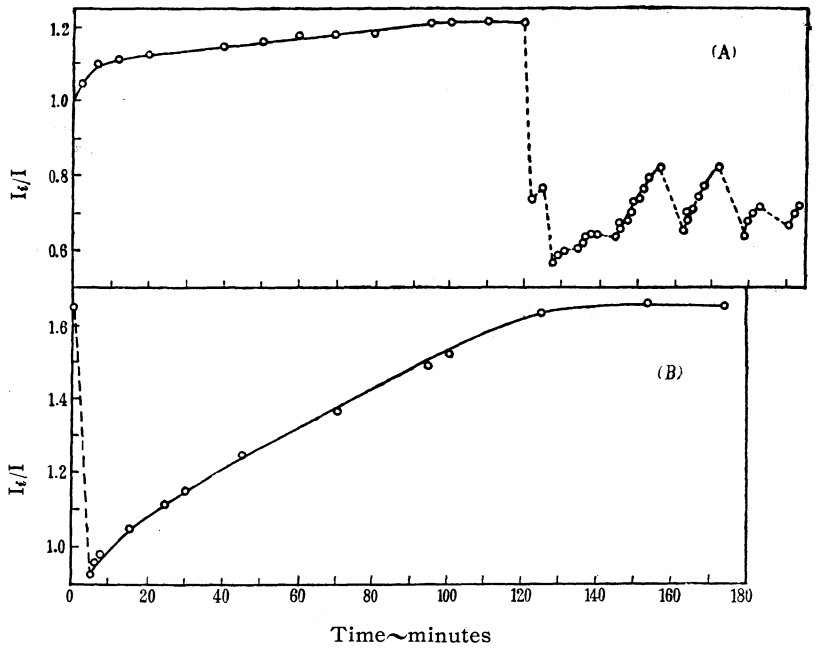



Fig. 7 (A) Formation and phototropy of pigment-thioglycollic acid complex. $2.5 \times 10^{-4}$ M pigment and 1.5 M thioglycolic acid in 3 N NaOH.
(B) Phototropy followed after standing for about 15 hours from the terminal of Fig. 7A.

cysteine. The absorption maxima of pigment-thioglycollic acid complex were initially at 470 and 495 mμ, but later changed to 520 mμ on illumination (Fig. 8). Since this spectral shift to 520 mμ due to some photochemical reaction took place more easily than that of cysteine-complex, the same change to a deep color as in the case of glutathione was observed in the third irradiation of Fig. 7A. The phototropy was observed in both complexes of different spectra. The regeneration degree was 100% and the regeneration time about two hours at room temperature, which was longer by about one hour than in the case of cysteine.

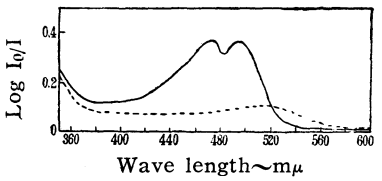



Fig. 8. Absorption spectra of pigment-thioglycolic acid complex:—, before irradiation of light;....., after irradiation and regeneration. $10^{-4}$ M pigment and 0.6 M thioglycolic acid in 1.2 N NaOH.

It was found, moreover, that this dark regeneration is generally a thermal reaction accelerated by heat. The relation between temperature and regeneration time in the case of thioglycolic acid is shown in Table I. Since the initial absorption maximum, the degree of regeneration, and the time required for regeneration are very different with each SH-compound, the summary of these experimental results is shown in Table II.

Table I
Relation between temperature and regeneration time after irradiation for five minutes

| Temp. (°C) | Reg. time (min.) |
|---|---|
| 15 | 120 |
| 30 | 85 |
| 50 | 60 |

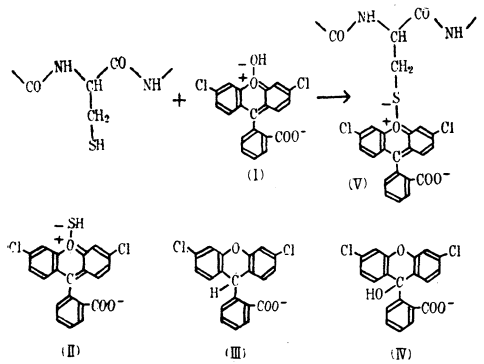
Table II
Various properties of pigment-SH compound complexes

| Properties SH-compound | Absorp. Max. (mμ) | Reg. Deg. (%) | Reg. time* (min.) |
|---|---|---|---|
| Egg albumin | 520 | 30–8 | about 2 |
| Glutathione | 520 | — | 10 |
| Cysteine | 505→520 | 100 | 60 |
| Thioglycolic acid | 470. 495→520 | 100 | 120 |

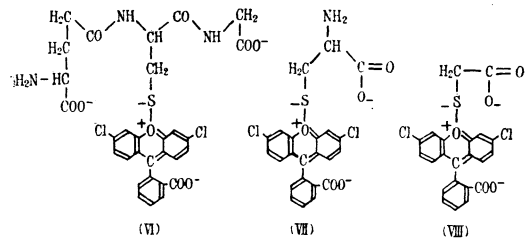
* Regeneration time at room temperature after irradiation for fiver minutes.

## Discussion

The evidence that oxonium hydroxide of the pigment (I) reacts with SH-group in these reactions is obvious from the experimental facts that sodium sulfide also reacted to produce the non-fluorescent red compound (II) with the absorption maximum at 520 mμ and that such a reaction could not occur at all in the reduction product (III) and OH-transition product (IV) of the pigment (I). It is certain, therefore, that the reaction with protein should be represented by the following schema:



The reaction products with glutathione, cysteine, and thioglycolic acid would be (VI), (VII), and (VIII), respectively.



In egg albumin and glutathione, both of which are polypeptides, the absorption maximum is at 520 mμ from the beginning, while in cysteine and thioglycolic acid with free carboxyl group adjacent to the SH-group it is at a shorter wave length than 520 mμ and shifts to 520 mμ by light absorption. This fact seems to suggest some photochemical change of intramolecular orientation, namely photochemical isomerization, in these complexes and some effect of the adjacent free carboxyl ion upon this.

Since these red complicated complexes show the same absorption maximum at 520 mμ and non-fluorescence as in the more simple SH-pigment (II), the discussion described in the previous paper[3] will be true for the present complexes between a fluorescent pigment and complicated SH-compounds; thus the ionic combination of oxonium oxygen of the pigment (I) with SH-group, resulting in the formation of $-S^{-}-{}^{+}O=$ bond, would bring the remarkable deactivation of fluorescence and the shift of absorption spectrum into a longer wave length range. Moreover, the mechanism of this remarkable deactivation of fluorescence in these complexes will be analogous to that, in the SH-pigment (II), considered in connection with the instantaneous quenching of OH-pigment (I) fluorescence by SH-compounds; i. e., it may probably be due to the electron-transfer based on the reducing power of SH-group. Such a remarkable deactivation of fluorescence and a shift of absorption spectrum is likely to be observed in a static molecular complex formed in the ground state. In such a case, the transfer of excitation energy may sometimes bring about a specific photosensitivity. The present series of complexes seems to belong to this category.

Although (II) shows neither fluorescence nor photochemical change under irradiation, the pigment-SH compound complex is bleached in light, stays in some bleaching metastable state with the lifetime made longer by the specific effect of combined $^{-}$S-R, and is regenerated slowly to the original state in the dark as shown in the experiments. As such a bleaching state, a diradical and especially a semiquinone radical with an ·S-R free thiol radical may be of significance. If so, this phototropy of oxidizing oxonium pigment-reducing SH-compound complexes will be regarded as a sort of photo-reversible oxidation-reduction reaction where intramolecular electron transfer takes place through the diradical and semiquinone radical with the formation of ·S-R radical by light absorption.

The dark and light reactions of the pigment ant pigment-SH-compound complexes discussed above, including the previous results on the bleaching reaction of the pigment itself, will presumably be summarized by the following various model equations according to the above assumption:

| | | |
|---|---|---|
| 1 | $D—OH+h\nu_a \rightarrow D^*—OH$ | Light absorption of the pigment |
| 2 | $D^*—OH \rightarrow D—OH+h\nu_f$ | Fluorescence of the pigment |
| 3 | $D—OH \rightarrow HO—D$ | Dark bleaching reaction of the pigment |
| 4 | $D^*—OH \rightarrow HO—D$ | Light bleaching reaction of the pigment |
| 5 | $D^*—OH+{}^-S-R \rightarrow (\cdot D \cdot —OH+{}^-S-R) \rightarrow \cdot D^-—OH+\cdot S-R$ | Quenching of the fluorescence |
| 6 | $\cdot D^-—OH+\cdot S-R \rightarrow D—OH+{}^-S-R$ | Reverse reaction |
| 7 | $D—OH+{}^-S-R \rightarrow D—S—R_I+OH^-$ | Formation of the complex |
| 8 | $D—S—R_I+h\nu_{a'} \rightarrow D^*—S—R_I$ | Light absorption of the complex |
| 9 | $D^*—S—R_I \rightarrow \cdot D \cdot —S—R_I \rightarrow \cdot D^- \cdot S—R_I$ | Bleaching reaction of the complex |
| 10 | $\cdot D^- \cdot S—R_I \rightarrow \cdot D \cdot —S—R_I \rightarrow D—S—R_I$ | Regeneration reaction of the complex |
| 11 | $D^*—S—R_I \rightarrow D—S—R_{II}$ | Photo-isomerization |
| 12 | $D—S—R_{II}+h\nu_{a''} \rightarrow D^*—S—R_{II}$ | Light absorption of the isomer |
| 13 | $D^*—S—R_{II} \rightarrow \cdot D \cdot —S—R_{II} \rightarrow \cdot D^- \cdot S—R_{II}$ | Bleaching reaction of the isomer |
| 14 | $\cdot D^- \cdot S—R_{II} \rightarrow \cdot D \cdot —S—R_{II} \rightarrow D—S—R_{II}$ | Regeneration reaction of the isomer |
| 15 | $D—S—R_I+{}^-S—R_{III} \rightarrow D—S—R_{III}+{}^-S—R_I$ | Exchange reaction of SH-compound |

where D-OH is the pigment (I); D*-OH, the normal excited state (singlet); HO-D, the colorless OH-transition product (IV); $^-$S-R, the negative ion of SH-compound; D-S-$R_I$, the initial complex; D-S-$R_{II}$, an isomer produced by light; $\cdot D \cdot$, a diradical (tiplet state); $\cdot D^-$, a semiquinone radical; and ·S-R, also a free radical. The complex between $\cdot D^-$ and ·S-R, $\cdot D^- \cdot$S-R, will be regarded especially as a complex diradical responsible for the bleaching metastable state with a longer lifetime and seems to be closely related to the diradical, $\cdot D \cdot$-S-R, so as to stabilize it and the diradical by forming a resonance complex.

Thus this phototropy seems to be based on the photochemical formation of pigment free radicals and ·S-R free radical, especially $\cdot D^- \cdot$S-R complex through $\cdot D \cdot$-S-R. Although the formation of ·S-R free thiol-radical was assumed by Waters[4] or Barron[5] in the function of SH-enzymes, e. g., FAD- or DPN-SH protein enzyme, and ascertained by Crawshaw and Speakman[6] in the photolysis of disulfides, there are several studies on pigment free radicals in the field of photochemistry. In 1940, the phototropy due to the formation of a semiquinone radical was studied by Rabinowitch[7] in thionine-ferrous ion system. Schenck[8] suggested the possibility of a diradical in vision, and Livingston[9),10] showed that the formation of a diradical and a semiquinone free radical in the illuminated solution of chlorophyll is the cause of its phototropy.

4) W. A. Waters, "The chemistry of free radicals", Clarendon Press, Oxford, (1946), P. 257–283.
5) E. S. G. Barron, *Advances in Enzymol.*, **11**, 201, (1951).
6) G. H. Crawshaw and J. B. Speakman, *J. Soc. Dyers and Colourists*, **70**, 81 (1954).
7) E. Rabinowitch, *J. Chem. Phys.*, **8**, 551, 560 (1940).
8) G. O. Schenck, *Naturw.* **40**, 212 (1953); *Z. Elektrochem.*, **57**, 675 (1953).
9) R. Livingston and V. A. Ryan, *J. Am. Chem. Soc.*, **75**, 2176 (1953).
10) R. Livingston, G. Porter and M. Windsor, *Nature*, **173**, 485 (1954).


## Summary

The absorption maximum of all pigment-SH compound complexes shifted to a longer wave length range than that of the pigment itself. Although in protein and glutathione the absorption maximum was at 520 m$\mu$ from the beginning, in cysteine and thioglycolic acid it was in a shorter wave length range than 520 m$\mu$ and shifted to 520 m$\mu$ after some photochemical reaction. These complexes with their absorption maxima in a shorter wave length range than 520 m$\mu$ fluoresced more weakly than the original pigment, while those at 520 m$\mu$ showed the almost complete disappearance of fluorescence. Before these SH-compounds combined with the pigment, its fluorescence was partly instantaneously quenched by them. Both complexes of different spectra showed a phototropy; i. e., bleaching in light and regeneration in darkness. The regeneration reaction was thermal: its velocity was parallel to the molecular weight of the SH-compound in these SH-compounds used in the present experiment. The degree of regeneration was low in protein but about 100% in cysteine and thioglycolic acid. The concentration of protein influenced the degree of regeneration but not the velocity of regeneration. This phototropy was discussed from the point of view of an ·S-R free radical and pigment radicals.


*Department of Chemistry and Metallurgy,*
*Institute of Industrial Science,*
*University of Tokyo, Chiba*

# The Effect of Concentration and Valency of Added Salts on the Critical Micelle Concentration of Sodium and Calcium Dodecyl Sulfates

By Kōzō SHINODA

(Received February 21, 1955)

## Introduction

In the preceding report[1], the theoretical equation for the critical micelle concentration (CMC) was derived, and it has been shown that the electrical charges of micelle forming ions play an important role in the process of micellization. In order to criticize this equation the following experiments are needed: to investigate (1) the effect of added salts on the CMC[2-5], (2) the effect of added alcohols on the CMC[6-8], (3) the CMC of soap mixtures[9-11], (4) the CMC of the surfactants which possess two or three dissociable groups at one end of their hydrocarbon chains[12], etc. As for the investigation (1), a number of papers have been published on the effect of uni-valent counterions on the CMC, and the effect of bi- or tri-valent counterions has been measured by H. Lange[3], but, so far as we know, no quantitative explanation has been published.

The present investigation was undertaken to derive the theoretical formula for the CMC values as a function of the concentration and valency of added salts and to compare it with the experimental results given by Lange[3,13].

## Electrical Potential at the Charged Surface of the Micelle

If it is assumed that the surface of a micelle is plane (or at least the double layer thickness is small in comparison with the radius of curvature of micelle surface) and the charge layer on the micelle surface is homogeneous, the counterions distribute homogeneously and parallel to the micelle surface, and the electrical potential is only a function of the normal coordinate. Now the Poisson-Boltzmann equation is applied for the micelle of a plane uniformly charged surface in contact with a solution of strong electrolytes, and the following equation is obtained:

$$\Delta\phi=\frac{\mathrm{d}^2\phi}{\mathrm{d}x^2}=-\frac{4\pi}{D}\sum z_i n_i \mathrm{e}\exp(-z_i\mathrm{e}\phi/kT), \quad (1)$$

where $\phi$ is the electrical potential, $x$ the coordinate normal to the surface, $D$ the dielectric constant of the medium, e the elementary charge, $z_i$ the valencies of the positive and negative ions, $n_i$ the numbers of respective ions per cc. in the bulk of the solution ($n_i=C_iN/1000$, $C_i$ mole number of ions per liter, N Avogadro number), $k$ the Boltzmann constant and $T$ the absolute temperature.

Considering the boundary conditions, $\phi=0$ and $\frac{\mathrm{d}\phi}{\mathrm{d}x}=0$ for $x=\infty$, we obtain;

$$\frac{1}{2}\left(\frac{\mathrm{d}\phi}{\mathrm{d}x}\right)^2=\frac{4\pi kT}{D}\sum n_i\{\exp(-z_i\mathrm{e}\phi/kT)-1\}, \quad (2.1)$$

and therefore,

$$\frac{1}{2}\left(\frac{\mathrm{d}\phi}{\mathrm{d}x}\right)_{x=0}^2=\frac{4\pi kT}{D}\sum n_i\{\exp(-z_i\mathrm{e}\phi_0/kT)-1\}. \quad (2.2)$$

The surface charge density, $\sigma$, may be obtained directly from the potential function. To this end we make use of the general equation[14],

$$\sigma=-\int_0^\infty \rho\,\mathrm{d}x=\frac{D}{4\pi}\int_0^\infty\frac{\mathrm{d}^2\phi}{\mathrm{d}x^2}\mathrm{d}x=-\frac{D}{4\pi}\left(\frac{\mathrm{d}\phi}{\mathrm{d}x}\right)_{x=0} \quad (3)$$

The latter quantity may be read from equation (2.2)

$$\left(-\frac{4\pi\sigma}{D}\right)^2=\left(\frac{\mathrm{d}\phi}{\mathrm{d}x}\right)_{x=0}^2=\frac{8\pi kT}{D}\sum n_i\{\exp(-z_i\mathrm{e}\phi_0/kT)-1\}. \quad (4)$$

1) K. Shinoda, *Bull. Chem. Soc. Japan*, **26**, 101 (1953).
2) M. L. Corrin and W. D. Harkins, *J. Am. Chem. Soc.*, **69**, 683 (1947).
3) H. Lange, *Kolloid-Z.*, **121**, 66 (1951).
4) E. D. Goddard, O. Harva and T. G. Jones, *Trans. Faraday Soc.*, **49**, 980 (1953).
5) H. B. Klevens, *J. Phys. Chem.*, **52**, 130 (1948).
6) M. L. Corrin and W. D. Harkins, *J. Chem. Phys.*, **14**, 640 (1946).
7) S. H. Herzfeld, M. L. Corrin and W. D. Harkins, *J. Phys. Chem.*, **54**, 271 (1950).
8) K. Shinoda, *J. Phys. Chem.*, **58**, 1136 (1954).
9) H. B. Klevens, *J. Chem. Phys.*, **14**, 742 (1946).
10) H. Lange, *Kolloid-Z.*, **131**, 96 (1953).
11) K. Shinoda, *J. Phys. Chem.*, **58**, 541 (1954).
12) K. Shinoda, *J. Phys. Chem.*, **59**, No. 5 (1955).
13) H. Lange, a private communication.
14) E. J. W. Verwey and J. Th. G. Overbeek, "Theory of the Stability of Lyophobic Colloids" Elsevier Publishing Co. Inc. 1948.

Equation (4) gives the electrical potential, $\phi_0$, at the charged surface of the micelle.

If the micelle forming ion is anion, $\phi$ will be negative and $-z_i e\phi_0$ will be positive for cations, and negative for anions. As pointed out later the condition $\exp(-z_i e\phi_0/kT) \gg 1$ is satisfied[15], and the contribution of the anions and 1 in the right hand side of equation (4) can be neglected. It is apparent from (4) that the valencies or kinds of ions of the same sign as that of the long chain ions have no effect and only the valencies of ions of the opposite sign are important.

Then equation (4) gives electrical potentials in each of the following cases:

**(1) for long chain salts of uni-univalent type,**

1) with no added salt,

$$\phi_0 = \frac{kT}{e} \log \frac{2000\pi\sigma^2}{C_1 DNkT}, \tag{5.1}$$

where

$$C_1 = \mathrm{CMC} = 1000\, n_1/N,$$

2) with added uni-valent cation salt,

$$\phi_0 = \frac{kT}{e} \log \frac{2000\pi\sigma^2}{C_1 DNkT}, \tag{5.2}$$

where

$$C_1 = \mathrm{CMC} + C_1',$$

3) with added bi-valent cation salt,

$$\frac{2000\pi\sigma^2}{DNkT} = C_1 \exp(e\phi_0/kT) + C_2 \exp(2e\phi_0/kT), \tag{5.3}$$

where

$$C_1 = \mathrm{CMC},$$

4) with added tri-valent cation salt,

$$\frac{2000\pi\sigma^2}{DNkT} = C_1 \exp(e\phi_0/kT) + C_3 \exp(3e\phi_0/kT), \tag{5.4}$$

where

$$C_1 = \mathrm{CMC},$$

**(2) for long chain salts of uni-bivalent type,**

1) with no added salt,

$$\phi_0 = \frac{kT}{2e} \log \frac{2000\pi\sigma^2}{C_2 DNkT}, \tag{5.5}$$

where

$$C_2 = \mathrm{CMC}/2.$$

2) with added uni-valent cation salt,

$$\frac{2000\pi\sigma^2}{DNkT} = C_1 \exp(e\phi_0/kT) + C_2 \exp(2e\phi_0/kT), \tag{5.6}$$

where

$$C_2 = \mathrm{CMC}/2,$$

3) with added bi-valent cation salt,

$$\phi_0 = \frac{kT}{2e} \log \frac{2000\pi\sigma^2}{C_2 DNkT}, \tag{5.7}$$

where

$$C_2 = \mathrm{CMC}/2 + C_2',$$

## Comparison with Experimental Observations

For a given chain length the cohesive energy contribution will be constant; however, it is clear that in the presence of added electrolytes the ions of charge opposite to that of the long chain ions have a marked influence on micelle formation by reducing the electrical repulsive forces between the head groups of the long chain ions; or, in other words, by reducing the electrical potential on the micelle surface.

Formulae (5.1)—(5.7) can be tested by the experimental data for the CMC as a function of the concentration and valency of added salts[3,13]. The CMC of long chain salts is given as[1]

$$\log \mathrm{CMC} = \log \frac{1000}{N\nu} - \frac{m\omega}{kT} + \frac{E_{el.}}{kT} - 1, \tag{6}$$

where $\nu$ is the free volume per molecule in the micellar state, $m$ the number of carbon atoms in hydrocarbon chain, $\omega$ the surface energy change per methylene radical, passing from the bulk of the solution into the micelle, $E_{el.}$ the electrical energy change per micelle forming ion, and would be given as $Ke\phi_0$.

A reasonable alternative is to assume that the dissociation degree of the micelle forming ion is not 1 but $K$.

Considering this alternative and combining equations (5.2), (5.7) and (6), we obtain,

$$\log \mathrm{CMC} = \log \frac{1000}{N\nu} - \frac{m\omega}{kT} + \frac{K}{Z_i} \log \frac{2000\pi K^2\sigma^2}{C_i DNkT} - 1, \tag{7}$$

where $Z_i$ is the valencies of respective counterions and $C_i$ the concentrations of counterions in moles per liter.

It is expected from equation (7) that the log CMC is a linear function of log $C_i$ and the slope of this line is K for sodium dodecyl sulfate and $K/2$ for calcium dodecyl sulfate. Comparing the experimental data measured by Lange[13] with the theoretical equation, it has been found that the slope of the plot

15) A. B. D. Cassie and R. C. Palmer, *Trans. Faraday Soc.*, **37**, 156 (1941).

of log CMC versus log $C_i$ is a linear function and the slope is 0.503(=$K$) for sodium dodecyl sulfate and 0.286(=$K/2$) for Calcium dodecyl sulfate, showing good agreement with the theory*.

Introducing the CMC values of sodium and calcium dodecyl sulfates into equation (7) and substituting $K=0.54$, we obtain at $T=343°K$,

$$\frac{2000\pi K^2\sigma^2}{DNkT}=0.654\,.$$

This value is somewhat smaller than that expected from the values of $\sigma$**, $K$, $D$, $N$, $k$, and $T$, but this will be attributed to the fact that each ion contribute less charge than e to the micelle because of the accompanying counterion with the introduction of another charge.

Introducing these values into equations (5.1)—(5.7) and (6), the comparison between the theory and the experimental CMC values as a function of the concentration and valency of added salts was attained. The results are shown in Table I.

TABLE I

COMPARISON BETWEEN THE OBSERVED (BY LANGE) AND CALCULATED CMC VALUES AS A FUNCTION OF THE CONCENTRATION AND VALENCY OF ADDED SALTS AT 70°C.

| Concn. of added salt in equivalent/liter | obs. CMC | calc. CMC (moles/1.) |
|---|---|---|
| KCl or NaCl | Sodium Dodecyl Sulfate | |
| 0 | 0.0066 | 0.0067 |
| 0.01 | 0.0045 | 0.0045 |
| 0.02 | 0.00315 | 0.0030 |
| 0.05 | 0.00235 | 0.0023 |
| 0.1 | 0.0016 | 0.0016 |
| 0.2 | 0.0012 | 0.00115 |
| 0.5 | 0.00075 | 0.00065 |
| $MgCl_2$ or $CaCl_2$ | | |
| 0.0001 | 0.0060 | 0.0057 |
| 0.0003 | 0.0051 | 0.0048 |
| 0.0005 | 0.0043 | 0.0043 |
| 0.001 | 0.0039 | 0.0038 |
| 0.002 | 0.0030 | 0.0032 |
| 0.005 | 0.0022 | 0.0026 |
| 0.012 | 0.0018 | 0.0020 |
| 0.025 | 0.0015 | 0.0017 |
| 0.05 | 0.0012 | 0.0014 |
| 0.1 | 0.0010 | 0.0011 |
| 0.3 | 0.00077 | 0.0009 |
| $AlCl_3$ | | |
| 0.0007 | 0.0038 | 0.0024 |
| 0.001 | 0.0022 | 0.0022 |
| 0.002 | 0.0016 | 0.0014 |
| 0.005 | 0.0011 | 0.0011 |
| 0.01 | 0.0008 | 0.0008 |

* The value of K in the case of fatty acid soap is 0.56.

** $\delta$ is equal to the elementary charge divided by the cross sectional area of micelle forming ions.

| Concn. of added salt in equivalent/liter | obs. CMC | calc. CMC (moles/1.) |
|---|---|---|
| NaCl | Calcium Dodecyl Sulfate | |
| 0 | 0.0029 | 0.0029 |
| 0.001 | 0.00285 | 0.00285 |
| 0.004 | 0.0028 | 0.0028 |
| 0.01 | 0.0027 | 0.0027 |
| 0.02 | 0.0026 | 0.0026 |
| 0.03 | 0.0026 | 0.0024 |
| 0.05 | 0.0024 | 0.0021 |
| 0.1 | 0.0017 | 0.0015 |
| 0.2 | 0.00125 | 0.0011 |
| 0.5 | 0.00073 | 0.0006 |
| $CaCl_2$ | | |
| 0.001 | 0.0026 | 0.0028 |
| 0.005 | 0.00215 | 0.0023 |
| 0.025 | 0.00145 | 0.0016 |
| 0.1 | 0.00102 | 0.0011 |
| 0.3 | 0.00077 | 0.0008 |

It is apparent from Table I that the CMC values calculated using relations (5.1)—(5.7) show good agreement with the experimental ones. In the case of the large ionic radius of counterions or of the more concentrated system of counterions, the agreement between the theory and experiments is not so satisfactory.

## The CMC of the Mixture of Sodium and Calcium Dodecyl Sulfates

The CMC of the mixture of sodium and calcium dodecyl sulfates can also be tested with the equation (5.3) or (5.6). In this case, however, the sum of the equivalent concentration of sodium and calcium ions is equal to the CMC, i.e., $C_1+2C_2=$CMC. The comparison between the experimental and the calculated CMC values are given in Table II.

TABLE II

COMPARISON BETWEEN THE OBSERVED (BY LANGE) AND CALCULATED CMC VALUES OF MIXTURES OF SODIUM AND CALCIUM DODECYL SULFATES AT 70°C.

| mole fraction of the calcium dodecyl sulfate | obs. CMC (moles/1.) | calc. CMC (moles/1.) |
|---|---|---|
| 0 | 0.0066 | 0.0067 |
| 0.02 | 0.0057 | 0.0056 |
| 0.05 | 0.0053 | 0.0050 |
| 0.1 | 0.0049 | 0.0046 |
| 0.25 | 0.0040 | 0.0037 |
| 0.5 | 0.0034 | 0.0033 |
| 0.75 | 0.0031 | 0.0031 |
| 1 | 0.0029 | 0.0029 |

## Conclusion

Formulas for the electrical potentials of the micelle surface in various conditions are derived. Using these formulas, the comparison between the theory and the experiments was undertaken. From the good agreement between the theory and experiments, the CMC of sodium and calcium dodecyl sulfates as a function of the concentration and valency of added salts was explained quantitatively. The present investigation is applicable not only to the study of the micelle, but to the elucidation of the outstanding colloid chemical fact of the predominating influence of oppositely charged ions upon the electrical double layer.

The author wishes to express his sincere thanks to Dr. H. Lange (Henkel U. Cie, Deutschland) for his kindness in sending the numerical data of CMC to him.

*Department of Physical Chemistry, Faculty of Engineering, Yokohama National University, Minamiku, Yokohama*

# *On the Oxidation of Cellulose. II. On Celluronic Acid Prepared by a Simple Method**

By Seishi MACHIDA and Mitsumasa INANO

(Received February 24, 1955)

During the course of chemical research of natural polyuronides[1], it became desirable to obtain celluronic acid[2] for purposes of comparison.

Pigman[3] oxidized cellulose by concentrated nitric acid added with sodium nitrite. The authors[4], using his method, obtained an oxidized cellulose containing one glucuronic residue per five glucose residues. But the mean degree of polymerisation of the oxidized cellulose was about one-fourth of the original cellulose and its copper value was very high.

The present paper presents the results obtained in the oxidation of cellulose by phosphoric acid added with sodium nitrite.

## Experimental Results and Discussion

In 150 cc. of 90% phosphoric acid, 5 g. of pulp cellulose was placed and a definite quantity of solid sodium nitrite was added. The suspension was stirred and kept at constant temperature for a definite time. The suspension was then diluted with 50 cc. of water and filtered. The oxidized cellulose was suspended in 500 cc. of water, stirred, kept at least 12 hrs., and filtered. The washing was repeated in the same manner until the acidity of the filtrate vanished. The oxidized cellulose was then washed several

TABLE I

| Sample Number | Reaction time (hr.) | Reaction temp. (°C) | $NaNo_2$ (g.) | Carboxyl content (%) | Glucuronic content (%) | Glucurono lacton / Glucose |
|---|---|---|---|---|---|---|
| 1 | 1 | 10 | 0 | 0.08 | 0.31 | 1/311 |
| 2 | 1 | 10 | 2 | 2.09 | 8.17 | 1/12 |
| 3 | 1 | 10 | 5 | 2.30 | 9.00 | 1/12 |
| 4 | 1 | 15 | 10 | 7.90 | 30.90 | 1/4 |
| 5 | 1 | 20 | 15 | 16.07 | 62.85 | 3/5 |
| 6 | 1 | 20 | 20 | 18.32 | 71.65 | 2/3 |
| 7 | 1 | 20 | 2 | 4.17 | 16.31 | 1/7 |
| 8 | 1 | 25 | 5 | 11.92 | 46.62 | 1/2 |
| 9 | 1 | 20 | 10 | 9.75 | 38.13 | 1/3 |

* A portion of this paper was presented before the Annual Meeting of the Chemical Society of Japan in April, 1953 at Kyoto.

1) Reviewed in "A Summary of Chemical Studies on Polyuronides", *Bulletin of the Faculty of Textile Fibres, Kyoto University of Industrial Arts and Textile Fibres*, **1**, 116 (1954) (in English).

2) W. O. Kenyon et al., *J. Am. Chem. Soc.*, **64**, 121, 127 (1942); **69**, 342, 349, 355 (1947); **70**, 270 (1948).

3) W. W. Pigman et al., *J. Am. Chem. Soc.*, **71**, 2200 (1949).

4) S. Machida, N. Uchino and M. Inano, *J. Chem. Soc. Japan*, **74**, 204 (1953).

times with acetone and finally with ether and dried in a vacuum desiccator.

The oxidized cellulose thus obtained was a white powder, and the yield was about 90%. Carboxyl group contents determined by the calcium acetate method and the calculated theoretical glucuronic residue contents of the oxidized cellulose obtained in various reaction conditions are shown in Table I.

As is shown in the table, the highest value of the carboxyl content is 18.32%, which means that one uronic residue is present per 1.5 glucose residue in the chain molecule. The presence of the uronic group in the oxidized cellulose was confirmed by the naphthoresorcinol test. Its content was actually determined by heating the sample with 12% hydrochloric acid and estimating the furfural liberated from it. For example, Sample No. 9, was found to contain 36.5% glucurono lactone in this actual determination. The theoretical uronic residue content calculated for the same sample is 38.13%, assuming that the 9.75% value of carboxyl content is wholly due to uronic groups. Therefore, it is found that carboxyl groups of this substance are largely of the glucuronic type and only a few of them are of other types, such as the aldonic.

The mean degree of polymerisation of the oxidized cellulose was determined by the viscosity measurement of acetone solution of its nitric ester. The results obtained are shown in Fig. 1.

The solubilities of the oxidized cellulose in 1% caustic soda solution at 20°C and 100°C were determined, and are shown in Fig. 2.

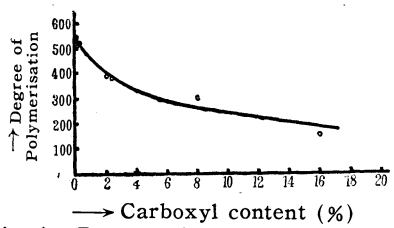



Fig. 1. Degree of polymerisation of the celluronic acids.

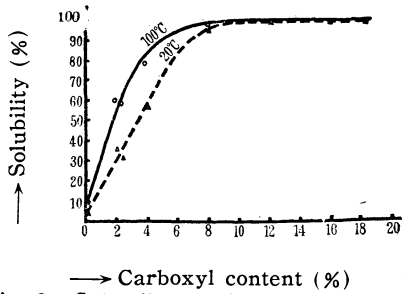



Fig. 2. Solubility of the celluronic acids in 1% caustic soda solution.

As is shown in Fig. 2, the oxidized cellulose, whose carboxyl content was more than 8%, is almost entirely soluble; and, by referring to Fig. 1, it is found that the mean degree of polymerisation of such oxidized cellulose is 322, which is nearly two-thirds that of the untreated cellulose.

These facts indicate that the oxidation of cellulose by concentrated phosphoric acid added with sodium nitrite is much more convenient; that is, the cellulose is not apt to be hydrolyzed heavily and the oxidation proceeds smoothly. The reason, perhaps, is that phosphoric acid as compared with nitric acid has weak acidity and strong ability to make cellulose swell. As the phosphoric acid group was not detected in the oxidized cellulose, it could not be considered that the phosphoric acid group combined chemically with the oxidized cellulose enhanced its solubility.

The alkaline solution of the oxidized cellulose was fluid. Furthermore it was coagulated by adding salts of alkali earth or heavy metal or a large volume of alcohol or acetone. By neutralization with acid, about 85% of the oxidized cellulose was recovered from the alkaline solution. The recovered oxidized cellulose had almost the same carboxyl group content as the original oxidized cellulose and still indicated the color reaction with naphthoresorcinol. However, it can easily be imagined that the molecules must have disintegrated.

## Summary

Cellulose was conveniently oxidized by concentrated phosphoric acid added with sodium nitrite; that is, the cellulose was not apt to be hydrolyzed heavily and the oxidation proceeded smoothly.

It was found that carboxyl groups of the oxidized cellulose were largely of the glucuronic type.

The oxidized cellulose, whose carboxyl content was more than 8%, was almost soluble in dilute caustic soda solution; and the mean degree of polymerisation of such oxidized cellulose was nearly two-thirds of that of the untreated cellulose.

Some properties of the alkaline solution of the oxidized cellulose were investigated.

The expense of this study was defrayed in part by a grant from the Hattori Hokokai, to which the authors' thanks are due.

*Chemical Laboratory of Textile Fibres, Kyoto University of Industrial Art and Textile Fibres, Kyoto*

# *Three Prototypes for the Cathodo-luminescence Spectra of Praseodymium in Various Forms of Alumina*

By Eiichi IWASE, Seijiro NISHIYAMA and Toshiaki ISONO

(Received February 23, 1955)

## Introduction

The structures of aluminas and alumina-hydrates have recently been the subject of extensive researches, the X-ray diffraction method being, as is well known, almost always employed for this purpose. The present authors have tried, in the course of the studies on the similar problems, to apply a spectrographic method of the cathodo-luminescence brought about by a certain rare earth, either praseodymium or samarium, which was imbedded in the various specimens of alumina, and have found this method fairly effective in solving such yet indistinct problems. This paper presents the finding of the three prototypes for the cathodo-luminescence spectra given by the praseodymium-bearing alumina, and at the same time the structural interpretations as well as the preparations for the samples of alumina corresponding to the yielding of these three luminescence prototypes.

## Materials and Experimental Procedures

Three samples of alumina containing praseodymium were prepared as follows.

**Sample 1.**—The hydrous alumina gel was precipitated with ammonia from the solution of aluminium sulphate, washed by decantation, filtered, and dried at about 110°C. This dried gel was soaked with a solution of praseodymium nitrate and then ignited at about 900°C for 1 hr.

**Sample 2.** — Crystals of aluminium nitrate ennea-hydrate were partially calcined at about 180°C until they became fine powders, which were then soaked with a solution of praseodymium nitrate and ignited at 1200–1300°C.

**Sample 3.** — Crystals of alumina-trihydrate produced by Bayer process, namely hydrargillite were previously calcined at about 800°C for 1 hr. The thermally decomposed product was soaked with a solution of praseodymium nitrate and then ignited at about 900°C for 1 hr.

The amount of praseodymium to be introduced was always made about 1% as oxide to the resulting sample of alumina.

The three samples mentioned above were submitted to the cathode-ray bombardment in a small Urbain tube and their luminescences thus yielded were spectrographically investigated by employing a glass-prism spectrograph of Feuss.

## Experimental Results

Fig. 1, (a), (b) and (c) shows schematically the results of the investigations on the cathodo-luminescence spectra given by the samples 1, 2 and 3 respectively. The relative intensities of the luminescence bands were estimated visually, and indicated by the heights in the figures.

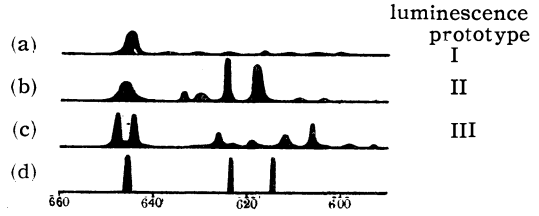



Fig. 1. Cathodo-luminescence spectra of praseodymium-bearing aluminas.

These three luminescence spectra have quite different and readily distinguishable appearances, and may be regarded as the three prototypes for the cathodo-luminescence spectra due to the praseodymium ions exisiting in various kinds of alumina.

The luminescence spectra given by the samples 1, 2 and 3 are, for convenience, called the luminescence prototypes I, II and III respectively.

## Discussions

It has generally been considered that a certain rare earth element imbedded in a colorless inorganic ground-material of definite chemical composition, will give rise to a fixed luminescence spectrum. A few exceptions have, however, been reported: When the europium or samarium is present in either magnesia or calcium sulfide, the luminescence spectrum given by one of these rare earths differs in its details rather widely, depending on the manner of preparations for the luminescent materials, although the ground-materials have the same chemical composition[1].

1) P. Pringsheim; "Fluorescence and Phosphorescence", Interscience publishers, Inc., New York, (1949), p. 470.

The luminescence of praseodymium mentioned here may provide a further noteworthy example of these interesting exceptional cases.

Rohden[2] described a definite luminescence spectrum for the praseodymium-bearing alumina as shown in Fig. 1, (d). It is concluded, from the comparison of Rohden's data with the three luminescence prototypes found by the present authors, that Rohden's spectrum seems to correspond to the prototype II.

The feature of the luminescence bands yielded by a rare earth, which has been introduced in a crystalline ground-material, is mainly determined by the transitions between electronic levels of the rare earth ion. The individual luminescence bands corresponding to these transitions may be influenced by the Stark effect owing to the electric field of the surrounding ions, and also to some extent by the lattice vibrations of the ground-material[3]. Thus the crystal structure of the ground-material would be expected to produce, in some cases, rather remarkable effects upon the feature of luminescence spectrum.

X-ray diffraction photographs have been taken of the samples 1, 2 and 3 in a Debye-Scherrer powder camera using copper $K_\alpha$ filtered radiation, and the results obtained are schematically illustrated in Fig. 2.

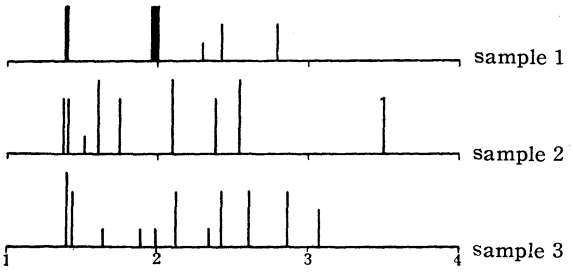



Fig. 2. Graphical representations of X-ray diffraction data for aluminas.

It will be seen that the X-ray diffraction patterns for the samples of alumina 1, 2 and 3 coincide almost entirely with those of $\gamma$-[4], $\alpha$-[5] and $\kappa$-[6] modifications of alumina respectively.

The oxygen arrangement in alumina is hexagonal close-packed for $\alpha$-modification, while it is cubic close-packed for the $\gamma$- and $\kappa$-modifications.

The aluminium ions of the $\alpha$-modification are situated in the octahedral interstices of the oxygen networks, and this configuration of alumina yields decisively the luminescence prototype II of the praseodymium.

In the case of $\gamma$-modification the aluminium ions are said to be situated statistically in the octahedral and tetrahedral interstices of the cubic close-packed oxygen networks evenly, and it may therefore be assumed that the praseodymium ions introduced in this modification of alumina will also be distributed at random through these two kinds of interstices. The luminescence prototype I of the praseodymium given by the $\gamma$-modification of alumina may accordingly be considered as the luminescence spectrum of the praseodymium in solution.

It is also found that the praseodymium contained in an optically isotropic substance, namely ordinary glass emits the cathodo-luminescence spectrum almost similar to that of the prototype I. This fact seems to support the above reasoning.

Ervin[7] has recently postulated the position occupied by aluminium ions in the oxygen networks of cubic close-packing, by taking the intensity of the line at 1.985–2.03 Å observed in X-ray diffraction patterns into considerations. This line is caused by the reflection from (400) planes of the spinel lattice, which include all the oxygen positions and the octahedral aluminium positions, but not the tetrahedral aluminium positions. It is to be remarked that this line is found to be weak in the $\kappa$-modification of alumina as compared with the $\gamma$-modification. Provided the postulation described above is valid for the $\kappa$- and $\gamma$- modifications of alumina, the conclusion may then be drawn that the aluminium ions in the $\kappa$-modification should be situated much more predominantly in the tetrahedral rather than the octahedral interstices of oxygen networks.

The praseodymium-luminescence of the prototype III can be seen distinctly only in the case of the praseodymium-bearing alumina, which has been derived from the hydrargillite through the special previous heat treatment.

The practical thermal decomposition of hydrargillite is, at the present, considered to proceed simultaneously through dual routes[8], the one through boehmite followed by a

2) A. de Rohden, *Ann. chim.*, [9] 3, 361 (1915).

3) R. Tomaschek, *Acta Phys. Polonica*, 6, 401 (1936).

4) H. C. Stumpf, A. S. Russell, J. W. Newsome, and C. M. Tucker, *Ind. Eng. Chem.*, 42, 1402 (1950).

5) H. Thibon, J. Charrier and R. Tertian, *Bull. soc. chim. de Fr.*, [5] 18, 387 (1951).

6) J. F. Brown, D. Clark and W. W. Elliott, *J. Chem. Soc.*, 1953, 86.

7) G. Ervin, *Acta Cryst.*, 6, 106 (1953).

8) J. F. Brown, D. Clark and W. W. Elliott, *J. Chem. Soc.*, 1953, 85; M. R. B. Day and V. J. Hill, *Nature*, 170, 539 (1952); *J. Phys. Chem.*, 57, 946 (1953).

series of virtually anhydrous alumina, namely $\gamma$-, $\delta$- and $\theta$-modifications, and the other directly through a sequence of other virtually anhydrous alumina, namely $\chi$- and $\kappa$-modifications, both of these routes leading eventually to a common product, the $\alpha$-modification. Irrespective of whether the formation of boehmite is of primary[9] or of secondary origin[10], it seems to be almost certain that the thermal decomposition of hydrargillite forks off in practice into two branches on the way of the transformation to the $\alpha$-modification of alumina. In the route of conversion directly via the anhydrous aluminas, for example the $\kappa$-alumina, the aluminium ions tend to be arranged in the tetrahedral interstices of the cubic close-packed oxygen networks. This arrangement seems to be characteristic of the thermal transformation sequence derived from the hydrargillite and responsible for giving rise to the luminescence prototype III of praseodymium.

## Conclusion

Almost all the cathodo-luminescence spectra given by the various preparations of the praseodymium-bearing alumina can be regarded as belonging to either one of the three prototypes (I, II and III) or their combinations.

The occurrence of these three fundamental spectral types for the praseodymium-luminescence may closely be related with the three ways for the reciprocal arrangements of oxygen and aluminium in the configuration of alumina.

The prototype II of the praseodymium-luminescence spectrum is obtained for the alumina with the oxygen network of hexagonal close-packing, namely the $\alpha$-modification.

The alumina with the oxygen network of cubic close-packing, shows either the luminescence prototype I or III, depending upon the location of aluminium ions. The prototype I is seen in the $\gamma$-modification of alumina, where the aluminium ions are statistically distributed evenly throughout the two sorts of interstices of the oxygen network, namely octahedral and tetrahedral interstices, while the luminescence prototype III is yielded with the $\kappa$-modification of alumina, in which the aluminium ions take their seats in the tetrahedral rather than in the octahedral interstices.

In connection with the X-ray investigations here included thanks are due to Dr. M. Nakahira. The authors are also grateful to the Ministry of Education for the Scientific Research Encouragement Grant in aid of this work.

*The Institute of Scientific Researches, Komagome, Bunkyo-ku, Tokyo*

9) J. E. Brown, D. Clark and W. W. Elliott, *J. Chem. Soc.*, **1953**, 85.
10) M. K. B. Day and V. J. Hill, *Nature*, **170**, 539 (1952); *J. Phys. Chem.*, **57**, 946 (1953).

# *Cathodo-luminescence as Applied to the Detection of Rare Earths Contained in Some Natural Calcareous Substances*

By Eiichi IWASE

(Received February 23, 1955)

## Introduction

Crookes detected minute amounts of yttrium and samarium in calcareous portions of some marine organisms. It has been said that this fact led him to a confirmation of the presence of rare earths in sea water.[1] Goldschmidt found rare earths also in the calcium carbonate, which constitutes reef corals.[2] As is well known, some of the rare earths contained in calcium oxide behave as activators in giving the characteristic luminescence under the cathode-ray bombardment, the spectra of which consist of fairly sharp line-like bands. This phenomenon proved already to be an efficacious aid in making some geochemical researches: Rare earths sparingly present in anorthite and

1) Cited in V. M. Goldschmidt, *J. Chem. Soc.*, **1937**, 667.

2) V. M. Goldschmidt, *J. Chem. Soc.*, **1937**, 667.

TABLE I

CATHODO-LUMINESCENCE SPECTRA DUE TO RARE EARTHS CONTAINED IN CONVERTED CALCIUM-OXIDE SAMPLES

| Wave-length | Miyako Main Isle | | Akiyoshi | Hiroshima |
|---|---|---|---|---|
| (mμ) | *Acropora* | *Pocillopora* | Stalactite | *Licina* |
| 648.0 | w | — | wwb | — |
| 639.5 | w | — | wwb | — |
| 633.4 | m | w | m | — |
| 626.0 | s | w | s | — |
| 620.0 | ww | — | w | — |
| 616.0 | w | ww | w | — |
| 613.2 | w | — | w | — |
| 606.6 | ss | m | ss | w |
| 604.6 | m | — | s | — |
| 596.5<br>594.0 | ww | — | w | — |
| 590.3 | ww | — | — | — |
| 588.0 | w | w | w | — |
| 585.2 | ss | m | s | w |
| 583.4 | w | — | w | — |
| 580.5 | w | — | ww | — |
| 578.5 | w | — | ww | — |
| 575.9 | w | w | w | — |
| 571.3 | w | — | w | — |
| 568.3 | — | — | ww | — |
| 558.6 | — | — | ww | — |
| 555.0<br>552.1 | ww | — | ww<br>w | — |
| 549.2 | — | — | w | — |
| 546.3 | w | — | ww | — |
| 543.3 | — | — | w | — |
| 537.0 | — | — | w | — |
| 517.0 | — | — | ww | — |
| 500.0<br>499.0 | ww | — | ww | — |
| 494.6 | ww | — | ww | — |
| 489.8 | w | — | ww | — |
| 486.9 | ww | — | w | — |
| 483.8 | ww | — | ww | — |
| 481.7 | ww | — | ww | — |
| 479.9 | w | w | ww | — |
| 477.0 | ww | ww | — | — |
| 460.5 | — | — | ww | — |
| 457.2 | — | — | w | — |
| 454.3 | — | — | ww | — |
| 448.5 | — | — | ww | — |
| 439.0 | — | — | ww | — |
| 436.9 | — | — | w | — |
| 421.8 | — | — | ww | — |
| 421.0 | — | — | ww | — |
| 419.5 | — | — | ww | — |
| 418.0 | — | — | ww | — |
| 416.0 | — | — | ww | — |
| 415.0 | — | — | ww | — |
| 413.5 | — | — | ww | — |
| 411.8 | — | — | ww | — |

ordinary augite from Taga volcanoes in Shizuoka Pref. were investigated by means of the cathodo-luminescence spectra, which appeared in one paper[3] entitled "A short note relating to the evolution of magma", and the detection of rare earths was also made by the inspection of cathodo-luminescence spectra, which is seen in another paper[4] entitled "On the crystallisation of fluorites," regarding two kinds of samples of fluorite from Tateiwa village, Fukushima Pref. one is a green octahedral crystal crystallised at an earlier stage and the other a violet cubic one at a later stage.

In the present paper the applicability of the cathodo-luminescence method to the detection of rare earths is revealed on such natural calcareous substances as reef coral, stalactite, molluscan fossil and calc-sinter.

## Materials and Experimental Procedures

Seven specimens were used in the experiments; two reef corals, one stalactite, one molluscan fossil, and three calc-sinters. Two kinds of reef corals from Miyako Main Isle, *Pocillopora Sp.* and *Acropora variabilis Verrill* are reproduced in Figs. 1 and 2 respectively. The former is of amber white antler form and the latter has an appearance closely resembling a group of small flower clusters, like those of a cauliflower. It is to be mentioned that the *Acropora* is soluble in hydrochloric acid without any perceptible residues,

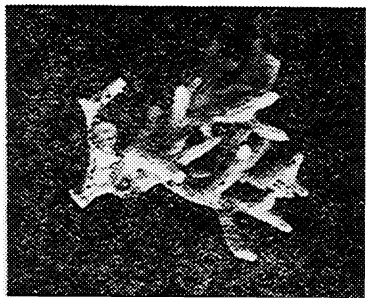


Fig. 1. *Pocillopora sp.*

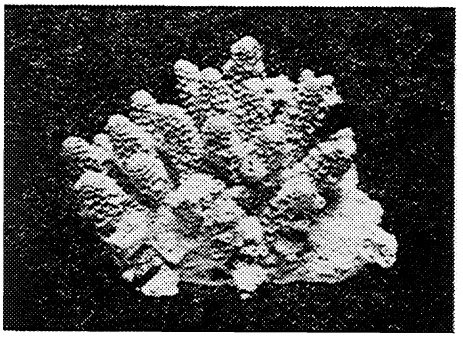


Fig. 2. *Acropora variabilis verrill.*

3) E. Iwase, *J. Chem. Soc. Japan*, **63**, 633 (1941).
4) E. Iwase, *Bull. Inst. Phys. Chem. Researches* (Tokyo), **21**, 61 (1942).

while the *Pocillopora* leaves a thin transparent yellow cuticular sack after the same treatment.

An ochrey stalactite from Akiyoshi in Yamaguchi Pref. shows, when cut crosswise, onyx-like banding near the periphery and radiated structures in the center portion.

A molluscan fossil, *Licina (Anodontia) Sp.*, which was found at Hiroshima city, is greasy, translucent and stained with reddish brown tint.

Calc-sinters occurring at Senami springs in Niigata Pref., Miné springs is Shizuoka Pref. and Shirahone springs in Nagano Pref. were also delivered to the author.

About 10 g. of each specimen were dissolved in hydrochloric acid, the solution thus produced was made slightly acidic by the controlled addition of ammonia, and then 2 g. of oxalic acid were added. Rare earths, if present in the original specimen, would have been coprecipitated with calcium as oxalates, which would then be converted to the oxide-form by the calcination. The same procedure is repeated once more, the only difference being the application of a much smaller amount of oxalic acid (0.5 g.). In this way the concentration of rare earths in calcium oxide is increased about fifty times, compared with that in the original specimen. The converted calcium oxide thus obtained is subjected to the cathode-ray bombardment in a small Urbain tube and the luminescence brought about is spectrographically investigated by employing a glass-prism spectrograph of Feuss.

## Experimental Results and Discussions

The results of cathodo-luminescence spectra given by the converted calcium-oxide samples from reef corals, stalactite and molluscan fossil are summarised in Table I. Relative intensities are estimated visually and indicated by the following symbols: ss(very strong), s(strong). m(medium), w(weak), ww(very weak) and b(broad).

TABLE II
RARE EARTHS DETECTED BY CATHODO-LUMINESCENCE BANDS

| Localites | Specimens | Rare earths identified |
|---|---|---|
| Miyako Main Isle | *Acropora* | Dy, Pr, (Sm), (Tb) |
| | *Pocillopora* | Dy, Pr, (Sm) |
| Akiyoshi | stalactite | Dy, Pr, Sm, Tb |
| Hiroshima | *Licina* | Dy, Pr |

The presence of dysprosium and praseodymium in these four specimens is confirmed, as illustrated in Table II, by comparing the wave-lengths of the observed luminescence bands with Fagerberg's data[5], which give the precise numerical figures for the wave-lengths of the cathodo-luminescence bands yielded by the calcium oxide containing each individual rare earth element. Furthermore,

5) S. Fagerberg, *Nova Acta Regiae Societatis Scientiarum Upsaliensis*, Ser. IV, Vol. 7, No. 6 (1931).

samarium and terbium are distinctly detected in the stalactite and also perceptible in the *Acropora*, whereas not at all in the molluscan fossil. Under the conditions of the present experimental work, none of the calc-sinters investigated here revealed the presence of rare earths.

To be precise, the concentration of rare earths in the samples of converted calcium oxide has been increased 45 and 67 times for the *Acropora* and the *Pocillopora* respectively. It is a remarkable fact that the luminescence bands due to dysprosium, samarium and terbium have been all distinctly visible in the case of *Acropora variabilis Verrill*, but have been, in the case of *Pocillopora Sp.*, found much weaker in intensity with the complete disappearance of the terbium bands, although the latter specimen has been subjected to a considerably higher concentrating treatment than the former one. These observations may possibly be interpreted by a distinction found between the surface conditions of the two reef corals; *Acropora variabilis Verrill* seems to be naked, while the surface of *Pocillopora Sp.* is covered by a thin superfacial membrane of organic nature, which would be expected to exercise various restricting influences on the assimilation of rare earths from sea water during the natural growing process of the reef corals.

**Summary**

Specimens of reef corals, stalactite, molluscan fossil and calc-sinters were converted to the form of oxide, in which rare earths, if present in the original specimens, would be concentrated by chemical means. Luminescence spectra given by these samples of calcium oxide were investigated under the cathode-ray bombardment and the presence of minute amounts of rare earths could be confirmed; dysprosium, praseodymium, samarium and terbium in a stalactite from Akiyoshi, dysprosium, praseodymium and presumably samarium in reef corals from Miyako Main Isle, and dysprosium and praseodymium in a molluscan fossil from Hiroshima. Not even slight traces of rare earths were perceived in calc-sinters from several springs, so far as this detecting method was concerned. Two kinds of specimens of reef corals from the same locality gave a remarkable difference in the rare-earth content and this observation may be explained by the different conditions of the surfaces found in these reef corals, during the growth of which the assimilation of the rare earth ions from sea water were possibly much more disturbed by the existence of an organic membrane covering the surface of one specimen as compared with another lacking such a membrane.

*The Institute of Scientific Researches,*
*Komagome, Bunkyo-ku, Tokyo*

# *A Relation between Bond-orders and Bond-lengths of C-Cl Bonds in Conjugated Systems: An Example of the Order-length Relation for Bonds other than C-C Bonds*

By Tosinobu ANNO and Akira SADÔ

(Received January 20, 1955)

## Introduction

By the method of molecular orbital, Coulson[1] has found a relation between bond-order and bond-length in C-C bonds in conjugated systems and derived the relation theoretically. If the order of a bond is known, this relation can be used to predict the bond distance except in special cases. However, as is mentioned by Coulson[2], such a theoretical order-length relation has not yet been derived for other bonds than C-C bonds.

It is the purpose of this paper to show that a relation similar to that for C-C bonds does exist also for C-Cl bonds. The theoretical relation which we present here is similar in form to that given by Coulson and predicts the bond-length from the bond-

1) C.A. Coulson, *Proc. Roy. Soc.* (London), **A169**, 413 (1939).

2) C.A. Coulson, *J. Phys. Chem.*, **56**, 311 (1952).

order which agrees very well with the observed length.

## Theoretical

We shall use the simple LCAO molecular orbital method. The total energy $E$ of $\pi$-electrons is shown to be

$$E=\sum_{r=1}^{k} q_r\alpha_r+2\sum\sum_{i<j} p_{ij}\beta_{ij},$$

where $\alpha_r$ and $\beta_{ij}$ are usual coulomb and resonance integrals and $q_r$ and $p_{ij}$ denote the formal charge and the mobile bond order, respectively.

Consider a hypothetical state where all $\pi$-electrons are localized at "original" atoms giving those $\pi$-electrons, i.e. where $\pi$-bonds are not formed. Then the total $\pi$-electron energy would be

$$E_0=\sum_{r=1}^{k} q_r^*\alpha_r,$$

where $q_r^*$ denotes the number of $\pi$-electrons localized at atom $r$. The binding energy of $\pi$-electrons is the energy difference between the actual and the hypothetical state. Allowing for the compression of the $\sigma$-bond, minimization of the total energy (including both the $\sigma$- and $\pi$-energies) with respect to the internuclear distance at constant $p_{ij}$'s and $q_r$'s gives,[1),3)]

$$\sigma_{ij}(x_{ij}-s_{ij})+2p_{ij}(\partial\beta_{ij}/\partial x_{ij})=0, \qquad (1)$$

where $x_{ij}$ is the bond-length of bond $i$-$j$, $\sigma_{ij}$ is its single bond force constant and $s_{ij}$ is the single bond distance.

For the C-Cl bond, we cannot use as standards the single and double bonds to obtain the functional variation of $\beta$ with $x$, since there is no double bond between carbon and chlorine atoms. Instead of the double bond, however, we can take up a C-Cl bond whose mobile order is as near to unity as possible. For this purpose we take the C-Cl bond in chloroacetylene, whose mobile order $p_a$ is calculated at 0.661 (see below). Let us consider a C-Cl bond whose mobile order and bond-length are $p_a$ and $x$, respectively. The $\pi$-electron energy of this bond can be expressed by $2p_a\beta_{C\text{-}Cl}$ where $\beta_{C\text{-}Cl}$ is the resonance integral in this C-Cl bond. On the other hand, taking the methyl chloride and chloroacetylene molecules as standards, considerations similar to the case of C-C bonds[1),3)] show that this $\pi$-electron energy is

$$E_a^0-E_s^0+(1/2)\kappa_a(x-d_a)^2-(1/2)\sigma(x-s)^2,$$

where $E_a^0$, $E_s^0$; $\kappa_a$, $\sigma$ and $d_a$, $s$ are the bond energies, force constants and the internuclear distances in C-Cl bonds in the chloroacetylene and methylchloride molecules, respectively. Equating this to $2p_a\beta_{C\text{-}Cl}$, differentiation with respect to $x$ gives

$$2p_a(\partial\beta_{C\text{-}Cl}/\partial x)=\kappa_a(x-d_a)-\sigma(x-s). \qquad (2)$$

Combining Eqs. (1) and (2) it follows that

$$x=s-\frac{s-d_a}{1+\frac{\sigma}{\kappa_a}\left(\frac{1-p'}{p'}\right)}, \qquad (3)$$

where $p'=p/p_a$.

## Test of the Theory

We have calculated the bond-order for the C-Cl bond in some molecules and the result is shown in Table I. In calculating the bond-order the following assumptions were made.

TABLE I

CALCULATED BOND-ORDERS AND OBSERVED BOND-LENGTHS OF SOME C-Cl BONDS

| Molecule | Bond-length*(Å) | Bond-order** |
|---|---|---|
| Chloromethane | 1.77 | (1.00) |
| *trans*-Dichloroethylene | 1.69 | 1.29 |
| 1,3,5-Trichlorobenzene | 1.69 | 1.32 |
| Dichloroacetylene | 1.64 | 1.55 |
| Chloroacetylene | 1.63 | 1.66 |

* These values are taken from reference 9 in text. All values are determined by electron diffraction except for chloroacetylene. The value for chloroacetylene is determined by microwave spectroscopy.

** It should be noted that the figures given here are for total bond orders defined by $(1+p_{ij})$, where $p_{ij}$'s are mobile orders.

(i) The coulomb integral at an atom is proportional to its electronegativity scale[4)] given by Pauling[5)].

(ii) The resonance integral $\beta_{ij}$ is zero when $i$ and $j$ refer to non-neighboring atoms. When $i$ and $j$ refer to neighboring atoms $\beta_{ij}$ is proportional to the overlap integral $S_{ij}$ between these two atoms[6)]. The overlap integral is available in the table by Mulliken et al.[7)].

(iii) The ratio of the coulomb integral $\alpha_C$ at the carbon atom in benzene to the resonance integral $\beta_{CC}$ for the C-C bond in the same molecule is

$$\alpha_C/\beta_{CC}=3.9^{8)}.$$

3) J. E. Lennard-Jones, *Proc. Roy. Soc.* (London), A158, 280 (1937).

4) C. Sandorfy, *Bull. soc. chim. France*, **1949**, 615.

5) L. Pauling, "The Nature of the Chemical Bond", Cornell University Press, Ithaca, New York, (1940).

6) G.W. Wheland, *J. Am. Chem. Soc.*, **64**, 900 (1942).

7) R.S. Mulliken, C.A. Rieke, D. Orloff and H. Orloff, *J. Chem. Phys.*, **17**, 1248 (1949).

8) S. Nagakura, This Bulletin, **25**, 164 (1952).

(iv) The overlap integral is negligible throughout. The empirical internuclear distances are also given in Table I.

If internuclear distances and bond-orders are plotted in a diagram we can expect a simple relation between them. In Fig. 1 the

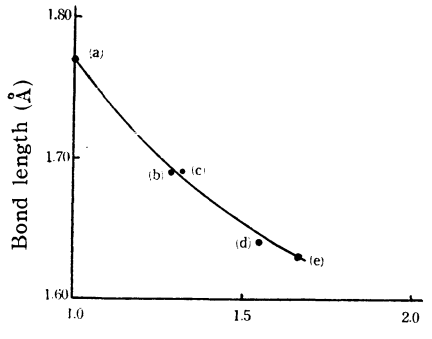



Fig. 1. Relation between bond-order and bond-length in C-Cl bonds. Points represent observed bond-lengths versus calculated bond-orders. Curve is the graphical representation of Eq. (3) (see text).

*a*, Chloromethane;
*b*, *trans*-Dichloroethylene;
*c*, 1,3,5,-Trichlorobenzene;
*d*, Dichloroacetylene;
*e*, Chloroacetylene.

curve of Eq. (3) is drawn, accepting the following numerical values.

$$s=1.77\ \text{Å}^{9)} \qquad d_a=1.63\ \text{Å}^{9)}$$
$$\sigma=3.64\times10^5\ \text{dynes/cm.}^{10)}$$
$$\kappa_a=5.52\times10^5\ \text{dynes/cm.}^{11)}$$

Points in the figure represent the calculated bond-orders and the observed bond-lengths. Fig. 1 shows that these points lie on the theoretical curve within experimental error. Therefore a similar equation as the one for the C-C bond can be seen to be available also for the other bond if the suitable reference molecule is chosen (for example, for C-Cl bonds the chloroacetylene molecule).

However, the effects of hybridization, charge distribution and the repulsion of non-bonding electrons must be taken into consideration.

Hybridization effect can be considered in the same way as in the case of the C-C bond. For various C-Cl bonds, the hybridization ratio of the $\sigma$-atomic orbital of the chlorine atom can be considered as approximately constant in all cases. Only the variation in the hybridization ratio of the carbon atomic orbital needs to be considered. Accepting Coulson's result (see Fig. 2 of reference 12) which shows carbon atomic radius as the function of the hybridization ratio, a separate order-length curve should apply according to the hybridization of the carbon $\sigma$-atomic orbital. However, our insufficient knowledge concerning the geometrical structure of polyatomic molecules will invalidate such a treatment. It is to be noted that Coulson's result shows that the difference between carbon atomic radii corresponding to $sp$ and $sp^3$ hybridizations is 0.035 Å.

It is true that the effect of the charge distribution must be taken into account in cases where the migration of the charge is large, but for C-Cl bonds in molecules whose bond-orders are calculated here, the effect of the charge distribution considered as described by Coulson[12] amounts only to a few thousandths of an angstrom which may be immaterial.

The effect due to the repulsion of non-bonding electrons would have to be considered in the absolute calculation of bond length. For bonds between a particular pair of atoms this type of effect can be considered as constant. Therefore in the relative calculation using the order-length curve, this effect may cancel out.

Thanks are due to Prof. S. Imanishi who read this manuscript.

*Department of Chemistry, Faculty of Science, Kyushu University, Fukuoka*

9) Landolt-Börnstein, "Zahlenwerte und Funktionen", Springer, Berlin, (1951).
10) G. Herzberg, "Infrared and Raman Spectra of Polyatomic Molecules," D. Van Nostrand Co. Inc., New York (1945), p. 193.
11) W. S. Richardson and J.H. Goldstein, *J. Chem. Phys.*, **18**, 1314 (1950).
12) C. A. Coulson, Contribution à l'étude de la structure moléculaire, Desoer, Liège (1948), p. 15.

# *Infrared and Raman Spectra of Pyridine N-Oxide*

By Mitsuo Ito and Norisuke Hata*

(Received January 13, 1955)

In a previous work[1], we have observed the ultra-violet absorption spectrum of pyridine N-oxide vapor with a complex vibrational structure. In order to carry out the vibrational analysis of this spectrum, assignments of the fundamental frequencies of pyridine N-oxide molecule are required, but we had no datum available for this.

In the present paper, infrared and Raman spectra of pyridine N-oxide have been measured under various conditions, and assignments based on these data are presented.

## Experimental

The sample of pyridine N-oxide was prepared according to the procedure of Ochiai[2] and was purified by repeated vacuum distillations. All precautions were taken to eliminate the absorption of atmospheric moisture by the sample.

The Raman spectrograph used in this investigation was a spectrograph with two dense flint glass prisms constructed in our laboratory, having a linear dispersion of 24 A/mm. at 4500 Å. Raman spectrum of pyridine N-oxide was obtained for both the liquid and the solution. For the liquid, hot water was circulated through the outer jacket of Wood's tube during the exposure in order to prevent the formation of crystal (the melting point of pyridine N-oxide is 59°C). For the solutions, chloroform, ethyl alcohol and water were used as solvents and concentration of each solution was about 20 g. pyridine N-oxide/20 cc. solvent. The Raman data for these conditions are listed in Table I, together with relative intensities based upon an arbitrary value of 5 for the strongest Raman line on the spectrogram. Although very broad Raman lines are also observed near 3000 $cm^{-1}$, they are not included in the table on account of their doubtful values.

Table I

Infrared and Raman frequencies of pyridine N-oxide ($cm^{-1}$)

| Infrared | | | Raman | | | | | |
|---|---|---|---|---|---|---|---|---|
| Solid | Chloroform solution | Ethyl alcohol solution | Liquid | Chloroform solution | Ethyl alcohol solution | Water solution | Average | Assignment |
| | | | 281 (1) | | 286 (1) | | 283 | $\nu_1$ non-planar O bending vib. |
| | | | 375 (1) | 371 (0) | | | 373 | $\nu_2$, ($B_2$), ring vib. |
| | | | | | 402 (1) | | 402 | $\nu_3$, ($A_2$), ring vib. |
| 482 w | | | 477 (0) | | 480 (1) | | 478 | $\nu_4$, planar O bending vib. |
| 512 w | | | | | | | 512 | |
| 546 w | | | | 548 (0) | 550 (1) | | 549 | $\nu_5$, ($A_1$), ring vib. |
| | | | 635 (1) | | 638 (3) | 641 (1) | 638 | $\nu_6$, ($B_1$), ring vib. |
| 679 s | | | 687 (1) | 660 (3) | | | 674 | $\nu_7$, ($B_2$), non-planer H bending vib. |
| | 803 m | | | | | | 803 | 2×402 |
| | 835 s | 835 s | 833 (4) | 832 (4) | 835 (4) | 829 (3) | 832 | $\nu_8$, ($A_1$), O stretching vib. |
| | 880 w | | | | | | 880 | 402+478 |
| | 902 m | 910 w | | | | | 906 | |
| | 1015 s | 1011 m | 1015 (5) | 1015 (5) | 1015 (5) | 1015 (5) | 1015 | $\nu_9$, ($A_1$), ring vib. |
| | 1044 w | | | | | | 1044 | 402+638 |
| | 1055 w | | | | | | 1055 | 512+549 |
| | 1096 w | | | | | | 1096 | 2×549 |
| | 1180 s | 1185 s | 1143 (2) | 1158 (3) | 1177 (3) | 1177 (3) | 1170 | $\nu_{10}$, ($A_1$), planar H bending vib. |
| | | 1240 s | 1239 (3) | 1250 (1) | 1240 (2) | | 1243 | $\nu_{11}$, ($B_1$), planar H bending vib. |
| | 1285 s | | | | | | 1285 | 2×638 |
| | | | 1312 (4) | 1318 (3) | 1329 (4) | 1327 (4) | 1321 | $\nu_{12}$, ($B_1$), planar H bending vib. |
| | 1386 w | | | | | | 1386 | 549+832, 373+1015 |
| | 1402 w | | | | | | 1402 | |

* Present address, Department of Pharmacy, Nagasaki University, Nagasaki.

1) M. Ito and N. Hata, This Bulletin, 28, 260 (1955).
2) E. Ochiai, *J. Org. Chem.*, 18, 534 (1953).

| Infrared | | | Raman | | | | | |
|---|---|---|---|---|---|---|---|---|
| Solid | Choro-from solution | Ethyl alcohol solution | Liquid | Choro-from solution | Ethyl alcohol solution | Water solution | Average | Assignment |
| | 1473 s | 1466 m | 1469 (2) | 1466 (2) | 1466 (2) | | 1467 | $\nu_{13}$, ($A_1$), ring vib. |
| | 1608 s | 1608 m | 1599 (5) | 1604 (5) | 1608 (5) | 1606 (5) | 1605 | $\nu_{14}$, ($A_1$), ring vib. |
| | 1720 m | 1680 m | | | | | 1700 | |
| | 1864 w | | | | | | 1864 | 832+1015 |
| | 1968 w | | | | | | 1968 | 638+1321 |
| | 2050 w | 2015 w | | | | | 2032 | 2×1015 |
| | 2100 w | | | | | | 2100 | |
| | 2472 m | 2435 w | | | | | 2452 | |
| | 2926 s | | | | | | 2926 | $\nu_{15}$, H stretching vib. |
| | | 2990 w | | | | | 2990 | |
| | 3084 m | | | | | | 3084 | 1467+1605 |
| | 3223 w | | | | | | 3223 | 2×1605 |

$\nu$ represents fundamental vibration.

An infrared spectrum was obtained with a Perkin-Elmer model 112 spectrometer with NaCl and KBr prisms. Measurements were made in the region of KBr for the solid sample and in the region of NaCl for the chloroform and alcohol solutions.* The frequencies of infrared absorption maxima are given in Table I, together with the Raman data. The abbreviated notations for absorption intensity, w, m and s represent weak, medium and strong, respectively.

## Discussion

If the oxygen atom of pyridine N-oxide lies on a straight line connecting the nitrogen atom with the opposite carbon atom in the pyridine ring, symmetry of this molecule belongs to a point group $C_{2v}$, like that of the parent molecule pyridine. This structure is the most possible one and the other structures (point group $C_2$ and $C_s$) are difficult to consider. Here, assignments of the fundamental frequencies are carried out on the basis of the $C_{2v}$ symmetry.

**Ring Vibration.**—As the heterocyclic ring of pyridine N-oxide is similar to that of pyridine, the ring vibration frequencies and their normal modes of the two molecules must also be similar to each other. On the other hand, the chemical similarity between benzene and pyridine is well known and electron diffraction[3], infrared and Raman data[4] show that the ring structures of benzene and pyridine are almost the same. Therefore, it is expected that the ring vibration frequencies of pyridine N-oxide should nearly coincide with those of benzene or its derivatives. That this is actually the case for the fundamental frequencies, 373($\nu_2$), 402($\nu_3$), 1015($\nu_9$), 1467($\nu_{13}$) and 1605 $cm^{-1}$($\nu_{14}$), can be recognized in Table II, where numbers in the first column denote the normal modes for the vibrations of monodeuterobenzene shown in Fig. 1[5]. Accordingly, it is evident that these vibrations belong to the ring vibrations with almost the same normal

TABLE II

RING VIBRATIONS OF BENZENE, MONODEUTEROBENZENE, PYRIDINE AND PYRIDINE N-OXIDE

| Normal mode[a] for monodeutero-benzene (Fig. 1) | Benzene[a] | Monodeutero-[a] benzene | Pyridine[b] | Pyridine N-oxide | Symmetry class ($C_{2v}$) |
|---|---|---|---|---|---|
| I | 405 | 380 | 374 | 373 ($\nu_2$) | $B_2$ |
| II | 405 | 405 | 404 | 402 ($\nu_3$) | $A_2$ |
| III | 605.6 | 601 | 604 | 549 ($\nu_5$) | $A_1$ |
| IV | 605.6 | 603 | 604 | 638 ($\nu_6$) | $B_1$ |
| V | 1010 | 1006.8 | 1028 | 1015 ($\nu_9$) | $A_1$ |
| VI | 1485 | 1480 | 1485 | 1467 ($\nu_{13}$) | $A_1$ |
| VII | 1596 | 1591.1 | 1580 | 1605 ($\nu_{14}$) | $A_1$ |

a) Reference 5) b) Reference 4)

* The authors are indebted to Prof. S. Akiyoshi and Mr. T. Matsuda of Engineering Department of Kyushu University for tracing the infrared spectra.

3) Schomaker and Pauling, *J. Am. Chem Soc.*, 61, 1769 (1939).

4) C.H. Kline and J. Turkevich, *J. Chem. Phys.*, 12, 300 (1944).

5) C.K. Ingold and his coworkers, *J. Chem Soc.*, 1946 299 and 316.

TABLE III
HYDROGEN BENDING VIBRATIONS OF BENZENE, MONODEUTEROBENZENE, PYRIDINE AND PYRIDINE N-OXIDE

| Normal mode[a] for monodeutero-benzene (Fig. 1) | Benzene[a] | Monodeutero-benzene[a] | Pyridine[b] | Pyridine N-oxide | Symmetry class ($C_{2v}$) |
|---|---|---|---|---|---|
| VIII | 671 | 698 | 652 | 674 ($\nu_7$) | $B_2$ |
| IX | 1110 | 1158.2 | 1139 | 1243 ($\nu_{11}$) | $B_1$ |
| X | 1178 | 1175.6 | 1139 | 1170 ($\nu_{10}$) | $A_1$ |
| XI | 1326 | 1292 | 1290 | 1321 ($\nu_{12}$) | $B_1$ |

a) Reference 5). b) Reference 4).

modes as those of the corresponding vibrations of monodeuterobenzene.

In addition to these, the vibrations of 549 $cm^{-1}(\nu_5)$ and 638 $cm^{-1}(\nu_9)$ are also the ring vibrations and can be interpreted as the $A_1$ and $B_1$ component vibrations deriving from the doubly degenerate $E_g^+$ vibration of benzene (605.6 $cm^{-1}$). This assignment seems to be reasonable from the fact that in monohalogenated benzenes, for example, $A_1$ component vibration shifts to lower frequency than 605.6 $cm^{-1}$ and $B_1$ component vibration to higher frequency[6].

**Hydrogen and Oxygen Bending Vibrations.**—The frequency 674 $cm^{-1}(\nu_7)$ is assigned to the non-planar hydrogen bending vibration (mode VIII in Fig. 1) on the basis of its frequency value and on analogy with the frequencies of the corresponding vibrations in other molecules (Table III). In the cases of benzene and pyridine derivatives, planar hydrogen bending vibrations generally possess their characteristic frequencies in the region of 1100~1300 $cm^{-1}$ [6]. Pyridine N-oxide have three fundamental frequencies, 1170 $cm^{-1}$ ($\nu_{10}$), 1243 $cm^{-1}(\nu_{11})$, and 1321 $cm^{-1}(\nu_{12})$, in this region. As seen from Fig. 1, the planar hydrogen bending vibrations with X and XI normal modes might be expected to be almost unchanged in their frequencies on passing from benzene to pyridine N-oxide, but the vibration frequency with IX normal mode should be greatly changed in pyridine N-oxide as the result of a considerable contribution of planar oxygen bending vibration. Therefore, as shown in Table III, 1170 $cm^{-1}(\nu_{10})$ and 1321 $cm^{-1}(\nu_{12})$ are assigned to X and XI normal modes ($A_1$ and $B_1$ classes) respectively, and 1243 $cm^{-1}(\nu_{11})$ is assigned to IX normal mode ($B_1$ class).

For 283 $cm^{-1}(\nu_1)$ and 478 $cm^{-1}(\nu_4)$, there are no comparable frequencies in the other molecules, so that these vibrations can be taken as oxygen vibration frequencies. Their frequency values suggest that 283 $cm^{-1}(\nu_1)$ is non-planar oxygen bending vibration and 478 $cm^{-1}(\nu_4)$ planar oxygen bending vibration.

**Oxygen Stretching Vibration.**—As 832 $cm^{-1}$ ($\nu_8$), which occur strongly in both infrared and Raman, has no corresponding frequency in benzene and pyridine, this vibration is also an oxygen vibration. In general, N-O stretching vibration in oxime compounds appears strongly in both infrared and Raman spectra in the region from 790 $cm^{-1}$ to 850 $cm^{-1}$.[6] For example, acetoxime have this vibration at 813 $cm^{-1}$ [7]. Therefore, 832 $cm^{-1}(\nu_8)$ can be assigned to a characteristic N-O stretching vibration, ($A_1$).

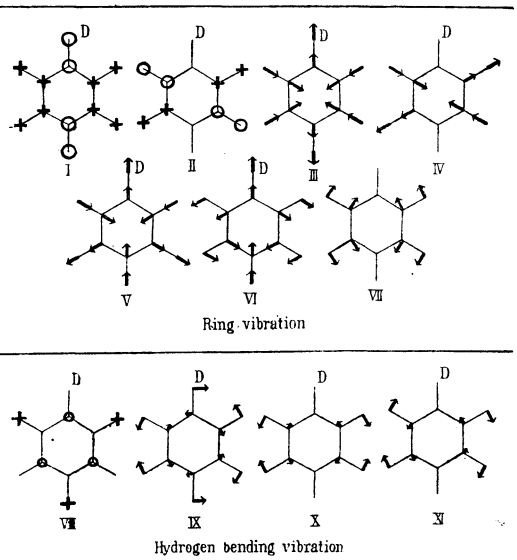



Fig. 1. Normal modes of vibrations of monodeuterobenzene (after C. K. Ingold, ref. 5).
Notes: (1) Vectors perpendicular to the plane of the ring are represented by + and ○.
(2) For each point-set ○ : ○ = ↑ : ↑ = 2 : 1.

The authors wish to express their sincere thanks to Prof. S. Imanishi for his kind guidance and helpful suggestions. They are also indebted to Prof. S. Akiyoshi and Mr. T. Matsuda of the Engineering Department of this University for the free use of the Perkin-Elmer infrared spectrometer.

*Department of Chemistry,*
*Faculty of Science,*
*Kyushu University,*
*Fukuoka, Japan*

6) See, for example, Landolt-Börnstein, "Atom u Molekularphysik," 2 Teil, Molekeln 1.

7) L. Kahovec and K. W. F. Kohlrausch, *Ber.*, 75, 627 and 1541 (1942).

# *Note on the Polymer-Mixed Solvent System. IV. Deviation from the Single Liquid Approximation in Osmotic, Viscometric and Swelling Measurements*

By Tōru KAWAI

(Received February 1, 1955)

## Introduction

In discussing the problems encountered in the treatment of the interaction of a polymer with a mixed solvent, the single liquid approximation is often used, assuming that the mixture of the two liquids behaves as a homogeneous liquid to the polymer. For the sake of its simplicity, the experimental results of osmotic pressure, viscosity, swelling ratio and other measurements for mixed solvents have been interpreted with considerable confidence by the terms usually employed in the binary system of a polymer and a liquid. In some polymer-mixed solvent systems, however, the deviation from the single liquid approximation cannot be ignored, due to selective adsorption. In the preceding paper[1], the relation between the liquid compositions in the two phases has been derived for the equilibrium between a mixed solvent and an isolated polymer molecule in solution. In this paper we shall apply this treatment to the equilibrium between a mixed solvent and a cross-linked polymer, or between a polymer-mixed solvent solution and a mixed solvent through a semi-permeable membrane, and shall investgate how the influence of the selective adsorption must be considered in osmotic, viscometric, and swelling measurements.

## Theoretical

In the two-phase systems, the thermodynamical condition for equilibrium requires that the partial molar free energy of each component (liquid 1 or liquid 2) be the same in both phases:

$$\Delta\bar{F}_1 = \Delta\bar{F}_1' \tag{1a}$$

$$\Delta\bar{F}_2 = \Delta\bar{F}_2' \tag{1b}$$

The partial molar free energies of the components in the binary phase of the two liquids may be written as[2]

$$\Delta\bar{F}_1 = \ln\theta_1 + \theta_2\{1-(V_1/V_2)\} + (V_1/RT)A_{12}\theta_2^2 \tag{2a}$$

$$\Delta\bar{F}_2 = \ln\theta_2 + \theta_1\{1-(V_2/V_1)\} + (V_2/RT)A_{12}\theta_1^2 \tag{2b}$$

where $\theta_1$ and $\theta_2$ are compositions (volume fractions), $V_1$ and $V_2$ molar volumes of the two liquids, and $A_{12}$ is a constant related to the heat interaction between the liquids 1 and 2.

For the ternary phase which consists of a cross-liked gel and the two liquids, Flory's expression for entropy change in swelling of a cross-linked gel in a single liquid may be applied to the present system in somewhat modified form. We may represent the entropy change associated with the swelling of a network of functionality $f$ formed from $\nu$ chains in a single liquid as the sum of two terms, the osmotic and elastic contributions, and according to Flory[3], may write,

$$\Delta S_{sw} = \Delta S_{osm} + \Delta S_{el} \tag{3a}$$

$$\Delta S_{osm} = -R\{n\ln(1-v_3)\} \tag{3b}$$

$$\Delta S_{el} = -R\{(3/2)\nu(v_3^{-2/3}-1)+(\nu/2)\ln v_3\} \tag{3c}$$

where $n$ is the number of solvent molecules and $v_3$, volume fraction of the polymer in the gel phase.

Since the effect of the segment size must be considered for the calculation of the entropy of dilution as in our previous treatments[1),4),5)], Eq. (3b) should be rewritten as

$$S_{osm} = -R[\{(n_1V_1+n_2V_2)/V_3\}\{\ln(1-v_3)+\mu_s' v_3\}] \tag{3b'}$$

for the present three component system, where $n_1$ and $n_2$ are the numbers of molecules of liquid 1 and liquid 2 respectively, $V_3$, molar volume of a polymer segment and $\mu_s'$ may be assumed to involve all the complicated factors except the effect of the segment size in the calculation of the entropy of dilution[5),6)]. Replacing $v_3$ in Eqs. (3b') and (3c)

1) T. Kawai, This Bulletin, **26**, 6 (1953).

2) J. H. Hildebrand and R. L. Scott, "Solubility of Non-electrolytes", 3rd Ed. Reinfold Publishing Corp., New York (1950).

3) P.J. Flory, *J. Chem. Phys.*, **18**, 108 (1950).

4) T. Kawai, This Bulletin, **25**, 336 (1952); **25**, 342 (1952).

5) T. Kawai, This Bulletin, **26**, 409 (1953).

6) The parameter $\mu_s'$ differs from the entropy contribution $\mu_s$ in the customarily used parameter $\mu$, since the effect of segment size is not considered in the usual treatment of polymer solutions ($\mu_s'$ is the same with $f$ in reference 5).

by $Z\nu V_3/(n_1V_1+n_2V_2+Z\nu V_3)$ ($Z$ is the number of segments between the cross links) and differentiating the resultant expressions of Eqs. (3b') and (3c) with respect to $n_1$ and $n_2$, the following equations are obtained,

$$\Delta\bar{S}_1=-R(V_1/V_3)[\ln(1-v_3)+\{1-(2/Zf)\}v_3+\mu_s'v_3^2+(1/Z)v_3^{1/3}] \quad (4a)$$

$$\Delta\bar{S}_2=-R(V_2/V_3)[\ln(1-v_3)+\{1-(2/Zf)\}v_3+\mu_s'v_3^2+(1/Z)v_3^{1/3}] \quad (4b)$$

Adding the terms for the mixing of the two liquids[4], and employing the expressions already given in the preceding paper [Eqs. (2a) and (2b) in the reference (4)] for the partial molar heat of mixing, the right hand sides of Eq. (1a) and (1b) are obtained, and then, combining them with Eqs. (2a) and (2b), Eqs. (1a) and (1b) may be written as follows,

$$\ln\theta_1+\{1-(V_1/V_2)\}\theta_2+(V_1/RT)A_{12}\theta_2^2=(V_1/V_3)[\ln(1-v_3')+\{1-(2/Zf)\}v_3'+\mu_s'v_3'^2+(1/Z)v_3'^{1/3}]+\ln\theta_1'+\{1-(V_1/V_2)\}\theta_2'+(V_1/RT)\{A_{12}v_2'^2+A_{13}v_3'^2+(A_{12}+A_{13}-A_{23})v_2'v_3'\} \quad (5a)$$

$$\ln\theta_2+\{1-(V_2/V_1)\}\theta_1+(V_2/RT)A_{12}\theta_1^2=(V_2/V_3)[\ln(1-v_3')+\{1-(2/Zf)\}v_3'+\mu_s'v_3'^2+(1/Z)v_3'^{1/3}]+\ln\theta_2'+\{1-(V_2/V_1)\}\theta_1'+(V_2RT)\{A_{12}v_1'^2+A_{23}v_3'^2+(A_{12}+A_{23}-A_{13})v_1'v_3'\} \quad (5b)$$

where the A's are the constants characteristic to each pair of the components (the gel phase being designated by a prime).

From Eqs. (5a) and (5b), there is easily obtained,

$$\ln(\theta_1/\theta_1')-(V_1/V_2)\ln(\theta_2/\theta_2')=(V_1/RT)[\{A_{13}-A_{23}-A_{12}(\theta_2'-\theta_1')\}v_3'+A_{12}\{(\theta_2'-\theta_1')-(\theta_2-\theta_1)\}] \quad (6)$$

If we write $\theta_1=\theta$, $\theta_1'=\theta+\Delta\theta$, $\theta_2=(1-\theta)$, and $\theta_2'=(1-\theta)-\Delta\theta$[7], Eq. (6) may be converted to the form,

$$(V_1/V_2)\ln\{1-(\Delta\theta)/(1-\theta)\}-\ln\{1+(\Delta\theta/\theta)\}=-(V_1/V_2)\{\Delta\theta/(1-\theta)\}-(\Delta\theta/\theta)-(1/2)(V_1/V_2)\{\Delta\theta/(1-\theta)\}^2+(1/2)(\Delta\theta/\theta)^2-\cdots\fallingdotseq(V_1/RT)[\{A_{13}-A_{23}-A_{12}(1-2\theta-\Delta\theta)\}v_3'-2A_{12}(\Delta\theta)] \quad (7)$$

Hence, to a satisfactory approximation[8],

$$\Delta\theta\fallingdotseq-(1/RT)\{A_{13}-A_{23}-A_{12}(1-2\theta)\}v_3'/\{[(1/V_1\theta)+\{1/V_2(1-\theta)\}]-(A_{12}/RT)(2-v_3')\} \quad (8a)$$

And when

$$(1/V_1\theta)+\{1/V_2(1-\theta)\}\gg(A_{12}/RT)(2-v_3'),$$

$$\Delta\theta\fallingdotseq\{-\theta(1-\theta)/[(\theta/V_2)+\{(1-\theta)/V_1\}]\}(1/RT)\{A_{13}-A_{23}-A_{12}(1-2\theta)\}v_3' \quad (8b)$$

Since $\Delta\theta/\theta$ is assumed to be a measure of the magnitude of selective adsorption, Eq. (8) shows the relation between its magnitude and the compositions, molar volumes of the two liquids or the interaction parameters. The magnitude of the selective adsorption for various types of the polymer-mixed solvent systems was discussed in details in the preceding paper[1]. It must be noted, however, that the effect of molar volumes of the two liquids should be considered also. The smaller the values of both $V_1$ and $V_2$, the smaller the magnitude of the selective adsorption. As seen from Eq. (8), however, the smaller $V_2$ values of nonsolvents would be effective in solvent-rich compositions to make the above magnitude smaller, and vice versa.

Now, the $\mu^*$ values, which are customarily used to express the polymer-solvent interaction, are often calculated from the experiments of swelling of cross-linked polymers, even in mixed solvents, by the equation,

$$-\mu^*v_3'^2=\ln v_0'+v_3'+(V_0/ZV_3)v_3'^{1/3} \quad (9)$$

which Flory presented for the cross-linked polymer-single liquid (designated by 0) system[9]. (For mixed solvents, the "single liquid approximation", assuming that the mixture of the two solvents behaves as a homogeneous liquid, is widely used. Then, $v_0=v_1+v_2$, and $V_0=x_1V_1+x_2V_2$, where the $x$'s are mole fractions of the two liquids). Let us consider how the calculation of the $\mu^*$ values from this equation must be corrected for the cross-linked polymer-mixed solvent system, owing to the effect of the selective adsorption.

Since the terms involving the $\theta$'s in Eqs. (5a) and (5b) can be expressed as $(\Delta\theta/\theta)-1/2(\Delta\theta/\theta)^2+\cdots$ and $-(\Delta\theta/1-\theta)-1/2(\Delta\theta/1-\theta)^2\cdots$ respectively, multiplying Eq. (5a) by $\theta V_0/V_1$ and Eq. (5b) by $(1-\theta)V_0/V_2$, and adding the resultant two equations, there is obtained,

7) It must be noted that the ratio of volume fractions of the two liquids was expressed by $\theta$ in reference 1.

8) Since $\Delta\theta$ is supposed to be far smaller than $\theta$ or $(1-\theta)$ in usual cases, and the second terms in the expanded equations of the logarithmic terms in Eq. (7) are inclined to be canceled with each other, Eq. (8a) may afford a satisfactory approximation, unless $\theta$ or $(1-\theta)$ is extremely small. Further more, the last terms $(A_{12}/RT)(2-v_3')$ in Eq. (8a) can be ignored so long as $\{(V_1/V_2)\theta_1+\theta_2\}/\theta_1\theta_2>2A_{12}V_1/RT$. (this condition is usually satisfied except in the systems having extremely large values of $A_{12}$) as mentioned also in reference 1.

9) P.J. Flory, J. Rehner, Jr., *J. Chem. Phys.*, **11**, 512 (1943).

$$(V_0/V_3)[\ln(1-v_3')+\{1-(2/Zf)\}v_3'+\mu_s'v_3'^2+(1/Z)v_3'^{1/3}]=-(V_0/V_1)\theta\ln\{1+(\Delta\theta/\theta)\}-(V_0/V_2)(1-\theta)\ln\{1-(\Delta\theta/1-\theta)\}+\{(V_0/V_1)-(V_0/V_2)\}\Delta\theta-(A_{12}V_0/RT)(\Delta\theta)^2-(V_0/RT)\{A_{13}(\theta+\Delta\theta)+A_{23}(1-\theta-\Delta\theta)-A_{12}(\theta+\Delta\theta)(1-\theta-\Delta\theta)\}v_3'^2-(V_0/RT)\{\theta(1-\theta-\Delta\theta)-(1-\theta)(\theta+\Delta\theta)\}[A_{13}-A_{23}-A_{12}\{1-2(\theta+\Delta\theta)\}]v_3'\fallingdotseq(V_0/2)[(1/V_1\theta)+\{1/V_2(1-\theta)\}](\Delta\theta)^2-(A_{12}V_0/RT)(1-2v_3'+v_3'^2)(\Delta\theta)^2-(V_0/RT)\{A_{13}\theta+A_{23}(1-\theta)-A_{12}\theta(1-\theta)\}v_3'^2+(V_0/RT)\{A_{13}-A_{23}-A_{12}(1-2\theta)\}v_3'(1-v_3')\Delta\theta \quad (10)^{10}$$

Substituting the expression of Eq. (8a) for $\Delta\theta$ in Eq. (10), and combining Eq. (9) with (10),

$$\mu^*v_3'^2\fallingdotseq[1/2-(V_0/V_3)(1/2-\mu'_s)+(V_0/RT)\{A_{13}\theta+A_{23}(1-\theta)-A_{12}\theta(1-\theta)\}]v_3'^2+[\{1-(V_0/V_3)\}\{(1/3)v_3'^3+(1/4)v_3'^4+\cdots\}-(2V_0/V_3Zf)v_3']+[\{1/(RT)^2\}\{A_{13}-A_{23}-A_{12}(1-2\theta)^2\theta(1-\theta)/\{(\theta/V_2)+(1-\theta)/V_1\}\{(\theta/V_1)+(1-\theta)/V_2\}]\times[1/2-v_3'+B\{1-4v_3'+(5/4)v_3'^2+\cdots\}+B^2\{2-12v_3'+(17/2v_3'^2)+\cdots\}+\cdots]v_3'^2 \quad (11)^{10}$$

where, $B=(A_{12}/RT)/[(1/V_1\theta)+\{1/V_2(1-\theta)\}]$ ($B$ is very small in usual cases[8]). The last bracketed terms are due to the selective adsorption, and the first and second bracketed terms correspond to the expresion for a single liquid, which usually may be written,

$$\mu=\mu_s+(V_0RT)A_{30} \quad (12)$$

where $\mu_s$ is a correction factor, mentioned in reference (6). It is easily seen from Eq. (11) that Eq. (12) must be replaced by

$$\mu=1/2-(V_0/V_3)(1/2-\mu_s')+(V_0/RT)A_{30}-(2V_0/V_3Zf)v_3'^{-1}+\{1-(V_0/V_3)\}\{(1/3)v_3'+(1/4)v_3'^2+\cdots\}. \quad (13)$$

On this point, strictly speaking, lies an important source of inaccuracy in the customary calculation of the $\mu$ values from swelling measurements, which will be discussed in detail elsewhere (In extremely poor solvents, the dependency of $\mu$ upon $v_3'$ can not be ignored).

Actually, even for single liquids, the $\mu$ values determined from swelling measurements are often larger than those obtained from osmotic pressure measurements[11),12)], and the influence of the molar volume of the solvent must be considered when the solvent power of the solvent is estimated from the $\mu$ value thus obtained[5)].

For the present three-component system, however, we shall confine ourselves to the investigation of the effect of the selective adsorption, and assuming that all the complicated factors, such as those seen from Eq. (13), are involved in the term $\mu_s$ in Eq. (12), may write for the "single liquid approximation"[4),13)],

$$\mu^{**}=\mu_{13}\theta+\mu_{23}(1-\theta)-\mu_{12}\theta(1-\theta) \quad (14)$$

where $\mu_{13}=\mu_s+(V_0/RT)A_{13}$, $\mu_{23}=\mu_s+(V_0/RT)A_{23}$, and $\mu_{12}=(V_0/RT)A_{12}$[14)] (Eq. (14) corresponds to the expression in Part II[4)], which is a somewhat improved form of Scott's[13)]). Thus, Eq. (11) reduces to

$$\mu^*=\mu^{**}+[\{(1/RT)^2\}\{A_{13}-A_{23}-A_{12}(1-2\theta)\}^2\theta(1-\theta)/\{(\theta/V_2)+(1-\theta)/V_1\}\{(\theta/V_1)+(1-\theta)/V_2\}]\times[1/2-v_3'+B\{1-4v_3'+(5/4)v_3'^2+\cdots\}+B^2\{2-12v_3'+(17/2)v_3'^2+\cdots\}+\cdots] \quad (15).$$

It may be notable that, as seen in Eq. (15), $\mu^*$ always gives a larger value than that expected for its original meaning due to the selective adsorption ($1/2>v_3'$, except in the case of swelling in an extremely poor solvent i.e. in the nonsolvent-rich region). Moreover, its deviation increases, of course, with the magnitude of the selective adsorption (accordingly, with the content of the nonsolvent), but, decreases rapidly in the neighbourhood of pure nonsolvent.

Several attempts[15),16)] have been made to correlate intrinsic viscosities with the thermodynamic properties of the solution. The writer[4)] has developed the procedure of Flory[15)], who treated the interaction of an isolated polymer molecule with solvent as a

10) For the same reason as mentioned in reference (8), Eqs. (10) and (11) would give a satisfactory approximation.

11) T. Kawai, This Bulletin, **24**, 69 (1951).

12) P. Doty, M. Brownstein, W. Schlener, *J. Phys. Colloid Chem.*, **53**, 213 (1949).

13) R.S. Scott, *J. Chem. Phys.*, **17**, 268 (1949).

14) Eq. (14) is merely a convenient representation of $\mu^{**}$ by employing $\mu_s$. And, strictly speaking, the parameter $\mu_{13}$, or $\mu_{23}$ employed here differs from that calculated from experiments in the polymer 3–single liquid 1 (or 2) system, also because $V_0$ is a function of $\theta$ (cf. Eqs. (16) and (17)).

15) P.J. Flory, *J. Chem. Phys.*, **17**, 303 (1949).

16) T.G. Fox, Jr., P.J. Flory, *J. Am. Chem. Soc.*, **73**, 1904; 1909; 1915 (1951)

swelling phenomenon, to the polymer-mixed solvent system, and formulated the relation between intrinsic viscosity and the parameter $\mu$ for the single liquid approximation. Now, we can apply the treatment developed in the preceding pages for the swelling of a cross-linked polymer in a mixed solvent to discuss the effect of the selective adsorption on intrinsic viscosities. In another treatment[5], which is developed in consideration of the effect of segment size, the writer pointed out a more satisfactory correspondence of the volume swelling ratio of polymer gels, or intrinsic viscosities of polymer solutions with the values of $(1/2-\mu)/V_0$ rather than with the $\mu$ values themselves. There[5], the parameter $\mu$ which has been usually interpreted in terms of Flory-Rehner's theory, was expresed by

$$\mu=1/2-(V_0/V_3)(1/2-\mu_s')+(V_0/RT)A_{30} \quad (16)$$

instead of Eq. (13)[17]. The last bracketed terms in the right hand side of Eq. (13) were ignored in Eq. (16), since this can afford a satisfactory approximation when the values of $v_3'$ is sufficiently small[18]. The similar approximation may be applied to the present problem on intrinsic viscosity, and we may write for the single liquid approximation,

$$\begin{aligned}\mu^{**}&=1/2-(V_0/V_3)(1/2-\mu_s')\\&+(V_0/RT)\{A_{13}\theta+A_{23}(1-\theta)\\&-A_{12}\theta(1-\theta)\}\end{aligned} \quad (17)$$

Considering the effect of the selective adsorption, the values of intrinsic viscosity in mixed solvents are expected to vary with

$$\begin{aligned}(1/2-\mu^{*})/V_0&=(1/V_3)(1/2-\mu_s')\\&-(1/RT)\{A_{13}\theta+A_{23}(1-\theta)-A_{12}\theta(1-\theta)\}\\&-\{1/(RT)^2\}[\{A_{13}-A_{23}\\&-A_{12}(1-2\theta)\}^2\theta(1-\theta)/\{(\theta/V_2)\\&+(1-\theta)/V_1\}]\times[1/2-v_3'\\&+B\{1-4v_3'+(5/4)v_3'^2+\cdots\}\\&+B^2\{2-12v_3'+(17/2)v_3'^2+\cdots\}+\cdots]\end{aligned} \quad (18)$$

Finally, the treatment developed above will be applied to the interpretation of osmotic pressure in mixed solvents. The expressions for osmotic pressure $\pi$ in the present system were already derived by Gee[19], Scott[13] and Scatchard[20]. Here, the errors introduced by employing the "single liquid approximation" in the customary calculations of the $\mu$ values will be discussed. The condition for equilibrium between both sides of the membrane in an osmometer may be expressed thus:

$$\begin{aligned}&\ln\theta_1+\{1-(V_1/V_2)\}\theta_2+(V_1/RT)A_{12}\theta_2^2\\&=(V_1/V_3)[\ln(1-v_3')+\{1-(1/x)\}v_3'\\&+\mu_s'v_3'^2]+\ln\theta_1'+\{1-(V_1/V_2)\}\theta_2'\\&+(V_1/RT)\{A_{12}v_2'^2+A_{13}v_3'^2\\&+(A_{12}+A_{13}-A_{23})v_2'v_3'\}+(\pi V_1/RT),\end{aligned} \quad (19a)$$

$$\begin{aligned}&\ln\theta_2+\{1-(V_2/V_1)\}\theta_1+(V_2/RT)A_{12}\theta_1^2\\&=(V_2/V_3)[\ln(1-v_3')+\{1-(1/x)\}v_3'\\&+\mu_s'v_3'^2]+\ln\theta_2'+\{1-(V_2/V_1)\}\theta_1'\\&+(V_2/RT)\{A_{12}v_1'^2+A_{23}v_3'^2\\&+(A_{12}+A_{23}-A_{13})v_1'v_3'\}+(\pi V_2/RT),\end{aligned} \quad (19b)$$

where $x$ is the number of segments (number average) in a polymer molecule. Meanwhile, the $\mu$ values for mixed solvents have been usually calculated by

$$\begin{aligned}-\pi V_0&=RT[\ln(1-v_3')+\{1-(V_0/xV_3)\}v_3'\\&+\mu^{*}v_3'^2]\end{aligned} \quad (20)$$

Combining Eqs. (19a, b) and (20), an entirely analogous evaluation to the derivation of Eq. (11) leads to

$$\begin{aligned}\mu^{*}&=1/2-(V_0/V_3)(1/2-\mu_s')\\&+(V_0/RT)\{A_{13}\theta+A_{23}(1-\theta)-A_{12}\theta(1-\theta)\}\\&+[\{1/(RT)^2\}\{A_{13}-A_{23}\\&-A_{12}(1-2\theta)\}^2\theta(1-\theta)/\{(\theta/V_2)\\&+(1-\theta)/V_1\}\{(\theta/V_1)+(1-\theta)/V_2\}]\\&\times[1/2-v_3'+B\{1-4v_3'+(5/4)v_3'^2+\cdots\}\\&+B^2\{2-12v_3'+(17/2)v_3'^2+\cdots\}+\cdots]\end{aligned} \quad (21)$$

The last bracketed terms in Eq. (21) give the contribution of the selective adsorption and the other terms are equivalent to those obtained for the binary system of a polymer and a solvent in consideration of the effect of the segment size.

Applications of the above treatment will be given in the next paper to the osmotic, viscometric, and swelling data in a few polymer-mixed solvent systems.

After this paper had been read at the Special Meeting on High polymers, held by the Chemical Society of Japan, and the Society of High Polymer, Japan, at Tokyo University, on 31st Oct., 1953, Dr. Krigbaum sent me a copy of the manuscript of his paper, which was due to appear on J. Polymer Sci., He dealt with the composition

17) The complications, which arise from the last bracketed terms in Eq. (13) and from Flory's modification of his own original equation (cf. Eqs. (3c) and (9)), are avoided in Eq. (16), and this approximation is equivalent to assuming an equal $\mu$ value for both osmotic and swelling measurements.

18) When the $v_3'$ values are considerably large (i.e. $v_3'>0.1$), it may be suitable to express $\mu$ by Eq. (13) instead of Eq. (16). Actually, the validity of the approximate treatment (Eq. (16)) in reference 5 fails when it is applied to the swelling in extremely poor solvents.

19) G. Gee, *Trans. Faraday Soc.*, **40**, 463 (1944).

20) G. Scatchard, *J. Am. Chem. Soc.*, **68**, 2315 (1946).

relationship of the two phases in equilibrium between a polymer and a mixed solvent, and drew the conclusion similar to that of my preceding paper[1], except for the effect of the difference in molar volumes of the two liquids. Also this effect of molar volumes of the liquids had been involved in this treatment, although somewhat different results had been obtained because the effect of the segment size was considered in this treatment. A few points of difference between my treatment and Krigbaum's will be explained elsewhere, after an exchange of views with him.

*Laboratory of Textile Chemistry,*
*Tokyo Institute of Technology,*
*Tokyo*

# *Alkylalkoxypolysiloxanes. III.*[1] *Lower Members of Ethylmethoxypolysiloxanes with One to Six Silicon Atoms*

By Rokuro ŌKAWARA

(Received February 16, 1955)

In the preceding papers, ethylethoxypolysiloxanes[2] and ethylisopropoxypolysiloxanes[1] have been prepared and characterized. This paper will describe a series of lower members of linear ethylmethoxypolysiloxanes as indicated by formula (I).

$$L_n;\quad CH_3O\left[\begin{array}{c}C_2H_5\\|\\SiO\\|\\OCH_3\end{array}\right]_n CH_3,\quad n=1\sim6 \quad (I)$$

As already described, the partially alcoholyzed ethyltrichlorosilane was easily polymerized by refluxing, liberating ethylalkoxypolysiloxanes. Thus ethylethoxy- and ethylisopropoxy- polysiloxanes have been prepared.

On the other hand, however, when the mixture of ethyltrichlorosilane and methanol in various mole ratios (1.6-2.5) was refluxed, the thermal reaction occurred with difficulty on prolonged refluxing. It was found that by the addition of sodium bicarbonate the condensation reaction occurred easily by evolving hydrogen chloride and carbon dioxide to the formation of polysiloxanes of the various polymer sizes.

$$C_2H_5Si(OCH_3)_xCl_{3-x}+\frac{(3-x)}{2}NaHCO_3$$

$$=C_2H_5Si(OCH_3)_xO_{\frac{3-x}{2}}+\frac{(3-x)}{2}NaCl$$

$$+\frac{(3-x)}{2}HCl+\frac{(3-x)}{2}CO_2 \quad (1)$$

This reaction takes place even at room temperature until the mixture becomes chlorine-free and a slight excess of sodium bicarbonate calculated from the above formula has been required to produce chlorine-free polysiloxanes. Furthermore, the chlorine-free product, such as ethyltrimethoxysilane, does not easily react with sodium bicarbonate in a short period of time even at the refluxing temperature.

On fractional distillation, a small amount of methanol and the lower members of the series (I) ($L_n$) were obtained. The amounts of these polymers were varied with the chlorine content of the mixture. The distribution of the lower members of series (I) was plotted against the mole ratios $x$ of methanol to ethyltrichlorosilane, and the results are shown in Fig. 1. By redistilling these polymers, the presence of a small amount of cyclocompounds of the series (II) ($C_n$) was also found between the succeeding plateaus of the linear polymers ($L_n$),

$$C_n;\quad \left[\begin{array}{c}C_2H_5\\|\\SiO\\|\\OCH_3\end{array}\right]_n \qquad n=3\sim6 \quad (II)$$

but they could not be accurately characterized. Analysis and physical properties of the linear polymers are given in Table II.

## Experimental

**Starting Materials.**—The ethyltrichlorosilane used in this experiment was prepared by the reaction of ethylchloride with copper-silicon and was purified by fractionation through a helices-

1) Part II of this series. R. Ōkawara and I. Ishimaru, This Bulletin, 27, 582 (1954).

2) R. Ōkawara, This Bulletin, 27, 428 (1954).

packed column of about 20 plates. The redistilled fraction having the boiling point 98°–99°C/760 mm Hg was taken as a starting material. Analysis of hydrolyzable chlorine was carried out by hydrolysis in water and titrating the liberated acid.

Anal. Calcd. for $C_2H_5SiCl_3$: Cl, 65.0 Found: Cl, 64.0.

### Preparation of Ethylmethoxypolysiloxanes

**(a) Partial Methanolysis.** — Ethyltrichlorosilane was placed in a 300 cc. three-necked flask equipped with an efficient stirrer, a dropping funnel and a reflux condenser and was cooled with an ice bath. Methanol was added drop by drop with vigorous stirring. After the addition the temperature of the mixture was gradually raised to 40°–50°C. Then the mixture was replaced in a 100 cc. flask equipped with a reflux condenser and heated gradually to its boiling point. The constant refluxing mixture was obtained. The refluxing temperature and the weight of the mixture scarcely changed even after refluxing 30 hours. In this experiment, the constant refluxing mixture was heated on its refluxing temperature for a few additional hours in order to completely remove any trace of free hydrogen chloride which resulted in the methanolysis. The yield and the refluxing temperature were slightly different according to its composition as shown in Table I.

**(b) Reaction of the Partial Methanolysis Product with Sodium Bicarbonate.**—To this mixture sodium bicarbonate was added. Hydrogen chloride may also be produced by the reaction, so it is desirable that sodium bicarbonate is added differentially to partially methanolyzed product and the free hydrogen chloride formed is removed successively from the reaction system. Since sodium bicarbonate powder causes a violent reaction even at room temperature, 1–2 g. of sodium bicarbonate powder, or more conveniently tabletted powder, was added differentially to the ethylmethoxychlorosilane at room temperature and the mixture was gradually heated to its refluxing temperature in order to expel the free hydrogen chloride after carbon dioxide had ceased to evolve. Then the mixture was cooled to room temperature and the same treatment was repeated until the fuming chlorine compound could not be detected in the mixture. The sodium chloride formed was filtered off and the filtrate was again tested with the Beilstein test to assure that no trace of chlorine compound was present in the mixture.

The amounts of bicarbonate required to produce chlorine-free mixture are given in Table I. It was found that the yields of the polymer based on the amount of the starting materials were 75–85%.

To test whether the ethylmethoxypolysiloxanes react with sodium bicarbonate or not, redistilled ethyltrimethoxysilane (21 g.) mixed with powdered sodium bicarbonate (5 g.) was refluxed for 10 hours. The filtrate (16 g.) was composed of methanol (1 g.), unreacted ethyltrimethoxysilane (12 g.) and the residue (3 g.). This reaction did not proceed smoothly, but with violent bumping.

**Distillation of the Polymer.**—The polymer thus formed was rigorously fractionated through a semi-micro Stedman column of about 20 theoretical plates. Methanol which may be formed

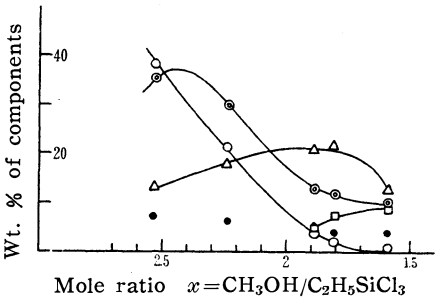
TABLE I

RESULTS OF THE SODIUM BICARBONATE TREATMENT

| | Starting Materials | | | Ethylmethoxychlorosilane | | | Sodium Bicarbonate | | Ethylmethoxypolysiloxane | |
|---|---|---|---|---|---|---|---|---|---|---|
| Exp. | A $C_2H_5SiCl_3$ | B $CH_3OH$ | $x$=B/A | Refluxing Temp. | Yield | | Added | Calcd. | Yield | |
| | g. (mole) | g. (mole) | (mole ratio) | °C | g. | %theory | g. | g. | g. | %theory* |
| 1 | 54.5 (0.333) | 27 (0.85) | 2.54 | 123 | 47 | 92 | 7.3 | 6.0 | 39.5 | 85 |
| 2 | 54.5 (0.333) | 24 (0.75) | 2.25 | 119 | 47 | 92 | 12.3 | 9.7 | 34.0 | 77 |
| 3 | 81.7 (0.5) | 30.5 (0.95) | 1.9 | 118 | 73 | 94 | 27.0 | 21.8 | 48.5 | 78 |
| 4 | 81.7 (0.5) | 29 (0.9) | 1.82 | 116 | 75 | 96 | 26.5 | 24.0 | 48.0 | 78 |
| 5 | 81.7 (0.5) | 25.6 (0.8) | 1.6 | 115 | 74 | 95 | 30.1 | 27.8 | 44.0 | 75 |

* Based on the amount of the starting materials.

by the fission of Si-$OCH_3$ in the bicarbonate treatment, distilled out at first; and then monomer, dimer, trimer and tetramer fractions were obtained as the succeeding plateaus. The relation between the percentage composition of these fractions and the composition of the starting materials are shown in Fig. 1.




Mole ratio $x=CH_3OH/C_2H_5SiCl_3$

Fig. 1. Composition of the chlorine-free products obtained from sodium bicarbonate treatment.
● Methanol, ○ Monomer,
◎ Dimer, △ Trimer,
□ Tetramer.

Monomer, dimer and trimer fractions were redistilled through the same column and the refractive index was observed throughout the distillation. The middle portion of the plateau having the constant refractive index was taken for the sample. Data on these polymers are given in Table II.

Between the plateaus of dimer and linear trimer, at the boiling point of 69°C/0.5 mm Hg, a knick point on the distillation curve was found and the higher refractive index ($n_D^{20}$ 1.4100) at this point than the other portions was also found. From analogy with the preceding papers, the presence of the cyclotrimer may be supposed at this point, but as the amount of this portion was very small, the rigorous separation could not be attained.

As the amount of the tetramer fraction was small in each experiment, the residues of each experiment of Table I and the similar several runs (120 g.) were simply distilled and the fraction distilled out under 200°C/0.3 mm Hg was collected (80 g.). Since the still temperature was not over 240°C it may be supposed that the thermal rearrangement of the polysiloxane[3], which has been reported to begin at above 350°C, did not occur. This distillate was rigorously fractionated through the same semi-micro Stedman column. It was found from the silicon content that the separation of cyclotetramer and linear tetramer was fairly good, but with the polymer higher than this, the rigorous separation could not be attained.

To attain the rigorous separation, the distillation was again carried out through a high efficient semi-micro Stedman column (packed length 54 cm., inner diameter 1.1 cm., 60 theoretical plates, hold-up 3 cc. and pressure drop 2 mm Hg at the total reflux rate of 80 cc./hour). The results with regard to the polymers except monomer and dimer are shown in Fig. 2.

Comparing the distillation curve and the refrac-

3) W. Patnode and D. F. Wilcock, *J. Am. Chem. Soc.*, **68**, 358 (1946).

TABLE II

ETHYLMETHOXYPOLYSILOXANES: $CH_3O\left[\begin{matrix}C_2H_5\\|\\SiO\\|\\OCH_3\end{matrix}\right]_nCH_3$

| Polymer Size | Boiling Point °C/mm Hg | Density $d_4^{20}$ | Refractive Index $n_D^{20}$ | Molar Refraction Found (Calcd.)** | Molecular Weight Found*** (Calcd.) | % Si Found (Calcd.) |
|---|---|---|---|---|---|---|
| Series I; $L_n$ | | | | | | |
| Monomer* ($n=1$) | 124.3/760 | 0.9488 | 1.3838 | 37.02 (37.19) | — (150.3) | 18.66 (18.69) |
| Dimer ($n=2$) | 97/20 | 1.0071 | 1.3979 | 60.95 (61.22) | 252 (254.4) | 22.05 (22.08) |
| Trimer ($n=3$) | 90/0.5 | 1.0335 | 1.4045 | 84.93 (85.25) | 359 (358.6) | 23.48 (23.50) |
| Tetramer ($n=4$) | 125/0.3 | 1.0499 | 1.4094 | 109.07 (109.28) | 462 (462.8) | 24.29 (24.28) |
| Pentamer ($n=5$) | 150/0.3 | 1.0621 | 1.4140 | 133.40 (133.31) | 554 (567.0) | 24.79 (24.77) |
| Hexamer ($n=6$) | 170/0.3 | 1.0744 | 1.4180 | 157.43 (157.34) | — (671,2) | 25.29 (25.11) |

* A. Ladenburg, *Ann.*, **173**, 143 (1874): Ber., **5**, 1081 (1872) b.p. 126/760, $d^0$ 0.9747.
J. Emeleus and S. R. Robinson, *J. Chem. Soc.*, **1947** 1592 b.p. 123.
** Calculated from bond refractivities by E. L. Warrick, *J. Am. Chem. Soc.*, **68**, 2455 (1946).
*** Cryoscopic measurements in benzene.

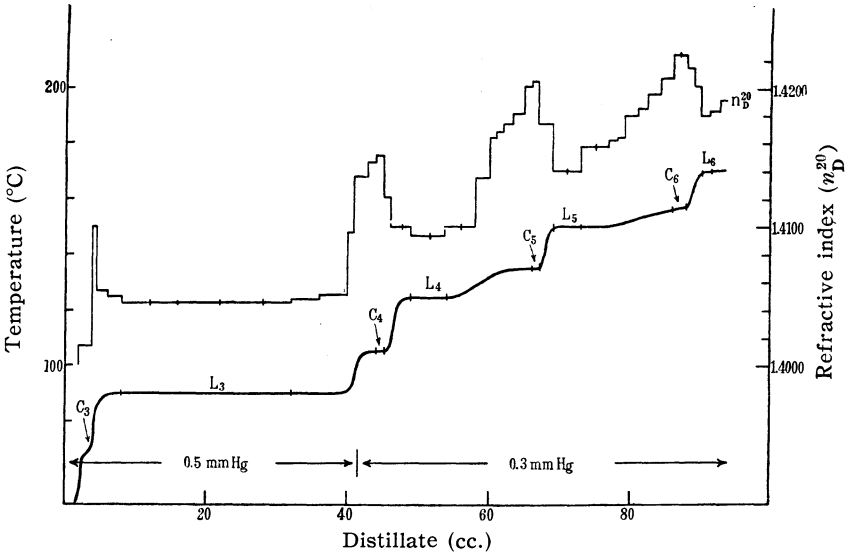



Fig. 2. Distillation curve of ethylmethoxypolysiloxanes.
$L_n$: Linear $n$-mer, $C_n$: Cyclo-$n$-mer

tive index of the distillate in Fig. 2, the plateaus of $L_3$, $C_4$, $L_4$, $C_5$, $L_5$, $C_6$ and $L_7$ were taken for the sample.

From the analytical data of $C_4$* and $C_5$* and from the analogy of a preceding paper[1], it was supposed that $C_n$ is the cyclocompound as indicated by formula (II), but the amount of these cyclocompounds is not enough to separate them from the neighbouring linear compounds. It was found in Fig. 2, that between the plateaus of linear trimer ($L_3$) and linear tetramer ($L_4$) there had appeared a plateau of cyclotetramer ($C_4$), having a higher refractive index than $L_3$ and $L_4$ and having a boiling point closer to $L_3$ than $L_4$. The similar relations may be seen with the other cyclocompounds.

**Analysis of Silicon.**—Monomer was weighed in gelatine capsule, the higher polymer were weighed in a platinum crucible and decomposed by concentrated sulfuric acid.

* Anal. Calcd. for $C_4$: Si, 26.96%. Found: Si, 25.31%.
Anal. Calcd. for $C_5$ (mol. wt. 521): Si, 26.96%.
Found: Si, 25.92% (mol. wt. 490, in benzene).

**Summary**

(1) Ethylmethoxypolysiloxanes have been prepared by the reaction of sodium bicarbonate with partially methanolyzed ethyltrichlorosilane.

(2) Distribution of the lower polymers was determined with regard to the composition of the partially methanolyzed product.

(3) Linear ethylmethoxypolysiloxanes containing from one to six silicon atoms have been prepared and characterized.

(4) Ethylmethoxycyclopolysiloxanes containing from three to six silicon atoms have been found, but they could not be accurately characterized.

The author wishes to express his hearty thanks to Mr. H. Osawa for his assistance in this investigation.

*Department of Applied Chemistry, Faculty of Engineering, Osaka University, Osaka*

# *Alkylalkoxypolysiloxanes. IV.*[1] *Lower Members of Methoxy End-blocked Dimethylpolysiloxanes with One to Six Silicon Atoms*

By Toshio TANAKA and Rokuro ŌKAWARA

(Received February 16, 1955)

In the preceding paper[1] ethylmethoxypolysiloxanes were synthesized by the condensation reaction of partially methanolyzed ethyltrichlorosilane using sodium bicarbonate. Here, the condensation reaction with sodium bicarbonate has been applied to partially methanolyzed dimethyldichlorosilane, and a series of lower members of methoxy end-blocked dimethylpolysiloxanes has been prepared as indicated below:

$$CH_3O\left[\begin{array}{c}CH_3\\|\\SiO\\|\\CH_3\end{array}\right]_n CH_3, \quad n=1\sim6.$$

Of these compounds the first member, dimethyldimethoxysilane ($n=1$), was previously obtained by Simpson[2] and by Kantor[3], but the boiling point only was reported.

Condensation reaction by the use of sodium bicarbonate is shown stoichiometrically in the following expression:

$$(CH_3)_2Si(OCH_3)_xCl_{2-x}+\frac{2-x}{2}NaHCO_3$$

$$\rightarrow (CH_3)_2Si(OCH_3)_xO_{\frac{2-x}{2}}+\frac{2-x}{2}NaCl$$

$$+\frac{2-x}{2}HCl+\frac{2-x}{2}CO_2$$

Just like the ethylmethoxychlorosilane described in the preceding paper[1] this reaction takes place even at room temperature and a slight excess of the amount of sodium bicarbonate calculated from the above formula has been required to produce chlorine-free polysiloxanes.

On fractional distillation of the condensation product, azeotropic mixture of dimethyldimethoxysilane and methanol, a small amount of methanol, and then the lower members of this series were obtained. The distribution of these distillates, varying with the mole ratio (0.9~1.7) of methanol to dimethyldichlosilane, was plotted against the mole ratios, and the results are shown in Fig. 1. By redistilling these polymers, the presence of a small amount of cyclo-compounds, $[(CH_3)_2SiO]_n$, was found between the succeeding plateaus of the linear compounds from the measurements of refractive index, but the cyclo-compounds have been too small in quantity to be characterized. Physical constants on these linear compounds were determined, and are shown in Table II together with the analytical data.

## Experimental

**Starting materials.** — Dimethyldichlorosilane used in these experiments were supplied from

TABLE I

| Exp. No. | Starting Material A $(CH_3)_2SiCl_2$ g. (mole) | Starting Material B $CH_3OH$ g. (mole) | $x$=B/A (mole ratio) | Dimethylmethoxychlorosilane Yield g. | Dimethylmethoxychlorosilane Yield % theory | Sodium Bicarbonate Calcd. g. | Sodium Bicarbonate Added g. | Methoxy End-blocked dimethylpolysiloxane Yield g. | Methoxy End-blocked dimethylpolysiloxane Yield % theory* |
|---|---|---|---|---|---|---|---|---|---|
| 1 | 64.5 (0.5) | 27.0 (0.84) | 1.68 | 52 | 87 | 5.6 | 7.0 | 40 | 73 |
| 2 | 64.5 (0.5) | 24.0 (0.75) | 1.50 | 53 | 87 | 9.1 | 10.5 | 39 | 74 |
| 3 | 65 (0.5) | 21.0 (0.66) | 1.31 | 51 | 83 | 12.0 | 13.0 | 38 | 74 |
| 4 | 129 (1.0) | 38.5 (1.20) | 1.20 | 105 | 85 | 28.6 | 31.0 | 73 | 74 |
| 5 | 65 (0.5) | 17.5 (0.55) | 1.10 | 54 | 86 | 16.8 | 20.5 | 37 | 76 |
| 6 | 65 (0.5) | 14.5 (0.45) | 0.90 | 56 | 88 | 20.5 | 22.5 | 34 | 72 |

* Based on the amounts of the starting materials.

1) Part III of this series, R. Ōkawara, This Bulletin, 28, 360 (1955).

2) P.W. Simpson, Brit. Patent, 635, 726 (April 12, 1950).

3) S.W. Kantor, *J. Am. Chem. Soc.*, 75, 2712 (1953).

the Shin-etsu Chem. Ind. Co. Analysis of hydrolizable chlorine was carried out by hydrolysis in water and titrating the liberated acid. Calcd. for $(CH_3)_2SiCl_2$: Cl, 54.9%. Found: Cl, 54.9%.

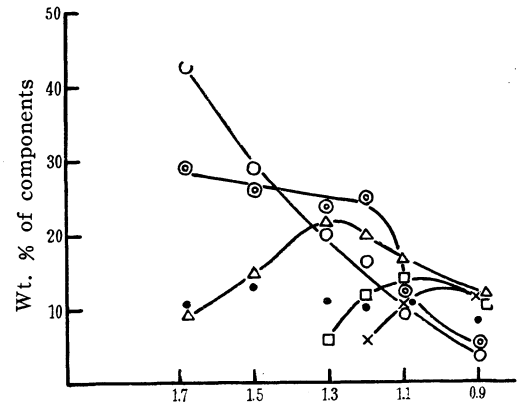
**Preparation of Methoxy End-blocked Dimethylpolysiloxanes.**—Partial methanolysis of dimethyldichlorosilane and the treatment by sodium bicarbonate were carried out as described in the preceding paper[1]. Before the treatment by sodium bicarbonate, the partially methanolyzed product was heated on its refluxing temperature (60°~65°C) for six to eight hours in order to remove free hydrogen chloride which resulted in the methanolysis.

The amounts of sodium bicarbonate required to obtain the chlorine-free product are given in Table I.

It was found that the yields of the products based on the amount of starting materials were 72~76%.

**Distillation of the Product.**—The products obtained in this manner were rigorously fractionated through a semi-micro Stedman column of about 20 theoretical plates. The azeotropic mixture of monomer and methanol was distilled out at first, and methanol which may be formed by the fission of Si-$OCH_3$, then monomer and dimer fractions, etc., were obtained as the succeeding plateaus. This azeotrope (b.p. 62°C, $n_D^{20}$ 1.3532) was broken with *n*-hexane to give the methanol-*n*-hexane azeotrope (b.p. 49°C). The composition was determined to be 53% dimethyldimethoxysilane and 47% methanol from the above distillation with *n*-hexane and the measurements of refractive index of the mixture of dimethyldimethoxysilane[4] and methanol in various ratios.

The relation between the percentage of each fraction and the mole ratio of the starting materials is shown in Fig. 1.




Mole ratio $x = CH_3OH/(CH_3)_2SiCl_2$

Fig. 1. Composition of the chlorine-free products obtained from sodium bicarbonate treatment.

● Methanol ○ Monomer
◎ Dimer △ Trimer
□ Tetramer × Pentamer

Here, the amounts of azeotrope were assigned to each component, and the middle fractions between two plateaus were also assigned to both side fractions.

Monomer[5], dimer and trimer fractions in each run were collected, respectively, and redistilled through the same column. The portions of each plateau having the constant refractive index were

4) This sample was obtained by the redistillation of monomer fraction, and the data are given in Table II.

5) Monomer fraction was found in the case of mole ratios 1.2~1.7.

TABLE II

METHOXY END-BLOCKED DIMETHYLPOLYSILOXANES: $CH_3O\left[\begin{matrix}CH_3\\|\\SiO\\|\\CH_3\end{matrix}\right]_n CH_3$

| Polymer Size | Boiling Point °C/mmHg | Density $d_4^{20}$ | Refractive Index $n_D^{20}$ | Molecular Weight Found[b] (Calcd.) | Molar Refraction Found (Calcd.)[c] | % Si Found (Calcd.) |
|---|---|---|---|---|---|---|
| Monomer ($n$=1) | 82/760[a] | 0.8646 | 1.3708 | — (120.2) | 31.51 (31.80) | 23.34 (23.36) |
| Dimer ($n$=2) | 139/760 | 0.9048 | 1.3835 | 195 (194.4) | 50.17 (50.44) | 28.83 (28.90) |
| Trimer ($n$=3) | 83/24 | 0.9241 | 1.3892 | 271 (268.5) | 68.67 (69.08) | 31.42 (31.38) |
| Tetramer ($n$=4) | 90/5 | 0.9346 | 1.3923 | 345 (342.7) | 87.37 (87.72) | 32.83 (32.79) |
| Pentamer ($n$=5) | 89/0.5 | 0.9424 | 1.3950 | 415 (416.9) | 106.06 (106.36) | 33.64 (33.69) |
| Hexamer ($n$=6) | 104/0.5 | 0.9470 | 1.3972 | 484 (491.0) | 124.91 (125.00) | 34.34 (34.32) |
| Heptamer ($n$=7) | 116/0.5 | 0.9492 | 1.4007 | — (565.2) | 144.57 (143.64) | — — |

a) b.p., 81.7°~82.2°C[2]; 80°~80.5°C[3].

b) Cryoscopic measurements in benzene.

c) Calculated from bond refractivities by E. W. Warrick, *J. Am. Chem. Soc.*, **68**, 2455 (1946).

used for the measurements of the physical constants and analysis. Data on these materials are given in Table II.

As the amounts of higher members than tetramer fraction were small in each run, the rigorous separation may not have been attained by the above distillation. Accordingly all of these fractions were collected together, then the distillation was again carried out through a high efficient semi-micro Stedman column (about 60 theoretical plates) as described in the preceding paper[1] and the refractive index was observed throughout the distillation. The results are shown in Fig. 2.

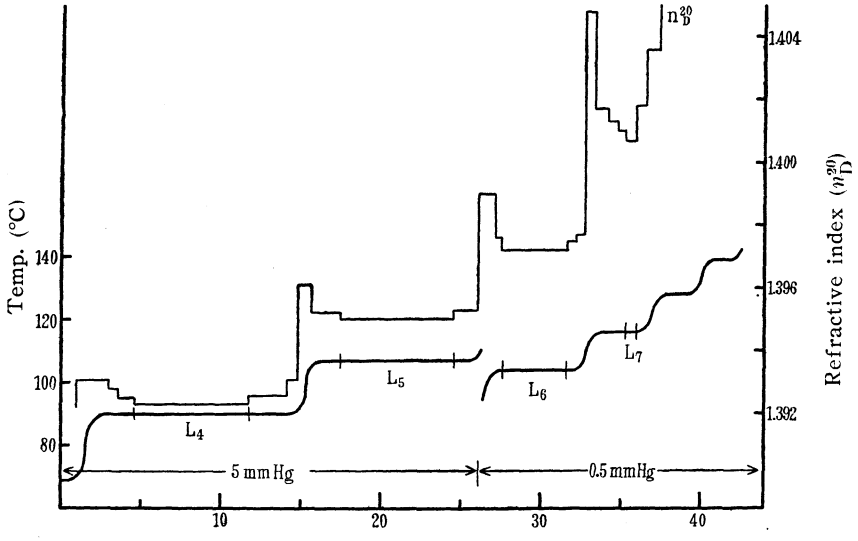



Fig. 2. Distillation curve of methoxy end-blocked dimethylpolysiloxanes.
$L_n$: Linear $n$-mer

Between the neighbouring plateaus, refractive index higher than that of the both side plateaus was found. From analogy with the preceding paper[1], the presence of the cyclo-compounds may be supposed. Comparing the distillation curve and the refractive index of the distillate in Fig. 2, the plateaus of $L_4$, $L_5$ and $L_6$ were taken as samples. Data on these polymers are also given in Table II. Judging from the refractive index, the members higher than heptamer may not have been separated from cyclo-compounds in this experiment. This fact has been ascertained by comparing the observed and calculated values of the molar refraction for the heptamer as shown in Table II.

**Analysis of Silicon.**—Silicon in these samples could not be determined by the usual digestion method with concentrated sulfuric acid, so the method using a gelatine capsule with concentrated sulfuric acid was developed. The analytical procedure, which will be soon published in detail, is as follows: 0.2 to 0.5 g. of sample weighed in a size 0 or 1 gelatine capsule was placed in a platinum crucible and the full amount of concentrated sulfuric acid to cover the capsule was added. At this time, the capsule floating on the sulfuric acid was pushed to the bottom of the platinum crucible by pressing it down with a glass rod, and it was left alone there at the room temperature. After two or three hours, the sulfuric acid decomposed the gelatine capsule and was mixed with the sample. This mixture in the covered crucible was heated with a small flame until a brown color appeared, then the acid was evaporated and the carbon was burned off using a low flame. The white residue was then ignited and weighed as silica.


## Summary

(1) Methoxy end-blocked dimethylpolysiloxanes have been prepared by the reaction of sodium bicarbonate with partially methanolyzed dimethyldichlorosilane.

(2) Distribution of the lower polymers was determined in regard to the composition of the partially methanolyzed dimethyldichlorosilane.

(3) Methoxy end-blocked dimethylpolysiloxanes from monomer (dimethyldimethoxysilane) to hexamer have been characterized.


*Department of Applied Chemistry,*
*Faculty of Engineering,*
*Osaka University,*
*Osaka*

# *Alkylalkoxypolysiloxanes. V.*[1] *Lower Members of Vinylmethoxypolysiloxanes with One to Five Silicon Atoms*

By Rokuro Ōkawara and Minoru Sakiyama

(Received February 16, 1955)

Recently, some data on vinylalkoxy-silanes and -disiloxanes[2] were presented, but no data on higher vinylalkoxypolysiloxanes have been reported. We wish now to report on the preparation and properties of vinylmethoxypolysiloxanes indicated by formula (I).

$$L_n;\ CH_3O\left[\begin{array}{c} HC=CH_2 \\ | \\ SiO \\ | \\ OCH_3 \end{array}\right]_n CH_3,\ (n=1\sim5)\quad (I)$$

For the preparation of the polymers, the method was used which is similar to that in the case of preparing ethylmethoxypolysiloxanes[3] and methoxy end-blocked dimethylpolysiloxanes.[1] Sodium bicarbonate was added to the partially methanolyzed vinyltrichlorosilane, which was prepared by mixing 1 mole of vinyltrichlorosilane and $x$ moles ($x=1.6$-$2.6$) of methanol. The liberated chlorine-free product was fractionated at as low a temperature as possible under reduced pressure to avoid the thermal polymerization of vinyl radical. A small amount of methanol was distilled out at first; then the lower members of the series (I) were obtained. The percentage composition of the lower members were plotted against the mole ratios $x$, and the results are shown in Fig. 1.

Monomer and dimer fractions were redistilled, respectively. The higher polymers were obtained from the residue of each experiment. To avoid the polymerization, the residue was rapidly distilled out at a pressure of 1 mm Hg until the stil-pot temperature reaches 220°C. The distillate thus obtained was rigorously fractionated through a high efficient column. Properties of the linear polymer are given in Table II. During the course of this fractionation, a long peroid of heating at high temperature (until 200°C/1 mm Hg) were required, but any polymeric changes such as gellation were not observed. The appearance of cyclo-compounds as indicated by formula (II) were also observed between the plateaus of the linear compounds, as in the case of preceding papers [1,3] but they could not be accurately characterized.

$$C_n;\ \left[\begin{array}{c} HC=CH_2 \\ | \\ SiO \\ | \\ OCH_3 \end{array}\right]_n \quad (n=4 \text{ and } 5)\quad (II)$$

## Experimental

**Starting Material.**—Vinyltrichlorosilane was presented from Linde Air Products Company.

### Preparation of Vinylmethoxypolysiloxanes

**(a) Partial Methanolysis and Polymerization with Sodium Bicarbonate.**—In this experiment, a procedure similar to that already described[1),3)] was used. To complete the reaction,

TABLE I

| | Starting Material | | | Vinylmethoxychlorosilane | | | | Sodium Bicarbonate | | Vinylmethoxypolysiloxane | |
|---|---|---|---|---|---|---|---|---|---|---|---|
| | A $CH_2=CHSiCl_3$ | B $CH_3OH$ | $x=B/A$ | Refluxing Temp. | Cl | Yield | | Added | Calcd*. | Yield | |
| | | | | | | Found | %theory | | | Found | %theory** |
| | g. | g. | mole ratio | °C | % | g. | % | g. | g. | g. | % |
| 1 | 40.4 | 20.9 | 2.6 | 122 | 4.5 | 35.5 | 94.7 | 2.7 | 2.5 | 28.5 | 82 |
| 2 | 40.4 | 18.4 | 2.3 | 122 | 12.3 | 35.0 | 92.5 | 5.5 | 5.0 | 27.0 | 82 |
| 3 | 80.8 | 32.0 | 2.0 | 122 | 20.0 | 70.0 | 91.7 | 17.8 | 17.5 | 45.0 | 73 |
| 4 | 40.4 | 15.2 | 1.9 | 123 | 16.0 | 34.0 | 88.8 | 7.9 | 7.4 | 21.0 | 68 |
| 5 | 80.8 | 28.8 | 1.8 | 121 | 23.5 | 71.0 | 92.4 | 20.0 | 19.5 | 43.0 | 71 |
| 6 | 40.4 | 12.8 | 1.6 | 120 | 22.0 | 34.0 | 88.1 | 10.5 | 10.0 | 12.0 | 42 |

* 1 Mol. of sodium bicarbonate was assumed to be equivalent to 2 g.-atoms of Cl contained in the chlorosilane mixture.

** Based on the amount of the starting materials.

1) Part IV of this series, T. Tanaka and R. Ōkawara, This Bulletin, 28, 364 (1955).

2) R. Nagel and H.W. Post, *J. Org. Chem.*, 17, 1382 (1952); R. Nagel, C. Tamborski and H.W. Post, ibid., 16, 1768 (1951).

3) R. Ōkawara, This Bulletin, 28, 360 (1955).

TABLE II

VINYLMETHOXYPOLYSILOXANES: $CH_3O\left[\begin{array}{l}CH=CH_2\\|\\SiO\\|\\OCH_3\end{array}\right]_n CH_3$

| Polymer Size | Boiling Point °C/mm Hg | Density $d_4^{20}$ | Refractive Index $n_D^{20}$ | Molecular Weiget Found* (Calcd.) | Molar Refraction Found (Calcd.)** | % Si Found (Calcd.) |
|---|---|---|---|---|---|---|
| Monomer ($n$=1)[a] | 122/760 | 0.9700 | 1.3930 | — (148.24) | 36.48 (36.72) | 18.85 (18.95) |
| Dimer ($n$=2)[b] | 86/11 | 1.0361 | 1.4107 | 248 (250.40) | 59.97 (60.28) | 22.55 (22.44) |
| Trimer ($n$=3) | 81/0.8 | 1.0636 | 1.4192 | 354 (352.57) | 83.74 (83.84) | 23.94 (23.90) |
| Tetramer ($n$=4) | 109/0.3 | 1.0784 | 1.4230 | 448 (454.73) | 107.36 (107.40) | 24.67 (24.71) |
| Pentamer ($n$=5) | 135/0.3 | — | 1.4284 | — (556.91) | — (130.96) | 24.94 (25.22) |

a) R. Nagel, C. Tamborski and H. W. Post, loc. cit b.p. 52.9/46, 59.5/62, $d_4^{25}$ 0.9669, $n_D^{25}$ 1.3910 and $MR_D$ 36.42.

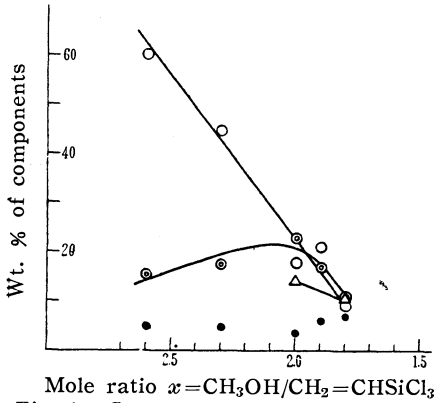
b) R. Nagel, C. Tamborski and H. W. Post, ibid. b.p. 120–20.6/46, $d_4^{25}$ 1.0627, $n_D^{25}$ 1.4172 and $MR_D$ 59.28.

* Cryoscopic measurements in benzene.

** Calculated from bond refractivities by E. L. Warrick, *J. Am. Chem. Soc.*, **68**, 2455 (1946).

the partially methanolyzed product was refluxed for 8–10 hours. The results are summarized in Table I.

The distribution of the lower polymers in the product was determined by fractionation through a semi-micro Stedman column of about 30 theoretical plates. The results are shown in Fig. 1.




Mole ratio $x = CH_3OH/CH_2=CHSiCl_3$

Fig. 1. Composition of the chlorine-free products obtained from sodium bicarbonate treatment.

● Methanol, ○ Monomer,
◎ Dimer, △ Trimer.

The product of Exp. 6 was a slightly viscous liquid and the composition could not be determined by fractionation, because the gellation occurred at 180°C/15 mm Hg in the stil-pot.

**(b) Redistillation of the Polysiloxanes.**— Monomer and dimer fractions were redistilled through the same column and the portions having the constant boiling point and refractive index were analyzed. The residues of Exp. 1–5 were simply distilled by a Claisen flask under 1 mm Hg until the stil-pot temperature reaches 220°C. The product distilled out below 170°C (40 g.) was fractionated rigorously through a high efficient semi-micro Stedman column of about 60 theoretical plates. The refractive index and the silicon content of the distillate are shown in Fig. 2.

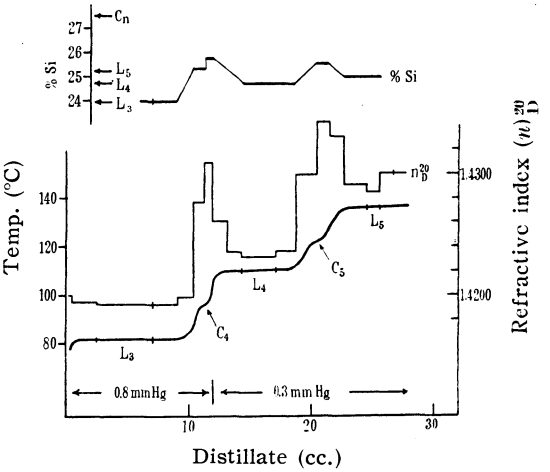



Fig. 2. Distillation curve of vinylmethoxypolysiloxanes.

$L_n$: Linear $n$-mer,
$C_n$: Cyclo-$n$-mer

The plateaus $L_3$, $L_4$ and $L_5$ were those of linear trimer, tetramer and pentamer, respectively. Between these plateaus the portions, $C_4$ and $C_5$, having a higher refractive index and a higher silicon content than the neighbouring portions were found.

From the silicon content and from the analogy of the preceding papers, $C_4$ and $C_5$ may be seen to be impure cyclotetramer and cyclopentamer respectively, indicated by formula (II). A slightly higher value of refractive index in front of the plateau of linear trimer was found in this experiment, but it may not be enough to suppose the presence of cyclotrimer.

**Analysis of Silicon.**—Monomer and dimer were weighed in gelatine capsule[1]; the higher polymers were weighed in a platinum crucible and decomposed by concentrated sulfuric acid.

## Summary

(1) Vinylmethoxypolysiloxanes have been prepared by the reaction of sodium bicarbonate with partially methanolyzed vinyltrichlorosilane.

(2) Distribution of the lower members was determined with regard to the composition of the partially methanolyzed product.

(3) Linear vinylmethoxypolysiloxanes containing from one to five silicon atoms have been prepared and characterized.

(4) Vinylmethoxycyclopolysiloxanes were found between the plateaus of linear polymer but they could not be accurately characterized.

The authors wish to express their hearty thanks to Mr. C. O. Strother of Linde Air Products Company for presenting them with vinyltrichlorosilane.

*Department of Applied Chemistry, Faculty of Engineering, Osaka University, Osaka*

# *Hyperconjugation. I. General Theory and Its Applications to Simple LCAO MO Calculations*

By Yasumasa I'HAYA

(Received March 16, 1955)

## I. Introduction[#]

It has been noticed by several writers that the alkyl group may have the power to conjugate with other resonating systems. In 1935, Baker and Nathan[1] introduced the concept later called hyperconjugation in order to explain the abnormal reaction rates of alkyl-substituted compounds. After that, the large increases in dipole moments of alkyl-substituted compounds were attributed by several authors[2-6] to a charge migration from the alkyl radical to the attached resonating systems. On the other hand, it has been found[7-9] that the length of the C-Me bond in such systems is less than the normal C-C bond length of 1.54Å. In 1939, Mulliken[10] has given a theoretical explanation on the basis of hyperconjugation to the red shifts of spectra and increases in the exaltation of molecular refractivity in alkylsubstituted resonating systems. Concerning the heats of hydrogenation of hyperconjugated systems, several investigations[11,13] have been published; for instance, Cullis, Hinshelwood and Mulcahy[12] state that the phenomenon of hyperconjugation seems to be significant in the oxidation of hydrocarbons.

[#] For reviews on experimental aspects, see C.L.Deasy, *Chem. Revs.*, **36**, 145 (1945), and more recently, V.A. Crawford, *Quart. Revs.*, **3**, 226 (1949).

1) J.W. Baker and W.S. Nathan, *J. Chem. Soc.*, 1840, 1844 (1935).
2) J.W. Baker and L.G. Groves, *J. Chem. Soc.*, 1144 (1939).
3) J.W. Baker, *J. Chem. Soc.*, 1150 (1939).
4) Mariott, Hobbs and Gross, *J. Am. Chem. Soc.*, **63**, 659 (1941).
5) H.C. Hurdis and C.P. Smyth, *J. Am. Chem. Soc.*, **64**, 2829 (1942).
6) H.C. Hurdis and C.P. Smyth, *J. Am. Chem. Soc.*, **65**, 89 (1943).
7) G. Herzberg, F. Patat and H. Verleger, *J. Phys. Chem.*, **41**, 123 (1937).
8) L. Pauling, H.D. Springall and K.J. Palmer, *J. Am. Chem. Soc.*, **61**, 927 (1939).
9) D.P. Stevenson, H.D. Burham and V. Schomaker, *J. Am. Chem. Soc.*, **61**, 2922 (1939).
10) R.S. Mulliken, *J. Chem. Phys.*, **7**, 121, 339, 356 (1939).
11) J.B. Conant and G.B. Kistiakowsky, *Chem. Revs.*, **20**, 181 (1937).
12) C. F. Cullis, C. N. Hinshelwood and M. F. R. Mulcahy, *Proc. Roy. Soc.* (London), **A196**, 160 (1949).

Mulliken, Rieke and Brown[13] give a description of an application of the molecular orbital method to the computation of hyperconjugation energies and bond orders in methylated hydrocarbon molecules. Explanations were given for the observed shortening of C-Me bonds and decrease in heats of hydrogenation in hyperconjugated molecules. They estimated an empirical exchange integral for C-$H_3$ bond, but assumed a coulomb integral for $H_3$ to be the same as for carbon atoms in a conjugated hydrocarbon. Thus, their new interpretations involve some bold assumptions, nevertheless their work seems to be very successful. Sklar[14] has computed the extent of migration of an electron from the methyl radical into the benzene ring by the method of antisymmetrized molecular orbitals, and obtained results which were in agreement with the experimental data. Roberts and Skinner[15] discussed the dissociation energies of carbon bonds in hydrocarbon radicals in terms of hyperconjugation

Herzfeld[16] and Matsen[17] independently discussed the effect of the migration of an electron from the substituent in the ring on the red shift and intensity of spectra; however they treat the methyl radical not as $-C\equiv H_3$ but as one group. More recently, Coulson and Crawford[18,19] have computed the hyperconjugation energies, charge distributions and red shifts in the spectra in methyl-substituted ethylenes and benzenes using the MO method.

Thus, although considerable work has been done in recent years in discussing hyperconjugation[20], no attempt has been made to compute the electronic structures of either methyl- or ethyl-substituted molecules with the common parameters. In this series, the effect of hyperconjugation is discussed in ethyl-substituted $\pi$-electron systems as well as in methyl-substituted ones using the LCAO MO method with common numerical parameters determined from the experimental aspects.

## II. General Theory of Hyperconjugation*

From the MO view point, the methyl group should have orbitals of $\pi$-character in order to conjugate with the $\pi$-orbitals of the resonating systems; namely it should have a structure of $-C\equiv H_3$. Now if the hydrogen atoms with 1s AO's $\psi_a$, $\psi_b$, $\psi_c$, ($\psi_a$ in yz plane) are called $H_a$, $H_b$, $H_c$, respectively, then we may form the following group orbitals with approximate contours (z-axis perpendicular to the paper) shown in Fig. 1#.

$$\begin{aligned} \phi_\sigma &= (\psi_a+\psi_b+\psi_c)/(3+6S)^{1/2} && \sigma\text{-type} \\ \phi_y &= (2\psi_a-\psi_b-\psi_c)/(6-6S)^{1/2} && \pi_y\text{-type} \\ \phi_x &= (\psi_b-\psi_c)/(2-2S)^{1/2} && \pi_x\text{-type} \end{aligned} \qquad (1)$$

where $S$ is the overlap integral between hydrogen atoms. The MO's such as $\phi_x$ and $\phi_y$ of Eq. (1), which may be called quasi-x and quasi-y MO's following Mulliken, are strictly equal in energy. Thus, in general, hyperconjugation is a two dimensional affair, namely in methylacetylene we have both x- and y- hyperconjugations, but in toluene we may have only one species of hyperconjugation for the reason that the other type of hyperconjugation perpendicular to the above one may be assumed to make no more contribution to the resonance energy for double bond than is present for simple unsaturated molecules like methylacetylene itself.

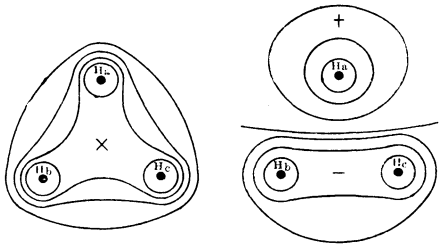



Fig. 1. $\sigma$ and $\pi_y$ group orbitals in methyl group.

Besides the $\pi$-character of the $-C\equiv H_3$ group, in ethylacetylene and ethylbenzene the quasi double bond between C and $H_2$ involves one $\sigma$-bond and one $\pi$-bond with the following quasi MO's:

13) R.S. Mulliken, C.A. Rieke and W.G. Brown, *J. Am. Chem. Soc.*, **63**, 41 (1941).

14) A.L. Sklar, *J. Chem. Phys.*, **7**, 184 (1939).

15) J.S. Roberts and H.A. Skinner, *Trans. Faraday Soc.*, **45**, 339 (1949).

16) K.F. Herzfeld, *Chem. Revs.*, **41**, 233 (1947).

17) F.A. Matsen, *J. Am. Chem. Soc.*, **72**, 5243 (1950).

18) C.A. Coulson and V.A. Crawford, *J. Chem. Soc.*, 2052 (1953).

19) V.A. Crawford, *J. Chem. Soc.*, 2058, 2061 (1953).

20) More interesting calculations concerning aromatic carbonium ions have recently been made; (a) E. Heilbronner and M. Simonetta, *Helv. Chim. Acta*, **35**, 1049 (1952), (b) N. Muller, L.W. Pickett and R.S. Mulliken, *J. Am. Chem. Soc.*, **76**, 4770 (1954).

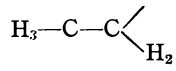
* The interpretation of hyperconjugation is a little different according to molecular orbital or valence bond descriptions. See, C. A. Coulson, "Valence", Oxford Univ. Press (1951), p. 310.

# This figure is reproduced from Professor Coulson's "Valence" with his kind permission.

21) The hyperconjugative effect may be accompanied with the inductive effect, as the former always causes polarities in various bonds to some extent. In this paper, however, the inductive effect except for next neighboring carbon atom is ignored because the hyperconjugative effect is to be chiefly dealt with.

$$\phi_\sigma=(\psi_a+\psi_b)/(2+2S)^{1/2}$$
$$\phi_\pi=(\psi_a-\psi_b)/(2-2S)^{1/2} \quad (2)$$

Here $\psi_a$ and $\psi_b$ refer to the two hydrogen atoms on opposite sides of the yz plane. If the orientation of the ethyl radical is assumed to be,



we have another type of hyperconjugation perpendicular to the above one. The proper quasi y-orbital would be

$$\phi_y=N\{2\times 2te\sigma-(\psi_a+\psi_b)/(2+2S)^{1/2}\} \quad (3)$$

where $2te\sigma$ is the tetrahedral orbital of the carbon atom of the methyl group which extends toward the other carbon atom of the ethyl group to make the C-C single bond within the ethyl group, and N is the normalization factor. This quasi y-orbital is to be hyperconjugated with the y-orbital of the carbon atoms of the attached conjugated systems, namely of the triple bond of acetylene. Thus in ethylacetylene we have two-dimensional hyperconjugation, but in ethylbenzene the treatment of x-hyperconjugation only is probably satisfactory just as it is in toluene.

After all, in the present study, it is assumed that the hyperconjugation of the substituted ethyl group is essentially the same as of the methyl group itself.

## III. Outline of Method and Empirical Parameters

It is convenient to express the molecular orbitals of the electrons as linear combinations of atomic orbitals (LCAO). If each MO is constructed out of n definite AO's $\phi_r(r=1,2,\ldots\ldots,n)$, we may write it down in the form,

$$\chi_j=\sum_{r=1}^{n} C_{jr}\phi_r \quad (4)$$

We have then following equations:

$$(\alpha_r-\varepsilon)C_r+\sum_{s\neq r}(\gamma_{rs}-S_{rs}\varepsilon)C_s=0 \qquad (r=1,2,\ldots\ldots,n) \quad (5)$$

where

$$a_r=\int\phi_r H\phi_r d\tau, \qquad \gamma_{rs}=\int\phi_r H\phi_s d\tau,$$
$$S_{rs}=\int\phi_r\phi_s d\tau \quad (6)$$

and $\varepsilon$'s are the energies of LCAO MO's. We write $\gamma_{rs}=\beta_{rs}+\frac{1}{2}S_{rs}(\alpha_r+\alpha_s)$ and assume that the Coulomb integral $\alpha_r$ has the same value $\alpha$ for all the carbon atoms in the system, and is $\alpha+\lambda_1\beta$ and $\alpha+\lambda_2\beta$ for pseudo atom $H_3$ or $H_2$ and next neighboring carbon atom respectively. Here $\beta$ corresponds to the benzene C-C, and $\lambda_1$ and $\lambda_2$ are empirical parameters to be determined from experimental aspects; particularly $\lambda_2$ is a measure of the inductive effect[21]. We also assume that $\beta_{rs}$ is proportional to the overlap integral between atoms r and s if r and s are bonded, otherwise zero[22,23]. That is

$$\beta_{rs}=(S_{rs}/S)\beta\equiv\rho_{rs}\cdot\beta \quad (7)$$

where S is the overlap integral between adjacent carbon atoms in benzene (C-C distance is 1.39Å).

With these assumptions and neglecting the overlap integrals, the equations (5) take the following forms,

$$(\alpha_r-\varepsilon)C_r+\sum_{s\neq r}\rho_{rs}\beta C_s=0 \quad (r=1,2,\ldots\ldots,n) \quad (8)$$

where the summation is carried out over all $s$ bonded to $r$. Then we get the sets of coefficients $C_{jr}$ corresponding to each eigenvalue $\varepsilon_j$. According to the definitions[24,25], the total $\pi$-electron density of atom $r$ is given by

$$q_r=2\sum_j C_{jr}^2 \quad (9)$$

and the bond order of a bond $r$-$s$ by

$$p_{rs}=2\sum_j C_{jr}C_{js} \quad (10)$$

where $q_r$ and $p_{rs}$ are given as a sum over all occupied MO's.

The overlap integrals needed to evaluate the $\rho$ values are computable from the table given by Mulliken et al[26]. using the experimental data for internuclear distances, and are shown in Table I. Although the overlap integral of the group orbitals such as C-$H_3$ and C-$H_2$ is also computable by the method of Mulliken et al. ($S=0.541$)[27], the parameter $\rho$ which was derived from the above overlap integral value was found to be not suitable for the present calculations probably because of neglecting all overlap integrals. If the

22) G.W. Wheland, *J. Am. Chem. Soc.*, **64**, 900 (1942).
23) R.S. Mulliken and C.A. Rieke, *J. Am. Chem. Soc.*, **63**, 1770 (1941).
24) G.W. Wheland and L. Pauling, *J. Am. Chem. Soc.*, **57**, 2086 (1935).
25) C.A. Coulson, *Proc. Roy. Soc.* (London), **A169**, 413 (1939).
26) R.S. Mulliken, C.A. Rieke, O. Orloff and H. Orloff, *J. Chem. Phys.*, **17**, 1248 (1949).
27) The overlap integral of the group orbital C-$H_3$ is computed as follows:

$$S(C,H_3)=\sqrt{\frac{2}{3}}\sin\alpha\,[1-S(1s,1s;H-H)]^{-\frac{1}{2}} \times S(1s,2te\sigma;C-H)$$

where $2\alpha$ is the tetrahedral valence angle 109.5°. See ref. 26), Section Vd.
28) See references 7) and 8).

overlap integral between C and $H_3$ or $H_2$ is estimated as the one between carbon $sp_3$ tetrahedral hybrid-AO and hydrogen 1s AO using the C-H internuclear distance 1.09Å[28], then we get $S(1s, 2te\sigma)=0.685$ and $\rho_{CH_3}$ or $\rho_{CH_2}=2.77$. The more suitable value was found to be chosen as 2.92[29] through calculations.

TABLE I

C($\pi$)-C($\pi$) OVERLAP INTEGRALS AND $\rho$ VALUES

| r(C-C), Å | S(2p$\pi$,2p$\pi$) | $\rho_r$* |
|---|---|---|
| 1.53 | 0.196 | 0.794 |
| 1.51 | 0.203 | 0.822 |
| 1.50 | 0.206 | 0.834 |
| 1.47 | 0.217 | 0.879 |
| 1.42 | 0.236 | 0.955 |
| 1.39 | 0.247 | 1.000 |
| 1.205 | 0.335 | 1.356 |

* $\rho_r=S(r)/S(1.39)$.

The overlap integral between the quasi $\pi_y$-orbital (3) and the tetrahedral orbitals of the attached carbon atom of the ethyl group is computed as 0.435[30] by the method of Mulliken et al., but the $\rho$ value derived from this was not adequate as mentioned above, $\rho_{CH_2-C}$ value is therefore taken as 2.35 in proportion to $\rho_{CH_3}$ or $\rho_{CH_2}$ (2.92).

As for another parameter $\lambda_1$, it seems certainly to be negative according to a theoretical explanation which was recently given by Muller, Pickett and Mulliken[20b], and probably in the neighborhood of $-0.5$. In this paper $-0.5$[31] was most suitable for reproducing experimental data, particularly dipole moments of hyperconjugated systems. Since the trigonal and digonal carbon atoms of the double and triple bonds are more electronegative than the tetrahedral carbon of the methyl group, parameter $\lambda_2$ will be also negative and is chosen as $-0.1$ taking account of the inductive effect from the adjacent $H_3$ group.

Since no precise method gives the numerical values of these quantities, the above assumed values involve considerable uncertainties. Therefore, as far as the reliability of these parameters is concerned, we should be contented with the agreement between predicted and observed values when these parameters are used in computations.

## IV. Application to Methyl and Ethylacetylenes

Following the ideas of Sec. II, methylacetylene has eight delocalized $\pi$-electrons and ethylacetylene ten delocalized ones. Therefore, the secular determinants are

$$\begin{vmatrix} z+\lambda_1 & \rho_{12} & 0 & 0 \\ \rho_{12} & z+\lambda_2 & \rho_{23} & 0 \\ 0 & \rho_{23} & z & \rho_{34} \\ 0 & 0 & \rho_{34} & z \end{vmatrix} = 0 \quad \text{twice} \qquad (11)$$

for methylacetylene, and

$$\begin{vmatrix} z+\lambda_1 & \rho_{12} & 0 & 0 & 0 & 0 \\ \rho_{12} & z+\lambda_2 & 0 & \rho_{24} & 0 & 0 \\ 0 & 0 & z+\lambda_1 & \rho_{34} & 0 & 0 \\ 0 & \rho_{24} & \rho_{34} & z+\lambda_2 & \rho_{45} & 0 \\ 0 & 0 & 0 & \rho_{45} & z & \rho_{56} \\ 0 & 0 & 0 & 0 & \rho_{56} & z \end{vmatrix} = 0,$$

$$\begin{vmatrix} z+\lambda_1 & \rho^* & 0 & 0 \\ \rho^* & z+\lambda_2 & \rho_{45} & 0 \\ 0 & \rho_{45} & z & \rho_{56} \\ 0 & 0 & \rho_{56} & z \end{vmatrix} = 0 \qquad (12)$$

for ethylacetylene. In Eqs. (11) and (12), $z=(\alpha-\varepsilon)/\beta$ and the numberings of atoms are shown in Fig. 2.

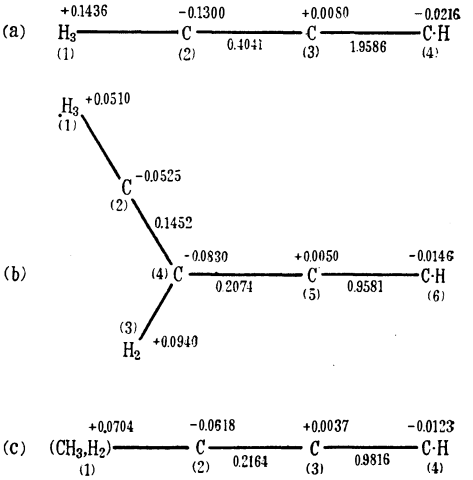



Fig. 2. The numberings of the atoms and the $\pi$-electron charge distribution and mobile bond order diagrams in methylacetylene (a) with both x and y-hyperconjugations and ethylacetylene (b) with x-hyperconjugation only and (c) with y-hyperconjugation only (taking the x-axis to be perpendicular to the plane of the paper and omitting bond orders between C and quasi-$\pi$ group orbitals).

29) In ref. 13), the $\rho_{CH_3}$ value was taken as 4: Pullman and Metzger took it as 2.5; *Bull. Soc. Chim.*, 57, 1021 (1948). The same value 2.5 was chosen by Coulson and Crawford in ref. 18) in calculations including overlap. Mulliken and Rieke found that if the overlap integral is included in the computations, the magnitude of the parameter $\rho_{CH_3}$ is reduced from 4 to about 2; see ref. 23) or R.S. Mulliken, *Rev. Modern Phys.*, 14, 265 (1942). The author has checked this evaluation, and obtained the value 2.19. The self-consistent computation including overlap integrals using such a parameter is in course of computation.

30) This value is obtained as follows:

$$S(CH_2,C)=N_1[\sin\alpha\times S(2te\sigma,2te\sigma;\ C-C) + 2N_2\cos^2\alpha\times S(1s,2te\sigma;\ C-H)],$$

where $N_1$ and $N_2$ are the normalization factors.

31) In ref. 18), Coulson and Crawford also took as $\lambda_1=-0.5$ and $\lambda_2=-0.1$ from the dipole moment evidence.

Using the following values of empirical parameters: for methylacetylene, $\lambda_1=-0.5$, $\lambda_2=-0.1$, $\rho_{12}=2.92$, $\rho_{23}=0.879$ (as 1.469 Å)[32], $\rho_{34}=1.356$ (as 1.205 Å)[32], and for ethylacetylene, $\lambda_1=-0.5$, $\lambda_2=-0.1$, $\rho_{12}=2.92$, $\rho_{24}=0.834$ (as 1.50 Å)[33], $\rho_{45}=0.879$ (as 1.47 Å)[33], $\rho_{56}=1.356$, $\rho^*=2.35$, computational results are given in Table II, and final charge distribution diagrams in Fig. 2.

TABLE II
THE OCCUPIED ENERGY LEVELS AND DIPOLE MOMENTS OF METHYL AND ETHYLACETYLENES

| | Occupied energy levels | μ (D) | |
|---|---|---|---|
| | $z$[a] | calcd. | obsd. |
| Methyl-acetylene | +1.260226[b] | 0.727 | 0.72[d] |
| | +2.915310[b,c] | | 0.77[e] |
| Ethyl-acetylene | +1.195202 | 0.783 | 0.80[e] |
| | +1.243628 | | |
| | +2.280381[c] | | |
| | +2.391106[c] | | |
| | +3.251446[c] | | |

a. Note $z=(\varepsilon-\alpha)/\beta$, where $\varepsilon$'s are the energies of MO's.
b. In methylacetylene, the occupied energy levels are doubly degenerate.
c. These are attributable to the hyperconjugated quasi-$\pi$ orbitals.
d. H. E. Watson and K. L. Ramaswamy, Proc. Roy. Soc. (London), **A156**, 130 (1936).
e. F. J. Krieger and H. H. Wenzke, J. Am. Chem. Soc., **60**, 2115 (1938).

**Bond Order and Bond Length.**—Using the bond order and bond length curve[34], we can estimate the approximate bond lengths from the calculated bond orders shown in Fig. 2. Thus we obtained $C_2$-$C_3$(1.47 Å), $C_3$-$C_4$(1.20 Å) in methylacetylene and $C_2$-$C_4$(1.52 Å), $C_4$-$C_5$ (1.47 Å), $C_5$-$C_6$(1.20 Å) in ethylacetylene. The experimental values of internuclear distance are given only for methylacetylene, and the agreements between the calculated and observed values are complete. Consequently, we may consider that the values of parameters assumed before are certainly adequate. In ethylacetylene, no appropriate experimental data for C-C length have been given, but the calculated values shown above might be very suggestive if experimental data could be available on the bond length of the carbon-carbon bond adjacent to the triple bond in ethylacetylene.

32) Spectroscopic data; G. Herzberg, "Infrared and Raman Spectra of Polyatomic Molecules" (D. Van Nostrand, New York, 1945).
33) These are estimated values.
34) C.A. Coulson, *Proc. Roy. Soc.*, A169, 413 (1939), A207, 91 (1951).

**Resonance Moment.**—The dipole moment due to the migration of electrons from alkyl group to carbon atoms of acetylene, assuming it to be a resonance moment only, may be calculated from the charge distribution diagrams. In Table II, the calculated values are compared with the observed ones and agreements are very satisfactory in both cases. Attention should be called to the neglect of dipole moment which may arise from the $\sigma$-electrons (mainly C-H moment).

The comparison of the computed and the empirical conjugation energies will be investigated in the subsequent paper including overlap integrals[35].

## V. Application to Methyl and Ethylbenzenes

When making computations by the MO method, the total effective number of $\pi$-electrons is taken to be eight and ten respectively for toluene and ethylbenzene each numbered as in Fig. 3. In these cases, the treatment of $\pi$-hyperconjugation only is probably satisfactory as mentioned in Sec. II.

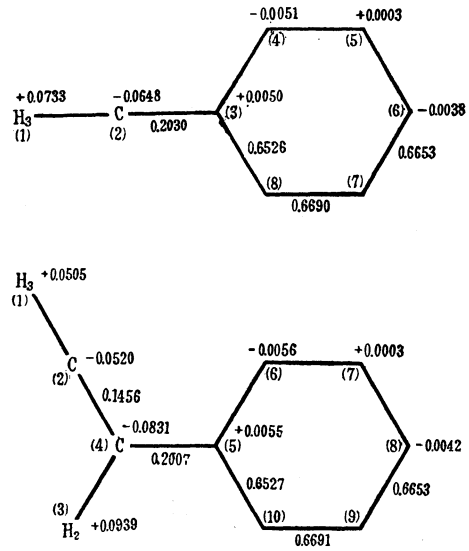



Fig. 3. The numberings of the atoms and the $\pi$-electron charge distribution and mobile bond order diagrams in toluene and ethylbenzene (omitting bond orders between C and quasi-$\pi$ group orbitals).

Using the same empirical parameters in secular equations as those for substituted acetylenes (cf. Sec. IV.), the energy levels of molecular orbitals (in Table III), charge distributions (in Fig. 3) and resonance moments (in Table IV) are obtained.

35) In ref. 13) and 18), Mulliken et al. and Coulson and Crawford computed the empirical conjugation energies from heats of combustion and compared with the theoretical values corrected for extension and compression of the $\sigma$-bonds. See Series II of this article.

TABLE III
THE CALCULATED ENERGY LEVELS OF TOLUENE AND ETHYLBENZENE

| Toluene | Ethylbenzene |
|---|---|
| $z$[a] | $z$[a] |
| −1.000000 | −1.000000 |
| −0.986142[b] | −0.994367[b] |
| +0.952463 | +0.950784 |
| +1.000000 | +1.000000 |
| +1.936516 | +1.914324 |
| +2.823428[c] | +2.324890[c] |
| | +3.156861[c] |

a. See foot-note (a) of Table II.
b. These correspond to the lowest unoccupied levels.
c. These are attributable to the hyperconjugated quasi—orbitals.

**The Red Shifts of the Near Ultraviolet Absorption Spectra.**—The above computed migration of electrons from alkyl group to the ring causes wave-length shift and the variation of intensity of 0–0 band in the absorption spectra of alkylsubstituted benzene. In order to compute the extent of these shifts, we must estimate the nature of the transition in alkylbenzene. In benzene, the excitation of the electron from the highest occupied orbitals in the ground state to the lowest unoccupied orbitals produced singlet and triplet states. Excitation energies computed without electron repulsion may be thought to give the average values of the actual levels[36]. In alkyl-substituted benzenes, the original orbital degeneracy is removed by the perturbation of the attached alkyl group. Therefore, in this case, we may assume that the average values of the theoretical excitation energies will give the approximate transition energy of alkylbenzene.

Thus for toluene, we assume a set of hypothetical states with the electron configurations as follows[37]:

$$\begin{array}{ll} \mathrm{Y}: & (\chi_0)^2\ (\chi_1)^2\ (\chi_2)\ (\chi_3)^2\ (\chi_5) \\ \mathrm{Y}': & (\chi_0)^2\ (\chi_1)^2\ (\chi_2)^2\ (\chi_3)\ (\chi_4) \\ \mathrm{Z}: & (\chi_0)^2\ (\chi_1)^2\ (\chi_2)\ (\chi_3)^2\ (\chi_4) \\ \mathrm{Z}': & (\chi_0)^2\ (\chi_1)^2\ (\chi_2)^2\ (\chi_3)\ (\chi_5) \end{array} \qquad (13)$$

For instance, a transition from the ground state N to the upper hypothetical state Y would involve transition of an electron from $\chi_2$ to $\chi_5$, leaving a second electron in $\chi_2$ and all other electrons in closed shells. Therefore,

$$\Delta\varepsilon_{\mathrm{av.}} = (1/2)(\varepsilon_5+\varepsilon_4-\varepsilon_3-\varepsilon_2) = h\nu \qquad (14)$$

where $\varepsilon_j$ is the $j$'th MO energy, and $\nu$ is the frequency of a transition from the ground state to an averaged hypothetical state which corresponds to the average height of the actual state.

Now we show that the relative shift in frequency between the $\nu$ of Eq. (14) and the corresponding mean frequency of benzene, $\nu' = -2\beta/h$, is given by

$$(\nu'-\nu)/\nu' = 1+(\varepsilon_5+\varepsilon_4-\varepsilon_3-\varepsilon_2)/4\beta \qquad (15)$$

These quantities are computed for toluene and ethylbenzene from the energy levels in Table III, and are shown in Table IV with the ones calculated from our observed 0–0 bands of the near ultraviolet absorption spectra (see Sec. VI). We find that they are in complete agreement with each other. A prediction for the 0–0 band frequencies in alkylbenzenes is also possible if the corresponding position in benzene is estimated. The calculated frequencies both in vapor and in solution are shown in Table IV, taking the values for benzene as 2625 Å[38] and 2640 Å[39] corresponding to vapor and solution states respectively.

TABLE IV
DIPOLE MOMENTS, ABSORPTION FREQUENCIES AND OSCILLATOR STRENGTHS OF TOLUENE AND ETHYLBENZENE

| | | Toluene | Ethylbenzene |
|---|---|---|---|
| $\mu$ (D) | calcd. | 0.362 | 0.549 |
| | obsd. | 0.37[a] | 0.58[a] |
| $\frac{\nu'-\nu}{\nu'}$ | calcd. | 0.016 | 0.014 |
| | obsd. | 0.019[b], 0.016[c] | 0.015[b] |
| Vapor $\lambda$, (Å) | calcd. | 2666 | 2661 |
| | obsd. | 2668[d] | 2664[d] |
| Solution $\lambda$, (Å) | calcd. | 2681 | 2678 |
| | obsd. | 2692[b] | 2680[b] |
| $f\times10^4$ | calcd. | 20.5 | 14.2 |
| | obsd. | 15[b], 10[e], 30[f] | 9[b] |

a. J. W. Baker and L. G. Groves, J. Chem. Soc., 1144 (1939).
b. Our experimental data. See Sec. VI and Fig. 4.
c. H. Sponer and E. Teller, Rev. Modern Phys., **13**, 75 (1941).
d. F. A. Matsen, W. W. Robertson and R. L. Chuoke, Chem. Revs., **41**, 273 (1947).
e. R. S. Mulliken and C. A. Rieke, "Reports on Progress in Physics", vol. 8, p. 331 (1941).
f. Sponer and Löwe, J. Opt. Soc. Am., **39**. 840 (1949).

36) C.C.J. Roothaan and R.S. Mulliken, *J. Chem. Phys.*, **16**, 118 (1948).
37) R.S. Mulliken, *J. Chem. Phys.*, **7**, 353 (1939).
38) H. Sponer, G. Nordheim, A.L. Sklar and E.Teller, *J. Chem. Phys.*, **7**, 207 (1939).
39) F.A. Matsen, W.W. Robertson and R.L. Chuoke, *Chem. Revs.*, **41**, 273 (1947).

**Oscillator Strength.**—Before calculation of the oscillator strength[40],

$$f=1.085\times10^{11}\nu Q^2 \qquad (16)$$

where $\nu$ is the frequency of the transition in $cm^{-1}$, we need to calculate the dipole strength $Q$ for the transition. In alkylbenzenes, the wave function of the lowest-lying singlet state is approximately given as follows by analogy with the corresponding one ($^1B_{2u}$) of benzene[41].

$$\psi(V)=[\psi(Z)-\psi(Z')]/2^{1/2} \qquad (17)$$

where $\psi(Z)$ and $\psi(Z')$ correspond to the electron configurations of third and forth lines shown in (13) respectively. The $Q$-values of the $N\rightarrow Z$ and $N\rightarrow Z'$ transitions in alkylbenzenes are z-polarized (figure axis is taken to be z), and

$$Q(N\rightarrow V)=[\int\psi_N(z_1+z_2)\psi_Z d\tau - \int\psi_N(z_1+z_2)\psi_{Z'}d\tau]/2^{1/2} \qquad (18)$$

where $z_1$ and $z_2$ refer to the two electrons occupied initially in the $\chi_2$ or $\chi_3$ orbitals (cf. (13)). The transition moments for the other axis which is perpendicular to $z$-axis in the benzene plane are zero. In the case of toluene, for example, this reduces to

$$Q(N\rightarrow V)=2^{1/2}[\int\chi_2 z\chi_4 d\tau-\int\chi_3 z\chi_5 d\tau] \qquad (19)$$

Using Eq. (4) and calculated coefficients $C_{jr}$, we get

$$Q(N\rightarrow V)=[1-2(C_{23}C_{43}+C_{24}C_{44}-C_{25}C_{45}-C_{25}C_{46})]r/2^{1/2} \qquad (20)$$

where $r$ is the carbon-carbon distance in benzene. Then we can calculate $f$ by Eq. (16). The $f$-value thus obtained theoretically is shown in Table IV with the one for ethylbenzene, in which the procedure of computation is the same as above.

The discussions for the conjugation energy are delayed in the subsequent paper.

## VI. The Near Ultraviolet Absorption Spectra of Alkylbenzenes

On account of the lack in the data of the near ultraviolet absorption spectra of alkylbenzenes, the solution spectra were obtained in normal hexane on a Beckman quartz spectrophotometer DU (see Fig. 4). The 0–0 band of benzene in solution was estimated to be 2640 Å (note the 0–0 band in benzene is forbidden). The oscillator strengths for the transitions were computed from the integrated areas under the extinction curves, by the following equation[42],

$$f=4.32\times10^{-9}\int\varepsilon_\nu d\nu \qquad (21)$$

where $\nu$ is the frequency in $cm^{-1}$. No correction was made for the effect of solution on the $f$-value.

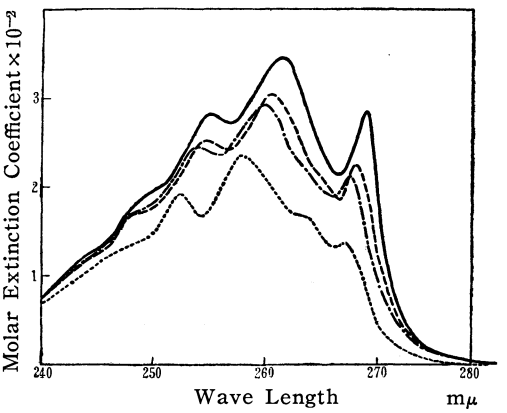



Fig. 4. The near ultraviolet absorption spectra in normal hexane of toluene (——), ethylbenzene (– – – –), iso-propylbenzene (–·–·–·–) and tert-butylbenzene (·····).

## VII. Critical Discussion

From the outset, it was our intention to calculate the electronic states of alkylbenzenes with a view to extending the theory of hyperconjugation. However, the precise computations of the electronic states in such complicated molecules are impossible for the present, so we cannot help making use of the empirical LCAO MO method with empirical parameters. Since no precise computations can be made for the Coulomb integrals of $H_3$ or $H_2$ groups or for the exchange integrals between C and $H_3$ or $H_2$, we meet first of all with a difficulty when we attempt to give reasonable values to these quantities. Consequently, values of these parameters which were chosen from several assumptions, so as to reproduce the observed dipole moments as well as possible were applied not only to alkylbenzenes but to alkyl-substituted acetylenes, and fairly satisfactory results were obtained. Therefore, these empirical parameters seem to be considerably reliable when the overlap integrals are ignored.

The calculations show that the theory of

40) R. S. Mulliken and C. A. Rieke, "Reports on Progress in Physics", Vol. 8, p. 231 (1941).

41) For benzene $\phi(Z)$ and $\phi(Z')$ are degenerated so that the coefficients of $\phi(Z)$ and $\phi(Z')$ should be equal in magnitude, for the alkylbenzenes, however, $\phi(Z)$, $\phi(Z')$ are no longer degenerate and the coefficients should be slightly unequal. This inequality will not affect the center of gravity of the excited states, but it must not give sufficiently correct $Q$-values for the transitions since equal mixing should not be expected. Matsen discussed the resulting errors in an appendix of ref. 17). See also reft. 37) and A.L. Sklar, *J. Chem. Phys.*, 5, 669 (1937), M. Goeppert-Mayer and A.L. Sklar, *J. Chem. Phys.*, 6, 645 (1938).

42) J.R. Platt and H.B. Klevens, *Rev. Modern Phys.*, 16, 182 (1944).

hyperconjugation introduced by Mulliken, Rieke and Brown has a real importance for the study of the electronic structure not only of methylated organic molecules but of other alkyl-substituted ones; namely even when the methyl group is substituted for a hydrogen atom of the methyl group, the hyperconjugation is recognized as being the same as in the case of methyl group only. For such a complicated organic molecule, the usual method consists of computing its electronic structure taking only $\pi$-electrons of carbon atoms involved; however the phenomenon of hyperconjugation suggests that to a large extent the 1s electrons of the hydrogen atoms and even the tetrahedral hybridized orbital of the carbon atoms in the alkyl group take part in $\pi$-conjugation. More accurate calculations are made in the subsequent papers using the LCAO MO and LCAO SCF MO methods including the overlap integrals.

## Summary

The theory of hyperconjugation has been extended and applied to computations of the electronic structures of methyl and ethyl-substituted acetylenes and benzenes using the empirical LCAO MO method not including the overlap integrals. The common empirical parameters introduced from experimental aspects were used consistently through the calculations. Charge distributions of the $\pi$-electrons, bond orders, resonance moments, relative shifts of near ultraviolet absorption spectra and oscillator strengths were calculated, and fairly satisfactory results, compared with the observed values, were obtained. Because of the lack of appropriate absorption data, the near ultraviolet absorption spectra of alkylbenzenes in normal hexane were obtained. The calculations show that when the methyl group is substituted for a hydrogen atom of the methyl group, the hyperconjugative effect is recognized as same as before.

The author wishes to thank Professor A. Kotera and Dr. S. Nagakura for many helpful discussions.

*Department of Chemistry, Tokyo University of Education, Tokyo*

# *Hyperconjugation. II. The Electronic Structures and Conjugation Energies of Alkylbenzenes*

By Yasumasa I'HAYA

(Received March 16, 1955)

## I. Introduction

It was shown in Part I[1] that even in ethyl-substituted acetylene and benzene the ideas of extended hyperconjugation could be also applied. In this paper, the author gives more detailed calculations of the electronic structures and conjugation energies not only in toluene and ethylbenzene but in *tert*-butylbenzene by the empirical LCAO MO method including overlap integrals for neighboring atoms. Since such a computation including overlap has been made only by Coulson and Crawford[2] for a series of methyl-substituted benzenes and ethylenes, it is desirable to investigate the electronic structures of the other alkyl-substituted resonating systems, particulary of alkylbenzenes which have long been a question, using the same method as in the case of toluene.

The models for the methyl and ethyl groups were already established in Sec. II of Part I, but a model for the *tert*-butyl group remains unsettled. In this case, it seems fairly reasonable to consider the three $CH_3$ as one group such as $H_3$ in toluene; that is

$$-C-(CH_3)_3.$$

Therefore, we have two dimensional hyperconjugation to be conjugated with an attached resonating system, but in *tert*-butylbenzene only one type of hyperconjugation is probably effective for just the same reason as in toluene.[3]

* A part of this work was presented at the 7th Annual Meeting of the Chemical Society of Japan, Tokyo University, April 3, 1954.

1) The preceding paper.

2) (a) C.A. Coulson and V.A. Crawford, *J. Chem. Soc.*, 2052 (1953); (b) V. A. Crawford, ibid., 2058, 2061 (1953).

3) See Sec. II of Part I.

## II. Method of Computations

The method of LCAO MO (Linear Combination of Atomic Orbitals Molecular Orbital) with inclusion of the overlap integrals between adjacent atomic orbitals requires certain changes in the forms of the equations and the definitions mentioned in Sec. III of Part I. If we denote different atoms by a Greek suffix $\mu$, $\nu$,..... and molecular orbitals (MO) by a Latin suffix i, j,....., each MO $\psi_j$ is represented by n AO's $\phi_\mu$ in the form

$$\psi_j=\sum_{\mu=1}^{n} x_{j\mu}\phi_\mu \qquad (1)$$

where tne coefficients $x_{j\mu}$ are determined by minimizing the total energy. The energy levels of MO's $\psi_j$ are given by the roots of the secular determinant

$$\det|H_{\mu\nu}-\varepsilon S_{\mu\nu}|=0 \qquad (2)$$

where

$$H_{\mu\mu}=\int\phi_\mu H\phi_\mu d\tau=\alpha_\mu,$$
$$H_{\mu\nu}=\int\phi_\mu H\phi_\nu d\tau=\tau_{\mu\nu},$$
$$S_{\mu\nu}=\int\phi_\mu\phi_\nu d\tau.$$

Neglecting interactions of non-neighbor atoms, making replacements $\beta=\tau-\alpha S$, $\xi_\mu=1-\lambda_\mu S$, and $z=(\alpha-\varepsilon)/(\tau-S\varepsilon)$, and assuming $\tau_{\mu\nu}$ is proportional to $S_{\mu\nu}$ [4], the above secular determinant is simplified as a polynomial of $z$. (note $\alpha$, $\beta$, $\tau$ and $S$ correspond to benzene).

Illustration for the case of toluene, the numbering of atoms shown in the diagram, is as follows; this molecule has eight $\pi$-electrons in orbitals made by combining the six $2p\pi$ carbon AO's and the two quasi-$\pi$ orbitals of the methyl group. Because of the $C_{2v}$ symmetry of the molecule[5], the MO's are divided into two groups, one is $a_2$ and the other is $b_1$ symmetries.

$$\Delta(a_2)=\begin{vmatrix} z & 1 \\ 1 & z \end{vmatrix}=0 \qquad (3)$$

$$\Delta(b_1)=\begin{vmatrix} \xi_1 z+\lambda_1 & \rho_{12} & 0 & 0 & 0 & 0 \\ \rho_{12} & \xi_2 z+\lambda_2 & \rho_{23} & 0 & 0 & 0 \\ 0 & \rho_{23} & z & 1 & 0 & 0 \\ 0 & 0 & 2 & z & 1 & 0 \\ 0 & 0 & 0 & 1 & z & 2 \\ 0 & 0 & 0 & 0 & 1 & z \end{vmatrix}=0 \qquad (4)$$

In these determinants, $\rho$'s are the proportional constants of the exchange integrals to overlap ($\rho_{\mu\nu}=S_{\mu\nu}/S$) and $\lambda$'s are the correction terms for the Coulomb integrals in units of $\beta$. Solution of above determinantal equations (3) and (4) provides us with the orbital energies $\varepsilon_j$ (shown in Table II) using the relation

$$\varepsilon_j=\alpha-\frac{z}{1-Sz}\beta \qquad (5)$$

and the corresponding coefficients $x_{j\mu}$'s.

TABLE I
EMPIRICAL PARAMETERS

| | $\lambda_1$ | $\lambda_2$ | $\rho_{12}$ | $\rho_{23}$ |
|---|---|---|---|---|
| Toluene | −0.5 | −0.1 | 2.92 | 0.834 |
| *tert*-Butylbenzene | −1.0 | −0.1 | 3.0 | 0.777 |
| | $\lambda_1,\lambda_3$ | $\lambda_2,\lambda_4$ | $\rho_{12},\rho_{34}$ | $\rho_{24},\rho_{45}$ |
| Ethylbenzene | −0.5 | −0.1 | 2.92 | 0.822 |

TABLE II
ORBITAL ENERGIES $w_i$ OF ALKYLBENZENES*

| | Toluene | Fthylbenzene | *tert*-Butylbenzene |
|---|---|---|---|
| $2a_2$ | −1.328021 | −1.328021 | −1.328021 |
| $4b_1$ | −1.297212 | −1.297330 | −1.320806 |
| $3b_1$ | +0.767269 | +0.768415 | +0.770480 |
| $1a_2$ | +0.801925 | +0.801925 | +0.801925 |
| $2b_1$ | +1.305127 | +1.290928 | +1.298214 |
| $1b_1$ | +1.623852 | +1.439167 | +1.515066 |
| $0b_1$ | | +1.745722 | |

* $w_i=(\varepsilon_i-\alpha)/\beta$, and orbital energies higher than $2a_2$ are not recorded.

The empirical parameters used are the same as that of Part I excepting *tert*-butylbenzene and some refinements made in $\rho_{23}$ both in toluene and ethylbenzene, and are recorded in Table I. Since the choice of parameters for *tert*-butylbenzene are quite arbitrary, considerable uncertainties remain. Judging from a result of calculations, however, they seem not to be very seriously wrong. The author of course wishes that further support will be provided for these numerical values of the empirical parameters.

The influences of the inductive effect to the Coulomb integrals of the ring carbon atoms are ignored.[6]

## III. Conjugation Energies and Hyperconjugation Energies

In order to obtain conjugation and hyperconjugation energies, the total energies $E(L)$ and $E(S)$ of the $\pi$-electrons in localized and semi-localized bond structures must be calculated, in addition to the total energy of the delocalized model $E(D)$. Here what is called the total energy of the semi-localized bond structure $E(S)$ is the total sum of each $\pi$-electron energies in $C-H_3$ group and the delocalized benzene. Now we get the vertical conjugation (or vertical $\pi$-resonance) energy

4) G.W. Wheland, *J. Am. Chem. Soc.*, **63**, 2025 (1941); ibid., **64**, 900 (1942).

5) In this paper, the benzene ring in ethylbenzene is approximately treated to be also $C_{2v}$ symmetry.

6) See foot-note 21) of Part I.

$E(\mathrm{CJ})$[7] and the vertical hyperconjugation energy $E(\mathrm{HCJ})$ as follows:

$$E(\mathrm{CJ})=E(\mathrm{L})-E(\mathrm{D})$$
$$E(\mathrm{HCJ})=E(\mathrm{S})-E(\mathrm{D}). \quad (6)$$

These energies computed theoretically for a series of alkylbenzenes are listed in column 3 of Table IV ($E(\mathrm{HCJ})$ is given in bracket).

On the other hand, it has been shown by Mulliken, Rieke and Brown[8] (hereafter called M. R. B.) that the following empirical formula for the heats of combustion fits the available data for saturated hydrocarbons with considerable accuracy:

$$-\Delta H_{298^\circ}=54.625N_{\mathrm{CH}}+48.25N_{\mathrm{CC}}-1.5N_{\mathrm{Me}}+22.18N_{\mathrm{C=C}}+56.6N_{\mathrm{C\equiv C}} \quad (7)$$

where $N_{\mathrm{CH}}$, $N_{\mathrm{CC}}$, $N_{\mathrm{Me}}$, $N_{\mathrm{C=C}}$ and $N_{\mathrm{C\equiv C}}$ are the numbers of C-H bonds, C-C bonds (counting each bond in a multiple bond; e.g., nine in benzene), methyl groups, C=C double bonds, and C≡C triple bonds, respectively. Then the difference $\Delta$ between the value empirically predicted by Eq. (7) and observed heat of combustion[9] is 39.46, 40.96 and 40.91 kcals. for benzene, toluene and ethylbenzene respectively. Therefore, the value $\Delta(\mathrm{HCJ})$, which is obtained after subtraction from the $\Delta$ of benzene, is 1.5 kcal. for toluene and 1.45 kcal. for ethylbenzene.

## IV. Third-Order Conjugation

It has been noticed that when comparing empirical and theoretically computed (vertical) conjugation energies, we should make two corrections; the one to the energy of compression and extension of the C-C bond length. the other to the energy of the third-order conjugation. The importance of doing the former correction for the empirically determined conjugation or resonance energies from the formula (7), has been demonstrated by several writers[10,11,12] and more recently Coulson and Crawford[2a] have recalculated the compression and extension energies using Morse functions. In this paper, the value C=35.49 kcal. for benzene which was given by above authors is used without revision.

The latter correction for the theoretically computed conjugation energies which was first stressed by M. R. B., is based upon the fact that ideal single (or double) bond is one which is slightly weaker and longer than that found in ethane (or ethylene), because the single (or double) bond in ethane (or ethylene) is strengthened by third-order conjugation. The corrected total conjugation energy is therefore given by the sum of the ordinary of first-order ($E(\mathrm{CJ})$ in Eq. (6)) and third-order conjugation energies; that is

$$E(\mathrm{CJ})=E_1(\mathrm{CJ})+E_3(\mathrm{CJ})$$

The third-order conjugation energies per bond are readily computed for various bond lengths on the basis of the variation method including overlap integrals between adjacent atomic orbitals:

$$\varepsilon(r)=2\left\{\frac{z_1(\mathrm{D})}{1-Sz_1(\mathrm{D})}+\frac{z_2(\mathrm{D})}{1-Sz_2(\mathrm{D})}-\frac{2z(\mathrm{L})}{1-Sz(\mathrm{L})}\right\} \quad (8)$$

per dimension where $-z_1(\mathrm{D})$ and $-z_2(\mathrm{D})$ are the lower two roots of the secular equation for both delocalized ethane and ethylene and take the following forms;

$$\left.\begin{matrix}z_1(\mathrm{D})\\ z_2(\mathrm{D})\end{matrix}\right\}=\frac{1}{2\xi_1\xi_2}[\xi_1\lambda_2+\xi_2\lambda_1\pm\xi_1\rho_{23}+\{(\xi_1\lambda_2+\xi_2\lambda_1\pm\xi_1\rho_{23})^2-4\xi_1\xi_2(\lambda_1\lambda_2-\rho_{12}^2\pm\lambda_1\rho_{23})\}^{1/2}] \quad (9)$$

and $-z(\mathrm{L})$ is a doubly degenerated root of the quadric secular equation for localized two $CH_3$ groups.

$$z(\mathrm{L})=\frac{1}{2\xi_1\xi_2}[\xi_1\lambda_2+\xi_2\lambda_1+\{(\xi_1\lambda_2+\xi_2\lambda_1)^2-4\xi_1\xi_2(\lambda_1\lambda_2-\rho_{12}^2)\}^{1/2}] \quad (10)$$

In Eqs. (9) and (10), $\rho_{12}$ and $\rho_{23}$ refer to the $C\equiv H_3$ or $C=H_2$ and C-C bonds respectively, and $\lambda$'s and $\xi$'s have the same meaning mentioned in Sec. II.

Taking the C-C overlap integral $S$ in benzene as 0.247, values of $\varepsilon(r)$ are evaluated for various bond lengths and are listed in Table III.

TABLE III

THIRD-ORDER CONJUGATION ENERGIES

| r(C-C), in Å | $\varepsilon(r)$, in units of $\beta$ |
|---|---|
| 1.54 | 0.001267 |
| 1.53 | 0.001308 |
| 1.52 | 0.001350 |
| 1.51 | 0.001396 |
| 1.50 | 0.001445 |
| 1.46 | 0.001659 |
| 1.39 | 0.002115 |
| 1.33 | 0.002595 |

7) This vertical conjugation energy corresponds to a quantum-mechanical resonance energy named by Coulson and Altmann in ref. 12).

8) R.S. Mulliken, C.A. Rieke and W.G. Brown, *J. Am. Chem. Soc.*, **63**, 41 (1941).

9) Heat of combustion for benzene, toluene and ethylbenzene is 789.08, 943.58 and 1101.13 kcals., respectively; W.C. Price, *Chem. Revs.*, **41**, 257 (1947). No appropriate data is given for *tert*-butylbenzene.

10) J. E. Lennard-Jones, *Proc. Roy. Soc.* (London), **A138**, 280 (1937).

11) D.F. Hornig, *J. Am. Chem. Soc.*, 72, 5772 (1950).

12) C.A. Coulson and S.L. Altmann, *Trans, Faraday, Soc.*, **48**, 293 (1952).

Now it has been shown (M. R. B.)

$$\Delta+C=E_1(\mathrm{CJ})+E_3(\mathrm{CJ})-2\varepsilon(1.54)N_{\mathrm{C-C}}-\varepsilon(1.33)N_{\mathrm{C=C}} \quad (11)$$

where $C$ is the conjugation energy correction due to compression and extension of the bonds, and $\varepsilon$ is the hyperconjugation energy per bond per dimension for bond distance 1.54 and 1.33 Å respectively. The right hand sides of Eq. (11) computed theoretically for three alkylbenzenes are given in Table IV together with the value for benzene, for the purpose of comparison between the theoretical and empirical conjugation energies $\Delta+C$ for benzene and of computing the hyperconjugation energies in three alkylbenzenes.

The value $\beta$ obtained by comparison of both $\Delta+C$ for benzen is $-70.0$ kcal.[13], and is somewhat larger than that of the spectroscopic value $-60$ kcal. Using the value for $\beta$ of $-70.0$ kcal., the corrected hyperconjugation energies for toluene, ethylbenzene and *tert*-butylbenzene are 1.45, 1.24 and 0.79 kcals. respectively, and this is the quite satisfactory order to be expected.

The third-order conjugation energies listed in Table III are appreciably less than the M. R. B., Roberts and Skinner[14] and even than the Coulson and Crawford[2a] values. This might be ascribed to including the corrected Coulomb integrals in Eqs. (9) and (10) but not including in the reference (2a)[15].

## V. Charge Distributions and Bond Orders

It was already mentioned in Sec. II that when overlap is included the definitions for the charge and the bond order must be changed. Following Chirgwin and Coulson[16], the total $\pi$-electron density $q_\mu$ on atom $\mu$ and the mobile bond order $p_{\mu\nu}$ between adjacent atoms $\mu$, $\nu$ are given by

$$q_\mu=\sum_{j=1}^{m} n_j x_{j\mu} y_{j\mu} \quad (12)$$

$$p_{\mu\nu}=\frac{1}{2}\sum_{j=1}^{m} n_j (x_{j\mu} y_{j\nu}+x_{j\nu} y_{j\mu}) \quad (13)$$

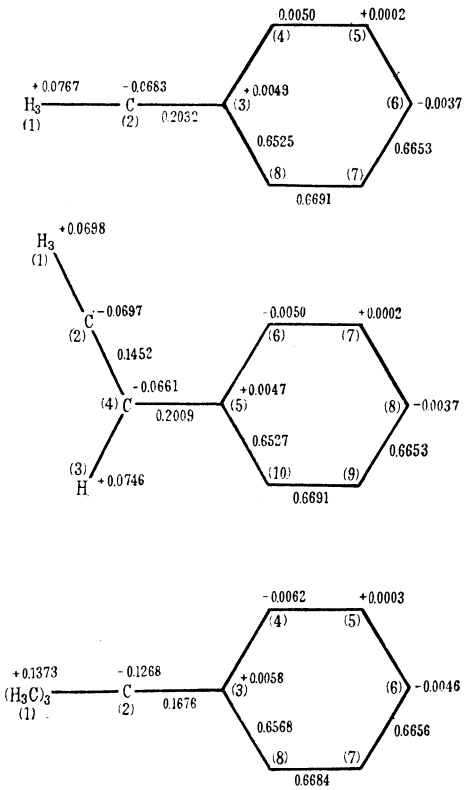
where $y_{j\mu}$ is the "covariant" coefficients associated with $\psi_j$ in contrast with the "contravariant" ones $x_{j\mu}$, and defined by the relation

$$y_{j\mu}=\sum_{\nu=1}^{n} S_{\mu\nu} x_{j\nu}$$

with the normalization condition

$$\sum_{\nu=1}^{n} x_{j\nu} y_{j\nu}=1 \quad (j=1, 2, \cdots\cdots n).$$

In Eqs. (12) and (13), the summation is carried over all the occupied molecular orbitals $j$, and $n_j$ is the number of electrons in the $j$'th MO. The computed values of the total $\pi$-electron charge densities and mobile bond orders thus obtained are shown in the following diagram.




The numberings of the atoms and the $\pi$-electron charge distribution and mobile bond order diagrams in toluene, ethylbenzene, and *tert*-butylbenzene, omitting bond orders between C and $H_2$ or $H_3$ group in toluene and ethylbenzene and between C and $(CH_3)_3$ in *tert*-butylbenzene.

The dipole moment due to the migration of electrons from alkyl group to benzene ring can be evaluated from the calculated charge densities and the bond lengths predicted from the bond orders (see column 2 of Table IV). Assumption of a resonance moment only is taken here as in Sec. IV of Part I. The results recorded in Table V show considerable agreements with the observed values.

13) Coulson and Crawford give the value $-71.6$ kcal. for $\beta$.

14) J. S. Roberts and H. A. Skinner, *Trans. Faraday Soc.*, **45**, 339 (1949).

15) The third-order conjugation energies computed in the present study were somewhat rescrutinized; Y. I'Haya, to be published.

16) B.H. Chirgwin and C.A. Coulson, *Proc. Roy, Soc.* (London), **A201**, 196 (1950).

TABLE IV

CONJUGATION ENERGIES OF ALKYLBENZENES, IN UNITS OF $\beta$

| | r(C–C), Å | $E_1$(CJ) | $E_3$(CJ)* | Deduction** | $\Delta$+C |
|---|---|---|---|---|---|
| Benzene | 1.39 | 1.073526 | 0.012690 | 0.015387 | 1.070829 |
| Toluene | 1.39 | 1.095352 | 0.014086 | 0.017921 | 1.091517 |
| | (2–3) 1.51 | (0.021826) | | | |
| Ethylbenzene | 1.39 | 1.093538 | 0.015394 | 0.020455 | 1.088477 |
| | (2–4) 1.53 | (0.020012) | | | |
| | (4–5) 1.51 | | | | |
| t-Butyl-benzene | 1.39 | 1.086034 | 0.014040 | 0.017921 | 1.082153 |
| | (2–3) 1.52 | (0.012508) | | | |

* $\sum_r \varepsilon(r) N_{C-C}(r)$

** $2\varepsilon(1.54)N_{C-C}+\varepsilon(1.33)N_{C=C}$.

TABLE V

DIPOLE MOMENTS, ABSORPTION FREQUENCIES AND OSCILLATOR STRENGTHS IN ALKYLBENZENES

| | | Benzene | Toluene | Ethylbenzene | t-Butylbenzene |
|---|---|---|---|---|---|
| $\mu$ (D) | calcd. | — | 0.372 | 0.491 | 0.746 |
| | obsd.* | — | 0.37 | 0.58 | 0.70 |
| Vapor $\lambda$, (Å) | calcd. | (2625) | 2666 | 2665 | 2649 |
| | obsd.** | 2625 | 2668 | 2664 | 2655 |
| Solution $\lambda$, (Å) | calcd. | (2640) | 2681 | 2680 | 2664 |
| | obsd.# | 2640 | 2692 | 2680 | 2672 |
| $f\times10^{-4}$ | calcd. | — | 16.1 | 11.0 | 8.2 |
| | obsd.# | — | 15 | 9 | 5 |

* J. W. Baker and L. G. Groves, *J. Chem. Soc.*, **1939,** 1144.

** F. A. Matsen, W. W. Robertson and R. L. Chuoke, *Chem. Revs.*, **41**, 273 (1947).

\# Y. I'Haya, the preceding Paper.

## VI. The Near Ultraviolet Absorption Spectra

**The Red Shifts Resulting from Alkyl Substitution.**—The general features have already been explained in Sec. V of Part I and it has been shown that the substitution of the hydrogen atoms of resonating molecules by alkyl groups cause the shift of the whole absorption curve to a longer wave-length (cf. Fig. 4 of Part I). We have also seen that this may result undoubtedly from a raising of the highest occupied level and a lowering of the lowest unoccupied level, and this lowering may be a characteristic feature of hyperconjugation. The simple LCAO MO calculations of $\pi$-electron transitions are also used here as done in Part I, and are compared with the observed values in Table V. In spite of using such a simple method instead of a more accurate method of anti-symmetrized molecular orbitals[17], the agreement between them is fairly satisfactory.

**Intensities of Spectra.**—The oscillator strength $f$ is computed for each of a series of alkyl benzens using the same equations as Eqs. (16) and (20) of Part I, and listed in Table V. Also in this case, therefore, the difficulty which was mentioned in foot note 41) of Part I is inevitable. However. the agreement between the computed and observed values shows that the omission of resulting errors from it is probably not too serious.

Although more detailed reasons for these wave-length shifts and intensities of the absorption spectra are not yet clear, a question which has long been unexplained seems to be semi-quantitatively solved; that is the absorption spectra representing $\pi$-electronic transitions allowed by the lower symmetries than benzene due to charge migrations from alkyl groups into benzene ring shift to longer wave-length and become stronger on passing from *tert*-butylbenzene to toluene. This result can also be explained by the computed hyperconjugation energies mentioned in the last paragraph of Sec. IV, for it is ascribed to increasing of hyperconjugation in a series of alkylbenzenes from *tert*-butylbenzene to toluene.

## VII. Critical Discussion

It has long been a question why the absorption spectra of a series of alkylbenzenes should become stronger and shift to longer wavelength but on the other hand the dipole moments should become smaller on passing from *tert*-butylbenzene to toluene. The re-

17) Sec A.L. Sklar, *J. Chem. Phys.*, 7, 984 (1939).

sults of computations obtained in the present study can explain this difficulty for the first time in spite of taking the simple LCAO MO method including overlap and choosing some unjustified empirical parameters.

However, here remains another difficulty to be settled; that is the inoization potential. That hyperconjugation plays a more important role here than any other alkyl-substituted resonating systems is indicated by the smaller lowering in ionization potentials on passing from *tert*-butylbenzene to toluene compared with the lowering in other systems[18]. In this connection, if more elaborated computations should be made as non-empirically as possible, an improvement would be made concerning this problem.

Attention should also be called to neglecting the inductive effect. The inductive effect has usually been regarded as being one of short range and is therefore unlikely to be of greater importance in large molecules such as alkylbenzenes than small ones[19]. However, Muller, Pickett and Mulliken[20] have recently stressed in the study of the benzenium ion that a joint inductive-hyperconjugative effect gives a considerably greater additional stabilization than the hyperconjugative effect only. This is likely to occur. Computations together with the inductive effect are in progress, and the result of both, including alkylbenzenes, will be presented before long.

18) See ref. 9).

19) Daub and Vandenbelt have concluded that the red-shifts of the absorption spectra are chiefly due to a resonance effect and that they are very insensitive to an inductive effect; *J. Am. Chem. Soc.*, **69**, 2714 (1947); ibid., **71**, 2414 (1949), and in ref. 2b) Crawford has obtained very satisfactory agreement with experimental data in computations of methyl-substituted benzenes using the same method without induction.

20) N. Muller, L.W. Pickett and R.S. Mulliken, *J. Am. Chem. Soc.*, **76**, 4770 (1954).

## Summary

The theory of hyperconjugation has been rescrutinized for a series of alkylbenzenes using the empirical LCAO MO method including overlap integrals for neighboring atoms. A detailed comparison of the theoretically computed and empirically determined conjugation energies of benzene gives a value of $-70.0$ kcal. for $\beta$, the reasonance integral for benzene C–C. Using this value, hyperconjugation energies for toluene, ethylbenzene and *tert*-butylbenzene are 1.45, 1.24 and 0.79 kcals. respectively. The third-order conjugation energies are found to be considerably less than any previous evaluations. Comparison of the predicted and observed dipole moments, absorption frequencies and oscillator strengths show fairly satisfactory agreements between them.

The author extends his thanks to Professor A. Kotera for his helpful comments.

*Department of Chemistry, Tokyo University of Education, Tokyo*

## SHORT COMMUNICATION

### *Anion Exchange Separation of Arsenic (V) and Phosphorus (V) from Arsenic (III) and Germanium (IV)**

By Yukichi YOSHINO

(Received May 6, 1955)

Present study on the anion exchange in hydrochloric acid solutions showed the existence of striking difference in adsorbability between As (III) and As (V), i.e., As (III) was found to be considerably adsorbed by Dowex 2 resin in concentrated hydrochloric acid, whereas that of As (V) was negligible at concentrations between 2 and 12 M of the acid. As was expected, P(V) (Phosphate) behaved just in the same way as As (V). On the other hand, Kakihana[1] reported the excellent adsorbability of Ge (IV) in concentrated hydrochloric acid solutions.

In order to clarify the conditions necessary for the separation of these elements, the author determined the distribution coefficients *Kd* (amount per gram resin/amount per ml. solution) of As (III) and Ge (IV) as a function of hydrochloric acid concentration. The results of the equilibrium experiments[2] are shown in Fig. 1 indicating that both elements can be considerably adsorbed in the range more than 6 M HCl with maximum adsorption at ca. 10 M.

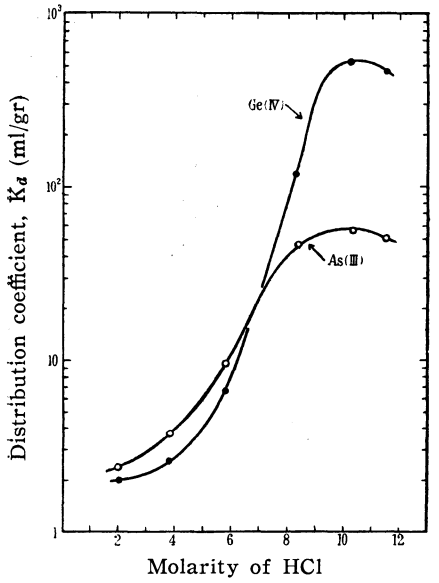



Fig. 1. Anion exchange adsorption of As (III) and Ge (IV). Dowex 2 (8% cross linked), 120-200 mesh, Cl-form. Less than 2% loading[2]. 9±1°C. As and Ge in the liquid phase were determined colorimetrically (molybdenum blue method[3] for As and phenylfluorone method[4] for Ge)

This behavior implies that the ready separation of As (V) and P (V) from As (III) and Ge (IV) should be possible. To demonstrate this, first of all, the separation of As (V) and As (III) was tried using 0.93 cm.²×9.0 cm. column of Dowex 2 and adding to it a 12 ml. of sample containing each 0.1 m mol. of As (V)

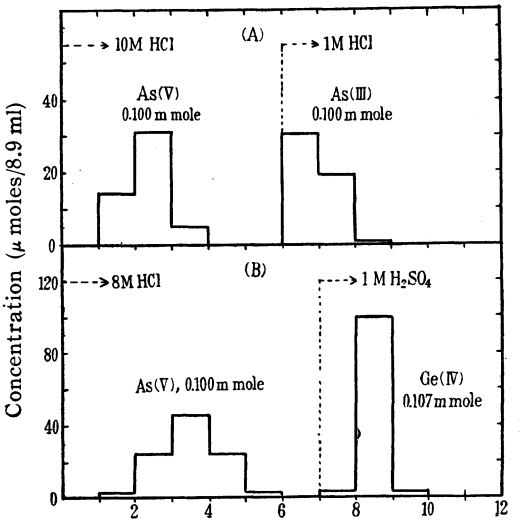



Fig. 2-(A) Separation of As (V) and As (III) Dowex 2-X 8, 80-120 mesh, Cl-form, 0.93 cm²×9.0 cm. Flow rate, 0.7 ml/min. As (V) and As (III) were determined iodometrically[5].

(B) Separation of As (V) and Ge (IV) Dowex 1-X 8, 80-120 mesh, Cl-form, 0.92 cm²×13 cm. Flow rate, 1.0 ml/min. Ge (IV) was determined by iodometry[6].

and As (III) in 10 M HCl. As shown in Fig. 2-(A), As (V) appeared rapidly in the effluent in 10 M HCl and then all the As (III) was removed with 1 M HCl. The same technique was found to be applicable to the separation

of P (V) and As (III) and to As (V) and Ge (IV). However, it was observed that if the HCl-concentration of Ge-containing sample exceeds 9 M, the quantitative removal of the element could not be achieved, which is presumably due to the irreversible precipitation of Ge (IV) in concentrated HCl. Detailed experiments revealed that the use of 8 M HCl sample was effective for the complete elution of Ge (IV) with dilute HCl or $H_2SO_4$. A typical run of the separation of As (V) and Ge (IV) was illustrated in Fig. 2-(B).

The author is indebted to Mr. Y. Sasaki for his valuable suggestion and to Miss M. Asada for her advice on colorimetric determination of germanium.

* Read before the Eighth Annual Meeting of the Chemical Society of Japan, April 3, 1955, Tokyo.

1) H. Kakihana, *Report of Germanium Research Committee of Japan*, No. 15 (1954).
2) See, for example, K.A. Kraus et al., *J. Phys. Chem.*, 58, 11 (1954).
3) Y. Kakida, *Sci. Rep. Research Inst.*, Tohoku Univ., **A-1**, 399 (1949).
4) H.J. Cluley, *Analyst*, **76**, 523 (1951).
5) J.T. Odencrantz and W. Rieman III, *Anal. Chem.*, 22, 1066 (1950); Y. Yoshino, This Bulletin, **24**, 39 (1950).
6) B. N. Ivanov-Emin, *Zavod. Lab.*, **13**, 161 (1947); *C.A.*, **42**, 480 (1948); D. A. Everest, *J. Chem. Soc.*, 1670 (1952), 4117 (1953).

*Department of Chemistry, College of General Education, University of Tokyo, Meguro-ku, Tokyo*

# *Studies on DNP-Protamines by Means of the Absorption Spectra**

By Chieko HASHIMOTO

(Received December 21, 1954)

Studies on chemical structures of protamine molecules, such as clupeine and salmine obtained from sperms of *Clupea pallasii* and *Oncorhynchus keta* respectively, which were purified as now possible, have been carried out from various quarters by many investigators in our laboratory and the summarizing results have been briefly reported[1-5]. From the results of such various methods, viz. qualitative analyses of the constituent amino acids, methoxyl determinations of the protamine methyl esters[5,6] and electrometric titrations of protamines[7],* it was found that both protamine molecules are probably constituted of one simple polypeptide chain, containing neither diamino acids except arginine, nor dicarboxylic acids and sulfur containing amino acids. The DNP-method by F. Sanger[8] for the identification of N-terminal amino acids in proteins in which the $\alpha$-amino groups are free, has already been applied to many proteins and peptides. The resulting yellow DNP-derivative either of protein or peptide has always a characteristic absorption spectrum which is associated with the presence of N-2,4-dinitrophenyl amino group. It is, therefore, likely that the determination of the wave lengths ($\lambda_{max.}$) and the absorption coefficients ($\epsilon_{\lambda max.}$) at their maxima, will lead in some cases to identify and estimate directly the N-terminal residue of the DNP-derivative, without laborious treatments of isolating DNP-amino acids after hydrolysis and fractionation.

In the present paper, the absorption spectra of DNP-derivatives of several amino acids and a few peptides were first determined and the differences among them were carefully investigated. Then, the absorption spectra of both DNP-protamines were observed, in order to compare them with those of the individual amino acids and peptides. Thus, such a method was found to be useful for the direct indentification of the N-terminal residue of clupeine or salmine. In fact, it was shown that the N-terminal residue of clupeine should be a mono amino acid while that of salmine should be proline, and moreover the calculation of the approximate values of the molecular weights of the protamines was enabled from their absorption coefficients.

## Experimental

**DNP-Amino Acids and -Peptides.**—These were prepared according to the methods of F. Sanger and R. R. Porter[8,9] (cf. Table I). Purifications and crystallizations of DNP-derivatives were repeated until they gave the constant absorption coefficients at their $\lambda_{max.}$ respectively. In the case of DNP-arginine derived from arginine hydrochloride, it was ascertained by means of electrometric titration and paper chromatographic methods that only the $\alpha$-amino group was replaced by DNP-group. Diglycylglycine used in this experiment was kindly supplied by the laboratory of Prof. Mizushima of the Chemical Institute in this University.

**2,4-Dinitrophenol.**—A material of commercial grade was purified by repeated recrystallizations from methanol using active charcoal, m.p. 114°C.

**2,4-Dinitroaniline.**—It was prepared by the method of O. Kym[10] by heating 2,4-dinitrochlorobenzene with acetamide at 200°C for ten hrs. It was then recrystallized from aqueous alcohol, m.p. 180°C.

**Protamine Sulfates.**—Each sample of protamines used, clupeine and salmine, was prepared and purified respectively by the method described in the previous papers,[1,2] and they were both the sulfate of the less soluble protamine of two fractions which were obtained using the solubility difference of their picrates in 67% aqueous acetone at

* The present work was presented to the 5th Annual Meeting of the Chemical Society of Japan held on April 3rd, 1952 in Tokyo Univ. and a part of the result of this work was briefly reported in this Bulletin (cf. reference 3).

1) T. Ando and K. Iwai, *Repts. Radiation Chem. Res. Inst.*, Tokyo Univ., No. 3, 14 (1948).

2) T. Ando and C. Hashimoto, *Repts. Radiation Chem. Res. Inst.*, Tokyo Univ., No. 4, 31 (1949).

3) T. Ando, S. Ishii, C. Hashimoto, M. Yamasaki and K. Iwai, This Bulletin, 25, 132 (1952).

4) T. Ando, K. Iwai, M. Yamasaki, C. Hashimoto, M. Kimura, S. Ishii and T. Tamura, This Bulletin, 26, 406 (1953).

5) T. Ando and C. Hashimoto, *Repts. Radiation Chem. Res. Inst.*, Tokyo Univ., No. 5, 56 (1950).

6) K. Iwai, The 5th Ann. Meeting of the Chemical Society, Japan (Tokyo, April, 1952).

7) C. Hashimoto, The 5th Ann. Meeting of the Chemical Society, Japan (Tokyo, April, 1952).

* The experimental results will be reported in the following paper.

8) F. Sanger, *Biochem. J.*, 39, 507 (1945).

9) F. Sanger and R. R. Porter, *Biochem. J.*, 42, 287 (1948).

10) O. Kym, *Ber.*, 32, 3539 (1899).

TABLE I
WAVELENGTHS AT ABSORPTION MAXIMA AND MOLECULAR ABSORPTION COEFFICIENTS OF DNP-DERIVATIVES§

| DNP-Derivative | Absorption Maxima $\lambda_{1max.}$ mμ | ($\lambda_{2max.}$) mμ | Molecular Absorption Coefficient at $\lambda_{1max.}$ |
|---|---|---|---|
| DNP-Glycine | 361 | (265) | $1.66\times10^4$ |
| 〃-Alanine | 361 | (265) | $1.63\times$ 〃 |
| 〃-Valine | 363 | (265) | $1.69\times$ 〃 |
| 〃-Isoleucine | 362 | (265) | $1.77\times$ 〃 |
| 〃-Arginine | 357 | (275) | $1.65\times$ 〃 |
| 〃-Serine | 359 | (265) | $1.72\times$ 〃 |
| 〃-Proline | 387 | (none) | $1.85\times$ 〃 |
| 〃-Glycylglycine | 354 | (265) | $1.52\times$ 〃 |
| 〃-Diglycylglycine | 352 | (265) | $1.52\times$ 〃 |
| 2,4-Dinitrophenol§§ | 361 | (257) | $1.48\times$ 〃 |
| 2,4-Dinitroaniline | 347 | (262) | $1.28\times$ 〃 |

§ Controlled in pH ca. 9.1 by using the 1% aq $NaHCO_3$.
§§ This absorption band is probably due to 2,4-dinitrophenolate ion.

0°C. These samples* were shown to be tentatively homogeneous by the diffusion measurement[11].

**Preparation and Purification of DNP-Protamine Sulfates.**—DNP-Protamine sulfates were prepared principally according to the method of F. Sanger[8]. Protamine sulfate (0.104 g.) and sodium bicarbonate (0.104 g.) were dissolved in water (5 ml.), a solution of 2,4-dinitrofluorobenzene (0.12 g.) in ethanol (3 ml.) was then added and the mixture was mechanically shaken for about 4 hr. at the room temperature (20—25°C). The glutinous yellow products obtained were cooled, a few drops of 2 N sulfuric acid were carefully added to them, and then alcohol was added. The mixture was then centrifuged and the precipitates were washed with absolute alcohol and ether. Since the crude DNP-protamine sulfate thus obtained still contained a small quantity of dinitrophenol, some inorganic salts and unsubstituted protamine, further purification of it through activated alumina was tried to eliminate them. The crude DNP-product (0.100 g.) was completely dissolved in water (80 ml.), and the solution was carefully passed through an activated alumina column (Wako Pure Chemical Industries, Ltd., especially prepared for chromatographic purpose, 13 g., 1×15 cm.). DNP-Protamine remained at the top of the column giving a sharp yellow band and the unsubstituted protamine seemed to stay in the lower part, while dinitrophenol and inorganic salts passed through rapidly. After the column was washed with water, the colorless part of the protamine was first eluted with 0.1 N hydrochloric acid, and then the yellow substance at the top was eluted. The collected eluate of the yellow band was once filtered, and one or two drops of 2 N sulfuric acid were added, followed by several volumes of alcohol. Precipitates of yellow crystal-like sulfate were thus obtained. By repeating the above treatment, they were purified until their absorption coefficient at $\lambda_{max.}$ gave constant values. Both DNP-clupeine and -salmine sulfates obtained were yellow crystal-like substances.

**Determination of Absorption Spectra.**—Absorption spectra of various DNP-derivatives above obtained were determined with a Beckman quartz spectrophotometer, model DU. In the case of protamine sulfates, their 0.5% aqueous solution was used (pH 3.3). In order to get rid of the pH effect, DNP-derivatives were dissolved in 1% aqueous solution of sodium bicarbonate to keep pH at 9.1±0.2. All measurements were made at 18—20°C. The concentration of DNP-derivative solution used in these absorption measurements was always below 50 μM, so that Beer's law held good in all cases.

## Results and Discussion

The results of measurements of absorption spectra for 2,4-dinitrophenol, 2,4-dinitroaniline and N-2,4-DNP-derivatives of several amino acids and peptides are shown in Fig. 1 and in Table I. As shown in Fig. 1, dinitroaniline

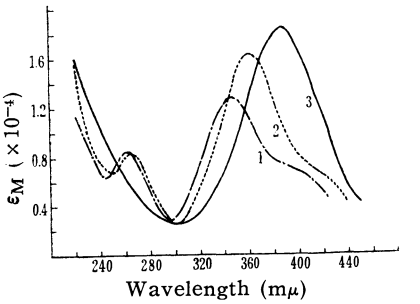



Fig. 1. Absorption spectra of some DNP-compounds in 1% aq.$NaHCO_3$.
Curve 1: Dinitroaniline; Curve 2: DNP-Alanine; Curve 3: DNP-Proline.

gave a characteristic absorption curve with maxima at the regions of 347 mμ and 262 mμ. But the absorption maxima of DNP-derivatives of monoamino acids, i. e. DNP-glycine, DNP-alanine etc., were observed at about 360 mμ and 265 mμ, being in longer wavelengths than those of dinitroaniline. α-DNP-Arginine also showed the absorption maxima at 357 mμ and 275 mμ, which were involved in nearly the similar regions as in the case of DNP-monoamino acids. In contrast with them, DNP-proline gave a characteristic absorption curve which had only a maximum at 387 mμ, a longer wavelength than DNP-derivatives of the above mentioned monoamino acids, and its absorption coefficient was higher than the latter, and no more absorption band could be seen near 265 mμ. The absorp-

11) K. Iso, T. Kitamura and I. Watanabe, *J. Chem. Soc. Japan*, **75**, 342 (1954).
* Further experiments are being made on the problem whether these samples are homogeneous or heterogeneous.

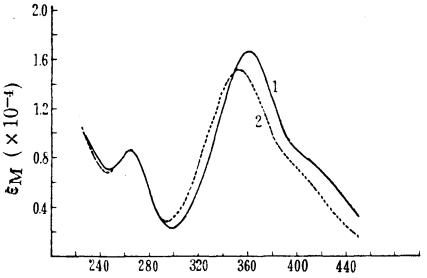



Fig. 2. Absorption spectra of DNP-glycine and DNP-diglycylglycine in 1% aq. $NaHCO_3$.
Curve 1: DNP-Glycine; Curve 2: DNP-Diglycylglycine.

tion spectra of DNP-glycylglycine and DNP-diglycylglycine showed the fairly similar shape to that of DNP-glycine, but both their maxima slightly shifted to the shorter wave-length side, and moreover their absorption coefficients were a little lower than that of DNP-glycine (cf. Fig. 2 and Table I). Sanger has also indicated that the DNP-glycyl peptides separated from insulin gave the same curve as DNP-glycine and DNP-glycylglycine at wave-lengths longer than 330 mμ[12].

From the measurements of these absorption spectra, it will be inferred that the difference among the curves of DNP-derivatives may mostly be attributed to the states of an amino group combining with the dinitrophenyl group, thus: in primary (dinitroaniline), secondary (DNP-monoamino acids or DNP-arginine), or tertiary amine (DNP-proline). The absorption maximum appearing in the longest wave-length region was found to shift to the longer wave-length side, in the order of primary < secondary < tertiary amine, and the absorption coefficient also was found to be higher in the same order. So far as the nitrogen combined with the DNP-group behaves as a secondary amine, the absorption curve of such a derivative seemed to show little difference whichever amino acid it may belong to. It was found also that the DNP-derivatives of glycylglycine and glycylpeptide gave absorption spectra essentially similar to that of the corresponding DNP-amino acid like DNP-glycine. Accordingly, from careful observations of the absorption spectra of the DNP-derivatives. it should at least be possible to determine whether proline or any other kind of monoamino acids occupies the α-N-terminal residue in the protein molecule, and further to estimate the number of N-terminal residues per 1 g. protein.

The absorption spectra of DNP-derivatives of clupeine and salmine are given in Fig. 3 and Table II.

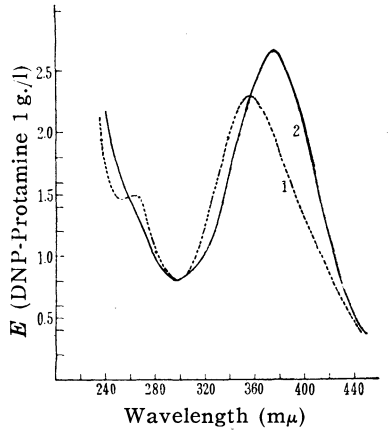



Fig. 3. Absorption spectra of DNP-Protamines in 1% aq. $NaHCO_3$.
Curve 1: DNP-Clupeine; Curve 2: DNP-Salmine.

As shown in the figure, DNP-clupeine gave two absorption maxima at about 357 mμ and 262 mμ, while DNP-salmine only one maximum at 375 mμ. Since neither clupeine nor salmine has absorption band with wave-length longer than 240 mμ, the absorption spectra

TABLE II
WAVELENGTHS AT ABSORPTION MAXIMA OF SOME DNP-PROTAMINES AND MOLECULAR WEIGHTS OF THE PROTAMINES

| Protamine | Absorption Maxima of DNP-Derivative $\lambda_{1max.}$ | ($\lambda_{2max.}$) | Extinction†† $E\lambda_1$(1 g./l) | Molecular weight†† | N-terminal residue |
|---|---|---|---|---|---|
| | mμ | mμ | | | |
| Clupeine (1951)† | 357 | (262) | $2.23_3$ | 7,100 | Ala |
| Clupeine (1947)† | 357 | (262) | $2.79_2$ | 5,600 | Ala |
| Salmine (1951)† | 375 | (None) | $2.64_4$ | 7,000 | Pro |
| Salmine††† (1951)† | 375 | (None) | $2.72_7$ | 6,600 | Pro |

† The number in parenthesis shows the year the material was caught.
†† These values are the averages of two or three experiments.
††† This sample was kindly supplied by Dr. Watanabe's Laboratory.

12) F. Sanger, *Biochem. J.*, 45, 563 (1949).

above observed for both DNP-protamines are surely associated with the presence of a DNP-group. Comparing the results with those for DNP-amino acids, therefore, it can be concluded with a high probability that the N-terminal residue of clupeine is a monoamino acid other than proline while that of salmine is proline. These results were consistent with the facts obtained in our laboratory; namely the N-terminal residue of our clupeine was shown to be alanine while that of salmine was proline by means of paper chromatography of DNP-protamine hydrolysates[3)4)], and partly by means of electrometric titration of both protamines.

Now, the number of DNP-groups per 1 g. of DNP-protamine* should be estimated from the absorption coefficient for the maxima at either 357 m$\mu$ or 375m$\mu$. An assumption was made that the molar absorption coefficient of DNP-clupeine at 357 m$\mu$ is equal to that of DNP-alanine at its absorption maximum 361 m$\mu$. As shown in Table II, the absorption coefficient of DNP-clupeine (1g./l) measured with an optical path-length 1 cm., at $\lambda_{max.}=$ 357 m$\mu$ was 2.233, while that of DNP-alanine (1 mol/l) with the same path-length, at $\lambda_{max.}=361$ m$\mu$ was $1.63\times10^4$ (Table I). Then it follows that there are $2.233/1.63\times10^4=1.37\times10^{-4}$ mol. DNP-groups in 1 g. of DNP-clupeine. As has already been shown, a clupeine molecule is a simple peptide chain consisting of arginine and several kinds of monoamino acids. The molecular weight for DNP-clupeine is thus $1/1.37\times10^{-4}=7{,}299$; accordingly that of free clupeine is 7,133. The molecular weight of clupeine is also calculated to 7,080 and 6,637, from the molecular absorption coefficients at 357 m$\mu$ of DNP-alanine ($1.62\times10^4$) and at $\lambda_{max.}=352$ m$\mu$ of DNP-diglycylglycine ($1.52\times10^4$) respectively.

Under the similar assumption that the molar absorption coefficient per DNP-group of DNP-salmine at $\lambda_{max.}=375$ m$\mu$, is equal to that of DNP-proline at $\lambda_{max.}=387$ m$\mu$, the following calculation may be made. The number of DNP-group in 1 g. of DNP-salmine is $2.644/1.85\times10^4=1.43\times10^{-4}$. It was already known that the salmine molecule also was a simple peptide chain consisting of arginines and other monoamino acids; consequently the molecular weight of DNP-salmine is calculated to $1/1.43\times10^{-4}=6{,}993$ and that of free salmine to 6,827. It also gives a value 6545, when calculated from the molar absorption coefficient of DNP-proline at 375 m$\mu$ ($1.78\times10^4$) instead of using the coefficient for $\lambda_{max.}=387$ m$\mu$.

Another sample of clupeine prepared from the ripe sperms of herrings caught in 1947 and that of salmine prepared in another laboratory*, also gave molecular weight 5,600 and 6,600 respectively, as shown in Table II.

From these results, it appears that both protamines, clupeine and salmine, probably have the molecular weights of the same order of 6,000–7,000. These values are also in fairly good agreement with those obtained by methoxyl determinations of the protamine methylesters, by electrometric titrations of the protamines, and by manometric determination of amino nitrogen in clupeine[4)] (cf. Table III).

TABLE III
MOLECULAR WEIGHTS OF CLUPEINE AND SALMINE

| Method | Clupeine§ | Salmine§ |
|---|---|---|
| Methoxyl determination of the esterified product. | | |
| Once esterification. | 10, 800 | 7, 300 |
| More repeated esterification. | 6, 100 | 6, 100 |
| Electrometric titration | 4, 600 | 4, 400 |
| Manometric van Slyke's method | 6, 400 | None |
| Present method | 5, 600–7, 100 | 6, 100–7, 000 |

§ The less soluble specimens of protamines were used.

## Summary

1) DNP-Derivatives of amino compounds gave the characteristic spectral absorption curves, according to the states of the amino groups combined with the DNP-group. It was found, that 2,4-dinitroaniline as a primary amine, DNP-monoamino acids in the case of secondary amine and DNP-proline in that of tertiary amine gave respectively the absorption spectra with different absorption maxima and absorption coefficients (cf. Table I and Fig. 1).

2) The absorption curve of DNP-clupeine was of the similar shape to DNP-derivatives in the states of secondary amines, while that of DNP-salmine in those of tertiary amines. From this fact the difference between the

13) K. E. Rasmussen, *Z. physiol. Chem.*, **224**, 97 (1934).

14) R.J. Block and D. Bolling, *Arch. Biochem.*, **6**, 419 (1945).

* In fact, sulfate was always used in these experiments. The sulfuric acid content in our protamine sulfate was tentatively supposed to be 20% according to the analyses by K.E. Rasmussen for his clupeine sulfate,[13)] and R. J. Block and D. Bolling for their salmine sulfate.[14)]

* This sample used for comparing with our sample was kindly supplied by Dr. Watanabe's Laboratory in this Institute, and was not fractionated by using the solubility difference of the picrate in 67% aqueous acetone.

N-terminal residues of clupeine and salmine molecules was evidently recognized, that of the former being monoamino acid while that of the latter proline.

3) By comparing the absorption of DNP-protamine with the molecular absorption coefficient of the corresponding DNP-amino acid which occupies the N-terminal residue in the molecule, the molecular weights of DNP-derivatives of clupeine and salmine were estimated. Both clupeine and salmine were shown to have the molecular weights of the same order, 6,000–7,000.

The author wishes to express her hearty thanks to Prof. T. Ando and Ass. Prof. S. Nagakura for their valuable advice and encouragement throughout this study, also to the Ministry of Education for the Scientific Research Encouragement Grant given to Prof. T. Ando in support of this research.

*Institute of Science and Technology, Tokyo University, Tokyo*

# *The Dipole Moment of the Polyhalocyclohexanes. II. The Calculated Values of Tetrachloro-, Hexachloro-, and Heptachlorocyclohexanes*

By Takashi SHIMOZAWA

(Received March 8, 1955)

The measurement of dipole moment is one of the authentic methods for the determination of the structure of polyhalocyclohexanes[1,2,4]. In order to determine the configuration of molecules by the dipole moment measurement, the observed values of the dipole moment must be compared with the calculated ones. With a view to providing the facility for the determination, the calculated values of the dipole moments of the polyhalocyclohexanes by the aid of Morino-Miyagawa's empirical rule are shown for all kinds of tetrachloro-, hexachloro-, and heptachlorocyclohexanes, in this article.

It is well established that the cyclohexane ring takes the chair form under ordinary condition[4]. The twelve hydrogen atoms, two to each carbon atom, are at the *a*- and *e*-positions, *a*-position being almost parallel to the molecular axis, while *e*-position is in a tetrahedral angle to it and is almost parallel to either of the C–C bonds in the molecule.

In hexachlorocyclohexane, in which the six hydrogen atoms are replaced by chlorine atoms, we have ninety-six isomers by the combination of the positions of the substitution. BHC is a one of the hexachlorocyclohexanes, in which one chlorine atom is attached to each carbon atom. Even in this case, we have eight isomers with respect to the order to the *a*- and *e*-position atoms in the cyclohexane ring. The spatial configuration of the six isomers of BHC already prepared has been determined by the dipole moment measurement[5], by the analysis of crystal structure by X-ray diffraction[6], and by electron diffraction investigation[7]. We have already many isomers of hexachlorocyclohexanes other than BHC. In the course of the determination of their configurations the dipole moment played an important role. Of course some of them were determined from the consideration of the relation to other compounds whose configuration had already been established, but in these cases we found no contradiction of the conclusions obtained from the dipole moments. As already described in the preceding articles[1], the simple rule of vector addition cannot provide enough information for the discussion of the configurations. An empirical rule suggested by Morino and Miyagawa[2,3], which formally took into consideration the moments induced by the bond moments, provided us with reasonable values for many molecules. Indeed, we never found isomers of polyhalocyclohexanes whose observed values were quite different from those computed by our rule.

1) I. Miyagawa, Y. Morino and R. Riemschneider; This Bulletin 27, 177 (1954).
2) Y. Morino, I. Miyagawa and T. Oiwa; *Botyu-Kagaku*, 15, 181 (1950).
3) I. Miyagawa; *J.Chem. Soc. Japan*, 75, 1061 (1654).
4) K. Kojima and T. Yoshino; *J. Am. Chem. Soc.*, 75, 166 (1953).
5) See reference 2) and 3), as examples.
6) R. G. Dickinson and C. Bilicke; *J. Am. Chem. Soc.*, 50, 764 (1928).
7) O. Bastiansen, $\phi$. Ellefsen and O. Hassel; *Research*, 2, 248 (1949); *Acta Chem. Scand.*, 3, 918 (1949).

Thus it will be useful to calculate the dipole moments from this rule, because reference to these values will enable us to determine the spatial configuration of a given isomer, or at least to confine our calculation to a number of configurations.

The Morino-Miyagawa rule was reported in detail in the preceding articles[2,3]. The calculated values for all kinds of hexachloro-, heptachloro-, and tetrachlorocyclohexanes are listed in Tables I, II, and III,

TABLE I

DIPOLE MOMENT OF HEXACHLOROCYCLOHEXANES

| | Configurations (stable form) | D | No. of the (1a, 3a) pairs | | Configurations (inverted isomers) | D | No. of the (1a, 3a) pairs |
|---|---|---|---|---|---|---|---|
| 1 | 1e2e3e4e5e6e($\beta$-BHC) | 0 | 0 | 1′ | 1a2a3a4a5a6a | 0 | 6 |
| 2 | 1a2a3e4e5e6e($\alpha$-BHC) | 2.25 | 0 | 2′ | 1e2e3a4a5a6a | 2.26 | 2 |
| 3 | 1a2a3a4e5e6e($\gamma$-BHC) | 2.93 | 1 | | | | |
| 4 | 1a2e3e4e5e6e($\delta$-BHC) | 2.25 | 0 | 4′ | 1e2a3a4a5a6a | 1.71 | 4 |
| 5 | 1a2e3e4a5e6e($\varepsilon$-BHC) | 0 | 0 | 5′ | 1e2a3a4e5a6a | 0 | 2 |
| 6 | 1a2e3a4e5e6e | 3.44 | 1 | 6′ | 1e2a3e4a5a6a | 2.59 | 3 |
| 7 | 1a2a3e4a5e6e($\gamma$-BHC) | 1.88 | 1 | | | | |
| 8 | 1a2e3a4e5a6e | 4.08 | 3 | | | | |
| 9 | 1ea2ea3ea | 3.71 | 1 | | | | |
| 10 | 1ea2ea4ea | 1.77 | 1 | | | | |
| 11 | 1ea3ea5ea | 1.84 | 3 | | | | |
| 12 | 1ea2ea3e4e | 2.74 | 0 | 12′ | 1ea2ea3a4a | 2.81 | 2 |
| 13 | 1ea2ea3e4a | 3.50 | 1 | 13′ | 1ea2ea3a4e | 2.42 | 1 |
| 14 | 1ea2ea3e5e | 2.12 | 0 | 14′ | 1ea2ea3a5a | 3.66 | 3 |
| 15 | 1ea2ea3a5e | 1.47 | 1 | 15′ | 1ea2ea3a5a | 3.31 | 1 |
| 16 | 1ea2ea3e6e | 2.97 | 0 | 16′ | 1ea2ea3a6a | 2.98 | 2 |
| 17 | 1ea2ea3e6a | 3.54 | 1 | | | | |
| 18 | 1ea2ea4e5e | 0.21 | 0 | 18′ | 1ea2ea4a5a | 2.44 | 2 |
| 19 | 1ea2ea4e5a | 2.15 | 1 | | | | |
| 20 | 1ea2e3ea4e | 3.42 | 1 | 20′ | 1ea2a3ea4a | 2.42 | 2 |
| 21 | 1ea2e3ea4a | 3.18 | 1 | 21′ | 1ea2a3ea4e | 2.48 | 1 |
| 22 | 1ea2e3ea5e | 1.65 | 1 | 22′ | 1ea2a3ea5a | 2.58 | 3 |
| 23 | 1ea2a3ea5e | 0.44 | 1 | 23′ | 1ea2e3ea5a | 3.98 | 3 |
| 24 | 1ea3ea4e5e | 2.03 | 1 | 24′ | 1ea3ea4a5a | 1.81 | 3 |
| 25 | 1ea3ea4a5e | 0.22 | 1 | 25′ | 1ea3ea4e5a | 3.04 | 3 |
| 26 | 1ea3ea4e6e | 2.17 | 1 | 26′ | 1ea3ea4a6a | 1.94 | 2 |
| 27 | 1ea3ea4e6a | 1.50 | 1 | | | | |
| 28 | 1ea2e3e4ea | 2.79 | 0 | 28′ | 1ea2a3a4ea | 0.93 | 2 |
| 29 | 1ea2e3a4ea | 2.20 | 1 | | | | |
| 30 | 1ea2e4ea5e($\alpha$-1,1,2,4,4,5) | 0 | 0 | 30′ | 1ea2a4ea5a | 0 | 2 |
| 31 | 1ea2a4ea5e | 1.88 | 1 | | | | |
| 32 | 1ea2e4ea6e | 1.45 | 0 | 32′ | 1ea2a4ea6a | 1.80 | 3 |
| 33 | 1ea2e4ea6a | 1.63 | 1 | | | | |
| 34 | 1ea2e3e4e5e | 1.65 | 0 | 34′ | 1ea2a3a4a5a | 1.51 | 4 |
| 35 | 1ea2e3e4e6e | 2.16 | 0 | 35′ | 1ea2a3a4a6a | 2.10 | 4 |
| 36 | 1ea2e3e5e6e | 1.56 | 0 | 36′ | 1ea2a3a5a6a | 2.08 | 4 |
| 37 | 1ea2a3e4e5e | 1.56 | 0 | 37′ | 1ea2e3a4a5a | 2.77 | 3 |
| 38 | 1ea2a3e4e6e | 0.49 | 0 | 38′ | 1ea2e3a4a6a | 2.70 | 2 |
| 39 | 1ea2a3e5e6e | 1.71 | 0 | 39′ | 1ea2e3a5a6a | 3.19 | 3 |
| 40 | 1ea2a4e5e6e | 2.54 | 0 | 40′ | 1ea2e4a5a6a | 2.43 | 2 |
| 41 | 1ea2e3a4e5e | 2.30 | 1 | 41′ | 1ea2a3e4a5a | 2.16 | 2 |
| 42 | 1ea2e3a5e6e | 3.39 | 1 | 42′ | 1ea2a3e5a6a | 1.82 | 2 |
| 43 | 1ea3a4e5e6e | 3.52 | 1 | 43′ | 1ea3e4a5a6a | 1.29 | 2 |
| 44 | 1ea2e3a4e6e | 3.54 | 1 | 44′ | 1ea2a3e4a6a | 3.16 | 3 |
| 45 | 1ea2e3e4a5e | 1.68 | 0 | 45′ | 1ea2a3a4e5a | 1.79 | 3 |
| 46 | 1ea2e3e4a6e | 2.68 | 0 | 46′ | 1ea2a3a4e6a | 0.21 | 2 |

| | Configurations (stable form) | D | No. of the (1a, 3a) pairs | | Configurations (inverted isomers) | D | No. of the (1a, 3a) pairs |
|---|---|---|---|---|---|---|---|
| 47 | 1ea2a3a4e5e | 1.27 | 1 | 47′ | 1ea2e3e4a5a | 2.87 | 1 |
| 48 | 1ea2a3a4e6e | 1.72 | 1 | 48′ | 1ea2e3e4a5a | 3.57 | 1 |
| 49 | 1ea2a3a5e6e | 2.90 | 1 | | | | |
| 50 | 1ea2a3e4a5e | 2.12 | 1 | 50′ | 1ea2e3a4e5a | 3.68 | 3 |
| 51 | 1ea2a3e4a6e | 2.41 | 1 | 51′ | 1ea2e3a4e6a | 1.81 | 1 |
| 52 | 1ea2a3e4e5a | 1.94 | 1 | 52′ | 1ea2e3a4a5e | 1.17 | 1 |
| 53 | 1ea2a3e5a6e | 1.88 | 1 | | | | |
| 54 | 1ea2a3e4e6a | 2.14 | 1 | 54′ | 1ea2e3a4a6e | 2.96 | 1 |
| 55 | 1ea2a3e5e6a | 2.15 | 1 | 55′ | 1ea2e3a5a6e | 4.50 | 3 |

TABLE II

DIPOLE MOMENT OF HEPTACHLOROCYCLOHEXANES

| | Configurations (stable form) | D | No. of the (1a, 3a) pairs | | Configurations (inverted isomers) | D | No. of the (1a, 3a) pairs |
|---|---|---|---|---|---|---|---|
| 1 | 1ea2e3e4e5e6e($\alpha$-Hepta) | 1.04 | 0 | 1′ | 1ea2a3a4a5a6a | 1.44 | 6 |
| 2 | 1ea2a3e4e5e6e($\gamma$-Hepta) | 1.26 | 0 | 2′ | 1ea2e3a4a5a6a | 2.36 | 4 |
| 3 | 1ea2e3a4e5e6e | 2.66 | 1 | 3′ | 1ea2a3e4a5a6a | 1.71 | 4 |
| 4 | 1ea2e3e4a5e6e($\zeta$-Hepta) | 1.45 | 0 | 4′ | 1ea2a3a4e5a6a | 0.68 | 4 |
| 5 | 1ea2a3a4e5e6e($\varepsilon$-Hepta) | 2.22 | 1 | 5′ | 1ea2e3e4a5a6a | 2.48 | 2 |
| 6 | 1ea2a3e4a5e6e | 2.20 | 1 | 6′ | 1ea2e3a4e5a6a | 1.73 | 3 |
| 7 | 1ea2a3e4e5a6e($\eta$-Hepta) | 0.86 | 1 | 7′ | 1ea2e3a4a5e6a | 1.41 | 2 |
| 8 | 1ea2a3e4e5e6a | 1.97 | 1 | 8′ | 1ea2e3a4a5a6e | 2.83 | 3 |
| 9 | 1ea2e3a4a5e6e($\delta$-Hepta) | 2.20 | 1 | 9′ | 1ea2a3e4e5a6a | 1.29 | 2 |
| 10 | 1ea2e3a4e5a6e | 3.44 | 3 | 10′ | 1ea2a3e4a5e6e | 2.44 | 2 |
| 11 | 1ea2ea3e4e5e | 1.42 | 0 | 11′ | 1ea2ea3a4a5a | 2.35 | 4 |
| 12 | 1ea2ea3e4e6e | 1.57 | 0 | 12′ | 1ea2ea3a4a6a | 2.76 | 4 |
| 13 | 1ea2ea3e5e6a | 1.99 | 1 | 13′ | 1ea2ea3a5a6e | 3.46 | 3 |
| 14 | 1ea2ea3a4e5e | 0.90 | 1 | 14′ | 1ea2ea3e4a5a | 2.70 | 2 |
| 15 | 1ea2ea4e5a6e | 1.97 | 1 | 15′ | 1ea2ea4a5e6a | 2.28 | 3 |
| 16 | 1ea2ea3e5a6e | 2.76 | 1 | 16′ | 1ea2ea3a5e6a | 1.59 | 2 |
| 17 | 1ea2ea4a5e6e | 2.82 | 1 | 17′ | 1ea2ea4e5a6a | 1.14 | 2 |
| 18 | 1ea2ea3a5e6e | 2.56 | 1 | 18′ | 1ea2ea3e5a6a | 2.66 | 2 |
| 19 | 1ea2e3ea5e6e | 1.36 | 1 | 19′ | 1ea2a3ea5a6a | 1.48 | 4 |
| 20 | 1ea2e3ea4e6e | 2.53 | 1 | 20′ | 1ea2a3ea4a6a | 2.39 | 4 |
| 21 | 1ea3ea4e5e6e | 2.06 | 1 | 21′ | 1ea3ea4a5a6a | 1.19 | 4 |
| 22 | 1ea2a3ea4e6e | 1.05 | 1 | 22′ | 1ea2e3ea4a6a | 3.07 | 2 |
| 23 | 1ea2a3ea5e6e | 1.25 | 1 | 23′ | 1ea2e3ea5a6a | 2.83 | 3 |
| 24 | 1ea2e3ea4e6a | 2.48 | 1 | 24′ | 1ea2a3ea4a6e | 2.64 | 2 |
| 25 | 1ea3ea4e5e6a | 1.62 | 1 | 25′ | 1ea3ea4a5a6e | 1.25 | 3 |
| 26 | 1ea2e3ea5e6a | 1.96 | 1 | 26′ | 1ea2a3ea5a6e | 1.91 | 3 |
| 27 | 1ea2e3ea5a6e | 3.47 | 3 | 27′ | 1ea2a3ea5e6a | 1.05 | 2 |
| 28 | 1ea3ea4e5a6e | 2.52 | 3 | 28′ | 1ea3ea4a5e6a | 0.97 | 2 |
| 29 | 1ea2e3e4ea6e | 1.06 | 0 | 29′ | 1ea2a3a4ea6a | 0.82 | 4 |
| 30 | 1ea2a3e4ea6e | 0.87 | 1 | 30′ | 1ea2e3a4ea6a | 0.75 | 2 |
| 31 | 1ea2a4ea5e6e | 2.60 | 1 | 31′ | 1ea2e4ea5a6a | 1.04 | 2 |
| 32 | 1ea2e4ea5a6e | 1.78 | 1 | 32′ | 1ea2a4ea5e6a | 2.23 | 3 |
| 33 | 1ea2ea3ea4e | 3.01 | 1 | 33′ | 1ea2ea3ea4a | 3.01 | 2 |
| 34 | 1ea2ea3ea5e | 1.14 | 1 | 34′ | 1ea2ea3ea5a | 3.30 | 3 |
| 35 | 1ea2ea3e4ea | 2.74 | 1 | 35′ | 1ea2ea3a4ea | 1.99 | 2 |
| 36 | 1ea2ea4ea5e | 0.85 | 1 | 36′ | 1ea2ea4ea5a | 1.41 | 2 |
| 37 | 1ea2ea4ea6e | 1.41 | 1 | 37′ | 1ea2ea4ea6a | 2.72 | 3 |
| 38 | 1ea2a3ea5ea | 1.00 | 3 | 38′ | 1ea2e3ea5ea | 2.09 | 3 |

TABLE III

DIPOLE MOMENT OF TETRACHLOROCYCLOHEXANES

| | Configurations (stable from) | D | No. of the (1a, 3a) pairs | | Configurations (inverted isomers) | D | No. of the (1a, 3a) pairs |
|---|---|---|---|---|---|---|---|
| 1 | 1e2e3e4e | 3.18 | 0 | 1′ | 1a2a3a4a | 0.93 | 2 |
| 2 | 1a2e3e4e | 4.14 | 0 | 2′ | 1e2a3a4a | 2.45 | 1 |
| 3 | 1e2a3e4e | 2.84 | 0 | 3′ | 1a2e3a4a | 2.20 | 1 |
| 4 | 1a2a3e4e | 3.03 | 0 | | | | |
| 5 | 1a2e3a4e | 4.17 | 1 | | | | |
| 6 | 1e2a3a4e | 0.93 | 0 | 6′ | 1a2e3e4a | 3.18 | 0 |
| 7 | 1e2e3e5e | 1.96 | 0 | 7′ | 1a2a3a5a | 2.50 | 3 |
| 8 | 1a2e3e5e | 1.91 | 0 | 8′ | 1e2a3a5a | 2.23 | 1 |
| 9 | 1e2a3e5e | 2.94 | 0 | 9′ | 1a2e3a5a | 4.22 | 3 |
| 10 | 1e2e3e5a | 3.65 | 0 | 10′ | 1a2a3a5e | 1.52 | 1 |
| 11 | 1a2a3e5e | 1.59 | 0 | 11′ | 1e2e3a5a | 4.24 | 1 |
| 12 | 1e2a3e5a | 2.11 | 0 | 12′ | 1a2e3a5e | 2.76 | 1 |
| 13 | 1e2e4e5e($\beta$-1,2,4,5) | 0 | 0 | 13′ | 1a2a4a5a | 0 | 2 |
| 14 | 1a2e4e5e | 2.65 | 0 | 14′ | 1e2a4a5a | 2.27 | 1 |
| 15 | 1a2a4e5e($\alpha$-1,2,4,5) | 2.65 | 0 | | | | |
| 16 | 1a2e4a5e | 0 | 0 | | | | |
| 17 | 1ea2e3e | 3.81 | 0 | 17′ | 1ea2a3a | 2.54 | 1 |
| 18 | 1ea2a3e | 2.76 | 0 | 18′ | 1ea2e3a | 4.10 | 1 |
| 19 | 1ea2e4e | 2.57 | 0 | 19′ | 1ea2a4a | 2.79 | 1 |
| 20 | 1ea2a4e | 0.48 | 0 | 20′ | 1ea2e4a | 3.08 | 0 |
| 21 | 1ea2e5e | 2.13 | 0 | 21′ | 1ea2a5a | 2.36 | 1 |
| 22 | 1ea2a5e | 2.25 | 0 | 22′ | 1ea2e5a | 4.11 | 1 |
| 23 | 1ea2e6e | 4.08 | 0 | 23′ | 1ea2a6a | 3.30 | 1 |
| 24 | 1ea2e6a | 3.34 | 0 | | | | |
| 25 | 1ea3e4e | 2.21 | 0 | 25′ | 1ea3a4a | 1.77 | 1 |
| 26 | 1ea3e4a | 2.24 | 0 | 26′ | 1ea3a4e | 2.82 | 1 |
| 27 | 1ea3e5e | 0.11 | 0 | 27′ | 1ea3a5a | 3.72 | 3 |
| 28 | 1ea3e5a | 2.15 | 1 | | | | |
| 29 | 1ea2ea | 3.36 | 0 | | | | |
| 30 | 1ea3ea | 2.90 | 1 | | | | |
| 31 | 1ea4ea | 0 | 0 | | | | |

where the forms which can be obtained by the inversion of the cyclohexane ring are listed on the same lines. The isomers which are shown in the right half of the tables are the less stable forms with regard to the steric repulsion and designated by primed numbers. The most important part of the steric repulsion of these molecules may be the forces between the chlorine atoms at the 1a-3a positions. The numbers of the pairs of atoms of this sort are listed also in configurations which have reasonable values of dipole moments.

The observed values of dipole moments of the isomers already prepared will be shown in the near future. It will be seen that the agreement between the observed and the calculated values is quite good in all cases, though the assumptions used are of very approximate nature.

It should be noted here that the resultant moment of the molecule arose from the addition of many large C-Cl bond moments (1.86 D). It follows often that the balancing of the large moments yields a small value of the total moment. In this case, the resultant moment largely depends upon the assumed values of induced moments. Actually, the Morino-Miyagawa rule had been proposed to correct the second order quantity. Therefore, we cannot trust the resultant moment, at least when it is smaller than 1.0 D. Of course, when the molecule has a center of symmetry, perfectly cancelling each moment with the corresponding one, a complete vanishing of the total moment results; this phenomenon will be seen, for instances, in the isomers 1,1′,5,30, and 30′ in Table I.

The author wishes to thank Professor Yonezo Morino and Doctor Ichiro Miyagawa for helpful discussions and for their detailed criticism of this paper, and is grateful for a Grant in Aid for Scientific Research given by the Ministry of Education.

*Department of Chemistry, Faculty of Science, Tokyo University, Tokyo*

# *The Dipole Moments of the Polyhalocyclohexanes. III**

By Takashi Shimozawa, Yonezo Morino and Randolph Riemschneider

(Received March 8, 1955)

In the previous report,[1] the configurations of some polyhalocyclohexanes and their related compounds by the dipole moment measurements were discussed, and the dipole moments of polyhalocyclohexanes were calculated by use of our empirical rule and listed in the second article[2].

The present work is a report on the result of the investigation of the configurations of some polyhalocyclohexanes; the process is the same as reported earlier[1].

## Experimental Results

**Materials.**—The samples were synthesized by one of the present authors (R.R). The dipole moments of these compounds were measured by another (T.S) without further purification.

**Dipole Moment Measurement.**—The process of the dipole moment measurement is the same as described in our previous article[1]. The values of the dielectric constant $\varepsilon$ and the specific density $d$ measured in different concentrations $\omega$ by use of the heterodyne beat apparatus and Ostwald's pycnometer, respectively, are listed in Table A.

The dipole moments were computed by the aid of the equation proposed by Halverstadt-Kumler, and the results are listed in Table B.

## Discussion of Results

The five compounds (I to V), which are to be discussed are a kind of chlorine substituted cyclohexanes. Let us discuss their confiigurations by comparing the observed values of their dipole moments with the calculated ones listed in our previous paper.

In the compound VI, there are two kinds of polar bonds, C-Cl and C-Br, so the observed dipole moment of the compound VI should not be directly referred to the calculated ones. But the difference between the bonds C-Cl (1.86D) and C-Br (1.79D) moments would cause only a small change in the dipole moment of the compound as a whole.

Table A

Dielectric constants and specific densities of benzene solutions at 25°C

| $\omega$ | $\varepsilon$ | $d$ | |
|---|---|---|---|
| I. Hexachlorocyclohexane, $C_6H_6Cl_6$ | | | |
| 0.0000 | 2.2725 | 0.8719 | $a=0.25_9$ |
| 0.0091 | 2.2746 | 0.8763 | $b=0.39_7$ |
| 0.0157 | 2.2753 | 0.8777 | |
| 0.0240 | 2.2775 | 0.8818 | |
| 0.0503 | 2.2856 | 0.8919 | |
| II. 1,1,2,4,4,5-Hexachlorocyclohexane, $C_6H_6Cl_6$ | | | |
| 0.0000 | 2.2743 | 0.8716 | $a=0.22_8$ |
| 0.0353 | 2.2820 | 0.8856 | $b=0.42$ |
| 0.0689 | 2.2902 | 0.9001 | |
| III. Heptachlorocyclohexane, $C_6H_5Cl_7$ | | | |
| 0.0000 | 2.2730 | 0.8732 | $a=0.42$ |
| $0.0064_7$ | 2.2758 | 0.8761 | $b=0.49$ |
| $0.0148_3$ | 2.2792 | 0.8803 | |
| $0.0196_6$ | 2.2813 | 0.8829 | |
| IV. Tetrachlorocyclohexane, $C_6H_8Cl_4$ | | | |
| 0.0000 | 2.2755 | 0.8745 | $a=5.02$ |
| $0.0065_5$ | 2.3087 | 0.8762 | $b=0.31$ |
| $0.0109_2$ | 2.3303 | 0.8778 | |
| V. Dodecachlorocyclohexane, $C_6Cl_{12}$ | | | |
| 0.0000 | 2.2724 | 0.8717 | $a=0.26_5$ |
| 0.0282 | 2.2808 | 0.8873 | $b=0.52_8$ |
| 0.0469 | 2.2852 | 0.8966 | |
| 0.0602 | 2.2880 | 0.9047 | |
| VI. *r*-Tetrachlorodibromocyclohexane, $C_6H_6Cl_4Br_2$ | | | |
| 0.0000 | 2.2724 | 0.8721 | $a=2.16$ |
| 0.0120 | 2.3012 | 0.8776 | $b=0.49_2$ |
| 0.0202 | 2.3159 | 0.8824 | |
| 0.0524 | 2.3860 | 0.8979 | |

Table B

Molecular, electronic, and atomic polarisations, and dipole moments at 25°C

| | Compounds | m.p. (°C) | $P$(cc.) | $P_E+P_A$ (cc.) | $\mu$ D |
|---|---|---|---|---|---|
| I. | Hexachlorocyclohexane | 109 | 68.4 | 59.8 | 0.65 |
| II. | 1,1,2,4,4,5-Hexachlorocyclohexane | 156 | 64.1 | 59.8 | 0.46 |
| III. | Heptachlorocyclohexane | 119 | 74.5 | 64.9 | 0.69 |
| IV. | Tetrachlorocyclohexane | 109 | 257.9 | 49.6 | 3.19 |
| V. | Dodecachlorocyclohexane | 285 | 92.0 | 90.4 | 0.28 |
| VI. | *r*-Tetrachlorodibromocyclohexane | 125 | 211.4 | 65.8 | 2.66 |

* The discussion described here was reported on the 7th Annual Meeting of the Chemical Society of Japan. April, 1 (1954).

1) I. Miyagawa, Y. Morino and R. Riemschneider, This Bulletin, 27, 177 (1954).

2) T. Shimozawa, This Bulletin., 28, 389 (1955).

## 1. Polychlorocyclohexanes

**I. Hexachlorocyclohexanes** $C_6H_6Cl_6$ (m.p. 109°C).—The observed value of this compound is 0.65D. Considering the accuracy of the dipole moment measurement, the following eleven configurations whose calculated values are less than 1 D, may be selected as the configuration corresponding to this molecule from the Table I in the previous paper;

| Corresponding Nos. in Table I | | Configurations | Calculated Moments D |
|---|---|---|---|
| 1 | 1 | 1e2e3e4e5e6e($\beta$-BHC) | 0 |
| 2 | 1′ | 1a2a3a4a5a6a | 0 |
| 3 | 5 | 1a2e3e4a5e6e($\varepsilon$-BHC) | 0 |
| 4 | 18 | 1ea2ea4e5e | 0.21 |
| 5 | 23 | 1ea2a3ea5e | 0.44 |
| 6 | 25 | 1ea3ea4a5e | 0.22 |
| 7 | 28′ | 1ea2a3a4ea | 0.93 |
| 8 | 30 | 1ea2e4ea5e | 0 |
| 9 | 30′ | 1ea2a4ea5a | 0 |
| 10 | 38 | 1ea2a3e4e6e | 0.49 |
| 11 | 46′ | 1ea2a3a4e6a | 0.21 |

The observed values of compound I is not completely zero, so the cases 1, 2, 3, 8, and 9 are excluded.

As the starting material of compound I is $\alpha$−1, 2, 4, 5-tetrachlorocyclohexane, the compound I must have the chlorine atoms at the la2a4e5e-positions on the cyclohexane ring, so that the cases 5, 6, 7, 10 and 11 are excluded. Thus, the only configuration compatible with the compound I is the case 4; 1ea2ea4e5e.

The same conclusion is obtained by another argument.

Since the compound I was synthesized by the chlorination of $\alpha$−1, 2, 4, 5-tetrachlorocyclohexane (1a2a4e5e) (m.p. 174°C),[3] its configuration was considered organochemically to be one of the following three;

| | | |
|---|---|---|
| a) | 1ea2ea4e5e | 0.21 D |
| b) | 1ea2ea4a5e | 2.15 |
| c) | 1ea2a4ea5e | 1.88 |

The calculated moments of these isomers are easily found in Table I in the previous paper; the values are given in the above.

The observed value (0.65D) shows that the configuration (a) corresponds to the compound I, while the other two have definitely too large values to correspond to the compound I.

Thus the configuration of hexachlorocyclohexane (m.p. 109°C) is concluded as 1ea2ea4e5e.

Recently, it was shown that the compound I was synthesized by the chlorination of the 1, 2-dichlorocyclohexadiene (1, 4), too.[4] This fact supports the above statement.

**II. Hexachlorocyclohexane** $C_6H_6Cl_6$ (m.p. 146°C).—It is sure that the positions of the six atoms of this compound on the cyclohexane ring are 1, 1, 2, 4, 4, and 5.[5]

The configuration of hexachlorocyclohexane, whose chlorine atoms are at the positions 1, 1, 2, 4, 4, 5, are listed below, together with their calculated dipole moment.

| Corresponding Nos. in Table I | | Configurations | Calculated Moment | No. of (1a, 3a) pairs |
|---|---|---|---|---|
| a) | 30 | 1ea2e4ea5e | 0 D | 0 |
| b) | 30′ | 1ea2a4ea5a | 0 | 2 |
| c) | 31 | 1ea2e4ea5a | 1.88 | 1 |

The case (c) in the above table is definitely excluded, because its dipole moment is too large compared with the observed one (0.46D). There are two pairs of (1a, 3a) polar bonds in the case (b), but no pairs in the case (a). Since the configuration with (1a, 3a) pairs, (b) is less stable than (a) that without such pairs, the configuration (b) is less plausible. As is well known, the measurement of the dipole moment becomes less accurate as the value approaches 0 D, the difference between the observed (0.46 D) and the calculated values may be ascribed to some error in the measurement.

Thus, the configuration of the hexachlorocyclohexane (m.p. 146°C) is determined as 1ea2e4ea5e.

**III. Heptachlorocyclohexane** $C_6H_5Cl_7$ (m.p. 119°C).—This compound was synthesized by the chlorination of the both hexachlorocyclohexane (m.p. 109°C, I) and $\alpha$-1, 2, 4, 5,-tetrachlorocyclohexane (m.p. 174°C).[6]

The dipole moment of this compound was observed to be 0.69D. The configurations whose calculated values of the dipole moment are smaller than 1D are as follows (taken from the Table II in the previous article).

3) R. Riemschneider and G. Ottmann, Mitt. II, *Z. Naturforschg.*, 5b, 248 (1950); Mitt. XXXI, 85, 453 (1954). About $\alpha$-1,2,4,5-Tetrachlorocyclohexane, see Mitt. XII, *Liebigs Ann. Chem.*, 576, 94 (1952).

4) R. Riemschneider, Mitt. XXXII, *Mh. Chem.*, 86, H, 1/2 (1955) and Mitt. XXXI, *Mh. Chem.*, 85, 453 (1954).

5) R. Riemschneider, Mitt, I, *Mitt. Physiolog. Chem. Inst. Bln.*, R33, März, 1949; Mitt. IV, V and VI, *Z. Naturforschg.*, 6b, 48, 410, 339 (1951). See also; G. Calingaret, A. J. Kolka, and N. O. Orloff, *J. Am. Chem. Soc.*, 73, 2359 (1951).

6) l.c. footnote 3).

| | Corresponding Nos. in Table II | Configurations | Calculated dipole moment |
|---|---|---|---|
| a) | 7 | 1ea2a3e4e5a6e | 0.86 D |
| b) | 14 | 1ea2ea3a4e5e | 0.90 |
| c) | 30 | 1ea2a3e4ea6e | 0.87 |
| d) | 36 | 1ea2ea4ea5e | 0.85 |

The synthetic process of this compound suggests that the position of the chlorine atoms were not changed during the reaction. Therefore, six chlorine atoms of the compound III must be at 1ea2ea4e5e, so the cases (a) and (c) are excluded.

However, one can exclude neither of the remaining two (b or d) from the result of the measurement of dipole moment only.

It is suggested, on the other hand in terms of organic chemistry[7], that the hydrogen atom of the group-CHCl is more easily substituted by chlorine than that of $-CH_2-$.

The configuration of the compound III, therefore, may be 1ea2ea4ea5e[8].

**IV. Tetrachlorocyclohexane** $C_6H_8Cl_4$ (m.p. 109°C).—As this compound was obtained by the partial chlorination of cyclohexane, the positions of the chlorine atoms were unknown.

The observed dipole moment was large (3.19 D).

From the Table III in the previous paper, the following five tetrachlorocyclohexanes (upper right) are selected, according to the magnitude of the observed moments (comparable with that of the observed values).

| | Corresponding Nos. in Table III | Configurations | Calculated Moment |
|---|---|---|---|
| 1 | 1 | 1e2e3e4e | 3.18 D |
| 2 | 4 | 1a2a3e4e | 3.03 |
| 3 | 6′ | 1a2e3e4a | 3.18 |
| 4 | 20′ | 1ea2e4a | 3.08 |
| 5 | 29′ | 1ea2ea | 3.36 |

have one of the following eight configurations.

Of these, the cases 2 and 8 would be inappropriate. For, in either case one of the inverted isomers is extremely unstable because of the three (1a, 3a) pairs, therefore, the other configuration without such pairs would be predominant, and this stable configuration has, as is seen, definitely smaller dipole moment than that observed for this compound. Nothing more is to be obtained from the result of the measurement of the dipole moment alone. (Table below)

**V. Dodecachlorocyclohexane** $C_6Cl_{12}$ (m.p. 285°C)[9].—The dipole moment of this molecule is expected to be zero, since this compound has a center of symmetry. The observed dipole moment, 0.28 D, is compatible with this expectation.

**2. Polychlorobromocyclohexane**

**VI. Tetrachlorodibromocyclohexane** $C_6H_6Cl_4Br_2$ (m.p. 123°C)[10].—The positions of halogene atoms of this molecule are, as in the case of BHC, 1, 2, 3, 4, 5, and 6 on the cyclohexane ring. It was hoped that the positions of bromine atoms by the dipole moment investigation could be determined, but it was found to be impossible, since the bond moment of C–Br is comparable to that of C–Cl bond.

| | Stable Forms | | | | Inverted Isomers | | | |
|---|---|---|---|---|---|---|---|---|
| | Correspond Nos. Table III | Configuration | calc. | No. of (1a 3a) | Correspond Nos. | Configuration | calc. | No. of (1a 3a) |
| 1 | 2 | 1a2e3e4e | 4.14 D | 0 | 2′ | 1e2a3a4a | 2.45 D | 1 |
| 2 | 9 | 1e2a3e5e | 2.94 | 0 | 9′ | 1a2e3a5a | 4.22 | 3 |
| 3 | 10 | 1e2e3e5a | 3.65 | 0 | 10′ | 1a2a3a5e | 1.52 | 1 |
| 3 | 11 | 1a2a3e5e | 1.59 | 0 | 11′ | 1e2e3a5a | 4.24 | 1 |
| 5 | 17 | 1ea2e3e | 3.81 | 0 | 17′ | 1ea2a3a | 2.54 | 1 |
| 6 | 18 | 1ea2a3e | 2.76 | 0 | 18′ | 1ea2e3a | 4.10 | 1 |
| 7 | 22 | 1ea2a5e | 2.25 | 0 | 22′ | 1ea2e5a | 4.11 | 1 |
| 8 | 27 | 1ea3e5e | 0.11 | 0 | 27′ | 1ea3a5a | 3.72 | 3 |

Another possibility is that the compound IV is a mixture of a pair of inverted isomers. If it were so, the observed value of the dipole moment (3.19 D) would be between the two values calculated for a certain pair of inverted isomers. In this case this compound must

7) l.c. footnote 4).

8) R. Riemschneider, T. Shimozawa and S. Bäker, Mitt. XXXIII, *Z. Naturforschg.*, 9b, 799 (1954).

9) R. Riemschneider and R. Oswald, Mitt. XXXVII, *Mh. Chem.*, 85, 972 (1954).

10) R. Riemschneider and S. Bäker, Mitt. XXIX, *Z. Naturforschg*, 9b, 751 (1954) and *Mh. Chem.*, 85, 1133 (1954). γ-$C_6H_6Cl_4Br_2$, m.p. 123°C shows insecticidal activity, see Table I, p. 1136.

The calculated moments of the hexachlorocyclohexanes with six chlorine atoms at the positions of 1, 2, 3, 4, 5, and 6 are listed below from the Table I in the previous paper (without considering inverted isomer).

| | | | |
|---|---|---|---|
| 1 | 1e2e3e4e5e6e($\beta$-BHC) | 0 | D |
| 2 | 1a2a3e4e5e6e($\alpha$-BHC) | 2.25 | |
| 3 | 1a2a3a4e5e6e($\gamma$-BHC) | 2.93 | |
| 4 | 1a2e3e4e5e6e($\delta$-BHC) | 2.25 | |
| 5 | 1a2e3e4a5e6e($\varepsilon$-BHC) | 0 | |
| 6 | 1a2e3a4e5e6e | 3.44 | |
| 7 | 1a2a3e4a5e6e($\eta$-BHC) | 1.88 | |
| 8 | 1a2e3a4e5a6e | 4.08 | |

It is seen that the case (3) correspounds to the observed value 2.66D, because the difference of the bond moments of C–Cl and C–Br makes the calculated values for the configuration (3) slightly smaller, but it can not be enough to reduce the next higher one, 3.44 D, to the observed value.

Thus, the configuration of the compound VI were determined as the $\gamma$-type (aaaeee).

*Department of Chemistry, Faculty of Science, Tokyo University, and Chemisches Institut der Freien Universität, Berlin-Dahlem*

# *Note on Polymer-Mixed Solvent System. V. Certain Consequences of the Previous Treatment*

By Tōru KAWAI

(Received February, 1, 1955)

## Introduction

In polymer-mixed solvent systems, thermodynamic properties of the ternary mixtures such as osmotic pressure and swelling, are usually explained by employing the approximation that the mixture of the two liquids can be treated as a hypothetical single liquid having intermediate properties. Sometimes, this single liquid approximation produces a considerable error in osmotic measurements due to non-uniform composition of a mixed solvent in both sides of a semi-permeable membrane. Similarly, swelling of a cross-linked gel or viscosity (especially intrinsic viscosity) of a polymer solution in a mixed solvent may have, more or less, the influence of this selective adsorption. The deviation of these properties from those for the single liquid approximation, have been formulated in Part IV. With the aid of the expressions of these deviations, several experimental results on osmotic, vicometric, and swelling measurements in polymer-mixed solvent systems will be investigated in this paper.

## The Magnitude of the Deviation from the Single Liquid Approximation

As mentioned in Part II[1] and Part III[2] there exist two types of interaction between polymers and mixed solvents. When a nonsolvent is added to a polymer solution, the solvent ability of the medium usually decreases uuiformly with its addition (in this case, $A_{23}-A_{13}>A_{12}$[1]). In some cases, however, the first portion of the addition of the nonsolvent improves the solvent ability of the medium, and the solvent power shows a maximum value at a certain composition, $\theta_c(=(1/2)+(A_{23}-A_{13})/A_{12})$,[1,2,3] and then, decreases (in this case, $A_{23}-A_{13}<A_{12}$[1]). Such behaviors are attributable to the repulsive force acting between solvent and nonsolvent molecules (which is expressed by the parameter $A_{12}$). The solvent ability of mixed solvent is improved by the strong repulsive force between the solvent and nonsolvent molecules in the latter case (hereafter, designated by Case II), whereas a stronger precipitating power of a nonsolvent overcomes the effect of the above repulsive force in the former case (designated by Case I).

If the phenomenon of the selective adsorption may be explained by the assumption that a polymer molecule exhibits a preferential adsorption to the solvent molecules in its statistical environments, the magnitude of the selective adsorption may be usually larger with the larger difference of the solvent powers of the two liquids. The repulsive force between the two liquids, however, act so as to drive the solvent molecules into the polymer-rich phase, and this tendency may be promoted as the content of the nonsolvent increases. For instance, Schulz and Jirgens-

1) T. Kawai, This Bulletin, **25**, 341 (1952).
2) T. Kawai, This Bulletin, **26**, 6 (1953).
3) As mentioned in Part IV, $\theta$ represents the composition of the solvent and not of the nonsolvent.

one[4] found that at 70% (by volume) of methanol the methanol-benzene ratio was 0.131 in a polystyrene gel phase and 3.00 in the solvent phase. In Case II, the magnitude of the selective adsorption depends considerably on the composition. In the composition range, $\theta>\theta_c$, the nonsolvent molecules are rather preferentially adsorbed by the polymer molecules owing to the fact that a majority of the solvent molecules drive the nonsolvent molecules into the environments of the polymer molecules through the strong repulsive force between the solvent and nonsolvent molecules. The magnitude of this "inverse" solective adsorption[5] decreases as the content of the nonsolvent increases until $1-\theta=1-\theta_c$, at which the solvent ability of the mixed solvent has a maximum value and at which the "inverse" selective adsorption vanishes. When the content of the nonsolvent becomes larger than $1-\theta_c$, many more solvent molecules are absorbed by the polymer molecules than the nonsolvent, and the magunitude of the solective adsorption increases with the increasing content of the nonsolvent as in usual cases.

Of course, the larger the manitude of the selective adsorption, the larger the deviation from the single liquid approximation. The deviation of the $\mu$ value is, however, to become smaller with increasing polymer concentration in the polymer-rich phase, whereas the magnitude of the selective adsorption must be larger with the polymer concentration (see Eqs. ($8_a$), ($8_b$) and (15) in Part IV). While, this deviation would increase with the addition of the nonsolvent until a certain nonsolvent-rich composition is reached, and then rapidly decrease to zero, although the effect of molar volumes of the two liquids is considerably comlicated. Therefore, the contribution of the selective adsorption to the $\mu$ value may be most remarkable when the solvent abilities of the two liquids differ very much from each other, and especially in a certain nonsolvent-rich composition. As will be shown later, this deviation sometimes amounts to 12% of the $\mu$ values observed in swelling measurements of a cross-linked gel in such a mixed solvent. In osmotic and viscometric measurements, however, this deviation exists generally in the range, 0~5% of the $\mu$ values, because the selective adsorption is not so remarkable at the compositions usually used in these measurements as in the swelling measurements. Intrinsic viscosity enables us, however, to detect the effect of the selective adsorption owing to its sensitivity to the solvent power.

4) G.V. Schulz and B. Jirgensone, *Z. physik. Chem.*, B46, 131 (1940).

5) Experimentally, Endo proved this phenomenon for polyvinyl acetate-acetone-water system. (Private communication from Mr. K. Endo, the Chemical Laboratory of Tokyo University).

### Osmotic Pressure

According to the treatment developed in Part IV, the second virial coefficient in osmotic pressure expression, $a_2$, may be expressed, to a satisfactory approximation, by

$$\begin{aligned}a_2&=(RT/\rho^2V_0)(1/2-\mu^*)\\&=(RT/\rho^2)[(1/V_3)(1/2-\mu'_s)\\&\quad-(1/RT)\{A_{13}\theta+A_{23}(1-\theta)-A_{12}\theta(1-\theta)\}]\\&\quad-\{1/(RT)\rho^2\}[\{A_{13}-A_{23}\\&\quad-A_{12}(1-2\theta)\}^2\theta(1-\theta)/\{(\theta/V_2)\\&\quad+(1-\theta)/V_1\}]\times[1/2-v_3'+B\{1-4v_3'\\&\quad+(5/4)v_3'^2+\cdots\cdots\}+B^2\{2-12v_3'\\&\quad+(17/2)v_3'^2+\cdots\cdots\}+\cdots\cdots]\end{aligned}\tag{1a}$$

(The notation is exactly the same as that employed in Part IV, and $\rho$ is the density of the polymer), which may be converted to the form,

$$\begin{aligned}a_2&=\{A^*_{13}\theta+A^*_{23}(1-\theta)+A^*_{12}\theta(1-\theta)\}\\&\quad-(\rho^2/RT)\{A^*_{13}-A^*_{23}+A^*_{12}(1-2\theta)\}^2\\&\quad\times[\theta(1-\theta)/\{(\theta/V_2)+(1-\theta)/V_1\}][1/2-v_3'\\&\quad+B\{1-4v_3'+(5/4)v_3'^2+\cdots\cdots\}\\&\quad+B^2\{2-12v_3'+(17/2)v_3'^2+\cdots\cdots\}+\cdots\cdots],\end{aligned}\tag{1b}$$

where

$A^*_{13}=(RT/\rho^2V_3)(1/2-\mu_s')-A_{13}/\rho^2$,
$A^*_{23}=(RT/\rho^2V_3)(1/2-\mu_s')-A_{23}/\rho^2$,
and $A_{12}^*=A_{12}/\rho^2$.

On the other hand, the expression for the single liquid approximation,

$$a_2=A^*_{13}\theta+A^*_{23}(1-\theta)+A^*_{12}\theta(1-\theta)\tag{2}$$

has been usually applied to the experimental data for its simplicity.

As was discussed in the preceding section, the contribution of the selective adsorption to the $\mu$ value is comparatively small (0~5%) in usual osmotic measurements. Considerable errors of the $a_2$ values, however, may often be introduced by employing the single liquid approximation. A few examples will be presented, in which this deviation may be supposed to be remarkable, considering such factors having effects upon it as discussed in the preceding section. Kawai and Furukawa[6] measured the osmotic pressure of cellulose acetate solution in acetone-alkyl phthalates mixtures at 20°C. In Table I, the $a_2$ values are given for a few different com-

6) T. Kawai and T. Furukawa, *J. Chem. Soc. Japan, Ind. Chem. Section*, 57, 436 (1954).

TABLE I

THE EFFECTS OF THE SELECTIVE ADSORPTION UPON THE $a_2$ VALUE AND THE INTERACTION PARAMETERS (CELLULOSE ACETATE-ACETONE-ALKYL PHTHALATES SYSTEMS)

at 20°C, $V_1=73.3$ cc $\rho=1.30$ g/cc $a_2$, $A^*$(atm.(cc./g.)$^2$)

| Nonsolvents | Dimethyl phthalate ($V_2=166.4$) | Diethyl phathalate ($V_2=197.9$) | Dibuthyl phthalate ($V_2=264.9$) |
|---|---|---|---|
| Interaction parameters from Eq. (2) | $A_{13}^*=1.43\times10$<br>$A_{23}^*=0.08_8\times10$<br>$A_{12}^*=1.48\times10$ | $A_{13}^*=1.43\times10$<br>$A_{23}^*=-0.99\times10$<br>$A_{12}^*=2.64\times10$ | $A_{13}^*=1.43\times10$<br>$A_{23}^*=-2.43\times10$<br>$A_{12}^*=0.26\times10$ |
| Interaction parameters from Eq. (Ib) | | $A_{13}^*=1.43\times10$<br>$A_{23}^*=-0.73_5\times10$<br>$A_{12}^*=2.32\times10$ | $A_{13}^*=1.43\times10$<br>$A_{23}^*=-2.60\times10$<br>$A_{12}^*=1.16\times10$ |

| Content of solvent by volume fraction | $a_2\times10$ (exp.) | $a_2\times10$ (calc.) | The contribution of selective adsorption $\times10$ | $a_2\times10$ (exp.) | $a_2\times10$ (calc.) | The contribution of selective adsorption $\times10$ | $a_2\times10$ (exp.) | $a_2\times10$ (calc.) | The contribution of selective adsorption $\times10$ |
|---|---|---|---|---|---|---|---|---|---|
| 0.856 | 1.42 | 1.42 | 0.0013 | 1.40 | 1.40 | 0.0019 | 0.91 | 0.91 | 0.085 |
| 0.750 | 1.35 | 1.36 | 0.0074 | 1.30 | 1.31 | 0.0092 | 0.51 | $0.51_5$ | 0.125 |
| 0.667 | | | | | | | 0.20 | $0.19_4$ | 0.150 |
| 0.500 | 1.10 | 1.09 | 0.0206 | 0.88 | 0.88 | 0.046 | | | |

The terms $[1/2-v_3'+B\{1-4v_3'+(5/4)v_3'^2+\cdots\cdots\}+B^2\{2-12v_3'+(17/2)v_3'^2+\cdots\cdots\}]$ in Eq. (Ib) are approximated by 1/2 in the above calculations. ($v_3'=0.005\sim0.02$)

positions. Since the contribution of the selective adsorption is supposed to be considerable when diethyl and dibutyl phthalates are used as the nonsolvent, the interaction parameters, $A^*_{13}$, $A^*_{23}$, and $A^*_{12}$, are calculated by employing Eq. (Ib) from the $a_2$ values for these two nonsolvent in Table I and are compared with those obtained by applying Eq. (2) in the same table. Merely for dimethyl phthalate, the interaction parameters are calculated only by Eq. (2), because this calculation does not seem to introduce any serious error. In order to estimate the contribution of the selective adsorption to the $a_2$ values, the last bracketed terms in Eq. (Ib) are evaluated for each composition of the three solvent-nonsolvent pairs also in Table I. Reasonable values of the parameters have been obtained by employing Eq. (Ib), whereas the $A^*_{12}$ value calculated by Eq. (2) is unacceptably small especially for acetone-dibutyl phthalate in consideration of the strong repulsive force between the two liquids. Furthermore, an extremely good agreement has been obtained between the experimental and calculated $a_2$ values in all the composition range investigated.

## Intrinsic Viscosity

As discussed in Part IV, intrinsic viscosities of a polymer in various liquids including mixed solvents might be correlated with the $(1/2-\mu)/V_0$ values. It is confirmed in Part IV and in another paper[7] that an entirely similar relationship may be expected between swelling ratio of a polymer gel in various liquids and the values of $(1/2-\mu)/V_0$[8]. Thus, a good correspondence is to be expected also between $[\eta]$ values and the equilibrium swelling ratio in a series of solvents or for various compositions of a mixed solvent. Actually, Staudinger and Heuer[9] found that the liquid which shows the greatest value of specific viscosity in the solvents for polystyrene, is the best swelling agent for polystyrene-divinyl benzene gels. Frith[10] also mentioned that $[\eta]$ values for a series of neoprence solutions in benzene-various esters mixtures are linearly related to the swelling of a vulcanized Neoprene in the corresponding esters[11]. Furthermore, the relationship between the equilibrium swelling ratio and the cohesive energy densities of the swelling agents, which was established by Gee[12] and has been widely used, can be well interpreted from the above procedure[7,13]. Also the $a_2$

7) T. Kawai, This Bulletin, **26**, 409 (1953).

8) Strictly speaking, the $\mu$ values for the swelling of a cross-linked polymer are somewhat different from those used in the discussion of intrinsic viscosity, as mentioned in Part IV.

9) H. Staudinger and W. Heuer, *Z. physik. Chem.*, A171, 129 (1934).

10) E.M.Frith and F.R.Tuckett, "Linear Polymers", p. 231 (1950).

11) Although the swelling agents are not the same as the liquids employed in the viscometric measurements, but are pure esters, it is not impossible to assume that this example may be interpreted by our procedure, as is seen from Eqs. (16) and (17) in Part IV.

12) G. Gee, "Advances in Colloid Science", Vol. II, Interscience Publishers, Inc., New York (1946), p. 179.

13) In the usual explanations for this relationship, the effect of segment size (see reference 7)) is not considered.

values would keep pace with the $[\eta]$ values in a series of solvents, as will be shown in the coming pages.

Now, the effect of the selective adsorption could be assumed to appear through the $(1/2-\mu^*)/V_0$ values upon intrinsic viscosities in mixed solvents. In case I, mentioned in the preceding section, $[\eta]$ value decreases with the addition of the nonsolvent, and its value may be somewhat smaller for each composition than that expected from the $(1/2-\mu^{**})/V_0$ values for the single liquid approximation. Although the magnitude of the selective adsorption may be notable in this case, its contribution to the $[\eta]$ value cannot be detected from the above procedure since only the $(1/2-\mu^*)/V_0$ value has been correlated with the selective adsorption, and $[\eta]$ itself has not yet been formulated in an analytical form in consideration of the above contribution.

In case II, however, this treatment leads to an interesting bit of information on the effect of the selective adsorption. It is evident Eqs. (17) and (18) in Part IV, that the $[\eta]$ values at the two compositions equally apart from the content of the solvent $\theta_c$ at which the solvent power of the mixed solvent shows a maximum, should be exactly equal to each other[14], if the single liquid approximation were valid. Namely, the $[\eta]\sim$composition curve is symmetrical with respect to the line $\theta=\theta_c$, as is shown by the dotted curve in Fig. 1. In actual system, the curve might

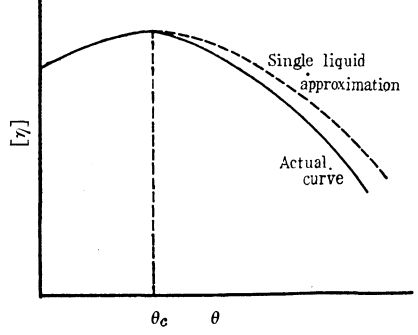



Fig. 1. Illustration of the effect of selective adsorption on the $[\eta]\sim\theta$ curve.

deviate from this symmetrical one as is given by the rigid curve in the same figure. It is easily seen from Eq. (18) in Part IV, that $[\eta]$ values may be somewhat smaller than those expected from the single liquid approximation, either when $\theta<\theta_c$ or $\theta>\theta_c$. However, these deviations are likely to be larger when $\theta<\theta_c$ than when $\theta>\theta_c$ as will be discussed later. Thus, the $[\eta]\sim\theta$ curve becomes an asymmetric one, the degree of which depends upon the magnitude of the selective adsorption. At the two compositions equally apart by $\delta$ from $\theta_c$, the contribution of the selective adsorption to the $(1/2-\mu^*)/V_0$ value may be written,

$$\Delta_1=\{1/(RT)^2\}(A_{12}\delta)^2(\theta_c+\delta)(1-\theta_c-\delta)(1/2-v_3'+C)/\{(\theta_c+\delta)/V_2+(1-\theta_c-\delta)/V_1\} \quad (3a)$$

at the composition, $\theta_1(=\theta_c+\delta)$, and

$$\Delta_2=\{1/(RT)^2\}(A_{12}\delta)^2(\theta_c-\delta)(1-\theta_c+\delta)(1/2-v_3'+C)/\{(\theta_c-\delta)/V_2+(1-\theta_c+\delta)/V_1\} \quad (3b)$$

at the composition, $\theta_2(=\theta_c-\delta)$, where the terms, $B\{1-4v_3'+(5/4)v_3'^2+\cdots\cdots\}+\cdots\cdots$ in Eqs. (1a) and (1b) are replaced by $C$ $(1-\theta_c>\delta>0)$.

As easily seen from Eqs. (3a) and (3b), the above asymmetry of the $[\eta]\sim\theta$ curve arises mainly from the fact that the values of the term $\theta(1-\theta)$ in Eq. (18) in Part IV, are greater in the composition, $\theta_2(=\theta_c-\delta)$ than in the composition, $\theta_1(=\theta_c+\delta)$, although the effect of molar volumes of the two liquids has to be taken into account. The smaller the $\theta_c$ values, the less the difference of the $\theta(1-\theta)$ values between the above two compositions for a constant value of $\delta$, and vice versa $(\theta_c\geqq 1/2)$. For instance, Palit, Colombo and Mark[15] obtained the $[\eta]\sim\theta$ relation, giving an almost symmetrical curve with respect to the line $\theta=\theta_c=0.56$ for polystyrene-methylcyclohexane-acetone system. In this system, the effect of the selective adsorption can be ignored due to the extremely small difference between the $\theta_1(1-\theta_1)$ and $\theta_2(1-\theta_2)$ values. In many cases the selective adsorption seems, however, to give a considerable deviation from the "ideal" symmetry of the $[\eta]\sim\theta$ curve, owing to the sensitive variation of the $[\eta]$ value to the solvent power. In Part II[1], the $[\eta]$ value was correlated with the value of $\mu$ for the single liquid approximation and was discussed from a few experimental data in mixed solvents. More precise knowledge on the $[\eta]\sim\theta$ relation will be obtained with the aid of the treatment developed here.

It is evident from Eqs. (3a) and (3b) that the $A_{12}$ value might also play an important role in the factors governing the asymmetry of the $[\eta]\sim\theta$ curve, when the degrees of the asymmetry are compared for various sys-

14) It is assumed, of course, that $[\eta]$ gives an equal value for the liquids having an equal value of $(1/2-\mu^*)V_0$ for a polymer.

15) S.R. Palit, G. Colombo and H. Mark, *J. Polym. Sci.*, **6**. 295 (1951).

tems[16]. In Fig. 2～5[17,18,19] the $[\eta]$～$\theta$ curves are given for several polymer-mixed solvent systems, which were cited also in Part II[1]. The $\theta_c$ and $\mu_{12}$ values are written for each system in the same figures, showing that the degree of the asymmetry of the curves is greater for the greater value of $\mu_{12}$ and for the smaller value of $\theta_c$. Strictly speaking,

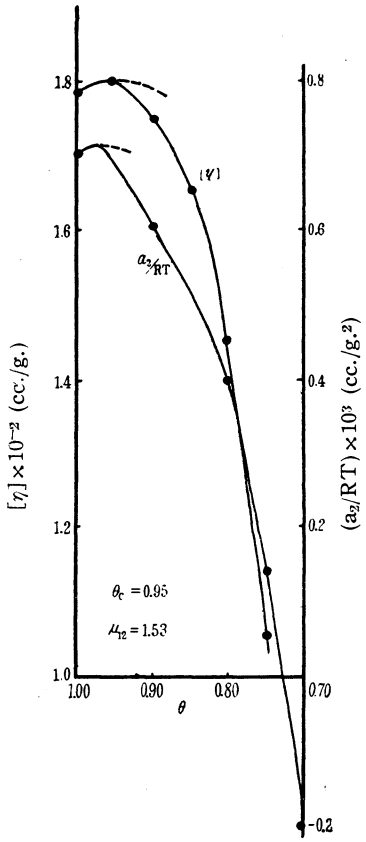



Fig. 2. $[\eta]$～$\theta$, and $a_2$～$\theta$ relationships for polyvinyl acetate-acetone-water system at 20°C.

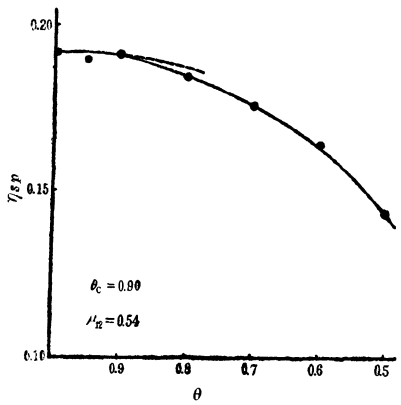



Fig. 4. The $\eta_{sp}$～$\theta$ relationship of 0.001 g./cc. polyvinyl acetate in acetone-ether mixture.

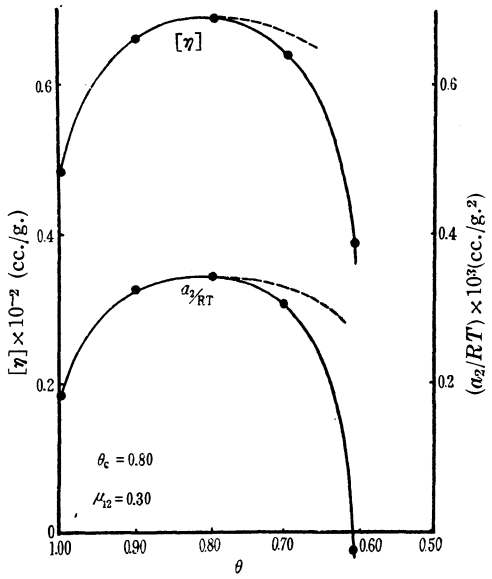



Fig. 3. $[\eta]$～$\theta$ and $a_2$～$\theta$ relationships for Polyvinyl acetate-methanol-watersystem at 20°C.

the $A_{12}$ values should be givin in these figures instead of $\mu_{12}$, as understood from the above treatment. For the present purpose, however the $\mu_{12}$ values[1] may be sufficient to represent the relative magnitude of the parameter $A_{12}$. In Fig. 2 and Fig. 3,

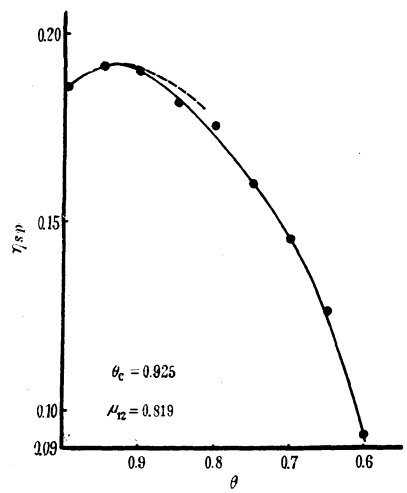



Fig. 5. The $\eta_{sp}$～$\theta$ relationship of 0.001 g./cc. polyvinyl acetate in acetone-petroleum benzin mixture.

16) Of cource, the deviation from the asymmetry of the $[\eta]$～$\theta$ curve increases with $\delta$. These discussions are those for a constant value of $\delta$.

17) K. Yoshioka, *J. Chem. Soc. Japan*, 72, 767 (1951).

18) K. Endo, *J. Chem. Soc. Japan*, 72, 885 (1951).

19) K. Yoshioka, *J. Chem. Soc. Japan*, 72, 664 (1951).

also the $a_2 \sim \theta$ curves are given from Endo's osmotic data[18,20], showing a satisfactorily good correspondence between the $[\eta]$ and $a_2$ values in all the composition ranges rather than between the $[\eta]$ and $\mu$ values[1], as is expected from the above treatment.

In order to investigate quantitatively the factors which have effects on the degree of the asymmetry in the $[\eta] \sim \theta$ curves, we have calculated numerically the right hand sides of Eqs. (3a) and (3b) in Table II,, having

TABLE II

ILLUSTRATION OF THE FACTORS RULING THE DEGREE OF THE ASYMMETRY IN THE $[\eta] \sim \theta$ CURVE (EXAMINATION OF EQS. (3a) AND (3b) FOR P.V.AC.-ACETONE-WATER[20] AND P.V.Ac.-METHANOL-WATER SYSTEMS[18])

| | P.V.Ac.-acetone-water system $\mu_{12}=1.53$[1], $\theta_c=0.95$[1] | | | | | P.V.Ac.-methanol-water system $\mu_{12}=0.30$[1], $\theta_c=0.80$[1] | | | | |
|---|---|---|---|---|---|---|---|---|---|---|
| $\delta$ | $(\mu_{12}\delta)^2 \times 10^4$ | $\theta(1-\theta) \times 10^2$ | $\frac{\{(\theta/V_1)+(1-\theta)/V_2\}^2}{(\theta/V_1)+(1-\theta)/V_2} \times 10^3$ | $\Delta^* \times 10^8$ | $(\Delta_2-\Delta_1)^* \times 10^8$ | $(\mu_{12}\delta)^2 \times 10^4$ | $\theta(1-\theta) \times 10^2$ | $\frac{\{(\theta/V_1)+(1-\theta)/V_2\}^2}{(\theta/V_2)+(1-\theta)/V_1} \times 10^3$ | $\Delta^* \times 10^8$ | $(\Delta_2-\Delta_1)^* \times 10^8$ |
| 0.01 | 2.34 | 3.84 | 4.35 | 1.95 | 1.30 | 0.09 | 15.39 | 19.85 | 1.38 | 0.09 |
| −0.01 | | 5.64 | 4.96 | 3.25 | | | 16.59 | 19.64 | 1.47 | |
| 0.02 | 9.36 | 2.91 | 4.08 | 5.57 | 10.33 | 0.36 | 14.76 | 18.11 | 4.80 | 1.42 |
| −0.02 | | 6.51 | 5.22 | 15.90 | | | 17.16 | 20.15 | 6.22 | |
| 0.03 | 21.06 | 1.96 | 3.84 | 7.91 | 34.96 | 0.81 | 14.11 | 17.63 | 10.08 | 4.76 |
| −0.03 | | 7.36 | 5.54 | 42.87 | | | 17.71 | 20.69 | 14.84 | |
| 0.04 | 31.44 | 0.99 | 3.64 | 6.74 | 82.67 | 1.44 | 13.44 | 17.18 | 16.61 | 11.27 |
| −0.04 | | 8.19 | 5.85 | 89.41 | | | 18.24 | 21.22 | 27.88 | |
| 0.10 | | | | | | 9.00 | 9.00 | 14.81 | 60.04 | 173.64 |
| −0.10 | | | | | | | 21.00 | 25.40 | 233.68 | |

* These $\Delta$ values are an approximate values, which were calculated by the relation, $\Delta=(1/2)(\mu_{12}\delta)^2\theta(1-\theta)\{(\theta/V_1)+(1-\theta)/V_2\}^2/\{(\theta/V_2)+(1-\theta)/V_1\}$.

compared the polyvinyl acetate-acetone-water system (Fig. 2) with the polyvinyl acetate-methanol-water system (Fig. 3). The difference of the $(\Delta_2-\Delta_1)$ values is remarkable between these two systems, mainly due to the superposed effects of the $\theta_c$ and $A_{12}$ values.

Now, the effect of the molar volumes of the two liquids should be considered. When the molar volume of the solvent is larger than that of the nonsolvent ($V_1 > V_2$), the asymmetry of the $[\eta] \sim \theta$ curve is increasingly promoted by this effect, since the terms represented by $1/\{(\theta/V_2)+(1-\theta)/V_1\}$, are greater in Eq. (3b) (at $\theta_2$) than in Eq. (3a) (at $\theta_1$). When $V_2 > V_1$, this effect of the molar volumes behaves as if it makes the degree of the asymmetry to be rather decreased. It is possible, however, to prove from Eqs. (3a) and (3b) that the deviation $\Delta_2$ at the composition $\theta_2$ is always greater than the deviation $\Delta_1$ at $\theta_1$ even when $V_2 > V_1$, owing to the predominant influence of the $\theta(1-\theta)$ values.

20) K. Endo, *J. Chem. Soc. Japan*, 71, 232 (1950).

When the degree of the asymmetry is compared for different systems, moreover, the magnitude of the terms, $1/\{(\theta/V_2)+(1-\theta)/V_1\}$ must be considered for the different systems. Therefore, it is no wonder that the degree of the asymmetry is sometime greater in the latter case ($V_2 > V_1$) than in the former case ($V_1 > V_2$) even if the comparison were made between the systems having equal $\theta_c$ and $A_{12}$ values. Naito[21] pointed out that the $[\eta] \sim \theta$ curves show a remarkable asymmetry in the ternary systems, which involve acetone, *n*-propyl alcohol, and dioxane as the nonsolvents in polyvinyl alcohol-water solutions. These systems belong to the case, $V_2 > V_1$, although the effects of the $\theta_c$ and $A_{12}$ values may predominate over the degree of the asymmetry.

## Equilibrium Swelling

Boyer and Spencer[22] measured equilibrium swelling of polysyrene-divinyl benzene gels in solvent-nonsolvent mixtures. Fig. 6 is a semilogarithmic plot of $\mu$, calculated by the Flory-Rehner equation (Eq. (9) in Part IV), against the composition of the solvent from their data for toluene-propanol mixture, which according to them, consists of three straight line portions, the first break occuring at $\mu \fallingdotseq 0.5$, the second at $\mu \fallingdotseq 1.0$. In the author's opinion, however, the $\mu \sim \theta$ relatino

21) R. Naito and T. Kominami, *Chem. of High Polymer, Japan*, II, 444 (1954).

22) R.F. Boyer and R.S. Spencer, *J. Polymer Sci.*, 3, 97 (1948).

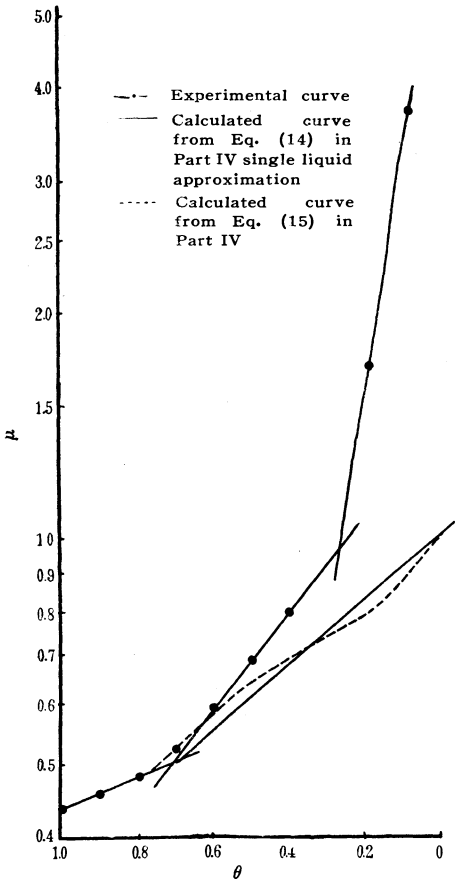



Fig. 6. Comparison of the theoretical $\mu\sim\theta$ curve considering the effect of selective adsorption with the experimental curve (Polystyrene-divinyl benzene gel-toluene-*n*-propanol).

should be represented by a smooth curve instead of the three straight lines. Although we can easily show that one of the origins of the break at $\mu=0.5$ resides in the choice of a semilogarithmic type of plot[23], the $\mu\sim\theta$ "curve" for this system clearly goes upward considerably in the neighbourhood of $\mu=0.5$ and also of $\mu=1.0$. These phenomena may imply the breakdown of the $\mu$ concept for poor solvents, as was pointed out by Boyer and Spencer[22]. This failure of the $\mu$ concept may be due to some complicated factors including those discussed in their paper[22], and may be due in part to the approximation of Eq. (12) applied instead of Eq. (13) in Part IV. For the present purpose, however, we shall confine ourselves to a discussion of the effect of the selective adsorption on the $\mu$ values. Also in order to make the other factors clear, it may not be meaningless, because this effect is supposed to be an important one of the above factors.

It is possible to calculate the contribution of the selective adsorption to the $\mu$ value from the equations derived in Part IV. Employing Eq. (14) in Part IV for the single liquid approximation[24], the interaction para-

23) It is derived from the condition, $\frac{d^2(\ln\mu)}{d\theta^2}=0$, that the point of inflexion of the $\ln\mu\sim\theta$ curve occurs at $\mu=0.5$, so long as the single liquid approximation and the relation, $(\mu_{12})^{1/2}=(\mu_{23})^{1/2}-(\mu_{13})^{1/2}$, which corresponds to Scott's approximation [*J. Chem. Phys.*, 17, 268 (1949)], hold their validity (cf. Eq. (14) in Part IV).

24) In these calculations of the interaction parameters, it is assumed that $\mu_{13}=1/2-(V_1/V_3)(1/2-\mu_S')+(V_1/RT)A_{13}$ and $\mu_{23}=1/2-(V_2/V_3)(1/2-\mu_S')+(V_2/RT)A_{23}$, where the last terms should be written $(V_0/RT)A_{13}$ and $(V_0/RT)A_{23}$ respectively, but these expressions may be permitted as approximate ones (cf. Eq. (14) in Part IV).

TABLE III

THE CONTRIBUTION OF THE SELECTIVE ADSORPTION EFFECT TO THE $\mu$ VALUE OBTAINED FROM EQUILIBRIUM SWELLING OF POLYSTYRENE-DIVINYL BENZENE GELS (0.0462% D.V.B.) IN TOLUENE-N-PROPANOL MIXTURES AT 23°C.

$V_1=107$, $V_2=75.1$, $\mu_{13}=0.434$, $\mu_{23}=1.02$, $\mu_{12}=0.451$

| $\theta$ | $v_3'$ | $\mu$ (experimental) | $\mu$ (calculated for the single liquid approximation) | Contribution of selective adsorption* |
|---|---|---|---|---|
| 1.0 | 0.0596 | 0.434 | 0.434 | 0 |
| 0.9 | 0.0650 | 0.452 | 0.452 | 0.0022 |
| 0.8 | 0.0780 | 0.479 | 0.479 | 0.0079 |
| 0.7 | 0.1225 | 0.523 | 0.505 | 0.0155 |
| 0.6 | 0.2362 | 0.592 | 0.562 | 0.0259 |
| 0.5 | 0.3880 | 0.688 | 0.614 | 0.0247 |
| 0.4 | 0.5195 | 0.800 | 0.677 | 0.0150 |
| 0.3 | 0.6256 | 0.925 | 0.750 | (−0.0011) |
| 0.2 | 0.8941 | 1.72 | 0.831 | (−0.0458) |
| 0.1 | 0.9906 | 3.80 | 0.921 | (−0.0480) |
| 0 | 0.9973 | 4.84 | 1.02 | 0 |

The contribution of the selective adsorption to the $\mu$ value has been calculated by $\{\mu_{23}-\mu_{13}+\mu_{12}(1-2\theta)\}^2[\theta(1-\theta)\{(\theta/V_1)+(1-\theta)/V_2\}/\{(\theta/V_2)+(1-\theta)/V_1\}]\times[1/2-v_3'+\mu_{12}\theta(1-\theta)\{1-4v_3'+(5/4)v_3'^2\}+\{\mu_{12}\theta(1-\theta)\}^2\{2-12v_3'+(17/2)v_3'^2\}]$ instead of Eq. (15) in Part IV, which may give a satisfactory approximation.

meters are evaluated from the $\mu$ values for 0, 10, and 20 percent propanol, since the errors due to the selective adsorption and other factors are supposed to be very slight in such solvent-rich compositions ($\mu_{12}=0.434$, $\mu_{23}=1.02$, and $\mu_{12}=0.451$[24]). The statement of Boyer and Spencer that this toluene-propanol mixture does not show a maximum swelling at any composition, is well explained from these values of the interaction parameters (i.e. this ternary system belongs to Case I mentioned in the preceding section), whereas it is unacceptable from Gee's treatment[25] as they pointed out[22].

Employing these values of the interaction parameters, the contribution of the selective adsorption to the $\mu$ value has been estimated from Eq. (15) in Part IV, and is given in Table III, being compared with the $\mu$ values calculated for the single liquid approximation, and with those from the experiments. These are also shown in Fig. 6. Until a certain composition is reached, the contribution of the selective adsorption increases with the addition of the nonsolvent, and amounts to a considerable percentage of the total $\mu$ value as was discussed in Part IV. It is interesting to note that this contribution begins to decrease from this composition, owing both to the increase of $v_3'$ and to the decrease of $\theta$ in Eq. (15) in Part IV, and finally, gives a negative value in the composition range above 80% propanol (the condition,

$1/2-v_3'+B\{1-4v_3'+(5/4)v_3'^2+\cdots\cdots\}+B^2\{2-12v_3'+(17/2)v_3'^2+\cdots\cdots\}+\cdots\cdots>0$ cannot be satisfied for the extremely great content of the nonsolvent. Thus, the dependency of the above contribution upon $v'_3$ and $B_1$ may appear in various complicated ways such as are represented by Eq. (15) in Part IV, whereas it can be ignored approximately in the treatments of osmotic pressure and intrinsic viscosity.

The writer wishes to thank Prof. H. Maeda, and Assist. Prof. K. Makishima for constant encouragement and many helpful suggestions.

*Laboratory of Textile Chemistry,*
*Tokyo Institute of Technology*
*Tokyo*

25) G. Gee, *Trans. Faraday Soc.*, **40**, 468 (1944).

# *Study of Reversible Photo-Chemical Reactions. III. Mechanism of the Phototropy of Mercuric Complex Salts (I). Changes of the Physical Properties in the Reversible Color Change Reaction of* $HgI_2 \cdot 2HgS$

By Kunio TAKEI

(Received December 22, 1954)

S. V. Raghava Rao[1] reported that $HgI_2 \cdot 2HgS$ rapidly turns black in sunlight owing to the formation of mercuric iodide and sulfide, which returns to the initial compound after a few days when left in the dark, and instantly when heated. However, according to the present author's earlier report[2] it appears more probable that mercuric complex salt is not decomposed by the action of light. Recently Lawrence Schow and George R. Pond[3] referred to a mechanism of phototropy of $HgI_2 \cdot 2HgS$ in a study of X-ray and optical absorption of $Ag_2S$-$HgI_2$ system. Mean-while we have investigated magnetic susceptibilities, X-ray diffraction patterns, possibility of phosphorescence or luminescence, as well as the effects of admixture of impurity and $CO_2$ or $O_2$ on it and related compounds. From the results obtained it was found that the degree of decomposition of $HgI_2 \cdot 2HgS$ in sunlight is small and a change of electronic structure of the crystal occurs. The sample studied was the yellow powder of $HgI_2 \cdot 2HgS$ prepared by the hydrogen sulfide method; however in the case of the study of the impurity effect, powder prepared in an electric furnace was used.

1) S. V. Raghava Rao and H. E. Watson, *J. Phys. Chem.*, 32, 1354 (1938).
2) Kunio Takei, *J. Chem. Soc. Japan*, 73, 202 (1952) (in Japanese).
3) Lawrence Schow and George R. Pond, *J. Phys. Chem.*, 58, 240 (1954).

## Experiments and Discussion of Results

**1. Magnetic Susceptibility.**—In a previous paper[2] the magnetic behaviour of $HgI_2 \cdot 2HgS$ was briefly reported. The Gouy method was employed for the measurement of magnetic susceptibility. About 1.5 g. of the sample ($HgI_2 \cdot 2HgS$, yellow powder) was packed as tightly as possible into a cylin-

drical glass tube 6 mm. wide and 130 mm. long. A Weiss type electromagnet (pole diameter 20 mm.: gap 15 mm.) was employed, which gave 9000 gausses field when excited with 10 amp. current. The accuracy of measurement was estimated to be about 3%. First the susceptibility of the yellow powder, $\chi_0$, was measured, then the powder was placed on a watch glass, turned uniformly black by exposure to daylight, and the susceptibility of this darkened powder, $\chi_1$, was measured. When this darkened powder was heated at 90°C for about 10 min., the color of the powder returned to the original, and the susceptibility of this powder, $\chi_2$, was measured. When the darkened powder was kept continually in the dark at room temperature for two days, the susceptibility, $\chi_3$, was measured. The susceptibility of mercuric iodide, sulfide, and silver bromide, which were treated similarly by daylight were measured. The results are shown in Table I.

TABLE I

MAGNETIC SUSCEPTIBILITY ($\times 10^6$ C.G.S.)

| Substance | $\chi_0$ | $\chi_1$ | $\chi_2$ | $\chi_3$ |
|---|---|---|---|---|
| $HgI_2 \cdot 2HgS$ (yellow) | −0.18 | +0.14, −0.044, +0.0060, −0.056 | −0.059 | −0.18 |
| $HgI_2$ (red) | −0.26 | +0.0067 | −0.0623 | −0.015* |
| HgS (black) | −0.23 | −0.23 | −0.23 | −0.23* |
| AgBr (yellow) | −0.33 | +0.00060 | −0.00060 | −0.13* |

From the above table it is evident that the initially diamagnetic yellow powder becomes paramagnetic after the blackening by sunlight. The extent of blackening was different according to the intensity of light, the time of exposure, and the degree of stirring; accordingly $\chi$ was not reproducible, but it was ascertained that the darkening causes a few paramagnetic characteristics. Mercuric iodide and sulfide are both diamagnetic, so that if the phototropy of $HgI_2 \cdot 2HgS$ were due to the decomposition into iodide and sulfide, the black powder must be diamagnetic with a negative value of $\chi$ on account of the additive law of magnetic susceptibility. The observed paramagnetism shows that the phototropic behaviour of this substance is not due to the decomposition but is due very probably to the change of the electronic structure of $HgI_2 \cdot 2HgS$. $\chi_2$ was nearly equal to $\chi_1$. $\chi_3$ returned to the original value, $-0.18 \times 10^{-6}$. On the other hand, when mercuric iodide and silver bromide were darkened by exposure to light, $\chi_1$ became paramagnetic and $\chi_2$ was nearly equal to $\chi_1$, but $\chi_3$ did not return to the original value even after a month. The mechanism of photodecomposition of silver bromide is well known. Comparing the above magnetic properties of $HgI_2 \cdot 2HgS$ with that of mercuric iodide and silver bromide, the magnetic behaviour of $HgI_2 \cdot 2HgS$ is explained as follows. Irradiation of $HgI_2 \cdot 2HgS$ by light elevates the electrons of $I^-$ or $S^{--}$ ion to the conduction band and leave positive holes in the crystal. Electrons move freely until captured by the centers. The observed paramagnetism is due to the existence of the spin of the trapped unpaired electrons. On heating the powder at 90°C, the trapped electrons return to the ground-states by enhanced thermal agitation and cannot recombine with positive holes, because most of the positive holes escape out of the crystal by heating. Therefore $\chi_2$ is nearly equal to $\chi_1$. However, when the darkened powder was kept in the dark, most of the holes remain in the crystal and the electrons released from the trapping centers react with these holes, so that $\chi_3$ will return to yellow value.

**2. Study of X-ray Diffraction of $HgI_2 \cdot 2HgS$ Powder.**—The commonly employed Debye-Scherrer diffraction method was used. Copper $K\alpha$ radiation filtered through a nickel plate was employed. The exposure length was 5—6 hr., at a potential of 30 kV and with a tube current of 20 m amp. Fig. 1 shows the powder diffraction pattern of $HgI_2 \cdot 2HgS$ (yellow), $HgI_2 \cdot 2HgS$ (black), 0.8[$HgI_2 \cdot 2HgS$(yellow)]+0.2[$HgI_2$+2HgS], 0.7[$HgI_2$-2HgS(yellow)]+0.3[$HgI_2$+2HgS], and 0.6[$HgI_2 \cdot 2HgS$ (yellow)]+0.4[$HgI_2$+2HgS] in comparison with those of mercuric iodide and sulfide. If the complex salt decomposes into mercuric iodide and sulfide in sunlight, the pattern of the darkened powder may consist of the degenerated lines of $HgI_2 \cdot 2HgS$ (yellow) and mercuric iodide and sulfide. However, in the pattern of the mixtures containing 20%, 30% and 40% of [$HgI_2$+2HgS], respectively, the intensity of the lines of 3.54, 3.37 and 1.78Å became very much stronger than that of the yellow powder. The line of 3.54 Å is due

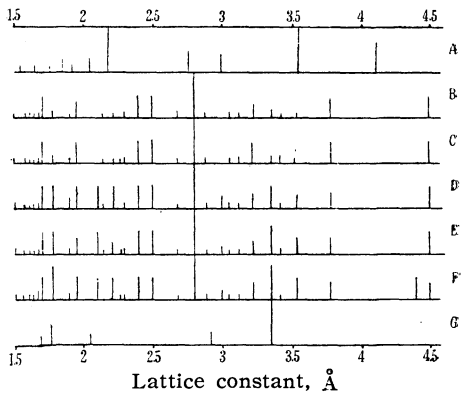



Fig. 1. X-ray diffraction pattern of powder:
(A) $HgI_2$, (B) $HgI_2 \cdot 2HgS$ (yellow),
(C) $HgI_2 \cdot 2HgS$ (black),
(D) 0.8[$HgI_2 \cdot 2HgS$ (yellow)]+0.2[$HgI_2$+2HgS],
(E) 0.7[$HgI_2 \cdot 2HgS$ (yellow)]+0.3[$HgI_2$+2HgS],
(F) 0.6[$HgI_2 \cdot 2HgS$ (yellow)]+0.4[$HgI_2$+2HgS],
(G) HgS (black).

* This value is for the darkened sample which was kept continually in the dark for a month.

to that of mercuric iodide and the lines of 3.37 and 1.78Å are due to that of mercuric sulfide. New lines of 3.00 and 2.10Å also are found in them. The former line is attributable to mercuric iodide. Therefore, even though the darkened powder contained mercuric iodide and sulfide, the lines of iodide and sulfide may not appear in the pattern of the darkened powder, if the powder contains [$HgI_2+2HgS$] less than 20% mole. From the fact that the black powder pattern of $HgI_2 \cdot 2HgS$ is identical with that of the yellow powder, it is evident that darkening does not change the crystal structure. Even if the change occurs, the degree may be below 20%.

**3. Fluorescence, Phosphorescence.**—From the measurements of magnetic susceptibility and X-ray diffraction it is considered that the yellow substance, specifically an electron belonging to its molecule is raised to an excited state by exposure to light; this substance returns slowly to the ground state while it is kept in the dark, presumably accompanied by emission of radiation. However, direct confirmation of fluorescence or phosphorescence could not be obtained by the eye nor by photographic observation.

**4. Impurity Effects.**—About 10 g. of a mixture of red mercuric iodide and black sulfide powder with 1.1: 2 mole ratio was heated in a porcelain crucible with lid, and placed in an electric furnace. The temperature of the furnace was kept at 170°C for one hour. After cooling slowly a yellow powder was obtained. Mercuric iodide melts at 250°C. and boils at 350°C, while mercuric sulfide could not have been fused, and at 170°C the vapor pressure of mercuric iodide is small. The yellow powder thus obtained was washed with methyl alcohol to remove unreacted mercuric iodide, and was dried under 80°C. The resulting substance was found to show the phototropy characteristic of the yellow $HgI_2 \cdot 2HgS$ completely prepared by the hydrogen sulfide method. Also the $\chi$ -value and X-ray pattern are entirely identical with those of the latter. On analysis it was found to 64.8% Hg and 6.4% S, while the values calculated as were $HgI_2 \cdot 2HgS$ are 65.4% Hg and 6.4% S respectively. The velocity of darkening of the above synthesized powder under the action of light was measured by the method previously reported[4]. It is also identical with that of $HgI_2 \cdot 2HgS$ obtained by the hydrogen sulfide method. To test the effects of impurity, a variously-determined amount of selenium was added to the 1.1: 2 mole mixture of mercuric iodide and mercuric sulfide, and the mixture was heated at 170°C for an hour. The darkening velocity of the product is shown in Fig. 2. With the sample containing 0.65–1.1% Se, the velocity is larger than with the pure $HgI_2 \cdot 2HgS$ or with the samples containing Se in any other percentage. From the above experiments it is evident that the photosensitivity increases by the addition of certain small amounts of foreign substances.

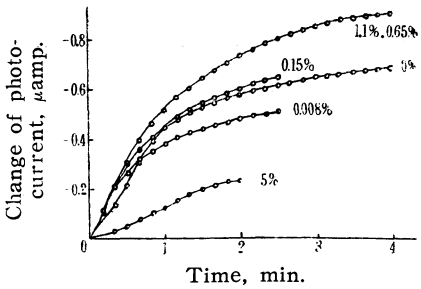



Fig. 2. Change of photo-current of mixed powder with time.

**5. Effects of Carbon Dioxide and Oxygen.**—No change of the darkening velocity of the yellow powder was observed either in carbon dioxide or oxygen atmosphere (760 mmHg) or in air. It was also the same in vacuum.

## Summary and Conclusion

From magnetic and X-ray experiments it is suggested that an electron belonging to the yellow $HgI_2 \cdot 2HgS$ is excited to an activated state by the action of light, without accompanying change in crystal structure. Even though a change of crystal structure may occur, it would be a degree below 20 mole %, the pattern of darkened form having almost the same form as the yellow one. As the oxygen has no influence at all on the darkening velocity, the darkening itself is not due to the oxidation-reduction process of mercuric ion. It is also sensitive to the existence of impurity. This suggests that the phototropy concerned has a structure sensitive factor. When the blackened powder is kept in the dark for two days at room temperature the color does not completely return to yellow, but the magnetic susceptibility becomes nearly equal to the value of the yellow form. Therefore the activated state seems to have a very long life at room temperature.

In conclusion the author wishes to express his hearty thanks to Professors S. Imanishi and K. Koshiyama, who suggested the theme of this report to the author and kindly encouraged him to publish it.

*Department of Applied Science,*
*Faculty of Engineering,*
*Kyushu University,*
*Fukuoka*

4) Kunio Takei, *J. Chem. Soc. Japan*, **73**, 204 (1952) (in Japanese).

# *Study of Reversible Photo-Chemical Reactions. III. Mechanism of the Phototropy of Mercuric Complex Salts (II). Absorption Spectrum and Microscopic Observation of Single Crystals of* $HgI_2 \cdot 2HgS$

By Kunio TAKEI

(Received December 22, 1955)

It is desirable to obtain a single crystal as large as possible for the study of the physical properties of $HgI_2 \cdot 2HgS$. The author made a comparably large single crystal by the vapor phase reaction of mercuric iodide and sulfide. In this paper the results of microscopic and absorption-spectroscopic observations of this single crystal will be reported.

## Materials

About 30 g. of a mixture of mercuric iodide and sulfide in powder form in 1.1:2 mole ratio was put in a glass test tube (1 cm. wide and 80 cm. long) buried in an electric furnace. Mercuric iodide, m.p. 250°C, b.p. 350°C; mercuric sulfide sublimes at 455°C. The furnace was slowly heated. Solid phase reaction takes place at 170°C between mercuric iodide and mercuric sulfide, forming $HgI_2 \cdot 2HgS$ which dissociates at 185°C into its components. At 250°C the iodide melts and at 330°C its vapor adheres to the upper cool part of the tube. At 480–500°C the sulfide sublimes and begins to react with the iodide in the vapor phase, and yellow crystals adhere to the wall. After keeping the furnace at 510–520°C for 30 min., the test tube was taken out and kept in the dark. Inside the tube it was observed there were red crystals of mercuric iodide at 50–60 cm. from the bottom, yellow crystals 10 cm. lower than this, black crystals of mercuric sulfide at the bottom. By analysis the yellow crystals of plate-form thus obtained were found to contain 64.8%Hg and 6.5%S (Calcd. for $HgI_2 \cdot 2HgS$: Hg, 65.4%; S, 6.9%). As they show the characteristic phototropy it is certain that they are $HgI_2 \cdot 2HgS$. The dimension of the largest single crystal obtained was $600 \times 500 \times 40 \mu^3$.

## Experiments and Results

To study the spectral absorption characteristics of this single crystal in the visible region, a Beckman Spectrophotometer was employed. A sheet of black paper with 17 pinholes (0.3 mm. in diameter), each hole being covered with a single crystal, was mounted. On the neighboring absorption cell frame a black paper sheet with equal number of pinholes, but not carrying crystals, was mounted. All the measurements were carried out at room temperature. The absorption curve obtained (Fig. 1-1) shows an apparent absorption edge at 510 mμ, and small absorption maxima at 430, 470, 560, 630, 650, 700 and 770 mμ. Fig. 1-1 shows

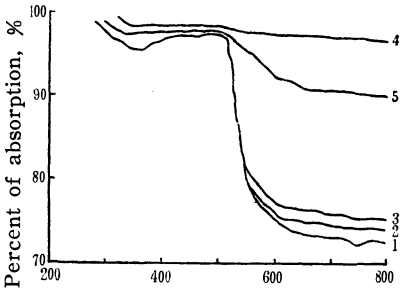



Fig. 1. Absorption spectra of single crystal, $HgI_2 \cdot 2HgS$.

also that the percentage absorption of wavelength shorter than λ 340 mμ becomes gradually larger than that of λ 350 mμ. In the course of the measurement the yellow crystals turned slightly black by the light from the tungsten lamp source and the percentage absorption slowly increased if we kept the position of the prism unchanged, for instance at 470 mμ for five min. With this in mind, we first measured the region between 510 and 800 mμ speedily, leaving the other region for separate experiments. In Fig. 1-2 is shown the absorption curve which was obtained after the crystals were irradiated by λ 470 mμ light by keeping the prism position constant for twenty five minutes. It is almost identical with the curve 1, except for the increased absorption of the wavelength region longer than 560 mμ. Curve 3 shows the same effect after two hr. irradiation. Curve 4 is for the sample blackened by daylight. It has no selective absorption in visible part. The crystals darkened in this experiment became yellow again if left in the dark at ordinary temp. for 2 months, after which they gave the curve 5, having the limit at 510 mμ. It shows an over-all decrease of absorption compared with curve 4, but an increase as compared with curve 1.

### Microscopic Observations

Micro- photograms of the darkening process of a $HgI_2 \cdot 2HgS$ single crystal were obtained in the following way. When a single crystal of a size $450 \times 250 \times 10\ \mu^3$ was exposed to a 60W tungsten lamp at 20 cm. distance, a few small black spots were produced on the surface of the crystal (photo. No. 1). After eighteen hr. the exposure crack increased, and the whole crystal turned darkish in appearance (phote. No. 2). If warmed at 90°C for twenty minutes the blackened crystal was bleached to yellow. But, under a microscope some small black spots were observed to remain still on its surface (photo. No. 3), and the bleaching was not complete. These spots did not disappear completely after several hr's warming at 90°C. This observation could be reproduced with several other specimens of $HgI_2 \cdot 2HgS$ single crystals, but the number of the spots produced by light differed with different specimens.




Photograph No. 1-Single crystal which was illuminated by tungsten lamp for 2 hrs.




Photograph No. 2-Single crystal which was illuminated by tungsten lamp for 18 hr.




Photograph No. 3-Single crystal which was warmed at 90°C for 20 mins.

To identify the black spots in photo. No. 2 the following experiment was performed. A few drops of conc. nitric acid were added to a darkened single crystal which was placed in a dish. Then it was observed by a microscope that most of the black spots in the darkened single crystal wer dissolved in the acid and some black spots were not dissolved. Simultaneously the existence of mercuric ion in the acid was recognized by violet color reaction of diphenylcarbazone. Mercury and its iodide dissolve easily in conc. nitric acid but mercuric sulfide does not dissolve. So, the soluble black spots seem to be mercury. We can assume the black spots in photo. No. 2 to be colloidal mercury. The evidence for the fact that the black spots in photo. No. 3 are mercuric sulfide was given by the following experiment. A quantity of the yellow powder of $HgI_2 \cdot 2HgS$ was placed in a glass mortar covered by a glass dish, darkened by daylight, and warmed at 90°C for ten minutes. These operations were repeated 20 times. Then some gray and red powders adhered to the cover glass. The former powder was found to be the mercury by violet color reaction of diphenylearbazone and the latter to be mercuric iodide, by the iodine-starch reaction. By the analysis of the powder left in the glassmortar thus obtained 7.6%S (mean of 3 values) was found (Calcd. for $HgI_2 \cdot 2HgS$ : S, 6.9%). The above result shows that, by warming the black powder, mercury and its iodide sublime and sulfide remains in the

powder. This phenomenon will also take place in a darkened single crystal. Therefore it is concluded that the black spots in photo. No. 3 are mercuric sulfide. On the othr hand, these spots did not dissolve in conc. nitric acid. This suggests that the spots are mercuric sulfide.

## Discussion

The strong absorption in the wavelength region shorter than 510 m$\mu$ and the sharp absorption edge at 510 m$\mu$ (Fig. 1-1) are the origin of the yellow color of the crystal. The minor absorption maxima at 560, 630, 650, 700 and 770 m$\mu$ are considered to be of no great importance. That the black $HgI_2 \cdot 2HgS$ has no selective absorption is shown by curve 4 in Fig. 1. Now, the question in point is the relation between the mechanism of the phototropy and light absorption. If the phototropy in this case be explained by electron excitation in the molecule, it must be due to the absorption of light of wavelengths shorter than $\lambda$ 300 m$\mu$, rather than $\lambda$ 430 m$\mu$ or $\lambda$ 470 m$\mu$, which have insufficient energies for the excitation. The existence of strong absorption of wavelengths shorter than 300 m$\mu$ is easily anticipated from Fig. 1.

On the other hand, it is considered from microscopic observation that the number of black spots produced on the crystal surface by illumination by a 60W tungsten lamp is small. This is due to the weakness of intensity of ultra-violet ray in the tungsten lamp. When a crystal is irradiated by daylight of very strong intensity of ultraviolet ray, many black spots are produced in a few seconds. It is clear from photo No. 1 and 2 that the darkening is due to the increase of the number of black spots on the crystal surface. These black spots are colloidal mercury. Curve 4 corresponds to the absorption curve of a single crystal whose surface is covered wholly by colloidal mercury. Colloidal mercury can vaporize rapidly by being heated. At room temp., however, its vaporization velocity is slow. Therefore we can point out that the percentage absorption for curve 5 decreases slightly as compared with that for curve 4 on account of slow vaporization of colloidal mercury.

## Conclusion

(1) Absorption spectra of yellow single crystal $HgI_2 \cdot 2HgS$ show an apparent absorption edge at 510 m$\mu$, and small absorption maxima at 430 and 470 m$\mu$.

(2) By the exposing a single crystal to daylight, colloidal mercury are produced on the crystal surface as black spots. By heating the black powder, mercury and mercuric iodide vaporize into the atmosphere and sulfide remains on the crystal surface.

The author would like to express his appreciation to Professor S. Imanishi in the Department of Science and K. Koshiyama in the Department of Applied Science of Engineering for their stimulating interest in this work.

*Department of Applied Science,*
*Faculty of Engineering,*
*Kyushu University,*
*Fukuoka*

# *Study of Reversible Photo-Chemical Reactions. IV. Phototropy of* $HgX_2 \cdot 2HgS$ *and* HgXCNS

By Kunio TAKEI

(Received December 22, 1955)

In the previous paper[1] the mechanism of phototropy of $HgI_2 \cdot 2HgS$ was reported. Now the author prepared mercuric complex salts, $HgX_2 \cdot 2HgS$ and HgXCNS and studied their phototropic phenomena. From the measurement of magnetic susceptibilities and X-ray diffraction of these powders, it was ascertained that the mechanism of their phototropy is identical with that of $HgI_2 \cdot 2HgS$. The reflectance spectra, darkening velocity, reverse reaction rate, activation energy in reverse reaction, decomposition temperature, discoloring temperature and specific weight were measured. The difference in the phototropy characteristics from the difference in halogen of complex salts will also be discussed.

1) Kunio Takei, This Bulletin, 28, 403 (1955).

## Materials

The materials $HgI_2 \cdot 2HgS$, $HgBr_2 \cdot 2HgS$ and $HgCl_2 \cdot 2HgS$ were prepared by the action of

hydrogen sulfide on the methyl alcoholic solution of mercuric iodide, mercuric bromide and mercuric chloride, respectively. When the mixture of mercuric halide and mercuric sulfide (black) in powder in a mole ratio of 1.1 : 2 was heated at 170°C for one hour in an electric furnace, the same complex salts as those of hydrogen method were also produced. When the mixture of mercuric halide and rhodanide in powder in the mole ratio of 1 : 1 was put in a porcelain crucible and heated at 160°C, stirring with a glass-rod and quickly cooled, an orange yellow powder, was produced from the mixture of mercuric iodide and rhodanide yellow white powder from mercuric bromide and rhodanide yellow-white powder from mercuric chloride and rhodanide. Impurity was removed by washing the powders with methyl alcohol. From chemical analysis of them, it was recognized that they were HgICNS (orange yellow), HgBrCNS (white yellow) and HgClCNS (white yellow), respectively. The materials obtained have phototropic characteristis. No large single crystal other than $HgI_2 \cdot 2HgS$ could be obtained.

## Experimental Results

**(1) Reflectance Spectra.**—The reflectance spectra of the above powders determined with a Shimazu Reflectance Spectrometer was shown in Fig. 1.

**(2) Physical and Phototropic Properties.**—The data of the physical and phototropic properties were shown in Table I.

**(1) Magnetic Susceptibility.**—For instance, the value of magnetic susceptibility, $\chi_0$, for the yellow powder $HgI_2 \cdot 2HgS$, was $-0.18 \times 10^{-6}$ and changed to $\chi_1$, i.e. $+0.030 \times 10^{-6}$, under action of daylight. After this darkened powder was heated at 90°C (discoloring temp.) for about ten minutes the susceptibility of this powder, $\chi_2$, was measured. When the darkened powder was kept in the dark at room temp. for 3 days, the value $\chi_3$ reversed to the original value, $\chi_0$. The words in the parenthesis in every column show the days during

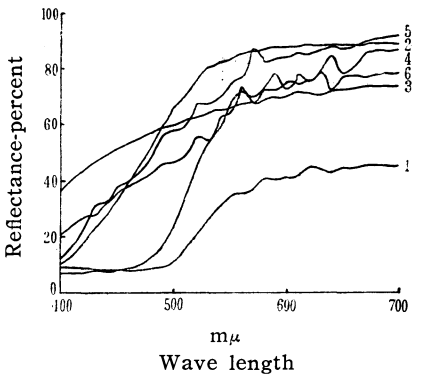



Fig. 1. Diffuse reflectance spectra:
(1) $HgI_2 \cdot 2HgS$, (2) $HgBr_2 \cdot 2HgS$,
(3) $HgCl_2 \cdot 2HgS$, (4) HgICNS,
(5) HgBrCNS, (6) HgClCNS.

which the darkened powder was kept in the dark. $\chi_1$ for darkened HgXCNS was paramagnetic, but it did not reverse to the original value when kept in the dark.

**(2) X-ray Diffraction Powder Pattern.**—The patterns of every powder which was not yet illuminated in sunlight were identical with that of the darkened powder. No new lines were found in the patterns of the darkened powder.

**(3) Darkening Velocity.**—The darkening velocity constants at +5°C obtained by the method of an earlier report[2] were larger in the following order: $HgI_2 \cdot 2HgS > HgBr_2 \cdot 2HgS > HgCl_2 \cdot 2HgS$ and HgICNS > HgBrCNS > HgClCNS. The order was identical with that of Rao's value[3]: the darkening time of $HgI_2 \cdot 2HgS$ < 1 min., $HgBr_2 \cdot 2HgS$ 3 min., $HgCl_2 \cdot 2HgS$ 10 min. and HgICNS 1 min., HgBrCNS 2 min., HgClCNS 20 min.

**(4) Activation Energy in Reverse Reaction.**

2) Kunio Takei, *J. Chem. Soc. Japan*, **73**, 294 (1952) (in Japanese).
3) S. V. Raghava Rao and H.E. Watson, *J. Phys. Chem.*, **32**, 1354 (1938).

TABLE I

PHYSICAL AND PHOTOTROPIC PROPERTIES

| Substance | | $HgI_2 \cdot 2HgS$ | $HgBr_2 \cdot 2HgS$ | $HgCl_2 \cdot 2HgS$ | HgICNS | HgBrCNS | HgClCNS |
|---|---|---|---|---|---|---|---|
| Magnetic suscep. $\times 10^{-6}$ C.G.S. Unit. | $\chi_0$ | −0.18 | −0.19 | −0.22 | −0.22 | −0.23 | −0.24 |
| | $\chi_1$ | +0.030 | −0.15 | −0.15 | +0.0020 | +0.0034 | −0.16 |
| | $\chi_2$ | +0.012 | −0.15 | −0.15 | +0.0020 | +0.0034 | −0.16 |
| | $\chi_3$ | −0.18 (3 days) | −0.19 (3 days) | −0.22 (1 month) | +0.0010 (3 days) | +0.0010 (13 days) | −0.16 (16 days) |
| Darkening velocity at 5°C per sec. | | 0.00234 | 0.000690 | 0.000184 | 0.00131 | 0.000253 | 0.00006 |
| Activation energy in reverse reaction, kcal./mol. | | 12.8 | 17.4 | 19.9 | 17.6 | 23.8 | —— |
| Decomposition temp., °C | | 185 | 200<br>332 | 200<br>347 | 213 | 288 | 290 |
| Discoloring temp., °C | | 90 | 197 | 225 | 136 | 202 | 260 |
| Specific weight | | 6.75 ±0.02 | 6.85 ±0.01 | 6.63 ±0.02 | 5.06 ±0.02 | 5.73 ±0.01 | 6.26 ±0.02 |
| Color | | orange yellow | pale yellow | white | orange yellow | white yellow | white yellow |

—The velocity constants in reverse reaction were measured at various temperatures by the method of 2nd report[2]. The activation energy in reverse reaction was calculated from temperature coefficient of logarithm of the velocity constants. The magnitudes obtained were in the following order: I<Br<Cl. The extent of darkening of HgClCNS in sunlight was very small, so that the activation energy for HgClCNS could not be calculated.

(5) **Decomposition Temperature.**—The decomposition temperature of the complex salts found by the method of thermal balance were in the following order in height: I<Br<Cl. For $HgBr_2 \cdot 2HgS$ and $HgCl_2 \cdot 2HgS$, there were first and second decomposition temperatures.

(6) **Discoloring Temperature.**—The blackened powder by daylight recovers instantly the original color on being heated. The bleaching temperature increases in the following order: I<Br<Cl.

(7) **Specific Weight.**—The mercuric complex salts were not wet in water. However, they were wet in a dilute solution of surface active agent. As an agent sodium-dodecylbenzene-sulfonate was used. When the above solution was used as a standered solution, sp. wt. of complex salts were determined at 30°C.

## Discussion

From the results that the powder patterns before darkening are identical with those after darkening, it is confirmed that the degree of decomposition of mercuric complex salts ($HgX_2 \cdot 2HgS$ and HgXCNS) is below 20 mole % as in the case of $HgI_2 \cdot 2HgS$. The value $\chi_1$ for darkened powder of $HgX_2 \cdot 2HgS$ was reversed to the original value in the dark after some days. However, $\chi_1$ for darkened HgXCNS did not reverse to the original value. This is explained as follows, Under the action of light, HgXCNS decomposes into its components. Simultaneously a positive hole remains in the crystal when an electron belonging to the molecule is raised to the conduction band. The positive hole diffuses to the outside of the crystal and escapes as gas in the atmosphere. In the case of HgXCNS most of the positive holes may escape in the atmosphere. However, in the case of $HgX_2 \cdot 2HgS$, most of the positive holes may remain in the crystal, for $\chi_1$ of $HgX_2 \cdot 2HgS$ reverses to the original value, $\chi_0$. An interstitial mercury is deposited as colloidal metal on the crystal surface. Comparing the values of activation energy with that of decomposition and discoloring temp., it is understood that the complex salts are more stable to heat in the following order: I<Br<Cl. From the difference in discoloring temp. due to the difference in halogen, it was found that the colloidal mercury deposit has still an interaction with the original molecule. The darkening velocity decreases in the following order: I<Br<Cl. The decrease of sensitivity to light in the above order may be not only due to the decrease of the quantity of interstitial mercuric ion in the same order, but also due to the increase of activation energy of diffusion of interstitial mercuric ion to the crystal surface.

The author wishes to express his thanks to professors S. Imanishi and K. Koshiyama for valuable discussions and suggestions in connection with this and preceding papers.

*Department of Applied Science, Faculty of Engineering, Kyushu University, Fukuoka*

# *Polymorphic Phase Transition of Barium-dicalcium Propionate* $BaCa_2(C_2H_5CO_2)_6$*

By Syûzô SEKI, Masanobu MOMOTANI,** Kazumi NAKATSU*** and Teruo ÔSHIMA.****

(Received February 9, 1955)

## Introduction

The crystal structure of barium-dicalcium propionate has been completely determined independently by Nitta and Watanabé[1a] and by Harris and Biefeld[1b] in 1935. According to their results, this crystal at room temperature belongs to the cubic modification and in order to satisfy the requirement of the symmetry properties of its space group, $O^4-F4_13$, it was found necessary to assume that the methyl group of the propionate ion should lie on the digonal axis including C–C bond of the $\alpha$- and carboxyl carbons. Considering the tetrahedral bond angle of the $\alpha$-carbon atom, this fact should be interpreted by assuming either the dynamical model in which the methyl group is making rotational motion, partial or free about the $C_\alpha$–$C_{carboxyl}$ bond, or the statical model which assumes that the crystal as a whole is a mixture of an equal number of ethanecarboxyl groups bent rightwards, as it were, and of those bent leftwards, each form being distributed in such a disordered way as to satisfy the digonal character mentioned above.

Now, it seems plausible to suppose that the methyl group would settle down in a definite orientation and as a result the crystal symmetry would become lower by forming an ordered lattice, if the crystal is cooled down below a certain critical temperature. We undertook this investigation to ascertain such a possibility and to elucidate the mechanism of the phase transition if it would really occur, in view of the recently recognized fact that the thermal motion as well as mutual interaction of molecules having methyl groups at their peripheries exhibit some interesting behaviour in the solid state; for example in the cases of $C(SCH_3)_4$,[2] $Pb(C_5H_5)_4$,[3] $Sn(C_2H_5)_4$,[3] $C_2(CH_3)_6$[4], etc.*

## Experimental

### 1) Sample

**a) Pure sample of barium dicalcium propionate (in the following referred to Ba-salt for brevity).**—Into aqueous solution of propionic acid, calcium carbonate and barium hydroxide were dissolved, each of which are in the molar ratio corresponding to the chemical formula, and then the Ba-salt was precipitated by slow evaporation of this solution in the thermostat at about 45°C. This sample was then recrystallized twice from water. Under the poralized microscope it was confirmed that they were homogeneous cubic crystals. The chemical composition was also checked by the chemical analysis of the content of $Ba^{++}$.

**b) Mixed crystal of the Ba-salt and $PbCa_2(C_2H_5CO_2)_6$ (Pb-salt for brevity).**—It is known[5] that the Ba-salt can form mixed crystal of cubic modification with the Pb-salt up to the concentration of 14.5 molar % of the latter. The region between 14.5–44.4 mole % of the concentration of Pb-salt is known as the miscibility gap, but beyond 44.4 mole % these two components form again a mixed crystal, although they now belong to the tetragonal system.

In order to clarify the mechanism of the phase transition, we have prepared the mixed crystal of various concentrations of the Pb-salt according to the method by Grenall[6]. The specimens of the molar ratios of $Ba^{++}$ and $Pb^{++}$ ions corresponding to (100: 2), (100: 5), (100: 8) and (100: 100) were used. The concentration of $Pb^{++}$ ion was determined by the chemical analysis and the real formation of the mixed crystal was ascertained by taking Debye photographs. To make the crystal as homogeneous as possible, the crystallized specimens were ground up to very fine powders and then they were again put into the mother liquors and left for a long time. These processes were repeated two or three times.

* A part of this investigation has been already published in *J. Chem. Phys.*, **19**, 1061 (1951).

** Present address: Momotani Juntenkan Co. Ltd., Osaka.

*** Present address: The Institute of Polytechnics, Osaka City University, Osaka.

**** Present address: Sumitomo Chemical Co., Osaka.

1a) I. Nitta and T. Watanabé, *Sci. Papers Inst. Phys. Chem. Research* (Tokyo) **26**, 164 (1935).

1b) L.P. Harris and P.M. Biefeld, *J. Am. Chem. Soc.*, **57**, 396 (1935).

2) H. J. Backer and W. G. Pedrock, *Rec. trav. chim.*, **61**, 553 (1943).

3) L.A.K. Staveley et al., *J. Chem. Soc.*, 2290 (1950).

4) F. Seyer, R. B. Bennett and F. C. Wiliams, *J. Am. Chem. Soc.*, **71**, 3447 (1949).

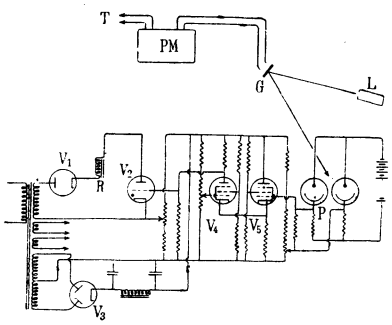
* As one part of a series of our investigation on the rotational transition, we have studied the phase transitions of $Be_4O(CH_3CO_2)_6$ and $C_6(CH_3)_6$. These results will be published shortly.

5) P. Groth, Chemische Krystallographie III, 203.

6) A. Grenall, *J. Chem. Phys.*, **17**, 1036 (1949).

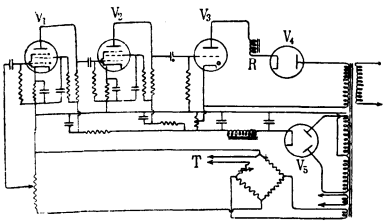
**2) Apparatus and Procedures**

**a) Specific heat measurements.**—For the preliminary study to ascertain the occurrence of the phase transition we carried out the differential thermal analysis using the Ba-salt and found in fact the existence of the phase change at about −6°C. To investigate further in detail we then measured the specific heats in the vicinity of this temperature in heating as well as in cooling directions by the conduction calorimeter, the description of which was already given precisely in the previous paper[7]. In the present investigation, we have improved the apparatus in the control of the temperature difference between the calorimeter heater and the cell containing the sample and also deviced an automatic regulator of the thermostat surrounding the calorimeter. The electric circuit used for the maintenance of the temperature head mentioned above is shown in Fig. 1. By use of this, we can regulate automatically the temperature difference at a constant value (we usually maintained it between 1°–5°C.) within the fluctuation of ±0.01°C. Special precaution was taken to prevent the effect on the photoelectric tube caused by the variation of the brightness of the room. The relay circuit employed for the thermostat is shown in Fig. 2.




L Lamp
PM Potentiometer
T to Thermocouple
G Galvanometer
R Magnetic Relay
$V_1$ KX-12F
$V_2$ 66G-GT
$V_3$ 5Y3-GT
$V_4$, $V_5$ 6AC7-GT
P Photoelctric Tube

Fig. 1. Electric circuit for the maintenance of the temperature head of calorimeter.




$V_1$, $V_2$ 6SJ7-GT
$V_3$ 66G-GT
$V_4$ KX-12F
$V_5$ 5Y3-GT
T to Thermister
R Magnetic Relay

Fig. 2. Relay circuit for the thermostat.

Thermister prepard from the mixture of cobalt- and nickel-oxides was used*. The temperature fluctuation was minimized within 0.1–0.01°C.

**b) Dilatometric measurements.**—By using a simple glass-made dilatometer with mercury as a dilometomer liquid[7] the thermal expansions below and above the said transition temperature were measured with the rate of 0.1°C/min. both in heating and cooling directions.

## Results and Discussion

The data of specific heats of the Ba-salt as well as of the mixed crystals of the Ba-

7) I. Nitta, S. Seki and M. Momotani, *Proc. Japan Acad.*, **26**, (9) 25 (1950).

* We are very much indebted to Mr. Saito of the physics department of this faculty who kindly prepared the present thermister for us.

TABLE I

SPECIFIC HEATS OF $BaCa_2(C_2H_5COO)_6$

| Heating direction | | | | Cooling direction | | | |
|---|---|---|---|---|---|---|---|
| t°C | $C_p$ cal/mole | t°C | $C_p$ cal/mole | t°C | $C_p$ cal/mole | t°C | $C_p$ cal/male |
| −17.60 | 179.96 | −5.05 | 298.86 | −16.25 | 182.4 | −6.00 | 399.4 |
| −16.25 | 176.96 | −4.49 | 301.72 | −14.85 | 184.8 | −5.34 | 848.9 |
| −14.84 | 177.28 | −4.00 | 332.60 | −13.50 | 190.2 | −4.67 | 1432.3 |
| −13.50 | 179.83 | −3.60 | 924.44 | −12.10 | 192.7 | −4.66 | 998.6 |
| −12.10 | 179.99 | −3.08 | 730.61 | −10.76 | 205.8 | −4.52 | 634.7 |
| −10.96 | 182.53 | −2.92 | 485.38 | −10.09 | 257.3 | −4.39 | 322.3 |
| −9.38 | 190.33 | −2.78 | 211.50 | −9.38 | 339.6 | −4.00 | 172.8 |
| −8.04 | 203.22 | −2.66 | 196.06 | −9.12 | 344.7 | −2.66 | 175.2 |
| −7.34 | 252.23 | −1.50 | 175.37 | −8.71 | 327.0 | 0.00 | 175.2 |
| −6.69 | 334.67 | −0.00 | 175.37 | −8.04 | 293.5 | | |
| −6.30 | 345.02 | | | −7.36 | 285.7 | | |
| −5.34 | 301.41 | | | −6.69 | 298.0 | | |

and Pb-salts (Ba: Pb=100:100 (mole)) are shown in Tables I and II and the specific heat curves of all kinds of mixed crystals investigated are illustrated in Figs. 3-7.

TABLE II
SPECIFIC HEATS OF (Ba, Pb)
$Ca_2(C_2H_5COO)_6$; Ba: Pb=100: 100 (mole)
Heating direction

| t°C | $C_p$ $\frac{cal}{mole}$ | t°C | $C_p$ $\frac{cal}{mole}$ |
|---|---|---|---|
| 107.45 | 181.55 | 162.38 | 221.11 |
| 109.66 | 182.03 | 164.45 | 220.14 |
| 111.85 | 182.28 | 166.45 | 217.95 |
| 114.05 | 182.28 | 168.41 | 215.77 |
| 118.35 | 182.76 | 170.43 | 212.61 |
| 122.74 | 182.76 | 172.43 | 208.73 |
| 127.04 | 183.00 | 174.44 | 205.09 |
| 131.26 | 183.97 | 176.46 | 200.24 |
| 135.47 | 184.46 | 178.45 | 197.32 |
| 137.56 | 184.70 | 180.46 | 194.41 |
| 141.72 | 197.32 | 182.45 | 190.04 |
| 143.79 | 200.24 | 184.41 | 188.10 |
| 145.85 | 208.00 | 186.39 | 187.13 |
| 147,90 | 211.40 | 188.36 | 187.37 |
| 149.96 | 213.83 | 190.30 | 187.61 |
| 152.03 | 216.74 | 192.00 | 186.89 |
| 154.60 | 218.20 | 194.20 | 185.92 |
| 156.18 | 222.57 | 196.20 | 186.16 |
| 158.25 | 223.54 | 198.20 | 183.97 |
| 160.33 | 221.84 | 200.00 | 184.22 |

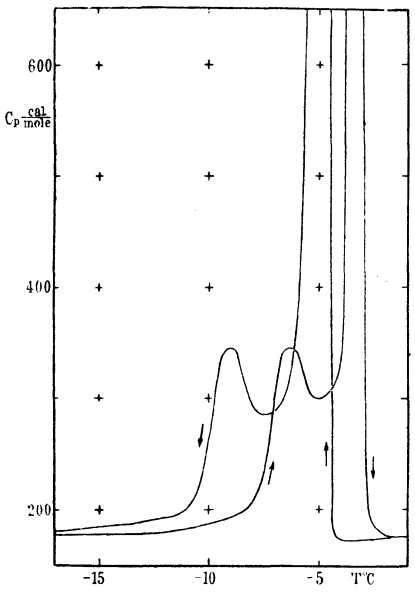



Fig. 3. Heat capacity vs. temperature curve (pure Ba-salt).

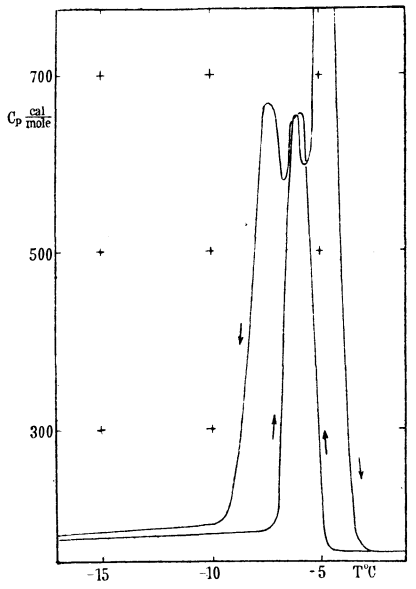



Fig. 4. Heat capacity vs. temperature curve (Ba-salt: Pb-salt=100: 2).

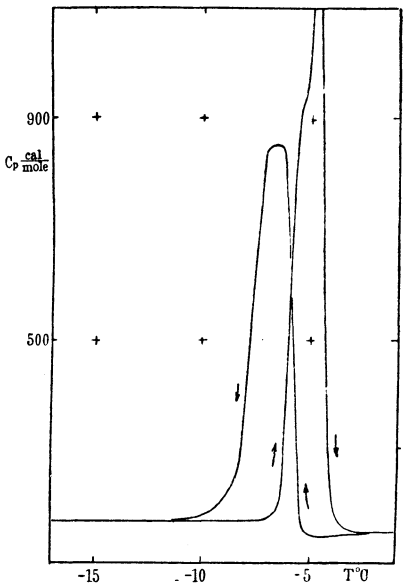



Fig. 5. Heat capacity vs. temperature curve (Ba-salt: Pb-salt=100: 5).

The tramsition temperatures, the heats and entropy changes at these transition temperatures of these salts are all summarized in Table III.

In this table and the figures given above, we can find that both the heat and entropy changes become smaller as the $Pb^{++}$ content increases and the general trends of the specific heat curves are not always the same in heating and cooling directions.

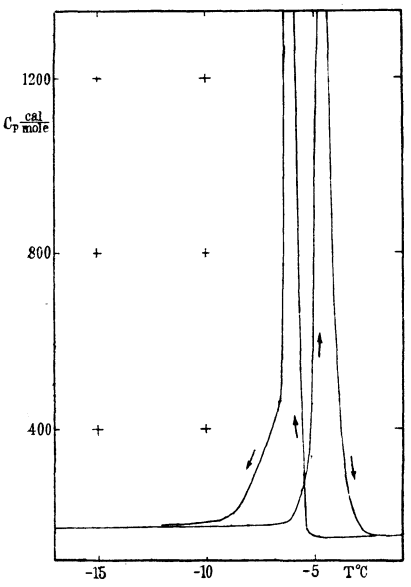



Fig. 6. Heat capacity vs. temperature curve (Ba-salt : Pb-salt = 100 : 8).

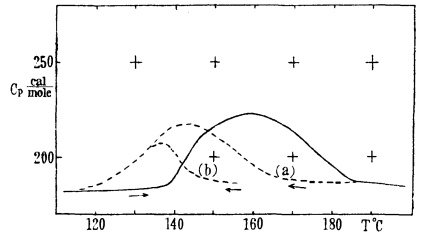



Fig. 7. Heat capacity vs. temperature curve (Ba-salt : Pb-salt = 100 : 100).

Now, let us consider the mechanism of the phase transition a little more in detail. For this purpose we should like to consider first the simpler case of the phase transition of the pure Ba-salt and thereafter to proceed to the effect of the substitution of the $Pb^{++}$ ion. It will be convenient for the following discussion, however, that we give a brief account of the relative molecular arrange-

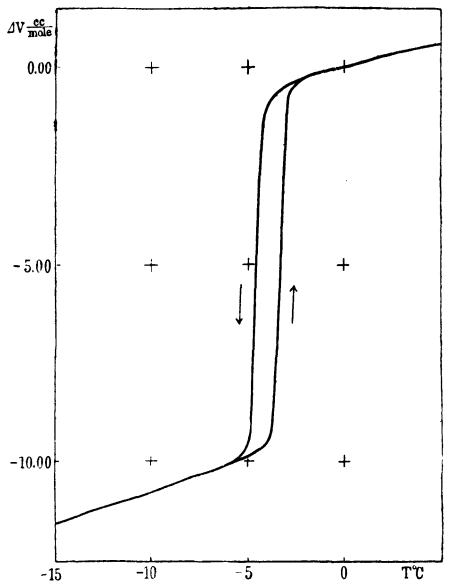



Fig. 8. Volume vs. temperature curve of pure Ba-salt.

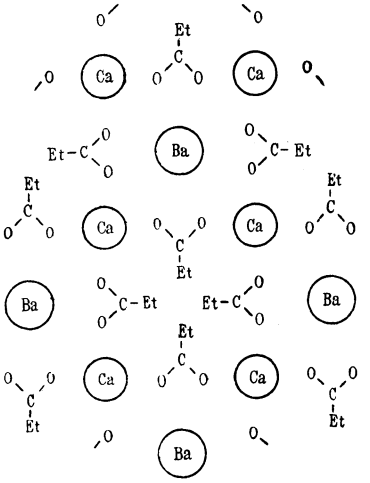



Fig. 9. Two dimensional schematic representation of relative arrangement of carboxyl radicals around metallic ions.

TABLE III

TRANSITION TEMPERATURE, HEATS AND ENTROPIES OF TRANSITION, AND VOLUME CHANGE AT TRANSITION OF Ba- AND MIXED SALTS

| | | | Ba-Salt | (Ba, Pb)$Ca_2(C_2H_5CO_2)_6$ | | |
|---|---|---|---|---|---|---|
| | | | | 100 : 2 | 100 : 5 | 100 : 8 |
| Transition Temperature t°C | Heating | LTS | −6.30 | −6.02 | −4.80 | −4.50 |
| | | HTS | −3.23 | −4.38 | — | — |
| | Cooling | LTS | −9.10 | −7.34 | −6.20 | −6.20 |
| | | HTS | −4.67 | −5.80 | — | — |
| Heat of Transition cal./mol. | Heating | | 1741 | 1464 | 1355 | 1260 |
| | Cooling | | 1745 | 1470 | 1356 | |
| Entropy of Transition e.u. | Heating | | 6.502 | 5.45 | 5.05 | 4.54 |
| | Cooling | | 7.00 | 5.50 | 5.08 | |
| Volume Change | $V_{cc}$/mol. | | 9.07 | — | — | — |

ment in this crystal. As shown schematically in Fig. 9, a barium atom is surrounded by twelve oxygen atoms of the six carboxyl radicals at the corners of an octahedron and a calcium atom is surrounded by six oxygen atoms at the corners of a nearly regular octahedron. Each oxygen atom of the carboxyl group is facing to barium on one side and to calcium on the other, and, while the behavior of the two oxygen atoms in a carboxyl group is the same towards the central barium atom, it is only one of these oxygen atoms that comes into contact with the same calcium atom. However this latter oxygen atom is taking an important part of mediator between the two kinds of metallic cations, as it were, and the whole crystal is joined together by them.

As is evident from the constitution of this crystal, we may point out two main contributions to the cohesive energy; viz, the electrostatic interaction between the positive metallic ion and the negative carboxyl radical and the van der Waal forces common in organic molecular crystals.

Taking these circumstances into consideration, we may put forward a tentative explanation of the mechanism of this transition phenomenon which seems to be not quite unreasonable. As already mentioned this transition is supposed to be intimately connected with the enhancement of the thermal motion of the methyl groups of the propionate ion. Although the complete crystal structure of the low temperature modification is not yet determined, it may be supposed that the six methyl groups which belong respectively to six different $Ba^{++}$ ions confront each other, so to say, nearly hexahedrally in this modification as in the cubic one. Below the transition point, these methyl radicals may be more or less fixed in definite orientations and as shown schematically in Fig. 10, the distance of the oppositely situated methyl groups, for instance, A–A, will be a little larger than those of the other two pairs, B–B, for the reason given above that the crystal system will become tetragonal or orthorhombic*. As the temperature rises, the rotational vibration of these methyl groups about the $C_{\alpha}$–$C_{carboxyl}$ bond will become more and more violent. In this case, if the distance between methyl groups are small enough to come in contact with each other, then we must assume that their mutual location should vary in phase just like meshing-gear-wheels and in such a case it will be realized that only the four of the six methyl groups can come into coupling as shown in Fig. 10. This situation may be said to be similar in a way to the rotational motion in long chain hydrocarbon crystals considered by Andrew[8]. We must recall here the fact that the LTS (low temperature side) hump in the spesific heat curve is more sensibly affected by the substitution of $Ba^{++}$ ion by $Pb^{++}$ ion. Such replacement of the metallic ion will probably cause a more remarkable effect on the electrostatic interaction than the Van der Waals forces. The movement of carboxyl radical attached to the substituted $Pb^{++}$ ion will be more limited, since the ionic radius of $Pb^{++}$ ion is smaller than $Ba^{++}$ ion. Indeed, we confirmed by taking Debye photographs of the two sorts of mixed crystals containing $Pb^{++}$ ion in molar ratios of (100 : 2) and (100 : 5), that the decrease of the lattice constant of the former amounts to 0.3% and that of the latter to 0.4%. Thus, the LTS phase transition will be more or less directly connected with the change of the thermal motion of the carboxyl radicals, this change influencing at the same time the rotational vibration of the methyl groups. When the temperature rises further, the rotational vibration will go over into a hindered rotational motion in which the six methyl groups will become equivalent and the crystal will be converted into the cubic modification. Thus, we may suppose that the HTS (high temperature side) large specific heat peak will be due to the equal participation in the rotational motion of all the six methyl groups which will be accompanied by a considerable volume change. Such explanation of the present two-step transition will be not unreasonable from the experimental fact that, while the LTS specific heat hump

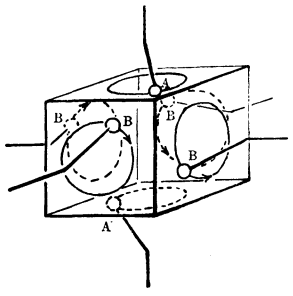



Fig. 10. Schematic illustration of the correlated molecular motion of six methyl groups.

* We confirmed by the observation of the appearence of the birefringence below the transition point that the low temperature one has no longer any cubic structure. According to the private communication of Professor Oda of Osaka University of Liberal Arts and Education, it is also confirmed by Debye-photograph that this low temperature phase has lower symmetry than the cubic modification.

8) E. R. Andrew, *J. Chem. Phys.*, 18, 607 (1950).

shows no appreciable volume change, the HTS one goes along with a considerable volume change (see Fig. 8).

Although the correlation between the thermal motions of the two different parts in one propionate ion is not clear in detail, it is rather remarkable that such a small content of $Pb^{++}$ ion causes a considerable effect. Probably the neighbouring lattice region surrounding the substituted $Pb^{++}$ ion would undergo a sort of lattice distortion, the effect of which will be propagated through the whole crystal by the action of carboxyl radical which plays the role of an mediator in the crystal structure as mentioned above. Anyhow, our discussion hitherto given may be only of qualitative nature and for the more quantitative discussion of such a complex phenomenon, crystal structure determination below as well as in the transition temperature region, study of nuclear magnetic reasonance absorption in respect to the movement of the methyl group, spectroscopic study of the part of the carboxyl radical, etc. are highly desirable.

Finally a few remarks may be added for the phase transition which occurs in the tetragonal mixed crystal having the composition of (100 : 100) molar ratio of $Ba^{++}$ and $Pb^{++}$ ions. As shown in Fig. 7, this phase transition takes place at around 160°C. In comparison with the cubic modification of the mixed crystal containing a small amount of $Pb^{++}$ ion, the transition temperature is displaced to much higher temperature and this phase transition occurs very gradually, the shape of its anomalous region being similar to that of $BaTiO_3$[9] at 393°K or of $C_6(CH_3)_6$ at 135–136°K[10]. The dotted line (a) is for cooling direction and the curve (b) corresponds also to the specific heat in the same direction starting from about 155°C where the phase transition is not completed yet in heating process. Hysteresis phenomenon is also very remarkable. It was ascertained by the microscopic observation that the high temperature form belongs to the cubic modification. In this respect, the above-mentioned phase transition, which occures at about −6°C, seems to be displaced to this higher temperature region by virtue of the large amount of the $Pb^{++}$ ion. However, for the detailed discussion on the relation between them, the crystal structure as well as other physicochemical properties should be studied further.

In conclusion, the authors wish to express their hearty thanks to Professor Nitta for his helpful suggestions and gracious encouragement throughout this work. A part of the cost of this research was defrayed from the funds of Taniguchi Kôgyô Shôreikai as well as from the Scientific Research Expenditure Grant from the Ministry of Education to which the thanks of the present authors are due.

*Department of Chemistry, Faculty of Science, Osaka University, Osaka*

9) H. Blattner and W. Merz, *Helv. Phys. Acta*, **21**, 210 (1948).

10) Huffman, Parks and Daniels, *J. Am. Chem. Soc.*, **52**, 1547 (1930).

# *Physicochemical Studies of Molecular Compounds. V. Heats of Solution of 1,3,5-Trinitrobenzene, Naphthalene and Anthracene in Benzene. Heats of Solution and Heats of Formation of Molecular Compounds of 1,3 5-Trinitrobenzene with Benzene, Naphthalene and Anthracene*

By Keisuke SUZUKI* and Syûzô SEKI

(Received March 14, 1955)

## Introduction

In the two previous papers we have reported the results of our investigations on the vapor pressure[1] and the heat of formation[2] of quinhydrone crystal which is one of the typical colored organic molecular compound. As is well known, on the other hand, there are a large number of organic molecular compounds which are formed between polynitrobenzenes and aromatic polynuclear hydrocarbons. Although phase diagram investigations and spectroscopic studies in the solution state of these molecular compounds have been hitherto accumulated, there is not yet known any energetic investigation in their crystalline state. In this respect, we have undertaken to study the substances mentioned above, to get further insight into the nature of the interaction energy between the component molecules.

## Experimental

### 1) Sample

**a) Naphthalene and Anthracene.**—These samples were given by the courtesy of Dr. M. Wayaku of the Central Research Institute of Osaka Gas Company. The purity of the sample determined by him was: 99.96% for naphthalene and 99.6% for anthracene.

**b) 1, 3, 5-Trinitrobenzene (TNB for brevity).**—This material was prepared from 2, 4, 6-trinitrobenzoic acid by the ordinary method* and then recrystallized twice from glacial acetic acid, m.p. 125.0–125.5°C.

**c) Molecular Compound (MC for brevity) of TNB with Naphthalene in (1: 1) Molar Ratio.**—This was prepared by slow evaporation of the solvent from acetone solution containing two components in the 1: 1 molar ratio. The precipitated small crystals on the bottom of the container were picked up. This MC decomposes slowly in the air, so we stored them in a disiccator with a small amount of naphthalene to prevent the preferred evaporation of naphthalene from the MC, m.p. 154.5–155.5°C.

**d) MC of TNB with Anthracene in 1: 1 Molar Ratio.**—By gradual cooling of the alcoholic solution containing two components in the 1: 1 molar ratio, we obtained this MC, m.p. 162.8–163.3°C.

**e) MC of TNB and Benzene in 1: 1** ** **Molar Ratio.**—By slow evaporation of benzene solution containing TNB we can obtain the precipitates of MC. This MC decomposed immediately, however, if we picked it up from the mother liquor at ordinary temperature, so we could not obtain pure MC having the 1: 1 ratio. Therefore, we divided the sample into six parts and sealed them as quickly as possible into six small glass bulbs having nearly the same volume. Then, a half of them were used for the analysis to determine the composition just at the beginning of the experiment. In order to determine the chemical composition of these samples, we weighed the sample together with the bulb, then made a small hole on its glass wall and placed it under high vacuum ($10^{-5}$mmHg) for about eight hours and then weighed it again. As the vapor pressure of TNB is very low at room temperature, we can ascertain by calculation that the loss of TNB during this procedure is negligible. After the decrease of the weight stopped, we confirmed finally by the chemical analysis of the nitrogen-content that the specimens were completely converted into TNB. Accordingly, all the samples employed for experiments are the mixture of MC and TNB (see Table VII).

### 2) Apparatus and Procedures

The calorimeter used for the determination of the heat of solution is essentially the same as before[2], only with some improvements for making it possible to measure the smaller heat effect. The main thermel for the measurement of temperature difference between the calorimeter

1) I. Nitta, S. Seki, H. Chihara and K. Suzuki, *Sci. Papers from Osaka Univ.*, No. 29 (1951).

2) K. Suzuki and S. Seki, This Bulletin, 26, 372 (1953).

* Present address; Department of Chemistry, Faculty of Science, Kobe University, Mikage, Kobe.

* See for example: Gilman, Organic Synthesis, Collected Vol. 1. P. 543.

** As to the composition of this MC, there are two alternative views of 1: 1 or 1: 2 molar ratio of TNB and benzene. We have been informed by private communication from Professor C.H. McGillavry at the University of Amsterdam that the 1: 1 compositions are much more reasonable by their preliminary crystal structure determination.

and fluctuation damper was made from 40 junctions of copper-constantan thermocouple. The fluctuation damper was made of a copper block cylinder 4 cm. in diameter and 7 cm. in height, in which 7 narrow wells (2 mm in diameter, 4 cm. in depth) are drilled for the insertion of the junctions of the thermel. By these improvements we could measure the temperature variation of 0.00005°C. When the glass bulb used as the container of the sample was destroyed, it was found that some amounts of heat were absorbed due to the evaporation of the solvent into the free space of the container. Using benzene as the solvent, we deter mined this heat $\Delta H$ by employing the empty bulbs of various sizes and found that it is expressed by the following equation,

$$\Delta H(\text{cal.}) = 0.038v,$$

where $v$ is the volume of the free space in the bulb in cc. All the measurements were carried out at 25°C. In order to check the amount of the heat of dilution, we measured the heats of solution at various concentrations.

## Results and Discussion

The heats of solution of the components as well as those of MC's are all given in Tables I~VI. It may be noticed here that the heats of solution of TNB decrease with the increase of the concentration of the solution, while those of naphthalene behave oppositely. For naphthalene and TNB (Table I and II) the extrapolated values to the infinite dilution are also given. They were

TABLE I

HEATS OF SOLUTION OF TNB

| No. | Weight of the Sample used. (g) | Concentration of Solution in Molar Ratio | | $\Delta H$ kcal./mol. |
|---|---|---|---|---|
| | | initial | final | |
| 1 | 1.3048 | 0.00000 | 0.00114 | 2.593 |
| 1′ | 1.3261 | 0.00000 | 0.00134 | 2.572 |
| 2 | 1.4032 | 0.0017 | 0.00234 | 2.560 |
| 2′ | 1.3718 | 0.00134 | 0.00256 | 2.572 |
| 3 | 1.4964 | 0.00230 | 0.00306 | 2.527 |
| | | Extraporated to zero concentration | | 2.601±0.011 |

TABLE II

HEATS OF SOLUTION OF NAPHTHALENE

| No. | Weight of the Sample used. (g) | Concentration of Solution in Molar Ratio | | $\Delta H$ kcal./mol. |
|---|---|---|---|---|
| | | initial | final | |
| 1 | 0.8507 | 0.00000 | 0.00134 | 4.212 |
| 2 | 0.8958 | 0.00134 | 0.00277 | 4.214 |
| 3 | 0.8486 | 0.00277 | 0.00420 | 4.272 |
| 4 | 0.8520 | 0.00420 | 0.00555 | 4.233 |
| 5 | 0.9100 | 0.00554 | 0.00690 | 4.257 |
| 6 | 0.8582 | 0.00690 | 0.00826 | 4.296 |
| | | Extraporated to zero concentration | | 4.205±0.013 |

TABLE III

HEATS OF SOLUTION OF ANTHRACENE

| No. | Weight of the Sample used. (g) | Concentration of Solution in Molar Ratio | | $\Delta H$ kcal./mol. |
|---|---|---|---|---|
| | | initial | final | |
| 1 | 0.6402 | 0.00000 | 0.00036 | 5.768 |
| 2 | 0.6693 | 0.00036 | 0.00130 | 5.858 |
| 3 | 0.6664 | 0.00130 | 0.00187 | 5.870 |
| 4 | 0.6738 | 0.00187 | 0.00266 | 5.853 |
| | | Average | | 5.812±0.020 |

TABLE IV

HEAT OF SOLUTION OF (1:1) MC OF NAPHTHALENE AND TNB

| No. | Weight of the Sample used. (g) | Concentration of Solution in Molar Ratio (MC/Benzene) | | $\Delta H$ kcal./mol. |
|---|---|---|---|---|
| | | initial | final | |
| 1 | 1.2016 | 0.00000 | 0.00063 | 7.893 |
| 2 | 1.4030 | 0.00062 | 0.00136 | 7.950 |
| 3 | 1.0532 | 0.00136 | 0.00206 | 7.957 |
| 4 | 1.1775 | 0.00207 | 0.00263 | 7.905 |
| | | Average | | 7.926±0.011 |

TABLE V

HEAT OF SOLUTION OF (1:1) MC OF ANTHRACENE AND TNB

| No. | Weight of the Sample used. (g) | Concentration of Solution in Molar Ratio (MC/Benzene) | | $\Delta H$ kcal./mol. |
|---|---|---|---|---|
| | | initial | final | |
| 1 | 0.8850 | 0.00000 | 0.00040 | 8.785 |
| 2 | 0.8647 | 0.00040 | 0.00080 | 8.770 |
| 3 | 0.8523 | 0.00080 | 0.00119 | 8.689 |
| | 0.4912 | 0.00119 | 0.00142 | 8.772 |
| | | Average | | 8.754±0.015 |

TABLE VI

HEAT OF SOLUTION OF THE MIXTURE OF TNB AND OF (1:1) MC OF BENZENE AND TNB

| No. | Weight of the Sample used. (g) | Concentration of Solution in Molar ratio (MC/Benzene) | | $\Delta H$ cal./g. |
|---|---|---|---|---|
| | | initial | final | |
| 1 | 1.6800 | 0 | 0.00141 | 12.73 |
| 2 | 1.1809 | 0 | 0.00081 | 12.02 |
| 3 | 1.3164 | 0 | 0.00089 | 13.10 |
| | | Average | | 12.74±0.18 |

calculated by assuming the following linear equation,

$$\Delta H_{\text{soln.}}(C) = \Delta H^{\infty}_{\text{soln.}} + C\Delta H_{\text{diln.}}$$

where $\Delta H_{\text{soln.}}(C)$ stands for the heat of solution at the concentration $C$, $\Delta H^{\infty}_{\text{soln.}}$ the heat of solution at infinite dilution, and $\Delta H_{\text{diln.}}$ the heat of dilution. The heats of solution of the other sub-

stances are independent of the concentrations within the experimental errors, so the average value for each material may be looked upon directly as the heat of solution at infinite dilution. Among these results, only that of naphthalene is known.[3] This reported result, however, is less accurate and without any description of the concentration and temperature at which the experiment was carried out, so we do not compare it with ours.

The results of analysis on the composition of the MC between TNB and benzene are given in Table VII. As is evident, the residue, after the evacuation, consists completely of pure TNB. In spite of the special care taken to avoid the preferred evaporation of benzene, it was found that the sample for the experiments was decomposed already to a considerable extent.

Table VII

Benzene contents of the samples in Table VI

| | | |
|---|---|---|
| Amount of benzene determined by the loss of weight on evaparation: | 18.7±0.4% | (average of three samples) |
| Amount of benzene in residue*: | 0.0±0.05% | |
| *Chemical analysis of $N_2$ in the residue: observed value | 19.63% | |
| calculated value (TNB) | 19.72% | |

Now, the heats of formation $\Delta H_f^c$, of MC from the components in their crystalline state except that between benzene and TNB, can be calculated as the difference of $\Delta H^{\infty}_{soln}$ of MC and the sum of those of component crystals, since at the infinite dilution the interactions between solute molecules may be negligible. In the above-mentioned case of MC of benzene and TNB pure MC can not be obtained, so that the data given in Table VI should correspond to the heats of the solution of the mixture of MC and TNB. The heat of formation $\Delta H_f^l$ of pure MC (1:1) from TNB and liquid benzene may be, therefore, calculated by the following relation

$$\Delta H_f^l = \{Q-(1-x)Q_0\}/(x/M_B)$$

where $Q$ is the observed heat of solution of the specimen in the unit of cal./g, $Q_0$ the heat of solution of pure TNB in the same unit, $x$ the weight fraction of benzene in the specimen and $M_B$ the molecular weight of benzene. The heats of formation $\Delta H_f^g$ from the gaseous components or the lattice energies of the crystalline MC's, were calculated from $\Delta H_f^c$ (or $\Delta H_f^l$) and the heats of sublimation (or vaporization) of each component.

The heats of formation of the three MC's measured by us are given in Table VIII, together with the binding energies of the MC's in the solution determined by Briegleb et al. for reference.[4]

In this table, the heat of formation of MC between benzene and TNB from the component crystals $\Delta H_f^c$ was calculated by subtracting the heat of fusion of benzene (2.351 kcal./mol.)[5] from the $\Delta H_f^l = 3.05 \pm 0.26$ kcal./mol. As shown in this table, $\Delta H_f^g$, the total interaction energies increase with the order of benzene, naphthalene and anthracene while $\Delta H_f^c$ the specific interaction energy between the component molecules, empirical net MC formation energy, is largest for the MC of TNB and naphthalene. As to the latter fact, we shall discuss later more in detail.

On examining the Table 8 it is worth while noticing the following two facts that (i) our values of heat of formation of these MC's determined above are different from those for solution and that (ii) binding energies in solution depend on solvents used and even their relative order of

3) G. Gehlhoff, *Z. Physik. Chem.*, 98, 252 (1921). $\Delta H$ 4.42 kcal./mol.

4) G. Briegleb and T. Schachowsky, *Z. Physik. Chem.*, B19, 255 (1932).

5) F. D. Rossini, K. S. Pitzer, W. J. Taylor, J. P. Ebert and J. F. Kilpatrick, Selected Values of Properties of Hydrocarbons (1947).

Table VIII

Heat of formation of MC in crystalline and in solution states (kcal./mol.)

| State | Benzene-TNB MC | Naphthalen-TNB MC | Anthracene-TNB MC |
|---|---|---|---|
| Heat of Formation of MC from gaseous molecules $\Delta H_f^g$ | −34.9 | −40.7 | −46.9 |
| Heat of Formation of MC from component crystals $\Delta H_f^c$ | −0.70±0.26 | −1.120±0.035 | −0.341±0.046 |
| Heat of Formation in Solution | | | |
| $CCl_4$ Solution* | − 0.6 | − 3.45 | − 4.4 |
| $C_2H_2Cl_4$ Solution | —— | —— | − 3.6 |
| Ether Solution* | —— | − 0.99 | − 2.1 |
| Benzene Solution* | —— | − 1.90 | − 0.98 |

* see ref. (4)

magnitude for the naphthalene MC and anthracene MC for different solvents shows a different trend. Although the latter fact (ii) seems to be a little unreasonable at first sight, it is natural if we consider the meaning of this binding energy more in detail. In the solution, all the solute molecules are not isolated as they are in the gaseous state, but surrounded by many solvent molecules, forming a kind of cluster with their neighbouring solvent molecules. Therefore, these energies do not correspond to the genuine binding energies of MC's, but to the heats of reaction of the following equation,

$$\text{Hydrocarbon (solvent)}_{Z_H} + \text{TNB}\cdot(\text{solvent})_{Z_T} = \text{MC}\cdot(\text{solvent})_{Z_M} + (Z_H + Z_T - Z_M)\ \text{solvent}$$

where $Z_H$, $Z_T$ and $Z_M$ are the numbers of solvated molecules on a molecule of the aromatic hydrocarbon, TNB and MC, respectively. Accordingly, to obtain a genuine binding energy of MC, all the heats of solvation in the equation must be known. At present, however, it is impossible to find out an adequate way of estimating the heat of solvation for the MC's, so we should be contented with the prediction that the contribution of these energies would not be ignored. The energies of solvation for the component molecules can be estimated by the following relation,

$$\Delta H^{\infty}_{\text{solv.}} = \Delta H^{\infty}_{\text{soln.}} - \Delta H_{\text{sub.}},$$

where $\Delta H^{\infty}_{\text{solv.}}$ and $\Delta H^{\infty}_{\text{soln.}}$ the heats of solvation and of solution at infinite dilution, $\Delta H_{\text{sub.}}$ the heat of sublimation, respectively. $\Delta H^{\infty}_{\text{solv.}}$ obtained by this way are given in Table IX.

tion the meaning of apparent binding energy in solution state.

In this connection, we should like to refer to the mode of the interaction between solvent and solute molecules at infinite dilution. For this purpose, we may define the quantity $\Delta H^{\infty}_{\text{solv.}}/V$ in which $V$ stands for the molecular volume of the solute in crystalline state*. This may be called the solvation energy density. In other words, this may be useful as one of the measures of the deviation from the ideal solution. In the last column of Table IX we can see that these quantities for the aromatic hydrocarbons are nearly equal, whreas those for nitro compounds are larger than those for hydrocarbons and increase with the number of nitro groups. This fact will indicate that the interactions between nitrocompounds and hydrocarbons should be discussed with cautions.

Finally a few remarks may be given below on the nature of the specific binding energy which appears on the formation of these MC's.

i) In comparison with the heat of formation $\Delta H^{c}_{f}$ of quinhydrone which comes out 5.387 kcal./mol., those of the present materials are much smaller. In the former, the energy contribution due to the enhancement of the strength of the hydrogen bond on the formation of the molecular compound and also the electrostatic force due to the migration of changes as suggested by Murakami might play a more or less important role. Judging from the order of magnitude of the heats of formation of the present MC's, we may conclude that the nature of the interaction in these MC's can neither be of a covalent bond nor of an ionic one, but rather it seems to be a kind of weaker interaction given by the theory of quantum-mechanical second order perturbation such as the induction or the intermolecular charge transfer forces.

ii) Diamagnetic properties[9] of these MC's indicate that the constituent molecules have no unpaired electron and the normal states of these molecules are in one of the singlet states. This fact excludes the possibility of any type of free radical with ion pair such as $TNB^-$ and $anthracene^+$.

TABLE IX

SOLVATION ENERGY DENSITIES AND SOME RELATED DATA OF SOME AROMATIC COMPOUNDS

| | $\Delta H_{\text{sub}}$ | $\Delta H^{\infty}_{\text{soln}}$ | $\Delta H^{\infty}_{\text{solv}}$ | $\rho$ | $V$ | $\Delta H^{\infty}_{\text{solv}/V}$ |
|---|---|---|---|---|---|---|
| Benzene | | | −8.09[8] | 1.08 | 72.2 | 0.112 |
| Naphthalene | 15.8[6a] | 4.205 | −11.6 | 1.158 | 110.6 | 0.105 |
| Anthracene | 22.8[6b] | 5.812 | −17.0 | 1.245 | 143.1 | 0.119 |
| Diphenyl | 17.9[6c] | 4.31[7] | −13.6 | 1.165 | 132.2 | 0.103 |
| TNB | 23.8[6d] | 2.601 | −21.2 | 1.687 | 126.4 | 0.168 |
| α-mononitro-naphthalene | 25.6[6d] | 5.38[7] | −20.2 | 1.331 | 130.1 | 0.155 |

$\rho$: density. $V$: molecular volume in c.c. $\Delta H$: kcal./mol.

Data for diphenyl and α-mononitronaphthalene are also given for reference. We can realize that the amount of $\Delta H^{\infty}_{\text{solv.}}$ is much larger than Briegleb's apparent binding energy between component molecules in MC, so that only a slight change in the number of the solvating molecules, which should occur on the MC formation from the component molecules, would cause a change of energy presumably amounting to a few kcal./mol. We must, therefore, discuss with sufficient precau

6) (a) K.L. Wolf et al, *Z. Physik. Chem.*, **B29**, 194 (1938); A.A. Zilberman and Granovskaya, *Chem. Abst.*, **35**, 3867 (1941). (b) I. Nitta, S. Seki and M. Momotani, *J. Chem. Soc. Japan*, **71**, 430 (1950). (c) S. Seki and K. Suzuki, This Bulletin, **26**, 209 (1953). (d) I. Nitta. S. Seki, M. Momotani and K. Sato, *J. Chem. Soc. Japan*, **71**, 378 (1950).

7) International Critical Table.

8) Heat of vaporization of benzene taken from ref (5).

* Strictly speaking, we must use the molecular volumes for the solutions at infinite dilution. However, they are not yet known at present.

9) R.C. Sahney, S. L. Aggarwal and M. Singh, *J.. Indian. Chem. Soc.*, **23**, 335 (1946).

iii) Nakamoto[10] measured the absorption spectrum of the crystalline anthracene-TNB MC and found that the absorption of light with electric vector perpendicular to the molecular plane is much stronger than that of the light with parallel vector. On the basis of this intensity ratio, two types of assignment for this absorption band may be possible, i.e. intermolecular charge transfer[11] and $n\rightarrow\pi$ transition spectra.[12] If we examine the intensity relation closely, however, the former seems to be more plausible. For, the order of magnitude of the absorption due to the $n\rightarrow\pi$ transition is ordinarily not so strong. In fact, the absorption due to the $n\rightarrow\pi$ transition of most of nitrobenzene derivatives has not been detected in crystalline state because of the overlapping with more intense absorption due to $\pi\rightarrow\pi$ transition[13]. From this point of view, the mechanism of intermolecular charge transfer may be more probable for the explanation of the interaction of these MC's.

iv) If we assume that the origin of interaction in this MC consists of an induction effect of polarizable electrons of aromatic hydrocarbons caused by the strong field of dipole moment of $NO_2$ groups as proposed by Briegleb[14], then we may expect the order of the relative strength of the interaction in *s*- trinitro- and *m*- dinitro benzene MC's as follows:

anthracene-TNB > naphthalene-TNB > benzene-TNB

and

anthracene-DNB > naphthalene-DNB > benzene-DNB

However, the magnitudes of the heats of formation of the MC's of TNB found by us do not go parallel with the above order and, moreover, in the latter series we can isolate only the MC of naphthalene-DNB as a stable crystal[15]. Accordingly it seems to be inappropriate to explain the origin of these MC's only by this view at least in the crystalline state.

For the discussion of the relative strength of interaction from the viewpoint of intermolecular charge transfer mechanism, data of ionization potential of these hydrocarbons are highly desirable. Unfortunately, the data for anthracene is not yet known, so we will not carry on the present discussion further.*

In conclusion the authors wish to express their sincere thanks to Professor Nitta for his kind suggestions and encouragement throughout this work and to Dr. Wayaku of the Central Research Laboratory of Osaka Gas Company for his gift of pure naphthalene and anthracene and also for pertinent data on them. Appreciation should be also expressed to Professor C. H. McGillavry for her kind information on the cell dimension of the Benzene-TNB MC in advance of publication and to Mr. Ônishi for his collaboration in the work of measurement. The expense of this research was partly defrayed from the funds of Taniguchi Kôgyô Shôreikai as well as from the Scientific Research Expenditure Grant from the Ministry of Education to which the thanks of the present authors are due.

*Department of Chemistry, Faculty of Science, Osaka University, Osaka*

10) K. Nakamoto, This Bulletin, **26**, 70 (1953).
11) R.S. Mulliken. *J. Phys. Chem.*, **56**, 801 (1952).
12) K. Nakamoto and K. Suzuki, *J. Chem. Phys.*, **20**, 1971 (1952),
13) K. Nakamoto, *J. Chem. Soc. Japan*, **71**, 621 (1949).
14) G. Briegleb, *Z. Physik. Chem.*, **B26**, 63 (1934).
15) See Landolt-Börnstein's Table.

* Recently, people calculated theoretically the ionization potentials of these unsaturated hydrocarbons; benzene, 9.76 e.v., naphthalene, 8.28 e.v. and anthracene, 7.38 e.v. (*Trans Faraday Soc.*, **49** 1375 (1953)). If we utilize his results, we can find that the order of the strength of interaction energies of these MC's can not be explained on the basis of the mechanism of intermolecular charge transfer, so far as we take only the ionization potential into consideration. We are indebted to Dr. Nagakura for his kind information on the reference given above.

# *Theoretical Analysis of Polarographic Waves. I. Reduction of Simple Metal Ions*

By Hiroaki MATSUDA and Yuzo AYABE

(Received December 24, 1954)

## Introduction

Theoretical analysis of the polarographic current-voltage curves was first attempted by J. Heyrovsky and D. Ilkovic[1], who assumed that the potential of the dropping mercury electrode was given by Nernst's equation. Although their treatment was successful in analysing the various types of reversible waves, it was soon shown that the numerous waves corresponding to the so-called irreversible electrode processes could not be analysed on the basis of Heyrovsky-Ilkovic's theory. Being promted by this inadequency, the theoretical treatments of the irreversible waves have been developed by various authors[2], who applied the absolute reaction rate theory to the polarographic problems. However, these authors assumed that the diffusion current was proportional to the difference between the concentration of the depolarizer in the bulk of the solution and that at the electrode surface, by using the concept of Nernst's diffusion layer. This assumption is valid only in the case in which the concentration of depolarizer at the electrode surface is independent of time, and consequently it cannot be adapted to the present problem.

Recently, T. Kambara and I. Tachi[3] and P. Delahay[4] have independently derived the equation of the instantaneous diffusion current during the drop age for any point along the wave, by solving the corresponding diffusion problem for the case of first-order electrode reaction. However, their results cannot be quantitatively applied to the dropping mercury electrode, since they assume that the diffusion process proceeds in a stationary medium.

In this paper, we shall derive a general equation of the instantaneous diffusion current, taking into account the movement of the solution caused by the expansion of the mercury drop with the same accuracy as Ilkovic's equation for the limiting diffusion current. Then, the general expression for the current-voltage curve will be given and its characteristics discussed upon being divided into three cases, i.e. reversible, "quasi"-reversible and irreversible.

## Theoretical Derivation of the Equation for the Instantaneous Diffusion Current

Consider the reduction to the metallic state (amalgam) of a simple ion of a metal that is soluble in mercury.

According to MacGillavry and Rideal[5], the concentration distributions of the simple metal ion (denoted by suffix *ox*) and of the amalgamated metal (denoted by suffix *red*) can be determined by solving the following system of differential equations.

$$\frac{\partial C_{ox}}{\partial t}=D_{ox}\frac{1}{r^2}\frac{\partial}{\partial r}\left(r^2\frac{\partial C_{ox}}{\partial r}\right)-\frac{a^3}{3r^2}\frac{\partial C_{ox}}{\partial r}\ (r\geqq r_0) \tag{1}$$

$$\frac{\partial C_{red}}{\partial t}=D_{red}\frac{1}{r^2}\frac{\partial}{\partial r}\left(r^2\frac{\partial C_{red}}{\partial r}\right)-\frac{a^3}{3r^2}\frac{\partial C_{red}}{\partial r}\ (r\leqq r_0) \tag{2}$$

In these equations, $D$ is the diffusion coefficient; $C$ is the concentration; $r$ is the distance from the center of mercury drop; $t$ is the time elapsed after the growth of the drop has begun; $r_0$ is the radius of the mercury drop, which is given by

$$r_0=(3m/4\pi d)^{1/3}t^{1/3}=at^{1/3} \tag{3}$$

where $m$ is the constant rate of flow of mercury out of the capillary and $d$ is the density of mercury.

The initial condition is given by

$$\left.\begin{aligned} &t=0,\ r>r_0 : C_{ox}={}^*C_{ox}\\ &t=0,\ r<r_0 : C_{red}=0\end{aligned}\right\} \tag{4}$$

where ${}^*C_{ox}$ is the concentration of the metal ion in the bulk of the solution. The bound-

1) J. Heyrovský and D. Ilkovič, *Collection Czechoslov. Chem. Communs.*, **7**, 198 (1935).

2) N. Tanaka and R. Tamamushi, This Bulletin, **22**, 187, 227 (1949); *Sbornik*, **1**, 486 (1951); H. Eyring, L. Marker and T.C. Kwoh, *J. Phys. Colloid. Chem.*, **53**, 1453 (1949); R. Goto and I. Tachi, *J. Electrochem. Soc. Japan*, **18**, 207 (1950); *Sbornik*, **1**, 69 (1951); M. Kalousek and A. Tockstein, *Sbornik*, **1**, 563 (1951).

3) T. Kambara and I. Tachi, This Bulletin, **25**, 135 (1952).

4) P. Delahay, *J. Am. Chem. Soc.*, 75, 1430 (1953).

5) D. MacGillavry and E. K. Rideal, *Rec. trav. chim.*, **56**, 1013 (1937).

ary condition is controlled by the current $i(t)$ flowing through the surface of the dropping mercury electrode and is manifested by

$$t>0,\ r=r_0 :\ D_{ox}\frac{\partial C_{ox}}{\partial r}=D_{red}\frac{\partial C_{red}}{\partial r}=i(t)/nF\cdot q\ , \tag{5}$$

where $n$ is the number of faradays of electricity required per mole of electrode reaction, $F$ is the faraday and $q$ is the surface area of the dropping mercury electrode, which is given by $4\pi r_0^2$.

In order to integrate the system of the differential equations, it is convenient to perform a substitution of the variables to simplify the calculation. Let

$$x=r^3-r_0^3=r^3-a^3t \tag{6}$$

$$y=t^{7/3} \tag{7}$$

Then

$$\frac{\partial}{\partial t}=-\frac{7}{3}t^{4/3}\frac{\partial}{\partial y}-a^3\frac{\partial}{\partial x}$$

$$\frac{\partial}{\partial r}=3r^2\frac{\partial}{\partial x}=3(x+a^3t)^{2/3}\frac{\partial}{\partial x}\ . \tag{8}$$

Owing to the very small values of the diffusion coefficients of metal ion and amalgamated metal, the inhomogeneities of concentration distributions occur only in the regions which are very close to the surface of the dropping mercury electrode, and since in these regions $r$ differs only slightly from $r_0$, it follows that $|x|$ is very much smaller than $a^3t$. When $|x|\ll a^3t$, we have

$$\frac{\partial}{\partial r}\cong 3a^2t^{2/3}\frac{\partial}{\partial x}=3a^2y^{2/7}\frac{\partial}{\partial x} \tag{9}$$

Substituting the relations expressed by Eqs. (6), (7), (8) and (9) into Eqs. (1), (2), (4) and (5) leads to

$$\frac{\partial C_{ox}}{\partial y}=\frac{27}{7}a^4D_{ox}\frac{\partial^2C_{ox}}{\partial x^2}\quad (x\geqq 0) \tag{1}'$$

$$\frac{\partial C_{red}}{\partial y}=\frac{27}{7}a^4D_{red}\frac{\partial^2C_{red}}{\partial x^2}\quad (x\leqq 0) \tag{2}'$$

with the following initial and boundary conditions

$$\left.\begin{aligned} &y=0,\ x>0 :\ C_{ox}={}^*C_{ox}\\ &y=0,\ x<0 :\ C_{red}=0\end{aligned}\right\} \tag{4}'$$

$$y>0,\ x=0 : 3a^2y^{2/7}D_{ox}\frac{\partial C_{ox}}{\partial x}$$

$$=3a^2y^{2/7}D_{red}\frac{\partial C_{red}}{\partial x}=i(y)/nF\cdot q \tag{5}'$$

The above derived differential equations (1)′ and (2)′ can be easily solved by using the method of the Laplace transformation. The solutions of Eqs. (1)′ and (2)′, which fulfil the initial and boundary conditons (4)′ and (5)′, are shown to be

$$C_{ox}={}^*C_{ox}-\sqrt{\frac{3}{7\pi}}\frac{1}{\sqrt{D_{ox}}}\int_0^y e^{-\frac{x^2}{4(27/7)a^4D_{ox}(y-s)}}\cdot \times\frac{s^{-2/7}[i/nF\cdot q]}{\sqrt{y-s}}\,ds\ (x\geqq 0)$$

$$C_{red}=\sqrt{\frac{3}{7\pi}}\frac{1}{\sqrt{D_{red}}}\int^y e^{-\frac{x^2}{4(27/7)a^4D_{red}(y-s)}}\cdot \times\frac{s^{-2/7}[i/nF\cdot q]}{\sqrt{y-s}}\,ds\ (x\leqq 0)$$

Therefore, the concentration of the amalgam formed on the surface of the mercury drop, designated by ${}^\circ C_{red}$, and the concentration of the reducible metal ion in the layer of solution at the surface of the drop, designated by ${}^\circ C_{ox}$, can be expressed as

$${}^\circ C_{ox}={}^*C_{ox}-\sqrt{\frac{3}{7\pi}}\frac{1}{\sqrt{D_{ox}}}\int^y\frac{s^{-2/7}[i/nF\cdot q]}{\sqrt{y-s}}\,ds \tag{10}$$

$${}^\circ C_{red}=\sqrt{\frac{3}{7\pi}}\frac{1}{\sqrt{D_{red}}}\int^y\frac{s^{-2/7}[i/nF\cdot q]}{\sqrt{y-s}}\,ds\ , \tag{11}$$

respectively.

The current flowing through the electrode surface depends on the electrode potential and the concentrations of the metal ion and of the amalgam at the electrode surface. According to the reaction rate theory[6], the current flowing can be expressed as

$$[i/nF\cdot q]=k_f^0(f_{ox}{}^\circ C_{ox})e^{-\frac{\alpha nF}{RT}E}$$

$$-k_b^0(f_{red}{}^\circ C_{red})e^{\frac{(1-\alpha)nF}{RT}E}\ , \tag{12}$$

where $f$ is the activity coefficient; $E$ is the electrode potential, measured with respect to the normal hydrogen electrode; $\alpha$ is the transfer coefficient; $k_f^0$ and $k_b^0$ are the rate constants of the reduction process and of the oxydation process at the potential of the normal hydrogen electrode, respectively.

Eliminating ${}^\circ C_{ox}$ and ${}^\circ C_{red}$ from Eqs. (10), (11) and (12) leads to Volterra's integral equation of the second kind with respect to the unknown function $[i/nF\cdot q]$,

$$[i/nF\cdot q]=k_f^0f_{ox}{}^*C_{ox}e^{-\frac{\alpha nF}{RT}E}$$

$$-\sqrt{\frac{3}{7\pi}}\lambda\int_0^y\frac{s^{-2/7}[i/nF\cdot q]}{\sqrt{y-s}}\,ds\ ,$$

where

6) S. Glasstone, K. J. Laidler and H. Eyring: The Theory of Rate Processes, p. 575 (1941).

$$\lambda=\frac{k_f^0 f_{ox}}{\sqrt{D_{ox}}}e^{-\frac{\alpha nF}{RT}E}+\frac{k_b^0 f_{red}}{\sqrt{D_{red}}}e^{\frac{(1-\alpha)nF}{RT}E}. \quad (13)$$

In order to obtain a description of our problem formulated by means of dimensionless parameters, we perform the following substitution

$$[i/nF\cdot q]=k_f^0 f_{ox}{}^*C_{ox}e^{-\frac{\alpha nF}{RT}E}\cdot\psi \quad (14)$$

$$\xi=\lambda y^{3/14}=\lambda t^{1/2} \quad (15)$$
$$\eta=\lambda s^{3/14}.$$

Then we obtain

$$\psi(\xi)=1-2\sqrt{\frac{7}{3\pi}}\int_0^{\xi}\frac{\eta^{7/3}\psi(\eta)}{\sqrt{\xi^{14/3}-\eta^{14/3}}}d\eta \quad (16)$$

By the method of successive substitution, the solution of the integral equation (16) can be expressed by the equation in form of power series,

$$\psi(\xi)=1+\sum_{p=1}^{\infty}(-1)^p\left\{\prod_{l=1}^{p}\frac{\Gamma\left(\frac{3l+7}{14}\right)}{\Gamma\left(\frac{3l+14}{14}\right)}\right\}\left(\sqrt{\frac{3}{7}}\xi\right)^p, \quad (17a)$$

where $\Gamma$ represents Euler's Gamma function. This power series is convergent for any value of $\xi$, but it shows a very slow convergence for the value of $\xi$ larger than about $\sqrt{7/3}$. For the large values of $\xi$, as shown in the Appendix, the following asymptotic expansion is applicable,

$$\psi(\xi)\sim\frac{1}{\sqrt{\pi}}\left(\sqrt{\frac{3}{7}}\xi\right)^{-1}\left\{1+\sum_{p=1}^{\infty}(-1)^p\left[\prod_{l=1}^{p}\left(\frac{7-3l}{14}\right)\frac{\Gamma\left(\frac{14-3l}{14}\right)}{\Gamma\left(\frac{21-3l}{14}\right)}\right]\left(\sqrt{\frac{3}{7}}\xi\right)^{-p}\right\} \quad (17b)$$

Therefore, considering the relations expressed by Eqs. (13), (14) and (15), we obtain the general expression showing the instantaneous diffusion current for any point along the wave,

$$i=4\pi\left(\frac{3m}{4\pi d}\right)^{2/3}\cdot nF.$$
$$\times(f_{ox}\cdot{}^*C_{ox})k_f^0 e^{-\frac{\alpha nF}{RT}E}t^{2/3}\psi(\lambda\sqrt{t})$$
$$=i_d\left[1+\frac{k_b^0 f_{red}/\sqrt{D_{red}}}{k_f^0 f_{ox}/\sqrt{D_{ox}}}e^{\frac{nF}{RT}E}\right]^{-1}$$
$$\times\sqrt{\frac{3\pi}{7}}(\lambda\sqrt{t})\psi(\lambda\sqrt{t}), \quad (18)$$

where the surface area of the dropping mercury electrode $q$ is replaced by $4\pi r_0^2=4\pi\left(\frac{3m}{4\pi d}\right)^{2/3}t^{2/3}$, and $i_d$ represents Ilkovic's equation for the instantaneous limiting diffusion current, which can be written as

$$i_d=4\sqrt{\frac{7\pi}{3}}\left(\frac{3}{4\pi d}\right)^{2/3}nF\cdot D_x^{1/2}\cdot m^{2/3}{}^*C_{ox}t^{1/6}.$$

In Table I, the values of function $\sqrt{\frac{3\pi}{7}}(\lambda\sqrt{t})\psi(\lambda\sqrt{t})$ evaluated by means of Eqs. (17a) and (17b) are given for various values of $\lambda\sqrt{t}$.

TABLE I

VALUES OF THE FUNCTION $\sqrt{\frac{3\pi}{7}}\cdot(\lambda\sqrt{t})\cdot\psi(\lambda\sqrt{t})$ FOR VARIOUS VALUES OF $\lambda\sqrt{t}$.

| $\lambda\sqrt{t}$ | $\sqrt{\frac{3\pi}{7}}(\lambda\sqrt{t})\psi(\lambda\sqrt{t})$ | $\lambda\sqrt{t}$ | $\sqrt{\frac{3\pi}{7}}(\lambda\sqrt{t})\psi(\lambda\sqrt{t})$ |
|---|---|---|---|
| 0.0 | 0.000 | 4.0 | 0.865 |
| 0.05 | 0.0555 | 4.5 | 0.879 |
| 0.1 | 0.106 | 5.0 | 0.890 |
| 0.2 | 0.195 | 5.5 | 0.900 |
| 0.3 | 0.271 | 6.0 | 0.907 |
| 0.4 | 0.336 | 7.0 | 0.920 |
| 0.5 | 0.391 | 8.0 | 0.930 |
| 0.6 | 0.439 | 9.0 | 0.937 |
| 0.7 | 0.481 | 10 | 0.943 |
| 0.8 | 0.518 | 12 | 0.953 |
| 0.9 | 0.551 | 14 | 0.959 |
| 1.0 | 0.579 | 16 | 0.964 |
| 1.2 | 0.628 | 18 | 0.968 |
| 1.4 | 0.668 | 20 | 0.971 |
| 1.6 | 0.700 | 25 | 0.977 |
| 1.8 | 0.728 | 30 | 0.981 |
| 2.0 | 0.750 | 40 | 0.986 |
| 2.2 | 0.770 | 50 | 0.988 |
| 2.4 | 0.786 | 60 | 0.990 |
| 2.6 | 0.801 | 80 | 0.993 |
| 2.8 | 0.813 | 100 | 0.994 |
| 3.0 | 0.824 | | |
| 3.5 | 0.847 | $\infty$ | 1.000 |

## Theoretical Derivation of the Equation for the Current-Voltage Curve

Upon integrating Eq. (18) with respect to $t$ from zero to the drop time $\tau$ and dividing by $\tau$, the mean diffusion current is given by

$$\bar{i}=4\pi\left(\frac{3m}{4\pi d}\right)^{2/3}nF\cdot(f_{ox}\cdot{}^*C_{ox})$$
$$\times k_f^0 e^{-\frac{\alpha nF}{RT}E}\frac{1}{\tau}\int_0^{\tau}t^{2/3}\psi(\lambda\sqrt{t})\,dt$$

Then, after writing $\xi=\lambda\sqrt{t}$ and rearranging, we obtain

$$\bar{i}=\bar{i}_d\left[1+\frac{k_b^0 f_{red}/\sqrt{D_{red}}}{k_f^0 f_{ox}/\sqrt{D_{ox}}}e^{\frac{nF}{RT}E}\right]^{-1}$$
$$\times\sqrt{\frac{7\pi}{3}}(\lambda\sqrt{\tau})^{-7/3}\int^{\lambda\sqrt{\tau}}\psi(\xi)\xi^{7/3}d\xi,$$

where $\bar{i}_d$ represents Ilkovic's equation for the average value of the limiting diffusion current and can be written as

$$\bar{i}_d=\frac{24}{7}\sqrt{\frac{7\pi}{3}}\left(\frac{3}{4\pi d}\right)^{2/3}\cdot nF\cdot{}^*C_{ox}\cdot m^{2/3}\cdot D_x^{1/2}\cdot\tau^{1/6}. \quad (19)$$

If we use the following expression for the half-wave potential in the case in which the electrode reaction takes place reversibly,

$$E^r_{1/2}=(RT/nF)$$
$$\times\ln(k_f^0\cdot f_{ox}\cdot\sqrt{D_{red}}/k_b^0\cdot f_{red}\cdot\sqrt{D_{ox}}), \quad (20)$$

$\frac{k_b^0 f_{red}/\sqrt{D_{red}}}{k_f^0 f_{ox}/\sqrt{D_{ox}}}e^{\frac{nF}{RT}E}$ and $\lambda\sqrt{\tau}$ can be written as follows, respectively,

$$\frac{k_b^0 f_{red}/\sqrt{D_{red}}}{k_f^0 f_{ox}/\sqrt{D_{ox}}}e^{\frac{nF}{RT}E}=e^{\zeta}$$
$$\lambda\sqrt{\tau}=\Lambda(e^{-\alpha\zeta}+e^{(1-\alpha)\zeta}),$$

where

$$\zeta=(nF/RT)(E-E^r_{1/2}), \quad (21)$$

and

$$\Lambda=(k_f^0 f_{ox}/\sqrt{D_{ox}})^{1-\alpha}(k_b^0 f_{red}/\sqrt{D_{red}})^{\alpha}\sqrt{\tau}, \quad (22)$$

or by using the rate constant $k_s$ at the standard potential of the electrode reaction,

$$\Lambda=k_s(f_{ox}/\sqrt{D_{ox}})^{1-\alpha}(f_{red}/\sqrt{D_{red}})^{\alpha}\sqrt{\tau}. \quad (22)'$$

Accordingly, it is shown that the above derived equation for $\bar{i}$ can be transformed into the form,

$$\bar{i}=\frac{\bar{i}_d}{1+e^{\zeta}}\varphi(\Lambda e^{-\alpha\zeta}[1+e^{\zeta}]).$$

In this equation, the function $\varphi$ is defined as

$$\varphi(z)=\sqrt{\frac{7\pi}{3}}z^{-7/3}\int_0^z\psi(\xi)\xi^{7/3}d\xi,$$

with $z=\Lambda e^{-\alpha\zeta}(1+e^{\zeta})$. The values of $\varphi(z)$ calculated by performing numerically the indicated integration with the aid of Eqs. (17a) and (17b) are given in Table II. By comparing the values of $\varphi(z)$ with the values of function $z^{1.04}/(1.13+z^{1.04})$, which are also given in Table II, it is seen that the function $\varphi(z)$ can be, with sufficient accuracy, written as

TABLE II

COMPARISON OF THE VALUES OF FUNCTION $\varphi(z)$ WITH THE VALUES OF FUNCTION $\frac{z^{1.04}}{1.13+z^{1.04}}$ FOR VARIOUS VALUES OF $z$.

| $z$ | $\varphi(z)$ | $\frac{z^{1.04}}{1.13+z^{1.04}}$ | $z$ | $\varphi(z)$ | $\frac{z^{1.04}}{1.13+z^{1.04}}$ |
|---|---|---|---|---|---|
| 0.0 | 0.000 | 0.000 | 4.0 | 0.791 | 0.789 |
| 0.1 | 0.0759 | 0.0747 | 4.5 | 0.811 | 0.809 |
| 0.2 | 0.142 | 0.142 | 5.0 | 0.827 | 0.825 |
| 0.3 | 0.201 | 0.202 | 5.5 | 0.840 | 0.839 |
| 0.4 | 0.252 | 0.254 | 6.0 | 0.852 | 0.851 |
| 0.5 | 0.298 | 0.301 | 7.0 | 0.871 | 0.870 |
| 0.6 | 0.339 | 0.342 | 8.0 | 0.885 | 0.885 |
| 0.7 | 0.376 | 0.379 | 9.0 | 0.897 | 0.897 |
| 0.8 | 0.410 | 0.412 | 10 | 0.907 | 0.907 |
| 0.9 | 0.440 | 0.442 | 12 | 0.921 | 0.921 |
| 1.0 | 0.467 | 0.470 | 14 | 0.932 | 0.932 |
| 1.2 | 0.515 | 0.517 | 16 | 0.940 | 0.941 |
| 1.4 | 0.556 | 0.557 | 18 | 0.946 | 0.947 |
| 1.6 | 0.590 | 0.591 | 20 | 0.951 | 0.952 |
| 1.8 | 0.620 | 0.620 | 25 | 0.961 | 0.962 |
| 2.0 | 0.646 | 0.645 | 30 | 0.967 | 0.968 |
| 2.2 | 0.669 | 0.668 | 35 | 0.972 | 0.973 |
| 2.4 | 0.689 | 0.688 | 40 | 0.975 | 0.976 |
| 2.6 | 0.707 | 0.705 | 50 | 0.980 | 0.981 |
| 2.8 | 0.723 | 0.721 | 60 | 0.983 | 0.984 |
| 3.0 | 0.737 | 0.735 | 80 | 0.987 | 0.988 |
| 3.5 | 0.767 | 0.765 | 100 | 0.990 | 0.991 |
| | | | $\infty$ | 1.000 | 1.000 |

$$\varphi(z)\cong\frac{z^{1.04}}{1.13+z^{1.04}}. \quad (24)$$

Therefore Eq. (23) becomes

$$\bar{i}=\frac{\bar{i}_d}{1+e^{\zeta}}\frac{\{\Lambda e^{-\alpha\zeta}(1+e^{\zeta})\}^{1.04}}{1.13+\{\Lambda e^{-\alpha\zeta}(1+e^{\zeta})\}^{1.04}}. \quad (25)$$

This is the general equation of the current-voltage curve for the reduction of the simple metal ion. It is easily shown from Eq. (25) that $\bar{i}$ approaches to the limiting diffusion current $\bar{i}_d$ as the electrode potential becomes sufficiently negative.

In the following, we discuss the characteristics of the polarographic waves, upon dividing into three cases, viz., reversible, irreversible and "quasi"-reversible, corresponding to the magnitude of the parameter $\Lambda$ (or $k_s$).

## Reversible Waves

Consider the case in which the value of $\Lambda$ is larger than $50\times\alpha^{\alpha}(1-\alpha)^{1-\alpha}$. Then, since it can be easily shown that

$$\exp(-\alpha\zeta)+\exp(1-\alpha)\zeta\geqq\alpha^{-\alpha}(1-\alpha)^{-(1-\alpha)}$$

for any value of $\zeta$, Eq. (25) can be transformed into the following form,

$$\bar{i}=\bar{i}_d/(1+e^{\zeta})$$

or

$$E=E^r_{1/2}-\frac{RT}{nF}\ln\frac{\bar{i}}{\bar{i}_d-\bar{i}}. \tag{26}$$

This is the well-known equation for the reversible waves. Consequently, the condition under which the reversible waves are observed, can be written as

$$\Lambda>50\times\alpha^{\alpha}(1-\alpha)^{1-\alpha}.$$

Assuming that $f_{ox}=f_{red}=1$, $D_{ox}=D_{red}=10^{-5}$ cm²/sec., $\tau=3$ sec. and $\alpha\approx0.5$, the above condition becomes

$$k_s>2\times10^{-1}\ (\text{cm./sec.}). \tag{27}$$

## Irreversible Waves

In case of $\Lambda<2\times10^{-2(1-\alpha)}$, $\bar{i}$ is smaller than about 2 per cent of the limiting diffusion current $\bar{i}_d$ in the range of

$$\zeta>-4.6,$$

and the appreciable values of $\bar{i}$ are observed only for the values of $\zeta$ for which the condition

$$\zeta<-4.6$$

is satisfied. Then, since it is found that

$$\exp\zeta<10^{-2}\ \text{for}\ \zeta<-4.6,$$

Eq. (25) becomes

$$\bar{i}=\bar{i}_d(\Lambda e^{-\alpha\zeta})^{1.04}/|1.13+(\Lambda e^{-\alpha\zeta})^{1.04}|$$
$$=\bar{i}_d\frac{\left\{\frac{k_f^0 f_{ox}}{D_{ox}}\sqrt{\tau}\exp\left(-\frac{\alpha nF}{RT}E\right)\right\}^{1.04}}{1.13+\left\{\frac{k_f^0 f_{ox}}{D_{ox}}\sqrt{\tau}\exp\left(-\frac{\alpha nF}{RT}E\right)\right\}^{1.04}}. \tag{28}$$

By solving the equation derived above with respect to $E$, it will be found that

$$E=\frac{RT}{\alpha nF}\left\{2.3\log\frac{k_f^0 f_{ox}}{\sqrt{D_{ox}}}\sqrt{\tau}-0.12-2.2\log\frac{\bar{i}}{\bar{i}_d-\bar{i}}\right\} \tag{28}'$$

Since Eq. (28) or (28)′ can be obtained by ignoring the effect of the reverse process (oxydation process), the waves for such cases may be called as irreversible. Thus the condition under which the irreversible waves appear, can be written as

$$\Lambda<2\times10^{-2(1+\alpha)},$$

or

$$k_s<4\times10^{-5}\ (\text{cm./sec.}) \tag{29}$$

assuming that $f_{ox}=f_{red}=1$, $D_{ox}=D_{red}=10^{-5}$ cm²/sec., $\tau=3$ sec. and $\alpha\approx0.5$.

Eq. (28)′ is the equation of the current-voltage curves for the irreversible waves. As it comes from Eq. (28)′, the plot of $-E$ versus $\log(\bar{i}/\bar{i}_d-\bar{i})$ must be linear, and the inclination of this line is found to be 2.2 $RT/\alpha nF$ ($=57/\alpha n$ mV. at 25°C). Consequently, if this plot is carried out and the tangent of this line is determined, the value of $\alpha n$ can be calculated.

From Eq. (28)′ the half-wave potential $E_{1/2}$ can be obtained as

$$E_{1/2}=\frac{RT}{\alpha nF}\left\{2.3\log\frac{k_f^0 f_{ox}}{\sqrt{D_{ox}}}+\frac{2.3}{2}\log\tau-0.12\right\}. \tag{30}$$

Therefore, by introducing the values of $D_{ox}$, $f_{ox}$, $\tau$ and $\alpha n$ into Eq. (30), the rate constant $k_f^0$ can be calculated from the observed value of $E_{1/2}$. Eq. (30) shows that the half-wave potential of the irreversible wave varies with the drop time as follows:

$$\Delta E_{1/2}/\Delta\log\tau=29.6/\alpha n\ (mV) \tag{31}$$

at 25°C. But this shift in $E_{1/2}$ is appreciably small, i.e. $14.1/\alpha n$ mV. at 25°C, as the drop time varies from 2 sec. to 6 sec.

In the following, we will determine the inflection point $E_p$ of the current-voltage curve (i.e. the potential corresponding to the maximum value of the corresponding derivative curve). By deriving the second derivative of Eq. (28) with respect to $E$ and by putting this derivative equal to zero, $E_p$ can be calculated as

$$E_p=E_{1/2} \tag{32}$$

i.e., the inflection point is identical with the half-wave potential. Furthermore, the maximum value of the derivative curve can be shown as

$$[d\bar{i}/d(-E)]_{E=E_p}=0.26\,\bar{i}_d(\alpha nF/RT) \tag{33}$$

by calculating the first derivative of Eq. (28) with respect to $E$ at $E=E_p$.

## "Quasi"-Reversible Waves

According to Delahay[4], the polarographic waves for the case of $50\times\alpha^{\alpha}(1-\alpha)^{1-\alpha}>\Lambda>2\times10^{-2(1+\alpha)}$ (or $2\times10^{-1}$ cm./sec.$>k_s>4\times10^{-5}$ cm./sec.) may be called "quasi"-reversible in order to distinguish them from reversible and irreversible waves. In such cases, the equation for the current-voltage curve can not be reduced to a simple form as well as in the reversible and irreversible cases. In order to analyse the characteristics of the "quasi"-reversible wave, we must therefore use Eq. (25) which is a complicated function containing the unknown parameters $\Lambda$ and $\alpha$. For the several assumed values of $\Lambda$ and

$\alpha$, the current-voltage curves have been numerically calculated by the aid of Eq. (25). The results are shown in Fig. 1. As

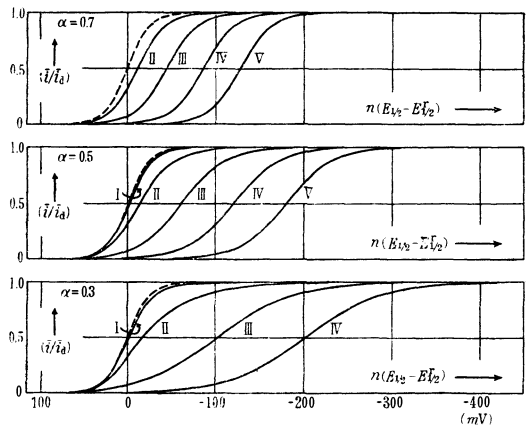



Fig. 1. Current-voltage curves for various values of $\Lambda$ and $\alpha$. Currents are in per cent of the limiting diffusion current $i_d$.
I: $\Lambda=10$, II: $\Lambda=1$, III: $\Lambda=10^{-1}$, IV: $\Lambda=10^{-2}$, V: $\Lambda=10^{-3}$, Dotted curve: $\Lambda=\infty$ (reversible).

illustrated in Fig. 1, the wave shifts towards more negative potentials with regard to the corresponding reversible wave, as $\Lambda$ decreases. Furthermore it is found that the value of $\alpha$ has a remarkable effect on the wave form.

From Eq. (25) it is easily shown that the half-wave potentials of the "quasi"-reversible waves can be numerically calculated by the following equation,

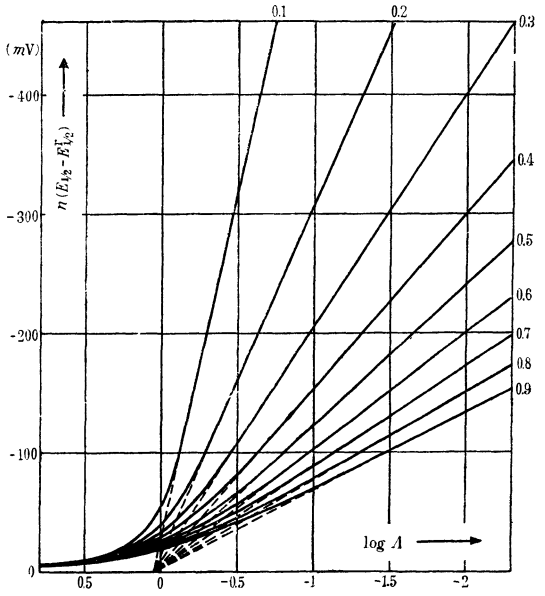



Fig. 2. Variations of $n(E_{1/2}-E^r_{1/2})$ with the values of $\log\Lambda$. Number on each curve is the value of $\alpha$. Dotted lines are the ones given by Eq. (30).

$$\alpha\zeta_{1/2}-2.2\log(1-e^{\zeta_{1/2}})-0.09\log(1+e^{\zeta_{1/2}})=2.3\log\Lambda-0.12$$

where $\zeta_{1/2}=(nF/RT)(E_{1/2}-E^r_{1/2})$.

$n(E_{1/2}-E^r_{1/2})$ versus $\log\Lambda$ diagram is illustrated in Fig. 2.

## Polarographic Waves of Organic Substances

Consider the waves due to the reductions of organic substances and suppose that the reactions which take place at the electrode surface, are shown by

$$R+ne \underset{k_b^0}{\overset{k_f^0}{\rightleftarrows}} R^{n-} \qquad (34)$$

$$R^{n-}+nH^+ \xrightarrow[\text{rapid process}]{} RH_n .$$

Then, the equations derived above are all applicable to this case, by using the following expressions for $\Lambda$ and $E^r_{1/2}$ in place of the above defined ones,

$$\Lambda=(k_f^0\cdot f_R/\sqrt{D_R})^{1-\alpha}\times(k_b^0K\cdot f_{RH}/\sqrt{D_{RH}})^{\alpha}(C_H)^{-\alpha n}\sqrt{\tau}$$

$$E^r_{1/2}=2.3(RT/nF)\times\log\{(k_f^0/k_b^0\cdot K)(f_R/f_{RH})\sqrt{D_{RH}/D_R}\}-2.3(RT/F)\mathrm{pH},$$

where $K$ is the equilibrium constant of the reaction (35); $C_H$ is the concentration of the hydrogen ion in the solution, which is assumed to be well buffered.

In the present case, it must be noticed that the classification into three cases, viz., reversible, irreversible and "quasi"-reversible, depends on pH of the solution, since the value of $\Lambda$ varies with pH. It must be also kept in mind that the half-wave potential varies linearly with pH in the reversible case but is independent of pH in the irreversible case.

## Summary

In the present paper, the general equation of the instantaneous diffusion current has been derived, by taking into account the expansion of the mercury drop with the same accuracy as Ilkovic's equation. Then, the general expression of the current-voltage curve for the reduction of simple metal ion has been given and its characteristics discussed upon being divided into three cases,

i.e. reversible, irreversible and "quasi"-reversible. Reversible waves are given by electrode processes for which the value of $k_s$ is larger than $2\times10^{-1}$ cm./sec., and on the other hand, irreversible waves are observed when the value of $k_s$ is smaller than $4\times10^{-6}$ cm./sec. In the irreversible case, it has been shown that the rate constant $k_f^0$ and the transfer coefficient $\alpha$ can be calculated from the observed values of the half-wave potential and the tangent of log-plot, respectively.

At last, the equation of the current-voltage curve due to the reduction of organic substance has been derived.

Addendum.—Recently J. Koutecky[7] reported a theoretical treatment of the instantaneous and mean diffusion current for any point along the wave, in which the present diffusion problem was solved by an other method. The present work has been independently carried out.

## Appendix

If we write $u$ in place of $\xi$ in Eq. (16), then multiply both sides of Eq. (16) by $\frac{14}{3}u^{11/3}/\sqrt{\xi^{14/3}-u^{14/3}}$ and integrate from zero to $\xi$ with respect to $u$, we obtain,

$$\frac{14}{3}\int_0^{\xi}\frac{u^{11/3}\psi(u)}{\sqrt{\xi^{14/3}-u^{14/3}}}du = 2\xi^{7/3}-2\sqrt{\frac{7\pi}{3}}\int_0^{\xi}\psi(\eta)\eta^{7/3}d\eta\,.$$

By differentiating both sides of the above derived equation with respect to $\xi$, we have after rearranging,

$$\psi(\xi)=\sqrt{\frac{7}{3\pi}}\xi^{-1}-\sqrt{\frac{7}{3\pi}}\xi^{-7/3}\frac{d}{d\xi}\int_0^{\xi}\frac{u^{11/3}\psi(u)}{\sqrt{\xi^{14/3}-u^{14/3}}}du\,.$$

By the method of successive substitution, it is found that the solution of the above derived integro-differential equation can be expressed by the following asymptotic expansion,

$$\psi(\xi)\sim\frac{1}{\sqrt{\pi}}\left(\sqrt{\frac{3}{7}}\xi\right)^{-1}\times\left\{1+\sum_{p=1}(-1)^p\prod_{l=1}^{p}\left(\frac{7-3l}{14}\right)\frac{\Gamma\left(\frac{14-3l}{14}\right)}{\Gamma\left(\frac{21-3l}{14}\right)}\left(\sqrt{\frac{3}{7}}\xi\right)^{-p}\right\}$$

The present authors wish to express their thanks to Dr. T. Kambara who has kindly read the manuscript of this paper and given them helpful advise. The authors' thanks are also due to Dr. Y. Kotera for his interest in this research.

*Government Chemical Industrial Research Institute, Tokyo*

7) J. Koutecky: Chem. Listry. 47, 323 (1953); Collection Czechoslov. Chem. Communs., 18, 597 (1953). These papers of J. Koutecky have been here cited at the suggestion of the editor.

# *Ortho-localisation Energies for Methyl-1 : 2 benzanthracenes*

By Takeshi NAKAJIMA

(Received February 18, 1955)

## Introduction

Various theories have been advanced with a view to examining the hypothesis proposed by Pullman[1] that the carcinogenic activity of the polycyclic hydrocarbons is due to the high $\pi$-electron density of the so-called K region (the 3–4 bond, for example, of 1 : 2-benzanthracene (B. A.) in Fig. 1). In addition to the electron densities, mobile-bond orders and net free valence values with regard especially to the 3–4 bonds of several methyl-benzanthracenes (M.B.A.) have been calculated rather in the rough approximations by Pullman and Pullman[2], and Daudel and Daudel[3]. Recently, based on the per-

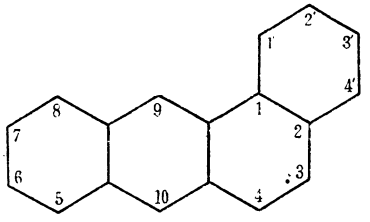



Fig. 1. 1 : 2-Benzanthracene.

1) A. Pullman, *Ann. Chim.*, 2, 5 (1947).

2) A. Pullman and B. Pullman, *Bull. Soc. Chim. Biol.*, XXXI, 343 (1949).

3) P. Daudel and R. Daudel, *J. Chem. Phys.*, 16, 639 (1950).

turbation method, Greenwood[4] has made the more rigorous calculations of these quantities. All these quantities as the criteria of the reactivity of a conjugated bond are concerned with the $\pi$-electron configuration in the non-reacting ground state.

The other method of approach for the discussion of bond reactivity is the localisation (polarisation) method due originally to Wheland[5] and extended by Brown[6]. According to this method reactivity of a conjugated bond is correlated with the ortho (bond) localisation energy (O.L.E.), defined as the energy required to convert the conjugated bond in question into a double bond. Recently, Pullman, Pullman, and Berthier[7] have calculated O. L. E. for the 3-4 bonds of several M.B.A. and reached the conclusion that the reaction homolytic in nature should occur at the 3-4 bond in contradiction to the conclusion put forward by Greenwood that the reaction should be heterolytic in nature. In virtue of the rough approximation made by Pullman and others[8] in their treatment, however, it seems desirable to carry out an independent calculation of O.L.E. for M.B.A.

## Method of Calculation

Let us suppose that the reare two conjugated systems $R$ and $S$ initially separate, and then joined by a bond between atoms $r$ of $R$ and $s$ of $S$, forming a composite system $RS$. The delocalisation energy $\Delta\varepsilon(RS)$ across the connecting bond $r$-$s$ may be defined as the difference between the $\pi$-electronic energy of the complete system $RS$ and the sum of the $\pi$-electronic energies of the systems $R$ and $S$ taken separately. Formally then

$$\Delta\varepsilon(RS)=\varepsilon(RS)-\varepsilon(R)-\varepsilon(S). \tag{1}$$

On the other hand, employing the variation method for the orbital interactions between $R$ and $S$, we can express $\Delta\varepsilon(RS)$ as a function of orbitals and their energies of $R$ and $S$ as follows[9]:

$$\Delta\varepsilon(RS)=2\sum_{i}^{occu}\sum_{j}^{un}\frac{C^2_{ir}\,C^2_{js}}{\epsilon_i{}^R-\epsilon_j{}^S}k^2 + 2\sum_{j}^{occu}\sum_{i}^{un}\frac{C^2_{js}\,C^2_{ir}}{\epsilon_j{}^S-\epsilon_i{}^R}k^2 \text{ (in } \beta \text{ units)}, \tag{2}$$

where $\epsilon_i{}^R$ denotes the energy of the $i$th MO of $R$, $C_{ir}$ the coefficient of the $r$th atomic orbital in the $i$th MO and so on, and $k$ is the resonance integral of $r$-$s$ bond in $\beta$ units. Thus, if the MO's and their energies of $R$ and $S$ are known, we can calculate $\Delta\varepsilon(RS)$ without the tedious procedure due to the straightforward application of LCAO MO method for $RS$.

In discussing the effect of a substituent on O.L.E., consider that $R$ denotes a parent molecule, $S$ a substituent, and $R'$ a parent residual molecule for the transition state in which the requisite number of electrons appropriate to a given type of reaction are assumed to be localised at both the ends of the bond of $R$ in question. An expression similar to Eq. (1) may be written for the energy $\varepsilon(R'S)$ of the substituted residual molecule, so that we can immediately derive,

$$\begin{aligned}\text{O.L.E.}&=\varepsilon(R'S)+\varepsilon(=)-\varepsilon(RS)\\&=\varepsilon(R')+\varepsilon(=)-\varepsilon(R)+\Delta\varepsilon(R'S)-\Delta\varepsilon(RS),\end{aligned} \tag{3}$$

where $\varepsilon(=)$ is the energy of the ethylenic double bond. As we are concerned only with the effect of a substituent with the position of substitution on O.L.E.o f a given molecule, it is convenient to have an expression for the change in O.L.E. $\Delta$O.L.E.$_r$ caused by the substitution at the $r$th atom. This expression is

$$\Delta\text{O.L.E.}_r=\Delta\varepsilon_r(R'S)-\Delta\varepsilon_r(RS), \tag{3'}$$

With a substituent such as methyl, besides the above considered effect due to delocalisation, the effect due to induction should be taken into account. Induction causes a change in $\alpha_r$, the coulomb term for atom $r$ to which the substituent is attached. Then, the effect due to induction on O.L.E. is treated by the perturbation method as follows:

$$\Delta\text{O.L.E.}r \text{ due to induction} = (q_r'-q_r)\delta\alpha_r+\frac{1}{2}(\pi_{rr}'-\pi_{rr})\delta\alpha_r{}^2, \tag{4}$$

where $q_r$ and $\pi_{rr}$ denote the electron density and self-polarisability of the $r$th atom respectively and the $'$ refers to the residual molecule.

In calculating O.L.E. for the 3-4 bonds of several M.B.A., consider that $R$ represents the parent molecule, B.A., $R'$ the parent residual molecule, $\beta$-phenyl-naphthalene (P.N.), and $S$ the methyl substituent. The MO's and their energies of $R$, $R'$ and $S$ are calculated by the standard LCAO MO method with overlap omitted. The additional parameters related to the methyl substituent are taken according to Pullman and Pullman[10] as follows:

4) H. H. Greenwood, *Brit. J. Cancer*, 5, 441 (1951).
5) G. M. Wheland, *J. Am. Chem. Soc.*, 64, 900 (1942).
6) R. D. Brown, *J. Chem. Soc.*, **1950**, 3249 and **1951**, 1950, 1955.
7) A. Pullman, B. Pullman, and G. Berthier, *Compt. rend.*, 236, 2067 (1953).
8) B. Pullman, personal communication; "Dewar's method (*J. Am. Chem. Soc.*, 74, 3357 (1952)) used in our treatment is erroneous when applied to the calculation of the effect of substituents on O.L.E."
9) T. Nakajima, *Sci. Rep. Tohoku Univ.*, Ser. I, in press.
10) B. Pullman and A. Pullman, "Les Theories Electroniques de la Chimie Organique", 1952, p. 410.

$\alpha_{H_8}=\alpha-0.2\beta$, $\beta_{C\equiv H_8}=2.5\beta$,
$\delta\alpha_{C_{aron}}=-0.1\beta$, $k=0.7$.

## Result and Discussion

In Table I are given the delocalisation energies $\Delta\varepsilon_r$ produced by methylations in each of the ten possible positions of B.A. containing 20 $\pi$-electrons and of P.N. containing 18 $\pi$-electrons. Table I lists also

TABLE I
DELOCALISATION ENERGIES $\Delta\varepsilon_r$ AND SELF-POLARISABILITIES $\pi_{rr}$ FOR B.A. AND P.N.

| B.A. | | | P.N. | | |
|---|---|---|---|---|---|
| $r$ | $\Delta\varepsilon_r$ (in $\beta$ units) | $\pi_{rr}\times\beta$ | $r$ | $\Delta\varepsilon_r$ (in $\beta$ units) | $\pi_{rr}\times\beta$ |
| 10 | 0.16023 | 0.513 | 9 | 0.15820 | 0.480 |
| 9 | 0.15901 | 0.495 | 8 | 0.15498 | 0.447 |
| 5 | 0.15528 | 0.452 | 5 | 0.15454 | 0.441 |
| 8 | 0.15511 | 0.449 | 10 | 0.15422 | 0.439 |
| 4′ | 0.15439 | 0.439 | 1′ | 0.15309 | 0.425 |
| 1′ | 0.15340 | 0.429 | 3′ | 0.15139 | 0.412 |
| 7 | 0.15111 | 0.410 | 6 | 0.15093 | 0.408 |
| 2′ | 0.15111 | 0.410 | 7 | 0.15063 | 0.405 |
| 6 | 0.15098 | 0.409 | 2′ | 0.14971 | 0.396 |
| 3′ | 0.15051 | 0.404 | 4′ | 0.14971 | 0.396 |

the self-polarisabilities $\pi_{rr}$ of B.A. and P.N. It has been shown by the present author[9] that the delocalisation energy per a connecting bond between a given molecule and a given substituent is correlated linearly with $\pi_{rr}$ of the substituted atom of the molecule. It will be seen that there exists a fairly good correlation of this kind between $\Delta\varepsilon_r$ and $\pi_{rr}$ in Table I.

$\Delta$O.L.E.$_r$ are calculated by taking account merely of the delocalisation effect from Eq. (3). The contribution due to the inductive effect is ignored because in Eq. (4) the first term vanishes as the electron density is unity at every position of B.A. and P.N. and the actual values of the second term are very small. $\Delta$O.L.E.$_r$ thus calculated are compared with $\pi_{rr}'-\pi_{rr}$ in Table II. The linear correlations

TABLE II
HOMOLYTIC $\Delta$O.L.E.$_r$, DIFFERENCES IN SELF-POLARISABILITIES $\pi_{rr}'-\pi_{rr}$, AND RELATIVE CHANGES IN BOND ORDER $\delta p_{3-4}$

| $r$ | $\Delta$O.L.E.$_r$ (in $\beta$ units) | $(\pi_{rr}'-\pi_{rr})\times\beta$ | $\delta p_{3-4}$ |
|---|---|---|---|
| 3′ | 0.00088 | 0.008 | 0.0007 |
| | 0.00000 | 0.000 | 0.0000 |
| 6 | −0.00005 | −0.001 | −0.0002 |
| 8 | −0.00013 | −0.002 | −0.0002 |
| 1′ | −0.00031 | −0.004 | −0.0005 |
| 7 | −0.00048 | −0.005 | −0.0016 |
| 5 | −0.00074 | −0.011 | −0.0023 |
| 9 | −0.00081 | −0.015 | −0.0021 |
| 2′ | −0.00140 | −0.014 | −0.0050 |
| 4′ | −0.00468 | −0.043 | −0.0092 |
| 10 | −0.00601 | −0.074 | −0.0175 |

seen between $\Delta\varepsilon_r$ and $\pi_{rr}$ in Table I and between $\Delta$O.L.E.$_r$ and $\pi_{rr}'-\pi_{rr}$ in Table II lead to the conclusion that in discussing the effect of the substituent, the delocalisation effect may be replaced effectively by a virtual inductive effect by the suitable choice of the value of $\delta\alpha_r$ in Eq. (4), in which, in this case, only the second term is effective.

Brown[6] has shown that it is possible to correlate bond order with O.L.E., suggesting that bond order also should be a useful index of bond reactivity. The relative changes in mobile order $\delta p_{3-4}$ of the 3-4 bond of B.A. caused by methylations have been calculated by Greenwood[4] and are arranged also in Table II. Considering that Greenwood's calculations have been made by taking account merely of the inductive effect by the second order perturbation method, it is remarkable that there exists a close parallelism between $\Delta$O.L.E.$_r$ and $\delta p_{3-4}$ as seen in Table II. This parallelism is a further evidence of the above deduction that the delocalisation effect may be replaced effectively by a virtual inductive effect.

It is clear that we cannot correlate decrease in O.L.E. of the 3-4 bond of M.B.A. with the experimentally determined increase in the rate of addition of $OsO_4$ to the 3-4 bond[11], since an increase in reactivity consequent upon methylation is in fact accompanied by an increase in O.L.E. (except the methylation at 3′-position). It has been established by Brown[5] that O.L.E. provides a very satisfactory interpretation of the relative reactivities of conjugated bonds toward bond reagents such as $OsO_4$ for a system of alternant hydrocarbons. As we have seen, in the case of substituted hydrocarbons, however, this correlation no longer holds. Agreeing to Greenwood's suggestion deduced from the decrease in $\delta p_{3-4}$ this suggests that although for alternant hydrocarbons $OsO_4$ may react by a largely homolytic mechanism, the reactions for substituted hydrocarbons may be not homolytic but heterolytic in nature.

At this point we must distinguish two types of bond localisation as in the case of atom localisation. In the homolytic and heterolytic (electrophilic or nucleophilic) atom localisations, 1 and 2 or 0 $\pi$-electrons respectively are assumed to be localised at the site of reaction. By analogy with this we assume that in the homolytic and heterolytic bond localisations 2 and 4 or 0 $\pi$-electrons respectively are localised at the reaction sites of the bond in question. Thus, O.L.E. so far considered is that for the homolytic type of bond localisation.

11) G. M. Badger, *J. Chem. Soc.*, 1950, 456.

Next the heterolytic (electrophilic) O.L.E. for several M.B.A. will be calculated. For the calculation of heterolytic O.L.E. the inductive effect contributes much because the electron density at every atom of the parent residual molecule which, in this case, is P.N. with two $\pi$-electrons lost is not necessarily unity. The contribution due to induction is calculated by Eq. (4) in which, in this case, the first term is effective and the second term is ignored. Then, for the heterolytic (electrophilic) bond localisation Eq. (4) may be rewritten as follows:

$$\Delta\text{O.L.E.}_r \text{ due to induction} = (q_r' - q_r)\delta\alpha_r = -q_r^f \delta\alpha_r, \quad (5)$$

where $q_r^f$ denotes the electron density in the frontier orbital (the highest occupied orbital) of P.N.[12].

From the results given in Table III we can notice the following points. (1) There exists a close parallelism between the heterolytic $\Delta$O.L.E.$_r$ due to delocalisation and induction, so that the resultant sum is closely correlated with $q_r^f$. This suggests that heterolytic $\Delta$O.L.E.$_r$ may be calculated effectively by taking account merely of the virtual induction by the suitable choice of the value of $\delta\alpha_r$ in Eq. (5). (2) Except with regard to the 4'-position, both the delocalisation and inductive effect decrease heterolytic O.L.E.; for details, the former lowers relatively the energy of the transition state and the latter raises that of the ground state. (3) We can correlate the decrease in heterolytic O.L.E. with the experimentally determined increase in the rates of addition of $OsO_4$ to the 3–4 bond though the experimental data are not sufficient. (4) The changes in heterolytic O.L.E. with the position of substitution are remarkable compared with those in homolytic O.L.E.

Table III lists also the relative carcinogenic powers of M.B.A[13]. It may be seen that there exists a satisfactory correlation between heterolytic O.L.E. and the activity especially with regard to M.B.A. substituted in the angular ring and at the 9-position. In this respect, it should be remembered that the especially high electron densities for 2'- and 4'-M.B.A. which are inactive and the relatively low density for 9-M.B.A. which is highly active have provided the results in direct contradiction to the attempt to correlate the electron density of the 3–4 bond of M.B.A. with the activity[4),9)].

TABLE III

HETEROLYTIC $\Delta$O.L.E.$_r$, RATE CONSTANTS OF ADDITION OF $OsO_4$, $10^3$K AND CARCINOGENIC ACTIVITIES

| $r$ | $\Delta$O.L.E.$_r$ (in $\beta$ units) | | | $10^3$K | carcinogenic activity |
|---|---|---|---|---|---|
| | due to delocalisation | due to induction | total | | |
| 9 | 0.04301 | 0.04169 | 0.08470 | 0.96 | ++ |
| 8 | 0.03137 | 0.02996 | 0.06133 | | + |
| 5 | 0.02400 | 0.02353 | 0.04753 | | ++ |
| 10 | 0.02089 | 0.02559 | 0.04648 | 0.91 | +++ |
| 6 | 0.01689 | 0.01611 | 0.03300 | 0.64 | + |
| 3' | 0.01248 | 0.01104 | 0.02352 | | 0 |
| 1' | 0.00788 | 0.00780 | 0.01568 | | 0 |
| 7 | 0.00653 | 0.00667 | 0.01320 | | + |
| 2' | −0.00048 | 0.00088 | 0.00040 | | 0 |
| | 0.00000 | 0.00000 | 0.00000 | 0.48 | 0 |
| 4' | −0.00376 | 0.00088 | −0.00288 | | 0 |

## Summary

(1) The effects of the methyl substituent on O.L.E. for the 3–4 bond of B.A. have been calculated. The effect may be discussed by the perturbation method taking account of the virtual inductive effect through the suitable choice of the value of $\delta\alpha$ of the substituted position.

(2) The homolytic and heterolytic O.L.E. were defined. The former predicts the bond reactivity only for a system of alternant hydrocarbons. With substituted hydrocarbons the latter should be used as a criterion of bond reactivity.

(3) The heterolytic O.L.E. for the 3–4 bonds of several M.B.A. have been successfully correlated with the experimental evidences on rates of addition of $OsO_4$ and the carcinogenic activities.

(4) The method of calculation of the effect of the methyl substituent on O.L.E. used in the present note may be applicable, with due caution, to other substituents in general.

12) K. Fukui, T. Yonezawa, and H. Shingu, *J. Chem. Phys.*, **20**, 722 (1952).

13) G. M. Badger, *Brit. J. Cancer.*, **2**, 309 (1949).

In conclusion, the author is grateful to Prof. H. Azumi for his continued interest in this problem. The author's thanks are also due to Prof. B. Pullman in the Institut du Radium, Paris for his helpful criticism and kind encouragement.

*Department of Chemistry, Faculty of Science, Tōhoku University, Sendai*

# *Separation of RaD, RaE and RaF by Ion Exchange*

By Tatsujiro ISHIMORI

(Received July 14, 1955)

There are several well-known procedures for the separation of RaD, RaE and RaF, e.g., coprecipitation with a suitable carrier, electrochemical separations, extractions of some complex compounds formed with organic reagents, and methods using radiocolloid formation. Recently Polonium has been extracted as dithizonate[1], and ThC has been separated from ThB by the use of radiocolloid formation[2]. These elements can also be separated from each other by means of paper partition chromatography[3]. As anion exchange resins are reported to be very effective for the separations of Zr, Hf, Nb, Ta and Pa[4], rare earths[5] and transition elements[6], etc.[7], the author studied the carrier-free separation of RaD, RaE and RaF using anion exchangers. It was found, in the hydrochloric acid solutions of suitable concentrations, that remarkable differences in the degree of adsorption of these elements for the resin could be successfully utilized for the ion exchange separation.

These ions adsorbed on the top of the column of Amberlite XE-98 (IR-411), a lower cross-linked strongly basic type resin, can be eluted successively, using 2 or 3N hydrochloric acid for RaD, conc. hydrochloric acid for RaE and finally dil. nitric acid or perchloric acid for RaF, respectively. Radioactive assay proved the radioactive purity of each fraction to be nearly 99.9%.

1) T. Ishimori and H. Sakaguchi, *J. Chem. Soc. Japan*, Pure Chem. Sect., **71**, 327 (1950).
2) M. Ishibashi, Y. Kusaka and M. Oyabu, presented at Annual Meeting of the Chemical Society of Japan (Kyoto, April, 1953).
3) W. J. Friesln and J. W. Jones, *Anal. Chem.*, **23**, 1447 (1951). E. E. Dickey, *J. Chem. Education*, **30**, 525 (1953).
4) K. A. Kraus and G. E. Moore, *J. Am. Chem. Soc.*, **73**, 2900 (1951).
5) E. H. Huffman and R. L. Osawlt, *J. Am. Chem. Soc.*, **72**, 3323 (1950).
6) K. A. Kraus and G. E. Moore, *J. Am. Chem. Soc.*, **75**, 1460 (1952).
7) K. A. Kraus, F. Nelson and G. H. Smith, *J. Phys. Chem.*, **58**, 11 (1954).

## Experimental

**Preparation of The Stock Solution of the Mixture of RaD, RaE and RaF.**—The mixture of carrier-free RaD, RaE and RaF was extracted by digestion with aqua regia from a radon tube which had been used over these two years. From the extracted solution, stock solution of the mixture in conc. nitric acid (14N) was prepared by repeated evaporations and additions of nitric acid.

**Radioactive Measurement.**—Radioactive measurement was performed with a Geiger-Muller counter and a Lauritsen electroscope. The Geiger-Muller tube used was an end-window type, with thin mica window of 1.8 mg/cm² thickness.

Preparation of samples for radioactive assay: The radioactive substances were collected with ferric hydroxide. One ml. of 1 mole/l ferric nitrate solution was added to the radioactive solution, and ferric hydroxide precipitate, produced by the addition of dil. ammonium hydroxide solution, was filtered through a Gooch crucible and was collected on a disk of filter paper. The precipitate was dried using an infrared lamp and was used for assays. Ferric hydroxide was found to be a suitable carrier for the collections of RaE and RaF, but not fitted for RaD. One of the experiments showed that about 20% of RaD was retained in the solution without being carried down. But, since the procedure of preparing the samples is simple and time-saving this hydroxide was usually used as a carrier for RaD whenever a complete recovery was not necessary. Lead sulphide, if necessary, was used instead of ferric hydroxide.

The differences in disintegration properties of RaD, RaE and RaF favoured the identification of each species*.

**Preliminary Experiments.**—In order to find a good condition for the separation, the elution of the individual ion was investigated, using.

* The radioactive properties of these species have been sammarized as follows by G. T. Seaborg et al. (1953):

| Symbol | Element | Half-life | Type of disintegration (Mev) |
|---|---|---|---|
| RaD | Pb | 22 years | $\beta$ (0.018) $\gamma$ (0.047) |
| RaE | Bi | 5.0 days | $\beta$ (1.17) |
| RaF | Po | i40 days | $\alpha$ (5.3) $\gamma$ (.077) |

hydrochloric acid solutions of various concentrations. The columns used were of Amberlite XE-98 (65-120 mesh), 3 cm. × 0.9 cm. diameter in size, and were preliminarily conditioned with 3NHCl. One drop of the stock solution was taken as a sample. The radioactive ions in the effluents were successively collected by coprecipitation with ferric hydroxide and their activities were measured. While the isolated RaD is expected to show an increase in the $\beta$-activity, the $\beta$-activity of RaE has to decrease because of its decay. So RaD and RaE are easily identified by duplicate measurements of their $\beta$-activities within a interval of a few days. RaF was identified by means of a Lauritsen electroscope because on its $\alpha$-emitting property. The data of the elution experiments with 3N, 6N and conc. HCl are illustrated in Fig. 1 (No. 1-No. 3). Since RaF is

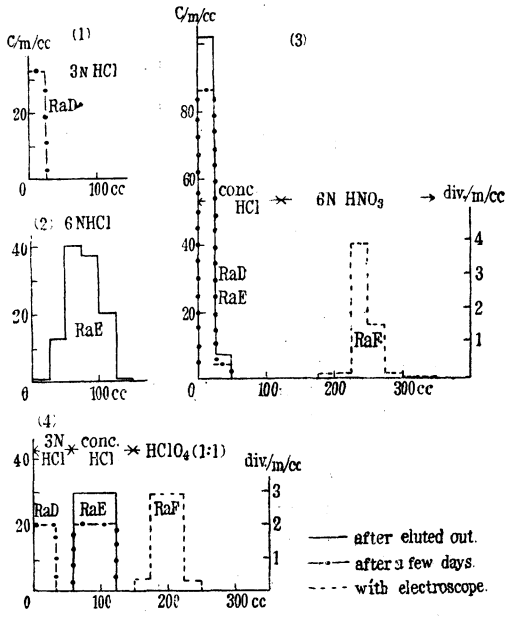



Fig. 1.

not detected in the effluents of the hydrochloric acid solution, in Experiment No. 3 6NHNO$_3$ was used to elute it. The considerable differences in the rate of elution of these ions indicate the desired separation as being possible. Thus, in Experiment No. 4 fractional elution of these ions were performed, i.e., RaD was eluted out with 3NHCl, RaE with conc. HCl and then RaF with $HClO_4$ (1 : 1). Perchloric acid was used because on its slight tendency to form a complex anion. The experimental results were parallel with this anticipation.

**Separation for the Samples of Stronger Activities.**—The experiments with samples of stronger activities were tried and each fraction of effluent was to check the extent of the separation. As a sample, one drop was taken out of the hydrochloric acid solution which had been prepared by evaporating the stock solution, followed by digesting it with conc. HCl. The activity of a sample was about $4 \times 10^4$ c/m. The columns used were of Amberlite XE-98 (65-120 mesh), 3 cm × 0.85 cm. diameter in size, and preliminarily conditioned with 2NHCl. Solutions of 2NHCl, conc. HCl and $HNO_3$ (1 : 1) were used as the eluent for RaD, RaE and RaF, respectively. From the effluent, successive drops were taken at suitable intervals on a small glass pan or a disk of filter paper and after being dried, their activity was determined to obtain the elution curve. The resulting elution curve is shown in Fig. 2. From each fraction of effluents I, I′, II,

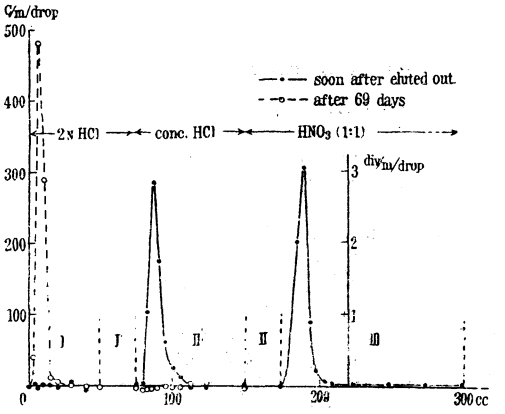



Fig. 2. Elution Curve.

Activities of each fraction were as following:

| activity c/m \ fraction | I | I′ | II | II′ | III |
|---|---|---|---|---|---|
| after eluted out | 390 | 1 | $41.5 \times 10^3$ | 1 | 0 |
| after 35 days | $39.7 \times 10^3$ | 0 | 270 | 2 | −3 |
| after 69 days | $40.0 \times 10^3$ | 0 | 0 | 0 | 0 |

II′ and III, as shown in Fig. 2, the radioactive ions were carried down with ferric hydroxide precipitates and their activities were measured. In the cases of fraction I and II, aliquots of 1/10 and 1/15 of the originals, respectively, were used because of their stronger activities.

### Examination of the Extent of Separation

**1. Elution Curve.**—From the elution curve illustrated in Fig. 2, the separation is considered to be satisfactory. Absence of activity in fraction I′ and II′ shows that the fractional elution was performed successfully. While it might be necessary to prevent the tailing of RaF, the quantity of RaF contained in the tailing of fraction III appears to be negligible when examined with some larger amounts of effluent.

**2. Detection of RaE Contaminating RaD Fraction.**—The activity of fraction I increased as shown in Fig. 3 due to the growth of the element, RaE. In this respect, the observed growth curve agrees with the theoretical one of RaE. Moreover, the observed activity $39 \pm 4$ c/m, of RaE grown after one handred minutes from the

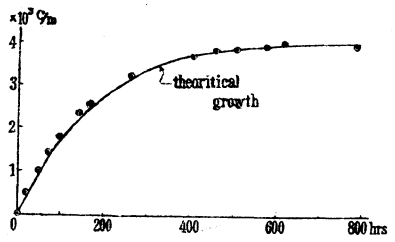



Fig. 3. Growth of RaE.

instant of the elution of RaD's peak, is in good agreement with the calculated value, 38.4 c/m:

$$4.02\times10^3(1-e^{-(0.693/5.0\times24\times60)}\cdot100)=38.4.$$

The value $4.02\times10^3$ c/m is the activity of RaE existing at radioactive equilibrium with RaD before the separation. It was obtained from the measurement after 69 days taking into account of RaD's decay. From the results mentioned above it is considered that at the moment of elution, RaD is, to a great extent, free from RaE which coexisted before the separation.

**3. Detection of RaD Contaminating RaE Fraction.**—A. Decay of RaE Fraction's Activity: The decay curve of RaE fraction (II) which was collected using ferric hydroxide is indicated in Fig. 4. Within the range of experimental error

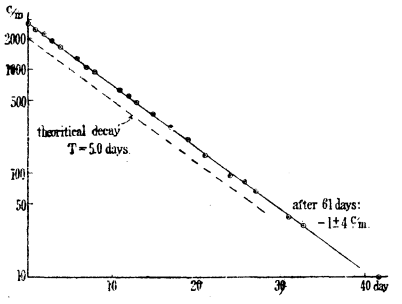



Fig. 4. Decay of RaE fraction.

the activity may be supposed to decrease in accordance with the half-life (5.0 days) of RaE. The sample was covered with a thin sheet of cellophane absorber and placed at 2 cm. under the window of a G.M. tube. So the $\alpha$-rays from RaF were cut off and the activity of RaF resulting from RaE does not interfere with this determination.

B. Fearing the possibility that the amounts of RaD in the RaE fration were not satisfactorily collected with ferric hydroxide in the above experiment, a further expriement was undertaken. Using RaE which was separated from RaD by fractional elution, the same procedure was repeated and the activity of the RaD fraction was measured. The produres and results are shown in Table I. It may be said that contaminants in RaE separated as above are in the order of less than $1:10^4$.

**4. Detection of RaD and RaE Contaminating RaF Fraction.**—The radioactivity of ferric hydroxide precipitated from the aliquot of RaF

TABLE I
DETECTION OF RaD CONTAMINATING RaE FRACTION

Procedure:

Sample→RCl → (2N HCl 75 cc.) → RaD fr. → evap. → *
Sample→RCl → (conc. HCl 100 cc.) → RaE fr.

* 10 cc. of 2N HCl → RCl → (2N HCl 75 cc.) → RaD fr.**
RCl → (conc. HCl 100 cc.) → RaE fr.***

** (PbS) .....A
*** ($Fe(OH)_3$) .....B

| activity c/m / sample | after a day | after 5 days |
|---|---|---|
| A | −1 | −2 |
| B | $14.6\times10^3$ | $9.5\times10^3$ |

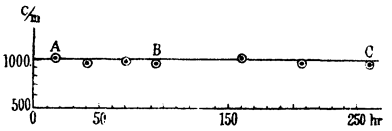



Fig. 5. Activities of RaF measuree with G.M. counter.

When the absorber (3.3 mg/cm² cellophane) is used, the activities are following:

| at the time of | A | B | C |
|---|---|---|---|
| activity c/m | −1 | −1 | 0 |

fraction was measured with a G.M. counter. As shown in Fig. 5, activities did not show any decrease for 10 days. The RaF radiations may be completely cut off when a cellophane sheet (3.3 mg./cm²) is used as an absorber. Hence it may be concluded that this fraction is not contaminated with RaD and RaE.

**5. Detection of RaF Eluted in RaD and RaE Fraction.**—Since it is difficult to detect the presence of a small amount of RaF in the presence of RaD and RaE, a pure sample of RaF was prepared by preliminary fractional elution and was tested with respect to the absence of RaD and RaE. The sample was treated again by the fractional elution method: 25 cc. of RaF solution (2NHCl) were passed through a column and then fractionation was performed with 50 cc. of 2NCHI, 50 cc. of conc. HCI and 150 cc. of $HNO_3$ (1:1). From each fraction, RaF was collected with ferric hydroxide and measured using a Lauritsen electroscope. The results are the following:

| fraction | RaD | RaE | RaF |
|---|---|---|---|
| div./min. | 0.10 | 0.12 | 104 |

It was found that about 0.1% of RaF leaked and contaminated both the fractions of RaD and RaE.

**6. Ash of the Exchanger after the Experiment.**—The exchange resins were burnt to ashes

and examined after the fractional elution experiment in order to investigate whether the radioactive components had been quantitatively removed or not. The results given in Table II indicate that 0.8% of RaF remained in the exchange resin and the other two species were eluted out quantitatively.

TABLE II
ASH OF EXCHANGER AFTER THE EXPERIMENT

| sample / activity | eluted RaD and RaE | eluted RaF | ash of exchanger |
|---|---|---|---|
| c/m | $8.28\times10^3$ | — | 2 |
| c/m[1] | — | — | 0 |
| div./m | — | 227 | 1.74 |

Each sample was prepared with carrier of ferric hydroxide (Fe (III) 0.4 m. eq.)
1) with 7.2 mg/cm$^2$ Al absorber.

**Summary**

RaD, RaE and RaF may be satisfactorily separated from each other by means of an anion exchanger, Amberlite XE-98. Carriers are not necessary. The use of an anion exchanger and strong acidities of eluents helps to prevent the formation of radiocolloids. This separation technique seems to be highly suitable for the preparation of carrier-free RaE and RaF tracer. It is efficient in separation and easy to manipulate.

The author gratefully acknowledges the helpful discussions and continual encouragement given him by Prof. H. Okuno and Dr. M. Honda. He also expresses heartfelt thanks to Dr. N. Saito for presenting the randon tube used in this experiment.

*Department of Chemistry,*
*St, Paul's University, Tokyo*

# *On the Rate of the Sluggish Inversion of Silica Stone Kinetics of the Polymorphous Transition of Silica*

By Taneki TOKUDA

(Received March 3, 1955)

## Introduction

Quite a few qualitative investigations have been reported on the sluggish inversion of silica stone. However, only few publications on the rate of conversion* have appeared.

Mellor and Campbell[1] have studied the speed of conversion of quartz into cristobalite by making 15 successive burns in a china biscuit kiln to cone 10, and measuring the density of the product after each burn. The authors proposed the following experimental formula,

$$x = e^{-kn} \tag{1}$$

where $x$ is the fraction which remains unchanged at the number of burns $n$, and $k$ is a constant.

Nakai and Fukami[2] had determined precisely the density of the Merk's silica stone powder after firing several hours in an electric furnace. As a result, they proposed the following experimental formula,

$$1 - x = k \log t \tag{2}$$

where $t$ is the time required for firing. This formula, however, is not in good agreement with the experimental data.

Avgustinik and Kurdevanidge[3] determined the rate of conversion of $\alpha$-quartz into metastable $\alpha$-cristobalite at 1200°, 1300°, 1400° and 1500°C±15°C through pycnometric determinations of the density after 0.5, 1, 3 and 6 hrs. heating at the given temperatures. Assuming a unimolecular, a bimolecular, or the Jander rate equation, and by application of the Arrhenius' equation, linearity between $\log k$ and $1/T$ ($T$ is a firing temperature in °K) is fulfilled only for the bimolecular reaction. Thereby the following experimental formula was proposed.

$$k = e^{(a/\delta^{0.064} - b \times 10^4/T)} \tag{3}$$

where $\delta$ is the diameter of the grain, and $a$ and $b$ are constants.

Segawa[4] measured the linear expansion of silica stone rod by heating it at a uniform

* In this report, the word "conversion" means the sluggish inversion of $\alpha$-quartz to $\alpha$-cristobalite.

1) J. W. Mellor and A. J. Campbell, *Trans. Engl. Ceram. Soc.*, **15**, 77 (1915).

2) T. Nakai and Y. Fukami, *J. Soc, Chem. Ind., Japan*, **38**, Supple. binding, 340 (1935).

3) A. I. Avgustinik and O. K. Kurdevanidge, *J. Appl. Chem. (U.S.S.R.)*, **19**, 1189 (1946).

4) K. Segawa, *Tech, Rep. Yawata Iron Works*, **26**, 1 (1951).

rate of temperature rise. Assuming that the reaction is of the primary nature, he showed the linearity between $\log k$ and $1/T$.

According to the results of Mellor and Campbell, Nakai and Fukami, and Segawa, the conversion of $\alpha$-quartz to $\alpha$-cristobalite have the nature of primary reaction. On the contrary, Avgustinik and Kurdevanidge claimed that it is of the secondary nature. In order to clarify the contrariety between these two hypotheses, the following experiments are carried out using many sorts of silica stone of different geological origin.

TABLE I
SILICA STONE SAMPLES

| Silica stones | Type of occurence | Locality | Size of single crystals |
|---|---|---|---|
| A | Radiolarian chert | Kuroda, Japan | 0.2 mm-submicroscopic, mostly 0.005 mm |
| B | Chert | Tamba, 〃 | 0.2 mm-submicroscopic, |
| C | Recrystallized chert | 〃 〃 | 0.02-0.002 mm, mostly 0.01 mm |
| D | Vein quartz with chert | Youra, 〃 | 2.5 mm-submicroscopic |
| E | Vein quartz | Tamba, 〃 | 1.0–0.05 mm, mostly 0.5 mm |
| F | Pegmatite quartz | Fukushima, 〃 | 1.0–0.01 mm |
| G | Rock crystal | Yamanashi, 〃 | Single crystal |

TABLE II
CHEMICAL ANALYSIS OF SILICA STONES

| | A | B | C | D | E | F |
|---|---|---|---|---|---|---|
| $SiO_2$ | 94.12 | 95.68 | 97.23 | 98.35 | 99.13 | 99.72 |
| $Al_2O_3$ | 1.87 | 2.87 | 0.20 | 0.52 | 0.01 | 0.00 |
| $Fe_2O_3$ | 1.89 | | 2.17 | 0.43 | 0.63 | 0.14 |
| CaO | 0.25 | 0.81 | 0.09 | 0.05 | 0.09 | 0.10 |
| MgO | 0.66 | 0.24 | 0.03 | 0.28 | 0.01 | 0.00 |
| MnO | 0.24 | — | — | — | — | — |
| Alkalis | — | — | 0.18 | — | 0.11 | — |
| Ig. loss | 0.77 | 0.19 | 0.09 | 0.35 | 0.10 | 0.00 |
| Total | 99.80 | 99.79 | 99.99 | 99.98 | 100.08 | 99.96 |

## Experimental

Several silica stones of different geological origins were adopted as samples (Table I, II). And experimental results were shown in Table III.

TABLE III

| (1) Silica stone sample | Firing atmosphere | (2) Firing temp. (°C) | (3) Hours heated (hr.) | (4) Apparent density after firing | (5) Residual quartz (%) | (6) Rate constant $k_1$ | (7) Half life time (hr.) | (8) Energy of activation (kcal.) | (9) Frequency coeff. ($sec^{-1}$) | $d_\alpha$ | $d_\alpha$ | $d_\beta$ |
|---|---|---|---|---|---|---|---|---|---|---|---|---|
| B | in air | 1203 | 2 | 2.658 | 96 | 0.0201 | 34 | 81 | $6.3\times10^{6}$ | 2.689 | 2.673 | 2.339 |
| | | 1300 | 2 | 2.598 | 80 | 0.113 | 6.1 | | | | | |
| | | 1431 | 2 | 2.394 | 19 | 0.838 | 0.8 | | | | | |
| | | 1540 | 2 | 2.338 | 0 | — | — | | | | | |
| | | 1540 | 4 | 2.339 | 0 | — | — | | | | | |
| C | in air | 1311 | 3 | 2.628 | 96 | 0.012 | 57 | 120 | $2.2\times10^{11}$ | 2.659 | 2.641 | 2.320 |
| | | 1395 | 3 | 2.510 | 62 | 0.158 | 4.4 | | | | | |
| | | 1450 | 3 | 2.363 | 15 | 0.633 | 1.1 | | | | | |
| | | 1550 | 1 | 2.319 | 0 | — | — | | | | | |
| | | 1550 | 4 | 2.321 | 0 | — | — | | | | | |
| D | in air | 1400 | 3 | 2.545 | 75 | 0.0953 | 7.3 | 123 | $1.05\times10^{15}$ | 2.666 | 2.638 | 2.300 |
| | | 1449 | $3\frac{8}{60}$ | 2.434 | 43 | 0.270 | 2.6 | | | | | |
| | | 1498 | 3 | 2.333 | 11 | 0.734 | 0.94 | | | | | |
| | | 1530 | 1 | 2.302 | 0 | — | — | | | | | |
| | | 1530 | 4 | 2.298 | 0 | — | — | | | | | |
| E | in air | 1240 | $3\frac{5}{60}$ | 2.615 | 98 | 0.00722 | 96 | 145 | $2.1\times10^{15}$ | 2.642 | 2.624 | 2.289 |
| | | 1277 | 3 | 2.599 | 94 | 0.0224 | 31 | | | | | |
| | | 1411 | 3 | 2.334 | 4 | 0.630 | 1.1 | | | | | |
| | | 1537 | 1 | 2.288 | 0 | — | — | | | | | |
| | | 1537 | 4 | 2.290 | 0 | — | — | | | | | |

| (1) Silica stone sample | Firing atmosphere | (2) Firing temp. (°C) | (3) Hours heated (hr.) | (4) Apparent density after firing | (5) Residual quartz (%) | (6) Rete constant $k_1$ | (7) Half life time (hr.) | (8) Energy of activation (kcal.) | (9) Frequency coeff. ($sec^{-1}$) | $d_0$ | $d_\alpha$ | $d_\beta$ |
|---|---|---|---|---|---|---|---|---|---|---|---|---|
| F | in air | 1448 | $5\frac{1}{2}$ | 2.609 | 92 | 0.0159 | 44 | 205 | $6.03\times10^{20}$ | 2.652 | 2.635 | 2.322 |
| | | 1498 | 3 | 2.559 | 78 | 0.084 | 8.2 | | | | | |
| | | 1520 | 3 | 2.498 | 60 | 0.171 | 4.1 | | | | | |
| | | 1538 | 3 | 2.443 | 42 | 0.292 | 2.4 | | | | | |
| | | 1650 | 1 | 2.320 | 0 | — | — | | | | | |
| | | 1650 | 4 | 2.324 | 0 | — | — | | | | | |
| B | in reducing atmosphere (0.2 atm. press. CO & 0.8 atm. press. $N_2$) | 1201 | 2 | 2.635 | 90 | 0.0534 | 13 | 68 | $1.8\times10^{5}$ | 2.690 | 2.673 | 2.340 |
| | | 1300 | 2 | 2.531 | 61 | 0.251 | 2.8 | | | | | |
| | | 1350 | 2 | 2.455 | 38 | 0.489 | 1.4 | | | | | |
| | | 1431 | 2 | 2.358 | 6.2 | 1.38 | 0.5 | | | | | |
| | | 1600 | 1 | 2.338 | 0 | — | — | | | | | |
| | | 1600 | 4 | 2.341 | 0 | — | — | | | | | |
| D | in water vapor | 1298 | 3 | 2.604 | 91 | 0.0310 | 22 | 96.2 | $0.79\times10^{12}$ | 2.666 | 2.638 | 2.299 |
| | | 1350 | 3 | 2.562 | 81 | 0.0752 | 9.2 | | | | | |
| | | 1400 | 3 | 2.449 | 47 | 0.248 | 2.8 | | | | | |
| | | 1451 | $3\frac{8}{60}$ | 2.356 | 19 | 0.538 | 1.3 | | | | | |
| | | 1500 | $3\frac{2}{60}$ | 2.314 | 4.7 | 1.006 | 0.69 | | | | | |
| | | 1540 | 1 | 2.297 | 0 | — | — | | | | | |
| | | 1540 | 4 | 2.301 | 0 | — | — | | | | | |

The sample stones (**1**) were fired at the given temperatres (**2**) during given hours (**3**). The fluctuation of the furnace temperature was ±5°C. Platinum boat was used when the stone was fired in air or in steam. When the stone was fired in the reducing atmosphere, samples were enclosed in a carbon capsule, and fired in the furnace tube which was packed with carbon granules. The density of the fired samples was determined by a pycnometer at 25±0.02°C (**4**). The experimental error in density determinations was 0.002 (0.1%). The difference between the apparent density and the true density was less than 0.01. The amount of the residual quartz (**5**) after firing was calculated from,

$$x = \frac{d_\alpha}{d_\alpha - d_\beta}\left(1 - \frac{d_\beta}{d}\right)\times 100 \qquad (4)$$

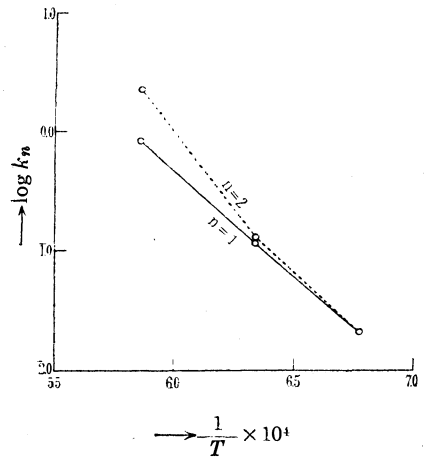



Fig. 1. Chert fired in air (Sample B).

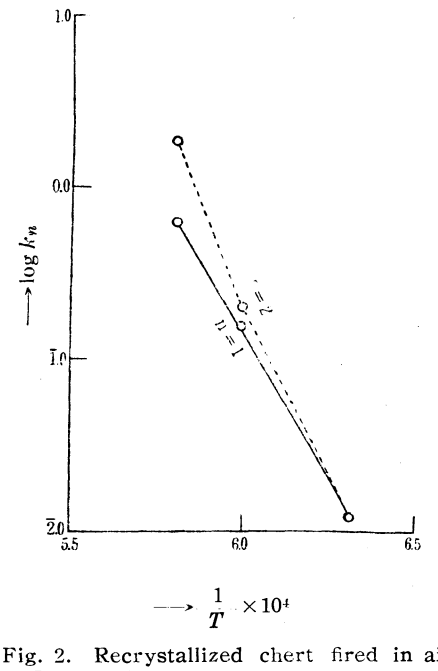



Fig. 2. Recrystallized chert fired in air (Sample C).

where $d_\alpha$ is the density when no quartz is converted (corrected as related later), $d_\beta$ is the density when all quartz is converted, and $d$ is the density at any time of firing. As is shown in the Figures 1, 2, 3, 4 and 5 linearity between

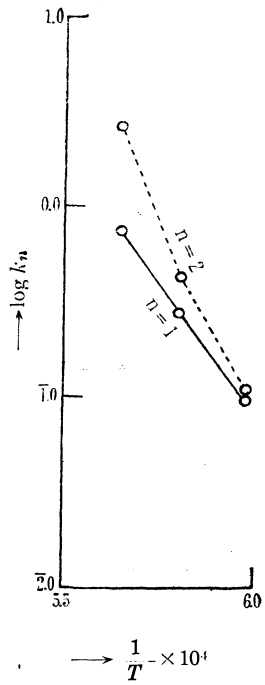



Fig. 3. Vein quartz with chert fired in air (Sample D).

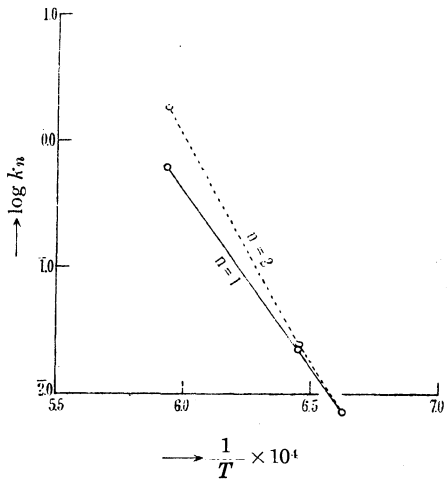



Fig. 4. Vein quartz fired in air (Sample E).

$\log k$ and $1/T$ is satisfied only for the primary reaction for all sorts of silica stone. Differential rate equations of the higher order, namely those of the third and 4th order etc., were calculated, but a larger deviation from the straight line was found to occur. Accordingly, the half life time (**7**), the energy of activation (**8**) and the frequency

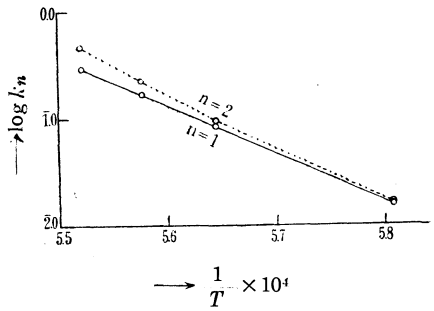



Fig. 5. Pegmatite quartz fired in air (Sample F).

coefficient (**9**) were calculated only from the rate constants of the primary reaction ($k_1$).

## Discussion

What is noteworthy is the contrast between vein quartz (Sample E) and recrystallized chert (Sample C). Vein quartz includes far less impurities, and its crystals are developed to such an extent as about one hundred times larger in diameter than those of recrystallized chert. Therefore, though intuitively the rate constant of vein quartz may seem smaller than that of the recrystallized chert, the experimental results indicate that the former is about three fold of the latter. Therefore, vein quartz is proved to be excellent as a refractory material; because of its extremely high rate of conversion notwithstanding its chemically high purity.

The rate of the chemical reaction of silicates is affected by reducing firing[5,6,7,8]. The conversion rate of silica stone was

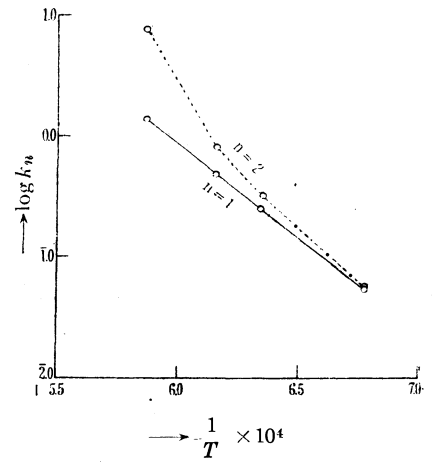



Fig. 6. Chart fired in reducing atmosphere (Sample B).

5) F. Thomas, *Chem. Ztg.*, **36**, 25 (1912).
6) S. Kondo, *J. Japan Cer. Ass.*, **29**, 367 (1918).
7) A. E. Vickers and L. S. Theobald, *Trans. Cer. Soc., (Engl.)*, **24**, 86, 98 (1924-5).
8) A. E. Badger, *J. Am. Cer. Soc.*, **16**, 107 (1933).

determined in reducing atomospher also. Linearity between $\log k$ and $1/T$ existed only for the primary reaction (Fig. 6). The rate was compared with that in air (Fig. 7.). In

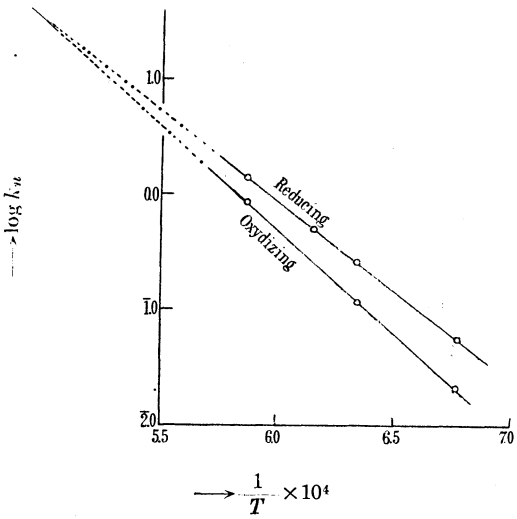



Fig. 7. Rate of conversion of chert in reducing firing compared with that in oxidizing firing (Sample B).

reducing atmosphere, the rate constant had always higher value than that in air (oxidizing). The difference is decreased as the temperature rises, and at about 1730°C, diminishes to zero.

The reaction rate of silicates is considerably

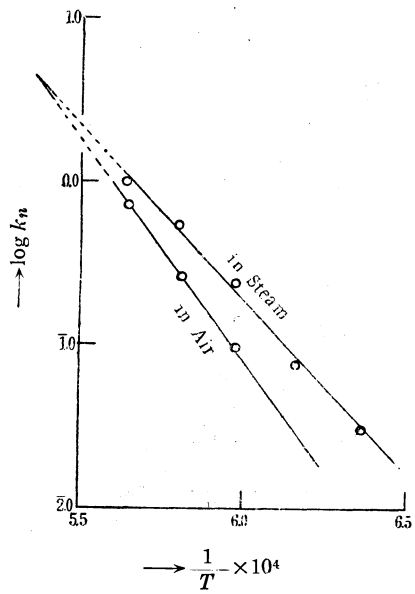



Fig. 8. Comparison of conversion rate of silica stone in steam with that in air (Sample D).

accelerated by the presence of water vapor[9]. It was attempted to find the rate constant of the conversion of silica stone in water vapor. Linearity between $\log k$ and $1/T$ is satisfied also for the primary reaction in the presence of water vapor of one atmospheric pressure. The rate of the conversion in water vapor of one atmospheric pressure was compared with that in air which contains water vapor of about ten mm Hg (Fig. 8). In steam, the rate constant had higher value than that in air. The difference is decreased as the temperature rises, and at about 1600°C, diminishes to zero.

From the density determinations by Nakai and Fukami[2], the rate constants $k$ were calculated using a primary ($k_1$) or secondary ($k_2$) rate equation, whereby the uniformity of the rate constants could be obtained only when the primary rate equation was adopted (Table IV). Jander's rate constant $k_J$ was

TABLE IV
FIRING AT A CONSTANT TEMPERATURE
(1400°C±10)

| Hours heated | Density[2] | $k_1$ | $k_2$ | $k_J$ |
|---|---|---|---|---|
| 0 | 2.648 | — | — | — |
| 5 | 2.553 | 0.063 | 0.073 | 0.0020 |
| 10 | 2.483 | 0.065 | 0.092 | 0.0038 |
| 15 | 2.415 | 0.079 | 0.149 | 0.0067 |
| 20 | 2.388 | 0.076 | 0.18 | 0.0075 |
| 30 | 2.368 | 0.064 | 0.19 | 0.0066 |
| 40 | 2.354 | 0.056 | 0.21 | 0.0064 |
| 50 | 2.340 | 0.057 | 0.33 | 0.0069 |
| 60 | 2.332 | 0.062 | 0.67 | 0.0072 |
| 70 | 2.327 | 0.059 | 0.87 | 0.0066 |
| 80 | 2.322 | — | — | — |

also calculated using his well-known equation,

$$(1-\sqrt[3]{x})^2=k_J t \qquad (5)$$

and tabulated in Table IV. The deviation of $k_J$ was large at the early stage of the reaction. According to his diffusion theory, closer agreement between his equation and experimental results is to be expected in the earlier period of the reaction. On the contrary, however, greater deviations have appeared in an earlier period of the reaction. This proves that his theory is not applicable to the conversion of silica stone.

**Grain size.**—Influence of grain size on the reaction rate must be considered when solid reaction is treated. The writer obtained the following results. As a sample, the author used grains of vein quartz washed by concentrated hydrochloric acid and water repeat-

9) R. Smoluchowski, "Phase Transformations in Solids", John Willy & Sons, Inc., New York, 1951, p264, 267, 276.

edly. Coarse grains were mixed with fine grains of the same quantity, put in a platinum boat, and the mixture was fired twice in the furnace. After cooling down, the grains were separated from each other, and densities were determined (Table V). For

TABLE V
INFLUENCE OF GRAIN SIZE ON THE RATE OF THE CONVERSION

| | Coarse grains | Fine Grains |
|---|---|---|
| Diameter (mm.) | 9–7 | 1–0.4 |
| Apparent density (unfired) | 2.640 | 2.642 |
| Apparent density (fired once) | 2.608 | 2.608 |
| Apparent density (fired twice) | 2.572 | 2.571 |

particles of diameter between 9 and 0.4 mm., decrease of density was equal within the experimental error; accordingly, the rate of conversion is uniform. Particles of these sizes were used all through our experiments. Jander's relation[10]

$$k \backsim 1/\delta^2 \qquad (6)$$

was not applicable to the conversion of silica stone.

For the rate of the conversion of silica stone (polycrystal aggregates), the following five factors are significant.

1. Area of the macroscopic surface of grains.
2. Distribution of imperfections in crystals.
3. Degree of solid solution.
4. Liquid and gaseous inclusions.
5. Area and condition of boundary surface between single crystals.

(A) When the factor 1. is the rate-determining step, Jander's relation (5) is applicable. For example, when fine powder of very pure, perfect, single crystals is used as a sample, or when very effective liquid mineralizer is used, this is perhaps true.

(B) When the factors 2., 3., and 4. were the rate-determining steps, the rate of conversion would have nothing to do with grain size.

(C) When the factor 5. is the rate-determining one,

($C_1$) if the grain is polycrystalline, the rate of conversion follows (B),

($C_2$) if the grain is a single crystal, the rate of conversion follows (A).

Silica stones as raw materials for fire bricks, the writer supposes, belong to group (B) or ($C_1$).

**Irreversible Expansion of Aggregates.**— Silica stone is an aggregate made up of anisotropic quartz crystals. Therefore, correction must be made on the irreversible thermal expansion of aggregates[11,12] when we wish to determine the quantity of residual quartz by the apparent density determinations. As is shown in Fig. 9[13] above 800°C, the value

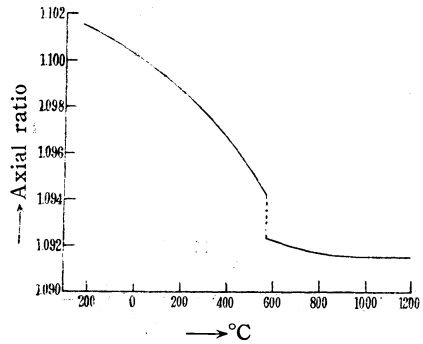



Fig. 9. The thermal variation of the axial ratio of quartz after Sosman[13].

of axial ratio is kept almost constant. On the other hand, it is hardly possible for the sluggish inversion of silica stone without mineralizer to proceed below 1100°C. Therefore, when fired within the temperature interval of 800—1100°C, they show the diminution of density ($\Delta d$), in spite of the fact that no sluggish inversion occurred.

Now $\Delta d$ was determined experimentally, and it was found that silica stone always shows about the same degree of density diminution (0.60–0.64%) when fired in the temperature interval mentioned above, regardless of its mode of occurrence and origin. Assuming that the orientation of each crystal is completely random, this density diminution is calculated to be 0.75% from the data[13] of the axial ratio. Therefore, experimental data and calculated value are in good agreement. From this $\Delta d$, $d_\alpha$ was calculated by the following formula,

$$d_\alpha = d_0 - \Delta d \qquad (7)$$

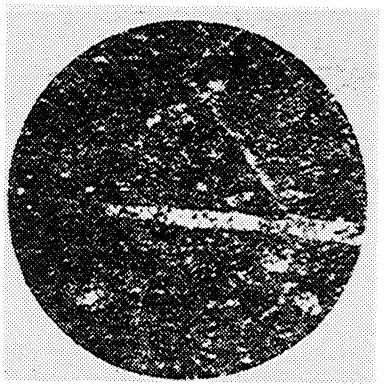
in which, $d_0$ is the density of the unfired sample.

10) W. Jander, *Z. anorg. allg. Chem.*, **163**, 1 (1927).

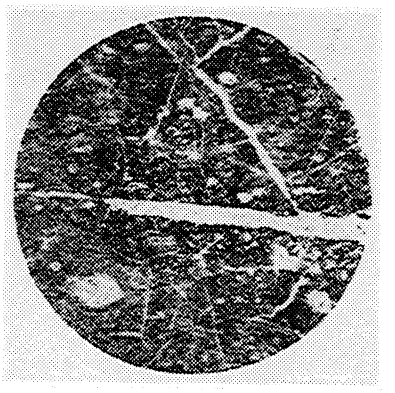
11) J. B. Austin, *J. Am. Cer. Soc.*, **35**, 243 (1952).

12) R. B. Sosman, "The Properties of Silica", The Chemical Catalog Company, New York, 1927, p. 388.

13) ibid., p. 375.

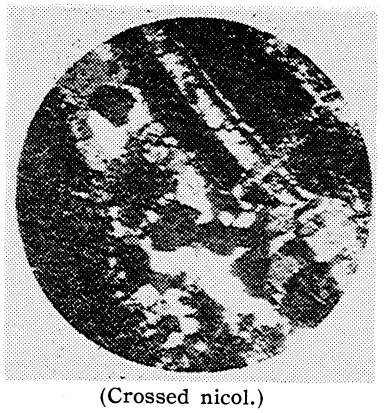


(Crossed nicol.)

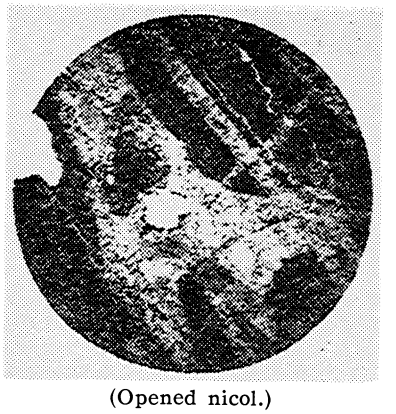


(Opened nicol.)

Fig. 10. Photomicrographs of radiolarian chert. (×40, Sample A; Kuroda, Japan.)
Elliptical spots of various sizes is the pseudomorphs of Radiolaria by substitution.

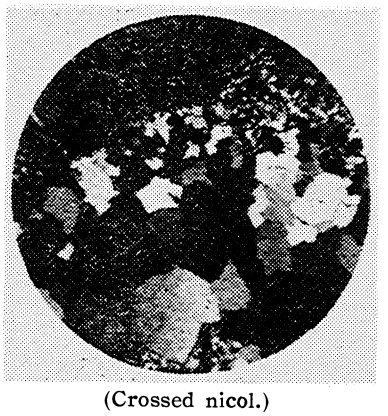


(Crossed nicol.)

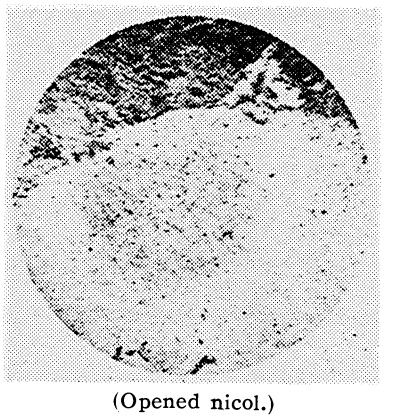


(Opened nicol.)

Fig. 11. Photomicrographs of chert. (×50, Sample B; Tamba, Japan.)

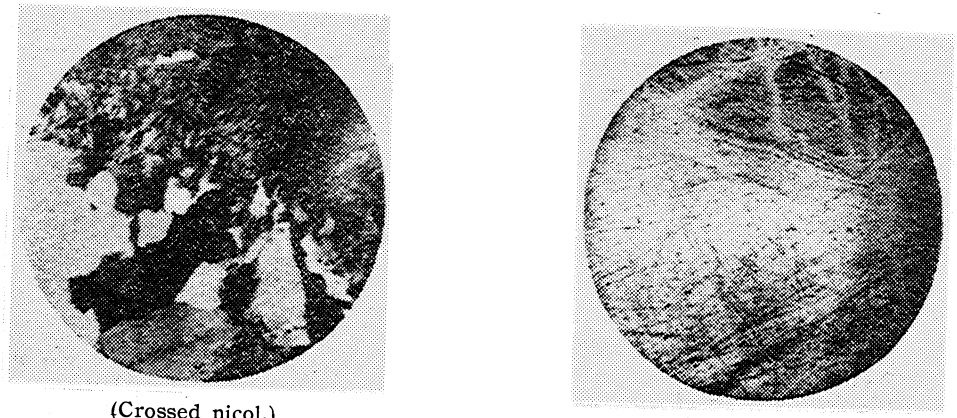


(Crossed nicol.)



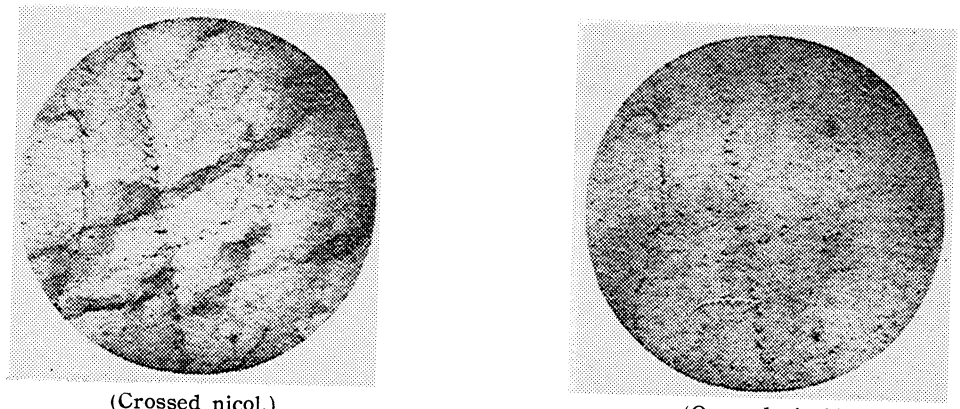
(Opened nicol.)

Fig. 12. Photomicrographs of recrystallized chert with vein quartz. (×40, Tamba, Japan.)
Upper part of the photographs show recrystallized chert (Sample C), and lower part of the photographs show vein quartz (Sample E).



(Crossed nicol.) (Opened nicol.)

Fig. 13. Photomicrographs of vein quartz with chalcedonic chert. (×40, Sample D; Youra, Japan.)
Upper part of the photographs is chalcedonic chert, and lower part is vein quartz.



(Crossed nicol.) (Opened nicol.)

Fig. 14. Photomicrographs of pegmatite quartz. (×40, Sample F; Fukushima, Japan.)
The photograph by crossed nicol reveals mosaic structures.

## Summary

(1) It was found that the soluggish inversion of silica stones of different geological origins, from quartz to cristobalite, was the primary reaction when fired in air, in steam or in reducing atmosphere of carbon monoxide.

(2) Effect of firing atmosphere on the conversion rate of silica stone was investigated.

(3) Influence of grain size on the rate of conversion was investigated, and it was found that Jander's, relation $k \backsimeq 1/\delta^2$ was not applicable to the conversion of silica stone.

(4) Irreversible thermal dilatation of anisotropic aggregates was examined, and the necessary correction to determine the conversion rate by determination of the density was devised.

The author would like to express his hearty thanks to Prof. Takeo Ao of Osaka University for his kind guidance and encouragement throughout this work.

*The Institute of Scientific and Industrial Researches, Osaka University, Osaka*

# SHORT COMMUNICATIONS

## *Reaction of Si-Si Bond in Hexaisopropoxydisilane with Sodium Methylate*

By Ukiko TAKAHASHI

(Received March 10, 1955)

Recently, Ōkawara and his co-workers[1] reported on the preparation of alkoxydisilanes in pure state, and they pointed out the uncertainty of volumetric determination of hydrogen evolved by the cleavage of the Si-Si bond with basic reagents. I wish to report on the possibility of determining the Si-Si bond by volumetric method when the bond is cloven by sodium methylate.

Isopropoxydisilane is the only reliable alkoxydisilane to be taken as a standard sample, for it is obtained in crystalline state and can be purified by recrystallization from the contaminating liquid materials, especially, hexaisopropoxydisiloxane which has the boiling point close to that of disilane. In this experiment, the recrystallized isopropoxydisilane having the melting point 86.0°C (reported[1], 84.7°C) was used. Calcd. for $(C_3H_7O)_6Si_2$: Si, 13.68%. Found: Si, 13.73%. Sodium methylate solution was prepared by edding sodium metal to the completely dehydrated methanol. Methanol was dehydrated with magnesium and distilled through a Stedman column of about 20 theoretical plates, any contamination of moisture being carefully prevented.

With 2.8N$CH_3ONa$ solution and isopropoxydisilane the reaction proceeded rapidly in Zerewitinoff apparatus at 13°C, but with 0.6 N-$CH_3ONa$ the reaction was slow and completed in forty hours at the same temperature.

Anal. $H_2$ evolved from 0.3554 g. of $(C_3H_7O)_6Si_2$ and 6 cc. of 2.8 N-$CH_3ONa$ solution: Calcd. vol., 19.39 cc. Found vol. 19.40 cc. (corrected), 21.97 cc. (uncorrected).

Since the hydrogen evolved was replaced by methanol, the vapor pressure of methanol was taken account of in the volume correction.

In this experiment, care should be taken to use completely dehydrated methanol in preparing sodium methylate solution. For if an incompletely dehydrated methanol is used, the solution becomes turbid at the early stage of the reaction with disilane and the volume of hydrogen can not attain the calculated value. It is to be considered that, for the same reason, the volumetric determination of alkoxydisilanes will give inconsistent results[1] with the basic reagents containing water which will cause flocculent precipitate or gelation of disilanes.

1) R. Ōkawara, T. Tanaka and K. Maruo, This Bulletin **28**, 189 (1955).

*Osaka Prefectural Kozu Senior High School, Higashi-Kozu Kitanocho, Tennoji-ku, Osaka*

## *Influence of Substituent Groups on Nuclear Reactivity in Formation of Substituted Biphenyls through Reactions of Aromatic Diazo and Cognate Compounds with Aromatic Liquids. IV*[1]*. The Methyl Group*

By Osamu SIMAMURA and Takashi INUKAI

(Received May 24, 1955)

In a paper, which has very recently become available, Hey, Pengilly and Williams[2] reported partial rate factors for the phenylation of toluene by phenyl radicals generated from benzoyl peroxide at 80°. This prompts us to publish the results of our study which we have been carrying out on a similar subject. Our experimental methods were different from those of the British workers in that our source of the phenyl radical was N-nitrosoacetanilide and that the competition between toluene and benzene for the radical generated was investigated.

N-Nitrosoacetanilide (6.7 g., 40.8 millimoles) was dissolved in a mixture of 225 cc. of benzene and 271 cc. of toluene (both 2.55 moles) at 21°; the decomposition of the nitroso compound set in immediately evolving nitrogen. After a few days, when the reaction had been completed, the reaction mixture was washed successively with aqueous sodium hydrogen carbonate, 10% sodium hydroxide, dilute hydrochloric acid and water. The solvent was then removed from the solution dried with calcium chloride by distillation through a Vigreux column 30 cm. in length. The residue was subjected to steam distillation, and the distillate, combined with the residue from the redistillation of the solvent recovered mentioned above, was fractionally distilled under reduced pressure, giving a small amount of toluene and then a fraction (I, 1.891 g.) boiling at 122–135° at 20 mmHg which consisted of biphenyl and methylbiphenyls. The residue (30 mg.) was almost pure *p*-methylbiphenyl, m.p. 46–48°. The fore- and after-runs of fraction I, which were combined together, amounted to 0.326 g. (fraction II). The compositions of fractions I and

II as determined by infra-red spectrophotometry were found to be as follows:

| Fraction | Methylbiphenyls (%) | | | Biphenyl (%) |
|---|---|---|---|---|
| | *o* | *m* | *p* | |
| I | 51 | 9.2 | 4.1 | 37 |
| II | 31 | 25 | 15 | 28 |

Thus, the total quantities of *o*-, *m*- and *p*-methylbiphenyls and biphenyl itself amounted to 1.053, 0.255, 0.156 and 0.782 g., respectively; and consequently the ratio of the isomeric methylbiphenyls was *o*: *m*: *p*=72: 17.4: 10.6[3]. From these data, the relative reactivities of the ortho, meta and para positions of toluene are calculated to be 3.7, 0.9 and 1.1, respectively, the reactivity of one nuclear position of benzene itself being taken as unity. These values are to be compared with those found by Hey and his collaborators, i.e., 4.1, 1.0 and 1.4. The general agreement between the two sets of values is of interest in view of the difference in experimental methods.

1) Part III, O. Simamura and T. Migita, This Bulletin, 27, 228 (1954).

2) D. H. Hey, B. W. Pengilly and G. H. Williams, *J. Chem. Soc.*, **1955**, 6.

3) Note added in proof—After the submission of this communication two papers by R.L. Dannley and B. Zaremsky *J. Am. Cnem. Soc.*, 77, 1588 (1955), and by C.S. Rondestvedt and H.S. Blanchard, ibid., 1769, came to our attention. The former reported the isomer composition of methylbiphenyls obtained by phenylation of toluene by the decomposition of benzoyl peroxide to be *o*: *m*: *p*=65: 19: 16; and the latter gave very similar values, *o*: *m*: *p*=62: 20: 18, for phenylation by nitrosoacetanilide.

*Department of Chemistry,*
*Faculty of Science,*
*Tokyo University,*
*Tokyo*

## *A Note on the Preparation of Alkali Cyanide from Barium Carbonate*

By Masaru Hasegawa, Naoki Inamoto and Osamu Simamura

(Received May 24, 1955)

Numerous methods[1] have hitherto been described of the preparation of alkali cyanide-$C^{14}$ from radioactive carbon dioxide or carbonate, because that cyanide is one of the most important materials for the synthesis of organic compounds labelled with carbon-14. No available methods are, however, satisfactory in every respect, for it is desirable that the apparatus and operation should be simple and the yield high on a micro or small-scale preparation suitable for work with radioactive carbon-14. Jeanes[2] has recently reported a convenient synthesis of sodium cyanide directly from barium carbonate. In his synthesis, barium carbonate, zinc dust and sodium were heated at 650° in a stream of ammonia which had been passed over hot iron; and it was claimed that the yield of sodium cyanide was quantitative. This method appeared very attractive, involving only a simple apparatus and eliminating the need for intermediate preparation of carbon dioxide or alkali carbonate. In our hands, however, it gave yields ranging only from 63 to 65%, in spite of repeated trials closely following Jeanes's procedure. We have now found that the use of potassium instead of sodium gives invariably 90 to 100% yields of potassium cyanide.

Our procedure, which is essentially similar to that of Jeanes[2], is as follows: An intimate mixture of 200 mg. of barium carbonate and 1 g. of zinc dust is placed in a porcelain boat together with 0.40 g. of potassium cut in small pieces. The boat is inserted into a quartz tube (700 mm. in length and 17 mm. inside diameter) until it touches a loosely wound prolate ball of iron wire (10 g., 0.3 mm. in diameter), which has been placed beforehand at the middle of the tube. Anhydrous ammonia is introduced into the tube at the end nearest the iron wire, and the tube is heated at 650° for four hours. It is then allowed to cool while ammonia is being passed through it. Subsequently, the product is worked up according to the usual procedure: hydrogen cyanide is distilled by heating the reaction mixture with dilute sulfuric acid and is absorbed in 1N alkali hydroxide. Yields were estimated by titration with a standard silver nitrate solution.

Typical results are given in the accompanying table, which also includes the results of experiments without zinc dust. Zinc does not seem to be essential for the preparation, but in its presence the highest yield of cyanide is secured.

Experimental conditions and yields of alkali cyanide

| No. | $BaCO_3$ (mg.) | Zn (g.) | Alkali metal (g.) | Yield based on $BaCO_3$ (%) |
|---|---|---|---|---|
| 1 | 200 | 1.0 | Na 0.29 | 63.3 |
| 2 | 202 | 1.0 | Na 0.28 | 64.5 |
| 3 | 201 | 1.0 | K 0.40 | 100.0 |
| 4 | 200 | 1.0 | K 0.35 | ca. 93 |
| 5 | 201 | 0 | K 0.41 | 83.2 |
| 6 | 200 | 0 | K 0.38 | 82.2 |
| 7 | 199 | 0 | Na 0.24 | 61.7 |

We are indebted to the Ministry of Education for a Grant-in-Aid for Scientific Research.

1) See, e.g., F. L. J. Sixma, H. Hendriks, K. Helle, U. Hollstein and R. Van Ling, *Rec. trav. chim.*, **73**, 161 (1954), in which are summarized the available methods.
2) J. K. Jeanes, *Science*, **118**, 719 (1953).

*Department of Chemistry,*
*Faculty of Science,*
*Tokyo University,*
*Tokyo*

## *A New Preparation of Catalytic Nickel*

By Yoshiyuki URUSHIBARA, Shigeo NISHIMURA, and Hideo UEHARA

(Received June 17, 1955)

The nickel catalyst which is now named Urushibara nickel B or U-Ni-B in abbreviation is prepared by adding aqueous nickel chloride to an excess of zinc dust and digesting the precipitated nickel with aqueous caustic alkali[1),2)]. The activity of the catalyst depends largely on the method of precipitation. A high temperature, a concentrated solution of nickel chloride, and a quick addition of the solution to the zinc dust with vigorous stirring, namely conditions favoring the precipitation of finely divided nickel, produce a high activity. The precipitated nickel shows a high catalytic activity only after being treated with caustic alkali. The nature of the activating effect of caustic alkali, however, has not yet been elucidated.

In this paper another new hydrogenating nickel catalyst, named Urushibara nickel A or U-Ni-A in abbreviation, is announced.

The solids from aqueous nickel chloride and zinc dust, prepared in the same way as in the preparation of U-Ni-B[2)], are collected on a glass filter, washed with hot distilled water, and treated with acetic acid or propionic acid instead of caustic alkali. For instance, the solids from 4.04 g. of nickel chloride and 10 g. of zinc dust, after being washed with hot distilled water, are quickly transferred into 160 cc. of 13% acetic acid without heating. When the generation of hydrogen gas subsides, the solids are again collected on a glass filter, washed with distilled water of 50–60° and then with the solvent of hydrogenation, and transferred into the hydrogenating vessel. Contact with air is avoided as far as possible. In this way very active U-Ni-A is obtained.

While the U-Ni-B contains a large proportion of metallic zinc, the U-Ni-A contains only a little, if any, and has a much smaller bulk. The new U-Ni-A acts very well, for instance, in the catalytic reduction of nitrobenzene to aniline and of ethyl cinnamate to ethyl hydrocinnamate. The U-Ni-B is very active in the reduction of ketones and also in the reduction of nitrobenzene if it is washed thoroughly, while the U-Ni-A exhibits excellent activity in the reduction of ketones if a small amount of caustic alkali is added.

The same precipitated nickel acquires a high activity on treatment with either caustic alkali or acetic acid. Thus, it is very probable that the activating effect of these reagents consists in uncovering the inherently active nickel surfaces, but not in creating any active substances or state on the surfaces. The precipitated nickel, as it is precipitated, contains zinc hydroxide and basic zinc chlorides besides excessive metallic zinc. It is concluded from the facts stated below that the basic chlorides must be removed in order to recover the active surfaces.

Caustic alkali quickly removes the basic chlorides from the precipitated nickel, and digestion with an amount of aqueous caustic alkali insufficient to dissolve completely the colloidal hydroxide and metallic zinc gives a quite active catalyst. On the other hand, the far less active solids prepared with an insufficient amount of acetic acid release again chloride ions on further treatment with acetic acid and become highly active[3)]. For obtaining a highly active nickel with acetic acid, such an amount as is sufficient to dissolve nearly completely the metallic zinc and partly even the nickel is necessary. Stronger acids, for instance, formic acid and hydrochloric acid, are not suitable for producing catalytic activity.

1) Y. Urushibara, This Bulletin, 25, 280 (1952).
2) Y. Urushibara, and S. Nishimura, ibid., 27, 480 (1954). For the exact procedure see loc. cit.
3) Added in proof: Basic zinc acetate also diminishes the activity, because the U-Ni-B loses partly its activity on treatment with insufficient acetic acid but regains the original activity when treated with sufficient acetic acid.

*Department of Chemistry, Faculty of Science, Tokyo, University, Tokyo*

## *Absorption Spectra of Molecular Compounds of Diethyl Ether with Several Metallic Chlorides*

By Sohachiro HAYAKAWA

(Received March 22, 1955)

Some metallic chlorides such as aluminum chloride or stannic tetrachloride produce stable molecular compounds with diethyl ether. Dipole moments of some of them were measured in non-polar solvents by several investigators[1]; however, no spectroscopic data are obtainable at all. The author measured the absorption spectra of the molecular compounds in solutions of ether and *n*-heptane.

**Apparatus.**—Shimadzu Photoelectric Spectrophotometer Type QB-50 (the measured range of wave number, 45,000-17,000 kayser[2]; quartz cell length, 1.00 cm.; temperature, 10-15°C).

**Materials.**—Anhydrous aluminum chloride, of commercial highest class, was sublimed in a current of dry nitrogen gas, and the product was resublimed directly into sample tubes. Anhydrous ferric chloride was purified similarly in an atmosphere of chlorine instead of nitrogen. Anhydrous zinc chloride, of highest purity, was heated in dry air and dehydrated by phosphoric pentoxide. Anhydrous stannic and titanium tetrachlorides were fractionally distilled twice. Diethyl ether of the commercial product was distilled fractionally several times in an atmosphere of dry air by a Wydmer's distillator. Heptane was purified by the Potts' method[3].

### Results and Discussion

Absorption spectra of the solutions of aluminum chloride, zinc chloride and titanium

tetrachloride in diethyl ether are shown in Fig. 1. Absorption spectra of the solutions of aluminum chloride-ether, stannic chloride-

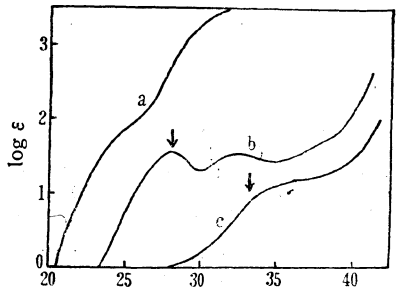



Fig. 1. Absorption curves of solutions of $TiCl_4$ (curve a), $AlCl_3$ (curve b) and $ZnCl_2$ (curve c) in diethyl ethep expressed in extinction coefficient. (ε's are expressed as values per mole of chlorides)

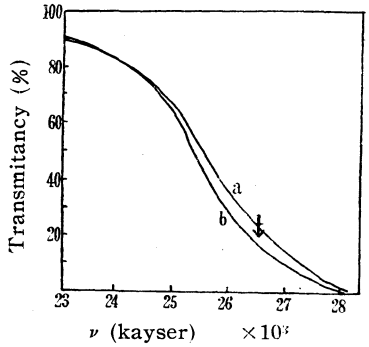



Fig. 2. Absorption curves of solutions in heptane, which is saturated by $AlCl_3$, of 0.02M ether (curve a) and of 0.2M ether (curve b).

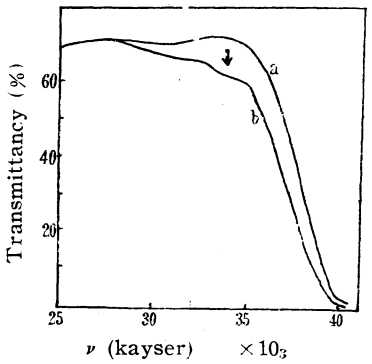



Fig. 3. Absorption curves of solutions in heptane of 0.01 M $SnCl_4$ and 0.01 M ether (curve a) and of 0.01 M $SnCl_4$ and 0.1 M ether (curve b).

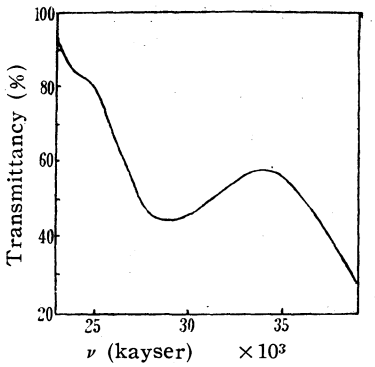



Fig. 4. Absorption curve of saturated soluton of $FeCl_3$ in heptane containing 0.1 M ether.

ether and ferric chloride-ether in heptane are shown in Fig. 2, 3 and 4 respectively. The extinction coefficient could not be determined from the spectra of solutions in heptane because of slight solubilities of the chlorides in heptane.

The author regards the absorption bands marked by arrows in the figures as the characteristic absorption of the molecular compounds. However, for the solutions of titanium tetrachloride and ferric chloride, none could be concluded for lack of exact informations about the spectra of titanium and ferric chlorides themselves, although their solutions showed remarkable absorptions. The ultra-violet absorptions obtained for the molecular compounds of aluminum, stannic and zinc chlorides are considered to correspond to the intermolecular charge transfer spectra defined by R.S. Mulliken[4].

The author expresses his hearty thanks to Prof. S. Makishima for his kind guidance throughout this work.

1) H. Ulich et al, *Z. Angew. Chem.*, **44**, 750 (1931); *Z. phys. Chem.*, **B17**, 21 (1932); W. Nespital, *Z. phys. Chem.*, **B16**, 153 (1932); T. J. Lane et al, *J. Am. Chem. Soc.*, **64**, 2076 (1942); L. A. Woodward and D. A. Long, *Trans. Farady Soc.*, **45**, 1131 (1949).

2) Kayser (formerly $cm^{-1}$). See Transactions of the Joint Commission for Spectroscopy, *J. Opt. Soc. Am.*, **43**, 410 (1953).

3) W. J. Potts, *J. Chem. Phys.*, **20**, 809 (1952).

4) R. S. Mulliken, *J. Am. Chem. Soc.*, **74**, 811 (1952), **76**, 386 (1954); *J. Phys. Chem.*, **56**. 801 (1952).

*Institute of Science and Technology,*
*Tokyo University,*
*Tokyo*

# *Alkaline Iodine as an Oxidant for Uranium. IV.*

By G. S. DESHMUKH and M. K. JOSHI

(Received January 10, 1955)

New volumetric methods of estimating uranium based on the reduction of U(VI) to U(IV) and re-oxidation of the latter by selenious acid or alkaline ferricyanide have been recently reported from our Laboratories[1,2]. In these procedures uranium was actually determined by performing iodometric titrations of the excess oxidising agents and also by estimating the products. Thus in the selenious acid method the metallic selenium was weighed and in the ferricyanide procedure the $K_4Fe(CN)_6$ formed was titrated directly with standard solution of $Ce(SO_4)_2$.

The oxidising action of iodine in alkaline medium is well known[3,4]. Its use as an oxidant for tetravalent uranium, however, finds little mention in the existing literature. Preliminary experiments showed that when an aqueous solution of iodine in KI was added to uranous sulphate solution followed by NaOH, rapid oxidation of U(IV) to U(VI) occurred. It was interesting therefore to study this redox process in some detail and utilize it for the quantitative determination of uranium.

## Experimental

Uranyl sulphate solution was prepared by dissolving E. Merck's extra pure sodium uranate in sulphuric acid. Its uranium content was determined by the classical oxinate method. An aliquot volume of the uranyl sulphate solution was taken in a stoppered flask and reduced by means of pure zinc and $H_2SO_4$ in the cold. It was allowed to stand for about 15 minutes until the yellow colour of the uranyl sulphate changed to apple green characteristic one of the uranous sulphate. The contents of the flask were filtered through a Gooch crucible and the unreacted zinc was washed several times with dilute $H_2SO_4$ and then with distilled water. A stream of air was now bubbled through the cold uranous solution for five minutes to oxidise any U(III) formed to U(IV)[5].

An inert atmosphere was maintained by passing a slow stream of nitrogen gas, and a measured excess of standard iodine solution was added and then followed by 3N NaOH solution until a yellow precipitate was obtained. The contents of the flask were left over for 15~20 minutes, acidified and the unreacted iodine was determined in the usual way by titration with standard thiosulphate to the starch end point. In another set, the alkali was just neutralised with dilute $H_2SO_4$, followed by an excess of borax-boric acid buffer to maintain a pH 8~10 appropriate for iodine-arsenite reaction. The buffer solution was prepared by dissolving 8% and 4% by weight of crystallised borax and pure boric acid respectively in water as recommended by Chapin[6]. The unused iodine was then titrated with standard $As_2O_3$ solution to the starch end point.

The difference in the volume of thiosulphate and arsenious oxide before and after the reaction thus corresponds to the iodine consumed for the

TABLE I

| Expt. No. | Normality of $Na_2S_2O_3$(N) | Vol. of Thio$=I_2$ reacted (ml.) | Normality of $As_2O_3$(N) | Vol. of $As_2O_3=I_2$ reacted (ml.) | Weight of uranium (g.) Oxinate method (x) | $Na_2S_2O_3$ Method (a) | $As_2O_3$ Method (b) | Difference x—a | x—b |
|---|---|---|---|---|---|---|---|---|---|
| 1. | 0.09781 | 25.80 | 0.1000 | 25.25 | 0.3008 | 0.3006 | 0.3007 | 0.0002 | 0.0001 |
| 2. | 0.1000 | 20.20 | 〃 | 20.20 | 0.2406 | 0.2406 | 0.2406 | nil | nil |
| 3. | 0.08322 | 21.30 | 〃 | 17.75 | 0.2118 | 0.2113 | 0.2113 | 0.0005 | 0.0005 |
| 4. | 0.1030 | 15.20 | 〃 | 15.65 | 0.1866 | 0.1866 | 0.1864 | nil | 0.0001 |
| 5. | 0.1000 | 10.10 | 〃 | 10.10 | 0.1203 | 0.1203 | 0.1203 | nil | nil |
| 6. | 0.08320 | 10.65 | 〃 | 8.85 | 0.1059 | 0.1056 | 0.1054 | 0.0003 | 0.0005 |
| 7. | 0.1030 | 7.60 | 〃 | 7.825 | 0.09330 | 0.09330 | 0.09320 | nil | 0.0002 |
| 8. | 0.1000 | 5.05 | 〃 | 5.05 | 0.06015 | 0.06015 | 0.06015 | nil | nil |
| 9. | 0.1030 | 4.15 | 〃 | 4.55 | 0.05401 | 0.05403 | 0.05419 | 0.0002 | 0.00018 |
| 10. | 0.05000 | 5.05 | 0.05000 | 5.05 | 0.03006 | 0.03007 | 0.03007 | 0.00001 | 0.00001 |
| 11. | 0.06035 | 3.65 | 〃 | 4.40 | 0.02635 | 0.02624 | 0.02620 | 0.00011 | 0.00011 |

1) G. S. Deshmukh and M. K. Joshi, *Z. anal. Chem.*, **143**, 334—339 (1954).
2) G. S. Deshmukh and M. K. Joshi, *Ber.* **88**. 186—187 (1955).
3) E. Rupp, *Arch. Pharmaz*, **245**, 6 (1907).
4) Abel, *Z. anorg. allgem. Chem.*, **76**, 396 (1912).
5) A. I. Vogel, "A Text-Book of Quantitative Inorganic Analysis", Longmans, Green and Co., London, p. 318 (1951).
6) R. M. Chapin, *J. Am. Chem. Soc.*, **41**, 351 (1919).

oxidation of U(IV) to U(VI). The amount of uranium was calculated as follows,

$I_2+2NaOH \longrightarrow 2NaI+H_2O+O$ .....(i)

$UOSO_4+O \longrightarrow UO_2SO_4$. .....(ii)

Thus, $1U \equiv I_2 \equiv 2Na_2S_2O_3 \equiv 2/1As_2O_3$.

It follows that 1 ml. of 0.1 N $Na_2S_2O_3$ or $As_2O_3$ is equal to 0.01191 g. of uranium. Results of a series of experiments are returned in Table I. It will be seen that they are in fair agreement with those obtained by the classical oxinate procedure.

Iodine reacts with hydroxyl ions to form iodide and the extremely unstable hypoiodite; the latter is rapidly converted into iodate and iodide by self-oxidation-reduction[7].

$I_2+2OH^- \rightleftarrows I^-+IO^-+H_2O$ .....(iii)

$3IO^- \rightleftarrows 2I^-+IO_3^-$ .....(iv)

Since reaction (ii) is very fast and iodate rarely acts as an oxidising agent in alkaline medium, it is evident that tetravalent uranium is oxidised to the hexavalent state by hypoiodite, which in turn is reduced to iodide. After the oxidation process is completed and the system is acidified, an amount of iodine equivalent to the iodate formed is libereted according to the following equation,

$5NaI+NaIO_3+3H_2SO_4 \longrightarrow 3I_2+3Na_2SO_4+3H_2O$ (v)

This is titrated with standard $Na_2S_2O_3$ or $As_2O_3$ which corresponds to the unreacted iodine.

Titrations of U(IV) to U(VI) are generally carried out at elevated temperatures and involve the risk of aerial oxidation[8,9]. Since in the present method an excess of the oxidant is used in an inert atmosphere this possibility is eliminated. An additional advantage of this method, besides its simplicity and accuracy, is the use of $As_2O_3$, as a primary standard.

## Summary

A new method for the determination of uranium based on the reduction of U(VI) to U(IV) and re-oxidation of the latter by alkaline iodine is described. The excess iodine is titrated with standard $Na_2S_2O_3$ or $As_2O_3$ and the results are found to be accurate and reproducible.

The authors are indebted to Prof. S. S. Joshi for facilities given to them and kind interest in the work. The award a U. P. Scientific Research Committee Scholarship (to M. K. J.) is also gratefully acknowledged.

*Department of Chemistry, Banaras Hindu University, Banaras, India*

7) A. I. Vogel, "A Text-Book of Quantitative Inorganic Analysis", Longmans, Green and Co., London, p. 329 (1951).

8) N. Birnbaum and S. M. Edmonds, *Ind. Eng. Chem., Anal. Ed.*, **12**, 155 (1940).

9) E. Miller and A. Flath, *Z. Elektrochem.*, **29**, 500 (1923).

# *A New Method of Drawing the Potential Energy Surface*

By Shin SATO

(Received March 8, 1955)

## Introduction

The calculation of the potential energy of a polyatomic system, which is necessary for the discussion of molecular structure or chemical reaction, is mathematically so difficult that the so-called "semi-empirical method" devised by Eyring and his collaborators has been widely used to interpret many chemical reactions[1]. The results obtained by this method, however, are found to have several weak points when being compared with the experimental data. In the present paper a new method of drawing the potential energy surface for the system of three atoms is proposed and compared with Eyring's method.

1) S. Glasstone, K. J. Laidler and H. Eyring, "The Theory of Rate Processes" McGraw-Hill Book Company, Inc., New York and London (1941).

## Approximate Function for the Anti-bonding State of Two Atoms

When two atoms approach each other, there appear two energy states generally; the one is bonding and the other anti-bonding. The potential energy of the bonding state can be obtained experimentally as a function of the distance between two atoms. As is well known, the curves for many diatomic molecules are conveniently approximated by the Morse function[2],

$$E_{\text{bond}}=D_e\left[e^{-2\beta(r-r_e)}-2e^{-\beta(r-r_e)}\right]. \qquad (1)$$

For the anti-bonding state, however, the curves cannot be obtained experimentally and the function is not yet proposed. The present author researched the function and found that the equation

2) P. M. Morse, *Phys. Rev.* **34**, 57 (1929).

$$E_{\text{ant}}=\frac{D_e}{2}[e^{-2\beta(r-r_e)}+2e^{-\beta(r-r_e)}], \qquad (2)$$

where $D_e$, $\beta$ and $r_e$ are constants which appear in the equation (1), is in good agreement with results calculated by James-Coolidge-Present[3] and Hirschfelder-Linnett[4] for the $^3\Sigma_u$ state of hydrogen molecule, which is shown in Fig. 1. Their results seem to be

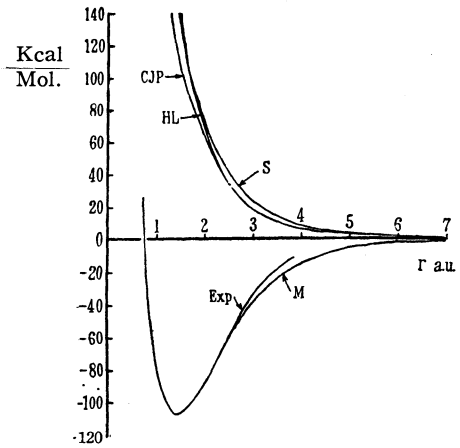



Fig. 1. Potential energy curve of hydrogen molecule.
Exp=Experimental; M=Morse curve; CJP = Coolidge, James and Present calculations; HL = Hirschfelder and Linnett calculations; S=Curve used by the present author.

the best ones at present. The applicability of this function for the anti-bonding states of other diatomic molecules cannot be ascertained because of no existing data. In the present method, one needs the energy curve for the anti-bonding state and the relation of (2) is assumed until the more suitable function is found.

## Potential Energy for the System of Three Atoms

On the other hand, the potential energy curve of the system of two atoms $A$ and $B$ is approximated from the analogy of the well-known Heitler-London method for hydrogen molecule, as follows.

$$E_{\text{bond}}=(Q_{AB}+\alpha_{AB})/(1+S^2_{AB})$$
$$=(Q_{AB}+\alpha_{AB})/(1+k) \qquad (3)$$

and

$$E_{\text{ant}}=(Q_{AB}-\alpha_{AB})/(1-S^2_{AB})$$
$$=(Q_{AB}-\alpha_{AB})/(1-k) \qquad (4)$$

where $k=S^2_{AB}$ and $Q_{AB}$, $\alpha_{AB}$ and $S_{AB}$ are Coulomb, exchange and overlap integrals respectively, all of which are functions of the distance between two atoms $A$ and $B$.

For the potential energy of the system of three atoms $A$, $B$ and $C$, London derived an equation by making some approximations and his equation has been used by Eyring et al. to interpret many simple chemical reactions[1]. The present author, by making a slightly different assumption $S^2_{AB}=S^2_{BC}=S^2_{CA}=k$, has derived the equation

$$E=\frac{1}{1+k}\left\{Q_{AB}+Q_{BC}+Q_{CA}-\sqrt{\frac{2}{1}[(\alpha_{AB}-\alpha_{BC})^2+(\alpha_{BC}-\alpha_{CA})^2+(\alpha_{CA}-\alpha_{AB})^2]}\right\}, \qquad (5)$$

where $Q_{ij}$, $\alpha_{ij}$ and $k$ have the same meanings as in equations (3) and (4). The London equation does not contain the term $k$, which corresponds to the square of overlap integral and may be so small compared with unity in the range of the internuclear separation under consideration that the equation (5) does not differ very much from London's equation.

Thus one can calculate the potential energy of the system of three atoms $A$, $B$ and $C$ as functions of $r_{AB}$, $r_{BC}$ and $r_{CA}$ from the above equations; assuming $k$ as a constant for the system considered, one can obtain $Q_{ij}$ and $\alpha_{ij}$ as functions of $r_{ij}$ by substituting eqs. (1) and (2) in eqs. (3) and (4) respectively and these functions are substituted in the equation (5).

In Eyring's method $Q_{ij}$ and $\alpha_{ij}$ are calculated by putting $k=0$ and by assuming that the Coulomb fraction $\rho$ is a constant for the system of two atoms, while the present method is based on the relation of (2) and the assumption of $k$.

## Potential Energy Surface for Hydrogen Atom-molecule Reaction

As a first attempt to make use of the method just described, the author has drawn the potential energy surface for hydrogen atom-molecule reaction, which has been already treated by Eyring's method[1].

The calculation for two configurations of an equilateral triangle (a) and a straight-line (b) indicates that the latter configuration is more stable than the former one as is seen from Fig. 2. Since only the lowest state is necessary for the present discussion, the surface has been drawn in the linear configuration. The result of calculation on the assumption of $k=0.18$ is given in Fig. 3,

3) H. M. James, A. S. Coolidge and R. D. Present, *J. Chem. Phys.*, **4**, 187 (1936).
4) J. O. Hirschfelder and J. W. Linnett, *J. Chem. Phys.*, **18**, 130 (1950).

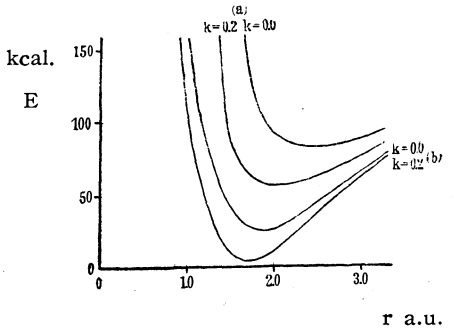



Fig. 2. Comparison of two configurations.
(a) equilateral triangle; (b) straight-line

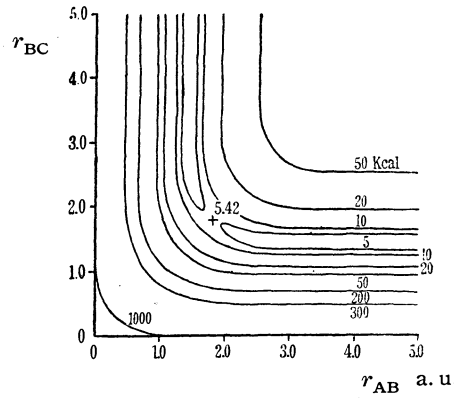



Fig. 3. Potential energy surface for the system of three hydrogen atoms in the linear configuration.

where $r_{AB}$ is the distance between hydrogen atoms $A$ and $B$ and $r_{BC}$ is the distance between $B$ and $C$ in the linear configuration of $A$-$B$-$C$. The vicinity of the saddle point in Fig. 3 is enlarged in Fig. 4. The diagram

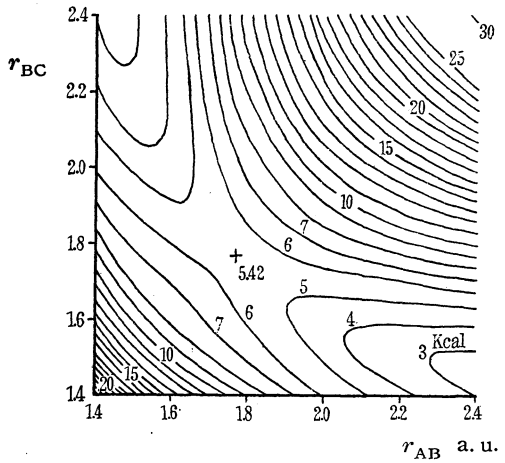



Fig. 4.

obtained differs essentially from Eyring's one which has two saddle points and a basin[1]; the present result has only one saddle point and no basin, coinciding with that of the non-empirical calculation[5]. The calculations with various values of $k$ show the same situation, which seems, then, to be accompanied by the present method.

## Comparison of the Two Methods

According to the theory of absolute reaction rates, the energy value at the saddle point, after allowing for zero-point energies, corresponds to the activation energy of hydrogen atom-molecule reaction. The results calculated by the two methods are given in Table I together with the experimental data.

TABLE I
ACTIVATION ENERGY OF HYDROGEN ATOM-MOLECULE REACTION

(kcal./mol.)

| Observed | Calculated: Eyring | | | Calculated: Present | | |
|---|---|---|---|---|---|---|
| | $\rho$ | $E_c$ (a) | $E_a$ (b) | $k$ | $E_c$ | $E_a$ |
| 5.0±0.5[5] | 0.14 | 14 | ... | 0.0 | 23.8 | ... |
| | | | | 0.1 | 13.4 | ... |
| 7.0±0.5[7] | 0.20 | 7.63 | 8.50 | 0.18 | 5.42 | 4.99 |
| | | | | 0.2 | 3.59 | ... |

a) without allowing for zero-point energies.
b) after allowing for zero-point energies.

Inspecting the table one can easily find that if $\rho > 0.20$ is used in Eyring's method the better value may be obtained. If this is done, however, the minimum of the basin which appears in Eyring's diagram becomes lower than the minimum of the hydrogen molecule. This result might suggest the possibility of a stable linear complex H-H-H which has not been observed. Moreover Eyring's method cannot be applied in the range of $r < 1.0$ a.u., as is seen from Fig. 5,

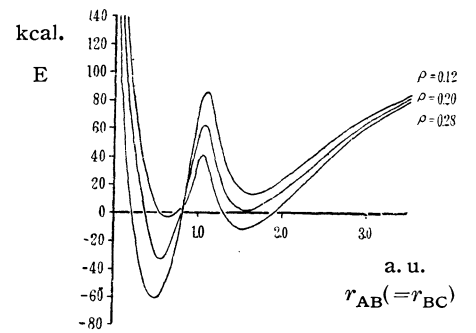



Fig. 5. Potential energy curves along the diagonal section of the surface for various values of $\rho$ by Eyring's method.

5) J. O. Hirschfelder, H. Diamond and H. Eyring, *J. Chem. Phys.* 5, 697 (1937).
6) A. Farkas and L. Farkas, *Proc. Roy. Soc.* (London) *A*152, 124 (1935).
7) K.H. Geib and P. Harteck, *Z. physik. Chem.* (Bodenstein Festband) 849 (1931).

which shows the potential energy curves along the diagonal section of the surface for the various values of $\rho$. The minimum of the curves at 1.5 a.u. in Fig. 5 corresponds to the basin described above.

On the other hand, the present method gives a more reasonable value for the activation energy of hydrogen atom-molecule reaction and is bearable even in the range of $r<1.0$ a.u., as in seen from Fig. 6.

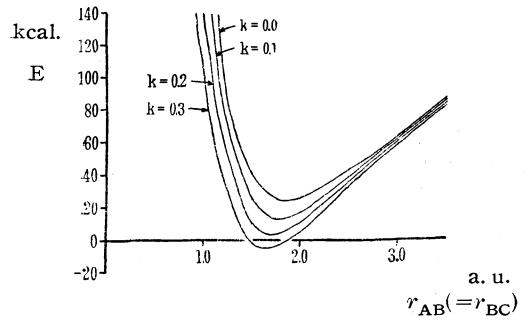



Fig. 6. Potential energy curves along the diagonal section of the surface for various values of $k$ by the present method.

## Summary

A new method of drawing the potential energy surface has been devised and compared with Eyring's semi-empirical method. The points different from the latter method are that an appropriate function for the anti-bonding state of a diatomic molecule is assumed and the overlap integral is not ignored. The so-called Coulomb fraction in Eyring's method is not used and the London equation has been slightly modified.

As an example the activation energy of hydrogen atom-molecule reaction has been calculated. So far as this reaction is concerned, the present method gives more reasonable value than Eyring's method.

The present author wishes to express his hearty gratitude to Prof. S. Shida for his interest and advice and to Mr. I. Yasumori, Mr. J. Higuchi and Mr. K. Fueki for their helpful discussions and suggestions.

*Laboratory of Physical Chemistry,*
*Tokyo Institute of Technology,*
*Tokyo*

# *Rheology of Surface Films. IV. Viscoelastic Properties of 6-Nylon Films at Air/Water Interface*[1]

By Kiyoshi INOKUCHI

(Received March, 22, 1955)

## Introduction

For the study of the fundamental rheological properties of surface films, it is desirable to investigate first a simple elastic film, being formed by a substance of known structure, which facilitates the interpretation of the experimental data in terms of molecular structure. Second, it is also necessary to extend the research to the viscoelastic films, in order to complete the investigation of surface rheology. In the course of this study, the author found[2] that the spread film of 6-nylon is a favorable material for our present purpose mentioned above, since it behaves as a purely elastic body at large areas, whereas it became viscoelastic when the compression advanced beyond a certain area. The aim of this report is to describe the rheological characteristics of 6-nylon film in detail in relation to their dependence to the degree of compression, magnitude of stress, temperature, and molecular weight of the sample, and to attempt some discussions thereupon.

## Experimental

**Materials.**—Samples of poly-ε-capramide (6-nylon), whose molecular weights were controlled with benzoic acid, were kindly furnished from the Research Laboratory of Toyo Rayon Co. The average molecular weights were viscometrically determined[3], and the following results were obtained: 17300, 9100, 4600, 2800, and 1000. Unless otherwise stated, the sample of molecular weight 17300 was mainly used. Prior to the measurement, all the samples were washed with water, alcohol, and benzene, and dried in vacuum.

1) Presented at the Annual Meeting of the Chemical Society of Japan, April, 1954, Tokyo.

2) T. Tachibana and K. Inokuchi, *J. Colloid Sci.*, 8, 341 (1953).

3) M. Watanabe, *J. High Polymer* (Japan), 6, 216 (1949).

**Spreading Condition.**—The sample was spread from a mixed solution of benzene and phenol (3 : 1 in volume) on distilled water. The film was initially spread to 90 Å²/residue from 0.05% solution. Before compression, about twenty minutes were allowed for the equilibrium to be attained. Unless otherwise stated, the film was compressed down to a desired area at a rate of 60 cm²/min. and held at least for two hours before measurement. Film compression mainly studied was attained down to about a few Å²/residue.

**Apparatus.**—Surface rheometer used was the electromagnetic driving type reported in the foregoing paper[4]. The size of the trough and the detailed measures of the apparatus were the same as shown there. The apparatus was set in an air-thermostatted cabinet and the humidity in it was maintained at an almost saturated state by hanging up some water-immersed cloths in the cabinet. The temperature control of water in the trough was carried out by passing the thermostatted water into the jacket at the bottom of the trough. The temperature near the surface of the water was measured by means of a thermistor. Accuracy of temperature control was about ±0.5°C. The stress being applied to the film at all compressions was always controlled so that a suitable amount of strain (within 2 degrees of angle) occurred under shearing stress. The duration of the measurement was limited within about thirty minutes.

For the numerical evaluation of the viscoelastic quantities, equations (4) and (5) in the previous paper[4] were used with the implicit assumption that the film under test is isotropic and homogenous. With less compressed films, this assumption may be approximately valid. With highly compressed films, however, in which the films are no longer isotropic, and this assumption will not necessarily be valid, no accurate evaluation but more approximation of the viscoelasticity was attained.

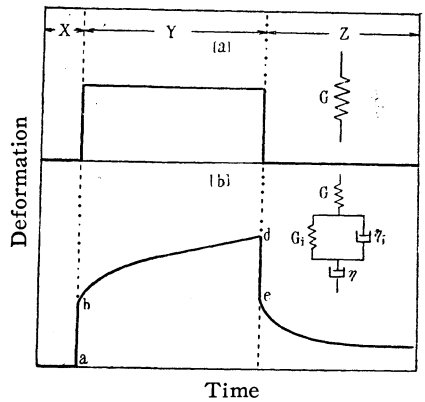



Fig. 1. Strain-time curves of 6-nylon. (a), at less compressed film, (b), at compressed film beyond about 40 Å²/residue. X represents the dead time, Y, the time, the stress being applied, and Z, the time after the stress is removed.

4) K. Inokuchi, This Bulletin, 27, 432 (1954).

## Results and Discussion

**General Remarks on the Rheological Properties.**—As shown in Fig. 1, the strain-time curve of 6-nylon film was divided into two types according to the degree of compression of the film, i.e., a simple elastic type of less compressed film (about 75–40 Å²/residue) and a viscoelastic type of considerably compressed film (less than about 40 Å²/residue). For convenience' sake, the descriptions will be divided into two parts: time-independent mechanical property and a time-dependent one.

### Part I. Time-independent Mechanical Property (Instantaneous Elasticity)

#### (1) Effect of Stress

It was found that the stress-strain relation generally depends upon the past history of shearing when the stress was first applied to the film. So, experiments, involving repeated process of application and removal of stress, were performed. Successive strains were thus obtained, stresses being gradually increased. Typical examples of these patterns, determined with the film at 42 Å²/residue were shown in Fig. 2. It is seen that,

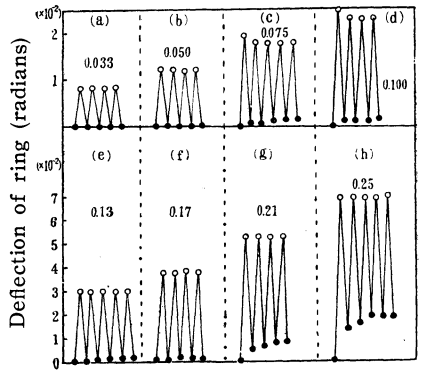



Fig. 2. Pattern of successive straining of the film at 42 Å²/residue at 28°C, stress being varied in each run, the values of which are indicated above each figure in dyne per cm. Open circles represent the instantaneous strain under stress, and full circles, the strain under removal of the stress.

at moderately small stress, each strain was perfectly identical, no hysteresis being observed as in Fig. 2 a-b. Under large stresses, however, considerable shortening of each strain was evident at the first one or two cycles, though it became less marked upon further repetition of straining tending to a limiting value as in Fig. 2 c-h, especially in h.

It is worthy of noticing that the film become more rigid as the rhythmic strain was

applied to the film. Such a phenomenon may well be compared to "rheopexy" or "work hardening" at bulk. It is plausible to consider that the elasticity of film, simply set up by compression, involves certain unstability in bond formation. Thus, it is presumable that the rhythmic motion, applied to the film, orients and aligns the film molecules, thereby accelerating the attainment of more stable bond formation. Such a mechanism may also be inferred from the property of the ordinary fibre, in which the increase of the tensile strength develops under extension.

When the plots were made using the first value of each strain series, a linear stress-strain relationship was obtained which bent down at larger stress as in Fig. 3. On the

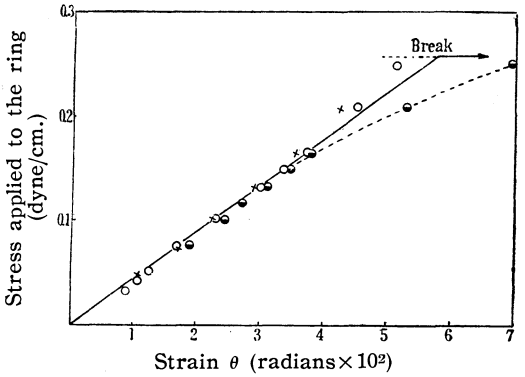



Fig. 3. Stress-strain relation obtained from Fig. 2. Half circle plots were obtained from the first strain of each group of the strain cycles, open circles, from the fourth strain. Crosses represent the plots obtained five minutes after rupture of the film.

other hand, if the curve were plotted using the fourth value of strain series, the nearly straight line was obtained almost up to the point of rupture. Even once the rupture took place under too large stress, only several minutes were sufficient for recovering the film structure. In Fig. 3, crosses indicate that the strain, determined five minutes after rupture, is in good coincidence with those before rupture.

Nearly linear relation between stress and strain was generally observed with films at large areas, where only an instantaneous elastic response appeared under stress. On the other hand, with films at small areas, where creep appeared under stress, the plots tended to bend towards the strain-axis above a certain value of stress, though they produced a good straight line at moderately small stresses. Hysteresis was negligible as far as the linear portion was concerned. It was thus presumed that the film at all compressions would be Hookean for at least moderately small stress.

The stress-strain curves at constant rate of strain were also determined, since they are significant for studying the film properties, especially the properties of weakening or fatigue preceding the rupture, which cannot adequately be analysed in terms of viscoelastic deformation alone. The form of the curves are of course dependent on the rate of strain, and the family of the curves depicted in Fig. 4, were obtained under a

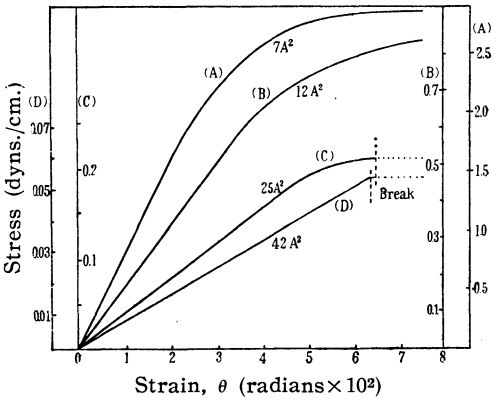



Fig. 4. Stress-strain curves of 6-nylon at constant rate of strain ($1.05\times10^{-2}$ radian per minute). Curve (A), 7 Å²/residue; (B), 12 Å²/residue; (C), 25 Å²/residue; and (D), 42 Å²/residue. Temperature 20°C.

fixed rate of strain. In this figure, it is seen that at large areas, e.g., at 42 Å²/residue, a good straight line up to the film rupture was obtained, whereas as the area decreased, the plastic portion became evident before rupture set in. In addition, we see that with reducing area, elastic modulus (the slope of the linear portion) remarkably increased, but the strain at yield (length of the elastic portion) became shorter and shorter. Moreover, it is noticed that with highly compressed films (12 and 7 Å²/residue), the creep after yield was well-definable, without causing any gross rupture. Such behavior clearly represents that the film which was simply "brittle" at less compressed state, transformed to "tough" as the compression proceeded, the mechanical properties becoming closer to that of bulk.

It is really surprising that the film at less compressed state, not at highly compressed one, actually exhibits an ideal elastic behavior, which can hardly be seen at the ordinary bulk materials, upon which some discussions will be made in the next paper.

### (2) Effect of Aging Time at Constant Temperature

Time effect of elasticity was examined. In Fig. 5, instead of the actual value of the

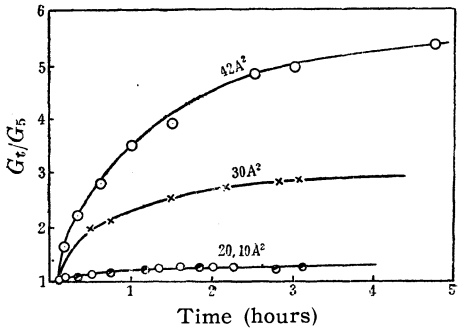



Fig. 5. Effect of aging time on the instantaneous modulus of rigidity at temperature 20°C. Abscissa indicates the aging time, $t$, defined as the time measured from the end of compression, ordinate, the ratio of rigidity at time $t(G_t)$ for that at 5 minutes of $t(G_5)$.

elastic modulus, ratio of instantaneous elastic modulus at time $t$ for that of five minutes after the end of the compression, was plotted against the gelation time. It is seen that within the first ten minutes, there occurred a rapid increase in the modulus of elasticity, but this was followed by a very gradual approach to a steady state. Moreover, it was found that such an aging effect was remarkable with films at large areas, whereas it became less serious with highly compressed films. The large effect of aging at less compressed films may well be accounted for by the greater ease of orientation and alignment of the film molecules, which tends to form the stable bond than in the case of high compression. It is also noticed from these curves that the time of about two hours, which was allowed to elapse before all the measurements other than this were started, is practically sufficient to attain the steady state of elasticity.

### (3) Effect of Temperature

When the temperature was raised to 38°C and chilled at the initial temperature, considerable increase in rigidity was noted, indicating that the temperature hysteresis does exsist. But when the sample was spread at moderately high temperature (38°C), and cooled and held at about 7°C for about ten hours, hysteresis was practically eliminated between the curves for increasing and decreasing temperature as seen in Fig. 6.

Temperature dependence of the instantaneous elastic modulus $G$, defined as $S/\theta$, was depicted in Fig. 6. It was seen that the plots may yield a straight line, with negative inclination which was similar for films at all compressions. Thus, the following equation may hold between $G$ and temperature, $T$.

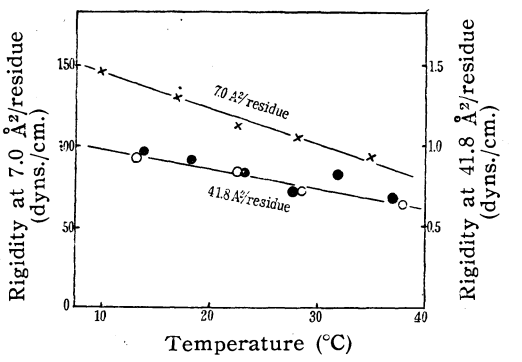



Fig. 6. Effect of temperature on the instantaneous modulus of rigidity. Rate of temperature change, 0.1°C per minute. Crosses show the plots at 7.0 Å²/residue, circles, those at 41.8 Å²/residue. The degree of temperature hysteresis was seen by the open and full circles, the former being those obtained with increasing temperature, the latter with decreasing temperature.

$$G=a+bT \tag{1}$$

where $a$, and $b$, are constants, $b$ being negative. Such a temperature dependence is the same as the bulk material of nylon whose tensile strength decreased with increase in temperature[5].

According to Wieland and Snyder[6], the stress, $F$, can be resolved as follows

$$F=F_u+F_s, \tag{2}$$

where $F_u$ represents energy term, and $F_s$, entropy term. The entropy term, $F_s$, is given by the relation

$$F_s=T(\partial F/\partial T)_\theta. \tag{3}$$

Since our present discussion is confined to the Hookean elastic part,

$$F=G\cdot\theta$$

Thus,

$$F_s=T\cdot\theta\cdot(dG/dT). \tag{4}$$

Assuming that $F_u$ is independent of temperature, it follows from the equation (1), (2), and (4) that $F_s$ is negative because of the negative sign of $dG/dT$ (or $b$), and this term decreased, as the strain increased, whereas the stress due to energy, $F_u$ possesses increasing positive value with increasing strain.

5) T. Alfrey, "Mechanical Behaviors of High Polymers", p. 518 (1948).

6) W. B. Wiegand and I. W. Snyder, *Trans. Inst. Rubber Ind.*, 10, 234 (1934).

If we compare this thermal data with that of rubber[7], this film corresponds to that of highly stretched rubber in which advanced degree of crystallization occurs. When this film is compared to that of resting muscle[8], in which $F_u$ is increased, and $F_s$ decreased with advancing strain, the property is analogous to the highly organized structure of resting muscle. From those observations, it is suggested that 6-nylon film is not rubber-like, but of rather orderly arranged crystalline structure. Such a view may also be inferred from the property of crystallite formation in bulk.

### (4) Relation between Elastic Modulus and Film Concentration

Change in modulus of rigidity with reducing area was quantitatively examined. By performing the compression at constant rate, it was possible to overcome the hysteresis of elasticity and to characterize the transformation of the film phase. Fig. 7

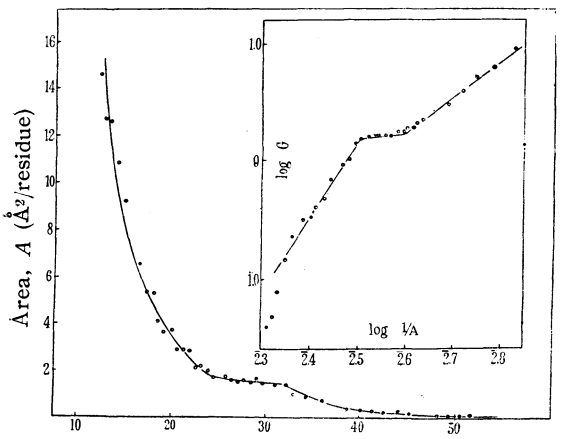



Fig. 7. Rigidity-area ($G$-$A$) curve obtained under a constant rate of compression (9.6 cm²/minute). Inset indicates the log $G$—log $1/A$ relation.

shows the rigidity-area curve, which was determined at a compression rate of 9.6 cm²/min. It is seen in this figure that the modulus increased continuously as the compression proceeded down to about 33 Å²/residue, where a plateau started. Further compression did not appreciably increase the rigidity until the areas of 24 Å²/residue was reached after which the rigidity was found to increase again with reducing area, this time more steeply. To make clear this relation, the logarithm of both modulus of rigidity $G$, and the reciprocal of area, $1/A$—a surface concentration—was plotted as seen in the inset of the figure. It is seen that these plots at larger areas than the plateau fall on a straight line with slight deviation, while those at smaller areas than the plateau produced a fairly good straight line. Thus, it was found that the experimental results were charcterized by the slopes of the lines, namely by the value $p$ of the following equation

$$G=c(1/A)^p \qquad (5)$$

where $c$ and $p$ are constants. At larger and smaller areas than the plateau, $p$'s were approximately calculated as 6 and 3, respectively. It may be that a film structure, once established at large areas, transformed to another type according to the degree of compression. The plateau region is thought to be a transition state of film structure under compression. As will be mentioned in the next paper, the plateau in the rigidity-area curve was consistent with the plateau which appeared in the pressure-area curve.

If we assume an approximate value as the thickness of the film under test, the modulus of rigidity in bulk would be calculated from the value of surface modulus of rigidity, $G$. The film thickness was presumed from the spreading amount and the density of the solid. The modulus of rigidity in bulk, corresponding to the area of 40 Å²/residue was calculated as $1.2\times10^7$ dyns./cm², whereas those corresponding to the area of 20 Å²/residue and 7.0 Å²/residue, were $4.6\times10^7$, and $5\times10^8$ dyns./cm², respectively. Uéno and Fuchino[9] obtained 55 kg./cm² as Young's modulus of elasticity of unstretched fibre of 6-nylon, from which the modulus of rigidity in bulk was calculated as $1.9\times10^9$ dyns./cm², assuming the poisson ratio 0.4. Although, with the film of high compression, precise evaluation of the film rigidity is impossible because of the failure of the isotropy of the film, the general trend is that the value calculated from the surface modulus at large areas was considerably smaller than that in bulk, whereas the values became closer to each other with reducing area. Such a disagree- ment of rigidity modulus between the bulk and the surface film would not be surprising, because the structure of spreading film is generally not the same as that in bulk. Such a difference in structure, however, is thought to be less pronounced as the compression advanced to form multimolecular layers, since the values at high compression became close to that of bulk.

7) E. Guth, *Ann. N.Y. Acad. Sci.*, 47, 723 (1947).
8) E. Guth, *Ann. N.Y. Acad. Sci.*, 47, 743 (1947).
9) S. Ueno and K. Fuchino, *J. Textile Research (Sen'i-gakukai-shi)*, 45, 324 (1951).

### (5) Molecular Weight Dependence of Gelation Area

The area, at which the film first manifests elasticity under compression is significant for the study of the film structure, and is called here "gelation area" ($A_g$), the unit being Å²/residue. Fig. 8 shows how the gelation

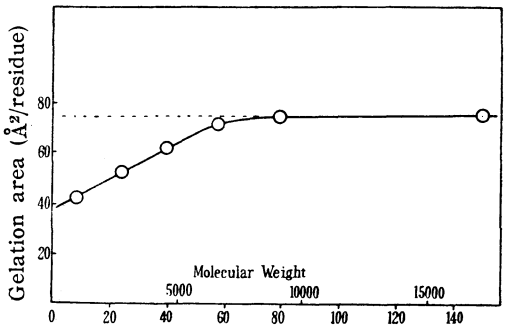



Fig. 8. Gelation-area versus molecular weight relation.

area is affected by the molecular weight of the spead material. It was found that the gelation area versus degree of polymerisation *D. P.* plots yielded a straight line showing an increase in $A_g$ with increase in *D. P.*, so long as *D. P.* is not very high. However, with *D. P.* above a certain value, it tended to a maximum value of about 75 Å²/residue.

It is apparent that the gelation area inevitably necessitates the mutual contact of the neighboring molecules. So, the gelation area must closely be related to the degree of molecular extension. Since at the gelation point, the molecules are linked together, the degree of molecular extension would chiefly be determined by the flexibility of molecular chain.

With molecules, whose chain length is relatively short, the smaller value of $A_g$ would be expected, the lower *D. P.* is, because the moleculer extension due to the flexibility of the molecular chain might be come less pronounced with decreasing chain length. In an extreme case of monomer films, $A_g$ would be very close to the co-area of the residue itself. As seen in Fig. 8, extrapolation of the $A_g$-*D. P.* curve to zero *D. P.* yielded about 37 Å²/residue, which is fairly consistent with the co-area of residue, lying flat on water surface (molecular model gives 40.2 Å²/residue).

On the other hand, with the molecule, whose chain length is sufficiently long, it will be expected that the area per residue is independent of *D. P.*, since further increase in *D. P.* beyond a certain limit, would merely cause repetition of the flexible unit of chain. This was experimentally verified as shown in Fig. 8, in which $A_g$ became independent of *D. P.*, when *D. P.* was over about 80.

It is generally accepted that chain polymers in solution take a spatial configuration of nearly random coiling, if there is no special interaction between chains. Applying this analogy to the surface, and assuming a two-dimensional random-coil model for the chain configuration of the film molecules, it can be deduced from simple statistical calculations that the mean area occupied by one molecule is proportional to *D. P.*, that is, the mean area per residue is independent of *D. P.* except for the chains of extremely short length. This seems to explain the above experimental result.

It must be noticed, however, that the maximum value of $A_g$ is only twice as the co-area of residue, which is too small if we assume the two-dimensional random coil of a molecular chain. Moreover, it is surmised that, if the random coil of the molecular chain might be assumed, the value of *D. P.* at point of levelling off of the curve should be far small, being less than one-tenth of that in Fig. 8, at most. These results lead us to the postulation that the configuration of molecular chains at water surface is not likely in the case of random-coil, but may presumably be an extremely stretched one, possessing less flexibility. Such a molecular configuration may rather be favorable for the alignment and association between adjacent molecular chains which lead to the formation of rigid gel-structure.

### (6) Molecular Weight Dependence of the Film Elasticity

Instantaneous modulus of rigidity was plotted against the molecular weight of the

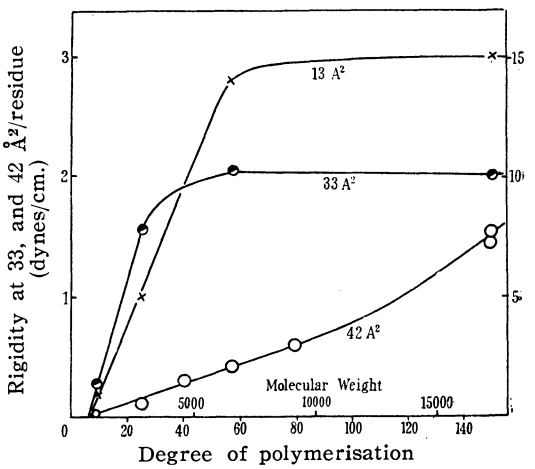



Fig. 9. Rigidity versus molecular weight relations at various areas.

sample at various areas. As depicted in Fig. 9, two types of the curve were obtained. At a highly compressed state (13 and 33 Å²/residue), rigidity increased proportionally with *D. P.* as far as *D. P.* is relatively low, but they approached asymptotically to a maximum value when *D. P.* was over about 80. Moreover, it was found that extrapolation to zero rigidity failed to pass through the origin, cutting the *D. P.* axis by about 5. Such a form of the curve is entirely similar to that obtained with material in three-dimensional state[10]. Kanamaru and Koyama[11] also obtained the similar curve with nylon fibre.

On the other hand, the spreading at a less compressed state, 42 Å²/residue, failed to exhibit the saturation curve as shown above. That is, the rigidity increased linearly with *D. P.* up to *D. P.* value of about 150. Extrapolation of the curve to zero rigidity coincided with the same point for the more compressed film.

Although the current view[12,13] of the strength-*D. P.* relation of the fibre or yarn is that the mechanical strength of material is affected by the two factors, the one is a frictional force between the chains (*D. P.*-dependent), and the other a primary valence force of the main chain (*D. P.*-independent)., it is not suggested that the strength of the spread film can readily be explained from this view point. The author should like to consider that the degree of cristallite formation is intimately related to this phenomenon. As is generally accepted, fine structure of the crystalline polymers are considered to consist of the dense, tightly packed crystalline regions interspersed with less-dense amorphous regions, and the latter, being weaker than the former in mechanical strength, may be determinant for the establishment of the overall mechanical property. It is further believed that one and the same molecule may pass through two or more amorphous regions. Thus, it will be expected that the mechanical strength becomes independent of *D. P.*, when *D. P.* is sufficiently high. A similar consideration may also be applied for the case of the compressed film of 6-nylon, for instance at 13 and 33 Å²/residue, since, as will be described in the next paper, the structure of the compressed film is thought to bear considerable resemblance to that in bulk.

10) A. M. Sookne and M. Harris, *Ind. End. Chem.*, 37, 478 (1945).
11) K. Kanamaru and F. Koyama, *J. Chem. Soc. Japan (Ind. Chem. Sec.)*, 1273, **46**, (1943).
12) K. H. Meyer, and H. Mark, Der Aufbau der Hochpolym. org Naturstoffe (Leipzig, 1930), p. 153.
13) R. R. Sulivan, *J. Appl. phys*, **13**, 157 (1947).

With the films at large areas, however, the condition may be somewhat unfavorable for the crystallite formation, because the molecular configuration is confined within the two-dimensional plane, and the molecules are more loosely packed than in the above case. It follows that, due to the imperfect crystallite formation, amorphous region extends to a longer part of the molecule, and the mechanical strength may become dependent of *D. P.* up to a higher value of *D. P.* Thus, the simple increase in rigidity with *D. P.* at 42 Å²/residue may result. Such a view must be verified further with various kinds of material, and experiments with spreading films, which facilitate the control of the concentration of molecules with the same material, may be very useful for the investigation of this problem.

**(7) Effect of pH of the Substrate Water**

Gelation areas were measured under various pH of the substrate water (Fig. 10). Control

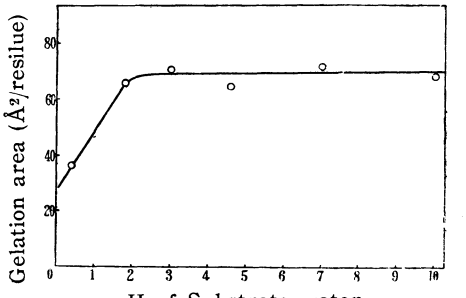



Fig. 10. Effect of pH of the substrate water upon the gelation-area, temperature 13–16°C.

of pH was carried out with hydrochloric acid and sodium hydroxide, and a glass electrode system was used to measure pH values. It was found that gelation area markedly decreased on the acidic substratum, though no remarkable influence was observed in the pH range between 2 and 10. On the 2 N sulfuric acid aqueous solution, the film failed to exhibit the elasticity above the areas of about 40 Å²/residue. Below this area, the film elasticity was found to decrease on the strong acidic solution. Such a result may well be consistent with the plausible view that the hydrogen bridge between the iminogroup of one residue and the carbonyl of another is respon sible for the film elasticity, since such a bond would be very weak on high acidic substratum.

## Part II. Time-dependent Mechanical Properties

**(1) Formal Analysis of the Strain-time Curve under Constant Shear Stress**

Since, as mentioned above, the mechanical properties of the film at compressed state was complicated, it seemed convenient to represent the behavior with a series of the mechanical models: an instantaneously recoverable spring having an elastic modulus $G$, atime-dependent slowly recoverable spring of elastic modulus $G_i$ set in parallel with a dashpot of viscosity, $\eta_i$, and a non-recoverable viscosity, $\eta$ (see the inset of Fig. 1). The delayed elastic response is generally represented by a series of definite numbers of retardation times. So we now examine how many retardation mechanisms are necessary to represent practically the form of the experimental curve for delayed elasticity. As a typical example of the analysis, the strain-time curve at the area of 7.0 Å²/residue was used.

According to the usual analysis of rheology[14], the form of the curve for the delayed elastic response is expressed by the following equation

$$\gamma=\sum_{i=1}^{n} A_i(1-e^{-t/\tau_i}), \qquad (6)$$

where $\gamma$ represents the delayed elastic strain at time t, $A_i$, a constant, and $\tau_i$ a retardation time. Letting $Q$ be equal to $(\Sigma A_i-\gamma)$, which corresponds to the distance between "b-c" curved line and "p-c" straight line measured along the strain axis of Fig. 11 (shadow region), the equation (6) follows,

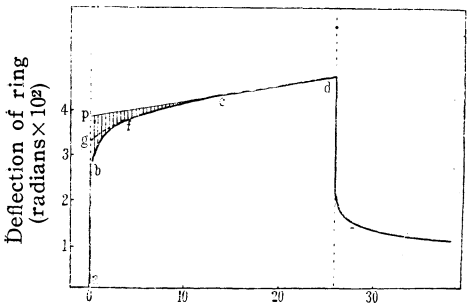



Fig. 11. Strain-time curve at 7.0 Å²/residue, temperature 35°C. Stress applied to the ring, 5.0 dynes per cm.

$$Q=\sum_{i=1}^{n} A_i e^{-t/\tau_i} \qquad (7)$$

Letting $\tau_1$, $\tau_2$,..., a series of the retardation times involved in the film, be arranged in the decreasing order of magnitude and assuming that $\tau_1$ is preferentially large compared with the other retardation times, $\tau_2$, etc., log $Q$, when plotted against time, should give a straight line for large value of $t$. Except for the region of the initial several minutes, the above relation was valid in Fig. 12 (circle plots), which shows a straight

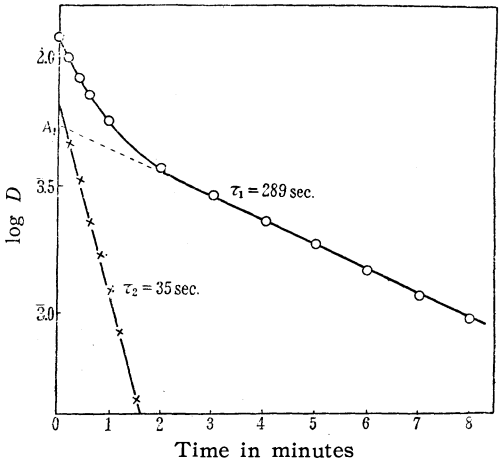



Fig. 12. Log $Q$ versus time plots, corresponding to the curve in Fig. 11.

line intersecting log $Q$ axis at $A_1$. Putting this straight line back into Fig. 11, the dotted line "f-g" was obtained, which represents the equation (7) involving single retardation time. From this figure, it can readily be seen that single retardation mechanism does not serve to represent the experimental data with sufficient accuracy.

If the relation mentioned above proved to hold, equation (7) further predicts that log $(Q-A_1e^{-t/\tau_1})$ should also become linear with large value of t, provided $\tau_1>\tau_2$. This was also valid as shown in the lower part of Fig. 12 (cross plots), from which $\tau_2$, and $A_2$ were obtained from the inclination of the linear part of the line and the intercept on the ordinate axis, respectively. Since, in the present experimental conditions, it was difficult to determine the accurate form of the curve of the initial period of several seconds, a further series of retardation times following $\tau_2$, was not taken into our consideration.

In brief, it was found that duplicate retardation mechanisms, in which longer and shorter retardation times are involved, seem adequate to describe the delayed elastic response of this film. If the initial displacement of the ring due to an instantaneous elasticity and the creep of constant rate of motion are represented by $\theta_0$, and $\lambda t$, respectively, where $\lambda$ stands for the rate constant of motion, the overall strain of the ring, $\theta$, would be expressed by the following equation of the six parameter model,

$$\theta=\theta_0+A_1(1-e^{-t/\tau_1})+A_2(1-e^{-t/\tau_2})+\lambda t. \qquad (8)$$

A similar degree of agreement between equa-

14) T. Alfrey, "Mechanical Behaviour of High Polymers," Intersci. Publ. New York, (1948), p. 58.

tion (8) and the observed curve was found to hold for all the data obtained with films at high compression, though films at less compression, e.g., 20 to 30 Å²/residue, where the contribution of the time-dependent strain was comparatively small, single retardation time was found to be practically adequate to express the delayed elastic strain. Such a form of the creep curve was just similar to that of the three-dimensional hydrogels of agar-agar, reported by Fujita and others[15].

Assuming that $G=KS/\theta_0$, $G_1=KS/A_1$, $G_2=KS/A_2$, $\eta_1=G_1\tau_1$, $\eta_2=G_2\tau_2$, and $\eta=KS/\lambda$, $S$ represents the stress applied, and $K$, a constant involving shape factor, numerical values of the various areas, were obtained as shown in Table I.

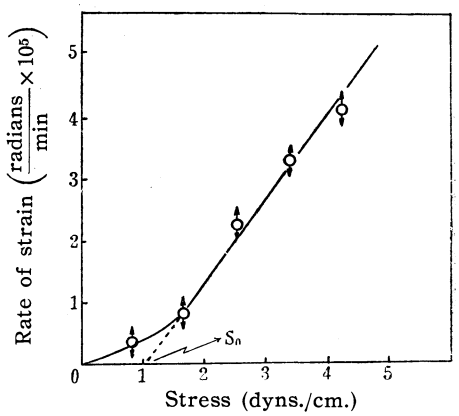



Fig. 13. Stress dependence of the rate of stationary flow at the film of 7.0 Å²/residue.

TABLE I

VARIOUS PARAMETES IN THE MECHANICAL MODEL IN c.g.s. UNIT TEMPERATURE 20°C

| C.G.S. unit / Area Å²/residue | Instantaneous Elasticity | Delayed Elastic Parameters | | | | | | Stationary Flow Viscosity |
|---|---|---|---|---|---|---|---|---|
| | $G$ | $G_2$ | $\tau_2$ | $\eta_2$ | $G_1$ | $\tau_1$ | $\eta_1$ | $\eta$ |
| 42 | 0.38 | — | — | — | — | — | — | — |
| 25 | 1.6 | — | — | — | 19.5 | 113 | $2.2\times10^3$ | $7.8\times10^3$ |
| 12 | 11.2 | 109 | 17 | $1.9\times10^3$ | 107 | 72 | $7.7\times10^3$ | $1.3\times10^4$ |
| 7 | 112.3 | 1590 | 27 | $4.3\times10^4$ | 675 | 126 | $8.5\times10^4$ | $7.0\times10^5$ |

Although the observed values obtained with the same film were considerably reproducible, those obtained with a different run of experiments were found to scatter to a considerable extent. This seemed to be more pronounced at highly compressed film, while it was less serious at large areas. This may be due to the difficulties of obtaining conditions of forming exactly the same gel-structure.

(2) **Stationary Flow Properties**

(a) **Effect of Stress.**—Stress effect on $\lambda$ of equation (8) was examined. As shown in Fig. 13, $\lambda$-$S$ plots curved at small stress, with convex curvature against the strain axis, while, at higher stress, $\lambda$ increased linearly with increasing stress, although the experimental plots scattered to some extent. If the intercept of the straight line on the stress axis was represented by $S_0$, such plots would be approximated by the equation,

$$\theta_f=K(S-S_0)t/\eta \qquad (9)$$

where $\theta_f$ is the displacement due to the flow, $\eta$, a parameter having the dimension of surface viscosity. Such a flow behavior, which is well-known as Bingham's plastic flow, was always observed in all the flow region of the films.

(b) **Effect of Temperature.**—The effect of temperature on $\eta$ was also studied. It was found that the viscosity decreased with increasing temperature as should be expected. To make this clear, the logarithm of $\eta$ was plotted against the reciprocal of the absolute temperature ($1/T$) as depicted in Fig. 14.

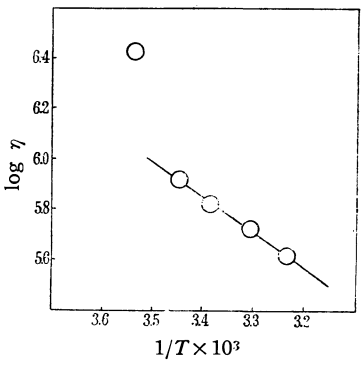



Fig. 14. Temperature dependence of the viscosity coefficient ($\eta$) at the film at 7.0 Å²/residue.

We see that the temperature dependence of the viscosity follows the well-known Andrade

15) H. Fujita, K. Ninomiya and T. Homma, This Bulletin, 26, 20 (1953).

equation and the corresponding apparent activation energy $E$ was approximately estimated as 6.4 kcal./mole. This value is in good agreement with that obtained in bulk[16], and, from this, it is assumed that the flow mechanism of such films is similar to that in bulk. Although it is difficult to know what this means, such a magnitude of energy may suggest that the strength of flow unit involved in it is the interaction of a secondary nature as would be expected from the molecular structure of 6-nylon, which permits the hydrogen bondings between NH and CO of adjacent chains of molecules.

Such a temperature dependence was almost the same for all compressions of the film. It was found, however, that the films, which were compressed to the areas of 12—15 Å²/residue, were the exception. Although the films of such a degree of compression took no special attitude as far as the stress effect was concerned, the viscosity of this film decreased far more markedly with rise of temperature than that of the other compressions. The author[17] reported a surface film of ovalbumin which suffered melting at room temperature under a certain condition. The fact observed here with 6-nylon may have some similarity with this phenomenon. Detailed mechanism requires further studies.

### (3) Transcient Creep Properties

As is understood from the equation (8), these properties can be characterized by the parameters $A_i$, and $\tau_i$. It was found that the values of both parameters was considerably less reproducible compared with the instantaneous elasticity and stationary flow, the experimental errors amountung to about 30% or more. In Fig. 15, instead of $A_1$, the modulus of retarded elasticity $G_1$, defined by $KS/A_1$, was plotted, together with $\tau_1$, against stress. Fig. 16 gives the temperature dependence of $G_1$ and $\tau_1$. We can see in these figures that the values of $G_1$ decreased with increasing stress. It is to be noted that the delayed elasticity is non-Hookean unlike the instantaneous elasticity. The value of $G_1$ decreased with increasing temperature, in a manner just similar to $G$. Because of the negative sign of the temperature dependence of $G_1$, the nature of the delayed elasticity was considered to be energy effect rather than entropy effect, as was the case with instantaneous elasticity.

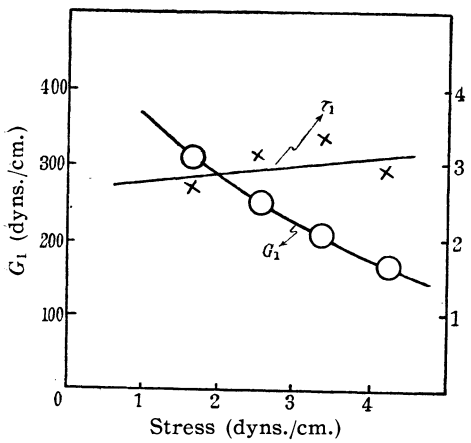



Fig. 15. Stress dependence of parameters in the delayed elastic mechanism. The area, 7.0 Å²/residue. Circles represent the delayed elasticity ($G_1$), crosses, the retardation time ($\tau_1$).

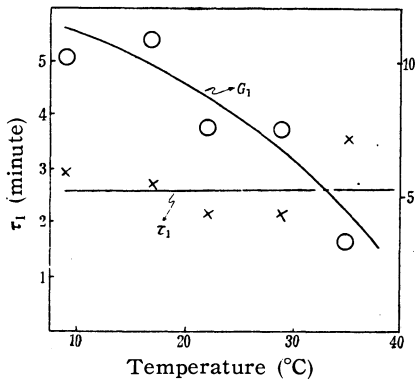



Fig. 16. Temperature dependence of each parameters in the delayed elastic mechanism. The area, 7.0 Å²/residue. Circles represent the delayed elasticity $G_1$, crosses, retardation time, $\tau_1$.

The dependence of $\tau_1$ upon the stress as well as temperature was considerably scattered, being similar to the Fujita's[15] data obtained with agar-agar hydrogel. Although definite conclusion could not be drawn on either stress or temperature effect on the retardation times, it would be likely that the retardation time is little influenced by temperature or stress. Such charactersitics of $A_1$ and $\tau_1$ were similar also in the case of $A_2$ and $\tau_2$.

### (4) Stress-relaxation Test at Constant Shear Strain

(a) **Formal Analysis of the Curves.**—This test was carried out by reading the microammeter of the circuit of the rheometer at suitable intervals of time, when the current passed through the coil was controlled by adjusting the potentiometer so that the deflection of the ring, which occurred instantaneously after applying the stress, was held

16) K. Fuchino, H. Okada, and N. Sagane, *J. High Polymer Chem.* (Japan), **7**, 19 (1950).

17) K. Inokuchi, This Bulletin, **26**, 500 (1953).

constant throughout the experiment. A family of the curves in Fig. 17, obtained at different

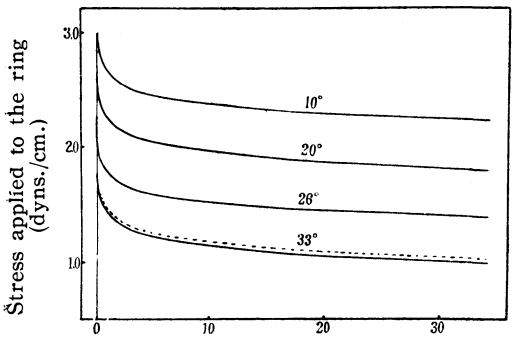



Fig. 17. Stress-relaxation curves at constant shear strain of the film at 7.0 Å$_2$/residue at varying temperatures. Deflection of the ring, $2.5\times10^{-2}$ radians.

temperatures showed that considerably fast decay of the stress appeared at the early stage of time, followed by a slow decay at longer periods of time. Results of duplicate experiments are also indicated with a dotted line for the curve of 33°C. In general, relaxation of slow decay is relatively reproducible, whereas that of fast decay showed less reproducibility.

It was considered here that the experimental curves obtained could be expressed by a series of several Maxwellian relaxations as being written by the following equation

$$S=A\Sigma_i' e^{-t/\tau_i'}$$

where $S$ represents the stress applied, $\tau_i'$ a constant termed as a relaxation time, and $A'_i$, a constant. Check of the equation was made just in the same manner as was the case of the creep test in the foregoing section. As a result, it was found that three elements of Maxwellian relaxation were at least necessary to fit the whole data of the experimental plots except for the initial stage several seconds. In the present film, $\tau_1'$, $\tau_2'$ and $\tau_3'$, have the order of magnitude of $10^4$, $10^2$ and $10^1$ second, respectively. Such a trend was always found with each curve obtained. Assuming that $G'_i=S_i/A'_i$, where $S=\sum S_i$, each value of the parameters, $G$ and $\tau$, were calculated as seen in Table II. Accurate determination of the numerical values of the third relaxation mechanism was, however, rather difficult, so we had to be contented with approximations.

(b) **Temperature Dependence of the Relaxation Times.**—Assuming Arrhenius equation, apparent activation energies, $E'_1$ and $E'_2$, corresponding to $\tau_1'$ and $\tau_2'$, respectively were obtained by plotting logarithms of $\tau_1'$ and $\tau_2'$ against $1/T$. It is to be noticed that temperature dependence of both relaxation times markedly differed, that is, longer relaxation time, $\tau_1'$, is considerably temperature-dependent, giving $E'_1\fallingdotseq5$ kcal./mole, whereas shorter relaxation time, $\tau_2'$, exhibited almost no temperature dependence, namely $E'_2\fallingdotseq0$.

TABLE II
VARIOUS PARAMETERS OF THE MECHANICAL MODEL OBTAINED FROM THE STRESS-RELAXATION CURVES IN Fig. 17

| Temperature (°C) \ Parameters in C. G. S. unit | $G_1'$ | $G_2'$ | $G_3'$ | $\tau_1'$ | $\tau_2'$ |
|---|---|---|---|---|---|
| 10 | 44.9 | 5.6 | 3.9 | $2.1\times10^4$ | $1.4\times10^2$ |
| 20 | 37.6 | 5.2 | 5.2 | $1.5\times10^4$ | $1.6\times10^2$ |
| 26 | 29.4 | 4.6 | 7.8 | $1.4\times10^4$ | $1.3\times10^2$ |
| 33 | 22.2 | 4.8 | 4.8 | $0.9\times10^4$ | $1.4\times10^2$ |

Activation energy of longer relaxation time, 5 kcal./mole, is fairly consistent with that of flow obtained with the creep curve in the preceding section. This value of activation energy for relaxation is in good harmony with the view that the gel-structure of this film consists of cross-linking at points of contact of a secondary strength. The fact that the shorter relaxation time was independent of temperature, is inferred from the result of the creep test that the retardation time, $\tau_1$, failed to exhibit any definite temperature dependence.

Although, at the present stage, molecular interpretation of the temperature-independent relaxation mechanism is not clear, it would be reasonable to suppose that this relaxation is chiefly associated with the frequency factor in Arrhenius equation, presumably with the activation entropy for relaxation. In any case, it was pointed out here that the compressed film under test involves at least two kinds of relaxation mechanism of different modes.

**(5) Correspondence between the Two Mechanical Models**

In the above description, two types of mechanical model were presented: the one (model A), obtained from the creep test, the other (model B), from the stress relaxation test. If each parameter operating in the models is linear in nature, both models should be equivalent to each other, and values of parameters of one model are obtainable, when those of the other are known. In order to study the extent of correspondence of the mechanical models, duplicate measurements of creep and stress-relaxation were carried out with one and the same film, since the data

obtained from the experiments on different films scattered considerably even when the same experimental conditions were considered to be secured. The results obtained were arrayed by means of the mechanical models in Fig. 18, in which respective numerical


## Summary

(1) Using a surface-rheometer, the strain-time curves at constant shear stress, the stress-relaxation curves at constant strain, and the stress-strain curves at constant rate of strain were determined with the spread films of 6-nylon at air/water interface, and the rheological data were measured in relation to their dependence upon stress, temperature, and molecular weight of the sample under varying compressions, and were arrayed in the light of the mechanical models.

(2) It was found that the rheological characteristics of the film were classified into two types according to the degree of compression, i.e., a simple elastic type at large areas which involves a Hookean elasticity alone, and a viscoelastic type at considerably small areas, which is characterized by an instantaneous elasticity, the delayed elasticity, and stationary flow under constant stress.

(3) The stress-strain curves at constant rate of strain revealed that the film, which was simply brittle at large areas transformed to tough as the compression proceeded, the mechanical properties resembling to that in bulk.

(4) It was also observed that the film strength, which was readily set up after compression, was considerably improved by the rhythmic strains applied to it, indicating the two-dimensional rheopexy.

(5) Instantaneous elastic modulus versus area curve showed a conspicuous plateau at the areas from about 33 to 24 Å²/residue, which suggests that at least two different phases are experienced during the process of compression.

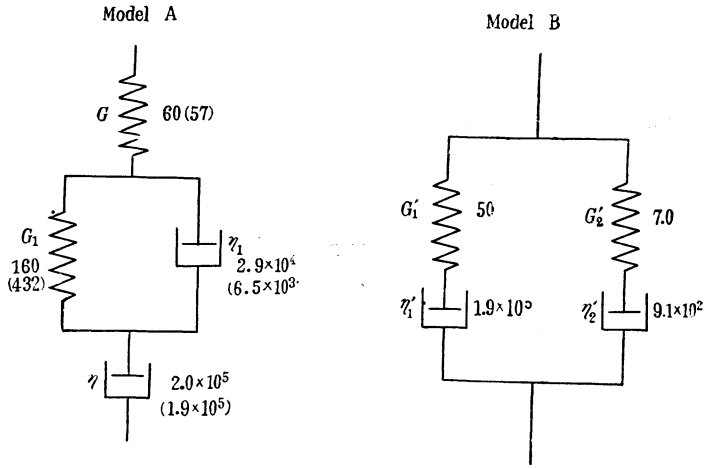




Fig. 18. Mechanical models of 6-nylon.

values of each parameter were given in c.g.s. unit. It was stated above that six parameters were adequate to express the overall form of the curves up to the initial several seconds. For the sake of simplicity, however, the mechanical models of four parameters were used in this connexion, parameters belonging to the shortest retardation times (within one minute) being neglected. In this figure, blackets in model (A) give the values calculated from model (B).

It is indicated that satisfactory agreement was obtained between the observed and calculated values, so far as instantaneous elasticity and stationary flow viscosity are concerned. As to the delayed elastic part, however, considerable disagreement of the values was seen. Such a degree of departure may well be expected, since it was shown above that parameters operating in the delayed elastic mechanisms as well as those in the shorter relaxation ones were considerably irreproducible, and that the delayed elasticity is non-Hookean (non-linear).

Such a state of affairs makes it difficult to draw a definite conclusion as to the consistency of the model of delayed elastic mechanism. It may, however, be said that our mechanical models presented above are sound for describing the static viscoelastic behaviors of the film, so far as the simple elastic part and stationary flow part are concerned.

(6) Temperature dependence of the instantaneous elasticity suggests that the elasticity is mainly due to the energy effect rather than entropy effect.

(7) Molecular weight variations of the film elasticity and of the gelation area were examined together with their pH dependence of the substratum, and discussions were made in molecular terms.

(8) The stationary flow under constant stress behaved as a plastic flow, which is characterized by a yield stress above which flow practically begins to occur. Apparent activation energy of flow was estimated as about 6 kcal./mol.

(9) Overall forms of the strain-time curves and of the stress-relaxation ones were found to be well fitted by the mechanical models of six parameters.

(10) From the temperature dependence of the relaxation times, it was suggested that at least two different modes of relaxation mechanism do exist within the films of high compression.

The author wishes to express his hearty thanks to Prof. T. Tachibana for his helpful advice and encouragement throughtout this work. The author is also indebted to Prof. S. Oka (Gakushuin University), Dr. K. Suzuki (Tokyo University of Education), and Dr. T. Nakagawa (University of Tokyo) for valuable criticism of this work.

*Department of Chemistry, Faculty of Science, Ochanomizu University, Tokyo*

# *Spectrochemical Study of Microscopic Crystals. VIII.*[1] *Absorption Spectra of Dicyclopentadienyl-compounds of Iron and Cobalt*

By Shoichiro YAMADA, Akitsugu NAKAHARA and Ryutaro TSUCHIDA

(Received April 7, 1955)

Since the first preparation of dicyclopentadienyl-iron[2], a number of reports have appeared on the dicyclopentadienyl-compounds of various metals. Although the measurement of pleochroism is expected to afford valuable information about the linkages within the complexes, none of the former investigators have dealt with this property. In this paper we will report on the quantitative dichroism measurement with crystals of dicyclopentadienyl-iron (II) and dicyclopentadienyl-cobalt (III) perchlorate, and discuss the results of the measurements.

## Experimental

**Materials.**—Dicyclopentadienyl-iron was prepared from cyclopentadienyl-magnesium bromide and tris-(2,4-pentanediono)-iron (III) in orange, monoclinic needles elongated along the [100] m.p. 173°C. The optical measurements were made on the prism face with polarized light having its electric vector along and perpendicular to the (100)-plane.

Dicyclopentadienyl-cobalt (III) perchlorate was prepared according to the method of Wilkinson et al.[3] from tris-(2,4-pentanediono)-cobalt (III) and cyclopentadienyl-magnesium bromide. The yellow, prismatic crystals thus obtained exhibit a straight extinction on the prism face. The optical measurements were made on this face with the electric vector along the directions of extinction.

**Measurements.**—Quantitative dichroism measurements were performed at room temperature in the region covering from 2400 to 7000 Å by Tsuchida-Kobayashi's microscopic method[4]. The symbol, $\alpha$, represents absorption coefficient per mm. of a crystal. Molecular absorption coefficients, $K$, were estimated from the relation, $K = 10\,\alpha M/\rho$, where $M$ and $\rho$ denote formula weight of a compound and density of a crystal, respectively.

## Results and Discussion

**Dicyclopentadienyl-iron (II).**—The results of the measurements are shown in Fig. 1 and Table I. The A- and B-absorption represent the absorption with the electric vector along and perpendicular to the $a$-plane of the crystal, respectively. Based on the

1) Paper VII of this series, S. Yamada, A. Nakahara, Y. Shimura and R. Tsuchida, This Bulletin, 28, 222 (1955).

2) T. J. Kealy and P. L. Pauson, *Nature*, 168, 1039 (1951); S. A. Miller, J. A. Tebboth and J. F. Tremayne, *J. Chem. Soc.*, 1952, 632.

3) G. Wilkinson, *J. Am. Chem. Soc.*, 74, 6148 (1952).

4) R. Tsuchida and M. Kobayashi, "The Colours and the Structures of Metallic Compounds." Zoshindo, Osaka, 1944, p. 180. See also the previous papers of this series.

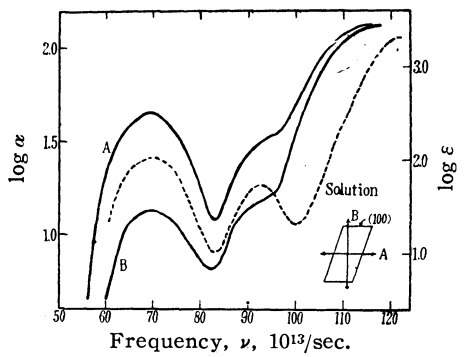



Fig. 1. Absorption spectra of $Fe(C_5H_5)_2$. The spectra of the aqueous solution (dotted curve) is taken from Ref. (7).

rings. Taking into consideration the orientation of the molecules in the crystal[5,6], the components of the molecular absorption coefficients (Fig. 2) were estimated, and shown in Table II. Dicyclopentadienyl-iron in the crystalline state is seen to exhibit in the region of the present measurement three band maxima at about 70, 94 and $120\times10^{13}$/sec., which almost correspond with the maxima observed for the solution of the compound[7]. Comparing the absorption curves of dicyclopentadienyl-iron with those of other compounds of iron[8], it is supposed that the absorption bands at 70 and $94\times10^{13}$/sec. should correspond to such absorption bands as would appear when the iron atom comes into co-ordinate linkage with ligands. Those bands, therefore, may be considered as due mainly to the co-ordinate linkages around the central metal atom of the complexes. Based on the former investigations on the absorption spectra of metallic complexes[9], it is also supposed that the band at about $120\times10^{13}$/sec. should be due to the electronic transitions in the cyclopentadienyl rings in coordination with the metal atom, being designated as a specific band.

TABLE I

ABSORPTION MAXIMA OF DICYCLOPENTADIENYL-IRON IN THE CRYSTALLINE STATE

| | Band I | | | Band II | | | Specific Badd | | |
|---|---|---|---|---|---|---|---|---|---|
| | $\nu$, $10^{13}$/sec. | log $\alpha$ | $K$ | $\nu$, $10^{13}$/sec. | log $\alpha$ | $K$ | $\nu$, $10^{13}$/sec. | log $\alpha$ | $K$ |
| A-abs. | 69.1 | 1.65 | $558\times10^2$ | 93.4 | 1.47 | $368\times10^2$ | 117 | 2.15 | $176\times10^3$ |
| B-abs. | 69.6 | 1.14 | $172\times10^2$ | 93.0 | 1.14 | $172\times10^2$ | 120 | 2.15 | $176\times10^3$ |
| | $\alpha_A/\alpha_B=3.24$ | | | $\alpha_A/\alpha_B=2.14$ | | | | | |

crystal analysis[5,6], it is seen that the A-absorption represents the main characteristic of the component absorption of the molecule with the electric vector perpendicular to the cyclopentadienyl-rings, and the B-absorption represents the one along the pentagonal

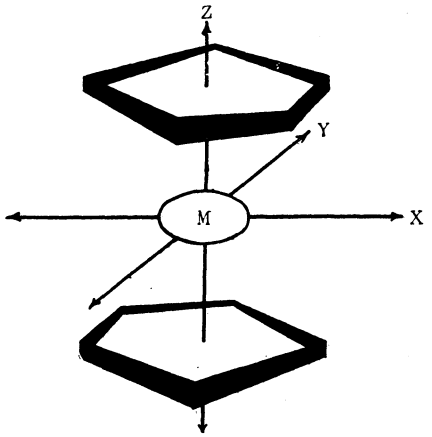



Fig. 2. Configuration of the metallic dicyclopentadienyl-compounds.

TABLE II

| | Band I | Band II |
|---|---|---|
| $K_z$ | 94400 | 56400 |
| $K_x$ | 17200 | 17200 |
| $K_z/K_x$ | 5.48 | 3.28 |

For the bands at 70 and $94\times14^{13}$/sec., *Z-absorption, the absorption with the electric vector perpendicular to the pentagonal rings, has much larger intensity than X-absorption, absorption with the electric vector parallel to the pentagonal rings;* $K_z/K_x=5.48$ for the band at $70\times10^{13}$/sec., and $K_z/K_x=3.28$ for the band at $94\times10^{13}$/sec.

As to the specific band at about $120\times10^{13}$/sec., which may be ascribed to transitions in the cyclopentadienyl-radicals in coordination with the metal atom, *the absorption with electric vector along the rings is slightly hypsochromic to that perpendicular to the above.*

**Dicyclopentadienyl-cobalt (III) Perchlorate.**—Results of the measurements are shown in Fig. 3 and Table III. A-absorption

5) E. O. Fischer and W. Pfab, *Z. Naturforsch.*, 7b, 377 (1952).

6) P. F. Eiland and R. Pepinsky, *J. Am. Chem. Soc.*, 74, 4971 (1952); J. D. Dunitz and L. E. Orgel, *Nature*, 171, 121 (1953).

7) L. Kaplan, W. L. Kester and J. J. Katz, *J. Am. Chem. Soc.*, 74, 5531 (1952).

8) K. Sone, This Bulletin, 25, 1 (1952), etc.

9) Absorption bands of such a kind were previously named "specific bands." See R. Tsuchida and M. Kobayashi, This Bulletin, 13, 476 (1938).

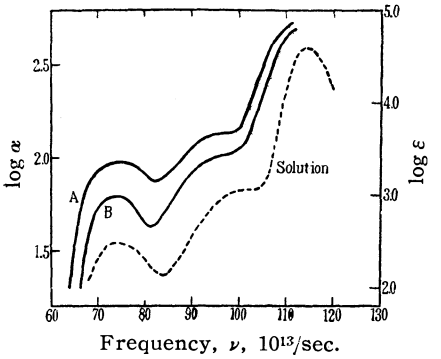



Fig. 3. Absorption spectra of $Co(C_5H_5)_2ClO_4$. The spectra of the aqueous solution (dotted curve) is taken from Ref. (3).

TABLE III

ABSORPTION MAXIMA OF DICYCLOPENTADIENYL-COBALT (III) PERCHLORATE IN THE CRYSTALLINE STATE

| | Band I | | Band II | |
|---|---|---|---|---|
| | $\nu$, $10^{13}$/sec. | $\log \alpha$ | $\nu$, $10^{13}$/sec. | $\log \alpha$ |
| A-abs. | 74.4 | 2.0 | 97.0 | 2.2 |
| B-abs. | 74 | 1.79 | 97 | 2.06 |
| | $\alpha_A/\alpha_B=1.62$. | | $\alpha_A/\alpha_B=1.38$ | |

and B-absorption denote absorption with electric vector along and perpendicular to the direction of elongation. The compound exhibits three absorption bands at 74, 96 and about $115\times10^{13}$/sec., which almost coincide with the band maxima reported for the solution[10]. By analogy with dicyclopentadienyl-iron (II), the band at $115\times10^{13}$/sec. may be readily assigned to the specific band, which is due to the electronic transitions in the cyclopentadienyl-rings of the cobaltic compound. The two bands at the longer wave-length of dicyclopentadienyl-cobalt are supposed to be due to the electronic transitions of co-ordination electrons or electrons closely related to the co-ordinate linkages. The crystal structure of the present compound has not yet been determined. But it is reasonable that we should expect for this compound a similar rule on dichroism to that for the corresponding iron-compound. Thus, for the bands directly connected with the co-ordinate linkages in the dicyclopentadienyl-cobalt (III)-complex, the *Z*-absorption should be stronger than the *X*-absorption. The results of the present measurements, therefore, indicate that the *B*-absorption represents the main characteristic of the component absorption with the electric vector along the pentagonal rings. On the basis of the above assumption, the dichroism of this compound is seen to be quite similar to that of the corresponding iron-compound. Thus for both the bands, *absorption is stronger with electric vector perpendicular to eth pentagonal rings than with the vector along the cyclopentadienyl-rings.*

For the specific band at $115\times10^{13}$/sec., *absorption with electric vector along the rings is slightly hypsochromic to that perpendicular to the above.*

**General Rules on the Dichroism.**—From what is described in the foregoing part of this paper may be derived the following rules on the dichroism which are common for dicyclopentadienyl-iron (II) and -cobalt (III) complexes: (1) *For the two bands at the longer wave-length, due mainly to the co-ordination electrons around the metal atom, Z-absorption is highly hyperchromic to X-absorption, and* (2) *for the specific band, Z-absorption is slightly bathochromic to X-absorption.*

Rule (1) means that, for the bands which are considered as due mainly to the co-ordination electrons around the metal atom, the electronic transitions occur much more readily with the electric vector along the direction binding the metal atom and the centres of the pentagonal rings than with the vector along the plane. In the previous reports on planar quadri-co-ordinate complexes[11], it was found that for the band, considered to be due to the co-ordinate linkages, the oscillator strength was much greater with the electric vector along the complex-plane in which co-ordinate linkages exist than with the vector perpendicular to the plane. Hence, the above rule (1) may be compatible with the previously derived relation[11], assuming that there should exist firm linkages between the metal atom and cyclopentadienyl-radicals. Furthermore, the remarkable difference in absorption coefficient between the *Z*- and *X*-absorption seems to indicate that the $\pi$-electrons of the cyclopentadienyl-radicals may be involved considerably in the linkages between the metal atom and the pentadienyl-rings.

Rule (2) is concerned with the specific band, which may be ascribed to transitions in the cyclopentadienyl-radicals in co-ordination with the metal atom. It may be expected that the compounds would exhibit similar dichroism to that of the benzene rings if the pentagonal rings in these compounds would hold their aromatic property. For the $\pi$-band of the benzene rings in such compounds as hexamethylbenzene, absorption with the

10) G. Wilkinson, *J. Am. Chem. Soc.*, **74**, 6148 (1952).

11) S. Yamada and R. Tsuchida, This Bulletin, **26**, 489 (1953). See also S, Yamada, *J. Am. Chem. Soc.*, **73**, 1182 (1951), etc.

electric vector along the benzene rings was found to be far more hyperchromic and slightly bathochromic to that with the electric vector perpendicular to the benzene rings[12], and for the specific bands of cupric complexes with β-diketones, such as tropolone, salicylaldehyde or acetyl-acetone, each involving π-electronic systems, absorption with the electric vector along the plane of π-electronic systems was found to be far more bathochromic to the absorption with the electric vector perpendicular to the plane[13]. It is seen that the above rule (2) on the specific band of the metallic dicyclopentadienyl-compounds is not compatible with the dichroism for the π-band of the benzene rings, nor with that for the specific band of π-electronic systems within ligands in co-ordination with the metal atoms. It is supposed, therefore, that *the electronic state of the cyclopentadienyl-radicals in the above compounds differs from that of the π-electronic systems in the metallic complexes of an ordinary type as well as from that of the benzene-derivatives. Thus, as far as dichroism is concerned, the cyclopentadienyl-raaicals in the metal-compounds exhibit little aromatic property.* The above relations on the dichroism with the present metal-compounds may be comprehensible, assuming that the π-electrons in the pentagonal rings may be greatly attracted toward the metal atom to form co-ordinate linkages with the metal atom[14].

Rules (1) and (2) can be elucidated also in terms of the group theory. The details of the quantum-theoretical treatment will be submitted later.

**Electronic State of the Cyclopentadienyl-groups in the Metallic Complexes.**—The electronic state of the cyclopentadienyl-groups in the metallic compounds of the above type may be judged also from the wave-length at the maxima of the specific band. When one metal atom in some compound of the above type is replaced by another, the electronic state of the cyclopentadienyl-radicals would change to a greater or less extent according to the change in the linkages between the metal atom and ligands. At the same time, as the π-electrons of the pentagonal rings are attracted toward the metal atom more strongly, π-bond character of the pentagonal rings would be lost more and more, the specific band being displaced hypsochromically corresponding to the change in the electronic state of the cyclopentadienyl-radicals. Thus it is seen from the data reported by former investigators that the Fe(II)- and Co(III)-comlexes exhibit their specific bands at a much shorter wave-length than the Ni(II)-compound (Table IV). This fact suggests that the π-electrons

TABLE IV

MAXIMA OF SPECIFIC BANDS OF DICYCLOPENTADIENYL-COMPOUNDS IN SOLUTION

| | $\nu$, $10^{13}$/sec. | $\log \varepsilon$ |
|---|---|---|
| $Fe(C_5H_5)_2$[a] | 120 | 3.08 |
| $Co(C_5H_5)_2ClO_4$[b] | 114.5 | 4.6 |
| $Ni(C_5H_5)_2$[c] | 97.5 | 4.0 |
| $Ru(C_5H_5)_2$[d] | 142.9 | 3.5 |

(a) Ref. 7. (b) Ref. 3.
(c) E. O. Fischer, *Z. Naturforsch.*, 8b, 217 (1953).
(d) G. Wilkinson, *J. Am. Chem. Soc.*, 74, 6146 (1952).

in the former two compounds would be attracted toward the metal atom more strongly than in the Ni(II)-compound. Such a presumption seems to be in good agreement with the order in stability of the compounds: the Fe(II)- and Co(III)-compounds are far more stable than the Ni(II)-compound. According to the same criterion, the π-electrons are supposed to be attracted rather firmly toward the metal atom in the Ru(II)-compound, which is known, as would be expected, to be very stable. It may be supposed from the above consideration that the electronic state of the cyclopentadienyl-radicals would change greatly from a compound of one metal to that of another. Moreover, there might be some possibility that the linkages or bonding orbitals in the compounds of the above type would change essentially with changing the central metal atom.

As described above, the pentagonal rings in the above compounds would involve a different electronic state from the benzene rings. Their electronic state, however, would not be quite identical with those of cycloparaffines either. Thus the fact that the metal compounds in question exhibit their specific bands in the region between 2500 and 3000 Å might be taken as indicating that the cyclopentadienyl-radicals in the above compound would involve some π-electronic character, since the ordinary cycloparaffines would show no such specific bands in the corresponding region. The dichroism, reverse to that of the ordinary benzene rings, was also observed with aromatic molecular compounds, in which π-π interaction is supposed to exist between benzene rings in the direc-

12) R. Tsuchida, M. Kobayashi and K. Nakamoto, *J. Chem. Soc. Japan*, 70, 12 (1949); K. Nakamoto, *J. Am. Chem. Soc.*, 74, 390 (1952), etc.; G. Scheibe, S. Hartwig and H. Müller, *Z. Elektrochem.*, 49, 372 (1943).

13) R. Tsuchida and S. Yamada, read before the sixth annual meeting of the Chemical Society of Japan, Kyoto, April, 1953; to be published soon.

14) S. Yamada, A. Nakahara and R. Tsuchida, *J. Chem. phys.*, 22, 1620 (1954).

tion perpendicular to the benzene plane[15]. By assuming a similar effect, the dichroism of the present compounds may be understood in the same way, if the $\pi$-electrons of the pentagonal rings would be attracted toward the metal atom.

It is interesting to note that the absorption spectra of dicyclopentadienyl-iron (II) and cobalt (III) bear a close resemblance to those of tris (acetylacetono) iron (III) and cobalt (III)[16] in which $\pi$-electrons of the ligands are supposed to be involved in the co-ordinate linkages with the metal atoms. This fact, which seems to indicate similarity in linkages between the metal atom and ligands in the complexes of the above two types, may be in harmony with the above presumption that the $\pi$-electrons of the cyclopentadienyl-radicals should be greatly involved in the metal-ligand linkages.

## Summary

Dichroisms of dicyclopentadienyl-iron (II) and dicyclopentadienyl-cobalt (III) perchlorate in the crystalline state have been quantitatively determined. For the two compounds, the common rules on the dichroism have been obtained. (1) For the two bands at the longer wave-length, absorption perpendicular to the pentagonal rings is very hyperchromic to absorption parallel to the rings. (2) For the specific band, absorption perpendicular to the rings is slightly bathochromic to absorption parallel to the rings.

Consideration of the results has led us to the conclusion that the cyclopentadienyl-radicals in these compounds may be different from the $\pi$-electronic systems of ordinary benzene rings, suggesting that the $\pi$-electrons would be greatly attracted toward the metal atom to form co-ordinate linkages.

The authors wish to express their hearty thanks to Mr. C. Holstein of the Firm Holstein for a sample of dicyclopentadiene, and to Miss I. Föppl (Dipl. Chem.) for her kind interest and valuable help in the present work. This work was supported in part by a grant from the Ministry of Education.

*Department of Chemistry, Faculty of Science, Osaka University, Osaka*

15) R. Tsuchida, M. Kobayashi and K. Nakamoto, *Nature*, **167**, 726 (1951); K. Nakamoto, *J. Am. Chem. Soc.*, **74**, 1739 (1952), etc.

16) K. Sone, I. Miyake, K. Yamasaki and H. Kuroya, *J. Chem. Soc. Japan*, **69**, 70 (1948).

# *Sterols and Other Unsaponifiable Substances in the Lipids of Shell Fishes, Crustacea and Echinoderms. XVI. Reinvestigation of Hitodesterol and its Identity with α-Spinasterol*

By Yoshiyuki TOYAMA and Toru TAKAGI

(Received April 11, 1955)

Hitodesterol[1], m.p. 167–168°C, was found first in *Asterina pectinifera* and subsequently in *Asterias amurensis* (formerly *Asterias rollestoni*) in this laboratory. The formula for this sterol was deemed at that time to be $C_{28}H_{42}O$ or $C_{29}H_{44}O$, its tetra-unsaturation being inferred mainly from its iodine value determined by the pyridine sulfate dibromide method. It became, however, known that $\Delta^7$-sterols generally give abnormally high iodine values by halogen absorption methods, and after having had experienced such an abnormally high iodine value for corbisterol, a $\Delta^{5,7,22}$-sterol of the $C_{29}$-series, the authors came to believe that hitodesterol shouldbe a di-unsaturated $\Delta^{7,22}$-sterol of the formula $C_{29}H_{48}O$ or $C_{28}H_{46}O$ which has a close resemblance to spinasterol, stellasterol and chondrillasterol, and is possibly identical with one of them[2]. Matsumoto and Wainai[3] have recently come to a similar conclusion that hitodesterol is a $\Delta^{7,22}$-sterol of the $C_{29}$- or $C_{28}$-series, the derivatives of which have the closest resemblance to the corresponding derivatives of α-spinasterol. Although a di-unsaturated sterol, named stellasterol, of m.p. 149–150°C, was reported to occur in *Astropecten auruntiacus*[4], this sterol appears not to be a uniform com-

1) T. Matsumoto and Y. Toyama, *J. Chem. Soc. Japan*, **64**, 1069 (1943); T. Matsumoto, M. Yajima and Y. Toyama, ibid., **64**, 1203 (1943).

2) Y. Toyama and T. Takagi, This Bulletin, **27**, 39 (1954).

3) T. Matsumoto and T. Wainai, *J. Chem. Soc. Japan, Pure Chem. Sect.*, **75**, 1147 (1954).

4) A. Kossel and S. Edelbacher, *Z. physiol. Chem.*, **94**, 264 (1915).

pound. Bergmann and Stansbury[5] separated from *Asterias forbesi* a sterol mixture which was found to consist of $\Delta^{7,22}$- and $\Delta^{7}$-sterols of the $C_{28}$-series, and they proposed to retain the name stellasterol for the former and assign the name stellastenol to the latter. Although a complete separation of these two sterols was not attained, ozonolysis of a mixture of stellasteryl and stellastenyl acetates yielded *d*-methylisopropylacetaldehyde which was identified as its 2, 4-dinitrophenylhydrazone of m.p. 119–120°C and $[\alpha]_D^{24} = +14.1°$. Hence these authors regarded stellasterol as a C-24 epimer of 5-dihydroergosterol.

The present paper records the results of our reinvestigation on hitodesterol. As for sterol components other than hitodesterol, such as mono-unsaturated sterols, in *Asterina pectinifera*, our investigation is now in progress, and the results will be reported in near future.

The crude sterol mixture of the star fish, *Asterina pectinifera*, was acetylated, and the acetylation product was subjected to repeated recrystallizations from acetone by which a steady rise of the melting point was brought about until finally a steryl acetate fraction (A) of m.p. 182–183°C was obtained. This fraction was found to be still contaminated with a minor amount of steryl acetate having a lower melting point, but the melting point and specific rotation of this fraction was not altered substantially by further recrystallizations. This fraction showed a saponification value which agrees with the calculated value for $C_{31}H_{50}O_2$ and an iodine value corresponding to 1.9 double bonds per molecule by the perbenzoic acid method, and was regarded as hitodesteryl acetate in the following. The melting points and specific rotations of hitodesterol and its derivatives are compared with the corresponding compounds of $\alpha$-spinasterol, chondrillasterol and 5-dihydroergosterol in Table I.

The Liebermann-Burchard test for hitodesteryl acetate developed a blue coloration in which the change of absorption at 620 m$\mu$ with the reaction period was quite similar to that of the $\Delta^{7}$-sterol type. A further evidence for the presence of double bond between C-7 and C-8 in hitodesterol was afforded by converting hitodesteryl acetate by the action of mercuric acetate to a product which showed the absorption characteristic to $\Delta^{7,9(11)}$-steryl acetates.

In order to obtain an insight into the structure of the side chain attached to C-17 of hitodesterol, its acetate was subjected to ozonolysis. Among the products of ozonolysis, *l*-ethylisopropylacetaldehyde was identified as its 2, 4-dinitrophenylhydrazone; m.p. 116–117°C and $[\alpha]_D^{14} = -4.6°$. Hence hitode sterol is established as a $\Delta^{7,22}$-sterol of the $C_{29}$-series and is identical with $\alpha$-spinasterol, both having the same optical configuration at C-24.

Steryl acetate fractions having melting points between 171°C and 175°C were recovered from the mother liquors of the recrystallizations which were performed to obtain hitodesteryl acetate. These fractions were united, and the united fraction (B) was subjected to ozonolysis. 2, 4-Dinitrophenylhydrazones prepared from the products of ozonolysis were separated into several fractions, including a fraction of m.p. 115–116°C together with a small amount of a fraction of m.p. 124–126°C. The scarcity of the material did not permit us to determine the optical rotation. While the fraction of m.p. 115–116°C was regarded as 2, 4-dinitrophenylhydrazone of ethylisopropylacetaldehyde, the fraction of m.p. 124-126°C was considered to be 2, 4-dinitrophenylhydra-

TABLE I
COMPARISON OF HITODESTEROL AND SOME RELATED STEROLS

| | Free sterol | | Acetate | | Benzoate | | 3, 5-Dinitrobenzoate | |
|---|---|---|---|---|---|---|---|---|
| | m.p. (°C) | $[\alpha]°_D$ | m.p. (°C) | $[\alpha]°_D$ | m.p. (°C) | $[\alpha]°_D$ | m.p. (°C) | $[\alpha]°_D$ |
| Hitodesterol | 167–168 | −3.0 | 182–183 | −5.8 | 197–199 | +3.8 | 195 | ±0 |
| Hitodesterol[6] | 167–168 | ±0 | 181–182 | ±0 | — | — | — | — |
| Hitodesterol[7] | 168–169 | −2.6 | 182–183 | −2.8 | 198.5 | ±0 | 195 | ±0 |
| $\alpha$-Spinasterol[8] | 168–169 | −3.6 | 186 | −4.5 | 200 | +1.8 | — | — |
| $\alpha$-Spinasterol[9] | 167–168 | −3 | 185 | −5 | 201 | +2 | — | — |
| Chondrillasterol[10] | 168–169 | −1.1 | 175–176 | −1 | 194–195 | +4.0 | — | — |
| 5-Dihydroergosterol[9] | 176 | −19 | 181 | −19 | 200 | −10 | — | — |

5) W. Bergmann and H. A. Stansbury, Jr., *J. Org. Chem.*, 9, 281 (1944).
6) l.c., 1).
7) l.c., 3).
8) L. F. Fieser, M. Fieser and R. N. Chakravarti, *J. Am. Chem. Soc.*, 71, 2226 (1949).
9) D. H. R. Barton and J. D. Cox, *J. Chem. Soc.*, 1948, 1354.
10) W. Bergmann and F. H. McTigue, *J. Org. Chem.*, 13, 738 (1948).

zone of methylisopropylacetaldehyde. Accordingly the steryl acetate fraction (B) seems to contain a small proportion of the acetate of $C_{28}$-sterol, which gives methylisopropylacetaldehyde by ozonolysis, besides hitodesteryl acetate.

It is thus seen from the foregoing that the di-unsaturated sterol components of *Asterina pectinifera* consist mainly of hitodesterol, although $C_{28}$-sterol, possibly $\Delta^{7,22}$-sterol, seems to be present in a lesser amount. Whether this sterol of the $C_{28}$-series corresponds to stellasterol or not, remains undetermined in the present study. The fact that hitodesterol constitutes the main component of the di-unsaturated sterols of *Asterina pectinifera*, whereas the di-unsaturated sterol of *Asterias forbesi* was found by Bergmann and Stansbury to be stellasterol, is by no means difficultly explicable if it is taken into consideration that the content of some sterol components in the total sterol mixture of the same species of aquatic invertebrates often differs widely as has been found in the case of corbicula, chiton and *Asterias amurensis*[11]. It may also be worthy of mention that some sterols formerly found only in the vegetable kingdom have been found to occur not seldom in aquatic invertebrates too. Thus the occurrence of brassicasterol in oyster[12], mussel[13], corbicula[14] and clam[15], and β-sitosterol in *Spisula sachalinensis*[16] and *Ophiopholis aculeata*[17] has been reported in previous studies, and now the occurrence of α-spinasterol or hitodesterol in *Asterina pectinifera* has been demonstrated in the present study.

## Experimental

Several lots of the sun-dried star fish, *Asterina pectinifera* (Müller et Troschel) were united. The united material, 15.7 kg. in total, was cut into small pieces and extracted with ether, yielding 268 g. (1.7%) of a dark reddish orange viscous lipid. On treating the lipid with 2.7 liters of acetone, an acetone-soluble oil (180 g.) with the following constants were obtained: $d_4^{20}$ 0.9441, $n_D^{20}$ 1.4906, acid value 92.0, saponification value 117.5, iodine value (Wijs method) 173.9, unsaponifiable matter 44.06%.

**Recrystallization of steryl acetate mixture.**—The unsaponifiable matter of the acetone-soluble oil was separated by saponification of the oil with alcoholic potash followed by extraction of the diluted soap solution with ether. It was a reddish orange mixture of solid and liquid, and contained 43.5% of sterol (digitonide method). The unsaponifiable matter (72 g.) was recrystallized from 200 cc. of acetone under cooling, and the solid material (49 g.) obtained was refluxed with acetic anhydride. The acetylated product was then recrystallized from 200 cc. of acetone-ether, yielding 26.5 g. of crystalline solid (crude steryl acetate mixture). Further recrystallization of this material from acetone brought about a steady rise of the melting point and iodine value as shown in Table II.

TABLE II

RECRYSTALLIZATION OF STERYL ACETATE MIXTURE

| No. of recrystallization | Steryl acetate crystallized out | | Steryl acetate recovered from mother liquor | |
|---|---|---|---|---|
| | Yield (g.) | m.p. (°C) | m.p. (°C) | I.V. by the perbenzoic acid method |
| 2 | 19.5 | 141–147 | 110–117 | — |
| 4 | 14.0 | 145–151 | 132–134 | — |
| 6 | 8.5 | 159–165 | 142–145 | 71.2 |
| 8 | 5.0 | 168–172 | 153–158 | 89.5 |
| 11 | 2.8 | 178–179 | 167–168 | — |
| 12 | 2.5 | 182–183 | 171–173 | 99.6 |
| 13 | 2.2 | 182–183 | 173–175 | |

The fraction (A) obtained after 13 recrystallizations had $[\alpha]_D^{12} = -6.0°$*. A portion (0.67 g.) of this fraction was subjected to further recrystallizations by which the melting point, 182–183°C, was unaltered, but the melting point of the material recovered from the mother liquor of recrystallization was raised until finally 0.1 g. of a uniform steryl acetate of m.p. 182–183°, $[\alpha]_D^{18} = -5.8°$ and iodine value by the perbenzoic acid method 108.1 was obtained. The fraction (A) had saponification value 124.6 which agrees with the calculated value (123.4) for $C_{31}H_{50}O_2$, and its iodine value (106.9) by the perbenzoic acid method corresponded to 1.9 double bonds per molecule (I.V. calcd. for $C_{31}H_{50}O_2$, 111.6).

**Hitodesterol and its derivatives.**—Saponification of the fraction (A) gave free sterol which showed m.p. 167–168°C and $[\alpha]_D^{12} = -3.0°$ after recrystallization from acetone. Benzoate prepared from the free sterol by using benzoyl chloride and pyridine had m.p. 197–199°C, $[\alpha]_D^{11} = +3.8°$ and saponification value 109.2 (calcd. for $C_{36}H_{52}O_2$, 108.6) after recrystallization from acetone. 3,5-Dinitrobenzoate prepared from the free sterol was light yellow laminae of m.p. 195°C and $[\alpha]_D^{11} = \pm 0$.

11) Cf. Y. Toyama and T. Takagi, This Bulletin, **27**, 421 (1954).
12) T. Matsumoto and Y. Toyama, *J. Chem. Soc. Japan*, **65**, 310 (1944).
13) W. Bergmann and R. C. Ottke, *J. Org. Chem.*, **14**, 1085 (1949).
14) T. Matsumoto and Y. Toyama, *J. Chem. Soc. Japan*, **65**, 258 (1944).
15) Y. Toyama, T. Takagi and T. Tanaka, This Bulletin, **26**, 154 (1953).
16) Y. Toyama and T. Takagi, *J. Chem. Soc. Japan, Pure Chem. Sect.*, **75**, 1238 (1954).
17) Y. Toyama and T. Takagi, *J. Chem. Soc. Japan, Pure Chem. Sect.*, **76**, 237 (1955).

*) Optical rotations were measured with the samples dissolved in chloroform.

Calcd. for $C_{36}H_{50}N_2O_6$: N, 4.62%. Found: N, 4.45%.

The change of color developed in the Liebermann-Burchard reaction for the fraction (A) with the period of reaction is shown in Fig. 1 in which the absorption at 620 mμ is plotted against the period of reaction. The curve for hitodesteryl acetate is quite similar to the curve for a typical $\Delta^7$-sterol.

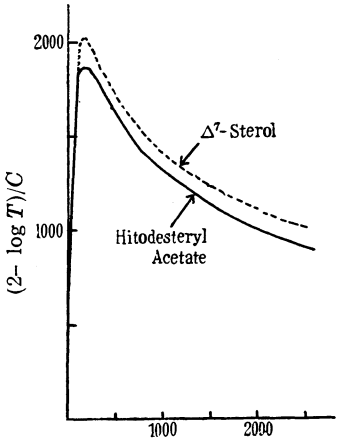



Fig. 1. Libermann-Burchard test for hitodesteryl acetate. $T$: Transmittance, $C$: Concentration ($10^{-3}$ mole)

A solution of 0.1 g. of the fraction (A) was mixed with a solution of 0.3 g. of mercuric acetate in 10 cc. of glacial acetic acid, and the mixture was stirred for twelve hours. The product, after two recrystallizations from acetone, showed m.p. 168°C and $[\alpha]_D^{15}=+31.5°$. It exhibited an ultraviolet absorption in ethanol, as shown in Fig. 2, with the characteristic absorption maxima of $\Delta^{7,9(11)}$-sterol; $\log \varepsilon_{235}=4.02$, $\log \varepsilon_{243}=4.07$ and $\log \varepsilon_{250}=3.88$.

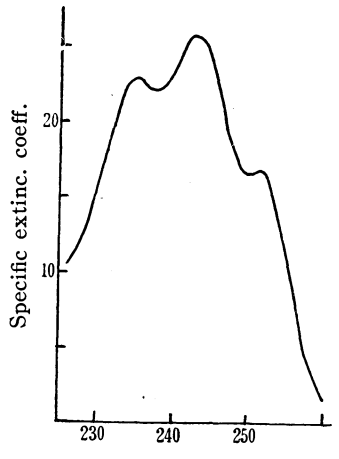



Fig. 2. Absorption curve of the conjugated product of hitodesteryl acetate.

**Ozonolysis of hitodesteryl acetate and a fraction of lower melting point.**—One g. of the fraction (A) was suspended in 20 cc. of glacial acetic acid, and a current of ozonized oxygen was passed through the suspension. After the suspension had become a clear solution, ozonization was continued for ten minutes more. One g. of zinc dust and a few drops of silver nitrate solution were then added, and the mixture was agitated for thirty minutes. Zinc was then removed by filtration. The liquid was diluted with water, and the solution was subjected to steam distillation. The distillate was collected in a trap containing 500 cc. of a 0.2% solution of 2,4-dinitrophenylhydrazine in 2 N hydrochloric acid. An orange yellow crystalline precipitate was formed in the trap, which was filtered after standing for twenty four hours. The precipitate (191 mg.) was dissolved in 10 cc. of chloroform, and the solution was passed through a 2 cm. x 22 cm. column of silica gel. The adsorption zone was then eluted with isohexane, yielding three eluates of 300 cc. each. Isohexane was distilled off from each eluate. The residues from the first, second and third eluates were 94 mg., 43 mg. and 15 mg. with m.p. 109–112°C, 108–111°C and 95–106°C, respectively. On recrystallizing the first and second fractions from ethanol, 118 mg. of orange yellow needles of m.p. 116–117°C and $[\alpha]_D^{14}=-4.6°$ were obtained. The melting point was unaltered by a further recrystallization. Its absorption curve in ethanol exhibited a maximum and a minimum characteristic to 2,4-dinitrophenylhydrazone of saturated aliphatic aldehyde as shown in Fig. 3 ($k_{359}=23.6$ and $k_{300}=1.6$).

Calcd. for $C_{13}H_{18}N_4O_4$: C, 53.05; H, 6.16; N, 19.04%. Calcd. for $C_{12}H_{16}N_4O_4$: C, 51.42; H, 5.76; N, 19.99%. Found: C, 53.03; H, 6.28; N, 18.48%.

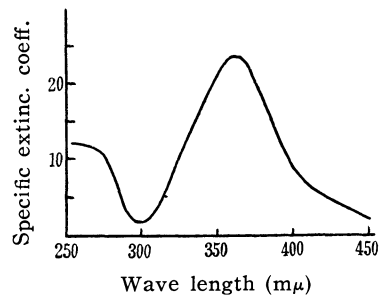



Fig. 3. Absorption curve of 2,4-dinitrophenylhydrazone.

Steryl acetate fractions, which were recovered from the mother liquors of recrystallizations in Table I and had melting points between 171°C and 175°C, were united. The united fraction (B), 0.7 g., was subjected to ozonolysis, and crystalline precipitates of 2,4-dinitrophenylhydrazone (90 mg.) were chromatographed in a similar way as described above, excepting that the adsorption zone was eluted first with isohexane and then with isohexane containing 1% of ether. The precipitates were thus separated into five fractions, the

fifth fraction being obtained by extraction of the silica gel with ethyl acetate. The first fraction (16 mg.) gave, on recrystallization from ethanol, orange yellow needles of m.p. 124–126°C. Calcd. for $C_{12}H_{16}N_4O_4$: N. 19.99%. Calcd. for $C_{13}H_{18}N_4O_4$: N, 19.04%. Found: N, 19.71%.

Recrystallization of the third, fourth and fifth fractions, 15 mg., 10 mg. and 25 mg., respectively, gave orange yellow needles of m.p. 115–116°C, 114–115°C and 114–115°C, respectively. These were united and once more recrystallized from ethanol giving orange yellow needles of m.p. 115–116°C. Calcd. for $C_{13}H_{18}N_4O_4$: N, 19.04%. Calcd. for $C_{12}H_{16}N_4O_4$: 19.99%. Found: N, 18.91%.

## Summary

1. A fraction having m.p. 167–168°C and consisting mainly of hitodesteryl acetate was separated from the steryl acetate mixture of *Asterina pectinifera*. Hitodesterol was found to have an ethylenic linkage between C–7 and C–8. Among the products of ozonolysis of hitodesteryl acetate, *l*-ethylisopropylacetaldehyde was identified in the form of its 2, 4-dinitrophenylhydrazone. Hence hitodesterol has been found to be a $\Delta^{7,22}$-sterol of the $C_{29}$-series and identical with $\alpha$-spinasterol.

2. Among the products of ozonolysis of a lower melting steryl acetate fraction, the presence of a small amount of methylisopropylacetaldehyde besides ethylisopropylacetaldehyde was indicated. Hence it appears that a $C_{28}$-sterol having at least an ethylenic linkage between C–22 and C–23, possibly of $\Delta^{7,22}$-type, is also present in a lesser amount in the unsaturated sterol components of *Asterina pectinifera*.

*Department of Applied Chemistry, Faculty of Engineering, Nagoya University, Nagoya*

# *Studies on Dimethylglyoximato cobalt (III) Complexes. III. Direct Evidence for the Planar Coördination of Two Dimethylglyoximate Ions in Bis-(dimethylglyoximato)-cobalt (III) Complexes*

By Akitsugu NAKAHARA

(Received April 16, 1955)

In the former papers[1),2)] the author discussed on the high stability of bis-(dimethylglyoximato)-cobalt (III) complexes. Then, an elucidation was suggested that the most important origin of the high stability is attributable to the O-H-O hydrogen bonds in the complex radical. However, the strong hydrogen bonds of this kind will be reasonably expected only when the two dimethylglyoximate ions coördinate to a cobalt atom with planar configuration. On the other hand, there has never been found any paper which dealt with the direct evidence for the planar coördination of two dimethylglyoximate ions in bis-(dimethylglyoximato)-cobalt (III) complexes. Thus, it seems to be desirable to afford not chemical but direct evidence for the above configuration. In this work, therefore, the author measured infrared absorption spectra of the so-called Feigl-Rubinstein's bis-(dimethylglyoximato)-cobalt (III)-derivative[3),4)] and the tris-(dimethylglyoximato)-cobalt (III)[1),5)], confirming the planar coördination of two dimethylglyoximate ions in the former compound.

## Experimental

### Materials

**Hydrogen Dichloro-bis-(dimethylglyoximato)-cobaltate (III), (Feigl-Rubinstein's complex), $H[Co(DH^*)_2Cl_2]$**[3),4)].— The method of Cambi et al.[4)] was applied in preparing the compound. To a concentrated aqueous solution of cobaltous acetate was added a slight excess of dimethylglyoxime, and the solution was oxidized by passing air through it. On adding concentrated hydrochloric acid, the compound was precipitated in dark green rhombs. It was recrystallized from aqueous solution by adding concentrated hydrochloric acid. For optical measurements the crystal had to be freed from accompanying moisture and hydrochloric acid.

**Tris-(dimethylglyoximato)-cobalt (III), [Co (DH)$_3$]**[1),5)].—The compound was prepared according to the previously described procedure[1),5)].

1) A. Nakahara, This Bulletin, **27**, 560 (1954).
2) A. Nakahara, This Bulletin, **28**, 207 (1955).
3) F. Feigl and H. Rubinstein, *Ann.*, **433**, 183 (1923).
4) L. Cambi and C. Coriselli, *Gazz. Chim. ital.*, **66**, 81 (1933).
5) A. Nakahara and R. Tsuchida, *J. Am. Chem. Soc.*, **76**, 3103 (1954).

* The following symbols are used: the ion of dimethylglyoxime (DH), $H_3CC(NO)C(NOH)CH_3$; the undissociated molecule of dimethylglyoxime ($DH_2$), $H_3CC(NOH)C(NOH)CH_3$.

The pure product was heated on a water bath under reduced pressure in order to remove the water molecules of crystallization.

**Dimethylglyoxime, $DH_2$.**—The compound was recrystallized from 94%-ethanol, and dried in a vacuum desiccator over calcium chloride.

**Measurements**

The infrared absorption spectra were obtained with a Perkin-Elmer Model 21 Recording Spectrophotometer using sodium chloride prisms and a Nujol suspension of the compound in question.

## Results

The results of the measurements are shown in Fig. 1 and Fig. 2. There is also inserted,

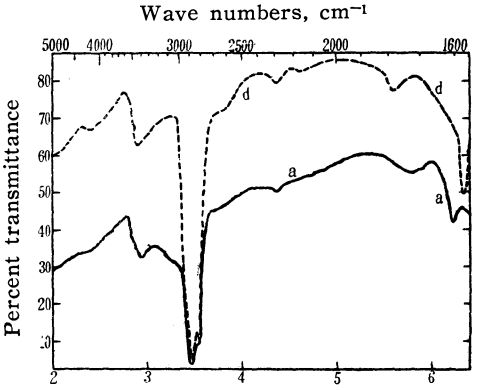



Fig. 1. Infrared absorption spectra of : (a), $H[Co(DH)_2Cl_2]$; (d), $[Ni(DH)_2]$.

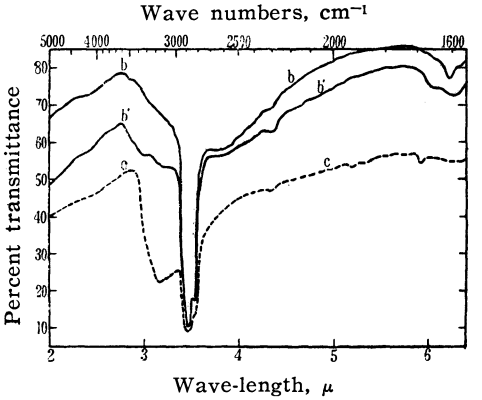



Fig. 2. Infrared absorption spectra of: (b), $[Co(DH)_3]$; (b'), $[Co(DH)_3]\cdot 2.5H_2O$; (c), Dimethylglyoxime.

in Fig. 1, the curve of bis-(dimethylglyoximato)-nickel (II), (d), which was obtained by Rundle and Parasol[6], for the purpose of comparison with the present results. As is clear from those Figures, the curve of bis-(dimethylglyoximato)-cobalt (III)-derivative, (a), is quite similar to that of the bis-(dimethylglyoximato)-nickel (II), (d). On the contrary, the curve of tris-(dimethylglyoximato)-cobalt (III), (b), differs to a considerable degree from those of (a) and (d). The difference between those two types of curves can be found, for instance, in the region from 3600 to 3300 $cm^{-1}$ or from 1800 to 1670 $cm^{-1}$. Especially, the band found at 1725 $cm^{-1}$ on the curve of (a) shows a very important meaning as discussed below.

## Discussion

Recently Rundle and his co-workers[6,7,8] have presented trustworthy data concerning the crystal structure of bis-(dimethylglyoximato)-nickel (II).

According to their X-ray analysis, the complex molecule is planar and contains four five-membered rings as shown in Fig. 3. Of

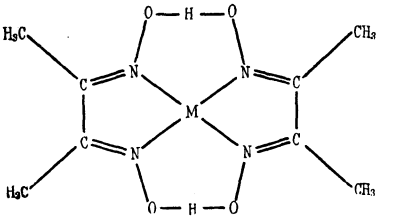



Fig. 3. The structure of planar bis-(dimethylglyoximato)-metal complex with O-H-O hydrogen bonds.

special interest was the very short O-H-O hydrogen bond, 2.44Å, shorter than any O-H-O hydrogen bond, heretofore reported. Furthermore, it was noteworthy that the O-H stretching frequency for this hydrogen bond is only 1775 $cm^{-1}$, about half the normal 3500 $cm^{-1}$, and that spectroscopic arguments have been presented indicating that the hydrogen lies symmetrically between the two oxygens in this case.

As can be seen in Fig. 1, the curve, (a), has a strong resemblance to the curve, (d), of the above bis-(dimethylglyoximato)-nickel (II) in the region from 5000 to 1670 $cm^{-1}$, suggesting the planar coördination of the two dimethylglyoximate ions about a cobalt atom in the bis-(dimethylglyoximato)-cobalt (III)-complex. This interpretation is supported by the fact that the curve, (b), of tris-(dimethylglyoximato)-cobalt (III) in which the planar coördination of two dimethylglyoximate ions could not be expected differs to a considerable extent from those of (a) and (d). In addition to that, the O-H stretching frequency for the above hydrogen bond can be found on (a) at 1725 $cm^{-1}$, and not on (b). This is

6) R. E. Rundle and M. Parasol, *J. Chem. Phys.*, **20**, 1487 (1952).
7) L. E. Godycki, R. E. Rundle, R. C. Voter and C. V. Banks, ibid., **19**, 1205 (1951).
8) L. E. Godycki and R. E. Rundle, *Acta Cryst.*, **6**, 487 (1953).

the direct evidence for the planar coördination of the two dimethylglyoximateions in the bis-(dimethylglyoximato)-cobalt(III)-derivative, since the existence of such a kind of hydrogen bond as described above could not be expected with any other configuration except the planar coördination. The appearance of the O-H stretching band on the curve, (a), is, however, somewhat broad and shifted a little towards a longer wave-length compared with the case of nickel (II)-complex, (d). This may be perfectly understandable by taking into consideration the action of an additional proton which is contained only in the Feigl-Rubinstein's bis-(dimethylglyoximato)-cobalt(III)-complex, $H^{*}[Co(DH)_2Cl_2]$, and not in the bis-(dimethylglyoximato)-nickel (II). It coincides also with Rundle's opinin[9] that there are indications that very broad bands, characteristic of strong hydrogen bonds, become sharper as the O-H-O bond becomes symmetric. But the difference between the ionic radii of nickelous- and cobaltic-ion may be also concerned with the above facts. At any rate, it can be said that the O-H-O hydrogen bond in bis-(dimethylglyoximato)-cobalt(III)-complexes has been proved to be the same kind of the nature as established in the bis-(dimethylglyoximato)-nickel(II).

Rundle and Parasol[5] have also discussed the relation between the bond length and the stretching frequency for O-H-O hydrogen bonds. If it be applied their investigation to the present O-H stretching frequency, 1725 $cm^{-1}$, the bond length of below 2.5 Å a very short hydrogen bond, will be forecasted.

As is seen in Fig. 1 and Fig. 2, some other differences between the curves of bis- and tris-(dimethylglyoximato)-complex can be also found. But the assignments of those bands are very difficult without more detailed research. The author is, at present, investigating the fruits which are obtained by the substitution of deuterium for hydrogen atom concerned with the above O-H-O hydrogen bond[9].

## Summary

Infrared absorption spectra of bis- and tris-(dimethylglyoximato)-cobalt(III)-complex were measured. Some discussions concerning the O-H stretching band of the former complex were given, and they reached the conclusion that the band at 1725 $cm^{-1}$. corresponds to the band at 1775 $cm^{-1}$ of the bis-(dimethylglyoximato)nickel (II) and is characteristic of the planar bis-(dimethylglyoximato)-complexes.

The author wishes to thank Professor R. Tsuchida for his kind guidance and encouragement throughout this work. Appreciation is also expressed to Mr. J. Fujita for his helpful discussions.

This work was supported in part by a grant from the Ministry of Education.

*Department of Chemistry, Faculty of Science, Osaka University, Osaka*

* Although the hydrogen atom has been written conventionally as the external cation of the comeplex anion, it is highly probable that the real structure of the complex should be considered to be "dichloro-dimethylglyoximato-dimethylglyoxime-cobalt (III)" molecule, $[Co(DH_2)(DH)Cl_2]$. If this proves to be the case, it seems to be most probable that the proton attaches to an oxygen atom.

9) To be submitted later.

# *Magnetochemical Study of Violanthrene-iodine System*

By Yoshio MATSUNAGA

(Received April 23, 1955)

## Introduction

As reported in the preceding paper[1], it has been found that polycyclic aromatic hydrocarbons form molecular complexes with bromine or iodine, and these complexes behave as typical semiconductors with high conductivity. For instance, the electrical resistivity of perylene-bromine complex is as low as several ohm-cm. at room temperature with the energy gap for conductivity of 0.13 e.v., and that of violanthrene-iodine complex is about 40 ohm-cm. with the energy gap of 0.15 e.V.

In connection with the investigation for the electrical conductivity of these molecular

1) H. Akamatu, H. Inokuchi and Y. Matsunaga, *Nature*, **173**, 168 (1954), see also This Bulletin to be published.

complexes, we have studied the magnetic susceptibility of violanthrene-iodine complex as a function of iodine concentration in it. Included also are the following complexes, benzanthrone-bromine, perylene-bromine, perylene-iodine, and violanthrene-bromine.

## Experimental

### Materials

**Benzanthrone-bromine.**—Brass and Clar prepared this complex by addition of bromine to benzene solution of benzanthrone[2], but our sample was prepared by direct absorption of bromine vapor to a known quantity of crystalline powder of benzanthrone. The complex containing excess bromine was left in a desiccator, and its weight was measured from time to time. The change of composition with time shows that a complex is formed containing one molecule of benzanthrone and one atom of bromine (cf. Fig. 1). This result agrees well with that reported by Brass and Clar, though we prepared it by a different method.

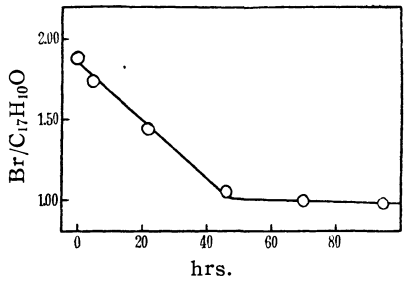



Fig. 1. Change of bromine content of benzanthrone-bromine complex by preservation in a desiccator.

**Perylene-bromine.**—The sample used in this study was prepared by direct absorption of bromine vapor[3]. The complex containing excess bromine was left over potassium hydroxide in a desiccator for a week. Therefore, the sample may be dibromoperylene-bromine complex with a little amount of free dibromoperylene[1].

**Perylene-iodine.**—This complex was prepared by addition of iodine to benzene solution of perylene[4]. To determine the composition of complex, we dissolved its known quantity in benzene, added potassium iodide and water, and titrated the liberated iodine with the standard solution of sodium thiosulfate.

**Violanthrene-bromine.**—This complex was also prepared by absorption of bromine vapor, and left in a desiccator until the change of weight due to the decomposition became so small that we could ignore it during the time required for the magnetic measurement. We have not yet prepared the complex which can be considered to have a definite composition. However, it is sure that a part of bromine which combines with violanthrene is used for substitution and the other part for the formation of molecular complex.

**Violanthrene-iodine.**—The crystalline powder of violanthrene was treated with benzene solution of iodine for some minutes at boiling point, or with carbon tetrachloride solution for a few days at room temperature. The precipitated complex was filtered and dried in vacuo at room temperature. The samples which have varied compositions were obtained by the change of iodine concentration of solution. Solubility of violanthrene and its complex to cold benzene and carbon tetrachloride is very small, so that in the calculation of its composition, we can leave out of consideration the loss of violanthrene during this treatment.

### Magnetic measurement

The susceptibilities were measured using a Gouy balance as previously described[5]. The field was calibrated at two current strengths with distilled water. Fields of about 16 and 23 kilooersteds were used, and each sample was measured in two field strengths to detect any ferromagnetic impurities. The samples which exhibited field strength dependence of susceptibility were discarded.

Taking water as the standand substance ($-0.720\times10^{-6}$), the susceptibility of a sample per gram ($\chi$) is calculated by

$$-\chi\cdot10^{6}=0.749\times\frac{V}{M}\times\frac{F}{F_0}-\frac{0.029}{D}\qquad\text{(at 20°C)}$$

where $F_0$ and $F$ are the resultant forces on water and the sample in g., respectively, $V$ is the volume of water in cc. and the same volume is occupied by $M$ g. of the sample, and $D$ is the true density of the sample.

## Results

The hydrocarbons and complexes under consideration together with the experimental molar susceptibilities are given in Table I

TABLE I

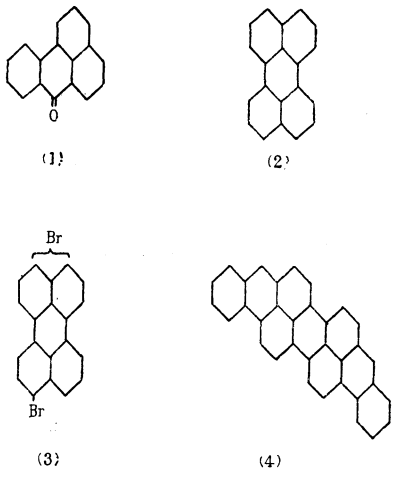
MOLAR SUSCEPTIBILITIES OF SOME MOLECULAR COMPLEXES AND RELATED COMPOUNDS

| Substance | Formula | Molar suscept. $(-\chi_M\times10^6)$ observed | estimated |
|---|---|---|---|
| benzanthrone | (1) | 143 | |
| benzanthrone-0.97 Br. | | 171 | 173 |
| perylene | (2) | 167 | |
| dibromoperylene | (3) | 216 | 215 |
| perylene-3.87 Br. | | 62 | 286 |
| perylene-2.67 I. | | 210 | 286 |
| violanthrene | (4) | 304* | |
| violanthrene-4.36 Br. | | 180 | 437 |
| violanthrene-4.00 I. | | 308 | 482 |
| bromine (1/2 $Br_2$ or Br)** | | 30.6 | (Pascal's constants) |
| iodine (1/2 $I_2$ or I)** | | 44.6 | (Pascal's constants) |

* The previously reported value is 273, the new datum may be more correct.

** The constant for halogen is half the molar susceptibility.

2) K. Brass and E. Clar, *Ber.*, **69**, 690 (1936).
3) A. Zinke and A. Pongratz, ibid., **69**, 1591 (1936).
4) K. Brass and E. Clar, ibid., **65**, 1660 (1932).
5) H. Akamatu and Y. Matsunaga, This Bulletin, **26**, 364 (1953).




columns one and two. The molar susceptibilities of complexes estimated from the measurements on hydrocarbons and Pascal's constants for halogens by direct application of the additivity law are given in column three.

The experimental molar susceptibilities of benzanthrone-bromine complex and dibromoperylene are in accordance with the estimated ones within the errors of the experiments and the estimations. But, in the others, the estimated values are all in serious disagreement with the experimental ones.

Most of complexes which show such a large discrepancy are not stable, bromine complexes change spontaneously to brominated hydrocarbons evolving hydrogen bromide, and perylene-iodine complex loses iodine slowly and leaves the original hydrocarbon. Only violanthrene-iodine complex is so stable that we have no need to consider the change of composition with time. In Fig. 2, its susceptibility per gram is plotted against the concentration of iodine varied from 0 to 67.1 per cent in twelve steps. The dotted line shows the calculated susceptibility derived by the additivity law, and the susceptibility of iodine ($-0.36\times10^{-6}$) is taken from "International Critical Tables"[6]. The actual susceptibility decreases lineary as a function of iodine concentration, but deviates remarkably from the dotted line. When iodine concentration exceeds 55 per cent, the susceptibility increases very slowly and approaches that of pure iodine. The maximum deviation amounting to over 35 per cent occurs at 55 per cent iodine, suggests that a complex is formed containing one molecule of violanthrene and two of iodine. The molecular complex which has this composition will show the most typical properties of this two-component system. If we assume merely the existence of the compound which has the above mentioned concentration of iodine, the linearity of susceptibility-composition curve below and above 55 per cent iodine will be explained. The linearity, whilst consistent with the assumption, can not be regarded as the evidence for non-existence of other complexes in this two-component system.

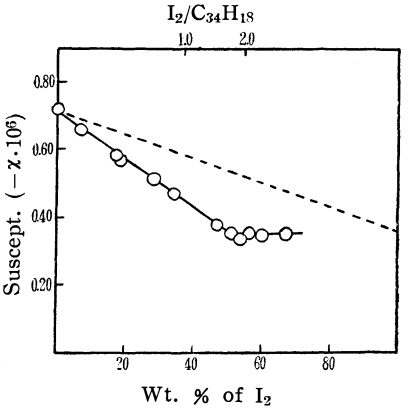



Fig. 2. Magnetic susceptibility of violanthrene-iodine complex as a function of iodine concentration.

## Discussion

It is apparent that benzanthrone-bromine complex and the other complexes shown in Table I belong to different types of molecular complexes from each other. In the former case, the susceptibility follows the additivity law strictly, although stoichiometrical formula of this complex $C_{17}H_{10}O\cdot Br$ suggests the existence of unpaired electron, as Brass and Clar named these complexes "unpaarige Halogenide"[2,4]. For this reason, benzanthrone-bromine complex should be represented by doubled formula. The same conclusion had already been obtained by Müller and Wiesemann within the limits of their rather large experimental errors[7]. Schwab and Schwab-Agallidis applied the ortho-para conversion of hydrogen, and concluded also that this compound was not a radical[8].

On the other hand, the complexes between perylene or violanthrene and halogens, which are colored almost black and show surprisingly high electrical conductivities, are also very anomalous in magnetic behavior. In view of the peculiar and characteristic change of these properties, there can be little doubt

6) International Critical Tables, vol. 6, p. 355.

7) E. Müller and W. Wiesemann, *Ber.*, 69, 2173 (1936).

8) G. M. Schwab and E. Schwab-Agallidis, *Z. physik. Chem.*, B. 49, 196 (1941).

that in their complexes, hydrocarbons and halogens are present with very large changes in their electronic states. Dibromoperylene does not show such anomalies, and we can analyse perylene-iodine complex by titration with standard solution of sodium thiosulfate, so in these complexes, there is no doubt that halogens are not substituted in aromatic nuclei.

The decrease of molar susceptibility in these complexes is not explainable by the localization of $\pi$-electrons which have large orbital radii in aromatic molecules, as the contribution of these electrons to the susceptibilities of original hydrocarbons are no more than $-65\times10^{-6}$ in perylene and $-137\times10^{-6}$ in violanthrene. Therefore, these large decreases must be attributed to the occurrence of constituents or complex as a whole in the paramagnetic state, such as atomic halogen, hydrocarbon positive ion, triplet state or free electrons.

To make further examination of magnetic state, we estimate the depression of diamagnetism at the apparent composition containing one molecule of hydrocarbon and four atoms of halogen in each complex from the data shown in Table I, assuming that perylene-bromine, perylene-iodine and violanthrene-bromine behave like violanthrene-iodine in the susceptibility-composition curve. This assumption is not improbable in perylene-bromine and perylene-iodine, as the composition of the former complex is $C_{20}H_{12}\cdot2Br_2$ or $C_{20}H_{10}Br_2\cdot Br_2$ as described in the previous paper and that of the latter complex reported by Pestemer and Treiber is $C_{20}H_{12}\cdot2I_2$[9]. Violanthrene-bromine complex shown in Table I contains more halogen compared to the standard composition, so that the required value may be equal to the observed decrease. The estimated depressions are shown in Table II. In this Table, we regarded perylene-bromine complex as pure dibromoperylene-bromine complex, so the depression was estimated for $C_{20}H_{10}Br_2\cdot Br_2$.

TABLE II

THE ESTIMATED DEPRESSION OF MOLAR SUSCEPTIBILITY OF COMPLEX AT THE APPARENT COMPOSITION OF ArH-4X

| Substance | Estimated depression of molar suscept. |
|---|---|
| perylene-bromine | $240\times10^{-6}$ |
| perylene-iodine | $110\times10^{-6}$ |
| violanthrene-bromine | $260\times10^{-6}$ |
| violanthrene-iodine | $170\times10^{-6}$ |

We can find from Table II that bromine is more effective to the depression of diamagnetism than iodine, and violanthrene is affected more than perylene by these two halogens. Consequently, it is not probable that the occurrence of paramagnetism is due to the dissociation of halogen molecule, as the bond energy of bromine is larger than that of iodine, and if so, iodine should be more effective. The order of depression of diamagnetism is not compatible with that of the electronegativity of halogen and besides probably with that of the ionization potential of aromatic molecule. The partial ionization of constituents may be sufficient to explain the above data. But this explanation is inconsistent with the data on the electronic conduction described in the previous paper.

Nowadays, it is well known that aromatic hydrocarbons as benzene[10], naphthalene[11], and phenanthrene[12] form complexes with halogens. The bonding power in these complexes is named by Mulliken as "intermolecular charge-transfer force"[13]. He showed also that the theory predicts the possibility of highly intense absorption even for very loose complexes. Benzene, naphthalene and their derivatives form only loose complexes in solutions, so that the charge-transfer may be limited in one complex molecule. If the complex molecules are packed together closely as in our solid complexes, the charge-transfer will not be limited in one complex molecule, but spread out more widely and strongly. In such a case, the complexes have to be extremely deeply colored and show very intense absorption. The occurrence of the excited form with unpaired electrons by thermal excitation may be plausible. The order of difference between observed and estimated molar susceptibilities seems to be consistent with this theory We are not yet ready to state whether the electrical conductivity is explainable by triplet state or not, but we can conclude confidently that the excited state relates to the electrical conductivity of these complexes from its temperature dependence.

If we assume that the difference between observed and estimated molar susceptibilities is equal to the paramagnetic contribution of unpaired electrons and all unpaired electrons behave as free electrons, the excitation energy 0.17 e.V. for violanthrene-iodine complex ($C_{34}H_{18}\cdot2I_2$) is anticipated from it[14].

9) M. Pestemer and E. Treiber, *Ber.*, **74**, 964 (1941).

10) H. A. Benesi and J. H. Hildebrand, *J. Am. Chem. Soc.*, **71**, 2703 (1949).

11) N. W. Blake, H. Winston and J. A. Patterson, ibid., **73**, 4437 (1951).

12) L. J. Andrews and R. M. Keefer, ibid., **74**, 4500 (1952).

13) R. S. Mulliken, ibid., **74**, 811 (1952), *J. Phys. Chem.*, **56**, 801 (1952).

14) Assuming that the paramagnetic contribution of one mole of free electron is equal to $1270\times10^{-6}$, the relation between the depression of molar susceptibility ($\Delta\chi_M$ and the excitation energy ($\Delta\varepsilon$) is approximated by $\Delta\chi_M/2\times1270\times10^{-6}=2\cdot\exp(-\Delta\varepsilon/2kT)$.

This is in good accordance with that obtained from the temperature dependence of electrical conductivity.

Bhatnagar and Lakra[15], and Rao and Govindarajan[16] studied the magnetic susceptibility of benzene solution of iodine. Both of them found that the susceptibility of solution is more diamagnetic than expected from the additivity law. The apparent susceptibility per gram of iodine reported by the former investigators is $-0.51\times10^{-6}$. This increase of apparent susceptibility is not inconsistent with the above explanation, as, in this case, the interaction between complex molecules may be negligibly small and the charge-transfer in a complex molecule will bring about only the expansion of the orbital radii of $\pi$-electrons, namely, the increase of diamagnetism, and not the occurrence of a paramagnetic state.

If we take into consideration the expansion of the orbital radii of $\pi$-electrons in our complexes, the contribution of paramagnetism to molar susceptibility will increase and the excitation energy will decrease to a little extent. For example, if we take the apparent susceptibility of iodine in violanthrene-iodine complex for $-0.60\times10^{-6}$, calculated from the apparent susceptibility in benzene solution and the formation constant of benzene-iodine complex[10], assuming that the susceptibility of iodine not tied up as complex is equal to $-0.36\times10^{-6}$, the magnitude of paramagnetism will be $300\times10^{-6}$, and the excitation energy 0.15 e.V. The agreement between the final estimated value of excitation energy and that obtained from the temperature dependence of electrical conductivity is surprisingly good.

15) S. S. Bhatnagar and C. L. Lakra, *Indian J. Phys.*, 8, 43 (1933).
16) S. R. Rao and S. R. Govindarajan, *Proc. Indian Acad., Sci.*, 15, A. 35, (1942).

**Summary**

The magnetic susceptibility of violanthrene-iodine complex was measured as a function of iodine concentration. This complex shows the large discrepancy between the observed susceptibility and the estimated one which was derived by direct application of the additivity law. Perylene-bromine, perylene-iodine, and violanthrene-bromine show a similar behavior also. The susceptibility-composition curve in violanthrene-iodine system suggests the existence of molecular complex containing one molecule of violanthrene and two of iodine. At that composition, the discrepancy exceeds 35 per cent. This depression of diamagnetism is so large that we can not explain it by the localization of $\pi$-electrons in aromatic molecule. The occurrence of paramagnetic state is taken into consideration, and the nature of this state is discussed. The large difference between observed and estimated susceptibilities is attributed to the partial cancellation of diamagnetism by the paramagnetic contribution of free electrons produced by the intermolecular charge-transfer force which spreads out widely and strongly in this solid complex.

The author expresses his hearty thanks to Prof H. Akamatu for his kind direction of this study. The cost of this research has been defrayed from the Grant in Aid for Fundamental Scientific Research from the Ministry of Education, to which the author's thanks are due.

*Department of Chemistry,*
*Faculty of Science,*
*Tokyo University,*
*Tokyo*

# *The Selenium Dioxide Oxidation of Substituted Acetophenones*

By Tadashi SATO and Masaki OHTA

(Received April 26, 1955)

It is widely known that the methyl group adjacent to the carbonyl group can conveniently be oxidized to aldehyde group by selenium dioxide. In this way many arylglyoxals (I) have been obtained from substituted acetophenones (II).

$ArCOCHO$ (I) $ArCOCH_3$ (II)

As we came to the need of *o*-nitro- and *o*-acetamino-phenylglyoxal for further synthesis in our study, we carried out the oxidation of *o*-nitro- and *o*-acetamino-acetophenone. It has been reported[1] that the oxidation of *p*-nitro- and *p*-acetamino-acetophenone gives corresponding phenylglyoxal derivatives. We found, however, that the oxidation of the *o*-acetaminoacetophenon did not give *o*-acetaminophenylglyoxal, while that of *o*-nitroacetophenone gave *o*-nitrophenylglyoxal. In the case of the oxidation of *o*-acetaminoacetophenon, its methyl group was oxidized to the carboxylic group, and the product was a mixture of almost equal amount of *o*-acetaminophenylglyoxylic acid (III) and isatin (IV). The presence of (IV) is considered to be the result of deacetylation of (III) and ensuing cyclization. Isatin was, in fact, formed by heating (III) in 10% hydrochloric acid.

(III) reacted with 2,4-dinitrophenylhydrazine, semicarbazide, and thiosemicarbazide to give crystalline products. But they were not the ordinary condensation products (V) at all, though their structures have not been confirmed here.

*o*-Nitrophenylglyoxal was also identified by analysis, of its 2,4-dinitrophenylhydrazone and thiosemicarbazone.

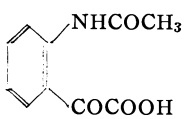
*o*-Nitrophenylglyoxal gave the condensation product, *o*-nitrobenzoylacrylic acid (VI), on treatment with malonic acid in acetic acid solution containing a small amount of sulfuric acid, while in pyridine solution, only a small amount of crystals could be obtained, which melted at 233–4°, and had the empirical formula of $C_{15}H_{10}N_2O_6$.

## Experimental

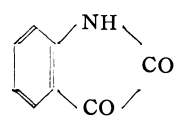
***o*-Nitrophenylglyoxal.**—Fourteen grams of selenium dioxide were dissolved in the mixture of 70 cc. of dioxane and 3 cc. of water with heating. To this warm solution, 19 g. of *o*-nitroacetophenone was added at one time and refluxed for seven hours with constant stirring. After the metallic selenium was filtered off, the most part of dioxane was evaporated, water was added and extracted with ether. After drying over anhydrous sodium salfate, ether was evaporated. From the residue a deep yellow oil distilled at 124-4.5° at a pressure of 3.5 mmHg, yield 13 g. Found: N, 8.24. Calculated for $C_8H_5NO_4$: N, 7.82%.

***o*-Nitrophenylglyoxal thiosemicarbazone.**—The thiosemicarbazone was prepared from *o*-nitrophenylglyoxal (1 g.) and thiosemicarbazide (0.6 g) in dilute ethanol by refluxing for one hour. Recrystallization from ethanol gave light needles, m.p. 172°. Found: N, 22.11. Calculated for $C_9H_8N_4O_3S$: N, 22.2%.

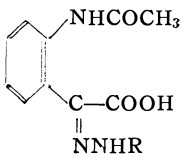
1) C. Musante et al., *Gazz. Chim. Ital.*, **81**. 451 (1951). C. A. **46**, 5549 (1952).



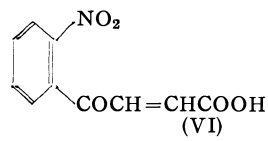

(III)




(IV)




(V)




(VI)

***o*-Nitrophenylglyoxal 2,4-dinitrophenylhydrazone.**—Small amounts of *o*-nitrophenylglyoxal and 2,4-dinitrophenylhydrazine were heated in ethanol for thirty minutes. Upon recrystallization from ethanol, this hydrazone melted at 186–8°. Found: N, 19.82. Calculated for $C_{14}H_9N_5O_7$: N, 19.6%.

**The oxidation of *o*-acetaminoacetophenone.**—Thirty five grams of *o*-acetaminoacetophenone were oxidized with 22 g. of selenium dioxide in dilute dioxane (120 cc. of dioxane and 4 cc. of water) and extracted with ether in the same way as described above in the case of *o*-nitro derivative. After evaporating ether, a red oily substance remained which soon solidified. This was washed with benzene and added to the aqueous sodium carbonate solution. The insoluble substance was filtered (filtrate A), washed with water and recrystallized from acetone-benzene. The red needles of isatin were obtained., m.p. 200°C. Found: C, 64.88; H, 3.51; N, 10.16. Calculated for $C_8H_5NO_2$: C, 65.3; H, 3.40; N, 9.54%. Filtrate A, when acidfied with hydrochloric acid, gave white crystals. Recrystallization from water gave white needles of *o*-acetaminophenylglyoxylic acid, m.p. 162°C. Found: N, 7.09. Calculated for $C_{10}H_9NO_4$: N, 7.78%.

**The change of *o*-acetaminophenylglyoxylic acid into isatin.**—*o*-Acetaminophenylglyoxylic acid, when heated with 10% hydrochloric acid, went gradually into solution. The hot solution was filtered off from a small amount of insoluble matter and cooled. Red needles were obtained. The mixed melting point with isatin showed no depression.

**The reaction of *o*-nitrophenylglyoxal with malonic acid.**—To a solution of 12 g. of *o*-nitrophenylglyoxal in 24 cc. of gracial acetic acid, 10 g. of malonic acid and 5 drops of concentrated sulfuric acid were added. The mixture was heated at 70°C for thirty minutes and then refluxed for ten minutes, water was then added and extracted several times with saturated sodium carbonate solution. The acidification of the combined water layer with hydrochloric acid gave white crystal accompanied by resinous matter. This was washed with dilute ethanol and recrystallized from dilute ethanol, yield 3 g., m.p. 170°C. Found: C, 53.85; H, 3.48; N, 6.27. Calculated for $C_{10}H_7NO_5$: C, 54.3; H, 3.16; N, 6.33%.

*Laboratory of Organic Chemistry,*
*Tokyo Institute of Technology*

# *The Estimation of the Thioethoxyl Group of a Sugar Diethylmercaptal*

By Susumu HIRASE and Choji ARAKI

(Received April 26, 1955)

In the course of our investigation on the mercaptolysis[1,2] of a polysaccharide, it has become necessary to estimate the thioethoxyl group of a sugar diethylmercaptal. This group has been usually estimated by the conversion to a sulfate group by the nitric acid oxidation according to the Carius' method. But the Carius' method is somewhat time-consuming, and in addition, it can not be applied to the mercaptolysates of such polysaccharides as those of sea weeds, which contain the sulfate group in their molecules. The present paper offers a convenient method, by which the direct estimation of the thioethoxyl group of a sugar diethylmercaptal and its acetylated and methylated derivatives has been made without any possibility of the interference of the originally present sulfate group.

The method involves the acid hydrolysis[3] of the mercaptal followed by the distillation and the subsequent iodometrical titration of the liberated ethylmercaptan, as shown by the equations (1) and (2)[4].

$$R-CH(SC_2H_5)_2+H_2O=R-CHO+2C_2H_5SH \quad (1)$$

$$2C_2H_5SH+I_2=C_2H_5-S-S-C_2H_5+2HI \quad (2)$$

## Experimental

**Materials.**—Sugar diethylmercaptals and their derivatives used in this study were prepared according to original papers. Melting point or boiling point of each compound used is included in Tables I and II.

1) C. Araki and S. Hirase, This Bulletin, **26**, 463 (1953).
2) S. Hirase and C. Araki, This Bulletin, **27**, 109 (1954).
3) E. Fischer, *Ber.*, **27**, 673 (1894).
4) P. Klason and J. Carlson, *Ber.*, **39**, 738 (1906); J. W. Kimball, R. L. Kramer and E. E. Reid. *J. Am. Chem. Soc.*, **43**, 1199 (1921).

**Apparatus and General Procedure.**—The apparatus (Fig. 1) was essentially the same as that used for the estimation of the ordinary methoxyl or ethoxyl group. The trap (B) was charged with distilled water (about 20 cc.), to keep

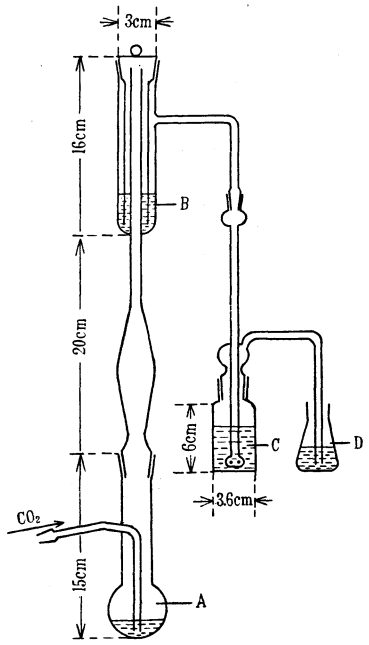



Fig. 1. The apparatus for the thioethoxyl estimation.

any hydrolysing agent from getting into the receiver. The receiver (C) and the sub-receiver (D), in which the reaction shown by the equation (2) occurred, were charged with an excess 0.1N-potassium iodide-iodine solution (20 cc. and 5 cc., respectively), and equal volumes of ethanol were respectively added to each receiver to increase the solubility of ethylmercaptan. An exactly weighed sample (0.1~0.2 g.) to be analysed was placed in the reaction flask (A), and hydrolysing agent, aqueous N-hydrochloric acid (10 cc.) was added.

Then the apparatus was immediately assembled as shown in Fig. 1, all ground joints being moistened with distilled water. A slow stream of carbon dioxide free from any hydrogen sulfide was bubbled through the solution at a rate of about two bubbles a second. The reaction flask was gradually heated in a glycerol bath during thirty minutes to a gentle boiling (bath temperature 115~120°C). After keeping a gentle boiling for two hours, the excess iodine remaining in the receiver and the sub-receiver was individually titrated with a 0.1N-sodium thiosulfite solution without using a starch indicator, which is no use in the high concentration of ethanol. In most cases ethylmercaptan was perfectly absorbed in the receiver C. The quantity of the thioethoxyl group was calculated from the iodine consumed: $SC_2H_5$ g. $=0.06113\times 0.1$N-$I_2$ cc. consumed.

## Results

**Sugar Diethylmercaptals.**—The analysis of several sugar diethylmercaptals, carried out by the above method, gave satisfactory results as shown in Table I. Considerable lite-

TABLE I

THE ESTIMATION OF THIOETHOXYL GROUPS OF SUGAR DIETHYLMERCAPTAL

| Diethylmercaptal of | Sample g. | 0.1N-$I_2$ cc. consumed | $SC_2H_5$% found | Error |
|---|---|---|---|---|
| D-Galactose[3] | 0.1394 | 9.75 | 42.75 | +0.06 |
| [141~143°] | 0.1384 | 9.71 | 42.89 | +0.20 |
| | 0.1293 | 9.07 | 42.88 | +0.19 |
| D-Glucose[3] | 0.1471 | 10.30 | 42.80 | +0.11 |
| [127~128°] | 0.1246 | 8.70 | 42.68 | −0.01 |
| | 0.1247 | 8.73 | 42.79 | +0.10 |
| D-Mannose[3] | 0.1207 | 8.42 | 42.64 | −0.05 |
| [131~133°] | 0.1776 | 12.32 | 42.41 | −0.28 |
| | 0.1338 | 9.31 | 42.53 | −0.16 |
| L-Arabinose[3] | 0.1377 | 10.69 | 47.46 | −0.18 |
| [124~126°] | 0.1165 | 9.10 | 47.75 | +0.11 |
| | 0.1300 | 10.10 | 47.49 | −0.15 |
| L-Rhamnose[3] | 0.1173 | 8.68 | 45.23 | +0.02 |
| [135~137°] | 0.1184 | 8.80 | 45.43 | +0.22 |
| | 0.1421 | 10.57 | 45.47 | +0.26 |
| 3,6-Anhydro- | 0.1557 | 11.65 | 45.74 | +0.19 |
| L-galactose[1] | 0.1046 | 7.83 | 45.76 | +0.21 |
| [110~111°] | 0.1378 | 10.29 | 45.65 | +0.10 |
| Agarobiose[2] | 0.1234 | 5.75 | 28.49 | +0.09 |
| [171~172°] | 0.1517 | 7.01 | 28.25 | −0.14 |
| | 0.1524 | 7.04 | 28.24 | −0.15 |

[ ]: m.p. of the sample used for the analysis.

rature[5] has recorded the difficult hydrolytic cleavage of the carbon-sulfur bonds of mercaptals. This may be due to the incomplete elimination of the liberated ethylmercaptan by distillation[6].

**Acetylated and Methylated Sugar Diethylmercaptals.**—Pentaacetyl and pentamethyl D-galactose diethylmercaptal were tentatively analysed by the same method as above mentioned, but analytical figures obtained were 14.7% and 30.6% (theoretical values 24.6% and 34.3%) respectively. This may be attributed to the low solubility of the sample in the hydrolysing agent, and to the resistance of

5) E. Stuffer. *Ber.*, 23, 3241 (1890); E. Fisher and K. Delbrück, *Ber.*, 42, 1476 (1909); W. Schneider, J. Sepp and O. Stiehler, *Ber.*, 51, 220 (1918); E. Pacsu, *Ber.*, 58. 509 (1925).

6) D. S. Tarbell and D. P. Harnish, *Chem., Rev.*, 49, 1~90 (1951).

TABLE II

THE ESTIMATION OF THIOETHOXYL GROUPS OF FULLY ACETYLATED AND METHYLATED SUGAR DIETHYLMERCAPTALS

| Diethylmercaptal of | Sample g. | 0.1N-$I_2$ cc. consumed | $SC_2H_5$% found | Error |
|---|---|---|---|---|
| Pentaacetyl | 0.1404 | 5.63 | 24.51 | −0.10 |
| D-galactose[7] | 0.1505 | 6.01 | 24.41 | −0.20 |
| [77～79°] | 0.1446 | 5.80 | 24.53 | −0.10 |
| Pentaacetyl | 0.1326 | 5.30 | 24.45 | −0.16 |
| D-glucose[8] | 0.1148 | 4.61 | 24.55 | −0.06 |
| [46～48°] | 0.1774 | 7.07 | 24.36 | −0.25 |
| Tetraacetyl | 0.1324 | 6.18 | 28.53 | −0.26 |
| L-arabinose[9] | 0.1608 | 7.54 | 28.66 | −0.13 |
| [78～80°] | 0.1473 | 6.89 | 28.59 | −0.20 |
| Pentamethyl | 0.2022 | 11.30 | 34.16 | −0.11 |
| D-galactose[10] | 0.1591 | 8.93 | 34.31 | +0.04 |
| (175～180°/4mm.) | 0.1187 | 6.62 | 34.09 | −0.18 |
| Pentamethyl | 0.1368 | 7.65 | 34.18 | −0.09 |
| D-glucose[10] | 0.1421 | 7.95 | 34.20 | −0.07 |
| (175～180°/4mm.) | 0.1244 | 6.94 | 34.10 | −0.17 |
| Hexaacetyl | 0.1258 | 3.71 | 18.03 | +0.09 |
| agarobiose[2] | 0.1456 | 4.42 | 18.01 | +0.07 |
| [101～103.5°] | 0.1361 | 4.04 | 18.15 | +0.21 |

[ ]: m.p., ( ): b.p. of the sample used for the analysis.

the sample against hydrolysis. These difficulties, however, have been overcome by putting glacial acetic acid (2 cc.) into the hydrolysing agent to increase the solubility and prolonging the heating period up to four hours. The analysis by this modified method gave good results as shown in Table II.

*Institute of Chemistry, Faculty of Industrial Arts, Kyoto Technical University, Matsugasaki, Kyoto*

7) M. L. Wolfrom, *J. Am. Chem. Soc.*, **52**, 2464 (1930),
8) M. L. Wolfrom, *J. Am. Chem. Soc.*, **51**, 2188 (1929),
9) M. L. Wolfrom and M. R. Newlin, *J. Am. Chem. Soc.*, **52**, 3619 (1930).
10) P. A. Levene and G. M. Meyer, *J. Biol. Chem.*, **69**, 175 (1926).

# *On the Color-reactions of the Condensed Polycyclic Aromatic Hydrocarbons and their Related Quinones in the Solutions of the Concentrated Sulfuric Acid*

By Takashi HANDA

(Received April, 12, 1955)

## Introduction

The condensed polycyclic aromatic hydrocarbons and their related quinones develop deep beautiful color from yellow to green in the concentrated sulfuric acid. It is understood that these reactions are ascribed to the interaction between the $\pi$-electrons of these compounds and the protons in the sulfuric acid, and with the under-standing that these reactions are those of the so-called "between acids and bases" in the sense of Brönsted, the basicity of these compound is evaluated in terms of Hammett's $pK_B$-values by varying the acidity of the sulfuric acid, and measuring the adsorption-spectrum of these compounds at various concentrations of the acid after the method of L. P. Hammett, with the assumption that the equilibria are obtained between bases and their complexes with protons in the sulfuric acid.

## Experimental

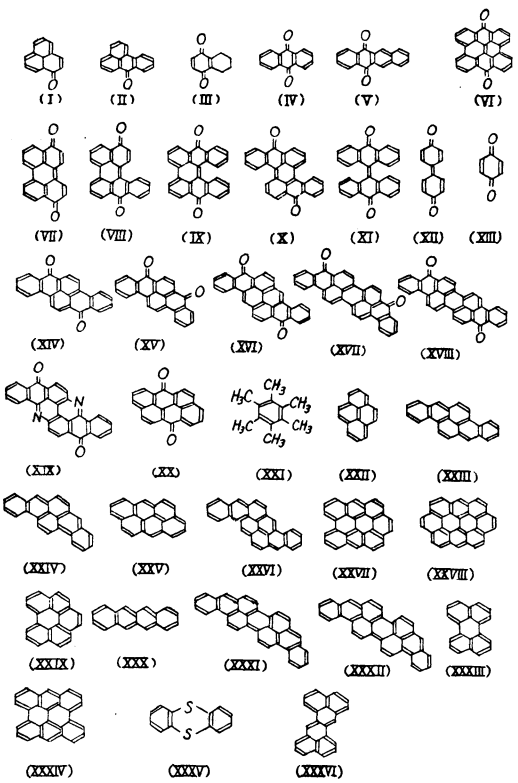
The measurement of the absorption-spectra was done with Beckmanntype spectrophotometer, with quartz-cell of which dimensions were $1.0\times 1.0\times 3.0\,cm^3$, at room temperature. The evaluation of pK-value was done after the method of L. P. Hammett[1], and reasonably the same result was obtained with anthraquinone, of which value was described on the Table V. On this account, this method of measurement is extended to the longer side of the visible region of spectrum, although, owing to the low dispersion of spectrum in this region, the accuracy of the measurement was not so good. The concentrated sulfuric acid used in this measurement was the commercially chemical pure product, not having any traces of peroxides, or nitric acid, or any impurities in the visible region of spectrum in which the measurement had been carried out. The specimens used in this measurement were as follows: perinaphthoindenone (I), benzoanthrone (II), *p*-naphthoquinone (III), anthraquinone (IV), naphthacene-

1) Leo. A. Flexser, Louis P. Hammett and Andrew Dingwall, *J. Am. Chem Soc.*, 57, 2103 (1935).

buinone (V), mesonaphthodianthrone (VI), 3, 10-perylenequinone (VII), 1, 2-benzoperylene-3, 10-quinone, (VIII), helianthrone (IX), 1, 2, 7, 8-dibenzoperylene-3, 9-quinone (X), dianthrone (XI), diphenoquinone (XII), *p*-benzoquinone (XIII), dibenzopyrenequinone (XIV), isodibenzopyrenequinone (XV), pyranthrone (XVI), violanthrone (XVII), isoviolanthrone (XVIII), flavanthrone (XIX), anthanthrone (XX) hexamethylbenzene (XXI), pyrene (XXII), dibenzopyrenee (XXIII), isodibenzopyrene (XXIV), pyranthrene (XXV), anthanthrene (XXVI), dibenzocoronene (XXVII), ovalene (XXVIII), benzoperylene (XXIX) tetracene (XXX), violanthrene (XXXI), isoviolanthrene (XXXII), perylene (XXXIII), mesonaphthodianthrene (XXXIV), thianthrene (XXXV), zethrene (XXXVI)[2]. The structual formula of these compounds is illustrated on the Table I. These compounds are synthesized after the usual manner described in the literature of this subject. They were recrystallised from preferable sorts of solvents, for instance, 1-methylnaphthalene and were further purified by the repeated sublimation in *vacuo* at $10^{-3}$–$10^{-4}$ mm Hg[3]. Each of these compounds was extremely fine, even from the viewpoint of spectroscopy. The solutions of these compounds used in this measurement were prepared, at first, by dissolving from 4 mg. to 7 mg. of specimens in the concentrated sulfuric acid of which concentration was known, and after that, by diluting the original standard solutions with sulfuric acid of the same quality to the appropriate concentration of both specimens and acidity for the measurement. Beer's law was held for these kinds of specimens and for this method of the preparation of the solutions. It is not necessary to consider the effect of sulfonation at room temperature during the time of measurement after certifying the fact that the filtrate of the diluent of the original solution with aquo., is clear, having no extinction of light in the visible region, and the effect of the influence of peroxides is eliminated with the fact that the evidence for the non-existence of peroxides is certificated by iodometry and the color of the solutions are quite different from those of the corresponding quinones in the cases of hydrocarbons.

TABLE I

STRUCTURAL FORMURA OF SPECIMEN USED IN THIS EXPERIMENT




The state of the existence of these complexes may be considered to be the following form, that, with ketones or quinones each proton ($H^+$) is attached to the carbonyl group and forms hybride resonance between $(\rangle C=OH)^+$ and $(\rangle \overset{\cdot\cdot}{C}-O-H)^+$. It was partially supported by the cryoscopic method to measure the depression of the freezing point of the 100% sulfuric acid by L. P. Hammett and J. Dyrup[4]. It was partially supported by the fact that there exists equilibrium between bases and their complexes in the sulfuric acid, which is shown in Fig. 1 and Fig. 2, and it also exists between complexes and their reduced forms with chromous ion ($Cr^{++}$). Some of the shapes of the absorption-spectra of the fully reduced forms of the complexes are similar to those of the vatted forms of the original compounds ($\rangle C-O-H$), which are shown in Fig. 3, with flavathrone.

For the state of the existence of the complexes between condensed polynuclear aromatic hydrocarbons and the protons ($H^+$) in the sulfuric acid, it may be reasonable to consider that there exist equilibria between hydrocarbons (bases) and their complexes. It will be supported empirically from the shapes of the absorption-spectra in various degrees of the acidity of the sulfuric acid, which meet nearly at one definite wavelength with a little correction, considering the solvent effect and which vary regularly showing the so-called existence of equilibria between bases and their complexes, as is shown in the cases of quinones, which are illustrated in Fig. 5 and Fig. 6 and Fig. 7. The absorption-spectra of these compounds in the concentrated sulfuric acid shift towards the longer side of the visible region compared with those of the original ones taken in the non-polar solvents, for instance, 1-methylnaphthalene. For these reasons above mentioned, it may be reasonable to consider the existence of equi-

2) see E. Clar. "Aromatishe Kohlenwasserstoff," Springer Verlag, Berlin, (1952), p. 387. This substance was not used in this experiment. It was previously reported in this paper that it was very basic.

3) Purification of specimens was done by H. Inokuchi in our laboratory, to which the author's sincere thanks are due. H. Inokuchi, This Bulletin, 24, 222 (1951).

4) L. P. Hammett and J. Dyrup, *J. Am. Chem. Soc.*, 54, 2721 (1932); ibid., 55, 1900 (1933),

libria between these compounds and their complexes with protons in the sulfuric acid, and estimate the basicity as the function of $pK_B$ from the absorption curves after L. P. Hammett, putting that;

$$C=C_B+C_{BH^+} \quad (1)$$

$$\varepsilon=\log I_0/I/dc \quad (2)$$

$$C_{BH^+}/C_B=\frac{\varepsilon_{BH^+}-\varepsilon}{\varepsilon-\varepsilon_B} \quad (3)$$

$$pK_B=-\log\frac{a_{H^+}a_B}{a_{BH^+}} \quad (4)$$

$$H_0=-\log(a_{H^+}) \quad (5)$$

$$H_0=pK_B-\log C_{BH^+}/C_B \quad (6)$$

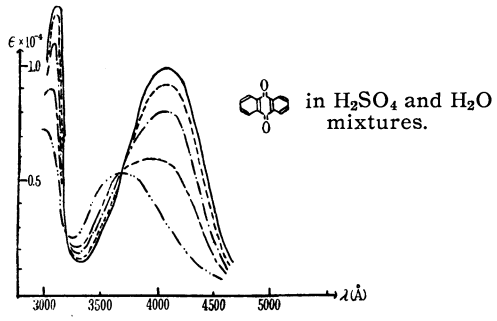
$C$; Molar concentration of specimen, suffix B means unprotonated base, $BH^+$ means protonated base.

$\varepsilon$; Molar extinction-coefficient of specimen.

$a$; Molar activity coefficient of each component.

$H_0$; Logarithm of the activity of the hydrogen ion.

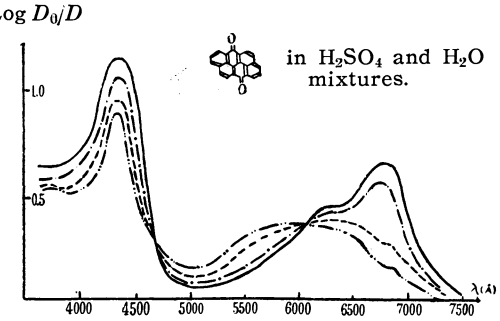
$H_0$ being the Kolthoff's acidity-function which really means the value of $\log a_{H^+}$. Equation (2) means that Beer's law is held. $K$ is the dissociation constant of the ionized base. So from the equation from (1) to (6), the base-strength $pK_B$ is defined. The $pK_B$ of each of these compounds have been estimated in this manner. Among the results obtained, for instance, the result for anthraquinone was in good agreement with that of L. P. Hammett. The former value is $-7.5$, the latter is $-8.0$. In this case the absorption curves are corrected approximately against the influence of the solvent-effect by the lateral shift of spectrograph with the isobestic-point or the sharp peak of the absorption-curve as standards after L. P. Hammet. The small difference of $pK_B$ to that of L. P. Hammett was found, when the Kolthoff's table was used unlike in the case of him, who had used his own table. In this sense the result obtained agreed well with that of L. P. Hammett. The absorption-spectra of anthraquinone in various acidity of sulfuric acid is illustrated in Fig. 1.




——— 100% $H_2SO_4$ – – – – – 89% $H_2SO_4$
– – – – – 96% $H_2SO_4$ —·—·— 86% $H_2SO_4$
—·—·— 93% $H_2SO_4$

Fig. 1. The absorption spectrum of anthraquinone in $H_2SO_4$ and $H_2O$ mixtures (corrected by the lateral schift).

Another example in the longer side of the visible region is illustrated with anthanthrone of which $pK_B$ is estimated on the Table II, and of which absorption-curves are shown in Fig. 2. The state of existence of equilibrium between the complex and it's reduced form with chromous ion ($Cr^{++}$), which suggests the nature of this type of complex, is shown in Fig. 3, with flavanthrone in which protons ($H^+$) may be assumed to be attached to both the carbonyl group and nitrogen atoms. In Fig. 3, curve (I) shows that of the completely




——— 100% $H_2SO_4$ – – – – – 92% $H_2SO_4$
—·—·— 96% $H_2SO_4$ —··—·· 85% $H_2SO_4$

Fig. 2. The absorption spectrum of anthanthrene in $H_2SO_4$ and $H_2O$ mixtures (corrected by the lateral schift).

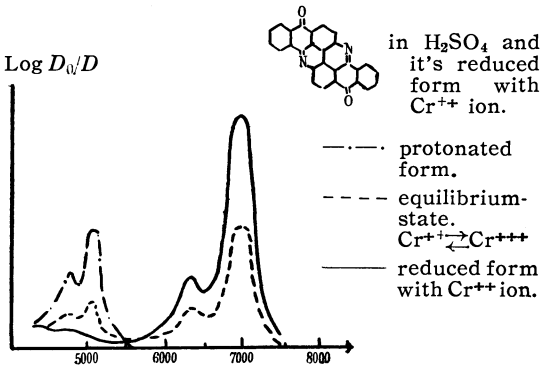



Fig. 3. The absorption spectrum of flavanthrone in $H_2SO_4$ and it's reduced form with chromous ion.

reduced form, curve (II) shows that of the complex-form which may be called the oxidized form, With other complexes of quinones, they may be said to be similar to those of the vatted states, which are shown in Fig. 4. With mere hydrocarbons in this series, the same may be said as those of quinones. However, in these cases, it will be necessary to consider how many numbers of protons are attached to the hydrocarbon molecule and to what positions in the molecule they are attached. In this report, we have as-

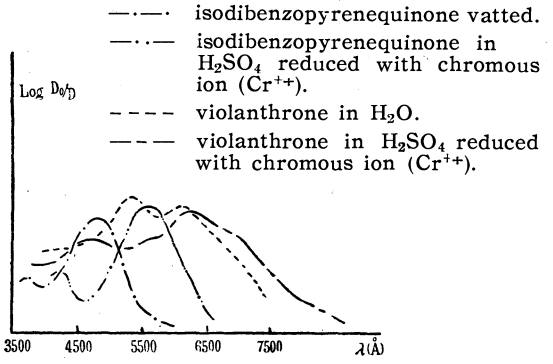



Fig. 4. The absorption spectra of isodibenzoquinone and violanthrone vatted in $H_2O$, and reduced with chromous ion ($Cr^{++}$) in $H_2SO_4$.

TABLE II

$pK_B$ VALUES FOR ANTHANTHRONE BY ISOBESTIC-POINT METHOD

| Wavelenghth (Å) | Optical density in $H_2SO_4$ and $H_2O$ mixtures 100% | 96% | 92% | 85% | $pK_B$* | $pK_B$** |
|---|---|---|---|---|---|---|
| 6500 | 0.50 | 0.45 | 0.36 | 0.31 | −7.6 | −7.5 |
| 6600 | 0.56 | 0.51 | 0.34 | 0.25 | −7.5 | −7.7 |
| 6700 | 0.63 | 0.55 | 0.30 | 0.20 | −7.7 | −8.0 |
| 6800 | 0.66 | 0.55 | 0.26 | 0.15 | −7.8 | −8.1 |
| 6900 | 0.58 | 0.44 | 0.22 | 0.12 | −8.0 | −8.1 |
| 7000 | 0.38 | 0.28 | 0.17 | 0.09 | −8.1 | −8.0 |
| | | | | average | −7.8 | −7.9 |
| | | | | Total average | −7.8 | |

* means the $pK_B$ values from the absorption-curves observed in 96% $H_2SO_4$ and 100% $H_2SO_4$. It is assumed that in 100% $H_2SO_4$ the specimen is completely protonated.

** means the $pK_B$ values from the absorption-curves observed in 92% $H_2SO_4$ and 100% $H_2SO_4$.

sumed the numbers of protons attached or dispatched from the hydrocarbon molecule reversibly, empirically from the shapes of the absorption-curves of the complexes in the acid, as is shown in Fig. 5 and Fig. 6 and Fig. 7, which are considered to be in equilibria with the original hydrocarbons. These are usually one, and in several cases two protons which contribute to $pK$ or basicity. The problem, to what positions in the molecule the protons are attached can not be discussed in this method of measurement. Even, it may be inferred from the whole result of this report as follows; they may be attached to the positions in the molecule where the $\pi$-electrons are localized. In Fig. 5 which is the case of anthanthrene molecule, it is shown from it's shapes of absorption-curves as in the case of quinones, that there exist equilibrium between hydrocarbon and its complex. There exist three isobestic-points above 4000Å which support the existence of equilibrium-state and in this case in one definite range of wave-length between the isobestic-points, there is only mere increase or decrease of extinction of light with the elevation

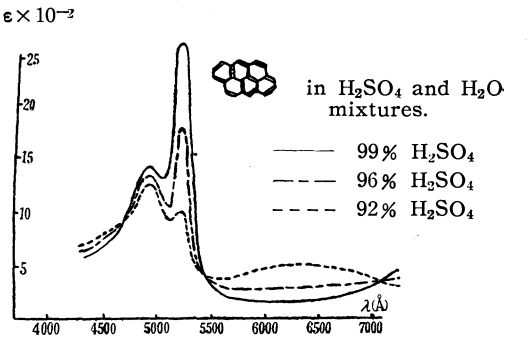



Fig. 5. The absorption spectrum of anthanthrene in $H_2SO_4$ and $H_2O$ mixtures (corrected by the lateral schift).

of the concentration of the acid. In this case, it is assumed that there is only one proton which takes parts in the complex-formation, or in other words, there is only one phase of substance or complex. In Fig. 6 which is the case of dibenzopyrene (XXIII), there are also isobestic-points, but in this case in one definite range of wavelength from 5000 to 6000 Å, there are both increase and decrease of extinction of light with the elevation of the degrees of acidity. In this case, it is assumed that there exist two final states of complexes (one-proton-complex, and two-proton-complex in the sense mentioned above.). The complex-formation proceeds by two steps in this case. On the Table III, the evaluation of $pK$ is shown

TABLE III

$pK_B$ VALUES FOR VIOLANTHRENE BY ISOVESTIC-POINT METHOD

| Wavelenghth (Å) | Extinction-coefficient in $H_2SO_4$ and $H_2O$ mixtures ($\varepsilon\times10^{-4}$) 99.5% | 96% | 92% | 85% | $pK_B$ |
|---|---|---|---|---|---|
| 6500 | 27.5 | 26.5 | 25.5 | 18.0 | |
| 6600 | 27.0 | 26.0 | 25.0 | 18.0 | |
| 6700 | 26.3 | 25.5 | 24.5 | 17.6 | −7.0 |
| 6800 | 33.0 | 30.0 | 26.0 | 16.3 | −7.4 |
| 6900 | 44.0 | 40.0 | 34.0 | 18.0 | −7.4 |
| 7000 | 62.0 | 56.0 | 45.0 | 21.0 | −7.4 |
| 7100 | 74.0 | 66.0 | 56.0 | 23.0 | −7.4 |
| 7200 | 60.0 | 52.0 | 41.0 | 21.0 | −7.3 |
| 7300 | 32.0 | 30.0 | 26.0 | 16.0 | −7.1 |
| 7400 | 21.0 | 20.0 | 18.0 | 13.0 | −7.0 |
| | | | | average | −7.2 |

with violanthrene. In every case, when we add very small amounts of chromous ion ($Cr^{++}$), the shape of the absorption-curve changes, there stands another peak towards the shorter side of the spectrum, which seems to be in equilibrium with the former one, and the solution be comes to possess fluorescence. But, it is not studied quantitatively here. In this report, the color-change of a specimen is described, when $Cr^{++}$ ion is added, on the Table IV. This color-change is reversible, when hydrogenperoxide or free radical is added.

TABLE IV

THE COLOR-REACTIONS OF CONDENSED POLYNUCLEAR AROMATIC HYDROCARBONS AND THEIR RELATED QUINONES IN THE CONCENTRATED SULFURIC ACID

| Index No. of structural formula of specimen | Name of specimens | Color-change in $H_2SO_4$ ($+H_2O_2$) $\rightleftarrows$ ($Cr^{++}$) | |
|---|---|---|---|
| XX | anthanthrene | green | red brown |
| VI | mesonaphthodianthrene | red viollet | colorless |
| XIV | dibenzopyrenequinone | viollet | pale brown |
| IX | helianthrone | orange | greenish yellow |
| XVIII | violanthrone | red viollet | green |
| XVIII | isoviolanthrone | green | blue |
| XVI | pyranthrone | blue | orange-red |
| XV | isodibenzopyrenequinone | dark orange | red-viollet |
| XIX | flavanthrone | orange | green |
| | indanthrone | dark brown | pale brown |
| | perylene-tetracerboxylic acid | scarlet | green |
| XXXI | violanthrene | blue green | sky blue |
| XXXIII | perylene | green red viollet | blue green |
| XXVIII | ovalene | green | red viollet |
| XXVII | dibenzocoronene | dark green | red viollet |
| XXXV | thianthrene | red | colorless |
| XXIII | dibenzopyrene | blue-green | red violet |
| II | benzanthrone | red | red (No Change) |

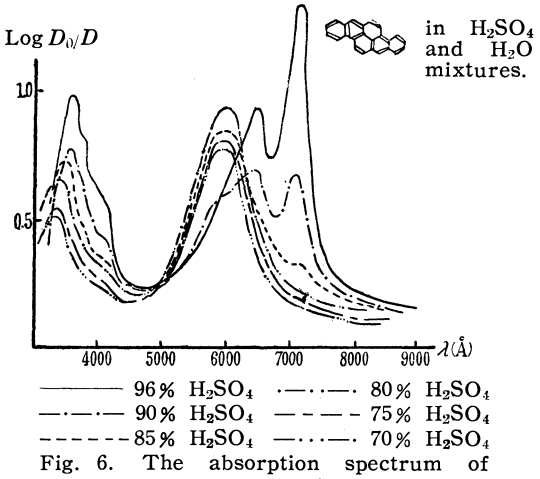



Fig. 6. The absorption spectrum of dibenzopyrene in $H_2SO_4$ and $H_2O$ mixtures.

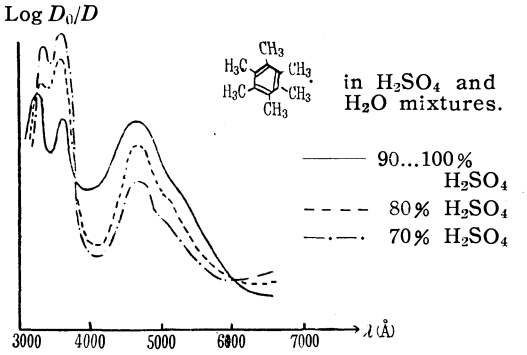



Fig. 7. The absorptionspectrum of hexamethylbenzene in $H_2SO_4$ and $H_2O$ mixtures (corrected by the lateral schift).

## Results and Discussions

The estimated $pK_B$ with various condensed polynuclear aromatic hydrocarbons and their related quinones are shown on the Table V. It seems from that table that $pK_B$ becomes smaller as the molecular-weight becomes larger. However, as in the case of dibenzopyrene, there exist two values of $pK_B$ which means that two protons actually take parts in the complex-formation. The smaller value is $-7.4$, which is comparatively equivalent to that of anthanthrene, ovalene, dibenzocoronene, etc. The relatively larger value is $-5.1$, which is equivalent to hexamethylbenzene, pyrene, tetracene. To explain the contradiction between the experimental results, and the general understanding which suggests that the basicity or freee energy of complex-formation becomes larger as the molecular weight increases, it may be reasonable to think that the smaller value of anthanthrene, ovalen, dibenzocoronene, which are found in the experiment is the smaller one of the two $pK_B$ values, the larger one not being able to be found in this measurement, perpaps owing to the low solubility or unstability of these compounds in the sulfuric acid. In the case of smaller molecules such as hexamethylbenzen, or tetracene, it may be considered that one proton takes part in the complex-formation. In the case of larger molecules such as anthanthrene,

TABLE V

$pK_B$ VALUES FOR CONDENSED POLYNUCLEAR AROMATIC HYDROCARBONS AND THEIR RELATED QUINONES BY ISOBESTIC-POINT METHOD

| Index No. of structural formura of specimens | Name of speciment | $pK_B$ |
|---|---|---|
| I | peri-naphthoindanone | −0.4 |
| II | benzanthrone | −3.2 |
| III | *p*-naphthoquinone | −7.2 |
| IV | anthraquinone | −7.5 |
| V | naphthacenequinone | −8.4 |
| VI | mesonaphthodianthrone | −6.0 |
| VII | perylenequinone | −5.5 |
| VIII | 1.2-benzoperylene-3.10-quinone | −4.7 |
| IX | helianthrone | −5.2 |
| X | 1.2.7.8.-dibenzo-3.9.-quinone | −5.1 |
| XI | dianthrone | * |
| XII | diphenoquinone | ** |
| XIII | *p*-benzoquinone | *** |
| XIV | dibenzopyrenequinone | −7.4 |
| XVI | pyranthrone | −6.0 |
| XVII | violanthrone | −7.6 |
| XX | anthanthrone | −7.9 |
| XXI | hexamethylbenzene | −5.0 |
| XII | pyrene | −4.7 |
| XXIII | dibenzopyrene | −5.1<br>−7.4 |
| XXV | anthantrene | −7.4 |
| XXVI | pyranthrene | −8.2 |
| XXVII | dibenzocoronene | −8.7 |
| XXVIII | ovalene | −8.9 |
| XXX | tetracene | −6.6 |
| XXIX | benzoperylene | −8.3 |
| XXXI | violanthrene | −7.3 |
| XXXIII | perylene | −5.2**** |
| XXXIV | mesonaphthodianthrene | −6.0***** |

*, **, ***. It is not yet possible to measure the value owing to the destruction of specimens in the concentrated sulfuric acid.

****, *****. New trials are being attempted with other appropriate solvents and at low temperature.

ovalene, violanthrene, dibenzopyrene, it may be considered that two protones take part in the complex-formation. It may be thought that there is a relatively small difference of $pK_B$ value with the shape of the molecule in such smaller molecules as hexamethylbenzene, tetracene etc., as in the cases of aza-aromatic hydrocarbons such as pyridine, quinoline, and acridine. When one proton is added to the molecule, the aromaticity for the rest of the molecule is reasonably destroyed and so the basicity corresponding to the next proton becomes much smaller than that corresponding to the first one, as in the case of diazine such as pyrimidine, pyrazine, cinnoline etc[5]. It may be possible, on the same way of consideration, to explain the difference of $pK_B$ value, or the basicity between the monoketones such as perinaphhtoindenone, benzoanthrone, and quinones such as anthraquinone, violanthrone etc. In the cases of quinones, it seems unreasonable to consider that there exist two values of $pK_B$ from the cryoscopic data of L. P. Hammett and J. Dyrup, who had determined the number of protons attached to the anthraquinone molecule from the depression of the freezingpoint of the sulfuric acid. However, in the present measurement, one value (−7.5) is found, which seems to be considerably smaller compared with that of benzoanthrone of which $pK_B$ value is −3.2. To explain the considerably large difference, it may be considered that in the present measurement it is unable to find the larger one of two $pK$ owing to the stability of one-proton-complex, or the low-solubility of that in the sulfuric acid. The relatively small difference between the $pK$ values of various quinones may be ascribed to the molecular structure of each molecule. The relatively larger $pK_B$ observed in violanthrene, mesonaphthodianthrene molecule compared with that observed in ovalene, anthanthrene molecule, suggests that the proton is easily attached to the molecule which is more or less easily excited, or which seems to have localized $\pi$-electron. Such sorts of molecules are known to have more or less localized $\pi$-electron from the magnetic study by H. Akamatu and Y. Matunaga in our laboratory[6]. It is reported by E. Clar that zethrene is easily soluble in the glacial acetic acid to be protonated by it, which means its $pK_B$ is relatively very large, or it is relatively very basic compared with other hydrocarbons of this sort. It is explained that zethrene possesses localized $\pi$-electron from the standpoint of organic chemistry and may be a little para-magnetic, if measured. From this standpoint pentacene, and hexacene may be more basic than tetra-

5) A. Albert, R. Goldacre and J. Phillips., *J. Chem. Soc.*, **1948**, 2240.

6) H. Akamatu and Y. Matsunaga, This Bulletin **26**, 364 (1953).

cene, if they are measured. In addition, the molecular extinction-coefficient of violanthrene in the sulfuric acid is about twenty times larger than that taken in non-polar solvent.

## Summary

The basicity of the condensed polynuclear aromatic hydrocarbons and their related quinones with higher molecular weight have been measured after the method of L. P. Hammett and J. Dyrup, and it is approximately estimated in terms of $pK_B$. In dibenzopyrene molecule two values of $pK_B$ have been found. The larger seems to correspond to that of the smaller molecules such as hexamethylbenzene, tetracene. The smaller one seems to be equivalent to that of ovalene, anthanthrene etc. approximately, with which molecules the larger $pK_B$ value seems to be unable to be found, owing to the unstability or the low-solubility of them in the sulfuric acid in the present method of measurement. The relatively large difference of $pK_B$ between monoketones and quinones seems to be explained on the same considerations as above. The relatively small difference of $pK_B$ seems to be dependent on the molecular structure as in the case of azaaromatic hydrocarbons such as pyridine, quinoline and acridine. From the results of such series of molecules as violanthrene, mesonaphhtodianthrene, zethrene, compared with the series of circulartype of molecules such as ovalene, anthanthrene, it is suggested that the proton is more easily attached to the molecule which seems to have localized $\pi$-electron in some sense.

The author expresses his hearty thanks to Prof. H. Akamatu, who has directed him throughout this study and to Dr. Inokuchi and M. Kobayashi and to Mr. Matsunaga for their collaboration and advice in this study. The cost of this study was defrayed from the grant of the Ministry of Education, to which the author's thanks are due.

*Department of Chemistry, Faculty of Science, Tokyo University, Tokyo*

# *A Note on the Measurement of the Absorption Coefficient in Infra-red Region. Influence of the Thickness of Layer on the Measurement of Absorption Coefficient*

By Masasi YASUMI

(Received November 30, 1954)

## Introduction

In order to determine the absorption coefficient $k$ (or absorption index $\kappa$) in infra-red region, the transmission method is usually used. In the most of the researches, it is assumed that the Beer's rule holds strictly, For the gases and dilute solutions, this assumption may be valid, but inadequate to the liquids and solids which are highly absorbing. The invalidity of the Beer's law is due to the boundary reflexion and to the multiple reflexion of the substance layer whose thickness is comparable to the wavelength.

Recently, Simon[1] has investigated the surface reflexion of the highly absorbing substances including carbon tetrachloride and has obtained the values of refractive indices and of the absorption indices from the reflexion coefficients.

We have calculated the transmission coefficient of the infra-red beam passing through a thin layer of liquid carbon tetrachloride according to the correct formula using Simon's data, and have compared this with the value calculated from simple Beer's law.

The effect of the thickness of the layer is very marked, and it is concluded that we cannot obtain the correct value of the absorption coefficient for the highly absorbing materials by the simple transmission method usually used.

## The Formula of Transmission Coefficient for the Single Plane Layer

A plane electromagnetic wave of the wavelength $\lambda$ is considered to be linearly polarized and to be propagated in the medium 1. An absorbing dielectric layer with plane boundary surface is placed as shown in Fig. 1.

1) I. Simon, *J. Opt. Soc. Am.*, **41**, 336 (1951).

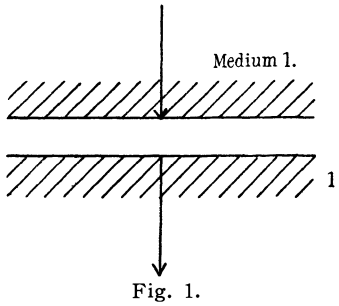



Fig. 1.

The direction of the propagation of incident wave is considered to be normal to the boundary surface. A part of the wave will be transmitted through the sheet characterized by refractive index $n$, absorption coefficient $k$ ($=n\kappa$, where $\kappa$ is absorption index) and thickness $d$. The medium 1 is considered to be non-absorbing and to be characterized by refractive index $n_1$.

The transmission coefficient of the sheet $D^2$ is expressed as follows[2]:

$$D^2=e^{-\frac{4\pi kd}{\lambda}}\times\frac{1+R_{12}^4-2R_{12}^2\cos 2\gamma}{1+R_{12}^4e^{-\frac{8\pi kd}{\lambda}}-2R_{12}^2e^{-\frac{4\pi kd}{\lambda}}\cos\left(\frac{4\pi nd}{\lambda}+2\gamma\right)}$$

$$=\frac{\sinh^2(-\ln R_{12})+\sin^2\gamma}{\sinh^2\left(\frac{2\pi kd}{\lambda}-\ln R_{12}\right)+\sin^2\left(\frac{2\pi nd}{\lambda}+\gamma\right)} \qquad (1)$$

where

$$R_{12}^2=\frac{(n-n_1)^2+k^2}{(n+n_1)^2+k^2} \qquad (2)$$

$$\tan\gamma=\frac{2n_1k}{(n^2-n_1^2)+k^2} \qquad (3)$$

**Transmission Coefficient for the Thin Layer of Liquid Carbon Tetrachloride**

The calculation is made for the thin layer of carbon tetrachloride placed between rock salt plates.

The refractive indices and the absorption coefficients of carbon tetrachloride for the infra-red waves in the wave number 760–815 $cm^{-1}$ region are tabulated in Table I. The data are taken from Simon's paper[1]. Using these values, the values of $R_{12}$, and $\tan\gamma$ are calculated. In this calculation, $n_1$ is taken to be 1.52. The calculated values are tabulated also in Table I.

Carbon tetrachloride shows marked absorption and dispersion in the region 760–815 $cm^{-1}$ [1]. The suitable thickness of the layer for the measurement of the absorption coefficients by transmission method in this region would be, therefore, very small and would be comparable to the wave-length. We have calculated the transmission coefficients $D^2$ for the layer of the thickness $d=2.5\times10^{-5}$ cm., $5\times10^{-5}$ cm. and $10^{-4}$ cm. respectively. On the other hand, the values of hypothetical transmission coefficient $T^2=\exp(-4\pi kd/\lambda)$, are also calculated. These values are tabulated in Tables II, III, and IV. The values of $(-\ln D^2)$ and $4\pi kd/\lambda$ are also given in Tables II, III and IV.

2) M. Yasumi, This Bulletin, 24, 54 (1951).

TABLE I

REFRACTIVE INDICES, ABSORPTION COEFFICIENTS AND RELATED CONSTANTS OF CARBONTETRACHLORIDE IN INFRA-RED REGION

| $\bar{\nu}$(cm.$^{-1}$) | $n$ | $k$ | $R_{12}$ | $\tan\gamma$ |
|---|---|---|---|---|
| 760 | 1.30 | 1.20 | 0.40 | −21.5 |
| 765 | 1.30 | 1.25 | 0.41 | −76.1 |
| 770 | 1.30 | 1.25 | 0.41 | −76.1 |
| 775 | 1.45 | 1.30 | 0.41 | + 2.65 |
| 780 | 1.85 | 1.75 | 0.51 | + 1.29 |
| 785 | 2.15 | 3.10 | 0.66 | + 0.79 |
| 790 | 1.70 | 3.50 | 0.74 | + 0.78 |
| 795 | 1.20 | 2.00 | 0.60 | + 1.94 |
| 800 | 0.80 | 0.80 | 0.44 | − 2.38 |
| 805 | 0.85 | 0.45 | 0.34 | − 0.99 |
| 810 | 0.95 | 0.25 | 0.25 | − 0.52 |
| 815 | 1.05 | 0.15 | 0.16 | − 0.41 |

The value of refractive index of rock salt is taken as $n_1=1.52$.

TABLE II

TRANSMISSION COEFFICIENTS AND RELATED QUANTITIES FOR THE LAYER OF CARBON TETRACHLORIDE

$d=2.5\times10^{-5}$ cm.

| $\bar{\nu}$(cm$^{-1}$) | $D^2$ | $\exp(-4\pi kd/\lambda)$ | $-\ln D^2$ | $4\pi kd/\lambda$ |
|---|---|---|---|---|
| 760 | 0.818 | 0.751 | 0.201 | 0.287 |
| 765 | 0.796 | 0.740 | 0.228 | 0.301 |
| 770 | 0.796 | 0.740 | 0.228 | 0.303 |
| 775 | 0.740 | 0.728 | 0.301 | 0.317 |
| 780 | 0.635 | 0.674 | 0.454 | 0.395 |
| 785 | 0.394 | 0.465 | 0.931 | 0.766 |
| 790 | 0.377 | 0.418 | 0.976 | 0.873 |
| 795 | 0.624 | 0.605 | 0.471 | 0.502 |
| 800 | 0.884 | 0.812 | 0.123 | 0.208 |
| 805 | 0.935 | 0.892 | 0.067 | 0.114 |
| 810 | 0.955 | 0.938 | 0.046 | 0.064 |
| 815 | 0.964 | 0.963 | 0.037 | 0.038 |

TABLE III

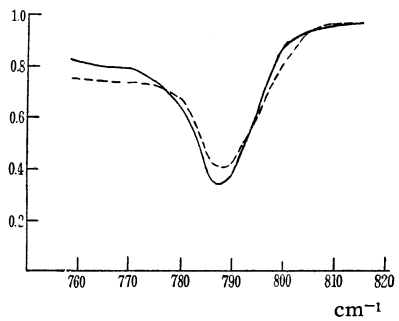
$d=5\times10^{-5}$ cm.

| $\bar{\nu}$(cm$^{-1}$) | $D^2$ | $\exp(-4\pi kd/\lambda)$ | $-\ln D^2$ | $4\pi kd/\lambda$ |
|---|---|---|---|---|
| 760 | 0.663 | 0.563 | 0.411 | 0.575 |
| 765 | 0.639 | 0.547 | 0.448 | 0.603 |
| 770 | 0.635 | 0.546 | 0.454 | 0.606 |
| 775 | 0.565 | 0.530 | 0.571 | 0.634 |
| 780 | 0.442 | 0.452 | 0.892 | 0.792 |
| 785 | 0.182 | 0.217 | 1.70 | 1.53 |
| 790 | 0.160 | 0.174 | 1.83 | 1.75 |
| 795 | 0.444 | 0.367 | 0.812 | 1.00 |
| 800 | 0.761 | 0.657 | 0.273 | 0.417 |
| 805 | 0.886 | 0.799 | 0.121 | 0.224 |
| 810 | 0.902 | 0.880 | 0.103 | 0.127 |
| 815 | 0.936 | 0.927 | 0.066 | 0.076 |

TABLE IV

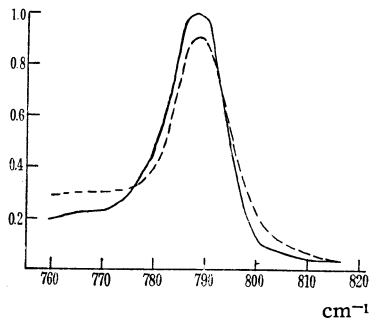
$d=10^{-4}$ cm.

| $\bar{\nu}$(cm$^{-1}$) | $D^2$ | $\exp(-4\pi kd/\lambda)$ | $-\ln D^2$ | $4\pi kd/\lambda$ |
|---|---|---|---|---|
| 760 | 0.415 | 0.317 | 0.879 | 1.15 |
| 765 | 0.391 | 0.301 | 0.939 | 1.20 |
| 770 | 0.390 | 0.298 | 0.942 | 1.21 |
| 775 | 0.348 | 0.281 | 1.06 | 1.27 |
| 780 | 0.224 | 0.206 | 1.50 | 1.58 |
| 785 | 0.044 | 0.047 | 3.12 | 3.06 |
| 790 | 0.030 | 0.030 | 3.51 | 3.50 |
| 795 | 0.187 | 0.135 | 1.68 | 2.00 |
| 800 | 0.553 | 0.434 | 0.592 | 0.834 |
| 805 | 0.725 | 0.639 | 0.322 | 0.448 |
| 810 | 0.797 | 0.776 | 0.227 | 0.254 |
| 815 | 0.866 | 0.858 | 0.144 | 0.153 |




——— $D^2$
- - - - $T^2$

Fig. 2.




——— $-\ln D^2$
- - - - $44\pi kd/\lambda$

Fig. 3.

The values of $D^2$ and $T^2$ versus wave numbers for the thickness of $d=2.5\times10^{-4}$ cm. are illustrated in Fig. 2. The behavior of $(-\ln D^2)$ and $4\pi kd/\lambda$ versus wave numbers are shown in Fig. 3.

## Discussion

As shown in Tables I—III, and Figs. 2—3, it is concluded that the values of the transmission coefficients for the thin layer of carbon tetrachloride calculated with the exact formula are markedly different from the hypothetical transmission coefficient calculated with simple Beer's law. In the case of $d=10^{-4}$ cm., the maximum deviation amounts about 30%.

If we calculate the absorption coefficients from the values of $D^2$, which will be identical with the experimental transmission coefficients in ideal cases, according to simple Beer's law, the obtained values would be $-\ln D^2/(4\pi d/\lambda)$. As shown in Table I—III, the values of $(-\ln D^2)$ are markedly different from $4\pi kd/\lambda$.

The situation will be more serious when the relative absorption coefficient is concerned, for the deviation will have plus sign in one wave-length region and minus sign in another region.

It can be said that the transmission method based upon the simple Beer's law cannot be applied for the highly absorbing substances and an erroneous conclusion would be drawn if we calculate absorption coefficient according to Beer's law.

It may not be unexpected that the absorption coefficient is dependent on the thickness of the layer and that the unexisting lines appear in some case or existing lines disappear in another case[3].

For the less absorbing materials the effect of the thickness will be less important, but for the lines whose absorption coefficient is about 0.5[4] the effect is not negligible[5].

## Summary

The transmission coefficient of a thin layer of carbon tetrachloride is calculated according to the exact formula and compared with the

3) Earle K. Plyer and Nicola Aquista, *J. Opt. Soc. Am.*, **44**, 505 (1954).

4) e. g. k is ca. 0.6 for 8.90 $\mu$ of ethyl ether, 0.5 for 5.8 $\mu$ of ethyl acetate.

5) This conclusion is drawn from the calculation made by K. Kuratani.

value calculated by simple Beer's rule.

The usual transmission method which is based upon the Beer's law is inadequate to the determination of the absorption coefficient of highly absorbing substances such as carbon tetrachloride.

We are grateful to Prof. San-ichiro Mizushima for his kind advice and the encouragement throughout this work, and to Dr. Kenji Kuratani for his valuable advice.

Our thanks are also due to the Ministry of Education for a grant in aid of this research.

*Institute of Science and Technology,*
*Tokyo University,*
*Tokyo*

# *A Rapid Colorimetric Determination of Vanadium in Carbon Materials*

By Ken SUGAWARA, Motoharu TANAKA and Akiya KOZAWA*

(Received February 9, 1955)

## Introduction

Among heavy metal impurities found in the "electrolyte" (a concentrated sodium chloride solution), the undesirable effect of vanadium upon the chlorine-caustic electrolysis is particularly marked even at a low concentration.[1] Hence, the establishment of a reliable and rapid method of vanadium determination is desirable to estimate the quality of anode carbon and its raw materials and to improve upon it. Indeed, there have been many method tested and others proposed by various investigators. Some, however, are unsatisfactory because insufficient attention was paid to the possible escape of vanadium in the ashing process[2], while others involve some tedious processes unsuitable for use in industrial laboratories.

By overcoming these difficulties, the authors devised a new method having the following characteristics.

(1) Addition of sodium carbonate to the sample accelerates the ashing and guards against the escape of vanadium during the process.

(2) The use of ferric hydroxide gives a simple method for separation of vanadium which replaces E.B. Sandell's tedious processes of leaching the sodium carbonate cake and extracting the vanadium oxinate in the original phospho-tungstate method[3].

## Procedure

Pulverize a 0.5–1.0 g. sample so that it can pass through a 100 mesh sieve. Grind the sieved sample in an agate mortar with 2 g. of sodium carbonate for a few minutes and transfer it into a quartz dish so as to make a thin layer. Place it in an electric furnace at 650–750°C and reduce it to ash. After complete ashing, dissolve the ash in sulfuric acid and boil for about five minutes.

Add 5 mg. of ferric iron and 50 ml. of distilled water to the solution thus obtained. Neutralize the solution roughly with sodium hydroxide (3N) while stirring constantly. The neutralization is completed by using six drops or less of ammonia (3N) to B. C. P. or *p*-nitrophenol as indicator. Filter and dissolve the precipitate into 20 ml. of a hot phosphoric acid (1 : 3). Add one ml. of sodium tungstate reagent (0.5M) and keep the solution boiling for about five minutes. After cooling to room temperature, transfer the solution into a 25 ml. measuring flask and fill it with distilled water to the 25 ml. mark. Then the optical density is measured spectrophotometrically at the wavelength of 410 m$\mu$ to determine the vanadium, using the working curve described by one of the authors.[4]

When the vanadium content of the sample is below 30 $\mu$g., it is advisable to prepare a standard solution of a concentration approximate to that of the sample, and to compare the color of the sample with the standard, using ordinary Nessler tubes of 8 mm. caliber and 35 cm. height. In this way even 5 $\mu$g. of vanadium can be determined.

* Department of Applied Chemistry, Faculty of Engineering, Nagoya University.

1) G. Angel and T. Lundén, *J. Electrochem, Soc.*, **99**, 435 (1952).

2) I. Iwasaki and I. Ukimoto, *J. Chem. Soc. Japan*, **63**, 1678 (1942).

3) E. B. Sandell, *Ind. Eng. Chem.*, Anal. Ed., **8**, 336 (1936).

4) M. Tanaka, This Bulletin, **27**, 10 (1954).

## Discussion

1) **Ashing.**—As shown in Table I, the presence of sodium carbonate hinders the escape of vanadium in the ashing process, which is considerable when it is absent. At the same time the carbonate accelerates ashing. Thus, in the presence of the salt, the ashing process which would otherwise require a full hour, is completed within twenty minutes at 650–750°C.

TABLE I

ANALYSES OF SEVERAL SAMPLES

| Sample | Sample taken g. | V added μg. | V found μg. | V found* μg. |
|---|---|---|---|---|
| Coke No. 1 | 0.50 | 0 | 8 | 8.5 |
| 〃 | 0.50 | 23 | 30 | — |
| Coke No. 2 | 0.50 | 0 | 226 | 230 |
| Coke No. 2† | 0.50 | 0 | 158 | — |
| Coke No. 2† | 0.50 | 0 | 181 | — |
| Coke No. 3 | 1.00 | 0 | 18 | 16 |
| 〃 | 0.50 | 46 | 57 | — |
| Graphite No. 4 | 0.50 | 0 | 128 | 133 |
| 〃 | 0.50 | 46 | 176 | — |
| 〃 | 0.50 | 92 | 224 | — |
| Grrphite No. 4† | 0.50 | 0 | 100 | — |
| Graphite No. 4† | 0.50 | 0 | 119 | — |
| Graphite No. 5 | 0.50 | 0 | 8 | 9 |
| Cathode of "AD" cell (containing Mn) | 0.50 | 0 | 10 | 12 |
| 〃 | 0.50 | 23 | 34 | — |
| 〃 | 0.50 | 46 | 57 | — |

* Determined after the ashed mixture was once put to fusion.

† Ashed without sodium carbonate.

The process of ashing, here mentioned, is sufficient to bring the vanadium in the sample completely into a soluble form. As shown in the same table, the vanadium values do not increase after the ashed sample is once put to fusion. Consequently, fusion is dispensable in the present procedure.

Also it must be added that the wet method of combustion using sodium iodate[5] can successfully replace the ashing. The sieved sample (0.5 g.) is put into 10 ml. of concentrated sulfuric acid contained in a 100 ml. beaker. While the beaker is kept slightly heated, 8—9 g. of sodium iodate powder is added. A violent reaction occurs with a considerable sublimation of iodine, giving a yellowish color to the solution. Diluted with 30 ml. of distilled water, the solution is kept boiling until the iodine is completely expelled. Then the solution is ready for the procedure described above from the point of addition of ferric salt.

The iodate method may be recommended because of its rapidity, but it must be noted that it requires iodate which is expensive and considerable skill for the manipulation.

2) **Ferric Hydroxide as Vanadium Collector**[6].—In the present method, vanadium is collected and separated by ferric hydroxied from the ions of ammonium and potassium which may interfere with the final colorimetry. The following experiment shows that the vanadium collection is complete when it is conducted under the conditions prescribed in the procedure. A series of sulfuric acid solutions was prepared containing various amounts of vanadium, tetra- and quinque-valent in addition to 5 mg. iron. These solutions were processed according to the directions given in the procedure. Table II shows that the result is quite satisfactory. Also it is noticeable that during the process the tetravalent vanadium is completely oxidized into quinque-valent.

TABLE II

COLLECTION OF VANADIUM BY FERRIC HYDROXIDE

| No. of experiment | V taken μg. | Valency | V found μg. | Recovery % |
|---|---|---|---|---|
| 1 | 50 | IV | 50 | 100 |
| 2 | 125 | IV | 123 | 97 |
| 3 | 250 | IV | 248 | 99 |
| 4 | 200 | V | 201 | 100 |
| 5 | 300 | V | 295 | 98 |

3) **Interference by Large Amounts of Iron and/or Manganese and its Avoidance.**—When more than one mg. of manganese is present in the sulfuric acid solution, it is partly coprecipitated with ferric hydroxide and oxidized by the air into the tri-valent state, forming pink colored manganic phosphate by later treatment with phosphoric acid. Further, the color is intensified by the addition of sodium tungstate, causing remarkable error in the colorimetry. Also more than 10 mg. of iron cause a considerable error. E.B. Sandell avoided such interferences by sodium carbonate fusion and leaching of the cake obtained. In our procedure, the interfering manganese and iron can be separated as given in the following example: a series of 60 ml. of sulfuric acid solution (0.5N) was prepared in which various amounts of vanadium are contained in addition to 5 mg. each of iron and manganese. After the addition of one ml. of 30% hydrogen peroxide, the

5) T. Kiba, S. Ohashi, T. Takagi and Y. Hirota, *Japan Analyst* 2, No. 5, 446 (1953).

6) K. Sugawara, M. Tanaka and H. Naito, This Bulletin, 26, 417 (1953).

solutions were neutralized with sodium hydroxide solution (3N) and 3—5 ml. of the same reagent were added in excess. After being stirred well, they were left standing at 70°C for about ten minutes until the decomposition of the hydrogen peroxide was complete. The precipitate was filtered off through a glass filter and the filtrate was processed according to the direction in the procedure. Table III proves that the separation was successful.

TABLE III
SEPARATION OF VANADIUM FROM MANGANESE AND IRON

| No. of experiment | V taken μg. | V found μg. | Recovery % |
|---|---|---|---|
| 1 | 0 | 0 | — |
| 2 | 11.5 | 12 | 104 |
| 3 | 23 | 23 | 100 |
| 4 | 115 | 118 | 103 |
| 5 | 230 | 237 | 103 |

4) **Other Interfering Elements.**—Ti, Zr, Bi, Sb, and Sn are considered possible as other interfering elements. Their contents in anode samples, however, are negligible so that a discussion on them can be dispensed with.

5) Table I shows some results of the application of the proposed method to coke and graphite samples and particularly a cathode sample of air depolarized cell. The latter was remarkably contamined with manganese. Consequently their analyses were carried out under the special directions given in the preceding article.

*Faculty of Science, Nagoya University, Nagoya*

# *A New Method of Spectrophotometric Determination of Iodine in Natural Waters*

By Ken SUGAWARA, Tadashiro KOYAMA and Kikuo TERADA

(Received February 16, 1955)

## Introduction

Because no appropriate method is available for the determination of a small amount of iodine found in ordinary natural waters, the determination of this element has been limited to special kinds of water which are iodine-rich. In order to fill this lack, the present method was established.

The characteristics of this method are the following:

1) By the use of silver nitrate solution, together with a large amount of silver chloride, iodide ions are precipitated as silver iodide and are completely gathered into the chloride precipitate.

2) The precipitated iodide is converted into iodate by bromine. Then the reaction between the iodate and cadmium iodide liberates the iodine, in a quantity six times that of the original sample. Thus the minimum amount of determinable iodide is lowered to one-sixth.

3) Finally, the liberated iodine is determined spectrophotometrically as starch-iodine-chromogen. Thus 0.2 $\mu$g. of iodine can be determined with an error of only $\pm 5\%$.

## Analytical Method

### Reagents

1) Sodium chloride solution, about 0.1 N, free from iodine.

The addition of a small amount of silver nitrate solution can remove any trace of iodine in the form of silver iodide involved in a large amount of silver chloride.

2) Silver nitrate solution, about 0.1 N.

3) Sulfuric acid, about 3 N.

4) 1/2 M acetate buffer with pH 2.8 saturated with bromine.

1000 parts of 1/2 M acetic acid are mixed with 20 parts of 1/2 M sodium acetate. A suitable amount of bromine is added.

5) Cadmium iodide solution, about 5%.

Cadmium iodide crystals are dissolved in distilled water and boiled for five minutes before they are stored in a brown glass bottle.

6) Starch solution, about 0.5%.

After being prepared in the usual way, the solution is put to centrifuge at 3000 r.p.m. for ten minutes. Then it is filtered through a filter paper of fine texture.

7) Sodium acetate solution, about 25%.

8) Sodium sulfite solution, about 1%.

### Procedure

1) Take a suitable amount of sample, usually

3—5 litres, depending upon the iodine content, filter it through a piece of absorbent cotton previously washed with 3 N hot hydrochloric acid and distilled water. And a sufficient amount of 0.1 N sodium chloride solution to the filtrate to adjust the chloride concentration to about 15 mg. per litre. While vigorously stirring, add an amount of silver nitrate solution equivalent to the chloride. After the silver chloride is completely precipitated, add 3 N sulfuric acid in the proportion of 1 ml. to 1 litre of the solution. Allow the solution to stand in a dark place for about twenty hours. After the precipitate has completely settled, the supernatant is siphoned off and the remaining precipitate is transferred to a small beaker (50 ml.). Rinse the precipitate with distilled water several times and pour the washings on a filter paper so that any suspended precipitate will be collected on it. Transfer the collected precipitate with a small amount of water back into the original beaker.

2) To the content of the beaker, add 2 ml. of 0.1 N sodium chloride solution and then and 10 ml. of 1/2 M acetate buffer previously saturated with bromine. Dilute the total volume with distilled water to about 25 ml. Stir and allow it to stand for one hour at a temperature below 20°C with occasional stirring. At this step, the iodine is completely oxidized into iodate.

3) Warm the beaker on a boiling water bath until excess bromine is expelled and the solution turns pale yellow. After cooling by tap water, filter the liquid through a small filter paper of fine texture. Wash the residue on the filter paper three times with small portions of distilled water. Gather the filtrate and washings into a 50 ml. beaker.

4) Warm the beaker on a boiling water bath until all trace of bromine is expelled and the solution is colorless. Leaving it to cool to room temperature, add 0.2 ml. of 1% sodium sulfite solution to remove any bromous acid which might have been formed during the above oxidation process.

5) Add 10 ml. of 1/2 M acetate buffer and keep the solution at a temperature below 20°C. Oxidation is complete within thirty minutes. Evaporate the solution on a boiling water bath to a volume of about 10 ml.

6) Cool and transfer the solution into a 25 ml. measuring flask of brown glass. Dilute the solution to about 20 ml. And 1 ml. of 0.5% starch solution and cool by tap water for five minutes. Then add 1 ml. of cadmium iodide solution, shake vigorously, and allow it to stand for fifteen minutes until a deep blue color fully develops. Adjust the pH to 4.2 by the addition of 0.3 ml. of 25% sodium acetate solution. After filling distilled water to the mark, the contents of the flask is mixed well.

The optical density of the solution is determined spectrophotometrically, using a wavelength of 580 mμ.

## Discussion

1) The usual evaporation method[1] for iodine enrichment has many tedious dfficulties which are accompanied by unavoidable loss in iodine and by contamination with other interfering elements. The proposed silver iodide method is absolutely free from such difficulties and moreover, gives a result of 100% accuracy for a tenth mg. of iodine from a sample of 3–5 litres as will be shown later. The addition of sulfuric acid perfects the coagulation of silver iodide.

2) The idea introducing the iodide-bromine reaction for minimizing the least determinable iodine to one-sixth, originally occurred to H. Ballczo[2] who recommended that the oxidation of iodide by bromine be carried out at pH 4.3. The authors obtained a satisfactory result when steps from the iodide oxidation by bromine up to the addition of starch solution and cadmium iodide are processed at pH 2.8 and then the pH is adjusted to 4.2 for colorimetry.

3) In some cases samples are left for a long time without further treatment after silver nitrate solution was added, when some amount of metallic silver may be produced due to photochemical decomposition. This silver reacts with bromine at a later step by the following equation

$$Ag^+ + Br_2 + H_2O = HBrO + AgBr + H^+$$

with the production of hypobromous acid. This hypobromous acid liberates iodine in the cadmium iodide treatment, causing a considerable error in the final colorimetry. The treatment by sodium sulfite is naturally given whereby hypobromous acid and iodate are reduced to bromide and iodide. Thus in the second oxidative treatment by bromine, iodate alone is produced.

4) For the liberation of iodine, cadmium iodide was preferred to the potassium iodide currently used[3,4] because the latter compound tends in an acid medium to liberate iodine even in the absence of iodate, thus causing a considerable error in the precise determination at which the authors are aiming.

Cadmium iodide solution keeps for at least two months without any liberation of iodine when it is stored in a brown glass bottle after being boiled for five minutes.

1) American Public Health Association, "Standard Methods for the Examination of Water and Sewage", New York, (1946), 9th Ed., p. 47.
2) H. Ballczo und G. Mondl, *Mikrochem. ver. Mikrochim. Acta*, 39, 247 (1952).
3) W.G. Gross. L.K. Wood and J.S. McHargue, *Anal. Chem.*, 20, 900 (1948).
4) F.G. Houston, *Anal. Chem.*, 22, 493 (1950),

5) Starch-iodine-chromogen gives a maximum absorption at a wave length of 580 mμ. (See Fig. 1) and strictly obeys the Beer's law covering a range of 0.00–120 μg. of iodine.

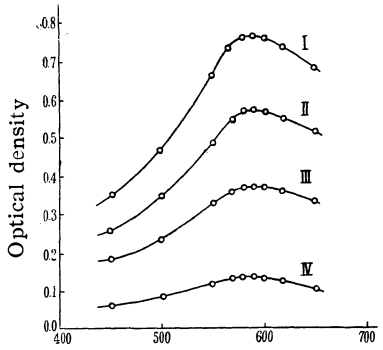



Fig. 1. Absorption curves.
I: 100 μg. of I in 25 cc.
II: 75 μg. of I in 25 cc.
III: 50 μg. of I in 25 cc.
IV: 20 μg. of I in 25 cc.

When the authors use Coleman Model 14 Universal Spectrophotometer with an accessory "round cuvette" of an effective cell thickness 13.06 mm., the following relation holds:

$$X=\frac{E-0.006}{0.0074},$$

where $X$ is the amount of iodine in 25 ml. and $E$ is the optical density for 580 mμ.

The amount of iodine in the original sample can be calculated by dividing $X$ by 6[5].

Starch species and temperature affect somewhat the standard curve. Therefore, the curve sometimes should be constructed for several starch species and at various temperatures (See Fig. 2).

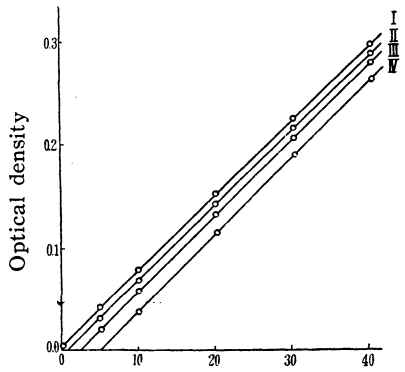



Fig. 2. Effect of temperature on color intensity at a wavelength of 580 mμ.
I: at 10–20°C III: at 25°C
II: at 23°C IV: at 28°C

The color undergoes no measurable change for at least two hours if the pH of the solution is adjusted to 4.2 after the color developed at pH 2.8. Fig. 3 shows the effect of pH on the rate of color development.

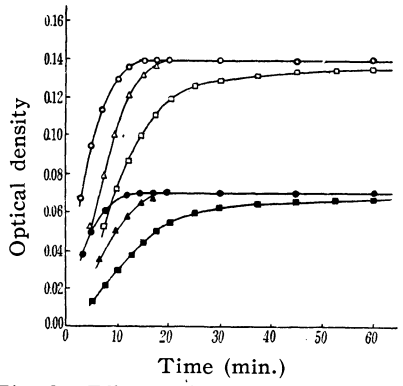



Fig. 3. Fffects of pH on rate of color development at a wave length of 580 mμ.
—○— pH: 2.8 —○— 20 μg. of I in 25 cc.
—△— pH: 3.6
—□— pH: 4.2 —●— 10 μg. of I in 25 cc.

6) Among common elements in ordinary natural waters, chloride, bromide, nitrate and sulfate cause interference which at least is not up to the concentrations 200, 10, 30 and 30 mg., respectively.

TABLE I
ACCURACY OF THE METHOD

| Cl added mg. | I used μg. | I found μg. | Error % |
|---|---|---|---|
| 17.5 | 0.00 | 0.00 | — |
| 17.5 | 0.20 | 0.19 | −5.0 |
| 17.5 | 0.20 | 0.20 | 0.0 |
| 17.5 | 0.20 | 0.21 | +5.0 |
| 17.5 | 0.99 | 0.95 | −4.0 |
| 17.5 | 0.99 | 0.96 | −3.0 |
| 17.5 | 0.99 | 1.03 | +4.0 |
| 17.5 | 1.98 | 1.95 | −1.5 |
| 17.5 | 1.98 | 1.91 | −3.5 |
| 17.5 | 1.98 | 1.99 | +0.9 |
| 17.5 | 4.95 | 4.99 | +0.8 |
| 17.5 | 4.95 | 4.92 | −0.6 |
| 17.5 | 4.95 | 4.98 | +0.6 |

7) The accuracy of the proposed method was tested using various amounts of a standard solution of potassium iodide. Table I gives the result.

The fact that the oxidation of silver iodide is complete was also shown by the following experiment: Various amounts of the standard solution of potassium iodide were similarly processed and the iodine liberated at pH 2.8

5) L.W. Andrews, *J. Am. Chem. Soc.*, 25, 756 (1903).

was determined using standard solution of thiosulfate. Table II shows the result.

TABLE II

OXIDATION OF SILVER IODIDE BY BROMINE*

| Cl added mg. | I used mg. | I found mg. | Recovered % |
|---|---|---|---|
| 35.5 | 0.00 | 0.00 | — |
| 35.5 | 0.19 | $0.19_2$ | 101.0 |
| 35.5 | 0.19 | 0.19 | 100.0 |
| 35.5 | 0.19 | $0.19_1$ | 100.5 |
| 35.5 | 0.39 | 0.39 | 100.0 |
| 35.5 | 0.39 | $0.38_9$ | 99.7 |
| 35.5 | 0.39 | $0.38_9$ | 99.7 |
| 35.5 | 0.49 | $0.49_1$ | 100.0 |
| 35.5 | 0.49 | $0.48_3$ | 99.2 |
| 35.5 | 0.49 | $0.48_3$ | 99.2 |
| 35.5 | 0.49 | $0.48_9$ | 100.0 |

* Determination was carried out volumetrically.

Table III shows examples of the result from natural waters to which the present method was applied.

The present study was accomplished by using Coleman Model 14 Universal Spectrophotometer supplied by the Elizabeth Thompson Science Fund. The authors express their appreciation to the Trustees of that fund.

TABLE III

EXAMPLES OF ANALYSIS

| Description | Sample taken l. | I found μg./l. | Cl found mg./l. |
|---|---|---|---|
| Rain water collected at Higashiyama area, Nagoya City (June, 1954) | 4.0 | $0.9_0$ | 0·18 |
| | 4.0 | $1.3_1$ | 0.89 |
| | 2.0 | $1.1_5$ | 0.58 |
| | 2.0 | $1.0_5$ | 0.36 |
| Ground water from a well in the campus of Nagoya University (June, 1953) | 5.0 | $0.8_5$ | 3.83 |
| Surface water of Lake Biwa-ko, Shiga Prefe- (Oct., 1953) | 5.0 | 1.3 | 4.69 |
| Surface water of Lake Gongen-ike, Mt. Norikura, Gifu Prefecture (Sept., 1953) | 10.0 | 0.2 | 0.13 |
| A spring water from Higashiyama area, Nagoya City (Aug., 1954) | 3.0 | 2.2 | 5.58 |

*Chemical Institute, Faculty of Science, Nagoya University, Nagoya*

# *Electron Transfer Spectra in the Crystals of Hexamminecobalt(III) Salts*

By Yukio KONDO

(Received April 25, 1955)

## Introduction

The formation of the ion-pairs of hexammine and tris-(ethylenediamine) complex cations of cobalt(III) and chromium(III) with various anions in aqueous solutions and the consequent appearance of a new absorption band in the ultraviolet were first observed by Linhard[1], and the thermodynamical study of the ion-pair formation was spectrophotometrically done by him[1], Evans and Hancollas[2] and Kubota[3]; this so-called association band has been attributed to the transfer of an electron from an anion to a complex ion[2,3,4]. It will be natural to suppose that in crystals in which a complex ion is closely surrounded by anions, this absorption band will acquire more intensity than in solutions, and indeed Linhard and Weigel[4] suggested in their paper that the deepening in the color of the crystals of hexamminecobalt(III) chloride, bromide and iodide in this order is attributable to the presence of this band. Actually, in 1936, in the study of the absorption spectra of cobalt(III) ammine salt crystals, Kobayashi[5] observed the new absorption band which was absent in solutions. But he attributed it to the transition of an electron from a ligand to the central atom.

On the other hand, studying theoretically the absorption spectra of the first transition metal complexes by the crystalline field ap-

1) M. Linhard, *Z. Elektrochem.*, **50**, 224 (1944).
2) M.G. Evans and G.H. Hancollas, *Trans. Faraday Soc.*, **49**, 363 (1953).
3) T. Kubota, *J. Chem. Soc. Japan (Pure Chem. Sec.)*, **75**, 552 (1954).
4) M. Linhard and M. Weigel, *Z. anorg. Chem.*, **266**, 49 (1951).
5) R. Tsuchida and M. Kobayashi, *J. Chem. Soc. Japan (Pure Chem. Sec.)*, **64**, 1268 (1943); "The Colors and the Structures of Metallic Compounds", Zoshindo Co., Osaka, Japan (1944), p. 180.

proximation, Tanabe and Sugano[6] have recently suggested the possibility of the appearance of the absorption band due to the two-electron jump within a metal ion in the case of nickel(II), cobalt(III) and chromium(III) complexes. Thus, concerning the origin of the new absorption band appearing in crystals, there are three different possibilities, namely, the transitions of electrons of the central atom, a ligand and an anion.

The present study was undertaken for the purpose of confirming the existence of this band in the spectra of various hexamminecobalt(III) salt crystals, as only the chloride was investigated by Kobayashi, and also to determine which of the above mentioned theories is correct.

## Experimental

**Materials.**—Hexamminecobalt(III) salts investigated in the present study are listed in Table I. The chloride was prepared by the air oxidation of the ammonical solution of cobalt(II) chloride and ammonium chloride using activated charcoal as a catalyst according to the method of Bjerrum and McReynolds[7]. The iodide selenate was prepared by the oxidation of the ammoniacal solution of cobalt(II) selenate and ammonium selenate with iodine after Hassel and Bödtker Naess[8]. The others were derived from the chloride by the method described briefly in the table[9-17]. These were, in general, recrystallized from slightly acidic, hot aqueous solutions.

**Apparatus and Procedure.**—The optical system of the microscope used is shown in Fig. 1, in

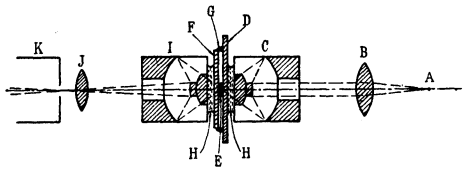



Fig. 1. Optical system (schematic) of the reflecting microscope used for measuring the absorption spectra of microscopic crystals.

which A, B, C, I and J are fixed to the body of a usual microscope. As a light source A, a hot cathode hydrogen discharge tube was used except in the case of the iodide in which a tungsten lump was used. A fused quartz lens B of a focal distance 8 cm. was used to parallelize the light from the source. A reflecting condenser*1C has the similar abilities with a reflecting objective*1I with the exceptions of having some aberrations and providing an iris diaphragm and centering screws. The reflecting objective has the abilities of numerical aperture max. 1.0, magnification 100×, and working distance 1 mm. In addition to the merit of having no color aberration, the reflecting objective has practically neither spherical aberration nor coma by means of making its sur face non spherical[18].

TABLE I

| Crystal | Thickness (mm.) | Exposure time (min.) | Wave length of the 2nd band max. (mμ) | Wave length of absorption edge (mμ) | Method for preparation |
|---|---|---|---|---|---|
| $[Co(NH_3)_6](ClO_4)_3$ | 0.058 | 60 | 332 | 254 | chloride+$HClO_4$, Ref. 8 |
| $[Co(NH_3)_6]_2(SO_4)_35H_2O$ | 0.076 | 60 | 336 | 265 | chloride+$H_2SO_4$, Ref. 9 |
| $[Co(NH_3)_6]_2(HPO_4)_34H_2O$ | 0.032 | 30 | 336 | 274 | chloride+$Na_2HPO_4$, Ref. 10 |
| $[Co(NH_3)_6]Cl_3$ | 0.021 | 30 | 330 | 299 | Ref. 7 |
| $[Co(NH_3)_6]Br_3$ | 0.01 | 30 | — | 357 | chloride+HBr, Ref. 11 |
| $[Co(NH_3)_6]I_3$ | 0.038 | 5 | — | 505 | chloride+KI, Ref. 12 |
| $[Co(NH_3)_6]Cl(ClO_4)_2$ | 0.040 | 20 | 331 | 259 | chloride+$NH_4ClO_4$, Ref. 13 |
| $[Co(NH_3)_6]Cl(SO_4)3H_2O$ | 0.045 | 30 | 334 | 265 | chloride+$Na_2SO_4$, Ref. 14 |
| $[Co(NH_3)_6]Br(SO_4)$ | 0.040 | 30 | 336 | 287 | bromide+$H_2SO_4$, Ref. 10 |
| $[Co(NH_3)_6]I(SO_4)$ | 0.056 | 30 | — | 354 | sulfate+KI, Ref. 15 |
| $[Co(NH_3)_6]I(SeO_4)$ | 0.035 | 30 | — | 364 | Ref. 8 |
| $[Co(NH_3)_6]_2(C_2O_4)_34H_2O$ | 0.041 | 30 | 332 | 292 | chloride+$(NH_4)_2C_2O_4$, Ref. 16 |
| $[Co(NH_3)_6](NO_3)_3$ | 0.048 | 30 | — | — | chloride+$HNO_3$, Ref. 9 |
| $[Co(NH_3)_6](NO_2)_3$ | 0.022 | 30 | — | — | chloride+$NaNO_2$, Ref. 17 |

6) Y. Tanabe and S. Sugano, *J. Phys. Soc. Japan*, **9**, 753, 766 (1954).
7) J. Bjerrum and J. P. McReynolds, "Inorganic Syntheses", Vol. II, p. 217.
8) O. Hassel and G. Bödtker Naess, *Z. anorg. Chem.*, **174**, 25 (1928).
9) S. M. Jörgensen, *Z. anorg. Chem.*, **17**, 457 (1898).
10) S. M. Jörgensen, *J. prakt. Chem.*, (2) **35**, 431 (1887).
11) W. Biltz, *Z. anorg. Chem.*, **83**, 178 (1914).
12) E. Fremy, *Ann.* **83**, 290 (1892).
13) H. Alvisi, *Gazz. chim. ital.*, **31**, II, 291 (1901).
14) T. Klobb, *Bull. soc. chim. France*, (3) **25**, 1025 (1901).
15) F. Ephraim and W. Flügel, *Helv. chim. Acta*, **7**, 739 (1924).
16) E. Birk and W. Biltz, *Z. anorg. Chem.*, **153**. 124 (1926).
17) E. Birk. *Z. anorg. Chem.*, **164**, 243 (1927).
*1 Made by Olympus Optical Co, Ltd., Tokyo.
18) S. Miyata, S. Yanagawa and N. Noma, *J. Optical Soc. Am.*, **42**, 431 (1952).

A crystal E is chosen from a sample and its thickness is determined under a travelling microscope. This is placed on a fused quartz slide glass D and is covered with a fused quartz cover glass F and then the latter is sealed with paraffin G to the former. These are brought into the apparatus. As the microscope is a liquid immersion type, the space between C and I is filled with the glycerin water mixture H whose glycerin content is about 90% and the refractivity of which is identical with that of quartz, $n_d=1.458$. Focusing is carried out by inspecting through a glass eyepiece J, which is then removed. The image of the crystal magnified by the microscope is projected on the slit of a Jobin-Yvon medium type quartz spectrograph K and an absorption spectrum is photographed on a dry plate together with a wave length scale, the slit width being fixed at 0.2 mm. throughout this study. A qualitative absorption curve is obtained by tracing the plate photographed with a recording microphotometer. The thicknesses of the crystals used and the time exposed are shown in Table I. As our condenser has the numerical aperture of 1.0, its condensed light falls on the samples, not parallel, but with the angles of max. 43°18′ to the center line. Therefore, the thicknesses shown in the table do not indicate the actual thicknesses of the crystals passed by the light, the true values being a little larger than those reported.

**Schwarzschild-Villiger Effect.**—Although the reflecting objective is stated to have less Schwarzschild-Villiger (S-V) effect[19] which is very important in microspectrophotometry, than the usual transmission microscope, the stray light entering the objective from the exterior of a sample may still produce a large error in the result obtained. To avoid this, crystals which had larger areas than 0.1 mm.×0.1 mm. were used throughout this study with a few exceptions, considering the image of the light source projected on the crystals was the circle whose diameter was about 0.03 mm. It was proved that the stray light had no effect on the spectra obtained, since the highly absorbed part of the dry plate photographed was perfectly blank after long exposure.

## Results

From the smooth microphotometer traces of blanks shown in Fig. 2, it will be apparent

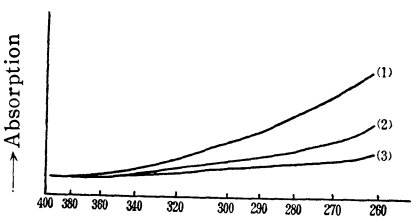



Fig. 2. Microphotometer traces of blanks; exposure time: 10 min. (1), 30 min. (2). 60 min. (3).

19) See for example: H. Naora, *Science*, **114**, 279 (1951); **115**, 248 (1952); *Biochim. Biophys. Acta*, **9**, 582 (1952).

that the light source, the optical system and the dry plate give no selective absorption on the spectra obtained, and that our qualitative method is satisfactory for the detection of absorption bands. In the spectra of the perchlorate, the sulfate and the hydrogen phosphate shown in Fig. 3*2, the second

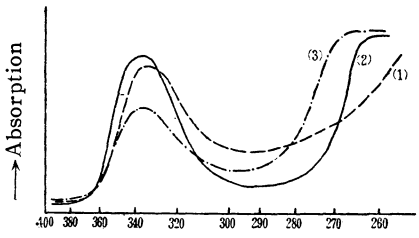



Fig. 3. Absorption spectra of the crystals of hexamminecobalt(III) perchlorate (1), sulfate (2) and hydrogen phosphate (3).

absorption band due to a *d* electron appears clearly, the position of which is about the same in these salts and is almost identical with that in aqueous solutions. There is practically no absorption in the range between the second band and the intense absorption edges*3 found at shorter wave lengths. It is apparent that these absorption edges are not due to the anions, since these disply no absorption down to 220 mμ[20].

In the spectra of the halogenides shown in Fig. 4, the edge absorption moves to

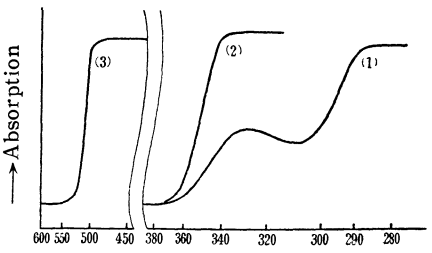



Fig. 4. Absorption spectra of the crystals of hexamminecobalt(III) chloride (1), bromide (2) and iodide (3).

longer wave lengths in the following order: iodide > bromide > chloride, thus covering

*2 The flattened upper and lower parts of the spectra indicate the perfect absorption and transmission of light, respectively.

*3 The term, edge absorption or absorption edge, is used, for convenience, throughout this study to designate our band in question, since it is beyond the ability of our apparatus to determine the stronger part of the spectra using thinner crystals than those used here, because thin crystals usually are attended with smaller sizes, which result in the increase of the S-V effect as stated above. To avoid this, the use of the microscope having much larger magnifying power than the one used here is necessary.

20) S. Kato, *Sci. Papers Inst. Phys. Research*, Tokyo, **13**, 7 (1950).

perfectly the second band in the bromide and the iodide. This red shift is the feature of the spectra in crystals, as the second band appears clearly in dilute aqueous solution even in the case of the iodide. In the series of the chloride perchlorate, the chloride sulfate, the bromide sulfate, the iodide sulfate and the iodide selenate shown in Fig. 5, the

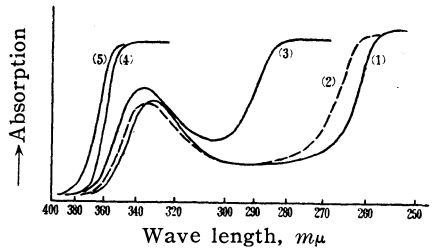



Fig. 5. Absorption spectra of the crystals of hexamminecobalt(III) chloride perchlorate (1), chloride sulfate (2), bromide sulfate (3), iodide sulfate (4) and iodide selenate (5).

absorption edge behaves like the simple halogenides, but is shifted to a shorter wave length as compared with that of the corresponding halogenide. The absorption spectrum of the oxalate shown in Fig. 6 resembles

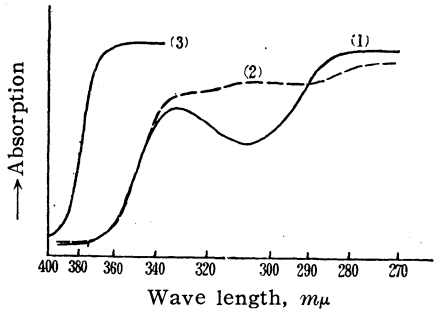



Fig. 6. Absorption spectra of the crystals of hexamminecobalt(III) oxalate (1), nitrate (2) and nitrite (3).

that of the chloride. Here again, it is apparent that the edge absorption is not attributable to the anion, as it absorbs at a shorter wave length (ca. 270 mμ)[21]. In the spectra of the nitrate and the nitrite shown in the same figure, the absorption bands due to the anions make it impossible for one to determine exactly the positions of the absorption edges.

The positions*4 of the absorption edges are listed in Table I. The results obtained are summarized as follows; in the absorption spectra of the crystals of hexamminecobalt (III) salts, there are strong edge absorptions, the positions of which are shifted to longer wave lengths as compared with those in aqueous solutions and are largely affected by anions.

## Discussion

**Comparison of the Present Results with Kobayashi's.**—In the spectrum of the crystal of hexamminecobalt(III) chloride, Kobayashi[5] found the distinct absorption maximum at 282 mμ which had a little lower intensity than that of the second band. In the present study, however, this absorption peak which had been called by Tsuchida and Kobayashi the third band was not found not only in the chloride, but was also absent in the mixed chlorides with the perchlorate or the sulfate, in which the content of the chloride ions was diminished to one-third of the pure chloride. In place of absorption peaks we have obtained absorption edges which indicate the existence of much stronger absorption bands than the second band.

This discrepancy will be interpreted by considering the S-V effect in the apparatus used by Kobayashi, in which the condenser having small magnifying power and the transmission microscope, which are both apt to produce stray light, are employed Since the stray light increases as the wave length becomes shorter, it is expected that the sum of the light really transmitted and the stray light may produce a spurious maximum at a given wave length. It should also be pointed out that the error due to the S-V effect gets greater as the optical density of a sample becomes larger, and according to Naora[19], in some extreme cases, a sample having the transmittance of 1% indicated the erroneous value of 20%.

The above statement will also apply to the spectra of other cobalt(III) ammine in which Kobayashi found either no absorption bands or weak ones in crystals, even in the case where complexes showed strong absorption in aqueous solutions. In fact, the discrepancy has been found recently in the crystals of dinitrotetramminecobalt(III) salts investigated by Faust and Quagliano[22]. In place of only one broad weak band reported by Kobayashi, they obtained the strong absorption bands corresponding to those in aqueous solutions using a potassium bromide disk method.

21) H. Ley and B. Arends, *Z. physik. Chem.*, B17, 177 (1932).

*4 These were obtained by subtracting a corresponding blank curve from each absorption spectrum, and taking, for convenience, the wave length of the edge absorption which had the same intensity as that of the maximum of the second band. Where the latter was unknown, it was calculated from another salt assuming Lambert's law to be valid.

22) J. P. Faust and J. V. Quagliano, *J. Am. Chem. Soc.*, 76, 5346 (1954).

**Origin of the Edge Absorption.**— The dependence of the edge absorption on anions is understood only by considering the strong interaction between a complex ion and an anion in a crystal. We shall first consider the possibility of interpreting the edge absorption by the transitions of the electrons within a complex ion.

According to Tanabe and Sugano[6], a possible transition responsible for the third band in cobalt(III) complexes is a two-electron excitation, $(d\varepsilon^6)^1A_1 \rightarrow (d\varepsilon^4 d\gamma^2)^1F_2$. The degree of the energy change in the upper level, $^1F_2$, by the change in a crystalline field is, though a little larger, not so different from those in the levels, $(d\varepsilon^5 d\gamma)^1F_1$ and $(d\varepsilon^5 d\gamma)^1F_2$, which are responsible for the first and the second bands, respectively, in so far as we assume that, even in crystals, the field acting on the cobalt ion is of cubic symmetry as a first approximation. Therefore, the fact that the edge absorption is remarkably affected by anions, in contrast to the almost unchanged second band, suggests that the former is not due to the above transition. Moreover, the intensity criterion made by Tanabe and Sugano that as the mixing with another configuration may be small, the third band must have a much lower intensity than those of the first two bands, makes the two-electron jump hypothesis more inadequate for the origin of the edge absorption. Further evidence substantiating the above conclusion will be given in the last section of the discussion.

Tsuchida and Kobayashi[5] proposed the idea that the ammonias in ammine complexes dissociated into amino radicals and protons as a result of the hydrogen bonds with anions, and that the transition of the electron of the amino radical thus formed to the central atom was the very one responsible for the third band in crystals. Actually, in the crystals of metal complexes the possibility of hydrogen bonding is very large. For example, we can find it in trinitrotriamminecobalt(III) and chlorodinitrotriamminecobalt (III) for which the hydrogen bonds between ammonias of one molecule and oxygens of the others were suggested by Tanito et al.[23], and in dichlorotetrammineplatinum(IV) chloride and chloropentammineplatinum(IV) chloride monohydrate in which the hydrogen bonds between nitrogens and anionic chlorines were found by Bokij et al.[24]. On the other hand, the partially dissociated character of strongly hydrogen bonded NH and OH groups, which results in the formation of non-bonding electrons, has recently been shown by Tsuboi[25]. The effect of an anion on the electron of the hydrogen bonded NH bond will be larger than on *d* electrons and largely determined by the hydrogen bonding power or the electro-negativity of the anion. Therefore if the edge absorption were due to the electron of the dissociated ammonia, it should shift to longer wave lengths and increase its intensity in the following order: chloride>bromide>iodide, since the approach of the anion will facilitate the transition and increase its probability. As the order in the shifts is contrary to the results obtained, the dissociation hypothesis must be abandoned.

The explanation of the far ultraviolet intense edge absorption of the hexamminecobalt(III) ion in aqueous solutions ($\log\varepsilon=4$) by the transition of the bonding electron of a Co-N bond proposed by Linhard[1] is interesting because of the facts that our band in question also absorbs strongly, and that the transition of bonding electrons usually produces intense absorptions. However, it is easy to show that if the edge absorption in crystals were due to the red shift of the one in aqueous solution, it should shift to longer wave lengths in the following order: bromide sulfate> iodide sulfate>iodide selenate>iodide>perchlorate, since the potential energy of an hexamminecobalt(III) ion in a crystal, $A'''e^2/r_\alpha$, increases in this order (see Table II). Here again, this order is inconsistent with our results. Therefore, all the possible transitions within the complex ion stated above are inadequate to account for the edge absorption.

Secondly, we must consider the possibility of the red shift of the absorption band due to an anion which was taken up by Linhard[1] in an early stage and by Yoneda[26] recently to explain the association band in solutions. In oxy-acidic anions, sulfate, hydrogen phosphate, perchlorate, oxalate, nitrate and nitrite ions, there are the non-bonding electrons which were shown, in some cases, to be rather strongly affected by an outer field. For example, according to Schaumann[27], the weak band of nitrate ion in aqueous solutions at 302 m$\mu$ with $\varepsilon=7$ which is said to arise from an $n\rightarrow\pi$ transition[28,29], suffers in the crystal a large shift in its position, the

23) Y. Tanito, Y. Saito and H. Kuroya, This Bulletin, **25**, 188 (1952); **26**, 420 (1953).
24) G. B. Bokij and M. A. Poraj-Koshits, *Doklady Akad. Nauk S.S.S.R.*, **64**, 337 (1949); G.B. Bokij and L.A. Popova, ibid., **67**, 73 (1949).
25) M. Tsuboi, This Bulletin, **25**, 385 (1952).
26) H. Yoneda, This Bulletin, **28**, 125 (1955).
27) H. Schaumann, *Z. Physik*, **76**, 106 (1932).
28) H. McConnell, *J. Chem. Phys.*, **20**, 700 (1952).
29) W.G. Trawick and W.H. Eberhardt, ibid., **22**, 1462 (1954).

values of which are 304 mμ for potassium nitrate, 291 mμ for sodium nitrate and 278 mμ for barium nitrate. Another example is the weak band of sodium nitrite at 350 mμ which is said to arise from the transition of the non-bonding electron of nitrogen to an anti-bonding orbital[29]. It was shown that the crystal of silver nitrite lacked this band on account of probable existence of the weak covalent binding between the nitrogen and the silver[29]. But, the present measurements on the crystals of hexamminecobalt(III) nitrate and nitrite suggest that the shift of the absorption band of the anions due to the complex ion is not sufficiently large to explain the remarkable shift of the edge absorption. The same is also observed in the absorption bands of chromate and permanganate ions which are both said to arise from $n\rightarrow\pi$ transitions[30] and are almost equal in aqueous solution and in mixed crystals[31].

Although we can not draw any definite conclusion as to whether the red shift of the absorption band of an anion can explain the edge absorption from the above discussion, the situation is simpler in the halogendies than in the oxy-acidic salts, as will be seen in the following paragraphs.

Absorption spectra of alkali halogenides in gaseous molecules, aqueous solution and crystals were studied extensively by many workers[32], and the results showed that there was no evidence of the transition within an anion and the absorption spectra were due to the transfer of an electron from an anion to a cation or water. That this is also true in our crystals containing halogen ion is shown by the following consideration: if the edge absorption of the iodide sulfate and the iodide were the absorption band of the iodide ion perturbed by a crystalline field, the former should be more bathochromic than the latter, since the potential energy of the iodide ion in the crystals, $A'e^2/r_\alpha$, is larger in the iodide sulfate than in the iodide as is seen from Table II. As this is contrary to the experimental results, the possibility of the red shift of the absorption band of an anion must be excluded at least in the halogenides and the edge absorption must be interpreted by the transfer of an electron from an anion to the complex ion, as in the association band in aqueous solution.

Such an electron transfer is also expected in the oxy-acidic anions, since the far ultraviolet intense absorption bands of nitrate, nitrite, chlorate ions etc. have been attributed to the transfer of an electron from an anion to its hydration sphere[33], although the alternative interpretation which assigned $\pi\rightarrow\pi$ transitions to them also exists[29].

**Calculations of the Differences Between the Wave Lengths of the Absorption Edges by the Energy Cycle Method.**—If the edge absorption is an electron transfer spectrum, it should correspond to the first absorption band of ionic crystals due to an exciton, the wave length of which can be calculated by the energy cycle method as is usually performed. We shall do this below to the bands of the iodide, the iodide selenate, the iodide sulfate and the bromide sulfate.

We perform the following cycle[34,35,36].

1) Remove a halogen ion*5 from a crystal; the work necessary is $A'e^2/r_\alpha$, where $A'$ is the crystal potential constant at the lattice point of the halogen ion and $r_\alpha$ the lattice constant of the crystal.

2) Remove an electron from the halogen ion; the work necessary is $E$, the electron affinity of the corresponding halogen atom.

3) Replace the halogen atom; the work necessary is zero.

4) Remove a neighbouring hexamminecobalt(III) ion from the crystal; the work necessary is $(A'''-B)e^2/r_\alpha$, where $A'''$ is the crystal potential constant at the lattice point of the hexamminecobalt(III) ion and $B$ the potential constant at that point due to a neighbouring halogen ion.

5) Add the electron to the hexamminecobalt(III) ion; the work necessary is $-I$, where $I$ is the ionization potential of an hexamminecobalt(II) ion.

6) Replace the hexamminecobalt(II) ion; the work necessary is $-2(A'''-B)e^2/3r_\alpha$.

7) The movement of the electron from the halogen ion to the hexamminecobalt(III) ion will polarize the surrounding medium; the polarization energy is denoted by $-\omega$.

8) It will also polarize the halogen atom and the hexamminecobalt(II) ion; we denote the polarization energy of the former by $-\Omega_X$ and that of the latter, plus the decrease in the energy due to the dipole formed in the latter, by $-\Omega_L$.

Adding the contributions of covalent binding, the van der Waals force and hydrogen bonding designated by $\Delta U$, the total energy $h\nu$ of an edge absorption is thus given by

30) M. Wolfsberg and L. Helmholz, *J. Chem. Phys.*, **20**, 837 (1952).
31) J. Teltow, *Z. physik. Chem.*, **B43**, 198 (1939).
32) E. Rabinowitch, *Revs. Modern Phys.*, **14**, 112 (1942).
33) H.L. Friedman, *J. Chem. Phys.*, **21**, 319 (1953); see also Ref. 32.
34) W. Klemm, *Z. Physik*, **82**, 529 (1933).
35) N.F. Mott, *Trans. Faraday Soc.*, **34**, 500 (1938).
36) Y. Uehara, *J. Chem. Soc. Japan (Pure Chem. Sec.)*, **63**, 597 (1942).

$$h\nu = \psi + E - I - \omega - \Omega_X - \Omega_L + \Delta U, \quad (1)$$

where $\psi = A'e^2/r_\alpha + (A''' - B)e^2/3r_\alpha$.

Unfortunately, even the approximate calculations of $h\nu$'s are impossible for the reason that the values of $I$ and $\Delta U$ are unknown, and also the estimations of $\omega$ and $\Omega_L$ are impossible since the estimation of the former requires the unknown polarizabilities of hexaminecobalt(III) and sulfate or selenate ions and that of the latter requires the unknown polarizability of hexamminecobalt(II) ion, according to the method of Klemm[34].

Thus, we must content ourselves only with calculating the differences of the $h\nu$'s between those salts. Taking into account the fact that the sum of $\omega$ and $\Omega_L$ are a few eV in alkali halogenides, the differences between the halogenides of a same cation being much smaller[34,35], the values of $\Omega_X$ are less than 0.1 e.V. in our crystals*6, and the values of $\Delta U$ are also a few eV, even in the silver halogenides[37] which have considerable covalent character, we neglect these terms in Eq. 1, which then becomes

$$h\nu = \psi + E - I \quad (2)$$

Then, we have only to calculate the crystal potential constants. The crystal structures of hexamminecobalt(III) iodide and perchlorate were determined by Meisel and Tiedje[38], et al. being an anti- $(NH_4)_3FeF_6$ type (see Fig. 7). On the other hand, the iodide selenate, iodide sulfate and bromide sulfate have an anti- $K_2PtCl_6$ type structure according to Hassel and Bödtker Naess[8], et al. (Fig. 8).

Now, we assume that the +3 charges on the hexamminecobalt(III) ion are concentrated on the cobalt. The assumption is justified in so far as potential constants are concerned, since the calculation based on the assumption that the charge is zero on the cobalt, therefore +1/2 on each nitrogen atom, according to Pauling's neutrality principle[39], gives the potential constant of 6.88 which is very close to that of 6.93 calculated on the former assumption, even for the nearest

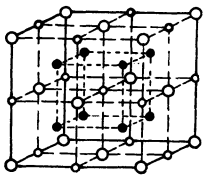


Fig. 7.

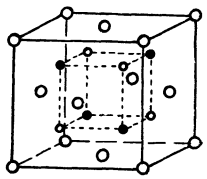


Fig. 8.

Fig. 7. Crystal structure of hexamminecobalt(III) iodide and perchlorate; the large circles are the hexamminecobalt (III) ions, and the small ones, open and solid, are the iodide or perchlorate ions.

Fig. 8. Crystal structure of hexamminecobalt(III) iodide sulfate, iodide selenate and bromide sulfate; the large circles are the hexamminecobalt(III) ions, the small open circles are the halogen ions and the small solid ones the sulfate or selenate ions.

halogens. Thus, we are justified for treating our crystals as having a $BiF_3$ or a $CaF_2$ type structure. Their crystal potential constants can easily be obtained using the potential data calculated for the cubic lattice by the method of Ewald. The potential, $a\psi(xyz)$, at the lattice point (000) due to the simple cubic lattice situated on lattice points $a(xyz)$ are given as follows[40]:

$$a\psi(000) = \varphi_0 = -2.83729$$
$$a\psi(00\tfrac{1}{2}) - \varphi_0 = \varphi_1 = 2.7414$$
$$a\psi(0\tfrac{1}{2}\tfrac{1}{2}) - \varphi_0 = \varphi_2 = 2.2548$$
$$a\psi(\tfrac{1}{2}\tfrac{1}{2}\tfrac{1}{2}) - \varphi_0 = \varphi_3 = 2.0354$$
$$a\psi(\tfrac{1}{4}\tfrac{1}{4}\tfrac{1}{4}) - \varphi_0 = \varphi_4 = 2.6368.$$

From Figs. 7 and 8 and taking into consideration the +3 charges on the hexamminecobalt(III) ions and the −2 charges on the sulfate and selenate ions, our expressions for the crystal potential constants are given as follows:

for the iodide and the perchlorate,

$$A' = -3\varphi_1 - 3\varphi_2 - \varphi_3 + 8\varphi_4$$
$$A''' = 9\varphi_1 - 27\varphi_2 + 3\varphi_3 + 24\varphi_4;$$

for the iodide selenate, the iodide sulfate and the bromide sulfate,

$$A' = -6\varphi_1 - 3\varphi_2 - 2\varphi_3 + 12\varphi_4$$
$$A''' = -27\varphi_2 + 36\varphi_4.$$

$B$ is easily calculated to be 6.9282. The values of $A'$ and $A'''$ are listed in Table II, together with $r_\alpha$, $\psi$ and $E$. The differences of the $h\nu$'s calculated between four salts are also given as well as the observed values.

Table II indicates that there is fairly good agreement between the $\Delta h\nu$'s calculated and

*5 In the crystal of hexamminecobalt (III) iodide, there are two kinds of iodide ions, whose distances from the complex ion are not the same (see Fig. 7). We assume that the edge absorption in this crystal is due to the transition of the electron of the iodide ion nearer to the complex ion.

37) Y. Uehara, *J. Chem. Soc. Japan(Pure Chem. Sec.)*, **63**, 1041 (1942); S. Kikuchi and S. Umano, ibid., **70**, 94 (1949).

*6 According to Klemm, $\Omega_x$ is represented by $\Omega_x = e^2\alpha_x/2r_0^4$, where $\alpha_x$ is the polarizability of a halogen atom which is assumed to be 70% of that of the corresponding ion, and $r_0$ is the shortest cation-anion distance.

38) K. Meisel and W. Tiedje, *Z. anorg. Chem.*, **164**, 223 (1927).

39) L. Pauling, *J. Chem. Soc.*, **1948**, 1461.

40) T. Nagamiya and T. Matsubara, "The Theory of Solids", Vol. I, Kyoritsu Shuppan Co., Tokyo (1951), p. 234.

TABLE II

| Crystal | $A'$ | $A'''$ | $r\alpha$(A) | $\phi$(e.V.) | $E$(e.V.) | $\Delta h\nu_{calc.}$ | $\Delta h\nu_{obs.}$ |
|---|---|---|---|---|---|---|---|
| $[Co(NH_3)_6](ClO_4)_3$ | 4.0704 | 33.1824 | 11.38 | 16.20 | | | |
| $[Co(NH_3)_6]I_3$ | 4.0704 | 33.1824 | 10.91 | 16.90 | 3.12 | >0.96 | 0.96 |
| $[Co(NH_3)_6]I(SeO_4)$ | 4.3580 | 34.0452 | 10.79 | 17.86 | 3.12 | >0.13 | 0.09 |
| $[Co(NH_3)_6]I(SO_4)$ | 4.3580 | 34.0452 | 10.71 | 17.99 | 3.12 | >0.74 | 0.82 |
| $[Co(NH_3)_6]Br(SO_4)$ | 4.3580 | 34.0452 | 10.51 | 18.33 | 3.52 | | |

observed. Thus, the red shift of the edge absorption in the order listed in the table could be interpreted using the theory of the exciton. Unfortunately, the lattice structures of the chloride, the bromide and the chloride sulfate are unknown*7. The complete explanation of the observed order in $h\nu$ is, therefore, impossible, but it will be suggested that the increase in $E$ and the probable decrease in $r_\alpha$ will be the major factors determining the increasing tendency of $h\nu$, though potential constants are necessarily different from that of a cubic lattice in the monoclinic lattice of the chloride and the rhombic one of the bromide.

As was stated previously, in the crystals containing oxy-acidic anions, the possibility of interpreting the edge absorption by the red shift of the anion's absorption was not excluded. However, it must be pointed out here that the fact that the edge absorptions exist at shorter wave lengths in those salts shown in Fig. 3 than those of the halogenides will be interpreted by the electron transfer theory, since the large ionization potential of oxygen (10 e.V. in perchlorate ion[30]) may be the principal factor determining the increase in $h\nu$.

**Effect of a Crystaline Field on the Second Absorption Band.**—In the preceding paragraphs, we neglected to discuss the behavior of the second band in crystals. Now, we shall briefly consider below the effect of a crystalline field on this band. The crystalline field theory mentioned above tells us that the stronger the crystalline field becomes, the larger the splitting of a $d$ level, say in our case, the difference between the excited level, $(d\varepsilon^5 d\gamma)^1F_2$, which is responsible for the second band and the ground one, $(d\varepsilon^6)^1A_1$, becomes. The expectation is attained in our crystals, as the second band exists at shorter wave lengths in crystals (330–336 m$\mu$) than in aqueous solutions (339 m$\mu$). This is also true for the larger shifts of the second band in the chloride and the chloride perchlorate than that of the others, since the crystalline field in these complexes is expected to be stronger than in the others.

It is of interest to note here that if the edge absorption were of similar origin with the second band, it must shift to shorter wave lengths as compared with the one in aqueous solutions, contrary to our results. This is another reason why the two-electron jump hypothesis must be discarded.

*7 In the famous W. Hückel's "Anorganische Strukturchemie", Ferdinand Enke Verlag, Stuttgart (1948), p. 548, Fig. 68b, hexamminecobalt(III) chloride is illustrated as having a cubic lattice. This is incorrect, since its crystal form is monoclinic. It seems to the present author that its lattice structure has not so far been analysed as well as that of the bromide.

## Summary

(1) The ultraviolet absorption spectra of the crystals of fourteen hexamminecobalt(III) salts were qualitatively measured using a reflecting microscope (magnification 100×), a quartz spectrograph and a recording microphotometer.

(2) All the crystals investigated showed, besides the weak absorption bands due to the complex ion, the strong absorption edges which were situated at longer wave lengths than those in aqueous solutions, and the positions of which were largely affected by anions. The most remarkable example was the iodide, the absorption edge of which extended to the visible region.

(3) It is concluded that, at least in the case of the halogenides, all the possible transitions within the complex ion and an anion are inadequate explanations and the electron transfer from an anion to the complex ion is most statisfactory for the origin of these strong absorption bands.

(4) The differences between the wave lengths of the absorption edges of hexamminecobalt(III) iodide, iodide selenate, iodide sulfate and the bromide sulfate were calculated by the energy cycle method and the results agreed fairly well with the experimental values, thus showing that these bands corresponded to the excition bands in ionic crystals.

Special acknowledgment is due to M. Linhard, R. Tsuchida and M. Kobayashi whose works stimulated this investigation. The author wishes to express his sincere thanks to Prof. T. Uemura and Prof. Y. Inamura for their kind encouragement and advice. The author's thanks are also due to Prof. K. Kozima who gave him a chance to use the recording microphotometer, and to Mr. W. Suetaka and Mr. M. Nakahara for their kind help in the microphotometer tracing.

*Laboratory of Inorganic Chemistry,*
*Tokyo Institute of Technology,*
*Tokyo*

# *Studies on Molecular Structure by the Measurement of the Dielectric Constants of Gases. III. The Dipole Moment and the Structure of Alkyl Nitrites*

By Takehiko CHIBA

(Received April 18, 1955)

Studies on molecular structure concerning the internal rotation have been made on many compounds such as ethane derivatives[1] but in these compounds both ends of internal axis have three atoms or groups which contribute to the forces determining the structure of these compounds. In alkyl nitrites both ends of the internal axis N-O have only an oxygen atom and a group R respectively, which will make the treatment easier. Recently Tarte made infrared investigation on alkyl nitrites[2] and found that there are two rotational isomers in these compounds.

This paper reports the results of the dipole moment measurement on some of the alkyl nitrites: ethyl, isopropyl, and tertiarybutyl nitrites in the gaseous state at various temperatures.

## Preparation of the Materials

The samples were prepared by dropping concentrated hydrochloric acid in the mixture of corresponding alcohol and 35% aqueous solution of sodium nitrite in cooling. The raw products of the *i*-propyl and *t*-butyl nitrites seemed to decompose when washed with water; they were therefore first dried over calcium chloride and distilled, and then dry air was passed though them to exile the remaining NO and $NO_2$ gases, and finally redistilled. Ethyl nitrite was washed with sodium carbonate solution and distilled over calcium chloride. Ethyl nitrite b.p. 17°C, *i*-propyl nitrite b.p. 39.2–.4°C, *t*-butyl nitrite b.p. 63.0°C.

## The Procedure and the Results of the Measurement

Because of the instability of the alkyl nitrites the measurement was made at temperatures below about 60°C. The electric part of the apparatus is that described in the previous paper[3], but some improvements were made on the thermostat, the gas cell, and the gas filling devices. A Dewar-vessel filled with insulating oil was used for the thermostat at low temperature (down to −20°C). Ethyl and propyl nitrites have vapor pressures high enough for the measurement of dielectric constant at these temperatures. The dimensions of the gas cell are the same as the cell "D" of the previous paper, but in order to keep the lead from contact with oil in the bath, a new cell was constructed which is shown in Fig. 1. To reduce the

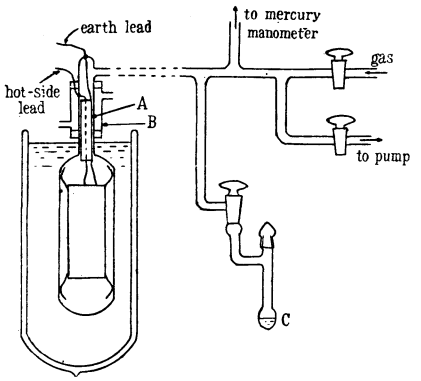



Fig. 1. Gas cell and vapor filling system.

stray field the hot-side lead was covered with a nickel cylinder (A) of earth-side which itself formed a part of the earth lead. The part (A) was covered with a glass mantle (B) through which dry air was allowed to flow to avoid the condensation of moisture on it.

The cell constant was calibrated many times by measuring the dielectric constant of carbon dioxide, and further checked with carbon tetrachloride and benzene. The correction due to the capacity of the part (A) was computed as a coaxial cylinder. Samples were introduced into the reservoir (C) by vacuum distillation. After each run of observations of $\Delta\epsilon$ and $\Delta p$, the cell was pumped out, and a fresh sample was used for each observation to avoid the errors due to the decomposition of the sample.

The results of the observations are summarized in Table I, Though these compounds are appreciably yellow colored, the extrapolation of the refractive index in visible region to infinite wave length shows no

1) S. Mizushima, "Molecular Structure and Internal Rotation", (1954).
2) P. Tarte, *J. Chem. Phys.*, 20, 1570 (1952).
3) T. Chiba, This Bulletin, 28, 19 (1955).

TABLE I

OBSERVED POLARIZATIONS AND DIPOLE MOMENTS OF ETHYL, *i*-PROPYL AND *t*-BUTYL NITRITES

Ethyl nitrite

$P_E+P_A=1.05MR_D$(assumed)$=18.5$ cc.

| $T$(°K) | $n$ | $p$(mmHg) | $P$(cc.) | $\Delta P$(cc.) | $\mu$(D) |
|---|---|---|---|---|---|
| 253.3 | 8 | 64–85 | 158.1 | 0.4 | $2.40_9$ |
| 266.7 | 6 | 70–82 | 151.8 | 0.2 | $2.41_4$ |
| 295.9 | 7 | 85–131 | 139.0 | 0.4 | $2.41_7$ |
| 298.0 | 6 | 69–90 | 138.2 | 0.3 | $2.41_8$ |
| 316.1 | 6 | 70–104 | 130.5 | 0.4 | $2.41_0$ |
| 333.8 | 8 | 70–97 | 124.8 | 0.4 | $2.41_2$ |

*i*-Propyl nitrite

$P_E+P_A=1.05MR_D$(assumed)$=23.3$ cc

| $T$ | $n$ | $p$ | $P$ | $\Delta P$ | $\mu$ |
|---|---|---|---|---|---|
| 256.1 | 7 | 33–52 | 181.6 | 0.6 | $2.57_8$ |
| 267.4 | 8 | 25–56 | 174.9 | 0.3 | $2.57_8$ |
| 284.2 | 7 | 46–63 | 164.7 | 0.5 | $2.56_8$ |
| 300.3 | 8 | 51–74 | 157.2 | 0.2 | $2.56_8$ |
| 314.3 | 8 | 54–70 | 151.2 | 0.5 | $2.56_8$ |
| 332.4 | 7 | 56–83 | 143.8 | 0.4 | $2.56_2$ |

*t*-Butyl nitrite

$P_E+P_A=1.05MR_D$(assumed)$=28.1$ cc.

| $T$ | $n$ | $p$ | $P$ | $\Delta P$ | $\mu$ |
|---|---|---|---|---|---|
| 288.8 | 5 | 45–51 | 183.2 | 0.6 | $2.71_1$ |
| 291.0 | 6 | 41–63 | 181.1 | 0.7 | $2.70_1$ |
| 301.4 | 4 | 51–63 | 175.1 | 0.4 | $2.69^5$ |
| 313.2 | 5 | 65–77 | 169.2 | 0.4 | $2.69_1$ |
| 330.1 | 5 | 57–67 | 161.2 | 0.3 | $2.68_4$ |

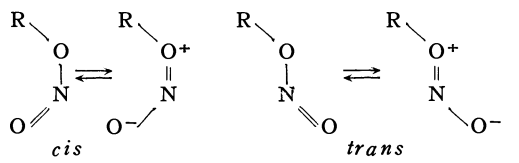
$n$: number of the observations.
$p$: pressure range of the observations.
$\Delta P$: average deviation of $P$.

abnormality; for instance, for ethyl nitrite, $MR_D=17.60$ cc., $MR_\infty=17.32$ cc. (extrapolated), and a sum of atomic refractions $\Sigma AR_D=16.9$ cc. Therefore, $P_E+P_A$ is taken as $1.05MR_D$ as in the usual cases.

The moment of ethyl nitrite in the gaseous phase was given by Czerlinsky[4] to be 2.38D at 17°C, and the dielectric constant of ethyl nitrite at 15°C and 760 mmHg given by Cordonier[5] is 1.0182, which corresponds to the dipole moment of 2.43D. The present results are in good agreement with these two.

## Discussion

According to the infrared study of Tarte[2] the absorption lines assigned to $\nu_{N=O}$, $\nu_{N-O}$, $\nu_{C-O}$, and $\delta_{ONO}$ have doublet structure, the ratio of the intensity of each doublet line depending on alkyl radical, as well as on temperature. This phenomenon was explained adequately by the existence of the rotational isomers. It is, however, difficult to attribute the effect of giving two isomers to the forces such as steric or dipole one, since these forces should vary monotonously from the *cis* to the *trans* position. The possible explanation of this is to take into account resonances such as




which stabilizes the planar structure, i.e., the *trans* and the *cis*. A calculation of resonance energy was made by a simple MO method to estimate barrier height at 90°C position. This calculation was made for a four-electron system of the skeleton of $-O^{++}-N^{+}-O^{+}$ and for the corresponding localized system, and the potential barrier is taken as a difference in resonance energy between them. This was made after the procedure employed by Kurita and Kubo[6] for the case of tropolone except exchange integral $\beta_{ij}$ between atoms $i$ and $j$, i.e., $\beta_{ij}$ was taken as $\beta_{ij}=\beta\cdot s_{ij}/s$, where $\beta$ is an exchange integral of benzene $\pi$-electron, $s_{ij}$ and $s$ are corresponding overlap integrals. Bond distances used were those given by Rogowski[7] for methyl nitrite: that is N-O: 1.37Å, N=O: 1.22Å. From this calculation the barrier height of $0.34\beta$ can be obtained; therefore if we assume 30 kcal./mole for $\beta$, this barrier is as high as about 10 kcal./mole. This is only an approximate value, but as shown later, it is a reasonable order of magnitude compared with the case of HONO, and therefore, it can be said that the resonance force is large enough to separate these molecules into two isomers.

Since there is a small temperature dependence of the moments of *i*-propyl and *t*-butyl nitrite (see Table I), it must be concluded that an energy difference exists between the *cis* and the *trans* forms. The energy difference can be calculated by use of the well-known formula of the average moment $\bar{\mu}$ at the temperature $T$:

$$\bar{\mu}^2=\frac{\mu_c^2+\mu_t^2 s e^{\Delta E/RT}}{1+s e^{\Delta E/RT}}, \qquad (1)$$

where $s$ denotes the ratio of the entropy factor of the *trans* form to that of the *cis* form. Its value cannot be computed since the curvatures at the potential minima are not known. Therefore, it is left as an un-

4) E. Czerlinsky, *Z, Physik*, 88, 515 (1934).
5) Cordonier and Guinchaut, *Compt. rend.*, 185, 1449 (1927).
6) Y. Kurita and M. Kubo, This Bulletin, 24, 13 (1951).
7) F. Rogowski, *Ber.*, 75B, 244 (1942).

known parameter which should be determined by the experiments.

Now, if the temperature dependence of the moment is small and $d\bar{\mu}/dT$ is constant in the range of the observation, then from Eq. (1) it is easily seen that

$$\Delta E = -2RT^2 \frac{(\mu_t^2 - \mu_c^2)\bar{\mu}}{(\bar{\mu}^2 - \mu_c^2)(\mu_t^2 - \bar{\mu}^2)} \cdot \frac{d\bar{\mu}}{dT}. \quad (2)$$

Thus the energy difference can be evaluated if we know the values of $\mu_c$ and $\mu_t$ without the knowledge of $s$. The value of $s$ is calculated from Eq. (1), using the value of $\Delta E$ thus obtained[8].

The diple moments of the *cis* and the *trans* forms are calculated to be $\mu_c = 1.27$D, and $\mu_t = 2.97$D respectively, using $\mu_{N=O} = 2.0$D, $\mu_{N-O} = 0.3$D, $\mu_{R-O} = 1.1$D, and $\angle$RON = tetrahedral and $\angle$ONO = 120°.[9] The values of $\Delta E$ and $s$ which give the best fit with the observed temperature dependence of the dipole moments using $\mu_c$ and $\mu_t$ obtained above are given in Table II. As mentioned above, the $\mu_t$, it can safely be said that $\Delta E$ of *i*-propyl nitrite is estimated to be less than about 140 cal., and that of *t*-butyl nitrite to be less than 340 cal. Thus $\Delta E$ increases in the order of methyl, ethyl, *i*-propyl and *t*-butyl nitrites, although $\Delta E$ is not great in the last two compounds.

Tarte[11] obtained $\Delta E$ from the measurements of the temperature dependence of the intensity of absorption lines assigned to both isomers. His result is −350 cal. for methyl nitrite and nearly equal to zero for ethyl and *i*-butyl nitrites, and $\Delta E \gg 0$ in *t*-butyl nitrite. In the last case accurate value was not obtained since the *cis* absorption line is very weak. The constant moment of ethyl nitrite in the present work agrees well with his result.

We shall next consider these $\Delta E$ values from the theoretical considerations. First of all, it should be mentioned that the resonance effect is not a main cause of the energy difference between the isomers because the

TABLE II

$\Delta E$ AND $s$ VALUES OF ALKYL NITRITES ESTIMATED FROM THE OBSERVED DATA OF DIPOLE MOMENT

| | $\mu_t = 2.97$D, $\mu_c = 1.27$D, | | $\mu_c = 1.40$D. $\mu_t = 3.27$D. | |
|---|---|---|---|---|
| | $s$ | $\Delta E$ cal./mol. | $s$ | $\Delta E$ cal./mol. |
| $CH_3ONO$ | 1.5[a] | (−350) | 0.9[a] | (−350) |
| $C_2H_5ONO$ | 1.4 | 0 | 0.8 | 0 |
| $(CH_3)_2CHONO$ | 1.8 | 140 | 1.0 | 100 |
| $(CH_3)_3CONO$ | 2.1 | 340 | 1.1 | 200 |

*a*: These values are estimated using dielectric constant data for methyl nitrite given by Cordonier (Ref. 5).

contribution of the resonance forms is considerable in these molecules. Hence in calculating $\mu_c$ and $\mu_t$ it will be more reasonable to take into account the polar structures[10]. However, the simple MO calculation does not provide a reliable estimate to the augmentation of the moments, since it has usually a trend to give considerably high values. In Table II there are also shown the values obtained by assuming 10% higher values for $\mu_c$ and $\mu_t$. It is seen from this table that, if we take higher values for $\mu_c$ and $\mu_t$, $\Delta E$'s of *i*-propyl and *t*-butyl nitrites becomes smaller. Hence, although there are some ambiguities in the values of $\mu_c$ and effect of alkyl radical R on the resonance is that of a higher order. Therefore we have to look for the origin of the energy difference in some other effect. It is seen that the dipole-dipole interaction between R-O and O-N stabilizes the *cis* position whereas the steric force between the radical R and the end O atom has an opposite effect. Since dipole interaction energy does not vary so much by replacing R, the difference obtained for different radicals may be mainly due to the steric effect. It can easily be understood that $\Delta E$ of steric nature is higher in (Et..... O) than in (Me.....O) because in the former a hydrogen atom of a methyl radical is replaced by another methyl and, in the same way $\Delta E$ in (*i*-Propyl,.....O) is higher than in (Et.....O), and in (*t*-Butyl.....O) higher than in (*i*-Propyl.....O). If we replace one hydrogen atom of a methyl radical by another methyl or by other alkyl radical with longer chain, the steric energy may remain nearly

8) $\Delta E$ is taken here to be positive when the *trans* form is more stable than the *cis* one.

9) $\mu_{N=O} = 2.0$D was given by Smyth from the value 2.5D of *t*-nitrosobutyl (Smyth, *J. Am. Chem. Soc.*, 60, 183 (1938)). The moment of N=O bond presumably varies with the extent of resononce, but on account of the lack of other available data, the above value is tentatively used.

10) There is a possibility of larger $\mu_c$ and $\mu_t$ in higher alkyl nitrites by induction effect.

11) P. Tarte, unpublished.

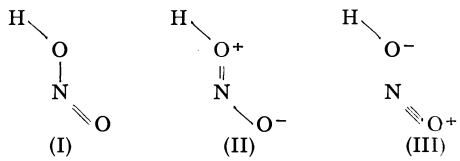
the same, because the atoms in the radical are far apart from the oxygen atom and the steric energy is probably determined by the interaction between the end oxygen atom and the atoms in $\alpha, \beta$-position of R. Really a similar situation has already been found in ethane derivative hydrocarbons. The hindering barrier against the internal rotation around C-C axis in propane is considerably higher than that in ethane, but the difference does not increase so much in *n*-butane, or *n*-pentane[12]. By these considerations, the observed change in $\Delta E$ by replacing $R$ and the spectroscopic result of nearly equal $\Delta E$ in ethyl and in *i*-butyl nitrite can be adequately explained.

A peculiar feature of the spectrum of alkyl nitrites is that the ratio of the extinction coefficients ($\ln I_t/\ln I_c$) of the $\nu_{N=O}$ band in the *cis* and the *trans* isomers is constant in esters of same $\alpha$-carbon class of $R$, but differs appreciably in different classes[2]. Now the ratio of the extinction coefficients is given by a product of the ratio of the number of molecules $N_t/N_c$ and the square of the ratio of the change of the dipole moments with the normal mode of vibration:

$$\ln I_t/\ln I_c=(N_t/N_c)|(d\mu/dQ)_t/(d\mu/dQ)_c|^2. \quad (3)$$

It is easily seen that the change of the ratio $N_t/N_c$ is small, because it is given by the expression $s\cdot\exp(\Delta E/RT)$ and the difference of $\Delta E$ is small. Therefore the large change of the extinction coefficients must be attributed to a large change of the ratio $(d\mu/dQ)_t/(d\mu/dQ)_c$. However, from the ordinary concept of the normal vibration, such a large change cannot be expected at all, since the inner vibration of the N=O group is hardly affected by the structure of the outer part of that group. One explanation is the change of the amount of resonance, but this must bring about a considerable change of $\Delta E$, contrary to the observed result. Thus the explanation of the above fact requires further study.

Lastly a few words should be added with regards to HONO molecule. This molecule is too unstable for the measurement of the dipole moment, but several authors reported the infrared spectrum. It is interesting to compare these results with those of RONO. According to the studies of Jones[13] and of D'Or[14] the characteristic frequencies of this molecule $\nu_{N=O}$, and $\nu_{N-O}$, and $\delta_{ONO}$ have doublet structure, from which the molecule is considered to have also two rotational isomers, the *trans* and the *cis* forms. From the measurement of the temperature dependence of band intensity, Jones concluded that the *trans* form is about 500 cal. more stable than the *cis* form. This conclusion seems to be unlikely at first sight, since the steric force between O and H in the *cis* position is smaller than that between O and R. Actually, however, in the spectrum of HONO there are several points different from that of RONO; namely, $\nu_{N=O}$ of RONO is lower than that of HONO, on the contrary, $\nu_{N-O}$ of the former is higher than that of the latter. From these results, Jones suggested that in HONO the central N-O bond is much weaker than in RONO, which is a result of a contribution of the resonance form (III) besides (I) and (II).




(I) (II) (III)

The potential barrier of internal rotation of HONO is found to be 9–10 kcal., using the torsional frequencies given by these authors, and assuming the cosine type potential ($V=\frac{1}{2}V_0(1-\cos\varphi)$). In RONO this frequency is not observed, but it is very interesting to compare the value 9–10 kcal. of HONO with the value 10 kcal. of RONO derived from the MO calculation described earlier.

## Summary

The dipole moment measurement was made at various temperatures on ethyl, *i*-propyl and *t*-butyl nitrites. Observed moments are 2.41D for ethyl, 2.57D for *i*-propyl, 2.70D for *t*-butyl nitrite at room temperature. The moment of the latter two compounds decrease slightly with temperature while ethyl compound remains constant. These esters are considered to consist of two isomers: the *trans* and the *cis* separated by a barrier of several kcal. due to a resonance effect. The energy difference $\Delta E$ between the two isomers is found to be zero in ethyl, $<140$ cal. in *i*-propyl, and $<340$ cal. in *t*-butyl nitrite; in the latter two the trans from being more stable.

This change in $\Delta E$ with replacing $R$ is satisfactorily explained as due to the steric energy between $R$ and the end oxygen atom.

12) K. S. Pitzer, *Faraday Soc. Disc.*, **10**, 66 (1951); G. Herzberg, "Infrared and Raman Spectra", (1945), p. 520.
13) I.H. Jones et al., *J. Chem. Phys.*, **19**, 1599 (1951).
14) L. D'Or and P. Tarte, *Bull. soc. roy. sci. Liege*, **1951**, 478.

The author wishes to express his sincere thanks to Prof. Y. Morino and to Dr. Miyagawa for the kind guidance and valuable advice through this study and to Dr. P. Tarte of the University of Liège, who kindly informed the author of his spectroscopic results including some of the unpublished data. The cost of this research has been defrayed from the Grant in Aid for Fundamental Scientific Research from the Ministry of Education to which the author's thanks are also due.

*Department of Chemistry, Faculty of Science, Tokyo University, Tokyo*

# *Estimation of the Geologic Age of Radioactive Sediment Containing Radium Isotopes*

By Hitoshi SAKAI

(Received February 18, 1955)

## Introduction

The determination of the geologic age of sediment is one of the important and very difficult problems in geochemistry. Generally the complex conditions governing the sedimentation process present many difficulties for researchers.

So far as radioactive sediments are concerned, however, it is sometimes possible to estimate their geologic age. The ionium-radium method[1] proposed for the determination of the geologic age of deep-sea sediments is the best known example of this. But this method is only applicable to appreciably old sediments of several hundred years. Recently, Koczy[2] estimated the sedimentation intensities[3] of some sorts of clay by statistical calculations using the content of radium, manganese and titanium in these samples. In this case, however, it is obvious that the degree of accuracy is limited by the number of samples analyzed.

When a fairly young sediment contains isotopes of radium which are not supported by their long-lived parents, the abundance ratios of these isotopes should vary with the age of the sediment. Based upon this relation, three new methods are proposed for the estimation of sedimentation rate and intensity of young sediments which are approximately one to two hundred years old.

1) C. S. Piggot and W. D. Urry, *Amer. J. Sci.*, 240, 1 and 93 (1942).

2) F. F. Koczy, *Geochim. et Cosmochim. Acta*, 1, 73-85 (1951).

3) Sedimentation intensity means the sedimentation velocity in gram per unit area per unit time, see koczy loc. cit.

## Assumptions

In our methods, the following conditions are assumed to persist during the period of sedimentation.

(1) The abundance ratios of radium isotopes keep constant in the water precipitating sediments.

(2) There is no way for the elements once precipitated in the sediments to be lost by any process.

(3) Within the sediments, no migration of elements occurs.

(4) Sedimentation intensity of an element keeps constant and consequently the intensity is uniform at least in that part of the sediments which we examine.

The conditions (1) to (4) are necessary to develop the following methods (a) and (b), while in the method (c), the condition (3) is not necessary.

In this paper the following values are used as the decay constants of radioactive elements: $4.3\times10^{-4}$, 68.7, $3.1\times10^{-2}$, 0.10, 0.36 and 69.3 per year for $Ra^{226}$, $Ra^{222}$, $Pb^{210}$, $Ra^{228}$, $Th^{228}$ and $Ra^{224}$, respectively. These values are calculated on the basis of nuclear data which appeared in the Table of Isotopes by Hollander, Perlman and Seaborg.

## Principle of the Methods

**(a) The Method Based on the Vertical Variation of the Ratios of Radium Isotopes.** —Let us consider an infinitely thin layer in a sediment perpendicular to the direction of growth. The number of atoms of radium isotopes present in the layer at the time $t$

from the beginning ($t=0$) of sedimentation can be represented by the following equations.

$$[Ra^{226}]^t=[Ra^{226}]\,e^{-\lambda_1 t}, \quad (1)$$

$$[Ra^{228}]^t=[Ra^{218}]\,e^{-\lambda_2 t}, \quad (2)$$

$$[Ra^{224}]^t=[Ra^{224}]\,e^{-\lambda_4 t}+\lambda_2\lambda_3/\lambda_4(\lambda_3-\lambda_2),\ [Ra^{228}]\,(e^{-\lambda_2 t}-e^{-\lambda_3 t}), \quad (3)$$

where $[Ra]'$ and $[Ra]$ stand for the number of atoms of radium in the layer at $t=t$ and $t=0$, respectively, $\lambda_1$, $\lambda_2$, $\lambda_3$ and $\lambda_4$ being the decay constants of $Ra^{226}$, $Ra^{228}$, $Th^{228}$ and $Ra^{224}$, respectively. Deriving the above equations the contributions by $Th^{228}$ and other long-lived parents are neglected because, as will be given later, the $Th^{228}$ content in the water precipitating the sediment is negligibly small and because the effect by other long-lived parents is also negligibly small so far as a short period of from 100 to 200 years is concerned. In addition, the first term of the equation (3) can be neglected if $t$ is longer than about thirty days as in our samples described later.

From equations (1) and (3), equation (4)′ is obtained.

$$[Ra^{224}/Ra^{226}]^t=[Ra^{224}/Ra^{226}]\,e^{(\lambda_1-\lambda_2)t}+\lambda_2\lambda_3/\lambda_4(\lambda_3-\lambda_2)[Ra^{228}/Ra^{226}]\,(e^{-\lambda_2 t}-e^{-\lambda_3 t})/e^{-\lambda_1 t} \quad (4)'$$

where the first term can be neglected because it is much smaller than other terms when $t$ is longer than about thirty days. Then by introducing numerical values for constants, equation (4) is obtained.

$$[Ra^{224}/Ra^{226}]^t=2\times10^{-3}[Ra^{228}/Ra^{226}]'\,(e^{-0.10t}-e^{-0.36t})/e^{-0.43\times10^{-4}t} \quad (4)$$

Here, according to condition (1), the ratio $[Ra^{228}/Ra^{266}]'$ can be represented by the corresponding ratio in the water at the present time, which can be determined experimentally. Also the ratio $Ra^{224}/Ra^{226}$ in the layer now in qnestion can be determined. Thus the time elapsed after the layer was formed and consequently the rate of sedimentation for the sediment laying above the layer are calculated.

**(b) The Method Based on the Vertical Variation of the Beta-activity of the Daughter Nuclides from Radium Isotopes.**—The equation for the beta-activity in the same layer as considered in the method (a) can be similarly derived. Here, the contributions by short-lived nuclides originally precipitated from the water are neglected, and only the secondarily produced activities from $Ra^{226}$, $Pb^{210}$ and $Ra^{228}$ are taken into consideration. The activity due to beta particles from $Pb^{210}$ can also be neglected because of their extremely low maximum energy. Then the beta activity of a layer is given by the following equations at the time $t$,

$$[\Sigma Ra^{226}]^t=3\lambda_1[Ra^{226}]'e^{-\lambda_1 t}+(\lambda_5[Pb^{210}]'-\lambda_1[Ra^{226}]')e^{-\lambda_5 t}$$

$$[\Sigma Ra^{228}]^t=\lambda_2[Ra^{228}]'\{(1+2/(\lambda_3-\lambda_2))e^{-\lambda_2 t}-1/(\lambda_3-\lambda_2)\cdot e^{-\lambda_3 t},$$

where $[\Sigma Ra^{226}]^t$ and $[\Sigma Ra^{228}]^t$ stand for the beta-activity of $Ra^{226}$-series and of $Ra^{228}$-series, respectively, and $\lambda_5$ expresses the decay constant of $Pb^{210}$. Then by the summation of the two equations the total beta-activity of the layer, $A_\beta^t$, is obtained as follows:

$$A_\beta^t=4.3\times10^{-4}[Ra^{226}]'\{3-(1-q)e^{-3.1\times10^{-2}t}+8.7pe^{-0.10t}-3.9pe^{-0.36t} \quad (5)$$

where $p=\lambda_2[Ra^{228}]'/\lambda_1[Ra^{226}]'$ and $q=\lambda_5[Pb^{210}]'/\lambda_1[Ra^{226}]'$.

By the same consideration as in the method (a) we can calculate the geologic age of a layer by measuring the total beta-activity of the layer, assuming $q$ is also constant during the period of sedimentation.

**(c) The Method Based on the Total Time Variation of the Abundance Ratios of Radium Isotopes in Sediments.**—Let us consider a column parallel to the direction of growth of the sediment. The concentration of a radium is controlled by two factors, an increase of the isotope by sedimentation and a decrease by radioactive decay.

When $dk$ and $d[Ra]^t$ express the increase of an isotope of radium by sedimentation and the total change of the isotope in the column, respectively, in a small time, $dt$, at $t=t$, the increase of the amount of the isotope at $t=t$ can be written by the following equation:

$$d(Ra)^t=dk-\lambda(Ra)^t\,dt,$$

where $(Ra)^t$ stands for the total amount of an isotope of radium in the column at $t=t$.

According to the condition (4), $dk$ or $dk/dt=K$ in this equation is constant and we can solve the differential equation obtaining the total amount of the isotope in the column at $t=t$. Thus for $Ra^{226}$ and $Ra^{228}$ the following equations can be given:

$$(Ra^{226})^t=K_1(1-e^{-\lambda_1 t})/\lambda_1 \quad (6)$$

$$(Ra^{228})^t=K_2(1-e^{-\lambda_2 t})/\lambda_2 \quad (7)$$

When the determination is carried out at a

time $t'$ after sample has been collected and when the time $t'$ is sufficiently large in comparison with the half-life of $Ra^{224}$ so that the sedimented $Ra^{224}$ has completely decayed off at the time of determination, the total amount of $Ra^{224}$ at this time will be obtained by integrating the equation (3) from $t'$ to $t+t'$ giving the equation (8).

$$(Ra^{224})^{t+t'}=\{K_2/\lambda_4(\lambda_3-\lambda_2)\}\{\alpha(\lambda_3-\lambda_2-\lambda_3e^{-\lambda_2 t}+\lambda_2 e^{-\lambda_3 t})+\beta\lambda_3(1-e^{-\lambda_3 t})\}, \quad (8)$$

where $\alpha=e^{-\lambda_3 t'}$, and $\beta=e^{-\lambda_2 t'}-e^{-\lambda_3 t'}$, respectively.

From the equation, (6) and (8), the total variation of the ratio, $Ra^{224}$ to $Ra^{226}$, v.s. time in the column is represented by the following equation when we insert numerical values for constants:

$$(Ra^{224}/Ra^{226})^{t+t'}=(K_2/18K_1)\{\alpha(0.26-0.36e^{-0.10t}+0.10e^{-0.36t}\}+0.36\beta(1-e^{-0.36t})\}/t+t' \quad (9)$$

where $e^{-\lambda_1(t+t')}$ is approximated to $1-\lambda_1(t+t')$.

In this equation $K_2/K_1$ is considered to be equal to the abundance ratio of the two isotopes in the water. Then the geologic age of the sediment as well as the mean rate of sedimentation can be estimated by measuring the ratio, $Ra^{224}$ to $Ra^{226}$, in the total mass of the columnar sample.

**The Rough Estimation of the Sedimentation Rate as well as the Sedimentation Intensity of Hokutolite.**

Hokutolite is one of the radioactive sinter deposits from hot springs[4,5] and is being precipitated from spring waters at temperatures ranging from 98°C to 40°C. In most cases, it is growing layer by layer on the surface of the base rock, andesite and is considered to be the most suitable sample for our methods.

The content and the ratios of radium isotopes in the spring water are shown in Table I. $Pb^{210}$ is also supposed to be present, but the content in the water has not yet been determined. In Table II are shown the mean content of $Ra^{226}$ and ratio, $Ra^{224}$ to $Ra^{226}$, in the two samples, Hokutolite A and Hokutolite B. The Hokutolite A is of a thickness of eleven millimeters and is grow-

TABLE I
CONTENTS AND RATIOS OF RADIUM ISOTOPES IN THE SPRING WATERS

| Date | Content of $Ra^{226}$ | The Atomic Ratio $Ra^{224}/Ra^{226}$ | $Ra^{228}/Ra^{226}$ | Content of $Th^{228}$ |
|---|---|---|---|---|
| October '53 | $2.0\times10^{-11}$ g./l. | $5.9\times10^{-5}$ | ca. $5\times10^{-2}$ | ca. 0 |
| July '54 | 1.4 „ | 5.0 „ | — | ca. 0 |

TABLE II
CONTENT AND RATIO OF RADIUM ISOTOPES IN HOKUTOLITE

| Sample | Age observed | Content of $Ra^{226}$ | The Atom Ratio $Ra^{224}/Ra^{226}$ |
|---|---|---|---|
| Hok.—A | unknow | $1.0\times10^{-9}$ g./g. | 1.0 0.2 |
| Hok.—B | 5 yr. | 1.6 „ | 4.0 0.2 |

TABLE III
VERTICAL CHANGE OF RADIOACTIVE PROPERTIES IN HOKUTOLITE A

| Nos. of pieces | Depth from the Surface (mm.) | Cont. of $Ra^{226}$ ($10^{-9}$g./g.) | Atom. Ratio $Ra^{224}/Ra^{226}$ ($10^{-5}$) | Specific—Activity (c.p.m./g.) |
|---|---|---|---|---|
| 1 | | 1.9 | 6.0 | 6010 |
| 2 | | 0.8 | 6.0 | 3500 |
| 3 | | 1.9 | 3.5 | 2400 |
| 4 | | 0.9 | 2.7 | 1480 |
| 5 | | 1.8 | 0.87 | 960 |
| 6 | | — | — | 820 |
| 7 | | 1.5 | 0.10 | 555 |
| 8 | 3 | — | — | — |
| 9 | | 1.4 | 0 | — |
| 10 | 4 | 1.1 | 0 | — |
| 11 | | — | — | 710 |
| 13 | | 0.9 | 0 | — |
| 14 | 6 | — | — | 350 |
| 16 | | 0.7 | 0 | — |
| 17 | | — | — | 330 |
| 19 | | 0.8 | 0 | — |
| 20 | | — | — | 455 |
| 23 | | — | — | 460 |
| 25 | | 0.8 | 0 | — |
| 26 | 9 | — | — | 410 |
| 29 | | — | — | — |
| 32 | | 0.8 | 0 | 310 |
| 33 | 11 | 1.5 | 0 | 405 |

4) R. Ohashi, Mineralogical Mag., **19**, 73 (1920); I. Suganuma, Bull. Chem. Soc. Japan, **3**, 69 (1928); E. Minami, Kobutsugaku Zasshi (J. Mineralogical Soc. Japan), **2**, 1 (1954).

5) Hokutolite is composed of the mixed crystal of barium sulfate and lead sulfate, and was found first at the Hokuto springs in Formosa and then at the Tamagawa Springs (formerly called Shibukuro Springs) in Akita perfecture in Japan. The molecular ratio, lead sulfate to barium sulfate, in Hokutolite from Tamagawa is found to fluctuate between 0.2 and 0.02. The spring waters of Tamagawa contain radioactive elements of both uranium- and thorium-series which make the mineral distincly radioactive. The main constituents of the water are $Al^{+++}$, $Fe^{++}$, and $Cl^-$, with smaller quantities of $SO_4^{--}$, $F^-$ and $Fe^{+++}$. Barium and lead are also contained in the water but their concentrations are in the order of p.p.m.

ing on the large base rock. It is deposited from the flowing water with a temperature as high as 45°C. A small column is made carefully from this sample, and is cut, layer by layer, into thirty-three pieces from the surface to the bottom. The measurements of the content and the ratio of radium isotopes as well as the specific beta activity are performed on each of these pieces and the results are summarized in Table III.

Hokutolite B is, on the other hand, about 0.75 mm. thick and is known to be about five years old. This sample is growing on a small andesite block on which the spring water, with a temperature of 75°C, splashes vigorously.

The content and the ratio of radium isotopes of the water are determined by the following method. One hundred milligrams of barium are added to the sample water as barium chloride and barium sulfate is precipitated by the usual method. Barium chloride method reported by Ames et al[5] is employed in order to eliminate other radioactive elements coprecipitated with radium. The alpha-activity of the barium sulfate is measured continuously by a Lauritsen type electroscope and the variation with time of the activity is plotted on a graph paper. The content of $Ra^{226}$ and the ratio, $Ra^{224}$ to $Ra^{226}$, are easily calculated from the curve, but the calculation of the ratio, $Ra^{228}$ to $Ra^{226}$, is not so easy because of the somewhat long half-life of $Ra^{228}$. As described later, the ratio, $Ra^{228}$ to $Ra^{226}$, in the spring water, is evaluated by the more convenient way. In the determination of these values in Hokutolite, the same method is employed but barium chloride need not be added to the sample in this case.

(1) **The Estimation of the Rate of Growth Near the Surface of Hokutolite.**—From the equations, (4) and (5), it is calculated that the ratio, $Ra^{224}$ to $Ra^{226}$, or the total beta-activity of a layer becomes zero or constant when about fifty years has passed since its precipitation. From Table III, it is shown that in the case of Hokutolite A this time corresponds to the period of sedimentation of the layer about 3 mm. thick. The mean rate of growth above this layer is then calculated to be about $6\times10^{-2}$ mm. per year.

This fact is more clearly shown in Fig. 1 and Fig. 2, which are constructed on the basis of the following considerations: the experimentally determined ratio of radium isotopes as well as beta-activity for each piece shown in Table III are not the values for infinitely thin layers, but the mean values for the layers with some thickness. Considering the above estimated rate of growth, the thickness of each layer seems to correspond to about seven years sedimentation. To compare these facts with theoretical data, therefore, we must use mean "theoretical" values for every seven years. The ratio, $Ra^{228}$ to $Ra^{226}$, in the water is evaluated by equalizing the mean theoretical ratio, $Ra^{224}$ to $Ra^{226}$, for the first seven years to the observed ratio and this gives $8\times10^{-2}$ for the value. This value is considered to be more reliable than the one experimentally determined in Table I and will be used in the following discussion.

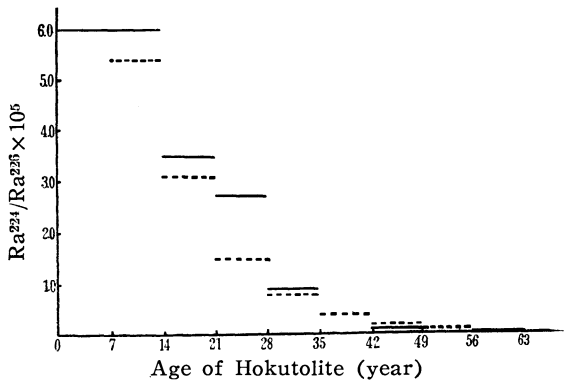



Fig. 1. Vertical change of the ratio, $Ra^{224}/Ra^{226}$, in Hokutolite-A.
Solid lines: Observed ratio, $Ra^{224}/Ra^{226}$, in each piece of Hokutolite-A up to No. 9 in Table III.
Dotted lines: Theoretical mean ratio for every seven years. Theoretical. value for first seven years is equalized to the observed one.

From Fig. 1 and Fig. 2, it is concluded that the rate of growth estimated above is approximately valid near the surface of the sample.

(2) **The Estimation of the Mean Rate and Intensity of Sedimentation of Hokutolite for the Past One to Two Hundred Years.**—From the above discussion the value for $K_2/K_1$ in the equation (9) is $8\times10^{-2}$ and the time $t'$, is known as 0.25 years for Hokutolite A and Hokutolite B, respectively. Using these data the theoretical time variation of the ratio, $Ra^{224}$ to $Ra^{226}$, in the total mass of the deposit is plotted in Fig. 3 in a solid line. Comparison of the data in Table II with the curve in Fig. 3 gives the age and

6) D.P. Ames, J. Sedlet, H.H. Anderson and T.P. Kohman, The Transuranium Elements, (Natl. Nuclear Energy Series IV-14B) p. 1700 (1949).

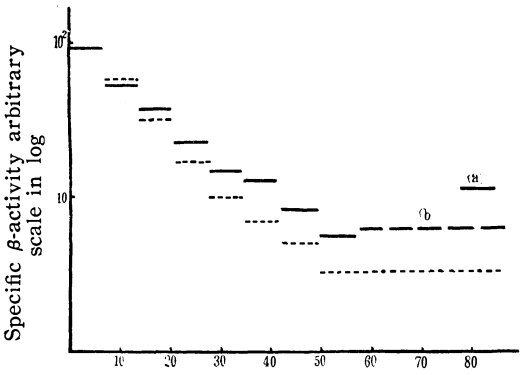



Fig. 2. The Vertical change of β-activity of Hokutolite.

Solid lines: Observed specific β-activiteis of each pieces of Hokutolite-A up to No. 11 in Table III.

Dotted lines: Theoretical mean β-activities for evry seven years. $Pb^{210}$ is assumed to be in equilibrium with $Ra^{226}$ in the water and the value for the first seven years is equalized to the observed one.

(a): observed value for No. 11, exceptionally high.

(b): observed mean value from No. 14 to No. 33.

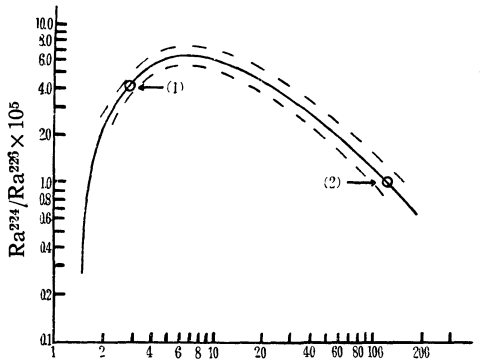



Fig. 3. The variation with time of the mean ratio, $Ra^{224}/Ra^{226}$, in total mass of Hokutolite.

Solid line: $K_2/K_1=8\times10^{-2}$

Dotted lines: above $K_2/K_1=9\times10^{-2}$, below $K_2/K_1=7\times10^{-2}$

(1) and (2): observed values for Hokutolite-B and-A, respectively.

the mean rate of sedimentation. Combining these results with the content of each element in Hokutolite and weight of the sample, the sedimentation intensity of each element can be estimated. Here the sedimentation intensities of radium and of Hokutolite as a whole are given. In the calculation of the sedimentation intensity of Hokutolite, the water content in the sediment is neglected. The reason is that the weight of Hokutolite A is approximately 4.5 gr./cm³ while the specific gravity of Hokutolite is 4.5. These results are summarized in Table IV.

## Discussion

The accuracy of the values calculated depends largely on the validity of assumptions first proposed. Among them assumption (4) is the most unlikely. A remarkable discrepancy between the values for the growth rate of Hokutolite A, between the values by the first two methods and the value by the third method, is evidently due to this. The fact that most of the Hokutolite samples consist of alternating white and brown layers suggests that sedimentation has proceeded not uniformly. Really it was shown by Mr. Sasaki[7] in our laboratory using the nuclear emulsion method that white layers are richer in radio-active elements than brown layers.

From these observations it is probable that the mean rate of growth of Hokutolite is smaller in recent years than in the older period.

On the other hand, the difference of the rate of growth between the sample A and sample B is considered mainly due to the difference of the conditions governing the sedimentation process. Some of them are shown in the beginning of this chapter. In addition, the content of $Ra^{226}$ in the water precipitating Hokutolite A is about one-half of that in the water near Hokutolite B. The contents of barium and lead are probably decreased by the same proportion as radium though not yet assured.

As for the first assumption, that is, the constancy of the abundance ratio of radium

7) Symposium on Geochemistry held in Fukuoka October, 1954.

TABLE IV

THE SEDIMENTATION RATE AND INTENSITY OF HOKUTOLITE

| Sample | Age calcd by the Method (c) yr. | Sedimentation Rate by the Method (a) & (b) Method (c) mm./yr. | | Sedimentation Intensity by the Method (c) of Ra $10^{-11}$ g./cm²/yr. | Hokutolite $10^{-2}$ g./cm²/yr. |
|---|---|---|---|---|---|
| Hok.—A | 120±20 | 0.06 | 0.09±0.015 | 4±0.7 | 4±0.7 |
| Hok.—B | 3± 0.2 | — | 0.25±0.03 | 18±1 | 11±0.7 |

The Density of Hok.—B is assumed to be 4.5.

Experimental error in the determination of the ratio $Ra^{224}$ to $Ra^{226}$, is only considered here.

isotopes, its validity cannot be ascertained experimentally within a short period. If radium isotopes are introduced into the spring water from the same mother rocks, sudden and appreciable change of their ratios would not take place in such a short period as one or two hundred years. In this case, however, the steady increase or decrease of the ratios, probably in both directions, may occur to some extent. In Fig. 3, the limit of the error is shown in two dotted lines as the ratio, $Ra^{228}$ to $Ra^{226}$, in the water varies from $7\times10^{-2}$ to $9\times10^{-2}$.

Uncertainties arising from other assumptions may be minimized by taking samples near the center of gross sediment.

The determination of the ratio, $Ra^{224}$ to $Ra^{226}$, is done by the rather inconvenient method described before. The error is estimated to be about fifteen per cent when the ratio is less than $1\times10^{-5}$, while it decreases to about five per cent as the ratio increases. In our purpose, however, the uncertainty of this order could be allowed if one considers non-validities of the conditions assumed.

In the methods, (a) and (b), another important error is introduced by the crystalization of Hokutolite. The surface of Hokutolite becomes uneven as the crystalization takes place and it is very difficult to measure accurately the depth of a layer from the surface. This error is considered to amount to about ten per cent at the depth of 3 mm.

Comparing three methods with each other, (a) ond (b) are better than (c) in that the assumption for the uniform growth is not necessary to them and the time $t$ is obtained rather distinctly, when the ratio, $Ra^{224}$ to $Ra^{226}$, or the total beta activity becomes zero or constant. In the method (b), however, the uncertainty from the ratio, $Pb^{210}$ to $Ra^{226}$, must be taken into consideration. In the case of the method (c), on the other hand, it is possible to estimate the mean rate of growth in the period ranging from a few years to one or two hundred years, while the first two methods can estimate the value only for about sixty years.

From these discussions it can be concluded that compared to the observed rate of growth, 0.15 mm./year the calculated rate for Hokutolite B, 0.25 mm./year, is fairly satisfactory. Perhaps, the value for Hokutolite A is also satisfactory with good approximation.

## Summary

Under some assumptions, three methods for the estimation of sedimentation rate as well as sedimentation intensity of radioactive sediments are proposed. These methods are based on the time variation of the abundance ratios of radium isotopes in the sediments. The rate of sedimentation of a radioactive sediment, Hokutolite, is estimated for two samples by these methods. The result is 0.25 mm./year for one sample for which the observed value is known to be 0.15 mm./year. For the other sample of unknown age, the rate is estimated to be 0.09 mm./year.

The author wishes to express his sincere thanks to Prof. E. Minami and Dr. N. Saito, the University of Tokyo, for their encouragement and valuable suggestions. The work was supported financially by a scientific grant from the Ministry of Education as well as a grant from Research Association of Tamagawa Hot Springs, to which the author's thanks are due.

*Department of Chemistry, Faculty of Science, Tokyo University, Tokyo*

# *Some Remarks on the New Equation of State as Applied to the Critical Region*

By Tetsuya ISHIKAWA

(Received March 9, 1955)

The indefiniteness of the critical state has been an interesting question for as long a time as since 1880, but the exact nature of the critical point does not yet seem to be established. The shape and the degree of flatness of the isotherms in the critical region are not those predictable from a van der Waals' type of equation which is conditioned by $(\partial p/\partial V)_{T=T_c}=0$, $(\partial^2 p/\partial V^2)_{T=T_c}=0$, and $(\partial^3 p/\partial V^3)_{T=T_c}=0$, but could be reconciled with either of the current theories: (1) Mayer-Harrison's "derby hat" theory[1] which predicts below the true critical temperature, $T$, flat, horisontal isotherms above the temperature of meniscus disappearance, $T_m$; (2) Rice's modified "derby hat" theory[2] which predicts a flat, horizontal critical isotherm with linear but sloping isotherms immediately above $T_c$; and (3) Zimm's singular point theory[3] which describes the critical point as a singularity at which not only $(\partial p/\partial V)_{T=T_c}=0$, $(\partial^2 p/\partial V^2)_{T=T_c}=0$, but also all the higher derivatives are zero. The precise $pVT$ measurements in the critical region of xenon done by Habgood and Schneider[4], however, offer no support for Mayer-Harrison's theory since there is no obvious region of flat, horizontal isotherms above $T_m$, and also for Rice's theory since the observed coexistence border curve appears to be definitely rounded at the apex.

The present author[5] put forward a modified form of van der Waals' equation available for both gaseous and liquid phases:

$$p+a/V^{2-\epsilon}=RT/(V-b),\ a=3p_cV_c^2,\ b=V_c/3,$$

where $\epsilon$ is a constant independent of pressure to the extent that the applied pressure affects no appreciable change in molecular association.

The introduction of $\epsilon$ into van der Waals' equation is sufficient to allow the critical factor, $RT_c/p_cV_c$, to be consistent with experiments, i.e., the reduced equation at the critical point, $RT_c/p_cV_c=2(1+3V_c^{\epsilon})/3$, $\epsilon=0.077\pm0.008$ when $V$ is expressed in cc./mol., is valid for 66 kinds of normal and slightly polar substances, but such transformation of equation results in separating a simple van der Waals' critical point, which is conditioned by either of $b=V_c/3$ or $b=RT_c/8p_c$ with $a=27p_cb^2$, into a maximum and a minimum with never realizable portion, $\partial V/\partial p>0$, and with supersaturated vapour portion, the former being supposed to correspond with generally accepted phenomena in the liquid-vapour coexistence region. The divergency in the portion of $(\partial V/\partial p)_{T=T_c}>0$ may be saved, if the critical point is assumed to be the limiting case of liquid-vapour coexistence region by combining the equation of critical isotherm, $p+a/V^{2-\epsilon}=RT_c/(V-b)$, with the horizontal line passing through the critical pressure, $p_c=3RT_c/2V_c(1+3V_c^{\epsilon})$, where $\epsilon$ is not the value at the critical point, but the mean at the critical isotherm, provided that the continuity of state is true.

It is the fact, however, that there occurs no appreciable difference between $\epsilon$ at the critical point and the mean of $\epsilon$ values in the critical region, e.g., from Habgood and Schneider's data of xenon at the critical point, $t_c=16.590$°C, $p_c=57.636$ atm., and $d_c=1.099$ g./cc., $\epsilon$ is evaluated to be 0.06932, whereas the mean of $\epsilon$ values out of 29 measurements in their observed density range of 0.91503 to 1.30705 g./cc. is 0.06941; also from their preliminary data[6], the mean of $\epsilon$ values out of 16 measurements in the density range of 0.9934 to 1.2463 g./cc., for the range of which a meniscus is expected to disappear, is 0.06932; again from Beattie, Douslin, and Levine's data[7] for neopentane, $C(CH_3)_4$, $\epsilon$ at the critical point, $t_c=160.60$°C, $p_c=31.57$ atm., and $V_c=303$ cc./mol., is 0.07411, whereas the mean of $\epsilon$ values out of 17 measurements in their observed volume range of 259.7 to 377.4 cc./mol. is 0.07495.

1) T.E. Mayer and S.F. Harrison, *J. Chem. Phys.*, **6**, 87, 101 (1938).
2) O.K. Rice, *J. Chem. Phys.*, **15**, 314 (1947).
3) B.H. Zimm, *J. Chem. Phys.*, **19**, 1019 (1951).
4) H. W. Habgood and W. G. Schneider, *Can. J. Chem.*, **32**, 98 (1954).
5) T. Ishikawa, This Bulletin, **26**, 78, 530 (1953); ibid., **27**, 226, 570 (1954); ibid., **28**, 89 (1955); T. Ishikawa and M. Ikeda, ibid., **26**, 516 (1953).
6) W.G. Schneider and H.W. Habgood, *J. Chem. Phys.*, **21**, 2080 (1953).
7) J. A. Beattie, D.R. Douslin and S. W. Levine, *J. Chem. Phys.*, **19**, 948 (1951).

In the present case, to evaluate $p$(atm.) against a given $V$(cc./mol.) from the new equation of state, we take $\varepsilon$'s at the respective critical points: for Xe, $2-\varepsilon=1.93068$, $b=V_c/3=39.82$cc./mol., $\log a=6.3923491$, and $T_c=16.590+273.16$°K; and for $C(CH_3)_4$, $2-\epsilon=1.92589$, $b=101.0$ cc./mol., $\log a=6.9392811$, and $T_c=160.60+273.16$°K, their results being illustrated (in full line) with the observed pressures (circles) in Fig. 1 and Fig. 2, in which are also shown, for the sake of comparison, the corresponding volumes of the maximum and the minimum.

With these consistent results for both cases, one is not able to deny the fact that the new equation has some intimate relationship with the actual state, but one can not elucidate any more, so long as $(2-\varepsilon)$ in the critical region is assumed to keep constant, so that, in the following case, we shall analyze the variation of $\varepsilon$ with respect to the volume.

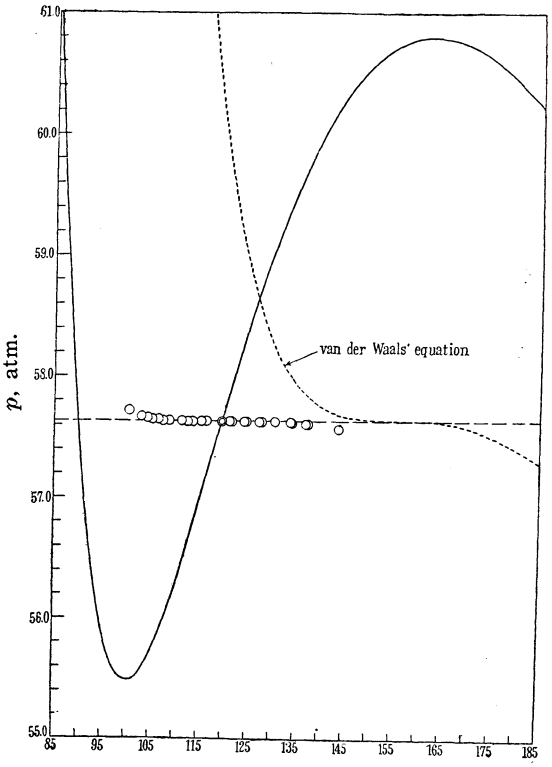



Fig. 1. $p$-$V$ Diagram of xenon at the critical temperature.

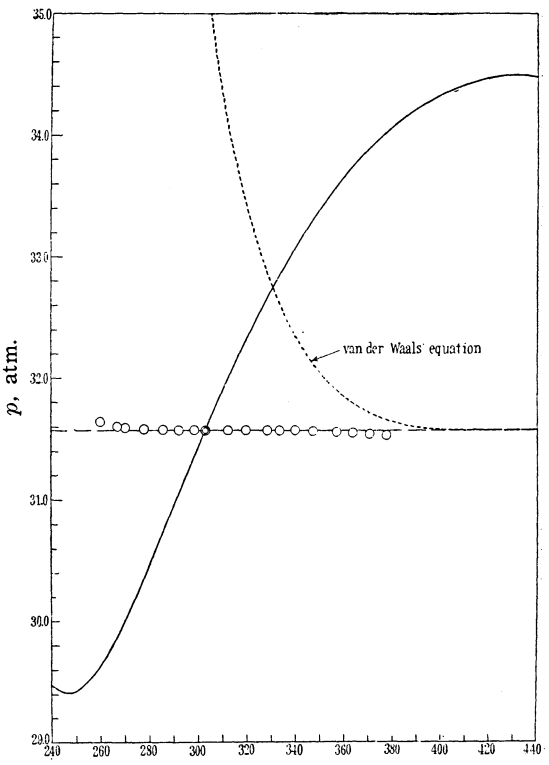
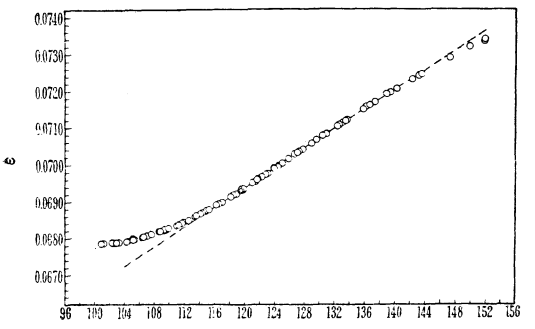



Fig. 2. $p$-$V$ Diagram of neopentane at the critical temperature.

curves from van der Waals' equation (in dotted line) by putting $b=RT_c/8p_c=51.57$ cc./mol., $\log a=6.6168073$ for Xe, and $b=140.93$ cc./mol., $\log a=7.2286712$ for $C(CH_3)_4$.

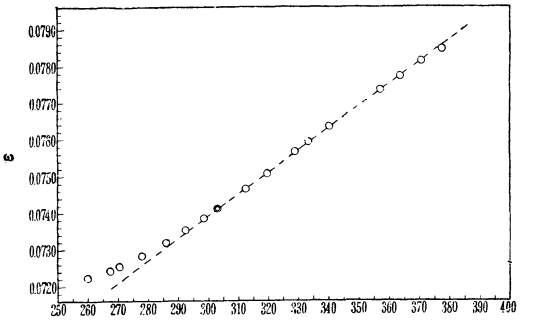
As seen from Figs. 1 and 2, it can be acknowledged (1) that the inflection point in the portion of $(\partial p/\partial V)_{T=T_c}>0$ nearly coincides with the actual critical point (double circle), (2) that the minimum point is situated near the least volume in the liquid-vapour critical region, (3) that the maximum point is situated at the critical volume corresponding to van der Waals' equation ($b=RT_c/8p_c$), and (4) that the liquid-vapour critical region is the horizontal line which passes through the inflection point and ends close to the

For each substance, isothermal $\varepsilon$ values at the critical temperature and at most 0.10° above and below the critical temperature have been computed from the measurements of the same workers cited above (see Tables I and II), and are diagrammatically shown in Figs. 3 and 4. As seen from Figs. 3 and 4, $\varepsilon$ values within these temperature ranges seem to converge upon the respective unique curves, which are quite similar with each other, and each curve appears to consist of three parts, the first part being concave up to the critical point (double circle), or more precisely speaking, at first horizontal, or probably a minimum which is situated at the corresponding volume of the minimum




$V$, cc./mol.

Fig. 3. $\varepsilon$-$V$ Diagram of xenon in the critical region.




$V$, cc./mol.

Fig. 4. $\varepsilon$-$V$ Diagram of neopentane in the critical region.

TABLE I

ISOTHERMAL $\varepsilon$ VALUES OF XENON IN THE CRITICAL REGION

| 16.550°C | | 16.585°C | | 16.590°C | | 16.590°C | |
|---|---|---|---|---|---|---|---|
| $V$ cc./mol. | $\varepsilon$ | $V$ cc./mol. | $\varepsilon$ | $V$ cc./mol. | $\varepsilon$ | $V$ cc./mol. | $\varepsilon$ |
| 102.27 | 0.06789 | 100.90 | 0.06787 | 100.46 | 0.06785 | 100.87 | 0.06786 |
| 104.33 | 0.06794 | 102.68 | 0.06789 | 104.30 | 0.06792 | 102.94 | 0.06787 |
| 106.44 | 0.06804 | 104.82 | 0.06793 | 106.48 | 0.06804 | 105.13 | 0.06797 |
| 108.62 | 0.06819 | 107.02 | 0.06807 | 108.74 | 0.06819 | 107.46 | 0.06811 |
| 110.94 | 0.06836 | 109.37 | 0.06825 | 111.16 | 0.06837 | 109.90 | 0.06828 |
| 113.36 | 0.06859 | 111.91 | 0.06847 | 113.50 | 0.06862 | 112.47 | 0.06849 |
| 115.87 | 0.06887 | 114.44 | 0.06872 | 116.18 | 0.06893 | 115.22 | 0.06879 |
| 118.49 | 0.06919 | 116.87 | 0.06900 | 118.83 | 0.06922 | 118.09 | 0.06914 |
| 121.13 | 0.06953 | 119.83 | 0.06937 | 121.61 | 0.06959 | 120.95 | 0.06950 |
| 123.94 | 0.06990 | 122.78 | 0.06973 | 124.40 | 0.06994 | 123.94 | 0.06989 |
| 126.75 | 0.07026 | 125.87 | 0.07014 | 127.33 | 0.07036 | 127.09 | 0.07032 |
| 129.65 | 0.07066 | 129.04 | 0.07056 | 130.30 | 0.07076 | 130.32 | 0.07076 |
| 132.66 | 0.07106 | 132.40 | 0.07102 | 133.58 | 0.07117 | 133.71 | 0.07120 |
| 135.80 | 0.07149 | 135.84 | 0.07148 | 136.64 | 0.07159 | 137.36 | 0.07168 |
| 138.95 | 0.07190 | 139.45 | 0.07194 | 143.49 | 0.07246 | | |
| | | 143.35 | 0.07244 | | | | |
| | | 147.20 | 0.07289 | | | | |

| 16.600°C | | 16.620°C | | 16.490°C | | 16.690°C | |
|---|---|---|---|---|---|---|---|
| $V$ cc./mol. | $\varepsilon$ | $V$ cc./mol. | $\varepsilon$ | $V$ cc./mol. | $\varepsilon$ | $V$ cc./mol. | $\varepsilon$ |
| 101.17 | 0.06787 | 103.27 | 0.06791 | 103.25 | 0.06790 | 103.25 | 0.06790 |
| 103.09 | 0.06789 | 105.32 | 0.06797 | 111.44 | 0.06844 | 111.44 | 0.06842 |
| 105.11 | 0.06798 | 107.43 | 0.06810 | 114.83 | 0.06877 | 114.83 | 0.06875 |
| 107.26 | 0.06808 | 109.61 | 0.06823 | 119.70 | 0.06937 | 119.70 | 0.06931 |
| 109.41 | 0.06824 | 111.97 | 0.06847 | 121.68 | 0.06961 | 121.68 | 0.06958 |
| 111.66 | 0.06842 | 114.39 | 0.06870 | 123.05 | 0.06979 | 123.05 | 0.06975 |
| 114.08 | 0.06867 | 116.90 | 0.06898 | 136.27 | 0.07156 | 136.27 | 0.07151 |
| 116.52 | 0.06895 | 119.53 | 0.06935 | 151.89 | 0.07336 | 151.89 | 0.07339 |
| 119.05 | 0.06926 | 122.21 | 0.06965 | 175.21 | 0.07563 | 175.21 | 0.07558 |
| 121.78 | 0.06960 | 125.04 | 0.07003 | | | | |
| 124.53 | 0.06996 | 127.86 | 0.07040 | | | | |
| 127.29 | 0.07034 | 130.69 | 0.07079 | | | | |
| 130.12 | 0.07071 | 133.63 | 0.07119 | | | | |
| 133.06 | 0.07112 | 136.82 | 0.07162 | | | | |
| 136.03 | 0.07151 | 140.25 | 0.07204 | | | | |
| 142.25 | 0.07230 | 143.21 | 0.07241 | | | | |
| | | 149.83 | 0.07320 | | | | |

TABLE II

ISOTHERMAL ε VALUES OF NEOPENTANE IN THE CRITICAL REGION

| $V$ cc./mol. | 160.50°C | 160.58°C | 160.60°C | 160.62°C | 160.70°C | mean |
|---|---|---|---|---|---|---|
| | | | ε | | | |
| 259.7 | 0.07224 | 0.07224 | 0.07224 | 0.07223 | 0.07223 | 0.07224 |
| 266.7 | 0.07243 | 0.07243 | 0.07242 | 0.07242 | 0.07241 | 0.07242 |
| 270.3 | 0.07255 | 0.07255 | 0.07255 | 0.07355 | 0.07253 | 0.07255 |
| 277.8 | 0.07283 | 0.07283 | 0.07283 | 0.07283 | 0.07282 | 0.07283 |
| 285.7 | 0.07320 | 0.07319 | 0.07319 | 0.07318 | 0.07317 | 0.07319 |
| 292.4 | 0.07353 | 0.07353 | 0.07352 | 0.07352 | 0.07351 | 0.07352 |
| 298.5 | 0.07386 | 0.07385 | 0.07384 | 0.07385 | 0.07383 | 0.07385 |
| 304.9 | 0.07423 | 0.07422 | 0.07422 | 0.07421 | 0.07419 | 0.07421 |
| 312.5 | 0.07467 | 0.07467 | 0.07466 | 0.07466 | 0.07465 | 0.07466 |
| 319.5 | 0.07509 | 0.07509 | 0.07508 | 0.07508 | 0.07504 | 0.07508 |
| 328.8 | 0.07566 | 0.07566 | 0.07565 | 0.07565 | 0.07562 | 0.07565 |
| 333.3 | 0.07594 | 0.07593 | 0.07593 | 0.07592 | 0.07590 | 0.07592 |
| 340.1 | 0.07639 | 0.07635 | 0.07633 | 0.07633 | 0.07631 | 0.07634 |
| 357.1 | 0.07735 | 0.07735 | 0.07733 | 0.07731 | 0.07730 | 0.07733 |
| 363.6 | 0.07773 | 0.07772 | 0.07771 | 0.07770 | 0.07767 | 0.07771 |
| 370.4 | 0.07814 | 0.07813 | 0.07812 | 0.07811 | 0.07808 | 0.07812 |
| 377.4 | 0.07850 | 0.07847 | 0.07846 | 0.07845 | 0.07844 | 0.07846 |

of $p$-$V$ curve, and finally a nearly straight line, the second part being undoubtedly a long straight line starting from the critical point, or in other words, at the critical point, the second, third, and higher derivatives of ε with respect to the volume appear to be zero, and the third part being convex up to the maximum corresponding to the volume at which the other form of van der Waals' equation ($b=V_c/3$) takes the critical pressure. The volume coincidences of the minimum with the minimum of $p$-$V$ curve, and of the maximum with the inflection point of this form of van der Waals' equation have been confirmed by making use of Beattie, Barriault, and Brierley's data[8] for Xe, and of Beattie, Douslin, and Levine's data[9] for $C(CH_3)_4$. On the whole, it is clear that in the critical region $(\partial\varepsilon/\partial V)_T$ is always positive.

According to the Le Chatelier principle of mobile equilibrium[10], if the volume occupied by the molecules is increased, the state will tend to occur in the direction of increased number of molecules, or, if molecular association[11] is taken into account, in the direction of diminishing the degree of molecular association which will result in pressure increase, whereas in the critical region where the pressure is, by experience constant over a finite volume range, the state will occur to increase the degree of molecular association, i.e., to increase ε which depends on molecular association, so as to annul, as far as possible, the effect of volume increase, and if so, so long as a differential shift of ε occurs to be proportional to a differential shift of $V$ in the same direction, the pressure will continue to be constant, or in other words, $(\partial^2\varepsilon/\partial V^2)_T=0$, $(\partial^3\varepsilon/\partial V^3)_T=0$, and so on at the critical point should be the necessary condition that the pressure in the critical region is constant over a finite volume range.

That the above condition is satisfied can clearly be acknowledged by comparing the observed constant pressure range in Fig. 1 or 2 with the straight line portion in Fig. 3 or 4 for each substance, and at the same time, the fact that there occurs no change of ε with respect to the volume just above and below the critical temperature in each case is a strong proof of the existence of a critical region, at least, within 0.10°C above the critical temperature.

The maximum point of ε which appears in the supersaturated vapour portion has been estimated to have the value of 14.4% increase for Xe, and the value of 17.5% increase for $C(CH_3)_4$ as referred to the respective critical values, each maximum corresponding to $V=341.62$ cc./mol. and $V=975.3$ cc./mol. respectively as computed from van der Waals' equation ($b=V_c/3$).

In conclusion, the author expresses his hearty thanks to Nagasaki American Cultural Center who has furnished him with American journals at his request.

*Sasebo Commercial Junior College, Sasebo, Nagasaki*

8) J.A. Beattie, R.J. Barriault and J.S. Brierley, *J. Chem. Phys.*, **19**, 1219 (1951).
9) J. A. Beattie, D. R. Douslin and S. W. Levine, *J. Chem. Phys.*, **20**, 1619 (1952).
10) H.L. Chatelier, *Compt. rend.*, **100**, 441 (1885).
11) refer to T. Ishikawa, This Bulletin, **27**, 570 (1954).

# *High Viscous Alginic Acid*

By Takeo TAKAHASHI and Koji KIMOTO

(Received March 4, 1955)

## Introduction

Algin industry is a chemical industry newly developed in postwar Japan, and is regarded as a promising export industry in which seaweed is used as its raw material.

Many problems; however, remain to be solved. Especially maintaining the high viscosity of alginate through manufacturing processes is of great importance since this is the property to be utilized in most practical applications. The purpose of the present research is, by studying some properties of pure alginic acid and its salts, to confirm what causes the high viscosity and thus to make a contribution to the algin industry.

Alginie acid is a highly polymerized mannuronic acid in which the aldehyde groups of *d*-mannuronic acid are linked in $\beta$-glucoside bindings. The characteristic of this compound is the fact that in that one carboxyl group on each unit of monomer is free to react.

Owing to the various characteristics of alginic salts, this substance has lately been most effectively put in practical uses extensively in many fields, as foodstuffs, industrial and medical uses, toilet articles, etc.

## Viscosity Measurement

A new viscosimeter of constant shearing force type (modified type of Ostwald's capillary viscosimeter) has been designed for a solution of alginate by Dr. Hajime Okada, and universally used in the algin industry of Japan. Experiments with various solutions revealed the fact that a viscosimeter of this type was suitable for measuring the viscosity of non-Newtonian fluid such as alginate. This apparatus is shown in Fig. 1. The liquid level head can be adjusted to obtain the desired shearing force, by moving up or down the capillary tube.

In this viscosimeter, the maximum shearing force is taken to be 27.6 dyne/cm. and in accordance with the length and diameter of capillary, the level head is determined as follows and the mark is graduated on the capillary tube

$$\text{Maximum shearing force} = 27.6 = PR/2L = H \cdot g \cdot R/2L = 980 \cdot H \cdot R/2L \quad (1)$$

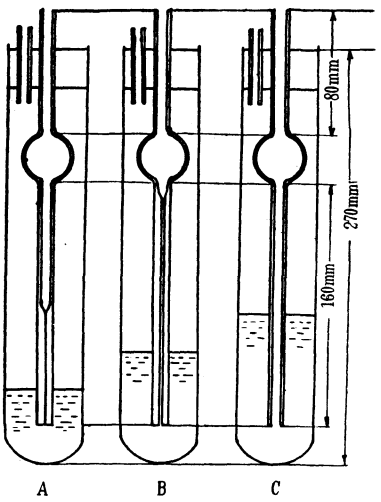



Fig. 1. A new viscosimeter of constant shearing force.
Each tube (A, B, C) should have a definite level head, which can be calculated from diameter and length of capillary.

$$H = 27.6 \times (2/980) \times L/R = 0.05633\, L/R \text{ cm.} \quad (2)$$

here, $P$=pressure
$H$=head of level
$R$=radius of capillary
$L$=length of capillary

Since the magnitude of viscosity of alginate solution changes from a few centipoises to poises, the viscosimeter tubes with different diameter of capillary are necessary. In such cases, each tube should have a definate level head, which can be calculated from diameter and length of capillary according to the above equation (2).

## Viscosity Characteristics

Sodium alginate is a typical heteropolar high-molecular electrolyte having the following viscosity characteristics:

(1) The viscosity of the aqueous solution of alginate becomes maximum at the vicinity of neutral point. According to E. Heen[1], the electric charge of colloidal particles becomes maximum, so that the polar adsorption, hydrating property and viscosity suc-

1) E. Heen, *Koll. Z.*, 83, 204 (1938).

cessively increase. This is the theory which explains the enormous viscosity due to "Elektroviskosen Effect".

Otherwise, H. Staudinger[2] estimated the phenomenon to be "Poly-ionische Viskositätserscheinung", i.e., by electrostatic action of high-valency colloidal ions, they agglomerate and viscosity increases.

(2) In the relation between reduced viscosity and concentration, the minimum point occurs at a certain diluted concentration. This phenomenon is not found on the homopolar high-molecular substance, so that it is due to the effect of ionized ions.

(3) If low-molecular electrolyte such as sodium carbonate or sodium chloride is added, the above minimum vanishes. This example is shown in Eig. 2. According to W. Kern[3],

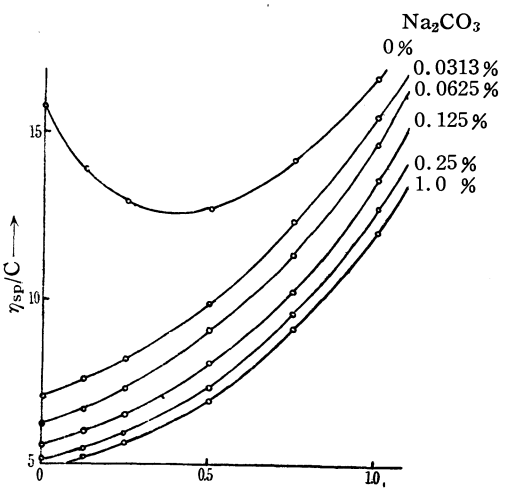



Fig. 2. Effect of addition of sodium carbonate on the relation between reduced viscosity and concentration.

reduced viscosity increases in the region of sol and gel, and then at the boundary becomes minimum. In the sol region "Ionaler Faktor" and in the gel region "Makromolekular Faktor" act powerfully.

Reduced viscosity = ("Ionaler Faktor") × ("Makromolekulaler Faktor")

In the existence of low-molecular electrolyte, the "Ionaler Faktor" approaches to one, so that "Makromolekulaler Faktor" controls all the region.

The critical viscosity (at the transition point between sol and gel) of the aqueous solution of sodium alginates of different origin was measured and found to be about 3.5 to 3.6 c.p. The fact verifies the Staudinger's theory that the critical viscosity has the same value in lower-molecular as well as in high-molecular compound, if the compounds belong to the same homologue,

When the sodium carbonate is added until its concentration attains to 0.031%, the aqueous solution of sodium alginate shows no more minimum point in reduced viscosity-concentration curve. The reason is that the electric charge of the alginate particle is discharged by sodium ion added and has no characteristics of heteropolar high-molecule.

## Viscosity and Temperature

Generally, according to Andrade[4], the viscosity of fluid has a relation against temperature as following equation:

$$\eta = Ae^{Q/RT} \quad (3)$$

here, $\eta$ = relative viscosity
$T$ = absolute temperature
$R$ = gas constant
$Q$ = activation energy
$\log \eta = \log A + Q/4.574T$

The viscosity measurement of an aqueous solution of sodium alginate at various temperature shows that the relation between the viscosity and temperature of such a non-Newtonian fluid may be expressed by Andrade's equation. The Fig. 3 shows the examples.

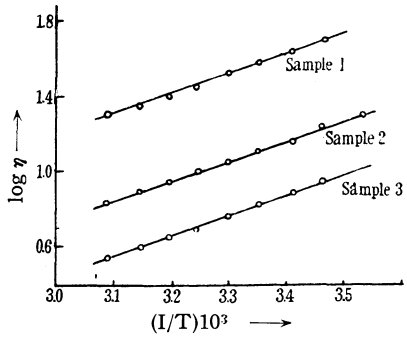



Fig. 3. Relation between $\log \eta$ and I/T. From inclination of staight line against abscissa, the activation energy can be calculated.

The activation energy ($Q$) for the fluidity of 1% solution of sodium alginate, when computed from the above equation, is approximately 5,000 cal. with some variations according to the concentration and viscosity of the solution.

## Viscosity and Concentration

Many equations had been proposed by Einstein, Mark and Fikentscher, Arrhenius[5],

2) H. Staudinger, *Ann.*, **502**, 201 (1938).
3) W. Kern, *Z. Phys. Chem.*, A, **153**, 391 (1931).
4) Andrade, *Nature*, **125**, 580 (1930).
5) Arrhenius, *Z. Phys, Chem.*, I, 285 (1887).

Baker, Philippoff and Hess, Bredee Bergenand Booys, etc.

When applied to sodium alginate solution, Arrhenius' equation (4) gives value appropriate only at a high concentration. Especially when the alginate solution does not contain low molecular electrolyte, the deviation from the Arrhenius' equation becomes conspicuous.

$$\log \eta = k \cdot c \qquad (4)$$

The Arrhenius' equation can not express the relation of viscosity and concentration (c) of the solution of heteropolar high-molecule such as sodium alginate, of which the viscosity is due to the ionic high molecule.

The Baker's equation[6],

$$\eta = (1+ac)^k \qquad (5)$$

gives values that agree fairly with observed ones. However, the Baker's equation is not satisfied at a high concentration, contrary to Arrhenius' equation.

From the point of view of the two regions of sol and gel, there is no identical equation applicable through high and low concentration.

According to the author[7], in the lyophile colloidal solution such as alginate or carrageen, of which the viscosity is due to hydration with water, the viscosity may behave against concentration such as the depression of surface tension versus concentration. According to Freundlich's equation, it is able to express as following:

$$\eta_{sp} = \eta - 1 = \alpha \cdot c^{1/n} \qquad (6)$$

$$\log \eta_{sp} = \log \alpha + (1/n) \cdot \log c \qquad (7)$$

Schematically the relation between viscosity and concentration has two equations of the same type, only the value of constant, being different, as shown in Fig. 4.

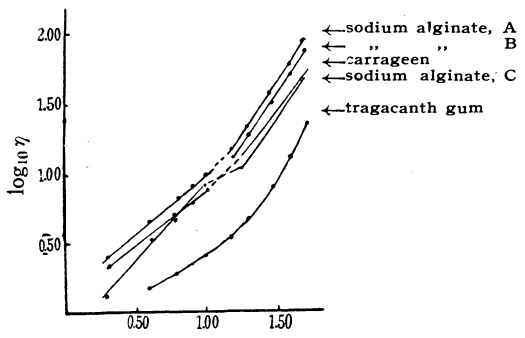



Fig. 4. Relation between viscosity and concentration has two equations of the same type, only differing the value of constants.

The critical concentration, which divides the equation into two, is about 0.15% and it coincides with the concentration, at which the hydration of alginate reaches maximum.

Recently Tetsuro Seiyama[8] proposed the following equation:

$$\eta = 1 + (a \cdot \phi \cdot c + A \cdot c^{1/2})/(100 - a \cdot c) \qquad (8)$$

In this equation, the viscosity is assumed to be a linear function of $c^{1/2}$ under the assumption that the ionic atmosphere of high-molecular electrolyte is like that of low molecular electrolyte.

## Colloidal State of Sodium Alginate in Aqueous Solution

In an aqueous solution of sodium alginate, the colloidal particle hydrates and swells. The Einstein's equation is derived dynamically from volume occupied by the solute particle, so that conversely, the specific volume of solute in solution can be computed theoretically from the equation.

According to Ichiro Sakurada[9], it follows by expansion of Baker's equation,

$$\eta = (1+ac)k = 1 + akc + [k(k-1)/2]a^2c^2 + \qquad (9)$$

In diluted concentration, it may be allowed to neglect the term $c^2$ and follows,

$$\lim_{c \to 0} \eta = 1 + akc \qquad (10)$$

also from Einstein's equation,

$$\lim_{c \to 0} \eta = 1 + 2.5\ (fc/100) \qquad (11)$$

so that it follows,

$$ak = (2.5/100) \cdot f, \text{ or } f = 40 \cdot a \cdot k \qquad (12)$$

By applying the equation (12) on alginate solution, the authors calculated the specific volume ($f$), which is shown in Fig. 5. The

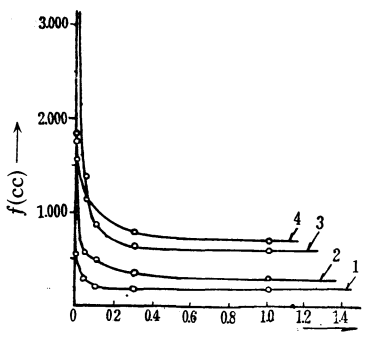



Fig. 5. Relation between specific volume and concentration of $Na_2CO_3$.

value of $f$ decreases radically until the concentration of sodium carbonate approaches

6) F. Baker, *J. Chem. Soc.*, **103**, 1653 (1913).
7) T. Takahashi, *Report of Imperial Industrial Research Laboratory*, **28**, No. 5 (1933).
8) T. Seiyama, *J. Ind. Chem. Japan*, **52**, 300 (1949).
9) I. Sakurada, *J. Ind. Chem. Japan*, **35**, 1103 (1932).

0.3% and then takes the constant value, differing with the polymerization degree.

Computing from the above value, we know that 1 g. of pure highly-polymerized sodium alginate can fix water of about 3,500 cc. in volume.

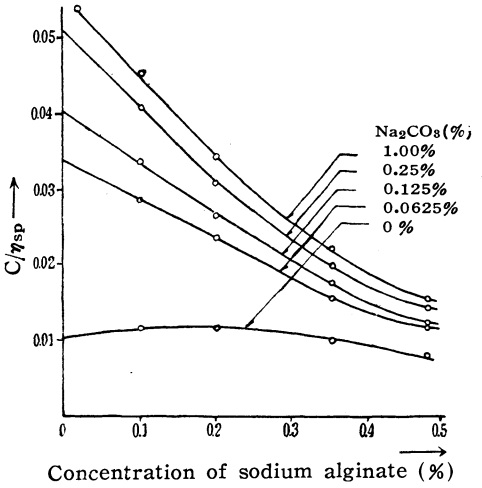
Fikentscher's equation[10],

$$\eta=1+a\cdot\phi\cdot c/(100-\phi\cdot c) \quad (13)$$

is transformed as follows:

$$c/\eta=100/a\phi-c/a \quad (14)$$

From the $c/\eta-c$ curve shown in Fig. 6, the values of $100/a\phi$ and $1/a$ can be calculated respectively.




Eig. 6. Relation between reciprocal of reduced viscosity and concentration.

As a result, the value of a takes 6.5 to 8 at 1% of sodium carbonate, even if the polymerization degree of alginate differs greatly. If the particle is a spherical and non-electric body, the value of a is 2.5, according to Einstein's equation. This result shows distinctly that the particle of alginate must be in a bar shape.

Kuhn's equation (15)[11] refers to a bar molecule.

$$\eta=1+[2.5+(1/16)(1/d)^2]\cdot\phi\cdot c/100 \quad (15)$$

here, $1$=length of a bar particle

$d$=longitudinal diameter in cross section of a bar particle

Placing

$$a=2.5+(1/16)\cdot(1/d)^2 \quad (16)$$

or $$1/d=4\sqrt{a-2.5}$$

and putting the above value of $a$ into equation (16), the value of $1/d$ of sodium alginate becomes 8 to 9. The colloidal particle of alginate, therefore, seems to change its shape into a spheroid with major axis about 8 to 9 times the minor axis, if electrolyte, for example sodium carbonate, is added by 1% to the solution.

10) H. Mark and H. Fikentscher, *Koll. Z.*, **49**, 135 (1929).

11) W. Kuhn, *Z. Phys. Chem., A*, **158**, 78 (1931).

## Electric Conductivity

The high molecular electrolyte is poly-valent as well as colloidal, and therefore its behaviour differs from the common electrolyte. The dissociation property can be studied by measuring either hydrogen ion concentration or electric conductivity, but on the high molecular electrolyte such as sodium alginate, the electric conductivity is the only method for investigation of dissociation.

On the purification of sodium alginate for measurement of conductivity, the method of coagulation by methanol is the most effective in removing the foreign minerals and other impurities. It takes at least three times of operation for purification to obtain alginate pure enough for electric conductivity measurement.

From the observed conductivity, the equivalent conductivity is computed according to the following formula:

Equivalent conductivity $=1{,}000\,k/c$

here, $k$=specific conductivity

$c$=equivalent concentration

The examples of experiments are shown in Fig. 7. Alkali metals and ammonium

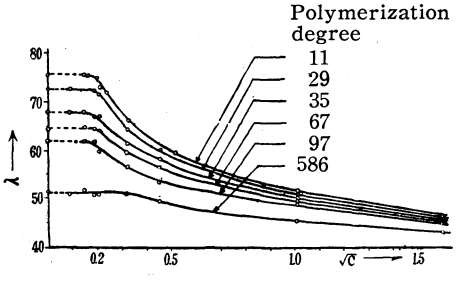



Fig. 7. Relation between equivalent conductivity and square root of concentration of sodium alginates having different polymerization degree.

salts of alginate in aqueous solution were found to show the typical characteristics of poly-valent colloidal electrolytes, i.e., the equivalent conductivity ($\lambda$) increases with the dilution of the solution, while, if furthermore diluted, it becomes constant or decreases.

The above phenomenon was already indicated as showing characteristics of high molecular electrolyte such as sodium alginate by Pauli and Sternbach[12] and Seiyama[13].

12) W. Pauli and Sternbach, *Koll. Z.*, **84**, 291 (1938).

13) T. Seiyama, *J. Ind. Chem. Japan*, **53**, 122 (1950).

According to the present authors[14] the equivalent conductivity decreases with increase of polymerization degree. If the equivalent conductivity takes a constant value at very much diluted solution, the ultimate equivalent conductivity ($\lambda_0$) may be extrapolated. When the $\lambda_0$ is plotted against a logarithm of polymerization ($n$), as shown in Fig. 8, the linear relation exists between

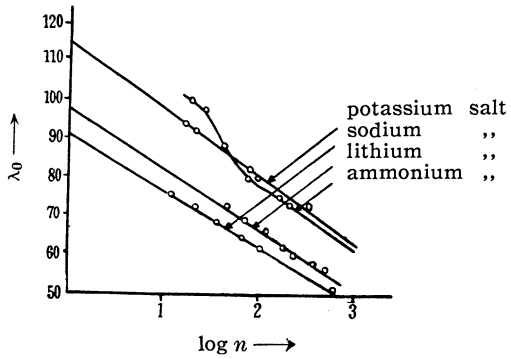



Fig. 8. Relation between equivalent conductivity at infinite dilution and logarithm of polymerization degree.

equivalent concuctivity and logarithm of polymerization degree.

$$\lambda_0^n = \lambda_0^1 - k \log n \qquad (17)$$

Here $\lambda_0^n$, $\lambda_0^1$ are equivalent conductivities at infinite dilution of alginate of polymerization degree $n$ and 1, and $k$ is the constant.

The above relation fits in case of alkali metals as well as magnesium and triethanolamine alginates.

## Dissociation of Alginate

The equivalent conductivity decreases as the polymerization degree increases. This fact is to be interpreted as a result of change of ionic activity in high molecular electrolyte. Generally, the high molecular electrolyte has numerous ionic valency, so that it dissociates step by step, and it is impossible to apply the mass action law to dissociation of high molecular electrolyte as in the case of low molecular electrolyte.

According to Pauli and Valko[15], the dissociation degree is defined as average dissociation degree, and it is varied by distance between ionic radicals, i.e., density of ionic radicals in yarn-like molecule.

Furthermore, the ionic activity has a great role in dissociation of high molecular electrolyte. The alginate particle is not in the shape of a straight bar, but may dissolve in form of "Knäuel". As the polymerization degree increases, the density of ionic radicals increases and ionic activity decreases. This relation is shown in Fig. 9.

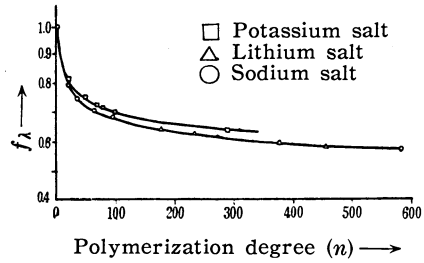



Fig. 9. Relation between coefficient of ionic activity ($f\lambda$) and polymerization degree.

The sodium ion may be restricted in inner structure of colloidal ion of alginic acid, and as the polymerization degree increases, the activity of sodium ion decreases.

The ionic activity of alkali alginates decreases with increases of $n$, and this relation may be represented by equation (18):

$$f_\lambda^n = f_\gamma^l - K \log n \qquad (18)$$

here $f_\lambda^n$ and $f_\lambda^l$ denote the coefficients of ionic activity when $n=n$ and $n=1$ respectively, and $K$ is a constant that depends on the concentration.

Furthermore, by measuring ashes in sodium alginate, the relation between the degree of ionization and $n$ of alginic acid was also proved to be represented by an equation similar to the above.

The alginic acid dissociates partially in the aqueous solution and its chain molecule forms a "Knäuel". In its central part, the ionic radical is suppressed to ionize under the influence of ionic charge on the surrounding part, and retains the form of its inactive state.

When alkali acts upon alginic acid, at first the neutralization occurs on free and active ionic radicals in the outer part of alginic acid. As the neutralization proceeds, the ionic radical which formed salt, dissociates completely and the molecule expands owing to repulsive action among the negatively charged ions. Thus, the molecule decreases its ionic density, and approaches to the complete dissociation.

The authors gratefully acknowledge the generous grant for scientific research from the Ministry of Education, Japan, which made this study possible. They also wish to express appreciation to the collaborators in their laboratory.

*Institute of Industrial Science, Tokyo University, Chiba*

14) T. Takahashi and K. Kimoto, *Rep. of the Institute of Industrial Science* (Tokyo Univ.), **1**, No. **4** (1951).

15) W. Pauli and Valko, *Elektrochemie der Kolloide*, 73 (1929).

# *Structure of Sulphamic Acid Molecule from a Three-dimensional Fourier Analysis*

By Kenji OSAKI, Hiroyuki TADOKORO and Isamu NITTA

(Received May 9, 1955)

## Introduction

Physical and chemical properties of sulphamic acid, or aminosulphonic acid $HSO_3NH_2$, stand in highly interesting contrast with those of sulphuric and other sulphonic acids. A crystal structure investigation of sulphamic acid has recently been undertaken by Brown, Cox and Llewellyn[1] who determined the dimensions of the unit cell as well as the space group but did not give any further detailed account of the structure. As it is of significance to know the molecular structure and arrangement in crystals of this substance, we have carried out the determination of atomic parameters by means of the three-dimensional Fourier syntheses. The present paper, of which an abstract was sent to the Stockholm Congress of the International Union of Crystallography in 1951, deals with some account of this investigation. After having sent our abstract we were informed of the paper by Kanda and King[2] of the determination of sulphamic acid and on later study of their paper we found that our results were in general agreement with theirs. However, as to the detailed structure of the molecule, there are some points of difference, which seem to be worth discussing here.

## Determination of the Structure

**Crystal Data.**—Sulphamic acid, $HSO_3NH_2$; molecular weight, 97.09; the dimensions of the unit cell, from a series of symmetrical back-reflexion photographs, $a=8.066\pm0.001$ Å, $b=8.115\pm0.001$ Å, $c=9.255\pm0.003$ Å (Cu $K\alpha_1$, $\lambda=1.5405$ Å);* density, calculated 2.129, observed 2.126 gm/cm$^3$ (in toluene at 25°C) 2.03 gm/cm$^3$ (in ether at 12°C) (Cupery)[3]; eight molecules per unit cell, space group $D_{2h}^{15}-Pcab$.

In view of the conflicting circumstances in the Patterson projections of this space group, we computed the three-dimensional Patterson function $P(u\,v\,w)$ near the origin besides its sections at $w=0$, $\frac{1}{2}$, $\frac{1}{4}$ and $\frac{3}{4}$. Comparison among these functions together with ordinary Patterson projections immediately led us to an unambiguous solution of the spatial arrangement of the molecules, of which the structure was preliminarily assumed to be a regular tetrahedron similar to the $SO_4$-ion. Parameters thus obtained were improved through the calculation of structure factors and Fourier projections on the principal planes. As the refinement seemed insufficient, we calculated electron densities about each

TABLE I

ATOMIC PARAMETERS

| | $x/a$ | $y/b$ | $z/c$ | $x$(in Å) | $y$(in Å) | $z$(in Å) |
|---|---|---|---|---|---|---|
| S | 0.0940 | 0.1668 | 0.1719 | 0.758 | 1.354 | 1.591 |
| | | | | (−0.003) | (−0.004) | (0.007) |
| $O_I$ | −0.0486 | 0.0601 | 0.1767 | −0.392 | 0.488 | 1.635 |
| | | | | (0.001) | (0.011) | (0.002) |
| $O_{II}$ | 0.0750 | 0.3057 | 0.0757 | 0.605 | 2.481 | 0.701 |
| | | | | (−0.002) | (0.015) | (0.015) |
| $O_{III}$ | 0.1758 | 0.2025 | 0.3055 | 1.418 | 1.643 | 2.827 |
| | | | | (−0.001) | (0.021) | (0.011) |
| N | 0.2377 | 0.0438 | 0.0790 | 1.917 | 0.355 | 0.731 |
| | | | | (−0.046) | (0.036) | (−0.024) |

Atomic parameters listed here are already corrected for finite series summation by the values in brackets.

1) C.J. Brown, E.G. Cox and F.J. Llewellyn, *J. Chem. Soc.*, **1940**, 1.

2) F.A. Kanda and A.J. King, *J. Am. Chem. Soc.*, **73**, 2315 (1951).

* Tne data of Kanda and King, if multiplied by the factor 1.0020, become $a=8.116$Å, $b=8.065$Å, $c=9.246$Å, *Pbca*, in good agreement with our values.

3) M.E. Cupery, *Ind. Eng. Chem.*, **30**, 627 (1938).

atomic centre using three-dimensional data. After two stages of refinement, $F_c$-corrections were introduced, the effect of which was considerable as given in brackets in Table I of the corrected parameters.

The nitrogen atom was first recognized in our case from the presence of single atom at a particularly larger distance~1.7 Å from the central sulphur atom, while the other three are at essentially same distance~1.4 Å. This choice was later verified by the electron density plot using the three-dimensional data; namely the peak corresponding to the nitrogen atom was found to be sensibly lower and broader than those for oxygen atoms (Fig. 1).

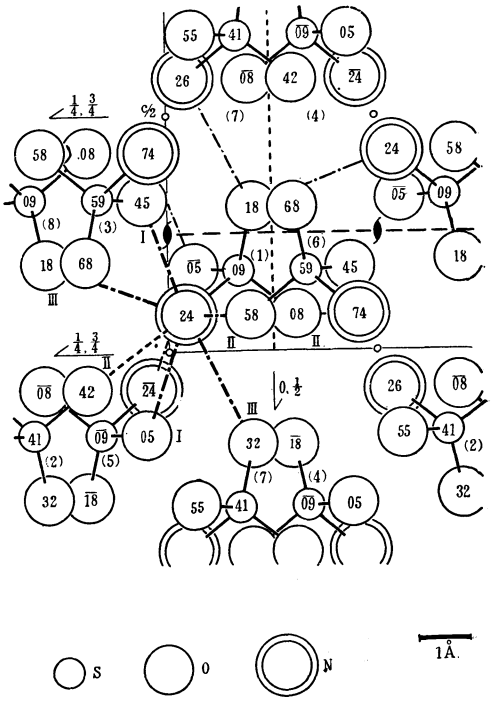



Fig. 2. Projection of part of unit cell upon (100). N-H·····O bonds only between molecule (1) and its neighbours are shown in chain lines, while dotted one show another close approach (2.84 Å) between O and N.

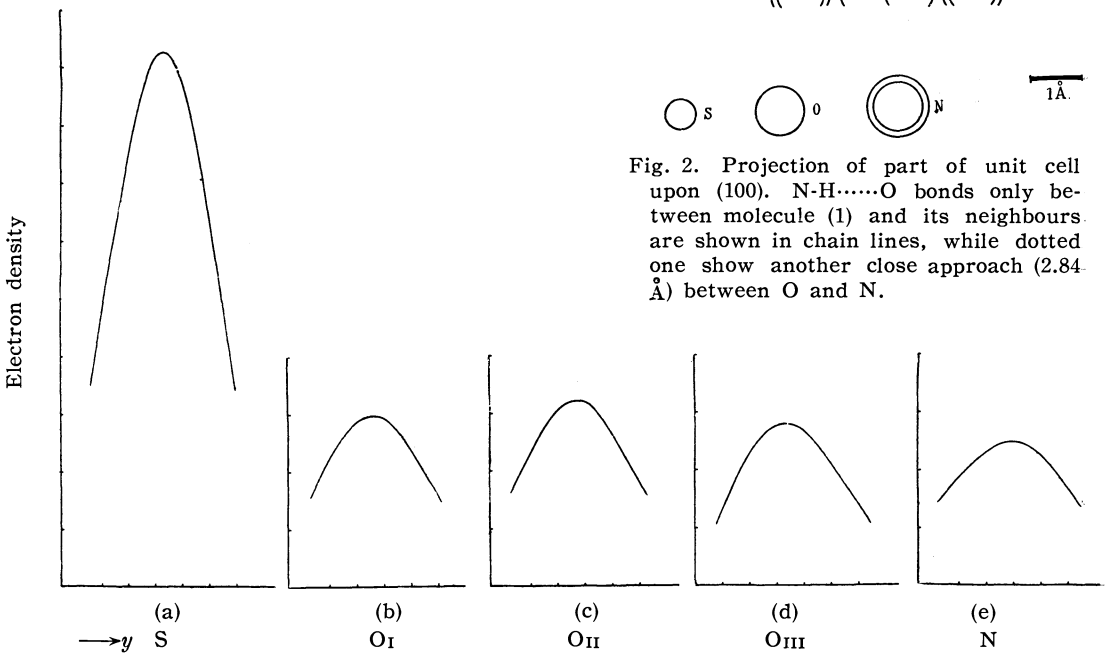



Fig. 1. Electron density plot along lines through atomic positions. Only curves along *b*-axis are shown.

## Description of the Structure

The one nitrogen and the three oxygen atoms in the molecule of sulphamic acid constitute a nearly regular tetrahedron, and such tetrahedra are linked three-dimensionally to each other through hydrogen bonds of the type N-H·····O as shown partially in Fig. 2. The nitrogen atom of the molecule (1) (see Fig. 2) is surrounded, besides the three oxygen atoms of the same molecule, by six oxygen atoms, each from one of the neighbouring molecules, five being at distances ranging from 2.93 to 3.01 Å and the sixth at a distance of 2.84 Å. In spite of such a short distance, the sixth atom does not seem to be concerned with the hydrogen bond formation subst antially, because it lies rather in the extended direction of the sulphur-nitrogen axis of the molecule. The arrangement of the oxygen atoms around the nitrogen is illustrated by Fig. 3, in which the atoms are projected upon the plane of three oxygen atoms of the molecule (1). The five N-O directions except the sixth all make angles ranging from 100° to 114° with the N-S axis and this would

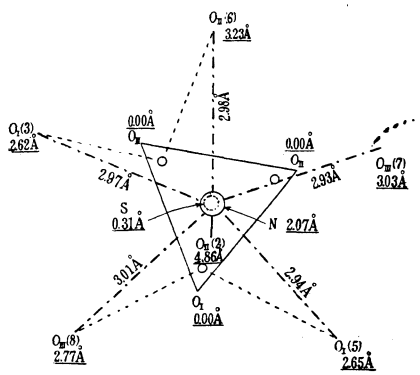



Fig. 3. Arrangement of the oxygen atoms surrounding a nitrogen atom of molecule (1), projected on the plane $O_I$ $O_{II}$ $O_{III}$. Underlined figures show the height of corresponding atoms measured from the plane of projection. Chain lines indicate the atom pairs linked by N-H·····O bonds.

suggest that all these N·····O pairs take part in the hydrogen bonding. A tentative location of three hydrogen atoms, which leads to one single and two bifurcated hydrogen bonds, are indicated in Fig. 3.* As for the non-hydrogen bonded nature of the sixth N·····O distance, it may be added that, in the case of potassium sulphamate crystal determined by Brown, Cox and Llewellyn[1] and by Jeffrey and Stadler[4] they have already found a short N·····O distance 3.04 Å, which they did not consider to be hydrogen bonded. Another instance is found in the case of orthorhombic hydrazonium sulphate[5], where a similarly disposed oxygen atom was not considered to be hydrogen bonded in spite of a shorter distance of 2.82 Å.

## Discussion of the Molecular Structure

Though further refinements of atomic coordinates have not been carried out, the values of standard deviations $\sigma$ listed in Table II seem to indicate already that we may discuss the molecular structure in some detail. The determined dimensions of the molecule are listed in Table III.

TABLE II
STANDARD DEVIATIONS

| | S | | O(average) | N |
|---|---|---|---|---|
| $\sigma(r)$ | 0.008Å | | 0.024Å | 0.028Å |
| | S-O | S-N | O-O | O-N |
| $\sigma$(distance) | 0.025Å | 0.029Å | 0.034Å | 0.037Å |

As to the shape of the $NO_3$ tetrahedron, the mutual deviations observed within the values of the three O-O's, or within those of the three O-N edges (see Table III) will be regarded as insignificant, whereas there is observed significant difference between the averaged values for the set of O-O and that for O-N. Thus we have in this crystal a somewhat elongated, but nearly regular tetrahedron.

The observed differences within three S-O distances are also insignificant and their mean value comes out 1.44 Å,* which deviates considerably from those given by Kanda and King[2], but agrees perfectly with the refined values obtained by Jeffrey and Stadler[4] in the case of potassium sulphamate.

TABLE III
BOND LENGTHS AND BOND ANGLES

| Substances | S-N | S-O | O-O | N-O | ∠NSO | ∠OSO |
|---|---|---|---|---|---|---|
| Sulphamic acid | | | | | | |
| present work | $1.75_5$ | 1.43 | 2.42 | 2.48 | 102° | 114° |
| | | 1.44 | 2.42 | 2.50 | 102° | 115° |
| | | 1.45 | 2.46 | 2.51 | 103° | 118° |
| Kanda & King[2] | 1.73 | 1.47 | 2.54 | 2.33 | 92° | 114° |
| | | 1.48 | 2.57 | 2.49 | 100° | 117° |
| | | 1.49 | 2.60 | 2.53 | 102° | 119° |
| $NH_4O_3S$-NO·NO | 1.791 | 1.464 | | | 102.2° | 114.2° |
| Jeffrey & Stadley[4] | | 1.434 | | | 102.2° | 114.2° |
| | | 1.434 | | | 105.7° | 116.0° |
| $KO_3S$·$NH_2$ | 1.60 | 1.42 | 2.38 | 2.45 | 107° | 111° |
| Jeffery & Stadler[4] | | 1.45 | 2.38 | 2.49 | 107° | 112° |
| | | 1.45 | 2.38 | 2.49 | 108° | 112° |
| β-isoprene sulphone Jeffery[6] | | 1.436 | 2.403 | | | 113.7° |
| $SO_2$ (microwave spectroscopy)[17] | | 1.433 | | | | |

* This location turned out to be similar to that obtained by Kanda and King.

4) G.A. Jeffrey and H.P. Stadler, *J. Chem. Soc.*, 1951, 1467.

5) I. Nitta, K. Sakurai and Y. Tomiie, *Acta Cryst.*, 4, 289 (1951).

6) G.A. Jeffrey, *Acta Cryst.*, 4, 58 (1951).

The mean value of the three bond angles O-S-O is 116° which is considerably greater than the tetrahedral angle.

Our determined value of the S-N bond length is $1.75_5$ Å in rather good agreement with that found by Kanda and King[2]. On the other hand Jeffrey and Stadler[4] have obtained a value 1.791 Å for the S-N distance in the dinitrososulphite ion and 1.60 Å for that in the sulphamate ion, of which the former was regarded by them to correspond very closely to the length of a pure single $\sigma$ bond and the latter to that associated with a double bond. They discussed the accordance of their value 1.79 Å for $N^+-S$ with that calculated from the well established values C-N=1.48 Å, C-S=1.81 Å and N-N=1.48 Å. A similar discussion to that of the case of dinitrososulphite ion will also be applied to the present case, although here the bond length is somewhat shorter and there are some differences in the distribution of valence forces around the nitrogen atom; for example, this is more or less tetrahedral and the configuration of three oxygen and three hydrogen atoms seems to be such as to form a trigonal prism, as shown in Fig. 3. As shown in Table III the observed N-S-O bond angles are nearly equal to each other and their mean value 102° is sensibly smaller than that 107° found by Jeffrey and Stadler[4] in the case of potassium sulphamate, of which the latter is more close to the tetrahedral angle 109.5°.

As to the bonding characteristics of the molecule as a whole, there are two extreme ideal structures conceivable; the one containing a hydroxyl and an amino group, $(H_2N)-SO_2-(OH)$, and the other of a zwitterion type, $(H_3N)^+-(SO_3)^-$. In the former case the lone pair of $2p$ electrons on the neutral amine nitrogen atom will be expected to possess a tendency to form a linkage of a partial double bond character with the central sulphur atom, as actually observed by Brown and Cox[1] and by Jeffrey and Stadler[4] in the case of sulphamate ion $(H_2NSO_3)^-$ in the potassium and ammonium salts. In the other case of zwitterion structure, on the contrary, the absence of such a lone pair of electrons will prevent double bond formation with the sulphur atom. The observed value $1.75_5$ Å of the S-N bond distance, which corresponds more closely to a single covalent $S-N^+$ bond, will thus be accounted for essentially by the zwitterion structure $(H_3N)^+-(SO_3)^-$. In this respect our conclusion is in agreement with that of Kanda and King[2]. The location of three hydrogen atoms around the ammonium nitrogen was not determined directly. However, assuming that they are arranged so that the bond angles S-N-H and H-N-H form approximately tetrahedral angles and that they are all linked by forming hydrogen bonds with adjacent oxygen atoms of the surrounding molecules, it is possible to assign probable positions for them which are shown in Fig. 3 as already mentioned. It may be added that such assignment makes one hydrogen atom $H_{II}$ lie on the line connecting the central nitrogen and an oxygen $O_{III}(7)$ and each of the other two, $H_I$ or $H_{III}$, on the plane of $NO_I(5)O_{III}(8)$ or $NO_I(3)O_{II}(6)$, thus the latter $H_I$ or $H_{III}$ forming bifurcated bonds. Moreover, such configuration of the hydrogen atoms may be an electrostatically stable one because each hydrogen atom comes very near to each of the three oxygen atoms in the molecule.* Turning to the part $SO_3$, it has already been remarked that the S-O bond length found is in the mean to be 1.44Å, which is consistent with the remarkably constant values reported for S-O bonds in various molecules, and a similar discussion on the nature of the bond to that given by Jeffrey and Stadler[4] will also apply to the present case. Only it will be of some interest to notice that this zwitterion type of sulphamic acid molecule may be regarded as an addition compound of pyramidal ammonia molecule $NH_3$ and planar sulphur trioxide $SO_3$, as in the cases of $NH_3$-$BF_3$ and the like which have been extensively studied by Hoard, Geller and others.[7-14] The flat shape of the $SO_3$ pyramid may suggest a considerable contribution of the $\pi$-bond

* The values given in the Abstracts of the Second International Congress (I.U.C., 1951) are those before the correction for finite series and refinement of lattice parameters.

* Quite recently (at a meeting of the Physical Society of Japan held in Nagoya in April, 1955) K. Sano of the Yamanashi University, Japan, reported his nuclear magnetic resonance absorption experiment of this crystal. In this connection it is remarked that the above-mentioned location of the three hydrogen atoms as forming a regular triangle is only a tentative one and the possibility of a deviation from such a regular arrangement is not excluded.

7) S. Geller and J.L. Hoard, *Acta. Cryst.*, **3**, 121 (1950).

8) J. L. Hoard, T. B. Owen, A. Buzzell and O. N. Salmon, *Acta Cryst.*, **3**, 130 (1950).

9) S. Geller and O.N. Salmon, *Acta Cryst.*, **4**, 379 (1951).

10) S. Geller, R. E. Hughes and J. L. Hoard, *Acta Cryst.*, **4**, 380 (1951).

11) S. Geller and M.E. Miberg, *Acta Cryst.*, **4**, 381 (1951).

12) J. L. Hoard, S. Geller and W. M. Cashin, *Acta Cryst.*, **4**, 396 (1951).

13) S. Geller and J.L. Hoard, *Acta Cryst.*, **4**, 399 (1951).

14) J. L. Hoard, S. Geller and T. B. Owen, *Acta Cryst.*, **4**, 405 (1951).

nature in the S-O linkage. Recently Pauling[15] gave an interesting discussion on the interatomic distances and bond character in the oxygen acids and related substances. He gave for the S-O distance in the flat molecule of $SO_3$ the calculated value of 1.44Å, which also suggest the view that the nature of the S-O bond in sulphamic acid molecule is not very different from that in $SO_3$ molecule.

In order to obtain some further information on the structure of the molecule, we have carried out a dielectric measurement of this crystal at various temperatures using the alternating field of the frequency of 3 Mc. The results are $\varepsilon_a=5.2$, $\varepsilon_b=5.2$ and $\varepsilon_c=5.0$ (at 12~15°C), which are sensibly constant at various temperatures. By combining these data, comparable with those of ordinary ionic crystals of NaCl type, with those of refractive indices $n_a=1.568$, $n_b=1.563$ and $n_c=1.553$ (at 25±3°C) for 5461 Å of this crystal given by Bryant,[16] it is obvious that the infrared polarisabilities are fairly large, by far larger than ordinary molecular crystals containing amino or hydroxyl group, standing thus not in contradiction to the view of the zwitterion structure of the molecule in the crystalline state.

15) L. Pauling, *J. Phys. Chem.*, **56**, 361 (1952).

16) W. M. D. Bryant, *J. Am. Chem. Soc.*, **61**, 2551 (1939).

17) B. P. Dailey, S. Golden and E. B. Wilson, Jr., *Phys. Rev.*, **72**, 871 (1947).

## Experimental Remarks

Crystals obtained from neutral aqueous solution were ground into thin rods of cylindrical shape as far as possible, the cross sections being 0.24×0.31 mm. for [100], 0.27×0.25 mm. for [010], 0.12×0.10 mm. for [001].

Oscillation photographs were taken using the multiple film technique with the Cu-$K$ radiations. Intensities were estimated by comparing with standard density scales. Atomic scattering factors for $S^{+6}$, $O^{-2}$, $N^{-2}$ were taken from the International Tables. The effect of outer electrons was found to be small when all (*hkl*) data were taken into account. Three-dimensional Fourier summations were carried out along lines parallel to the three principal axes using 120-section cosine tables, these lines passing in no case more than 0.10 Å apart from the peak obtained.

The authors express their gratitude to Dr. S. Uchida of Government Chemical Industrial Research Laboratory of Tokyo, who directed our attention to the importance of the X-ray investigation of this substance and gave us good crystals for this purpose, to Dr. R. Kiriyama for the measure ment of the dielectric constants of the crystal, and to Mr. Y. Sasada for his help in numerical computations. Grateful acknowledgment is made to the Ministry of Education for a grant.

*Department of Chemistry, Faculty of Science, Osaka University, Osaka*

# *The Michael Addition of Diethyl Malonate to Ethyl Crotonate-(carbonyl-$C^{14}$)*[1]

By Osamu SIMAMURA and Naoki INAMOTO

(Received May 24, 1955)

Michael and Ross have shown[2] that whereas diethyl methylmalonate adds to ethyl crotonate in the presence of one sixth equivalent of sodium ethoxide to yield diethyl $\alpha$-ethoxycarbonyl-$\alpha$, $\beta$-dimethylglutarate (normal product), the product is, with one equivalent of sodium ethoxide, diethyl $\alpha$-ethoxycarbonyl-$\beta$, $\gamma$-dimethylglutarate (abnormal product). In a previous work[3] it has been established by a tracer technique with radioactive carbon-14 that the abnormal product is formed by the migration of an ethoxycarbonyl group from the diethyl methylmalonate moiety to the $\alpha$-carbon atom of the crotonate in the course of the addition reaction. A mechanism of the formation of the normal or abnormal product according to experimental conditions has been put foward and the structural features which lead to the migration of the ethoxycarbonyl group have been discussed.

Work has now been extended to the Michael addition between diethyl malonate and ethyl crotonate-(carbonyl-$C^{14}$). In this case, the migration of an ethoxycarbonyl group from diethyl malonate should result in structurally the same product as the one formed without the migration. But, similarly to the case with diethyl methylmalonate described previously, the tracer method would reveal any migration which might take place.

Labelled ethyl crotonate (activity 8.6±0.6 $\mu$c/mol.) was refluxed with diethyl sodiomalonate in ether and the resulting diethyl $\alpha$-ethoxycarbonyl-$\beta$-methylglutarate was hydrolyzed with sodium hydroxide to the corresponding tricarboxylic acid (activity 8.4± 0.6 $\mu$c/mol.). The decarboxylation of this acid by heating at 165° gave carbon dioxide which was found to be only slightly active, and $\beta$-methylglutaric acid with an activity of 8.0±0.5 $\mu$c/mol. The sequence of the reactions carried out is shown below and the measured activities (with standard errors) of the products at each step are also given under the formulae.

If the migration of an ethoxycarbonyl group had taken place freely in the course of the Michael addition from an adding molecule of diethyl malonate to the carbon atom $\alpha$ to the labelled ethoxycarbonyl group of ethyl crotonate, the tricarboxylic acid

$$\underset{8.6\pm0.6\ \mu c/mol.}{CH_3CH{=}CHC^{14}OOC_2H_5}+CH_2(COOC_2H_5)_2 \xrightarrow{C_2H_5ONa} \underset{9.5\pm1.1\ \mu c/mol.}{CH_3CHCH_2C^{14}OOC_2H_5 \\ | \\ CH(COOC_2H_5)_2}$$

$$\longrightarrow \underset{8.4\pm0.6\ \mu c/mol.}{CH_3CHCH_2C^{14}OOH \\ | \\ CH(COOH)_2} \longrightarrow \underset{8.0\pm0.5\ \mu c/mol.}{CH_3CHCH_2C^{14}OOH \\ | \\ CH_2COOH} + \underset{0.12\pm0.08\ \mu c/mol.}{CO_2}$$

1) Presented at the Meeting of the Kanto Section of the Chemical Society of Japan, in Tokyo, Sept. 18, 1954.

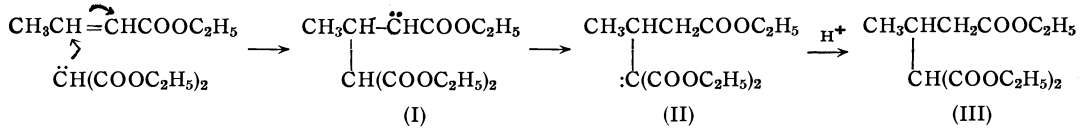
2) A. Michael and J. Ross, *J. Am. Chem. Soc.*, 52, 4598 (1930).

3) O. Simamura, N. Inamoto and T. Suehiro, This Bulletin, 27, 221 (1954).

Added in proof—D. Samuel and D. Ginsburg, *J. Chem. Soc.*, **1955**, 1288, have come to the same conclusion by the use of $O^{18}$ as tracer.

obtained by hydrolysis of the addition product would have included a labelled malonic acid grouping, and therefore the carbon dioxide evolved on decarboxylation would have contained half the amount of the radioactivity in the original ethyl crotonate. Most of the activity being actually found in β-methylglutaric acid, it was demonstrated that such a migration of the ethoxycarbonyl group occurred only to an extremely limited extent and the addition proceeded almost normally.

According to the theory set forth previously, the non-migration of the ethoxycarbonyl group in the present case is due to the presence of an acidic hydrogen atom on the carbon with two activating ethoxycarbonyl groups in an adduct anion (I) initially formed from diethyl sodiomalonate and ethyl crotonate. This hydrogen atom immediately migrates to the carbon atom carrying a lone pair of electrons, giving rise to an isomeric anion (II), which is more stable than structure (I) owing to the conjugation of the lone pair of electrons thus produced with two ethoxycarbonyl groups. In the process of working up of the reaction mixture, anion (II) picks up a proton from the aqueous medium to give the final product (III). The present result demonstrates that the migratory aptitude of a proton to an atom with a lone pair of electrons exceeds by far that of an ethoxycarbonyl group.




Added in Proof—After the submission of this article our attention has been drawn to the work of G. A. Swan, *J. Chem. Soc.*, 1955, 1039, who reported the results of similar experiments, which are in full accord with ours.

## Experimental

**Materials.**—Ethyl crotonate-(carbonyl-$C^{14}$) was prepared as reported previously[3]. Diethyl malonate was purified by fractional distillation under diminished pressure.

**The Michael Addition.**—Sodium (0.24 g.) was melted by heating in xylene and powdered by shaking, the xylene decanted, the sodium washed with ether, and 50 cc. of ether and 0.5 g. of absolute ethyl alcohol added to prepare sodium ethoxide. To this mixture 1.52 g. of diethyl malonate was added. Ethyl crotonate-(carbonyl-$C^{14}$) (1.09 g., 8.6±0.6 μc/mol.) in 30 cc. of ether was then added to the stirred mixture and the mixture was refluxed for five hours. Acetic acid (0.7 g.) in 14 cc. of water was added with stirring, the ethereal layer separated, dried with anhydrous sodium sulfate, the ether removed on a water bath and the residue subjected to distillation under diminished pressure, giving 0.9 g. of diethyl α-ethoxycarbonyl-β-methylglutarate boiling at 127~128° at 4 mmHg. This was heated with 0.6 g. of sodium hydroxide in a mixture of 6 cc. each of water and alcohol for three hours on a boiling water bath. The alcohol was removed from the reaction mixture and the residue diluted with water to 40 cc. and passed through a column of Amberlite IR 120. A fraction with pH 2.2 was collected and evaporated to dryness over concentrated sulfuric acid in a vacuum desiccator, giving 0.6 g. of crude acid. This acid was recrystallized four times from ether and benzene, yielding 0.4 g. of α-carboxy-β-methylglutaric acid, m.p. 138–139°C (Found: neutralization equivalent 63.4; activity 8.4±0.6 μc/mol.).

**Decarboxylation of α-Carboxy-β-methylglutaric Acid.**—The decarboxylation of the labelled α-carboxy-β-methylglutaric acid described above and the absorption of the evolved carbon dioxide by aqueous sodium hydroxide were carried out in an apparatus similar to that for the Van Slyke-Folch oxidation[4]. The labelled acid (173 mg.) was placed in one limb of the apparatus and aqueous sodium hydroxide in another. The apparatus was evacuated and the limb containing the acid was heated gradually to 165°C and kept at that temperature for one hour. When the reaction was completed, ammonium chloride was added to the sodium hydroxide solution, and barium carbonate was precipitated by barium chloride, collected on a filter paper and assayed for radioactivity (Found: 0.12±0.08 μc/mol.). The residue from the decarboxylation was recrystal-

4) M. Calvin et al., "Isotopic Carbon", John Wiley & Sons, Inc., New York, 1949, p. 93.

lized three times from benzene, giving 60 mg. of β-methylglutaric acid, m.p. 86–87°C (Found: activity 8.0±0.5 μc/mol.).

**Radioactivity Determinations.** — Radiocarbon assays were carried out by oxidizing samples according to Van Slyke and Folch[5], and converting the resulting carbon dioxide to barium carbonate, which was counted with an end-window Geiger-Müller counter on an "infinite thick" layer, the counts being all corrected for background and compared with the count of a standard barium carbonate with a known molar activity.

## Summary

The Michael addition of diethyl malonate to ethyl crotonate-(carbonyl-$C^{14}$) was carried out with one equivalent of sodium ethoxide. The addition product, diethyl α-ethoxycarbonyl-β-methylglutarate, was hydrolyzed to the corresponding acid. It was decarboxylated by heating to give β-methylglutaric acid, which was found to contain most of the radioactivity originally present in the ethyl crotonate. Thus, it was demonstrated that the migration of an ethoxycarbonyl group did not take place in contrast to the case with diethyl methylmalonate. The mechanism is discussed.

The authors are indebted to the Ministry of Education for a Grant-in-Aid for Scientific Research.

*Department of Chemistry,*
*Faculty of Science,*
*Tokyo University,*
*Tokyo*

5) D.D. Van Slyke and J. Folch, *J. Biol. Chem.*, **136**, 509 (1940).

# SHORT COMMUNICATIONS

## *Isotopic Exchange Reaction Between Heavy Oxygen and Carbon Dioxide on Silver Catalyst*

By Hisashi Mori, Kozo Hirota and Yasushi Kobayashi

(Received March 17, 1955)

As reduced silver can catalyze the oxidation reaction of carbon monoxide even at such a low temperature as 80°C[1], it is of interest to study the behavior of oxygen and carbon dioxide on this metal. It was attempted, therefore, to ascertain whether or not the catalytic isotopic exchange reaction:

$$OO^* + CO_2 \rightleftarrows COO^* + O_2$$

(O* denotes heavy oxygen)

was measurable by the static method, as done with platinum by use of slightly shifted oxygen[2]. The heavy oxygen was obtained by thermal diffusion column constructed in our laboratory by Mr. Y. Horibe[3] (total column length=15 m.).

The catalyst was prepared by the reduction of precipitated silver oxide at 120–240°C using the hydrogen gas, followed by repeated activation at 240°C. Throughout this research one and the same catalyst was used, but it was reduced again before each run. The original gas consisted of heavy oxygen (OO* being 2.12% of total $O_2$) and carbon dioxide in nearly equal molar amount. Its total pressure was 127–148 mmHg, the partial pressure of $O_2$ being less than the decomposition pressure[4] of $Ag_2O$ at 175–250°C. In the measurement of chemisorption of $O_2$ and $CO_2$, their initial pressure was taken to be 76–78 mmHg. As the volume of reaction tube was about 120 cc. (STP), the volume of oxygen in the original gas was about 7 cc. (STP), which was fairly little as compared with the catalyst quantity (74 g.). Such a proportion was adopted, so as to make the amount

Table I

| Run No. | React. temp. °C | React. time min. | $OO^{18}$ % | $COO^{18}$ % | $\frac{CO_2}{O_2}$ | Initial pres. mmHg | Adsorb. gas amount mmHg | Remark |
|---|---|---|---|---|---|---|---|---|
| 1 | 175 | 90 | $2.1_4$ | $1.0_4$ | 0.99 | 141 | 19 | b |
| | | 270 | $2.1_1$ | $1.1_1$ | | | 25 | |
| 2 | 188 | 20 | — | — | 0.97 | 142 | 17 | b |
| | | 60 | $2.0_4$ | $0.9_9$ | | | 22 | |
| | | 210 | $1.8_8$ | $1.1_0$ | | | 26 | |
| 3 | 200 | 15 | $2.0_7$ | $0.8_9$ | 1.08 | 127 | 15 | a |
| | | 90 | $2.0_3$ | $1.1_1$ | | | 21 | |
| | | 270 | $1.4_3$ | $1.1_8$ | | | 21 | |
| 4 | 200 | 15 | $1.5_4$ | $1.0_5$ | 1.28 | 130 | 0 | c |
| | | 60 | $1.5_7$ | $1.0_6$ | | | 0 | $CO_2$ after $O_2$ |
| | | 180 | $1.2_6$ | $1.1_4$ | | | 0 | |
| 5 | 200 | 15 | $2.0_7$ | $1.1_4$ | 1.15 | 133 | 21 | c, |
| | | 60 | $1.9_5$ | $1.2_0$ | | | 22 | $O_2$ after $CO_2$ |
| | | 180 | $1.5_3$ | $1.2_1$ | | | 22 | |
| 6 | 200 | 15 | $1.7_7$ | — | — | 78 | $16._5$ | c, $O_2$ only |
| | | 180 | $1.6_4$ | — | | | $16._5$ | |
| 7 | 200 | 180 | — | $0.4_1$ | — | 76 | 0 | c, $CO_2$ only |
| 8 | 220 | 60 | $1.8_0$ | $0.8_0$ | 1.03 | 137 | 16 | a |
| | | 180 | $1.0_2$ | $0.8_7$ | | | — | |
| 9 | 220 | 10 | $2.0_0$ | $1.0_1$ | 0.93 | 148 | 16 | b |
| | | 50 | $1.3_4$ | $1.0_9$ | | | 18 | |
| | | 180 | $1.2_0$ | $1.1_2$ | | | 18 | |
| 10 | 250 | 15 | $1.6_2$ | — | — | 76 | 6 | b, $O_2$ only |
| | | 210 | $1.4_0$ | — | | | 7 | |

of gaseous oxygen comparable to that chemisorbed.

Besides the continuous manometric reading, the progress of the reaction was investigated intermittently by mass-spectrometric analyses of the samples (about one cc. STP) taken out from the reaction tube at recorded times. Abundance ratios of $O^{18}/O^{16}$ in $O_2$ and $CO_2$ contained in them were determined by the same mass-spectrogram (Type of the mass-spectrometer: Hitachi-RMB-1). The ratio could be determined within the accuracy of $\pm 0.05\%$ for $O_2$ and $\pm 0.03\%$ for $CO_2$.

Summarized results are shown in Table I, where a, b, and c in the last column denote the reducing temperatures 220,250, and 300°C, respectively. In runs 1, 2, 3, and 5 there is this curious result that the increase of $O^{18}$ in $CO_2$ from its natural abundance, 0.40% as $COO^{18}$, is greater than the corresponding decrease of $O^{18}$ in $O_2$. This tendency becomes more marked as the reaction temperature decreases. It can be explained, however, if we assume that, following the rapid adsorption of $O_2$ and $CO_2$, the exchange reaction and desorption of $CO_2$ soon occur before the desorption of a considerable amount of oxygen takes place. This assumption is plausible, because the chemisorbed amount of oxygen cannot be neglected in reference to the initial gas volume.

Though the data are not yet reproducible, due to the gradual increase of catalytic activity, the following conclusion can be derived.

i) Even when the catalyst is reduced at 300°C for five hours, some chemical species containing oxygen atoms remain in the subsurface or bulkphase of the catalyst; see runs 10, 6, 7, and 8.

ii) The exchange reaction proceeds evidently at 175–220°C, though the desorption of $O_2$ is very slow at 175–188°C; thus the rate-determining step is the desorption of oxygen atoms; see runs 1, 2, 3, 4, 5, 7, 8 and 9.

Detailed studies are now going on.

1) A.F. Benton and R.P. Bell, *J. Am. Chem. Soc.*, **56**, 501 (1934). T. Titani et al., *J. Chem. Soc. Japan*, **55** 13, 224, 305 (1934). N. Yamada, This Bulletin, **27**, 36, (1954).

2) N. Morita and T. Titani, This Bulletin, **12**, 104 (1937); **13**, 357 (1938).

3) Y. Horibe and S. Nishizawa, *J. Chem. Soc. Japan*, **76**, 26 (1955).

4) E.g., A.F. Benton and L.C. Drake, *J. Am. Chem. Soc.*, **54**, 2186 (1932); **56**, 255 (1934).

*Chemical Department, Science Faculty,*
*Osaka University, Osaka*

# *Isotopic Composition of the Common Lead in Japan*

By Hitoshi Sakai, Masatake Honda and Eiichi Minami

(Received June 28, 1955)

Fourteen lead samples, mainly consisting of galenas, from the various parts of Japan are analyzed for their isotopic compositions of lead. Using a commercial mass-spectrometer, Model 21-103A of Consolidated Engineering Co., the samples are analyzed in the form of lead tetra-methyl as described by Collins et al.[1] and Dibeler and Mohler[2]. Of four main peak groups in the mass-spectrogram of lead tetra-methyl, the first group consisting of $Pb^+$ and $PbH^+$ is used for the isotopic analysis. Since $Pb^{204}$ peak is usually very small compared to those of other isotopes of lead, the superposition of $Hg^{204}$ peak to that of $Pb^{204}$ must be accurately corrected. For this purpose mercury dimethyl is synthesized from the same mercury as used in the pumping system of the instrument and the peak ratio of $Hg^{204}$ to $Hg^{202}$ is found to be $0.231\pm0.001$ for the same machine. This correction factor is used throughout the research.

The time variation of working conditions of the mass-spectrometer is checked by a standard sample and is proved to be negligibly small in the course of the experiment.

The results are summarized in Table I, and the maximum standard deviation is $\pm0.5\%$ of the values.

A standard sample, galena, from Broken Hill, New South Wales, is analyzed by the same method and the values 16.07, 15.41 and 35.87 are obtained for the ratios $Pb^{206}/Pb^{204}$, $Pb^{207}/Pb^{204}$ and $Pb^{208}/Pb^{204}$, respectively. They are in good agreement with Nier's data[3], 16.07, 15.40 and 35.5, respectively, for the corresponding ratio's obtained for a galena from the same district.

A number of lead ores of recent geologic ages from the various parts of the world has been analyzed by many researchers. For example, Tilton et al.[4] calculated the average composition of lead ores formed within the last 50 m.y. by least squares analysis of the data by Collins et al.[5]. They

TABLE I

ISOTOPIC COMPOSITION OF ORE LEAD IN JAPAN

| No. | Locality | Mineral | Isotopic Composition of Lead $\frac{Pb^{206}}{Pb^{204}}$ | $\frac{Pb^{207}}{Pb^{204}}$ | $\frac{Pb^{208}}{Pb^{204}}$ | Geologic Age |
|---|---|---|---|---|---|---|
| | | | (Atomic Ratio) | | | |
| 1 | Kamioka Mine, Gifu Prefecture | Galena | 18.20±0.05 | 15.55±0.05 | 38.71±0.15 | Cretaceous |
| 2 | Daira Mine, Akita Prefecture | Galena | 18.32±0.05 | 15.43±0.05 | 38.45±0.15 | Tertiary |
| 3 | Hanaoka Mine, Akita Prefecture | Galena | 18.55±0.05 | 15.57±0.05 | 38.61±0.15 | Tertiary |
| 4 | Arakawa Mine, Akita Prefecture | Galena | 18.44±0.05 | 15.57±0.05 | 38.74±0.15 | Tertiary |
| 5 | Hosokura Mine, Akita Prefecture | Galena | 18.59±0.05 | 15.59±0.05 | 38.73±0.15 | Tertiary |
| 6 | Tamagawa Hotsprings, Akita Prefecture | Hokutolite | 18.63±0.05 | 15.61±0.05 | 39.04±0.15 | — |
| 7 | Osaruzawa Mine, Akita Prefecture | Galena | 18.54±0.05 | 15.58±0.05 | 38.82±0.15 | Tertiary |
| 8 | Taishuu Mine, Nagasaki Prefecture | Galena | 18.47±0.05 | 15.59±0.05 | 39.02±0.15 | Cretaceous |
| 9 | Budō Mine, Niigata Prefecture | Galena | 18.42±0.05 | 15.50±0.05 | 38.60±0.15 | Tertiary |
| 10 | Mikawa Mine, Niigata Prefecture | Galeha | 18.58±0.05 | 15.66±0.05 | 39.00±0.15 | Tertiary Probably |
| 11 | Chichibu Mine, Saitama Prefecture | Galena | 18.71±0.05 | 15.83±0.05 | 39.20±0.15 | Tertiary |
| 12 | Ogoya Mine, Ishikawa Prefecture | Pyro-morphite | 18.82±0.05 | 15.67±0.05 | 39.32±0.15 | Tertiary |
| 13 | Sani-mura, Shioya, Ibaragi Prefecture | Galena | 18.36±0.05 | 15.53±0.05 | 38.59±0.15 | — |
| 14 | Tōya Mine Hokkaidō | Galena | 18.52±0.05 | 15.56±0.05 | 38.68±0.15 | Tertiary |
| | The average value of Galena sample: | | 18.48 | 15.59 | 38.76 | |

are 18.5, 15.6 and 38.4 for the ratios, $Pb^{206}/Pb^{204}$, $Pb^{207}/Pb^{204}$ and $Pb^{208}/Pb^{204}$, respectively, and in good agreement with the average value of the recent lead from Japan. From Table I, however, it is seen that "secondary" lead ores, Hokutolite and Pyromorphite, as well as some of the galena have comparatively high content of thorium lead, of which the geological meanings are not yet known.

The samples in this research are kindly presented by Prof. T. Watanabe and Assist. Prof. K. Imai of the University of Tokyo and Mr. Sugizaki of the University of Nagoya. Prof. S. Araki and his associates of the University of Tokyo have given us useful suggestions on the operation of the mass spectrometer. The authors wish to express their sincere thanks to them.

1) C. B. Collins, R. D. Russell and R.M. Farquhar, *Can. J. Phys.*, **31**, 402-418 (1953).
2) V.H. Dibeler and F.L. Mohler, *J. Res. Nat. Bur. Standards* V. **47**, 337-342 (1951).
3) A.O. Nier, *J. Am. Chem. Soc.*, **60**, 1571 (1938).
4) G.R. Tilton et al., *Bull. Am. Geal. Soc.*, in Press.
5) loc. cit.

*Department of Chemistry, Faculty of Science, Tokyo University*
*Tokyo*

## *Low-temperature Sublimation of Polonium Dithizonate*

By Kenjiro KIMURA and Hisao MABUCHI

(Received June 28, 1955)

The formation of polonium dithizonate was first reported in 1950 by T. Ishimori and H. Sakaguchi[1], and, independently, by G. Boussière and C. Ferradini[2]. In the course of study on polonium chemistry using polonium-210, the present authors observed the following phenomenon.

A thin layer of ultra-micro quantities of polonium dithizonate was prepared in a stainless steel dish by evaporating the solution of the compound in carbon tetrachloride. When the dish was heated on a hot plate, the $\alpha$-activity of the sample in the dish was rapidly diminished.

Since such a phenomenon has never been reported, it was explored in detail.

In order to know the cause of decrease in activity of the sample, a platinum plate was placed 3 cm. above the dish and heating of the sample was carried out in a closed system. The platinum plate was checked for its radioactivity with a Lauritsen electroscope. The presence of $\alpha$-activity of polonium-210 was detected and approximately 25% of the lost activity was found on the plate.

From this fact it is likely that the decrease in the activity is caused by the sublimation of polonium-210 in some chemical form, although further study is necessary to confirm whether or not this phenomenon is the sublimation in the strict sense.

The heating was carried out in a range of temperatures between 80°C and 200°C, and attempts were made to identify the sublimate by chemical procedures combined with the measurement of radioactivity.

The result of the experiment is summarized as follows:

(1) The sublimation occurs at temperatures above approximately 120°C under atmospheric pressure.

(2) When the sample is treated with hydrogen peroxide before heating, the $\alpha$-activity of the sample in the dish does not decrease even at temperatures above 120°C.

(3) The sublimate on the platinum plate is very soluble in carbon tetrachloride, but only slightly soluble in water. Moreover, it is remarkable that the partition of polonium $\alpha$-activity between carbon tetrachloride and water is dependent on the hydrogen ion concentration of the water layer. This is one of characteristic properties of metal chelate compounds.

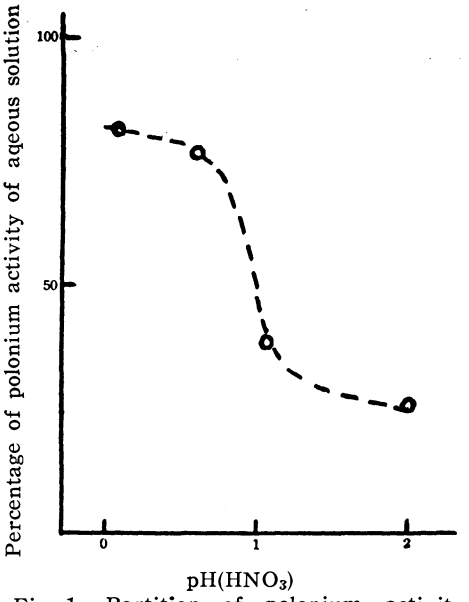



Fig. 1. Partition of polonium activity between carbon tetrachloride (2 cc.) and aqueous solution (20 cc.).

The figure shows the partition of polonium-210 between carbon tetrachloride and aqueous solution as a function of the pH of aqueous solution. In the study of the dithizone extraction of polonium the authors observed a similar change of the partition of polonium between carbon tetrachloride and aqueous solution.

From these results, the authors came to the conclusion that the sublimate is probably polonium dithizonate itself.

This phenomenon may be applied to the carrier-free separation as well as to the purification of polonium.

The detail of this study will be reported in a separate paper.

The authors would like to express their sincere thanks to Dr. Nobufusa Saito and Mr. Yuji Yokoyama for their valuable advice.

1) T. Ishimori and H. Sakaguchi; *J. Chem. Soc. Japan*, **71**, 327 (1950).
2) G. Boussière et C. Ferradini; *Anal. Chim. Acta*, **4**, 610 (1950).

*Department of Chemistry, Faculty of Science, Tokyo University, Tokyo*

## *Paramagnetic Resonance Absorption of Coals and Coal Extracts*

By Yasaburo YOKOZAWA, Isao MIYASITA, Masao KUGO and Keniti HIGASI

(Received June 29, 1955)

Distinct paramagnetic resonance absorption has been observed in British and French coals[1,2,3]. As the nature of Japanese coal is regarded to be particular in many respects as compared with European one, it was considered worth while to enquire whether or not Japanese coal shows this absorption.

The paramagnetic resonance absorption was measured for a British coal as well as for eighteen samples from Hokkaido mines by use of a micro-wave of 3.2 cm. wavelength[4], the dielectric properties of Hokkaido coals having been reported elsewhere[5,6].

Paramagnetic resonance absorption peak with high intensity and narrow width was detected in all the samples examined. The amplitude of Japanese coal was somewhat less than that of the British specimen (Compare the height of the peaks on the left side of the photographs).

By heating the coals at 270°, 330°, 380°, 430° and 460°C, the height of the line was increased gradually with the elevation of temperature. The extracts and residues of the coals by pyridine, as well as the coal specimens heated up to 460°C were also examined and all of them showed the paramagnetic absorption.

It would be premature to discuss whether or not this absorption is ascribed to 'free radicals' of broken bonds[1] or to some other paramagnetic compounds similar to violanthrone and violanthrene[4,7], but it appears certain from this experiment that the problematic substance embracing unpaired electrons is fairly stable against the attack of pyridine solvent.

The writers wish to thank Professor G. Takeya for his kind interest in the present work.

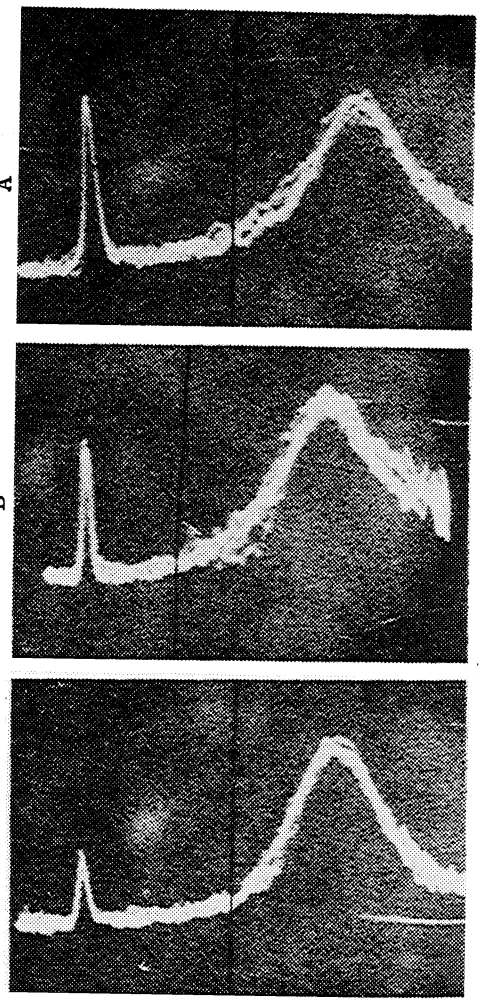



Fig. 1. Oscilloscope trace: absorption spectrum of coal and its pyridine extract. The hills seen on the right side are due to the absorption of cupric sulfate which was added as a standard.
A, British coal (Durham): fixed carbon 71.31, volatile matter 26.14, moisture 0.85, ash 1.70%.
B, Japanese coal (Yubari): fixed carbon 49.41, volatile matter 41.98, moisture 1.50, ash 7.11%.
C, Pyridine extract of B: C 84.50, H 6.48, O+N+S 7.73, ash 1.29%.

1) J.E. Bennett, D.J.E. Ingram and J.G. Tapley, *J. Chem. Phys.*, 23, 215 (1955).
2) J. Uebersfeld, A. Étienne and J. Combrisson, *Nature*, 174, 614 (1954).
3) A. Etienne and J. Uebersfeld, *J. Chim. Phys.*, 51, 328 (1954).
4) Y. Yokozawa and I. Tatsuzaki, *J. Chem. Phys.*, 22, 2087 (1954).
5) I. Miyasita, R. Miura and K. Higasi, This Bulletin, 28, 148 (1955).
6) I. Miyasita, *Bull. Res. Inst. Appl. Elec.*, 5, 123 (1953); 6, 117 (1954); 7, 17 (1955).
7) H. E. Blayden, J. Gibson and H. L. Riley, *J. Inst. Fuel*, Wartime Bulletin, 117 (1945).

*Research Institute of Applied Electricity and the Faculty of Engineering, Hokkaido University, Sapporo*

# *Determination of Nitrogen in Nitro and Oxime Compounds by the Iodic Acid Decomposition Method*

By Shigeru OHASHI

(Received May 11, 1955)

In the previous investigation[1] on the determination of nitrogen in organic compounds by the iodic acid decomposition method the author has found that for analyses of ammonium salts, amines, azo-compounds, pyrroles, thiazoles, etc., satisfactory results are obtained by means of this new method, but nitro and oxime compounds, etc. do not give good results.

The outline of this method is as follows. An organic compound containing nitrogen is decomposed by heating with a potassium iodate-strong phosphoric acid mixture in a special reaction vessel. By sending the liberated nitrogen with carbon dioxide into an azotometer, which is filled with potassium hydroxide solution, the nitrogen can be determined gas-volumetrically. The reason why the nitrogen in nitro and oxime compounds can not be directly estimated by this method may be due to the fact that the nitrogen in these compounds is already in an oxidized state and is liberated by the iodic acid decomposition, at least partially, merely as nitrogen monoxide, or dioxide, which is absorbed in potassium hydroxide solution in the azotometer.

The purpose of the present investigation is to extend this method to the determination of nitrogen in nitro and oxime compounds. It has previously been shown that the nitrogen in amine compounds can be easily determined by this method. Therefore, if the nitrogen of a nitro or oxime form could be reduced to an amine form by a somewhat simple treatment, it may be possible to determine the nitrogen in nitro or oxime compounds by the reduction and the subsequent iodic acid decomposition.

For this reason, the present study was mainly aimed at finding out the most suitable reducing agent against these compounds. From the results of the experiments described later, it was concluded that iron metal with diluted sulfuric acid is the best reducing agent for the present purpose.

In this paper the discussion of the reducing agents, the recommended procedure of this method, and the analytical results of several nitro and oxime compounds are described.

In the author's laboratory strong phosphoric acid has been used not only for the determination of nitrogen in organic compounds, but also for the determination[2] of the oxidation value of organic compounds and the determination[3] of elementary carbon such as active carbon and graphite. Since hitherto the property of strong phosphoric acid has not been stated in these papers, the specific gravity and the chemical composition of strong phosphoric acid used in these studies are also described complementally.

## Reducing Agents

The reducing agent used in this method must have the following properties: A nitro or oxime radical is quantitatively reduced by it to an amino radical; the reduction should be done at temperatures lower than 100°C, because many nitro and oxime compounds are easily volatilized at higher temperatures; and after the reduction the remaining reducing agent does not interfere with the subsequent decomposition procedure of the reduced product and the estimation of nitrogen.

Since the decomposition process is carried out in a strong phosphoric acid medium, it seems to be convenient for the reduction process also to be done in the same medium. Therefore, at first, zinc metal in strong phosphoric acid was used as a reducing agent. But, using this agent, the analyses for *p*-nitroacetanilide and *α*-dinitrophenol gave low results. Probably it may be due to the fact that zinc metal does not easily dissolve in strong phosphoric acid at a relatively low temperature.

Next, tin(II)-strong phosphoric acid was tested, because it was found in the anthor's laboratory that this agent can reduce sulfates[4] or various organic sulfurs[5] to hydrogen sulfide. But it was

1) S. Ohashi. This Bulletin, **28**, 177 (1955).

2) S. Ohashi, This Bulletin, **28**, 171 (1955).

3) T. Kiba, S. Ohashi, T. Takagi and Y. Hirose, *Japan Analyst*, **2**, 446 (1953).

4) T. Kiba, T. Takagi, and Y. Yoshimura, Presented at the Symposium of Analytical Chemistry at Kinki University, October 30, 1954.

5) S. Ohashi, I. Kishi, Presented at the same Symposium described above.

not favorable, as it produces, when heated, a certain gas, probably hydrogen, which can not be absorbed in potassium hydroxide solution in the azotometer.

Glucose was used by J. Noguchi[6] as a buffer agent in the micro-Dumas method for the analyses of nitro compounds. Accordingly as an example α-dinitrophenol was decomposed with iodic acid-strong phosphoric acid in the presence of glucose, but the test also failed, because too much iodine was liberated by the oxidation of glucose and the sample.

Hypophosphorous acid in strong phosphoric acid was not suitable for the present purpose, since it liberates, when heated, phosphine, which can not be absorbed in alkali solution in the azotometer.

In view of the above facts the reduction methods using strong phosphoric acid were given up. Then the reduction in diluted mineral acids was investigated.

Iron metal powder in hydrochloric acid was tested, since it has been commonly used to reduce nitro compounds. The results for picric acid gave values which were almost correct. But it was not favorable, because the liberated chlorine reacts with iodine and mercury in the azotometer to produce iodine chloride and mercuric chloride, which block the capillary of the azotometer.

Finally it was found that iron metal powder in diluted sulfuric acid does not possess the various defects described above and is the most suitable reducing agent.

## Apparatus and Reagents

The same apparatus described in the previous paper[7] was used. Only the reaction vessel is illustrated in Fig. 1.

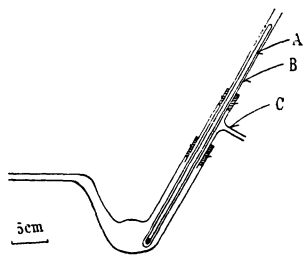



Fig. 1. Reaction vessel
A: Thermometer
B: Thermometer-protecting Tube
C: Gas-introducing Tube

The following reagents were the same ones that were used in the foregoing paper[8]; strong phosphoric acid, potassium iodate, carbon dioxide, and potassium hydroxide solution. Acetone, 6 N sulfuric acid, and iron metal powder were all of extra pure grade.

## Procedure

Weigh accurately a 10 to 30 mg. sample, depending upon its nitrogen content, into a small weighing tube; choose the sample weight so that the volume of the nitrogen formed will be 1 to 5 ml. Place the weighing tube containing the sample in the reaction vessel, add 1 to 1.5 ml. of acetone, and dissolve the sample in it. Next, add 50 to 60 mg. of iron metal powder and 1 ml. of 6 N sulfuric acid. Gently heat the mixture on a water bath. By this treatment the nitro or oxime compound is reduced to the corresponding amine compound and at the same time the excess of iron is dissolved in sulfuric acid. Continue heating on the water bath until all the acetone and the greater part of the water are expelled. At the end of this time the dissolution of the iron is almost always complete.

After cooling the contents of the vessel, add 3 to 5 ml. of strong phosphoric acid and two or three times as much of the theoretically required amount of potassium iodate in it.

Now insert a gas-introducing tube, a thermometer, and a thermometer-protecting tube into the reaction vessel, and connect the vessel with a carbon dioxide generator and a calcium carbonate-filled guard tube. After removing the air present in the reaction vessel, connect it to an azotometer.

Heat the mixture in the vessel on a small electric heater at 200°C to 250°C. After the complete decomposition of the sample, transfer the gas in the vessel into the azotometer and carbon dioxide is then allowed to be introduced. Read the volume of the nitrogen, the room temperature, and the atmospheric pressure at this time and calculate the percentage of the nitrogen by using these values.

## Results of Analyses and Discussion

Analyses of various known nitro and oxime compounds were carried out by this method. These results are summarized in Table I. As shown in Table I analyses for *p*-nitrophenol, α-dinitrophenol, picric acid, *p*-nitroacetanilide, sodium hexanitrodiphenylamine, *m*-nitro-*o*-anisidine, dimethylglyoxime, cyclohexanone oxime, and α-oxime of phenylpropionic acid gave satisfactory results. In the case of *p*-nitroacetanilide, sodium hexanitrodiphenylamine, and *m*-nitro-*o*-anisidine, the total nitrogen contents of both the nitro and amino radicals were determined.

The accuracy of the results obtained is within ±2%. The time required for an analysis is fifty minutes.

It is necessary for a rapid and complete reaction between a sample and a reducing agent that the sample be homogeneously dissolved in acetone.

If the quantity of sulfuric acid to be added is deficient, the reduction can not be carried out completely and if it is in too excess, after the reduction, strong phosphoric acid is so much diluted that the sample can not be decomposed perfectly.

6) J. Noguchi, Scientific Papers from the Osaka University, No. 22, February 1951.
7), 8) S. Ohashi, This Bulletin, 28, 177 (1955).

TABLE I

DETERMINATION OF NITROGEN IN VARIOUS NITRO AND OXIME COMPOUNDS

| Substance | Nitrogen Content % | Sample Weight mg. | Nitrogen Content Found % | Nitrogen Content Deviation % |
|---|---|---|---|---|
| *p*-Nitrophenol $C_6H_4(OH)NO_2$ | 10.01 | 13.1 | 9.99 | −0.02 |
| | | 13.7 | 9.98 | −0.03 |
| | | 11.1 | 10.09 | +0.08 |
| | | 14.5 | 10.07 | +0.06 |
| | | 10.8 | 10.02 | +0.01 |
| | | 10.9 | 10.11 | +0.10 |
| *a*-Dinitrophenol $C_6H_3(OH)(NO_2)_2$ | 15.19 | 14.9 | 15.30 | +0.11 |
| | | 13.3 | 15.33 | +0.14 |
| | | 12.9 | 15.15 | −0.04 |
| | | 11.1 | 15.23 | +0.04 |
| | | 11.5 | 15.20 | +0.01 |
| | | 13.9 | 15.20 | +0.01 |
| | | 13.0 | 15.14 | −0.05 |
| Picric acid $C_6H_2(OH)(NO_2)_3$ | 18.34 | 7.8 | 18.30 | −0.04 |
| | | 11.4 | 18.32 | −0.02 |
| | | 10.3 | 18.49 | +0.15 |
| | | 11.0 | 18.36 | +0.02 |
| | | 7.7 | 18.21 | −0.13 |
| | | 9.1 | 18.04 | −0.30 |
| *p*-Nitroacetanilide $C_6H_4(NO_2)NHCOCH_3$ | 15.55 | 13.3 | 15.55 | 0.00 |
| | | 15.7 | 15.58 | +0.03 |
| | | 14.6 | 15.63 | +0.08 |
| | | 15.0 | 15.69 | +0.14 |
| | | 14.3 | 15.69 | +0.14 |
| | | 13.9 | 15.74 | +0.19 |
| Sodium hexanitrodiphenylamine $NaN(C_6H_2(NO_2)_3)_2$ | 21.26 | 10.5 | 21.21 | −0.05 |
| | | 11.4 | 20.95 | −0.31 |
| | | 12.4 | 21.25 | −0.01 |
| | | 10.1 | 21.14 | −0.12 |
| | | 10.9 | 21.27 | +0.01 |
| | | 11.1 | 21.07 | −0.19 |
| *m*-Nitro-*o*-anisidine $C_6H_3(NO_2)(NH_2)(NH_2)OCH_3$ | 16.66 | 11.4 | 16.58 | −0.08 |
| | | 8.1 | 16.66 | 0.00 |
| | | 14.8 | 16.60 | −0.06 |
| | | 16.7 | 16.45 | −0.21 |
| | | 11.2 | 16.62 | −0.04 |
| Dimethylglyoxime $HON(CH_3)C\cdot C(CH_3)NOH$ | 24.13 | 12.6 | 24.16 | +0.03 |
| | | 12.1 | 24.20 | +0.07 |
| | | 23.3 | 24.08 | −0.05 |
| | | 16.7 | 24.22 | +0.09 |
| | | 16.4 | 24.04 | −0.09 |
| | | 20.4 | 24.14 | +0.01 |
| Cyclohexanone oxime $C_6H_{10}NOH$ | 12.38 | 24.7 | 12.37 | −0.01 |
| | | 28.0 | 12.27 | −0.11 |
| | | 24.6 | 12.33 | −0.05 |
| | | 26.5 | 12.36 | −0.02 |
| | | 24.3 | 12.40 | +0.02 |
| | | 24.0 | 12.40 | +0.02 |
| *a*-Oxime of phenylpropionic acid $C_6H_5CH_2C(NOH)COOH$ | 7.82 | 26.4 | 7.67 | −0.15 |
| | | 28.6 | 7.85 | +0.03 |
| | | 22.6 | 7.66 | −0.16 |
| | | 23.9 | 7.86 | +0.04 |
| | | 26.1 | 7.97 | +0.15 |
| | | 28.4 | 7.77 | −0.05 |
| | | 28.6 | 7.79 | −0.03 |

On many occasions excess iron metal powder is all dissolved in sulfuric acid by means of the above mentioned procedure. If it remains, the hydrogen formed by the reaction between iron and strong phosphoric acid may be transferred with nitrogen to the azotometer and gives a serious error. Therefore, in such a case, before the addition of potassium iodate the remaining iron powder should be dissolved by heating with strong phosphoric acid.

### Strong Phosphoric Acid

The strong phosphoric acid used in the experiments below was prepared from common 89% orthophosphoric acid by using an apparatus shown in Fig. 2. About 18 g. of the orthophosphoric

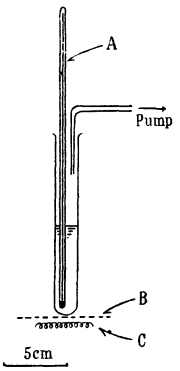



Fig. 2. Dehydration Apparatus
A: Thermometer
B: Wire Gauze
C: Electric Heater

acid was dehydrated by heating until the temperature of the liquid attained various points, ranging from 200° to 320°C at intervals of about 20°C.

The specific gravity of the strong phosphoric acid obtained in this manner at 15°C was estimated by means of a specific gravity bottle.

Since some phosphoric acid is expelled with water during the dehydration, a percentage of phosphorus pentoxide in the prepared strong phosphoric acid can not be calculated from the decrease of the total weight of the sample. As pyro- or triphosphoric acid is not completely converted into orthophosphoric acid even by heating with water for thirty minutes, it is undesirable to use a direct titrimetric method with a standard sodium hydroxide solution for the determination of the total phosphorus pentoxide. Therefore it was determined gravimetrically as magnesium pyrophosphate.

From the obtained percentage of phosphorus pentoxide and the diagram reported by R. N. Bell[9], which shows the relation between the content of phosphorus pentoxide and the chemical composition of strong phosphoric acid, the content of ortho-, pyro-, and triphosphoric acid in the sample can be estimated respectively.

All of the above-mentioned results are shown in Table II. According to R. N. Bell strong phosphoric acid is defined as phosphoric acid containing more than 72.4% phosphorus pentoxide, which corresponds to the phosphorus pentoxide content of 100% orthophosphoric acid. According to this definition, in Table II, only the acids having a specific gravity higher than 1.882 are the true strong phosphoric acid.

If the dehydration condition changes, a different strong phosphoric acid is formed, even though heated to the same temperature. For example, when 400 g. of 89% orthophosphoric acid is dehydrated until its temperature reaches 300°C, the resulting strong phosphoric acid has a specific gravity of 1.932, which is greater than that obtained in the above-mentioned experiments. This is probably due to the fact that, when the larger amount of the acid is used, the dehydration takes place more effectively than in the case of the smaller amount. The so-called "300°C strong phosphoric acid" used in the author's laboratory has a specific gravity of about 1.93.

### Summary

(1) The iodic acid decomposition method for the determination of nitrogen in organic compounds, which has been reported already by the author, was extended to analyses of nitro and oxime compounds.

9) R.N. Bell, *Ind. Eng. Chem.*, 40, 1464 (1948), L.F. Audrieah, "Inorganic Syntheses, Volume III", McGraw-Hill Book Company, Inc., New York, (1950), p. 89.

TABLE II

SPECIFIC GRAVITY AND CHEMICAL COMPOSITION OF VARIOUS STRONG PHOSPHORIC ACIDS

| Dehydration Temp. °C | Initial Weight g. | Final Weight g. | Remains Weight % | Specific Gravity at 15°C | $P_2O_5$ % | $H_3PO_4$ % | $H_4P_2O_7$ % | $H_5P_3O_{10}$ % |
|---|---|---|---|---|---|---|---|---|
| 202 | 17.574 | 16.570 | 94.28 | 1.805 | 69.23 | 95.6 | — | — |
| 218 | 17.684 | 16.276 | 92.04 | 1.833 | 70.52 | 97.4 | — | — |
| 241 | 17.657 | 15.971 | 90.46 | 1.865 | 72.21 | 95 | 1 | 4 |
| 259 | 17.910 | 15.969 | 89.18 | 1.882 | 72.97 | 90 | 5 | 5 |
| 281 | 17.974 | 15.767 | 87.72 | 1.909 | 74.15 | 82 | 12 | 6 |
| 300 | 17.315 | 15.022 | 86.78 | 1.925 | 74.63 | 76 | 18 | 6 |
| 320 | 17.873 | 15.274 | 85.51 | 1·948 | 75.75 | 65 | 28 | 7 |
| 300 | 400 | — | — | 1.932 | — | — | — | — |

(2) In a reaction vessel, a samplew as dissolved in acetone, reduced with a reducing agent to the corresponding amine, and then decomposed by heating with a mixture of iodic acid and strong phosphoric acid. The liberated nitrogen was determined by means of an azotometer.

(3) After testing many reducing agents it was concluded that a mixture of iron metal powder and diluted sulfuric acid was the best.

(4) For various nitro and oxime compounds satisfactory results were obtained by means of this modified method.

(5) The specific gravity and the chemical composition of strong phosphoric acid prepared in the various conditions have been described complementally.

The author wishes to thank Prof. T. Kiba for his encouragement and valuable advice during the course of this investigation, Prof. J. Noguchi and Prof. Y. Kurata for supplying some of the samples used in this study, and Mr. T. Takagi and Mr. Y. Sasaki for their helpful assistance. The cost of this research has been partly defrayed from the Scientific Research Grant from the Ministry of Education.

*Department of Chemistry,*
*Faculty of Science,*
*Kanazawa University,*
*Kanazawa*

# *Lower Members of Diethoxycyclopolysiloxanes from Diethoxydichlorosilane*

By Rokuro Ōkawara, Saburo Hotta and Toshiro Shimura

(Received May 14, 1955)

Many series of synthesized compounds of linear and cyclopolysiloxanes have been described in the literature[1]. Diorganocyclopolysiloxanes, $(RR'SiO)_n$ and organohydrocyclopolysiloxanes, $(RHSiO)_n$ have been prepared by the hydrolysis of the corresponding dichlorosilanes or dialkoxysilanes. In these cyclopolysiloxanes, cyclotrimer (n=3) was found to be the first member of the series. In the mineral silicates of natural source, skeletal structure of cyclotrisiloxane was also found[2]. Among the alkoxycyclopolysiloxanes which may be considered to be similar to the mineral silicates in their structure, only a seris of dibutoxycyclopolysiloxanes[3], $((C_4H_9O)_2SiO)_n$ (n=3, 4, .....) was studied. In a series of diethoxycyclopolysiloxanes, only cyclotetramer[4], $((C_2H_5O)_2SiO)_4$ was prepared and the other members of this series have not been reported. This paper will describe the preparation and properties of the lower members of diethoxycyclopolysiloxanes (n=3, 4 and 5).

Diethoxydichlorosilane reacts vigorously with water or water vapor instantaneously and the liberated hydrogen chloride causes the fission of ethoxy group from silicon and there remain silica and ethanol as the hydrolysis products. In the previous paper[5] the hydrolysis of triethoxychlorosilane, $(C_2H_5O)_3SiCl$ against the bound water of inorganic salts such as $NiCl_2\cdot 6H_2O$ and $CuCl_2\cdot 2H_2O$ was carried out to assure whether the selective hydrolysis of Si-Cl without the fission of ethoxy group could occur or not. The result obtained showed that the selective hydrolysis occurred in part but the accompanying fission of ethoxy group could not be prevented.

In this experiment, the reaction of diethoxydichlorosilane with sodium bicarbonate, which has the ability to convert Si-Cl to Si-O-Si and the acid accepting function in a molecule, was carried out in the hope of acquiring silanediol or siloxanes by the following reaction.

$$(C_2H_5O)_2SiCl_2+2NaHCO_3 = (C_2H_5O)_2Si(OH)_2+2NaCl+2CO_2.$$

But the result of this experiment showed that the product was mainly composed of tetraethoxysilane and a high boiling viscous liquid. This reveals that the fission of ethoxy group occurred in the course of the reaction. Then the hydrolysis was car ried out by us-

1) E. Rochow, "An Introduction to the Chemistry of the Silicones" John Wiley & Sons, New York, 1951.
2) W. L. Bragg, "Atomic Structure of Minerals" London, 1937.
3) R.K. Iler, *Ind. Eng. Chem.*, 39, 1384 (1947).
4) T. Takatani, *J. Chem. Soc. Japan, Pure Chem. Sec,*, 72, 765 (1951); 74, 890 (1953) (in Japanese).
5) R. Ōkawara, *J. Chem. Soc. Japan. Ind. Chem, Sec.*, 55, 678 (1952) (in Japanese).

ing pyridine as an acid acceptor and the lower members of diethoxycyclopolysiloxanes could be isolated. The conditions of hydrolysis are given in Table I.

At first, the hydrolysis was carried out at the constant temperatures of 0°C, 30°C, 50°C and 70°C, respectively. On fractionation, a small amount of the cyclotrimer was found to be formed accompanying the linear trimer in limited ranges of the hydrolysis temperature, e. g., at 30°C and 50°C, while the cyclotetramer was found to appear at each hydrolysis temperature except 70°C. At 70°C, only the linear polymers could be obtained owing to the increasing fission of the ethoxy group. As it seemed very difficult to separate the cyclotrimer from the linear trimer by fractionation, the hydrolysis conditions have been pursued which liberate each one of these compounds independently. It was found that when the hydrolysis was rapidly carried out by adding chlorosilane to the ice-cooled hydrolyzing medium with vigorous stirring, good yield of the cyclotrimer could be obtained without the formation of the linear trimer. From the residue of these hydrolyzates, the cyclopentamer was also obtained. Data of these cyclocompounds are given in Table III.

The cyclotrimer reserved in a sealed glass ampulla became viscous on prolonged standing. The changes of refractive index, density and molecular weight were determined after 200 and 300 days. Trimethylcyclotrisiloxane, $(CH_3HSiO)_3$[6] has been the only example of an unstable cyclotrimer. Now, hexaethoxycyclotrisiloxane seems to be another example of the unstable cyclotrimer.

## Experimental

**Starting Materials.**—Diethoxydichlorosilane used in our experiments was prepared by adding 2 moles of absolute ethanol to 1 mole of silicon tetrachloride with vigorous stirring. After the addition, the mixture was heated gradually to 80°C with stirring. Then the mixture, which was mainly composed of ethoxytrichlorosilane, diethoxydichlorosilane and triethoxychlorosilane was fractionated through a helices packed column of about 20 theoretical plates. The crude diethoxydichlorosilane having the boiling point 130°C to 140°C was rigorously fractionated through the same column and the middle portion of the constant boiling fraction (136°C) was taken as the starting material. Analysis for hydrolyzable chlorine by hydrolysis in water and titration of the liberated acid indicated that our sample was pure diethoxdichlorosilane.

Anal. Found: Cl, 37.2%. Calcd. for $(C_2H_5O)_2SiCl_2$: Cl, 37.5%.

6) S.D. Brewer, *J. Am. Chem. Soc.*, 70, 3962 (1948).

**Hydrolysis with Sodium Bicarbonate.**—Sodium bicarbonate (25 g., 0.3 mole) was added to the mixture of diethoxydichlorosilane (19 g., 0.1 mole) and 100 cc. of benzene. The violent reaction did not occur differently from the case of partially alkolyzed alkylchlorosilanes[7]. The mixture was heated to refluxing with stirring, but the fuming chlorine compound was stil found in the benzene layer after refluxing for two to three hours and it was not easy to make a trace of the fuming compound disappear with a short time.

From the similar three runs 18 g. of the chlorine free product was obtained. On fractionation, 8 g. of tetraethoxysilane and a small amount of hexaethoxydisiloxane were found. The residue was a high viscous liquid. This reaction was not further examined, for the formation of a large amount of tetraethoxysilane in the product reveals the fission of the ethoxy group during the course of reaction.

**Hydrolysis in Pyridine Solution.**—(a) *Hydrolysis and fractionation of the hydrolyzate.*—As described above, the hydrolysis of diethoxydichlorosilane with sodium bicarbonate failed to obtain the lower members of cyclocompounds; the hydrolysis in a wet pyridine was therefore carried out. After several experiments the most convenient method of hydrolysis was adopted.

In a 2 *l* three-necked flask equipped with an efficient stirrer, a reflux condenser and a dropping funnel, distilled pyridine which was dehydrated on the solid sodium hydroxide, a slight excess of water required to convert $(C_2H_5O)_2SiCl_2$ to $(C_2H_5O)_2SiO$ and benzene as a diluent were placed. To this hydrolyzing mixture, diethoxydichlorosilane was added with vigorous stirring. The amount of the reagents and the conditions of hydrolysis are given in Table I. After the addition of chlorosilane, the mixture was stirred until the odor of hydrogen chloride or chlorosilane had completely disappeared from the mixture. The product was filtered from pyridine hydrochloride and thoroughly washed with ca. 500 cc. of water over five times to separate the product from pyridine hydrochloride and dehydrated on a calcinated sodium sulfate. When the pyridine hydrochloride was present in the product, it caused the product to decompose in the course of fractionation at a high temperature. After benzene and a slight excess of pyridine were distilled off, the product amounted to Pg. as is shown in Table I. The oily product was simply distilled under 10 mmHg by using a Claisen flask. Tetraethoxysilane ($L_1$) distilled out, then the remaining oily product was further distilled under 1 mmHg and the distillate coming out below 200°C was collected. Since in these distillations, the stil-pot temperature was not over 300°C, it may be supposed that the thermal rearrangement of polysiloxanes[8] did not occur. The total amount of the distillate obtained under 10 and 1 mmHg (T) and the remaining residue ($R_1$) in weight percent of P. are also given in Table I.

7) R. Ōkawara et al., This Bulletin, 28, 360, 364 and 367 (1955).

8) W. Patnode and D.F. Wilcock, *J. Am. Chem. Soc.*, 68, 358 (1946).

The distillate under 1 mmHg was rigorously fractionated through a high efficient semi-micro Stedman column of about 60 theoretical plates and the refractive index and the silicon content of the distillate were determined throughout the distillation. The amount of the succeeding plateaus including the intermittent fractions cut on the distillation curve and the silicon content of these plateaus are given in Table II.

that of cyclotetramer ($C_4$). In Expt. 2 and 3, the trimer fraction may be seen to be composed of cyclotrimer ($C_3$) and linear trimer ($L_3$) and the following fraction may also be seen to be composed of $C_4$ and a small amount of linear tetramer ($L_4$). From its silicon content, the trimer fraction found in Expt. 4 was $L_3$ and the following plateau was that of $L_4$. The higher the reaction temperature, the larger the amount of the fractions

TABLE I

HYDROLYSIS OF DIETHOXYDICHLOROSILANE

In each experiment, diethoxydichlorosilane (150 g., 0.8 mole) was added to the mixture of pyridine (140 g., 1.8 moles), water (15 g., 0.83 mole) and the indicated amount of benzene.

| | | Hydrolysis | | | | Simple Distillation of P. | |
|---|---|---|---|---|---|---|---|
| Expt. No. | $C_6H_6$ | Temp. | Dropping Rate of Chlorosilane | Product (P.) | | ~200°C/1 mm. (T) | Residue ($R_1$) |
| | g. | °C | g./min. | g. | %Theory | %P. | %P. |
| 1 | 155 | 0 | 1.7 | 82 | 77 | 30 | 70 |
| 2 | 250 | 30 | 2.2 | 94 | 89 | 62 | 38 |
| 3 | 250 | 50 | 2.0 | 90 | 85 | 70 | 30 |
| 4 | 250 | 70 | 2.0 | 73 | 70 | 82 | 18 |
| 5 | 145 | 0–(—) | 6.0 | 90 | 85 | 55 | 45 |
| 6* | 250 | -5–(31)** | 12.0 | 90 | 85 | 46 | 54 |
| 7* | 250 | 0–(52) | 20.0 | 98 | 92 | 54 | 46 |
| 8 | 250 | 0–(54) | 37.5 | 89 | 84 | 43 | 57 |
| 9* | 250 | 0–(—) | 150.0 | 87 | 83 | 58 | 42 |

* Diethoxydichlorosilane was cooled to 0°C before hydrolysis.

** The value in parentheses indicates the highest temperature attained by the reaction.

TABLE II

COMPOSITION OF THE LOWER BOILING FRACTION

(T in Table I)

| | Fraction | | | | | | |
|---|---|---|---|---|---|---|---|
| Expt. No. | Monomer ($L_1$)* 60°C/10 mm. | Dimer ($L_2$) 73°C/1 mm. | Trimer ($C_3$, $L_3$) 105°–10°C/1 mm. | | Tetramer ($C_4$, $L_4$) 130°–45°C/1 mm. | | Residue ($R_2$) 145°C~/1 mm. |
| | %P. | %P. | %P. | %Si | %P. | %Si | %P. |
| 1 | 2 | 0.5 | 0 | — | 21 | 20.95 | 6 |
| 2 | 15 | 11 | 12 | 18.3–18.1 | 9 | 19.6–19.2 | 15 |
| 3 | 23 | 12 | 11 | 20.0–18.0 | 7 | 19.9–19.6 | 17 |
| 4 | 27 | 12 | 10 | 17.82 | 6 | 18.81 | 27 |
| 5 | 3 | 3 | 8 | 21.0–20.9 | 16 | 21.0–20.8 | 25 |
| 6 | 2 | 1 | 4 | — | 12 | 21.1–20.5 | 27 |
| 7 | 4 | 1 | 6 | 21.00 | 13 | 20.8–20.6 | 30 |
| 8 | 1 | 1 | 6 | 20.95 | 16 | 20.61 | 19 |
| 9 | 8 | 1 | 4 | 17.52 | 15 | 21.0–19.9 | 30 |

* $L_n$ and $C_n$ indicate the linear n-mer and cyclo-n-mer.
Anal. Calcd. for $L_1$, $L_2$, $L_3$, $L_4$ and $C_n$: Si, 13.48, 16.40, 17.67, 18.39 and 20,93% respectively.

(b) *Composition of the hydrolyzate.* (i) *Hydrolyzate obtained from the slow hydrolysis at a constant temperature* (Expt. 1–4).—In Expt. 1–4, hydrolysis was carried out at 0°C, 30°C, 50°C and 70°C by adding chlorosilane slowly (2 g./min.) to the hydrolyzing mixture. In Expt. 1, the trimer fraction was not found and the following plateau was

of monomer ($L_1$) and dimer ($L_2$) obtained and the more the contamination of the linear compounds in the trimer and tetramer fractions. It was supposed to be caused by the fission of ethoxy group with temperature. From the distillation curve of Expt. 3, the appearance of $C_3$ in front of the plateau of the trimer fraction was clearly

shown by its silicon content and a high refractive index at this portion as shown in Fig. 1.

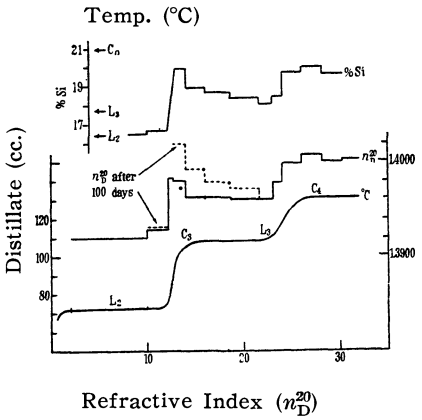



Fig. 1. Distillation curve of Expt. 3 under 1 mmHg.
$L_n$: Linear n-mer,
$C_n$: Cyclo-n-mer.

From Fig. 1, $C_3$ and $L_3$ may have a close boiling point and it was supposed to be difficult to separate these compounds by the distillation.

(ii) *Hydrolyzate obtained from the rapid hydrolysis* (Expt. 5–9).—From the results obtained in Expt. 1–4, the formation of $C_3$ was observed, only at the temperature range of 30°C to 50°C and the amount of $C_3$ was very small by the reaction at the constant temperature. $C_3$ was successfully obtained without formation of $L_3$ by the following rapid hydrolysis. The results are given in Table I from Expt. 5 to 9.

By adding the chlorosilane rapidly to the hydrolyzing mixture which was cooled by an ice-salt bath at 0°C, the temperature of the mixture rapidly rose by the reaction. The temperature was observed by the thermometer dipped in the mixture and the highest temperature attained is shown in parentheses in some experiments. After the temperature of the mixture fell down to the temperature of the bath in which ice still remained, stirring was further continued until the chlorosilane odor disappeared completely from the mixture.

In Expt. 5–8, a small amount of $L_1$ and $L_2$ was obtained. In the trimer fraction, $L_3$ was not found, while in the tetramer fraction, $C_4$ was supposed to be contaminated with a small amount of $L_4$ at the back part of the plateau. Too rapid addition of chlorosilane to the hydrolyzing mixture as in Expt. 9, may also causes the fission of ethoxy group owing to an instantaneous rise of the reaction temperature, and there was obtained a relatively large amount of $L_1$ and further only $L_3$ was found in the trimer fraction and the contamination of $L_4$ was observed in the tetramer fraction.

(c) *Characterizationof the Cyclopolysiloxanes.*—After redistillation, $C_3$ was reserved at the room temperature (10°C) and the measurement of its physical properties and analysis were carried out during a week. For the characterization of $C_4$, the tetramer fractions in Table II having the silicon content 19.6 to 21.1 were gathered and redistilled rigorously through the efficient column described above. To obtain the cyclocompounds higher than $C_4$, the residues ($R_2$) of Expt. 5–8 were fractionated as above. The gradually rising plateau (b.p. 148°–150°C/0.3 mmHg) with the distillate (12 cc.), having the silicon content of 20.18 to 20.85%, was obtained. From these data, $C_5$ may seem to be somewhat contaminated with the neighbouring linear compounds. Properties of these cyclopolysiloxanes are given in Table III.

**Stability of the Cyclotrimer.**—The cyclotrimer obtained above was sealed in a soft glass ampulla and the refractive index, density and molecular weight were measured after 200 and 300 days. The typical results obtained were as follows.

| After days | $n_D^{20}$ | $d_4^{20}$ | Mol. Wt. (in benzene) |
|---|---|---|---|
| — | 1.3981 | 1.0764 | 398 |
| 200 | 1.4032 | 1.1083 | ca. 1000 |
| 300 | 1.4052 | — | — |
| | (1.4070)* | | |

* Value obtained after the sample had been left open at room temperature for thirty minuites. This change may be caused by the escaping of some volatile matter formed by the decomposition of $C_8$, for the weight of the sample in a platinum crucible was reduced by about 3.1% of its weight after two hours.

TABLE III

DIETHOXYCYCLOPOLYSILOXANES

$C_n$: $((C_2H_5O)_2SiO)_n$

| Name | Boiling Point °C/mmHg | Refractive Index $n_D^{20}$ | Density $d_4^{20}$ | Molecular Weight Found* (Calcd.) | %Si Found (Calcd.) |
|---|---|---|---|---|---|
| Hexaethoxycyclotrisiloxane ($C_3$) | 106/0.7 | 1.3982 | 1.0764 | 400 (402.6) | 20.95 (20.93) |
| Octaethoxycyclotetrasiloxane** ($C_4$) | 125/0.3 | 1.4015 | 1.0971 | 534 (536.8) | 20.99 (20.93) |
| Decaethoxycyclopentasiloxane ($C_5$) | 150/0.3 | 1.4042 | 1.1039 | 660 (671.1) | 20.85 (20.93) |

* Cryoscopic measurements in benzene.

** T. Takatani, loc. cit., b.p. 138–40/1.5, $n_D^{20}$ 1.4001 and $d_4^{20}$ 1.0946.

As it was of interest to know the compounds which have been formed by the decomposition of $C_3$, the sample (10 g.) was carefully fractionated through a semi-micro Stedman column of about 30 theoretical plates after 350 days. About 3% of the volatile compound, 2% of $L_2$ (b.p. 78°C/1 mmHg) and 20% of the trimer fraction (b.p. 106°C/1 mmHg, $n_D^{20}$ 1.3966 and $d_4^{20}$ 1.0364. Anal. Found: Si, 18.19%) were obtained. From the silicon content, this trimer fraction was supposed to be composed of about 84% of $L_3$ (Reported: b.p. 107°C/0.8 mmHg[9], $n_D^{20}$ 1.3952[9] and $d_4^{20}$ 1.0301[10]) and 16% of unchanged $C_3$. The higher fraction could not be obtained until the stil-pot temperature reaches 235°C. The residue was a viscous liquid and the silicon content of it was found to be 22.00%.

With all the samples which were contaminated by $C_3$, the elevation of the refractive index was also observed. For example, it is shown in Fig. 1 in dotted lines. But the change was not observed by the other compounds within one year.

**Analysis of Silicon.**—Silicon was determined by decomposing the sample with concentrated sulfuric acid.

9) R. Ōkawara, T. Tanaka and K. Maruo, This Bulletin, **28**, 189 (1955).

10) T. Takatani, *J. Chem. Soc. Japan, Pure Chem. Sec.*, **73**, 409 (1952) (in Japanese).

## Summary

(1) Diethoxydichlorosilane did not easily react with sodium bicarbonate.

(2) Diethoxycyclopolysiloxanes beginning with cyclotrimer could be obtained from the hydrolysis of diethoxydichlorosilane by using pyridine as an acid acceptor.

(3) The lower members of diethoxycyclopolysiloxanes having three to five silicon atoms have been characterized.

(4) The cyclotrimer was found to be formed only in the limited conditions of hydrolysis and it was decomsosed spontaneously in a sealed soft glass ampulla.

The authors wish their hearty thanks to Dr. Watase for his encouragement during this work.

*Department of Applied Chemistry Faculty of Engineering, Osaka University, Osaka*

# *Dielectric Studies on Colloidal Solutions. I. High-frequency Conductivity of Aqueous Solutions of Paraffin-chain Salts*

By Michio SHIRAI and Bun-ichi TAMAMUSHI

(Received May 24, 1955)

It is a well-known fact that the equivalent electrical conductivity of aqueous solutions of the various types of paraffin-chain salts shows a sudden fall when the concentration is increased beyond a certain value corresponding to the micelle formation and then, after passing through a minimum point, it increases gradually with increasing concentration. This latter phenomenon was considered by McBain[1] to be due to the change in the dissociation state of the electrolyte contained in micelles. On the other hand, Hartley[2] pointed out that it should come out from the electrostatic interaction.

Some years ago, Schmid and Larsen[3] measured the electrical conductivity of aqueous solutions of some paraffin-chain salts at frequencies of 15 and 25 Mc./sec. by means of Deubner's method[4], and found that the high-frequency effect showed itself at the concentration corresponding to the sudden fall of the equivalent low frequency conductivity. Recently, the authors have investigated the high-frequency conductivities of sodium dodecyl sulphate, sodium oleate, and dodecyl amine hydrochloride at frequencies of 15 and 30 Mc./sec. by means of the resonance method over a wider range of concentration. Our experimental method and result may be useful for further discussion of the problem of micelle structures.

## Experimental

**Method of measurement.** — The method of measurement lies in the determination of the

1) J.W. McBain and M.D. Betz, *J. Am. Chem. Soc.*, **57**, 1905 (1935).
2) G.S. Hartley, ibid., **58**, 2347 (1936).
3) G. Schmid and E.C. Larsen, *Z. Elektrochem.*, **44**, 651 (1938).
4) A. Deubner, *Physik. Z.*, **30**, 946 (1929).

width of the resonance curve of a resonant circuit coupled to a high-frequency oscillator[5]. The stabilized oscillator supplies a high-frequency wave of constant amplitude and of fixed frequency to a resonator, to which is connected a valve voltmeter. The block diagram of the whole apparatus is indicated in Fig. 1.

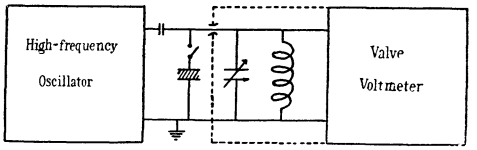



Fig. 1. Block-diagram of the apparatus.

The resonator consists of a parallel plate condenser containing the test liquid parallel to a variable condenser across an inductance. This variable condenser is an eccentric cylindrical one adjusted by a micrometer. The condenser containing the test liquid is immersed in a thermostatically controlled bath. Each part is screened in a metal box. The coupling of the resonator to the oscillator is so loose as to eliminate any pulling of the oscillator by the resonator. The high-frequency voltage of the resonator tuned to the oscillator is measured by the valve voltmeter. The circuit of the valve voltmeter is indicated in Fig. 2. The sensitivity of the galvanometer used is $2.8\times10^{-9}$ amp./mm., and its deflection must be proportional to the square of the input voltage. This can be done by adjusting the grid bias of the valve.

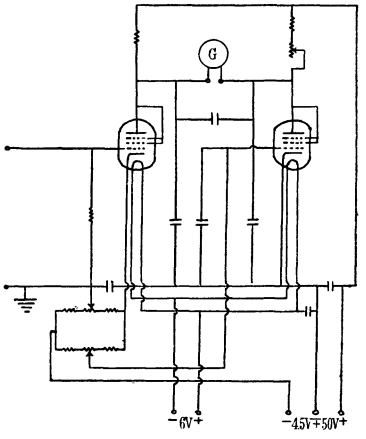



Fig. 2. Circuit of valve voltmeter.

Thus, the shape of the resonance curve for various test liquids placed in the parallel plate condenser is determined. The conductance of the resonator, $G$, is determined by the following formula[5]:

$$G=\frac{\omega(C-C_R)}{\sqrt{\left(\frac{V_R}{V}\right)^2-1}},$$

where, $\omega$ = frequency at which measurement is made.
$V_R$ = voltage at resonance.
$C_R$ = capacitance at resonance.
$V$ = voltage at any other point.
$C$ = capacitance at any other point.

In the manner stated above, the conductances of the resonator both with and without the test liquid in the parallel plate condenser can be determined, the difference of those being the conductance of the test liquid. In order to obtain specific conductivities from these conductances, we need a "cell constant". This can be determined by making use of the aqueous solution of potassium chloride as the standard. The whole operation is repeated for a series of concentrations at each frequency-setting of the oscillator. The probable error of the measurement of conductance at each frequency is $\pm0.2\%$.

**Materials.** — Sodium dodecyl sulphate was a "pure" sample prepared at Nezu Chemical Laboratory, Tokyo.

Oleic acid was purified from a commercial sample by vacuum distillation. Sodium oleate was prepared by neutralizing pure oleic acid with sodium hydroxide.

Dodecyl amine hydrochloride was obtained by neutralizing dedecyl amine which came from Armour and Co., U.S.A. with hydrochloric acid, which was then recrystallized.

The dissolution and dilution of these substances were made with distilled water free from carbon dioxide and thus solutions of various concentrations were obtained.

## Results and Discussion

In Tables I—III and in Figs. 3—5, the high-frequency effects of the three substances under investigation are indicated. Here the high-frequency effect is expressed by

$$H=100\frac{(\Lambda_h-\Lambda_l)}{\Lambda_l},$$

where $\Lambda_l$ is the low-frequency equivalent conductivity and $\Lambda_h$ is the high-frequency equivalent conductivity. $\Lambda_l$ was measured at 700 c./sec. In Figs. 3—5, the low-frequency equivalent conductivity is also shown for comparison.

TABLE I
SODIUM DODECYL SULPHATE
Temp. 25°C

| Concentration mol./l. | Equivalent conductivity 700c./sec. | High-frequency Effect 30Mc./sec. | 15Mc./sec. |
|---|---|---|---|
| 0.0025 | 79 | 0 | 0 |
| 0.005 | 76 | 0 | 0 |
| 0.008 | 71 | 0 | 0 |
| 0.01 | 60 | 1.1 | 0 |
| 0.015 | 46 | 2.4 | 0.8 |
| 0.025 | 37 | 2,5 | 0.3 |
| 0.05 | 29 | 2.0 | 0 |

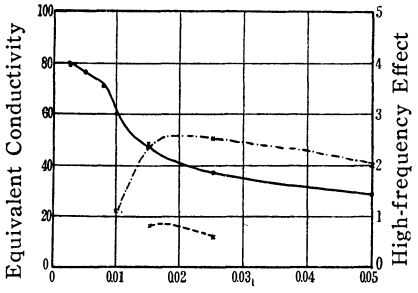
5) Report of the Sub-Committee of Japan Society for the Promotion of Scientific Research, *J. I. E. E. Japan*, 59, 519 (1939).

TABLE II
SODIUM OLEATE

| Concentration mol./l. | Equivalent conductivity 700c./sec. | High-frequency Effect (Temp. 25°C) 30 Mc./sec. | 15 Mc./sec. |
|---|---|---|---|
| 0.005 | 52 | 4.1 | 1.8 |
| 0.0075 | 42 | 5.0 | 2.0 |
| 0.01 | 39 | 4.5 | 1.7 |
| 0.015 | 37 | 3.2 | 1.3 |
| 0.02 | 34 | 2.5 | 1.1 |
| 0.025 | 33 | 2.2 | 1.0 |

TABLE III
DODECYL AMINE HYDROCHLORIDE

| Concentration mol./l. | Equivalent conductivity 700c./sec. | High-frequency Effect (Temp. 25°C) 15 Mc./sec. | 30 Mc./sec. |
|---|---|---|---|
| 0.0008 | 99 | 0 | 0 |
| 0.001 | 96 | 0.6 | 0.3 |
| 0.0015 | 85 | 2.0 | 1.5 |
| 0.0025 | 60 | 4.3 | 2.8 |
| 0.005 | 35 | 4.0 | 2.6 |
| 0.01 | 36 | 2.7 | 2.3 |
| 0.015 | 44 | 1.8 | 1.5 |




-·-·× 30 Mc./sec.
---× 15 Mc./sec. } high-frequency effect.
———· 700c./sec. equivalent conductivity.

Fig. 3. Sodium dodecyl sulphate.

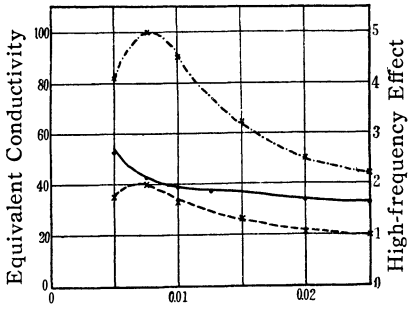



Fig. 4. Sodium oleate.

The Fig. 3 for sodium dodecyl sulphate shows that in the range of very low concentrations the high-frequency effect is very small. We were unable to confirm its existence. But with increasing concentration, the high-frequency effect becomes greater and arrives at its maximum at the concentration where the low frequency equivalent conductivity is decreasing. Then it shows a gradual decrease, but on account of the high conductance of the solution we could not make a measurement at very high concentrations.

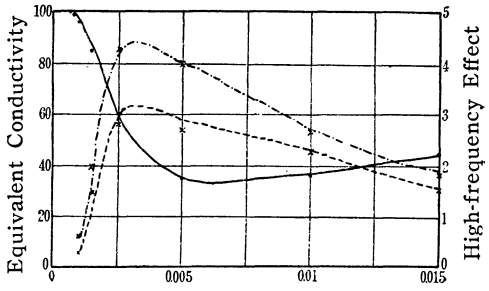



Fig. 5. Dodecyl amine hydrochloride.

The high-frequency effects of sodium oleate and sodium dodecyl amine hydrochloride show similar curves, as shown in Figs. 4 and 5.

The abnormally large values of the high-frequency effect of these solutions at the concentration corresponding to the micelle formation can be interpreted in terms of Debye-Falkenhagen's theory[6] of the dependence of the conductivity on frequency. Of course, the effect of the dielectric relaxation due to the orientation of molecules of the solvent and the solute must be considered, too. The critical frequency of the dielectric relaxation of the water molecule is about $1.5\times10^{4}$ Mc./sec., and that of the carboxyl group is about $3\times10^{3}$ Mc./sec.[7]. The critical frequencies of the sulphate group and the amino group have not been measured, but it is quite conceivable that they are nearly the same as that of the carboxyl group, considering that these polar groups have nearly the same dimensions. Thus, the critical frequencies of these groups are very high, and therefore the dielectric losses due to their orientation are negligible at frequencies of 15 and 30 Mc./sec., at which our measurement has been performed. Moreover, as molecules contained in a micelle may be rather in a liquid state of aggregation as is shown from the solvent properties of the micelle[8], the orientation of the micelle itself may not take place.

According to Debye-Falkenhagen's theory, the high-frequency effect incraeses with in-

6) P. Debye and H. Falkenhagen, *Physik. Z.*, **29**, 121, 401 (1928); *Z. Elektrochem.*, **34**, 562 (1928).
7) T.J. Buchanan. *J. Chem. Phys.*, **22**, 578 (1954).
8) cf. A.E. Alexander and P. Johnson, "Colloid Science", Oxford Press (1949), p. 685.

creasing valency of the electrolyte. Considering that ions in the solution under investigation join into a polyvalent ion on account of the formation of micelles, the high-frequency effect can be fairly great in the solutions under investigation, in spite of the loose structure of micelles. The critical fall of the low-frequency equivalent conductivity is probably due to this electrostatic interaction which comes into play with the formation of polyvalent micelle ions.

With further increasing concentration, the high-frequency effect shows a gradual decrease, as shown in Figs. 3—5. This decrease may be partly due to the shortening of the relaxation time of the ionic atmosphere with the increase of concentration, it being impossible to detect the effect at the frequency corresponding to the relaxation time at the applied frequency of 30 Mc./sec.. However, as shown in Fig. 5, there are cases where the low-frequency equivalent conductivity gradually increases with increasing concentration, and in order to account for the dependence of the low-frequency equivalent conductivity and that of the high-frequency effect on concentration consistently, we must conclude that the electrostatic interaction decreases as a whole with the concentration. Such reduction of the electrostatic interaction is presumably due to a loosening of counter ions due to the overlap of ionic atmospheres and consequently a change in the structure of micelles with increasing concentration.

## Summary

The high-frequency conductivity of solutions of sodium dodecyl sulphate, sodium oleate, and dodecyl amine hydrochloride was measured at frequencies of 15 and 30 Mc./sec.. The high-frequency effect remarkably appeared at the concentration corresponding to the critical micelle concentration and the effect can be interpreted in terms of Debye-Falkenhagen's theory of strong electrolytes.

The appearance of maximum and gradual decrease in high-frequency effect may be explained by the shortening of the relaxation time or by the reduction of the electrostatic interaction due to the change of micelle structures with the increase of concentration.

We are grateful to Nezu Chemical Laboratory, Tokyo and Armour & Co. U.S.A. for their kind supply of samples of detergents. A part of the expense for the experiment has been defrayed from a grant given by the Ministry of Education.

*Chemistry Department, College of General Education & Instiute of Science and Technology, The University of Tokyo, Tokyo*

# *Diffusion of Hydrocarbon, Alcohols and Esters through the Aqueous Solutions of Cationic Detergent*

By Haruhiko OKUYAMA

(Received May 12, 1955)

## Introduction

There have been many reports since the Graham-age about the diffusion of solute in colloidal solutions, for example through gelatine or agar solution. In these cases, it has been shown that the velocity of diffusion is only slightly affected in the presence of gelatine if the solute molecules or ions are small and non-reacting with them, but deeply influenced if there are interactions between the solute and the gelatine[1].

1) T. Graham, *Liebig Ann.*, **121**, 1 (1862); L. Friedman and E.O. Kraemer, *J. Am. Chem. Soc.*, **52**, 1295, 1305, 1311 (1930).

Investigations have been made in this paper, as to how the diffusion of a certain substance is influenced by the presence of a detergent. In general the detergent has an amphipathic structure, which is composed by hydrophilic and oleophilic part in the molecule. According to this amphipathic property, they associate in the aqueous solution and micelle formation occurs. The association occurs between not only detergent molecules themselves but also the other substances added to the solution, for instance, non-polar compounds such as hydrocarbon occupying the non-polar loci of micelles, viz. inside the micelles, resulting in swollen micelles. On

the other hand the polar compounds such as alcohol take a position which is essentially similar to the detergent molecules which make up the micelles.

It will be expected in this case that the kinetic unit is different according to the absence or presence of a detergent. In the latter case the diffusion is considerably delayed. Some results have been reported by Dean and Vinograd[2] in regard to the diffusion of solubilized dyes in Aerosol OT micelles, where diffusion was measured through sintered glass and cellophane membrane. However, this porous disc method has disadvantages in many respect and the solubilizate also has a complicated chemical structure in their experiments. In this paper the diffusion of some simple compounds in detergent solution has been investigated by the free boundary method which is much more free from theoretical objection.

## Experimental Methods and Samples

The diffusion coefficient was measured in 2.37% aqueous solution of trimethyldodecylammonium chloride (TMDA). This sample was the pure grade product of Nihon Yushi Co. To obtain the concentrated aqueous solution, TMDA was dialysed[3] by cellophane membrane to remove the low molecular substances or ions supposed to be contained in this sample. Some TMDA escaped through the membrane but the portion retained was pure enough for our present purpose. The solution inside the membrane was diluted to 2.37% by weight, of which relative viscosity was 1.352 and pH was about 5.4. The diffusing substances which were recrystallized or redistillated before use were of the highest market grade.

The diffusion coefficient was measured by the method of refractive index. The diffusion-cell was Neurath-type, made of Ni-Cr stainless steel 18-8 manufactured by Kobe Steel Factory, the thickness being 30 mm. The optical system was the diagonal Schlieren type, the same as described in other papers[4]. The cell was placed in a thermostat at 25.0°C More than ten diffusion patterns (concentration-gradient curves) were photographed at almost the same time intervals in each experiment. In the case of the most rapid diffusion the time interval was about three minutes while it was about an hour for the slowest one. The diffusion coefficient was calculated from the breadth between two inflection points in diffusion pattern whose ordinate could easily be found from the maximum height of the pattern[5].

2) R.B. Dean and J.R. Vinograd, *J. Phys. Chem.*, **46**, 1091 (1942).
3) J.T. Yang and J.F. Foster, *J. Phys. Chem.*, **57**, 628 (1953); B.S. Harrap and I.J. O'Donnell, *J. Phys. Chem.*, **58**, 1099 (1954).
4) N. Sata, H. Okuyama and K. Tyuzyo, *Kolloid-Z.*, **121**, 46 (1951); H. Okuyama and K. Tyuzyo, This Bulletin, 27, 259 (1954).
5) H. Neurath, *Chem Rex.*, **30**, 357 (1942).

## Results and Some Considerations

**(1) Experiments with completely soluble solute in water.** — In Table I, the diffusion coefficients of some solutes in water and in the TMDA solution are listed.

TABLE I
DIFFUSION COEFFICIENTS OF SOME SOLUBLE SUBSTANCES IN TMDA-SOLUTION AND IN WATER

| Substance | $C_1$ | $C_2$ | $D_S \times 10^7$ cm²/sec. | $D_W \times 10^7$ cm²/sec. |
|---|---|---|---|---|
| Urea | 2.0% | 1.0% | 137 | 135 |
| Fructose | 0.1% | 0,0% | 76.0 | 73.4 |
| Potassium Chloride | 0.1N | 0.0N | 202 | 192 |

$C_1$ and $C_2$ show the initial concentration of the solute in lower and upper solutions on the diffusion cell respectively. $D_s$ and $D_w$ indicate the diffusion coefficient of the solute in TMDA 2.37% solution and in water respectively.

The equation of Onsager and Fuoss[6]

$$D=\frac{RT}{f}\left(1+\frac{d\ln\gamma}{d\ln c}\right)$$

was derived from a general treatment of the diffusion problem which may be used to explain the above results. In this equation, $f$ is the frictional coefficient and $\gamma$, the activity coefficient, $c$ the concentration of the solute. The hydrodynamic factor, $f$ and the thermodynamic factor, $\frac{d\ln\gamma}{d\ln c}$ also may be increased by the presence of TMDA. It is thus seen that both factors approximately may cancel one another and roughly account for the fact that $D_s$ differ only slightly from $D_w$ as seen in Table I. Similar phenomena are reported[7] in which the diffusion coefficients of certain high-polymer solutions are not sensitively dependent on concentration, since hydrodynamic and thermodynamic factors both increased with the concentration of the high polymer. Potassium chloride affects the state of micelles greatly[8], however this has no relation to the present subject.

**(2) Experiments with nonpolar substance.** —The diffusion coefficient of hexane solubilized in TMDA solution is shown in Table II.

The diffusion coefficient is far less than that of Exp. 1. At the constant concentration gradient, $D_s$ becomes somewhat greater as the concentration of hexane decreases.

6) L. Onsager and R.M. Fuoss, *J. Phys. Chem.*, **36**, 2689 (1932).
7) C.O. Beckmann and J. L. Rosenberg, *Ann. N. Y. Acad. Sci.*, **46** (5), 329 (1945).
8) v.g. P. Debye and E.N. Anacker, *J. Phys. Chem.*, **53**, 1 (1949).

TABLE II

DIFFUSION COEFFICIENTS OF HEXANE SOLUBILIZED IN TMDA-SOLUTION

| $C_1$ | $C_2$ | $D_s \times 10^7$ cm²/sec. | $(D_1-D_2)\times 10^7$ cm²/sec. |
|---|---|---|---|
| 0.1%[9] | 0.6%[9] | 1.90 | 1.62 |
| 0.3 | 0.8 | 1.68 | 1.50 |
| 0.5 | 1.0 | 1.30 | 1.37 |
| 0.7 | 1.2 | 1.31 | 1.25 |
| 1.0 | 1.5 | 0.98 | 1.07 |
| 0.1 | 1.0 | 3.00 | 2.69 |
| 0.5 | 1.5 | 2.72 | 2.44 |
| 0.1 | 1.5 | 4.21 | 3.76 |

and $D_s$ considerably increases with increasing concentration gradient of hexane.

In these cases the kinetic units of diffusion must exclusively be micelles swollen by hexane molecules, because the hexane molecules exist only in solubilized micelles and the molecularly dispersed hexane is negligible. The homogenization of hexane-containing micelles must occur initially in such a manner that the more swollen micelles sink and the less swollen micelles rise. Then the observed diffusion coefficient in Table II may be considered as the difference of the diffusion coefficients of both micelles in water.

Assuming the micelle as spherical, the relation between the radius of the micelle and diffusion coefficent is shown by Einstein and Sutherland, as follows:

$$D=\frac{RT}{6\pi\eta rN} \qquad (1)$$

$R$ represents gas constant, $T$, absolute temperature, $\eta$, solvent viscosity, $N$, Avogadros' number, $D$, diffusion coefficient and $r$, radius of diffusing particles. Evaluating Eq. (1), we obtain.

$$rD=2.43\times 10^{-13} \text{ C.G.S.} \qquad (2)$$

The radius of the micelle can be calculated from Eq. (2) by the measurement of the difusifon coefficient alone of the TMDA solution. However the diffusion coefficient cannot be obtained owing to the influence of diffusion potential caused by the charged large micelles and small gegenions. On the other hand, in order to suppress this potential it is necessary to add sufficient amounts of electrolyte, which would change the state of micelles completely. For the same reason as mentioned above the radius of the swollen micelle cannot be obtained directly.

From the X-ray data[10] it is supposed that the diameter of the micelle of TMDA is about 35 Å and the diameter of the swollen micelle is increased linearly with the solubilized amount of solubilizate. The maximum (saturated) increment is reported to be 15 Å. In this experiment 1.5% hexane solution is nearly the saturation-value.

Assuming that the X-ray data also hold in this experiment, we can calculate the true diffusion coefficient as shown in Table III.

TABLE III

CALCULATED RADII AND DIFFUSION COEFFICIENTS OF THE SWOLLEN MICELLES BY HEXANE

| Hexane % | 0.0 | 0.1 | 0.3 | 0.5 | 0.6 | 0.7 | 0.8 | 1.0 | 1.2 | 1.5 |
|---|---|---|---|---|---|---|---|---|---|---|
| $r$(A) | 17.5 | 18.0 | 19.0 | 20.0 | 20.5 | 21.0 | 21.5 | 22·5 | 23.5 | 25.0 |
| $D\times 10^7$ | 13.88 | 13.49 | 12.80 | 12.17 | 11.87 | 11.57 | 11.30 | 10.80 | 10.32 | 9.73 |

From Table III the difference between two diffusion coefficients of swollen micelles at $C_1$ and $C_2$ can be obtained, and the values $(D_1-D_2)$ are listed in the last column of Table II. Fairly good coincidence with the experimentally obtained diffusion coefficients is found.

(3) **Experiments with polar compounds.**— Table IV exhibits the diffusion coefficients of alcohols in TMDA- solution.

TABLE IV

DIFFUSION COEFFICIENTS OF VARIOUS ALCOHOLS IN TMDA-SOLUTION

| Alcohols | $C_1$ | $C_2$ | $D_s\times 10^7$ cm²/sec. | Solubility[11] in water |
|---|---|---|---|---|
| *n*-Amyl- | 1.0%[9] | 2.0%[9] | 15.8 | 2.20 |
| *n*-Octyl- | 1.0 | 2.0 | 6.15 | 0.059 |
| *n*-Lauryl- | 1.0 | 2.0 | 0.915 | 0.00 |
| *n*-Lauryl- | 0.1 | 1.0 | 4.87 | 0.00 |

The diffusion coefficient of iso-amylalcohol in water is $93.2\times 10^{-7}$cm²/sec. So *n*-amylalcohol diffuses much more slowly in the detergent solution than iso-amylalcohol in water in spite of the same molecular weight.

In Table IV, it is seen that the longer the chain length of alcohol the slower is the diffusion velocity. In these cases, however, the solubility in water has a somewhat closer relation to the diffusion velocity than the chain length of alcohols. The concentration gradient curves of diffusion obtained from *n*-amylalcohol deviate remarkably from the ideal Gaussian curves and assume the shape

9) volume %.

10) W.D. Harkins, R.W. Mattoon and M.L. Corrin, *J. Colloid Sci.*, **1**, 105 (1946). W. D. Harkins, R. W. Mattoon and R. S. Stearns, *J, Chem. Phys.* **15**, 209 (1947); **16**, 646, 652 (1948).

11) Grams of the substances in 100 g. water.

of two (at least) ideal curves superimposed, of which one is very sharp and the other very diffuse. The diffused one may be caused by simple alcohol molecules and the sharp one by complicated mixed micelles composed of alcohol and detergent molecules.

The present method of calculating the diffusion coefficient gives only the complex average value of two different diffusion coefficients of these. It is impossible to analyze the value in greater detail at the present stage.

If there were rapid equilibrium between amylalcohol in swollen micelles and that in the extra-micellar solutions, diffusion would be performed chiefly by molecularly dissolved *n*-amylalcohol; then the concentration-gradient curves would show a different patterns.

Therefore, the sorption or desorption of dissolved alcohol molecules by micelles may not occur so easily in this case as Winsor's equilibrium theory[12] of micelles suggests. The slow exchange between swollen micelles and solutes may be similar to the phenomena of surface aging which exhibit hindered diffusion to the surface by monomolecular film of surface active substances[13].

Laurylalcohol diffuses like hexane but in this case the circumstances are more complex owing to the penetration and the least diffusion coefficient value and the highest viscosity, has been obtained presumably as the result of large sandwich-micelles.

In Table V, the diffusion coefficients of esters are listed. The hydrolysis was not observed at least.

TABLE V

DIFFUSION COEFFICIENTS OF VARIOUS ESTERS IN TMDA-SOLUTION

| Esters | $C_1$ | $C_2$ | $D_s \times 10^7$ cm²/sec. | Solubility[11] in water |
|---|---|---|---|---|
| Ethylacetate | 1.0%[9] | 2.0%[9] | 102 | 7.56 |
| Butylacetate | 1.0 | 2.0 | 15.9 | 2.3 |
| Dimethylphthalate | 1.0 | 0.5 | 18.2 | 0.24 |
| Diethylphthalate | 1.0 | 0.5 | 8.25 | — |
| Dibutylphthalate | 1.0 | 0.5 | 4.36 | — |

Ethylacetate which is completely soluble at this concentration diffuses ordinarily, but $D_s$ of butylacetate is very small and the concentration gradient curves of diffusion of this are the composite curve of at least two parts just as in the case of *n*-amylalcohol mentioned above.

12) P.A. Winsor, *J. Phys. Chem.*, **56**. 391 (1952).

13) A.F.H. Ward and L. Tordai, *Rec. Trav. Chim. Pays-Bas*, **71**, 396, 482, 572 (1952); A.E. AIexander and P. Johnson, "Colloid Science", Clarendon press, Oxford 1949, p. 529.

McBain found unusual behaviours in the case of solubilization of dimethylphthalate[14] in detergent solution which is insoluble both in water and in hydrocarbon and suggested that the rearrangement of micelles takes place and the solubilization of dimethylphthalate molecules is achieved by polar groups of small micelles. In such a case it will be expected that the circumstances are somewhat different in diffusion process. But the numerical value of the diffusion coefficient on Table V shows no anomaly. A parallelism is rather found between the solubility and the diffusion coefficient. McBain took up dimethylphthalate only, diethylphthalate and dibutylphthalate are also investigated in these experiments.

In Table VI the diffusion coefficients of partly water-soluble polar substances in various mean concentrations are listed.

TABLE VI

CONCENTRATION DEPENDENCE OF DIFFUSION COEFFICIENTS IN TMDA-SOLUTION

| | $C_1$ | $C_2$ | $D_s \times 10^7$ cm²/sec. |
|---|---|---|---|
| *n*-Amylalcohol | 1.0%[9] | 2.0%[9] | 15.8 |
| | 2.0 | 3.0 | 11.8 |
| | 3.0 | 4.0 | 6.22 |
| *n*-Butylacetate | 0.5 | 1.5 | 15.9 |
| | 1.0 | 2.0 | 15.1 |
| | 2.0 | 3.0 | 12.6 |
| | 3.0 | 4.0 | 9.75 |
| | 4.5 | 5.5 | 5.76 |
| Ethylacetate | 1.0 | 2.0 | 102 |
| | 3.0 | 4.0 | 93.8 |
| | 5.0 | 6.0 | 86.1 |
| | 7.0 | 8.0 | 63.4 |
| | 8.0 | 10.0 | 22.4 |
| | 10.0 | 13.0 | 15.7 |
| Dimethylphthalate | 1.0 | 0.5 | 18.2 |
| | 1.5 | 0.5 | 15.6 |
| | 2.7 | 1.5 | 5.16 |

These polar compounds dissolve somewhat in water but in the detergent solution much more through solubilization. The higher the concentration of these polar compounds, the smaller becomes the valueof the diffusion coefficient. This is explained by assuming that the contribution of complicated micelles to the diffusion becomes more dominant compared with the single molecules of the solute as the concentration is increased. This is also found in the diffusion curve since the diffuse part of the diffusion pattern tends to vanish as the concentration of the solute approaches saturation.

14) J.W. Mc Bain and Mc Han, *J. Am. Chem. Soc.*, **70**, 3838 (1948).

No quantitative relation between concentration and diffusion coefficient can be found, since the obtained diffusion coefficient is a complicated mean of two components.

## Summary

(1) Urea, fructose and potassium chloride which are completely soluble in water, diffuse in the TMDA solution at about the same rate as in water notwithstanding the fact that the former has higher viscosity than the later.

(2) The diffusion coefficient of hexane is in a fairly good coincidence with the difference of the calculated diffusion coefficient from X-ray data between more and less swollen micelles.

(3) The diffusion of alcohols and esters is generally governed by their solubility in water. From the concentration gradient curves of diffusion, they are considered to diffuse on two different mechanisms, one as the single molecule and the other as the complex group associated with the detergent micelles.

(4) The equilibrium between solute in micelles and in water is rather slower process when the mechanical disturbance or convection is absent in the solution.

(5) The anomalies reported on the solubilization of dimethylphthalate is not observed in these diffusion experiments.

In conclusion, the author thanks Prof. Dr. N. Sata for his kind instruction and also expresses sincere thanks to Mr. Y. Seno of Nihon Yushi Co. who afforded valuable samples and suggestions.

*Department of Chemistry, Faculty of Science, Osaka University, Osaka*

# *A Kinetic Study on the Vinylation of Alcohol**

By Teiji TSURUTA, Hiroyuki KOMATSUBARA and Junji FURUKAWA

(Received May 23, 1955)

Previous interpretations[1] of the vinylation reaction of alcohol are not satisfactory, because few of them are based upon kinetic studies. In the present study, the course of the vinylation was traced under atmospheric pressure using phenylacetylene and benzyl alcohol as reactants, so that inaccuracies inherent in the autoclave reaction were eliminated.

In the first place, it was synthetically ascertained that the acetylene and the alcohol react to give a corresponding vinylation product, styryl benzyl ether, under a condition similar to that in the present kinetic measurement. Secondly, the volumetric analysis of phenylacetylene was examined and modified. Thirdly, dependences of the rate of reaction upon the concentration of phenylacetylene and the activity of the alcoholate were examined. And finally, a possible mechanism of the vinylation is proposed.

* Presented at the 7th Annual Meeting of the Chemical Society of Japan in Tokyo, April 2, 1954.

1) A review on the vinylation mechanism: S. Murahashi, *J. Soc. Org. Synth. Chem. Japan*, **10**, 485 (1952) (in Japanese).

## Experimental

**1. Materials.**—Commercial C.P. benzyl alcohol was treated with anhydrous potassium carbonate and rectified at a reduced pressure under nitrogen. A cut boiling at 110–111°/30 mm. was used. Phenylacetylene was prepared from cinnamic acid according to the literature[2]. A cut boiling at 50–51.5°/30 mm. was used.

**2. Styryl benzyl ether.**—A solution of 2 g. of metallic sodium in 125 g. of benzyl alcohol was placed in a 500-cc. four-necked flask equipped with a stirrer, thermometer, reflux condenser and dropping funnel. The solution was heated to 130°C in an oil bath and 20 g. of phenylacetylene in 50 g. of benzyl alcohol was added. The addition was controlled so that the temperature of the solution did not exceed 135°C. After being stirred at that temperature for two hours, to the solution was added 100 cc. of water and the separated organic layer was extracted with ether. The ether layer was washed with water, dried on anhydrous potassium carbonate, the solvent evaporated and the residue was distilled in vacuo under nitrogen. Thus, besides unreacted phenylacetylene, 23 g. of an oily product (A) boiling at

2) H. Gilman, "Organic Syntheses, Collective Vol. I", John Wiley and Sons, Inc., New York, N.Y. (1948), p. 438.

183°/9 mm. was obtained. A small quantity of residue remained in the distillation flask. On being cooled, the adduct (A) solidified into white crystals which showed m.p. 72–73°C on being recrystallized three times from ethanol.

*Anal.* Found: C, 85.68; H, 6.68; Mol. Wt., 203. Calcd for $C_{15}H_{14}O$: C, 85.71; H, 6.67; Mol. Wt., 210.

**3. A Modified Volumetric Analysis of Phenylacetylene.**—The principle[3] of the analysis is represented as

$$C_6H_5C{\equiv}CH+Cu^{(+)} = C_6H_5C{\equiv}CCu+H^{(+)} \quad (1)$$

$$C_6H_5C{\equiv}CCu+Fe^{(3+)}+H_2SO_4 = C_6H_5C{\equiv}CH+CuSO_4+Fe^{(2+)}+H^{(+)} \quad (2)$$

$$10Fe^{(2+)}+2KMnO_4+8H_2SO_4 = K_2SO_4+2MnSO_4+10Fe^{(3+)}+5SO_4^{(2-)}+8H_2O \quad (3)$$

1 mol. of $C_6H_5C{\equiv}CH$ (102.13 g.) corresponds to 1 N $KMnO_4$ (31.606 g.).

Since cuprous chloride in saturated ammonium carbonate solution[4] was found to give poor results for the precipitation reagent of phenylacetylene, we applied Ilosvay's method[3] with some modifications to the present analysis.

A solution of 1 g. of $CuSO_4{\cdot}5H_2O$ in 5 cc. of water was added to 5.5 cc. of 10.61 N $NH_4OH$. Into this deep blue solution, 3 g. of $NH_2OH{\cdot}HCl$ was dissolved and diluted with water to 50 cc. The blue color disappeared completely in a few minutes[5].

The precipitation of the acetylide was seriously affected by the concentration of $NH_4OH$. The most suitable pH for the precipitation was found to be 8.6–8.7. To examine the accuracy of the analysis, known quantities (9.039, 4.520, 1.792 and 0.897 ($\times10^{-4}$ mol.)) of the acetylene in 5 cc. of ethanol were treated with 20 cc. of the cuprous solution. The yellow precipitates of the acetylide were filtered on a glass filter (No. 4). To remove the excess hydroxylamine, the precipitates were washed with water several times until the filtrate did not decolorize one drop of N/10 $KMnO_4$. During these operations, the precipitates should be covered with the mother liquid in order to keep the acetylide from the air oxidation.

For dissolving the precipitates, a solution of ferric sulfate in sulfuric acid was prepared; 100 g. of ferric sulfate[6] was dissolved in 250 g. of sulfuric acid (sp. gr., 1.85), which was diluted with water to 1 l. Twenty cc. of the ferric solution was mixed with 10 to 15 cc. of $H_2SO_4$, added to the precipitates and was digested for 10 to 20 minutes on a steam bath to complete solution. There was obtained a clear light-green solution involving ferrous ion, which was cooled to the room temperature, and to this was added a few cc. of 85% phosphoric acid[7], and then titrated with N/20 $KMnO_4$. The average of errors for 16 measurements was −0.8% with standard deviation 4.12%.

For the precipitation of the acetylide from benzyl alcohol solution some modifications were required because of the slight solubility of the alcohol in water. Known quantities (10.626, 5.313 and 2.125 ($\times10^{-4}$ mol.)) of phenylacetylene in 10 to 15 cc. of benzyl alcohol were mixed with 20 to 30 cc. of the precipitating agent under vigorous shaking. The mixing was effected by the addition of some ethanol. When the precipitation was completed, the precipitates were filtered and washed successively with water, aqueous ethanol, and with ethanol and water to remove hydroxylamine and benzyl alcohol. The average of errors for 11 measurements was −0.51% with standard deviation 4.96%.

**4. Kinetic Measurement.**—The reactions were carried out in test tubes immersed in an oil bath, the temperature of which was controlled to 130± 0.5°C. A typical run of the measurements is as follows:

A 5.4-cc. solution of sodium benzylate in benzyl alcohol was placed in a 15-cc. test tube and heated to 130°C. To this solution, a 5-cc. solution of phenylacetylene in benzyl alcohol was added. The initial concentrations of phenylacetylene, sodium benzylate and benzyl alcohol were 0.001, 0.010 and 0.100 (in mol. ratio), respectively. After a definite time interval, the reaction solution was added to a slight exess 1 N HCl solution to interrupt the reaction. The excess of hydrochloric acid was neutralized with 1 N NaOH using methyl red as indicator and the unreacted phenylacetylene in the mixture was analyzed. In one run, the analysis was done with respect to four to eight test tubes with the reaction time varied.

## Results and Discussion

The results obtained are summarized in Table I. The rates of vinylation estimated

TABLE I

REACTION BETWEEN PHENYLACETYLENE* AND BENZYL ALCOHOL IN BENZYL ALCOHOL AT 130±0.5°

| Exp. No. | Sodium Benzylate (M) | Sodium Benzylate ($a_r$) | $k_1=v/p$ ($\times10^{-2}$) | $k_2=k_1/a_r$ ($\times10^{-2}$) | No. of Tests |
|---|---|---|---|---|---|
| 1 | 0.48 | 2.17 | 1.34±0.08 | 0.66 | 7 |
| 2 | .72 | 3.50 | 2.33±0.03 | .67 | 7 |
| 3 | .86 | 4.85 | 4.36±0.32 | .90 | 7 |
| 4 | .87 | 4.93 | 4.91±0.19 | .99 | 7 |
| 5 | .97 | 6.35 | 5.75±0.07 | .91 | 6 |
| 6 | 1.00 | 6.97 | 6.75±0.14 | .97 | 4 |
| 7** | 1.01 | 7.01 | 6.73±0.19 | .96 | 6 |
| 8 | 1.04 | 7.95 | 7.28±0.34 | .92 | 4 |
| 9 | 1.13 | 10.77 | 9.05±0.14 | .84 | 5 |
| 10 | 1.37 | 20.35 | 17.71±0.77 | .87 | 5 |
| | | | | Mean: | 0.87±0.08 |

* The initial concentration $p_0$ of the acetylene is 0.096 mol./l.

** $p_0$: 0.048 mol./l.

3) L. Ilosvay and N. Ilosva, *Ber.*, **32**, 2697 (1899).

4) Fr. Hein, A. Meyer, *Z. anal. Chem.*, **72**, 30 (1927).

5) The solution should be kept from contact with air. In this study, the solution was prepared immediately before the analysis.

6) The ferric alum solution, which appeared in Hein's paper[4] as the reagent for solution of the acetylide, was not satisfactory, because it was difficult to obtain a clear ferric solution even if sulfuric acid was used in great excess.

7) F.P. Treadwell, "Lehrbuch der anal. Chem. II. Band", Franz Deuticke, Leipzig (1937), p. 523.

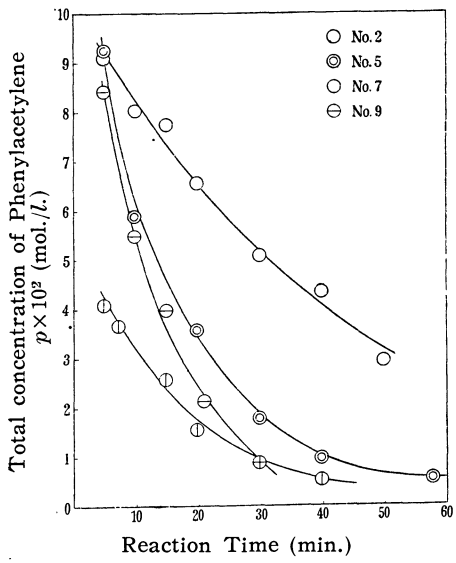



Fig. 1. Typical runs of the reaction with the initial concentration of phenylacetylene 0.096 (mol./l.)[a]. The concentrations of sodium benzylate: 2) 0.72; 5) 0.97; 7) 1.01; 9) 1.13 (mol./l.)
[a] In No. 7, the initial concentration of the acetylene is 0.048 (mol./l.).

from straight line portions of the reaction curves, some examples of which are shown in Fig. 1, were found to be first order with respect to the total concentration of the acetylene as shown in Table I. Thus the rate $v$ is expressed as

$$v = k_1 p \tag{4}$$

where $p$ denotes the total concentration of phenylacetylene and $k_1$ is a constant. From Table I, it can be seen that the constant $k_1$ is proportional to the relative mean ionic activity[8] $a_r$ of the alcoholate but not to the analytical concentration. Thus Eq. (4) is reduced to Eq. (5):

$$v = k_2 p a_r \tag{5}$$

where $k_2$ is a constant.

If we assume that the addition of the alcoholate ion to the acetylene is the rate determining stage, the rate $v$ of the vinylation is expressed as Eq. (6).

$$v = k_3[RO^{(-)}][R'C{\equiv}CH] \tag{6}$$

where $k_3$ is a constant. In the reaction system, an equilibrium between the alcoholate and the acetylide is present:

$$RO^{(-)} + R'C{\equiv}CH \overset{K_1}{\rightleftarrows} ROH + R'C{\equiv}C^{(-)} \tag{7}$$

where $K_1$ is an equilibrium constant, and

$$[RO^{(-)}] + [R'C{\equiv}C^{(-)}] = [Na] \tag{8}$$

$$[R'C{\equiv}CH] + [R'C{\equiv}C^{(-)}] = p \tag{9}$$

From Eqs. (6)—(9),

$$v = k_3 p[Na][ROH]^2 / \{[ROH] + K_1[RO^{(-)}]\}\{[ROH] + K_1[R'C{\equiv}CH]\} \tag{10}$$

Under the present condition, the reaction was carried out in benzyl aclohol in large excess, so that Eq. (10) is reduced to

$$v = k_4 p[Na] \tag{11}$$

where $k_4$ is a constant. Since the relative mean ionic activity $a_r$ of sodium benzylate is little varied under the condition even if the formation of acetylide is taken into consideration, Eq. (11) is equivalent to Eq. (5)[9]. These results are essentially in accordance with Rigamonti and Bernardi's[10].

In a previous paper[11], we reported a rate expression:

$$v = k[Ac.]^{1.5}[Na]^1[Al.]^{1.4} \tag{12}$$

where Ac. and Al. denote acetylene and ethanol. The reaction was examined with low concentration of sodium alcoholate so that Eq. (10) was transformed to Eq. (13).

$$v = k_3 p[Na][ROH] / \{[ROH] + K_1[R'C{\equiv}CH]\} \tag{13}$$

Equation (12) was interpreted by Eq. (13).

Recently Otsuka[12] found that the dependence of the rate upon the concentration of alcohol or of acetylene decreased, to a degree less than first order, with increasing concentrations of the reactants. He accounted for the kinetic data in terms of a complex formation from acetylene, alcohol and alcoholate. However, there seem to be no experimental evidences for such complex intermediates.

In his experiment, the concentration of the alkali is so small that Eq. (13) still holds well. Considering the order of magnitude of $pK_a$[13], the tendency of decrease in the reaction order of alcohol or of acetylene is well accounted for by Eq. (13).

Equation (5) may be derived from an alternative mechanism in which an addition between benzyl alcohol and phenylacetylide is assumed as the rate determining step.

8) The relative mean ionic activity $a_r$ of the alcoholate in benzyl alcohol was potentiometrically determined according to the Harned method:
a) H.S. Harned and J. C. Hecker, *J. Am. Chem. Soc.*, 55, 4838 (1933).
b) H.S. Harned and M.A. Cook, ibid., 59, 496 (1937).

9) $[Na] = k_5 a_r$

10) R. Rigamonti and L. Bernardi, *Chime. Ind. (Milan)*, **34**, 561 (1952); *C.A.*, **47**, 2583b (1953).

11) A. Onishi, N. Saito and J. Furukawa, *Repts. Chem. Research. Inst., Kyoto Univ.*, **19**, 85 (1949) (in Japanese).

12) S. Otsuka, presented at the 8th Annual Meeting of the Chemical Society of Japan in Tokyo, April 1, 1955.

13) For example, $pK_a$ of phenylacetylene and benzyl alcohol are 21 and 19. J.B. Conant and G.W. Wheland, *J. Am. Chem. Soc.*, **54**, 1212 (1932).

Otsuka[14] found that the rate of vinylation of phenol was much slower than that of alcohol; if a mixture of alcohol and phenol was reacted with acetylene in the presence of alkali, only phenol was vinylated until the latter[15] was completely converted to the vinyl ether. This supports the assumption that alcoholate and acetylene participate in the rate determining step.

## Summary

To elucidate the vinylation mechanism, a liquid phase reaction between phenylacetylene and benzyl alcohol was kinetically studied. The reaction was found to proceed along a second order mechanism between the acetylene and the alcoholate. A possible mechanism of the reaction was proposed.

The authors are grateful to Dr. S. Otsuka for private communications and discussion and to Professor S. Okada, Professor S. Yoshizawa and Mr. Hine for their help with the electrochemistry. This work was supported by a grant in aid for Miscellaneous Scientific Research from the Ministry of Education.

*Institute for Chemical Research, Kyoto University, Takatsuki, Osaka*

14) S. Otsuka, private communication.

15) In the reaction mixture, the concentration of $C_2H_5O(^-)$ is negligibly small compared with that of $C_6H_5O(^-)$.

# *The Interaction of Gelatin Molecule with Surface Active Ions*

By Kunio TAMAKI and Bun-ichi TAMAMUSHI

(Received May 24, 1955)

## Introduction

The interaction between proteins and synthetic detergents has been the subject of discussion of many investigators[1]. It has been reported that the interaction depends upon some factors, among which the ratio of detergent to protein seems to be of importance in elucidating its mechanism[2]. It has also been observed that cationic detergents precipitate only anionic proteins, namely, proteins on the alkaline side of the isoionic point, while anionic detergents precipitate only cationic proteins, namely, proteins on the acidic side of the isoionic point, and that the precipitate initially formed is dissolved when excess detergent is added. Pankhurst and Smith[3] assumed, basing their assumption on their investigation of the complex formation between gelatin and sodium dodecyl sulphate, that the precipitation took place when the monolayer of dodecyl sulphate ions was formed at basic groups of gelatin molecules and the precipitate was led to dissolve when the second adsorption layer was built up. Lundgren[4] also suggested such a mechanism of complex formation between proteins and detergents. Furthermore it has been evidenced that certain stoichiometric combinations can also take place between cationic detergents and proteins on the acidic side of an isoionic point as well as between anionic detergents and proteins on the alkaline side of the isoionic point[5,6,7,8,9].

In this paper we describe our experiment on the interaction of dodecyl amine hydrochloride and sodium dodecyl sulphate on gelatin at various values of hydrogen ion concentration, whereby we studied the phenomena first by determining the combined detergent to the precipitated gelatin and then by measuring flow properties of the mixed solutions.

## Experimental

**Materials.**—The sample of gelatin used in this experiment was a commercial one, its ash content

1) F.W. Putnam, "Advances in Protein Chemistry", **4**, 80 (1948).
2) F.W. Putnam and H. Neurath, *J. Am Chem. Soc.*, **66**, 692 (1944).
3) K.G.A. Pankhurst and R. C. M. Smith, *Trans. Faraday Soc.*, **40**, 565 (1944); **41**, 630 (1945); "Surface Chemistry" London (1949) p. 109.
4) H. P. Lundgren, *Textile Research J.*, **13**, 335 (1945).
5) H.P. Lundgren, D.W. Elam and R.A. O'Connell, *J. Biol. Chem.*, **149**, 183 (1943).
6) F. W. Putnam and H. Neurath, ibid., **159**, 195 (1945).
7) H. Neurath and F.W. Putnam, ibid., **160**, 397 (1945).
8) S.N. Timasheff and F.F. Nord, *Arch. Biochem. Biophys.*, **31**, 309 (1951).
9) B.S. Harrap and J.H. Schulman, *Discussions Faraday Soc.*, No. 13, 197 (1953).

having been found to be 2.6% and the pH of its solution 5.3. This sample was purified by using ion exchange resins by which means the ash content of the gelatin was reduced to less than 0.09% and the pH at the isoionic point of the purified gelatin was found to be 4.8.

Dodecyl amine hydrochloride (DAH) was prepared from dodecyl amine supplied by Armour and Co. U.S.A., and recrystallized twice from acetone.

Sodium dodecyl sulphate (SDS) was a sample of the highest purity supplied by Nezu Chemical Laboratory, Tokyo.

**Method of Analysis of Detergents.** — SDS which remained uncombined in the mixed solutions was determined by volumetric precipitation process using DAH as a precipitant and eosin as an indicator. DAH was determined in the same manner by using SDS as a precipitant and rhodamin 6G as an indicator. In both cases, the concentration of the standard solutions was 0.001 mole per liter, and the end point of titration was determined by means of the disappearance of fluorescence of these indicators. Such method of analysis had been proposed by the investigators of Nezu Chemical Laboratory[10] and was proved to be applied to the solution containing gelatin with the error of about ±2% in our experiment.

**Measurement of Viscosity.**—The viscosity of the mixed solutions was measured by means of a horizontal capillary tube viscosimeter, the solution having been made to flow through the tube under suitable pressure diflerences at the two ends of the tube. The pressure difference was maintained constant during a set of measurements by means of a manostat. The radius of the capillary tube was equal to 0.031 cm. and its length 30.3 cm. The pressure range studied was from 0.5 cm. to 11 cm. in mercury manometer.

## Results and Discussion

**a) Complex formation.**—Various amounts of detergents were added to a 0.5% gelatin solution at various values of pH of the solution, which had been controlled by adding normal HCl or NaOH to the solution. It was found that gelatin was precipitated in a certain range of the concentration of any one of the detergents at a certain value of pH of the solution. DAH precipitated gelatin at pH values greater than that of the isoionic point, while SDS precipitated gelatin at pH values less than that of the isoionic point. When precipitates appeared, the resulting mixture, after being allowed to stand for twenty four hours, was centrifuged or filtered, and the concentration of detergent of the supernatant or filtered solution was determined as described above; the amount of detergent combined with the precipitant was thus obtained by taking the difference of concentration which existed before and after the process. Figs. 1a. and 1b. show the amount of the combined detergent in relation to the ratio of detergent to protein.

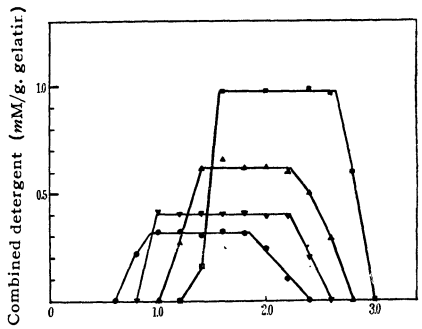



Fig. 1a. Amount of combined detergent (DAH) in relation to detergent/protein ratio.

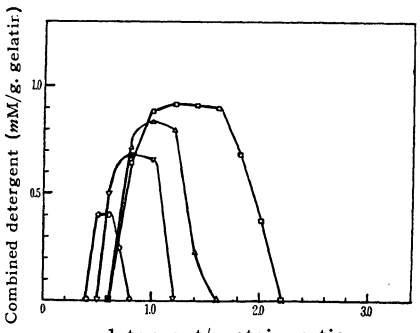
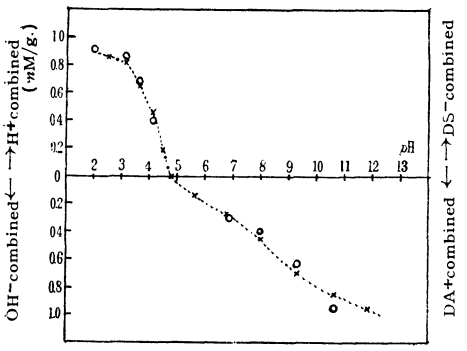



Fig. 1b. Amount of combined detergent (SDS) in relation to detergent/protein ratio.

As these figures indicate, the precipitation zone is greatly influenced by the pH of the mixed solution and, in the case of gelatin-dodecyl amine ion combination, the precipitation zone is displaced to the higher ratio of detergent to protein as pH becomes greater, while in the case of gelatin-dodecyl sulphate ion combination, the precipitation zone is displaced to the higher ratio of detergent to protein as pH becomes smaller. In both cases, it is to be remarked that the maximum precipitation and the complete dissolution of the precipitate take place at the definite ratio of the detergent concentrations, namely 1:2. It is also noticeable that SDS precipitates gelatin at much lower concentrations than DAH does.

10) T. Ino, T. Kondo, K. Meguro and O. Yoda, *J. Chem. Soc. Japan*, **76**, 220 (1955).




×···×··· Titration curve
○ Maximum value of combined detergent.

Fig. 2. Titration curve of gelatin and maximum value of combined detergent at each pH.

Fig. 2 shows that the maximum values of detergent combined at each pH are approximately corresponding to the acid or base combining power of gelatin, and therefore it is concluded that the first polar combination between gelatin molecules and detergent ions is accomplished at the point of the maximum precipitation.

**b) Flow Properties.**—The flow of gelatin solutions in presence and absence of detergent was found generally non-Newtonian, the rate of flow being expressed by the well known Bingham's equation[11], namely:

$$\frac{V}{t}=\frac{\pi\mu R^4}{8l}\left(P-\frac{4}{3}p+\frac{p^4}{3P^3}\right),$$

where, $V$ means the volume of the solution passed through the capillary tube in time $t$, $R$ the radius of the capillary tube, $l$ the length of the tube, $P$ the difference of pressures applied, $\mu$ the coefficient of mobility, $p$ a constant equal to $\frac{2l}{R}f$ in which $f$ means the yield value. When the applied pressure difference is large, the curve $V/t$ *vs.* $P$ becomes nearly linear, and it obeys the following equation:

$$\frac{V}{t}=\frac{\pi\mu R^4}{8l}\left(P-\frac{4}{3}p\right)$$

Putting herein $V/t=0$. we obtain the intercept at the axis $P$ and from this we get the value of the yield value. From the slope of the asymptote we obtain the value of $\frac{\pi\mu R^4}{8l}$ and consequently the value of the coefficient of mobility $\mu:\mu=1/\eta$, where $\eta$ means the coefficient of viscosity. In this paper, we conventionally use the relative viscosity to water, $\eta_r$, instead of $\mu$ or $\eta$.

The relative viscosity and the yield value obtained of the gelatin solution first in absence of detergent are shown in Fig. 3, both as a function of pH. As this figure demonstrates, $\eta_r$ and $f$ run completely parallel to each other. Both the values have the minimum at the isoionic point and the maximum on both sides of the isoionic point. Such a characteristic feature was formerly found by Freundlich and Neu kircher[12] and recently studied in some detail by Stainsby[13].

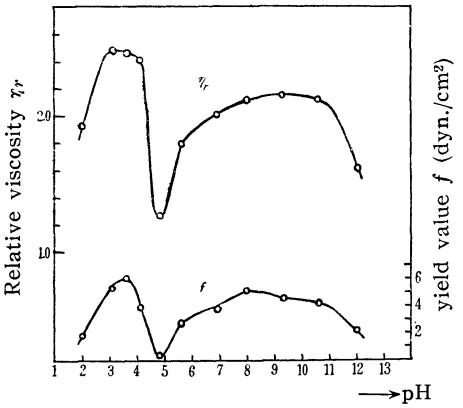
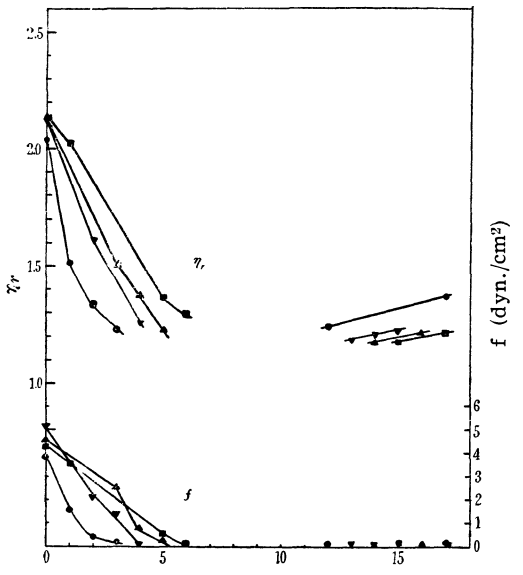



Fig. 3. Viscosity and yield value of gelatin solution as a function of pH. Solution: 0.5%, Temperature: 25°C.




● pH 6.9 ▼ pH 8.0 ▲ pH 9.3 ■ pH 10.6

Fig. 4a. Variation of viscocity and yield value of gelatin solution by addition of DAH. Solution: 0.5%, Temperature: 25°C.

11) E.C. Bingham, "Plasticity and Fluidity" New York, (1922) p. 222.

12) H. Freundlich and H. Neukircher, *Kolloid-Z.*, **38**, 180 (1926).

13) G. Stainsby, *Nature*, **169**, 662 (1952).

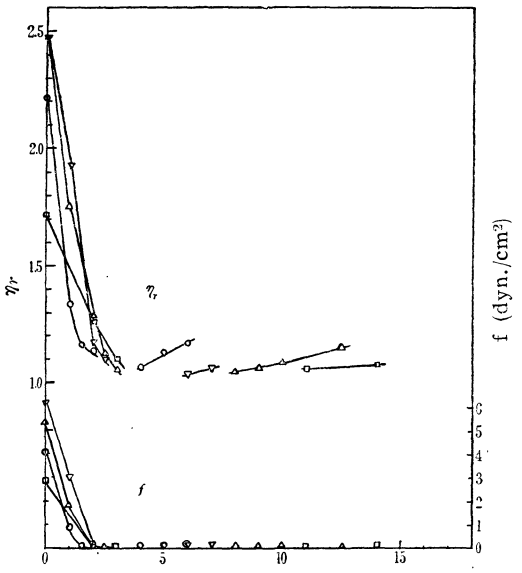



Fig. 4b. Variation of viscosity and yield value of gelatin solution by addition of SDS. Solution: 0.5%, Temperature: 25°C.

At the isoionic point, the macromolecule of gelatin is probably in the contracted form owing to the attractive forces between balanced charges, whereas, on both sides of the isoionic point, the molecule has a net charge, which may cause it to extend itself by repulsion. However, in more acidic or more basic solutions, the repulsive forces will be again reduced, owing to the increase of free ions in those solutions. The maximum of $\eta_r$ and $f$ on both sides of the isoionic point may be the result of the interplay of these two counter effects.

Fig. 4a shows how $\eta_r$ and $f$ of the solution change by the addition of DAH within certain range of detergent concentrations either before the precipitation or after the redissolution. Fig. 4b shows the similar change of $\eta_r$ and $f$ in the case of gelatin-SDS mixtures. In both cases, we find such a tendency that the values of $\eta_r$ and $f$ are greatly reduced as detergent is added until precipitation takes place and that, after redissolution of the precipitate initially formed, the mixture exhibits nearly Newtonian flow. The mechanism of the phenomena may be considered as follows. The more or less expanded gelatin molecule either at the acidic or alkaline side of the isoionic point may be changed into the folded, hydrophobic state by the continuous combination of detergent ions and consequently $\eta_r$ and $f$ decrease until precipitation takes place. On addition of excess detergent, however, the second adsorption layer of detergent ions will be formed by van der Waals attraction force between carbon chains, which makes the molecule hydrophilic and accordingly the precipitate once formed dissolves again into solution. The solution thus formed behaves itself similarly to the solution at the isoionic point without detergent.

It is remarkable that the relative viscosity of the mixed solutions, directly before the precipitate formation or directly after the dissolution of the precipitate, is somewhat less than that of the solution at the isoionic point. This suggests that the gelatin molecule in such mixtures may be in more folded state than the molecule at the isoionic point. It is further noticed from our experiment that SDS reduces the viscosity of the gelatin solution more effectively than DAH does and consequently that SDS is more effective than DAH in precipitating gelatin from the solution. This agrees with the general character of proteins that they interact more strongly with anions than with cations.

Furthermore, the combination of detergent ions with cationic or anionic groups of the macromolecules of gelatin would have taken place mainly at the side chains and probably not at the backbone in the case of our experiment, because the interaction was studied in absence of any other inorganic salts except that very small amount of sodium chloride formed by the neutralization of detergent ion with HCl or NaOH.

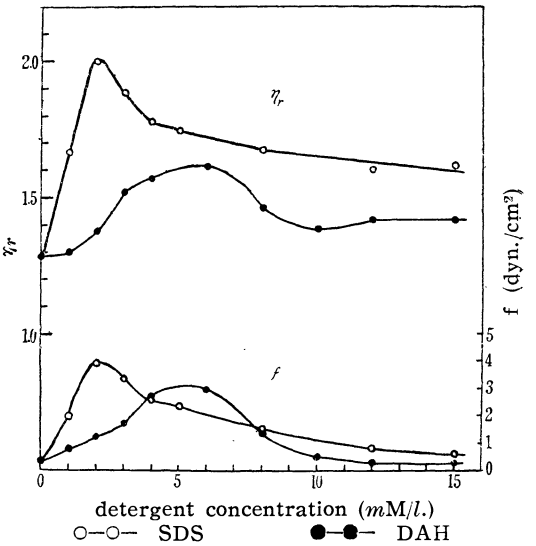



Fig. 5. Variation of viscocity and yield value of gelatin solution by addition of detergent at isoionic point. Solution: 0.5%, Temperature: 25°C.

Lastly, Fig. 5 indicates the change of $\eta_r$ and $f$ of the mixture in relation to the added DAH or SDS at the isoionic point of gelatin. As this figure shows, both $\eta_r$ and $f$ increase first with the addition of detergent, attain maxima and then decrease. Comparing these curves of $\eta_r$ or $f$ in this figure with those in Fig. 3, which show the change of $\eta_r$ or $f$ due to the addition of hydrogen ion or hydroxy ion to isoionic gelatin, we find a remarkable resemblance in the features of the corresponding curves. This suggests that the effect of detergent cations or anions upon gelatin bears a resemblance to that of hydrogen ion or hydroxy ion upon the same gelatin. It is thus quite presumable that either detergent cations or anions combine with a neutral gelatin molecule to some extent to give it net charges and consequently cause the molecule to extend itself. The appearance of maximum and decrease of $\eta_r$ or $f$ with increasing detergent concentration is probably due to the screening effect of counter ions.

## Summary

The action of dodecyl amine hydrochloride and sodium dodecyl sulphate on gelatin was studied at various hydrogen ion concentrations of the mixed solution, once by determining the combined detergent ions to the precipitated gelatin and then measuring flow properties of mixed solutions.

The determination of the combined detergent ions showed that the complex formation between detergent and gelatin should have taken place according to the mechanism proposed by Pankhurst and his co-workers.

The non-Newtonian flow character of gelatin solution at pHs on both sides of the isoionic point, was greatly influenced by the addition of detergent cations or anions and the flow of the mixed solutions directly before the precipitate formation or after the precipitate dissolution became approximately Newtonian, which suggested that the gelatin molecule would have been brought into a more folded state by the successive combinations of detergent ions.

The viscosity coefficient as well as yield value of the gelatin solution at the isoionic point were found to increase by the addition of detergent cations or anions. This suggested that the folded isoionic gelatin molecule would have been expanded by the combination with either one of the detergent ions.

We should like to express our sincere thanks to Armour and Co. U. S. A. and Nezu Chemical Laboratory, Tokyo, for their kind supply of pure detergents.

The present study was financially supported by a grant given by Ministry of Education.

*Chemistry Department, College of General Education; and Institute of Science and Technology, The University of Tokyo, Tokyo*

# *The Crystallinity of Solid High Polymers. I. The Crystallinity of Polyvinyl Alcohol Film*[*1]

By Hiroyuki TADOKORO, Syûzô SEKI and Isamu NITTA

(Received February 20, 1955)

## Introduction

The recent studies on solid high polymers have emphasized that the crystallinity is one of the most important factors to describe the state of them. The crystallinity is generally defined as the weight fraction of crystalline material. This definition is quite distinct if the polymer material is made of two distinct parts perfectly crystalline and perfectly amorphous. However, it is possible that there exist a transitional intermediate zone between these two perfect regions. In fact the same chain molecule may pass continuously from the one to the other region several times through such an intermediate zone. From this point of view the term "crystallinity" will be by nature an approximate one. During the past decade various methods of estimating crystallinity have been devised and developed, such as

*1 This paper was read at the discussion meeting on the high polymers under the auspices of the Kinki Branch of the Chemical Society of Japan and the Kansai Branch of the Society of Polymer Science (Japan) held in Kyoto on 9, Nov. 1954.

X-ray diffraction[1,2], density[3,4], infrared absorption spectrum[2,5], specific heat[6] etc. On the other hand some authors determine as a measure of this quantity the so-called "accessibility" by making use of the isotope exchange[7], hydrolysis[8] or sorption of water vapor[9,10]. In view of the conceptional limit of crystallinity mentioned above as well as the variety of detailed texture of polycrystalline high polymers, such as distribution of the size and shape of crystallites, their orientation, etc., it becomes of great importance to examine these methods of estimating crystallinity more critically as to what characteristic each of them possesses.

Although there exist a considerable number of reports on the crystallinity for cellulose[1a,3,7,8,9,10], polyethylene[1b,2,4,5a,6a,6b] nylon[2,6c,10], polyethylene terephthalate[2,5] etc., little work has been done with the same samples prepared under the same conditions by the comparative use of various kinds of existing methods estimating the crystallinity. In order to make some contribution to such a problem, we have undertaken to clarify the relationship among density, sorptive power for water vapor and infrared absorption spectrum as the proposed measures of the crystallinity, using the samples of polyvinyl alcohol (PVA) subjected to heat-treatments at different temperatures, each of which was prepared from one and the same source of material.

1a) P.H. Hermans and A. Weidinger, *J. Appl. Phys.*, **19**, 491 (1948); idem., *J. Polymer Sci.*, **4**, 135 (1949). b) S. Krimm and A.V. Tobolsky, *J. Polymer Sci.*, **7**, 57 (1951).

2) J.B. Nichols, *J. Appl. Phys.*, **25**, 840 (1954). (Review about the X-ray and infrared spectroscopic method).

3) P. H. Hermans, *J. Polymer Sci.*, **1**, 162 (1946); idem., "Contribution to the Physics of Cellulose Fibers", Elsevier Publishing Co., Inc., Amsterdam—New York, (1946), p. 70; "Physics and Chemistry of Cellulose Fibers", same publisher, (1949), p. 205.

4) E. Hunter and W.G. Oakes, *Trans. Faraday Soc.*, **41**, 49 (1945).

5a) R.B. Richards, *J. Appl. Chem.*, **1**, 370 (1951). b) W.H. Cobbs, Jr., and R.L. Burton, *J. Polymer Sci.*, **10**, 275 (1953). c) G.B.B.M. Sutherland and A. V. Jones, *Discussions Faraday Soc.*, **9**, 281 (1950). d) J.T. Maynard and M.B. Hall, *J. Polymer Sci.*, **12**, 235 (1954). Even in the case of ionic crystals this method can reveal the difference of the states of aggregation which cannot be differentiated by the X-ray method. (G. Chaudron, H. Mondange and M. Pruna, *Proc. Inter.n. Symposium Reactivity of Solids, Gothenburg* (1952) 9. *Chem. Abst.*, **48**, 13314a (1954).).

6a) H.C. Raine, R.B. Richards and H. Ryder, *Trans. Faraday Soc.*, **41**, 56 (1944). b) M. Dole, W.P. Hettinger, Jr., N.R. Larson and J.A. Wethington, Jr., *J. Chem. Phys.*, **20**, 781 (1952). c) R.C. Wilhoit and M. Dole, *J. Phys. Chem.*, **57**, 14 (1953). d) J.D. Hoffman, *J. Am. Chem. Soc.*, **74**, 1696 (1952).

7) V.J. Frilette, J. Hanle and H. Mark, *J. Am. Chem. Soc.*, **70**, 1107 (1948).

8) H. Maeda, *Chem. and Engineering (Japan)*, **4**, 429 (1951). (Review of the chemical methods).

9) J.A. Howsmon, *Text. Res. J.*, **19**, 152 (1949).

10) A.J. Hailwood and S. Horrobin, *Trans. Faraday Soc.*, **42B**, 84 (1946).

## Experimental

**a) Sample.**—The powdered specimen of PVA (average degree of polymerization: 1650) was used as a starting material. The method of purification of the sample and the procedure adopted for the preparation of film specimens were the same as those described already in the previous paper[11]. Several large films prepared were all 0.01–0.03 mm. thick and they were cut in pieces of about 5 mm. × 10 mm. These small pieces of films were then divided into four groups, and each group was placed on a paper in an air-thermostat and subjected to the heat-treatments, the conditions of which are given in Table I. A part

TABLE I

| Sample | Conditions of heat-treatments | Appearance |
|---|---|---|
| I | No heat-treatment | ——— |
| II | 100°C, 30 min. | Almost no change |
| III | 160°C, 15 min. | |
| IV | 193°C, 2.5 min. | Colored slightly brownish |

of the specimens of each group mentioned above were then cut further in smaller sizes of about 1 mm. × 5 mm. and they were used for the density measurements.

**b) Apparatus and Procedures.**—The sorption and desorption*2 isotherms were measured by the desiccator method and the measurements of the density were carried out by the flotation method. The apparatus and the procedures are essentially the same as before[11], so the description of them may be omitted here. The drying condition was about 60°C under a high vacuum ($10^{-4}$ mmHg or below) over phosphorous pentoxide, the vessel being connected to a liquid air trap. For the attainment of constant weight it took about five days. The experiments of sorption and desorption as well as the measurements of density were all performed at 25° ± 0.03°C. For the sorption equilibrium it required about three weeks.

Infrared (from 2 $\mu$ to 15 $\mu$) and ultraviolet absorption spectra (from 200 m$\mu$ to 550 m$\mu$) were also taken for reference to those experiments mentioned above, by using the Perkin-Elmer Model 21 Double Beam Recording Infrared Spectrophotometer with sodium chloride prism and the Beckman Model DU Quartz Spectrophotometer with ultraviolet accessaries respectively.

## Results and Discussion

**a) Density.**—The densities of the bone-dry samples at 25°C are given in Table II. They seem to increase with the rise of the temperatures of heat-treatments. In order to evaluate the crystallinity of a sample from the density data, it is necessary to know the densities of crystalline as well as amorphous

11) H. Tadokoro, S. Seki and I. Nitta, This Bulletin, **27**, 451 (1954).

*2 The details of our desorption experiments will be reported in the next paper.

TABLE II

| Sample | Density at 25°C. (g./cc.) | Crystallinity (From density and X-ray data) | $R/44$ |
|---|---|---|---|
| I | $1.291_0$ | 0.29 | 5.7 |
| II | $1.294_6$ | 0.34 | 5.9 |
| III | $1.300_7$ | 0.42 | 5.9 |
| IV | $1.306_6$ | 0.49 | 4.7 |

regions. The density of the former was calculated to be about 1.34 g./cc. from the lattice constants determined by X-ray investigation[12-15]. On the other hand, that of the latter cannot be measured directly, since the preparation of completely amorphous PVA has not yet been successful. By assuming that the ratio of the density of the amorphous to that of the crystalline state for PVA is of the same order of magnitude as that for other organic hydroxyl compounds, such as butyl alcohol (0.94)[16], as P. H. Hermans did in the case of cellulose[3], the density of the amorphous part was estimated to be about 1.26 g./cc. Recently I. Sakurada and his coworkers found that the crystallinity estimated by the X-ray method for the PVA film specimens, prepared under various conditions of heat- and stretching-treatments, shows an approximately linear relationship with their densities[17]. By extrapolation to zero for the crystallinity they found the density of the amorphous part of PVA to be 1.27 g./cc. This value coincides with that derived above by Hermans' method within experimental error. By use of the density values for the four groups of the specimens in column 2 of Table II together with the relationship of Sakurada et al., we can thus calculate their crystallinity, which is shown in column 3 of the same Table.

We measured also the densities of the samples at moist states for reference. As shown in Fig. 1, each density curve showed a conspicuous maximum at about 1.7, 1.5, 1.1 and 0.8% water content for the samples I, II, III and IV, respectively. This tendency is in good agreement with the discussion in the previous paper which indicated that the water content at which the density shows maximum, decreases in the reverse order to the crystallinity[11].

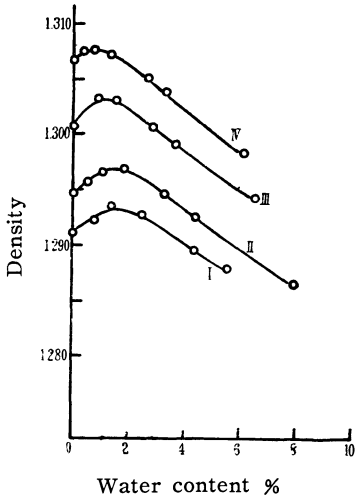



Fig. 1. Density-water content curves.

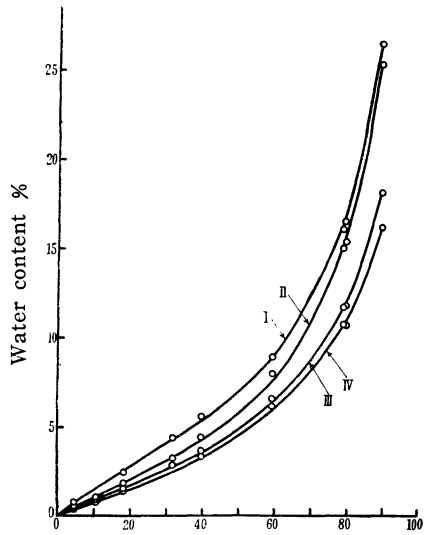



Fig. 2. Sorption isotherms at 25°C.
o Observed value
— Calculated value

**b) Sorption of water vapor.**—The sorption isotherms of water vapor by the PVA films are all given in Fig. 2 and Table III.

As is well known, there are two methods

TABLE III

| Relative humidity | Water content I | II | III | IV |
|---|---|---|---|---|
| 0.048 | 0.0079 | 0.0052 | 0.0046 | 0.0036 |
| 0.108 | — | 0.0107 | 0.0088 | 0.0075 |
| 0.184 | 0.0247 | 0.0182 | 0.0153 | 0.0132 |
| 0.318 | 0.0431 | 0.0323 | 0.0282 | — |
| 0.396 | 0.0553 | 0.0436 | 0.0364 | 0.0330 |
| 0.594 | 0.0890 | 0.0796 | 0.0652 | 0.0610 |
| 0.790 | 0.1606 | 0.1500 | 0.1165 | 0.1070 |
| 0.797 | 0.1650 | 0.1537 | 0.1175 | 0.1067 |
| 0.897 | 0.2640 | 0.2521 | 0.1807 | 0.1617 |

12) R.C.L. Mooney, *J. Am. Chem. Soc.*, **63**, 2828 (1941).
13) C.W. Bunn and H.S. Peiser, *Nature*, **159**, 161 (1947); C.W. Bunn, ibid., **161**, 929 (1948).
14) I. Sakurada and K. Fuchino, *X-Rays*, **6**, 66 (1950); *Rep. Sci. Res. Inst. (Tokyo)*, **20**, 890 (1941).
15) I. Nitta and I. Taguchi, *Ann. Report Inst. Fiber Res. (Osaka Univ.)* **6**, 3 (1952).
16) W. Biltz, *Z. physik. Chem.*, **A151**, 13 (1930).
17) I. Sakurada, Y. Sone and Y. Nukushina, Annual Meeting of the Chem. Soc. of Japan in April 1954.

of estimating the crystallinity of polymers, in a relative sense, from the sorption data: i) the sorption ratio method[9] and ii) the Hailwood-Horrobin method[10].

**i) Sorption ratio method.**[9]—Sorption ratio means the ratio of the water content of a sample to that of a standard sample at the same relative humidity. This ratio is thought to be proportional, in a rough sense, to the fraction of the amorphous region. In the present experiment, sample I was arbitrarily taken as the standard, whereas native cotton has been usually taken as the standard in the case of cellulose.

As for the relative humidity we selected 59.4%, where the swelling is not yet perceptible and the accuracy of the observed data is rather high. Fig. 3 shows the relation between the sorption ratio at this relative humidity and the density.

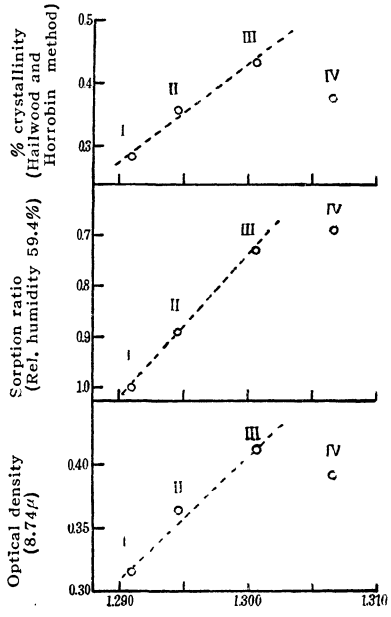



Fig. 3. Crystallinity-density curves (by water sorption and infrared absorption spectrum).

**ii) The Hailwood-Horrobin method.**[10]—Hailwood and Horrobin postulated that moist high polymer is an ideal solid solution of dissolved water, unhydrated polymer molecules, and hydrated polymer molecules, assuming:

$$\frac{W_i}{W_{i-1}a'}=K_i \qquad i=1,\ 2,\ \ldots\ldots \tag{1}$$

where $a'$ is the activity of the dissolved water in the soild phase, $W_i$ is the activity of the $i$-th hydrate of the polymer, and $K_i$ is the appropriate equilibrium constant. It follows that:

$$W_i=W_0(a')^iK_1K_2\ldots\ldots K_i \tag{2}$$

where $W_0$ is the activity of the unhydrated polymer. Using:

$$a'=\bar{K}x \tag{3}$$

where $x$ is the activity of the water in the vapor phase and $\bar{K}$ is a constant, they then equate the activities of the various species to their mole fractions assuming the formation of an ideal solution. This leads them to the following three-parameter equation, neglecting the second and higher hydrates,

$$\frac{Mr}{1800}=\frac{\bar{K}h}{1-\bar{K}h}+\frac{\bar{K}K_1h}{1+\bar{K}K_1h} \tag{4}$$

where $M$ is the "molecular weight" of the operative polymer unit, $r$ is the regain, i.e. the total grams of water absorbed per 100 grams of bone-dry polymer, and $h$ is the relative humidity. Further (4) can be put into the following form:

$$A+Bh-Ch^2=h/r \tag{5}$$

All the curves shown in Fig. 2 were drawn by using three parameters $A$, $B$ and $C$ which were calculated from the data of Table III by the method of least squares. We could find that this equation fit the observed values well.

Assuming that water molecule is not accessible to the interior of the crystalline region, Hailwood and Horrobin then correlated the constant $M$ in this equation (4) with the accessible fraction $\theta$ by the following relation:

$$M\theta=R \tag{6}$$

where $R$ ($\leq M$) is the molecular weight of the "unit" of the polymer molecule which is capable of combining with one molecule of water to form a monohydrate and is equal to $M$ when the polymer is completely amorphous. They assumed further that the value of $R$ is equal to the molecular weight of the unit which contains one characteristic polar group. In our previous paper[11], we assumed that the monohydrate consists of one polymer unit -($CH_2CHOH$)- and one water molecule according to the method of Hailwood and Horrobin. However, since the value of $R$ cannot be checked as such from the measurement of water sorption only, the crystallinity on the basis of the assumed $R$ would be used at most only as a relative measure. In order to see if the value of $R$ comes out to be corresponding to the monomer unit, we calculated it by utilizing the crystallinity shown in column 3 in Table II and the value of $M$ obtained from $A$, $B$ and $C$. In column 4 of Table II, are shown the values of $R/44$ which correspond to the

number of monomer units per one monohydrate (molecular weight of monomer unit =44). It is rather remarkable that these values for samples I, II and III are nearly constant (5.7–5.9) in spite of the rather naïve and crude theoretical treatment by Hailwood and Horrobin, and at the same time the value for sample IV (4.7) is considerably different from the other three, being parallel to the experimental evidences of sorption ratio and others which will be mentioned below. These results will show that this method may be utilized for estimating the relative crystallinity of this material. However, the questions why these values come out nearly constant and whether their magnitude has a definite physical meaning or not, might be solved first by further experiments; the measurement of the adsorption at very low humidity may be useful in this respect.

By taking $R/44=5.8$ for all samples, the crystallinities are then calculated and plotted against the density in Fig. 3.

c) **Infrared absorption spectrum.**—Fig. 4 shows a part of the infrared absorption spec-

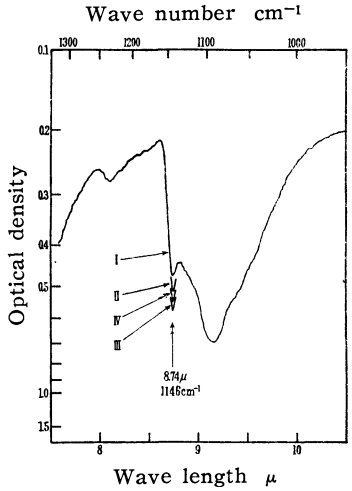



Fig. 4. Infrared absorption spectra of PVA films.

tra of our samples. The curve covering the whole region in this figure is for sample I, while for the other samples only the absorption band at $8.74\mu$($1146\ cm^{-1}$) is given by adjusting the intensity of absorption of seven other bands ($3.4\mu$, $7.0\mu$, $7.40\mu$, $8.06\mu$, $9.15\mu$, $10.9\mu$ and $11.75\mu$) to fit with those of sample I. Although the optical density of the broad and very strong $3.0\mu$ band changes sensitively with the amount of bound water as some investigators reported[18,19], we have confirmed that those of the above-mentioned seven bonds do not depend on the water content. We have also found that the intensity of the $8.74\mu$ band is not affected by the bound water so long as the water content does not exceed several percent. According to the investigation by A. Elliott et al., this band shows striking effect of dichroism, and they also inferred that this band may be due to a kind of absorption mechanism relating to the presence of the oxygen atoms[20]*3. Recently, E. Nagai and his coworkers found further that this band becomes stronger and stronger as the heat-treatment proceeds until the sample becomes colored[21]. As shown in Fig. 4, the intensity of absorption of this band increases in the order of samples I, II and III, and then decreases in IV. The optical density of this band vs. the density is given in Fig. 3. By the linear relationship of the intensity variation of this absorption band to the density and also by other facts mentioned above, we confirmed that this band is really the so-called "crystallization-sensitive" band[2].

Now we proceed to the relationship among these results obtained above. In Fig. 3 the values given in ordinates for the samples I, II and III lie nearly on straight lines, whereas remarkable deviations are found for the sample IV. As the sample IV was subjected to the heat-treatment at the highest temperature, and got colored considerably, so it may be conceived that such an abnormality is due to the occurrence of some chemical changes.

In order to ascertain whether it is really the case or not, the ultraviolet absorption spectra were measured. Our results are shown in Fig. 5, in which the absorption bands at 280 m$\mu$ and 330 m$\mu$ are particulary distinguished for the sample IV. These two bands are considered to be attributed to carbonyl group and carbon-carbon double bond conjugated with the carbonyl group respectively. This conclusion is also in agreement with the results obtained by J. Ukita and his coworkers using the chemical method[22]. As the occurrence of chemical changes in

18) H. W. Thompson and P. Torkington, *Trans. Faraday Soc.*, **41**, 246 (1945).

19) L. Glatt, D.S. Webber, C. Seaman and J.W. Ellis. *J. Chem. Phys.*, **18**, 413 (1950).

20) A. Elliott, E.J. Ambrose and R.B. Temple, *J. Chem. Phys.*, **16**, 877 (1948).

*3 The elucidation of the origin of this band seems to have considerable significance for clarifying the nature and structure of the crystalline part. To get further information we are now studying this point by means of deuterium exchange (H. Tadokoro, S. Seki and I. Nitta, *J. Chem. Phys.*, **23**, 1351 (1955)).

21) E. Nagai, S. Mima, S, Kuribayashi and N. Sagane, *Chem. High Polymers (Japan)*, **12**, 199 (1955).

22) J. Ukita, S. Usami and T. Kominami, *Chem. High Polymers (Japan)*, **11**, 300 (1954).

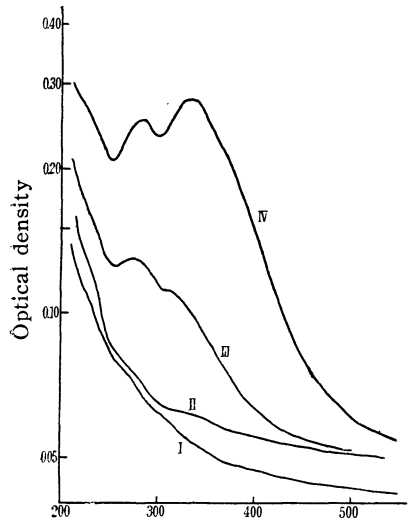



Fig. 5. Ultraviolet absorption spectra of PVA films.

the sample IV were thus ascertained, it may be of less significance to discuss the crystallinity of this sample in comparison with the other three samples on the same grounds. In passing, it may be added here that we found recently the fact that when the heat-treatment was carried out above the temperature of about 180°C, the density-time curve at constant temperature for such a sample shows a maximum in contrast to those treated at lower temperatures*4. This fact may also be explained by the occurrence of chemical changes.

After all, it is ascertained in the present investigation that the crystallinity measured by the X-ray, density, water sorption and infrared absorption methods go approximately parallel with each other as far as chemical change on heating is not appreciable, so the methods we have adopted in the present work may be used for determining the crystallinity.

Although we can correlate the four above-mentioned methods estimating the crystallinity with each other, it would be necessary to carry out further investigation in relation to the detailed texture of solid high polymers in order to obtain deeper insight into the nature of this quantity, "crystallinity". From such a standpoint, we are led to investigate such problems as given below and examine the results with systematical and synthetical criticism:

i) the application of the method for measuring the accessibility, e. g. deuterium exchange*3,

ii) the application of the method for studying the texture, e. g. X-ray small angle scattering*5,

iii) the assignment of the crystallization-sensitive band in infrared absorption spectra*3,

iv) the application of a new method for localizing hydrogen atoms, e. g. proton magnetic resonance absorption, chemical shift,

v) the comparative investigations with other high polymers, e. g. cellulose, nylon, etc.

*4 Details of this experiment will be published later.

## Summary

i) Densities, sorption of water vapor and infrared absorption spectra were measured on four kinds of PVA films, which were prepared from the same PVA powder specimen and subjected to different heat-treatments.

ii) It was found by the present investigation that the 1146 $cm^{-1}$ (8.74$\mu$) band is the so-called crystallization-sensitive band.

iii) Since the degrees of crystallinity determined by these methods went in parallel, it was found that they may be used as relative measures for the crystallinity.

iv) Samples subjected to the heat-treatment at about 193°C, behave abnormally from the other three groups of samples. This deviation was found to be due to chemical changes occurring in the heat-treatment. This was confirmed by the measurement of ultraviolet absorption spectra.

The authors express their sincere thanks to Mr. Y. Sone of the Institute for Chemical Research of Kyoto University for helpful advice and criticism, to Messrs. E. Nagai and S. Kuribayashi of the Osaka Industrial Research Institute and Dr. M. Momotani of Momotani Juntenkan Co., Ltd. for preparing charts of infrared absorption spectra, to Mr. S. Fukushima of this Faculty for preparing data of ultraviolet absorption spectra, to Mr. K. Kôzai for his collaboration in our experiments, and to Kurashiki Rayon Co., Ltd. for kindly giving them the PVA samples.

*Department of Chemistry, Faculty of Science, Osaka University, Osaka*

*5 For the elucidation of the texture, the X-ray small angle scattering method seems to be very helpful. For this purpose Dr. M. Kakudo of the Faculty of Engineering of this University is now studying this problem in relation the to same materials we are using at present in accordance with our request.

Note added in Proof: According to Fig. 1 of the paper by E. Nagai, S. Mima, S. Kuribayashi and N. Sagane[21] the fourth point (of the specimen of the density 1.306$_6$) lies on the straight line. This is in contradiction to our result. Such discrepancy might be due to the fact that they have chosen 3.0 $\mu$ absorption band as the standard, which does not seem to be adequate judging from our observation.

# *Studies on Several Phosphates from the View-point of Analytical Chemistry. IV. A Radioactive Paper Chromatography on Several Meta- and Poly-Phosphates labelled with $P^{32}$**

By Mutsuaki SHINAGAWA, Junichi TAKANAKA, Yoshiyuki KISO, Aiko TSUKIJI and Yōko MATAMA

(Received November 15, 1954)

Recently the studies on several meta- and poly- phosphoric acids and their phosphates have been carried on by many investigators, but it appears that no definite method for separational analysis has been yet established. Therefore, the authors synthesized several phosphates labelled with $P^{32}$ and investigated their chromatograms at various rates using pyridine-water as solvent.

## Material and Reagents

### (1) Samples

Samples were obtained by synthesizing sodium ortho-, pyro-, tripoly-, trimeta- and hexametaphosphates, each labelled with $P^{32}$.

As there was only a little radioactive material, it was impossible to synthesize the labelled substances to a great degree. Hence we were unable to use it as a purified sample.

*a) Disodium-hydrogen-orthophosphate* ($Na_2HPO_4$)[1]. —With reference to Richard C. Vogel and H. Podall's report[1], the preparation was made by adding 10 ml. of "carrier-free" phosphate (by diluting 2 mc. of "carrier-free" to 50 ml. of distilled water slightly acidified by hydrochloric acid) to 1 g. of disodium-hydrogen-orthophosphate. After agitation at 110°C it was used as a dehydrated salt.

*b) Sodium-pyrophosphate* ($Na_4P_2O_7$)[2].—About 1 g. of sodium-dihydrogen-orthophosphate was heated in a platinum-crucible and maintained at 210°C for twelve hours. The purity was more than 97%.

*c) Sodium-trimetaphosphate* ($Na_3P_3O_9$)[2].—About 1 g. of sodium-dihydrogen-orthophosphate was heated in a platinum-crucible and maintained at 300°C for one hour and then at 610°C for three hours, lowered to 390°C slowly in that same condition, and then allowed to stand for fourteen hours. After the finely powdered substance was placed in a desiccator, this was lowered to room temperature.

*d) Sodium-tripolyphosphate* ($Na_5P_3O_{10}$)[2].—Sodium-dihydrogen-orthophosphate and disodium-hydrogen-orthophosphate were mixed in the proportion of 1:2. This was heated to 800°C and maintained at this temperature for a period of eighteen hours, so it could completely melt. The temperature was then lowered gradually from 650°C to 250°C, which required about eight hours, and then cooled in a desiccator.

*e) Sodium-hexametaphosphate* ($Na_6P_6O_{18}$)[2].—Monosodium-dihydrogen-orthophosphate was heated to about 900°C and maintained at this temperature for three hours in a platinum crucible and then the melted mass was cooled rapidly. Different batches of the resulting glassy product contained from 90% to 95% sodium-hexametaphosphate.

Each phosphate was dissolved in water and about 0.1 mol. solutions were prepared.

### (2) Solvents

The solvents were prepared by mixing *n*-$C_4H_9OH$, and $H_2O$ and 11 N $NH_4OH$ in the ratio of 8:1:1 in volume respectively and by mixing pyridine and water in the ratios of 0:1, 1:4, 3:7, 1:2, 2:3, 1:1, 3:2, and 1:0 in volume.

### (3) The Method of Development

The chromatograms were developed by the ascending method on Toyo Rosi No. 50 paper for six to ten hours in a chromatographic cylinder, which was kept at 25±1°C in the thermostat. The making of the cylinder was based on W. H. Longenecker[3] and Otosai's apparatus[4]: The size of paper was 1 cm.×40 cm. and sufficiently long to provide a chromatograph path of 30 cm. On this about 0.02 micro-mol. of samples were placed with capillary on each sheet approximately 4 cm. above the surface of the solvent.

### (4) The Method for Detection

Recently studies on application of chromatography by using the radioactive method were made by H. Muller[5] and H. H. Strain[6], who also devised a convenient apparatus for measuring radiation. The authors devised a simple apparatus, which was used in the test as shown in Fig. 1.

The following were used in this apparatus.

Hundred scaling G. M. Counter (Kobe Tech. Co.).

Two sheets of stainless steel (10 cm.×10 cm.×2 mm.) for slit.

A glass plate (10 cm.×30 cm.×2 mm.) upon which the papers were slid. A 30 cm. ruler.

* Presented at the 7th. Annual Meeting of Chem. Soc. of Japan, April 1954.

1) R.C. Vogel and H. Podall, *J. Am. Chem. Soc.*, **72**, 1420 (1950).

2) L.T. Jones, *Ind. Eng. Chem. Anal. Ed.*, **14**, 536 (1942).

3) W.H. Longenecker, *Anal. Chem.*, **11**, 402 (1949).

4) K. Otosai, *Kagaku no Ryoiki*, **8**, No. 8, 25 (1950).

5) R.H. Muller, *Anal. Chem.*, **23**, 208 (1951).

6) T.R. Sato, W.P. Norris and H.H. Strain, *Anal. Chem.*, **24**, 776 (1952).

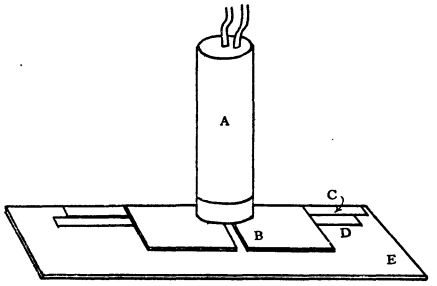



Fig. 1. Counting technique. A, counter tube holder; B, stainless steel slit; C, 30 cm. ruler; D, paper; E, glass-plate.

As shown in Fig. 1 the position of the G. M. tube is fixed. Two sheets of stainless steel were used to make a slit, the width of which was adjustable from 0.25 to 0.5 cm. These steel plates were placed over the glass plate, between which the paper could be moved at intervals of 0.25 or 0.5 cm. At each interval the count was made for one minute. The measured counting rates per minute were plotted against the developed distances.

During the measurement, there was no possibility of contamination on the surface of the slit or elsewhere. This was proved from the results of various tests.

Rf's were determined from the positions which are shown as the maximum counting rate.

Several phosphate ions came to their characteristic places regularly in the paper according to the differences of mobilities.

## Results and Discussion

a) Although the separation of several phosphate ions was examined with the solvent of $n$-$C_4H_9OH-H_2O-11$ N $NH_4OH$ (8 : 1 : 1), the result was not successful. Rf's were approximately zero.

b) The developed states of a crude hexameta-phosphate at the various rates of pyridine-water solvent are shown in Fig. 2, in which the greatest peak should be hexametaphosphate, the main component, while others having the smaller peaks should be some impurities of the other types of phosphates.

From Fig. 2 it could easily be recognized that the most satisfactory result was obtained in the case of pyridine-water (1 : 1) and the result was found to be reproducible. Fig. 3 was introduced from the relation of Rf's of several phosphates ions with the various rates of pyridine-water solvent.

The results showed the following. When samples were developed only with water, all Rf's were nearly 1.0, but trimetaphosphate ions could be separated a little from other ions. Consequently, the other mutual ions except trimeta-ion could not be separated completely.

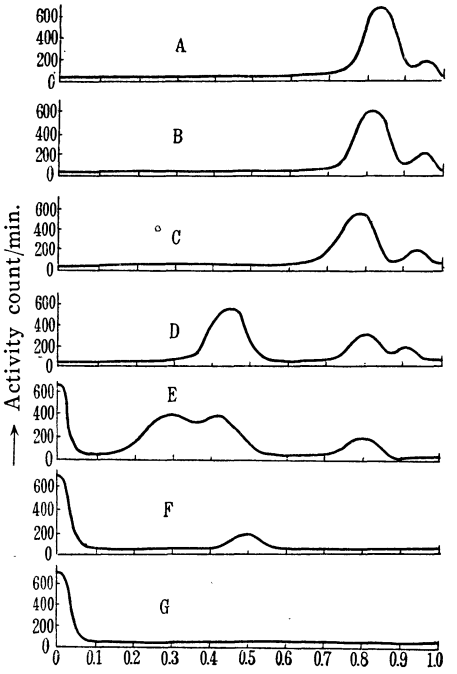



Fig. 2. Radioactive chromatograms of synthesized hexametaphosphate at various rate of pyridine-water.

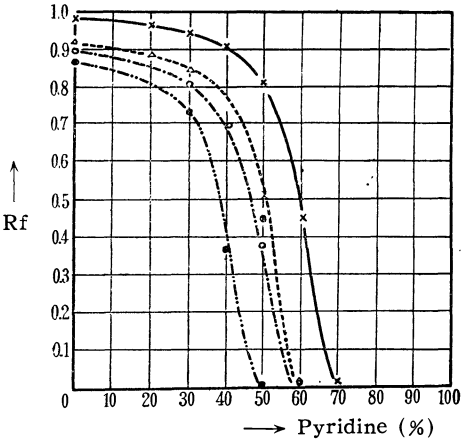



Fig. 3. Diagrams of Rf-amount of pyridine (%). △, orthophosphate ion; ⊙, pyrophosphate ion; ×, trimetaphosphate ion; ○, tripolyphosphate ion; ●, hexametaphosphate ion.

Corresponding to the increase of pyridine the mutual separation among several phosphate ions gradually became possible. Pyridine-water (1 : 1) appeared to be the most desirable solvent for separation.

When the rate of pyridine was increased further, Rf's of each phosphate ion decreased and approached zero. However, the decrease of trimeta ions was comparatively delayed.

A in Fig. 4 shows the peak of trimeta-

phosphate ion. B in Fig. 5 shows the case in which hydrolysis of hexametaphosphate did not occur. The small peak at the right hand side in the figure indicates an impurity of the hexametaphosphate. This can be quite conceivable from the results of the other investigators[7]. C in Fig. 4 shows the result of the tripolyphosphate ion having a indistinct double peak. The peak having smaller Rf-value was due to tripolyphosphate ion and the other was due to orthophosphate ion, according to the peak shown in G in Fig. 4 which was due to orthophosphate ion. A peak of similar nature can be seen in D in Fig. 4, which was obtained with the mixed sample of several phosphate ions. E in Fig. 4 shows the result of pyrophosphate ion.

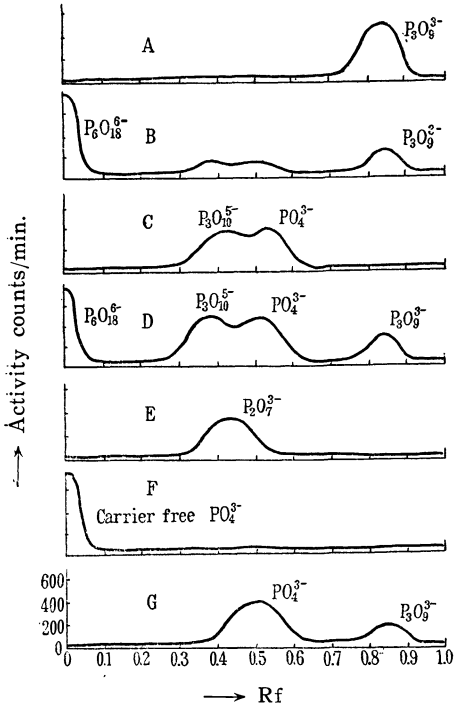



Fig. 4. Radioactive chromatogrames for several phosphates at 1-pyridine-1-water.
A. trimetaphosphate
B. hexametaphosphate C. triphosphate
D. trimeta-, ortho-, tri- and hexametaphosphate E. Pyrophosphate
F. "carrier free" orthophosphate
G. orthophosphate labelled with 'carrier free' orthophosphate.

Especially interesting cases are shown in F, G in Fig. 4. In the case of F, "carrier-free" orthophosphate was developed. The peak can be seen only at the position of its origin. In the case of G the figure was obtained with the orthophosphate ion labelled with the "carrier-free" phosphate ion just mentioned, and showed two peaks. The same result was also obtained when the trimetaphosphate was used as carrier. Judging from the results of A, B and D, the right-side peak must be due to trimetaphosphate ions and the left-side peak is large enough to be considered due to the main component; i.e. the orthophosphate ions. The peak of trimetaphosphate ion must be an impurity of the "carrier-free" orthophosphoric acid which was imported from U. S. A.

Strain[8] has already made a report on a similar fact in the case of electrochromatographic separation for calcium phosphate, but he did not clearly mention what type of ions the impurity had.

## Summary

1) To separate various meta-and poly-phosphate ions respectively, pyridine-water (1 : 1) was found to be the most desirable developing solvent. Especially, both trimeta- and hexameta-phosphate ions can be separated from the ortho-, pyro-, and tripoly-phosphate ions, but the latter were not completely separated. The authors plan to separate them after further study of solvents.

However, by using labelled radioactive substances, it may possible to detect the impurity in synthesized phosphate or the traces of other phosphates in the main component. If the radioactive dilution method should be applied, this method may be used in determining nonactive substances. No special care was necessary in this case concerning the atom-exchange of phosphorus between active phosphate ions and non-active[1].

2) As shown in Fig. 4 it may be possible to determine hydrolysis products by the present simple method.

3) There is a certain regular relationship between the ionic structures and their Rf's. That is to say, Rf's will decrease in proportion to the increase of the number of phosphorus atoms contained in each kind of ions with chain structure, while trimetaphosphate having a cyclic structure has greater Rf value than others with chain structure.

*Chemical Laboratory, Faculty of Science, Hiroshima University, Hiroshima*

7) M. Kobayashi and M. Shinagawa, *Kagaku no Ryoiki*, 8, No. 2, 39 (1954).

8) T.R. Sato, W.E. Kisieleski, W.P. Norris and H.H. Strain, *Anal. Chem.*, 25, 438 (1953).

# *Studies on Several Phosphates from the View-point of Analytical Chemistry. V. An Electro-Chromatography on Several Meta- and Poly-phosphates labelled with $P^{32}$*

By Mutsuaki SHINAGAWA, Junichi TAKANAKA, Yoshiyuki KISO, Aiko TSUKIJI, and Yōko MATAMA

(Received November 15, 1954)

In the previous paper[1] we reported on the separation by paper chromatography of several meta- and poly-phosphates. In this paper the behaviour of several phosphate ions in electro-chromatography is discussed. The detection of the positions to which several phosphate ions migrated was carried out with active phosphates labelled with $P^{32}$ and was found to be made possible by decolorization caused by the formation of complex metal phosphates.

## Material and Apparatus

Samples used were sodium ortho-, pyro-, trimeta-, tripoly-, and hexameta-phosphate[1,2]. Almost all the separations reported here were performed on paper moistened with a single supporting electrolyte, i.e. aqueous acetic acid or ammonium acetate. Filter paper (Toyo Rosi No. 50, size 20 cm. × 20 cm.) was employed in all the experiments described herein. Aqueous solutions permeate this paper exceptionally well and hence it was found useful in the formation of chromatograms which may be developed quickly by flow of solvant.

The control of temperature of the paper during the electrical migration was not necessary because there was no remarkable change of temperature. A dry sheet of filter paper was placed on the glass sheet (the size was equal to that of the paper) and the acetic acid solution was added until an excess was present in the paper. After a few minutes, the excess electrolytic solvent was removed with a piece of blotting paper and the mixed solutions to be investigated were then added by a sharp-pointed capillary to pencilled circles on the paper.

Platinum wire electrodes were placed along both ends of the paper on which a glass sheet of the same size was placed. These two glass plates were firmly pressed together with clamps. Potential (0 to 300 V.) from an electronic rectifier was applied to these electrodes.

## Detection and Identification of Several Ions

**a) Tracer Method.** — The migration of radioactive ions in the moist paper was followed with a thin-window G. M. Counter[1]. When the separation was complete, the moist filter paper was placed in a warm (25°~30°C) well ventilated hood and dried on a table shielded from radioactive contamination by a thick nonactive paper placed on glass sheets. The filter paper was then cut along pencilled lines and it was found that the ions had migrated parallel to the lines and had been separated. The cut papers were treated by the method reported previously[1] and hence radioactive ions separated in the filter paper were detected directly with a G. M. tube and scaler. Non-radioactive ions and acidic and basic zones in the paper were detected with suitable reagents and acid-base indicators.

**b) Chemical Method.** — In spot tests of phosphate ions, Feigl[3], Hanes, and Isherwood[4] have already applied the formation of molybdenum blue from complex phosphomolybdate. We were able to detect phosphate ions (0.1 to 0.05 M) simply, by using Fe (III) (0.01 to 0.005 M) and $[Fe(CN)_6]$ (IV) (0.01 to 0.05 M) as reagents. Concentrations of reagents were adjusted so they could correspond with that of the samples. Sample solutions were dropped on the filter paper and dried in air. Then iron alum solution was sprayed on uniformly and again after drying in air, $[Fe(CN)_6]$ (IV) ion solution was sprayed on. Instantly the paper turned prussian blue in colour, but the parts where phosphate ions were present remained unchanged or developed somewhat different colours as compared with the colour of the

1) M. Shinagawa, T. Takanaka, Y. Kiso, A. Tsukiji and Y. Matama, This Bulletin, **28**, 565 (1955), Presented at the 7th Annual Meeting of Chem. Soc. of Japan, April 1954.

2) L.T. Jones, *Ind. Eng. Chem. Anal. Ed.*, **14**, 536 (1942).

3) F. Feigl, "Qualitative analysis by spot test" 3rd English edition, 1947, p. 251. F. Feigl, *Z. Anal. Chem.*, **61**, 454 (1922); **74**, 386 (1928).

4) C.S.I. Isherwood, *Nature*, 164, 1107 (1949).

background. If the reagent solution were sprayed in reverse, it was possible to detect and identify phosphate ions by the difference in colours of the discoloured spots and in the widths of spot-rings, as shown in Table I.

TABLE I

SPOT TEST FOR SEVERAL PHOSPHATE IONS

| Phophate ion | Colour of spot | Width of ring | Identif. Lim. |
|---|---|---|---|
| $PO_4^{3-}$ | thin violet | narrow | 10 $\gamma$ |
| $P_2O_7^{4-}$ | thin violet | diffuse | |
| $P_3O_9^{3-}$ | deep blue | diffuse | |
| $P_3O_{10}^{5-}$ | thin violet | wide | 1.3 $\gamma$ |
| $P_6O_{18}^{6-}$ | thin blue | narrow | 20 $\gamma$ |

Identification limit of tripolyphosphate ion was the smallest among several phosphates. Identification limits shown in Table I are minimum quantities that permit the specific detection of each ion. However when the detection was not restricted to specificity, the detection limits were much smaller.

These methods for detecting phosphate ions proved satisfactory in procedure and in specific detection and were comparable to Feigl's method[4].

This method could be applied to paper chromatography and electro-chromatography.

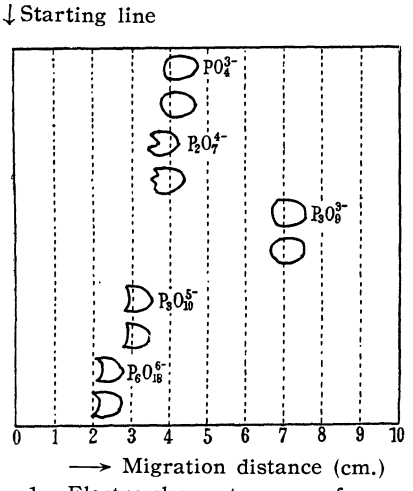



Fig. 1. Electro-chromatograms of several phosphate ions. Potential, 300 volts per 20 cm.; migration time, 2 hours; electrolyte, 0.1 mol. ammonium acetate.

## Result

Fig. 1 was obtained by the detection method reported previously[3].

The vertical axis indicates the counting rate per minute and horizontal axis the migration distances of each phosphate ion. Sample concentration was about 0.05 M; the migration time, two hours; and the electrolyte concentration, 0.1 M.

Fig. 2 shows the decolorization patterns of phosphate ions which was gotten from the method of decolorization.

Fig. 1 and Fig. 2 were obtained from same experimental results.

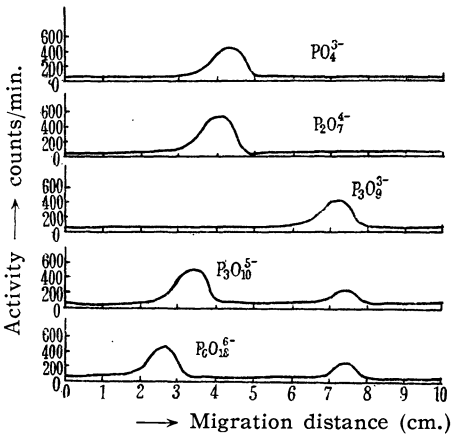



Fig. 2. Electro-chromatograms of several phosphate ions. Potential, 300 volts per 20 cm.; migration time, 2 hours; electrolyte, 0.1 mol. ammonium acetate.

## Summary

1) Several phosphate ions can be separated by the present electro-chromatographic method. This method of separation is a vast improvement over the paper chromatography.

2) The smaller the number of phosphorus atoms contained in a phosphate ion, the greater the migration rate of ion in the case of chain ionic structure. Trimetaphosphate ion which has ring ionic structure showed the greatest migration rate among all of them.

3) The test by means of prussian blue was more distinct in electro-chromatography than in paper chromatography.

*Chemical Laboratory, Faculty of Science, Hiroshima University, Hiroshima*

# *The Effect of Pressure on the Semi-conductivity of Isoviolanthrone*

By Hiroo INOKUCHI

(Received April 18, 1955)

On the semiconductive properties of violanthrene and related polycyclic aromatic compounds reports have been presented in the previous papers[1,2]. Since the preparations of single crystals of those compounds are very difficult and the specimens are obtained in powdered form, the measurements of electrical resistivity were usually made under compressed states. In such a condition, the apparent resistivity is likely to depend strikingly upon the compressive pressure. The relation between resistivity and pressure up to 300 kg./cm² has been reported in a preceding paper[3]. The results showed that resistivity decreases remarkably with increasing pressure up to 80 kg./cm²; however, thereafter it becomes approximately constant. A similar result was also reported by D. D. Eley et al.[4] For this and other reasons, we have assumed that the observed resistivity is an intrinsic one, excluding the contact resistance between the crystalline particles, when measurement was made beyond 80 kg./cm².

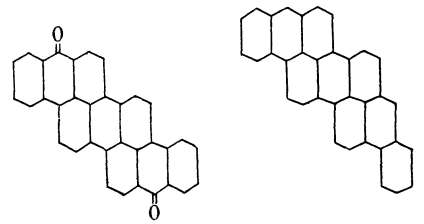
There is an interesting point concerning the pressure effect on the conductivity of organic semi-conductors. Polycyclic aromatic compounds are made of a typical molecular lattice, wherein the intermolecular force is none other than van der Waals type and not so great as compared with that in ionic or valence bond crystals. From the measurements of the heat of sublimation, the intermolecular force is found to depend on the molecular weight and 30.2 kcal./mol. for perylene and 52.3 kcal./mol. for violanthrene[5]. The compressibility is not known; however, it is presumably rather high*.

Therefore, it could be presumed that when these organic semi-conductors are compressed under high pressure, the molecules would be brought nearer to each other than the equilibrium positions and this is accompanied by further overlapping of the electron clouds (diffuse $\pi$-orbitals) or every molecule; this would have an effect on the semi-conductivity.

In this paper the effect of hydrostatic pressure up to 8,000 kg./cm² is presented.

## Experimental Procedures

Among the condensed polycyclic aromatic compounds, violanthrene ($C_{34}H_{18}$) and isoviolanthrone ($C_{34}H_{16}O_2$) were selected for measurements (Fig. 1). These samples were purified as already described[6], and made into a rod, 2 mm. diameter and 6 mm. height, under ca. 300 kg./cm² pressure. This rod was supported by copper wire in a silicon oil as is shown in Fig. 2. In order to prevent silicon oil from flowing out from a gap between piston and cylinder, this contact was made carefully air-tight. Subsequently, this rod




isoviolanthrone violanthrene

Fig. 1. Isoviolanthrone and violanthrene.

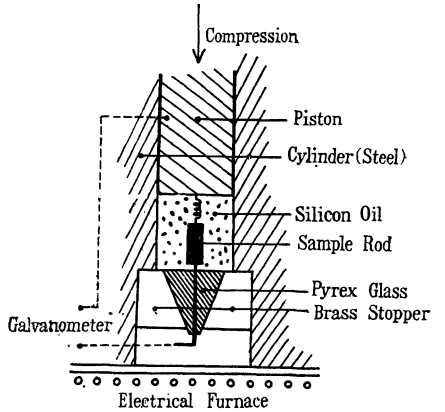



Fig. 2. A diagram of compression apparatus.

1) H. Akamatu, *Kagaku* (Iwanami), 282 (1954).
2) H. Inokuchi, This Bulletin, **24**, 222 (1951); **25**, 29 (1952); **27**, 22 (1954).
3) H. Akamatu and H. Inokuchi, *J. Chem. Phys.*, **18**, 810 (1950).
4) D.D. Eley et al., *Trans. Farad. Soc.*, **49**, 79 (1953).
* The compressibility of benzene (solid) and naphthalene is $20\sim30\times10^{-6}$ (range 100 kg./cm²~1,000 kg./cm² compression)[7,8], then the volume change is 2% of its initial value under 1,000 kg./cm².
5) H. Inokuchi, S. Shiba, T. Handa and H. Akamatu, This Bulletin, **25**, 299 (1952).
6) H. Akamatu and K. Nagamatsu, *J. Colloid Sci.*, **2**, 593 (1947).
7) T.W. Richards et al., *J. Am. Chem. Soc.*, **43**, 1538 (1921).
8) H. Essex, *Z. anorg. Chem.*, **88**, 200 (1914).

was compressed by hydrostatic power with hydraulic press.

Since the compressed specimen has pretty good conductivity, the conductivity measurement was made directly without using D.C. amplifier. To know the temperature dependency of conductivity, samples were heated by electrical furnace from a room temperature up to 130°C as shown in Fig. 2.

## Results and Discussion

The electrical resistivity of these organic semi-conductors decreased with compression above 300 kg./cm². The resistivity of isoviolanthrone was lowered to one five-hundredth of its value at an ordinary compression (under 80 kg./cm²~300 kg./cm² pressure). This relation is shown in Fig. 3. This decrease of resistance is of the same order as in the case of phosphorus[9] or selenium[10], that is, the decrease of resistivity of the former being to 1/1000 of its initial value with 20,000 kg./cm² compression, and that of the latter being to 1/50~1/200 under 3,000 kg./cm².

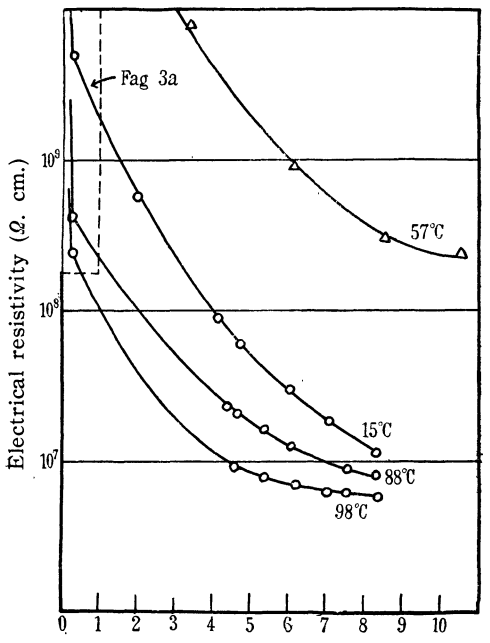



Fig. 3. The relation between electrical resistivity ($\rho$) and pressure ($p$).
△ Violanthrene
○ Isoviolanthrone

As shown in Fig. 3a, the resistivity-pressure relation curve seems reasonably to divide into two parts. The former one (I) has a deep descent between the pressure range of 0 to 80~100 kg./cm² and the latter part (II) has a mild descent above the pressure of 80~100 kg./cm². The kink point of this curve is coincident with one in which electrical resistivity is constant against pressure approximately[3]. Then it seems to be possible to suppose that the curve (I) is due to the plastic deformation of a specimen with the increasing pressure and latter part (II) is an elastic deformation of the compound.

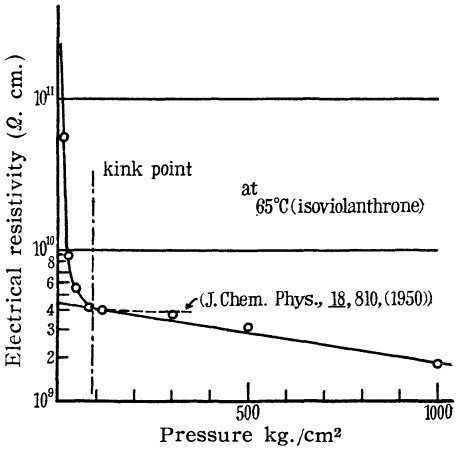



Fig. 3a. The $\rho$-$p$ curve between the pressure range of 0 to 1,000 kg./cm².

Therefore, for the reason mentioned above, it seems that the intrinsic value of electrical resistivity of this group is obtained by the extrapolation of the curve (II) at the section of the axis of pressure 0 kg./cm². This value is coincident approximately with the observed one of electrical resistivity under 80 kg./cm² ~300 kg./cm² compression, and these results are consistent with the previous reports[3].

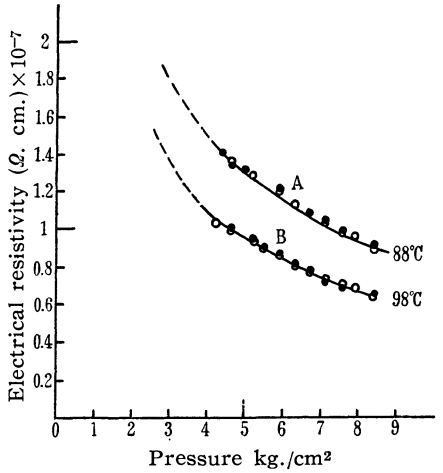



Fig. 4. The reversible curve of $\rho$-$p$ relation of isoviolanthrone.
○ increasing pressure
● decreasing pressure

9) P.W. Bridgman, *Proc. Nat. Acad. Sci.*, **21**, 109 (1935).
10) F. Montén, Diss., Upsala (1909).

The change of resistivity was quite reversible to the pressure. Fig. 4 shows this relation between the electrical resistivity and the pressure from 3,000 kg./cm² to 8,000 kg./cm². From this relation, I think also that the observed decrease of electrical resistivity is an intrinsic one due to the elastic deformation of crystals, but not due to the change of crystal packing nor to any other plastic deformation.

The temperature dependency of the electrical resistivity ($\rho$) of these specimens has the semi-conductive character, that is,

$$\rho = \rho_0 \exp(\Delta\epsilon/2kT) \qquad (1)$$

where $k$ is the Boltzmann's constant, $T$ is the absolute temperature and $\Delta\epsilon$ is the activation energy. $\Delta\epsilon$, corresponds to the energy gap between the occupied level and the empty level, decreased too with increasing pressure, but as shown in Table I the change was rather small.

TABLE I

THE VALUE OF $\rho_{15}^{\circ}$ AND $\Delta\epsilon$ OF ISOVIOLANTHRONE WITH A COMPRESSION

| Compression kg./cm² | $\rho_{15}^{\circ}\Omega$. cm. | $\Delta\epsilon$ kcal./mol. | $\Delta\epsilon$ e.V. |
|---|---|---|---|
| $3\times10^2$ | $5\times10^9$ | 17.3 | 0.75 |
| $4.2\times10^3$ | $8.4\times10^7$ | 17.0 | 0.74 |
| $6.3\times10^3$ | $2.6\times10^7$ | 15.9 | 0.69 |
| $8.4\times10^3$ | $1.2\times10^7$ | 15.0 | 0.68 |

From the above results, the author inclines to assume that the increment in electrical conductivity with high pressure is contributed by electron clouds overlappings between molecules in the molecular lattice.

If the elastic constants of these organic crystals are known, and if these compounds are more compressed, we may have very interesting results.

## Summary

The electrical resistivity of isoviolanthrone ($C_{34}H_{16}O_2$) and violanthrene ($C_{34}H_{18}$) decreased with compression. The resistivity of isoviolanthrone was lowered to 1/500 of its value ($5\times10^9$ Ω.cm.) at an ordinary pressure, that is, $8.4\times10^7$ Ω.cm. at $4.2\times10^3$ kg./cm² and $1.2\times10^7$ Ω.cm. at $8.4\times10^3$ kg./cm² at 15°C. Further it is possible to suppose that the observed decrement of electrical resistivity is an intrinsic one, due to elastic deformation of crystals.

The author desires to express his hearty thanks to Prof. H. Akamatu for his kind direction of this study. The cost of this research has been defrayed from the Grant in Aid for Fundamental Scientific Research from the Ministry of Education, to which the author's thanks are also due.

*Department of Chemistry, Faculty of Science, The University of Tokyo, Tokyo*

# *Absorption Spectra of Co(III) Complexes. I. Curve Analyses of the First and Second Absorption Bands*[1)]

By Yoichi SHIMURA and Ryutaro TSUCHIDA

(Received April 25, 1955)

## Introduction

There have been offered two experimental equations of some applicability for the broad absorption band such as the first or second absorption band[2)] of metallic complexes. The one is the equation of Kuhn and Braun[3)], and the other, Lowry and Hudson's[4)]:

Kuhn and Braun's equation

$$\varepsilon=\varepsilon_{\max}\exp\left(-\left[\frac{\nu_{\max}-\nu}{\theta}\right]^2\right), \qquad (1)$$

Lowry and Hudson's equation

$$\varepsilon=\varepsilon_{\max}\exp\left(-\left[\frac{\nu_{\max}}{\nu}\cdot\frac{\nu_{\max}-\nu}{\theta}\right]^2\right), \qquad (2)$$

1) Presented at the Symposium on Co-ordination Compounds, Tokyo, November 14, 1954.

2) For general discussion of the first and second bands of co-ordination compound the reader is requested to refer to the following literature. a) R. Tsuchida, This Bulletin, **13**, 388, 436 (1938). b) R. Tsuchida, "The Colours and Structures of Metallic Compounds", (in Japanese), Osaka, 1944. c) Y. Inamura and Y. Kondo, *J. Chem. Soc. Japan*, **72**, 843 (1951).

3) W. Kuhn and E. Braun, *Z. phys. Chem.*, **B 8**, 281 (1930).

4) T.M. Lowry and H. Hudson, *Phil. Trans.*, **A 232** 117 (1933).

where $\varepsilon$ and $\varepsilon_{max}$ are the formal extinction coefficients at frequencies $\nu$ and $\nu_{max}$, $\nu_{max}$ being the frequency of maximum absorption. The value of $\theta$ is determined by the relation

$$\theta=\frac{l}{2\sqrt{\ln 2}}=\frac{l}{1.665}, \quad (3)$$

where $l$ is the half-value width of the band, i.e., the difference between the two frequencies, $\nu_k$ and $\nu_l$, where the formal extinction coefficients are equal to the half of $\varepsilon_{max}$:

$$l=\nu_l-\nu_k \ (\nu_l>\nu_k). \quad (4)$$

The equation (1) is based upon the assumption of a symmetrical distribution in frequencies, while the equation (2) postulates a symmetrical distribution in wave-lengths.

Kuroya[5] and Shimura[6] employed the equation of Kuhn and Braun in the analyses of the spectra of Co(III) nitro- or isothiocyanato-complexes, and the Lowry and Hudson's equation was used by Mead[7] and Mathieu[8] in studying Cr(III) and Co(III) complexes. All these authors, however, adopted the equations with some modifications of the values of $\theta$'s in order to get agreement with experimental curves.

As will be seen in this paper, in fact, the first and second bands of the Co(III) complex compounds are not symmetrical either on the scale of frequency or of wave-length. An unsymmetrical equation of absorption band had been offered by Bielecki and Henri[9], but this was not superior to the equation (1) or (2). In this report, a new unsymmetrical equation has been developed and the general applicability has been substantiated by the analyses of absorption curves of the typical Co(III) complexes.

## Experimental

The visible and ultraviolet absorption spectra of about fifteen typical Co(III) complexes were measured in aqueous solutions. The numerical data for the first and second bands of the complexes are collected in Table I, and typical absorption curves are shown in Figs. 1-4. The

TABLE I

ABSORPTION DATA OF THE FIRST AND SECOND BANDS OF Co(III) COMPLEXES

| Type | Complex Salt | First Band | | | | Second Band | | | | $\Delta(\nu_{max})$ | $\Delta(\log\varepsilon_{max})$ |
|---|---|---|---|---|---|---|---|---|---|---|---|
| | | $\nu_{max}$ ($10^{13}$/sec.) | $\log\varepsilon_{max}$ | $l$ ($10^{13}$/sec.) | $\delta$ ($10^{13}$/sec.) | $\nu_{max}$ ($10^{13}$/sec.) | $\log\varepsilon_{max}$ | $l$ ($10^{13}$/sec.) | $\delta$ ($10^{13}$/sec.) | ($10^{13}$/sec.) | |
| 6N | $[Co(NH_3)_6](ClO_4)_3$ | 62.9 | 1.68 | 10.3 | 0.45 | 88.3 | 1.60 | 12.5 | 0.35 | 25.4 | −0.08 |
| | $[Co\ en_3](ClO_4)_3$ | 63.9 | 1.94 | 10.4 | 0.55 | 88.4 | 1.90 | 12.0 | 0.4 | 24.5 | −0.04 |
| | *trans*-$[Co\ en_2(NH_3)_2](ClO_4)_3\cdot H_2O$ | 64.2 | 1.77 | 10.8 | 0.8 | 89.2 | 1.73 | 12.3 | 0.55 | 25.0 | −0.04 |
| | *cis*-$[Co\ en_2(NH_3)_2](ClO_4)_3\cdot H_2O$ | 64.4 | 1.79 | 10.7 | 0.65 | 89.4 | 1.74 | 12.6 | 0.5 | 25.0 | −0.05 |
| 5N1O | $[Co\ en_2\ glycine'](ClO_4)_2$ | 61.3 | 2.00 | 11.2 | 0.7 | 86.4 | 2.04 | 12.5 | 0.3 | 25.1 | +0.04 |
| | $[Co\ en_2\ leucine'](ClO_4)_2$ | 61.5 | 2.02 | 11.3 | 0.65 | 86.1 | 2.06 | 12.4 | 0.5 | 24.6 | +0.04 |
| 4N2O | $[Co(NH_3)_4\ ox]ClO_4\cdot H_2O$ | 58.7 | 1.91 | 10.4 | 0.5 | 84.0 | 2.11 | 12.3 | 0.35 | 25.3 | +0.20 |
| | $[Co\ en_2\ ox]Cl\cdot 3H_2O$ | 60.1 | 2.05 | 10.1 | 0.45 | 84.3 | 2.16 | 12.7 | 0.45 | 24.2 | +0.11 |
| | $[Co(NH_3)_4CO_3]ClO_4$ | 57.4 | 2.01 | 9.8 | 0.35 | 82.6 | 2.02 | —* | —* | 25.2 | +0.01 |
| | $[Co\ en_2\ CO_3]ClO_4$ | 58.4 | 2.13 | 9.4 | 0.3 | 83.0 | 2.09 | 13.3 | 0.0 | 24.6 | −0.04 |
| 3N3O | α-[Co glycine'$_3$]** | — | — | — | — | 80.4 | 2.16 | 12.1 | 0.35 | — | — |
| | β-[Co glycine'$_3$]*** | 57.7 | 2.20 | 9.1 | 0.55 | 80.2 | 2.14 | 12.7 | 0.6 | 22.5 | −0.06 |
| 2N4O | $[Co\ ox_2(NH_3)_2]NH_4\cdot H_2O$ | 54.0 | 2.04 | 9.6 | 0.6 | 78.2 | 2.30 | 11.4 | 0.3 | 24.2 | +0.26 |
| | [Co edta] $Na\cdot 4H_2O$**** | 55.9 | 2.51 | 10.4 | 0.2 | 78.1 | 2.36 | 10.6 | 0.5 | 22.2 | −0.15 |
| 1N5O | No example. | | | | | | | | | | |
| 6O | $[Co\ ox_3]K_3\cdot 3H_2O$ | 49.7 | 2.17 | 8.0 | 0.35 | 70.9 | 2.30 | 10.8 | 0.65 | 21.2 | +0.18 |
| | $[Co(O_6Mo_6O_{18}H_6)](NH_4)_3\cdot 7H_2O$ | 49.2 | 1.29 | 9.0 | 0.3 | 72.8 | 1.30 | 12.3 | 0.2 | 23.6 | +0.01 |
| | Mean..... | | | 10.0 | 0.5 | | | 12.2 | 0.4 | | |

* Omitted because of uncertainty. For the details, see the next paper of this series.
** The first absorption of this complex is split into two bands. The details will be reported separately.
*** Measured in 60% perchloric acid.
**** edta represents a ethylenediaminetetraacetate ion (quadrivalent).

5) H. Kuroya, *J. Inst. Polytech., Osaka City Univ.* C 1, No. 1, 29 (1950).
6) Y. Shimura, *J. Am. Chem. Soc.*, 73, 5079 (1951).
7) A. Mead, *Trans. Farad. Soc.*, 30, 1052 (1934).
8) J.-P. Mathieu, *Bull. soc. chim.*, [5] 3, 463 (1936).
9) J. Bielecki and V. Henri, *Phys. Z.*, 14, 516 (1913).

experimental details will appear in the next paper of this series.

In Fig. 5, the spectrum of [Co $en_2$ $Cl_2$] Cl is given. This was determined in methyl alcoholic solution with concentration of $3.3\times10^{-3}$ F. A Beckman DU spectrophotometer was used.

## Inclination of Absorption Band

Lowry and Hudson[4] previously stated that absorption spectra of most organic compounds are not symmetrical but steeper on the side of longer wave-lengths. As will be seen in Figs. 1–5, this is also true of the first and second bands of Co(III) complexes.

In order to obtain precise information about the unsymmetrical nature of these absorption bands, a new parameter, $\delta$, was introduced (see, Fig. 1):

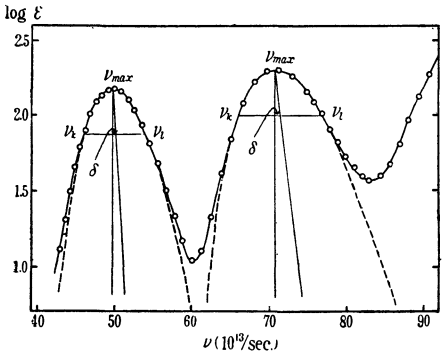



Fig. 1. $[Co\ ox_3]^{3-}$:
-o-o-o-, experimental curve;
-----, first and second bands calculated by the new equation.

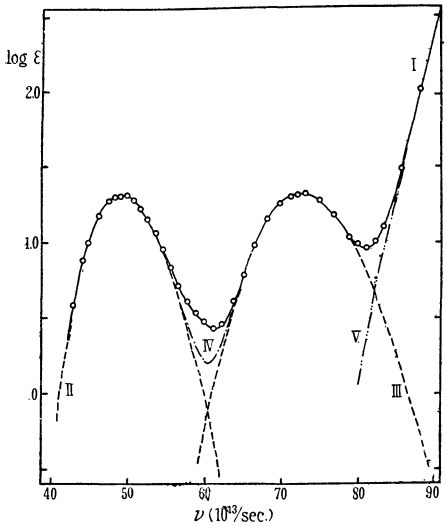



Fig. 2. $[Co(O_6Mo_6O_{18}H_6)]^{3-}$:
I, experimental curve; II, calculated first band; III, calculated second band; IV, II+III; V, I−III.

$$\delta=\frac{\nu_k+\nu_l}{2}-\nu_{max.} \qquad (5)$$

This is a measure of the inclination of the absorption band. The values of the parameters determined are given in Table I. The following conclusions were drawn from these data: (a) the values of the inclination parameters vary from 0.0 to $+0.8(\times10^{13}$/sec.). Thus the first or second bands of these complexes are almost always steeper on the side of longer wave-lengths. (b) Among the values of $\delta$'s no apparent regularities were recognized. (c) In summary, these bands are not symmetrical either on the scale of frequency or wave-length.

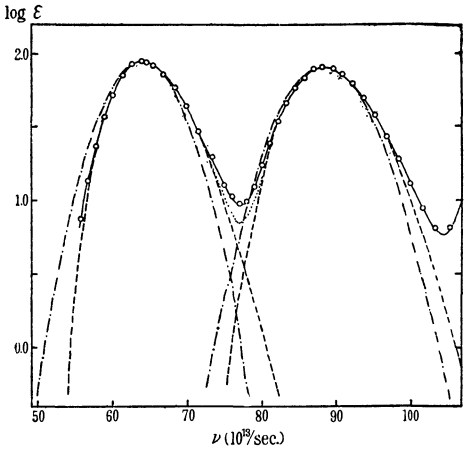



Fig. 3. $[Co\ en_3]^{3+}$:
-o-o-o-, experimental curve;
-----, calculated by the new equation;
——-——, calculated by Kuhn and Braun's equation.

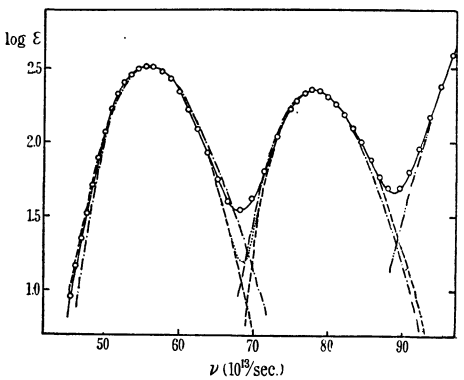



Fig. 4. $[Co\ edta]^{-}$:
-o-o-o-, experimental curve;
-----, calculated by the new equation;
——-——, calculated by Lowry and Hudson's equation.

### Experimental Equation

To fit the unsymmetrical absorption bands, a new absorption equation (6) was developed:

$$\varepsilon=\varepsilon_{max}\exp\left(-\left[\frac{\theta-\sqrt{\theta^2-2\delta'(\nu_{max}-\nu)}}{\delta'}\right]^2\right) \quad (6)$$

where

$$\delta'=2\times0.434\times\frac{\delta}{0.3} \quad (7)$$

As in equation (1) and (2), $\theta$ is defined by the relation (3).

The principal feature of the new equation is that it is a modification of Kuhn and Braun's equation by the addition of a correction term, which contains the inclination parameter $\delta$. Thus the equation (6) becomes

$$\nu=\nu_{max}\pm\theta'\sqrt{\log\varepsilon_{max}-\log\varepsilon}+\frac{\delta}{0.3}(\log\varepsilon_{max}-\log\varepsilon), \quad (8)^*$$

where $\theta'=\dfrac{\theta}{\sqrt{0.434}}$. If the third term is neglected, the equation (8) is reduced to the equation (1). The expression (8) has practical conveniences because it is applicable to either symmetrical or unsymmetrical bands ($\delta=0$ for symmetrical and $\delta\neq0$ for unsymmetrical).

The curve of equation (8) passes the three points ($\nu_{max}$, $\varepsilon_{max}$), ($\nu_k$, $\frac{1}{2}\varepsilon_{max}$) and ($\nu_l$, $\frac{1}{2}\varepsilon_{max}$), and adequately represents the essential characteristics of the experimental curve. Both the calculated and experimental curves for some of the Co(III) complexes are shown in Figs. 1–4. The agreement is now so close as to approach the limits of experimental error throughout the first and the second bands except where there is serious overlapping of the two bands. The values calculated by the equations (1) or (2) are also plotted for comparison (Figs. 3 and 4). From these figures, it is clear that the new equation shows a closer resemblance to the observed curves than the equation (1) or (2), especially on the side of shorter wavelengths.

The new equations are also applied successfully to the analyses of the specific absorption bands, for example, the isothiocyanato specific bands of Co(III) complexes, which will be the subject of a later paper of this series.

It should be added that integration of the equation (6) gives for the total intensity $F$ of a broad absorption band:

$$F=\int\varepsilon d\nu=\int\varepsilon_{max}\exp\left(-\left[\frac{\theta-\sqrt{\theta^2-2\delta'(\nu_{max}-\nu)}}{\delta'}\right]^2\right)d\nu \fallingdotseq\varepsilon_{max}\theta\int_{-\infty}^{\infty}e^{-t^2}dt=\varepsilon_{max}\cdot\theta\cdot\sqrt{\pi}=1.06\,\varepsilon_{max}\cdot l \quad (9)$$

This formula is useful for determining experimentally the oscillator strengths of broad absorption bands.

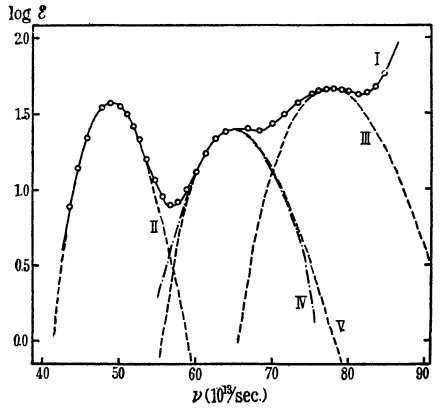



Fig. 5. *trans*-[Co $en_2Cl_2$]$^+$:
I, experimental curve; II, calculated first component of first bands; III, calculated second band; IV, I−(II+III); V, calculated second component of first bands.

### *Application to the spectra of trans-*[*Co en₂ Cl₂*]$^+$

Recently[10,11] it was confirmed that the first absorption of *trans*-[Co $en_2$ $Cl_2$]$^+$ was spilit into two peaks, overlapping the second component on the second absorption band. The analyses of these bands using equation (8) are shown in Fig. 5. As with the first peak of the first bands, the curve II was calculated by the use of the parameters determined experimentally. For the second band, by using the mean values of the half-value widths and inclination parameters for the second bands ($l=12.2$, $\delta=0.4\times10^{13}$/sec., as listed in Table I), curve III has resulted. After subtracting curves II and III from the experimental curve I, a peak appeared at 64.9 ($\times10^{13}$/sec.) with intensity of $\log\varepsilon=1.41$. The resultant band IV was exactly reproduced by the curve V, which was calculated using the values, $l=10.5$ and $\delta=0.45$. The parameters of these bands are given in Table II.

* $\varepsilon>\varepsilon_{max}e^{-(\theta/\delta')^2}$, for $\nu<\nu_0$ if $\delta>0$ and for $\nu>\nu_0$ if $\delta<0$.

10) M. Linhard and M. Weigel, *Z. anorg. allg. Chem.*, **271**, 101 (1952).
11) S. Yamada, A. Nakahara, Y. Shimura and R. Tsuchida, This Bulletin, **28**, 222 (1955).

TABLE II
FIRST AND SECOND BANDS OF *trans*-[Co en$_2$ Cl$_2$]$^+$

| Band | $\nu_{max}$ ($10^{13}$/sec.) | log $\varepsilon_{max}$ | $l$ ($10^{13}$/sec.) | $\delta$ ($10^{13}$/sec.) |
|---|---|---|---|---|
| First Bands | | | | |
| First component | 48.8 | 1.58 | 7.8 | 0.3 |
| Second component | 64.9 | 1.41 | 10.5 | 0.45 |
| Second Band | 77.5 | 1.68 | (12.2) | (0.4) |

## Relation between the First and the Second Bands

**i) Frequency of Maximum Absorption.**—Some close relationships have been recognized between the first and the second bands of metallic complexes[12]. As regards the Co(III) complexes, Kuroya[5] and Sone[12] derived each an experimental formula for the positions of the first and the second bands:

Kuroya's formula $\nu_2=\nu_1+25.0$ (10)

Sone's formula $\nu_2=1.189\,\nu_1+13.31$, (11)

where $\nu_1$ and $\nu_2$ are the frequencies in $10^{13}$/sec. of absorption maxima of the first and the second bands.

In Fig. 6, both the formulae are plotted

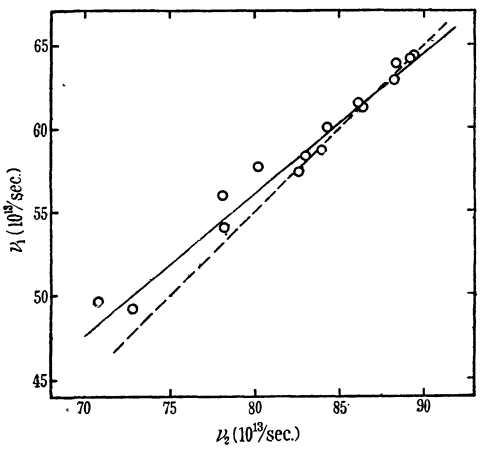



Fig. 6. Frequency of absorption maximum of the first band vs. that of the second band:
o , experimental data;
-----, plot of Kuroya's formula;
———, plot of Some's formula.

with the new data listed in Table I. It is seen that Sone's formula shows excellent agreement with the experimental data. From the values of $\Delta(\nu_{max})$ listed in Table I, which is the frequency difference between the maxima of the second and the first bands, it is also shown that Kuroya's formula is useful for the complexes of hexammine-, pentammine- and tetrammine-types. But the values of $\Delta(\nu_{max})$ for complexes of triammine-, diammine- and hexacido-types deviate considerably from 25.0. Such a condition is also clearly observed in Fig. 7, on the left

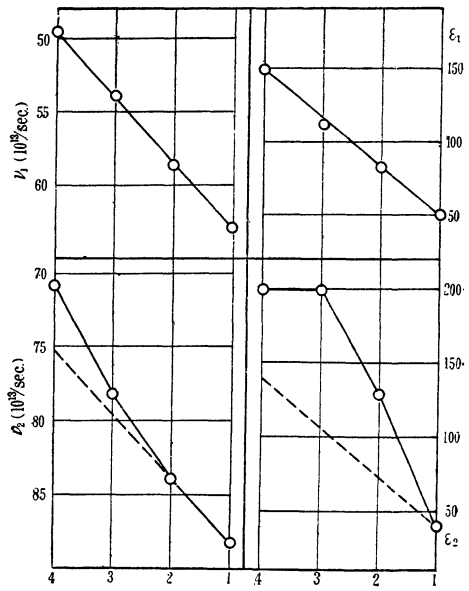



Fig. 7. Frequency positions and formal extinction coefficients of the ammine-oxalato Co(III) complexes:
1, $[Co(NH_3)_6]^{3+}$;
2, $[Co(NH_3)_4\ ox]^+$;
3, $[Co(NH_3)_2ox_2]^-$;
4, $[Co\ ox_3]^{3-}$.

part of which are plotted the frequency values for the first and second bands of Co(III) complexes belonging to an ammine-oxalato series. From the diagrams it has been confirmed that the successive substitutions of ammonia molecules by oxalate ions cause the shifts in the first absorption bands which are directly proportional to the degree of the substitution. On the other hand, the shifts in the second bands are not proportional to the degree of substitution; the greater shifts were observed for the second bands as compared with the first bands.

It is interesting to note that a similar relation exists among the absorption intensities of these complexes (See right part of Fig. 7). In view of these relations it should be suggested that the first and the second bands arise from some what different origins.

**ii) Intensity.**—Many previous authors recognized that the intensities of the first and the second bands are nearly of the same order. This is also supported by the values of $\Delta(\log \varepsilon_{max})$ listed in Table I ($\Delta(\log \varepsilon_{max})$ denotes the difference between $\log \varepsilon_{max}$'s of

12) K. Sone, *J. Chem. Soc. Japan*, **71**, 270, 316 (1950).

the second and the first bands. It should be added, however, that all oxalato-complexes studied are stronger in the second bands than in the first bands.

**iii) Half-value Width.** — The half-value widths of the first bands are always smaller than those of the second bands (see Table I).

**iv) Inclination Parameter.**—The inclination parameters of the first bands are almost always greater than those of the second bands (see Table I).

## Summary

The measurements of the visible and ultraviolet absorption spectra of about fifteen Co(III) complex compounds have revealed that the first and second bands of these complexes are not symmetrical either on the scale of frequency or wave-length, and that these bands cannot be represented by the equation of Kuhn and Braun, nor of Lowry and Hudson.

To fit the unsymmetrical absorption bands, a new experimental absorption equation has been developed and its adequacy substantiated.

Some relationships between the first and the second bands of Co(III) complexes are also investigated.

*Department of Chemistry, Faculty of Science, Osaka University, Osaka*

# *Intermolecular Charge-Transfer Spectra. IV. Electronic Structure of Molecular Complexes*

By Hideo MURAKAMI

(Received March 30, 1955)

As was mentioned in the previous paper[1], the observed molar extinction coefficient $\epsilon_c$ of intermolecular charge-transfer spectra decreases by a considerable amount with the increase of donor character of B-component (or that of acceptor character of A-component) in spite of the appreciable decrease of the factor $(W_1-W_0)$. In order to solve this apparent contradiction and caculate the absorption intensity $f_{EN}$ or $\epsilon_c$, it was pointed out that one should take the following factors into account:

1) Electron density distribution in the molecular orbitals which are essential to the intermolecular charge-transfer spectra.

2) The degree of extension of each atomic orbital.

For example, as was stated in the previous paper, it is easy to show that these two factors make the value of resonance integral $|H_{01}|$ and consequently that of $\epsilon_c$ smaller for the substituted benzene complex than that for benzene complex. Somewhat later, Kuboyama and Nagakura also suggested the smaller value of resonance integral for naphthalene complex than for benzene complex in order to explain their own experimental results concerning heat of formation[2]. It is obvious that this suggestion can be included in the afore-mentioned statement 1) as special case.

In the present paper, the previous idea will be shown in the more concrete and quantitative form. Moreover, the predicted relative value of $\epsilon_c$ will be compared with some of the experimental results.

## General Theory

In the third paper of this series[1], the simple relation between resonance energy and absorption intensity is given as follows:

$$H_{01}^2/(W_1-W_0)\simeq(3h^2/8\pi^2m)f_{EN}/(r_B-r_A)^2 \quad (1)$$

where $f_{EN}$ is the oscillator strength of intermolecular charge-transfer spectra and $(r_B-r_A)$ is the distance between the respective electronic center of B- and A-component. The left hand side of the above equation represents the resonance energy between two hypothetical electronic structures $\Psi_0=\Psi(A\cdot B)$ and $\Psi_1=\Psi(A^--B^+)$.

Since the resonance intergral $H_{01}$ and the overlap integral $S$ is given respectively by

$$H_{01}=(\Psi_0|H|\Psi_1),\quad S=(\Psi_o\Psi_1),$$

it is reasonable to postulate the approximate

1) H. Murakami, This Bulletin, 27, 268 (1954).

2) A. Kuboyama and S. Nagakura, *J. Chem. Soc. Japan*, 75, 1082 (1954).

proportionality between them; that is*,

$$H_{01} \simeq const.\, S \qquad (2)$$

Now it is desirable to introduce the simple molecular orbitals $\phi_A$ and $\phi_B$ which are essential to the resonance interaction or the intermolecular charge-transfer spectra. According to Mulliken[3], the charge-transfer process involves essentially the jump of one electron in a molecular orbital $\phi_B$ of the B-component into a previously unoccupied molecular orbital $\phi_A$ of the A-component, and there exists the relation

$$S \simeq 2^{1/2} S_{AB}/(1+S_{AB}^2)^{1/2} \simeq 2^{1/2} S_{AB} \qquad (3)$$

where

$$S_{AB} = (\phi_A | \phi_B).$$

In order to estimate the overlap integral $S_{AB}$, one should consider that the overlapping part of $\phi_A$ and $\phi_B$ in actual molecular complex is rather localized and consequently $\phi_A$ and $\phi_B$ can be devided into two parts, respectively, as follows:

$$\begin{aligned} \phi_A &= \phi_\alpha + \phi_{\alpha'} \\ \phi_B &= \phi_\beta + \phi_{\beta'} \end{aligned} \qquad (4)$$

where $\phi_\alpha$ and $\phi_\beta$ is the partial molecular orbital of A- and B-component, respectively, which are overlapping with each other for a given relative configuration. Accordingly, $\phi_{\alpha'}$ and $\phi_{\beta'}$ is defined as the remaining part of them, respectively, which are not overlapping with each other. Under such a definition as above, $S_{AB}$ is given by

$$S_{AB} = (\phi_\alpha | \phi_\beta) \qquad (5)$$

In order to develop the calculation, we introduce the following simplifing approximation:

$$\begin{aligned} \phi_\alpha &= \sum_l^l C_l^{(\alpha)} \phi_l^{(\alpha)} \simeq C_l^{(\alpha)} \sum_l^l \phi_l^{(\alpha)} \\ \phi_\beta &= \sum_j^m C_j^{(\beta)} \phi_j^{(\beta)} \simeq C_m^{(\beta)} \sum_j^m \phi_j^{(\beta)} \end{aligned} \qquad (6)$$

where $\phi_i^{(\alpha)}$ and $\phi_i^{(\beta)}$ is the constitutent atomic orbital in the partial molecular orbital $\phi_\alpha$ and $\phi_\beta$ respectively. In Eq. (6), the mean effective coefficient $C_l^{(\alpha)}$ and $C_m^{(\beta)}$ is defined respectively by

$$\begin{aligned} [C_l^{(\alpha)}]^2 &= \sum_l^l [C_l^{(\alpha)}]^2 / l \\ [C_m^{(\beta)}]^2 &= \sum_j^m [C_j^{(\beta)}]^2 / m \end{aligned} \qquad (7)$$

In the present approximation, $S_{AB}$ is given as follows,

$$S_{AB} \simeq C_l^{(\alpha)} C_m^{(\beta)} S_{\alpha\beta} \qquad (8)$$

where

$$S_{\alpha\beta} = (\sum_l^l \phi_i^{(\alpha)} | \sum_j^m \phi_j^{(\beta)}).$$

The combination of Eq. (8) with Eqs. (1), (2) and (3) provides us with the formula

$$\begin{aligned} &[C_l^{(\alpha)}]^2 [C_m^{(\beta)}]^2 S_{\alpha\beta}^2 / (W_1 - W_0) \\ &\quad \simeq const.\, f_{EN}/(r_B - r_A)^2 \end{aligned} \qquad (9)$$

If the rather insensitive terms $(W_1 - W_0)$ and $(r_B - r_A)^2$ are ignored, Eq. (9) reduces to a very simple relation

$$[C_l^{(\alpha)}]^2 [C_m^{(\beta)}]^2 S_{\alpha\beta}^2 \simeq const.\, f_{EN}. \qquad (9a)$$

Remembering the well known formula

$$f_{EN} \simeq 4.32 \times 10^{-9} \epsilon_c \Delta\nu$$

and assuming the approximate constancy of the half width $\Delta\nu$ of the absorption band, Eq. (9a) is rewritten in the form

$$[C_l^{(\alpha)}]^2 [C_m^{(\beta)}]^2 S_{\alpha\beta}^2 \simeq const.\, \epsilon_c \qquad (9b)$$

where $\epsilon_c$ is the molar extinction coefficient of the intermolecular charge-transfer spectra. Thus, the evaluation of the relative value of $\epsilon_c$ is reduced to the electron density calculation of the molecular orbitals which are essential to the intermolecular charge-transfer spectra.

## Application to Some Examples

In Eq. (9b), the numerical values of $S_{\alpha\beta}^2$ and *const.* are not known. Consequently, the theoretical prediction is limited in the relative value of $\epsilon_c$ for various complexes in which A- or B-component is the same. In the present paper, we consider the former case and define the relative value $k$ of $\epsilon_c$ as follows:

$$k = \frac{\epsilon_c \text{ of } (A \cdot Ar)}{\epsilon_c \text{ of } (A \cdot Bz)}$$

where A represents the common A-component, and Ar, Bz respectively represents any aromatic molecule and benzene as B-component.

In case of quinhydrone-type molecular complexes, it is reasonable to assume the most compact relative configuration between two components in which the ring portion of each component is facing and contacting with the other and the substituted groups in both components are also facing with each other so long as such a configuration is allowed (see the discussion in the preceding paper[1]). Since the spatial extension of $2p$-atomic orbital of oxygen or nitrogen is considerably smaller than that of carbon, we can expect very small overlap integrals between substituted groups even in the above-described

* In the following, the numerical value and the physical dimension of *const.* should be considered for the respective case and it is not necessary to be equal throughout the every cases.

3) R.S. Mulliken, *J. Am. Chem. Soc.*, **74**, 811 (1952).

configuration and can neglect them. Consequently, $\phi_B$ corresponds to the appropriate linear combination of $2p\pi$-atomic orbitals of ring carbon and does not contain the atomic orbitals in the substituted groups. When B-component is benzene, there exists the relation

$$\phi_B=\phi_\beta, \quad \sum_j^6[C_j^{(\beta)}]^2=1$$

as special case.

Moreover, it is reasonable to assume that $S_{\alpha\beta}$ is approximately the same regardless of the molecular size of B-component since the electronically interacting area is the same throughout the molecular complexes considered so long as the A-component is common. which is essential to the intermolecular charge-transfer process is the highest occupied one. Fortunately, the electron density distribution of the highest occupied molecular orbital have been calculated by Fukui et al. for various aromatic compounds in relation to their reactivity as frontier electron theory[5]. From Eq. (10), it is easy to see that $k$ is given by the half of the total electron density in the partial molecular orbital $\phi_\beta$ since the complete orbital $\phi_B$ is filled by two electrons. By using the numerical value of Fukui et al., one can easily predict the approximate value of $k$ for various molecular complexes. Some examples are shown in Table I together with the experimental results. The agreement between

TABLE I

OBSERVED AND CALCULATED VALUES OF THE RATIO $k$ OF MOLAR EXTINCTION COEFFICIENT $\epsilon_c$ IN VARIOUS MOLECULAR COMPLEXES

| A-Component | B-Component | $\epsilon_c$ | $k_{obs.}$ | $k_{calc.}$ | Reference |
|---|---|---|---|---|---|
| *p*-Quinone | Benzene | (2800)[a] | 1.00 | 1.00 | (1) |
| | Phenol | 1200 | 0.43 | 0.66[b] | (2) |
| | Hydroquinone | 890 | 0.32 | 0.32 | (2) |
| Maleic anhydride | Benzene | 3140 | 1.00 | 1.00 | (1) |
| | Styrene | 1940 | 0.62 | 0.50 | (1) |
| | Dimethylaniline | 1590 | 0.51 | 0.66[b] | (1) |
| Iodine | Benzene | 16400 | 1.00 | 1.00 | (3) |
| | Dibenzyl | 11200 | 0.68 | 1.00 | (3) |
| | Bromobenzene | 10400 | 0.63 | 0.66[b] | (3) |
| | Styrene | 7350 | 0.45 | 0.50 | (3) |
| | Stilbene | 7140 | 0.44 | 0.31 | (3) |
| | Naphthalene | 7640 | 0.47 | 0.50 | (3) |

a) Extrapolated value (not so exact)

b) Estimated from Fig. 5 in reference 5) assuming the equal electron density at 1- and 4-positions. (Assumed values of parameter are $a\simeq 0.6$, $b=1.0$. Of course, these values may differ more or less for the different compounds and consequently the predicted values of $k$ may also deviate from the listed value 0.66.)

(1) L. J. Andrews and R. M. Keefer, *J. Am. Chem. Soc.*, **75**, 3776 (1953).
(2) H. Tsubomura, This Bulletin, **26**, 304 (1953).
(3) L. J. Andrews and R. M. Keefer, *J. Am. Chem. Soc.*, **74**, 4500 (1952).

These situations enable us to give a simple expression for $k$, that is,

$$k=\sum_j^m[C_j^{(\beta)}]^2. \qquad (10)$$

This formula is also applicable to the halogen-aromatic complexes since the dimension of the halogen molecule is almost the same as that of the benzene ring.

As was discussed by McConnell et al., there is an excellent correlation between the wavelengths of absorption maximum of intermolecular charge-transfer spectra and the estimated ionization potentials of B-components[4]. Therefore, it is almost certain that the molecular orbital in the B-component predicted and observed values are relatively good at least qualitatively. From the quantitative point of view, however, one should remember the existence of the following situations which prevent the exact comparison:

1) The simplifing assumption such as Eq. (6) is introduced.

2) The insensitive terms $1/(W_1-W_0)$ and $1/(r_B-r_A)^2$ are neglected although in some cases they might not be negligible.

3) In the present consideration, $k$ is defined as the ratio of $\epsilon_c$ for convenience, sake although it should be defined as that of $f_{EN}$ from the more exact point of view.

4) The statistical situation on the relative

4) McConnell, Ham and Platt, *J. Chem, Phys.*, **21**, 66 (1953).

5) Fukui, Yonezawa, Nagata and Shingu, *J. Chem. Phys.*, **22**, 1433 (1954).

configuration between two components is neglected.

At any rate, it is almost certain that the interesting behavior of $\epsilon_c$ among such molecular complexes as shown in Table I is explainable by the consideration of their electronic structures.

## Appendix

In case of iodine-benzene complex, the observed value of oscillator strength ($f_{EN} \simeq 0.38$) is very large. Consequently, Eq. (1) seems to predict the much larger resonance energy than the observed heat of formatian ($\Delta H \simeq 1.4$ Kcal./mol.[6]). This apparent contradiction can be solved by the examination of its electronic structure.

According to Mulliken, the attractive resonance energy in halogen-benzene complex (symmetry $C_{2v}$) is essentially given by the electronic interaction between antibonding $\sigma$-orbital $b_2\sigma_u$ in halogen molecule and the molecular orbital which has the same symmetry $b_2$ in benzene[3]. Therefore, the electronic interaction between any other pair of orbitals (especially that of $\pi$-orbitals) which are occupied by electrons contribute to exchange repulsive interaction. (In the rough approximation, the contribution of excited electronic configurations can be neglected since the degree of contribution of them is expected to be small.)

Now we examine the geometrical situation of each atomic orbital in halogen molecule. As is well known, the electron density distribution of $\sigma$-orbital is rather concentrated on the molecular axis, on the contrary, that of $\pi$-orbital is extended to the direction which is normal to the molecular axis. Taking this fact into account and assuming the most compact relative configuration, it is quite reasonably expected that the attractive resonance energy is negligibly small even at the region (distance between two components) in which the exchange repulsive energy amounts to considerable value. This situation is expressed

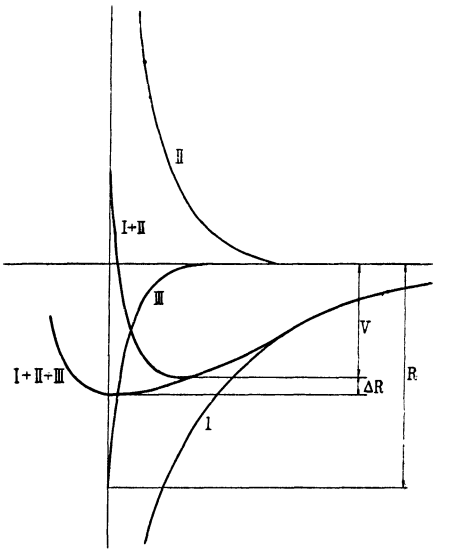



Fig. 1.

in Fig. 1 diagramatically. In this figure, the curve I, II and III represents, respectively, the ponential energy curve of van der Waals type attraction, exchange repulsion and resonance attraction. Comparing the resultant curve (I+II) and (I+II+III), it is easy to see that the contribution of resonance attraction ($\Delta R$) to the total binding energy ($V+\Delta R$) is small enough although the absolute value of resonance energy ($R$) in equilibrium position is very large. This situation seems to suggest the special importance of the repulsive term in the charge-transfer type interaction.

The author wishes to express his sincere thanks to Prof. S. Akabori for his encouragement and interest in the course of this study.

*Department of Chemistry, Faculty of Science, Osaka University, Osaka*

6) T.M. Cromwell and R.L. Scott, *J. Am. Chem. Soc.*, 72, 3825 (1950).

# *Intermolecular Charge-Transfer Spectra. V. Halogen-Polymethylbenzene Complexes*

By Hideo MURAKAMI

(Received March 30, 1955)

In the first paper of this series[1], we studied the spectroscopic features of halogen-aromatic complexes such as $X_2 \cdot C_6H_{(6-n)}(CH_3)_n$ in which $n=0, 1, 2$. Now we extend the previous discussions over the cases of $n=3, 4, 5, 6$ and compare the predicted value of molar extinction coefficient $\epsilon_c$ of intermolecular charge-transfer spectra with the observed results. Next, the foregoing idealized treatment will be discussed from the more general point of view in relation to the previous discussions on pressure effect[2,3] and the recent result by Ham[4].

## Statistical Consideration

As can easily be seen, the electronic structure of $\pi$-electron system in methyl-benzene is practically the same as that in benzene itself. Consequently, in case of halogen-alkylbenzene complex, the observed behaviour of $\epsilon_c$ cannot be explained from the viewpoint of the electronic structure of the aromatic component. In order to solve this difficulty, we have already introduced the statistical treatment on the relative configuration between the two components[1]. That is, we considered the two relative configurations such as Model ($\alpha$) and Model ($\beta$). In Model ($\alpha$), the halogen molecule is resting on the benzene ring with its axis parallel to the plane of benzene and its center on the six-fold axis of benzene. In Model ($\beta$), the center of the halogen molecule is shifted towards the methyl group on account of van der Waals attraction of it (see Fig. 1 in reference 1). Since the degree of overlapping between orbital functions which are essential to charge-transfer interaction is considerably different for Models ($\alpha$) and ($\beta$), it is reasonable to assume that each configuration has its own molar extinction coefficient $\epsilon_c^{(\alpha)}$ and $\epsilon_c^{(\beta)}$, respectively.

Next we postulate, as we have already done in our previous paper[1], that these two configurations ($\alpha$) and ($\beta$) have almost the same stability and exist in solution with almost equal statistical weight. This assumption is reasonable so long as the contribution of the van der Waals type interaction is predominant compared with that of the charge-transfer type interaction[5]. Considering these conditions, we can give the following general formula for the observed molar extinction coefficient $\epsilon_c$ of molecular complexes as statistical mean,

$$\epsilon_c=(\epsilon_c^{(\alpha)}+n\epsilon_c^{(\beta)})/(1+n) \qquad (1)$$

where $n$ is the number of substituted methyl groups and arbitrary integer between 0 and 6. At the present stage, the exact evaluation of $\epsilon_c^{(\beta)}$ is somewhat difficult and remains as parameter. Hence, we retain the previous relation[1]

$$\epsilon_c^{(\beta)} \simeq \epsilon_c^{(\alpha)}/2 \qquad (2)$$

as a reasonable one. The value of $\epsilon_c^{(\alpha)}$ is approximated by the observed molar extinction coefficient of halogen-benzene complex ($n=0$). Then, Eqs. (1) and (2) enable us to predict the observed molar extinction coefficient $\epsilon_c$ for any value of $n$. The results are shown in Table I together with the experimental results. At present, we have two sets of experimental results. The one is by Andrews and Keefer[6] and the other is by Tamres et al.[7]

As is seen in Table I, the order of magnitude of predicted values corresponds well to either of the two observations. The most essential feature of theoretical prediction is the decrease of $\epsilon_c$ with the increase of $n$. This interesting feature is well established in the data of Tamres et al. although it is not established in those of Andrews and Keefer. Strictly speaking, the rate of decrease of observed $\epsilon_c$ is greater than that of theoreticol prediction. If this difference is significant, it may probably be due to the contribution of the configurations in which the halogen molecule is rather resting on the

1) H. Murakami, This Bulletin, **26**, 441 (1953).
2) R.E. Gibson and H. Loeffler, *J. Am. Chem. Soc.*, **62**, 1324 (1940).
3) H. Murakami, This Bulletin, **26**, 446 (1953).
4) J. Ham, *J. Am. Chem. Soc.*, **76**, 3881 (1954).
5) H. Murakami, This Bulletin, **28**, 577 (1955).
6) L.J. Andrews and R.M. Keefer, *J. Am. Chem. Soc.*, **74**, 4500 (1952).
7) M. Tamres, D.R. Virzi and S. Searles, *J. Am. Chem. Soc.*, **75**, 4358 (1953).

TABLE I
EXPERIMENTAL AND THEORETICAL MOLAR EXTINCTION COEFFICIENTS OF IODINE-POLYMETHYLBENZENE COMPLEXES (IN $CCl_4$ SOLUTION)

| Aromatic Component | $\epsilon_c$ (obs.) Andrews et al.[5] | $\epsilon_c$ (calc.) | $\epsilon_c$ (obs.) Tamres et al.[7] | $\epsilon_c$ (calc.) |
|---|---|---|---|---|
| Benzene | 16400 | (16400) | 14700 | (14700) |
| Mesitylene | 8850 | 10250 | 10200 | 9190 |
| Durene | 9000 | 9840 | 8700[a] | 8820 |
| Pentamethylbenzene | 9260 | 9570 | 7770 | 8580 |
| Hexamethylbenzene | 8200 | 9370 | 6690 | 8400 |

a) The value for isodurene.

two adjacent methyl groups and its own molar extinction coefficient is smaller than $\epsilon_c^{(\beta)}$.

If methyl groups are replaced with ethyl groups, one can expect the larger contribution of such configurations (which have smaller $\epsilon_c$ than $\epsilon_c^{(\beta)}$). Moreover, as was pointed out by Andrews and Keefer and also by Tamres et al., the steric hindrance of ethyl groups prevent the configuration such as Model ($\alpha$) (which has greater $\epsilon_c$ than $\epsilon_c^{(\beta)}$). Consequently, one can predict the smaller $\epsilon_c$ for $X_2 \cdot C_6(C_2H_5)_6$ than for $X_2 \cdot C_6(CH_3)_6$. In fact, Tamres et al. observed the much smaller $\epsilon_c$ for $X_2 \cdot C_6(C_2H_5)_6$ ($\epsilon_c \sim 4570$) than for $X_2 \cdot C_6(CH_3)_6$ ($\epsilon_c \sim 6690$). On the contrary, Andrews and Keefer observed the reverse, that is, $\epsilon_c \sim 16700$ for the former complex. Judging from the regular behaviour of the observed $\epsilon_c$ and $K$, the results by Tamres et al. seem to be more reliable. At any rate, further experimental study is very desirable.

### Generalization and Pressure Effect

In the foregoing discussion, we considered only two configurations such as Model ($\alpha$) and Model ($\beta$). This corresponds to the idealized limiting case and is not exact enough. From the more general point of view, the observed molar extinction coefficient $\epsilon_c$ is given as follows:

$$\epsilon_c = \sum_i W_i \epsilon_c^{(i)} / \sum_i W_i \qquad (3)$$

where $\epsilon_c^{(i)}$ is the molar extinction coefficient for the any configuration ($i$) and $W_i$ is the statistical weight of this configuration in solution. In case of non-substituted benzene complex, the value of $W_i$ which corresponds to such a configuration as Model ($\beta$) may be much smaller than that of Model ($\alpha$). On the other hand, in case of substituted benzene complex, the former value may become comparable to the latter one. Then, if one assumes that $W_i$ of all the configurations except those of Model ($\alpha$) and Model ($\beta$) are equal to zero, Eq. (3) reduces essentially to Eq. (1)*. In practice, any of $W_i$ may be unequal to zero although it may be small enough. Consequently, when one uses the observed $\epsilon_c$ of halogen-nonsubstituted benzene complex as the value of $\epsilon_c^{(\alpha)}$ in Eq. (1), one should always remember that such a value of $\epsilon_c^{(\alpha)}$ has already included the statistical effect more or less (the assumed value of $\epsilon_c^{(\beta)}$ should also be considered as effective value which includes statistical effect).

This situation seems to have special importance for the explanation of pressure effect. In fact, it is reasonable to consider that the high pressure favours the compact configurations and makes the values of $W_i$ of compact configurations greater. In case of halogen-aromatic complexes, the more compact configuration may have the greater $\epsilon_c^{(i)}$. Taking these factors into account, one can predict the increase of $\epsilon_c$ with increase of pressure. These considerations correspond to the special case of pressure effect which was discussed in the second paper of this series and seems to explain the recent work by Ham in which he observed the slight increase of optical density under the high pressure for iodine-aromatic complexes in $n$-heptane solution.

According to our opinion, the above-described explanation is more correct than that of Ham which postulated the alteration of equilibrium constant $K$ and the constancy of $\epsilon_c$ with increase of pressure. At least, we should emphasize that Ham's explanation is rather macroscopic or phenomenological and does not take the microscopic situation into account: such as relative configuration between two components which seems to be essential to the value of $\epsilon_c$. Especially, Ham's discussion seems to be inadequate for the case of Gibson and Loeffler's experiment in

* If one takes the contribution of Model ($\gamma$) into account—see Part I of this series—the contribution of Model ($\alpha$) and Model ($\beta$) should decrease by the corresponding amount.

which 50%, 50% mixture of nitrobenzene and aniline was used (without solvent). In such a condition as the above, the degree of intensification of $\epsilon_c$ may become much greater than that in Ham's experiment which was performed as dilute solution (solvent was *n*-heptane). Moreover, Gibson and Loeffler observed that the elevation of temperature at constant volume causes the same result as the high pressure at constant temperature. It is almost certain that the elevation of temperature tends to break up the molecular complex in the usual concept even at constant volume. Consequently, the concept or definition of molecular complex should be generalized as was discussed by Gibson and Loeffler from the kinetic point of view. If one admits this generalization, the previous explanation in the second Part of this series seems to be most probable.

The author wishes to express his sincere gratitude to Prof. S. Akabori for his ceaseless interest and encouragement throughout the course of this series.

*Department of Chemistry, Faculty of Science, Osaka University, Osaka*

# *On the Molecular Rotations of Polypeptides of Alanine. II.*

By Hideo MURAKAMI

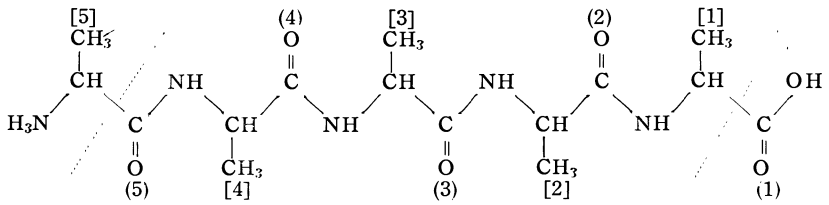
(Received April 1, 1955)

## Introduction

In the previous paper, the molecular rotations $[M]_D$ of a series of polypeptides of alanine were calculated theoretically assuming the folded $\alpha$-type configuration[1]. More precisely, the seven membered ring due to intramolecular hydrogen bond was assumed so as to satisfy Kauzmann and Eyring's suggestion in which the rigid ring structure of polypeptides was required[2]. The recent viewpoint, however, is that one can expect a rather rigid nature even in the extended $\beta$-type configuration[3]. Therefore, it seems to be desirable to calculate the molecular rotation for the extended configuration assuming the complete rigidity. As was already shown, the contribution of the one-electron effect is much smaller than that of the dynamical coupling effect. Consequently the calculation will concern only the latter effect.

## Method of Calculation

As a molecular model, the extended $\beta$-type configuration is used. For example, the configuration of tetra-alanyl-alanine is given by the formula:




Here, one can consider two idealized models. First, the structure completely rigid from one end to the other, $\beta_{(1)}$. Second, the stracture in which only the two terminal groups (COOH and $CH(CH_3)(NH_3)$) are in the state of free rotation and the remaining part being completely rigid, $\beta_{(2)}$.

The method of calculation and the degree of approximation are the same as before* and the following pairs of interactions are taken

1) H. Murakami, This Bulletin, **27**, 246 (1954).

2) W. Kauzmann and H. Eyring, *J. Chem.Phys.*, **9**, 41 (1941).

3) M. Laskowski, Jr., and H.A. Scheraga, *J. Am. Chem. Soc.*, **76**, 6305 (1954). In this paper, the authors stated as follows: "For rotation in hydrocarbons the potential barriers are quite high compared to $RT$ at room temperature. Further, since the potential curves for internal rotation in higher hydrocarbons are, in general, asymmetric and the various potential minima differ appreciably, we can assume that the majority of non-hydrogen bonded molecules are confined to the lowest minimum and that the entropy associated with the distribution among various possible minima is small." (See p. 6308).

* In order to simplify the calculation, the bond angles in the main chain are all assumed to be 120°. This is the only difference from the previous approximation.

into account.*

$A$: {(1)[1]} {(2)[2]} {(3)[3]} {(4)[4]} {(5)[5]}
$B$: {(2)[1]} {(3)[2]} {(4)[3]} {(5)[4]}
$C$: {(3)[1]} {(4)[2]} {(5)[3]}
$D$: {(1)[2]} {(2)[3]} {(3)[4]} {(4)[5]}

The molecular rotations $[M]_D$ are given for $\beta_{(1)}$ and $\beta_{(2)}$, respectively, as follows:

| | | |
|---|---|---|
| $\beta_{(1)}$ | alanine | $A$ |
| | alanyl-alanine | $2A+B+D$ |
| | di-alanyl-alanine | $3A+2B+C+2D$ |
| | tri-alanyl-alanine | $4A+3B+2C+3D$ |
| | tetra-alanyl-alanine | $5A+4B+3C+4D$ |
| $\beta_{(2)}$ | alanine | 0 |
| | alanyl-alanine | $B$ |
| | di-alanyl-alanine | $A+2B+C$ |
| | tri-alanyl-alanine | $2A+3B+2C+D$ |
| | tetra-alanyl-alanine | $3A+4B+3C+2D$ |

The numerical results are shown in Tables I and II together with the previous results on the $\alpha$-type cofiguration and the observed results[4].

TABLE I

| Polypeptides | Calculated values $[M]_D^{\alpha}$ | $[M]_D^{\beta(1)}$ | $[M]_D^{\beta(2)}$ | Observed values $[M]_D$ |
|---|---|---|---|---|
| alanine | 0° | − 182° | 0° | − 13° |
| alanyl-alanine | 169° | − 521° | − 143° | + 58° |
| di-alanyl-alanine | 380° | − 823° | − 431° | +179° |
| tri-alanyl-alanine | 609° | −1125° | − 733° | +347° |
| tetra-alanyl-alanine | 837° | −1427° | −1035° | +494° |

TABLE II

| Polypeptides | Calculated values $[M]_D^{\alpha}\times 0.591$ | $-([M]_D^{\beta(1)}-A)\times 0.382$ | $-[M]_D^{\beta(2)}\times 0.491$ | Observed values $\lvert[M]_D\rvert+13°$ |
|---|---|---|---|---|
| alanine | 0° | 0° | 0° | 0° |
| alanyl-alanine | 100° | 129° | 70° | 71° |
| di-alanyl-alanine | 225° | 245° | 212° | 192° |
| tri-alanyl-alanine | 360° | 360° | 360° | 360° |
| tetra-alanyl-alanine | 495° | 476° | 508° | 507° |

## Discussion on the Results

The noticeable features of the theoretical predictions are as follows:

1) The signs of $[M]_D$ for $\alpha$-and $\beta$-type configurations are reverse (see Table I).

2) Except for the sign, the qualitative tendency of the predicted $[M]_D$ agrees relatively well with the observed one for either the configurations of $\alpha$ and $\beta$ (see Table II).

3) The absolute values of the predicted $[M]_D$ are too great for either the configurations of $\alpha$ and $\beta$** (see Table I).

These results may probably require the existence of equilibrium between $\alpha$-and $\beta$-type configurations***. Especially, it is interesting to observe that the predicte values based on $\beta_{(2)}$ agree very well with the experimental results in its qualitative tendency (see Table II). This fact seems to suggest the rather predominant contribution of $\beta_{(2)}$-type configuration in water solution (if this situation is proved to be correct, some statements in the previous paper must be revised within the suitable range). At the present stage, however, it is difficult to give a decisive conclusion about the direction and the degree of shift of equilibrium among various rotational isomers. In order to obtain the detailed knowledge about this equilibrium, further refinement of calculation is necessary and the determination of the absolute configuration of alanine or related amino acid is very desirable. This is a task for future study.

The author wishes to express his sincere gratitude to Prof. S. Akabori for his kind guidance and encouragement throughout the course of this study.

*Department of Chemistry, Faculty of Science, Osaka University, Osaka*

* Pairs $E\{(4)[1]\}\{(5)[2]\}$ are neglected since these pairs correspond to too large separation in case of $\beta$-type configuration.

4) P.A. Levene and P.S. Yang, *J. Biol. Chem.*, **99**, 405 (1932). See also E. Abderhalden and W. Gohdes, *Ber.*, **64**, 2070 (1931).

** At the present stage, the values of parameters are not conclusive. Moreover, the degree of rigidity of $\beta$-type configuration is still a matter of doubt. Therefore, one should remember that the absolute value of the predicted $[M]_D^{\beta(1)}$ and $[M]_D^{\beta(2)}$ are also inconclusive.

*** Strictly speaking, the contribution of intermediate type configurations—folded and extended configurations are mixed in the one polypeptide chain—should also be considered. In the rough approximation, however, one can replace the intramolecular distribution of $\alpha$- and $\beta$-type configurations by the statistically equivalent intermolecular ones.

# *Determination of Carbon in Organic Compounds by the Iodic Acid Decomposition Method*

By Shigeru OHASHI

(Received June 21, 1955)

In the previous papers the author and his co-workers have already reported that by using a mixture of potassium iodate and strong phosphoric acid, elementary carbons[1], oxidation values of organic compounds[2], and nitrogen in organic compounds[3,4] can be simply and rapidly determined. Among these methods the determinations of carbon contents in elementary carbons, such as graphite, active carbon and so on, containing some inorganic substances, and those of oxidation values of organic compounds composed of carbon, hydrogen, and oxygen are based on the following reactions, respectively,

$$5C+4HIO_3=5CO_2+2H_2O+2I_2$$

$$5C_kH_mO_n+2(2k+m/2-n)HIO_3 = 5kCO_2+(2k+3m-n)H_2O + (2k+m/2-n)I_2.$$

Carbon contents in elementary carbons as well as oxidation values of organic compounds can be indirectly determined by titrating the liberated iodine in the above reactions.

If it is possible to estimate the liberated carbon dioxide by any suitable method in the above-mentioned reactions, it may be possible to determine directly the carbon contents in elementary carbons and in organic compounds.

The present investigation has aimed at establishing a new direct method for the determination of carbon in organic compounds by means of iodic acid decomposition followed by titrimetric estimation of the liberated carbon dioxide. The investigation on the direct determination of carbon in elementary carbons is now undertaken in this laboratory and will be reported later.

For the present study the investigation of direct semimicrodetermination of oxygen in organic substances achieved by R. D. Hinkel and R. Raymond[5] serves as a good reference. They described the fact that carbon monoxide formed in the pyrolysis of an organic compound is oxidized with iodine pentoxide, the resulting carbon dioxide is absorbed in a measured excess of 0.05 N alkali, and the excess is back-titrated with 0.025 N acid after precipitation of the carbonate formed with barium chloride.

In the present investigation, using a carbon dioxide absorber of a special type and an anhydrous sodium thiosulfate-filled iodine absorber, which were devised by Hinkel and Raymond, satisfactory results have been obtained. In this paper the recommended apparatus, reagents, and procedure for this method, the analytical results of several organic compounds, and the discussion concerning them are described.

## Apparatus

The apparatus used in this study is illustrated in Fig. 1. It is mainly composed of three parts, a reaction vessel A, a carbon dioxide absorber B, and an iodine absorber K.

Into the reaction vessel A a gas-introducing tube H and a thermometer F, which is covered with a thermometer-protecting tube G, are inserted. These tubes are attached to the vessel A with rubber tubes. After passing through a concentrated solution of sodium hydroxide, a soda lime-filled tube, and concentrated sulfuric acid in turn, the air free from carbon dioxide is introduced by means of a suction pump into the vessel A through the three-way stopcock D of a water-addition funnel C, which is used to add water to the vessel A after the decomposition of a sample. The vessel A is heated at the bottom with a samll electric heater J, the temperature of which can be regulated with a transformer. The left arm of the vessel A is connected to the absorber B through the iodine absorber K filled with anhydrous sodium thiosulfate and a stopcock L.

The carbon dioxide absorber B is the same one that was used by Hinkel and Raymond. The tube B is closed at the top by means of a rubber stopper, through which the capillary tips of two burets, Q and N, containing standard solutions of hydrochloric acid and sodium hydroxide, respectively, and the tip of a reagent-addition tube R are inserted. The standard solution of sodium hydroxide is introduced from its reservoir to the buret by the compressed air. At the top of the buret N and the left side arm of the absorber B there are soda lime-filled guard tubes, P and S.

1) T. Kiba, S. Ohashi, T. Takagi, and Y. Hirose, *Japan Analyst*, **2**, 446 (1953).
2) S. Ohashi, This Bulletin, **28**, 171 (1955).
3) S. Ohashi, ibid., **28**, 177 (1955).
4) S. Ohashi, ibid., **28**, 537 (1955).
5) R.D. Hinkel and R. Raymond, *Anal. Chem.*, **25**, 470 (1953).

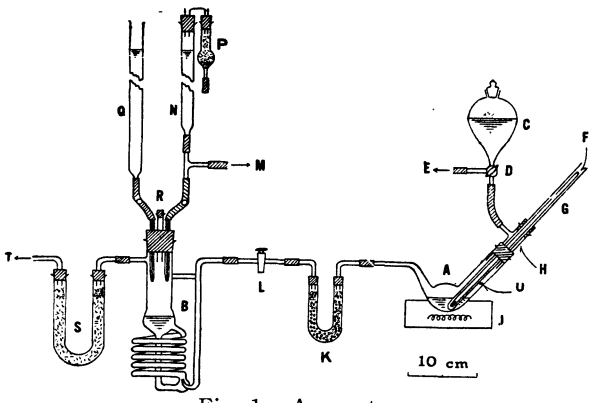



Fig. 1. Apparatus

A: Reaction Vessel
B: Carbon Dioxide Absorber
C: Water-Addition Funnel
D: Three-Way Stopcock
E: To an Apparatus Preparing the Carbon Dioxide-Free Air
F: Thermometer
G: Thermometer-Protecting Tube
H: Gas-Introducing Tube
J: Electric Heater
K: Iodine Absorber
L: Stopcock
M: To a Sodium Hydroxide Reservoir
N: Buret of Sodium Hydroxide
P: Soda Lime-Filled Guard Tube
Q: Buret of Hydrochloric Acid
R: Reagent-Addition Funnel
S: Soda Lime-Filled Guard Tube
T: To a Suction Pump
U: Small Glass Hook

## Reagents

*Potassium Iodate.*—Extra pure grade potassium iodate was used.

*Strong Phosphoric Acid.*—About 400 g. of extra pure grade 89% orthophosphoric acid was dehydrated by heating until the temperature of the liquid reached 320°C. Its specific gravity was 1.96.

*Anhydrous Sodium Thiosulfate.*—Sodium thiosulfate having 5 mol. of water of crystallization was dehydrated in vacuo at 40°C on a water bath. The resulting white anhydrous salt was crushed and its coarse fraction was used.

*Standard Solution of Hydrochloric Acid.*—A 0.1 N hydrochloric acid solution standardized against pure anhydrous sodium carbonate was used.

*Standard Solution of Sodium Hydroxide.*—A 0.1 N sodium hydroxide solution standardized against 0.1 N hydrochloric acid described above was used. According to Hinkel and Raymond, the sodium hydroxide pellets used must contain at least 2.5% by weight of sodium carbonate. If this quantity is not present, an appropriate amount should be added to the solution. The standardization was carried out by means of the method described in the section of procedure.

*Barium Chloride.*—A 10% solution of extra pure grade barium chloride was used.

*Thymol Blue.*—A 0.1 % solution of thymol blue was used.

## Procedure

Weigh accurately a 10 to 60 mg. of sample, depending upon its carbon content, into a small weighing tube; choose the sample weight so that the liberated carbon dioxide will consume about 50% of the sodium hydroxide used. Add 4 to 5 ml. of strong phosphoric acid and two or three times as much of the theoretically required amount of potassium iodate into the vessel A. Into the carbon dioxide absorber, and 3 drops of the indicator solution of thymol blue. Hang the weighing tube containing the sample on the small glass hook U of the thermometer-protecting tube G. Connect all of the apparatus and make sure that it is tight. Sending carbon dioxide-free air from E through the apparatus by a suction pump, expel all the air containing carbon dioxide, present in it. Then add 25 ml. of 0.1 N sodium hydroxide to the absorber B from the buret N.

Stop the suction, close the stopcock D, and open the stopcock L a little. Let the weighing tube containing the sample fall in the reaction medium by rotating the thermometer-protecting tube G. Then, gently heat the bottom of the vessel A with a small electric heater J. During the decomposition reaction keep the temperature of the reactants between 180° and 230°C, and regulate the stopcock L so that 2 bubbles of gas per second pass through the inlet of the absorber B. The greater part of the liberated iodine is sublimed and condensed on the inside wall of the vessel A. The small part of it is sent to the tube K and absorbed on anhydrous sodium thiosulfate. After the end of the decomposition reaction, stand the vessel A aloof from the heater until the temperature of the reaction medium falls to about 140°C. Apply gentle suction and open the stopcock D to introduce about 10 ml. of carbon dioxide-free water into the vessel A. Then heat once more the aqueous solution in the vessel A on the heater to expel the remaining carbon dioxide in the reaction medium. Then take away the heater and continue drawing air through the apparatus, at the rate of 2–3 bubbles per second for about fifteen minutes, in order to

get all the carbon dioxide into the absorber B.

From the reagent-addition tube R quickly add 10 ml. of 10% barium chloride to the absorber solution and close the top of the tube R. Then, applying rapid suction, titrate the remaining sodium hydroxide with 0.1 N hydrochloric acid until the blue color of thymol blue is changed to the light yellow one.

From the volumes of 0.1 N sodium hydroxide and 0.1 N hydrochloric acid used in the experiment the carbon content of the sample is calculated.

The standardization of 0.1 N sodium hydroxide is carried out as follows. After removing the air containing carbon dioxide from the apparatus, 25 ml. of 0.1 N sodium hydroxide, 3 drops of the indicator solution, and 10 ml. of 10% barium chloride are added to the absorber B and this solution is titrated with 0.1 N hydrochloric acid, stirring the contents of the absorber B by letting the carbon dioxide-free air flow rapidly.

## Results and Discussion

At first, in order to examine the purity of the carbon dioxide-free air used in this study, after passing the air through a measured amount of 0.1 N sodium hydroxide in the absorber B for twenty to forty minutes, it was titrated with 0.1 N hydrochloric acid in the same manner as in the standardization of sodium hydroxide described above. As shown in Table I the ratios of the volumes

Table I
Examination of the Purity of the Carbon Dioxide-Free Air Used

| Aeration min. | 0.1 N HCl ml. / 0.1 N NaOH ml. |
|---|---|
| 0 | 1.000 |
| 20 | $0.999_8$ |
| 30 | $0.996_7$ |
| 30 | $1.002_4$ |
| 40 | $1.000_4$ |

of 0.1 N sodium hydroxide and 0.1 N hydrochloric acid were almost equal to that in the case without aeration.

If the vapor of phosphoric acid is expelled from the reaction medium by heating and if it is absorbed in sodium hydroxide solution, it causes a serious error. In order to examine this point, two kinds of strong phosphoric acid having the specific gravity 1.93 and 1.96 were used. To the vessel A 5 ml. of the strong phosphoric acid was added and heated at various temperatures for fifteen minutes, while the vapor expelled from the medium was sent by the air stream into a definite amount of 0.1 N sodium hydroxide. From the results shown in Table II it was found that the strong phosphoric acid of the specific gravity 1.93 can not be used for the present

Table II
Effect of the Vaporization of Strong Phosphoric Acid

| Specific Gravity of Strong Phosphoric Acid | Temp. °C | 0.1 N HCl ml. / 0.1 N NaOH ml. |
|---|---|---|
| 1.93 | Room Temp. | 1.000 |
| 〃 | 167 | $0.989_8$ |
| 〃 | 181 | $0.998_6$ |
| 〃 | 200 | $0.987_9$ |
| 1.96 | Room Temp. | 1.000 |
| 〃 | 230 | $1.000_6$ |
| 〃 | 235 | $1.000_9$ |

purpose and that of the specific gravity 1.96 should be used.

Next, using sodium carbonate as a sample, preliminary experiments were undertaken to examine some conditions. The results obtained are shown in Table III. These experiments indicated that after the decomposition reaction, the reaction medium should be diluted with water and heated once more to expel the carbon dioxde dissolved in strong phosphoric acid. Also the time required to expel the carbon dioxide present in the apparatus is within fifteen minutes.

Table III
Determination of Carbon in Sodium Carbonate

Carbon Content Calculated: 11.33%

| Sample Weight | Carbon Content | | Expelling Time | Remarks |
|---|---|---|---|---|
| | Found | Deviation | | |
| mg. | % | % | min. | |
| 52.5 | 10.5 | −0.8 | 15 | Without additon of water |
| 55.6 | 10.6 | −0.7 | 30 | |
| 74.7 | 10.6 | −0.7 | 15 | |
| 77.0 | 11.1 | −0.2 | 30 | |
| 52.8 | 11.2 | −0.1 | 15 | With addition of water |
| 55.5 | 11.3 | 0.0 | 15 | |
| 57.4 | 11.3 | 0.0 | 13 | |
| 66.4 | 11.4 | +0.1 | 15 | |
| 70.5 | 11.2 | −0.1 | 15 | |
| 72.5 | 11.3 | 0.0 | 15 | |

Analyses of various known organic compounds, oxalic acid, sodium oxalate, tartaric acid, dulcitol, arabinose, alanine, urea, and methylred were carried out by this method. Thess results are summarized in Table IV. The accuracy of the data is within ±2%. The time required for one analysis is about fifty minutes.

The absorption tube used in this method is very advantageous for the determination of carbon dioxide, because the addition of alkali solution as well as the titration with acid solution can be done under the condition in which carbon dioxide present in the

TABLE IV
DETERMINATION OF CARBON IN ORGANIC COMPOUNDS

| Substance | Carbon Content | Sample Weight | Carbon Content | |
|---|---|---|---|---|
| | | | Found | Deviation |
| | % | mg. | % | % |
| Oxalic Adid $C_2H_2O_4 \cdot 2H_2O$ | 19.05 | 40.2 | 19.2 | +0.1 |
| | | 41.5 | 19.2 | +0.1 |
| | | 51.1 | 19.5 | +0.4 |
| | | 57.4 | 19.1 | 0.0 |
| | | 44.2 | 18.8 | −0.3 |
| Sodium Oxalate $Na_2C_2O_4$ | 17.93 | 40.3 | 18.0 | +0.1 |
| | | 44.0 | 18.0 | +0.1 |
| | | 46.9 | 18.0 | +0.1 |
| | | 54.2 | 17.9 | 0.0 |
| Tartaric Acid $C_4H_4O_6$ | 32.01 | 23.1 | 32.1 | +0.1 |
| | | 25.3 | 32.1 | +0.1 |
| | | 27.1 | 32.4 | +0.4 |
| | | 28.2 | 31.9 | −0.1 |
| Dulcitol $C_6H_{14}O_6$ | 39.56 | 20.4 | 39.6 | 0.0 |
| | | 21.5 | 39.6 | −0.6 |
| | | 27.5 | 39.4 | −0.2 |
| | | 27.5 | 39.4 | −0.2 |
| Arabinose $C_5H_{10}O_5$ | 40.00 | 23.5 | 39.6 | −0.4 |
| | | 24.5 | 40.0 | 0.0 |
| | | 27.3 | 39.7 | −0.3 |
| | | 32.1 | 39.6 | −0.4 |
| Alanine $C_3H_7O_2N$ | 38.70 | 11.7 | 39.1 | +0.4 |
| | | 15.7 | 38.5 | −0.2 |
| | | 18.9 | 38.9 | +0.2 |
| | | 25.6 | 38.7 | 0.0 |
| Urea $CH_4ON_2$ | 20.00 | 33.8 | 20.0 | 0.0 |
| | | 35.9 | 19.8 | −0.2 |
| | | 36.6 | 20.4 | +0.4 |
| | | 40.8 | 19.9 | −0.1 |
| | | 47.7 | 19.9 | −0.1 |
| Methylred $C_{15}H_{15}O_2N_3$ | 66.90 | 13.4 | 65.9 | −1.0 |
| | | 14.2 | 66.4 | −0.5 |
| | | 15.0 | 66.0 | −0.9 |

atmosphere is excluded perfectly from the titrating system.

For the determination of carbon in organic substances Pregl's dry combustion method has so far been commonly used. However various wet combustion methods have been recently developed to overcome the defects of Pregl's method. Among others the investigations of D. D. Van Slyke and his coworkers[6] are very remarkable. The present method reported by the author is also one of the wet combustion methods for the determination of carbon in organic compounds. As regards the time required for analysis and the accuracy of data the author's method is inferior to that of Van Slyke, but as regards the inexpensiveness of the apparatus and the simplicity of the analytical techniques the former is superior to the latter. The present method can not be applied to volatile compounds. The applicability of the author's method should be further investigated and the improvement of the apparatus is also a problem remaining for the future.

6) e.g., D.D. Van Slyke, *Anal. Chem.*, 26, 1706 (1954).

## Summary

(1) A new wet combustion method for the determination of carbon in organic compounds has been developed.

(2) A sample is decomposed by heating with a mixture of potassium iodate and strong phosphoric acid. The liberated carbon dioxide is absorbed in 0.1 N sodium hydroxide, using a spiral type absorber. After adding barium chloride solution the excess sodium hydroxide is titrated with 0.1 N hydrochloric acid, using thymol blue as indicator, in the absorber.

(3) A part of the liberated iodine is absorbed into the tube filled with anhydrous sodium thiosulfate in order to avoid the absorption of the iodine in the alkali solution in the absorber.

(4) Analyses for several organic compounds gave satisfactory results. Using 10 to 60 mg. of samples, the accuracy was within ±2%. Analysis time for one sample is about fifty minutes.

The author wishes to express his hearty thanks to Prof. T. Kiba for his advice and encouragement and to Mr. J. Ono and Mr. T. Takagi for their helpful assistance. This study was supported in part by a grant from the Ministry of Education.

*Department of Chemistry, Faculty of Science, Kanazawa University, Kanazawa*

# *Hydrogen Deformation Vibrations*[1]

By Ichiro NAKAGAWA and San-ichiro MIZUSHIMA

(Received May 18, 1955)

## Introduction

The normal vibrations of molecules can conveniently be grouped into hydrogen vibrations and skeletal vibrations[2]. Of the former the stretching vibrations are observed in the 3 $\mu$ region sufficiently separated from skeletal frequencies, whereas the deformation vibrations appear in a region in which many skeletal vibrations give infrared and Raman frequencies. Therefore, it is desirable to distinguish the hydrogen deformation vibrations from the skeletal vibrations for the interpretation of the vibrational spectra in relation to the structure of molecules[3]. The present calculation has been made with the object of aiding in the assignment of these hydrogen deformation vibrations.

## Outline of the Calculation

The calculation was made by Wilson's method[4], according to which we set up a secular equation of the type:

$$|\boldsymbol{GF}-\boldsymbol{E}\lambda| = 0,$$

where $\boldsymbol{G}$ and $\boldsymbol{F}$ are, respectively, the kinetic and the potential energy matrices. In this calculation we consider only that part of a molecule which is directly connected to the CH, $CH_2$, and $CH_3$ groups under consideration, because Nakagawa has shown that there is, in general, not much coupling between the hydrogen deformation vibrations and the skeletal vibrations[5]. For example, when we calculate the $CH_2$ deformation frequencies of $CH_3CH_2Cl$, we reduce the problem to the vibrations of C-$CH_2$-Cl.

The symmetry coordinates $\boldsymbol{S}$ obtained from the internal coordinates $\boldsymbol{R}$ by a linear transformation:

$$\boldsymbol{S} = \boldsymbol{UR}$$

are shown in Table I. Here $\boldsymbol{U}$ is an orthogonal matrix, $\alpha$ is a carbon valence angle, and 1, 2, 3, and 4 (subscripts) refer to the four bonds of carbon atom (see Fig. 1). For example, $\alpha_{12}$

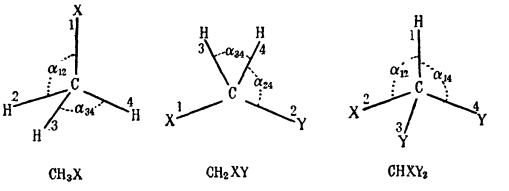



Fig. 1. Internal coordinates of $CH_3X$, $CH_2XY$ and $CHXY_2$.

denotes the carbon valence angle formed by the first and second bonds. The mode of each hydrogen deformation vibration is understood from the mathematical expression of the corresponding symmetry coordinate shown in Table I[6].

TABLE I
SYMMETRY COORDINATES OF HYDROGEN DEFORMATION VIBRATIONS

| Molecule | Vibrational mode | Symmetry coordinate |
|---|---|---|
| $CH_3X$ | $CH_3$ degenerate | $\Delta(2\alpha_{34}-\alpha_{23}-\alpha_{24})/\sqrt{6}$<br>$\Delta(\alpha_{23}-\alpha_{24})/\sqrt{2}$ |
| | $CH_3$ symmetric | $\Delta(\alpha_{12}+\alpha_{13}+\alpha_{14}-\alpha_{23}-\alpha_{24}-\alpha_{34})/\sqrt{6}$ |
| | $CH_3$ rocking | $\Delta(2\alpha_{12}-\alpha_{13}-\alpha_{14})/\sqrt{6}$<br>$\Delta(\alpha_{13}-\alpha_{14})/\sqrt{6}$ |
| $CH_2X_2$, $CH_2XY$ | $CH_2$ bending | $\Delta(4\alpha_{34}-\alpha_{13}-\alpha_{14}-\alpha_{23}-\alpha_{24})\sqrt{20}$ |
| | $CH_2$ wagging | $\Delta(\alpha_{13}+\alpha_{14}-\alpha_{23}-\alpha_{24})/2$ |
| | $CH_2$ twisting | $\Delta(\alpha_{13}-\alpha_{14}-\alpha_{23}+\alpha_{24})/2$ |
| | $CH_2$ rocking | $\Delta(\alpha_{13}-\alpha_{14}+\alpha_{23}-\alpha_{24})/2$ |
| $CHX_3$, $CHXY_2$ | CH bending | $\Delta(2\alpha_{12}-\alpha_{13}-\alpha_{14})/\sqrt{6}$<br>$\Delta(\alpha_{13}-\alpha_{14})/\sqrt{2}$ |

The matrices $\boldsymbol{G}_S$ and $\boldsymbol{F}_S$ in symmetry coordinates are obtained from the matrices $\boldsymbol{G}_R$ and $\boldsymbol{F}_R$ in internal coordinates through the transformations:

$$\boldsymbol{G}_S = \boldsymbol{UG}_R\boldsymbol{U}'$$
$$\boldsymbol{F}_S = \boldsymbol{UF}_R\boldsymbol{U}'$$

1) A part of this paper was presented at Gordon Research Conference on Infrared Spectroscopy, Meriden, New Hampshire, U.S.A. August, 1954.

2) See, e.g., S. Mizushima, "Structure of Molecules and Internal Rotation", Academic Press, New York (1954 ; I. Nakagawa and S. Mizushima, *J. Chem. Phys.*, **21**, 2195 (1953).

3) As to previous researches on hydrogen deformation vibrations, see, e.g., N. Sheppard, *J. Chem. Phys.*, **16**, 690 (1948); **17**, 74 (1949); R.S. Rasmussen, *J. Chem. Phys.*, **16**, 712 (1948).

4) E.B. Wilson, *J. Chem. Phys.*, **7**, 1047 (1939); **9**, 76 (1941).

5) I. Nakagawa, *J. Chem. Soc. Japan*, **75**, 178, 535 (1954).

6) The modes of these deformation vibrations are shown diagramatically in reference 5.

where $U'$ is the transpose of $U$.

The diagonal terms $G_{SS}$ of $G$-matrices are shown in Table II, where $\mu_C$, $\mu_H$, $\mu_X$ and $\mu_Y$ are the reciprocals of masses of the C, H, X and Y atoms, and $r_H$, $r_C$, $r_X$ and $r_Y$ are the reciprocals of the C-H, C-C, C-X and C-Y bond lengths. Furthermore, all the carbon valence angles are assumed to be tetrahedral. The underlined parts of the expressions of $G_{SS}$ are independent of X and Y and contain $\mu_H$ which makes the diagonal terms much larger than the cross terms containing the reciprocals of masses of heavier atoms. Therefore, we may neglect the cross terms of $G$-matrices in the approximate calculation of hydrogen deformation frequencies.

In the case of $F$-matrices the ratio of diagonal terms to cross terms depends on the nature of the potential function. We used the function of the Urey-Bradley type[7], from which the diagonal terms of $F$-matrices are calculated as shown in Table II, where

$$J_{HH}=R_H^2(H_{HCH}+2/5F_{H\ldots H}),$$
$$J_{HX}=R_HR_X(H_{HCX}+c_{HX}F_{H\ldots X}).$$

and

$$c_{HX}=tt_1+1/10\,ss_1$$
$$t=(2\sqrt{2}/3)R_X/q_{HX},$$
$$t_1=(2\sqrt{2}/3)R_H/q_{HX},$$
$$s=(1/q_{HX})(R_H+1/3\,R_X),$$
$$s_1=(1/q_{HX})(R_X+1/3\,R_H),$$
$$q_{HX}=(R_H^2+R_X^2+2/3\,R_HR_X)^{\frac{1}{2}}.$$

Here $H_{HCH}$ and $H_{HCX}$ are force constants for the deformation of the HCH and HCX angles, $F_{H\ldots H}$ and $F_{H\ldots X}$ those for the changes of distances between the two nonbonded H atoms and between the nonbonded H and X atoms, $R_H$ and $R_X$ the C-H and C-X bond lengths, and $k$'s the intramolecular tensions[7]. The values of force constants and intramolecular tensions are shown in Table III[2,8].

7) T. Shimanouchi, *J. Chem. Phys.*, **17**, 245, 734, 848 (1949).

8) See also T. Shimanouchi, *J. Chem. Soc. Japan*, **74**, 266 (1953); I. Nakagawa and S. Mizushima, *J. Chem. Phys.*, **22**, 759 (1954); I. Nakagawa, *J. Chem. Soc. Japan*, **76**, 540 (1955).

TABLE II

DIAGONAL TERMS OF $G$- AND $F$-MATRICES, $G_{SS}$ AND $F_{SS}$

| Molecule | Vibrational mode | $G_{SS}$ | $F_{SS}$ |
|---|---|---|---|
| $CH_3X$ | $CH_3$ degenerate | $\underline{[(5/2)\mu_H+(8/3)\mu_C]r_H^2}$ | $J_{HH}+(1/2\sqrt{2})k_1$ |
| | $CH_3$ symmetric | $\underline{[2\mu_H+(16/3)\mu_C]r_H^2}$ | $(1/2)(J_{HH}+J_{HX})+(3/2\sqrt{2})k_1$ |
| | $CH_3$ rocking | $\underline{[\mu_H+(1/6)\mu_C]r_H^2}+(3/2)\mu_Xr_X^2+\mu_C[(3/2)\times r_X^2+r_Hr_X]$ | $J_{HX}+(1/2\sqrt{2})k_1$ |
| $CH_2X_2$ | $CH_2$ bending | $\underline{[(5/2)\mu_H+(10/3)\mu_C]r_H^2}+(1/10)\mu_Xr_X^2+(2/15)\mu_Cr_X^2-(4/3)\mu_Cr_Hr_X$ | $(4/5)J_{HH}+(1/5)J_{HX}+(3/10\sqrt{2})k_2$ |
| | $CH_2$ wagging | $\underline{[(3/2)\mu_H+3\mu_C]r_H^2}+(1/2)\mu_Xr_X^2+\mu_C[(1/3)r_X^2+2r_Hr_X]$ | $J_{HX}+(3/2\sqrt{2})k_2$ |
| | $CH_2$ twisting | $\underline{(3/2)\mu_Hr_H^2}+(3/2)\mu_Xr_X^2$ | $J_{HX}-(1/2\sqrt{2})k_2$ |
| | $CH_2$ rocking | $\underline{[(1/2)\mu_H+(1/3)\mu_C]r_H^2}+(3/2)\mu_Xr_X^2+\mu_C(3r_X^2+2r_Hr_X)$ | $J_{HX}+(3/2\sqrt{2})k_2$ |
| $CH_2XY$ | $CH_2$ bending | $\underline{[(5/2)\mu_H+(10/3)\mu_C]r_H^2}+(1/20)(\mu_Xr_X^2+\mu_Yr_Y^2)+(1/20)\mu_C(r_X^2+r_Y^2)+(1/30)\mu_Cr_Xr_Y-(2/3)\mu_C(r_Hr_X+r_Hr_Y)$ | $(4/5)J_{HH}+(1/10)(J_{HX}+J_{HY})+(3/10\sqrt{2})k_2$ |
| | $CH_2$ wagging | $\underline{[(3/2)\mu_H+3\mu_C]r_H^2}+(1/4)(\mu_Xr_X^2+\mu_Yr_Y^2)+(1/4)\mu_C(r_X^2+r_Y^2)-(1/6)\mu_Cr_Xr_Y+\mu_C(r_Hr_X+r_Hr_Y)$ | $(1/2)(J_{HX}+J_{HY})+(3/2\sqrt{2})k_2$ |

| Molecule | Vibrational mode | $G_{SS}$ | $F_{SS}$ |
|---|---|---|---|
| | $CH_2$ twisting | $(3/2)\mu_H r_H^2+(3/4)(\mu_X r_X^2+\mu_Y r_Y^2)$ $+(3/4)\mu_C(r_X^2+r_Y^2)-(3/2)\mu_C r_X r_Y$ | $(1/2)(J_{HX}+J_{HY})-(1/2\sqrt{2})k_2$ |
| | $CH_2$ rocking | $[(1/2)\mu_H+(1/3)\mu_C]r_H^2+(3/4)(\mu_X r_X^2+\mu_Y r_Y^2)$ $+(3/4)\mu_C(r_X^2+r_Y^2)+(3/2)\mu_C r_X r_Y$ $+\mu_C(r_H r_X+r_H r_Y)$ | $(1/2)(J_{HX}+J_{HY})+(3/2\sqrt{2})k_2$ |
| $CHX_3$ | CH bending | $[(3/2)\mu_H+(3/2)\mu_C]r_H^2+\mu_X r_X^2+\mu_C[(1/6)r_X^2$ $+r_H r_Y]$ | $J_{HX}+(1/2\sqrt{2})k_3$ |
| $CHXY_2$ | CH bending (A′) | $[(3/2)\mu_H+(3/2)\mu_C]r_H^2+(2/3)\mu_X r_X^2$ $+(1/3)\mu_Y r_Y^2+\mu_C[(2/3)r_H r_X$ $+(1/3)r_H r_Y+(2/3)r_X^2-(10/9)r_X r_Y$ $+(11/18)r_Y^2]$ | $(2/3)J_{HX}+(1/3)J_{HY}+(1/2\sqrt{2})k_3$ |
| | CH bending (A″) | $[(3/2)\mu_H+(3/2)\mu_C]r_H^2+\mu_Y r_Y^2+\mu_C[(1/6)r_Y^2$ $+r_H r_Y]$ | $J_{HY}+(1/2\sqrt{2})k_3$ |
| $CH_3$–$CH_3$* | $CH_3$ degenerate | $(G_{SS})_0$ | $J_{HH}+(1/2\sqrt{2})k_1$ |
| | $CH_3$ symmetric | $(G_{SS})_0$ | $(1/2)(J_{HH}+J_{HC})+(3/2\sqrt{2})k_1$ |
| | $CH_3$ rocking | $(G_{SS})_0\pm\mu_C(3r_C^2+r_C r_H)\cos\theta$ | $J_{HC}+(1/2\sqrt{2})k_1$ |
| $XCH_2$ –$CH_2X$** | $CH_2$ bending | $(G_{SS})_0\pm[-2\mu_C\{(2/3)r_C r_H-(1/10)r_C^2$ $-(1/30)r_C r_X\}\cos\theta]$ | $(4/5)J_{HH}+(1/10)(J_{HX}+J_{HC})$ $+(3/10\sqrt{2})k_2$ |
| | $CH_2$ wagging | $(G_{SS})_0\pm(1/2)\mu_C[r_C^2+2r_C r_H-(1/3)r_C r_X]\cos\theta$ | $(1/2)(J_{HX}+J_{HC})+(3/2\sqrt{2})k_2$ |
| | $CH_2$ twisting | $(G_{SS})_0\pm[-(3/2)\mu_C(r_C^2-r_C r_X)\cos\theta]$ | $(1/2)(J_{HX}+J_{HC})-(1/2\sqrt{2})k_2$ |
| | $CH_2$ rocking | $(G_{SS})_0\pm[-(3/2)\mu_C\{r_C^2+r_C r_X$ $+(2/3)r_C r_H\}\cos\theta]$ | $(1/2)(J_{HX}+J_{HC})+(3/2\sqrt{2})k_2$ |

* $(G_{SS})_0$ signifies $G_{SS}$ of $CH_3X$ for X=C. The signs+and−refer, respectively, to the symmetric (A) and the anti-symmetric (B) vibrations to the $C_2$ axis. The azimuthal angle $\theta$ is taken as zero for the trans position.

** $(G_{SS})_0$ signifies $G_{SS}$ of $CH_2XY$ for Y=C.

TABLE III

VALUES OF FORCE CONSTANTS $H$ AND $F$ IN $10^5$ dyn./cm. AND INTRAMOLECULAR TENSION $k$ IN $10^{-11}$ dyn. cm.

| Deformation constant $H$ | | Repulsion constant $F$ | | Intramolecular tension $k$ | | | | | | | |
|---|---|---|---|---|---|---|---|---|---|---|---|
| H–C–H | 0.40 | H..(C)..H | 0.10 | | | | | | | $CH_4$ | 0.00 |
| H–C–F | 0.06 | H..(C)..F | 1.15 | $CH_3F$ | 0.10 | $CH_2F_2$ | 0.20 | $CHF_3$ | 0.35 | $CF_4$ | 0.45 |
| H–C–Cl | 0.05 | H..(C)..Cl | 0.80 | $CH_3Cl$ | 0.05 | $CH_2Cl_2$ | 0.10 | $CHCl_3$ | 0.20 | $CCl_4$ | 0.26 |
| H–C–Br | 0.04 | H..(C)..Br | 0.65 | $CH_3Br$ | 0.03 | $CH_2Br_2$ | 0.07 | $CHBr_3$ | 0.15 | $CBr_4$ | 0.25 |
| H–C–I | 0.04 | H..(C)..I | 0.52 | $CH_3I$ | 0.02 | $CH_2I_2$ | 0.04 | $CHI_3$ | 0.10 | | |
| H–C–$CX_3$ | 0.15 | H..(C)..$CX_3$ | 0.40 | $CH_3CX_3$ | 0.05 | | | | | | |
| H–C–$CH_3$ | 0.25 | H..(C)..$CH_3$ | 0.50 | | | | | $CH(CH_3)_3$ | 0.03 | $C(CH_3)_4$ | 0.04 |
| H–C–C(≡) | 0.21 | H..(C)..C(≡) | 0.50 | $CH_3CN$ | 0.04 | $CH_2(CN)_2$ | 0.07 | | | | |
| H–C–N | 0.20 | H..(C)..N | 0.60 | $CH_3NC$ | 0.05 | | | | | | |

Although the diagonal terms of $F$-matrices are not always large as compared with the cross terms, approximate calculations of hydrogen deformation frequencies have been made from the product $G_{ss}F_{ss}$ of the diagonal terms shown in Table II. The difference between the computed and the observed frequencies has been found to be less than 5%[9].

In the higher approximations we have taken into account the effect of the cross terms in the following form:

$$(GF)_{ss}=G_{ss}F_{ss}+a,$$
$$\lambda=(GF)_{ss}+b,$$

where $a$ and $b$ are the correction terms[9].

## Results for CH Deformation Frequencies

The calculations have been made for many molecules, including those of methane and ethane derivatives and their deuterated compounds. The computed values have been shown to be in good agreement with those observed[10]. The frequency ranges of hydrogen deformation vibrations thus obtained are shown in Table IV, where those of fluorine compounds have been omitted, because they show abnormal values[10].

The inspection of the expressions of $G_{ss}$ and $F_{ss}$ shown in Table II, together with the numerical values given in Table IV, gives us information on the specific features of hydrogen deformation vibrations, which are useful in the assignment of these vibrations. Some of these features are listed in the following:

(1) The $CH_3$ degenerate deformation vibrations and the $CH_2$ bending vibrations appear in narrow frequency regions. Furthermore, these regions are separated from those of other hydrogen deformation vibrations.

(2) The $CH_3$ symmetric deformation vibrations also appear in a narrow frequency range, when this group is directly connected to a carbon atom as $CH_3$–C–.

(3) The frequency values of the hydrogen deformation vibrations in the same series (e.g. $CH_3X$, $CH_2X_2$ and $CHX_3$) decrease in the following order: $CH_3$ degenerate deformation $>CH_2$ bending $>CH_3$ symmetric deformation $>CH_2$ wagging $>CH$ bending $>CH_2$ twisting $>CH_3$ rocking $>CH_2$ rocking. In some cases

TABLE IV

THE FREQUENCY RANGES OF HYDROGEN DEFORMATION VIBRATIONS IN $cm^{-1}$

| Molecule* | Vibrational mode | Frequency range |
|---|---|---|
| $CH_3X$ | $CH_3$ degenerate | ca. 1450 |
| | $CH_3$ symmetric | 1250–1400 |
| | $CH_3$ rocking | 900–1150 |
| $CH_2X_2$ & $CH_2XY$ | $CH_2$ bending | 1350–1450 |
| | $CH_2$ wagging | 1100–1350 |
| | $CH_2$ twisting | 1000–1300 |
| | $CH_2$ rocking | 700–1000 |
| $CHX_3$ & $CHXY_2$ | CH bending | 1100–1350 |
| $CH_3CX_3$ | $CH_3$ degenerate | ca. 1450 |
| | $CH_3$ symmetric | 1370–1390 |
| | $CH_3$ rocking | 1000–1100 |
| $CH_3CHX_2$ & $CH_3CH_2X$ | $CH_3$ degenerate ($A'$ & $A''$) | ca. 1450 |
| | $CH_3$ symmetric | 1370–1390 |
| | $CH_3$ rocking ($A'$ & $A''$) | 1000–1100 |
| $CH_3COX$ | $CH_3$ degenerate ($A'$ & $A''$) | ca. 1420 |
| | $CH_3$ symmetric | ca. 1360 |
| | $CH_3$ rocking ($A'$ & $A''$) | 1000–1100 |
| $(CH_3)_2CHX$ | $CH_3$ degenerate ($A'$ & $A''$) | ca. 1450 |
| | $CH_3$ symmetric ($A'$ & $A''$) | 1370–1390 |
| | $CH_3$ rocking ($A'$ & $A''$)** | 900–1150 |
| | C–C stretching** | 870–890 ($A'$), 1120–1140 ($A''$) |
| | CH bending | variable ($A'$), 1320–1340 ($A''$) |
| $(CH_3)_3CX$ | $CH_3$ degenerate ($A_1$ & $E$) | ca. 1450 |
| | $CH_3$ symmetric ($A_1$ & $E$) | 1370–1390 |
| | $CH_3$ rocking ($A_1$ & $E$)** | 900–1150 |
| | C–C stretching ($A_1$ & $E$)** | 800–810 ($A_1$), 1220–1240 ($E$) |
| $XCH_2CH_2X$ | $CH_2$ bending | 1400–1450 |
| | $CH_2$ wagging | 1150–1350 |
| | $CH_2$ twisting | 1000–1300 |
| | $CH_2$ rocking | 700–1000 ($B_g > A > B > A_u$) |

* Fluorine compounds are excluded.

** The C–C stretching and $CH_3$ rocking vibrations are coupled with each other considerably in these cases.

9) I. Nakagawa, *J. Chem. Soc. Japan*, **75**, 1259 (1954).

10) I. Nakagawa, ibid., **76**, 540 (1955).

the order of the $CH_2$ wagging frequency and the $CH_3$ symmetric deformation frequency may be reversed.

(4) The CH bending frequencies of $CHX_3$ and $CHY_3$, which are degenerate, are split into two frequencies $A'$ and $A''$ in $CHXY_2$ where $A''$ has nearly the same frequency as the degenerate frequency of $CHY_3$ and $A'$ has a value lying between those of $CHX_3$ and $CHY_3$ but closer to that of $CHX_3$.

(5) According to the result of the similar calculation made for molecules of the type, $XH_2C-CH_2X$, the two deformation frequencies, one symmetric and the other antisymmetric to the $C_2$ axis, are not much different from each other and are not sensitive to the change of azimuthal angle of the internal rotation about the C-C axis, except for the $CH_2$ rocking frequencies. Furthermore, the selection rules for the rocking frequencies are quite different for the trans, gauche and cis forms. The frequency values of the rocking vibrations decrease in the following order: $B_g(trans) > A(gauche) > B(gauche) > A_u(trans)$. The observation of rocking frequencies provides important experimental data of the optical isomerism of a new type described in previous notes[11].

## $NH_3$-Deformation Frequencies in Ammine Complexes

When the $NH_3$ group is coordinated about a central metal atom in coordination complexes such as $[Co(NH_3)_6]Cl_3$, we expect the appearance of three deformation frequencies similar to those of the $CH_3$ deformation frequencies. Actually we have found in these complexes three frequencies at about 1610, 1330 and 830 $cm^{-1}$ and these are assigned, respectively, to the degenerate deformation, symmetric deformation and rocking vibrations as shown in a previous paper[12]. There we did not describe the procedure of the calculation at all, but it is easily seen that this is quite similar to that of the calculation of $CH_3$ deformation vibrations of $CH_3X$ shown in Table I. The force constants used in this calculation are shown in Table V.

It is to be noted that of these five constants $H_{HNH}$, $F_{H\,..\,(N)\,..\,H}$ and $k$ can also be used for the calculation of the normal frequencies of ammonia, $NH_3$, ammonium ion, $NH_4^+$ and their deuteration products, $ND_3$ and $ND_4^+$. Therefore, the reasonableness of their values can be checked by the normal frequency calculations for these compounds and ions. As shown in Table VI the calculated values are in good agreement with the observed values and consequently, these constants are concluded to have reasonable values.

TABLE VI*

CALCULATED AND OBSERVED FREQUENCIES IN $cm^{-1}$ OF $NH_3$, $ND_3$, $NH_4^+$ AND $ND_4^+$

| | $NH_3$ | | $ND_3$ | |
|---|---|---|---|---|
| | Calc. | Obs. | Calc. | Obs. |
| $A_1$ | 3333 | 3336 | 2374 | 2419 |
| | 951 | 950 | 724 | 749 |
| $E$ | 3410 | 3414 | 2506 | 2555 |
| | 1630 | 1628 | 1188 | 1191 |

| | $NH_4^+$ | | $ND_4^+$ | |
|---|---|---|---|---|
| | Calc. | Obs. | Calc. | Obs. |
| $A_1$ | 3041 | 3041 | 2150 | 2214 |
| $E$ | 1710 | 1710 | 1209 | 1215 |
| $T$ | 3138 | 3138 | 2321 | 2350 |
| | 1403 | 1403 | 1049 | 1066 |

* Evidently for the calculation of these frequencies the N-H stretching force constants ($6.30\times10^5$ dynes/cm. for $NH_3$ and $5.26\times10^5$ dynes/cm. for $NH_4^+$) are needed in addition to the three constants mentioned above.

Using the force constants shown in Table V, the frequencies of the $NH_3$ degenerate deformation, symmetric deformation and rocking vibrations of $[Co(NH_3)_6]Cl_3$ have been calculated and compared with the observed values in Table VII. The agreement between the computed and observed values is good and consequently our assign-

TABLE V

THE VALUES OF FORCE CONSTANTS $H$ AND $F$ IN $10^5$ DYNES/CM. AND INTRAMOLECULAR TENSION $k$ IN $10^{-11}$ dyn. cm.

| $H$ | | $F$ | | $k$ |
|---|---|---|---|---|
| H-N-H | 0.54 | H..(N)..H | 0.06 | −0.04 |
| H-N-Co | 0.18 | H..(N)..Co | 0.10 | |

TABLE VII

CALCULATED AND OBSERVED DEFORMATION FREQUENCIES IN $CM^{-1}$ OF THE $NH_3$ AND $ND_3$ LIGANDS

| Vibrational mode | $[Co(NH_3)_6]Cl_3$ | | $[Co(ND_3)_6]Cl_3$ | |
|---|---|---|---|---|
| | Calc. | Obs. | Calc. | Obs. |
| Degenerate | 1579 | 1610 | 1156 | 1162 |
| Symmetric | 1340 | 1330 | 1021 | 1024 |
| Rocking | 854 | 835 | 628 | outside the NaCl region |

11) J.V. Quagliano and S. Mizushima, *J. Am. Chem. Soc.*, 75, 6084 (1953). See also S. Mizushima, I. Nakagawa, I. Ichishima and T. Miyazawa, *J. Chem. Phys.*, 22, 1614 (1954).

12) S. Mizushima, I. Nakagawa and J.V. Quagliano, *J. Chem. Phys.*, 23, 1367 (1955).

ment has been shown to be correct. Furthermore, this assignment has been checked by observing the isotopic shift of these frequencies[12]. As shown in the same table, the observed frequencies of the deformation vibrations of the $ND_3$ ligand are in good agreement with those calculated from the isotopic relations.

Some authors have explained these bands as arising from the metal-ligand vibrations of the octahedral cation[13]. However, from our calculation it has been shown that the assignment made in this paper is more reasonable.

From the result of the present research we can conclude that the metal-to-ligand bond should be fairly covalent in metal ammine complexes. If this bond were ionic, we could conclude that there are no rocking vibrations of the $NH_3$ group.

13) H.G. Hill and A.F. Rosenberg, *J. Chem. Phys.*, 22, 148 (1954).

**Summary**

The CH, $CH_2$ and $CH_3$ deformation frequencies in various organic compounds and the $NH_3$ deformation frequencies in metal ammine complexes have been calculated based on the Urey-Bradley field. The fact that diagonal terms of $G$-matrices for these vibrations are much larger than the cross terms makes the approximate calculation quite easy. The frequency range of each of these vibrations has been tabulated and their specific features have been pointed out, which will aid in the assignment of the frequencies observed for many organic compounds and metal ammine complexes.

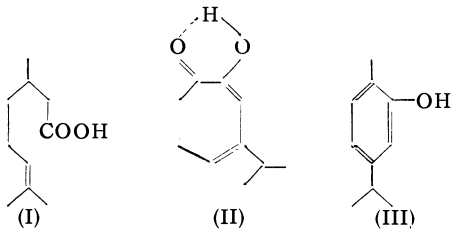
*Chemical Laboratory, Faculty of Science,*
*The University, of Tokyo,*
*Tokyo*

# *The Structure of Chamenol**

By Tetsuo NOZOE, Yoshio KITAHARA, and Tomio ARAI

(Received May 18, 1955)

Some time ago, Nozoe and others[1] isolated two different phenolic substances from the acid portion of the essential oil of *Chamaecyparis taiwanensis Masamune et Suzuki*, together with *l*-rhodinic acid (I) and hinokitiol (II) (or β-thujaplicin), and designated the phenolic substances chamenol-A (oil) and chamenol-B (m.p. 41–42°, b.p. 122–124°/15 mmHg, $C_9H_{12}O_2$ or $C_{10}H_{14}O_2$). Later studies by Nozoe and others[2] revealed that chamenol-A is carvacrol (III).




(I) (II) (III)

By studies[2] on the acid portion of *Thujopsis dolabrata Sieb. et Zucc.*, *l*-rhodinic acid (I), hinokitiol (II) and carvacrol (III) were isolated; however the fraction (b.p. 122–125°/15 mmHg) that seemed to be chamenol-B, on seeding with crystals of chamenol-B, afforded crystals of α-thujaplicin, and chamenol-B could not be isolated from the essential oil of *Thujopsis*. Luckily, however, a minute amount of chamenol-B was brought back to Japan on repatriation from Formosa and its structural studies were again carried out.

Since chamenol-A has been found to be identical with carvacrol, chamenol-B will henceforth be referred to simply as *chamenol*.

The infrared spectra[3] (Figs. 1 and 2) of chamenol point to the presence of the following groups[4].

2.80 μ: hydroxyl group
3.24 μ (shoulder): probably C-H of benzene nucleus
3.37 and 3.45 μ: aliphatic C-H
6.24 and 6.60 μ: benzene nucleus
6.87, 7.32, 8.52 and 8.72 μ: isopropyl group[5]

* This work was presented at the XIIIth International Congress of Pure and Applied Chemistry at Stockholm, July 31st, 1953.

1) T. Nozoe, *Science of Drugs*, **3**, 174 (1949); *Science Repts. Tohoku Univ., First Ser.*, **34**, 199 (1950).

2) T. Nozoe, A. Yasue and K. Yamane, *Proc. Japan Acad.*, **27**, 15 (1951).

3) Infrared absorption spectrum was measured by Dr. M. Tsuboi of Faculty of Science, Tokyo University.

4) a) H.W. Thompson, *J. Chem. Soc.*, 328 (1948).
b) N.B. Colthup, *J. Optical Soc. Am.*, **40**, 397 (1950).
c) H.M. Randall, R.G. Fowler, N. Fuson and J.R. Dangl, *Infrared Determination of Organic Structures*. D. Van Nostrand Co., N.Y. (1949).

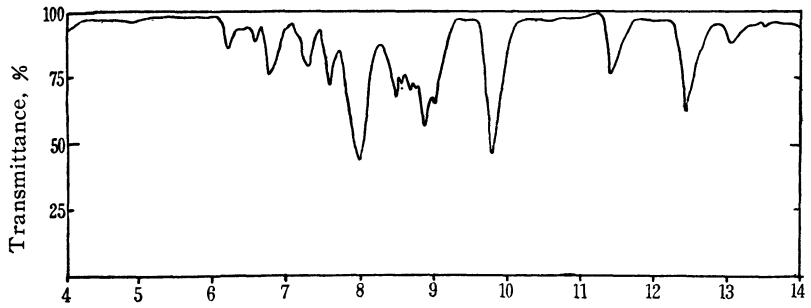
5) D.M. Simpson and G.B.B.M. Sutherland, *Proc. Roy. Soc.* (London), **A 199**, 169 (1949); *Chem. Abstr.*, **44**, 2372 (1950).

8.05 and 8.85 $\mu$: aromatic ether (the absorption band due to C-O-C in trimethoxybenzaldehyde is at 8.87 $\mu$[4c])

11.43 and 12.49 $\mu$: 1, 2, 4-trisubstituted benzene.

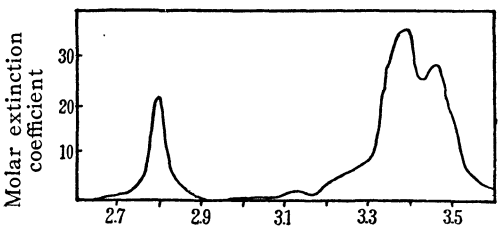
The fact that the 5.5–6.1 $\mu$ region lacks any absorption clearly shows that the molecule does not contain any carbonyl function.

Analytical values of chamenol correspond to the formula $C_{10}H_{14}O_2$, containing one methoxyl group. It is a phenolic substance and colors deep green with ferric chloride but did not give a red color in organic solvents (chloroform or benzene), characteristic of tropolones. It gives a monobenzoate, m.p. 64–65° and a *p*-nitrobenzoate, m.p. 87°. Chamenol shows a blue green coloration by the Liebermann reaction[6] and therefore the para-position of the phenol is apparently free of a substituent.




Wave length in microns

Fig. 1. Infrared absorption spectrum of chamenol (solid).




Wave length in microns

Fig. 2. Near infrared absorption spectrum of chamenol in 0.01 mol./l. $CCl_4$ solution.

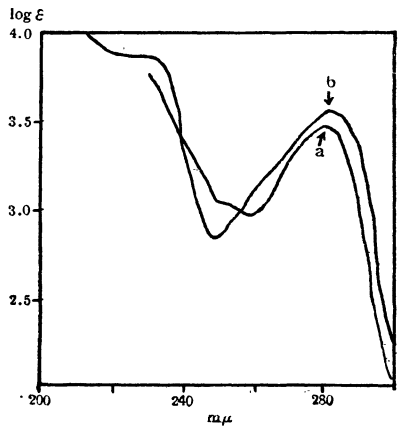


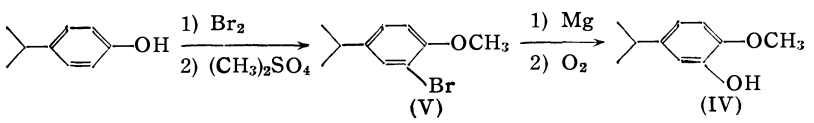

Fig. 3. Ultraviolet absorption spectra in methanol.

a) chamenol b) dihydroeugenol

From the analytical results and infrared determination, chamenol may be assumed to be a phenol possessing a methoxyl and an isopropyl group. The ultraviolet spectrum of chamenol, as shown in Fig. 3, possesses an absorption maximum at 281 m$\mu$ while the maximum of dihydroeugenol is 281 m$\mu$.

These results suggest that chamenol is an isopropyl derivative of guaiacol and could reasonably be represented by structure (IV).

Based on this surmise, the synthesis of (IV) was initiated from 2-bromo-4-isopropylanisole (V), obtained from *p*-isopropylphenol[7]. The bromide (V) was converted to the Grignard reagent in the presence of isopropyl bromide and followed by oxidation with oxygen to afforded 5-isopropylguaiacol, m.p. 41-42°. Both this substance and its *p*-nitrobenzoate showed no depression of the melting points on admixture with chamenol and its *p*-nitrobenzoate respectively; thus the structure of chamenol was confirmed as (IV).




6) C. Liebermann, *Ber.*, 7, 806, 1098 (1874); W.B. Deichmann, *Ind. Eng. Chem. Anal. Ed.*, 16, 37 (1944).

7) R.A. Smith, *J. Am. Chem. Soc.*, 56, 718 (1934).

## Experimental

*Chamenol*[1]—Colorless scales from petroleum ether, b.p. 122–124°/15 mmHg, m.p. 41–42°. Anal. Found: C, 72.44; H, 8.31; Mol. wt. (Rast method), 169; $OCH_3$ (by Zeisel method), 18.01. Calcd. for $C_{10}H_{14}O_2$: C, 72.44; H, 8.48; Mol. wt., 166; $OCH_3$, 18.67. *p-Nitrobenzoate*: Pale yellow prisms from ethanol, m.p. 86–87°. Anal. Found: C, 64.42; H, 5.46; N, 4.65. Calcd. for $C_{17}H_{17}O_5N$: C, 64.76; H, 5.40; N, 4.44. *Benzoate*: Colorless scales from ethanol, m.p. 64–65°. Anal. Found: C, 75.24; H, 6.95. Calcd. for $C_{17}H_{18}O_3$: C, 75.53; H, 6.71.

*2-Bromo-4-isopropylphenol*—To a solution of 12 g. of 4-isopropylphenol[7] in 40 cc. of chloroform, 17 cc. of chloroform containing 14 g. of bromine was added under ice-cooling. Removal of the solvent followed by distillation furnished monobromo compound (15.7 g., 83%), b.p. 119–120°/15 mmHg. *p-Nitrobenzoate*: Colorless prisms from ethanol, m.p. 83–84°. Anal. Found: N, 4.08. Calcd. for $C_{16}H_{14}O_4NBr$: N, 3.87.

*2-Bromo-4-isopropylanisole* (V)—To a stirred mixture of 16.5 g. of 2-bromo-4-isopropylphenol, and 6 g. of sodium hydroxide in 30 cc. of water, 10.5 g. of dimethyl sulfate was added dropwise, the reaction mixture was heated at 60–70° for five hours after the last addition, and extracted by ether. Removal of the solvent from the extract followed by distillation furnished the anisole (V, 11.9 g., 68%), b.p. 113–116°/4 mmHg. Anal. Found: C, 52.38; H, 5.53. Calcd. for $C_{10}H_{13}OBr$: C, 52-42; H, 5.72.

*5-Isopropylguaiacol* (IV)—Grignard reagent prepared from 4 g. of (V), 3.2 g. of isopropyl bromide, and 1 g. of activated magnesium was oxidized by the introduction of dry oxygen for four hours. After standing for fifteen hours, the reaction mixture was refluxed with dilute sulfuric acid for one hour. The ethereal layer was extracted with 20 cc. of 5% sodium hydroxide solution and the alkali layer was acidified and extracted with ether. Removal of the solvent from dried ether solution followed by distillation furnished colorless solid (1.1 g. 38%, b.p. 115–124°/10 mmHg, m.p. 38–40°), which after recrystallization from petroleum ether, afforded colorless scales, m.p. 41–42°, 5-isopropylguaiacol (IV). (IV) and its derivatives (*benzoate*, m.p. 64–65°, *p-nitrobenzoate*, m.p. 86–87°) were respectively found by admixture to be identical with chamenol and its derivatives.

## Summary

The structure of chamenol, a phenolic substance isolated from the acid fraction of the essential oil of *Chamaecyparis taiwanensis*, was proved to be 2-methoxy-5-isopropylphenol.

*Chemical Institute, Faculty of Science, Tohoku University, Sendai*

# *Cathodo-luminescence of Samarium as Applied to the Structural Studies of Alumina. I. Three Prototypes for the Luminescence Spectra of Samarium in Alumina*

By Eiichi IWASE

(Received April 25, 1955)

## Introduction

Studies on the structures of alumina and alumina-hydrate as well as their structural variations during dehydration and calcination have made steady and marked progress in recent years, being based mainly on the results of X-ray diffraction investigations. The present author has carried out over a number of years extensive investigations on the cathodo-luminescence spectra of certain rare earths, such as praseodymium and samarium, which were impregnated into a great variety of anhydrous alumina, derived from hydrargillite, bayerite and boehmite, or from hydrous alumina gels, or from hydrated crystals of aluminium salts.

Rohden[1] as well as the present author[2] have already made spectrographic studies on the cathodo-luminescence of samarium imbedded in alumina and a different set of luminescence bands was assigned for it respectively. These two sets of the luminescence spectra for the samarium-bearing alumina are likely to correspond to an observation described in Lecoq de Boisbaudran's[3] classical work; namely the samarium imbedded in alumina gave two different cathodo-luminescence spectra, according as the calcination temperature was varied.

1) Ch. de Rohden, *Ann. chim.*, [9] **3**, 362 (1915).
2) E. Iwase, *Sci. Papers Inst. Phys. Chem. Research* (Tokyo), **34**, 770 (1938).
3) Lecoq de Boisbaudran, *Compt. rend.*, **105**, 258 (1887).

Rohden[4] proposed, on the other hand, one definite kind of cathodo-luminescence spectrum for praseodymium-bearing alumina. Three prototypes have, however, been brought forward quite recently by the present author and his collaborators[5] for cathodo-luminescence spectra of the praseodymium imbedded in various kinds of alumina, and some interpretations have also been given for their occurrences from a structural standpoint.

This paper presents three prototypes of the cathodo-luminescence spectra owing to samarium existing in three different kinds of alumina respectively, and shows the interdependence of the alumina-structure and the samarium-luminescence spectrum, since cathodo-luminescence bands due to the samarium ions are, in general, much more intense than those due to the praseodymium ions in solid inorganic ground-materials.

TABLE I

CATHODO-LUMINESCENCE SPECTRA OF SAMARIUM-BEARING ALUMINA

| Prototype I | | Prototype II | | Prototype III | |
|---|---|---|---|---|---|
| Wave-length (mμ) | Intensity | Wave-length (mμ) | Intensity | Wave-length (mμ) | Intensity |
| 656 | | 661 | | 656 | |
| 651 | w | 658.5 | w | 654 | w |
| 646 (maximum) | s | 650 | | 649.5 | w |
| 644 | | 648 | ww | 644.5 | w |
| 635 | w | 644.5 | | 625 | |
| | | 642 | ww | 623 | s |
| | | 637 | | 621.5 | |
| | | 635 | ww | 620 | s |
| 621 | | 624.5 | | 616 | |
| | | 623 | s | 615 | m |
| | | 622 | | 613 | |
| | | 620.5 | m | 612 | s |
| | | 619 | | 611 | |
| | m | 616.5 | ss | 609.5 | s |
| | | 614.5 | | 609 | |
| | | 612 | w | 607 | s |
| | | 610 | s | 606 | |
| | | 608.5 | m | 604 | m |
| | | 606.5 | | | |
| 604 | | 604.5 | | 603 | |
| | | 602 | ww | 602 | m |
| 599.5 (maximum) | ss | 600 | | 600 | |
| | | 596 | ww | 598 | w |
| | | 595 | | 596.5 | ss |
| 594 | | 593.5 | m | 593 | w |
| | | 591 | | | |
| | | 590 | m | 589.5 | |
| | | 590 | | | |
| | | 589 | m | | ww |
| | w | 588.5 | s | | |
| | | 587 | | 587 | |
| | | 586 | ww | | |
| | | 585 | ww | 583.5 | |
| | | 582.5 | | 582.5 | w |
| 581 | | 581 | s | 581 | |
| | | 580 | | 580 | w |
| | | 578 | | 578 | |
| | | 576.5 | ww | 577 | ww |
| | | 575 | | | |
| | | 573.5 | ww | | |
| 574 | | | | | |
| | s | 572 | w | 571.5 | m |
| 568 | | | | 568 | ww |
| 567 | ww | | | 566 | ww |
| 565 | | | | 562.5 | m |
| 560.5 | m | | | 561 | m |
| 551 | | | | 553.5 | ww |
| 547 | w | | | 548.5 | ww |
| 545 | w | | | | |
| 542.5 | | | | 542.5 | ww |
| 541 | m | | | | |
| 540.5 | ww | | | | |

4) Ch. de Rohden, *Ann. chim.*, [9] 3, 360 (1915).

5) E. Iwase, S. Nishiyama and T. Isono, This Bulletin, 28, 345 (1955).

## Experimental

Three samples of samarium-bearing alumina were prepared by the following methods.

Sample 1: The hydrous alumina gel was precipitated by the addition of ammonia to a cold solution of aluminium sulphate. After being washed with water and dried at 110°C, the gel was soaked with a solution of samarium nitrate and then ignited at about 900°C for one hour.

Sample 2: Crystals of aluminium nitrate enneahydrate were partially calcined at about 180°C until they became porous masses, which were ground to fine powders, soaked with the solution of samarium nitrate and roasted at 1200°C or above.

Sample 3: Fine granular crystals of the hydrargillite obtained by the Bayer process, namely crystals of alumina-trihydrate, were previously calcined at a suitable temperature, for example 800°C for one hour. The anhydrous alumina thus obtained was, after the solution of samarium nitrate had been added, ignited at about 900°C for one hour.

The samarium introduced into the above-mentioned samples of alumina, serves as an activator to cause the cathodo-luminescence, and its concentration was adjusted to be nearly 1% calculated as oxide for a ground-material, namely alumina in the present cases.

These samples of samarium-bearing alumina were subjected to cathode-ray bombardment in a small Urbain tube and their luminescence was spectrographically investigated by employing a Feuss glass-prism spectrograph.

## Results

Table I shows results of the cathodo-luminescence spectra given by the samples 1, 2 and 3. Relative intensities of the luminescence bands were estimated visually and indicated by the following symbols; ss(very strong), s(strong), m(medium), w(weak) and ww(very weak).

These luminescence spectra are reproduced in Photos. 1, 2 and 3. They are schematically given in Fig. 1, (a), (b) and (c) in order to facilitate comparisons. Luminescence spectra of the samples 1, 2 and 3 have quite different and readily distinguishable appearances, and thus may be designated as the three prototypes I, II and III respectively for the cathodo-luminescence spectra due to the samarium ions, which have been imbedded in different modifications of alumina. The prototype I of samarium-luminescence spectrum is composed of several broad diffuse bands, while the prototypes II and III are composed of a number of relatively sharp line-like bands.

## Discussion

The sample 1 of samarium-bearing alumina is found, on one hand, giving the cathodo-luminescence spectrum of the prototype I (Fig. 1, a, and Photo. 1) and, on the other

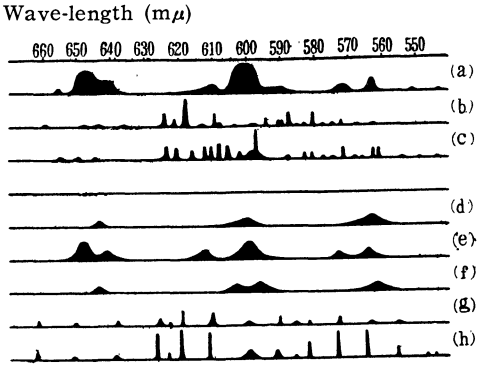



Fig. 1. Schematic representation of luminescence spectra due to samarium in alumina and in water.

Cathodo-luminescence spectrum of prototype I (a), of prototype II (b), and of prototype III (c), Luminescence spectrum of $Al_2O_3$-Sm calcined at low temperatures (Lecoq de Boisbaudran) (d), of $Al_2O_3$-Sm (Iwase) (e), of aqueous solution of $SmCl_3$ (Lecoq de Boisbaudran) (f), of $Al_2O_3$-Sm calcined at elevated temperatures (Lecoq de Boisbaudran) (g), and of $Al_2O_3$-Sm (Rohden) (h).

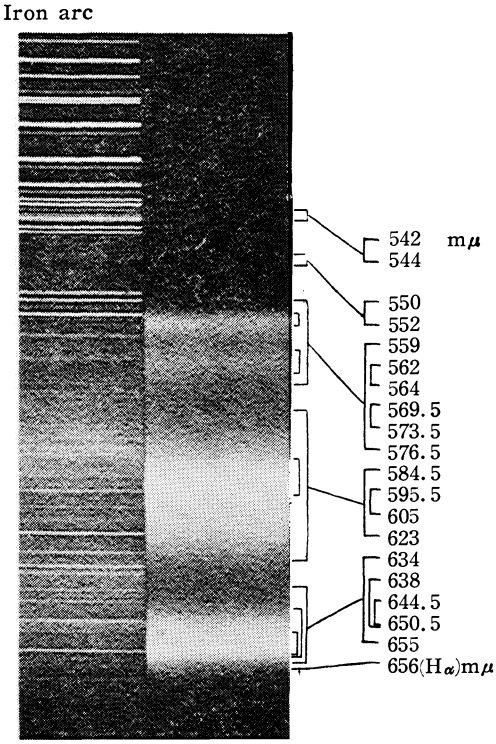



Photo. 1. Prototype I of the cathodo-luminescence spectrum of samarium-bearing alumina.

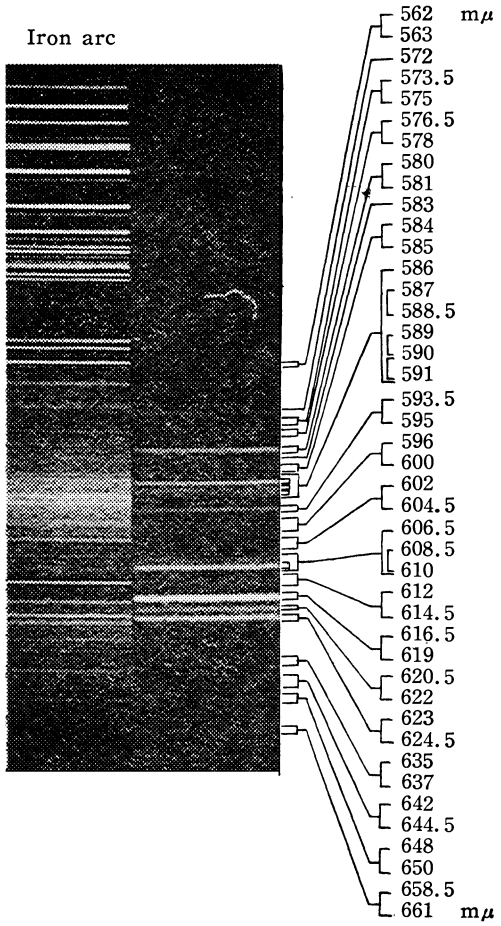



Photo. 2. Prototype II of the cathodo-luminescence spectrum of samarium-bearing alumina.

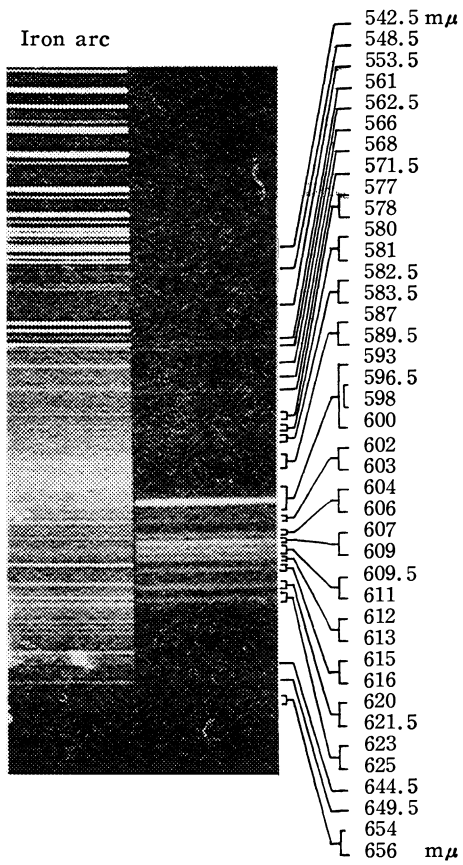



Photo. 3. Prototype III of the cathodo-luminescence spectrum of samarium-bearing alumina.

hand, having the structure of $\gamma$-modification as revealed by an X-ray investigation[5]. This luminescence prototype may simply accounted for by the luminescence spectrum caused by the excitation of samarium ions in solution, since the present author has confirmed that samarium ions distributing at random in an optically isotropic substance, for example in an ordinary glass, show a cathodo-luminescence spectrum quite akin to that of the prototype I (Photo. 4). The $\gamma$-modification of alumina is considered to be, in harmony with the above statement, constructed from the oxygen-ion network of cubic close-packing with aluminium ions distributing in a statistical way over its whole interstices evenly[6].

Additional examples for this luminescence prototype are supplied by samarium-bearing alumina prepared by means of the calcination at low temperatures, as already described by Lecoq de Boisbaudran[3] (Fig. 1, d) as well as the present author[2] (Fig. 1, e), and by a solution of samarium chloride, as shown by Lecoq de Boisbaudran[3] (Fig. 1, f).

The luminescence spectrum of the prototype II (Fig. 1, b and Photo. 2) is decisively produced by samarium ions imbedded in a corundum structure, in which oxygen ions are arranged in hexagonal close-packing, because a study of the X-ray diffraction pattern has revealed that the sample 2 is really $\alpha$-modification of alumina[5]. The cathodo-luminescence spectrum of samarium-bearing alumina calcined at greatly elevated temperatures belongs to this prototype, according to observations by Lecoq de Boisbaudran[3] (Fig. 1, g) and Rohden[1] (Fig. 1, h).

In addition to the above-mentioned two luminescence prototypes another conspicuous luminescence spectrum is obtained, which seems overlooked by the investigators. This new luminescence spectrum may be designated as the prototype III for the luminescence spectrum of samarium ions existing in an

6) E.J.W. Verwey, *Z. Krist.*, **91**, 68 (1935).

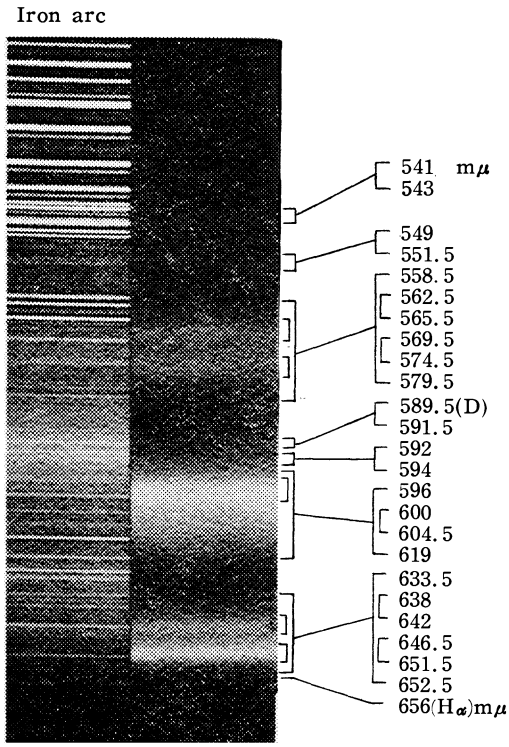



Photo. 4. Cathodo-luminescence spectrum of samarium-bearing glass.

alumina, and is seen in its pure form only with a sample of samarium-bearing alumina, which has been yielded from the hydrargillite by a suitable heat treatment, prior to the addition of samarium (Fig. 1, c and Photo. 3). Brown[7] and Day[8] have recently proposed that the hydrargillite should thermally be decomposed to the $\alpha$-alumina through dual routes simultaneously, one proceeding directly through a sequence of virtually anhydrous aluminas, namely $\chi$-and $\kappa$-modifications, and the other through boehmite followed by a series of other virtually anhydrous aluminas, namely $\gamma$-, $\delta$-, and $\theta$-modifications. Both of these two routes lead eventually to a common product, the $\alpha$-alumina. There remains much to be proved, as to whether or not the formation of the boehmite is of primary nature[7,8,9,10] in this case, and further precise investigations seem necessary in this connection.

It has been confirmed, from an X-ray powder diffraction analysis[5], that the sample 3 of samarium-bearing alumina is almost completely composed of $\kappa$-modification. This $\kappa$-modification is assumed to be an intermediate alumina produced in one route of the dual thermal transformation from the hydrargillite to the $\alpha$-alumina. Provided that the X-ray diffraction line in the immediate vicinity of 2.0 Å is caused by the reflection from (400) planes of a spinel lattice[11], its estimated relative intensity would allow us to elucidate whether most of the aluminium ions take their seats in tetrahedral or octahedral interstices of the oxygen network of cubic close-packing. It may probably be concluded, for structural reasons quite similar to those previously made concerning the three prototypes for cathodo-luminescence spectra of praseodymium-bearing aluminas[5] that aluminium ions would fill tetrahedral in preference to octahedral interstices in the decomposition sequence leading directly through anhydrous aluminas. This is likely to be the reason why the luminescence spectrum of the prototype III appears in its genuine form only in the case of samarium-bearing alumina derived from the hydrargillite by a suitable previous heat treatment.

Almost all the luminescence spectra caused by samarium ions existing in numerous samples of anhydrous alumina, which have been obtained in various ways of preparation, may be interpreted as belonging to either one of the three prototypes mentioned above or their combinations.

## Conclusion

Cathodo-luminescence spectra given by samarium ions, which have been imbedded in various samples of anhydrous alumina can, according to circumstances, be regarded as belonging to either one of the three luminescence prototypes, namely I, II and III, or their combinations.

It is concluded that the three ways of the reciprocal arrangements for oxygen and aluminium in the configuration of a ground-material, namely alumina in the present cases, may be closely related to the occurrence of these three fundamental spectral types for the samarium-activated luminescence.

The luminescence prototype II mentioned above is obtained with an alumina having the oxygen network of hexagonal close-packing, namely $\alpha$-modification of alumina, while the luminescence prototypes I and III are caused by aluminas possessing the oxygen network of cubic close-packing.

Which of the last two prototypes of lumi-

7) J.F. Brown, D. Clark and W.W. Elliott, *J. Chem. Soc.*, **1953**, 84.
8) M.K. Day and V.J. Hill, *Nature*, **170**, 539 (1952); *J. Phys. Chem.*, **57**, 946 (1953).
9) T. Sato, *J. Chem. Soc. Japan, Ind. Chem. Section*, **55**, 66 (1952).
10) H.T. Tran et M. Prettre, *Compt. rend.*, **234**, 1366 (1952).
11) G. Ervin, *Acta Cryst.*, **5**, 106 (1952).

nescence is produced, depends probably upon the manner of aluminium ions in occupying the two sorts of interstices of the cubic close-packed oxygen network, namely octahedral and tetrahedral interstices. The luminescence prototype I is seen with $\gamma$-modification of alumina, in which aluminium ions are statistically distributed evenly throughout the two sorts of interstices mentioned above, whilst the luminescence prototype III is observed with $\kappa$-modification of alumina, where aluminium ions take, for the most part, their seats in the tetrahedral rather than in the octahedral interstices.

This research has been financed by the Scientific Research Encouragement Grant of the Ministry of Education, to which the author's thanks are due.

*The Scientific Research Institute, Ltd*
*Komagome, Bunkyo-ku, Tokyo*

# *Cathodo-luminescence of Samarium as Applied to the Structural Studies of Alumina. II. On the Alumina Produced from Hydrous Alumina Gels*

By Eiichi IWASE and Seijiro NISHIYAMA

(Received April 25, 1955)

## Introduction

Investigations of X-ray powder diffraction patterns showed that hydrous alumina gels freshly produced by a rapid precipitation from cold solutions of aluminium salts are amorphous[1,2]. The hydrous alumina gels are, on calcination, converted to $\gamma$-alumina in a wide sense[3,4] through poorly crystallised boehmite, and with progressively increased temperatures, a gradual ordering of cubic close-packed oxygen network takes place, aluminium ions entering into the network by thermal diffusion preferably much more into octahedral than tetrahedral interstices. A low-temperature form of the $\gamma$-alumina may be regarded as a modification possessing imperfect and disordered lattices. A complete ordering of aluminium ions is achieved in the cubic close-packed oxygen network by a heat treatment at just below the temperature required for producing $\alpha$-alumina. This state was called $\theta$-alumina by Stumpf et al.[5] and is considered to be a well-crystallised form of the $\gamma$-alumina[6]. The arrangement of oxygen ions varies, on further heating at much elevated temperatures, from cubic to hexagonal close-packing, resulting in the $\alpha$-alumina or corundum modification of alumina. In this paper an account is given on the mode of changes in a cathodo-luminescence spectrum of samarium ions brought about by heat treatments of samarium-bearing aluminas which have been derived from various alumina hydrogels, and effects of the heat treatments upon the so-called $\gamma$-$\alpha$ transformation of alumina are explained.

1) R. Fricke, *Kolloid-Z.*, 69, 314 (1934).
2) Gmelins Handbuch anorg. Chem., 35, Aluminium Teil B, 8 Aufl., Verlag Chemie, Berlin, 1934, S. 103.
3) G. Ervin, *Acta Crystal.*, 5, 103 (1952).
4) Gmelins Handbuch anorg. Chem., 35, Aluminium Teil B, 8 Aufl., Verlag Chemie, Berlin, 1934, S. 114.
5) H.C. Stumpf, A.S. Russell, J.W. Newsome, and C.M. Tucker, *Ind. Eng. Chem.*, 42. 140 (1950).
6) G. Ervin, *Acta Crystal.*, 6, 107 (1952).

## Experimental Procedure and Results

Hydrous alumina gels were precipitated by means of neutralisation with ammonia from the solution of one of the following aluminium salts, namely nitrate, sulphate and chloride. These precipitates were washed with water several times on filters, and dried at about 110°C. One gram of each sample of the hydrous alumina gels thus obtained was soaked with 1 ml. of a samarium nitrate solution (the concentration of samarium in this solution is 1% calculated as samarium oxide), dried on a water bath, and ignited at a certain elevated temperature. The resulting samples of samarium-bearing alumina were subjected to cathode-ray bombardment, and cathodo-luminescence spectrograms were taken with a small glass-prism spectrograph of Feuss. The alumina obtained by the ignition at about 930°C for thirty minutes showed, when the aluminium nitrate was employed for the preparation of hydrous alumina gel, broad diffuse luminescence bands belonging to the luminescence prototype I[7], while that at 1000°C for one hour comparatively sharp line-like bands characteristic of the luminescence prototype II[7] (Photo. 1, a). The luminescence spectrum of the prototype I was, however, seen persistently in

7) E. Iwase, This Bulletin, 28, 596 (1955).

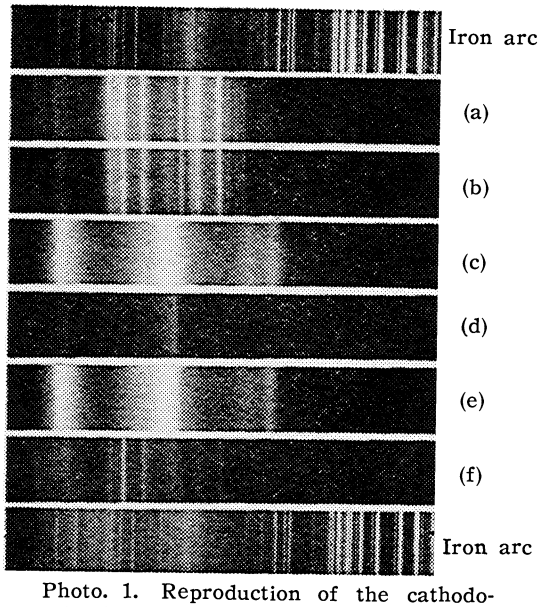



Photo. 1. Reproduction of the cathodo-luminescence spectra of samarium-bearing aluminas derived from various precipitated alumina hydrogels.

Alumina hydrogels were prepared by adding ammonia to solutions of aluminium nitrate (a), (b), of aluminium chloride (c), (d) and of aluminium sulphate (e), (f) respectively. The hydrogels were, after being soaked with a solution of samarium nitrate, converted to alumina by calcination at 1000°C (a), (c), (e) and by roasting in a direct flame of coal gas mixed with oxygen.

the case of alumina derived from either aluminium chloride or aluminium sulphate, without accompanying any band of the prototype II, even though heat treatment had been done at 1000°C for one hour or 1100°C for fifteen minutes (Photo. 1, c and e).

Extremely remarkable differences were observed in cathodo-luminescence spectra of samples of alumina derived from the various alumina hydrogels mentioned above, after being roasted intensely in a direct flame of coal gas mixed with oxygen. The alumina produced by neutralisation of aluminium nitrate solution showed, needless to say, the luminescence spectrum of the pure prototype II (Photo. 1, b), since this had already been attained by calcination at 1000°C, a much lower temperature than that of the present calcination. The alumina derived from the solution of aluminium chloride exhibited, however, a mixed luminescence spectrum of the prototypes I and III (Photo. 1, d), and that from the solution of aluminium sulphate a mixed luminescence spectrum of the prototypes II and III (Photo. 1, f).

It is worthy of note that the most intense luminescence band of the prototype III situated at 596.5~598.0 mμ was seen in the cases of alumina, which had been prepared by precipitation from the solution of aluminium chloride and that of sulphate, and by subsequent ignition in a direct flame of coal gas mixed with oxygen. This luminescence band commenced to appear, after heat treatment had been made at 1200°C for fifteen minutes in the case of alumina derived from the solution of aluminium sulphate. The intensity of cathodo-luminescence bands belonging to the prototype I was decreased in the case of alumina produced from the solution of aluminium chloride, when roasting had been repeated in a direct flame of coal gas mixed with oxygen.

There were observed two luminescence bands at 648~650 mμ and 642~644.5 mμ in a spectral region between 640 and 650 mμ. It is to be mentioned that the former band was more intense than the latter in the case of alumina derived from the nitrate solution, while the order of intensity was reversed in the case of alumina derived from the solution of chloride or sulphate.

Samarium was directly added to dried alumina hydrogels in the experiments so far described. Investigations of cathodo-luminescence spectra of samarium are now being carried out on samarium-bearing samples of alumina, which have been prepared by an addition of samarium at various intermediate stages of thermal decomposition from the hydrous to the anhydrous alumina.

The hydrous alumina gel produced by precipitation with ammonia, was submitted to a previous heat treatment at a certain temperature between 200 and 1000°C. The thermally decomposed samples thus obtained have been soaked with the solution of samarium nitrate and then ignited for one hour over a blast flame of coal gas mixed with air. The samarium-bearing samples of alu-

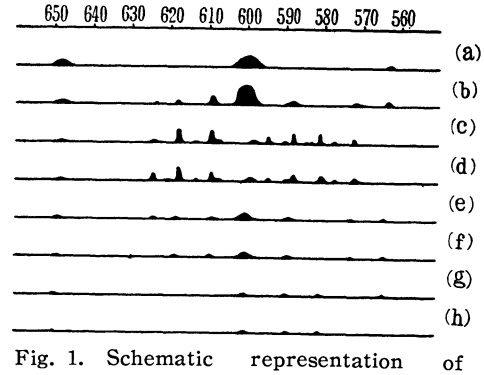



Fig. 1. Schematic representation of cathodo-luminescence spectrum of samarium-bearing alumina derived from the precipitated hydrogel.

Hydrous alumina gels were prepared from a solution of aluminium nitrate by precipitation with ammonia. Prior to the addition of samarium, the alumina gels were dried at 110°C (a), heated for 1 hr. at 200°C (b), at 230°C (c), at 270°C (d), at 300°C(e), at 400°C (f), at 700°C (g), and for 15 min. at 1000°C (h) respectively. All these were finally ignited in a blast flame of coal gas mixed with air.

mina derived from the solution of aluminium chloride or sulphate give always a cathodo-luminescence spectrum belonging to the prototype I, whereas this is not the case with those obtained from the solution of aluminium nitrate. A noteworthy phenomenon has been witnessed with the latter samples. Hydrous alumina gels yielded from the solution of aluminium nitrate, have been washed simply on filters as usual, heated at a temperature either below 200°C or above 400°C, soaked with the solution of samarium nitrate, and then ignited over a blast flame of coal gas mixed with air. These samples of alumina show samarium-luminescence spectra of the prototype I, as can be seen in Fig. 1, (a), (g) and (h).

When previous heat treatment was made at a moderately elevated temperature, namely between 230 and 270°C, and the other experimental conditions mentioned above were maintained, the resulting samples of samarium-bearing alumina give cathodo-luminescence spectra of the plain prototype II (Fig. 1, c and d), although the temperature of final heat treatment was considerably lower than that normally required for the $\gamma$-$\alpha$ transformation of alumina.

Experiments quite similar to those described above reveal, with thoroughly purified samples of hydrous alumina gels, that such a striking phenomenon is not encountered, the luminescence spectra being of the prototype I, so far as final ignition has been made over a blast flame of coal gas mixed with air.

Finally, results of investigations are described on hydrous alumina gels produced by immersing for a sufficiently long time crystals of aluminium nitrate enneahydrate, aluminium sulphate octodecahydrate, aluminium chloride hexahydrate and ammonium alum in concentrated solutions of ammonia respectively. The hydrous alumina gels resulting from these reactions were removed from the liquors, washed with water, dried at 110°C, soaked with the solution of samarium nitrate, and then ignited.

Cathodo-luminescence spectra of the prototype I were always obtained with samarium-bearing samples subjected to a moderate ignition over a blast flame of coal gas-air. These samarium-bearing samples showed, after ignited intensely in a direct flame of coal gas mixed with oxygen, cathodo-luminescence spectra of the prototype II, but a luminescence spectrum of the prototype III[7] appeared overlapping that of the prototype II in the cases of samarium-bearing alumina derived from hydrated crystals of aluminium chloride and aluminium sulphate.

## Discussion

According to Biltz's X-ray investigations[8], hydrous alumina gels yielded through neutralisation of a solution of aluminium sulphate with ammonia gave $\gamma$-modification of alumina, when subjected to heat treatments between 150 and 500°C. Hansen[9] also stated that hydrous alumina gels derived from a solution of aluminium chloride by precipitation with ammonia, was converted to the $\gamma$-alumina, when calcined at temperatures between 600 and 1000°C. A thermal transformation was said to proceed gradually from $\gamma$- to $\alpha$-alumina, and various temperatures were given for this transformation namely 950°C or higher[10], 1000°C[11], above 1000°C[12] and 1000~1200°C[13].

From the present authors' investigations on the feature of the cathodo-luminescence spectrum it is found that alumina gels derived from solutions of various aluminium salts show some differences in the temperature for the $\gamma$-$\alpha$ transformation, when samarium was added to the dried original hydrogels and the thermal transformation was caused in the presence of the samarium; the alumina hydrogel derived from a solution of aluminium nitrate is transformed into the $\alpha$-modification at temperatures between 930 and 1100°C, while that from a solution of aluminium chloride or sulphate is so far unable to be transformed by an intense heat treatment at 1100°C. Weiser[14] stated that a remarkable difference in the size of the constituting particles was confirmed by X-ray studies between the hydrous alumina gels produced from aluminium nitrate and those from either aluminium sulphate or chloride. This statement seems to deserve to be referred to in connection with the above-mentioned observations. There are also marked distinctions in the cathodo-luminescence spectrum between the alumina derived from a solution of aluminium chloride and that from a solution of aluminium sulphate, both samples of alumina being roasted at more elevated temperatures.

A peculiar configuration, namely the $\kappa$-modification of alumina, begins to be formed in some parts of the alumina derived from a solution of aluminium sulphate by heat treatment at 1200°C for fifteen minutes, the configuration being responsible for giving rise to the most intense luminescence band of the prototype III. This particular configuration is locally produced in corundum structure, when a much stronger heat treatment is made in a direct flame of coal gas

8) W. Biltz, A. Lemke und K. Meisel, *Z. anorg. Chem.*, **186**, 373 (1930).

9) W.C. Hansen and L.T. Brownmiller, *Am. J. Sci. Sill.*, (5), 15, 225 (1928).

10) E.J.W. Verwey, *Z. Krist.*, **91**, 65 (1935).

11) W. Biltz, A. Lemke und K. Meisel, *Z. anorg. Chem.*, **186**, 377 (1930).

12) G. Hägg und G. Söderholm, *Z. physik. Chem.*, B **29**, 93 (1935).

13) A.N. Winchell, "The Microscopic Characters of Artificial Inorganic Solid Substances or Artificial Minerals", John Willy & Sons, Inc., New York, p. 189 (1931).

14) H.B. Weiser and W.O. Milligan, "Advance in Colloid Sciences", **1**, 227 (1942)

mixed with oxygen. Thus the alumina obtained here does not consist of the simple corundum. The resulting alumina is composed of the mixture of $\gamma$- and $\kappa$-modifications, when the hydrogel derived from a solution of aluminium chloride has been subjected to an intense roasting in a direct flame of coal gas mixed with oxygen. The amount of its $\gamma$-ingredient is decreased by repeated heat treatments.

It was already presumed by one of the present authors[7] that the luminescence bands of the prototype III are perceptible, when the samarium ions exist in such an alumina that its constituting aluminium ions are situated favourably in tetrahedral rather than in octahedral interstices of cubic close-packed oxygen network. Verwey[15] compared the X-ray diagram of an ordinary spinel with that of the $\gamma$-alumina prepared by careful heating of aluminium hydroxide, which had been precipitated with ammonia, and thus arrived at a conclusion that octahedral interstices of the oxygen network are not filled up by aluminium ions in this $\gamma$-alumina. Hence, his conclusion is concordant with the postulation presented by one of the present authors, which has been deduced from investigations of the cathodo-luminescence spectra of samarium ions.

In short, the studies on the cathodo-luminescence spectra of samarium indicate that samples of alumina produced by neutralisation of solutions of aluminium nitrate, sulphate and chloride with ammonia, have constructions different from one another. This fact might naturally be related to the complicated characters shown by various kinds of alumina hydrogel, when they are employed as catalysts in some chemical reactions.

An impregnation of samarium ions may possibly stabilise the transient stage caused by thermal decomposition of hydrous alumina gels, and these stages would, in some cases, remain fixed in samples of anhydrous alumina obtained by the subsequent calcination at just below the temperature necessary for production of the $\alpha$-modification, since the large samarium ions might pack structural defects yielded during the course of thermal destruction of the hydrous alumina gels. This expectation is usually not fulfilled in the cases of hydrous alumina gels produced by precipitation with ammonia, irrespective of the different kinds of aluminium salts employed for the preparation of these alumina gels, the $\gamma$-modification of alumina being always obtained, which is confirmed by the feature of the cathodo-luminescence spectrum of the impregnated samarium. However, the intermediate configurations caused by suitable thermal treatments are, in the case of hydrous alumina gels derived from a solution of aluminium nitrate, likely made fixed by the impregnated samarium ions. The hydrous alumina gel in question was previously heated at a medium temperature, namely between 230 and 270°C for one hour, and the impregnation of samarium ions was made for the purpose of stabilising the intermediate configuration thus yielded. The samarium-bearing alumina resulting from a subsequent ignition in a blast flame of coal gas-air, gives a cathodo-luminescence spectrum of the plain prototype II, although the temperature of final heat treatment has been considerably lower than that normally required for the $\gamma$-$\alpha$ transformation of alumina. An X-ray diffraction investigation has also shown that this sample of alumina consists of the $\alpha$-modification. It should accordingly be presumed that the configuration yielded intermediately through the special heat treatment, closely resembles the structure of the $\alpha$-modification of alumina, which is fixed by the packing of the impregnated samarium ions.

The content of water and that of ammonium nitrate, the latter being the by-product of the neutralisation reaction, are estimated for the original sample of this hydrous alumina gel to be 1.00 and 0.39 g. of the resulting alumina respectively, while the water content is, in the samples partially decomposed by the special previous heat treatments at 230 and 270°C, reduced to 0.31 and 0.26 g. respectively and the ammonium nitrate content is also reduced to 0.30 and 0.06 g. respectively. The hydrous alumina gels mentioned above were produced by a simple washing on filters and not entirely free from the reaction by-products. In the case of hydrous alumina gel produced by neutralisation with ammonia, of a solution of aluminium nitrate, the reaction by-product, namely the ammonium nitrate remaining in the gel, seems to act, when its amount is moderate, as something like a mineraliser for accelerating the transformation into the $\alpha$-modification on being heated at much lower temperatures. A series of experiments indicates that such a striking effect is scarcely ever observed with the carefully purified samples of hydrous alumina gels.

The purified samples derived from a solution of aluminium nitrate were, after ammonium nitrate had been added to each of them in varying amounts, subjected to a mild heat treatment at 250°C for one hour, soaked

15) E.J.W. Verwey, *Z. Krist.*, **91**, 69 (1935).

with the solution of samarium nitrate, and then calcined over the flame of coal gas mixed with air. All the resulting samples of samarium-bearing alumina show nothing but the cathodo-luminescence spectrum of the prototype I. Thus it becomes apparent that no extraordinary effect is produced, once the ammonium nitrate intimately held in the original alumina hydrogel has been removed, and a subsequent addition of ammonium nitrate can no more act as a special mineraliser for yielding the $\alpha$-modification of alumina.

## Summary

Hydrous alumina gels were prepared from both solutions and crystals of a number of aluminium salts, in the former case by precipitation with ammonia and in the latter by direct immersion in concentrated ammonia liquor. Samarium ions were impregnated in these hydrous alumina gels or in their transition phases resulting from the previous thermal treatment of various temperatures. The feature of the cathodo-luminescence spectrum was investigated on the samarium-bearing alumina produced from the above-mentioned samples by a final heat treatment.

Spectrographic measurements of the cathodo-luminescence reveal that the heating of the hydrous alumina gels derived from a solution of aluminium nitrate results in their conversion to the $\alpha$-alumina, while the heating of those from solutions of aluminium chloride and sulphate does not give the genuine $\alpha$-modification. This was confirmed by the fact that the most intense band of a particular luminescence prototype III as designated by one of the present authors was observed in the cathodo-luminescence spectra.

The $\gamma$-$\alpha$ transformation of alumina occurs at temperatures far below its transition temperature when a suitable amount of ammonium nitrate, the by-product of the neutralisation reaction, was caused to remain by heating the precipitated hydrous alumina gel, which was derived from a solution of aluminium nitrate at a moderately elevated temperature.

Similar remarkable results were, however, not obtained with hydrous alumina gels derived from solutions of aluminium chloride and sulphate, and also with the gel derived from a solution of aluminium nitrate, if the latter gel had been made free from the reaction by-product. An addition of ammonium nitrate to the purified alumina gels can no more regenerate the ability to accelerate the $\gamma$-$\alpha$ transformation.

It is interesting to note that hydrous alumina gels obtained by immersing crystals of aluminium nitrate enneahydrate, aluminium chloride hexahydrate, aluminium sulphate octodecahydrate and ammonium alum in concentrated ammonia liquor for a sufficiently long time behave themselves, on being heated, in a somewhat similar way to those obtained by precipitation from the solutions of the foregoing aluminium salts.

This research has been financed by the Scientific Research Encouragement Grant of the Ministry of Education, to which the authors' thanks are due.

*The Scientific Research Institute, Ltd., Komagome, Bunkyo-ku, Tokyo*

# *The Structon Theory of Glasses and Solutions**

By Maurice L. HUGGINS**

(Received August 29, 1955)

## Introduction

Many properties of liquids and solids can usefully be considered as dependent on the kinds and numbers of "structon" present. This word, "structon," has been invented by the writer[1,2]. It may be defined as "an atom (or molecule or group of atoms of a given kind) in a given environment." The structon concept is especially valuable when considering properties which are approximately additive—that is, which can be made up of contributions of the different types of structon present. Volume and molar refraction are examples of such properties. Certain thermodynamic functions, such as energy and heat content, would also be expected to be approximately structon-additive. As would be expected, structon additivity is usually somewhat better than atomic or molecular additivity.

The "environment" referred to here is that of closest neighbors only. More distant atoms or molecules are considered to be of negligible influence on the properties dealt with.

This paper deals primarily with solutions—both solid solutions (such as ordinary glasses) and liquid solutions. The usefulness of the structon concept is most evident in dealing with solutions in which different structon types differ so much in stability that, over a composition range, only those few types exist, in significant relative amounts, which are the most stable.

## Glasses

Well-annealed sodium silicate glasses conform to this requirement, as will be shown. These glasses have a structural arrangement which was stable at a high temperature and which has been frozen in as the glass cooled. A graph of the volume as a function of the composition (Fig. 1[3-6]) shows straight-line segments, with sharp breaks between them. It has generally been assumed that behavior of this sort indicates compound formation, but x-ray studies[7] give no evidence of compounds.

The writer has proposed[1,2] the alternative explanation that in each composition range there are only a few types of structons, the breaks occurring at compositions at which one type of structon disappears and another appears.

Consider first the structure of pure silica, $SiO_2$. Many years ago the writer[8] showed that in crystalline silica (quartz) each silicon atom is surrounded by four close oxygen neighbors and each oxygen atom is adjacent to two silicons. The structure may be described as being composed of structons of the two types represented by the formulas Si(4.0) and O(2Si).

It does not matter, for present purposes, whether one considers the forces between adjacent silicon and oxygen atoms to be essentially covalent or ionic. Actually, there is good reason to believe that they are intermediate in character, involving electronpair bonds with a considerable degree of polarity.

In *vitreous* silica, x-ray and other evidence shows that the same two structon types exist, practically exclusively, as in crystalline silica.

If a little sodium oxide is added to silica and a glass is produced, there must of course be some new types of structons. The types to be considered may be limited to a few, either on the basis of simple theoretical considerations or, reasoning by analogy, making use of the large body of information which has been accumulated regarding the structures of *crystalline* silicates. All of the sodium atoms (or ions) would be expected to be surrounded by oxygens, with no sodium-silicon contacts. The number of oxygens around each sodium, for greatest stability, cannot be assumed *a priori*, but a good guess would be six. There would then be structons

* Communication No. 1746 from the Research Laboratories of the Eastman Kodak Company, Rochester 4, New York, U.S.A.

** Fulbright Exchange Professor, Osaka University, and Lecturer, Kyoto University, 1955-56.

1) M.L. Huggins, *J. Phys. Chem.*, **58**, 1141 (1954).

2) M. L. Huggins, *J. Am. Ceramic Soc.*, **38**, 172 (1955).

3) M.L. Huggins and K.H. Sun, *Glass Industry*, **24**, 472 (1943).

4) F.W. Glaze, J.C. Young and A.N. Finn, *Bur. Stand. J. Res.*, **9**, 799 (1932).

5) G.W. Morey and H.E. Merwin, *J. Opt. Soc. Am.*, **22**, 632 (1932).

6) S.R. Scholes, "Handbook of the Glass Industry", Ogden-Watney Publishers, Inc., New York, N.Y. (1941), p. 61.

7) See, for example, B.E. Warren, *J. Appl. Phys.*, **8**, 645 (1937). or *J. Am. Ceramic Soc.*, **24**, 256 (1941).

8) M.L. Huggins, *Phys. Rev.*, **19**, 363 (1922).

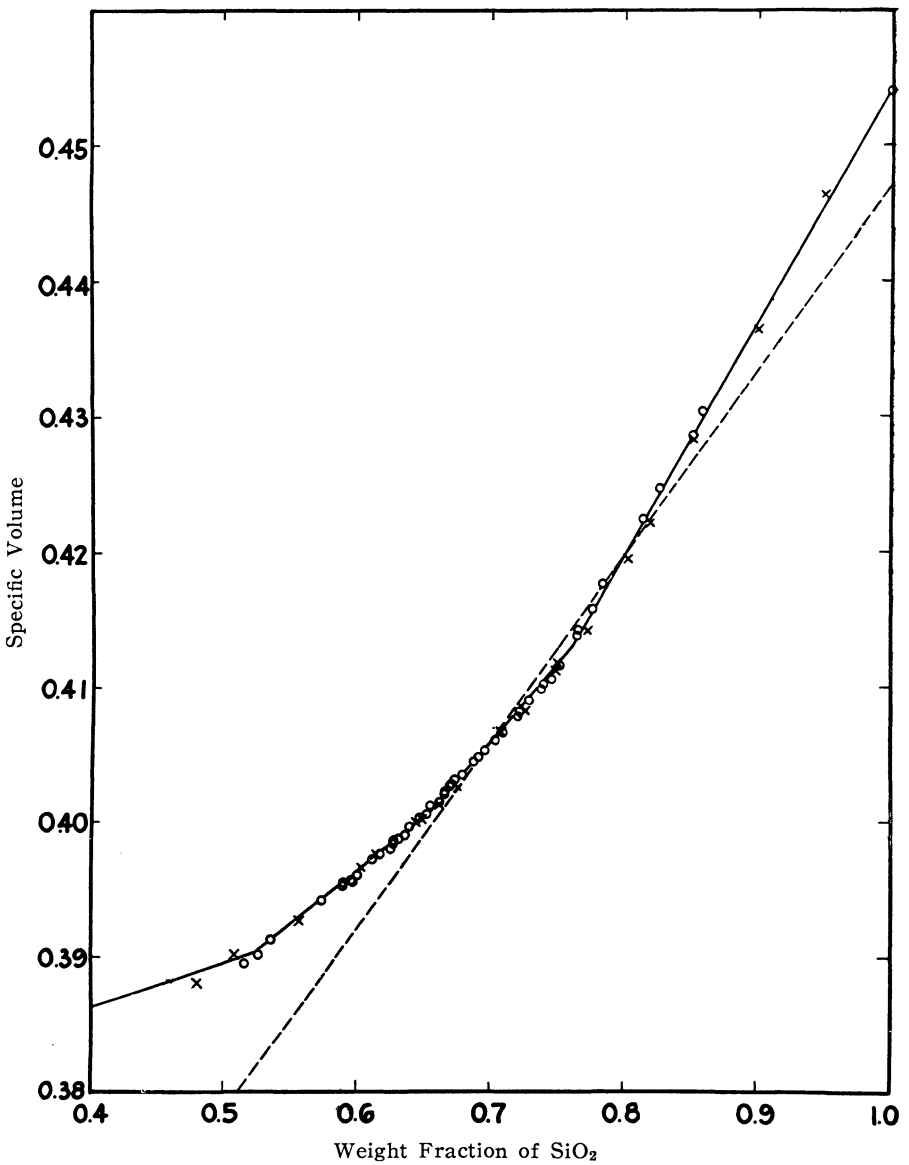



Fig. 1. Specific volumes of sodium silicate glasses[3]. Circles represent data by Glaze, Young, and Finn[4]; crosses denote data by Morey and Merwin[5]. The dashed line represents a relationship given by Scholes[6].

of formula Na(6.0). One would expect some oxygens to be surrounded by two silicons (as in pure silica), plus one sodium. An environment of two silicons and *two* sodiums would require a greater departure from short-range neutrality, and so would be less reasonable. As a rough measure of this departure, one can calculate a hypothetical "structon charge," by considering the structure as composed of sodium, silicon, and oxide *ions* and adding algebraically the charge on an oxygen (-2) and the appropriate shares of the charges on each of the ions surrounding that oxygen: +4/4 for each silicon neighbor and +1/(coordination number of the sodium) for each sodium neighbor.

There must also be oxygen-centered structons in which the central oxygen has less than two silicon neighbors. Oxygen-centered structons with only sodium neighbors (essentially oxide ions) have never been found in silicate crystals and would be unreasonable theoretically. Oxygen-centered structons with only one silicon neighbor would be expected to have some sodium neighbors, enough to give a close approach to regional

neutrality. The number is *a priori* unknown.

The minimum number of structon types capable of giving the over-all composition is five (See the section on "The Structon Number Rule"). For any given set of five types which one chooses to assume, it is easy to compute the limits of existence of the set and, within those limits, the relative numbers of structons of each type. The procedure may be illustrated for the following assumed set:

Si(4.0) Na(6.0) O(2Si) O(2Si, Na) O(Si, 3Na).

For convenience, an amount of glass which contains, on the average, one oxygen atom is considered. The number of structons of each type in this amount of glass is designated as $N$, with the appropriate structon formula as subscript. The numbers of silicon and sodium atoms in this amount of glass are represented as $N_{Si}$ and $N_{Na}$, respectively.

With these definitions, the sum of the numbers of oxygen-centered structons equals unity:

$$N_{O(2Si)}+N_{O(2Si,\ Na)}+N_{O(Si,\ 3Na)}=1 \quad (2)$$

The number of oxygen-to-silicon contacts equals the number of silicon-to-oxygen contacts. Hence,

$$2N_{O(2Si)}+2N_{O(2Si,\ Na)}+N_{O(Si,\ 3Na)} = 4N_{Si(4.0)}=4N_{Si} \quad (2)$$

Likewise, the number of oxygen-to-sodium contact equals the number of sodium-to-oxygen contacts:

$$N_{O(2Si,\ Na)}+3N_{O(Si,\ 3Na)}=6N_{Na(6.0)}=6N_{Na} \quad (3)$$

The valences must be balanced, to satisfy the requirement that the glass as a whole be electrically neutral. Hence,

$$4N_{Si}+N_{Na}=2 \quad (4)$$

By solving the foregoing equations simultaneously, the numbers of the different types of structon are obtained as functions of the composition. If the composition is expressed as $N_{Si}$, the equations are as follows:

$$N_{Si(4.0)}=N_{Si} \quad (5)$$
$$N_{Na(6.0)}=2-4N_{Si} \quad (6)$$
$$N_{O(2Si)}=-7+16N_{Si} \quad (7)$$
$$N_{O(2Si,\ Na)}=6-12N_{Si} \quad (8)$$
$$N_{O(Si,\ 3Na)}=2-4N_{Si} \quad (9)$$

The limits of the composition range, within which this assumed set of structons is capable of existence, are the compositions at which the numbers of one or more of the structon types become zero. The maximum value of $N_{Si}$ is 1/2, the value in pure silica. Then, according to Eqs. 6, 8, and 9, the number of structons of each of the types, Na(6.0), O(2Si, Na) and O(Si, 3Na), becomes equal to zero. The minimum value of $N_{Si}$ is 7/16, the composition at which the O(2Si) structons disappear. *This is at precisely the location of the first break in the curve representing the experimental volume data* (See Fig. 2[9,10,11]).

Similar calculations have been made for all other sets of structons which seem at all reasonable. All sets give a lower limit for $N_{Si}$ which is in disagreement with experiment, except those which are like the set just considered, except for replacement of Na(6.0) and O(Si, 3Na) by Na [$(w+3)$O] and O(Si, $w$Na), with $w$ equal to an integer. The choice of $w=3$, giving the structons tentatively assumed, seems to be the most reasonable. Moreover, other choices lead to disagreement with experiment in the next composition range. It seems necessary to conclude that the chosen set of structons is the one actually existing in these glasses in this composition range.

A similar analysis leads to the conclusion that in Range II, with $N_{Si}$ between 0.40 and 0.4375, the only structons present in significant amounts are the following:

Si(4.0) Na(6.0) O(2Si, Na)
O(2Si,2Na) O(Si, 3Na)

For $N_{Si}$ less than 0.40, there are several possibilities, between which the data now being considered do not enable one to distinguish. A reasonable set for the range $0.375<N_{Si}<0.40$ would be the following:

Si(4.0) Na(6.0) Na(5.0) O(2Si, 2Na) O(Si, 3Na)

This might be followed, for $0.333<N_{Si}<0.375$, by the set:

Si(4.0) Na(5.0) O(2Si, 2Na)
O(Si, 3Na) O(Si, 4Na)

At the sodium metasilicate composition, $N_{Si}=0.333$, the O(Si, 3Na) structons would necessarily disappear. The four remaining types are those occurring in the crystalline compound of this composition[12].

From these assumptions, or any of several others which also appear reasonable, one would expect a break in the property-composition curve at $N_{Si}=0.375$. The contributions of the different structon types might be such, however, as to make the break a very minor one. Experimentally (Fig. 2), the volume data are insufficient to tell whether or not a small break actually occurs at this composition.

From the slopes and intercepts of the straight-line segments of the experimental

9) F. Winks and W.E.S. Turner, *J. Soc. Glass Technol.*, **15**, 185T (1931).
10) M.L. Huggins, *J. Opt. Soc. Am.*, 30, 420 (1940).
11) M.L. Huggins, *Ind. Eng. Chem.*, 32, 1433 (1940).
12) P.A. Grund and M.M. Pizy, *Acta Cryst.*, **5**, 837 (1952).

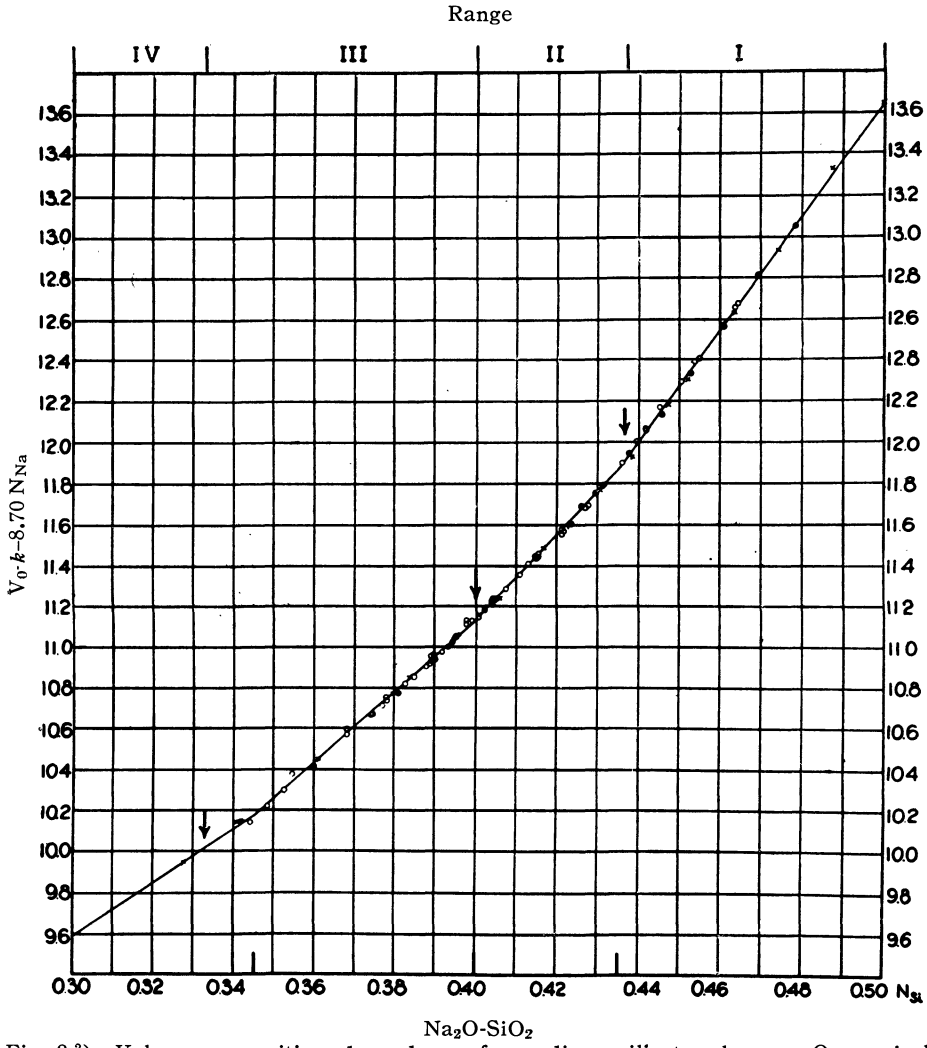



Fig. 2.[2] Volume-composition dependence for sodium silicate glasses. Open circles represent data of Glaze, Young, and Finn[4]; crosses denote data by Morey and Merwin[6]. Solid circles denote data by Winks and Turner[9] The small constant, $k$, is included to allow for difference in annealing techniques. The straight lines conform to relationships deduced empirically,[10,11] which differ very slightly from those recently obtained theoretically[1,2].

volume-composition curves, it is possible to deduce some relationships between the volume contributions of the different structon types. Their individual contributions, however, cannot be deduced from the data for this system alone. When suitable measurements are made for other systems containing some of the same types of structons, it should be possible to compute the individual structon contributions to the total volume. Similar remarks apply with respect to other additive properties.

## Liquid Solutions

The structon types existing in most liquid solutions include not only those in the set giving the lowest free energy, but also others, only slightly less stable, in dynamic equilibrium with them. It is possible, using well-known methods, to develop a quantitative theory of such solutions, relating the numbers of the different types of structons to their relative energies and to the over-all composition. These numbers can then be used as a basis for the theoretical calculation of various additive properties.

The present discussion, however, will be limited to consideration of a few molecular solutions which can be dealt with in much the same manner as the sodium silicate glasses. The essential requirement for this is that there are strong intermolecular inter-

actions of only one type or of only a few types, differing sufficiently in stability from one another. Many solutions in which their is strong intermolecular hydrogen-bonding conform to this requirement. Evidence for this is the observed broken-line dependence of certain properties on composition.

In these solutions it is the *molecular*, rather than the *atomic*, environment which is important for the present purpose, hence "molecular-structon" types will be discussed. Since the hydrogen-bond forces between molecules are much stronger than those of other types, only hydrogen-bonded neighbors need be specified in characterizing the structons.

As a first example, consider dilute solutions of dimethyl formamide and phenol in carbon tetrachloride. As is shown by Fig. 3[13], taken from a recent paper by Arshid et al.,[13] a

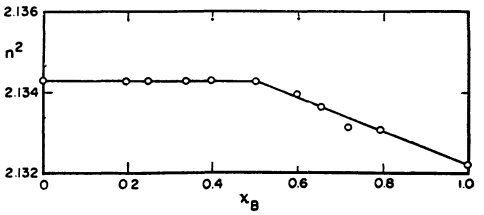



Fig. 3.[13] Variation of refractive index ($n$) with composition, for solutions of dimethyl formamide (A) and phenol (B) in carbon tetrachloride.

plot of the square of the refractive index against the relative proportions of dimethyl formamide and phenol shows two portions which are essentially straight, meeting at the equimolar composition.

This behavior is consistent with the assumption that the forces between like molecules are much weaker than those between unlike molecules, and that the latter produce a 1 : 1 complex, presumably by hydrogen-bonding:

$$\begin{matrix} R_2N-CH=O\cdots\cdots HO-C_6H_5 \\ A\cdots\cdots\cdots\cdots B \end{matrix}$$

The sets of structons can be represented as follows:

| | | | | |
|---|---|---|---|---|
| Range I: | A(O) | A(B) | B(A) | |
| Range II: | | A(B) | B(A) | B(O) |

Here, A(O) designates an A molecule which has no strong interaction with any of its neighbors, A(B) denotes an A molecule strongly attached to a single B neighbor, etc. (Note that "O" in these molecular-structon formulas represents "zero," not "oxygen").

The experimental curves might also be interpreted in terms of a complex of formula $A_2B_2$ or $A_3B_3$ or $A_iB_i$, with $i$ any integer, but in this case the simplest formula seems as reasonable as any.

The relative numbers of the different types of structons (in Range I, for example) are readily computed from the following relationships between the mole fractions:

$$x_{A(O)}+x_{A(B)}+x_{B(A)}=1 \qquad (10)$$

$$x_{A(B)}=x_{B(A)} \qquad (11)$$

The first of these is a normalizing equation, expressing the requirement that the sum of the mole fractions equals unity. The second shows that the sum of the A-B contacts equals the sum of the B-A contacts. The limits of this range, at mole fractions of phenol equal to zero and 1/2, are the concentrations at which, according to these equations, the mole fraction of at least one of the structon types equals zero.

In the equimolar solution, the only structons present are of the A(B) and B(A) types. From the properties of this solution, one can deduce the contributions of the A·····B complex, but not (without supplementary assumptions) those of the individual structons.

It may be noted that the refractive index squared, which is plotted in Fig. 3, is not itself an additive property, but is related[14,15] by the simple equation

$$n^2=1+\frac{R}{V} \qquad (12)$$

to the (Newton) refraction and the volume, both of which would be expected to be approximately structon-additive. Breaks in the plot of $n^2$ *versus* composition would be expected, at the same compositions as breaks in the $R$ and $V$ curves, i.e., at the points where changes of structon type occur.

Because of the proportionality between the dielectric constant and the square of the refractive index (for long wavelengths), one would expect dielectric constant *versus* composition curves to exhibit the same sort of

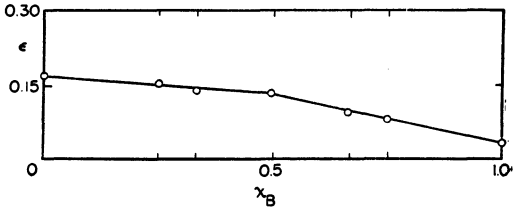


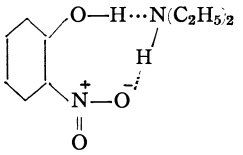

Fig. 4.[16] Variation of dielectric constant ($\varepsilon$) with composition, for solutions of $o$-nitrophenol (A) and diethylamine (B) in benzene.

13) F.M. Arshid, C.H. Giles, E.C. McLure, A. Ogilvie and T.J. Rose, *J. Chem. Soc.* (London), 1955, 67.

14) M.L. Huggins, *J. Opt. Soc. Am.*, 30, 495 (1940).

15) M.L. Huggins, *J. Am. Chem. Soc.*, 63, 116 (1941).

peculiarities as the corresponding squared refractive index curves. This is illustrated by Fig. 4[16], representing data for solutions of *o*-nitrophenol and diethylamine in benzene[16]. A 1:1 complex is again indicated. A reasonable structure would be that indicated by the formula.




With new definitions of A and B, the discussion given above for the (dimethylformamide)-phenol system is applicable.

The dielectric constant curve[16] (Fig. 5) for

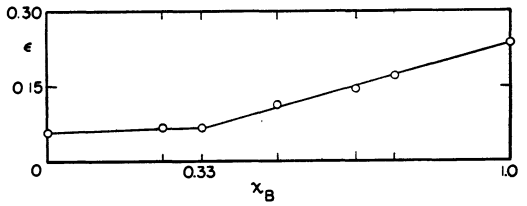



Fig. 5.[16] Variation of dielectric constant with composition, for solutions of azobenzene (A) and aniline (B) in benzene.

benzene solutions of azobenzene (A) and aniline (B) shows a sharp break at the 2:1 composition, indicating the formation of a complex of formula $A_{2i}B_i$, with $i$ indeterminate without further information. The structon sets in the two composition ranges are presumably the following:

Range I: A(O) A($i$B) B(2$i$A)
Range II: A($i$B) B(2$i$A) B(O)

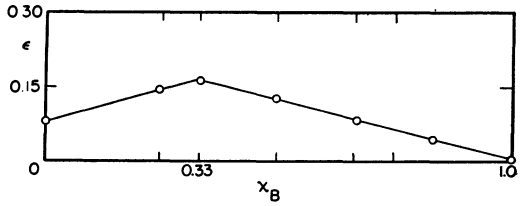



Fig. 6.[16] Variation of dielectric constant with composition, for solutions of phenol (A) and quinol (B) in diethyl ether.

The dielectric constant curve[16] (Fig. 6) for mutual solutions of phenol (A) and quinol (B) in diethyl ether also show a break at $x_B=1/3$. In this case, the most reasonable interpretation is that each phenol molecule is hydrogen-bonded to *two* quinol molecules and each quinol molecule to *four* phenol molecules. To account for the break in the curve, it seems necessary to assume that the hydrogen bonds to the ether molecules are considerably weaker and may be neglected.

An alternative way of looking at this system is to consider the hydroxyl hydrogen atoms (H), the phenol residues (P), and the quinol residues (Q) as the components of the structons, and to assume that every hydroxyl hydrogen is hydrogen-bonded to an oxygen of another hydroxyl. The observed break is then accounted for by the following sets of structon types and hydrogen-bond types:

Range I: P(2H) Q(4H) H(2P) H(P, Q)
H··· bonds: PHP PHQ
Range II: P(2H) Q(4H) H(P, Q) H(2Q)
H··· bonds: PHQ QHQ

The dielectric constant curve[16] for solutions of phenol (A) and azobenzene (B) in water shows two breaks, at $x_B=1/3$ and 1/2 (Fig. 7). This is most simply accounted for

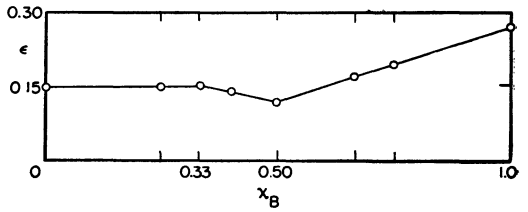



Fig. 7.[16] Variation of dielectric constant with composition, for solutions of phenol (A) and azobenzene (B) in water.

by the following sets of structons and aggregates:

Range I: A(O) A(B) B(2A)
Aggregates: $A_2B$
Range II: A(B) B(2A) B(A)
Aggregates: $A_2B$ AB
Range III: A(B) B(A) B(O)
Aggregates: AB

An especially interesting system is that of phenyl isothiocyanate (A) and diethylamine (B). The viscosity curve at 25°C, published by Kurnakov and Zemchuzny[17] in 1913, shows a very high, sharp maximum at the equimolar point, suggesting the presence of long-chain polymers (Fig. 8). As the temperature is raised, the height of the peak decreases, presumably because of decreasing average chain length. This indicates that the forces holding the units together in the molecular chain are either hydrogen-bond forces or others of similar magnitude.

The loss factor, $\varepsilon''$, of the microwave dielectric constant likewise shows a peculiar

16) C.H. Giles, T.J. Rose and D.G.M. Vallance, *J. Chem. Soc.* (London), 1952, 3799.

17) N. Kurnakov and S. Zemchuzny, *Z. Physik. Chem.*, 83, 481 (1913).

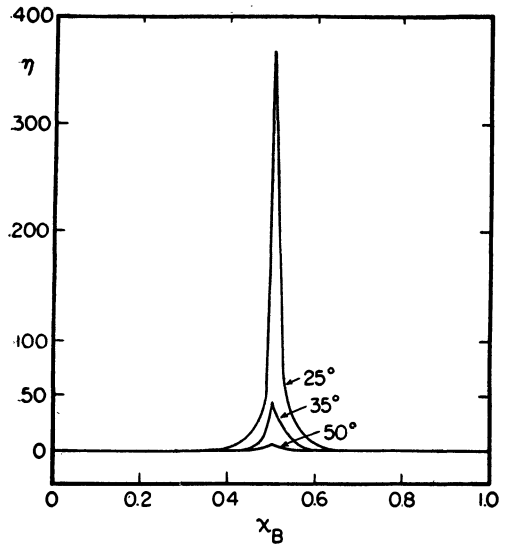



Fig. 8.[17] Variation of viscosity ($\eta$) with composition, for binary solutions of phenyl isothiocyanate (A) and diethylamine (B).

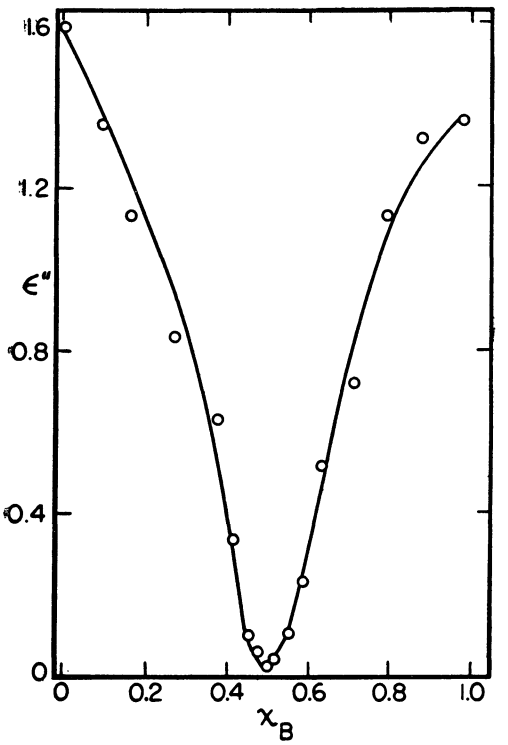



Fig. 9.[18] Variation of microwave dielectric loss ($\varepsilon''$) with composition, for binary solutions of phenyl isothiocyanate (A) and diethylamine (B).

behavior for this system[18]. A low, sharp minimum occurs at the equimolar point (Fig. 9).

18) P.K. Kadaba, *J. Chem. Phys.*, 22, 1465 (1954).

The following sets of structon and aggregate types are tentatively suggested, pending further experimental work, as reasonable ones to account for this behavior:

Range I: A(O) A(B) B(2A)
Aggregates: $A_2B$
Range II: A(B) B(2A) A(2B)
Aggregates: $(AB)_i$ $(AB)_iA$
Range III: B(2A) A(2B) B(A)
Aggregates: $(AB)_i$ $B(AB)_i$
Range IV: A(2B) B(A) B(O)
Aggregates: $AB_2$

On this basis, there are only small aggregates in Ranges I and IV, but Ranges II and III contain chain molecules (and perhaps ring molecules also). Assuming strict adherence to this scheme, but neglecting ring formation, the average molecular weight depends on composition as shown in Fig. 10.

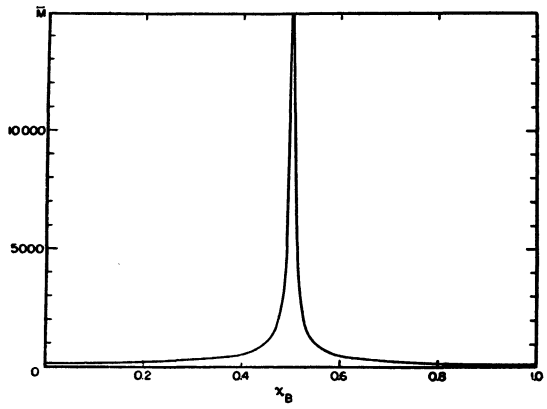



Fig. 10. Variation of calculated average molecular weight ($\bar{M}$) with composition, for binary solutions of phenyl isothiocyanate (A) and diethylamine (B).

The calculated molecular weight curve closely follows that of the 25°C viscosity curve, except that the former goes to infinity at the equimolar composition. This correspondence would be expected theoretically for solutions containing linear polymers[19].

Discussion of the nature of the association between the molecules in these polymer chains will be postponed until later.

In the literature, there are many other examples[13,16,20,21] of property-composition curves, for solution systems, which exhibit sharp breaks. In all cases of which the author is aware, it would be reasonable to assume association, usually involving hydro-

19) M.L. Huggins, *J. Phys. Chem.*, 42, 911 (1938); 43, 439 (1939).
20) V.S. Griffiths, *J. Chem. Soc.* (London), 1952, 1326.
21) G.N. Lewis and M. Randall, "Thermodynamics and the Free Energy of Chemical Substances," McGraw-Hill Book Co., New York, N.Y. (1923), p. 40.

gen bonds. Structon theory should be applicable, in most instances at least.

Although, in many cases, the breaks in the experimental curves can equally well be interpreted in terms of the formation of compounds or strong complexes of suitable compositions, the structon concept is more general and is more appropriate in cases in which linear or net work polymeric complexes are formed: for example, in the phenol-quinol, (phenyl isothiocyanate)-diethylamine, and sodium silicate systems. Another advantage of this point of view is that it makes possible the calculation of various properties of structon types, these properties presumably being transferable from system to system.

## The Structon Number Rule

The minimum number of structon types in a given system at a given concentration or over a given concentration range is given by a rule which can be called "the structon number rule," by analogy with the phase rule[22].

The minimum number ($S$) of structon types is equal to the number of equations required to fix the numbers of structons of each type. There is one equation for each of C types of contact between structon centers, representing the fact that there are as many B contacts to A centers as A contacts to B centers. There is a normalizing equation, expressing the requirement that the total amount of matter in the structons equals that in the quantity of matter being considered, or the requirement that the sum of the mole fractions equals unity. In many cases (e.g., in the glasses discussed above, other than pure silica), the relative numbers of structons of different types are also limited by a neutrality or valence-balancing equation. There is an additional equation for each degree of composition freedom ($F$).

The structon number rule can thus be expressed as

$$S=C+F+2 \qquad (11)$$

if the neutrality limitation is required, and

$$S=C+F+1 \qquad (12)$$

otherwise.

## Further Development

This theory can obviously be developed and extended in several ways. For example, the contributions of the individual structon types to specific properties of interest can be deduced and interpreted in terms of structon structure. It should be possible to relate the existence of structon types and of particular sets of them to energies of interaction between the atoms, ions, and molecules concerned. A quantitative treatment of these relationships should enable one to deal with systems showing departures from strict linearity of (structon-additive) property-composition curves, rounding at the breaks between ranges, etc., relating these phenomena quantitatively to the presence of structons other than those of lowest energy.

Another line of future extension of the theory is to polymer systems, in which the chief intermolecular interactions are strong attractions between atomic groups of specific kinds.

## Summary

In sodium silicate glasses and in many liquid solutions, curves representing the dependence of various properties on composition show distinct breaks. This behavior can be reasonably interpreted in terms of the types of environment around each atom or molecule or atomic group responsible for strong intermolecular interactions, together with the assumption that in these systems only the most stable environments are present in significant amounts. Only closest neighbors need be considered, hence the types of environment can conveniently be described in terms of "structons," each structon type being defined as a given kind of atom (or molecule or atomic group) surrounded by close neighbors in a given way.

The compositions at the breaks in the property curves limit, and in some cases determine uniquely, the types of structon present in and between the different composition ranges.

The structon theory has been applied to sodium silicate glasses and certain liquid solutions, in which there are strong hydrogen-bond interactions between molecules.

*The Research Laboratories of the Eastman Kodak Company, Rochester 4, New York, U. S. A.*

22) M. L. Huggins, *J. Am. Chem. Soc.*, 77, 3928 (1955).

# SHORT COMMUNICATIONS

## *Formation of Formoguanamine by the Reaction between Cyanamid and a Reduced Compound of Free Guanidine* (Studies on Some Derivatties of Cyanamide XLV**)*

By Keijiro Odo, Kozo Shirai and Kiichiro Sugino

(Received June 27, 1955)

It seemed to us that the reaction between cyanamide and free guanidine in alcoholic solution has hitherto not been studied. So, an investigation was made in order to clarify the products of this reaction.

First, the authors expected biguanide as a primary reaction product and melamine as a final product. But it was found that entirely different products were obtained in accordance with different procedures of the preparation of free guanidine. When a solution of free guanidine in ethanol was prepared by adding an equivalent amount of guanidine salt (for example, guanidine hydrochloride) to a sodium ethylate solution, it reacted with cyanamide to give biguanide just as we expected. But the reaction was found to proceed very slowly, so that only a trace of biguanide was formed even when the mixture was heated at 70–80°C for two hours[1]. And biguanide itself was found to give melamine when it was treated with cyanamide in ethanol. These reactions can be represented as follows.

$$NH_2\cdot C(NH)\cdot NH_2 + NH_2\cdot CN \longrightarrow NH_2\cdot C(NH)\cdot NH\cdot C(NH)\cdot NH_2$$

$$+NH_2\cdot CN \longrightarrow \text{(melamine)} + NH_3$$

But when a solution of free guanidine was prepared by adding an equivalent amount of metallic sodium to a solution of guanidine salt in ethanol, it reacted with cyanamide to give formoguanamine in a fair yield. This reaction seemed to be very rapid as compared with the formation of biguanide from guanidine.

For a typical run, 47.77 g. (0.50 mole) of thoroughly dried guanidine hydrochoride was dissolved in 250 cc. of absolute ethanol and 11.50 g. (0.50 mole) of clean sodium cuttings was added piece by piece with agitation, keeping the temperature at 20-30°C. A small quantity of ammonia was evolved during the dissolution of sodium (refer to Fig. 1). In the resulting solution, about 75% of guanidine used was found to remain as free base, but about 25% of it was supposed to be converted to a reduced form which could not be precipitated as picrate. 11.05 g. (0.25 mole) of cyanamide crystal (purity 95% was added to this solution without separating sodium chloride and the mixture was warmed gradually under reflux on the steam bath with slow stirring. When the temperature reached about 40°C, the reaction began to occur with the evolution of ammonia The reaction mixture was continued to heat till the temperature reached 80°C and maintained at that temperature for 30 minutes. (total reaction time: 3 hours and 20 minutes). In Fig. 1, are plotted the quantity of ammonia evolved and the reaction temperature against time which shows the proceeding of the over-all reaction accurately.

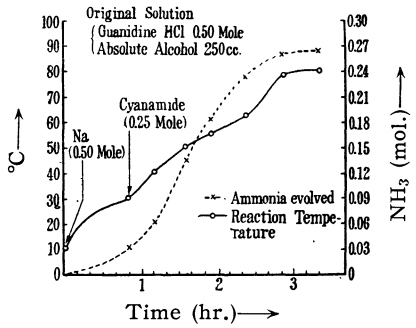


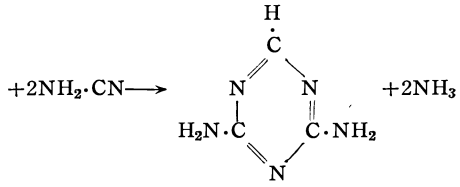

Fig. 1.

After the reaction, the solid (36.50 g.) was filtered off and treated with 100 cc. of water to dissolve sodium chloride only. The residue, washed with water and ethanol, dried, and weighed 7.00 g. (0.063 mole), m.p. 309–312°C, m.p. 316–7°C after crystallization from hot water. A mixture melting point with pure formoguanamine prepared from biguanide[2] showed no depression. Found: N, 62.73. Calcd. for $C_3H_5N_5$: N, 63.04%. The picrate melted at 248°C.

In the mother solution, about 58% of guanidine and 25% of cyanamide were found to remain unchanged together with a trace of biguanide formed[3]. Of course, a part of cyanamide was converted to dicyandiamide.

From these results, it was concluded that, in the latter case, guanidine was probably reduced to give an unstable reduced compound (triaminomethane (a part, formamidine $+NH_3$)?) and it reacted with cyanamide to give formoguanamine according to the following formula.

$NH_2 \cdot C(NH) \cdot NH_2$
$+2H \longrightarrow$ Reduced Compound of guanidine
($NH_2 \cdot CH(NH_2) \cdot NH_2$ or
$NH_2 \cdot CH{=}NH + NH_3$?)




The formation of formoguanamine was an unexpected result and seemed to be very interesting, because the possibility of the reduction of guanidine itself was proved.

*Laboratory of Organic Electrochemistry,*
*Department of Chemical Engineering,*
*Tokyo Institute of Technology,*
*Tokyo*

* This paper was presented at the 7th Annual Meeting of the Chemical Society of Japan, April 1, 1954.

** XLIV, K. Shirai, *J. Chem. Soc. Japan.*, Industrial Chemistry Section, 58, 343 (1955).

1) Under these conditions, cyanamide itself was converted in a considerable yield to dicyandiamide in the presence of guanidine.

2) This sample was prepared by Mr. M. Yamashita according to his procedure (*J. Chem. Soc. Japan*, Industrial Chemistry Section, 54, 786 (1951)) m.p. 318°C.

3) After standing for several months, the authors found a small amount of melamine crystallized out in the mother solution of this experiment.

## *Sur la Séparation de trois Éléments, l'Étain, l'Antimoine et Tellure, par la Résine échangeuse d'Anion*

Par Yukiyoshi SASAKI

(Reçu le 3 Août 1955)

En étudiant le dosage des éléments radioactifs produits par la fission nucléaire, et de l'étain irradié par neutron lent, nous nous sommes proposé de séparer trois métaux, l'étain, l'antimoine et le tellure. Dans ce but nous avons obtenu un bon résultat utilisant la résine échangeuse d'anion fortement basique.

Des essais préliminaires ont montré que ces métaux sont adsorbés sous les formes de chlorocomplexes, $SnCl_6^{2-}$, $SbCl_6^-$ et $TeCl_6^{2-}$ par la résine échangeuse d'anion en solution chlorhydrique concentrée. Lorsque l'acide se dilue, ces complexes commencent à se libérer de la résine se dissociant en cation ou chlorure de non-électrolyte et des anions de chlore.

Pour savoir l'affinité des métaux à la résine, nous avons mesuré des constants d'élution par des expériences chromatographiques utilisant une petite colonne remplie de la résine échangeuse d'anion Dowex 1-x4 fortement basique, sous la forme de chlorure.

Le chlorure du métal en question est mis au sommet de la colonne, et on laisse passer l'acide chlorhydrique pour déplacer le métal le long de la colonne. La courbe d'élution est obtenue par le dosage du liquide émergeante. Le constant d'élution s'exprime par le volume de la résine dans la colonne, divisé par le volume de l'acide chlorhydrique dépensé jusqu'au point de maximum de la courbe d'élution.

Tableau I montre les constants d'élution de ces trois éléments qui sont mesurés en solution chlorhydrique à diverses concentrations. La valeur de 1.3 signifie que le métal n'est pas adsorbé par la résine et passe librement la colonne.

TABLEAU I

CONSTANTS D'ELUTION

| Concentration de ClH | 0.1 | 1 | 2 | 3 | 4 | 6 N |
|---|---|---|---|---|---|---|
| Sn (IV) | 1.3 | <0.1* | <0.1 | <0.1 | <0.1 | <0.1 |
| Te (IV) | | 1.3 | 0.1 | <0.1 | <0.1 | <0.1 |
| Sb (V) | | 1.3 | 1.3 | 1 | 0.3 | <0.1 |
| In (III) | 1.3 | 0.5 | — | 0.3 | — | 0.3 |

* Le constant n'arrive pas à 0.1, mais la valeur précise n'a pas été obtenue.

Tandis que l'adorption et la désorption se réalisent rapidement et complètement pour le tellure et l'indium, l'adsorption irréversible a lieu pour l'antimoine-(V), à savoir, l'acide chlorhydrique à 3N ne peut eluer que 70% de l'antimoine qui était fixé sur la résine, ni l'acide nitrique, ni l'acide perchlorique n'est pas efficase à le désorber.

Etant donné que l'antimoine-(III) se fixe fermement sur la résine, cette adsorption anormale est interprétée en supposant la réduction de l'antimoine-(V) à l'antimoine-(III) dans la résine. Pour éviter la réduction de l'antimoine-(V), la résine à utiliser a été traitée par le brome jusqu'à ce qu'elle fût colorée en jaune*, et de plus, la durée où

l'antimoine serait en contact avec la résine a été minimée autant que possible.

Par ces traitements la quantité de l'antimoine resté dans la résine a été réduite jusqu'à 0.5% de l'antimoine total. L'etain n'est élué que moité par l'acide chlorhydrique à 0.1 N à cause de l'hydrolyse, mais l'acide perchlorique à 2 N le désorbe complètment.

Partant de ces résultats nous avons mis au point la séparation de ces trois métaux utilisant une colonne de verre de 0.85 cm. de diamètre, remplie de la résine Dowex 1-x4 de 50–100 mesh sous la forme de chlorure, traitée par le brome et lavé avec l'acide chlorhydrique à 3 N, jusqu'a une hauteur de 4 cm.

Un mélange à séparer est une solution chlorhydrique à 3 N, 1.5 $cm^3$ contenant 3 mg. de l'antimoine-(V) 1 mg. du tellure-(IV) 3 mg. de l'étain-(IV) avec les indicateurs radioactifs, $^{113}Sn$ (112 jours), son derive $^{113m}In$ (105 minutes), $^{129m}Te$ (30 jours) et $^{124}Sb$ (60 jours) de provenance des Etats-Unis. Après avoir laissé adsorber le mélange à étudier en haut de la colonne de la résine, on effectue l'elution avec l'acide chlorhydrique à 3 N pour éluer l'antimoine-(V). L'élution se pursuit pendant 20 $cm^3$ jusqu'à la disparition de la radioactivité dans le liquide émergeant. Dans ce cas, le constant d'élution a été un peu diminué par l'influence du brome.

Ensuite, l'acide chlorhydrique à 1 N est choisi pour enlever le tellure laissant adsorbé l'étain sur la résine. l'étain est désorbé par l'acide perchlorique à 1.8 N. La solution émergeante est receuillie par fraction de 1 $cm^3$. Les fractions du tellure et de l'étain sont évaporées à sec sur des assiettes de verre. Etant donné que le chlorure de l'antimoine se volatilise, l'antimoine est précipité et filtré comme sulfure.

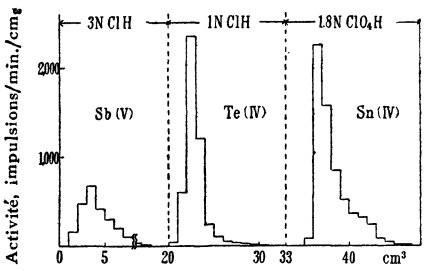



Fig. 1. Courbe d'elution.

Les dosages des métaux dans les fractions ont été réalisés en mesurant leur radioactivité par un conteur de Geiger-Müller après l'quilibre radioactif entre $^{113}Sn$ et $^{113m}In$ a été atteint. La Fig. 1 représente la courbe d'elution dans laquelle l'indium élué aux fractions de l'antimoine et du tellure n'existe plus,ma is de la Tableau I il resulte que si l'on désire à séparer l'indium de l'etain, l'acide chlorhydrique à 1–12 N élue l'indium et laisse l'étain sur la résine.

Nous avons repris le même procédé pour traiter les échantillons qui contiennent ces trois métaux dont l'un seul a été marquée avec l'indicateur radioactif.

Ces expériences ont montré que dans le procédé de la séparation donné ci-dessus, la quantité d'un élément qui contamine les fractions des deux autres métaux n'arrive pas à 0.05% de cet élément total.

*Laboratoire de Chimie, Faculté de Science*
*L'Université de Tokio*

* La résine échangeuse d'anion adsorbe du brome en solution chlorhydrique concentrée plus strictement qu'en solution peu concentrée. Il est probable que le brome est adsorbé comme $Br_2Cl^-$.

# *On 2-Arylaminotropones. I. The Syntheses of Several 2-Arylamino-4,7-dibromotropones and Their Dehalogenation Products*[1]

By Syun ISEDA

(Received March 3, 1955)

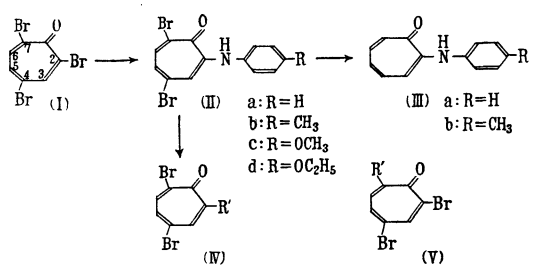
Nozoe and his co-workers reported[2] some time ago on the action of amines on 2, 4, 7-tribromotropone (I)[3]. In the case of aniline and *p*-toluidine, debromination of the reaction products without isolating the intermediates afforded liquid 2-anilinotropone (picrate, m.p. 142°C) and 2-(*p*-toluidino)-tropone, m.p. 108.5–109.5°C. The present writer followed these reactions and this paper describes the structure of the brominated products, their dehalogenation products, and similar reactions in several of the related compounds.

The reaction of 2, 4, 7-tribromotropone and aniline or *p*-toluidine proceeded well in benzene, in the presence of anhydrous sodium acetate, as has been described before[2]. The reaction products were obtained in a good yield and in pure state after several recrystallizations. The anilino derivative (II a) melted at 196–197°C and the *p*-toluidino derivative (II b) melted at 196°C, both crystallizing in fine yellow needles. None of their possible isomers was isolated.

The use of *o*-toluidine, *p*-bromoaniline, or *p*-nitroaniline as the anionoid reagent resulted in the recovery of the starting material possibly due to the steric hindrance in the case of *o*-toluidine and to lower basicity in the two latter reagents. When the *para*-position was occupied by an electron-releasing group other than the methyl, as in *p*-anisidine and *p*-phenetidine, crystalline products were obtained, though in an inferior yield, under the same conditions, affording (II c), m.p. 182°C, and (II d), m.p. 172°C.

Both (II a) and (II b) easily underwent hydrolysis by hot diluted ethanolic potassium hydroxide and afforded the same 3, 6-dibromotropolone (IV, R′=OH), indicating that (II a) and (II b) are 2-anilino- and 2-(*p*-toluidino)-4, 7-dibromotropone, respectively. As anticipated, the rate of hydrolysis of (II a) was greater than that of (II b).

It has been shown[2] that the hydrolysis of 2, 4, 7-tribromotropone in the presence of sodium acetate or the application of hydrazine hydrate yields a mixture (IV) and (V) of two kinds of dibromo compounds formed by the substitution of the bromine in $C_2$ or $C_7$. In the present series of experiments, however, only the $C_2$-substituted product was obtained. This was assumed to be due to the fact that the electron density at $C_2$ is lower than that at $C_7$ by the inductive effect of the bromine at $C_4$ and by the resonance effect, as well as to the steric condition between 2, 4, 7-tribromotropone and arylamines at the time of the reaction. In this connection, it would be interesting to study the reaction between 2, 4, 7-tribromotropone and alkylamines.




Catalytic debromination of (II a) and (II b) respectively yielded 2-anilinotropone (III a), m.p. 42–43°C, and 2-(*p*-toluidino)-tropone (III b), m.p. 109–110°C[2]. The respective picrates melting at 141–142°C and 117–118°C. (III a) dissolved in concentrated hydrochloric acid and perchloric acid but their salts could not be obtained in crystalline state. (III b) gives a crystalline hydrochloride of m.p. 175–180°C (decomp.) which was unstable in water and the original base was recovered on attempting its recrystallization from water. The perchlorate of the *p*-toluidino derivative was obtained in two different colors, red and yellow crystals, both melting at 176–177°C.

The ultraviolet absorption spectra (Fig 1)[4] show that the two pairs, (II a and II b) and (III a and III b) have a similar structure. The infrared spectra of these com-

1) This is part of a report presented at the Kyushu Local Meeting of the Chemical Society of Japan, Kumamoto, December 4, 1954.

2) T. Nozoe, Y. Kitahara, S. Masamune and K. Yamaguchi, *Proc. Japan Acad.*, 28, 85 (1952); T. Nozoe, Y. Kitahara, T. Ando, S. Masamune and H. Abe, *Sci. Repts. Tohoku Univ.*, Ser. I, 36, 166 (1952).

3) T. Nozoe, Y. Kitahara, T. Ando and S. Masamune, *Proc. Japan Acad.*, 27, 415 (1951).

4) Ultraviolet absorption spectra were determined by a Beckman spectrophotometer by members (especially by Miss Ayako Iwanaga) of the Chemical Institute, Faculty of Science, Tohoku University, Sendai.

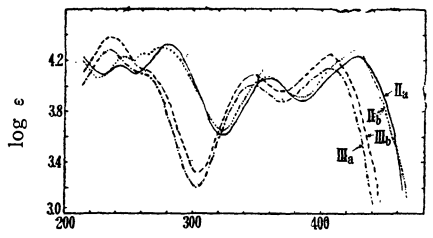



Fig. 1. Ultraviolet absorption spectra of 2-anilino-4, 7-dibromotropone (————), 2-anilinotropone (—·—·—), 2-(*p*-toluidino)-4, 7-dibromotropone (·····), and 2-(*p*-toluidino)-tropone (— — —). Solvent: methanol.

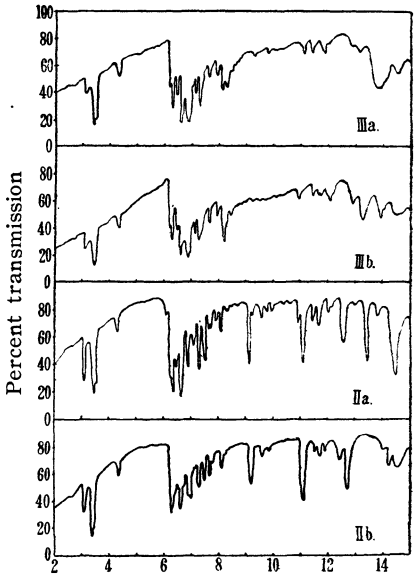



Fig. 2. Infrared absorption spectra of 2-anilino-4, 7-dibromotropone (II a), 2-(*p*-toluidino)-4, 7-dibromotropone (II b), 2-anilinotropone (III a) and 2-(*p*-toluidino)-tropone (III b).

pounds[5] (Fig. 2) all show absorption in 3.08–3.11 $\mu$, attritutable to the N-H bond (probably hydrogen bonded) but no absorption corresponding to the tropone carbonyl group (about 6.16 $\mu$).

## Experimental

**2,4,7-Tribromotropone (I)**[6].—Prepared according to the method of Nozoe, et al[2]. The crude product, m.p. 180–182°C, was dissolved in benzene and passed through a chromatographic column of alumina. Nearly colorless needles were obtained from the eluate and recrystallized from benzene, m.p. 182°C. It evolved a camphor-like odor when heated to 90°C or higher.

**2-Anilino-4,7-dibromotropone (II a)**.—To a mixture of 1.0 g. of 2,4,7-tribromotropone, 0.3 g. of anhydrous sodium acetate, and 20 g. of benzene, 0.4 g. of aniline was added under stirring at room temperature. The mixture was refluxed for two hours. After cooling, about 200 cc. of benzene was added to dissolve the separated crystals completely and the benzene solution was washed successively with water, diluted aqueous sodium hydroxide, diluted hydrochloric acid, and water. The filtered benzene solution was evaporated to dryness and the brownish residue was washed with a small amount of acetone. The yellow crystals thereby obtained, 0.85 g. (78%), were recrystallized three times from hot ethyl acetate to yellow needles, m.p. 196–197°C. Yield, 0.55 g. They were slightly soluble in cold ether, acetone, ethanol, and methanol. A solution of 0.50 g. of the crude crystals dissolved in 15 cc. of benzene was chromatographed on an alumina column. The initial fraction of colorless eluate afforded 10 mg. of 2,4,7-tribromotropone, m.p. and mixed m.p. with the authentic sample 182°C. Elution with benzene (total, 750 cc.) yielded 0.47 g. of yellow needles, m.p. 196–197°C, showing no depression on admixture with the sample of m.p. 196–197°C, obtained by the above method. Found: C, 44.22; H, 2.58; N, 4.16%. Calcd. for $C_{13}H_9ONBr_2$: C, 43.96; H, 2.56; N, 3.95%[7].

2-Anilino-4,7-dibromotropone failed to form any salts with hydrogen chloride in ether, saturated ethanolic solution of picric, flavianic, or picrolonic acid, or concentrated hydrochloric acid. On refluxing with one molar equivalent of aniline in benzene, the starting material was recovered.

**Hydrolysis of 2-anilino-4,7-dibromotropone. Isolation of 3,6-dibromotropolone.**—A mixture of 200 mg. of (II a) and 11 cc. of N ethanolic potassium hydroxide solution was refluxed for twenty minutes after the crystals completely dissolved to give a clear reddish brown solution. After adjusting the reaction mixture to pH 3.5 with 2 N hydrochloric acid, majority of ethanol was distilled off under a reduced pressure, cooled, 10 cc. of water was added to the residue, and the mixture was extracted several times with benzene. The combined benzene extract was evaporated under a reduced pressure and the residue was sublimed in vacuo (bath temperature, 110–120°C). The sublimate was crystallized from dilute ethanol or water to light yellow needles, m.p. 121–122°C. Yield, 70 mg. Admixture with an authentic sample of 3,6-dibromotropolone[2] did not show any depression of m.p.

The mother liquor was extracted with chloroform and a second crop of crystals was obtained. Total yield, 85 mg. (74%).

**2-Anilinotropone (III a)**.—A mixture of 5 g. of (II a) and 200 cc. of methanol was hydrogenated in the presence of 3 g. of anhydrous sodium ace-

5) Infrared spectra were determined by the Perkin-Elmer Model 21 double-beam instrument with NaCl prism, Nujol mull method, by Messrs. H. Kozuma and K. Kawasaki, Technical Department, Minamata Factory, Shin Nippon Chisso Hiryo K.K., Minamata, Kumamoto.

6) Suberone and a part of 2,4,7-tribromotropone were provided by the Chemical Institute, Faculty of Science, Tohoku University.

7) The microanalyses were carried out at the Institute of Polytechnics, Osaka City University, and at the Pharmaceutical Department, Kumamoto University. Some of the nitrogen analyses were carried out by Miss K. Kato of Tohoku University.

tate and 1 g. of 5% palladium-carbon. On a every hour, the vessel was immersed in a hot water bath for ten to fifteen minutes with occasional shaking to dissolve the remaining crystals. After absorption of 2.2 mol. of hydrogen, the reaction was stopped, the catalyst was removed by filtration, and the solvent was evaporated. The residue was extracted with benzene, the benzene layer was washed successively with water, diluted sodium hydroxide, and water, and dried over anhydrous sodium sulfate. Evaporation of the solvent under ordinary pressure left a viscous brown oil (yield, 1.86 g. or 67%) which was extracted several times with cold petroleum ether (b.p. 60–80°C). The extract was concentrated under reduced pressure and allowed to stand in an ice box for several days. Light yellow prisms, m.p. 42–43°C, were obtained. Yield 1.1 g. Slightly unstable to heat. Very easily soluble in all organic solvents, except petroleum ether. Presence of even a trace of solvent prevents crystallization. Found: N, 7.05%. Calcd. for $C_{13}H_{11}ON$: N, 7.10%.

The compound dissolved easily in hydrochloric acid and perchloric acid (70%), but their crystalline salts could not be obtained.

*Picrate.*—An ethanolic solution of picric acid was added to the base dissolved in a minimum amount of ethanol and the precipitate thereby formed was recrystallized from ethanol containing a few drops of picric acid to yellowish brown, short prisms, m.p. 141–142°C, which showed no depression on admixture with an authentic sample[2]. The picrate was resolved into components by chromatography through alumina and the base thereby recovered melted at 42°C.

**2-(*p*-Toluidino)-4,7-dibromotropone (II b).**—A mixture of 10 g. of 2,4,7-tribromotropone, 3.0 g. of anhydrous sodium acetate, 150 cc. of benzene, and 3.75 g. of *p*-toluidine was treated as in the case of aniline. The crude product (11.2 g.) was recrystallized twice from ethyl acetate to yellow needles, m.p. 196°C. Yield, 8.2 g. (76.2%). Admixture with the anilino compound (II a) melted at 175–185°C. Further purification by chromatography through alumina failed to any other product. Found: C, 45.79; H, 3.06; N. 4.12%. Calcd. for $C_{14}H_{11}ONBr_2$: C, 45.54; H, 3.01; N, 3.79%.

A residue (0.5 g.) obtained from the initial recrystallization mother liquor of ethyl acetate was dissolved in 150 cc. of benzene, chromatographed through 20 g. of alumina, and the eluate from 400 cc. of benzene was fractionated into 20 cc. each. Fractions 1–4 (colorless) yielded 10 mg. of 2,4,7-tribromotropone. Fractions 8–18 (yellow) yielded 150 mg. of crystals melting at 195°C, alone and in admixture with (II b). Residual fractions and elution with other solvents failed to give any other products.

**Hydrolysis of 2-(*p*-toluidino)-4,7-dibromotropone.**—A mixture of 100 mg. of (II b), 5 cc. of ethanol, and 2 cc. of 2 N ethanolic solution of potassium hydroxide was refluxed for 40 minutes on a water bath. The crystals that separated out on cooling melted at 192–194°C and were identified as the starting material (II b). After refluxing for two hours more, when the color of the solution turned wine-red, the solvent was evaporated under a reduced pressure, water was added to the residue, and the solution was extracted with ether. The ether-soluble portion had an odor resembling that of *p*-toluidine. The aqueous alkaline layer was acidified with hydrochloric acid, extracted with chloroform, and the solvent was evaporated from the chloroform extract. The residual, semicrystalline mass was sublimed in vacuo and the sublimate was recrystallized from water to slightly yellow needles, m.p. 120°C, alone and inadmixture with 3,6-dibromotropolone. Yield, 15 mg.

**2-(*p*-Toluidino)-tropone (III b).**—This compound was obtained by the catalytic debromination of (II b) (3.50 g.) with 5% palladium-carbon and hydrogen, as in the case of the anilino analog, and the reaction was completed in four hours. Evaporation of the benzene washing yielded some brownish yellow prisms which were recrystallized from benzene and showed m.p. and mixed m.p. with an authentic sample[2] of 109–110°C. Yield, 1.48 g. (73.7%). Found: N, 6.69%. Calcd. for $C_{14}H_{13}ON$: N, 6.63%.

*Hydrochloride.*—The base was dissolved in hot 5 N hydrochloric acid, allowed to stand over-night in an ice box, and the crystals that precipitated out were recrystallized from 5 N hydrochloric acid to reddish brown prisms, which softened at 120°C, solidified again, and decomposed at 175–180°C. The decomposed product solidified in the capillary tube when allowed to cool and melted at 108–109°C. On attempting to recrystallize this compound from water or when water was added to the hydrochloric acid solution, yellow crystals precipitated out and were identified as (III b), m.p. 109°C.

*Perchlorate.*—The base was added to cold 70% perchloric acid, warmed gradually, and filtered while warm. On cooling the filtrate, red prisms separated. These were recrystallized from absolute ethanol and melted at 177–178°C. The crystals were labile in water and recrystallization from water yielded yellow needles which softed at 160°C and melted at 177–178°C. Admixture with the foregoing red crystals showed no depression of the m.p. When the yellow crystals were treated with 70% perchloric acid, the red crystals regenerated. (III b) was recovered from both crystals by ammonia and identified as its picrate.

Found: (red), C, 63.92; H, 4.90% (yellow), C, 63.47, H. 4.77%. Calcd. for $C_{14}H_{13}ON$ 1/2 $HClO_4$: C, 64.30; H, 5.20%.

*Picrate.*—Prepared as in the case of the anilino compound. Yellow needles (from ethanol), m.p. 117–118°C; fairly soluble in ethanol. Found: C, 54.15; H, 3.65; N, 12.53%. Calcd. for $C_{20}H_{16}O_8N_4$: C, 54.55; H, 3.66; N, 12.72%.

*Other reactions.*—No crystalline products were obtained by reaction with acetic anhydride, either alone or in the presence of sodium acetate (refluxed for thirty minutes), or with one to three mol. equivalents of hydrazine hydrate in ethanol, heated for one hour in a water bath.

**2-(*p*-Methoxyphenylamino)-4,7-dibromotropone (II c).**—A mixture of 2.06 g. of 2,4,7-tribromotropone and 0.74 g. of *p*-anisidine was treated as in the case of (II a) and 1.25 g. (52.1%) of thick yellow rods were obtained. Recrystallized from acetone and then from ethyl acetate, m.p. 182°C. Found: C, 43.66; H, 3.14%. Calcd. for $C_{14}H_{11}O_2NBr_2$: C, 43.64; H, 2.86%.

**2-(*p*-Ethoxyphenylamino)-4,7-dibromotropone (II d).**—A mixture of 2.06 g. of tribromtropone and an equivalent amount (0.85 g.) of *p*-phenetidine was refluxed for four hours. The crude product obtained was dissolved in benzene, passed through an alumina column, and the column was eluted with benzene. The combined eluates were evaporated and the residue was recrystallized first from acetone and then from ethanol, to yellowish brown needles, m.p. 172°C. Yield, 1.01 g. (43.5%). Found: C, 44.91; H, 2.93%. Calcd. for $C_{15}H_{13}O_2NBr_2$: C, 45.12; H, 3.26%.

The majority of the experiments reported herein were carried out at the Chemical Institute, Faculty of Science, Tohoku University, Sendai, and the writer takes this opportunity to express his sincere gratitude to Professor Tetsuo Nozoe for his kind guidance and encouragement throughout the course of this work. The writer is also indebted to the members of the Institute for their friendly cooperation and kind criticisms, and to those who supplied analytical data.

The present series of studies constitute a part of the general research on troponoid compounds (Representative: Prof. T. Nozoe). Part of the expenses for the present work was defrayed by a Grant in Aid for Scientific Research provided by the Ministry of Education, which is gratefully acknowledged.

*Department of Chemistry, Kumamoto Women's University, Kumamoto*

# *Polarographic Behavior of Nitroammonocarbonic Acids in Aqueous Media. I. Nitrourea**

By Keiho NAMBA and Kyoichi SUZUKI

(Received February 18, 1955)

The principal organic compounds which possess $NO_2$ radicals are O-$NO_2$ compounds (nitric esters), C-$NO_2$ compounds (nitro compounds) and N-$NO_2$ compounds (nitramines). Among these compounds, the polarographic behavior of C-$NO_2$ compounds, especially, of aromatic nitro compounds has been studied considerably. However, the polarographic study published for N-$NO_2$ compounds, e. g., nitramines, which have a reduction mechanism similar to that of C-$NO_2$ compounds, was not found, except in the cases of the studies on the electrolytic reduction of nitroguanidine to aminoguanidine[1] and on the polarographic analysis of cyclotrimethylenetrinitramine[2]. Since the reduction mechanism of nitramine which has two N-$NO_2$ redicals is considered to be more complicated, we studied the polarographic behavior of nitroammonocarbonic acid which has one N-$NO_2$ radical and is water soluble. Nitrourea was studied at the first stage. However, the result was so complicated that it was impossible to clarify the reduction mechanism. We report here the experimental result mainly.

## Experimental

Nitrourea, prepared through the dehydration of urea nitrate by concentrated sulfuric acid[3] below 0°C and purified by recrystallizations from water and afterwards from aceton, had m.p. 155°C (decomp.) (Found: N, 39.97. Calcd. for $CH_3N_3O_3$: N, 40.00%).

The buffer solutions used as the supporting electrolyte are as follows;

| pH range | Buffer solution | |
|---|---|---|
| 1.0....4.7 | Walpole | (1N−HCl & 1N−$CH_3COONa$). |
| 5.2....8.0 | Sφrensen | (M/15−$KH_2PO_4$ & M/15−$Na_2HPO_4$). |
| 8.0....9.0 | 〃 | (M/20−Borax & N/10−HCl). |
| 9.2...12.0 | 〃 | (M/20−Borax & N/10−NaOH). |

The concentration of sample, temperature, sensitivity of galvanometer and the corrected value of shunt, were $1\sim5\times10^{-4}$ mol./l., 25.0±0.1°C, $1.49\times10^{-9}$ amp./mm./m. and 1 : 95.7, respectively. The oxygen gas solved in sample solution was removed by the bubbling stream of purified nitrogen gas, at the rate of 2~3 cc./sec. for twenty minutes, The Heyrovsky-Shikata type polarograph apparatus produced by Yanagimoto Manuf. Co. was used and every polarogram was taken

* The main part of this paper was presented at the 1st Symposium on Polarograph on Nov. 17, 1954, Kyoto.

1) K. Sugino and M. Yamashita, *J. Chem. Soc., Japan*, 70, 73 (1949).

2) W.H. Jones, *J. Am. Chem. Soc.*, 76, 834 (1954).

3) T.L. Davis, "The Chemistry of Powder and Explosives", John Wiley and Sons, Inc., New York, N. Y (1943), p, 373.

within thirty minutes after the preparation of the sample solution.

## Experimental Results and Discussion

**1) Effects of pH upon the Half-Wave Potential ($E_{1/2}$) and the Limiting Current ($i_l$).**—The polarographic waves of nitrourea at various pH are shown in Fig. 1.

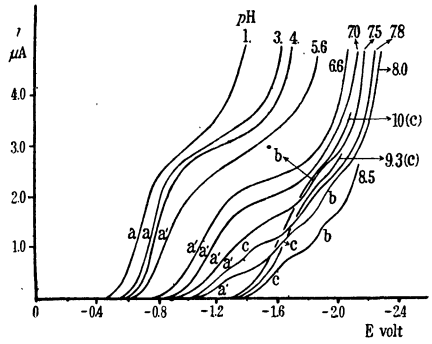



Fig. 1. Polarograms of $1\times10^{-4}$ mol./l. Nitrourea.

Relationships of pH–$E_{1/2}$ (vs. S.C.E.) and of pH–$i_l$ are shown in Fig. 2 and Fig. 3,

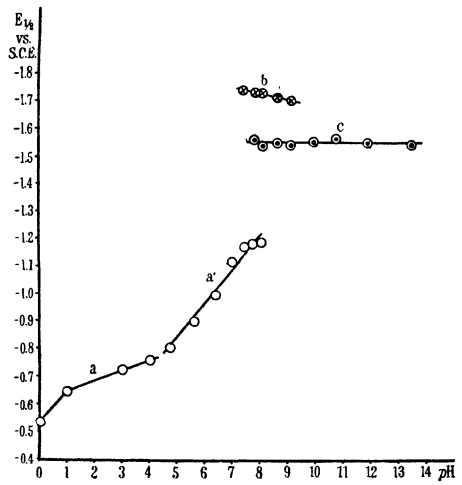



Fig. 2. Relationship between pH and $E_{1/2}$ (vs. S.C.E.)
○ —— (a) and (a') waves
⊗ —— (b) wave
⊙ —— (c) wave

respectively. The polarographic waves of urea and urea nitrate are not found at any pH under the same condition. It is evident that the above reduction waves are those of N-$NO_2$ radical. The wave symbolized as the (a) wave at pH 1–3, is the stable wave, and the relationship between concentration and $i_l$ is linear over the range $1\text{–}10\times10^{-4}$ mol./l.[4].

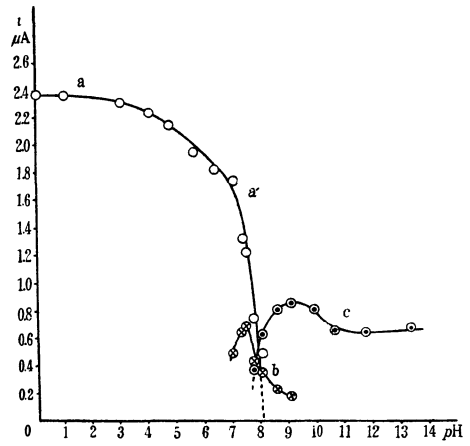



Fig. 3. Relationship between pH and $i_l$ (conc. $1\times10^{-4}$ mol./l.)

The (a') wave, appeared above pH 3, decreases in its height. The double waves, (a') and (b), appear above pH 7. Since the $E_{1/2}$ of (b) wave shifts considerably to the reduction potential of supporting electrolyte, it is presumed the polarogram below pH 7 is single wave in its appearance. After the (a') wave vanishes completely, the trace of (b) wave and the growing (c) wave exist around pH 9. The triple waves are found in range of pH 7.7–8.5. These are considered to be similar to the split polarographic waves reported in the studies of maleic and fumalic acids[5]. Only the (c) wave exists above pH 9.3 stably.

**2) Effects of the Height of Mercury Reservoir and of Temperature upon the Limiting Current.**—Table I represents the

TABLE I
DEPENDENCE OF THE EFFECTIVE HEIGHT OF MERCURY RESERVOIR ON THE LIMITING CURRENT OF $1\times10^{-4}$ mol./l. NITROUREA
TEMPERATURE: 25°C

| | | pH 1.04 | | pH 5.10 | | pH 7.01 | |
|---|---|---|---|---|---|---|---|
| $h_{eff}$ | $h_{eff}^{1/2}$ | $i_l$ | $i_l/h^{1/2}$ | $i_l$ | $i_l/h^{1/2}$ | $i_l$ | $i_l/h^{1/2}$ |
| cm. | | μa. | | μa. | | μa. | |
| 57 | 7.55 | 3.07 | 0.41 | 2.16 | 0.29 | 2.12 | 0.28 |
| 47 | 6.86 | | | 1.91 | 0.28 | | |
| 37 | 6.08 | 2.50 | 0.41 | 1.69 | 0.28 | 1.74 | 0.29 |
| 32 | 5.66 | 2.30 | 0.41 | | | | |
| 27 | 5.20 | 2.02 | 0.39 | 1.47 | 0.28 | 1.39 | 0.27 |
| 22 | 4.69 | 1.91 | 0.41 | 1.22 | 0.26 | 1.23 | 0.26 |
| 17.5 | 4.18 | | | 1.12 | 0.27 | 1.04 | 0.25 |
| 15.5 | 3.94 | 1.70 | 0.43 | | | | |

relationship between the effective height of mercury reservoir, $h_{eff}$, and the limiting current.

4) K. Namba and K. Suzuki, *Journal of the Industrial Explosives Society*, Japan, **15** 171. (1954).

5) P. J. Elving and I. Rosenthal, *Anal. Chem.*, **26**, 1454 (1954).

| | | pH 7.99 | | | | |
|---|---|---|---|---|---|---|
| | | (a) | | (b) | | (c) |
| $h_{eff}$ | $h_{eff}^{1/2}$ | $i_l$ | $i_l/h^{1/2}$ | $i_l$ | $i_l/h^{1/2}$ | $i_l$ |
| cm. | | μa. | | μa. | | μa. |
| 57 | 7.55 | 0.545 | 0.072 | 0.650 | 0.086 | 0.437 |
| 47 | 6.86 | 0.509 | 0.074 | 0.562 | 0.082 | 0.437 |
| 37 | 6.08 | 0.481 | 0.079 | 0.495 | 0.081 | 0.408 |
| 32 | 5.66 | 0.452 | 0.080 | 0.437 | 0.077 | 0.437 |
| 27 | 5.20 | 0.422 | 0.081 | 0.373 | 0.072 | 0.437 |
| 22 | 4.69 | 0.399 | 0.085 | 0.335 | 0.072 | 0.408 |
| 17 | 4.12 | 0.378 | 0.092 | 0.282 | 0.069 | 0.408 |

The fact that the limiting current at pH 1.05, 5.10 and 10.68 are proportional to $h^{1/2}$ means that these currents are controlled by the diffusion process; whilst the limiting current of the split polarographic wave such as the (c) wave at pH 7.99 is independent of the effective height of the mercurry reservoir, i.e., it can be concluded that the limiting current of the split wave shows the characteristics of kinetic current.

The relationships between the temperature and the limiting current at pH 2.20 and 5.20 is shown in Table II. Since the decomposition of nitrourea is acceralated in proportion

TABLE II
INFLUENCE OF THE TEMPERATURE ON THE LIMITING CURRENT OF $1\times10^{-4}$ mol./l. NITROUREA

| pH 2.20 | | | pH 5.20 | |
|---|---|---|---|---|
| t, °C | $i_l$, μa. | Temp. coeff., % | t, °C | $i_l$, μa. |
| 22.8 | 2.28 | | 26.4 | 2.15 |
| 26.7 | 2.42 | | 36.3 | 2.42 |
| 36.3 | 2.78 | av. 1.30 | 44.0 | 2.22 |
| 45.0 | 3.08 | | 51.9 | 1.98 |
| 54.7 | 3.44 | | | |

to the increase of both temperature and pH, particularly in alkaline[4], it is impossible to obtain the above relationship except in the case of comparatively strong acidic media where nitrourea is actually stable.

The temperature coefficient of the limiting current is about 1.30% per degree at pH 2.20 and it is almost equal to that of the diffusion current. At pH 5.20, it was impossible to account for the temperature coefficient in sake of the decomposition which induced the decrease of height in the limiting current despite the increase of temperature.

**3) Calculation of the Electron Number for Reduction ($n$).**—Since the reduction process of nitrourea in alkaline media seems to be kinetically controlled, it is not reasonable to calculate $n$ in such a region, by assuming a proper diffusion coefficient (D) in the Ilkovič equation. Therefore, we only calculated $n$ in the range of pH 1–3, where nitrourea is considered stable. We could not find out the proper value of the anion such as $NH_2{\cdot}CO{\cdot}NH{\cdot}COO^-$, the molecular size and weight of which are almost similar to those of nitrourea. The anion we chose was that of malonamic acid, $NH_2{\cdot}CO{\cdot}CH_2{\cdot}COO^-$, whose electroconductivity in infinite dilution was 35.5 $\Omega^{-1}$ cm$^2$ [6]. Inserting this value into the equation: $D_0 = 2.67\times10^{-7}\,\lambda_t^0/Z$ cm$^2$ sec$^{-1}$ (where $\lambda_t^0$ is the electroconductivity of ion in infinite dilution and the ionic value of ionized substance (Z) is 1), we obtained $9.49\times10^{-6}$ cm$^2$ sec$^{-1}$ for the $D_0$ value. The calculated $n$'s through this method, were 5.25 and 5.22 at pH 1.04 and 3.05, respectively (where $m^{2/3}$ is 1.98 mg./sec. and $t^{1/6}$ are 1.20 sec. in both cases).

Assuming the mechanism of reduction of nitrourea with five electrons, we must suppose the tetrazane compound such as that shown in the following formula

$$2NH_2{\cdot}CO{\cdot}NH{\cdot}NO_2+10H^++10e = NH_2{\cdot}CO{\cdot}NH{\cdot}NH{\cdot}NH{\cdot}NH{\cdot}CO{\cdot}NH_2+4H_2O$$

However, such tetrazane compound would be too unstable to exist. Further investigation on this problem by means of another direct method such as the controlled potential electrolysis will be necessary.

## Summary

1) The relationship of pH–$E_{1/2}$ (vs. S.C.E.) and of pH–$i_l$ of nitrourea under the dropping mercury electrode was studied.

2) It is presumed from the experiment on the effect of the effective height of the mercury reservoir and of temperature upon $i_l$ that $i_l$ will follow the diffusion law in acidic solution.

3) The electron number consumed for reduction was calculated by assuming the diffusion coefficient.

The authors wish to express their sincere thanks to Prof. I. Tachi, Mr. M. Suzuki and Mr. S. Koide, Faculty of Agriculture, University of Kyoto, for their kind discussions. The authors also express their sincere thanks to Prof. S. Yamamoto, Faculty of Engineering, University of Tokyo, for his encouragement and to Mr. T. Yamashita, Laboratory of Explosives, University of Tokyo, for his suggestion.

*Laboratory of Explosives, Faculty of Engineering, University of Tokyo, Tokyo*

6) Randolt-Börnstein, "Physikalisch-Chemische, Tabellen", Eg. III, Verlag von Julius Springer, Berlin (1936), S. 2044.

# *Polarographic Behavior of Nitroammonocarbonic Acids in Aqueous Media. II. Nitroguanidine**

By Keiho NAMBA and Kyoichi SUZUKI

(Received February 18, 1955)

In the preceding paper [1], the polarographic behavior of nitrourea in aqueous media was reported. We extended this study to the behavior of nitroguanidine, and obtained complicated results in this case as well as in the case of nitrourea. This report mainly consists of the experimental results.

## Experimental

The experimental method was described in Part I. Nitroguanidine, prepared through the dehydration of guanidine nitrate in concentrated sulfuric acid[2] and purified by recrystallization from water several times, was composed of colourless needles, m.p., 230°C (decomp.) (Found: N, 53.85. Calcd. for $CH_4N_4O_2$: N, 53.85%).

## Experimental Results and Discussion

**1) Effects of pH upon the Half-Wave Potential ($E_{1/2}$) and the Limiting Current ($i_l$).**—Polarographic waves at various pH are reproduced in Fig. 1. The relationship of

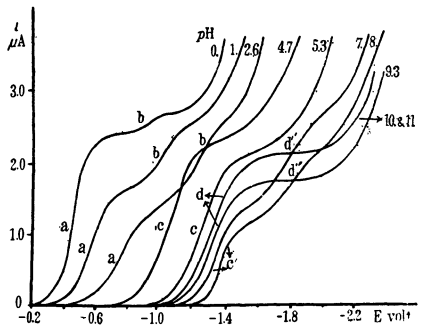



Fig. 1. Polarograms of $1\times10^{-4}$ mol./l. Nitroguanidine.

pH–$E_{1/2}$ (vs. S.C.E.) and of pH–$i_l$ is shown in Figs. 2 and 3, respectively. From these data, we can make the following summary:

a) in range of pH 0–3 double wave: (a) and (b) waves
b) in range of pH 4–5 single wave: (c) wave
c) in range of pH 5.6–8 double wave: (c′) and (d′) waves
d) above pH 9.3 single wave: (d) wave

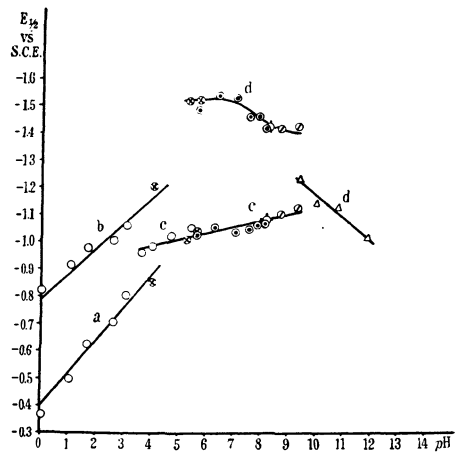



Fig. 2. Nitroguanidine: Relationship between pH and $E_{1/2}$ (vs. S.C.E.)
Species of buffer solution
○ Wolpole (1N-HCl & 1N-$CH_3COONa$)
⊗ Kolthoff (M/10-Citric Acid & M/5-$Na_2HPO_4$)
⊙ Sørensen (M/15-$KH_2PO_4$ & M/15-$Na_2HPO_4$)
-☼- Kolthoff (M/20-Borax & M/10-$KH_2PO_4$)
⊘ Sørensen (M/20-Borax & N/10-HCl)
△ Sørensen (M/20-Borax & N/10-NaOH)

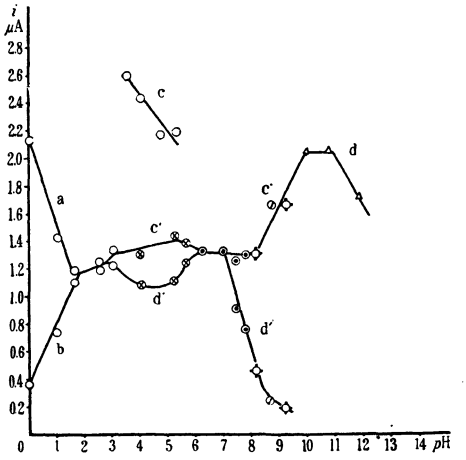



Fig. 3. Nitroguanidine: Relationship between pH and $i_l$ (conc. $1\times10^{-4}$ mol./l.)

* The main part of this paper was presented at the 1st Symposium on Polarograph on Nov. 17, 1954, Kyoto.

1) K. Namba and K. Suzuki, This Bulletin, 28, 620 (1955).

2) T.L. Davis, "The Chemistry of Powder and Explosives", John Wiley and Sons, Inc., New York, N. Y., (1943), p. 380.

Whether the wave is single or double in its shape depended upon the species of buffer solution as found in the range of pH 4–5 and at pH 9 in Fig. 2. The single wave obtained in the range of pH 4–5 in the Walpole solution will be the duplicated wave of the 1st and 2nd waves, due to the vicinity of reduction potential for both waves, while the total value of $i_l$ of the double wave in acidic media is almost the same. When we examined the polarogram of guanidine nitrate under the same condition, no reduction wave was found. From this fact, all reduction waves found are considered to be those of N-$NO_2$ radical.

In the previous paper[3], we examined the influence of concentration upon the limiting current and of temperature on the stability. A linear relationship between the limiting current and concentration was obtained over the concentration range of $1–10\times10^{-4}$ mol./l. in acidic media, where the nitroguanidine was stable.

**2) Effects of the Height of Mercury Reservoir and of Temperature upon the Limiting Current.**—Table I represents the relationship between the effective height of mercury reservoir, $h_{eff}$, and the limiting current.

TABLE I

DEPENDENCE OF THE EFFECTIVE HEIGHT OF MERCURY RESERVOIR ON THE LIMITING CURRENT OF $1\times10^{-4}$ mol./l. NITROGUANIDINE

Temperature 25°C

| | | pH 1.05 | | | | pH 3.49 | |
|---|---|---|---|---|---|---|---|
| | | (a) | | (b) | | (c) | |
| $h_{eff}$ | $h_{eff}^{1/2}$ | $i_l$ | $i_l/h^{1/2}$ | $i_l$ | $i_l/h^{1/2}$ | $i_l$ | $i_l/h^{1/2}$ |
| cm. | | μa. | | μa. | | μa. | |
| 57 | 7.55 | 1.80 | 2.38 | 1.25 | 1.66 | 3.47 | 4.60 |
| 47 | 6.86 | 1.63 | 2.38 | 1.02 | 1.49 | 3.04 | 4.43 |
| 37 | 6.08 | 1.48 | 2.43 | 0.86 | 1.41 | 2.94 | 4.83 |
| 27 | 5.20 | 1.25 | 2.40 | 0.71 | 1.37 | 2.32 | 4.46 |
| 22 | 4.69 | 1.11 | 2.37 | 0.67 | 1.43 | 2.10 | 4.48 |
| 17.5 | 4.18 | 1.02 | 2.44 | 0.61 | 1.46 | 1.82 | 4.36 |

| | | pH 5.10 | | | |
|---|---|---|---|---|---|
| | | (c') | | (d') | |
| $h_{eff}$ | $h_{eff}^{1/2}$ | $i_l$ | $i_l/h^{1/2}$ | $i_l$ | $i_l/h^{1/2}$ |
| cm. | | μa. | | μa. | |
| 57 | 7.55 | 1.69 | 2.24 | 1.74 | 2.31 |
| 47 | 6.86 | 1.48 | 2.16 | 1.48 | 2.16 |
| 37 | 6.08 | 1.30 | 2.14 | 1.32 | 2.17 |
| 27 | 5.20 | 1.05 | 2.02 | 1.09 | 2.10 |
| 22 | 4.69 | 0.96 | 2.05 | 1.02 | 2.18 |
| 17.5 | 4.18 | 0.82 | 1.96 | 0.91 | 2.18 |

| | | pH 7.01 | | | | pH 9.30 | |
|---|---|---|---|---|---|---|---|
| | | (c') | | (d') | | (d) | |
| $h_{eff}$ | $h_{eff}^{1/2}$ | $i_l$ | $i_l/h^{1/2}$ | $i_l$ | $i_l/h^{1/2}$ | $i_l$ | $i_l/h^{1/2}$ |
| cm. | | μa. | | μa. | | μa. | |
| 57 | 7.55 | 1.50 | 1.99 | 1.58 | 2.09 | 2.65 | 3.51 |
| 47 | 6.86 | 1.39 | 2.03 | 1.49 | 2.17 | 2.30 | 3.36 |
| 37 | 6.08 | 1.21 | 1.99 | 1.27 | 2.09 | 1.98 | 3.26 |
| 27 | 5.20 | 1.03 | 1.98 | 1.11 | 2.13 | 1.73 | 3.33 |
| 22 | 4.69 | 0.93 | 1.98 | 1.00 | 2.14 | 1.55 | 3.31 |
| 17.0 | 4.12 | 0.77 | 1.87 | 0.90 | 2.18 | 1.33 | 3.18 |

The fact that the limiting current at pH 1.05, 3.49, 5.10, 7.01 and 9.30 are proportional to $h^{1/2}$ means that these currents are controlled by the diffusion process.

The relationships between the temperature and the limiting current at pH 2.20, 5.05, 8.16 and 10.82 are shown in Table II.

TABLE II

INFLUENCE OF THE TEMPERATURE ON THE LIMITING CURRENT OF $1\times10^{-4}$ mol./l. NITROGUANIDINE

pH 2.20

| | (a) | | (b) | |
|---|---|---|---|---|
| $t$, °C | $i_l$, μa. | Temp. coeff., % | $i_l$ μa. | Temp. coeff., % |
| 26.2 | 1.22 | av. 1.14 | 1.17 | av. 1.65 |
| 35.8 | 1.42 | | 1.35 | |
| 45.3 | 1.69 | | 1.44 | |
| 53.9 | 1.86 | | 1.62 | |

pH 5.05

| | (c') | | (d') | |
|---|---|---|---|---|
| $t$, °C | $i_l$, μa. | Temp. coeff., % | $i_l$, μa. | Temp. coeff., % |
| 22.5 | 1.41 | av. 1.47 | 1.03 | av. 2.03 |
| 35.0 | 1.65 | | 1.38 | |
| 44.5 | 2.03 | | 1.60 | |
| 54.2 | 2.23 | | 1.85 | |

pH 8.16

| | (c') | | (d') | |
|---|---|---|---|---|
| $t$, °C | $i_l$, μa. | Temp. coeff., % | $i_l$, μa. | Temp. coeff., % |
| 26.7 | 1.41 | av. 1.32 | 0.51 | av. 1.73 |
| 36.0 | 1.60 | | 0.64 | |
| 45.5 | 1.86 | | 0.74 | |
| 52.6 | 1.93 | | 0.80 | |

pH 10.82

| $t$. °C | $i_l$, μa. | Temp. coeff., % |
|---|---|---|
| 26.0 | 2.12 | |
| 35.1 | 2.40 | 1.45 |
| 43.0 | 2.83 | 2.53 |
| 53.2 | 2.96 | 4.50 |

The temperature coefficient of (a) wave at pH 2.20 was comparatively less than those of other waves. In acidic and neutral solu-

3) K. Namba and K. Suzuki, *Journal of the Industrial Explosives Society*, Japan, **15**, 171 (1954).

tion, since we obtained reasonable values in the temperature coefficient, the limiting current seems to follow the diffusion law. However, at pH 10.82, as shown in Table II, the above value increases in proportion to temperature, acceleratively, and the limiting current at lower temperature seems to be controlled kinetically. It is easily assumed that a slight decomposition[3] will exist above 45°C through the character of nitroguanidine.

3) **Calculation of the Electron Number for Reduction ($n$).**—We could not find out the proper value of diffusion coefficient of anion such as $\begin{matrix}NH_2\\NH_2\end{matrix}>C=N\cdot COO^-$, whose molecular size and weight are almost similar to those of nitroguanidine. We chose anion of malonamic acid as the most adequate anion as we did in the case of nitrourea[1], the diffusion coefficient of which was estimated to be $9.49\times10^{-6}$ cm$^2$ sec$^{-1}$. The calculated value of $n$ by this method, $n_A$, was 2.64 for the 1st and 2.80 for the 2nd wave at pH 1.65, 3.08 for the 1st and 2.89 for the 2nd wave at pH 5.63 and 4.74 at pH 10.7.

From the application form of Stokes-Einstein's equation[4], by using the value of true density of nitroguanidine which was estimated to be 1.78[5], we obtained $8.55\times10^{-6}$ cm$^2$ sec$^{-1}$ as the $D$ value. The calculated $n_B$ by this method was 2.78 for the 1st and 2.96 for the 2nd wave at pH 1.65, 3.25 for the 1st and 3.20 for the 2nd wave at pH 5.63, and 5.00 at pH 10.7.

The total height of the 1st and 2nd wave in acidic solution is almost constant as was found in Fig. 3. It is also found that the total height in alkaline was less than in acidic. Since the (d) wave shown in Fig. 2 is completely different from the (a), (b), (c), (c') and (d') waves, the reduction mechanism of (d) wave must be considered in another aspect.

From the above results, the calculated $n$ was three for the 1st and 2nd wave at pH 1.65 and 5.63, respectively, and five at pH 10.7.

Assuming the mechanism of reduction of nitroguanidine with three electrons in acidic media, and with five electrons in alkaline media, we must imagine tetrazene compounds such as those shown in the following formula.

In acidic media:

(a) and (c')
$$2NH_2\cdot\overset{NH}{\overset{\ddot{}}{C}}\cdot NH\cdot NO_2+6H^++6e$$
$$=NH_2\cdot\overset{NH}{\overset{\ddot{}}{C}}\cdot NH\cdot N:\underset{\underset{O}{\downarrow}}{N}\cdot NH\cdot\overset{NH}{\overset{\ddot{}}{C}}\cdot NH_2+3H_2O$$

(b) and (d')
$$NH_2\cdot\overset{NH}{\overset{\ddot{}}{C}}\cdot NH\cdot N:\underset{\underset{O}{\downarrow}}{N}\cdot NH\cdot\overset{NH}{\overset{\ddot{}}{C}}\cdot NH_2+6H^++6e$$
$$=2NH_2\cdot\overset{NH}{\overset{\ddot{}}{C}}\cdot NH\cdot NH_2+H_2O$$

In alkaline media:

(d)
$$2NH_2\cdot\overset{NH}{\overset{\ddot{}}{C}}\cdot NH\cdot NO_2+10H^++10e$$
$$=NH_2\cdot\overset{NH}{\overset{\ddot{}}{C}}\cdot NH\cdot N:N\cdot NH\cdot\overset{NH}{\overset{\ddot{}}{C}}\cdot NH_2+4H_2O$$

However, such a tetrazene compound would be too unstable to exist, though one such tetrazene compound, the so-called "Tetracene", prepared by the interaction of aminoguanidine nitrate with natrium nitrite in neutral media, was used as initiators. Further investigation on this problem by another method will be necessary.

## Summary

1) The relationships of pH–$E_{1/2}$ (vs. S.C.E.) and of pH–$i_l$ of nitroguanidine under the dropping mercury electrode were studied.

2) From results about the influence of the effective height of mercury reservior and temperature upon $i_l$, it was found that $i_l$ will follow the diffusion law, and that the Ilkovič equation is applicable in this case.

3) Although the electron number consumed for reduction ($n$) was calculated by assuming a diffusion coefficient these were insufficient in discussion of reduction mechanism. Further investigation will be necessary.

The author wish to express their sincere thanks to Prof. I. Tachi, Mr. M. Suzuki and Mr. S. Koide, Faculty of Agriculture, University of Kyoto, for their kind discussions. The author also express their sincere thanks to Prof. S. Yamamoto, Faculty of Engineering, University of Tokyo, for his encouragement and to Mr. T. Yamashita, Laboratory of Explosives, University of Tokyo, for his suggestion.

*Laboratory of Explosives, Faculty of Engineering, University of Tokyo, Tokyo*

4) I.M. Kolthoff and J.J. Lingane, "Polarography", Interscience Publishers, New York, N. Y., (1952), p. 57.
5) W.C. McCrone, *Anal. Chem.*, **23**, 205 (1951).

# *On the Relation between the Hydrogen Overpotential and the Magnetic Susceptibility of Copper-Nickel Alloys**

By Mitsuru OIKAWA

(Received April 21, 1955)

## Introduction

In the case of the catalytic hydrogen electrode reactions, the present author paid special consideration to the influences of the two chief factors governing the general catalytic reactions, one of which is the so-called "geometric factor" and the other the "electronic factor." About the former the present author and Mukaibo previously discussed[1,2] the experiments on the variation of the slope of the Tafel line due to the steric hindrance caused by the adsorbed organic catalytic poisons.

It is the object of the present paper to explain how the latter-the "electronic factor"-has influences upon the catalytic electrode reaction.

Now, according to Couper and Eley[3] the metal *d*-orbital may be expected to give a stronger bond to a hydrogen atom than an *s*-orbital. On this standpoint, if the recombination process between two hydrogen atoms on the metal surface is the rate determining step of the hydrogen electrode reaction, it is reasonable to assume that the change of the adsorption energy of hydrogen atoms caused by the change of the electronic structure of *d*-band of the metal has a great effect upon the rate of the above reaction.

For this reason we can expect for the series of binary solid solutions containing one of the elements of the eighth group together with one of those of the first group, that the hydrogen overpotential depends largely on the number of holes in the *d*-bands of the alloy.

Since the values of the lattice constants of copper and nickel are very much alike and moreover nickel-copper alloys form a face-centred cubic lattice with no superstructure for any compositions, by selecting such alloys we are able to observe the effect of the "electronic factor" on the hydrogen overpotential without much anxiety about that of the "geometric factor."

## Experimental Procedures

### Hydrogen Overpotential

**Apparatus.**—The cell for the measurement of the hydrogen overpotential was divided into three rooms separated from each other by diaphragms of glass filter. The sample alloy cathode, having an available area of approximately 4.9 $cm^2$, was placed between two auxiliary platinum electrodes in the middle room. Hydrogen purified by passing over heated palladium asbestos was bubbled through the apparatus during measurements for removing air and oxygen. The alloy cathode was attached to the end of a glass tube and could be easily replaced. The tip of a fine capillary tube connected with the reference saturated calomel electrode was kept constantly at 1.0 mm. distance from the test cathode, so as to keep the ohmic fall of voltage involved in the measurement at a given current constant.

**Materials.**—As for the electrolyte normal sulphuric acid, saturated with hydrogen, was used during the experiments, which was produced from G. R. sulphuric acid and redistilled water.

Four nickel-copper alloys, which covered the whole composition range at 15–25% intervals together with the pure metals, were prepared by electrolytically refined nickel and copper; these alloys and the pure metals were rolled into sheets of 0.097 cm. thickness and were annealed at 900°C to remove strain. The Debye Scherrer rings of the needle samples polished out from the alloys were taken and it was observed that the measured lattice parameter-composition relationship does not depart from the Vegard's law appreciably as shown in Fig. 1. This shows the complete homogeneity of the composition of alloys.

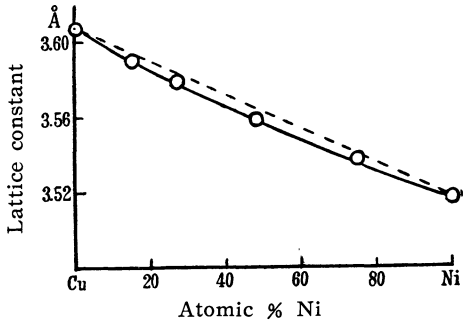



Fig. 1. The lattice constants of nickel copper alloys. (Verification to the Vegards law. ------)

* This paper was read at the discussion meeting of the Chemical Society of Japan and the Electrochemical Society of Japan on November 19, 1954.

1) M. Oikawa and T. Mukaibo, *J. Electrochem. Soc.*, Japan, 20, 568 (1952).

2) T. Mukaibo and M. Oikawa, *Bull. Chem. Soc. Japan*, 26, 524 (1953).

3) Couper and Eley, *Nature*, 164, 578 (1949).

**Procedure.**—It is most important to find a measuring method of the Tafel line which is satisfactorily reproducible. Prior to taking the data the present author tried the following two ways.

(1) The potential, whether constant or not, was measured one minute after the adjustment of the current. This method was rapid but the slope of the obtained Tafel line was rather abnormally large and could not be relied upon.

(2) The cathode was prepolarized at the current density of $1.1\times10^{-4}$ amp./cm$^2$ and continued until a steady potential value was attanined, usually after 1–3 hr. Steady potentials at the higher current densities were then measured within a few minutes after adjustment of current.

In the present work, method (2) was employed and found to give reproducible and reasonable $\eta$-log c.d. plots.

**Thermoelectric Power**

The thermoelectric power of the alloy ribbon cut out from the sample was measured by a student type potentiometer. In each case the test sample was welded to a pure copper wire and the thermal e.m.f. was taken at temperature range between minus 40 to plus 90°C under the basis of a Standard Chromel-Alumel thermocouple.

The two such junctions, the temperatures of which were fixed one at minus 40°C and the other at plus 90°C, were suspended in two glass tubes, one of which was dipped in Dewar's vessel filled up with ethyl alcohol saturated with dry-ice for the cold junction and the other in boiling water for the hot junction.

**Magnetic Susceptibilities**

The magnetic susceptibilities of nickel-copper alloys were determined by the inductance method, —the change of induction of a coil when the test piece was placed in the coil was measured by a flux meter. To eliminate the effect of oxygen, the alloy plates,—the section of which were made 10 mm. × 0.95 mm.—, were previously annealed at 300°C in pure hydrogen, followed by sufficient outgassing at the same temperature.

## Results

**Thermoelectric Power s.**—As shown in Fig. 2. the homogeneity of composition of these nickel-copper alloys was satisfactorily checked by the values of thermoelectric power s. If copper is added to nickel, the positive holes in the *d*-band are partially filled up, consequently the energy density of *d*-electron levels, will rapidly decrease with the increasing composition of copper and as in Fig. 2. s will become larger gradually until about 60 per cent composition of copper is reached, when the positive holes are all full. We should then expect[4] s to drop rapidly to a value comparable with that of copper, as the signs of s for nickel and copper are opposite to each other.

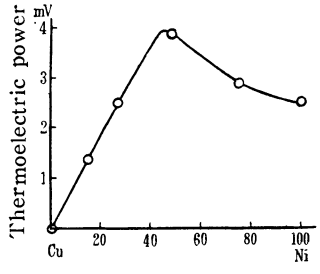



Fig. 2. Thermoelectric power s, in millivolts, of nickel copper alloys, at −40~+95°C, against pure copper.

**Magnetic Susceptibilities of Alloys.**—According to the theory of solid[8] the number of positive holes in the *d*-band of transition metals is equal to the saturation moment in Bohr magnetons. For this reason we are able to represent the number of positive holes by the value of the Bohr magneton. The magnetic susceptibilities of these alloys were obtained by the inductance method and are shown in Fig. 3. The point *x* in Fig. 3.

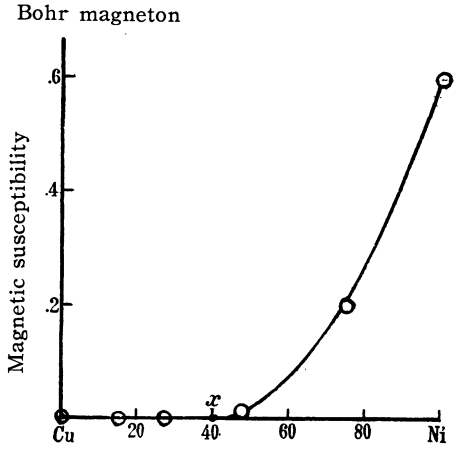



Fig. 3. The quenching of the magnetization of nickel by the addition of copper.

shows the experimental result agreeing with theoretical assumption[8] mentioning that in nickel there are about 9.4 electrons in the *d*-band (giving 0.6 holes, the vacant *d*-orbitals) and 0.6 electrons in the *s*-band. By alloying nickel with approximately 60 atomic per cent. of copper the *d*-band is filled with electrons completely as the copper atom contains one electron more than the nickel atom.

**Overpotential-log (Current Density) Relation.**—1. *Reproducibility*—The mean deviation from the mean value over the whole series of the experiment is ±0.01 V.

4) Mott and Jones, "The theory of the properties of metals and alloys," London, (1936) p. 314.

8) Mott and Jones, "The theory of the properties of metals and alloys," London (1936).

2. The plot of over potential against log (c.d.) is linear for all alloys. The mean value of b, the inclination of Tafel line, is about 0.11 for nickel rich alloys and 0.094 for copper rich alloys. These values and those

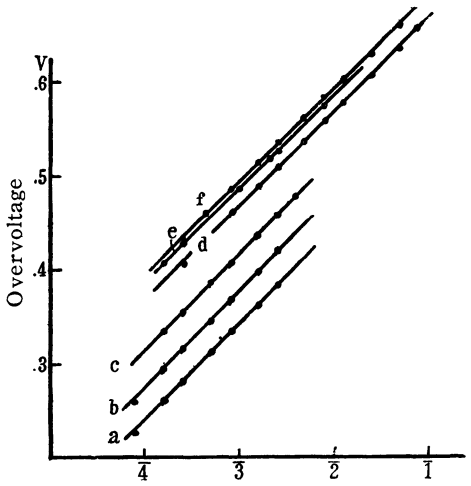



Fig. 4. Hydrogen overpotential on nickel copper alloys in N $H_2SO_4$ solution.
Variation with alloy composition.
a: 100% Ni d: 27% Ni
b: 75% Ni e: 15% Ni
c: 48% Ni f: pure copper

of the Tafel constant a, which were obtained in the present work, almost agree with the results of Hillson[5], Bockris[6] and Wetterholm[7].

## Discussion

In any attempts to apply the theories of solid to catalitic reaction, it is easiest to assume, in the first instance, that the electronic structures of the bulk metal persist unchanged into the surface layer where catalysis occurs.

Now the metal *d*-orbital would be expected to give a stronger bond to a hydrogen atom than an *s*-orbital because of[3] (a) its lower energy, (b) a possible greater overlapping with the *s*-electron of the H-atom. Moreover, according to the simplest Bloch-type picture of metals, which is chiefly due to Mott and Jones[8], it is supposed that in nickel-copper alloys the added copper atom passes its electron into the *d*-band of the nickel, because of the higher density of energy levels in this band, compared with that of the overlapping *s*-band as shown in Fig. 5.

Then, for nickel-copper alloys, we can except that the adsorption energy of the hydrogen

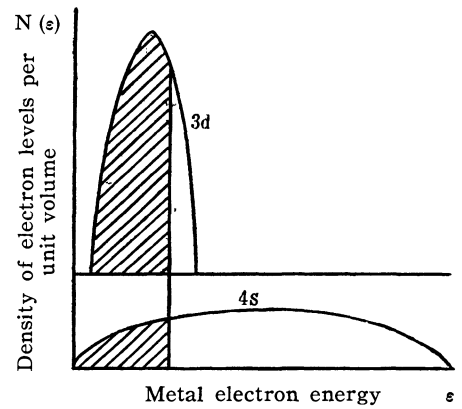



Fig. 5. The energy density of the s- and d-bands in nickel.
The shaded regions represent the levels that are filled by electrons.

atom decreases with the increasing composition of copper. For this reason, in the catalytic hydrogen electrode reaction as in the case of nickel[9], the richer the composition of copper in the alloy becomes the greater becomes the free energy forming the activated complex in the combination reaction between the two hydrogen atoms[10] and so the hydrogen overpotential becomes higher.

Fig. 6. shows the rate of hydrogen electrode

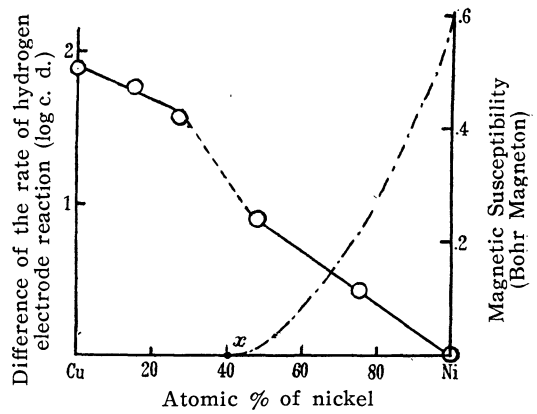



Fig. 6. Rate of hydrogen electrode reaction at the definite hydrogen overpotential, 0.42 volts, as a function of alloy composition.
The broken line (— · — · —) denotes the magnetic susceptibility in Bohr Magneton units.

reaction at the definite hydrogen overpotential, 0.42 volts, as a function of alloy composition. The broken line denotes the feromagnetic susceptibility, or the number of positive holes. As expected, the rate of hydrogen electrode

5) P.J., Hillson, *Trans. Farad. Soc.*, 48, 462 (1952).
6) J.O.M. Bockris, *Trans. Farad. Soc.*, 43, 417 (1947).
7) A. Wetterholm, *Trans. Farad. Soc.*, 45, 861 (1949).
9) J. Horiuti, G. Okamoto and K. Hirota, *Sci. Papers Inst. Phys. Chem. Res.*, (Tokyo), 29, 223 (1936).
10) Glasstone, Laidler and Eyring, "The Theory of Rate Processes," (1941).

reaction decreases with the increasing composition of copper until about 60 atomic per cent. composition of Cu is reached, when the positive holes are all full as denoted by point *x*. Then the reaction velocity approaches abruptly to that of copper as the energy of adsorption falls down to that of pure copper owing to the extinction of positive holes.

## Summary and Conclusion

Experiments were carried out on the relation between the hydrogen overpotential and the electronic structure of nickel-copper alloys.

We can classify these alloys into two groups, depending upon whether or not they contain more nickel than 60 atomic per cent., that is whether they have positive holes or not in their *d*-band.

The hydrogen overpotential of nickel rich alloys (more than 60 atomic percentages of nickel) is rather low because of their small activation energy caused by the large adsorption energy due to the strong bond between metal *d*-orbital and H-atom. For copper rich alloys the hydrogen overpotentials are high and are almost identical owing to the extinction of positive holes.

The author wishes to express his heartfelt thanks to Assistant Prof. T. Mukaibo, Tokyo University, for his kind advice and encouragement.

*Laboratory of Applied Electrochemistry, and Photochemistry, Faculty of Engineering, University of Tokyo, Tokyo*

# *Chemical Studies on Polyuronides. VI.*[1] *On the Mucilage of Nori-utsugi Plant, Hydrangea Paniculata, Sieb.* (*1*)[2]

By Seishi MACHIDA and Mitsumasa INANO

(Received May 6, 1955)

## Introduction

Nori-utsugi (*Hydrangea paniculata*, Sieb.), a species of Saxifragaceae, is a wild shrub growing widely in Japan. It contains a great amount of mucilage in the inner bark. The mucilagenous solution extracted from it with water, like that of the Tororo-aoi plant (*Abelmoschus Manihot*, Medic.), has been commonly used for the traditional paper-marking in Japan from olden times. In some cases the solution is said to have rather better properties than that of the Tororo-aoi plant, since the viscosity of the solution is not so easily decreased by stirring or heating. That is, the solution is suitable for paper-making in summer. These properties are due not only to the dispersing condition or molecular shape of the mucilage in the solution, but also to the chemical structure of the mucilage.

As the mucilage of the Tororo-aoi plant has been chemically studied in detail by the authors[1], the chemical structure of that of the Nori-utsugi plant was studied for purposes of comparison with it.

Formerly, Sawamura[3] found that the mucilage is a kind of polysaccharide, and Hara[4] showed that it is a galactoaraban. Komatsu[5] reported galactose, arabinose and rhamnose among the component sugars.

But the authors presumed that the mucilage is a polyuronide, seeing that the mucilagenous solution has very high viscosity and thread-forming ability even in low concentration. The chemical structure of the polyuronide was also studied.

## Experimental Results and Discussion

**1. Materials.**—The Nori-utsugi plant grown in Funagata-cho, Yamagata Prefecture was employed in the present study.

**2. Crude Mucilage.**—The inner bark (100 g.) stripped from the plant was extracted twice with cold water (1 *l*) for a day; the liquid collected was then filtered through linen. Using a portion of the clear solution, the viscosity was measured by an Ostwald's viscosimeter at 20°C and the re-

1) Part V: S. Machida and N. Uchino, *J. Chem. Soc. Japan*, **74**, 615 (1953). Works on this subject are reviewed by S. Machida and N. Uchino in "A Summary of Chemical Studies on Polyuronides Part I., "*Bull. of the Faculty of Textile Fibers, Kyoto Univ. of Ind. Arts & Text. Fibers*, **1**, 116 (1954), written in English.

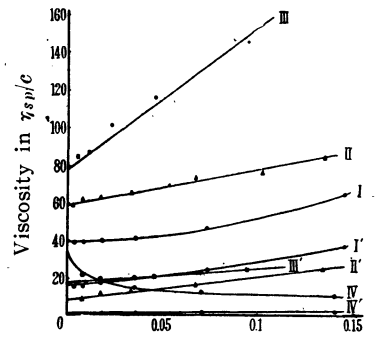
2) Read at the Ordinary Meeting of the Kinki Branch of the Chemical Society of Japan on May29, 1954.

3) M. Sawamura, *J. Chem. Soc. Japan*, **17**, 174 (1896); *Mem. Coll. Agri. Tokyo Imp. Univ.*, **5**, 259 (1902).

4) R. Hara, *Shigyo-zasshi*, **12**, No. 8, p. 1 (1918).

5) S. Komatsu, et al., *Mem. Coll. Sci. Kyoto Imp. Univ.*, **8**, 51 (1925).

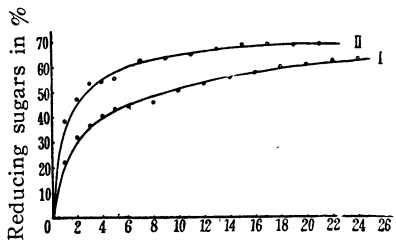
sults were shown in curve I in Fig. 1. The solution remaining was poured into acetone (ca. 2 *l*), and the mucilage, flocculated was filtered, washed by means of acetone, and then ether, and finally dried in vacuo over phosphoric oxide to give a white product of about 30% yield. The mucilage obtained did not reduce Fehling's solution, but gave the strong color reaction for uronic acid with naphthoresorcinol. It contained 12.13% moisture,1 4.85% ash and 0.80% nitrogen. The sample freed from water and ash was shown to contain 49.20% uronic acid lactone by the carbon dioxide evolution method, and to give 25.66 cc./g. acid value titrated with 0.1N NaOH. The viscosity of the solution was shown in curve II in Fig. 1.




Concentration of mucilage in g./100 cc.

Fig. 1. Viscosity of mucilagenous solution.

**3. Acid Hydrolysis.**—With a view to determining the component sugars, the mucilage was heated and hydrolysed with 4% sulfuric acid in a bath of boiling water, and the reducing sugars produced were determined by Bertrand's method from time to time. It was found, as shown in curve I in Fig. 2, that the sugar production reached a maximum after twenty four hours, whose value calculated as glucose was 62.6%. In order to make it hydrolyse in more severe conditions, 8% sulfuric acid was used at the same temperature. The maximum value of reducing sugars in this condition was 68.6%, which was attained after fifteen hours, as shown in curve II in Fig. 2.




Reaction time in hr.

Fig. 2. Hydrolysis of mucilage.
I. 4% $H_2SO_4$ II. 8% $H_2SO_4$

Under these conditions, the uronic acid and pentose produced seemed to be further decomposed to some extent, since furfural was detected in the hydrolysate by the test with aniline-acetic acid paper. The fact that the maximum value of the sugar content was at most within about 69%, suggests the presence of linkage not being apt to hydrolyse in the polysaccharide molecule. The reaction was stopped, and the hydrolysate solution was filtered from the remaining substance. The filtrate was neutralised with barium hydroxide, filtered, evaporated to a small volume and poured into methanol. The precipitate was filtered, redissolved in water, filtered through an active carbon layer several times, evaporated again in reduced pressure to a small volume and added to methanol. The precipitate was again purified by reprecipitation with methanol and finally dried. The white powder obtained reduced Fehling's solution in the hot state and gave a beautiful color reaction of uronic acid with naphthoresorcinol. (Found: Ba 26.05%. $(C_6H_9O_7)_2Ba$ requires Ba 26.24%). With cinchonine, the free acid gave a white crystal, m.p. 178°C, alone or mixed with authentic cinchonine salt of D-galacturonic acid; and by oxidizing with nitric acid, it gave crystals of mucic acid, m.p. and mixed m.p. 213°C. These facts indicate that the uronic acid obtained is D-galacturonic acid.

The methanol solution of the hydrolysate which was removed from the precipitated barium uronate by filtration was concentrated in vacuum to a syrup. The syrup was dissolved in water, de-ionised by Amberlite resin IR-4B and IR-120, and again concentrated. The mixture of sugars was separated into its components on a sheet of Toyo-Roshi No. 50 filter-paper by partition chromatography and the use of a mixture of phenol (80%) and water (20%) as the solvent and aniline hydrogen-phthalate as the spraying reagent. As the constant value of $R_f$ was not strictly expected due to some inconvenience of the experimental apparatus used, the value of $R_{GI}$ of the unknown sample was estimated by comparison with that of the known sample tested at the same time in each experiment. The sugars detected were galactose ($R_{GI}$ 1.07), arabinose ($R_{GI}$ 1.36) and rhamnose ($R_{GI}$ 1.48), where the known samples were galactose ($R_{GI}$ 1.10), arabinose ($R_{GI}$ 1.36) and rhamnose ($R_{GI}$ 1.50).

From these results, it was found that the mucilage was a polyuronide composed of arabinose, galactose, rhamnose, and D-galacturonic acid.

**4. The purified Mucilage.**—From the mucilagenous solution appeared, however, on standing for several days a deposit, which might be composed of impurities. As in the case of the mucilage of the Tororo-aoi plant[1], the supernatant solution removed from the precipitates was expected to contain a polyuronide, which was the essential part of the mucilage of the Nori-utsugi plant. The purified polyuronide was obtained by adding the supernatant solution to a large volume of acetone. It contained 9.37% moisture, 7.42% ash; and the sample freed from water and ash was found to contain 52.32% uronic acid lactone.

The component sugars besides D-galacturonic acid were shown by paper chromatography of the hydrolysate to be galactose ($R_{GI}$ 1.10) and rhamnose ($R_{GI}$ 1.48), which procedure was the same as that mentioned above. Arabinose was not found;

perhaps the linkage between arabinose and the skeleton in the mucilage molecule is so weak that it is apt to auto-hydrolyse and liberate[6].

The viscosity of the solution of the purified mucilage was very high, as shown in curve III in Fig. 1. The data showed that the more the impurity is removed from the mucilage, the more viscous the solution becomes.

**5. The degraded Mucilage.**—As the solution of the purified mucilage was too viscous to handle, a conventient method was devised to purify the polyuronide, disregarding some degradation. The extracted mucilagenous solution (ca. 10 *l*) was heated at 120–125°C in an autoclave. As the viscosity of the solution decreased to a constant value within about two hours, the solution was filtered from the precipitate and added to a saturated solution of copper sulfate. The precipitate was filtered and soaked in a quantity of ethanol containing a few drops of hydrochloric acid. The ethanol solution was renewed until the copper ion was eliminated, and the mucilage was washed with absolute alcohol and ether to eliminate the chlorine ion, and dried.

The degraded mucilage thus obtained was a white amorphous powder (yield ca. 32 g.). Analysis showed that it contained 4.64% moisture and 0.25% ash; the sample freed from water and ash contained 58.92% uronic acid lactone, and gave 34.42 cc./g. of acid value titrated with 0.1N-NaOH. The component sugars besides galacturonic acid were shown by paper chromatography to be galactose ($R_{GI}$ 1.07) and rhamnose ($R_{GI}$ 1.48). A very faint red spot ($R_{GI}$ 1.34?) was found with difficulty, which might be due to a trace of arabinose which still remained.

The degraded polyuronide was comparatively too hard to be dissolved in water, and owing to the degradation, the solution was found to have fairly low viscosity, as shown in curve IV in Fig. 1. The degraded polyuronide, however, is considered to represent the main molecular structure of the mucilage. It is further noticeable that curve IV indicates the characteristic feature of linear polyelectrolyte[7], which did not appear in the other curves. It may be explained on the basis of the presence of ionized carboxyl groups along the molecular chains. When sodium chloride was added to the mucilagenous solution, the viscosity decreased markedly and an almost linear curve was obtained. This is shown in the curves in Fig. 1, where I', II', III' and IV' indicate the addition of 1% sodium chloride to I, II, III and IV respectively. The essential part of the mucilage of the Nori-utsugi plant is, therefore, a polyuronide composed of galactose, rhamnose and D-galacturonic acid. In the crude solution, the properties of polyelectrolyte are perhaps interfered with some factors, for example metallic ion, and the viscosity curve of the crude solution gives a straight line.

**6. Composition of Mucilage.**—Then the quantitative relation between the component sugars in the polyuronide was determined. Boiling the purified mucilage with 12% hydrochloric acid solution gives rise to furfural and methyl furfural; the former is due to galacturonic acid and the latter to rhamnose, and both are precipitated as mixed phloroglucides. The amount of furfural-phloroglucide is calculated from the galacturonic acid content determined by the carbon dioxide evolution method. The quantity of furfural-phloroglucide is deducted from the total amounts of the mixed phloroglucides, and the amount of methyl furfural-phloroglucide is found, from which the rhamnose content of the mucilage is calculated. The glactose content is also directly found. The results thus obtained are shown in Table I.

TABLE I

COMPOSITION OF MUCILAGE

| Sample (water, ash free) | Total phloroglucide (g) | Furfural-phloroglucide (g) | Methyl furfural-phloroglucide (g) | Rhamnose (g) | Rhamnose (%) | Galactose (%) | Galacturonic acid (%) |
|---|---|---|---|---|---|---|---|
| 0.2123 | 0.0615 | 0.0465 | 0.0150 | 0.0274 | 12.92 | 34.76 | 52.32 |
| 0.2198 | 0.0639 | 0.0481 | 0.0158 | 0.0284 | | | |

It was found from these results that the essential part of the mucilage is a polyuronide composed of D-galacturonic acid, galactose and rhamnose in the molar ratio of 10:7:3; that is, the molecular formula is $[(C_6H_8O_6)_{10}\cdot(C_6H_{10}O_5)_7\cdot(C_6H_{10}O_4)_3]_x$. And the crude mucilage as it was extracted from the inner bark, is considered to have such a structure that the polyuronide skeleton is combined with some arabinose residues by some comparatively weaker linkages.

## Summary

1. The mucilage of the inner bark of the Nori-utsugi plant (*Hydrangea paniculata*, Sieb.) was found to be composed of arabinose, galactose, rhamnose and D-galacturonic acid.

2. When the crude mucilagenous solution had stood for several days, a deposit appeared which might be composed of impurities. The purified mucilage was obtained from the supernatant clear solution. The purified mucilage was a polyuronide composed of galactose, rhamnose and galacturonic acid and it was considered to be the essential part of the mucilage.

6) E.L. Hirst, E.G.V. Percival and C.B. Wylam, *J. Chem. Soc.*, **1954**, 189.

7) H. Staudinger, "Die Hochmoleculare Organische Verbindungen", S. 1344 (1932); Wo. Panli. L. Sternbach, *Helv. Chim. Acta*, **24**, 317 (1941); S. Machida, N. Uchino, *J. Chem. Soc. Japan*, **74**, 183 (1953).

3. Degraded mucilage was obtained by heating the crude mucilagenous solution at 120–125°C in an autoclave. It had the same component sugars as the purified mucilage, and represented the main structure of the mucilage.

4. The essential part of the mucilage was a polyuronide composed of D-galacturonic acid, galactose and rhamnose in the molar ratio of 10 : 7 : 3; that is, the molecular formula is $[(C_6H_8O_6)_{10}\cdot(C_6H_{10}O_5)_7\cdot(C_6H_{10}O_4)_3]_x$

5. The solution of the degraded mucilage exhibited the typical electroviscous behavior of polyelectrolyte.

The expense of this study was defrayed in part by a grant from the Hattori Hōkōkai, to which the author's thanks are due.

*Chemical Laboratory of Textile Fibers, Kyoto University of Industrial Arts and Textile Fibers, Kyoto*

# *Studies on A.C. Polarography. V. Theory of Reversible Wave**

By Mitsugi SENDA and Isamu TACHI

(Received May 18, 1955)

## Introduction

Recently Breyer and Hacobian[1] have developed an equation of the reversible polarographic wave. Their treatment, however, referred to the stationary state of the electrode process when a small sinusoidal alternating potential is superimposed upon the constant potential applied to the electrode. Grahame[2] has also shown the change of faradaic admittance against the applied constant potential, in which, however, Nernst's diffusion layer was assumed for the diffusion process of reactants.

In the first paper of this series[3] a general equation for the electrolytic current in a.c. electrolysis has been mathematically deduced. In the present paper an approximate solution of the general equation will be given for the case of the reversible redox-system, in which the electrode process at the transitionary state is also taken into account, and not only Breyer's polarogram but also Fournier's polarogram will be theoretically derived.

## Reversibility in A.C. Polarography

When an alternating voltage, $\Delta Ep(wt+\theta)$, is superimposed upon the constant voltage, $E$, applied to the steady plane electrode, the resulting current, $i$, is, after proper rearrangements, given as follows[3];

$$\frac{i}{nFq}=\phi(t)=\varphi_0(\xi)$$

$$=\varphi_1(\xi)+\varphi_2(\xi)\frac{1}{\sqrt{\omega}}\int_0^{\xi}\frac{\varphi_2(\xi)}{\sqrt{\pi(\xi-\eta)}}d\eta, \quad (1)$$

where the functions $\varphi_1(\xi)$ and $\varphi_2(\xi)$ are shown by

$$\varphi_1(\xi)=k_s\Big[f_O{}^*C_O\exp\Big\{-\frac{\alpha nF}{RT}(-E_0+E+\Delta Ep(\xi+\theta))\Big\}-f_R{}^*C_R\exp\Big\{\frac{(1-\alpha)nF}{RT}\times(-E_0+E+\Delta Ep(\xi+\theta))\Big\}\Big],$$

$$\varphi_2(\xi)=k_s\Big(\frac{f_O}{\sqrt{D_O}}\Big)^{1-\alpha}\Big(\frac{f_R}{\sqrt{D_R}}\Big)^{\alpha}\Big[\exp\Big\{\frac{-\alpha nF}{RT}\times(-E_{1/2}+E+\Delta Ep(\xi+\theta))\Big\}+\exp\Big\{\frac{(1-\alpha)nF}{RT}(-E_{1/2}+E+\Delta Ep(\xi+\theta)\Big\}\Big],$$

and $wt$ is transformed to $\xi$ by the equation,

$$wt=\xi. \quad (2)$$

In these equations $\Delta E$ is the amplitude of alternating voltage and $p(wt+\theta)$ is an arbituary periodic function, in which $w$ is the angular velocity, $t$ the time and $\theta$ the phase angle; $^*C$ is the concentration of reactant in the bulk solution, $f$ the activity coefficient, $D$ the diffusion coefficent, $n$ the number of

* A part of this paper was read at the 7th Annual Meeting of the Chemical Society of Japan, held in Tokyo on April 3, 1954.

1) B. Breyer and S. Hacobian, *Australian J. Chem.*, 7, 225 (1954).

2) D. C. Grahame, *J. electrochem. Soc.*, 99, 370C (1952).

3) I. Tachi and T. Kambara, This Bulletin, 28, 25 (1955).

faradays of electricity required per mole of the electron exchange reaction, $k_s$ the rate constant at the standard potential, $\alpha$ the transfer coefficient of forward reaction, and the suffixed $O$ and $R$ are referred to oxidized and reduced form, respectively. $F$, $R$, and $T$ are employed in the usual sense. $q$ is the surface area of electrode. $E_{1/2}$ is the half-wave potential of the reversible polarographic wave and is related to the standard potential, $E_o$, by the equation;

$$E_{1/2}=E_o+\frac{RT}{nF}\ln\frac{f_O\sqrt{D_R}}{f_R\sqrt{D_O}}$$

In deriving the above theoretical equation it was assumed that the electrolysis is carried out in the presence of excess amounts of supporting electrolytes, so that the depolarisers move exclusively by diffusion and the potential drop (ohmic and diffusion) in the solution is negligibly small. This condition also allows us to assume that the activity coefficient remains practically unchanged in the solution and that practically all of the potential drop between electrode and solution is limited to the Helmholz double layer, because the diffused electrical double layer is compressed.

For the greater value of $k_s$ eq. (1) can be transformed to a more convenient form[4];

$$\varphi_0(\xi)=g_0(\xi)-\lambda\frac{d}{d\xi}\int_0^\xi\frac{\varphi_0(\eta)}{\sqrt{\pi(\xi-\eta)}}\frac{1}{e^{\alpha\varepsilon}+e^{-(1-\alpha)\varepsilon}}d\eta, \tag{4}$$

where

$$\lambda=\sqrt{w}/k_s\left(\frac{f_O}{\sqrt{D_O}}\right)^{1-\alpha}\left(\frac{f_R}{\sqrt{D_R}}\right)^{\alpha}, \tag{5}$$

$$\varepsilon=\frac{nF}{RT}(E_{1/2}-E-\Delta Ep(\eta+\theta)),$$

and the function $g_0(\xi)$ is given by

$$g_0(\xi)=\sqrt{w}\frac{d}{d\xi}\int_0^\xi\frac{1}{\sqrt{\pi(\xi-\eta)}}[i_c(\eta+\theta)-i_a(\eta+\theta)]d\eta, \tag{6}$$

$$i_c(\eta+\theta)=\frac{1}{2}\sqrt{D_O}{}^*C_O(1+\tanh\frac{1}{2}\epsilon),$$

$$i_a(\eta+\theta)=\frac{1}{2}\sqrt{D_R}{}^*C_R(1-\tanh\frac{1}{2}\epsilon).$$

The integral equation (4) can be solved by the method of successive substitution and it is seen that

$$\varphi_0(\xi)=g_0(\xi)+\sum_{j=1}^{\infty}(-1)^j\lambda^j g_j(\xi), \tag{7}$$

where

$$g_j(\xi)=\frac{d}{d\xi}\int_0^\xi\frac{1}{\sqrt{\pi(\xi-\eta)}}\frac{g_{j-1}(\eta)}{e^{\alpha\varepsilon}+e^{-(1-\alpha)\varepsilon}}d\eta.$$

4) H. Matsuda, *Z. Elektrochem.*, in press.

When $$\lambda\ll 1, \tag{8}$$

the solution (7) is approximately reduced to

$$\varphi_0(\xi)\simeq g_0(\xi), \tag{9}$$

which is also derived when Peters' formula is assumed to be held at the interface of electrode[3] and should be called an equation for the reversible a.c. polarographic current. Thus it is seen that the parameter $\lambda$ defined by eq. (5) governs the a.c. polarographic behaviour of the redox-system and determines its characteristics whether it is reversible or not under the above stated conditions.

## Reversible Wave

For the sake of simplicity it is assumed that $^*C_R=0$, e.g., $i_a(\eta+\theta)=0$, in the following deduction. Thus from eqs. (6) and (9) the equation for the reversible a.c. polarographic current is rewritten as follows;

$$[\varphi_0(\xi)]_{rev.}=\sqrt{w}\frac{d}{d\xi}\int_0^\xi\frac{1}{\sqrt{\pi(\xi-\eta)}}i_c(\eta+\theta)d\eta$$

$$=\frac{\sqrt{w}}{\sqrt{\pi\xi}}i_c(\theta)-\int_\xi^\infty\frac{1}{\sqrt{\pi(\xi-\eta)}}\frac{d}{d\eta}i_c(\eta+\theta)d\eta$$

$$+\int_0^\infty\frac{1}{\sqrt{\pi(\xi-\eta)}}\frac{d}{d\eta}i_c(\eta+\theta)d\eta. \tag{10}$$

The third term in the right hand of this equation corresponds to the electrode process after a sufficiently long time has elapsed and should be called the stationary term. On the other hand the first term and the second should be called the transitionary term. The function $i_c(\eta+\theta)$ defined in the preceding section can always be developed in the Fourier series;

$$i_c(\eta+\theta)=\frac{a_0}{2}+\sum_{n=1}^{\infty}(a_n\cos[n(\eta+\theta)]+b_n\sin[n(\eta+\theta)]), \tag{11}$$

where

$$\frac{a_0}{2}=\frac{1}{2\pi}\int_0^{2\pi}i_c(\eta+\theta)d\eta,$$

$$a_n=\frac{1}{\pi}\int_0^{2\pi}i_c(\eta)\cos n\eta\,d\eta,$$

$$b_n=\frac{1}{\pi}\int_0^{2\pi}i_c(\eta)\sin n\eta\,d\eta.$$

Inserting this series into the above equation, (10), and using the well known formula;

$$\int_0^\infty\frac{1}{\sqrt{\pi(\xi-\eta)}}\begin{bmatrix}\sin\\ \cos\end{bmatrix}n\eta\,d\eta=\frac{1}{\sqrt{n}}\begin{bmatrix}\sin\\ \cos\end{bmatrix}\left(n\xi-\frac{\pi}{4}\right),$$

we obtain the stationary term, $\varphi_s(\xi)$, which corresponds to the a.c. component defined in Part I of this series[3], e.g.

$$\varphi_s(\xi)=\sqrt{w}\sum_{n=1}^{\infty}\left(\sqrt{n}a_n\cos\left[n(\xi+\theta)+\frac{\pi}{4}\right]+\sqrt{n}b_n\sin\left[n(\xi+\theta)+\frac{\pi}{4}\right]\right). \quad (12)$$

Upon employing the following approximate formula;

$$\int_{\xi}^{\infty}\frac{1}{\sqrt{\pi n}}\begin{bmatrix}\sin\\ \cos\end{bmatrix}n\eta\,d\eta\simeq\frac{1}{n\sqrt{\pi\xi}}\begin{bmatrix}\cos\\ -\sin\end{bmatrix}n\xi, \quad (13)$$

the transitionary term, $\varphi_t(\xi)$, which corresponds to the d.c. component defined in the first paper of this series[3], is given by

$$\varphi_t(\xi)\simeq\frac{\sqrt{w}}{\sqrt{\pi\xi}}-\frac{a_0}{2}. \quad (14)$$

It is easily shown that the approximate formula (13) is held in the errors less than 1%, when $\xi$ is greater than $4\pi$ or

$$t>\frac{2\pi}{w}=\frac{2}{\nu}, \quad (\nu:\ cycle/sec). \quad (15)$$

Thus the electrolytic current is given by the sum of a.c. and d.c. components. In practice, however, owing to the electric double layer present at the electrode interface, an alternating current will flow, which should be called capacity or base current. The double layer can be regarded as a constant capacitor when the amplitude of applied alternating potential does not exceed 30 mV.[5]. Thus by retransforming $\xi$ to $wt$ by Eq. (2) the total current is given by

$$[i]_{rev.}=nFq[\phi(t)]_{rev.}\simeq i_{a\cdot c.}+i_{a\cdot c.}+i_B,$$

where

$$i_{a\cdot c.}=nFq\varphi_s(wt),$$
$$i_{a\cdot c.}=nFq\varphi_t(wt),$$
$$i_B=wC_Dq\Delta E_p\left(wt+\theta+\frac{\pi}{2}\right).$$

The functions $\varphi_s(wt)$ and $\varphi_t(wt)$ are defined by eqs. (12) and (14). $i_B$ is the base current, where $C_D$ is the differential capacity of the double layer.

## Fournier's and Breyer's Polarograms

The above theoretical conclusion is derived with the assumption that the electrode is plane and the medium through which the depolarisers move, stays still. However, these results may be applied to the theoretical analysis of the electrode process at the dropping mercury electrode as a first approximation. At the dropping mercury electrode the surface area of the electrode, $q$, is given by[6]

$$q=4\pi\left(\frac{3m}{4\pi d}\right)^{2/3}t^{2/3},$$

where $m$ is the weight of mercury flowing out of the capillary per unit time, and $d$ the density of mercury. Accordingly Eq. (14) is a good approximation for the theoretical analysis of the electrode process at the dropping electrode, because the surface area of the mercury drop is very small at the beginning of the electrolysis and the mean value of the electrolytic current during each drop is observed. Usually it is also safe to assume that $q$ remains almost constant during each cycle of the alternating current. Accordingly the d.c. component, $i_{a\cdot c.}$, in Eq. (16) corresponds to Fournier's current, e.g., the mean value of the total electrolytic current. Furthermore it is possible by use of the so called Stackelberg's integral equation[7] to take into consideration the effect of expansion of the mercury drop. Thus the equation of reversible Fournier's polarogram[8] is given by

$$I_F=\frac{1}{\tau}\int_0^{\tau}\sqrt{\frac{7}{3}}i_{a\cdot c.}dt, \quad (18)$$

where $\tau$ is the drop time. From Eqs. (6), (11), (14), (16) and (17) it is seen that

$$I_F=\bar{i}_d\frac{1}{2\pi}\int_0^{2\pi}\frac{1}{2}\left[1+\tanh\frac{nF}{2RT}(E_{1/2}-E-\Delta E_p(\eta+\theta))\right]d\eta, \quad (19)$$

in which $\bar{i}_d$ is the polarographic limiting diffusion current originally derived by Ilkovic[9] and is given by

$$\bar{i}_d=\frac{24}{7}\left(\frac{7}{3\pi}\right)^{1/2}nFD_0^{1/2*}C_0\left(\frac{3m}{4\pi d}\right)^{2/3}\tau^{1/6}.$$

Since the condition that $\frac{1}{\tau}\ll\nu$ is satisfied in the usual experiments, it is easy to separate the a.c. component from the d.c. component by use of a current detector with proper frequency response. Thus is obtained Breyer's polarogram[10], which shows the change of the magnitude of a.c. component against the applied constant potential. From Eqs. (12), (16) and (17) the mean value of effective value of $i_{a\cdot c.}$ during each drop is given by

5) D.C. Grahame, *J. Amer. Chem. Soc.*, 68, 301 (1946).
6) I. Tachi, "Polarography", Iwanami Book Co., Tokyo (1954), p. 76.
7) M.v. Stackelberg, *Z. Elektrochem.*, 45, 466 (1939).
8) M. Fournier, *Compt Rend.* 232, 1673 (1951).
9) D. Ilkovic, *Coll. Czech. Chem. Communs.*, 8, 13 (1936).
10) B. Breyer, F. Gutmann and S. Hacobian, *Australian J. Sci. Research* A3 558, 567, 595 (1951); B. Breyer and S. Hacobian, ibid. 604, 610 (1951).

$$[I_{A\cdot C\cdot}]_{eff}=nF\frac{12}{5}\pi\left(\frac{3m}{4\pi d}\right)^{2/3}\tau^{2/3}\sqrt{\frac{w}{2}\sum_{n=1}^{\infty}(na_n^2+nb_n^2)}\ , \qquad (20)$$

where $a_n$ and $b_n$ are defined in Eq. (11).

## A.C. Polarography with Sinusoidal Alternating Potential

When the applied voltage is given by

$$V=E+\Delta E\sin(wt+\theta),$$

the function $i_c(\eta+\theta)$ is demonstrated by

$$i_c(\eta+\theta)=\frac{1}{2}\sqrt{D_0}^*C_0[1+\tanh\frac{nF}{2RT}(E_{1/2}-E-\Delta E\sin(\eta+\theta))] \qquad (21)$$

It is difficult to develop this function in the Fourier series. When the amplitude is so small that $-\beta=\frac{nF}{2RT}\Delta E$ is less than unity, however, this function is approximately expressed by the following series;

$$i_c(\eta+\theta)\simeq j_c(\eta+\theta)=\frac{A_0}{2}+B_1\sin[\eta+\theta]+A_2\cos[2(\eta+\theta)]+B_3\sin[3(n+\theta)]+A_4\cos[4(\eta+\theta)]+\cdots\cdots, \qquad (22)$$

where

$$\frac{A_0}{2}=j_0+\frac{1}{4}\beta^2j_2+\frac{3}{8}\cdot\frac{1}{4!}\beta^4j_4+\cdots\cdots,$$

$$B_1=\beta j_1+\frac{3}{4}\cdot\frac{1}{3!}\beta^3j_3+\cdots\cdots,$$

$$A_2=-\frac{1}{4}\beta^2j_2-\frac{1}{2}\cdot\frac{1}{4!}\beta^4j_4\cdots\cdots,$$

$$B_3=-\frac{1}{4}\cdot\frac{1}{3!}\beta^3j_3\cdots\cdots,$$

$$A_4=\frac{1}{8}\cdot\frac{1}{4!}\beta^4j_4+\cdots\cdots,$$

and

$$j_0=\left[\frac{1}{2}\sqrt{D_0}^*C_0(1+\tanh(-x))\right]_{x=-nF(E_{1/2}-E)/2RT}$$

$$j_1=\left[\frac{dj_0}{dx}\right]_{x=-nF(E_{1/2}+E)/2RT}$$

$$j_2=\left[\frac{d^2j_0}{dx}\right]_{x=-nF(E_{1/2}-E)/2RT},\cdots\cdots$$

It must be noted here that if we write $\bar{i}_d$ in place of $\sqrt{D_0}^*C_0$ in the above equation, the function $j_0$ coincides with the equation of reversible wave in classic polarography and $j_1$, $j_2$,……correspond to the first, second,…… derivative curve of it, respectively. From these equations being combined with Eqs. (12), (14) and (16) the electrolytic current is given by

$$j_{a\cdot c\cdot}=nFq\sqrt{w}\left\{B_1\sin\left[wt+\theta+\frac{\pi}{4}\right]+\sqrt{2}A_2\left[2(wt+\theta)+\frac{\pi}{4}\right]\right\}+\sqrt{3}B_3\left[3(wt+\theta)+\frac{\pi}{4}\right]+\cdots\cdots \qquad (23)$$

and

$$j_{a\cdot c\cdot}=nFq\sqrt{\frac{1}{\pi t}}\cdot\frac{A_0}{2} \qquad (24)$$

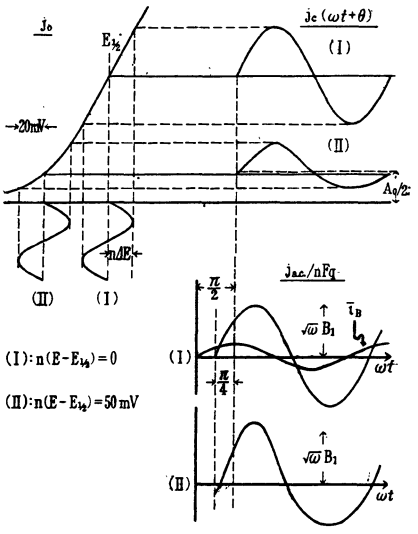



Fig. 1.

respectively. In Fig. 1 are illustrated the functions $j_0$, $j_c(wt+\theta)$, $j_{a\cdot c\cdot}/nFq$, and $A_0/2$ for the two values of applied constant potential, e.g. $E=E_{1/2}$ and $E=E_{1/2}+50/n\ mV$. At the half-wave potential the value of $A_0/2$ or $a_0/2$ agrees with that of $j_0$, which is always true for any type of alternating voltage being employed. When the amplitude is so small that $-\beta\ll1$, the a.c. component is approximately expressed by

$$j_{a\cdot c\cdot}\simeq nFq\sqrt{w}\frac{nF}{4RT}\Delta E\left(\sqrt{D_0}^*C_0+\sqrt{D_R}^*C_R\right)\times\cosh^{-2}\left[\frac{nF}{2RT}(E_{1/2}-E)\right]\sin\left(wt+\theta+\frac{\pi}{4}\right), \qquad (25)$$

in which the presence of reduced form is also taken into account. A similar result was reported by Breyer and Hacobian[1]. The-

value of Eq. (25) at the half-wave potential was also mathematically derived by Delahay and Adams[11]. Thus Breyer's polarogram coincides with the derivative curve of classical polarogram with respect to the applied constant potential when the amplitude is sufficiently small, but it begins to deviate from the derivative curve with increasing value of the amplitude as is expected from Eq. (23). Eq. (25) shows that the electrode interface is electrically equivalent to the series combination of Resistor, $R$, and capacitor $C$, which are given by

$$R=\frac{1}{wC}=\frac{1}{q}\frac{2\sqrt{2}}{(\sqrt{D_O}^*C_O+\sqrt{D_R}^*C_R)}\frac{RT}{n^2F^2}\frac{1}{\sqrt{w}}\left[\cosh^2\left[\frac{nF}{2RT}(E_{1/2}-E)\right]\right]$$

This is a more generalized expression for the faradaic impedance of reversible electrode interface[2] at the equilibrium d.c. potential

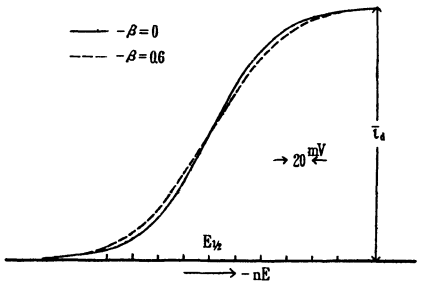



Fig. 2.

originally derived by Randles[12], Ershler[13] and Gerisher[14].

In Fig. 2 are shown the classical polarogram and Fournier's polarogram, which were calculated by substituting Eq. (24) in Eq. (18), when the amplitude is $30\,n\ mV$.

The theoretical conclusion described in this paper shows a good agreement with the experimental results given in the previous papers of this series[15] and of other investigators[10,16,17]. More detailed comparison with them will be given in the succeeding papers.

## Summary

The electrolytic current due to the superposition of an alternating potential upon a constant potential applied to the electrode is approximately derived for the case of reversible reaction. The parameter which determines the reversibility of the a.c. electrolysis is also given. Using the above derived results, the instateneous electrolytic current as well as current-voltage curves of reversible Breyer's and Fournier's polarogram are shown.

*Department of Agricultural Chemistry, Faculty of Agriculture, Kyoto University, Kyoto*

11) P. Delahay and T.J. Adams, *J. Amer. Chem. Soc.*, 74, 5740 (1952).

12) J. E. B. Randles, *Discuss Faraday Soc.*, 1, 11 (1947).

13) H. Ershler, ibid., 269.

14) H. Gerisher, *Z. physik. Chem.*, 198, 286 (1951).

15) M. Okuda and I. Tachi, This Bulletin, 28, 37 (1955).

16) E. Niki, *Study of Polarography*, 1, No. 4 p. 27 (1954).

17) J. van Cakenberghe, *Bull. Soc. chim. belge*, 60. 3 (1951).

# *On the Main Chemical Components dissolved in the Adjacent Waters to the Aleutian Islands in the North Pacific**

By Rinnosuke FUKAI and Fumiko SHIOKAWA

(Received May 23, 1955)

## Introduction

The authors have studied the main components dissolved in the sea water collected in the region adjacent to the Aleutian Islands. The chemical components dealt with in this paper are chloride, sulfate, sodium, magnesium, calcium and potassium ions.

Since Dittmar[1] reported the composition of oceanic salt obtained from various regions of the world, it has been well known that the abundance ratios between main ions dissolved in sea water are in good agreement for any locality of the whole ocean. Nevertheless, it has been also known that there are some exceptional cases where slight dis-

* Contribution B-No. 208 from the Tokai Regional Fisheries Research Laboratory, Tokyo, Japan.

1) W. Dittmar, "Challenger Report, Physics and Chemistry", Vol. 1 (1884).

agreement is found due to local circumstances such as inflow of a large river or explosion of a submarine volcano. At the present step of chemical oceanography, it is to such a local difference in the main dissolved components that attention has been called.

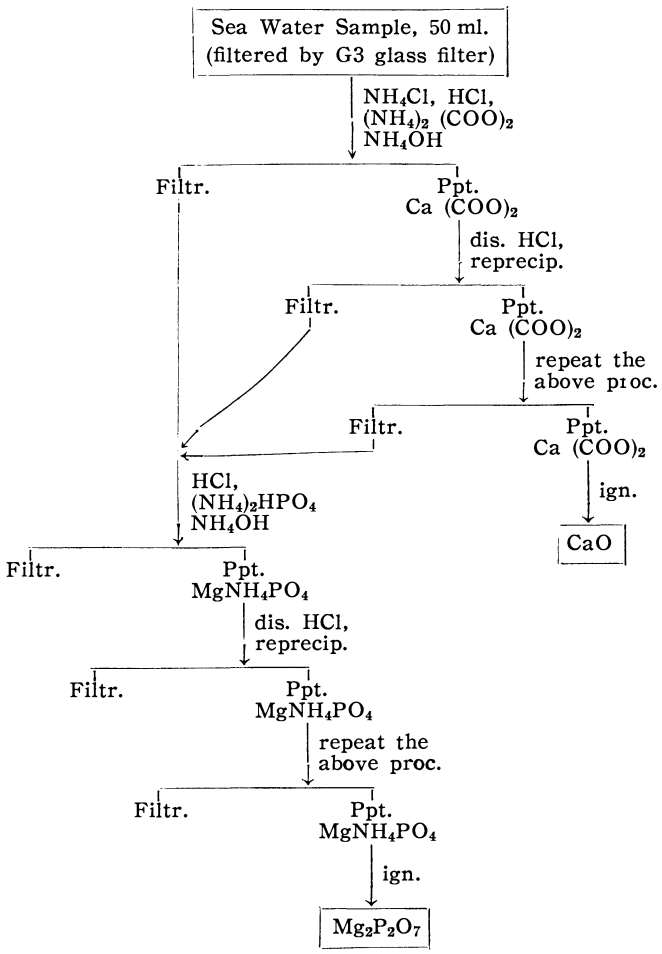
The region under study is located in the north end of the North Pacific, as shown in Fig. 1 of the previous report[2], being under the effect of polar conditions. In this paper, the authors mainly examined whether or not the ratios between the main components in the waters of this region show any difference when compared with those in other regions. Investigations concerning the subject in the region under study have scarcely been carried out except in the case of that made by Ratomanov et al[3], which seems to involve some results to be reexamined.

## Samples and Analytical Methods

As mentioned in the previous report, a marked minimum of water temperature is found in the region in question at a depth of about 100 m. It may accordingly be expected that the deviations from the normal values of the ratios between the main dissolved components presumably would be centered at the depth, if the deviations should be caused by freezing or other phenomena relating to low temperature. For this reason the following samples were selected from those collected in the areas under study, the Bering Sea area and the North Pacific area, keeping the above view in mind. They are respectively water samples from the surface layer (10–25 m.), the temperature minimum layer (75–100 m.) and the deep layer (about 1000 m.) in each area. Each sample was prepared by mixing equally water samples collected at several stations situated in the same area. In addition to these, two surface water samples were analyzed, one of which was

TABLE I

SCHEMES OF SEPARATION PROCEDURES FOR CALCIUM AND MAGNESIUM

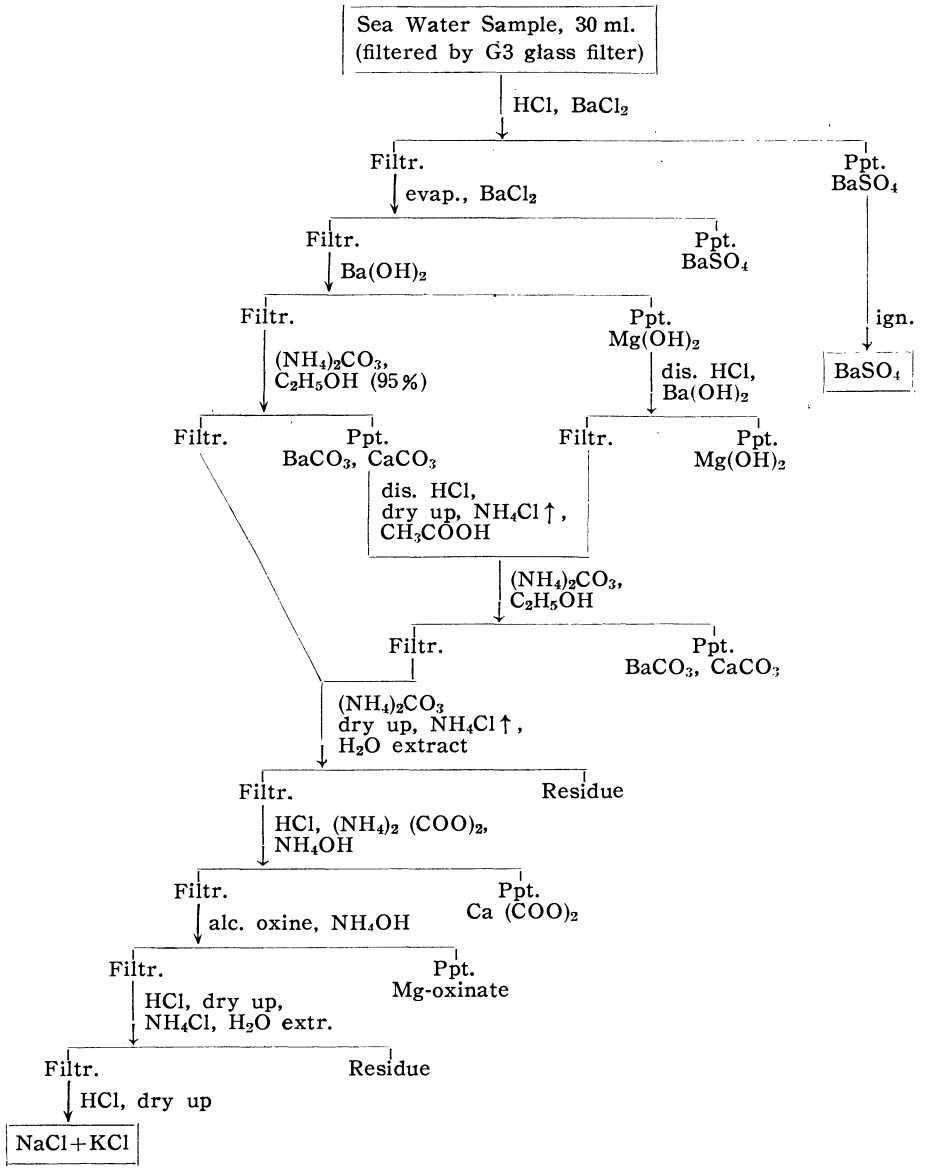



2) R. Fukai, This Bulletin, 27, 402 (1954).

3) C.E. Ratomanov et al, "Research of the Sea", Vol. 2, Moscow, 1936 (in Russian with English summary).

TABLE II

SCHEMES OF SEPARATION PROCEDURES FOR SULFATE, SODIUM AND POTASSIUM




obtained in the vicinity of an island and the other at Station 24 (just above Bowers Bank where upwelling was taking place).

Gravimetric methods of analysis have been adopted for all components except for chlorine determination. Ordinary procedures have been followed so that strict comparison with former data can be made. Outlines of procedures are shown schematically in Tables I and II. Accidental errors have been avoided by means of checking analyses from time to time on artificial sea water containing known quantities of each component.

Total amounts of alkali metals were determined as chlorides and potassium was precipitated by

TABLE III

PERCHLORATE METHOD FOR SEPARATION OF ALKALI METALS COMPARED WITH CHLOROPLATINATE METHOD

| Method | | K mg. (added) | K mg. (found) Perchlorate | K mg. (found) Chloroplatinate |
|---|---|---|---|---|
| KCl | solution | 13.04 | 13.03 | 13.30 |
| | | 〃 | 12.77 | 13.03 |
| KCl+NaCl | solution | 13.04 | 13.21 | 13.34 |
| | | 〃 | 13.18 | |

added NaCl: 842 mg.

perchloric acid instead of chloroplatinic acid. No significant difference was recognized between the values obtained by these two different methods as shown in Table III.

## Results and Discussion

Analyses have been carried out two or three times for each sample and the averaged values obtained are given in Table IV in terms of ratios to chlorinity.

TABLE IV

RESULTS OF ANALYSES IN TERMS OF RATIOS TO CHLORINITY

| Location and Depth | Cl ‰ | $SO_4$ | Na | K | Mg | Ca |
|---|---|---|---|---|---|---|
| Aleutian Region | | | | | | |
| Bering Sea Area | | | | | | |
| surface | 18.38 | 0.14054 | 0.5554 | 0.02090 | 0.06625 | 0.02137 |
| temp. min. 100 m. | 18.51 | .13853 | .5544 | .02087 | .06601 | .02113 |
| deep 1000 m. | 19.11 | .13963 | .5529 | .02011 | .06675 | .02136 |
| N. of Semisopochnoi I. (surface) | 18.43 | 0.13957 | 0.5587 | 0.02082 | 0.06580 | 0.02183 |
| S. of Amatignak I. | 18.04 | 0.14010 | 0.5570 | 0.02171 | 0.06623 | 0.02181 |
| North Pacific Area | | | | | | |
| surface | 18.41 | 0.14048 | 0.5572 | 0.02055 | 0.06687 | 0.02172 |
| temp. min. 100 m. | 18.45 | .13918 | .5512 | .02174 | .06648 | .02135 |
| deep 1000 m. | 19.17 | .13937 | — | — | .06632 | .02171 |
| Average | 18.56 | 0.13968 | 0.5553 | 0.02096 | 0.06632 | 0.02154 |
| Kuroshio Region | | | | | | |
| Average 33° 50'N 139° 45'E | 19.32 | 0.13993 | 0.5561 | 0.02125 | 0.06627 | 0.02128 |
| Rejection limit (level of sign. =0.05) | | ±0.00147 | ±0.0081 | ±0.00125 | ±0.00113 | ±0.00052 |

In Table IV are included also the averaged values for the Kuroshio region calculated from the results of the analyses carried out six times by the present authors. On the basis of the six values, rejection limits were computed for each component. Regarding the limits as a measure, no significant difference is found between the samples collected from the Aleutian region. However, systematic deviations from averaged values are noticed even within the limits. For example, the sulfate as well as sodium in the layer of temperature minimum are lower than each averaged value, both in the Bering Sea area and the Pacific area.

The fact may suggest that a small amount of sodium sulfate has been removed from the sea water by some process. Quantitatively, there is a considerable gap between the equivalents of sulfate and sodium depleted in the sample obtained from the Pacific area, while the equivalents in the Bering Sea area are in the same order, namely 0.44 and 0.66 milli-equivalents for sulfate and sodium, respectively. This may relate to the fact that microcrystals of sodium sulfate are deposited in lattices of ice crystal, upon being removed from sea water, when sea water is frozen in a refrigerator[4].

On the other hand, the tendency of relative increase in sulfate is recognized in the surface layer, suggesting the effect of dilution by melting ice.

Although the mechanism of the change in relative abundance of the dissolved components may be complicated, it may qualitatively be explained as follows. When sea water is cooled from the surface until it forms ice, the sea water should be separated into two phases, namely solid ice phase occluding a smaller amount of salts and a liquid phase containing a concentrated amount of salts. At this time the relative concentration of sodium and sulfate ions in the solid phase may occur. Owing to the concentration of salts in the liquid phase by the separation of the ice phase, the density of the sea water under the ice layer may increase and sink downward by convection process, until the balance of density will be acquired. Thus, the temperature minimum layer having lesser concentration of sodium and sulfate ions may be formed. On the other hand, when the ice is melted, water may have lower density remaining in the surface layer, thus, the relative concentration of sodium and sulfate ions may result.

In Table V the values obtained by the present authors for the Aleutian and Kuroshio regions were compared with those obtained by previous workers for various regions[5].

4) G.J. Lewis and T.G. Thompson, *Jour. Mar. Res.*, 9, 211 (1950); K.H. Nelson and T.G. Thompson, *Jour. Mar. Res.*, 13, 166 (1954).

5) T.G. Thompson and R.J. Robinson, "Geophysics of the Earth, V, Oceanography, Chemistry of the Sea" (1932).

TABLE V
AUTHORS' RESULTS COMPARED WITH OTHER DATA OBTAINED BY VARIOUS INVESTIGATORS

| Author | Lyman & Fleming (1940) | Thompson & Robinson (1932) | Miyake (1939) | Ratomanov et al. (1936) | Fukai & Shiokawa (1954) | |
|---|---|---|---|---|---|---|
| Location | Average | North Pacific | Kuroshio | Bering Sea | Kuroshio | Aleutian |
| $SO_4$ | 0.1394 | 0.1396 | 0.1397 | 0.1398 | 0.1399 | 0.1397 |
| Na | 0.5556 | 0.5495 | 0.5497 | 0.5533 | 0.5561 | 0.5553 |
| K | 0.0200 | 0.0191 | 0.0191 | 0.0187 | 0.0213 | 0.0210 |
| Mg | 0.06695 | 0.06694 | 0.0676 | 0.0659 | 0.06627 | 0.06632 |
| Ca | 0.02106 | 0.02150 | 0.02155 | 0.02277 | 0.02128 | 0.02154 |

The values for calcium in the table have been corrected for strontium on the basis of the value determined by Lyman and Fleming[6], although the strontium determination has not been carried out by the present authors.

Ratomanov mainly referred to Dittmar's values and stated that calcium, sodium and sulfate were higher as shown by the percentage of total salt, while magnesium and potassium were lower in the Bering Sea. However, these characteristics have not been revealed from the results of the present authors' analyses.

The results obtained by the present authors seem to be in close agreement with those obtained by previous authors both in the Aleutian and Kuroshio regions except for the higher potassium values. The cause of these systematic higher values for potassium is not obvious.

Whereas Miyake[7] pointed out that magnesium in the Kuroshio region was higher, the authors' result shows a rather lower value.

The facts mentioned above may indicate that the mixing of water masses is prevailing in the Aleutian region as a part of the oceanic circulation of the Pacific. Nevertheless, it should be noted that slight deviation from the normal composition may appear.

It has been open to doubt whether the results of freezing experiments of sea water in a laboratory can be applied to the interpretation of natural conditions[8]. As a conclusion, the possibility of change in relative abundance of dissolved components of sea water by natural freezing should be suggested.

6) J. Lyman and R.H. Fleming, *Jour. Mar. Res.*, 3, 134 (1940).
7) Y. Miyake, This Bulletin, 14, 29 (1939).
8) H.U. Sverdrup, M.W. Johnson and R.H. Fleming, "The Oceans, their physics, chemistry and general biology", Prentice-Hall, INC., New York, 1952, P. 219.

## Summary

The authors carried out the analyses of the main dissolved components of sea water on the samples collected from the Aleutian region in order to examine the local characteristics of the region under study. At the same time the samples collected from the Kuroshio region were analysed to check the systematic errors introduced. The results were expressed in terms of ratios to chlorinity.

As a result, the following conclusions have been deduced.

1. The relative decrease in sulfate and sodium equivalents was recognized on the samples collected from the layer of temperature minimum. This seems to relate to freezing phenomena of sea water.
2. A tendency of sulfate increase in the surface samples was noticed.
3. Averaged values for the Aleutian region were in close agreement with those for the Kuroshio region, both having been obtained by the present authors. The values also coincided with those obtained by other workers, except for higher potassium values.

These facts may indicate that although the water masses existing in the Aleutian region are, on the whole, a portion of the oceanic circulation of the Pacific, a slight deviation from the normal composition appears in the main components in some characteristic layers.

*Tokai Regional Fisheries Research Laboratory, Tokyo*

# *Tin (II)-Strong Phosphoric Acid. A New Reagent for the Determination of Sulfate by Reduction to Hydrogen Sulfide*

By Toshiyasu KIBA, Tomoo TAKAGI, Yooko YOSHIMURA and Ikuko KISHI

(Received July 22, 1955)

Although a number of methods for the determination of sulfate by reduction to hydrogen sulfide have previously been worked out[1], these methods are substantially based on dry heating[2] or fusion[3] of the sulfate-containing substances with adequate reductants. It has long been desired to develop a new method by which soluble or insoluble sulfate can be reduced to hydrogen sulfide in solution with simple treatment and apparatus. E. Rancke-Madsen[4] gives a procedure for the determination of sulfate by reduction to hydrogen sulfide in a mixture of tin (II)-chloride and phosphoric acid. By checking the method according to his procedure the present authors proved that the method can be applied only when the sulfate is present as sodium salt and moreover when the evolved hydrogen chloride on the reduction markedly acidifies the absorbing solution of zinc acetate and acetic acid, over the optimum range of pH that is adopted for zinc sulfide precipitation. C. M. Johnson and H. Nishita[5] reduced sulfates and organic sulfur compounds with a reducing mixture composed of hydroiodic acid, formic acid, and red phosphorus at a temperature of 115°C., and they determined the sulfur in plant materials, soils, and irrigation waters. However the reagents used in the method are not easily obtainable without accompanying impurity of sulfates and sulfur, especially for the purpose of micro-determination of sulfur.

In this laboratory for the last four years strong phosphoric acid has been used as a very excellent reaction medium for many analytical purposes, and the new methods for the determination of elementary carbon[6], oxidation value of organic compounds[7], and nitrogen in organic compounds[8,9], using a strong oxidizing action of potassium iodate in the medium have been already reported. The revealed fact that the strong phosphoric acid scarcely participates in the reaction carried on in it may also be utilized to the reduction by adding an adequate reductant in the medium. A new reagent for the reduction of sulfate to hydrogen sulfide was prepared by adding tin(II)-chloride into the strong phosphoric acid and boiling the mixture to expel the evolved hydrogen chloride perfectly. Very viscous and slightly turbid liquid thus obtained, named "Tin(II)-Strong Phosphoric Acid", can be stored in a desiccator of calcium chloride with slight decrease of reducing power for several months and be used as a conspicuous decomposing and reducing agent by heating above 120°C. for the determination of soluble and insoluble sulfates. In the following a method will be described in which the sulfate is determined by reduction to hydrogen sulfide with the above reagent, including details of preparation of the reagent and construction of apparatus.

## Apparatus

The set-up used for the preparation of the strong phosphoric acid and the tin(II)-strong phosphoric acid is illustrated in Fig. 1. For the critical purpose it is profitable to use a flask of fused silica instead of hard glass. A glass tube E plays as an outlet of water vapor in the preparation of strong phosphoric acid and as an inlet of carbon dioxide in the case of the preparation of tin (II)-strong phosphoric acid.

In Fig. 2 the apparatus for the reduction of sulfate and absorption of the evolved hydrogen sulfide is given as the assembly. All of these are hand-made in addition to Kipp's apparatus for production of carbon dioxide. Into the reaction vessel A, a gas-inlet B and a thermometer D, which is covered with a thermometer-protecting tube C, are inserted. These tubes are attached to the reaction vessel with suitable rubber tube as shown in Fig. 2.

## Reagents

**Strong Phosphoric Acid.**—Three hundred gram of commercial orthophosphoric acid of extra pure chemical grade (d=1.7) is placed in a flask in Fig. 1, and dehydrated by heating on a hot plate D, until a thermometer dipped in the liquid

1 A. Kurtenacker, "Analytische Chemie der Sauerstoffsäuren des Schwefels." Stattgart, (1938).
2) Y. Oka and T. Kanno, *J. Chem. Soc. Japan (Pure Chem. Sect.)* **72**, 161 (1951).
3) K. Bruger, *Angew. Chem.*, **54**, 479 (1941).
4) E. Rancke-Madsen, *Acta. Chim. Scand.*, **3**, 773 (1949); **6**, 305 (1952).
5) C.M. Johnson and H, Nishita, *Anal. Chem.*, **24**, 736 (1952).
6) T. Kiba et al., *Japan Analyst*, **2**, 446 (1953).
7) S. Ohashi, This Bulletin, **28**, 171 (1955).
8) S. Ohashi, ibid, **28**, 177 (1955).
9) S. Ohashi, ibid, **28**, 537 (1955).

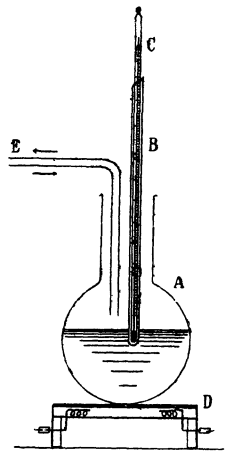



Fig. 1. Apparatus for the preparation of strong phosphoric acid and tin (II)-strong phosphoric acid.

A: Round bottom flask of 400 ml.
B: Thermometer-protecting tube.
C: Thermometer of 360°C.
D: Electric hot plate.
E: Glass tube.

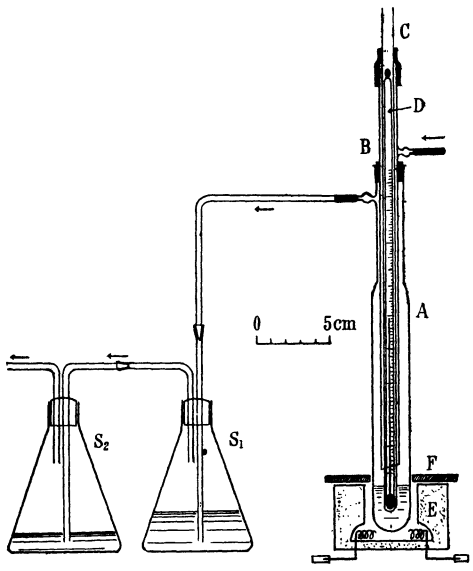



Fig. 2. Apparatus for reduction of sulfate and absorption of the evolved hydrogen sulfide.

A: Reaction vessel.
B: Gass-introducing tube.
C: Thermometer-protecting tube.
D: Thermometer.
E: Electric heater.
F: Asbestos plates·
$S_1$: Absorbing flask.
$S_2$: Absorbing flask.

shows 300°C. During the heating evaporated water vapor and mist of phosphoric acid should be rapidly removed from the liquid surface through a glass tube E which is connected to a suction pump. This makes the time for the evaporation shorter and contamination brought from the components of the glass smaller. The very viscous liquid thus obtained, strong phosphoric acid, is stored in a desiccator.

**Tin(II)-Strong Phosphoric Acid.**—Using the same apparatus shown in Fig. 1 tin(II)-strong phosphoric acid is prepared as follows. Twenty to eighty grams of crystals of tin(II)-chloride dihydrate of extra pure chemical grade, the amout of which is dependent upon that of sulfate to be analyzed, is placed in a flask A and covered with 200 g. of strong phosphoric acid obtained above. Introducing purified carbon dioxide from a Kipp's apparatus through a tube B, the content is gently heated to 300°C. Hydrogen chloride gas is evolved by the reaction and sometimes brownish color appears in the liquid. The color may be caused by the formation of tin(II)-sulfide, because a small quantities of sulfate which has been contained originally in commercial phosphoric acid as impurity or comes from the glass wares during the reaction are all reduced to hydrogen sulfide. In this case the temperature should be kept at 300°C. till the color disappears. The contents should be cooled under continuous passing of carbon dioxide. The obtained tin(II)-strong phosphoric acid can be stored in a desiccator of calcium chloride for several months.

**Zinc Acetate Solution.**—Dissolve 40 g. of zinc acetate dihydrate in distilled water of 100 ml. and add 30 ml. of gracial acetic acid,and dilute to 1 liter.

**Iodine, 0.02N.** Standardized accurately by ordinary procedure.

**Sodium Thiosulfate, 0.02N.** Standardized accurately.

**Various Sulfates Samples.** An aliquot from solution of a definite volume in which a known amount of sulfate has been dissolved, and a weighed sample of insoluble sulfate as barium sulfate are both used. The amounts of the sulfate ion in the sample were estimated gravimetrically as comparable standards.

## Procedure

Pipet accurately an aliquot from solution of sulfate as it contains 5 to 20 mg. of sulfate ion, or weigh 10 to 25 mg. of barium sulfate into the reaction vessel A in Fig. 2. The solution should be evaporated to dryness at the bottom of the vessel. From a buret pour about 6 to 10 ml. of tin(II)-strong phosphoric acid in the vessel; then connect all of the apparatus as shown in Fig. 2. In the absorbing flasks zinc acetate-acetic acid solution was previously added as 40 ml. in $S_1$ and 20 ml. in $S_2$. Pass carbon dioxide very rapidly through the apparatus for five minutes. The passage of the gas should be rapid enough to cause strong agitation of the surface of the liquid in the absorbing flasks. At the end of five minutes reduce the flow of carbon dioxide to a rate of 120 bubbles per minute in the absorbing flask. Gently heat the bottom of the reaction vessel A on a small electric heater E. Gas begins

to evolve from the bottom of the vessel when the temperature reaches 120°C. Continue the heating till it reaches 300°C. for about fifteen minutes, and then stop the heating. Carbon dioxide should be passed continuously through the apparatus to carry away the evolved hydrogen sulfide completely. Disconnect the absorbing flask from the side arm of the reaction vessel, add quickly 20 ml. of 0.02N iodine solution to the absorbing flask through the inlet tube, and swirl to mix thoroughly. Because some zinc sulfide may cling to the inlet tube of the absorbing flask, keep this tube in the absorbing flask when treating with the reagent. Back titrate the excess of iodine with 0.02N sodium thiosulfate solution using starch as indicator. The whole determination can be carried out in one hour. Further some blank tests are run by adding no sulfate. 1 ml. of 0.02N iodine consumed corresponds to 0.9607 mg. of $SO_4$, 0.3408 mg. of $H_2S$, and 0.3206 mg. of S, respectively.

## Results and Discussion

**Composition of Tin(II)-Strong Phosphoric Acid.**—Though the reagent has a remarkable reducing power, it is questionable from what component the reducing power occurs. In consequence of the reaction between tin(II)-chloride and strong phosphoric acid, not only stannous ion but phosphorous acid as well as hypophosphorous acid may be existing in the reagent. In order to estimate the composition of the tin(II)-strong phosphoric acid, the following experiment was carried out. A definite volume of tin(II)-strong phosphoric acid that has been prepared from 200 g. of strong phosphoric acid and 20 g. of tin(II)-chloride was weighed and dissolved in an adequate volume of 1.5N hydrochloric acid, and then titrated rapidly with 0.1N iodine solution using starch as indicator. The required volume of the iodine solution may correspond to the amount of stannous ion in the solution. The titrated solution was followed by the determination of phosphorous acid and hypophosphorous acid according to the method of E. H. Swift[10], in which each of them is estimated separately by iodometric titration at the different pH. The consumed volume of 0.1N iodine solution by each component of stannous ion, phosphorous acid, and hypophosphorous acid are tabulated in Table I. This indicates that the reducing power of the tin(II)-strong phosphoric acid is most attributed to stannous ion in it.

**Stability of Tin(II)-Strong Phosphoric Acid.**—Because tin(II)-strong phosphoric acid has an excellent reducing power only above the temperature of 120°C., it may be considered as a very convenient reductant from the point of view of its storage. The decrease

10) E.H. Swift, *Anal. Chem.*, 25, 1272 (1953).

Table I

Consumed volume of 0.1N iodine solution by three components of reductant in tin(II)-strong phosphoric acid (for 1.4915 g. of the acid)

| No. | 0.1N Iodine Consumed. ml. | | |
|---|---|---|---|
| | $Sn^{++}$ | $H_3PO_3$ | $H_3PO_2$ |
| 1 | 10.73 | 2.51 | 1.05 |
| 2 | 10.72 | 0.13 | 3.09 |
| 3 | 10.34 | 0.16 | 0.44 |

of the reducing power during standing at the room temperature of about 30°C. was estimated as a consumable volume of 0.02 N iodine solution by a definite volume of hydrochloric acid solution of 0.1 g. of tin(II)-strong phosphoric acid. For an example on 29th July, 1954, 4.65 ml. of the iodine solution was required and on 1st September, 4.07 ml., so the decrease rate of the reducing power is computed as 10% in a month but smaller in the cold.

**Determinable Amount of Sulfate.**—The recovery of sulfate as hydrogen sulfide by this method might be dependent upon both of the amounts of sulfate to be analyzed and that of tin(II)-strong phosphoric acid used as the reductant. To estimate the optimum range of quantitative recovery of sulfate the following experiments were carried out. Taking various aliquots from the working standard solution which contains 1 mg. of $SO_4$ in 1.00 ml. as sodium sulfate, the determination was worked for each of them using 6 and 10 ml. of tin (II)-strong phosphoric acid that has been prepared from 200 g. of strong phosphoric acid and 50 g. of stannous chloride dihydrate. The recovery of sulfate of various amount is illustrated in Fig. 3, in which the

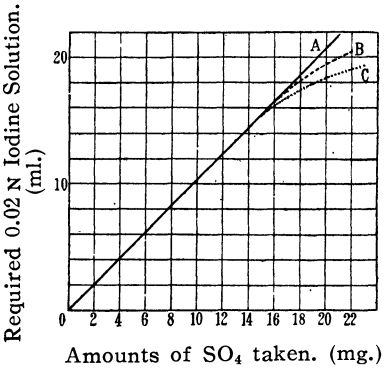



Fig. 3. Range of quantitative recovery of sulfate, using tin (II)-strong phosphoric acid prepared from 200 g. of strong phosphoric acid and 50 g. of $SnCl_2 \cdot 2H_2O$.
A: Theoretical.
B: Using 10 ml. of the reagent.
C: Using 6 ml. of the reagent.

ordinate indicates the values of 0.02N iodine solution required for titration of evolved hydrogen sulfide in ml. and the abscissa mg. of sulfate ion taken. In both cases the optimum range for the quantitative recovery of sulfate covers from 0 to 15 mg. of sulfate ion, so the substances to be analyzed should be taken as the amount of its sulfate ion which falls within the above range. The range will be extended to a larger amount of sulfate when we can prepare the tin(II)-strong phosphoric acid which contains a larger quantity of stannous ion. The problem is now being unraveled in the laboratory.

**Analytical Applications.**—Analyses of various sulfates were made with this method. These results are summarized in Table II.

TABLE II

DETERMINATION OF VARIOUS SULFATES

| Substance | Sample Weight mg. | $SO_4$ Content mg. | 0.02 N Iodine Required ml. | $SO_4$ Found mg. |
|---|---|---|---|---|
| | 10.41 | 7.03 | 7.30 | 7.01 |
| Sodium | 5.20 | 3.51 | 3.64 | 3.50 |
| sulfate | 9.94 | 6.71 | 6.96 | 6.69 |
| $Na_2SO_4$ | 9.94 | 6.71 | 6.96 | 6.69 |
| | 9.94 | 6.71 | 7.06 | 6.78 |
| Alum | 25.73 | 10.42 | 10.88 | 10.45 |
| KAl | 〃 | 〃 | 10.82 | 10.40 |
| $(SO_4)_2$· | 〃 | 〃 | 10.78 | 10.36 |
| $12H_2O$ | 〃 | 〃 | 10.87 | 10.44 |
| Chrome | | | | |
| alum | 26.00 | 10.00 | 10.48 | 10.07 |
| KCr | 〃 | 〃 | 10.49 | 10.08 |
| $(SO_4)_2$· | 〃 | 〃 | 10.49 | 10.08 |
| $12H_2O$ | | | | |
| | 31.22 | 10.43 | 10.86 | 10.43 |
| Zinc | 〃 | 〃 | 10.80 | 10.38 |
| sulfate | 33.37 | 11.15 | 11.15 | 11.09 |
| $ZnSO_4 \cdot 7H_2O$ | 〃 | 〃 | 11.15 | 11.09 |
| | 62.44 | 20.86 | 21.69 | 20.84 |
| Magnesium | 30.52 | 12.46 | 12.22 | 11.74 |
| sulfate | 〃 | 〃 | 12.21 | 11.73 |
| $MgSO_4$· | 〃 | 〃 | 12.24 | 11.76 |
| $7H_2O$ | | | | |
| Barium | 12.12 | 4.98 | 5.13 | 4.94 |
| sulfate | 23.20 | 9.55 | 9.73 | 9.35 |
| $BaSO_4$ | 24.70 | 10.16 | 9.70 | 9.32 |

Each of the weighed samples of sodium sulfate, alum, chrome alum, zinc sulfate, and magnesium sulfate was dissolved in water of a constant volume and pipetted into the reaction vessel as an aliquot of the solution. The pipetted solution in the vessel was evaporated to dryness and allowed to be analyzed. On the other hand, the content of sulfate ion in each of the solutions had been determined gravimetrically as barium sulfate as usual. As an example of insoluble sulfates, barium sulfate was analyzed by this method. The sample was weighed accurately using a micro-balance and allowed to be analyzed in the reaction vessel directly. The precision and accuracy of the data were subject to slight fluctuations with the kind of sulfate, but the errors rested within that of the usual gravimetric method. Further determinations were also carried out on other sulfates, like cupric sulfate and that of the second group metals, but the results were so much worse than those in Table II that only half of the sulfate ion could be reduced. The investigation on this fact and its cause is now being done in the laboratory. In the near future we will be able to report a more consummate method adoptable for all sulfates.

## Summary

A new reagent, "Tin(II)-Strong Phosphoric Acid", has been prepared to permit a rapid and simple determination of sulfates by reducing to hydrogen sulfide. The reagent is stable at a room temperature but reacts violently above 120°C. Evolved hydrogen sulfide after the reaction with this reagent is absorbed in zinc acetate-acetic acid solution and titrated iodometrically as usual. 1 ml. of 0.02N iodine solution corresponds to 0.9607 mg. of sulfate ion. The apparatus for the preparation of the reagent and reduction of sulfate are illustrated. The determination of sulfur in various sulfates was carried out by this method and satisfactory results were obtained. Moreover, it seems to be an advantage of this method that solid samples can be treated directly in the reaction vessel.

The expense of the present research has been paid in part by a Grant for Scientific Research from the Ministry of Education.

*Department of Chemistry, Faculty of Science, Kanazawa University, Kanazawa*

# *Rapid Determination of Sulfur in Organic Compounds by the Tin(II)-Strong Phosphoric Acid Reduction Method*

By Shigeru OHASHI

(Received July 22, 1955)

Sulfur in organic compounds is usually determined by the Pregl, the Carius, or the fusion method. In all these methods sulfur in organic compounds is oxidized to sulfate by the dry or wet combustion method and then commonly estimated gravimetrically as barium sulfate. In other cases for the determination of sulfate formed by combustion, various volumetric or colorimetric methods have been described. Since all these methods are composed of two step procedures, i.e. the decomposition of samples and the estimation of sulfate, they require patient time and skilful technique. Recently the new methods based on a reduction with metallic potassium[1] or lithium[2] have been reported on the determination of organic sulfur, but they are not yet generally accepted.

In this laboratory for the last four years strong phosphoric acid has been used as a very excellent reaction medium for many analytical purposes, and the new methods for the determination of elementary carbon[3], oxidation value of organic compounds[4], and nitrogen in organic compounds[5,6] using a strong oxidizing action of iodic acid in this medium have been already investigated. Recently in this laboratory it was also found that tin(II)-strong phosphoric acid has such a strong reducing action that sulfates can be quantitatively reduced to hydrogen sulfide by heating with it. By means of this reaction, sulfates can be very rapidly and simply determined volumetrically[7].

The present study has been carried out with the purpose of establishing a new rapid method for the determination of sulfur in organic compounds by means of this new reducing agent, tin(II)-strong phosphoric acid.

In this method sulfur in organic compounds is reduced to hydrogen sulfide by heating with the tin(II)-strong phosphoric acid reagent in the stream of carbon dioxide, and absorbed into zinc acetate solution. After the above reaction, by adding the definite amount of iodine solution into the absorbent solution and titrating the excess iodine with a standard solution of sodium thiosulfate, the sulfur is volumetrically determined. The procedure mentioned above in outline is for convenience called "Procedure A".

Since the sulfur contained in the compounds such as methylorange or cystine is easily reducible, it can be readily determined by the Procedure A. But the sulfur in the compounds such as thiourea or methionine can not be directly reduced by tin(II)-strong phosphoric acid. In such a case, after oxidizing the combined sulfur to sulfate or sulfonate by heating with chromium(VI)-strong phosphoric acid, the sulfur should be reduced to hydrogen sulfide by treating with tin(II)-strong phosphoric acid. This procedure is called "Procedure B". Chromium(VI)-strong phosphoric acid is also a new strong oxidizing agent which has been found in the author's laboratory.

## Apparatus

The apparatus used in this study is shown in Fig. 1. It is composed of two parts, a reaction vessel A and an absorption vessel B. The vessel A is closed at the top by means of a rubber stopper R, through which a gas-introducing tube and a thermometer-protecting tube are inserted. Both tubes are connected with a rubber tube T. In the middle of the vessel A, there is a constricted part above which a small glass lock is set to protect it against the backstream of gas. As at high temperature strong phosphoric acid has a strikingly corrosive action against glass, the bottom glass of the vessel A, after being used many times, will become thin and be broken at last. Therefore, when it becomes thin to a certain extent, it should be thicken by heating with a gas burner.

The absorption vessel B is composed of three 100 ml. Erlenmeyer flasks which are connected to each other with glass tubes and rubber tubes. The first flask is a guard one and the second and third are absorption flasks.

## Reagents

*Strong Phosphoric Acid.*—Extra pure grade 89% orthophosphoric acid was dehydrated by heating until the temperature of the liquid reaches 300°C.

1) W. Zimmermann, *Microchemie ver. Microchim. Acta*, 40, 162 (1952).
2) M. Vecera, *Chem. Listy*, 48, 613 (1954).
3) T. Kiba, S. Ohashi, T. Takagi and Y. Hirose, *Japan Analyst*, 2, 446 (1953).
4) S. Ohashi, This Bulletin, 28, 171 (1955).
5) S. Ohashi, ibid., 28, 177 (1955).
6) S. Ohashi, ibid., 28, 537 (1955).
7) T. Kiba, T. Takagi, Y. Yoshimura and I. Kishi, ibid., 28, 641 (1955).

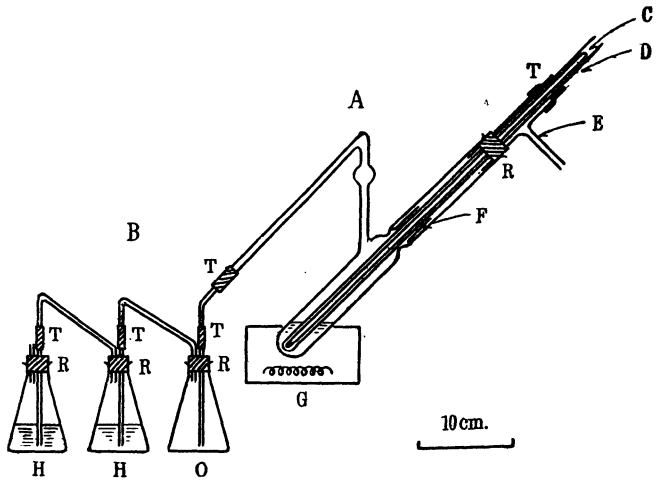



Fig. 1. Apparatus

A: Reaction Vessel
B: Absorption Vessel
C: Thermometer
D: Thermometer-Protecting Tube
E: Gas-Introducing Tube
F: Glass Lock
G: Electric Heater
H: Absorption Flasks
R: Rubber Stoppers
T: Rubber Tubes
O: Guard Flask

Its specific gravity was about 1.93[8].

*Tin(II)-Strong Phosphoric Acid.*—In a flask 20 g. of extra pure grade tin(II) chloride dihydrate was dissolved in 200 g. of strong phosphoric acid prepared as mentioned above and the mixture was heated at 300°C in the stream of carbon dioxide. By means of this treatment not only hydrogen chloride in the mixture was expelled, but also the trace of sulfur contained in tin(II) chloride was removed. The tin(II)-strong phosphoric acid thus prepared was stocked in a 100 ml. buret, which had an anhydrous calcium chloride-filled guard tube at the upper end, because strong phosphoric acid is very hygroscopic.

*Chromium(VI)-Strong Phosphoric Acid.*—In a beaker 15 g. of extra pure grade potassium dichromate was dissolved in 200 g. of strong phosphoric acid by heating on a water bath. This reagent was also stocked in the same manner as in the case of the tin(II)-strong phosphoric acid reagent.

*Zinc Acetate Solution.*—In about 200 ml. of water 40 g. of zinc acetate dihydrate and 30 ml. of glacial acetic acid were dissolved and the solution was diluted to 1 liter.

*Iodine Solution.*—About 0.02 N iodine solution prepared from iodine and potassium iodide was standardized against a 0.02 N standard solution of sodium arsenite.

*Sodium Thiosulfate Solution.*—About 0.02 N sodium thiosulfate solution was standardized against the above-mentioned 0.02 N iodine solution.

*Carbon Dioxide.*—Carbon dioxide was prepared from calcium carbonate and hydrochloric acid in a Kipp's apparatus and used after washing with potassium permanganate solution and the zinc acetate absorbent solution described above.

8) S. Ohashi, ibid., 28, 537 (1955).

## Procedure

*Procedure A.*—Weigh accurately a 10 to 30 mg. sample, depending upon its sulfur content, into a small weighing tube; choose the sample weight so that the liberated hydrogen sulfide will consume a half of the 0.02 N iodine solution, which will be used thereafter. Place the sample at the bottom of the reaction vessel and 7 ml. of tin(II)-strong phosphoric acid in it from the stock buret. Add each 20 ml. of the absorbent solution in both absorption flasks. Connect each part of the apparatus, expel the air in the reaction and absorption vessel by letting carbon dioxide flow, and heat the reaction medium at 250°–300°C for twenty minutes by means of a small electric heater. The hydrogen sulfide liberated from the medium is absorbed into the absorbent solution by sweeping with carbon dioxide and forms the white precipitate of zinc sulfide. After absorbing all of the liberated hydrogen sulfide, detach the absorption vessel from the reaction vessel and add 20 ml., the total amount, of the 0.02 N iodine solution in both absorption flasks at a suitable ratio. Usually the last flask does not contain zinc sulfide.

From a buret add the 0.02 N sodium thiosulfate solution to both absorption flasks until the greater part of the yellow color of iodine disappears. Transfer the solution in the flasks to a 300 ml. conical beaker, wash the flasks and the gas-conducting glass tubes with water, and titrate the excess iodine with the sodium thiosulfate solution in the presence of starch as indicator. If $t_1$ ml. is the volume of 0.02 N iodine solution used and $t_2$ ml. the volume of 0.02 N sodium thiosulfate, then,

$S\% = (t_1 - t_2)32.066/\text{sample weight (mg.)}$.

*Procedure B.*—Place a sample at the bottom of the reaction vessel, add 4 ml. of chromium(VI)-strong phosphoric acid in it from the stock buret, and warm the contents of the vessel on a water bath for about ten minutes. Next, gently heat the vessel on the electric heater for a few minutes. By this treatment all of the excess chromium(VI) compound, which will consume, if remains, the tin(II)-strong phosphoric acid, is decomposed to the green chromium(III) one. This chemical property of chromium(VI)-strong phosphoric acid is very interesting and advantageous for the present purpose. After the addition of tin(II)-strong phosphoric acid to the mixture in the reaction vessel, treat it subsequently in the same manner as in the Procedure A.

## Results and Discussion

Analyses of some known organic compounds containing sulfur were carried out by this method. The results obtained by using the Procedure A are listed in Table I. It shows that sulfonic acid (methylorange), amide of sulfonic acid (sulfur guanidine), and an easily reducible sulfur such as that of cystine can be determined by the direct reduction method with tin(II)-strong phosphoric acid.

TABLE I

DETERMINATION OF SULFUR IN ORGANIC COMPOUNDS BY THE PROCEDURE A

| Substance | Sulfur Content, % | Sample Weight, mg. | Sulfur Content: Found, % | Sulfur Content: Deviation, % |
|---|---|---|---|---|
| Sulfur guanidine $NH_2C_6H_4SO_2NHC(NH)NH_2$ | 14.97 | 22.7 | 15.0 | 0.0 |
| | | 〃 | 15.4 | +0.4 |
| | | 〃 | 15.3 | +0.3 |
| | | 〃 | 15.3 | +0.3 |
| | | 〃 | 14.9 | −0.1 |
| | | 〃 | 15.3 | +0.3 |
| | | 〃 | 15.1 | +0.1 |
| Methylorange $NaO_3SC_6H_4NNC_6H_4N(CH_3)_2$ | 9.80 | 29.4 | 9.7 | −0.1 |
| | | 30.0 | 9.6 | −0.2 |
| | | 30.5 | 10.0 | +0.2 |
| | | 22.2 | 10.3 | +0.5 |
| Cystine $(HOOCCH(NH_2)CH_2S\text{-})_2$ | 26.69 | 12.3 | 25.2 | −1.5 |
| | | 〃 | 25.8 | −0.9 |
| | | 〃 | 26.4 | −0.3 |
| | | 〃 | 26.5 | −0.2 |
| | | 〃 | 25.2 | −1.5 |

TABLE II

DETERMINATION OF SULFUR IN ORGANIC COMPOUNDS BY THE PROCEDURE B

| Substance | Sulfur Content, % | Sample Weight, mg. | Sulfur Content: Found, % | Sulfur Content: Deviation, % |
|---|---|---|---|---|
| Methionine $CH_3SCH_2CH_2CH(NH_2)COOH$ | 21.49 | 14.1 | 22.2 | +0.7 |
| | | 〃 | 21.9 | +0.4 |
| | | 〃 | 22.3 | +0.8 |
| | | 〃 | 21.7 | +0.2 |
| | | 〃 | 21.8 | +0.3 |
| | | 〃 | 22.2 | +0.7 |
| | | 〃 | 9.0[a] | — |
| | | 〃 | 6.4[b] | — |
| Thiourea $CS(NH_2)_2$ | 42.12 | 10.9 | 41.0 | −1.1 |
| | | 9.3 | 42.2 | +0.1 |
| | | 27.5 | 40.7 | −1.4 |
| | | 10.5 | 41.5 | −0.6 |
| | | 7.3 | 20.4[c] | — |
| | | 7.3 | 11.3[c] | — |
| Acetylmethionine $CH_3SCH_2CH_2CH(NHCOCH_3)COOH$ | 16.77 | 15.6 | 17.1 | +0.3 |
| | | 14.0 | 17.0 | +0.2 |
| | | 16.2 | 16.6 | −0.2 |
| | | 20.5 | 16.3 | −0.5 |
| | | 11.4 | 16.9 | +0.1 |

TABLE II (Contd.)

| Substance | Sulfur Content, % | Sample Weight, mg. | Sulfur Content Found, % | Sulfur Content Deviation, % |
|---|---|---|---|---|
| Thionalide | 14.76 | 16.7 | 15.1 | +0.3 |
| $C_{10}H_7NHCOCH_2SH$ | | 14.4 | 15.5 | +0.7 |
| | | 20.2 | 14.9 | +0.1 |
| | | 16.0 | 14.5 | −0.3 |
| | | 19.7 | 14.4 | −0.4 |
| | | 15.4 | 14.3 | −0.5 |
| | | 16.8 | 14.6 | −0.2 |
| | | 23.1 | 13.1[c)] | −1.7 |
| | | 15.4 | 13.6[c)] | −1.2 |

a) Oxidation with hydrogen peroxide.
b) Oxidation with a mixture of potassium permanganate and strong phosphoric acid.
c) Determination by the Procedure A.

The results of analyses carried out by the Procedure B are shown in Table II. Sulfur in methionine, thiourea, acetylmethionine, and thionalide can be determined by the oxidation with chromium(VI)-strong phosphoric acid followed by the reduction with tin(II)-strong phosphoric acid. The results obtained for methionine by using some oxidizing agents besides chromium(VI)-strong phosphoric acid and for thiourea by the direct reduction method (Procedure A) give all extremely low values as shown in Table II. For thionalide the Procedure A gives nearly correct values, but the Procedure B is more suitable.

For the analyses of sulfur guanidine, cystine, and methionine, dissolving the definite amounts of the samples in water or diluted hydrochloric acid, the aliquots of the obtained solution were evaporated in the reaction vessel and treated by the previously described procedure.

The determination of sulfur can be done by the Procedure A or B for thirty or forty minutes, respectively. With reference to rapidity of analysis this method is much more excellent than the various old ones. Accuracy of this method is not yet satisfactory, but it is useful enough for a routine analysis. The main source of the error may be probably due to the traces of sulfur contained in the reagents and apparatus used and of hydrogen sulfide remaining in the reaction medium.

The investigation on the chemical composition of tin(II)-strong phosphoric acid has been carried out in this laboratory[9)] and led to the conclusion that the reducing power of this reagent is practically based on tin(II) ion. It was also found that this reagent, if protected from the moisture in the air, can be stored for one month without any change of its composition.

Chromium(VI)-strong phosphoric acid is decomposed rapidly and completely, if heated at about 170°C, but it is not decomposed practically, at least for one month, at room temperature. This fact is shown in Table III. In this experiment, in order to determine

TABLE III
STABILITY OF CHROMIUM(VI)-STRONG PHOSPHORIC ACID AT A ROOM TEMPERATURE

| Date | Sample Weight, g. | 0.1 N $Na_2S_2O_3$, ml. | $K_2Cr_2O_7$, % |
|---|---|---|---|
| Nov. 22 | 1.233 | 11.35 | 4.53 |
| 〃 | 1.679 | 15.49 | 4.54 |
| Nov. 29 | 1.803 | 16.46 | 4.47 |
| 〃 | 1.714 | 15.76 | 4.50 |
| Dec. 4 | 2.545 | 23.14 | 4.46 |
| 〃 | 2.306 | 20.92 | 4.45 |
| Dec. 13 | 1.771 | 16.00 | 4.43 |
| 〃 | 1.652 | 14.85 | 4.41 |
| Dec. 24 | 2.119 | 18.71 | 4.33 |
| 〃 | 2.213 | 19.76 | 4.38 |

the content of Cr(VI) in chromium(VI)-strong phosphoric acid, potassium iodide was added to the solution, which was obtained by dissolving the definite amount of chromium(VI)-strong phosphoric acid in water, and the liberated iodine was titrated with 0.1 N sodium thiosulfate solution.

## Summary

1) A new method for the determination of sulfur in organic compounds has been established.

2) This method is based on the utillization of the reducing power of tin(II)-strong phos-

9) T. Kiba, T. Takagi, Y. Yoshimura and I. Kishi, ibid., 28, 641 (1955).

phoric acid and the oxidizing power of chromium(VI)-strong phosphoric acid.

3) Sulfur in organic compounds is reduced to hydrogen sulfide by heating with tin(II)-strong phosphoric acid directly (Procedure A) or after oxidizing with chromium(VI)-strong phosphoric acid (Procedure B).

4) The liberated hydrogen sulfide is absorbed in zinc acetate solution and estimated by the iodimetry.

5) The analytical results obtained for methylorange, sulfur guanidine, and cystine by the Procedure A and for thiourea, methionine, acetylmethionine, and thionalide by the Procedure B were given.

Acknowledgments are made to Prof. T. Kiba for his interest and encouragement and to Miss. I. Kishi for her helpful assistance. A part of the expence for the experiment has been defrayed from a grant given by the Ministry of Education, to which the author's thanks are due.

*Department of Chemistry, Faculty of Science, Kanazawa University, Kanazawa*

# *Studies on the Cooking Mechanism of Wood. XI.*[1] *On the Amount of B-group, and the Reactivity with Thioglycolic Acid*

By Hiroshi MIKAWA, Koichiro SATO, Chizuko TAKASAKI and Kiyo EBISAWA

(Received June 22, 1955)

Sulphonatable groups of lignin consist of different functional groups, namely, X, Z and B[2]. X and Z groups are sulphonatable even at neutral pH; B group is, however, only at low pH. B group, or at least a part of it, is thought to be a group of lignin, which is connected with carbohydrate of wood, or with another part of lignin by ether-linkage, or glycosidic linkage, or by other types of hydrolyzable linkages. The hydrolyzed B group is termed B' group[3].

**Reactivity of the B Group with Thioglycolic Acid.**—In the previous communication[4], it was shown that X and Z groups react with thioglycolic acid. It will, therefore, be very interesting to see if B group reacts also with thioglycolic acid or not. If one lets the low sulphonated lignosulphonic acid, and the acids obtained by further sulphonation of it, react with thioglycolic acid in homogeneous phase, and sees if the sulphonic acid group introduced to B group interferes with the reaction with thioglycolic acid or not, one can expect to obtain a definite conclusion of this question.

In order to be sure that the sulphonic acid group originally present in lignosulphonic acid is not split off by the treatment with thioglycolic acid–a condition which must be fulfilled in our case–it is necessary to know the content of sulphonic acid group of lignosulphonic acid treated with thioglycolic acid. Sulphonic acid group will be very easily estimated by conductometric titration. The estimation of the amount of the thioglycolic acid residue combined is, however, not so simple, because one can not calculate it from the difference of the total sulphur content and the sulphonic acid sulphur, as reportedly the sulphur atom of the lignosulphonic acid consists not only of acidic, but also non-acidic, so-called "excess sulphur"[5] the existence of which is also expected in the lignosulphonic acid treated with thioglycolic acid.

Hachihama, Shinra and Kyogoku[6] titrated conductometrically not only lignosulphonic acid, but also a mixture of lignosulphonic acid and acetic acid, and observed a distinct "break" in the titration curve of acetic acid, and the so-called weak acidic group of lignosulphonic acid itself. This fact suggests a possibility of estimating thioglycolic acid re-

1) Part X, H. Mikawa, This Bulletin, **24**, 53 (1954); Part IX, ibid., 50; Part VIII, H. Mikawa and K. Sato, *J. Chem. Soc. Japan, Ind. Chem. Sec.*, **57**, 639 (1954).

2) H. Erdtman, *Tech. Assoc. Pulp Paper Ind.*, 32, 71, 75 (1949); H. Mikawa, K. Sato, C. Takasaki and H. Okada, *J. Chem. Soc. Japan, Ind. Chem. Sec.*, **54**, 299 (1951); B. Lindgren, *Acta Chem. Scand.*, **5**, 603 (1951); E. Nokihara, *J. Agr. Chem. Soc. Japan*, **26**, 207, 236 (1952).

3) H. Erdtman, *Research*, 3, 83 (1950).

4) H. Mikawa and K. Sato, *J. Chem. Soc. Japan, Ind. Chem. Sec.*, **57**, 605 (1954).

5) O. Samuelson and A. Westlin, *Svensk Papperstidn.*, **50**, 141 (1947); **51**, 179 (1948).

6) Y. Hachihama, H. Shinra and Y. Kyogoku, *J. Soc. Chem. Ind. Japan*, **47**, 209, 212 (1944).

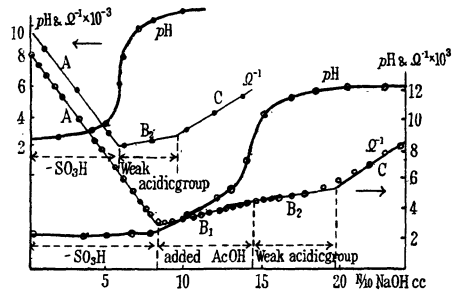



Fig. 1. Conductometric and potentiometric titrations of lignosulphonic acid (•) and a mixture of lignosulphonic acid and acetic acid (○).

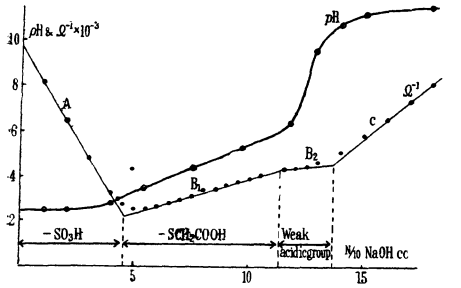



Fig. 2. Conductometric and potentiometric titration of lignosulphonic acid after reaction with thioglycolic acid.

sidue by conductometric titration, in spite of the presence of a weak acidic group of lignosulphonic acid itself. Examples of the conductometric and potentiometric titration curves of lignosulphonic acid, a mixture of lignosulphonic acid and acetic acid, as well as lignosulphonic acid treated with thioglycolic acid are shown in Figs. 1 and 2. The experiments of Fig. 1 were performed only in order to compare the curves with those of Fig. 2. As was reported by Hachihama, Shinra and Kyogoku, A-part of Fig. 1 corresponds to $SO_3H$ group, $B_2$-part to the weakly acidic group, and the acetic acid added was titrated at $B_1$-part. The titration curve of the lignosulphonic acid treated with thioglycolic acid showed completely the same shape as the titration curve of a mixture of lignosulphonic acid and acetic acid, in this case $B_1$-part being due to carboxyl group of thioglycolic acid residue attached to lignin. In this case, the separation of the carboxyl group of thioglycolic acid residue from the "weakly acidic group" is not very distinct, but is possible.

Low sulphonated lignosulphonic acids with $S/CH_3O = 0.25$–$0.3$, prepared in the usual manner, were sulphonated further at pH 1.8, for various periods of hours. Total sulphur content, and the sulphonic acid group content of the lignosulphonic acids obtained, are shown by curves I and II of Fig. 3, and the data are summarized in Table I. The difference

TABLE I

FURTHER SULPHONATION OF LIGNOSULPHONIC ACIDS

| | Condition of further sulphonation | | Analyses of Ba-LSA after further sulphonation | | | | | |
|---|---|---|---|---|---|---|---|---|
| | pH | hrs. | Total S | S in the form of $SO_3H$ | $CH_3O$ | weak acidic group equiv./$CH_3O$ | Total $S/CH_3O$ | $SO_3H/CH_3O$ |
| $LSLSA_a$ | — | — | 3.19 | 2.97 | 12.8 | 0.21 | 0.24 | 0.23 |
| | 1.8 | 3 | 5.80 | 5.49 | 11.6 | 0.27 | 0.48 | 0.45 |
| | | 8 | 6.46 | — | 11.2 | — | — | — |
| | | 16 | 8.16 | 6.98 | 10.5 | 0.30 | 0.75 | — |
| | | 24 | 7.76 | 5.73 | 10.2 | 0.32 | 0.74 | 0.55 |
| $LSLSA_b$ | — | — | 3.00 | 2.98 | 12.8 | 0.18 | 0.23 | 0.23 |
| | 1.8 | 3 | 5.31A | 4.87 | 10.8 | 0.25 | 0.48 | 0.44A |
| | | 8 | 6.10B | 5.72 | 10.1 | 0.26 | 0.59 | 0.57B |
| | | 24 | 8.21C | 6.68 | 10.4 | 0.30 | 0.77 | 0.63C |
| | | 10+10* | 6.70 | 6.12 | 10.2 | 0.26 | 0.64 | 0.58 |
| | | 10+10+16 | 7.65 | 6.09 | 9.9 | 0.28 | 0.75 | 0.60 |
| $LSLSA_c$ | — | — | 3.54 | 3.04 | 11.6 | 0.20 | 0.29 | 0.25 |
| | 5.8 | 20 | 5.73 | 4.99 | 9.8 | 0.20 | 0.57 | 0.49 |
| | | 20+20 | 6.20 | 4.76 | 11.2 | 0.24 | 0.54 | 0.41 |
| | 8.5 | 10 | 4.25 | 3.94 | 11.4 | 0.22 | 0.36 | 0.34 |
| | | 10+30 | 4.84 | 4.63 | 10.9 | 0.27 | 0.43 | 0.41 |
| | | 10+30+20 | 5.01 | 4.27 | 11.0 | 0.28 | 0.44 | 0.38 |
| LSA | — | — | 6.80 | 6.00 | 10.5 | 0.24 | 0.63 | 0.56 |
| (from | 1.8 | 3 | 6.24D | 5.71 | 10.8 | 0.24 | 0.56 | 0.52D |
| indust. | | 8 | 6.32E | 5.82 | 10.5 | 0.25 | 0.58 | 0.54E |
| waste | | 16 | 6.78F | 6.15 | 11.4 | 0.24 | 0.58 | 0.52F |
| liquor) | | 24 | 7.12G | 6.42 | 10.3 | 0.24 | 0.67 | 0.60G |

LSLSA=low sulphonated lignosulphonic acid, LSA=lignosulphonic acid *10+10 means that the sulphonation was continued another 10 hr. with fresh liquor after isolating and purifying LSA after the first 10 hr. of sulphonation.

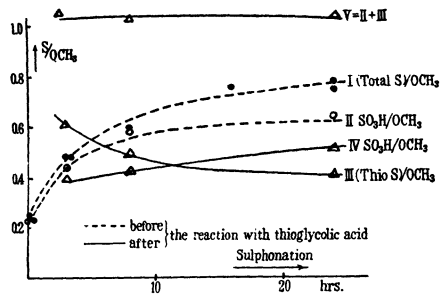



Fig. 3. Further sulphonation of low sulphonated lignosulphonic acid (LSLSA) and reaction of further sulphonated LSLSA$_b$ with thioglycolic acid.

of these two curves corresponds to the so-called "excess sulphur", which is not acidic in nature. Lignosulphonic acids with various degrees of sulphonation thus obtained, were heated with aqueous thioglycolic acid solution in 1 N hydrochloric acid, for ten hours at 100°C–the condition confirmed by the preliminary experiment, to be sufficient to complete the reaction. Because of the low solubility of the "low sulphonated lignosulphonic acid" in aqueous acidic solution of thioglycolic acid, this acid was not suitable for our purpose. Curves III and IV of Fig. 3 are the conductometrically obtained (Thio S)/$CH_3O$ and $SO_3H/CH_3O$, after the reaction with thioglycolic acid, where "Thio S" means the sulphur due to the thioglycolic acid residue in the sample.

From the results shown in Fig. 3, it is evident that the sulphonic acid group originally present in the lignosulphonic acid is split off by the treatment with thioglycolic acid, by the amount of the difference of curves II and IV. This amount is however not so large as to invalidate the following discussion. As the content of the total sulphur and the sulphonic acid group increases along with the curves I and II, the amount of the thioglycolic acid group introduced drops rapidly to about 0.4 Thio. S/$CH_3O$. Thus, the sulphonic acid group introduced to B'-group interferes with the reaction with thioglycolic acid, from which it may be concluded that thioglycolic acid is able to combine with the B'-group too. Thioglycolic acid reacts with some another group, however, even after the complete sulphonation of lignin. This fact is most clearly shown by the lignosulphonic acid isolated from industrial waste liquor. As is known the lignosulphonic acid obtained from the waste liquor of industrial cooking can not be sulphonated, which is also clear from the lowest part of the table. Such lignosulphonic acid is, therefore, completely sulphonated, but does react with thioglycolic acid to some extent as is shown in the third column from the right side of Table II.

TABLE II

ANALYSES OF Ba-SALT A-G AFTER REACTION WITH THIOGLYCOLIC ACID

| LSA | Total S | $SO_3H$ | Thio S | $CH_3O$ | $SO_3H/CH_3O$ | Thio S/$CH_3O$ | Total S/$CH_3O$ | Thio S+$SO_3H$ per $CH_3O$ |
|---|---|---|---|---|---|---|---|---|
| A | 8.47 | 3.37 | 5.11 | 8.20 | 0.40 | 0.61 | 1.00 | 1.01 |
| B | 8.56 | 3.90 | 4.55 | 8.95 | 0.42 | 0.49 | 0.93 | 0.91 |
| C | 8.22 | 4.59 | 3.57 | 8.73 | 0.51 | 0.40 | 0.91 | 0.91 |
| D | 7.34 | 4.20 | 3.34 | 8.98 | 0.45 | 0.36 | 0.79 | 0.81 |
| E | 7.61 | 4.33 | 3.02 | 8.89 | 0.47 | 0.33 | 0.83 | 0.80 |
| F | 7.48 | 4.56 | 3.02 | 8.95 | 0.50 | 0.33 | 0.81 | 0.83 |
| G | 7.42 | 4.56 | 2.82 | 8.88 | 0.50 | 0.31 | 0.81 | 0.81 |

The fact that the values of the last two columns of the table, i.e. those for analytically obtained (Total S)/$CH_3O$ and (ThioS +$SO_3H$)/$CH_3O$, coincide well after the reaction with thioglycolic acid, indicates that "excess sulphur" which had been contained in the original lignosulphonic acid was eliminated during the reaction with thioglycolic acid.

**On the Amount of the B-group.**—Among the three different sulphonatable groups, the amount of X and Z groups are found to be about 0.12–0.14/$CH_3O$[2]. The structure of these two groups are now almost clear, but that of B group is not so certain. The amount of this group was estimated by Lindgren[7] to be as much as 0.7/$CH_3O$. If this figure is correct, the sulphonatable groups with known structure, i.e. X and Z groups, are not more than one third of the total sulphonatable groups.

Further sulphonation of the low sulphonated lignosulphonic acid was studied by Leopold[8], and by his experiments it was made clear that the amount of sulphur introduced to lignin increased nearly up to one per methoxyl. Assuming the amount of the sum of X and Z groups as 0.3/$CH_3O$ the amount

7) B. Lindgren, *Svensk Papperstidn.*, **55**, 78 (1952).
8) B. Leopold, *Acta Chem. Scand.*, **6**, 64 (1952).

of B group was estimated as 1–0.3=0.7. This conclusion was drawn from the analytically obtained total sulphur content of the lignosulphonic acid. As stated before, it was however made clear by Samuelson that not all of the sulphur of lignosulphonic acid consisted of acidic sulphonic acid group, being partly non-acidic sulphur, which he called "excess sulphur". If this excess sulphur combines with B-group, the amount of this group must be estimated from the total sulphur of the completely sulphonated lignosulphonic acid. If, on the other hand, the excess sulphur does not combine with B group, the amount of this group must be estimated from the amount of the sulphonic acid group of the carefully and completely sulphonated lignosulphonic acid.

For this purpose the low sulphonated lignosulphonic acid was sulphonated further at pH 1.8, 5.8 and 8.5, and the data obtained are shown in Table I and in Fig. 4. Curves I and II are (Total S)/$CH_3O$, and $SO_3H/CH_3O$

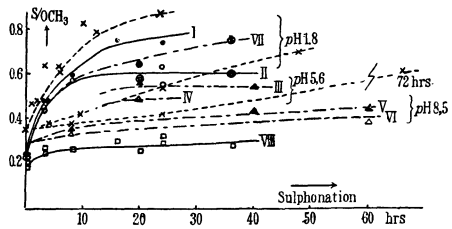



Fig. 4. Further sulphonation of low sulphonated lignosulphonic acid at three pH's.

| pH | 1.8 | 5.8 | 8.5 |
|---|---|---|---|
| Total S | ●I ⊙VII | ▲III | ▲V |
| $SO_3H$ | ○II ◎II | △IV | △VI |

Curves I ● and II ○ are the same with I and II of Fig. 3.
Curves VII ⊙ and II ◎ were obtained at pH 1.8 changing cooking acid repeatedly with fresh one and purifying lignosulphonic acid.
Curve VIII is the amount of weak acidic group of lignosulphonic acids obtained at pH 1.8 in (equiv.)/$OCH_3$ scale.
···×··· are the data reported by Erdtman and Leopold for (Total S)/$OCH_3$ at pH 1.8, 3.4 and 5.8.

of the lignosulphonic acids, obtained at pH 1.8. As the amount of sulphonic acid group is, however, considerably less than the total sulphur, and reaches its saturation value much earlier; the total amount of the sulphonatable group seems to be only about 0.6 per methoxyl, although it might not be impossible that some part of B' group had been changed to unsulphonatable structure during the reaction. Even if one carries out the sulphonation carefuly (curves VII and II), i.e. changing the cooking acid frequently with fresh acid and at the same time, isolating and purifying the lignosulphonic acid, the amount of the sulphonic acid group never exceeds 0.6– the value, obtained by ordinary one-step sulphonation. The difference between the total sulphur and the sulphonic sulphur is much smaller in this case, and consequently, the curve for the total sulphur (VII) approaches that of the sulphonic sulphur (II). If such were the case, many high values of the analytically obtained sulphur content of lignosulphonic acid reported in the literature might be due to the nonacidic "excess sulphur", which was introduced to some non-sulphonatable group, probably by thiosulphate formed during the sulphonation. From this point of view, the total amount of B group may be estimated, as only about 0.6–(X+Z)=0.3~0.35 per methoxyl. The low sulphonated lignosulphonic acid, obtained from the sulphonated wood by Kullgren process can not represent the total lignin, contained in the wood. Lignosulphonic acid prepared from industrial waste liquor has, however, also about 0.6 $SO_3H/CH_3O$.

The amount of the weakly acidic group of lignosulphonic acid (curve VIII, Fig. 4) seems to remain nearly constant, irrespective of the further sulphonation. It is remarkable that even the so-called low sulphonated lignosulphonic acid contains nearly the same amount of weakly acidic group. The nature of this weak acidic group will be investigated in the next communication.

## Experimental

**Preparation of the low sulphonated lignosulphonic acid.**—The method used is essentially the same with that of Erdtman[9]. Extractives free wood meal (100 mesh, 200 g.) was heated with neutral sulphite solution (pH 5.7, 1.5 l) to 135°C within 3 hrs. and kept at this temperature for 14 hrs. Sulphonated wood meal thus obtained was washed well with HCl (0.3%), and subsequently with distilled water, until free from $Cl^-$, heated twice with water for 4 hrs. each at 90°C, the combined extracts concentrated in vacuo, and the extracted low sulphonated lignosulphonic acid was precipitated by adding 1-(N-piperidinoacetylamino)-naphthalene sulphate[8]. The precipitate was washed with water until neutral pH, decomposed with 1% NaOH, and the free base separated, was filtered next day. The filtrate was passed through Amberlite IR 120 in hydrogen form, neutralized with $BaCO_3$, centrifuged, and the supernatant solution was poured into absolute

9) C. Kullgren, *Svensk Kem. Tid.*, **44**, 15 (1932); H. Erdtman, *Svensk Papperstidn.*, **48**, 75 (1945).

alcohol. The precipitated Ba-lignosulphonate was separated by centrifuge, washed well with alcohol, ether and petroleum ether successively.

**Further sulphonation of Ba-lignosulphonate.**—Ba-lignosulphonate (16 g.) to be sulphonated was dissolved in water, freed from barium by cation exchanger, sodium hydroxide (16 g.) added, and $SO_2$ was bubbled, until pH was lowered to the desired value (1.8–8.5), and the total volume was adjusted to 400 ml. by water. The solution was divided into four ampoules and heated at 135°C. After the sulphonation, the content was evacuated, passed through cation exchanger, evacuated again in order to expel $SO_2$, and the lignosulphonic acid was precipitated by 1-(N-piperidinoacetylamino)-naphthalene sulphate. The precipitate was treated as above.

**Preparation of Ba-lignosulphonate from industrial waste liquor.**—The waste liquor was dialyzed with cellophane membrane for 1–2 weeks, neutralized with $BaCO_3$, centrifuged, and the solution was poured into alcohol. The crude salt thus obtained was dissolved in water, passed through cation exchanger in hydrogen form, and the lignosulphonic acid was purified by the same precipitating agent as before.

**Reaction of lignosulphonic acid with thioglycolic acid.**—Ba-lignosulphonate (1 g.) was dissolved in water, passed through cation exchanger, thioglycolic acid (3 g.) and dil. HCl added, and the whole was made up to 30 ml. and adjusted to 1 N with respect to HCl. The solution was heated at 100°C for 10 hrs., extracted continuously with ether in order to remove excess thioglycolic acid, and the lignosulphonic acid was separated by the precipitating agent, and processed just the same as mentioned above.

**Analyses.**—Sulphur with micro Carius and $CH_3O$ according to Viebök-Blecher and Gran[10]. Conductometric and potentiometric titrations were performed with a solution of lignosulphonic acid, which was prepared by passing a solution (20 ml.) of Ba salt (500 mg.) through cation exchanger, and making up to 50 ml. with water.

## Summary

B-group of lignin reacts with thioglycolic acid. Total amount of the sulphonatable groups of lignin is about 0.6/$CH_3O$, the amount of B-group being consequently 0.3–0.35/$CH_3O$. Higher S/$CH_3O$ values reported in the literature may be due to the presence of non-acidic "excess sulphur".

The authors are indebted to Dr. H. Okada, the head of our laboratory, and to Miss. S. Suehiro for their encouragement.

*Research Laboratory of the Kokusaku Pulp Co., 184, 1-Chome, Kamiochiai, Shinjuku-ku, Tokyo*

10) G. Gran, *Svensk Papperstidn.*, 55, 255 (1952).

# *Studies on the Cooking Mechanism of Wood. XII*[1]. *On the Nature of the weakly Acidic Group of Lignosulphonic Acid*

By Hiroshi MIKAWA, Koichiro SATO, Chizuko TAKASAKI and Kiyo EBISAWA

(Received June 22, 1955)

It is a well known fact that the sulphite spent liquor shows considerable buffering action for neutralization. This phenomenon is clearly shown by the conductometric titration of the waste liquor. Among others, investigations of Hachihama[2], Samuelson[3], and Adler[4] made clear that this buffering action is due to the presence of sulphurous acid, organic acids, i.e. formic, acetic etc., so called loosely combined sulphurous acid, and some weakly acidic group of lignosulphonic acid itself. As the elucidation of the nature of the weakly acidic group of lignosulphonic acid is very interesting not only from the scientific, but also from the technical point of view, we will deal with this problem in the present communication.

It has been open to question, whether this group, which amounts to approximately one equivalent per 4–5 methoxyl groups, is carboxylic or phenolic in nature. Hachihama et al. assumed this to be phenolic, and Samuelson supposes that this may be carboxylic. As both carboxyl and phenolic hydroxyl groups are usually methylated by diazomethane to ester and phenol-ether groups respectively (some exceptions exist however : for example phenolic hydroxyl groups of conidendrin[5], and 3,3'-

1) Part XI, Preceeding Paper, p. 649.

2) Y. Hachihama, H. Shinra and Y. Kyogoku, *J. Chem. Soc. Japan, Ind. Chem. Sect.*, **47**, 209, 212 (1944).

3) S. Regestad and O. Samuelson, *Svensk Kem. Tid.*, **61**, 9 (1949).

4) E. Adler, *Svensk Papperstidn.*, **50**, 261, No. 11B 9 (1947).

5) F. Brauns, *J. Org. Chem.*, **10**, 216 (1945).

dimethoxy-4.4'-dihydroxy diphenylmethane[6]) were not methylated by diazomethane), it is expected that such a weakly acidic group must disappear after the methylation, and must reappear by alkaline hydrolysis, if the methylated group were carboxyl. Hachihama and Kyogoku observed recently that the weakly acidic group of lignosulphonic acid disappeared by methylation with dimethyl sulphate[7]).

$\alpha$-Lignosulphonic acid of spruce origin (lignosulphonic acid A, $S/CH_3O=0.44$) has a considerably large weakly acidic group (one equivalent per 4.7 $CH_3O$), as is evident from curve I Fig. 1, but this group disappears

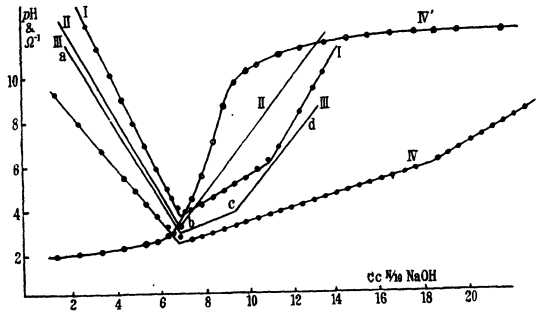



Fig. 1. Conductometric titration of lignosulphonic acid A (I), diazomethylated lignosulphonic acid A (II), diazomethane methylated lignosulphonic acid A after hydrolysis in nitrogen atmosphere at 30° for 72 hr. in 1 N NaOH (III) (Absorption spectra taken at a, b, c and d are shown in Fig. 2.) and the cond. and potent. titrations of lignosulphonic acid A after being kept in 1 N NaOH for 48 hr. at 30° in a closed vessel with air (IV, IV').

after methylation with diazomethane (curve II). This weakly acidic group which once disappeared was regenerated more than 50% after mild alkaline hydrolysis in nitrogen atmosphere, the hydrolysis condition being selected so as to be sufficient to hydrolyze ferulic acid methyl ester completely, i.e. 1 N NaOH, 30°C, 72 hr., for the reasons to be mentioned later (curve III). This result will most easily be explained by assuming that more than 50% of the weakly acidic group consists of carboxylic acid group. The diazomethylated lignosulphonic acid A shows completely the same UV-absorption in neutral and alkaline media (I, Fig. 2), which fact indicates that all phenolic hydroxyl groups are completely methylated. The UV-absorption curves were taken at point a,b,c and d of the conductometric titration curve of

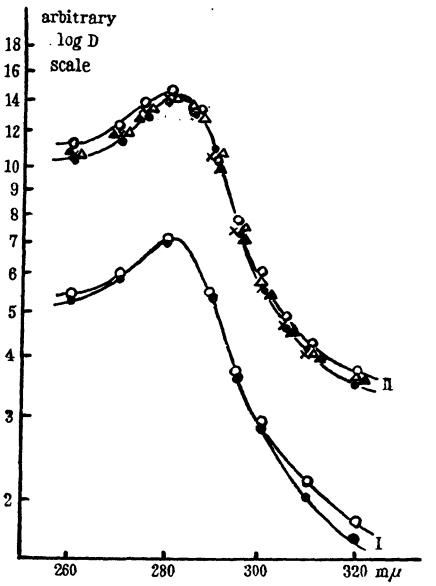



Fig. 2. Absorption spectra of diazomethylated lignosulphonic acid A (I) (● neutral, ○ 1 N NaOH) and of the diazomethylated lignosulphonic acid A after hydrolysis measured at points a, b, c and d of the conductometric titration (curve III, Fig. 1) (II) (● a, × b, ▲ c, △ d, ○ 1 N NaOH).

hydrolyzed diazomethylated lignosulphonic acid A (III, Fig. 1), without any dilution using a very thin cell. All curves superpose each other (II, Fig. 2), indicating that the phenolic hydroxyl group does not exist even after the hydrolysis. The weakly acidic group of this acid must, therefore, be carboxyl in nature. Even a slight increase in the number of weakly acidic group was not observed after keeping lignosulphonic acid A in 1 N sodium hydroxide for two days, and four days, at 30°C in nitrogen atmosphere. The carboxylic acid group observed after the hydrolysis of the methylated lignosulphonic acid must, therefore, be formed from the methylated carboxyl group by hydrolysis, and can not be a carboxylic acid group newly formed by oxidation during the hydrolysis.

Diazomethylation is able to be substituted by the methylation with dimethyl sulphate, as is shown in Fig. 3. Here, the conductometric and potentiometric titrations of another sample of $\alpha$-lignosulphonic acid (lignosulphonic acid B, $S/CH_3O=0.49$) (curves I and I', Fig. 3), conductometric tritration of this acid after methylation with dimethylsulphate (II, Fig. 3), and the conductometric, and potentiometric titrations of this methylated lignosulphonic acid, after hydrolysis for two-

6) I. Pearl, *J. Am. Chem. Soc.*, 68, 429 (1946).
7) Y. Hachihama and Y. Kyogoku, *Technology Reports of the Osaka Univ.*, 3, 375 (1953).

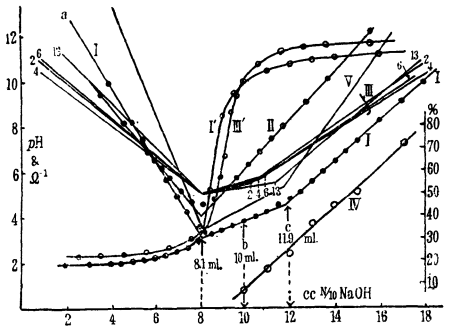



Fig. 3. Conductometric and potentiometric titration of lignosulphonic acid B (I, I') (Absorption spectra are shown in Fig. 4.), cond. titr. after methylation with dimethyl sulphate (II), cond. titr. of methylated acid after hydrolysis for 2–13 days at 30° in 1 N NaOH (III) and the potent. titr. after hydrolysis for 6 days (III'), percentage of the phenolic hydroxyl group ionized during the cond. titr. of lignosulphonic acid B along the curve I (IV) and the cond. titr. of sodium borohydride reduced lignosulphonic acid B (V).

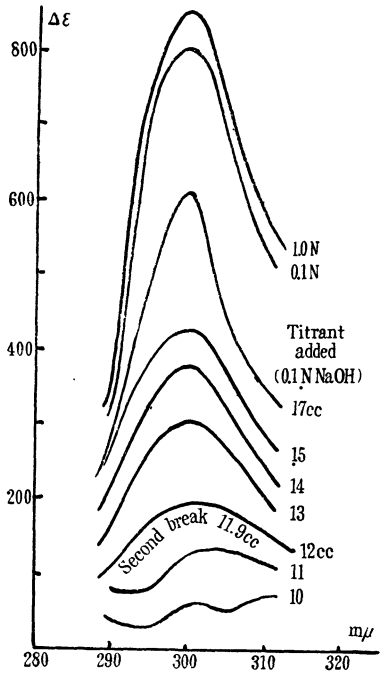



Fig. 4. Difference of the free acid spectrum and the spectra taken at various points of the conductometric titration of lignosulphonic acid B (cf. Fig. 3, Curve I).

thirteen days are shown (curves III and III', Fig. 3). The results are completely the same as in the case of diazomethylation mentioned above. This is quite understandable, as many examples are reported telling that the carboxyl group is esterified with dimethyl sulphate and alkali, for example, methylester from stearic acid[8], campholic acid[9], gallic acid[10] etc. More than 50% of the weakly acidic group seems again to be carboxyl in nature.

During the conductometric titration of the lignosulphonic acid B (Fig. 3, I), one drop of the solution was taken out at various points, and the UV-absorption of these solutions was measured without any dilution, using a very thin cell in order not to shift the condition of ionization of the lignosulphonic acid at these points. The UV-absorption curves thus obtained must therefore represent the condition of the lignosulphonic acid molecule at every stage of the titration. No change of the adsorption was observed from point "a" (free lignosulphonic acid) to "b" (half way of the weakly acidic part, titrant added, 10 ml.), corresponding to the neutralization of sulphonic acid group and the ionization of carboxyl group, which may not affect the absorption appreciably. After this point, the absorbancy at about 300 mμ rises slowly, and this rise is shown clearly by $\Delta\varepsilon$ curves of Fig. 4. $\Delta\varepsilon$ values were obtained by subtracting the absorption curve for point "a" from those for other points. Here in this figure, only the values obtained between 290 mμ to 310 mμ are shown. According to Aulin-Erdtman[11], the increase of the absorption at about 300 mμ is attributable to the ionization of the phenolic hydroxyl groups, and the total amount of the phenolic hydroxyl group is proportional to the difference of ε values, taken at 300 mμ in acidic or neutral and strong alkaline (1 N) media. $\Delta\varepsilon$ values obtained in 0.1 N and 1 N sodium hydroxide is also shown in Fig. 4. The increase of $\Delta\varepsilon$ value from the half way of the weakly acidic part of the conductometric titration, i.e. point "b" to the second "break" (point "c", titrant added, 11.9 ml.), is only about 24% of the $\Delta\varepsilon$ value which corresponds to the total amount of the phenolic hydroxyl groups ionizable in 1 N alkalinity. The percentage of the ionized phenolic hydroxyl groups during the titration thus obtained, is shown by curve IV of Fig. 3. Thus, one may be able to deduce also from such spectroscopic considerations, that about 50–75% of the weakly acidic group may be carboxyl, and the remaining 50–25% rather strong phenolic hydroxyl group.

8) A. Werner and W. Seybold, *Ber.*, 37, 3559 (1904).
9) J. Riedel, D.R.P. 187840, 196152.
10) P. Graebe and H. Martz, *Ann. d. Chem.*, 340, 219 (1905).
11) G. Aulin-Erdtman, *Svensk Papperstidn.*, 55, 745 (1952); 56, 91, 287 (1953).

Aqueous solution of vanillyl sulphonic acid was titrated conductometrically, and at the same time UV-absorption spectra were measured in the same manner as in the case of lignosulphonic acid. As seen from Fig. 5, the ionization of its phenolic hydroxyl group

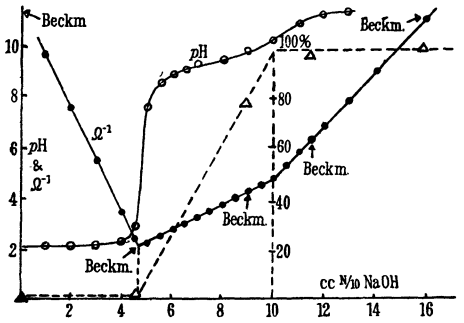



Fig. 5. Conductometric and potentiometric titrations of vanillyl sulphonic acid and the spectroscopically estimated percentage of the ionized phenolic hydroxyl group. Beckm. means the measurement of absorption by Beckmanspectrophotometer at the indicated points.

was complete already at the second "break". From this fact it may be certain that the phenolic hydroxyl group of the lignosulphonic acid, titrated before the second "break", must have been ionized before the "break", and the remaining part, which did not ionize before the second "break", did not contribute to the weakly acidic part of the conductometric titration.

As mentioned earlier, even up to 80–90% of the weakly acidic group was regenerated after prolonged hydrolysis. Judging from the amount of the spectroscopically estimated phenolic hydroxyl group, which contributed to the weakly acidic group of the lignosulphonic acid, however, it seemed improbable that so much carboxyl group existed in lignosulphonic acid. Lignosulphonic acid is very susceptible to oxidation in alkaline medium, which is clearly shown by curve IV of Fig. 1. Here, it is shown that the amount of the weakly acidic group of lignosulphonic acid A increases very much, after being kept in 1 N sodium hydroxide for forty eight hours at 30°C in a closed vessel with air. As lignosulphonic acid is so susceptible to oxidation, it may not be impossible that a slight increase of carboxylic acid group occurs, even in the case of the hydrolysis in nitrogen atmosphere.

The phenolic hydroxyl group, titrated before the second "break", must be stronger than the remaining phenolic hydroxyl groups. As the phenols with carbonyl group, conjugated with a benzene ring, in its para position are generally very strong, the lignosulphonic acid B was titrated conductometrically after the reduction with sodium borohydride. The amount of the weakly acidic group did not decrease appreciably by the reduction. The titration curve and the UV-absorption are shown by curve V of Fig. 3 and by Fig. 6 respectively.

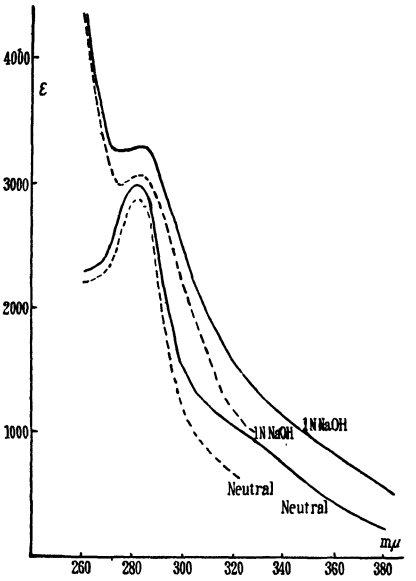



Fig. 6. UV-absorption spectra of lignosulphonic acid B (——) and sodium borohydride reduced lignosulphonic acid B (----).

Only lignosulphonic acids prepared from spruce were investigated so far, but the acids prepared from birch and beech have also considerable amount of weakly acidic group, the conductometric and potentiometric titration curves of these acids being essentially the same with the acids of gymnosperm origin. Since the lignosulphonic acid is very easily oxidized by air in alkaline solution as mentioned above, it will naturally be suspected, if the weakly acidic group is formed by air oxidation, during the isolation and purification, when the acid is treated with alkali. In order to confirm this, the birch lignosulphonic acid was isolated and purified without using alkali. during the whole process; i.e. after dialysis and ion exchange of the waste liquor, the lignosulphonic acid was precipitated by 1-(N-piperidino- acetylamino)-naphthalene as usual, the precipitate was dissolved in aqueous acetone containing some amount of sulphuric acid, the solution passed through IR 120 in hydrogen form, and the eluate was neutralized by barium carbonate. The lignosulphonic acid thus prepared had,

however, a weakly acidic group as indicated in Fig. 7.

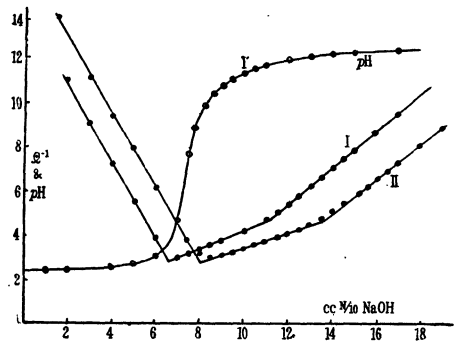



Fig. 7. Conductometric and potentiometric titration of birch lignosulphonic acid (I, I') and cond. titr. of beech lignosulphonic acid isolated and purified without being kept alkaline during the preparation (II).

Analytical data of the lignosulphonic acids used, are listed in Table I. Taking example acid A increased from 11.97% to 16.86% by methylation with diazomethane. The difference, 4.89%, must correspond to the methoxyl group mainly introduced to the phenolic hydroxyl group and the carboxyl group. If one neglects a slight increase of weight by methylation, the value of $\Delta CH_3O/CH_3O$ is about $0.4/CH_3O$. As the amount of the phenolic hydroxyl group must be much less, one must assume the existence of carboxyl group from such a point of view too.

## Discussion

The existence of a carboxyl group in lignin and lignosulphonic acid was advocated by some authors, but many others could not recognize it[12]. Friedrich and Diwald[13], and Moore, Wright and Hibbert[14] recognized a little amount of methyl ester group in alcohol lignin. Phillips[15] thought to have recognized carboxyl group in corncob lignin. On the basis of analytical composition of lignosulphonic acid salts, Hönig and Fuchs[16], and

TABLE I

ANALYSES OF LIGNOSULPHONIC ACIDS

| lignosulphonic acid | Anal. S% | Cond. $SO_3H$ S% | weakly acidic group equiv./$C_9$ | $CH_3O$ | $SO_3H/C_9$ | spectroscopically measured OH*/$C^9$ |
|---|---|---|---|---|---|---|
| A 1) | 6.81 | 5.45 | one/4.7 | 11.97 | 0.47 | — |
| after $CH_2N_2$ methylation | 5.63 | 5.10 | zero | 16.86 | — | zero |
| B 2) | 6.67 | 5.76 | one/4.8 | 11.32 | 0.51 | 0.21–0.17 |
| after methylation with $(CH_3)_2SO_4$ | — | 5.34 | zero | 16.70 | — | zero |
| beech 3) | 6.90 | 5.76 | one/2.5 | 15.01 | 0.56 | — |
| birch 4) | 8.00 | 4.75 | one/3.5 | 15.20 | 0.53 | 0.26–0.21 |

1) $C_9H_{10.4}O_{2.77}(CH_3O)_{1.06}(SO_3Ba/2)_{0.47}S^{neut.}_{0.12}Ba^{excess}_{0.04}$

2) $C_9H_{10.7}O_{3.2}(CH_3O)_{1.05}(SO_3Ba/2)_{0.51}S^{neut.}_{0.08}Ba^{excess}_{0.04}$

3) $C_9H_{9.82}O_{3.25}(CH_3O)_{1.53}(SO_3Ba/2)_{0.56}S^{neut.}_{0.11}Ba^{excess}_{0.05}$

4) $C_9H_{9.65}O_{2.87}(CH_3O)_{1.40}(SO_3Ba/2)_{0.53}S^{neut.}_{0.36}Ba^{excess}_{0.04}$

in the lignosulphonic acid B, this acid contains 0.04 mol. excess barium per $C_9$, which is not combined with the sulphonic acid group, and one equivalent weakly acidic group per 4.8 $CH_3O$, i.e. 0.22 equivalent per $C_9$ unit. Provided that the excess barium is combined with the carboxyl group, it is calculated from these data that the carboxyl group amounts to about 36% of the weakly acidic group. It will, however, be possible that only a part of the carboxyl group is neutralized with barium, as the neutralization was performed with barium carbonate, and the carboxyl group seems to be a very weak one.

As can be seen from Table I, the content of the methoxyl group of the lignosulphonic

Klason[17] thought to have recognized carboxyl group in some lignosulphonic acid preparations. Some barium salt had Ba/S values slightly higher than 0.5. Freudenberg et al.[18] reports that the lignosulphonic acid, prepared at relatively low temperature of 70°C, contained 1.8–2.8% of carboxyl groups.

12) Y. Hachihama and S. Jodai, "Chemistry of Lignin", Nihonhyoron Press., Tokyo (1946), p. 391.
13) A. Friedrich and J. Diwald, *Monatsh.*, **46**, 31 (1925).
14) R. Moore, G. Wright and H. Hibbert, *Can. J. Res.*, **15B**, 532 (1937).
15) M. Phillips, *J. Am. Chem. Soc.*, **53**, 768 (1931).
16) M. Hönig and W. Fuchs, *Monatsh.*, **41**, 215 (1920).
17) P. Klason, *Ber.*, **53**, 1864 (1920); **55**, 455 (1922); **56**, 300 (1923).
18) K. Freudenberg, W. Lautsch and G. Piazolo, *Cellulosechem.*, **22**, 97 (1944).

Kullgren[19] reports recently that the lignosulphonic acid in unbleached sulphite pulp seems to have carboxyl group. With many lignin preparations it is recognized, however, that Ba/S is practically 0.5, which fact was thought to suggest that the preparations did not contain carboxyl groups[20]. However, as Samuelson and Westlin[21] found that lignosulphonic acid contained a little amount of non-acidic sulphur, which he called "excess sulphur", one can not attribute the apparent equivalence of barium and sulphur in the lignosulphonic acid, directly to the non-existence of the carboxyl group.

As lignin contains cinnamic aldehyde side chain, $-CH=CH-CHO$, although in very limitted amount[22], it may not be improbable that a part of such a group is oxidized to cinnamic acid group, $-CH=CH-COOH$, just as the formation of aldonic acid from aldose, during the cooking reaction[23]. It may, however, be quite impossible, to ascribe so much carboxyl group as one per 8–9 methoxyl observed in $\alpha$-lignosulphonic acid, to such origin, as reportedly, the amount of cinnamic aldehyde side chain is so little as one per about 50 methoxyl, and, moreover, this group survives at least partly even after the sulphonation reaction. The carboxyl group of cinnamic acid type was, however, assumed tentatively in the present communication, and ferulic acid methyl ester was used to determine the condition of the hydrolysis, as was described previously. It remains open to question whether the carboxyl group exists even in lignin in situ, or it is formed during sulphonation. This fact will be a problem to be investigated in future.

The amount of the conductometrically titrable phenolic hydroxyl group was found to be only about 1/3–1/4 of the total phenolic hydroxyl group. The titrable one must be stronger than the remaining one. It is reported that phenolic hydroxyl group with carbonyl group in its para position is very strong in comparison with ordinary phenols. Some examples are listed in the Table II. Some of them are so strong that they are

TABLE II
pK OF SOME PHENOLS[23]

| phenols | pK |
|---|---|
| $\alpha$-hydroxypropiovanillone | 7.32 |
| $\alpha$-hydroxypropiosyringone | 7.45 |
| acetovanillone | 7.50 |
| guaiacol | 9.55 |
| phenols | 9.60 |

comparable to nitrophenols. According to Goldschmid[24] and Aulin-Erdtman[25], phenolate ion with carbonyl group in its para position, shows intensive absorption at about 350 m$\mu$, which is so strong that even so little amount as one such group per 50 methoxyl is spectroscopically still measurable. Although the absorption curves of our lignosulphonic acid do not show any clear maximum at this wave length in alkaline medium, as were shown in Fig. 6, considerable decrease of absorption was observed after reduction with sodium borohydride, which is sufficient to reduce such carbonyl group, if any[26]. The amount of the weakly acidic group of the lignosulphonic acid did not, however, decrease appreciably by the reduction. One can not, therefore, expect much contribution of such phenolic hydroxyl group with carbonyl group in its para position to the weakly acidic group.

As an example of the other type of strong phenolic hydroxyl group, one can cite the report of Sprengling[27]. According to him one of the phenolic hydroxyl groups of o,o'-dihyroxydiphenyl methane is very strong due to the hydrogen bonding of one of the two phenolic hydroxyl groups to the oxygen atom of the other resulting in an enhanced ionization of the hydrogen atom of the latter hydroxyl group. On the other hand Aulin-Erdtman recognizes that one of such phenolic hydroxyl groups is rather weak in comparison to the ordinary phenols[11,25]. Such diphenylmethane structure may not be so feasible to lignin structure.

According to her one of the phenolic hydroxyl groups, which belong to o,o'-diphenol, is very strong, and the remaining one is very weak. Such very strong phenolic hydroxyl group must have been titrated, if it existed in lignosulphonic acid, The existence of diphenyl structure in lignin is not, however, established as yet. The fact that

19) C. Kullgren, *Svensk Papperstidn.*, **55**, 1 (1952).
20) H. Erdtman, *Svensk Papperstidn.*, **45**, 315, 374, 392 (1942).
21) O. Samuelson and A. Westlin, *Svensk Papperstidn.*, **50**, 141 (1947); **51**, 179 (1948).
22) E. Adler, K. Björkqvist and S. Häggroth, *Acta Chem. Scand.*, **2**, 93 (1948); E. Adler and L. Ellmer, ibid., 839; K. Kratzl, *Monatsh.*, **78**, 173 (1948); T. Harada and J. Nikuni, *J. Agr. Chem. Soc. Japan*, **23**, 415 (1950); J. Pew, *J. Am. Chem. Soc.*, **73**, 1678 (1951); **74**, 2850, 5784 (1952); T. Nakamura and S. Kitaura, *Bulletin of the Institute of Sci. and Ind. Research, Kyushu Univ.*, **8**, 1 (1952).
23) E. Hägglund, *Ber.*, **62**, 84 (1929); E. Hägglund and H. Urban, ibid., 2046; T. Marusawa, *Bulletin of the Ryojun Institute of Technology*, **1**, 351 (1929).
24) O. Goldschmid, *J. Am. Chem. Soc.*, **75**, 3780 (1953).
25) G. Aulin-Erdtman, *Svensk Papperstidn.*, **57**, 745 (1954).
26) J. Gierer, *Acta Chem. Scand.*, **8**, 1319 (1954); S. Chaikin and W. Brown, *J. Am. Chem. Soc.*, **71**, 122 (1949).
27) G. Sprengling, *J. Am. Chem. Soc.*, **76**, 1190 (1954).

dehydro-diveratric acid[28], dehydro-divanillic acid[29] and dehydro-divanillin[30] are obtained by permanganate oxidation, cupric oxide oxidation and oxidation with nitrobenzene respectively, can not prove definitely, the existence of such structure, as one may be able to ascribe the formation of such degradation products to the secondary formation during the oxidation. Its existence seems, however, to be quite probable. By nitrobenzene oxidation, Leopold obtained dehydro-divanillin from lignin, but not from model compounds with guaiacyl nucleus. Phenols without double bond conjugated with benzene nucleus in its para position dimerize easily resulting in the formation of o,o′-diphenol structure[31]. As Freudenberg's dimeric intermediates of the biosynthesis of lignin, i.e. d,l-pinoresinol[32], dehydro-diconiferyl alcohol[33], and β-coniferyl ether of guaiacylglycerol[34], have such guaiacyl groups, it seems to be quite probable that some of such guaiacyl groups condense by further dehydrogenation, at 5th position in the process of the formation of DHP.

Jodai titrated conductometrically isoeugenol and hydrolignin, which was prepared by mild hydrogenation of *picea jezoensis* with Raney nickel in alkaline medium[35]. By back titration, the phenolic hydroxyl group of isoeugenol was conductometrically titrated. The phenolic hydroxyl group of hydrolignin, which was confirmed to be almost only simple guaiacyl type was also titrable by back titration. As mentioned before, the phenolic hydroxyl group of vanillyl sulphonic acid was titrated quantitatively. It seems, therefore, to be certain that such simple phenolic hydroxyl group of guaiacole type, contained in lignosulphonic acid, contributes also to its weakly acidic group. Recently Gierer[26] proved definitely that Brauns' native lignin as well as lignin in situ, contain about one 3-methoxy-4-hydroxy-benzyl alcohol type unit per seven to nine methoxyl groups.

More than half of the total amount of the phenolic hydroxyl group of lignosulphonic acid remains untitrated by conductometric titration. This phenolic hydroxyl group must be the weaker one. Hence, it appears that a comparatively small part of the total phenolic hydroxyl group belongs to simple guaiacol type. Recently Aulin-Erdtman have reported that phenolic hydroxyl group of guaiacyl nucleus with balky substituent at 5th position is rather weak. Such phenols were not ionized completely even at pH 12. In connection with the nature of the different phenolic hydroxyl groups of lignosulphonic acid, the conductometric titrations of various model compounds will be reported later.

28) K. Freudenberg, K. Engler, E. Flickinger, A. Sobeck and F. Klink, *Chem. Ber.*, **71**, 1817 (1938).
29) I. Pearl, *J. Am. Chem. Soc.*, **72**, 2309 (1950).
30) B. Leopold, *Acta Chem. Scand.*, **6**, 38 (1952).
31) H. Erdtman, *Biochem. Z.*, **258**, 172 (1933).
32) K. Freudenberg and H. Dietrich, *Chem. Ber.*, **86**, 4 (1953).
33) K. Freudenberg and H. Hübner, *Chem. Ber.*, **85**, 1181 (1952).
34) K. Freudenberg and W. Fuchs, *Chem. Ber.*, **87**, 1824 (1954).
35) S. Jodai, *J. Soc. Chem. Ind. Japan*, **47**, 958 (1944).
36) J. Fisher, W. Hawkins and H. Hibbert, *J. Am. Chem. Soc.*, **63**, 3031 (1941).

## Experimental

**Preparation of Ba-lignosulphonate, methylation with diazomethane or with dimethyl sulphate, and reduction with sodium borohydride.**—Barium lignosulphonate was prepared from the waste liquor of experimental cooking of spruce and birch, just in the same manner as was used in the previous communication[1].

In the case of birch lignosulphonic acid, the precipitate obtained by 1-(N-piperidinoacetylamino)-naphthalene was dissolved in 70% aceton, 2 N sulphuric acid added, untill a clear solution was obtained, and the solution was passed through IR 120 in hydrogen form. Acetone was distilled off in vacuo, and the solution was neutralized with barium carbonate and treated further as usual.

Barium lignosulphonate was kept in an etherial solution of diazomethane with occasional shaking, and changing the solution four times during thirty days, until constant methoxyl content was reached.

Barium lignosulphonate was methylated with dimethyl sulphate and alkali as usual, and separated by 1-(N-piperidinoacetylamino)-naphthalene sulphate.

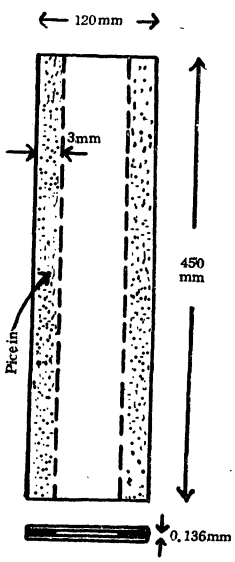



Fig. 8. Thin cell for UV-absorption mesurement.

Borohydride reduction of barium lignosulphonate was performed by dissolving the barium salt (15 g.) in water (200 ml.), adding sodium borohydride (2 g.), and keeping the solution at room temperature for four hours. The reduced barium lignosulphonate was precipitated by alcohol.

**Hydrolysis.**—Barium lignosulphonate (500 mg.) was dissolved in 1 N sodium hydroxide (20 ml.), kept at 30°C in an ampoule sealed carefully with nitrogen. After ion exchange, the solution was titrated.

**Measurement of UV-absorption with very thin cell.**—Two quartz plates of the same size, with the side wall of the ordinary cell for Beckman spectrophotometer, was put together with picein as Fig. 8. The washing of the inside was effected by applying slight suction on one end, and immersing the other end in suitable solvent. The cell is very easily filled with solution by attaching a drop of the solution to one end of the dried cell, the solution being sucked into it automatically by capillary action. The thickness was measured by the absorption of methylene blue (316 m$\mu$), methyl orange (458 m$\mu$) and lignosulphonic acid (280 m$\mu$), the average thickness being $0.136 \pm 0.001$ mm. Beckman spectrophotometer model DU was used.

## Summary

$\alpha$-Lignosulphonic acid has about one weak carboxyl group per 8–9 methoxyl, and about the same, or somewhat lesser amount of conductometrically titrable phenolic hydroxyl group, and both these groups correspond to the so-called weakly acidic group of lignosulphonic acid.

The authors are indebted to Dr. H. Okada, the head of our laboratory, and to Miss. S. Suehiro for their encouragement.

*Research Laboratory of the Kokusaku Pulp Co., 184, 1-Chome, Kamiochiai, Shinjuku-ku, Tokyo*

# *Modifications of Normal Fatty Acid Amides*

By Susumu KUROKAWA

(Received July 2, 1955)

## Introduction

It is well known that A. Müller[1] concluded, from his X-ray measurements, that molecules of normal paraffines with carbon numbers ranging from 21 to 27 rotate around their long axis above certain critical temperatures which are several degrees below their melting points. Similar rotational transformation has also been found in the experiments of X-ray diffractions[2,3], specific heats[4] and dielectric properties[5,6,7] of some normal alcohols. It seems interesting to confirm such transformation in some other long chain compounds, especially in those containing hydrogen bonds. The object of the present experiment is to examine if any discontinuous changes occur in X-ray diffraction lines of normal fatty acid amides of even carbon number from 4 to 18 between room temperature and the individual melting points.

1) A. Müller, *Proc. Roy. Soc. A.*, **138**, 514 (1932).
2) J.D. Bernal, *Nature*, **123**, 870 (1932).
3) K. Sano and Y. Kakiuchi, *J. Phys. Soc. Japan*, **4**, 365 (1949).
4) Y. Kakiuchi, T. Sakurai and T. Suzuki, *J. Phys. Soc. Japan*, **5**, 369 (1950).
5) Y. Kakiuchi, *Proc. Japan Acad.*, **23**, 65 (1947).
6) T. Sakurai, *J. Phys Soc.*, **6**, 431 (1949).
7) J.D. Hottman and C.P. Smyth, *J. Am. Chem. Soc.*, **71**, 431 (1949).

## Experimental

The acid amides were all synthesized by the following reaction.

$$2RCOOH + H_2NCONH_2 \longrightarrow RCONH_2 + CO_2 + RCOONH_4$$

After heating the mixture of equivalent fattty acid and urea for several hours in a flask, the amide was separated by distillation. All amides thus obtained were purified by vacuum distillation and by repeated recrystallization from adequate solvents, their melting points being shown in Table I.

The powdered specimens were enclosed in thin walled glass capillary tubes and their X-ray diffraction photographs were taken with the Cu $K_\alpha$ radiation filtered by nickel foil. The distance between the specimen and the film was 8.03 cm. The time of exposure was about five to ten minutes at about 30 *k*V. and 60–70 MA. using rotating copper anode.

The specimen was heated to the required temperature by a small electric furnace, which was placed so as to surround the capillary tube at the

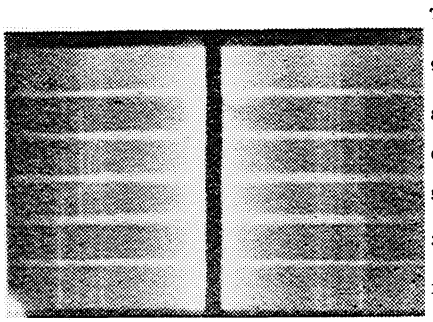



Photo. 1. $C_{12}$-amide

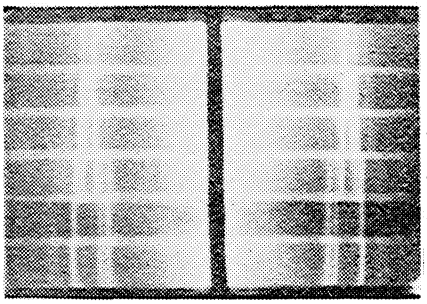



Photo. 2. $C_{16}$-amide Type I.

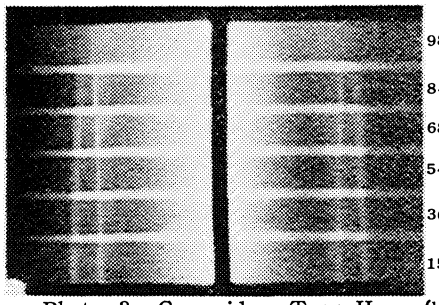



Photo. 3. $C_{18}$-amide Type II.

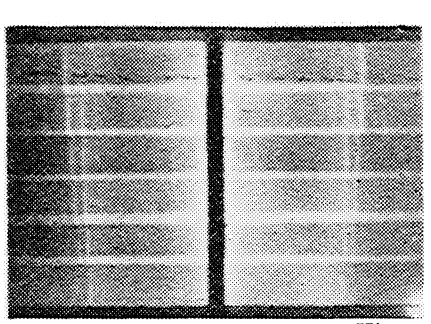



Photo. 4. $C_{18}$-amide Tpye II'.

center of the camera. The temperature of the specimen was measured by the thermometer, the bulb of which was close to the specimen. It was kept constant during the exposure within about 2°C. In order to find easily small shifts of diffraction lines due to the variation of temperature, the temperature of the specimen was varied stepwise and a whole series of photographs was recorded on the same film as shown in the Photos. 1–4.

## Experimental Results and Discussion

**Modification at Room Temperature.**—The measured values of short and long spacings at room temperature are summarized in Table I, their relative intensities of reflections estimated visually being given in five degrees as usual. In the cases of lower amides than $C_{16}$ the specimens crystallized from solvents show the same diffraction lines as those crystallized from the molten states. The general behaviours of the diffraction lines are close to those obtained by F. W. Matthews, G. G. Warren and J. H. Michell[8], though the individual values of reflection lines do not perfectly coincide.

In the case of $C_{16}$ amide four types of modifications exist at room temperature. The

TABLE I

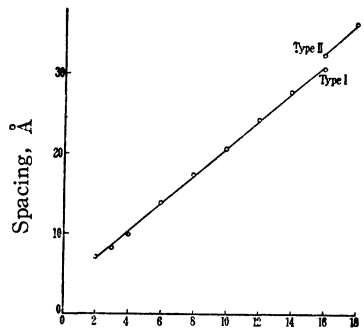
THE X-RAY DIFFRACTION DATA ON THE ACID AMIDES

| Acid amide | m.p. (°C) | Type | Short spacing (Å) | | | | | | | Long spacing (Å) |
|---|---|---|---|---|---|---|---|---|---|---|
| Butyric acid amide | $C_4$ 113 | | 3.79(s) | 4.05(m) | 4.20(w) | 4.68(vs) | | | | 9.95 |
| Caproic acid amide | $C_6$ 98 | | 3.56(s) | 4.30(vw) | 4.39(w) | 4.88(vs) | | | | 13.92 |
| Caprylic acid amide | $C_8$ 110 | | 4.07(s) | 4.36(m) | 4.55(m) | 4.94(s) | | | | 17.41 |
| Capric acid amide | $C_{10}$ 96 | | 3.33(w) | 3.48(vw) | 3.70(vs) | 4.19(m) | 4.45(s) | 4.94(s) | | 20.63 |
| Lauric acid amide | $C_{12}$ 97 | | 3.68(s) | 4.12(m) | 4.53(m) | 4.95(m) | | | | 24.32 |
| Myristic acid amide | $C_{14}$ 102 | | 3.51(vw) | 3.59(vw) | 3.76(w) | 3.96(s) | 4.51(m) | 4.92(m) | | 27.73 |
| Palmitic acid amide | $C_{16}$ 106 | I | 3.82(vs) | 4.58(s) | 4.95(s) | | | | | 30.62 |
| | | II | 3.39(vw) | 3.49(vw) | 3.78(vs) | 3.94(w) | 4.18(m) | 4.52(vs) | 5.02(w) | 32.41 |
| | | II' | 3.26(vw) | 3.77(s) | 4.16(vw) | 4.46(w) | | | | 32.46 |
| | | III | 3.82(vs) | 4.34(m) | 4.53(w) | | | | | 44.50 |
| Stearic acid amide | $C_{18}$ 107 | II | 3.77(s) | 3.86(m) | 4.54(s) | 5.09(vw) | | | | 36.22 |
| | | II' | 3.26(vw) | 3.71(s) | 3.87(m) | 4.10(vw) | | | | 36.26 |
| | | III | 3.80(vs) | 4.32(m) | 4.52(w) | | | | | 49.65 |

The symbols, vs., s., m., v., vw. show the relative intensities of reflections estimated visually, very strong, strong, medium, weak, very weak, respectively.

8) F.W. Matthews, G.G. Warren and J.H. Michell, *J. Anal. Chem.*, 22, 514 (1950).

specimen crystallized from solvents generally shows Type I, while that crystallized from the molten state show Type II (Table I). The relation between the long spacing and the number of carbon atoms in the chain is shown in Fig. 1. The linear relation existing




N. (carbon number)

Fig. 1. The long X-ray spacings for acid amides as a function of the number of C atoms.

usually in many other long chain compounds is seen also in the present case. It is noted, however, that the long spacing of Type I lies just on the linear extension of those of lower amides, while that of Type II shows a little greater value. T. Sakurai has recently concluded from his structural analysis that $C_{16}$ amide has two types[9], parallel chain and cross chain types, the former appearing in the crystal from molten state and the latter in that from solvents, and also suggested that in lower amides the cross chain type only may exist. Although this suggestion should be confirmed by the structural analysis of lower amides, the present result does not seen to contradict it. In the case of $C_{18}$ amide the distinction between Types I and II is not observed. The observed value of the long spacing, however, seems to correspond to that of Type II of $C_{16}$ amide as seen in Fig. 1.

Type II' appears when the molten $C_{16}$ and $C_{18}$ amides are solidified very slowly as written in the next section. Type III is observed in a thin flake obtained when the acetic acid solution of $C_{16}$ and $C_{18}$ amides are evaporated slowly on a glass plate. From their great values of long spacings it is considered that in the crystal of Type III the dimer linked together by hydrogen bonds between the amide ends stands perpendicular to the basal plane. If this is the case, the long spacing of $C_{18}$ amide will be greater than that of $C_{16}$ amide by four times the C-C distance projected on the chain axis; viz. $1.27\times4=5.08$ Å, the observed value 5.15 Å agreeing nearly with it. Among the four types, Type II seems to be the most stable from as seen below.

**Temperature Effects.**—In the cases of $C_{14}$-$C_{10}$ amides the diffraction lines do not present any discontinuous changes with temperatures up to the melting points. The long spacings increase continuously with the rise of temperature, while in short spacings some expand and some others contract. The amounts of these shifts are in the order of some per-

TABLE II

THE TEMPERATURE EFFECTS ON THE X-RAY DIFFRACTION DATA OF $C_{12}$ AND $C_{14}$-AMIDES (SHORT SPACINGS)

| temp. (°C) | Short spacings (Å) | | | | | | |
|---|---|---|---|---|---|---|---|
| | $C_{12}$-amide | | | | | | |
| 13 | 4.95(m) | | 4.53(m) | 4.12(m) | | 3.68(s) | |
| 31–32 | 4.93 | | 4.51 | 4.09 | | 3.67 | |
| 39 | 4.90 | | 4.48 | 4.11 | | 3.67 | |
| 45–46 | 4.91 | | 4.48 | 4.11 | | 4.66 | |
| 50–51 | 4.91(m) | 4.65(vw) | 4.46(w) | 4.19(s) | 3.74(w) | 3.61(vw) | |
| 68 | 4.90 | 4.68 | 4.47 | 4.20 | 3.76 | 3.63 | |
| 84–86 | 4.90 | 4.69 | 4.48 | 4.22 | 3.77 | 3.63 | |
| 99–100 | 4.93 | 4.69 | 4.47 | 4.24 | 3.78 | 3.64 | |
| | $C_{14}$-amide | | | | | | |
| 16 | 4.92(m) | 4.51(m) | 3.96(s) | 3.76(w) | 3.59(vw) | 3.51(vw) | |
| 34 | 4.91 | 4.50 | 3.96 | 3.76 | 3.58 | 3.52 | |
| 48–50 | 4.91 | 4.50 | 3.97 | 3.76 | 3.59 | 3.52 | |
| 55 | 4.89 | 4.49 | 3.95 | 3.75 | 3.57 | 3.50 | |
| 59 | 4.89 | 4.48 | 3.95 | 3.74 | 3.58 | 3.50 | 3.41(vw) |
| 63 | 4.90 | 4.48 | 3.95 | | 3.60 | 3.51 | 3.43 |
| 66 | 4.89 | 4.51 | 3.97 | | 3.60 | 3.53 | 3.46 |
| 86 | 4.91 | 4.52 | 3.98 | | 3.61 | 3.52 | 3.46 |
| 94–96 | 4.92 | 4.53 | 3.99 | | 3.61 | 3.53 | 3.45 |

9) T. Sakurai, *J. Phys. Soc. Japan*, (to be published soon).

centages between room temperature and the melting points and are completely reversible with temperature.

The long spacing as well as short spacings of $C_{12}$ amide present abrupt changes at about 48°C as shown in Table II and Photo. 1. This transformation is reversible with temperature. In the case of $C_{14}$ amide the expansion of long spacing is not observed, while in the reflection of short spacings one diminishes its intensity with the increase of temperature, disappearing at about 59°C and another one appears at the same time. These changes, however, are gradual and reversible with temperature, not showing a distinct transition point. (Table II)

Type I of $C_{16}$ amide and Type III of $C_{16}$ and $C_{18}$ amides both transform into Type II at high temperature. The former shows a distinct transformation point at 76°C, while the latter does not change abruptly. The very long spacing of the latter contracts gradually with temperature accompanying the gradual appearance of the characteristic long spacing of Type II, and Type II only remains above 80°C. It may be considered that in Type III the chain axis standing perpendicularly to the basal plane begins to tilt on heating, partially forming Type II. Type II, once formed by heating, does not return to Type I or III without recrystallization from solvents.

When Type II of $C_{16}$ amide is heated, the long spacing expands continuously. Among the short spacings the one which shows strong reflection at 3.78 Å, splits into a doublet between 49°C and 85°C, becoming again a singlet of 4.00 Å near the melting point as shown in Fig. 2. Another one, which shows strong reflection at 4.52 Å, contracts continuously, decreasing to 4.30 Å near the melting point. This approach of two strong reflection lines on heating appears to be similar apparently to the tendency observed by Müller in the case of paraffine. In the present case, however, the distinct transformation point to become a single reflection line can not be observed below the melting point.

It is interesting to note that contrary to the cases of lower amides a phenomenon of hysteresis is observed in the case of $C_{16}$ amide. When Type II is cooled after heating up to near the melting point, the temperature effects are just reversed with those of heating. When it is cooled slowly, however, after heating up to the molten state, new short spacings appear and they change continuously on cooling, forming a different type, Type II', at room temperature (Fig. 2). If it is cooled

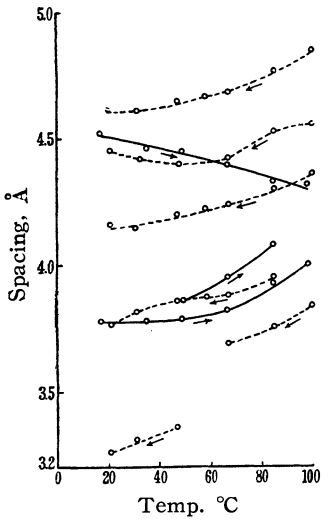



Fig. 2. The temperature effects on the X-ray spacings of $C_{16}$-amide. (Type II. & II'.)

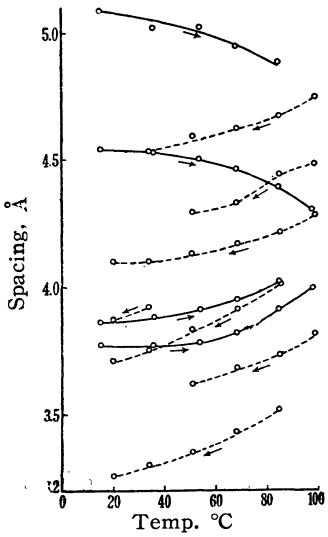



Fig. 3. The temperature effects on the X-ray spacings of $C_{18}$-amide. (Type II. & II'.)

rapidly to room temperature from the molten state, Type II always appears. As to the long spacing Type II' is not very different from Type II. The analogous phenomenon of hysteresis is observed also in the case of $C_{18}$ amide as shown in Fig. 3.

These phenomena are probably due to the following reasons: that the molecules are more loosely bound in higher amides than in lower amides, and also that different arrangements of atoms in the amide groups may occur on solidification from the molten state. The detailed discussion, however, must be postponed until the complete structural

analysis, now in progress, is accomplished.

In conclusion the author wishes to express his sincere thanks to Prof. S. Yoshida for his kind guidance throughout this experiment. A part of the expense for the experiment has been defrayed from a grant given by the Ministry of Education, to which the author's thanks are due.

*Department of Physics and Chemistry*
*Gakushuin University Mejiro,*
*Tokyo*

# *Spectrochemical Study of Microscopic Crystals. IX.*[1] *Absorption Spectra and Structure of Cobalt(II) Mercury(II) Tetrathiocyanate*

By Shoichiro YAMADA and Ryutaro TSUCHIDA

(Received July 14, 1955)

The structure of cobalt(II) mercury(II) tetrathiocyanate has long been discussed by a number of chemists[2,4]. In 1947 Jeffery[3] investigated the crystal structure with X-ray, showing that the sulphur atoms of the SCN-groups were attached to the mercury atom in tetrahedral co-ordination. However, he did not touch on the possibility of the linkage between the cobalt atom and NCS-groups, only stating that a cobalt atom is surrounded by nitrogen atoms. The present work was undertaken in order to clarify the structure of the compound in the crystalline state. In this paper polarized absorption spectra of the compound have been determined, and the results discussed in relation to the structure of the compound.

## Experimental

**Materials.**—Cobalt(II) mercury(II) tetrathiocyanate, $CoHg(SCN)_4$, was prepared by the method of Hantzsch and Shibata[4]. Indigo-blue, prismatic crystals thus obtained belong to the tetragonal system and show straight extinction on the prism face. A slight dichroism is observed on the prism face under the microscope. The measurements of the absorption spectra were made on the prism face with polarized light having its electric vector along and perpendicular to the needle axis.

Potassium tetrathiocyanato-mercurate(II) was prepared from mercuric thiocyanate and potassium thiocyanate according to the method of Rosenheim and Cohn[5]. Measurement of absorption spectrum was made with its aqueous solution containing an excess of potassium thiocyanate.

**Measurements.**—Quantitative measurements of absorption spectra of crystals were made by Tsuchida-Kobayashi's microscopic method[6] with polarized light in the region covering 7500 to 2400 Å. The notation, $\alpha$, represents absorption coefficient per mm. of a crystal. Molecular absorption coefficients of a crystal, $K$, were calculated from the relation, $K=10\alpha M/\rho$, where M and $\rho$ denote formula weight of a complex compound, and density of a crystal, respectively.

Absorption spectrum in solution was determined with a Beckman DU quartz-spectrophotometer. $\varepsilon$ represents molar extinction coefficient.

## Results and Discussion

The results of the measurements are shown in Fig. 1 and Table I. The a- and b-absorption represent absorption with the electric

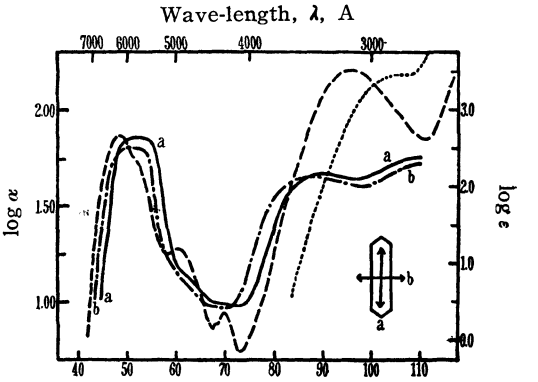



Fig. 1. Absorption spectra of $CoHg(SCN)_4$ in the crystalline state and its component complexes in solution. — — — —, $K_2[Co(NCS)_4]$, ·····, $K_2[Hg(SCN)_4]$. The curves in solution are taken from ref. 7.

1) Part VIII of this series, S. Yamada, A. Nakahara and R. Tsuchida, This Bulletin, **28**, 465 (1955).
2) For example, Y. Shibata, *J. Chem. Soc. Japan*, **35**, 807 (1914); T. Inoue, *J. Chem. Soc. Japan*, **48**, 177 (1927).
3) J.W. Jeffery, *Nature*, **159**, 610 (1947).
4) A. Hantzsch and Y. Shibata, *Z. anorg. Chem.*, **73**, 314 (1912).
5) A. Rosenheim and R. Cohn, ibid., **27**, 281 (1901).
6) R. Tsuchida and M. Kobayashi, "The Colours and the Structures of Metallic Compounds," Zoshindo, Osaka, 1944, p. 180; This Bulletin, **13**, 619 (1938).

vector parallel and perpendicular to the needle axis. The present measurement indicates that the crystal of the compound shows an absorption band at about $51\times10^{13}$/sec. and another band commencing at about $80\times10^{13}$/sec. Although the crystal analysis demonstrated the existence of the group, $Hg(SCN)_4$, the band at about $50\times10^{13}$/sec. can not be ascribed to the group, since the potassium salt, $K_2Hg(SCN)_4$, in aqueous solution shows absorption at far shorter wave-length. Alternatively, the band is considered to correspond to the band at the longer wave-length of the $Co(NCS)_4$-ion in the crystal of $K_2Co(NCS)_4\cdot4H_2O$ as well as alcoholic solution. It is concluded, therefore, that $CoHg(SCN)_4$ in the crystalline state should contain the group, $Co(NCS)_4$, as in the crystal of $K_2Co(NCS)_4\cdot4H_2O$[7,8]. In other words, four NCS-groups are attached to a cobalt atom through their nitrogen atoms. The linkage between the nitrogen atom and the cobalt atom is most likely to be largely electrostatic, judging from the tetrahedral configuration of the $Co(NCS)_4$-group[7].

The band at $50\times10^{13}$/sec. is found to be a little polarized. This fact shows that the co-ordination of four NCS-groups around a cobalt atom in the $Co(NCS)_4$-group deviates from regular tetrahedron. The similar conclusion was formerly obtained with the crystal of $K_2Co(NCS)_4\cdot4H_2O$[7]. Moreover, the dichroism for the band at $50\times10^{13}$/sec. of $CoHg(SCN)_4$ (Table I) is found to be similar

TABLE I

ABSORPTION MAXIMA OF $CoHg(SCN)_4$

| | $\nu$,$10^{13}$/sec. | $\log\alpha$ | $K$ | half width |
|---|---|---|---|---|
| a-abs. | 51.6 | 1.86 | $117\times10^2$ | 10.2 |
| b-abs. | 50.6 | 1.80 | $102\times10^2$ | 10.5 |

to the dichroism of the potassium salt. That is, the absorption with its maximum at the shorter wave-length has larger absorption coefficient than the absorption with its maximum at the longer wave-length. This also seems to support the above conclusion.

The absorption of $CoHg(SCN)_4$ at about $80\times10^{13}$/sec. and shorter wave-length may be considered as superposition of the absorption of $Hg(SCN)_4$- and $Co(NCS)_4$-groups, since both the $Hg(SCN)_4$ and $Co(NCS)_4$ ions in the potassium salts exhibit absorptions in the above regions.

Summarizing the above consideration, a NCS-group of $CoHg(SCN)_4$ in the crystalline state combines through its sulphur atom with a mercury atom and through its nitrogen with a cobalt atom. The effect of combination of the sulphur atom with a mercury atom on the Co-NCS linkage may be observed, for example, in the absorption bands due to the $Co(NCS)_4$-group. The absorption spectra of the crystal of $CoHg(SCN)_4$ is different from that for $K_2Co(NCS)_4\cdot4H_2O$ in the following respects. (1) The width of the band at the longer wave-length is larger than that of the crystal of the potassium salt. (2) The band is slightly more hypsochromic than that in the potassium salt. These differences may be understood as due to the change in the electronic state of the nitrogen atom and consequently in its linkage to the cobalt atom, which would be caused by co-ordination of the sulphur atom to a mercury atom.

## Summary

Polarized absorption spectra of $CoHg(SCN)_4$ in the crystalline state have been determined by Tsuchida-Kobayashi's microscopic method in the regions between 2400 and 7000 Å.

Absorption spectra of $HgCo(NCS)_4$ shows the existence of the $Co(NCS)_4$-group. Thus it has been concluded that the NCS-group is attached to a cobalt atom through a nitrogen atom, and to a mercury atom through a sulphur atom on the other end of the NCS-group.

The authors wish to thank Mr. T. Ninomiya for his assistance in the experiments and Mr. H. Matsuo of Hiroshima University for his interest in the present work. This work was supported by a grant from the Ministry of Education.

*Department of Chemistry, Faculty of Science, Osaka University, Nakanoshima, Osaka*

7) S. Yamada and R. Tsuchida, This Bulletin, **27**, 436 (1954).

8) G.S. Zhdanov and Z.V. Zvonkova, *Zhur. Fiz. Khim.*, **24**, 1339 (1950); C.A., **45**, 6001 (1951).

# *Syntheses of Adenosinesulfuric Acids*

By Fujio EGAMI and Noriko TAKAHASHI

(Received July 22, 1955)

As is well known, adenosinephosphoric acids play important roles in metabolism as such or as components of the coferments such as DPN, TPN, FAD, CoA etc. In 1953[1], I. Yamashina and one of us (Egami), considering the fact that the substances having sulfuric acids group in place of phosphoric acid group in these metabolites might compete with the latter in metabolism or in biochemical reactions in vitro, tried to synthesize adenosinesulfuric acids. In fact they have found in the preliminary experiments that adenosinemonosulfate (AMS) competes with DPN in the dehydrogenation of ethanol by alcohol dehydrogenase. However, AMS used in the experiments was not a chemical individual, but a mixture of adenoshine-5'-monosulfate and adenosine-3'- or/and 2'-monosulfate. It is quite clear that in order to carry out quantitative studies concerning the effects of adenosinesulfates on metabolism or on biochemical reactions, adenosinesulfate with a definite constitution must be used. So we tried to separate adenosinesulfates by ion-exchange resins. The present paper describes the separation of adenosinesulfates and especially the preparation of adenosine-5'-monosulfate.

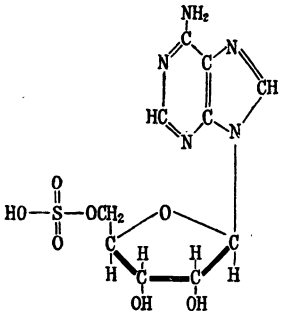


Fig. 1. Adenosine-5'-monosulfuric acid.

## Experimental

**1. Syntheses of Calcium Adenosinesulfates.**—Chlorosulphonic acid in dry chloroform was added slowly to adenosine solution in dry pyridine at 0°C with vigorous stirring and with strict prevention of moisture. After standing overnight at room temperature, the upper solvent layer was removed by decantation, and the remaining syrupy material was dissolved in water, then neutralized with calcium carbonate. After removal of calcium sulfate and the excess of calcium carbonate, the filtrate was evaporated in vaccuo (40°C/15mmHg) until it became syrupy. A crude calcium salt was obtained by addition of alcohol. As will be shown later, the crude product was composed of unchanged adenosine and a mixture of calcium adenosinemono-, di- and trisulfate. Experiments were carried out under several conditions. It was found that the proportion of each component varied according to the amount of chlorosulphonic acid used and to the reaction temperature. Two examples, which will be described later, were carried out with the following conditions:

(Example 1) 2 g. adenosine in 100 ml. pyridine, 1.3 ml. chlorosulphonic acid in 4 ml. chloroform, reaction temperature 0°C.

(Example 2) 2.5 g. adenosine in 130 ml. pyridine. 3 ml. chlorosulphonic acid in 7 ml. chloroform, reaction temperature 13~15°C.

**2. Analysis of the Crude Product.**—A method for the quantitative separation of AMP, ADP and ATP by ion-exchange chromatography has been devised by Cohn and Carter[2]. By slight modification of their method, the resolution of the mixture of adenosinemono-, di- and trisulfuric acid (AMS, ADS, ATS) and unchanged adenosine into the individual components has been achieved successfully. The aqueous solution of crude product was passed through a column of an anion exchanger, Dowex-1. Unreacted adenosine was removed by washing with water, but the other acidic components remained on the column. Subsequent elution of the adsorbed column, successively with 1) 0.01N hydrochloric acid (AMS), 2) 0.2 or 0.5N hydrochloric acid (ADS), and 3) 1N hydrochloric acid (ATS), gave each component completely in separate fractions. In spite of the three possible structures for AMS, the largest part (100-95%) of effluents with 0.01N hydrochloric acid was composed of only one sharp peak, which was later proved to be adenosine-5'-monosulfuric acid. The other minor components, observed in a few cases, were too small in quantity to be served for analysis and remained unidentified.

A Beckman ultraviolet spectrophotometer Model DU was used to detect and estimate adenosine derivatives in effluents, taking advantage of the characteristic ultraviolet adsorption at 260mμ.

Quantitative analysis of N and S content for each fraction, also served as a means of identification.

The results obtained with the products, synthe-

1) I. Yamashina and F. Egami, *J. Japan Biochem. Soc.*, 23, 281 (1953); F. Egami, *Medicina Revuo*, 2, 26 (1954).

2) W.E. Cohn and C.E. Carter, *J. Am. Chem. Soc.*, 72, 4273 (1950).

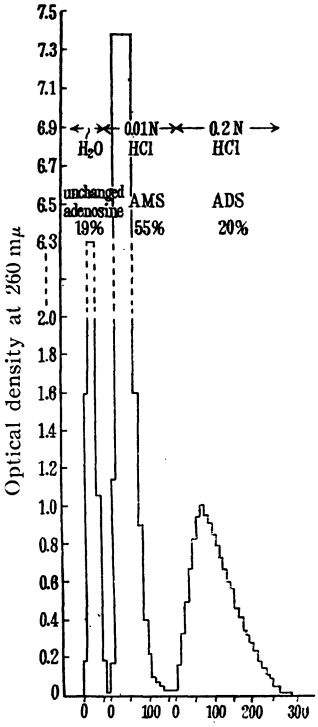



Fig. 2. (example 1). Ion-exchange separation of adenosinesulfates.
Exchanger: Dowex-1 (50~100 mesh), 0.8 $cm^2 \times 9$ cm. chloride form.
Flow rate: 1 ml./min./$cm^2$.
Test material: 30 mg.

sized under the conditions described above, was shown in Figs. 2 and 3, on which the experimental details for the analysis will be seen.

**3. Preparation of Calcium and Barium Adenosinemonosulfate.**—Two procedures were tried in order to obtain these components separately, one with hydrochloric acid as eluting solution, another with sulfuric acid. These were carried out as follows:

**(A) Elution with Hydrochloric Acid.**—Column of Dowex-1 (50~100 mesh) in the chloride form, 3.1 $cm^2 \times 20$ cm., flow rate 1 ml./min./$cm^2$ was used. 0.5 g. of the crude product in 100 ml. of water was passed through the column and the adsorbed materials were eluted with hydrochloric acid in a similar manner as used in the analytical procedure.

The pooled AMS fraction of the effluents (ca. 350 ml.) were neutralized with calcium carbonate and evaporated in vaccuo (40°C/15 mmHg) until it became syrupy. By addition of alcohol, the precipitate of Ca-AMS was obtained. The purification was achieved by reprecipitation with alcohol.

But, the similar procedure was not suitable for the preparation of di- and trisulfate in solid form, because of the high concentration of hydrochloric acid in ADS and ATS fractions, which brought about the formation of a large amount of calcium chloride interfering with the precipitation of Ca-

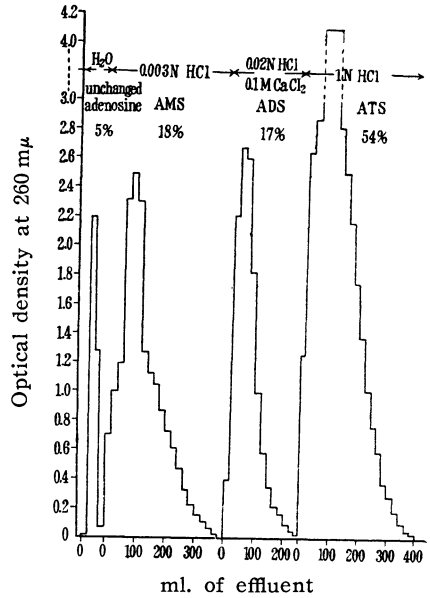



Fig. 3. (example 2). Ion-exchange separation of adenosinesulfates.
Exchanger: Dowex-1 (50~100 mesh), 1.77 $cm^2 \times 4$ cm. chloride form.
Flow rate: 0.5 ml./min./$cm_2$.
Test material: 60 mg.

ADS and Ca-ATS. However, this procedure was proved to be quite satisfactory for the analysis of these components, as described in the preceding paragraph.

**(B) Elution with Sulfuric Acid.**—Column of Dowex-1 (50~100 mesh) in the hydroxide form, 3.1 $cm^2 \times 31$ cm., flow rate 1 ml./min./$cm^2$ was used. 2 g. of the crude product in 100 ml. of water was served as starting material. Considerable amount of unreacted adenosine was adsorbed in this case, which was removed as a first fraction by elution with 0.03N sulfuric acid. Continuing elution with the same acid gave AMS as a sharply distinct fraction.

But, the other components did not show any difinite peaks with 0.5N, 1N, 2N, and even with 6N sulfuric acid. Therefore, application of this method to the elution of ADS and ATS was not satisfactory.

The pooled AMS fraction of the effluents (ca. 900 ml.) was neutralized with excess barium carbonate. By concentrating the filtrate in vaccuo (40°C/15 mmHg), Ba-AMS was obtained in colorless crystalline form. It was recrystallized from water.

**4. Nature of Ba-AMS.**—Crystalline Ba-AMS was found to contain 2 molecules of water which was lost by heating at 100°C in vaccuo over conc. sulfuric acid. The analytical results coincided with the formula $C_{10}H_{12}O_7N_5S$ Ba/2. Found: N, 16.5; S, 8.12; Ba, 16.4; Calcd.; N, 16.8; S, 7.73; Ba, 16.5%.

For the decision among possible positions 5′, 3′, and 2′ as the point of attachment of the sulfuric acid radical to ribose, the oxidation of Ba-AMS

with metaperiodate was examined. One mole of Ba-AMS consumed 0.94 moles of the oxidant. This indicates that the sulfuric acid radical is attached to the 5'-position of the ribose.

**Spectrographic Data:**[3] Measurements were made with a Beckman ultraviolet spectrophotometer Model DU. Comparisons of the ultraviolet absorption spectra from 220 mμ to 300 mμ of 0.1N hydrochloric acid solution of adenine, adenosine and Ba-AMS were shown in Fig. 4. It was clear from Fig. 4 that adenosine and Ba-AMS had a peak at 257mμ. But the maximum molecular extinction coefficient of AMS resembled more closely that of adenine than that of adenosine.

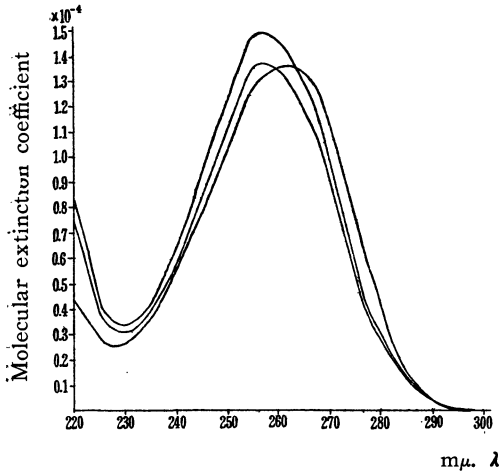



Fig. 4. Absorption spectra of adenosine (higher peak at 257 mμ), AMS (lower peak at 257 mμ) and adenine (peak at 262 mμ) respectively.

3) J.M. Gulland and E.R. Holiday, *J. Chem. Soc.*, 1936, 765.

## Summary

Syntheses of adenosinesulfuric acids were achieved by sulfation of adenosine with chlorosulphonic acid.

The crude product was a mixture of AMS, ADS and ATS, and the proportion of each component varied according to the amount of chlorosulphonic acid used and to the reaction temperature.

Quantitative separation of AMS, ADS and ATS has been achieved successfully by ion-exchange chromatography.

Barium adenosine-5'-monosulfate was obtained in crystalline form, and the ultraviolet absorption spectra were measured.

*Department of Chemistry, Nagoya University, Nagoya*

# *The State of Metal Ion in Aqueous Solutions and Its Surface Chemical Effects. I. Cobalt Ion-Stearic Acid Monolayer Interaction*

By Ryohei MATUURA and Hideo KIMIZUKA

(Received June 9, 1955)

It has been shown recently by Sasaki and Matuura[1,2] and by Schulman et al.[3,4,5] that certain metal ions interact with fatty acid monolayers specifically over a pH range characteristic of each ion. In the case of the monolayer of stearic acid this specific interaction has been observed through increase in the area per molecule of the acid, in compressibility and in rigidity of the monolayer. Metal ions which have been proved to give rise to such a remarkable change in the properties of the stearic acid monolayer are either ions of the transition elements or polyvalent ions, such as Co, Ni, Cu, Zn, Hg, Al, Fe, Ce or Th ions. The nature of the interaction between these metal ions and fatty acid monolayers has not yet been definitely postulated. Sasaki and Matuura proposed that metal soap of highly polymeric structure is produced in the monolayer by the interaction between fatty acid molecules and metal ions over a pH range characteristic of each ion. Schulman et al. presented the idea that the basic metal ions interact with the fatty acid monolayer at the pH of maximum interaction, and cross-linking results between neighboring molecules in the monolayer by hydrogen bonding. It is probable that the metal ion-monolayer interac-

1) T. Sasaki and R. Matuura, This Bulletin, **24**, 274 (1951).
2) R. Matuura, ibid., **24**, 278 (1951).
3) G.A. Wolstenholme and J.H. Schulman, *Trans. Faraday Soc.*, **46**, 475 (1950); **47**, 788 (1951).
4) J. H. Schulman and M. Z. Dogan, *Faraday Soc. Discussion*, **16**, 158 (1954).
5) J.G.N. Thomas and J.H. Schulman, *Trans. Faraday Soc.*, **50**, 1139 (1954).

tion has much to do with the state of the metal ion in aqueous solutions. It is known that certain metal ions of the transition elements or polyvalent ions exist in aqueous solutions as polynuclear cations in some cases, and sometimes the solution reveals rather colloidal behaviors around pH of hydroxide precipitation. In this respect information would be given from the studies of the radiocolloids of these elements which have been shown to be formed in dilute solutions under suitable conditions.[6,7] Although the mechanism of radiocolloid formation has not yet been established, it is interesting to note that in some metal ions (e.g., Th[8] or Ce[9] ions) the pH range of the specific interaction with fatty acid monolayers corresponds to that of colloid formation. It may be suggested also that in other metal ions in question their state in aqueous solutions would be much complicated in some cases and this complicated state would have a close connection with the specific interaction with the fatty acid monolayer. It is therefore necessary to study the metal ion-monolayer interaction with special reference to the state of the metal ion in aqueous solutions. In the present work the interaction between stearic acid monolayer and cobalt ion was investigated under various conditions along this line.

## Experimental

The surface pressure of the monolayer was measured by the modified Wilhelmy type surface balance described elsewhere[10]. The method of measurement of surface viscosity and rigidity was the same as that in the earlier work[11]. Except for the study of the effect of aging of the solution, the monolayer was formed on a freshly prepared $10^{-3}$ mol./l. solution of $CoCl_2$, which was purified by recrystallization. Unless otherwise stated, the compression of the monolayer was started ten minutes after spreading. The pH of the solution was adjusted by HCl and NaOH, changing from 2 to 10.

The effect of the aging of the solution on the cobalt ion-stearic acid monolayer interaction was studied by measuring surface pressures of the monolayer spread on the solution stored for periods of time in a large glass-stoppered bottle at room temperature. The pressure-area relations were determined for each aging time of the solution.

In order to know the effect of other electrolytes on the cobalt ion-monolayer interaction, sodium chloride, ammonium oxalate and sodium citrate were added before, or injected after spreading stearic acid, to the substrate solution at the pH of maximum interaction. All these salts were analytical reagents.

All the film experiments described above were carried out at room temperatures.

In relation to the film experiments, in order to obtain information as to the state of cobalt ion in aqueous solutions the self-diffusion coefficient of cobalt ion was measured in $CoCl_2$ solutions of $10^{-3}$ mol./l. and of varying pH values, using $Co^{60}$ as a radio-tracer. The capillary method[12] was used as shown in Fig. 1. The capillary used was

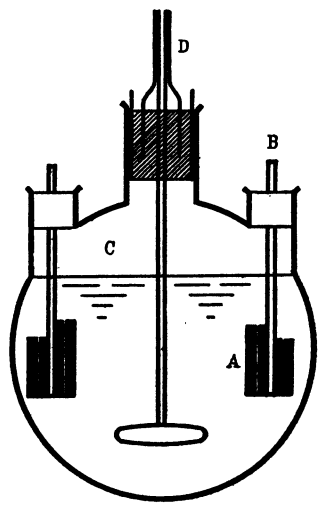



Fig. 1. Diffusion apparatus. A, diffusion cell; B, cell holder; C, three-neck flask (volume 1 liter); D, mercury-sealed stirrer (stirring rate 100rpm).

0.061 cm. in diameter and 1.8 to 2.5 cm. in length. Four capillaries of different lengths were used for each pH value, and the average of the diffusion coefficient was calculated from four values obtained for four different capillaries. The diffusion time was forty to fifty hours and the diffusion temperature was 35.0°C. The difiusion coefficient $D$ was calculated by the equation[13]

$$2.303 \log \frac{\pi^2}{8}\left(\frac{C}{C_0}\right) = -\frac{\pi^2 Dt}{4l^2},$$

where, $C$ is the average concentration of radioactive cobalt in a capillary after time $t$, $C_0$ is its initial concentration and $l$ is the length of the capillary.

## Results

**(1) Stearic Acid Monolayer on $10^{-3}$ mol./l. $CoCl_2$ Solution.**—Pressure-area curves of the monolayer of stearic acid on the surface of

6) A. C. Wahl and N.A. Bonner (editors), "Radioactivity Applied to Chemistry", John Wiley and Sons, Inc., New York, N.Y. (1951), p. 142.
7) G.K. Schweitzer and M. Jackson, *J. Chem. Education*, **29**, 513 (1952).
8) M.H. Kurbatov, H.B. Webster and J.D. Kurbatov, *J. Phys. & Colloid Chem.*, **54**, 1239 (1950).
9) J.D. Kurbatov and M.L. Pool, *Phys. Rev.*, **65**, 61 (1944).
10) R. Matuura and I. Hayasi, *Memoirs of the Faculty of Science, Kyushu University, Ser. C*, **1**, 31 (1948).
11) T. Sasaki and H. Kimizuka, This Bulletin, **25**, 318 (1952).
12) J.S. Anderson and K. Saddington, *J. Chem. Soc.*, **1949**, S.381.
13) A.C. Wahl and N.A. Bonner (editors), "Radioactivity Applied to Chemistry", John Wiley and Sons, Inc., New York, N.Y. (1951), p. 77.

$10^{-3}$ mol./l. $CoCl_2$ solution of varying pH values are shown in Fig. 2. From pH 2 to 4 the monolayer showed stable surface pressures and gave pressure-area curves similar to those without cobalt ion, the limiting area being about 25 Å$^2$ per molecule. The monolayer did not show appreciable rigidity over

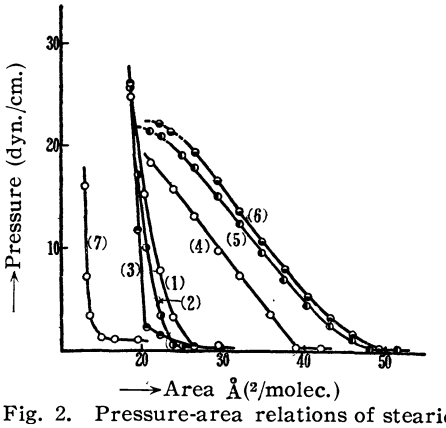



Fig. 2. Pressure-area relations of stearic acid monolayer on $10^{-3}$ mol./l. $CoCl_2$ solution. pH is (1) 2.0; (2) 5.2; (3) 6.3; (4) 7.6; (5) 8.0; (6) 8.3; (7) 9.6. Temperature 25–26°C.

this pH range. When the pH of the solution becomes larger than 4, the monolayer begins to show a little condensation until at pH 6.3 the limiting area reaches about 21 Å$^2$ per molecule. This condensation of the monolayer occurs at lower pH values than those in the case without cobalt ion, as shown in Fig. 3. It was observed that around pH 6 the monolayer did not show stable surface pressures soon after compression but the pressure dropped considerably when the monolayer was allowed to stand at a definite area after compression. At lower surface pressures the pressure dropped largely during the first minute and attained the constant value several minutes after compression, while at higher pressures the change of surface pressure with time was small. The condensed monolayer around pH 6 was observed to have some rigidity. When the pH of the solution exceeds 6.3, the monolayer begins to expand again, but this time it showed high rigidity. Maximum expansion and rigidity were reached at pH 8.3, where the limiting area attained as large as 50 Å$^2$ per molecule. The monolayer was very stable over this pH region of high expansion and rigidity and no such phenomenon of pressure dropping as was found around pH 6 was observed.

In Fig. 3 the limiting areas obtained by pressure-area relations are plotted against the pH of the substrate solution. In the same figure the areas which make viscosity (at pH's smaller than 4) and rigidity (at pH's larger than 4) of the monolayer suddenly large on compression are also shown as a function of the pH of the solution. It is

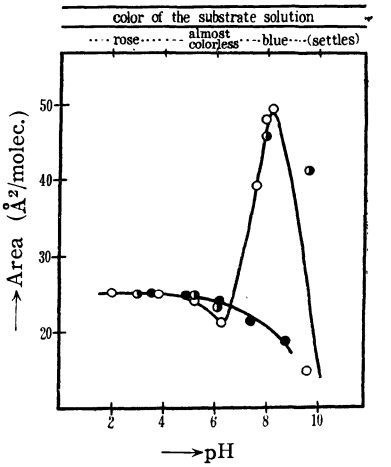



Fig. 3. Limiting area vs. pH of the monolayer of stearic acid on $10^{-3}$ mol./l. $CoCl_2$ solution. Temperature 25–26°C. ○ with cobalt ion (from surface pressure data); ◑ with cobalt ion (from rheological data); ● without cobalt ion (from surface pressure data).

observed that the limiting area obtained from the pressure-area relations is almost the same as that obtained from the rheological data at each pH value. The color of $10^{-3}$ mol./l. $CoCl_2$ solution of varying pH values is recorded in the upper part of Fig. 3. In the alkaline solution the color changed from blue to bluish green, then to yellow with the aging of the solution, and finally after some periods of time the precipitate of hydroxide settled out. Around pH 8.5 the precipitation was observed without aging.

**(2) Effect of Aging of $10^{-3}$ mol./l. $CoCl_2$ Solution.**—Fig. 4 shows pressure-area relations of the monolayer of stearic acid on the surface of $10^{-3}$ mol./l. $CoCl_2$ soluion which has been aged for the periods of time indicated in the figure. The initial pH of the solution was 8.3, but it decreased with time as shown in Table I, in which the change in appearance of the solution was also recorded. It was observed that the monolayer showed a little condensation on the solution in the earlier stage of aging, but it recovered or slightly exceeded the initial expansion by further aging of the solution. The monolayer maintained its high rigidity on the aged solution. No precipitation was observable in the $CoCl_2$ solution before 300 hours of aging;

TABLE I
AGING OF $10^{-3}$ MOL./L. $CoCl_2$ SOLUTION

| Aging time (hr.) | 0 | 0.5 | 3.5 | 24 | 72 | 144 | 336 |
|---|---|---|---|---|---|---|---|
| pH | 8.3 | 8.0 | 7.9 | 7.8 | 7.5 | 7.5 | 7.5 |
| Appearance | blue | greenish blue | yellowish blue | greenish yellow | yellow | yellow | brownish yellow |
| | clear solution | | | slightly turbid solution | | | precipitated |

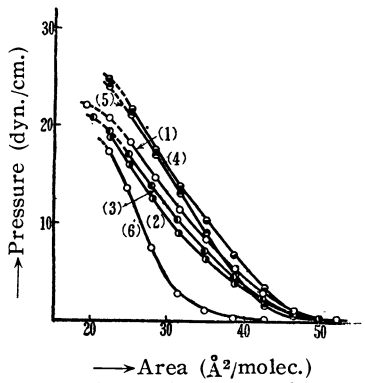



Fig. 4. Effect of aging of $10^{-3}$ mol./l. $CoCl_2$ solution of pH 8.3 on stearic acid monolayer on it. Aging time is (1) 0; (2) 0.5; (3) 3.5; (4) 24; (5) 72; (6) 336 hours. Temp. 22–27°C.

after that the area of the monolayer showed considerable decrease.

(3) **Effect of Other Electrolytes.**—sodium chloride, ammonium oxalate or sodium citrate was added to $10^{-3}$ mol./l. $CoCl_2$ solution and the pH of the solution was adjusted to 8.3. The concentration of each added electrolyte was $5\times10^{-3}$ mol./l. The pressure-area curves of stearic acid monolayer formed on these mixed solutions are shown in Fig. 5. It is seen that ammonium oxalate and sodium citrate make the expanded monolayer completely or almost completely condensed, while sodium chloride has no effect. On the other hand, when these electrolytes were injected into the substrate $CoCl_2$ solution after the monolayer had been formed on it, the condensing effect of ammonium oxalate and sodium citrate was small in the uncompressed state (0.1 dyn./cm.)and not observable in the compressed state (about 10 dyn./cm.) of the monolayer.

(4) **Self-diffusion of Cobalt Ion.**—In Table II self-diffusion coefficients of cobalt ion in $10^{-3}$ mol./l. $CoCl_2$ solution are recorded as a function of initial pH of the solution. In the acid and neutral solutions the diffusion coefficients obtained from four capillaries at the same pH coincided with one another within ±3 per cent. On the other hand in

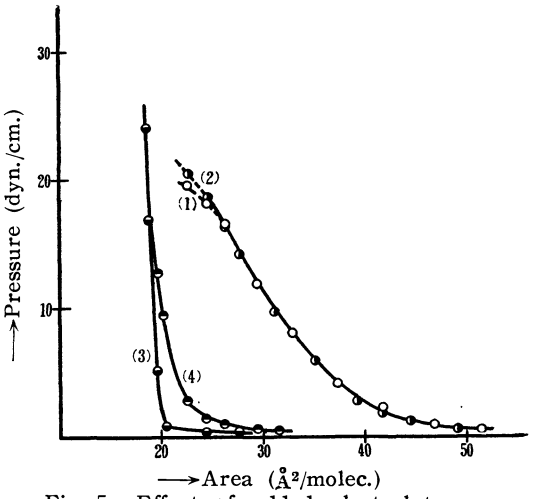



Fig. 5. Effect of added electrolytes on pressure-area relations of stearic acid monolayer on $10^{-3}$ mole./l. $CoCl_2$ solution at pH 8.3. (1) no salt; (2) sodium chloride; (3) ammonium oxalate; (4) sodium citrate. Temperature 26°C.

the alkaline solutions the fluctuation of maximum ±16 per cent was observed. Notwithstanding this large fluctuation, it is seen that the diffusion coefficient apparently decreases as the pH of the solution becomes larger than 7. When the Einstein-Stokes equation is assumed to hold, the radius of diffusing species regarded as spherical particles can be calculated from the observed values of the diffusion coefficient, as shown in the last column of Table II.

TABLE II
SELF-DIFFUSION COEFFICIENT AND RADIUS OF DIFFUSING SPECIES OF COBALT ION AT 35°C

| pH | $D\times10^6$ (cm²/sec.) | radius (Å) |
|---|---|---|
| 2.0 | 9.4±0.1 | 3.3 |
| 5.2 | 9.6±0.3 | 3.3 |
| 6.5 | 9.2±0.1 | 3.4 |
| 7.0 | 9.5±0.3 | 3.3 |
| 7.2 | 8.8±0.8 | 3.6 |
| 7.8 | 7.8±0.8 | 4.0 |
| 8.0 | 5.0±0.8 | 6.3 |
| 8.8 (precipitated) | — | — |

## Discussion

In the acid solution cabolt ion exists in the state of hydrated divalent ion which has rose color. When aqueous sodium hydroxide is added to this solution dropwise, the rose color fades gradually away to almost colorless around pH 6.3 in the case of $10^{-3}$ mol./l. $CoCl_2$ solution, then, by further addition of alkali, the solution turns to blue. It is probable that the change in color of the cobalt solution by addition of alkali corresponds to the change in the state of cobalt ion in the solution. By the addition of alkali to the neutral solution of $CoCl_2$ the first process which is assumed to take place will be that one of the hydrated water molecules is substituted by a hydroxyl group to form basic cobalt salt, which is considered to be blue in color[14]. The colorless solution around pH 6.3 may correspond to the region of transition from hydrated divalent ion to basic salt. The blue solution is not stable enough, because the color changes gradually to yellow by aging of the solution and precipitation takes place after some periods of time. This aging of the alkaline solution, which is accompanied by decrease in pH of the solution as shown in Table I, may be due essentially to transition from basic salt to hydroxide by further combination with hydroxyl group, accompanied by its oxidation to trivalent cobalt. It is to be noted that the solution in this state, before precipitation takes place, reveals colloidal nature. It is shown in Table II that the size of diffusing species at pH 8.0 is almost twice as large as that in the acid and neutral solutions. It is reasonable to assume that cobalt ion forms larger aggregates in the alkaline solution of $CoCl_2$. The large fluctuation of diffusion data in the alkaline solution of the same pH value suggests that the process of aggregation to larger particles depends sensibly upon conditions, the fact being usually the case with colloidal solutions.

The interaction between stearic acid monolayer and cobalt ion in alkaline solutions is closely related to the aggregated state of the ion in the solutions. When stearic acid is spread on the alkaline solution of $CoCl_2$, stearate ions in the monolayer, formed by the dissociation of the acid, will hold cobalt ion aggregates and produce a two-dimensional network structure, which causes large expansion and high rigidity of the monolayer. In the fresh solution the aggregates are considered to be composed mainly of basic ions interlinked by hydrogen bonding, but with aging of the solution the basic ion aggregates will decrease, due to the formation of hydroxide. Still the aged solution shows similar or sometimes greater, interaction with the stearic acid monolayer, as shown in Fig. 4. This seems to suggest that some aggregates are adsorbed physically to the monolayer so that they may offer some contribution to the expansion of the monolayer. On compression those physically adsorbed aggregates will be squeezed out of the monolayer and in the highly compressed state only strongly bound cobalt will remain in the film. It is difficult to explain such large expansion of the stearic acid monolayer as found in the present work only by the interaction with simple basic ion, without taking the aggregated state of ion into consideration.

The effect of complex-forming agents, such as ammonium oxalate and sodium citrate, on the cobalt ion-stearic acid monolayer interaction is remarkable, as shown in Fig. 5. Probably these agents form complex anions with cobalt in the alkaline solution, so that both large expansion and high rigidity of the stearic acid monolayer disappear. However, when these agents are injected into the substrate solution after the monolayer has been formed on it, they are not capable of taking cobalt from the compressed monolayer, because the cobalt atom is attached to the monolayer strongly. Small condensation by ammonium oxalate of the monolayer without compression may be due to extraction of physically adsorbed aggregates. It is interesting to note that these complex-forming agents hinder the formation of radiocolloids of lanthanum[15] and yttrium[16].

Around pH 6.3 the dissociation of stearic acid is not complete and also the formation of basic ion, accordingly, of aggregated state is not enough. The result would be that the monolayer is composed of free stearic acid, normal cobalt stearate and polymeric compound. In such a mixed monolayer the network structure as assumed in alkaline region would not be developed enough, because low-molecular cobalt stearate and stearic acid dispersed in the monolayer would hinder its development. On compression of the monolayer the partly developed network structure will be broken to some extent. This would be a cause of rapid dropping of surface pressure with time over this pH range. Finally the limiting area of 21 Å$^2$

14) J. W. Mellor, "A Comprehensive Treatise of Inorganic and Theoretical Chemistry", Longmans, Green and Co., London (1935), Vol. XIV, p. 628.

15) G.K. Schweitzer and W.M. Jackson, *J. Am. Chem. Soc.*, 74, 4178 (1952).

16) G.K. Schweitzer, B.R. Stein and W.M. Jackson, ibid., 75, 793 (1953).

per molecule is attained, and this is practically due to the condensing effect of divalent cobalt ion, just as that of calcium ion in the alkaline region[1].

Kurbatov et al.[17] showed in the experiment of adsorption of cobalt ion on hydrous ferric oxide that the number of the equivalent of hydrogen ion displaced by 1 gram-atom of cobalt on the adsorbent was 1.2. This seems to suggest that the complicated state of cobalt as considered in the present work also takes part in the adsorption on the solid surfaces. It is probable that other metal ions of the transition elements or polyvalent ions form the state of aggregates around pH of hydroxide precipitation, just as is the case with cobalt ion, and this state is responsible for the specific effect of these metal ions on various surface chemical phenomena. The behavior of these metal ions found in the adsorption on built-up film of stearic acid[18] and in wettability of solid stearic acid surfaces[19] are also accounted for by this fact. It is to be noted that in these experiments, including the present one, the extent of interaction, the pH range of specifc interaction, and other data are not necessarily reproducible. This indicates that the formation of aggregates is affected by a number of factors such as aging, method of preparation of the solution, purity of water, property of the glass vessel, and others, which are difficult to be put under perfect control.

17) M.H. Kurbatov, G.B. Wood and J.D. Kurbatov, *J. Phys. & Colloid Chem.*, 55, 1170 (1951).
18) M. Muramatsu, and T. Sasaki, This Bulletin, 25, 21, 25 (1952).
19) A. Inaba, ibid., 25, 174 (1952); 26, 43 (1953).

## Summary

The presence of aggregates of cobalt ion in the alkaline solution of $10^{-3}$ mol./l. $CoCl_2$ was shown by the measurement of self-diffusion coefficients. Large expansion and high rigidity of the stearic acid monolayer caused by cobalt ion in the alkaline solution were accounted for by the interaction of stearate ion in the monolayer with the aggregates of cobalt ion in the solution, resulting in the formation of two-dimensional network structure in the film. This idea was confirmed by the effect of aging of the substrate solution and also by the action of complex-forming agents such as ammonium oxalate and sodium citrate on the monolayer-ion interaction.

The authors wish to express their thanks to Prof. T. Sasaki, Tokyo Metropolitan University, for his advice and encouragement and also to Mr. M. Muramatsu, Fukuoka Gakugei University, for his discussion on this work.

*Department of Chemistry, Faculty of Science, Kyushu University, Fukuoka*

# *The Effect of Some Surface Active Substances on the Polarographic Reduction Process of Metallic Ions*[1]

By Reita TAMAMUSHI and Teruko YAMANAKA[2]

(Received May 24, 1955)

## Introduction

The use of some surface active substances such as gelatin and some sorts of organic dyes to suppress the so-called maximum has been widely known in polarography. The effect of such substances on the polarographic current-voltage ($c$-$v$) curve is of great importance from both the theoretical and practical standpoints. As the electrode process generally takes place at the interface between two separate phases, it is expected to have a close relation to the surface phenomena like adsorption of surface active substances. The structure of the electrical double layer at the electrode interface is evidently changed by the adsorption of such substances, and such an effect will appear on the electrode

1) Presented at the discussion on polarography held by the Chemical Society of Japan and the Electrochemical Society of Japan in November, 1954, and at the 8th Annual Meeting of the Chemical Society of Japan in April, 1955.

2) Present address: Department of Chemical Industry, Faculty of Engineering, Yokohama National University, Yokohama.

processes. In the polarographic method with the dropping mercury electrode (DME), it is possible to study both the electrode process and the electrocapillary phenomena at the same interface, which seems to be a great advantage in the study of the effect of surface active substances on the electrode process.

Some studies along this line have been published in the literature[3]. J. Heyrovsky mentioned the effect of the films of adsorbed molecules such as pyridine in the discussion on the mechanism of electrodeposition of metals[4], and J. E. B. Randles reported that the addition of small amounts of gelatin or methyl red changed the rate of some electrochemical processes[5]. The formation of micelles of some surface active substances and its effect on the polarographic reduction waves were discussed by E. L. Colichman, who proposed a new method for the determination of the critical micelle concentration (CMC) by the polarographic method[6]. To our best knowledge, however, there have been only few studies which concern the relation between the electrode processes and the electrocapillary phenomena at the DME. Furthermore, the recent rapid development in the synthetic detergents makes it possible to get some sorts of surface active substances with similar main aliphatic parts but different electrical property, which will be very desirable in such studies as mentioned above. Under these circumstances, we have planned to study the effect of three kinds of synthetic detergtnes on the polarographic reduction process of metallic ions and their electrocapillary (*E-C*) curves by using the DME[7].

## Experiments

**Materials.**—The detergents used in this study are listed in the following table. These detergents, which were kindly given by the Nezu Chemical Laboratory, Tokyo, were of the highest purity available and free from impurities which were reducible at the DME. All other chemicals were of reagent grade and used without further purification. The mercury of the DME was washed several times with dil. $HNO_3$ solution and distilled water, and was distilled three times under vacuum.

**Apparatus and Procedure.**—Both pen-recording polarograph (POL-I, Yokogawa Electric Works, Co.) and manually operating polarograph were used to obtain the *c-v* curve. The polarographic cell used throughout the present study is shown in Fig. 1, the resistance of which was about 40 Ω

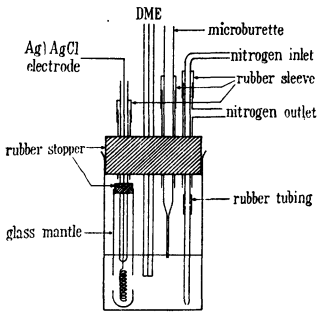



Fig. 1. Polarographic cell assembly.

in 0.1 N KCl solution. The capillary constant of the DME was 2.060 $mg^{2/3}$ $sec^{-1/2}$ in 0.1 N KCl solution without applied potential. A specially designed mercury reservoir using the principle of the Mariotte flask[8] was used to keep the level of the mercury column of the DME constant. The potential of the reference electrode (Ag-AgCl electrode) was occasionally checked against the normal calomel electrode (N. C. E.). Because the height of the polarographic maximum is very sensitive to a slight change in the condition of the system, the maximum suppression point (MSP) of the detergents was determined by observing the change of the maximum current with the successive addition of the solution of detergents from a microburette in Fig. 1, in order to maintain the condition of the system as constant as possible. The *E-C* curve was obtained in 0.1 N KCl solution with the various concentrations of the detergents by measuring the drop-time of 10 drops of mercury from the DME at each electrode potential under the assumption that the interfacial tension is approximately proportional to the drop-time[9]. All measurements were carried out at 25.0 ±0.1℃, and the dissolved oxygen in the solution was expelled by bubbling nitrogen through the solution.

TABLE I

| Detergent | | | Molecular Weight |
|---|---|---|---|
| Sodium dodecyl sulfate (SDS) | $C_{12}H_{25}SO_4Na$ | anionic | 288.4 |
| Dodecyl pyridinium bromide (DPB) | $C_5H_5NBrC_{12}H_{25}$ | cationic | 328.3 |
| Polyoxyethylene lauryl ether (LEO) | $C_{12}H_{25}O(C_2H_4O)_{15}OH$ | non-ionic | 862 |

3) For example: L. Meites and T. Meites, *J. Am. Chem. Soc.*, 73, 177 (1951); N. Tanaka and M. Kobayashi, This Bulletin, 24, 132 (1951); M. Dratovsky and M. Ebert, *Chem. Listy*, 45, 88 (1951); J.E. Strassner and P. Delahay, *J. Am. Chem. Soc.*, 74, 6232 (1952).

4) J. Heyrovsky, *Discussions Faraday Soc.*, 1947, 212.

5) J.E.B. Randles, ibid., 1947, 11.

6) E. L. Colichman, *J. Am. Chem. Soc.*, 72, 4036 (1950).

7) Recently, a similar study was independently carried out by Sj. L. Bonting and B.S. Aussen, which appeared in *Rec. trav. chim. pays-bas*, 73, 455 (1954).

8) E.F. Mueller, *Ind. Eng. Chem. Anal. Ed.*, 12, 171 (1940).

9) I.M. Kolthoff and J.J. Lingane, "Polarography" Vol. I, p. 84, 1952, Interscience Pub.

## Experimental Results

**Maximum Suppression Point.**—The effect of the detergents on the polarographic maximum was studied with the reduction waves of $Pb^{2+}$- and $Ni^{2+}$- ions in the medium of 0.1 N KCl solution. The MSP is defined as the minimum concentration of the detergents which is necessary to make $i_m/i_l$ equal to 1[6], where $i_m$ means the maximum current and $i_l$ the limiting current. It was determined graphically by plotting $i_m/i_l$ against the logarithm of the concentration of the detergents, log $C$ (Fig. 2 and Table II).

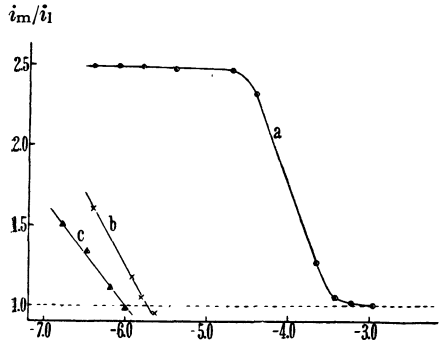



Fig. 2. The relation between $i_m/i_l$ and the logarithm of the concentration of detergents in the systems of 3*m*M $Ni^{2+}$-detergents in 0.1 N KCl solution.
a, SDS; b, DPB; c, LEO.

TABLE II
THE MSP OF THE DETERGENTS

| Detergent | MSP | |
|---|---|---|
| | $Pb^{2+}$-max. | $Ni^{3+}$-max. |
| SDS | $2.3\times10^{-6}$M | $1.1\times10^{-3}$M |
| DPB | $2.3\times10^{-6}$M | $1.9\times10^{-6}$M |
| LEO | $1.3\times10^{-6}$M | $1.0\times10^{-6}$M |
| (Gelatin | $1.1\times10^{-3}$%) | $1.2\times10^{-3}$%) |

**The Effect of Detergents on the *C-V* Curve.**—The half-wave potential and the relation between the electrode potential, $V$, and log $i/(i_l-i)$ (the log-plot analysis) were investigated with the reduction processes of $Tl^{+}$-, $Pb^{2+}$- and $Ni^{2+}$- ions in 0.1 N KCl solution with the various concentrations of the detergents. In general, the half-wave potential shifted to the more negative and the shape of the *c-v* curve was gradually distorted with the increase of the concentration of detergents. These tendencies were most clearly seen in the systems of $Ni^{2+}$-LEO and $Ni^{2+}$-DBP, then in the systems of $Pb^{2+}$-LEO and $Pb^{2+}$-SDS, and least in the system of $Tl^{+}$-DPB. If we plot the half-wave potential of the metallic ions in the systems of $Ni^{2+}$-LEO and $Pb^{2+}$-LEO against the logarithm of the concentration of detergents, an interesting relation is obtained as in Fig. 3, which shows a sudden change in the half-wave potential in a certain concentration range of the detergent.

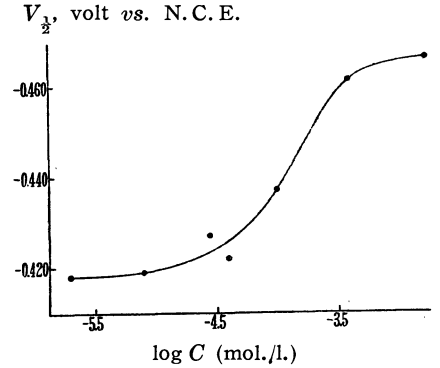



Fig. 3. The relation between the half-wave potential of $Pb^{2+}$-reduction wave and the logarithm of the concentration of LEO in 0.1 N KCl solution.

There was practically no effect of the presence of DPB or LEO on the shape of the *c-v* curve of $Tl^{+}$-ion, but it was slightly affected by the presence of SDS. In the case of $Pb^{2+}$-ion, an apparent change in the *c-v* curve was detected by the addition of a certain amount of SDS or LEO. The symmetrical property of the *c-v* curve of $Ni^{2+}$-ion was extensively disturbed by the presence of LEO or DPB in the system. The effect of DPB, however, could not be studied at its higher concentrations, because of the interference of the reduction wave of DPB itself on the *c-v* curve of $Ni^{2+}$-ion.

The limiting current of the metallic ions was approximately kept unchanged over a relatively wide concentration range of the detergents in each of the present systems.

Some of the typical experimental data are summarized in Table III. $\alpha$ in the third column of the table is a fractional number between zero and one, which appeared in the equation for the polarographic *c-v* curve of the activation-controlled type[10]:

$$V = const - \frac{RT}{n\alpha F}\ln\frac{i}{i_l - i} \qquad (1)$$

where $n$ is the number of electrons which participate in the redox reaction of the reducible substances at the DME. The value of $\alpha$ was calculated from the tangent of the

10) R. Tamamushi and N. Tanaka, This Bulletin, 22, 227 (1949).

TABLE III

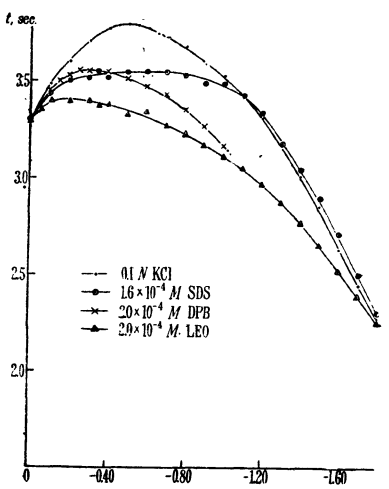
THE EFFECTS OF DETERGENTS ON THE POLAROGRAPHIC REDUCTION WAVES

| Concn., mol./l | $V_{\frac{1}{2}}$, volt *vs.* N. C. E. | | | log-plot analysis ($\alpha$) | | | $\partial t/\partial \log C$ | | *E-C* max. volt. *vs.* N. C. E. |
|---|---|---|---|---|---|---|---|---|---|
| | $Tl^+$ | $Pb^{2+}$ | $Ni^{2+}$ | $Tl^+$ | $Pb^{2+}$ | $Ni^{2+}$ | E-C max. | −1.12v. | |
| SDS | | | | | | | | | |
| $4.0\times10^{-6}$ | * | −.417 | * | * | .66 | * | −.10 | −.09 | −.49 |
| 8.0 〃 | * | — | * | * | — | * | −.10 | −.09 | — |
| $2.0\times10^{-5}$ | −.481 | −.442 | * | .79 | unsym(S) | * | −.10 | .05 | −.49 |
| 4.0 〃 | −.494 | −.447 | * | unsym(S) | 〃 (S) | * | −.65 | −.01 | −.57 |
| 8.0 〃 | −.487 | −.439 | * | .74 | 〃 (S) | * | −1.24 | 0 | ca. −.4 −.7 |
| $1.2\times10^{-4}$ | −.490 | −.429 | * | .68 | 〃 (S) | * | −.14 | .73 | ca. −.3 −.8 |
| 1.6 〃 | −.497 | −.442 | * | unsym(S) | 〃 (S) | * | −.47 | .23 | ca. −.3 −.8 |
| 2.7 〃 | −.503 | −.441 | * | 〃 (S) | 〃 (L) | * | −.97 | 0 | ca. −.3 −.8 |
| DPB | | | | | | | | | |
| $8.0\times10^{-6}$ | −.477 | −.417 | × | 1.02 | .76 | × | −.02 | × | −.48 |
| $2.8\times10^{-5}$ | — | −.419 | × | — | .74 | × | −.36 | × | ca. −.4 −.6 |
| 4.0 〃 | −.484 | −.419 | × | .92 | .76 | × | −1.46 | × | ca. −.4 |
| $1.0\times10^{-4}$ | −.482 | −.424 | × | .95 | .76 | × | −.74 | × | ca. −.3 −.4 |
| 2.0 〃 | — | −.423 | × | — | .74 | × | −.32 | × | −.3 −.4 |
| 4.0 〃 | −.483 | −.427 | × | .90 | .61 | × | −.66 | × | −.3 −.4 |
| $1.0\times10^{-3}$ | — | −.412 | × | — | .72 | × | −.33 | × | −.3 |
| 1.9 〃 | −.461 | −.397 | × | .87 | .80 | × | −.07 | × | −.3 |
| LEO | | | | | | | | | |
| $2.0\times10^{-6}$ | — | −.418 | — | — | .59 | — | — | — | — |
| 8.0 〃 | −.474 | −.419 | −1.055 | .94 | .60 | .40 | 0 | 0 | −.49 |
| $2.0\times10^{-5}$ | — | — | −1.111 | — | — | unsym(L) | −.63 | −.33 | −.45 |
| 2.8 〃 | −.492 | −.427 | −1.209 | .74 | unsym(L) | 〃 (S) | −4.78 | −3.68 | ca. −.2 −.5 |
| 4.0 〃 | −.493 | −.422 | −1.375 | .78 | 〃 (L) | 〃 (S) | −2.14 | −2.03 | ca. −.1 −.4 |
| $1.0\times10^{-4}$ | −.493 | −.437 | — | .74 | 〃 (L) | — | −1.14 | −.69 | ca. −.1 −.3 |
| 2.0 〃 | — | — | −1.576 | — | — | unsym(U) | −.78 | −.40 | ca. −.1 −.3 |
| 4.0 〃 | −.487 | −.461 | — | .80 | unsym(L) | — | −.46 | −.37 | ca. −.1 −.3 |
| $1.9\times10^{-3}$ | −.489 | −.465 | — | .73 | 〃 (L) | — | −.10 | −.12 | ca. −.1 −.3 |

* Can not be determined because of the presence of maximum.
× Can not be determined because of the interference due to the reduction wave of DPB.
unsym(S): The log-plot shows a S-shaped curve.
unsym(U); The upper half of the polarographic wave is steeper than the lower half.
unsym(L): The lower half of the polarographic wave is steeper than the upper half.

log-plots by assuming that $n=1$ in the case of $Tl^+$-ion and $n=2$ in the case of $Pb^{2+}$-or $Ni^{2+}$-ion.

**Electrocapillary Curve.**—The presence of a certain amount of these detergents changed both the position of the electrocapillary maximum (*E-C* max.) and the shape of the *E-C* curve as shown in Fig. 4. The addition of SDS more than $1\times10^{-4}$ M in its cocentration greatly flattened the curve and lowered the interfacial tension at the potential of the *E-C* max., the latter effect of which, however, was quite small at any potential more negative than about −1.2 volts. In the case of DPB, the *E-C* max. was shifted to the more positive and the interfacial tension was mainly lowered in the potential region of the negative branch. The presence of LEO lowered the interfacial tension over the whole potential region from 0 to −1.8 volts with the gradual shift of the *E-C* max. to the more




*V*, volt *vs.* Ag | AgCl electrode

Fig. 4. The electrocapillary curves of detergents in 0.1 N KCl solution.

positive potential. This suggests that LEO will be polarized at a polarized electrode surface, the positive end of the induced dipole being surface active.

If the drop-time at the *E-C* max., $t_{max.}$, is plotted against the logarithm of the concentration of detergents, log *C*, the curves as shown in Fig. 5 are obtained. The tangent of the

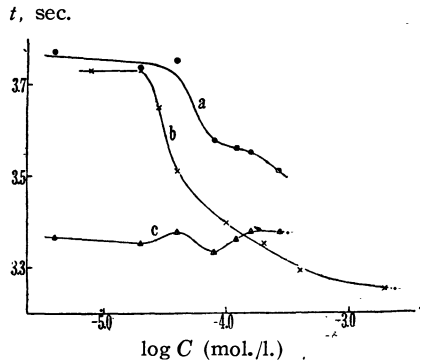



Fig. 5. The relation between the drop-time and the logarithm of the concentration of detergents in 0.1 N KCl solution. a, SDS at *E-C* max.; b, LEO at *E-C* max.; c, SDS at -1.12 volts *vs.* N.C.E.

relation between $t_{max.}$ and log *C* is shown to be approximately proportional to the surface excess of the neutral detergent molecule at the electrode surface at the potential of the *E-C* max., $\Gamma_{det.}^{max.}$, because, under the assumption that the surface excess of solvent is equal to zero,

$$\frac{d\sigma^{max.}}{d\mu_{det.}} = -\Gamma_{det.}^{max.}$$

is derived from the Gibbs adsorption equation applied to an ideal polarized electrode at constant temperature and pressure:

$$d\sigma = -qdE - qd(\Delta\psi) - \Sigma\Gamma_i d\mu_i \qquad (2)^{11)}$$

$\sigma$: The interfacial tension of phases between the electrode and the solution.
$\mu_i$: The chemical potential of a component represented by its subscript.
$\Gamma_i$: The surface excess of that component.
$q$: The surface charge density of electricity on the metallic phase.
$E$: The total applied potential difference between the working electrode and the reference electrode measured by a potentiometer.
$\Delta\psi$: The potential difference between the solution phase and the reference electrode.

It is also assumed in the present discussion that the activity coefficient of detergents in our systems is equal to one. This relation can be used in the discussion of the effect of the detergents on the reduction process of $Tl^{+}$- or $Pb^{2+}$- ion which is reduced at the electrode potential near the *E-C* max.

In the very low concentration range of the detergents, the value of the tangent is very small, which indicates a negligible amount of adsorption. Such a low concentration range is followed by the region of the almost constant inclination corresponding to the constant value of $\Gamma$. With the further increase of the concentration of the detergents, however, the drop-time is not decreased markedly, which does not necessarily mean the decrease in $\Gamma$ of the simple detergent molecule but will be interpreted by the change in the state of the system such as the micelle formation of the detergent molecules[12]. It must be mentioned here, with regard to the usual method of the determination of CMC from the data of the surface tension, that, in the relation between $t_{max.}$ and log *C*, non-ionic detergent LEO shows only one relatively smooth step but ionic detergents have a tendency to show two steps provided that the determination is carried out over a wide concentration range (Fig. 5).

The drop-time was also plotted against log *C* at a constant electrode potential of −1.12 volts, the result of which will be useful in the discussion of the effect of detergents on the reduction process of $Ni^{2+}$-ion which is reduced at this potential. It is shown from Eq. (2) that the tangent of such a relation is approximately proportional to the surface excess of detergent at this potential as in the case of the *E-C* max., i.e.,

$$\frac{d\sigma^{-1.12}}{d\mu_{det.}} = -\Gamma_{det.}^{-1.12}$$

provided that the value of $\Delta\psi$ in Eq. (2) is assumed unchanged with the change in $\mu_{det.}$ This assumption seems plausible because of the presence of KCl in excess as the indifferent electrolyte. In the case of LEO and DPB, the result at −1.12 volts was qualitatively similar to that at the *E-C* max., but SDS showed a quite different curve as in Fig. 5-c indicating a negligible adsorption of SDS at −1.12 voluts over the whole concentration range of SDS. This can be explained by considering the desorption of SDS at such a negative potential, which has been once adsorbed at the more positive potentials.

## Discussion

E. L. Colichman stated that the usual CMC "seems to be equal to the concentration

11) D.C. Grahame, *Chem. Revs.*, **41**, 441 (1947).

12) C.P. Roe and P.D. Brass, *J. Am. Chem. Soc.*, **76**, 4703 (1954).

of colloidal agent just sufficient to suppress maxima, the maximum suppression point (MSP)"[3]. However, Table II shows that the MSP of the detergents in our present systems, except one of SDS and $Ni^{2+}$-ion, are in the order of $10^{-6}$ mol./l. which is much lower than the generally accepted value of CMC of these detergents[13]. The very poor ability of SDS to suppress the maximum of $Ni^{2+}$-ion will be at first sight explained by considering that the adsorption of SDS on the DME is almost absent at such a negative potential as that of $Ni^{2+}$-maximum (Fig. 5-c and Table III). However, in the case of LEO or DPB, which are very active to both of $Pb^{2+}$- and $Ni^{2+}$-maxima, the lowering of the interfacial tension and the adsorption of these detergents are also shown to be quite small at such a low concentration range as their MSP from the result of the *E-C* curve. These experimental results suggest that the suppression of the polarographic maximum will not only concern the adsorption or the change in the interfacial tension due to the presence of surface active substances but also the slight change in the structure of the electrical double layer. At any rate, it can be concluded that these detergents are generally very effective to suppress the polarographic maximum and are preferable to gelatin in the following respects: 1) these detergents do not seem to have any tendency of complex-formation with metallic ions; 2) the viscosity of the solution does not change makedly by the addition of their small amount enough to suppress the maximum; 3) they are completely free from deterioration.

With regard to the difference in the electrical property of the detergents, which appears in their effect on the polarographic *c-v* curve, it can be said from the experimental results that the anionic detergent generally has a larger effect than the cationic one on the reduction process with the half-wave potential more positive than the *E-C* max., and *vice versa*. It must be mentioned that the non-ionic detergent, LEO, gives a relatively large influence to the polarographic *c-v* curve in all cases. The result of the *E-C* curve also reflects the difference in the electrical property of the detergents.

The apparent value of $\alpha$ in Table III, which should be equal to one under the simplest condition if the overall electrode process were diffusion-controlled[10], the distortion of the *c-v* curve, and the shift of the half-wave potential to the more negative suggest that the overall electrode process becomes more and more activation-controlled[10] and the reduction process is retarded with the increase in the concentration of the detergents. Such a tendency is the largest in the case of the so-called irreversible reduction process of $Ni^{2+}$-ion, then in the case of reversible reduction process of $Pb^{2+}$-ion, and the least in the case of completely reversible reduction process of $Tl^{+}$-ion in the present systems, which is in good agreement with Heyrovsky's theory on the mechanism of the reduction process of metallic ions[4]. It should be mentioned here, however, that even the reduction process of $Tl^{+}$-ion, which had been expected to be completely reversible and not influenced by the adsorption of the surface active substances according to J. Heyrovsky, was shown to be affected, although to a relatively small extent, by the presence of a certain amount of SDS (or LEO).

The relation between the effect of the detergents on the *c-v* curve and the results of the *E-C* curve must be emphasized at the end of the present discussion. Generally speaking, the concentration range of the detergents, in which the shift of the half-wave potential and the distortion of the *c-v* curve of the reduction process of the metallic ions clearly appear, almost coincides with the concentration range corresponding to the constant value of the surface excess of the detergents as shown in Fig. 5. Such a relation is most clearly seen in the one to one correspondence between the relation of half-wave potential *vs.* log *C* and that of the drop-time *vs.* log *C* in the system of $Ni^{2+}$-LEO or $Pb^{2+}$-LEO (Figs. 3. and 5-c).

It can be said from all these experimental results that the effect of the surface active substances on the electrode process of metallic ions at the DME has a very close relation to the adsorption phenomena of the surface active substances and the structure of the electrical double layer at the electrode interface. The difference in the effect, which was given to the polarographic *c-v* curve by the presence of the surface active substances with the different electrical property, will suggest, as pointed out by J. Heyrovsky[4], that the adsorption layer of these substances mainly affects the transfer of electrons at the electrode interface and not the diffusion process of metallic ions. The results of the present study are expected to provide some new experimental facts to the study of the polarographic maximum and the mechanism of the electrode processes.

13) For example, C.P. Roe and P.D. Brass gave the value of $1.45\times10^{-3}$ mol./l. for the CMC of SDS at *p*H 6.5 and $Na^{+}$-ion concentration of 0.1 mol./l.[12].

## Summary

The effect of three detergents on the polarographic electrode reduction processes of $Tl^{+}$-, $Pb^{2+}$- and $Ni^{2+}$-ions was studied together with the *E-C* curve of these detergents. It was shown that these detergents were very effective to suppress the polarographic maximum and their surface excess was shown to be very small at the concentration range of their MSP from the study of the *E-C* curve. The half-wave potential was shifted to the more negative and the shape of the *c-v* curve was distorted by the presence of these detergents, the degree of which was the largest in the case of $Ni^{2+}$-ion and the least in the case of $Tl^{+}$-ion. The anionic detergent seemed to have a larger effect than the cationic one on the electrode process with the half-wave potential more positive than the *E-C* max., and *vice versa*. It was shown that the effect of the detergents on the polarographic *c-v* curve was parallel to the result on their adsorption phenomena obtained from the *E-C* curve. From these results it was concluded that the polarographic electrode process is greatly influenced by the change in the structure of the electrical double layer and that it will be the electron-transfer process which is mainly affected by the presence of the adsorption layer of the surface active substances.


We thank to Prof. T. Tachibana for his great encouragement throughout this study. We also greatly appreciate the kindness of Mr. K. Meguro of the Nezu Chemical Laboratory in providing the samples of the synthetic detergents.

*Laboratory of Chemistry, Faculty of Science, Ochanomizu University, Tokyo*

# *The Third Virial Coefficient in Polymer Solutions*

By Tōru KAWAI

(Received July 19, 1955)

## Introduction

By means of grand partition functions, Mc Millan and Mayer[1] derived a rigorous series expansion for the osmotic pressure in terms of concentration. The first applications of their theory to polymer solutions were made by Zimm[2], who expressed the osmotic pressure $\Pi$ as:

$$\Pi/c=RT[(1/M)+A_2c+A_3c^2+\cdots\cdots], \quad (1)$$

where $c$ is the concentration of polymer in mass per unit volume of solution. $M$ is the molecular weight of the polymer and the $A_n$, so called virial coefficients, are constants at constant temperature. Since most measurements are made in fairly dilute solutions, the third and higher coefficients ordinarily need not be considered. To increase the accuracy of the extrapolation procedure, however, it would be desirable to make clearer the expression for the third virial coefficient. From the calculations of Bawn and Wajid[2], moreover, it can be seen that molecular weight dependency of $A_2$ depends strongly on the kind of expression that is used for the $\Pi$ vs. $c$ relation. An expression for $A_2$ had been given by Grimly[4], who deduced approximately in a limited interval of molecular weights,

$$A_2=CM^{-\varepsilon}, \quad (2)$$

where $C$ and $\varepsilon$ are constants depending on the molecular dimensions and the excluded volume of the representative chain element in that interval. In polystyrene-toluene system[3], the value 0.15 is found for $\varepsilon$ from a quadratic equation (cf. Eq. (I)), whereas a value of 0.33 is found when the relation of Flory and Krigbaum[5] is used for the third virial coefficient.

Flory and Krigbaum[5] have assumed, as an approximation, that $A_2$ bears the same re-

1) W.G. McMillan and J.W. Mayer, *J. Chem. Phys.*, **13**, 276 (1945).
2) B.H. Zimm, *J. Chem. Phys.*, **14**, 164 (1946).
3) C.E.H. Bawn and M.A. Wajid, *J. Polymer Sci.*, **12**, 109 (1954).
4) T.B. Grimly, *Prac. Roy. Soc. London*, **A212**, 339 (1952).
5) P.J. Flory and W.R. Krigbaum, *J. Chem. Phys.*, **18**, 1086 (1950).

lation to $A_3$ as in the case of hard sphere molecules, and have written

$$A_3=\frac{5}{8}A_2^2M. \quad (3)$$

This "hard sphere approximation" doubtless makes the third term too great, and actually gives more than ten times greater values for $A_3$ than those calculated by Bawn's graphical method[6] in the system cited above. Recently, Krigbaum and Flory themselves[7] have concluded from new osmotic measurements on polyisobutyrene in cyclohexane and polystyrene in toluene that this hard sphere treatment gives a greater value for $A_3$ than the data warrant.

At first sight, the above discrepancy of the $A_3$ value appears to be eliminated by Stockmayer and Casassa[8]. With the aid of approximate models for the intermolecular potential energy, they have obtained the third virial coefficient as a function of the second coefficient and Flory's parameter $\alpha$, which is obtainable from intrinsic viscosity. According to them,

$$\Gamma_3/\Gamma_2^2=A_3/A_2^2M=0.257\ A, \quad (\Gamma_2=A_2M,\ \Gamma_3=A_3M) \quad (4)$$

where $A$ can be calculated by a graphical method as a function of $\alpha$ only. Close inspection of this ratio $\Gamma_3/\Gamma_2^2$ obtained from experiments, however, reveals that their treatment must be in direct contradiction to the experimental results especially on the dependency of the ratio upon molecular weight of the polymer.

In this paper, the dependency of the parameter $\alpha$ on polymer concentrations will be considered, and it will be pointed out that the source of the above contradiction may be explained, at least qualitatively, by this procedure.

## The Dependency of the Ratio $\Gamma_3/\Gamma_2^2$ upon Molecular Weight

For the hard sphere molecular model[5], the ratio $\Gamma_3/\Gamma_2^2$ is 5/8, the value being markedly greater than the experimental, and is independent upon molecular weight of the polymer. If the results of Stockmayer and Casassa[8], the evaluation of the ratio in a more general and elegant manner, were acceptable, the ratio should be greatest at high molecular weight and in good solvents. On the other hand, the experimental results of Bawn et al., which are probably the most reliable osmotic pressure data available for this purpose, show that the ratio $\Gamma_3/\Gamma_2^2$ decreases markedly with increasing molecular weight. This is illustrated in Table I, the ratio being compared with the values of the ratio calculated by Eq. (4) ($(\Gamma_3/\Gamma_2^2)_{\text{stock.}}$). Furthermore, the ratio is greater in bad solvents than in good solvents, in contradiction of the results of the above authors, and its theoretical values are much too great especially in good solvents.

TABLE I

THE VIRIAL COEFFICIENTS OF POLYSTYRENE SOLUTION IN TOLUENE AND IN METHYL ETHYL KETONE[3]

| $\bar{M}_n\times10^{-4}$ | $A_2\times10^4$ (graphic) g.$^{-2}$ cc. | $A_2\times10^4$ (F. F. B. method) | $A_3\times10^3$ (graphic) g.$^{-3}$ cc. | $(\Gamma_3/\Gamma_2^2)_{\text{exp.}}$ (graphic) | $(\Gamma_3/\Gamma_2^2)_{\text{stock.}}$ | $\alpha_0$[13] |
|---|---|---|---|---|---|---|
| Toluene solution at 25°C: | | | | | | |
| 158 | 2.89 | 1.83 | 1.86 | 0.0141 | 0.315 | $1.51_6$ |
| 87 | 3.01 | 2.13 | 1.70 | 0.0216 | 0.284 | $1.43_3$ |
| 32 | 3.28 | 3.19 | 1.58 | 0.0472 | 0.248 | $1.31_9$ |
| 28.8 | 3.09 | 3.03 | 1.42 | 0.0516 | 0.247 | $1.31_2$ |
| 24.8 | 3.32 | 3.31 | 1.54 | 0.0563 | 0.240 | $1.29_6$ |
| 16.2 | 3.36 | 3.86 | 1.70 | 0.0930 | 0.215 | $1.25_7$ |
| 9.40 | 3.89 | 4.47 | 1.55 | 0.1090 | 0.188 | $1.22_1$ |
| 7.20 | 4.35 | 4.58 | 1.78 | 0.1307 | 0.165 | $1.21_0$ |
| Methyl ethyl ketone at 25°C | | | | | | |
| 32 | 0.75 | 1.22 | 0.60 | 0.333 | 0.105 | $1.11_1$ |
| 16.2 | 0.87 | 1.30 | 0.60 | 0.489 | 0.100 | $1.09_9$ |

## The Dependency of the Parameter $\alpha$ on Polymer Concentrations

In the highly dilute region, where osmotic measurements are most important, the concentration of the segments in solution is not uniform, but is much greater in the

6) C.E.H.Bawn, R.F.J.Freeman and A.R.Kamaliddin, *Trans. Faraday Soc.*, 46, 862 (1950).

7) W.R. Krigbaum and P.J. Flory, paper read at the meeting of the *Am. Chem. Soc.*, March 25, 1952.

8) W.H. Stockmayer and E.F. Casassa, *J. Chem. Phys.*, 20, 1560 (1952).

neighbourhood of the centers of the polymer molecules. Attempts have been made to account for this effect first by Flory and Krigbaum[5] and then others[4]. This is closely related to the (excluded) volume effect, which means the influence of the formation of polymer-polymer contacts between distant segments of a chain molecule (long range interference)[9,10]. Thus, the pair partition function for the Gaussian chains may be written as a function of $\alpha$, so long as the polymer is homogeneous[5].

Complications arising from non-uniformity in the distribution of segments over the volume, however, must become trivial as the concentration is increased owing to the forced overlapping of polymer molecules. The above theories, therefore, may be applied only to solutions so dilute thot overlapping of the excluded volume is slight. Actually, if the concentration is great enough to be supposed to show intense overlapping of molecules, the earlier theories of polymer solutions[11,12] may be available, although many questions remain unsettled on these theories. At intermediate concentrations neither theory is appropriate.

Here, let us consider the dependency of the parameter $\alpha$ upon the concentration of the polymer and introduce its effect on the partition function of this system. We are going to turn our attention to one polymer molecule and consider the influence of its environment on it. The actual domain pervaded by a polymer chain cannot be defined sharply. Here, the distribution of polymer segments in a polymer chain will be assumed to be Gaussian as usually and may be given by

$$x_j = x(\beta_0'/\pi^{\frac{1}{2}})^3 \exp(-\beta_0'^2 S_j^2) 4\pi S_j^2 \Delta S_j \quad (5)$$

in the absence of intramolecular interactions, where $x_j$ is the number of segments in the spherical shell of radius $S_j$ from the center of gravity and of thickness $\Delta S_j$, $x$, the total number of segments in a polymer chain, and

$$\beta_0' = 3/\sqrt{\bar{r}_0^2} = 3/\sqrt{6\bar{s}_0^2}, \quad (6)$$

where $\bar{r}_0^2$ is the mean-square distance between the ends of the chain, $\bar{s}_0^2$, that between the segments and the center of gravity, both in the absence of intramolecular interactions. It will be assumed that a given set of the segments given by Eq. (5) occupy the spherical shell between $\alpha S_j$ and $\alpha(S_j+\Delta S_j)$ in the equilibrium configuration.

The total free energy of dilution is

$$\Delta F_{\text{dil.}} = \sum_j \Delta F_j. \quad (7)$$

In an entirely analogous manner to Flory's treatment of intrinsic viscosities[13],

$$\partial \Delta F_{\text{dil.}}/\partial(\alpha^3) = (1/N)\sum(\mu_{1j}-\mu_{10})\{\partial n_{1j}/\partial(\alpha^3)\}, \quad (8)$$

where $\mu_{1j}$ and $\mu_{10}$ are the chemical potentials of solvent in the shell $j$ and of pure solvent, respectively, and $n_{1j}$, the number of solvent molecules in the shell $j$ ($N$: Avogadro's number). The terms in the right hand side of Eq. (8) may be written, to a satisfactory approximation, as follows:

$$\mu_{1j}-\mu_{10} = RT(\kappa_1-\varphi_1)v_{2j}^2, \quad (9)$$

where $\kappa_1$ and $\varphi_1$ are the parameters representative of heat and entropy terms respectively, and

$$v_{2j} = xV(\beta_0'/\alpha\pi^{1/2})^3 \exp(-\beta_0'^2 S_j^2) \quad (10)$$

($V$ is the volume of a segment). And

$$\partial n_{1j}/\partial(\alpha^3) \cong 4\pi S_j^2 \Delta S_j N/V_1, \quad (11)$$

where $V_1$ is the molar volume of the solvent. Substituting Eqs. (10) in (9), and (9) and (11) in (8), replacing the summation by an integral and integrating over $S_j$ from 0 to $\infty$, there is obtained

$$\partial \Delta F_{\text{dil.}}/\partial(\alpha^3) = kTK^*(\kappa_1-\varphi_1)/\alpha^6, \quad (12)$$

$$K^* = \{27/2\pi^{3/2}\}(\bar{v}^2/NV_1)(M/\bar{r}_2^0)^{3/2}M^{1/2}, \quad (13)$$

($\bar{v}$ is the specific volume of the polymer).

The configurational entropy $\Delta S_{\text{el.}}$ of the chain may be evaluated according to the method employed in the theory of rubber elasticity as follows[14]:

$$\Delta S_{\text{el.}}/k \doteqdot 3\ln\alpha - 3(\alpha^2-1)/2. \quad (14)$$

Hence, if the total free energy in the "domain" pervaded by a polymer chain may be written $\Delta F$, the following relationship may be derived from Eqs. (12) and (14):

$$\partial \Delta F/\partial(\alpha^3) = \partial \Delta F_{\text{dil.}}/\partial(\alpha^3) - \partial(T\Delta S_{\text{el.}})/\partial(\alpha^3)$$
$$= kT[K^*(\kappa_1-\varphi_1)/\alpha^3 + (1/\alpha) - (1/\alpha^3)]. \quad (15)$$

Now, it may be assumed that each molecule is distributed within an effective volume of sphere of radius $\alpha\sqrt{\bar{r}_0^2}$. Then,

$$(4/3)\pi\alpha^3(\bar{r}_0^2)^{3/2} = xV + (n_1V_1/N), \quad (16)$$

where $n_1$ is the number of the solvent molecules in this sphere[15]. Therefore, from Eqs. (15) and (16) the partial molal free energy of the solvent in this effective volume may be given by

9) B.H. Tompa, *Trans. Faraday Soc.*, **48**, 363 (1952).
10) A. Münster, *Mackromol. Chem.*, **2**, 227 (1948).
11) For instance, P.J. Flory, *J. Chem. Phys.*, **9**, 660 (1941); **10**, 51 (1942).
12) M.L. Huggins, *Ann. N.Y. Acad. Sci.*, **44**, 431 (1943).
13) P.J. Flory and T.G. Fox Jr., *J. Am. Chem. Soc.*, **73**, 1904; 1915 (1951).
14) P.J. Flory, *J. Chem. Phys.*, **17**, 303 (1949).
15) T. Kawai, This Bulletin, **24**, 69 (1951).

$$\Delta\bar{F}_1=\{\partial\Delta F/\partial(\alpha^3)\}\{\partial(\alpha^3)/\partial n_1\}$$
$$=RTB[K^*(\kappa_1-\varphi_1)/\alpha^6+(1/\alpha)-(1/\alpha^3)], \quad (17)$$

where $B=(V_1/N)/(4/3)\pi(\bar{r}_2^0)^{3/2}=C_B x^{-3/2}$. (18)

Next, that of the solvent in the environment region of this sphere (designated by prime) may be written as

$$\Delta\bar{F}_1'=-RT[(1/x)v_2+a_2v_2^2+a_3v_2^3+\cdots\cdots], \quad (19)$$

where $v_2$ is the volume fraction of the polymer in the whole region of the system.

Thus, the $\alpha$ vs. $v_2$ relation will be introduced from the condition of the equilibrium between the inside and outside of the above effective volume;

$$\Delta\bar{F}_1=\Delta\bar{F}_1'.$$

In Eq. (19) the activity of the solvent in the environment region is replaced to the mean value in the whole region. This approximation may be permitted as far as we deal with the equilibrium between one polymer chain and its environment in the vast region involving other molecules. Furthermore, the virial coefficients, $a_2$, $a_3$ and others in Eq. (19), should be a function of $\alpha$. As is shown later, however, this complication can be avoided to a satisfactory approximation, since this "reflection of $\alpha$" appears only in the higher terms in $v_2$[16].

At infinite dilution, we may write $\alpha=\alpha_0$, and from Eq. (17),

$$K^*(\kappa_1-\varphi_1)/\alpha_0^6+(1/\alpha_0)-(1/\alpha_0^3)=0. \quad (20)$$

Replacing $\alpha$ by $\alpha_0+\Delta\alpha$, and expanding the terms in the right hand side of Eq. (17) in the series of $\Delta\alpha$,

$$\Delta\bar{F}_1=RTB[(5\Delta\alpha/\alpha_0^2)-(3\Delta\alpha/\alpha_0^4)$$
$$-\{20(\Delta\alpha)^2/\alpha_0^3\}+\{15(\Delta\alpha)^2/\alpha_0^5\}+\cdots\cdots], \quad (21)$$

where the condition of Eq. (20) has been applied and then, $K^*$ in Eq. (17) has been able to be eliminated. Since $\Delta\alpha$ is supposed to be sufficiently smaller than $\alpha_0$[17], this series expansion would converge, and furthermore, it is possible to show that the terms beyond the first two in the right hand side of Eq. (21) may be neglected to a first approximation[18].

16) Strictly speaking, the $\alpha$ vs. $v_2$ relation must be obtained from the condition that the value of $\alpha$ minimizes the total free energy in the system, which were given a function of $\alpha$ and $v_2$.

17) The value of $\alpha_0$ is seldom greater than 1.8 apparently including all practical cases for any polymer-solvent pair so far investigated. However, even at the critical missibility point, $\alpha=1$. Thus, it is reasonable to suppose that $\alpha$ would not be much smaller than $\alpha_0$.

18) This series expansion reduces to $2\Delta\alpha-5(\Delta\alpha)^2+\cdots$ when $\alpha_0=1$, and is $(17/16)\Delta\alpha-(65/32)(\Delta\alpha)^2+\cdots$ when $\alpha_0=2$ ($\Delta\alpha$ may be supposed to be in the range, $0\sim0.2$).

Combining Eq. (19) with (21) from the above equilibrium condition,

$$B\{(5/\alpha_0^2)-(3/\alpha_0^4)\}\Delta\alpha\fallingdotseq-[(1/x)v_2+a_2v_2^2+\cdots\cdots]. \quad (22)$$

So long as the third coefficient is concerned, Eq. (22) may be written

$$\Delta\alpha\fallingdotseq-(\alpha_0^2/5Bx)v_2[1+(3/5\alpha_0^2)+(3/5\alpha_0^2)^2+\cdots\cdots]. \quad (23)$$

## The third Virial Coefficient

The partition function, $Z$ for a solution of the homogeneous polymer may be deduced by considering the volume available to each successive polymer molecule added to the solution;

$$\ln Z=N^*\ln v-\binom{N^*}{2}\mu_2/v-(N^*/6)\mu_3/v^2+\cdots\cdots, \quad (24)$$

where $v$ is the total volume of the solution, $N^*$, the total number of polymer molecules, and $\mu_2$ and $\mu_3$ are the excluded volumes for the pair and triplet of the molecules, respectively. For a sufficiently dilute solution to justify neglect of the influence of the other molecules, Flory and Krigbaum[5] evaluated the excluded volume $\mu_2$ for the pair as

$$\mu_2=2Jm^2F(\chi), \quad (25)$$

where

$$J=(\varphi_1-\kappa_1)\bar{v}^2/V_1, \quad (26)$$

$$\chi=4C_M(\varphi_1-\kappa_1)M^{1/2}/\alpha^3, \quad (27)$$

$$C_M=(27/2^{5/2}\pi^{3/2}N)(\bar{v}^2/V_1)(M/\bar{r}_0^2)^{3/2}=K^*/2M^{1/2}, \quad (28)$$

$$F(\chi)=1-\chi/2\ 2^{3/2}+\chi^2/3!\,3^{3/3}-\cdots\cdots, \quad (29)$$

and $m$ is the weight of a polymer molecule. Since Flory et al. had employed $\alpha$ as a parameter (although they assumed for $\alpha$ to be independent on the polymer concentration), and their calculation itself should be independent upon the effect of the concentration on $\alpha$, it may be permitted approximately[19] that the results of Eqs. (25)~(29) are available for the parameter $\alpha$ dependent on the polymer concentration.

We may now express Eq. (29) in the form of a Taylor series expansion around $\alpha_0$ from Eq. (27) and the relation, $[\chi]_{\alpha=\alpha_0}=2(\alpha_0^2-1)$[5];

$$F(\chi)=[F(\chi)]_{\alpha=\alpha_0}+[\partial F(\chi)/\partial\alpha]_{\alpha=\alpha_0}\Delta\alpha+\cdots\cdots, \quad (30)$$

where

$$[\partial F(\chi)/\partial\alpha]_{\alpha=\alpha_0}=\left[\frac{dF(\chi)}{d\chi}\frac{\partial\chi}{\partial\alpha}\right]_{\alpha=\alpha_0}$$
$$=-6\{\alpha_0-(1/\alpha_0)\}F'(\alpha_0) \quad (31)$$

$$\left(F'(\alpha_0)=\left[\frac{dF(\chi)}{d\chi}\right]_{\alpha=\alpha_0}\right).$$

Employing Eqs. (23)~(31), and noting that $v_2=m\bar{v}N^*/v$, Eq. (24) may be written

$$\ln Z=N^*\ln v-(N^*/2)\mu_{20}/v-(N^*/6)\mu_{30}/v^2 -[J(1/Bx)m^3\bar{v}N^{*3}/v^2]f(\alpha_0), \quad (32)$$

where

$$f(\alpha_0)=-[\partial F(x)/\partial\alpha]_{\alpha=\alpha_0}(\alpha_0^2/5) [1+(3/5\alpha_0^2)+(3/5\alpha_0^2)^2+\cdots\cdots], \quad (33)$$

and $\mu_{20}$ and $\mu_{30}$ are the excluded volumes for the constant value of $\alpha_0$ as are employed ordinarily (i.e. in the case of $\alpha=\alpha_0$)[5,8]. Since $\Pi=kT\partial\ln Z/\partial v$, the expression of the osmotic pressure is easily obtained from Eq. (32), and comparison of the resultant formula with Eq. (1) yields the third coefficient as follows:

$$A_3=(\bar{v}^3/V_1)[0.257Ax(\varphi_1-\kappa_1)^2\{F(\alpha_0)\}^2 +2(\varphi_1-\kappa_1)(1/Bx)f(\alpha_0)], \quad (34)$$

and

$$\Gamma_3/\Gamma_2^2=0.257A+2f(\alpha_0)/B(\varphi_1-\kappa_1)x^2\{F(\alpha_0)\}^2, \quad (35)$$

where the expression of Flory et al. (Eq. (39) in their paper[5]) for the second coefficient and that of Stockmayer et al. for the third, are assumed to correspond to the above excluded volumes, $\mu_{20}$ and $\mu_{30}$ respectively ($F(\alpha_0)\equiv[F(x)]_{\alpha=\alpha_0}$).

The above treatment is not a straightfoward evaluation of the virial coefficients, and it seems rather strange that the secont coefficients, is not influenced through the change of the $\alpha$ value with the concentration. As mentioned in reference (19), the molecules should flatten in the direction of their centers and expand in the perpendicular direction. According to Krigbaum's calculation[19], however, the change in the second coefficient was found to be very small even if such an effect was considered.

## Comparison with Experiments

Until the above theoretical treatment is applied to the experimental results, it would be well to bear in mind that the values of the third virial coefficient must be calculated from osmotic data with close attention. Fox, Flory and Bueche[20] proposed an approximate method for extrapolation of the experiments. Since they adopted Eq. (3) giving greater values for the third coefficient, the resultant values of $(\Pi/c)_0$ ($\Pi/c$ at infinite dilution) and $A_2$ are probably somewhat incorrect. Moreover, the values of the third coefficient thus obtained might fall into an error of great consequence, owing to the fact that the third term $A_3\ C^2$ in Eq. (I) ordinarily contributes little to the value of $\Pi/c$. Thus, it seems to be reasonable to adopt the empirical method of Bawn[6] for the calculation of $A_3$ rather than the above method of Flory et al. (designated F. F. B. method in Table I). In Bawn's method, however, appreciable variations of the $A_2$ and $A_3$ values were observed with the concentration range to which the method was applied; In the polystyrene-toluene system[6], the values of $RTA_2$ and $RTA_3$ were $7.0\times10^7$ (cm$^4$/g.) and $4.3\times10^9$ (cm$^7$/g.$^2$), respectively, for the concentration range up to 1.0 g./100 cc., whereas the values were $RTA_2=10\times10^7$, $RTA_3=1.6\times10^9$ for the concentrations from 1.0 to 2.5 g./100 cc..

Here, from the osmotic data of Flory[21] on a number of polyisobutylene in cyclohexane, the method of least squares was used for 4~5 concentrations in the most dilute region with the requirement that Eq. (I) holds its validity in the closed form terminated after the term in $C^2$. The values of $\Gamma_2$ and $\Gamma_3$ thus obtained are given in Table II, where the values for the fractions $B$(0–3) and $C$(4–9) are those calculated by Stockmayer and Casassa by the same method[8]. It is obvious that the ratio $\Gamma_3/\Gamma_2^2$ decreases considerably

TABLE II

THE VIRIAL COEFFICIENTS OF POLYISOBUTYRENE SOLUTIONS IN CYCLOHEXANE[21]

| Polymer fraction | $\bar{M}_n\times10^{-4}$ | $(\Pi/c)^{2*}$ | $\Gamma^{2*}$ | $\Gamma^{2*}$ | $(\Gamma_3/\Gamma_2^2)_{exp.}$ | $(\Gamma_3/\Gamma_2^2)_{stock.}$ | $\alpha_0$[24] |
|---|---|---|---|---|---|---|---|
| B(0—3) | 77 | 0.33 | 4.20 | 2.17 | 0.12 | 0.31 | 1.51 |
| C(4—9) | 25.6 | 0.99 | 1.51 | 0.58 | 0.25 | 0.27 | 1.39 |
| B(9—13) | 7.82 | 3.24 | $0.54_7$ | $0.11_1$ | 0.37 | 0.14 | 1.18 |
| A(14—25) | 2.92 | 8.67 | $(0.21_3)$ | $(0.31_2)$ | (6.92) | 0.11 | 1.12 |

* $\Pi$: g./cm$^2$, $C$: g./100 cc.

19) Strictly speaking, a mean potential of average force between the pair of molecules is affected otherwise than in the above treatment. For instance, the spherically symmetrical character of the molecules may be no longer preserved owing to the presence of the other molecules. Krigbaum investigated this theoretically using the cloud model, although the work has not been published (Reprint from Proceedings of the International Conference of Theoretical Physics, Kyoto, Sept. 1953). In my opinion, however, it may be prohibitively difficult to evaluate straightfowardly the partition function in consideration of these effects.

20) T.G. Fox, Jr., P.J. Flory and A.M. Bueche, *J. Am. Chem. Soc.*, 73, 285 (1951).

21) P.J. Flory, *J. Am. Chem. Soc.*, 65, 372 (1943).

with the increasing molecular weight, just as in the case of polystyrene in toluene cited in Table I. This tendency, however, cannot be explained quantitatively by the above treatment.

Considering the dependency of the ratio $\Gamma_3/\Gamma_2^2$ upon the molecular weight, Eq. (35) may be written as:

$$\Gamma_3/\Gamma_2^2=0.257A+\{12/[5C_B(\varphi_1-\kappa_1)x^{1/2}\{F(\alpha_0)\}^2]\}\times\{-F'(\alpha_0)\}\{(\alpha_0^3-\alpha_0)+(3/5)(\alpha_0-1/\alpha_0)+\cdots\cdots\} \quad (36)$$

(see Eqs. (18), (31), and (33)), which, employing the relation $\alpha_0^5-\alpha_0^3=2C_M(\varphi_1-\kappa_1)M^{1/2}$ [13], may be converted to

$$\Gamma_3/\Gamma_2^2=0.257\ A+C^*\{-F'(\alpha_0)\}\{(1/\alpha_0^2)+(3/5)(1/\alpha_0^4)+\cdots\cdots\}/\{F(\alpha_0)\}^2 \quad [C^*=(24/5)(C_M/C_B)(M/x)^{1/2}]. \quad (37)$$

Experimentally, the dependency of $F(\alpha_0)$ and $\alpha_0$ on the molecular weight can be determined from Eq. (2) and from the intrinsic viscosity~molecular weight relationship, respectively ($\alpha_0$ is given by the relation $\alpha_0^3=[\eta]/KM^{1/2}$ [13]). The value of $\{-F'(\alpha_0)\}$ does not vary sensitively with the molecular weight of the polymer, although it decreases to some degree with the increasing molecular weight[22].

Employing the relationships $A_2\propto M^{-0.10}$ [21,23] and $[\eta]=K_mM^{0.64}$ [21] for the polyisobutyrene-cyclohexane system, there, is obtained

$$\Gamma_3/\Gamma_2^2=0.257\ A+[C_1^{**}M^{0.1}+C_2^{**}+C_3^{**}M^{-0.1}+C_4^{**}M^{-0.2}+\cdots\cdots]\{-F'(\alpha_0)\}, \quad (38)$$

where

$$C_2^{**}/C_1^{**}=C_3^{**}/C_2^{**}=C_4^{**}/C_3^{**}=(3/5)(1/\alpha_0^2)=(3/5)(K/K_m)^{2/3}.$$

Since $K=1.08\times10^{-3}$ (at 24°C)[24] and $K_m=3.60\times10^{-4}$ [21] in this case, it may be no wonder that the ratio $\Gamma_3/\Gamma_2^2$ might decrease with the increasing molecular weight, even though not remarkably, if the term $0.257A$ in Eq. (38) is sufficienly small. However, such marked decrement with the molecular weight as is shown in Table I and II, cannot be interpreted by the above estimation of the ratio.

This discrepancy may be partly due to the uncertainty in the determination of the $A_2$ and $A_3$ values from experiments. As mentioned already, the smaller $\Gamma_3/\Gamma_2^2$ value was obtained when the higher concentration range was utilized in an empirical evaluation of the $A_2$ and $A_3$ values by the Bawn's method[6]. Also in the case where the method of least squares is used, considerable errors may be possible owing to the similer effect. Actually, a plot of the quantity, $[(\Pi/c)/(\Pi/c)_0-1]/c$ against $c$ shows the considerable scatter of the experimental data especially for the frac-($A$ 14—25) (although this graph is not given here). Thus, the determination of the ratio $\Gamma_3/\Gamma_2^2$ allows some scope for judgement as to what the true value is; the $\Gamma_3/\Gamma_2^2$ values quoted in Tables I and II should therefore not be taken too literally, and the values of the ratio and also its dependency upon the molecular weight thus obtained may be supposed to be too great due to the effect mentioned above.

The inconsistency of Eq. (4) may, however, be evident since the ratio must increase considerably with the increasing molecular weight if Eq. (4) were approvable. If the result of Eq. (35) holds its validity, the ratio $\Gamma_3/\Gamma_2^2$ should be greater than $0.257A$, that expected from the theory of Stockmayer et al. (designated by $(\Gamma_3/\Gamma_2^2)_{stock.}$ in Tables I and II). The fact that $(\Gamma_3/\Gamma_2^2)_{stock.}<(\Gamma_3/\Gamma_2^2)_{exp.}$, especially in the case of higher molecular weights, would mean the overestimation of this ratio by them. It has been pointed out by various authors[24,25,26], that, strictly speaking, current theories fail to account for abnormally low values of the entropy of dilution in actual polymer solutions. Possible reasons for this failure may exist in neglecting the orientation effect i.e. the effect of anisotropy in the force fields arround the molecules, and in not taking into account the influence of the geometrical character of the solvent in relation to that of the polymer segment; at any rate, the entropy of dilution, accordingly the ratio $\Gamma_3/\Gamma_2^2$ should become smaller, due to the above effects[27]. Thus, an apparent agreement of $(\Gamma_3/\Gamma_2^2)_{stock.}$ with the experimental values for a particular molecular weight, does not always mean the consistency of the theory of Stockmayer et

22) This function $\{-F'(\alpha_0)\}$ is expressed approximately by $\{-F'(\alpha_0)\}=0.195-0.146\log_{10}\{[\eta]_{\alpha=\alpha_0}\}$, where $[\eta]_{\alpha=\alpha_0}=2(\alpha^2{}_0-1)=\dfrac{2KC_M(\varphi_1-\kappa_1)M^{1-\beta}}{K_m}$ ($[\eta]=K_mM^{\beta}$).

23) This relation has been obtained from the $A_2$ values in Table II.

24) T.G. Fox, Jr. and P.J. Flory, *J. Am. Chem. Soc.*, 73, 1909 (1951).

25) H. Tompa, Discussion in reference 3); *J. Chem. Phys.*, 21, 250 (1953).

26) M.J. Schick, P. Doty and B.H. Zimm, *J. Am. Chem. Soc.*, 72, 530 (1950).

27) The expression of the second coefficient is not changed because the above complicated effects upon it are involved in the parameter $\varphi_1$ in the treatment of reference 5).

al. with experiments[8].

Furthermore, the ratio is greater in methyl ethyl ketone (a bad solvent) than in toluene (a good solvent) for polystyrene as is shown in Table I. This is consistent with what is predicted from our theory (see Eq. (37), where $\alpha_0$ is larger in a good solvent than in a bad solvent[28]), in direct contradiction of Stockmayer and Casassa's theory. It would be instructive to point out that the theories based on lattice models[11,12,29] imply the similar tendency on this ratio; the $\Gamma_3/\Gamma_2^2$ value is predicted to be greatest in poor solvents or at low molecular weights, although these theories involve some unsatisfactory approximations[24,25]. Our treatmet may be considered to be an intermediate one between the treatments developed in consideration of the volume effect[4,5] and the earlier theories in which the effect was not taken in to account[11,12,29]. So far as the third coefficient is concerned, the volume effect theory would have to be modified appreciably as is mentioned above.

In order to obtain confirmatory evidence on the quantitative interpretation for the third coefficient, there exist many difficulties to be resolved both experimentally and theoretically, and it seems, first of all, to be preferable to obtain additional data available for this purpose.

Finally, it may be remarked that a possibility may be predicted from our theory as to the existence of an inflexion point in the $H$ vs. $C$ curve. If the treatment of Stockmayer et al. were assumed to afford a legitimate representation of the third coefficient except the correction term arising from $\mu_2$ in Eq. (24), by empolying the parameter $\alpha$ dependent on the polymer concentration, instead of $\alpha_0$, it does not seem to be unlikely that the effect of this concentration dependency of $\alpha$ would make the fourth coefficient negative, since the ratio $(\Gamma_3/\Gamma_2^2)_{\text{stock.}}$ decreased with decreasing $\alpha$. Actually, experiments[8,26,30] over a wide concentration range indicate a negative deviation at high concentrations from the curve fitting the data well at lower values by employing Eq. (I) with the omission of the terms beyond the third. Also theoretically the existence of this inflexion point was pointed out by Rushbrooke et al.[31] from another point of view.

This paper was read at the Annual Meeting of Soc. of High Polymer, Japan, at Tokyo Institute of Technology, Tokyo, on June, 4th 1955.

The author expresses his appreciation to Professor H. Maeda and K. Makishima for their encouragement and support of this work.

*Laboratory of Textile Chemistry, Tokyo Institute of Technology, Tokyo*

28) Although $F(\alpha_0)$ in Eq. (37) is smaller for the larger value of $\alpha_0$, its change with $\alpha_0$ is very small ($F(\alpha_0)=1\sim0.8$ in the usual range of $\alpha_0$), and moreover, $\{-F'(\alpha_0)\}$ is smaller for the larger $\alpha_0$.

29) A.R. Miller, "Theory of Solutions of High Polymers", Oxford University Press, London (1948).

30) G.V. Browing and J.D. Ferry, *J. Chem. Phys.*, **17**, 1107 (1949).

31) G.S. Rushbrooke, H.I. Scoins and A.J. Wakefield, *Trans. Faraday Soc., Discussion*, **15**, 57 (1953).

# *Chemical Studies on Charoninsulfuric Acid**

By Fujio EGAMI, Tadashi ASAHI, Noriko TAKAHASHI, Sakaru SUZUKI, Shogo SHIKATA and Kazutosi NISIZAWA

(Received July 13, 1955)

## Introduction

T. Soda and his co-workers have found that several marine molluscs are the best materials for the preparation of sulfatases. For example, the visceral hump of *Charonia lampas* (*Tritonium nodiferm*) contains very active phenosulfatase, glucosulfatase and chondrosulfatase. So they considered that it obtained from the mucus of *Charonia lampas* by T. Soda and F. Egami[1] in 1938 and named

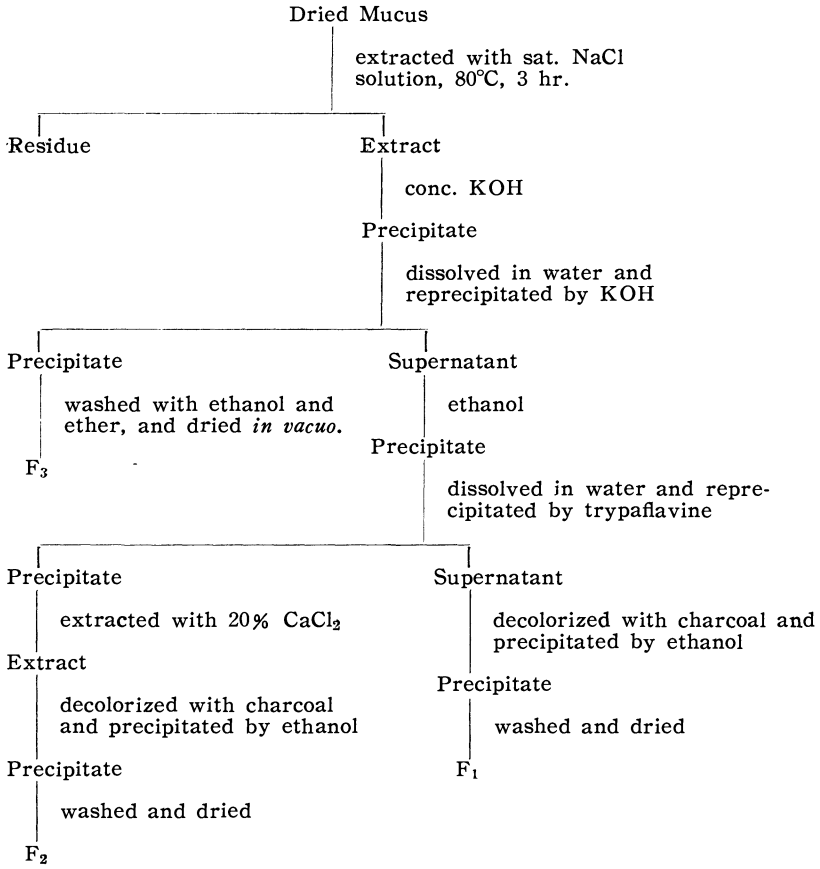
* Most part of this communication was already presented before the 27th Congress of the Biochemical Society of Japan (Kyoto, April 5, 1955) by S. Suzuki and before the 8th General Assembly of Physiolosists, Biochemists and Pharmacologists in USSR (Kiev, May 24, 1955) by F. Egami.

1) T. Soda and F. Egami, *Bull. Chem. Soc. Japan*, **13**, 652 (1938); *J. Chem. Soc. Japan*, **59**, 1417 (1938).

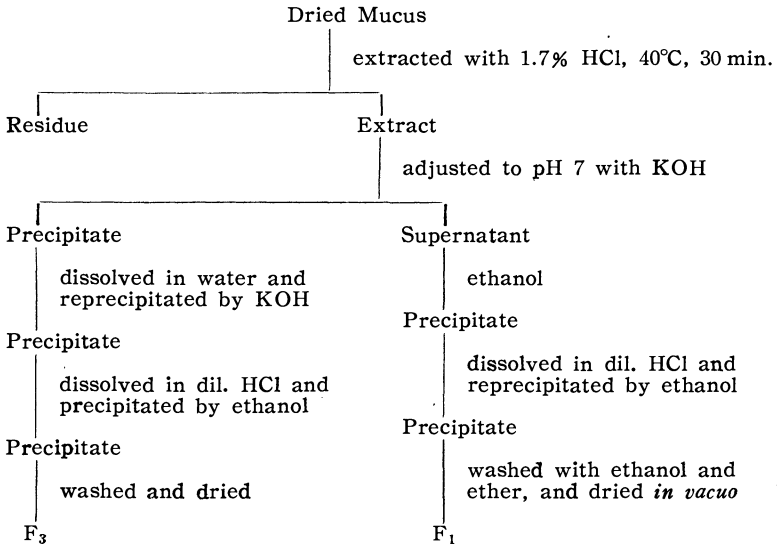
TABLE I

METHODS OF PREPARATION

Method 1.




Method 2.



charoninsulfuric acid. The chief characters of the preparation obtained by them were as follows:

Sodium charoninsulfate is free from N, and contains 15% of ethereal sulfate S and 36% of ash.

Lison's metachromatic reaction is intensely positive.

By sulfatase preparation of *Charonia lampas*, it liberates sulfuric acid and gives reducing sugars, one of which is regarded as D-glucose from the specific optical rotation and its fermentability by baker's yeast.

It has a strong inhibitory action on blood coagulation.

From these results, they considered charoninsulfuric acid to be a desamino-mucoitin polysulfuric acid.

In 1948, the further investigation on the chemical nature of charoninsulfuric acid was undertaken by T. Soda and H. Terayama[2]. The most important contribution by them was the discovery that the purified preparation did not contain uronic acid and the polysaccharide fraction gave only D-glucose after acid hydrolysis. Moreover they desulfated charoninsulfuric acid by heating it in methanolic hydrogen chloride and obtained a white powder, which gave an X-ray diffraction pattern identical to that of cellulose. From this and other qualitative results, they concluded that charoninsulfuric acid is a cellulose sulfate or sulfuric ester of a glucan quite similar to cellulose.

In 1954 we repeated this investigation in order to ascertain the conclusion of Soda by chemical and enzymatic methods. It is the purpose of the present paper to describe our experiments and results.

## Experimental*

### I. Preparation and General Properties

**Material.**—The mucus of *Charonia lampas* was defatted and dried by hot alcohol and acetone: N, 5~10%; ethereal sulfate S, 6~7%. The mucus may be regarded as a mucoprotein.

**Extraction.**—Charoninsulfuric acid can be extracted from the dried mucus by concentrated mineral salt solution or diluted mineral acid.

**Methods of Separation.**—As will be shown later, charoninsulfuric acid is not a definite chemical individual, but a mixture of glucan sulfates with different sulfur contents and different solubilities, and hence this had to be taken into consideration when preparing samples. Our methods of preparation were as follows:

1) Salting out by KCl: Charoninsulfuric acid with high sulfur content can be salted out by KCl as the potassium salt.
2) Precipitation by Trypaflavine: Charoninsulfuric acids, except those of very low sulfur content (ca 2%), are precipitated with trypaflavine, and then from this precipitate charoninsulfuric acid with a relatively low sulfur content may be extracted by concentrated $CaCl_2$ solution.
3) Precipitation by KOH: Charoninsulfuric acid with high sulfur content can be precipitated by KOH at the concentration of ca 0.5 N.
4) Precipitation by Benzidine: The benzidine salt of charoninsulfuric acid with high sulfur content is also difficultly (less difficultly than trypaflavine salt) soluble. Charoninsulfuric acid may be extracted from the precipitate by NaOH solution.
5) Precipitation by Ethanol: Charoninsulfuric acid is precipitated with an equal volume of ethanol from aqueous solutions.

Combining these methods of fractionation, various charoninsulfuric acids with different sulfur contents were obtained. Typical methods of preparation are shown in Table I. The properties of charoninsulfuric acids with different sulfur contents are summarized in Table II.

TABLE II
PROPERTIES OF CHARONINSULFURIC ACIDS

| Charoninsulfuric acids | S content % | Salting out by KCl | Precipitation by KOH | Precipitation by trypaflavine | $I_2$–KI reaction |
|---|---|---|---|---|---|
| $F_1$ | 1~ 2 | − | − | − | red |
| $F_2$ | 2~ 5 | + | − | + | − |
| $F_3$ | 10~18 | + | + | + | − |

The possibility that while charoninsulfuric acid itself is a substance with definite sulfur content, the preparations thus obtained are mixtures of charoninsulfuric acid and glycogen (or similarly nonsulfated glucans) need not be considered because of the following facts:

1) Charoninsulfuric acid with low sulfur content (2~5%) is precipitated by trypaflavine, and from the precipitate charoninsulfuric acid is extracted by $CaCl_2$ solution. Calcium charoninsulfate is obtained by alcohol precipitation. Even by repetition of this process, we could not separate any nonsulfated glucans and obtained the same charoninsulfate with a low sulfur content.
2) By Grassman's continuous electrophoresis on paper[3], we could confirm the fact that glycogen moves towards the cathode (probably owing to the electroendosmose) and charoninsulfuric acids towards the anode. The latter, when mixed with the former, can be separated easily by the apparatus.

Thus we have been led to the conclusion that there are various charoninsulfuric acids with different sulfur contents. Sodium charoninsulfate with the highest sulfur content obtained so far contained 20.3% ethereal sulfate sulfur.

### II. Investigation on the Chemical Nature of the Glycan.

**Desulfation.**—Charoninsulfuric acid with a high sulfur content (more than 5%) can be desulfated by heating it in methanol-HCl (1~1.5%) for several hours. The desulfated product was named "charonin". It is dissolved in Schweit-

2) T. Soda and H. Terayama, *J. Chem. Soc. Japan*, 69, 65 (1948).

* A part of the experiments was executed in the Marine Biological Laboratory of Nagoya University.

3) W. Grassman and K. Hanning, *Z. Physiol. Chem.*, 292, 32 (1953).

zer's reagent. When the solution was neutralized with acetic acid, a part of the charonin was precipitated. From the supernatant a further amount of precipitate was produced by adding methanol. The former was washed with diluted HCl, methanol and ether, and the white powder thus obtained was provisionally named Fraction A. The latter was purified by repeated reprecipitation and named Fraction B. So far the analysis for various charoninsulfuric acids with different sulfur contents showed that the less the sulfur content was the less the proportion of Fraction A to Fraction B (*vide infra*); fraction $F_1$ with the lowest sulfur content may be regarded as Fraction B itself. The properties of charonin, Fraction A, and Fraction B are summerized in Table III. It is remarkable that Fraction B gives a red color with iodine solution. Because Fraction A does not inhibit the color reaction of Fraction B, it seems that charonin is probably not a simple mixture, but a compound of Fraction A and Fraction B, which are combined with a rather weak bond and decomposed by the action of Schweitzer's reagent. The weak reducing power of Fraction A and B may be attributed to the hydrolysis by Schweitzer's reagent.

**Constitution of Fraction A.**—The desulfated preparation used for X-ray investigation by Soda and Terayama corresponds to this fraction.

It was confirmed by paper chromatography that sulfuric acid hydrolysis of this fraction resulted in the exclusive production of D-glucose:

Solvents, *n*-BuOH: AcOH: $H_2O$ (4:1:2), *n*-BuOH: Ether: $H_2O$: Ammonia (40:10:49:1), *n*-BuOH: Pyridine: $H_2O$ (6:4:3)

Aniline hydrogen phthalate was used to locate the sugar.

Octaacetylcellobiose (m.p. 220°C) was obtained by acetolysis of Fraction A. No melting point depression occured when mixed with octaacetylcellobiose prepared from filter paper. Moreover as shown in Table IV, it was hydrolysed by Irpex-cellulase prepared by the method of Nisizawa[5], but not at all by crystalline *α*-amylase (Taka-amylase) prepared by the method of Akabori[6] and sweet potato *β*-amylase prepared by the method of Balls[7]. In the reaction mixture after hydrolysis by Irpex-cellulase, glucose and cellobiose were detected by paper chromatography. Cellobiosazone (m.p. 210°C) was obtained after fermenting out the glucose by yeast (Rasse XII). It should be noted here that this Fraction A gives, similar to cellulose, a blue color reaction with $I_2$-KI-$H_2SO_4$ reagent.

Notwithstanding these findings confirming the existence of cellulose structure in Fraction A, several properties of the fraction are not consistent with a cellulose structure. For example, as shown in Table V, the periodate consumption was lower than expected from a cellulose structure.

TABLE III

PROPERTIES OF CHARONIN, FRACTIONS A AND B

| Substances | $I_2$–KI reaction | $I_2$–KI–$H_2SO_4$ reaction | $ZnCl_2$–$I_2$ reaction | Reducing power* |
|---|---|---|---|---|
| Charonin | negative | yellow | yellow | 0.00 |
| Fraction A | negative | blue | blue | 0.02 |
| Fraction B | red | red | red | 0.03 |
| Cellulose | negative | blue | blue | |
| Amylose | blue | blue | blue | |
| Starch | purple | purple | purple | |

* The value represents mg. glucose which corresponds to the reducing power per mg. of the substance (Somogyi's method (4)).

TABLE IV

HYDROLYSIS BY IRPEX-CELLULASE

| Substrate | Substrate concentration. % | Incubation time, hrs. | Increase of reducing power* per mg. of substrate |
|---|---|---|---|
| Charonin | 0.50 | 72 | 0.19 |
| Fraction A | 0.50 | 72 | 0.33 |
| Fraction B | 0.50 | 72 | 0.04 |
| Cellobiose | 0.12 | 137 | 0.00 |
| Soluble starch | 0.25 | 66 | 0.00 |
| Laminarin | 0.30 | 66 | 0.00 |
| Hydrocellulose | 0.50 | 24 | 0.18 |
| Carboxymethylcellulose | 0.25 | 24 | 0.45 |

Conditions: 0.1 M acetate buffer, pH 4.0, temp. 30°C.

* The reducing power was calculated as mg. cellobiose (Somogyi's method).

TABLE V

PERIODATE CONSUMPTION BY FRACTIONS A AND B

| Substance | Reaction time, hrs. | Periodate consumption, mol. per glucose unit |
|---|---|---|
| Fraction A | 120 | 0.65 |
| Fraction B | 68 | 0.93 |
| Cellulose | 93 | 1.08 |

4) M. Somogyi, *J. Biol. Chem.*, **160**, 61 (1945).

5) K. Nisizawa and T. Kobayasi, *J. Agr. Chem. Soc. Japan*, **27**, 239 (1953): K. Nisizawa, T. Kobayasi and N. Ichikawa, *Symposia on Enzyme Chem.*, **10**, 7 (1954).

6) S. Akabori, B. Hagihara and T. Ikenaka, *Proc. Japan Acad.*, **27**, 350 (1951).

7) A.K. Balls, R.R. Thompson and M.K. Walden, *J. Biol. Chem.*, **173**, 9 (1948).

So the constitution of Fraction A cannot yet be established completely and it must be further studied. However we may be able to conclude that the main part of Fraction A has a cellulose structure, i.e. β-1, 4′-glucan constitution.

**Constitution of Fraction B.**—Fraction B, which is soluble in water and gives a red iodine reaction, was also found to be composed entirely of glucose (by reducing power measurement and by paper chromatography after sulfuric acid hydrolysis). As previously shown in Table IV, this fraction was also, although far less easily than Fraction A, hydrolysed by Irpex-cellulase to give glucose and cellobiose. The most remarkable characteristic of this fraction is the fact that it was hydrolysed by α-and β-amylases (Table VI). In the reaction

TABLE VI

ACTIONS OF α-AND β-AMYLASES

| Substrate | Increase of reducing power* per mg. substrate | |
|---|---|---|
| | α-Amylase | β-Amylase |
| Charonin | 0.02 | 0.00 |
| Fraction A | 0.00 | 0.00 |
| Fraction B | 0.36 | 0.09 |
| Glycogen | 0.32 | 0.09 |

Conditions: Substrate conc. 0.13%, M/30 acetate buffer, pH 5.6 (α−), 4.7 (β−), incubation time 18 hrs., temp. 37°C; reaction mixtures contained 0.055% NaCl in the case of α-amylase.

* The reducing power was calculated as mg. maltose (Somogyi's method).

mixture after hydrolysis by both amylases, maltose and relatively small amounts of glucose were detected by paper chromatography. Because this fraction consumed periodate as expected from an 1, 4′-glucoside glucan structure (Table V), it seems to contain amylose structure. From these results, Fraction B may be regarded as containing both α-1, 4′- and β-1, 4′-glucoside bonds.

### III. Discussion on the Constitution of Charoninsulfuric Acid

From the foregoing results, it is quite certain that charoninsulfuric acid is a mixture of glucan polysulfates with different sulfur contents. The nature of the glucan seems to be very complex. A part of it has a cellulose structure and the other part an amylose structure; however the nature of the linkage combining the two parts are as yet unknown. At any rate, it is decomposed by Schweitzer's reagent after desulfation into two parts, i.e. Fraction A, insoluble in water, composed mainly of cellulose structure, and Fraction B, soluble in water, composed mainly of amylose structure. So far as we have analysed various charoninsulfuric acids, we have found that a parallelism exists between the sulfur content and the cellulose structure (Table VII). It seems that biological sulfation may be preceded or accompanied by biological transformation of amylose to cellulose.

TABLE VII

THE YIELDS OF FRACTIONS A AND B FROM VARIOUS CHARONINSULFURIC ACIDS WITH DIFFERENT SULFUR CONTENTS

| Material | S Content % | Yield* of Fraction A | Yield* of Fraction B |
|---|---|---|---|
| $F_3$ | 10.0 | 214 | 43 |
| | 9.2 | 200 | 50 |
| $F_2$ | 4.0 | 12 | 270 |
| $F_1$ | 1.1 | 0 | 390 |

* The values represent mg. each fractions obtained from 1 g. of charoninsulfulic acids.

The question might arise, whether a Walden inversion may take place during the desulfation process of charoninsulfuric acids. However, because the preparation $F_1$ with only one to two % of sulfur gave only glucose after direct hydrolysis by sulfuric acid, it is quite reasonable to assume that glucose must exist as such in charoninsulfuric acid.

## Summary

We have obtained charoninsulfuric acid free from glycogen (or similar glucans) and confirmed that it is a mixture of glucan polysulfates with different sulfur contents. The desulfated product (charonin) was decomposed by Schweitzer's reagent into two parts, Fractions A and B. From Fraction A, which is insoluble in water and gives a blue color reaction with $I_2$-KI-$H_2SO_4$, glucose (after hydrolysis by sulfuric acid), cellobiose (after hydrolysis by Irpex-cellulase) and octaacetylcellobiose (after acetolysis) were obtained. From Fraction B, which is soluble in water and gives a red iodine reaction, glucose, cellobiose and maltose (after hydrolysis by amylases) were obtained. This fraction consumed periodate as expected from 1, 4′-glucoside glucan. From these results, this glucan (charonin) may be regarded as having both cellulose and amylose structure. Moreover it was found by analysis of various charoninsulfuric acids that a close relation existed between the sulfur content of charoninsulfuric acid and the constitution of glucan, i.e. the less the sulfur content was, the less was the cellulose structure.

We wish to express our thanks to Prof. T. Soda for his kind encouragement and interest. We gratefully acknowledge the gift of amylases by Prof. S. Akabori and amylose by Prof. Z. Nikuni. The expense of this study was defrayed in part by a grant from Seikagaku-Kenkyujo Ltd., to which our thanks are due.

*Department of Chemistry and Department of General Education, Nagoya University, Nagoya* and
*Faculty of Textile and Sericulture, Shinshu University, Ueda*

# SHORT COMMUNICATION

## *The Solvent Effect on Fluorescence Spectrum. Change of Solute-Solvent Interaction during the Lifetime of Excited Solute Molecule*

By Noboru MATAGA, Yozo KAIFU and Masao KOIZUMI

(Received October 4, 1955)

The solvent effect on absorption spectrum is determined by the equilibrium ground state and the Franck-Condon excited state, while that of fluorescence spectrum depends upon the equilibrium excited state and the Franck-Condon ground state[1]. Therefore, the spectral shift of fluorescence due to the solvent effect may differ in general from that of absorption, and it is expected that from the investigation of this difference some informations may be derived concerning the excited electronic structure. But the theoretical treatment of the solvent effect of fluorescence spectrum seems not to have been undertaken so far. Now it was found that a reasonable formula for the difference of the spectral shifts between absorption and fluorescence conld be derived by applying Ooshika's theory[2] concerning the light absorption in solution to the case of fluorescence. The formula obtained is as follows.

$$hc(\Delta\sigma_f-\Delta\sigma_a)\cong-\left\{\frac{2(D-1)}{2D+1}-\frac{2(n^2-1)}{2n^2+1}\right\}\frac{(\vec{\mu}_e-\vec{\mu}_g)^2}{a^3}+\left\{\frac{2(D-1)}{2D+1}\right\}^2\frac{1}{a^3}\left[3\sum_{e\neq m}\frac{\{\vec{\mu}_e(e|\vec{\mu}_o|m)\}^2}{\varepsilon_e-\varepsilon_m}\right.$$
$$+3\sum_{m\neq g}\frac{\{\vec{\mu}_g(g|\vec{\mu}_o|m)\}^2}{\varepsilon_g-\varepsilon_m}-\sum_{m\neq g}\frac{\{\vec{\mu}_e(g|\vec{\mu}_o|m)\}^2}{\varepsilon_g-\varepsilon_m}-\sum_{m\neq e}\frac{\{\vec{\mu}_g(e|\vec{\mu}_o|m)\}^2}{\varepsilon_e-\varepsilon_m}-\sum_{m\neq e}\frac{\{\vec{\mu}_e(e|\vec{\mu}_o|m)\}\{\vec{\mu}_g(e|\vec{\mu}_o|m)\}}{\varepsilon_e-\varepsilon_m}$$
$$\left.-2\sum_{m\neq g}\frac{\{\vec{\mu}_g(g|\vec{\mu}_o|m)\}\{\vec{\mu}_e(g|\vec{\mu}_o|m)\}}{\varepsilon_g-\varepsilon_m}\right] \quad (1)$$

$\Delta\sigma_f$, $\Delta\sigma_a$; Wave number shifts of fluorescence and absorption spectra.

$D$, $n$; Dielectric constant and refractive index of the solvent.

$\vec{\mu}_e$, $\vec{\mu}_g$; Dipolemoments in the excited and ground states.

$a$: Radius of the cavity in Onsager's Theory[3].

$\varepsilon_m$: Electronic energy of the solute molecule in m state.

$\vec{\mu}_o$: Dipole operator.

The second term of Eq. (1) is relatively small in its order of magnitude compared with the first term, and can be neglected in the first approximation:

$$-hc(\Delta\sigma_f-\Delta\sigma_a)\simeq\left\{\frac{2(D-1)}{2D+1}-\frac{2(n^2-1)}{2n^2+1}\right\}\frac{(\mu_e-\mu_g)^2}{a^3} \quad (2)$$

This equation represents the effect of orientation polarization, and it is noteworthy that, if it really holds, it enables us to estimate the dipolemoment of the excited molecule.

In order to test the applicability of the equation, we have measured the spectral shifts of $\alpha$- and $\beta$-naphthols and $\beta$-naphthyl methyl ether in various solvents. It must be noted that, in the case of $\alpha$- and $\beta$-naphthols, the hydrogen bond is formed between the solute and solvent molecules in most cases. Hence a short range interaction due to hydrogen bonding must be taken into account in addition to a long range dipole interaction. But the contribution of the former to $(\Delta\sigma_f-\Delta\sigma_a)$ is negligibly small as was already confirmed by the measurement in mixed solvent[4].

The results obtained conform fairly well to with the Eq. (2) in all cases. If one assumes a$\sim$3 A for $\beta$-naphthyl methyl ether, the value of $\vec{\mu}_e-\vec{\mu}_g$ is calculated to be $\sim$0.5 $D$, from the inclination of a straight plot.

This enlargement of dipolemoment in the excited state may plausibly be due to the increase of electron migration in the excited state, because the value agrees fairly well with the one theoretically calculated by Baba[5] for phenol on the analogous assumption.

Quite recently, Lippert*[6] has made the treatment similar to ours regarding the

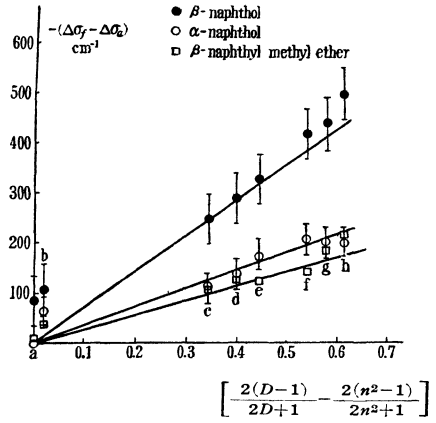



Fig. 1. $(\Delta\sigma_f-\Delta\sigma_a)\sim\left[\frac{2(D-1)}{2D+1}-\frac{2(n^2-1)}{2n^2+1}\right]$: relation for naphthols and β-naphthyl methyl ether.
Solvents
a, benzene; b, toluene; c, butyl acetate; d, ethyl acetate; e, methyl acetate; f, butanol; g, ethanal; h, methanol.

spectral shifts of 4-dimethylamino-4′-nitrostilbene and 4′-cyanostilbene, etc., and estimated the dipolemoments of these molecules in the excited state.

But the application of Onsager's theory to such long molecules would be too rough to except the satisfactory agreement between theory and experiment. Really, this agreement is much better in our case. The approximate nature of the theory, however, still does not allow the exact quantitative discussion of the problem, and a more refined theory should be needed. Full details of data and discussions will soon be published.

*Institute of Polytechnics, Osaka City University, Osaka*

1) See for example: N. S. Bayliss and E. G. McRae *J. Phys. Chem.*, **58**, 1002 (1954).
2) Y. Ooshika, *Rep. Kobayashi Inst. Phys. Research*, **2**, 99 (1952), ibid., **3**, 54 (1953); *J. Phys. Soc. Japan*, **9**, 594 (1954).
3) L. Onsager, *J Am. Chem. Soc.*, **58**, 1486 (1936).
4) N. Mataga, Y. Kaifu, and M. Koizumi, (to be published in this Bull.)
5) H. Baba, *Monograph Ser. Research Inst. Applied Electrocity*, Hokkaido, No. 4 61 (1954).
6) E. Lippert. *Z. Naturforsch.*, **10**a, 541 (1955).
* After we had finished the present work, Dr. Lippert, informed us of this work by a private communication which was kindly given to Mataga.